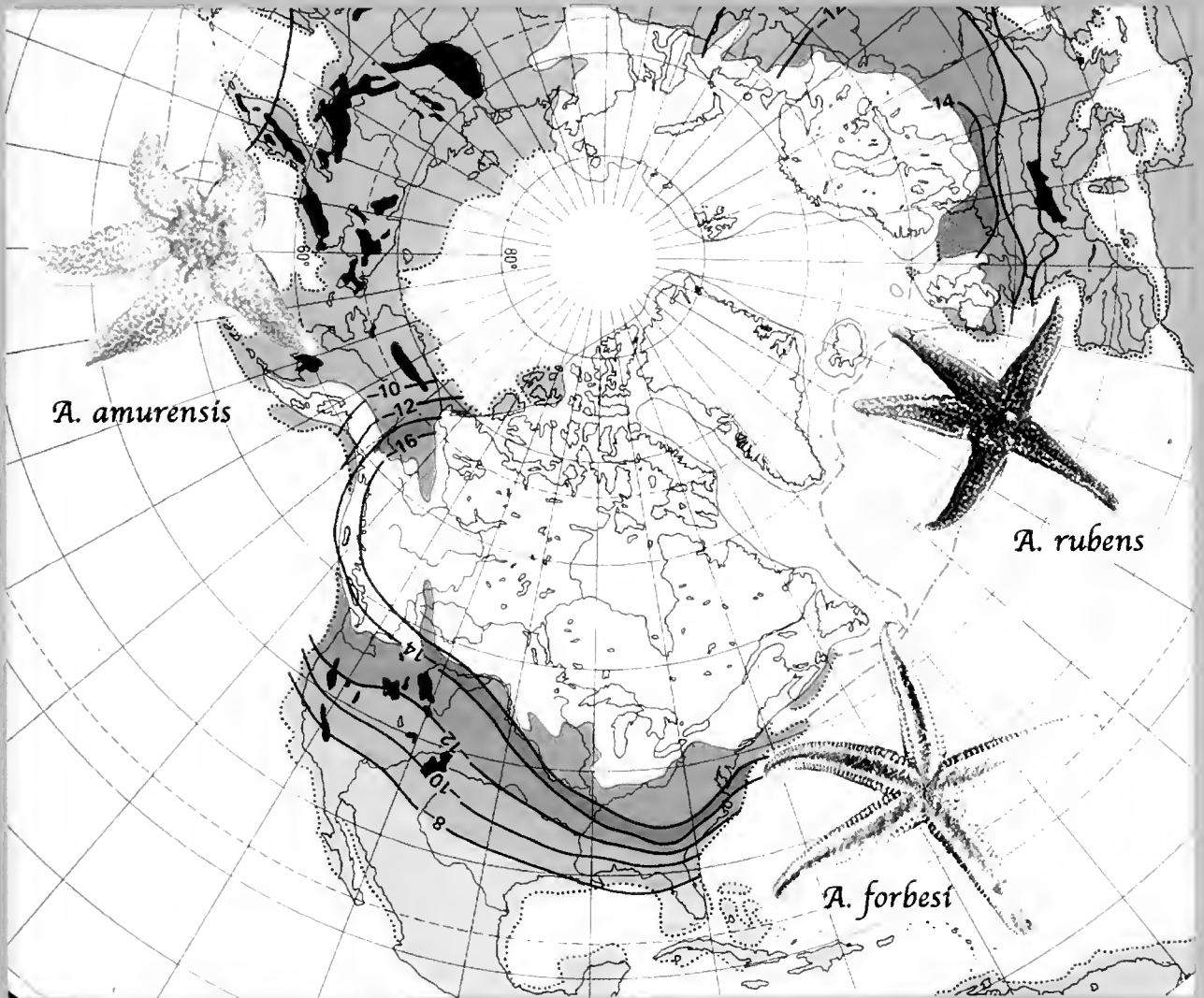


MBL



THE BIOLOGICAL BULLETIN



AUGUST 2001



Published by the Marine Biological Laboratory

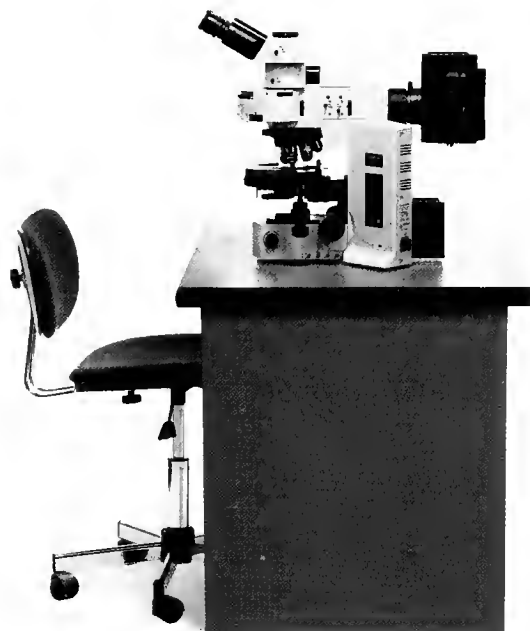
<http://www.biolbull.org>

Made to my exact

And yours.



Let's address my specs first, specifically high resolution, contrast and infinity-corrected optics. They've all reached Olympian standards thanks to Olympus. But even more to the point, here's how the BX2's modular design came through for me. First, the eight-position universal condenser offers the flexibility to choose from brightfield, darkfield and phase as well as DIC. Next, its assortment of prisms makes it possible to match the optical image shear to the specimen, achieving the optimal balance of contrast and resolution. Finally, the Plan APO objectives, with superb chromatic correction and contrast, provide extraordinary detail. Now let's move on.



Picture yourself sitting here, looking into your Olympus BX2 research microscope, your fluorescence requirements having been met. Specifically: The aspherical collector lens produces a fluorescence intensity that's twice as bright as others and more even across the field. The unique excitation balancers improve visualization of multiple labels by revealing details that would otherwise be unseen. The six-position filter turret makes single and multiband imaging faster and simpler. And the rectangular field stop, another Olympus exclusive, protects the specimen by exposing only the precise area being imaged in addition to enhancing the S/N ratio. Time to see what's next.

OLYMPUS
FOCUS ON LIFE

Visit us at www.olympusamerica.com or call 1-800-446-5967.

specifications.

And yours. And yours.



Here, imaging and automation is a must. And here, the BX2 responds as a high-performance, highly efficient, digital imaging machine. The motorized nosepiece, Z-drive, condenser, illuminator and filter wheels are fully integrated through the user-friendly software package. It's you who commands this automated imaging system with your PC, optional keypad or preset buttons located on the microscope frame itself. Digital images can now be acquired, processed and analyzed faster than before. And reports and documentation have never been this easy to generate. Which leaves one more set of specs.

Now modularity really is in high gear as the Olympus FLUOVIEW 500 is added, resulting in a complete confocal laser scanning microscope system. It provides five imaging channels and has an intuitive operation that makes it readily available to everyone so that productivity is greatly enhanced. By the way, the BX2 is the only microscope that offers a Metal Matrix Composite frame—the ultimate in static and thermal rigidity—making it the optimal solution for frequent use of 3D microscopy, time-lapse observations and high-end digital imaging. So you see, with all this modularity and flexibility, my BX2 microscope is also your BX2 microscope.

BX²

Research Microscope Series

Cover

About 3.5 million years ago (Ma), rising sea levels opened the Bering Strait, and the North Atlantic Ocean was invaded by hundreds of taxa from the North Pacific. Among the invaders was the seastar genus *Asterias*. At present, two species of *Asterias* are recognized in the North Atlantic: *A. forbesi* on the west coast of the Atlantic, from Cape Cod south to Cape Hatteras, and *A. rubens*, a European species that ranges from southern France to Norway and Iceland, but also occurs in the northwestern Atlantic, mainly from Cape Cod north. Representatives of these species are shown on the cover, as is a specimen of *A. amurensis*, which inhabits the North Pacific from British Columbia to Japan.

After entering the Atlantic, populations of *Asterias* were separated, and speciation subsequently occurred. The timing of the separation is critical, for it determined, in part, the mechanism involved in the speciation, and it is the basis for the present geographic distribution of *Asterias* species in the North Atlantic. However, as the map on the cover illustrates, the timetable of these events was constrained by habitat and oceanographic instability during the Pleistocene glaciation.¹ In particular, most of the current North American habitat of *Asterias rubens* was repeatedly covered by a kilometer of ice and was unavailable to this seastar until about 15,000 years ago—long after the opening of the Bering Strait.

¹ The map on the cover is a polar view of the North Atlantic and Pacific Oceans during the Wisconsin glacial maximum, about 20,000 years ago. The solid blue line marks the average glacial margin; the dashed blue lines show the extent of sea ice in summer (upper) and winter (lower); the dotted black line illustrates how lower sea levels during glacial maxima altered the Atlantic coastline; and the shades of blue and green represent isotherms, highly compressed in the northwestern Atlantic, and producing a strong temperature gradient.

The speciation of *Asterias* in the Atlantic has been explained by two hypotheses. Either the event occurred recently, with strong natural selection precluding hybridization; or the speciation into North American and European species occurred shortly after *Asterias* entered the North Atlantic, with a recolonization of the northwestern coast of the Atlantic by *A. rubens* taking place in recent times. The second hypothesis implies that speciation was due to prolonged isolation and was independent of observed adaptations to different water temperatures.

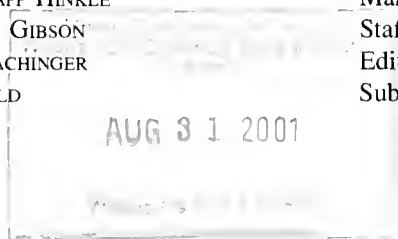
As reported in this issue (p. 95), John P. Wares has collected genetic sequence data from populations of *A. forbesi*, *A. rubens*, and *A. amurensis* and used them in phylogenetic and population genetic analyses to test the two hypotheses. He concludes that, although changes in climate and ocean currents—particularly the formation of the Labrador Current—were concomitant with the separation of *Asterias* populations in the North Atlantic 3 Ma, permanent colonization of New England and the Canadian Maritimes by *A. rubens* occurred very recently.

(Credits: map—from B. Frenzel, M. Pécsi, and A.A. Velichko, eds., 1992, *Atlas of Paleoclimates and Paleoenvironments of the Northern Hemisphere*, Geographical Research Institute, Hungarian Academy of Sciences, Budapest, p. 43; images of *Asterias forbesi* and *A. rubens*—from the George M. Gray Museum collection, formerly administered by the Marine Biological Laboratory, now at the Peabody Museum of Natural History of Yale University; image of *A. amurensis*—from a photograph by Jan Haaga, provided online by the Alaska Fisheries Science Center/National Marine Fisheries Service; cover design—by Beth Liles, MBL.)

THE BIOLOGICAL BULLETIN

AUGUST 2001

Editor	MICHAEL J. GREENBERG	The Whitney Laboratory, University of Florida
Associate Editors	LOUIS E. BURNETT R. ANDREW CAMERON CHARLES D. DERBY MICHAEL LABARBERA	Grice Marine Biological Laboratory, College of Charleston California Institute of Technology Georgia State University University of Chicago
Section Editor	SHINYA INOUÉ, <i>Imaging and Microscopy</i>	Marine Biological Laboratory
Online Editors	JAMES A. BLAKE, <i>Keys to Marine Invertebrates of the Woods Hole Region</i> WILLIAM D. COHEN, <i>Marine Models Electronic Record and Compendia</i>	ENSR Marine & Coastal Center, Woods Hole Hunter College, City University of New York
Editorial Board	PETER B. ARMSTRONG ERNEST S. CHANG THOMAS H. DIETZ RICHARD B. EMLET DAVID EPEL GREGORY HINKLE MAKOTO KOBAYASHI ESTHER M. LEISE DONAL T. MANAHAN MARGARET MCFALL-NGAI MARK W. MILLER TATSUO MOTOKAWA YOSHITAKA NAGAHAMA SHERRY D. PAINTER J. HERBERT WAITE RICHARD K. ZIMMER	University of California, Davis Bodega Marine Lab., University of California, Davis Louisiana State University Oregon Institute of Marine Biology, Univ. of Oregon Hopkins Marine Station, Stanford University Cereon Genomics, Cambridge, Massachusetts Hiroshima University of Economics, Japan University of North Carolina Greensboro University of Southern California Kewalo Marine Laboratory, University of Hawaii Institute of Neurobiology, University of Puerto Rico Tokyo Institute of Technology, Japan National Institute for Basic Biology, Japan Marine Biomed. Inst., Univ. of Texas Medical Branch University of California, Santa Barbara University of California, Los Angeles
Editorial Office	PAMELA CLAPP HINKLE VICTORIA R. GIBSON CAROL SCHACHINGER WENDY CHILD	Managing Editor Staff Editor Editorial Associate Subscription & Advertising Secretary



Published by
MARINE BIOLOGICAL LABORATORY
WOODS HOLE, MASSACHUSETTS

<http://www.biolbull.org>

Genomic Research Leaders Choose Microway® Scalable Clusters

Eos Biotechnology, Marine Biological Laboratory, Millennium Pharmaceuticals, Mount Sinai Medical School, NIH, Pfizer, and Rockefeller University All Choose Microway Custom Clusters and Workstations for Reliability, Superior Technical Support and Great Pricing.

- 1.4 GHz Dual Athlon, 1.7 GHz Pentium 4, or 1 GHz Dual Pentium III in 1U or 2U Clusters
- Dual Alpha 833 MHz Clusters and Towers
For maximum price/performance choose our Alpha 1U 833 MHz, 4 MB DDR Cache CS20, 4U UP2000+ or 4U 264DP RuggedRack™
- Myrinet, Gigabit Ethernet or Dolphin Wulfskit High Speed Low Latency Interconnects
- RAID and Fibre Channel Storage Solutions

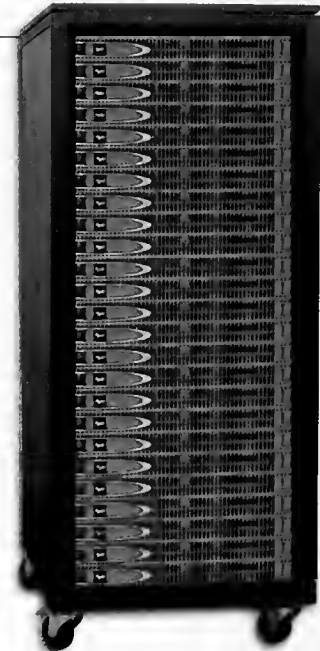


Microway® Screamer™
Dual Alpha UP2000+
833 MHz, 4MB Cache in
RuggedRack™ Chassis
with RRR™ Redundant
Power Supply

Microway has earned an excellent reputation since 1982. If you need a quality product that is fine tuned and built to last, from a company that will be around to support you for years to come, Microway is The Number One Choice.

Microway has delivered high-performance computing products since 1982, when our pioneering software made it possible to use an 8087 in the IBM-PC. In 1987 we created the world's first PC parallel processing systems. Since then, our QuadPutter™ architecture has migrated from Transputers to i860s and finally to Alphas in 1995. Over the past three years, we engineered and delivered over 300 clusters that utilized MPI running on Linux. As a software developer and hardware manufacturer, we know the value of extensive testing and validation. We are experts at configuring and validating the low latency interconnects we employ in our clusters. Our technical support is legendary — the systems we sell arrive at your site and WORK! Los Alamos chose Microway to maintain and upgrade its 144 node Alpha Avalon Cluster because of our reputation. Large clusters we have sold include 400+ nodes at the University of Wisconsin and 250+ nodes at Rockefeller University.

Microway offers three Athlon/Pentium enclosures—1U, 2U and tower, plus five Alpha configurations—1U, 3U, 4U RuggedRack™, QuadPutter™ and full tower. Our 264DP includes two 21264's with up to 4 GB of memory in our custom 4U RuggedRack, which features front accessible redundant power supplies and hard disks. This rugged configuration was chosen by the U.S. Navy for onboard use. We also offer a dual Alpha UP2000+ running at 833MHz with 2GB of memory. Our QuadPutter chassis holds 4 Alpha processors and up to 4GB memory. The 1U CS20 dual Alpha (at right) is the highest density computational platform available.



Microway is API-Networks' Top North American Channel Partner.



"Most Powerful, Highest Density Computational Platform On the Planet"

Microway Scalable 25 Node
50 Processor Cluster Using CS20 Dual
833 MHz Alphas and Myrinet Interconnect
Yielding Peak Throughput of 82.5 GigaFlop

"I have ordered numerous Alpha and Intel-based servers and workstations from Microway running both Tru64 UNIX and Linux. We have been very happy with both the performance and great value of Microway's products. The major UNIX vendors don't come close to Microway in this regard, and we have also found that Microway provides better value than other Linux hardware vendors. I have also used Microway's tech support and was pleased with their response. We've been using their systems for over a year and have had only a couple of minor incidents which were dealt with promptly."

— David Kristofferson, Ph.D., MBA,
Director of Information Systems, Eos Biotechnology, Inc.

Find out why over 75% of Microway's sales come from repeat customers. Please call 508-746-7341 for a technical salesperson who speaks your language!

Visit us at www.microway.com



Microway
Technology you can count on™

Research Park Box 79, Kingston, MA 02364 • 508-746-7341 • info@microway.com

AUG 31 2001

CONTENTS

VOLUME 201, No. 1: AUGUST 2001

RESEARCH NOTE

- Seibel, Brad A., and David B. Carlini**
Metabolism of pelagic cephalopods as a function of habitat depth: a reanalysis using phylogenetically independent contrasts 1

NEUROBIOLOGY AND BEHAVIOR

- Herberholz, Jens, and Barbara Schmitz**
Signaling *via* water currents in behavioral interactions of snapping shrimp (*Alpheus heterochaelis*) 6

PHYSIOLOGY AND BIOMECHANICS

- Reddy, P. Sreenivasula, and B. Kishori**
Methionine-enkephalin induces hyperglycemia through eyestalk hormones in the estuarine crab *Scylla serrata* . . . 17
- Mogami, Yoshihiro, Junko Ishii, and Shoji A. Baba**
Theoretical and experimental dissection of gravity-dependent mechanical orientation in gravitactic microorganisms 26

SYMBIOSIS AND PARASITOLOGY

- Hanten, Jeffrey J., and Sidney K. Pierce**
Synthesis of several light-harvesting complex 1 polypeptides is blocked by cycloheximide in symbiotic chloroplasts in the sea slug, *Elysia chlorotica* (Gould): A case for horizontal gene transfer between alga and animal? . . . 34
- McCurdy, Dean G.**
Asexual reproduction in *Pygospio elegans* Claparède (Annelida, Polychaeta) in relation to parasitism by *Lepocreadium setiferoides* (Miller and Northup) (Platyhelminthes, Trematoda) 45

DEVELOPMENT AND REPRODUCTION

- Stewart-Savage, J., Aimee Phillippi, and Philip O. Yund**
Delayed insemination results in embryo mortality in a brooding ascidian 52

CELL BIOLOGY

- Ballarin, Lorian, Antonella Franchini, Enzo Ottaviani, and Armando Sabbadin**
Morula cells as the major immunomodulatory hemocytes in ascidians: evidences from the colonial species *Botryllus schlosseri* 59

ECOLOGY AND EVOLUTION

- Halanych, Kenneth M., Robert A. Feldman, and Robert C. Vrijenhoek**
Molecular evidence that *Sclerolimum brattstromi* is closely related to vestimentiferans, not to frenulate pogonophorans (Siboglinidae, Annelida) 65
- Ponczek, Lawrence M., and Neil W. Blackstone**
Effect of cloning rate on fitness-related traits in two marine hydroids 76
- Meidel, Susanne K., and Philip O. Yund**
Egg longevity and time-integrated fertilization in a temperate sea urchin (*Strongylocentrotus droebachiensis*) . . . 84
- Wares, J. P.**
Biogeography of *Asterias*: North Atlantic climate change and speciation. 95

SYSTEMATICS

- Gershwin, Lisa-ann**
Systematics and biogeography of the jellyfish *Aurelia labiata* (Cnidaria: Scyphozoa) 104

* * *

- Annual Report of the Marine Biological Laboratory R1**

ANNOUNCEMENT

The Marine Biological Laboratory is pleased to announce that it has entered into an agreement with HighWire Press of Stanford University to publish *The Biological Bulletin* electronically. The online journal will be launched on 23 August 2001. It will be available free of charge to subscribers and the general public for the next six months. Subsequently, subscribers to *The Biological Bulletin* will receive both the print and electronic versions of the journal.

We invite you to visit *The Biological Bulletin* online at
<http://www.biolbull.org>

THE BIOLOGICAL BULLETIN

THE BIOLOGICAL BULLETIN is published six times a year by the Marine Biological Laboratory, 7 MBL Street, Woods Hole, Massachusetts 02543.

Subscriptions and similar matter should be addressed to Subscription Manager, THE BIOLOGICAL BULLETIN, Marine Biological Laboratory, 7 MBL Street, Woods Hole, Massachusetts 02543. Subscription per year (six issues, two volumes): \$235 for libraries; \$95 for individuals. Subscription per volume (three issues): \$117.50 for libraries; \$47.50 for individuals. Back and single issues (subject to availability): \$40 for libraries; \$20 for individuals.

Communications relative to manuscripts should be sent to Michael J. Greenberg, Editor-in-Chief, or Pamela Clapp Hinkle, Managing Editor, at the Marine Biological Laboratory, 7 MBL Street, Woods Hole, Massachusetts 02543. Telephone: (508) 289-7428. FAX: 508-289-7922. E-mail: pclapp@mbl.edu.

<http://www.biolbull.org>

THE BIOLOGICAL BULLETIN is indexed in bibliographic services including *Index Medicus* and MEDLINE, *Chemical Abstracts*, *Current Contents*, *Elsevier BIOBASE/Current Awareness in Biological Sciences*, and *Geo Abstracts*.

Printed on acid free paper,
effective with Volume 180, Issue 1, 1991.

POSTMASTER: Send address changes to THE BIOLOGICAL BULLETIN, Marine Biological Laboratory,
7 MBL Street, Woods Hole, MA 02543.

Copyright © 2001, by the Marine Biological Laboratory
Periodicals postage paid at Woods Hole, MA, and additional mailing offices.
ISSN 0006-3185

INSTRUCTIONS TO AUTHORS

The Biological Bulletin accepts outstanding original research reports of general interest to biologists throughout the world. Papers are usually of intermediate length (10–40 manuscript pages). A limited number of solicited review papers may be accepted after formal review. A paper will usually appear within four months after its acceptance.

Very short, especially topical papers (less than 9 manuscript pages including tables, figures, and bibliography) will be published in a separate section entitled "Research Notes." A Research Note in *The Biological Bulletin* follows the format of similar notes in *Nature*. It should open with a summary paragraph of 150 to 200 words comprising the introduction and the conclusions. The rest of the text should continue on without subheadings, and there should be no more than 30 references. References should be referred to in the text by number, and listed in the Literature Cited section in the order that they appear in the text. Unlike references in *Nature*, references in the Research Notes section should conform in punctuation and arrangement to the style of recent issues of *The Biological Bulletin*. Materials and Methods should be incorporated into appropriate figure legends. See the article by Lohmann *et al.* (October 1990, Vol. **179**: 214–218) for sample style. A Research Note will usually appear within two months after its acceptance.

The Editorial Board requests that regular manuscripts conform to the requirements set below; those manuscripts that do not conform will be returned to authors for correction before review.

1. **Manuscripts.** Manuscripts, including figures, should be submitted in quadruplicate, with the originals clearly marked. (Xerox copies of photographs are not acceptable for review purposes.) The submission letter accompanying the manuscript should include a telephone number, a FAX number, and (if possible) an E-mail address for the corresponding author. The original manuscript must be typed in no smaller than 12 pitch or 10 point, using double spacing (including figure legends, footnotes, bibliography, etc.) on one side of 16- or 20-lb. bond paper, 8 by 11 inches. Please, no right justification. Manuscripts should be proofread carefully and errors corrected legibly in black ink. Pages should be numbered consecutively. Margins on all sides should be at least 1 inch (2.5 cm). Manuscripts should conform to the *Council of Biology Editors Style Manual*, 5th Edition (Council of Biology Editors, 1983) and to American spelling. Unusual abbreviations should be kept to a minimum and should be spelled out on first reference as well as defined in a footnote on the title page. Manuscripts should be divided into the following components: Title page, Abstract (of no more than 200 words), Introduction, Materials and Methods, Results, Discussion, Acknowledgments, Literature Cited, Tables, and Figure Legends. In addition, authors should supply a list of words and phrases under which the article should be indexed.

2. **Title page.** The title page consists of a condensed title or running head of no more than 35 letters and spaces, the manuscript

title, authors' names and appropriate addresses, and footnotes listing present addresses, acknowledgments or contribution numbers, and explanation of unusual abbreviations.

3. **Figures.** The dimensions of the printed page, 7 by 9 inches, should be kept in mind in preparing figures for publication. We recommend that figures be about 1 times the linear dimensions of the final printing desired, and that the ratio of the largest to the smallest letter or number and of the thickest to the thinnest line not exceed 1:1.5. Explanatory matter generally should be included in legends, although axes should always be identified on the illustration itself. Figures should be prepared for reproduction as either line cuts or halftones. Figures to be reproduced as line cuts should be unmounted glossy photographic reproductions or drawn in black ink on white paper, good-quality tracing cloth or plastic, or blue-lined coordinate paper. Those to be reproduced as halftones should be mounted on board, with both designating numbers or letters and scale bars affixed directly to the figures. All figures should be numbered in consecutive order, with no distinction between text and plate figures and cited, in order, in the text. The author's name and an arrow indicating orientation should appear on the reverse side of all figures.

Digital art: *The Biological Bulletin* will accept figures submitted in electronic form; however, digital art must conform to the following guidelines. Authors who create digital images are wholly responsible for the quality of their material, including color and halftone accuracy.

Format. Acceptable graphic formats are TIFF and EPS. Color submissions must be in EPS format, saved in CMKY mode.

Software. Preferred software is Adobe Illustrator or Adobe Photoshop for the Mac and Adobe Photoshop for Windows. Specific instructions for artwork created with various software programs are available on the Web at the Digital Art Information Site maintained by Cadmus Professional Communications at <http://cjs.cadmus.com/da/home.html>

Resolution. The minimum requirements for resolution are 1200 DPI for line art and 300 for halftones.

Size. All digital artwork must be submitted at its actual printed size so that no scaling is necessary.

Multipanel figures. Figures consisting of individual parts (e.g., panels A, B, C) must be assembled into final format and submitted as one file.

Hard copy. Files must be accompanied by hard copy for use in case the electronic version is unusable.

Disk identification. Disks must be clearly labeled with the following information: author name and manuscript number; format (PC or Macintosh); name and version of software used.

Color: *The Biological Bulletin* will publish color figures and plates, but must bill authors for the actual additional cost of printing in color. The process is expensive, so authors with more than one color image should—consistent with editorial concerns, especially citation of figures in order—combine them into a single plate to reduce the expense. On request, when supplied with a copy of a color illustration, the editorial staff will provide a pre-publication estimate of the printing cost.

4. **Tables, footnotes, figure legends, etc.** Authors should follow the style in a recent issue of *The Biological Bulletin* in preparing table headings, figure legends, and the like. Because of the high cost of setting tabular material in type, authors are asked to limit such material as much as possible. Tables, with their headings and footnotes, should be typed on separate sheets, numbered with consecutive Roman numerals, and placed after the Literature Cited. Figure legends should contain enough information to make the figure intelligible separate from the text. Legends should be typed double spaced, with consecutive Arabic numbers, on a separate sheet at the end of the paper. Footnotes should be limited to authors' current addresses, acknowledgments or contribution numbers, and explanation of unusual abbreviations. All such footnotes should appear on the title page. Footnotes are not normally permitted in the body of the text.

5. **Literature cited.** In the text, literature should be cited by the Harvard system, with papers by more than two authors cited as Jones *et al.*, 1980. Personal communications and material in preparation or in press should be cited in the text only, with author's initials and institutions, unless the material has been formally accepted and a volume number can be supplied. The list of references following the text should be headed Literature Cited, and must be typed double spaced on separate pages, conforming in punctuation and arrangement to the style of recent issues of *The Biological Bulletin*. Citations should include complete titles and inclusive pagination. Journal abbreviations should normally follow those of the U. S. A. Standards Institute (USASI), as adopted by BIOLOGICAL ABSTRACTS and CHEMICAL ABSTRACTS, with the minor differences set out below. The most generally useful list of biological journal titles is that published each year by BIOLOGICAL ABSTRACTS (BIOSIS List of Serials; the most recent issue). Foreign authors, and others who are accustomed to using THE WORLD LIST OF SCIENTIFIC PERIODICALS, may find a booklet published by the Biological Council of the U.K. (obtainable from the Institute of Biology, 41 Queen's Gate, London, S.W.7, England, U.K.) useful, since it sets out the WORLD LIST abbreviations for most biological journals with notes of the USASI abbreviations where these differ. CHEMICAL ABSTRACTS publishes quarterly supplements of additional abbreviations. The following points of reference style for THE BIOLOGICAL BULLETIN differ from USASI (or modified WORLD LIST) usage:

A. Journal abbreviations, and book titles, all underlined (for *italics*)

B. All components of abbreviations with initial capitals (not as European usage in WORLD LIST e.g., *J. Cell. Comp. Physiol.* NOT *J. cell. comp. Physiol.*)

C. All abbreviated components must be followed by a period, whole word components *must not* (i.e., *J. Cancer Res.*)

D. Space between all components (e.g., *J. Cell. Comp. Physiol.*, not *J.Cell.Comp.Physiol.*)

E. Unusual words in journal titles should be spelled out in full, rather than employing new abbreviations invented by the author. For example, use *Rit Vísindafjélag Islandinga* without abbreviation.

F. All single word journal titles in full (*e.g.*, *Veliger*, *Ecology*, *Brain*).

G. The order of abbreviated components should be the same as the word order of the complete title (*i.e.*, *Proc.* and *Trans.* placed where they appear, not transposed as in some BIOLOGICAL ABSTRACTS listings).

H. A few well-known international journals in their preferred forms rather than WORLD LIST or USASI usage (*e.g.*, *Nature*, *Science*, *Evolution* NOT *Nature, Lond.*, *Science, N.Y.*; *Evolution, Lancaster, Pa.*)

6. **Reprints, page proofs, and charges.** Authors may purchase reprints in lots of 100. Forms for placing reprint orders are sent with page proofs. Reprints normally will be delivered about 2 to 3 months after the issue date. Authors (or delegates for foreign authors) will receive page proofs of articles shortly before publication. They will be charged the current cost of printers' time for corrections to these (other than corrections of printers' or editors' errors). Other than these charges for authors' alterations, *The Biological Bulletin* does not have page charges.

Metabolism of Pelagic Cephalopods as a Function of Habitat Depth: A Reanalysis Using Phylogenetically Independent Contrasts

BRAD A. SEIBEL^{1,*} AND DAVID B. CARLINI²

¹Monterey Bay Aquarium Research Institute, 7700 Sandholdt Road, Moss Landing, California 95039; and ²Department of Biology, 101 Hurst Hall, American University, 4400 Massachusetts Avenue, NW, Washington, DC 20016-8007

Metabolic rates of deep-living animals have been intensely studied (1). Within pelagic fishes, crustaceans, and cephalopods, a strong decline in rates of mass-specific metabolism with depth has been observed. Childress and Mickel (2) put forward the visual interactions hypothesis to explain this general pattern. Their hypothesis states that reduced metabolic rates among many deep-sea pelagic taxonomic groups result from relaxed selection for strong locomotory abilities for visual predator-prey interactions in the light-limited deep sea. This pattern has, however, been tested using mean metabolic rates for species as individual data points. Felsenstein (3) warned that, because species are descended in a hierarchical fashion from common ancestors, they generally cannot be considered as independent data points in statistical analyses. Statistical methods have recently been developed that incorporate phylogenetic information into comparative studies to create phylogenetically independent values that can then be used in statistical analyses. Reliable independent phylogenetic information has only recently become available for some deep-sea organisms. The present contribution reanalyzed the metabolic rates (4, 5) of pelagic cephalopods as a function of, for consistency with previous studies, MDO (minimum depth of occurrence) using phylogenetic independent contrasts derived from a recent molecular phylogeny (6). This analysis confirms the existence of a significant negative relationship between metabolism and minimum habitat depth in pelagic cephalopods but suggests that phylogenetic history also has

considerable influence on the metabolic rates of individual species.

Childress (1) argued against a phylogenetic basis for the observed relationships between metabolism and depth. He based the argument on the identification of convergence of metabolic rates at a given depth among distantly related taxa (fishes, crustaceans, cephalopods) as well as divergence within closely related groups as a function of depth. This pattern strongly suggests that species experience similar selective regimes at any given depth and that rates of metabolism are evolved in response to that selection. Seibel *et al.* (5) further argued, on the basis of an analysis of higher nodes, that most of the variation in metabolic rates among cephalopods is between families within an order, as opposed to between genera within a family or species within a genus. Therefore, families are more appropriate units for comparison. A decline in metabolic rates with increasing habitat depth was also observed when families were used as independent data points (5). Nevertheless, the degrees of freedom used for statistical analyses in these studies are elevated, to varying degrees, due to phylogenetic non-independence of the data.

Felsenstein (3) proposed computing weighted differences (“contrasts”) between the character values of pairs of sister species nodes, or both, as indicated by phylogenetic topology, thereby estimating an ancestral character value (*e.g.*, the ancestral states of log-transformed depth and metabolic data presented in Fig. 1). Insofar as the ancestral nodes are correctly determined, each of these contrasts is independent of the others in terms of the evolutionary changes that have occurred to produce differences between the two members of a single contrast (7). Felsenstein’s (3) method requires knowledge of the cladistic relationships between the species

Received 29 August 2000; accepted 12 April 2001.

* To whom correspondence should be addressed. E-mail: bseibel@mbari.org

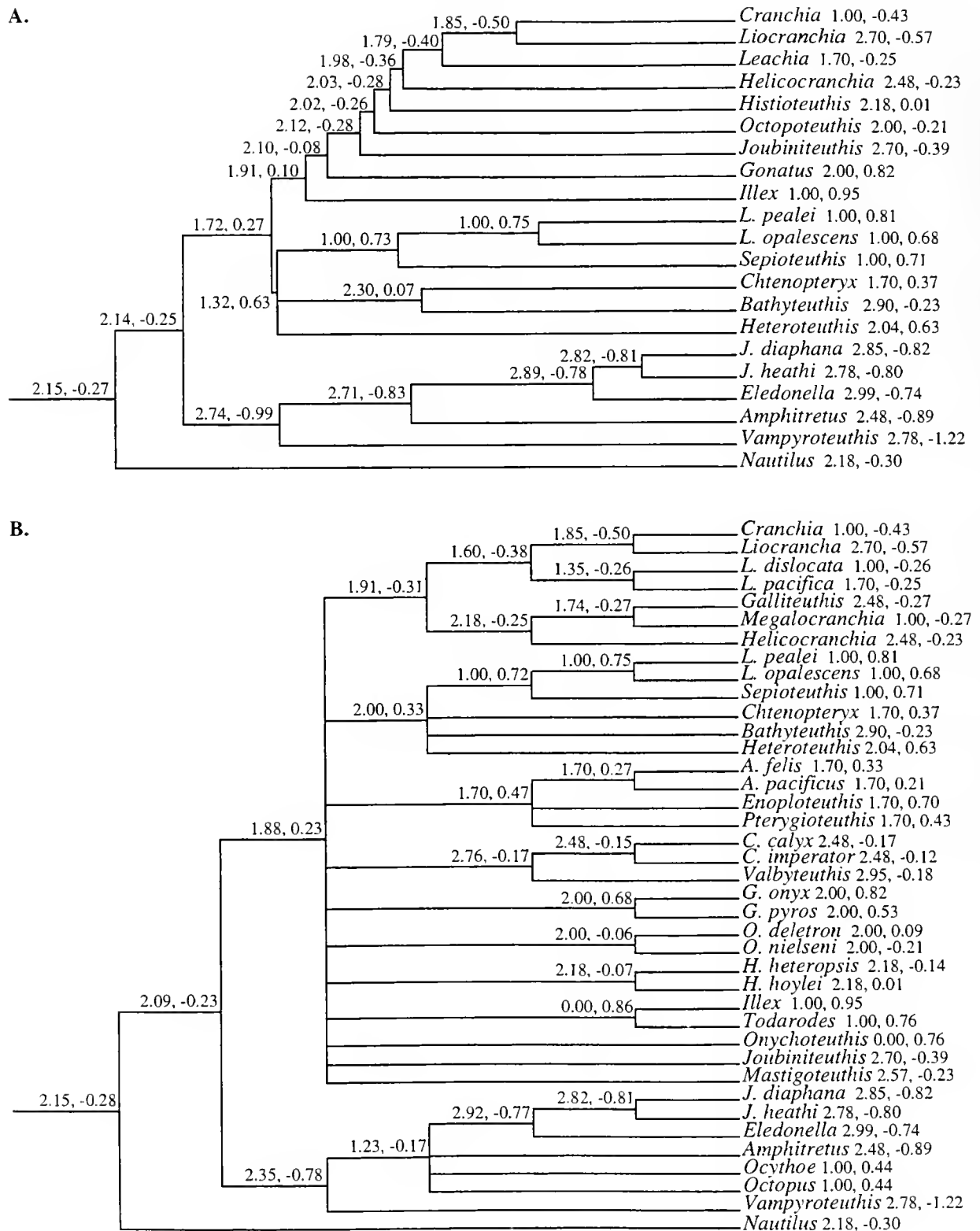


Figure 1. Phylogenetic trees used for calculating independent contrasts on metabolic rate data. Log-transformed minimum depth of occurrence (MDO) and metabolic rates, in that order, are shown to the right of taxon names. Ancestral states of log-transformed MDO and metabolic rate data (*i.e.*, weighted differences or "contrasts," see text), calculated using the CAIC software application (18), are also shown at the internal nodes. (A) A 21-taxon tree for which both COI sequences and metabolic rate data are available. Branch lengths

being analyzed. Several studies have attempted to construct phylogenies for cephalopods. However, only a single reliable family-level phylogeny exists that includes deep-water fauna. One previous phylogenetic analysis relied exclusively on morphological characters that are associated with buoyancy and locomotion and are thus confounded with metabolism and depth (8). We therefore felt that analysis was unsuitable for use in the present study. Other analyses have been unable to obtain sufficient resolution for familial relationships (9) or have included only shallow-living taxa (10, 11). Carlini and Graves (6) recently analyzed the higher level phylogenetic relationships of extant cephalopods by using a 657-bp sequence of the mitochondrial cytochrome *c* oxidase (COI) gene. The molecular sequence data from Carlini and Graves (6) provide an opportunity to test the visual interactions hypothesis directly, using a more valid statistical approach. An additional analysis based on actin gene sequences (12) was not included, primarily because there was very little overlap between taxa for which actin gene sequences were available and those for which metabolic data are available. Furthermore, the actin study provides a more accurate reconstruction of gene family evolution within the cephalopods than of specific relationships among taxa.

The phylogenetic trees presented here from which the independent contrasts were calculated include only those species for which metabolic data are available. Similar trees were constructed including species for which enzymatic data are available. Although it may have been preferable to "prune" the complete COI tree rather than reconstruct trees using only taxa for which metabolic data are available, we decided to calculate new trees so that we could include taxa for which COI sequences were obtained after the publication of the COI paper (6). The species we added were *Amphitretus pelagicus*, *Helicocranchia pfefferi*, and *Japetella heathi*. Pruning the tree would have had only a small effect on the values of the standardized contrasts and would not have significantly altered our conclusions.

A second requirement of Felsenstein's (3) method is knowledge of branch lengths in units of expected variance of change. Ideally, branch lengths should represent expected units of evolutionary change (gradual model). For this ap-

proach to be valid, independent contrasts must be adequately standardized so that they will receive equal weighting in subsequent regression analyses. We plotted the absolute value of each standardized independent contrast, generated from the fully resolved tree (Fig. 1a), versus its standard deviation (7) and found no relationship between the two variates (data not shown). Thus, the contrasts were adequately standardized and properly weighted in regression analysis.

However, even if a particular phylogenetic tree is well resolved and well supported, branch lengths are always estimates and are thus subject to error. A less optimal approach, but one that involves fewer assumptions about the evolutionary relationships of the taxa in question, is to assume that every branch in the phylogeny is the same length (punctuated model). The advantage of this approach is that it can be used for poorly resolved trees or for data sets where branch lengths cannot be estimated, such as those derived from both molecular (6) and morphological (13, 14) data. This allows more contrasts to be performed, increasing the power of subsequent statistical tests. On the other hand, the punctuated model is unrealistic for most data sets, as there is likely to be significant heterogeneity with respect to the evolutionary rates of the taxa under study. In any case, use of a punctuated model is far superior to any method that treats species values as independent data points.

In the present study we employed both gradual and punctuated models in constructing trees for comparison. The gradual model tree is depicted in Figure 1a (21 taxa, metabolic rates as a function of MDO). A similar tree was constructed including species for which enzymatic data are available (not shown, 18 taxa, enzymatic activities as a function of MDO). A tree constructed using the punctuated model for contrasts involving all taxa for which data are available is depicted in Figure 1b (39 taxa, metabolic rates versus MDO). A similar tree was constructed including species for which enzymatic data are available (not shown, 32 taxa, enzymatic activities versus MDO).

Independent contrasts for log-transformed, normalized mean oxygen consumption rates (4, 15–18) were produced, for both gradual and punctuated models, using CAIC v. 2.0.0 (19), and were regressed against those produced for

(molecular clock enforced) were calculated from the strict consensus of two most-parsimonious trees (Tree Length = 1432 steps; Consistency Index = 0.348; Retention Index = 0.334) derived from parsimony analysis of the COI data in PAUP* (28). (B) Partially resolved 39-taxon tree representing relationships between all pelagic taxa for which metabolic rate data are available. The conservative tree topology is based on a consensus of molecular and morphological evidence. In this case, branch lengths are unknown and a punctuated model of change was assumed; that is, all branches are of equal length. For example, the ancestral character state for log-transformed metabolic rate for the *Cranchia-Liocranchia* node, assuming a punctuated model of change, is calculated assuming a branch length equal to one and taking an average of the two species ($-0.43 + -0.57/2 = -0.50$, corresponding to a calculated ancestral oxygen consumption rate of $0.61 \mu\text{m O}_2 \text{g}^{-1}\text{h}^{-1}$). Determination of ancestral character states, assuming a gradual model of change, requires calculation of branch length using the CAIC software.

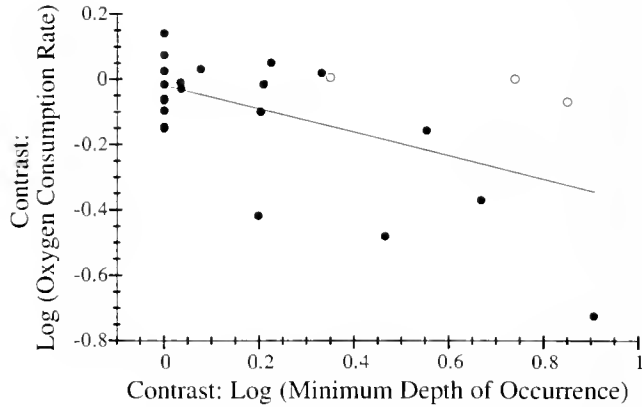


Figure 2. Standardized contrasts of log-transformed oxygen consumption data plotted as a function of standardized contrasts of log-transformed minimum depth of occurrence calculated from the 39-taxon tree (Fig. 1b; punctuated model). Contrasts for the three sister-species groupings within the cranchiid family (*Cranchia-Liocranchia*; *Leachia dislocata-L. pacifica*; *Galliteuthis-Megalocranchia*; Fig. 1b) are indicated with open symbols and are included in the plotted regression. The slope of the regression is significant ($P < 0.01$). See Table 1 and text for equation and related statistics.

MDO (Fig. 2, Table 1). We produced similar regressions for contrasts of activities of citrate synthase (CS) and octopine dehydrogenase (ODH) (5, 20–22), indicators of aerobic and anaerobic metabolic potential, respectively (Table 1). We tested the validity of log transformation by using a method suggested by Purvis and Rambaut (19), authors of the CAIC package. Regressions of the absolute values of the contrasts on the estimated nodal values were performed, and none had slopes significantly different from zero. We also performed

regressions of the absolute values of the contrasts against the standard deviations of the contrasts and detected no relationship in any case. These two tests ensure that we did not violate any of the assumptions of Felsenstein's (3) model of evolution of continuous characters as a random walk process.

Relationships between contrasts of metabolism and depth are summarized in Table 1. A significant decline in oxygen consumption rate with habitat depth was observed when all taxa were included and a punctuated model was assumed (Fig. 2; $y = -0.36x - 0.02$, $P = 0.01$). A similar relationship was observed using the gradual model ($y = -0.59x - 0.049$, $P = 0.03$), but only when the *Cranchia versus Liocranchia* contrast was excluded (see below). CS and ODH activities were weakly correlated with habitat depth when a gradual model was assumed, even with the *Cranchia versus Liocranchia* contrast excluded from analysis (Table 1; CS, $y = -1.01x + 0.46$, $P = 0.06$; ODH, $y = -1.26x - 0.22$, $P = 0.099$). Contrasts performed using the punctuated model for the CS and ODH data indicated a significant negative relationship between enzymatic activity and habitat depth with the *Cranchia versus Liocranchia* contrast excluded from analysis (Table 1; CS, $y = -0.64x + 0.08$, $P = 0.01$; ODH, $y = -1.02x - 0.04$, $P = 0.005$).

Although these results suggest a negative trend in metabolism with increasing depth independent of phylogeny, there are clearly phylogenetic influences on the data. For example, members of the family Cranchiidae (including *Cranchia* and *Liocranchia*, the contrast excluded from several of the analyses) have low metabolic rates regardless of

Table 1

Metabolism of pelagic cephalopods as a function of habitat depth

Parameter	Model	n	m	b	R^2	P
All contrasts included						
MO ₂	Punctuated	39	-0.36	-0.02	0.29	0.01
	Gradual	21				n.s.
CS	Punctuated	32				n.s.
	Gradual	18				n.s.
ODH	Punctuated	32				n.s.
	Gradual	18				n.s.
<i>Cranchia vs. Liocranchia</i> contrast excluded						
MO ₂	Punctuated	not performed				
	Gradual	21	-0.59	-0.05	0.27	0.03
CS	Punctuated	32	-0.64	0.08	0.32	0.01
	Gradual	18	-1.01	0.46	0.26	0.06
ODH	Punctuated	32	-1.02	0.04	0.40	0.005
	Gradual	18	-1.26	-0.22	0.21	0.099

Log-transformed contrasts (y) of oxygen consumption rates (MO₂ = $\mu\text{mole O}_2 \text{ g}^{-1} \text{ h}^{-1}$) and enzymatic activities (citrate synthase, CS, and octopine dehydrogenase, ODH, units g^{-1}) of pelagic cephalopods were regressed against minimum depth of occurrence (x), expressed as $y = mx + b$. Number of taxa (n), regression coefficients (R^2) and P values are also presented.

habitat depth. The Cranchiidae is a very diverse family, and our data set is slightly biased toward cranchiid species ($n = 7$ out of 39, MO_2 , punctuated model, Fig. 1b). Although many cranchiid species undergo ontogenetic vertical migrations in which successive developmental stages occupy progressively greater depths (12, 23), some species appear to remain near the surface until sexual maturity (24, 25). Seibel *et al.* (4) argued that the use of transparency (26) by the cranchiids reduces detection distances (27) at all depths and therefore allows them to employ sit-and-wait predation strategies, facilitating low metabolic rates, even in well-lit epipelagic waters. With the *Cranchia-Liocranchia* contrast removed, we consistently observed a much stronger relationship between metabolism and habitat depth. Several sources of depth-related variation in metabolism, such as buoyancy and body mass, exist in addition to phylogeny. These have been discussed elsewhere (4, 5).

Literature Cited

- Childress, J. J. 1995. Are there physiological and biochemical adaptations of metabolism in deep-sea animals? *Tree* 10: 30–36.
- Childress, J. J., and T. J. Mickel. 1985. Metabolic rates of animals from the hydrothermal vents and other deep-sea habitats. *Biol. Soc. Wash. Bull.* 6: 249–260.
- Felsenstein, J. 1985. Phylogenies and the comparative method. *Am. Nat.* 126: 1–25.
- Seibel, B. A., E. V. Thuesen, J. J. Childress, and L. A. Gorndezky. 1997. Decline in pelagic cephalopod metabolism with habitat depth reflects differences in locomotory efficiency. *Biol. Bull.* 192: 262–278.
- Seibel, B. A., E. V. Thuesen, and J. J. Childress. 2000. Light-limitation on predator-prey interactions: consequences for metabolism and locomotion of deep-sea cephalopods. *Biol. Bull.* 198: 284–298.
- Carlini, D. B., and J. E. Graves. 1999. Phylogenetic analysis of cytochrome c oxidase I sequences to determine higher-level relationships within the coleoid cephalopods. *Bull. Mar. Sci.* 64: 57–76.
- Garland, T. J., P. H. Harvey, and A. R. Ives. 1992. Procedures for the analysis of comparative data using phylogenetically independent contrasts. *Syst. Biol.* 41: 18–32.
- Clarke, M. R. 1988. Evolution of buoyancy and locomotion in recent cephalopods. Pp. 203–213 in *The Mollusca, Vol. 12: Paleontology and Neontology of Cephalopods*, M. R. Clarke and E. R. Trueman, eds. Academic Press, San Diego, CA.
- Young, R. E., and M. Vecchione. 1996. Analysis of morphology to determine primary sister-taxon relationships within coleoid cephalopods. *Am. Malacol. Bull.* 12: 91–112.
- Boucher-Rodoni, R., and L. Bonnaud. 1996. Biochemical and molecular approach to cephalopod phylogeny. *Am. Malacol. Bull.* 12: 79–85.
- Bonnaud, L., R. Boucher-Rodoni, and M. Monnerot. 1997. Phylogeny of cephalopods inferred from mitochondrial DNA sequences. *Mol. Phylogenet. Evol.* 7: 44–54.
- Carlini, D. B., K. S. Reece, and J. E. Graves. 2000. Actin family gene evolution and the phylogeny of coleoid cephalopods (Mollusca: Cephalopoda). *Mol. Biol. Evol.* 17: 1353–1370.
- Voss, N. 1988. Evolution of the cephalopod family Cranchiidae (Oegopsida). Pp. 293–314 in *The Mollusca, Vol. 12: Paleontology and Neontology of Cephalopods*, M. R. Clarke and E. R. Trueman, eds. Academic Press, San Diego, CA.
- Young, R. E., and R. F. Harman. 1988. Phylogeny of the “Enoptoteuthid” families. *Smithson. Contrib. Zool.* 586: 257–270.
- Segawa, S. 1995. Effect of temperature on oxygen consumption of juvenile oval squid, *Sepioteuthis lessoniana*. *Fish. Sci.* 61: 743–746.
- O’Dor, R. K., and M. J. Wells. 1987. *Energy and Nutrient Flow in Cephalopod Life Cycles*, P. R. Boyle, ed. Academic Press, London. Pp. 109–133.
- DeMont, M. E., and R. K. O’Dor. 1981. The effects of activity, temperature and mass on the respiratory metabolism of the squid, *Illex illecebrosus*. *J. Mar. Biol. Assoc. UK* 64: 535–543.
- Wells, M. J., and J. Wells. 1985. Ventilation and oxygen uptake by *Nautilus*. *J. Exp. Biol.* 118: 297–312.
- Purvis, A., and A. Rambaut. 1995. Comparative analysis by independent contrasts (CAIC): An Apple Macintosh application for analyzing comparative data. *Comput. Appl. Biosci.* 11: 247–251.
- Hochachka, P. W., K. B. Storey, and J. Baldwin. 1975. Squid muscle citrate synthase: Control of carbon entry into the Krebs cycle. *Comp. Biochem. Physiol.* 52B: 193–199.
- Baldwin, J. 1982. Correlations between enzyme profiles in cephalopod muscle and swimming behavior. *Pac. Sci.* 36: 349–356.
- Ballantyne, J. S., P. W. Hochachka, and T. P. Mommsen. 1981. Studies on the metabolism of the migratory squid, *Loligo opalescens*: enzymes of tissues and heart mitochondria. *Mar. Biol. Lett.* 2: 75–85.
- Young, R. E. 1975. Transitory eye shapes and the vertical distribution of two midwater squids. *Pac. Sci.* 29: 243–255.
- Young, R. E. 1975. *Leachia pacifica* (Cephalopoda, Teuthoidea): Spawning habitat and function of the brachial photophores. *Pac. Sci.* 29: 19–25.
- Voss, N. A., and R. S. Voss. 1983. Phylogenetic relationships in the cephalopod family Cranchiidae (Oegopsida). *Malacologia* 23: 397–426.
- Seapy, R. R., and R. E. Young. 1986. Concealment in epipelagic pterotracheid heteropods (Gastropoda) and cranchiid squids (Cephalopoda). *J. Zool. Lond.* 210: 137–147.
- Johnsen, S., and E. A. Widder. 1998. Transparency and visibility of gelatinous zooplankton from the Northwestern Atlantic and Gulf of Mexico. *Biol. Bull.* 195: 337–348.
- Swofford, D. L. 1998. *PAUP*: Phylogenetic Analysis Using Parsimony (* and Other Methods)*, Version 4.0. Sinauer, Sunderland, MA.

Signaling *via* Water Currents in Behavioral Interactions of Snapping Shrimp (*Alpheus heterochaelis*)

JENS HERBERHOLZ^{1,*} AND BARBARA SCHMITZ²

¹Georgia State University, Department of Biology, P.O. Box 4010, Atlanta, Georgia 30302; and

²Lehrstuhl für Zoologie, TU München, Lichtenbergstr. 4, 85747 Garching, Germany

Abstract. The snapping shrimp *Alpheus heterochaelis* produces a variety of different water currents during intraspecific encounters and interspecific interactions with small sympatric crabs (*Eurypanopeus depressus*). We studied the mechanisms of current production in tethered shrimp and the use of the different currents in freely behaving animals. The beating of the pleopods results in strong posteriorly directed currents. Although they reach rather far, these currents show no distinctions when directed toward different opponents. Gill currents are produced by movements of the scaphognathites (the exopodites of the second maxillae) and can then be deflected laterally by movements of the exopodites of the first and second maxillipeds. These frequent but slow lateral gill currents are most probably used to enhance chemical odor perception. The fast and focused, anteriorly directed gill currents, however, represent a powerful tool in intraspecific signaling, because they reach the chemo- and mechanosensory antennules of the opponent more often than any other currents and also because they are produced soon after previous contacts between the animals. They may carry chemical information about the social status of their producers since dominant shrimp release more anterior gill currents and more water jets than subordinate animals in intrasexual interactions.

Introduction

Alpheus heterochaelis of the family Alpheidae (Decapoda, Caridea) is one of the largest snapping shrimp, reaching a body length of up to 55 mm. It shows a large, modified

snapper claw on one (left or right) side and a small pincer claw on the other side in both sexes (Williams, 1984). The snapper claw allows the animals to produce an extremely fast water jet (of up to 25 m/s; Versluis *et al.*, 2000) by rapid claw closure after cocking the claw in the open position (Ritzmann, 1974). The high velocity of the water jet results in a pressure drop below vapor pressure that causes a cavitation bubble to grow to a size of about 3.5 mm in front of the snapper claw. The collapse of this bubble (and not as previously supposed the mechanical contact of both claw surfaces) causes the extremely loud (up to 215 dB re 1 μ Pa at 1 m distance; Schmitz, 2001) and short (about 500 ns) snapping sound (Versluis *et al.*, 2000). The strong effect of the water jet and the cavitation bubble collapse can be seen during interspecific encounters. Small prey (*e.g.*, worms, goby fish, or shrimp) can be stunned or even killed by the jet (MacGinitie, 1937; MacGinitie and MacGinitie, 1949; Morris *et al.*, 1980; Suzuki, 1986; Downer, 1989), and interspecific opponents (*e.g.*, small sympatric crabs, *Eurypanopeus depressus*) can be injured at interaction distances of on average 3 mm (Schultz *et al.*, 1998). Toward conspecifics the water jet was not observed to cause any damage but functions as a communicative signal (Herberholz and Schmitz, 1999), both opponents ensuring an interaction distance of on average 9 mm (Schmitz and Herberholz, 1998), which is far enough away from danger caused by implosion of the cavitation bubble. This hydrodynamic signal is analyzed by the receiving shrimp predominantly with the help of mechanosensory hairs on the snapper claw, and may contain information about the strength, motivation, and sex of the snapper (Herberholz and Schmitz, 1998; Herberholz, 1999).

The still rather small interaction distance of less than 1 cm in agonistic encounters between two snapping shrimp

Received 27 November 2000; accepted 10 April 2001.

* To whom correspondence should be addressed. E-mail: biojhh@panther.gsu.edu

also favors the exchange of chemical signals between the opponents. The literature on chemical orientation and communication in snapping shrimp is limited: Hazlett and Winn (1962) tested aggressive and defensive responses of *Synalpheus hemphilli* to crushed male or female extract, and Schein (1975) and Hughes (1996) investigated the choice of *Alpheus heterochaelis* toward extracts of male or female water in Y-maze experiments without clear-cut results. On the other hand, ablation of the chemosensitive antennules in *Alpheus edwardsii* strongly reduced pair formation and sex recognition, which may be due to impeded distant or contact chemoreception since the pairing frequency remained high when only the antennae were ablated (Jeng, 1994).

The importance of olfactory signals during hierarchy formation was shown in male American lobsters (Karavanich and Atema, 1998a). In these experiments, the recognition of urine-carried chemical signals, which were received by the antennules, allowed the subordinate animal to avoid the familiar dominant shrimp, and therefore reduced the duration and aggression of fights. The exchange of chemical signals is also assumed to play a major role in individual recognition and memory in male and female *Homarus americanus* (Karavanich and Atema, 1998b; Berkey and Atema, 1999). In lobsters, urine is released through a paired set of nephropores on the ventral sides of the basal segments of the second antennae (Parry, 1960). Agonistic behavior in lobsters causes an increase in the probability and volume of urine release (Breithaupt *et al.*, 1999). The released urine is then carried by the powerful anteriorly directed gill currents and may therefore transfer chemical information from one animal to another (Atema, 1985). In recent studies (Zulandt Schneider *et al.*, 1999; Zulandt Schneider and Moore, 2000), chemical cues were also described as an important source for recognition of the dominance status or stress condition of conspecifics in another crustacean, the red swamp crayfish (*Procambarus clarkii*).

In light of these examples, a similar mechanism of chemical signal exchange *via* gill currents in snapping shrimp seems likely. We cannot, however, exclude the possibility that the animals also exchange hydrodynamic signals. In fact, it has been shown that the antennules of crayfish (Mellon, 1996) and lobsters (Guenther and Atema, 1998; Weaver and Atema, 1998) are equipped with both chemical and mechanosensory receptors, and detailed morphological studies of antennule sensory hairs favor the same situation in snapping shrimp (Schmitz, unpubl. obs.). Therefore, snapping shrimp may also perceive hydrodynamic stimuli as well as chemical stimuli with their antennules. Previous studies (Herberholz and Schmitz, 1998, 1999) have shown that the transfer of hydrodynamic signals is realized by the powerful water jet that is formed by rapid closure of the large claw. In contrast, the much weaker gill currents appear to be more suitable for transferring chemical information.

Suspended plastic particles were successfully used to

visualize and quantify biological flow fields in lobsters and crayfish in a series of experiments by Breithaupt and Ayers (1996, 1998). Small floating particles of the same density as seawater were added to the aquarium water and illuminated in a horizontal or vertical plane in the vicinity of a tethered animal. Flow fields were then analyzed by tracking individual particles. It was shown that both lobsters and crayfish produce a great variety of flow fields by using the exopodites of the maxillipeds and by fanning the pleopods. The latter was also discussed with respect to chemical communication: male American lobsters commonly fan their pleopods at the second entrance of their shelter, thus creating a strong current that may contain chemical information about the female positioned at the first entrance (Atema, 1985, 1988). The pleopod fanning frequencies in males correlate with the frequencies of females checking the shelter. The existence of pheromones that control female choice and molting as well as male aggression was therefore assumed (Cowan and Atema, 1990; Atema, 1995; Bushman and Atema, 1997).

The possible exchange and use of different water currents during agonistic encounters has rarely been studied; but see Rohleder and Breithaupt (2000) for a preliminary study in the crayfish *Astacus leptodactylus*. To test the possibility that snapping shrimp use guided water currents as signals, we visualized and analyzed all water currents that the shrimp produced during their encounters with conspecifics of the same or different sex and in encounters with sympatrically living mud flat crabs (*Eurypanopeus depressus*).

Materials and Methods

We analyzed the behavior of 12 adult specimens of *Alpheus heterochaelis*, a species of snapping shrimp (6 males, 6 females; body size: 3.9 ± 0.4 cm, mean \pm SD). Each animal was tested in an encounter with a conspecific of equal size of either the same or different sex, as well as in an encounter with a small crab (*Eurypanopeus depressus*; mean length and width of carapace: $1.6 \pm 0.2 \times 1.2 \pm 0.2$ cm, mean \pm SD). All animals were caught in waters of the Gulf coast of Florida at the Florida State University Marine Laboratory near Panama. Prior to the experiments the animals were labeled with small numbers designated for marking queen bees and were kept individually in perforated plastic containers ($11 \times 11 \times 15$ cm) containing gravel and oyster shells for shelter. The containers were placed within a large tank ($90 \times 195 \times 33$ cm) with 330 l of circulating filtered seawater (salinity: 23‰–28‰; temperature: 22°–23°C). Proteins were removed from the water, and pH, carbonate, oxygen, CO₂, and NO₃ were regularly controlled. The shrimp were exposed to an illumination cycle of 12 h light/12 h dark and fed frozen shrimp, fish, or mussels three times a week.

For visualization of the different water currents, we pre-

pared the aquarium water (temperature: 22°–24°C, water level: 5 cm) with small, floating plastic particles (ABS-particles, Bayer, Leverkusen, diameter: 500–710 μm ; specific weight: 1.03 kg/l). The aquarium (30 \times 24 \times 24 cm; floor covered with black cloth to facilitate walking) was positioned on a platform isolated from vibrations (Breithaupt *et al.*, 1995). At the level of the interacting animals, the seawater was illuminated from one side by a slide projector holding a slide with a thin horizontal slit. Before each experiment fresh seawater and particles were added, and two animals (two snapping shrimp or one snapping shrimp and a crab) were placed in the aquarium for 10 min for acclimatization; the animals were separated by an opaque divider to prevent visual, tactile, and directed-chemical contact. After the partition was removed, all interactions between the animals during the following 20 min were videotaped from above (camera: Panasonic AG 455; video recorder: Panasonic AG 7355; monitor: Sony Trinitron). The reflexive characteristics of the suspended particles then allowed a precise tracking using standard video-frame analysis.

Each experiment (interactions between two snapping shrimp of the same or different sex or between a snapping shrimp and a crab) was characterized by the number of physical contacts between the opponents, regardless of their duration and strength, as well as by the number of water jets. Three different water currents were characterized, including a lateral gill current, an anterior gill current, and a pleopod current (Fig. 1a). The pleopod current was measured only when the shrimp was not in locomotion, because this current is also likely to be used in supporting the animal's walking. Moreover, no current was included in our analysis unless the single-frame video analysis gave clear evidence that it had moved two or more plastic particles. The following parameters were evaluated for all visualized water currents: frequency, duration (time between onset of movement of the first floating particle and end of movement of the last particle), range (total distance covered by an identified particle due to a certain current; possibly underestimated when the current hit an opponent or an aquarium wall), velocity and target of the currents, their potential to transfer chemical information (*i.e.*, entering the area of chemical perception at the receiver's side), the temporal correlation between currents and previous physical contacts, and the correlation between produced currents and water jets in winners and losers during intrasexual interactions. To determine a winner or loser, we counted the number of aggressive acts and the number of submissive acts after each physical contact between the conspecific opponents throughout the encounter. Aggressive acts include behaviors such as approach, aggressive stance, and grasping and opening of the claws. Submissive acts include moving backwards and turning and tail flipping away from the opponent. These definitions are largely adopted from Nolan and

Salmon (1970). In 11 out of 12 experiments, one animal produced more aggressive acts and fewer submissive ones than its opponent and was therefore determined to be the winner while the opponent was determined to be the loser.

Statgraphics Plus 6.0 (Manugistics Group, Inc.) and SPSS 6.0.1. (SPSS Science Software GmbH) were used for statistics. Mean and standard deviation were calculated for each variable of interest for each tested individual, and only one value per individual (grand mean) is included in each statistical test. The behavior of the respective opponents (male and female snapping shrimp, and crabs) was not analyzed and is not included in our results (exception: data presented in Fig. 7). If not otherwise stated, the Friedman rank test for repeated measurements (sample size >2) or the Wilcoxon rank test (sample size = 2) were used, and values with $P < 0.01$ and $P < 0.05$ are indicated in the text. We used nonparametric statistical tests because most of the data did not fulfill the requirements for the use of parametric tests *i.e.*, normality or equal variance.

To gain more insight into the mechanism of gill current production and redirection, two snapping shrimp were tethered upside down in a small petri dish filled with seawater and floating plastic particles, and the activity of the different mouth parts, which produced or deflected the currents, was videotaped using a CCD camera (Sony XC-77CE) mounted on a binocular microscope with high magnification. In addition, small drops of black ink (Brilliant Black 4001, Pelikan) were placed between the third and fourth walking legs of these shrimp as well as of animals tethered dorsal side up to a vertical holder and standing on a platform so that the gill currents could be visualized. (Fig. 1b).

Results

Visualization of water currents in tethered shrimp

A unique feature of snapping shrimp is the production of an extremely rapid water jet by fast closure of a specialized snapper claw. Apart from this water jet, the snapping shrimp *Alpheus heterochaelis* is able to produce four kinds of water currents (Fig. 1), which can be subdivided into two main categories. Fanning of the pleopods causes a strong, posteriorly directed *pleopod current*, and a *gill current* is produced by rhythmically beating the scaphognathites as revealed by our visualization experiments in two tethered shrimp. Beating of the scaphognathites produces a depression in the gill chamber; water is therefore sucked into this chamber and subsequently released anteriorly through two small openings in the carapace. This "normal" gill current can be visualized with ink in tethered animals, but it is too slow and weak to move floating particles and was therefore not analyzed during encounters of snapping shrimp and their opponents. It can, however, be accelerated and deflected into a *lateral gill current* (see Fig. 1B) by the exopodites of the second and third maxillipeds. The exopo-

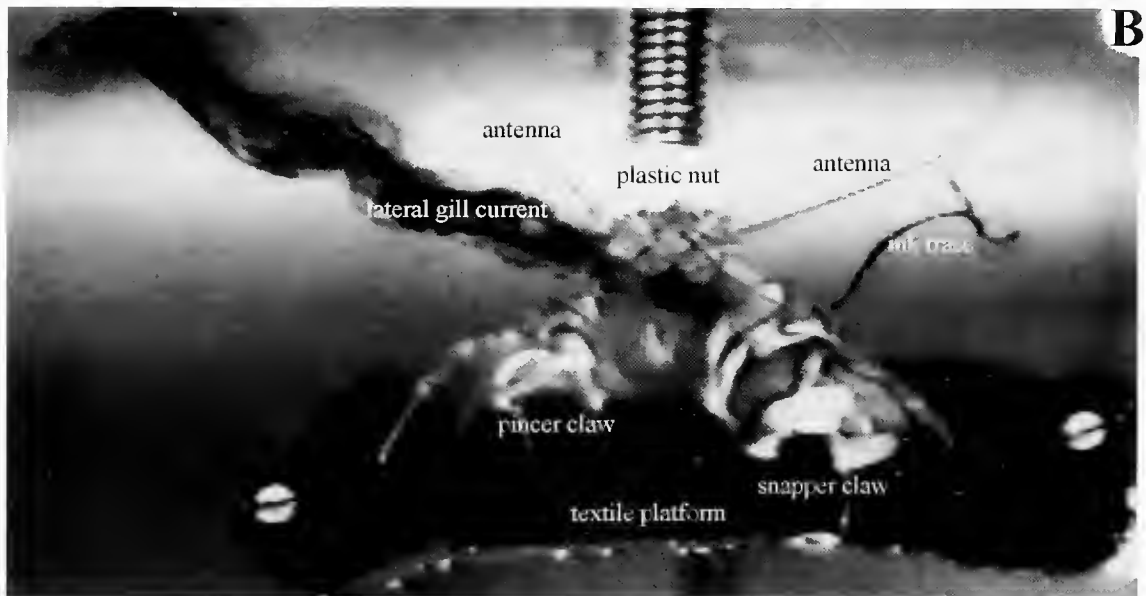
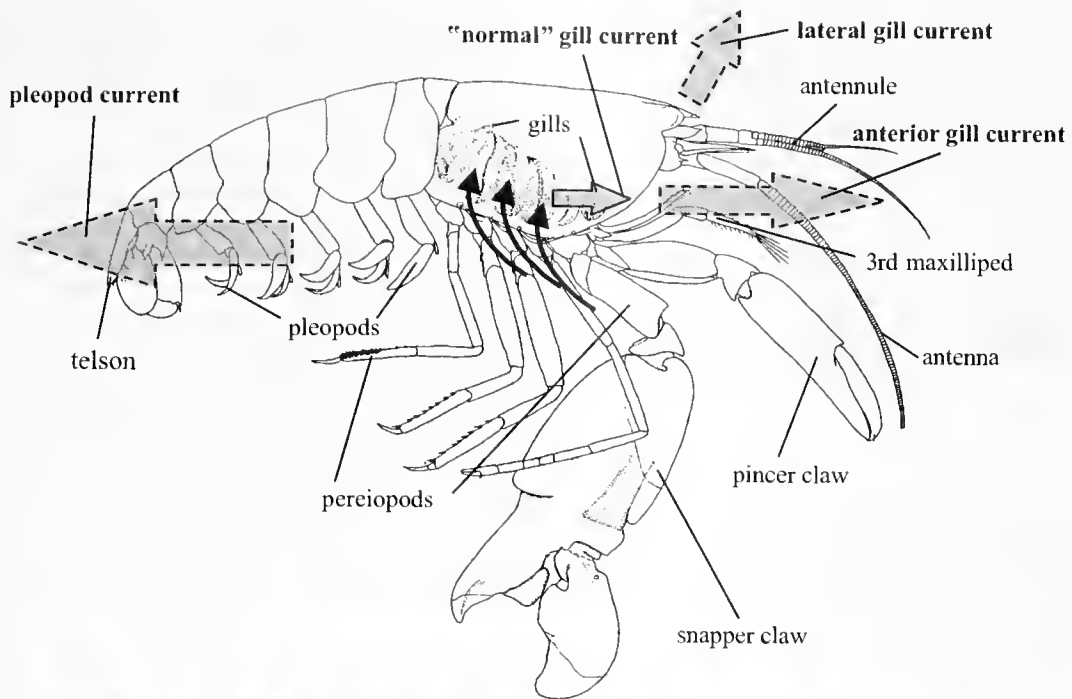


Figure 1. (A) Schematized drawing (lateral view) of a snapping shrimp modified after Kim and Abele (1988) showing four different water currents (gray arrows): the "normal" gill current, the lateral gill current, the anterior gill current, and the pleopod current. Black arrows show the direction of water entering the gill chamber. (B) Frontal view of an *Alpheus heterochaelis* snapping shrimp, tethered to a vertical holder by means of a plastic nut glued to the carapace and standing on a textile platform. Black ink was placed with a syringe between the third and fourth left pereopods (see ink trace) to visualize the gill currents. The shrimp is fanning the exopodites of the right second and third maxillipeds, thus producing an ink-stained lateral gill current to the right.

dites of the first maxilliped do not participate in this process. Fanning of the left exopodites results in acceleration and deflection of the released gill current to the left side, and fanning of the right exopodites results in deflection to the

right side. Tethered snapping shrimp never beat the exopodites of both sides simultaneously, and this was also never observed during interactions in which the illuminated particles were directed to only one side at a time. Interestingly,

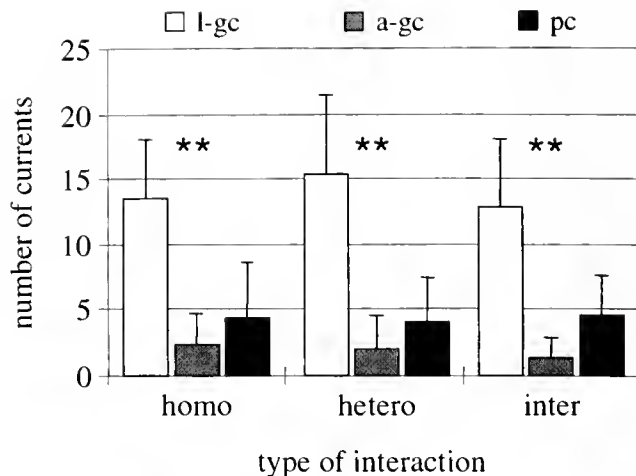


Figure 2. Frequency of three different water currents (l-gc, lateral gill current, a-gc, anterior gill current, pc, pleopod current) produced by *Alpheus heterochaelis* snapping shrimp in interactions with another shrimp of the same sex (homo), of different sex (hetero), and with a *Eurypanopeus depressus* crab (inter). Grand means and standard deviations for 12 snapping shrimp each are shown. Significant differences within interaction types with $P < 0.01$ are indicated by two asterisks (**).

a (fast) anterior gill current was restricted to encounters of freely moving animals; it could not be elicited in tethered shrimp. Its production obviously requires physical, chemical, or visual contact between the animals. As a result, we were not able to analyze the producing mechanism; that is, we did not identify the involved mouth parts.

General characteristics of released water currents

Encounters between two snapping shrimp of different sex (hetero) are characterized by a significantly higher number of physical contacts (23.9 ± 8.3 , $n = 287$; $P < 0.01$) than seen in encounters between two shrimp of the same sex (homo; 13.8 ± 6 , $n = 165$), or between a snapping shrimp and a crab (*Eurypanopeus depressus*) (interspecific; 12.7 ± 5.3 , $n = 157$). On the other hand, snapping (water jet production) of the tested shrimp is significantly increased after a contact with a crab ($38\% \pm 16\%$; $P < 0.01$) when compared to snapping after hetero and homo contacts ($5\% \pm 4\%$ and $11\% \pm 11\%$, respectively).

These differences in mind, we first evaluated the number of water currents (lateral gill currents, anterior gill currents, and pleopod currents) in each experiment. Figure 2 shows that there are no essential differences between interaction types (homo, hetero, or interspecific). Within each interaction type, however, the number of lateral gill currents significantly ($P < 0.01$) exceeds that of anterior gill currents as well as that of pleopod currents. In addition, in interspecific encounters with a crab, the frequency of anterior gill currents is significantly lower than the frequency of pleopod currents ($P < 0.01$).

The duration of the different water currents (Fig. 3A) tends to be longest for lateral gill currents, with no significant differences regarding the type of the opponent. The duration of anterior gill currents is generally shorter, with similar values in intraspecific interactions, yet almost twice as long as in interactions with a small crab. Anterior gill currents in interspecific encounters are significantly shorter in duration than lateral gill currents ($P < 0.05$). Pleopod currents, in contrast, reveal very consistent values for all types of interactions.

Figure 3B shows the range of the different currents in all interaction types. Regardless of the opponent, the snapping shrimp tend to produce lateral gill currents with small ranges. Anterior gill currents generally cover larger distances in intraspecific interactions, whereas the mean value is reduced in interactions with a crab. The most powerful current is the pleopod current, which covers long distances in all interaction types. Range differences within interaction types are significant at $P < 0.05$ and $P < 0.01$, respectively.

The velocity of the water currents during the first 120 ms (6 video frames) was evaluated for 10 examples for each current and interaction type (Fig. 3C). There are no significant differences in the velocities within and between different types of interactions. The lateral gill current shows the slowest velocities in all encounters. The anterior gill current and the pleopod current show similar values and are both more powerful than the lateral gill current. Initial velocities are higher, but their analysis has not proved satisfactory because of the standard video time resolution of 20 ms (50 frame/s).

Temporal relation of water currents to physical contact

Figure 4 compares the frequency of water currents that were elicited within 10 s after a physical contact between the opponents with those that were "spontaneously" produced—that is, emitted more than 10 s after a preceding contact. As shown in Figure 4A, in all interaction types the lateral gill current is significantly more often produced spontaneously than following a physical contact ($P < 0.01$). In homo interactions it occurs in only 6.2% of all cases ($n = 10$ of 162) shortly after a contact. During hetero interactions this current is elicited by a contact in 11.5% of all cases ($n = 21$ of 183); in interactions with a crab, the lateral gill currents occur within 10 s after a contact in only 8.5% of all cases ($n = 13$ of 153).

The analysis of the anterior gill current reveals a completely different frequency pattern, with more elicited currents than spontaneous ones (Fig. 4B). In homo interactions the anterior gill current is produced in 65.5% of all cases ($n = 19$ of 29) within 10 s after a preceding contact. Similarly, in hetero interactions this gill current is elicited by a contact in 62.5% of all cases ($n = 15$ of 24). Finally, during interactions with a crab, anterior gill currents are

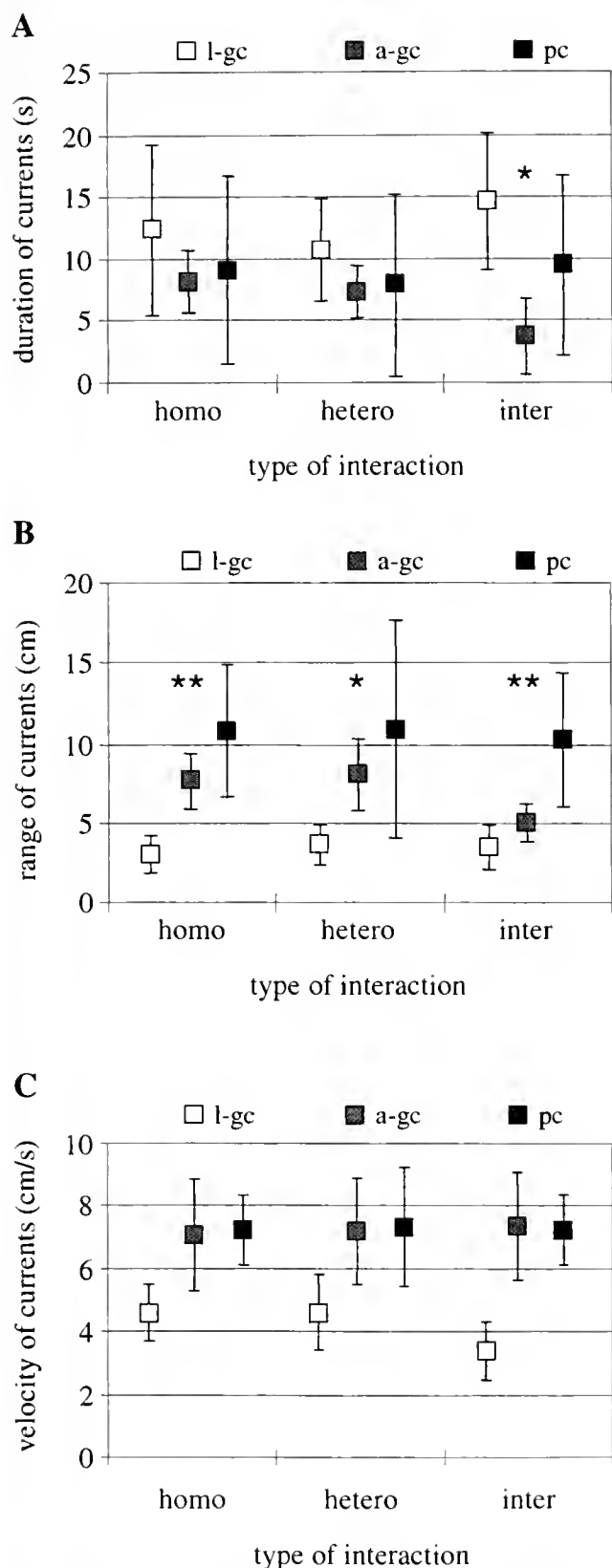


Figure 3. Duration (A), range (B), and velocity (C) of the lateral gill current (l-gc), the anterior gill current (a-gc), and the pleopod current (pc) in interactions of two snapping shrimp of the same sex (homo), of different

released within 10 s after a contact in 78.6% of all cases ($n = 11$ of 14).

In contrast, the pleopod current, like the lateral gill current, is significantly more often ($P < 0.01$) produced without an immediately preceding contact in all types of interactions (Fig. 4C). During homo interactions we observed only 7.7% of pleopod currents within 10 s after the last contact ($n = 4$ of 52). In hetero interactions this current is elicited in 16.7% of all cases ($n = 8$ of 48) by a preceding contact, and in interspecific interactions there are 13.0% of pleopod currents shortly after a previous contact ($n = 7$ of 54).

Possible chemosensory information transfer by water currents

If any of the water currents were used to transfer chemical information, one would expect them to be directed toward the chemoreceptive antennules of the opponent. We therefore evaluated the number of currents that reached the area between the opponents' claws—that is, an area mostly covered by the flicking antennules. This was possible by analyzing the video sequences and identifying the area of particle dispersion with respect to the animals' position. In fact, only the anterior gill current seems qualified to fulfill the function of possible information transfer (Fig. 5).

In all types of interactions, the mean number of lateral gill currents that miss the antennules is significantly higher ($P < 0.01$) than the mean number of those hitting the target (Fig. 5A). In homo interactions the lateral gill current reaches the antennule area in only 0.6% of the cases ($n = 1$ of 162). During hetero interactions lateral gill currents are never directed toward the opponent's antennules, but hit other targets ($n = 183$). In interactions with a crab, the snapping shrimp produce 0.7% ($n = 1$ of 153) of lateral gill currents, which could possibly transfer chemical information.

In comparison, a higher percentage of anterior gill currents reaches the antennule area in all interaction types (Fig. 5B). During homo interactions the anteriorly projected gill current reaches the antennules of the opponent in 35.7% of all cases ($n = 10$ of 28). In hetero interactions the percentage (66.7%, $n = 16$ of 24) of anterior gill currents directed toward the antennules is even higher than that of undirected anterior gill currents. During interspecific interactions the snapping shrimp projects 35.7% anterior gill currents toward the antennules of the crab ($n = 5$ of 14).

The frequency pattern for pleopod currents is similar to

sex (hetero), and of a snapping shrimp and a crab (inter). Grand means and standard deviations for 12 shrimp are shown in A and B; means and standard deviations of the velocity during the first 120 ms of 10 currents each are shown in C. A significant difference within an interaction type with $P < 0.05$ is indicated by one asterisk (*) and with $P < 0.01$ by two asterisks (**).

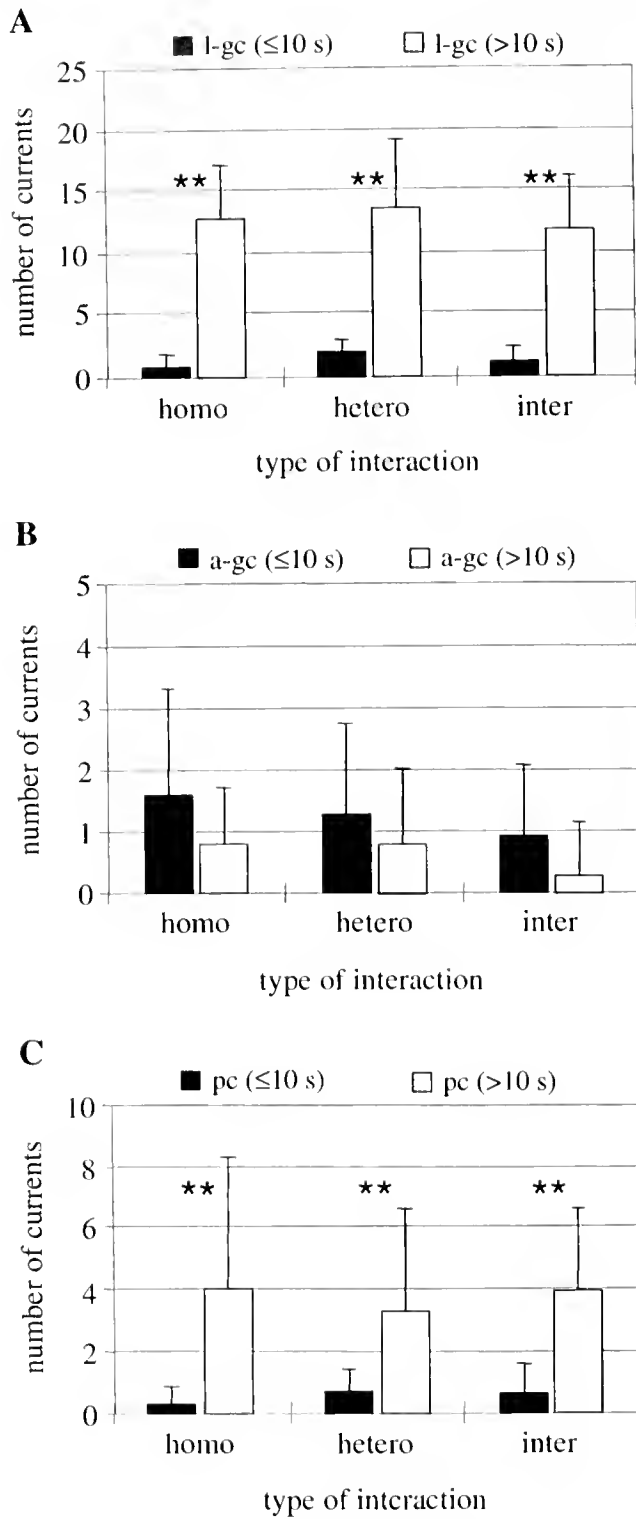


Figure 4. Mean number of lateral gill currents (A), anterior gill currents (B), and pleopod currents (C) within 10 s (black columns) or more than 10 s (white columns) after a physical contact between the opponents in interactions of two snapping shrimp of the same sex (homo), of different sex (hetero), and of a snapping shrimp and a crab (inter). Grand means and standard deviations for 12 shrimp are shown. Significant differences with $P < 0.01$ are indicated by two asterisks (**).

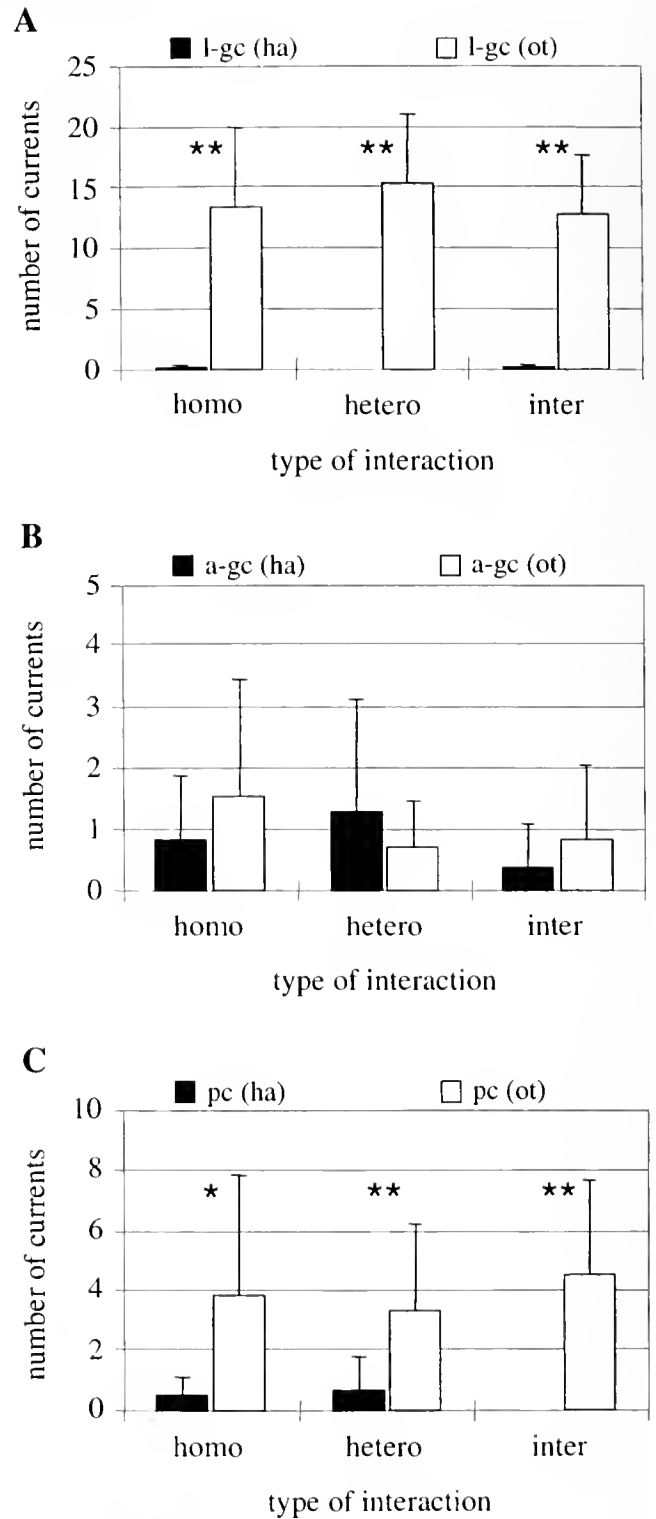


Figure 5. Mean number of lateral gill currents (A), anterior gill currents (B), and pleopod currents (C) hitting the antennules of the opponent (black columns, ha) or reaching other targets (white columns, ot) in interactions of two snapping shrimp of the same sex (homo), of different sex (hetero), and of a snapping shrimp and a crab (inter). Grand means and standard deviations for 12 shrimp are shown. A significant difference with $P < 0.05$ is indicated by one asterisk (*) and with $P < 0.01$ by two asterisks (**).

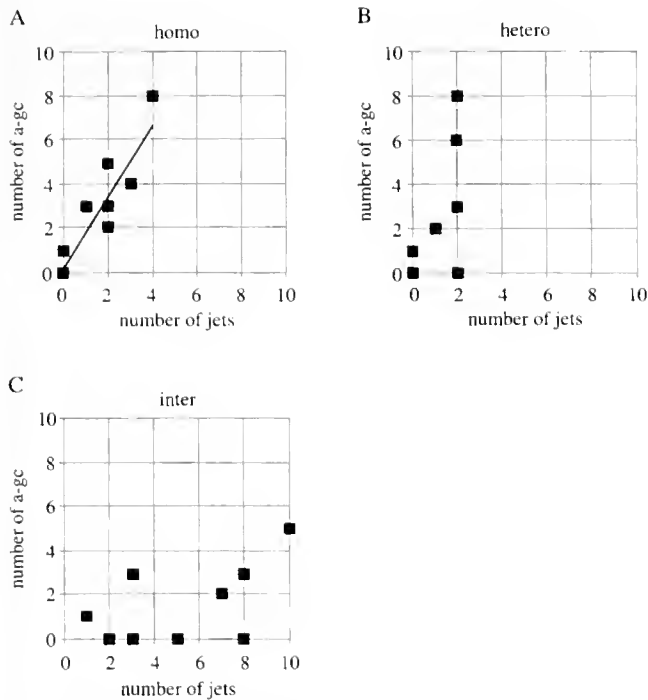


Figure 6. Correlation between the number of water jets and the number of anterior gill currents produced in interactions of two snapping shrimp (A) of the same sex (homo; Spearman's coefficient of rank correlation $r_s = 0.9$, $P < 0.01$), (B) of different sex (hetero), and (C) of a snapping shrimp and a crab (inter). Data of 12 shrimp each—some data points overlap.

that of lateral gill currents: the undirected currents significantly exceed the antennule-directed ones in each interaction type ($P < 0.05$ or 0.01 , respectively; Fig. 5C). In homo interactions an average of only 11.5% ($n = 6$ of 52) of all pleopod currents are projected towards the chemoreceptive antennules, and during hetero interactions 16.7% ($n = 8$ of 48) of all pleopod currents reach the antennule area. Finally, in interspecific interactions no pleopod current is aimed towards the antennules of the crab, but all ($n = 54$) are directed elsewhere.

Anterior gill currents and water jets

In view of the prominent role of the anterior gill current with respect to its timing after a physical contact and the increased possibility of chemosensory information transfer, we tested the correlation between these gill currents and emitted water jets (Fig. 6). As mentioned before, in comparison to intraspecific interactions, encounters with crabs are characterized by an increased number of water jets and a reduced number of anterior gill currents (Fig. 6C). In addition, more water jets are emitted in homo interactions between snapping shrimp (Fig. 6A) than in hetero encounters (Fig. 6B). Thus, the number of anterior gill currents significantly increases with an increasing number of water

jets only in interactions between two snapping shrimp of the same sex (Spearman rank correlation coefficient: $r_s = 0.9$, $P < 0.01$; Fig. 6A). This is not the case in interactions between two shrimp of different sex ($r_s = 0.5$, $P > 0.05$), though a noticeable trend is shown and the overall low number of water jets may have prevented a significant result. An even lower degree of correlation is seen in interactions with a crab ($r_s = 0.4$, $P > 0.1$).

As shown in Figure 7, winners of homo interactions (as defined by aggressive and submissive acts—see Materials and Methods) not only produce a significantly higher mean number of water jets ($N = 11$, $P < 0.01$) but also a significantly higher mean number of anterior gill currents than losers produce ($N = 11$; $P < 0.01$).

Discussion

Snapping shrimp (*Alpheus heterochaelis*) produce two main water currents, a strong posteriorly directed pleopod current and an anteriorly directed gill current. We show that the "normal" anteriorly directed gill current can be modified and redirected into a lateral and a fast anterior gill current. The production of the latter is restricted to social interactions, in which it represents a powerful tool for chemical signaling. Moreover, the use of the fast anterior gill currents varies for the winners and losers of individual encounters.

Mechanisms of gill current production

Our experiments in tethered snapping shrimp show that water is sucked into the gill chamber due to a depression elicited by the beating scaphognathites (Fig. 1A). A "normal" gill current is then released anteriorly with low velocity through two small openings of the carapace. Once the left or right exopodites of the second and third maxillipeds start fanning, the current is accelerated and deflected laterally to that side (Fig. 1B). As previously described in

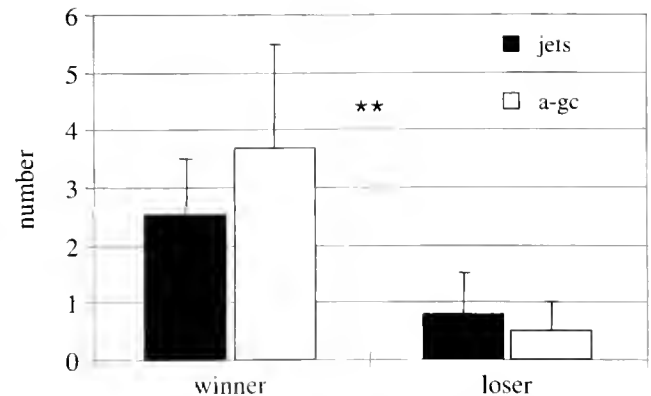


Figure 7. Frequency of water jets (jets, black columns) and anterior gill currents (a-gc, white columns) for winners and losers in interactions of two snapping shrimp of the same sex. The significant differences between winners and losers with $P \leq 0.01$ are indicated by two asterisks (**).

lobsters (*Homarus americanus*), the exopodites of the first maxillipeds do not contribute to these lateral gill currents in snapping shrimp, whereas in crayfish (*Procambarus clarkii*) these appendages are also involved (Breithaupt, 1998).

The production mechanism of the fast anterior gill current remains unclear, since this behavior obviously requires physical, chemical, or visual contact during intra- or inter-specific encounters of snapping shrimp, and thus was never seen in tethered animals. From our knowledge about the lateral gill current, we assume that the fast anterior gill current is created by high-frequency beating of the scaphognathites without contribution of the exopodites of the second and third maxillipeds. Since it is difficult to video-record the mouth parts with high magnification during social interactions, we are currently testing other methods of monitoring scaphognathite beating frequencies during encounters to verify this hypothesis.

Role of the fast anterior gill current during social interactions

The analysis of the fast anterior gill current revealed the most surprising and interesting results. Although anterior gill currents were observed and well described in lobsters (Atema, 1985, 1995) and crayfish (Breithaupt, 1998), we found decisive differences in snapping shrimp. First of all, *Alpheus heterochaelis* produces different types of anterior gill currents. The "normal" anterior current is a slow, weak release of water, which was sucked through the gill chamber, as opposed to the fast, strong, anteriorly directed gill current, which occurs during social interactions. The production of the fast anterior gill current is rare (Fig. 2) but strongly linked to previous contacts with a conspecific or a crab (Fig. 4B). Among the observed currents, only the fast anterior current is created shortly *after* a preceding contact, regardless of the type of opponent. In fact, this current never occurred *before* the first contact. Moreover, we show that only this current is suited to transfer chemical information towards the other animal (Fig. 5B): it reaches the antennules of the opponent in nearly 50% of all cases.

Of all analyzed currents, only the fast anterior gill current shows some peculiarities with respect to the shrimps' opponent. The number, duration, and range is smaller in encounters with a crab than in interactions with conspecifics (Figs. 2, 3). We assume that the shrimp collect information about the genus of their opponent and reduce the effort to communicate accordingly, if it is a crab.

Role of lateral gill currents during social interactions

During social interactions between snapping shrimp and conspecifics of the same or different sex as well as during interactions with small crabs, the lateral gill currents are most prominent and significantly outnumber all other observed currents (*i.e.*, pleopod currents and fast anterior gill

currents; Fig. 2). Moreover, they are produced for long intervals but have a short range and a low velocity (Fig. 3). They are barely elicited by physical contact (Fig. 4A) and hardly ever reach the antennules of their opponents (Fig. 5A). These properties of the lateral gill currents do not change with different opponents but appear to result from a stereotyped form of production. Thus, obviously lateral gill currents are not predestinated to play a prominent role in active (chemical) signaling between the animals.

Still, their function needs explanation. From our observations we conclude that the lateral gill current is used to improve the shrimps' ability to sense possible odor signals that occur at close distance. By redirecting the "normal" gill current, the shrimp refreshes the area around its chemical receptors from its own smell (released by the slow and permanent gill current) and thereby improves the detection of the chemical surrounding. This idea is supported by our knowledge that *Alpheus heterochaelis* naturally inhabits small, oyster-shell-covered areas with little water flow and that individuals of the species appear to be rather stationary within that area (Herberholz and Schmitz, pers. obs.). The lateral gill current produced by snapping shrimp seems to be used to remove water from the area around the antennules and to a much lesser extent to draw water toward that region as proposed for the posteriorly or laterally redirected gill currents of lobsters and crayfish (Atema, 1995; Breithaupt, 1998). In contrast to lobsters and crayfish, snapping shrimp were never observed to fan simultaneously with appendages on both sides. Instead, they beat the exopodites of *one* side at a time, and there are no obvious movements of particles from the opposite side toward the animal's anterior region.

Role of pleopod currents during social interactions

In lobsters (*Homarus americanus*), pleopod currents are used for chemical (possibly pheromonal) communication during courtship at a shelter (Atema, 1985, 1988, 1995; Cowan and Atema, 1990; Bushman and Atema, 1997). The snapping shrimp *Alpheus heterochaelis*, in addition to using its pleopods for locomotion and to provide an oxygen supply for attached eggs, uses them for shelter digging, fanning the substrate (sand or muddy-sand) backward behind it (Nolan and Salmon, 1970). These authors also mention (pleopod) fanning as an aggressive act, with a shrimp vigorously beating its pleopods and directing a water current posteriorly quite close to another shrimp. The frequency of pleopod fanning is not noted by Nolan and Salmon (1970), but the behavior was described to occur between two females at the entrance of a shelter. In our experiments, we did not provide a shelter, and all shrimp were in the middle of their molt cycle. In view of the finding that the actual impact of pleopod currents in lobsters depends to a high degree on the molt state of the animals as well as on their readiness to mate (Cowan and Atema, 1990), these condi-

tions may have affected our results. Though pleopod currents were rather often produced (Fig. 2) and (in comparison to gill currents) show an average duration, a large range, and high velocity (Fig. 3), there is a lack of correlation with previous contacts (Fig. 4C) and a low precision in hitting the antennules of the opponent (Fig. 5C). There are hardly any differences in the characteristics of these currents towards different opponents. All this indicates that pleopod currents are of little relevance for (chemical) signaling or communication among snapping shrimp and between shrimp and sympatric crabs under our conditions.

A specialized gill current for chemical signaling and communication?

The transfer of chemical signals between interacting lobsters (see *e.g.*, Atema, 1995; Bushmann and Atema, 1997) and crayfish (Breithaupt *et al.*, 1999) has been described in detail. In lobsters these signals can evoke long-term individual recognition (Karavanich and Atema, 1998a, b), and in crayfish they communicate dominance status or stress condition (Zulandt Schneider *et al.*, 1999; Zulandt Schneider and Moore, 2000). In all cases, urine-borne signals were assumed to be the source of chemical signaling (Breithaupt *et al.*, 1999; Breithaupt, pers. comm.). Since the urine is released through a paired set of nephropores on the ventral sides of the basal segments of the second antennae (Parry, 1960), it can be carried toward an opponent by the anterior gill current. Moreover, agonistic behavior in catheterized lobsters increases the probability and volume of urine release (Breithaupt *et al.*, 1999).

In the present study we show for the first time that the pattern of water current production actually changes with respect to the social situation of an aquatic animal. Although snapping shrimp have the ability to produce "normal" anterior gill currents, they create different, more powerful, anteriorly directed gill currents shortly after contacting their interaction partner. These elicited currents are then more likely to reach the opponents' area of chemical perception. The same may hold true for lobsters and crayfish, but their currents have not yet been quantified during social interactions. On the other hand, we still have to prove that the fast anterior gill current in snapping shrimp actually carries chemical signals toward the opponent. Although the data presented favor this assumption, we cannot exclude the possibility that hydrodynamic signals transferred by the gill currents participate in the communication between the animals. Judging by their sensory equipment, snapping shrimp—like crayfish (Mellon, 1996) and lobsters (Guenther and Atema, 1998; Weaver and Atema, 1998)—are most likely to perceive hydrodynamic stimuli as well as chemical stimuli with their antennules (Schmitz, unpubl.). We plan to test this possibility by deactivating the chemical receptors only.

In any case, the production of the fast anterior gill current may play a critical role during hierarchy formation in snapping shrimp. We show that in intrasexual encounters the numbers of water jets and anterior gill currents are positively correlated (Fig. 6) and that both are significantly higher in the winner than in the loser (Fig. 7). In the present study, winner and loser met in only a single 20-min experiment. Preliminary experiments show that repetitive pairing of winners and losers reduces the number of water jets and anterior gill currents (Obermeier and Schmitz, unpubl.). This supports the finding that these behaviors are most probably correlated with dominance and social status in snapping shrimp. Although the strength of the water jet represents the strength of the animal (see Herberholz and Schmitz, 1999), the signal transferred by the gill current may then allow recognition of the sender. This, in turn, can prevent two *Alpheus heterochaelis* shrimp of the same sex from engaging in more severe fighting during subsequent encounters, thus reducing the number of the "costly" water jets.

Acknowledgments

We would like to thank Maren Laube for help in data analysis. The experiments comply with the current laws of Germany. Supported by a grant of the Deutsche Forschungsgemeinschaft (Schm 693/5-2). The work of J.H. was additionally supported by a NIH grant (NS26457) to Donald H. Edwards at Georgia State University.

Literature Cited

- Atema, J. 1985. Chemoreception in the sea: adaptations of chemoreceptors and behaviour to aquatic stimulus conditions. *Soc. Exp. Biol. Symp. Ser.* **39**: 387–423.
- Atema, J. 1988. Distribution of chemical stimuli. Pp. 29–56 in *Sensory Biology of Aquatic Animals*, J. Atema, R. R. Fay, A. N. Popper, and W. N. Tavolga, eds. Springer Verlag, New York.
- Atema, J. 1995. Chemical signals in the marine environment: dispersal, detection and temporal signal analysis. *Proc. Natl. Acad. Sci. USA* **92**: 62–66.
- Berkey, C., and J. Atema. 1999. Individual recognition and memory in *Homarus americanus* male-female interactions. *Biol. Bull.* **197**: 253–254.
- Breithaupt, T. 1998. Flow generation by specialized appendages in lobsters and crayfish. Pp. 185–186 in *BIONA-Report 13*, R. Blickhan, A. Wisser, and W. Nachtigall, eds. Gustav Fischer Verlag, Stuttgart.
- Breithaupt, T., and J. Ayers. 1996. Visualization and quantitative analysis of biological flow fields using suspended particles. Pp. 117–129 in *Zooplankton: Sensory Ecology and Physiology*, P. H. Lenz, D. K. Hartline, J. E. Purcell, and D. L. Macmillan, eds. Gordon Breach Publishers, Amsterdam.
- Breithaupt, T., and J. Ayers. 1998. Visualization and quantification of biological flow fields through video-based digital motion-analysis techniques. *Mar. Freshw. Behav. Physiol.* **31**: 55–61.
- Breithaupt, T., B. Schmitz, and J. Tautz. 1995. Hydrodynamic orientation of crayfish (*Procambarus clarkii*) to swimming fish prey. *J. Comp. Physiol. A* **177**: 481–491.
- Breithaupt, T., D. P. Lindstrom, and J. Atema. 1999. Urine release in

- freely moving catheterised lobsters (*Homarus americanus*) with reference to feeding and social activities. *J. Exp. Biol.* **202**: 837–844.
- Bushman, P. J., and J. Atema. 1997.** Shelter sharing and chemical courtship signals in the lobster *Homarus americanus*. *Can. J. Fish. Aquat. Sci.* **54**: 647–654.
- Cowan, D. F., and J. Atema. 1990.** Moults staggering and serial monogamy in American lobsters, *Homarus americanus*. *Anim. Behav.* **39**: 1199–1206.
- Downer, J. 1989.** *Mit den Augen der Tiere. Teil: Laute der Natur.* [video recording]. Universum. BBC and WDR (Westdeutscher Rundfunk).
- Guenther, C. M., and J. Atema. 1998.** Distribution of setae on the *Homarus americanus* lateral antennular flagellum. *Biol. Bull.* **195**: 182–183.
- Hazlett, B. A., and H. E. Winn. 1962.** Sound production and associated behavior of Bermuda crustaceans (*Panulirus*, *Gonodactylus*, *Alpheus*, and *Synalpheus*). *Crustaceana* **4**: 25–38.
- Herberholz, J. 1999.** Die Bedeutung hydrodynamischer Signale in intra- und interspezifischen Interaktionen von Pistolenkrebsen (*Alpheus heterochaelis*). Ph.D. thesis, Technische Universität München, Germany.
- Herberholz, J., and B. Schmitz. 1998.** Role of mechanosensory stimuli in intraspecific agonistic encounters of the snapping shrimp (*Alpheus heterochaelis*). *Biol. Bull.* **195**: 156–167.
- Herberholz, J., and B. Schmitz. 1999.** Flow visualization and high speed video analysis of water jets in the snapping shrimp (*Alpheus heterochaelis*). *J. Comp. Physiol. A* **185**: 41–49.
- Hughes, M. 1996.** The function of concurrent signals: visual and chemical communication in snapping shrimp. *Anim. Behav.* **52**: 247–257.
- Jeng, M.-S. 1994.** Effect of antennular and antennal ablation on pairing behavior of snapping shrimp *Alpheus edwardsii* (Audouin). *J. Exp. Mar. Biol. Ecol.* **179**: 171–178.
- Karavanich, C., and J. Atema. 1998a.** Olfactory recognition of urine signals in dominance fights between male lobsters, *Homarus americanus*. *Behaviour* **135**: 719–730.
- Karavanich, C., and J. Atema. 1998b.** Individual recognition and memory in lobster dominance. *Anim. Behav.* **56**: 1553–1560.
- Kim, W., and L. Abele. 1988.** *The Snapping Shrimp Genus Alpheus from the Eastern Pacific (Decapoda: Caridea: Alpheidae)*. Smithsonian Institution Press, Washington, DC. 119 pp.
- MacGinitie, G. E. 1937.** Notes on the natural history of several marine Crustacea. *Am. Midl. Nat.* **18**: 1031–1036.
- MacGinitie, G. E., and N. MacGinitie. 1949.** *Natural History of Marine Animals*. McGraw Hill, New York. 473 pp.
- Mellon, DeF. 1996.** Behavioral responses of crayfish antennules to odorant and hydrodynamic stimuli. *Soc. Neurosci. Abstr.* **22**: 1406.
- Morris, R. H., D. P. Abbott, and E. C. Haderlie. 1980.** *Intertidal Invertebrates of California*. Stanford University Press, Stanford. 690 pp.
- Nolan, A. N., and M. Salmon. 1970.** The behaviour and ecology of snapping shrimp (Crustacea: *Alpheus heterochaelis* and *Alpheus narmani*). *Forma Function* **2**: 289–335.
- Parry, G. 1960.** Excretion. Pp. 341–366 in *The Physiology of Crustacea, Vol 1: Metabolism and Growth*. T. H. Waterman, ed. Academic Press, New York.
- Ritzmann, R. E. 1974.** Mechanisms for the snapping behavior of two alpheid shrimp, *Alpheus californiensis* and *Alpheus heterochaelis*. *J. Comp. Physiol.* **95**: 217–236.
- Rohleder, P., and T. Breithaupt. 2000.** Visualizing chemical communication in crayfish. *Zoology: Analysis of Complex Systems Suppl. III*: **103**: 72.
- Schein, H. 1975.** Aspects of the aggressive and sexual behaviour of *Alpheus heterochaelis* Say. *Mar. Behav. Physiol.* **3**: 83–96.
- Schmitz, B. 2001.** Sound production in Crustacea with special reference to the Alpheidae. Pp. 521–533 in *The Crustacean Nervous System*, K. Wiese, ed. Springer-Verlag, Berlin.
- Schmitz, B., and J. Herberholz. 1998.** Snapping behaviour in intraspecific agonistic encounters in the snapping shrimp (*Alpheus heterochaelis*). *J. Biosci.* **23**: 623–632.
- Schultz, S., K. Wuppermann, and B. Schmitz. 1998.** Behavioural interactions of snapping shrimp (*Alpheus heterochaelis*) with conspecifics and sympatric crabs (*Eurypanopeus depressus*). *Zoology: Analysis of Complex Systems Suppl. I*: **101**: 85.
- Suzuki, D. 1986.** *Stunning sounds*. Series: *The Nature of Things*. [video recording]. CBC (Canadian Broadcasting Corporation).
- Verluis, M., B. Schmitz, A. von der Heydt, and D. Lohse. 2000.** How snapping shrimp snap: through cavitating bubbles. *Science* **289**: 2114–2117.
- Weaver, M., and J. Atema. 1998.** Hydrodynamic coupling of lobster antennule motion to oscillatory water flow. *Biol. Bull.* **195**: 180–182.
- Williams, A. B. 1984.** *Shrimps, Lobsters, and Crabs of the Atlantic Coast of the Eastern United States, Maine to Florida*. Smithsonian Institution Press, Washington, DC.
- Zulandt Schneider, R. A., and P. A. Moore. 2000.** Urine as a source of conspecific disturbance signals in the crayfish *Procambarus clarkii*. *J. Exp. Biol.* **203**: 765–771.
- Zulandt Schneider, R. A., R. W. S. Schneider, and P. A. Moore. 1999.** Recognition of dominance status by chemoreception in the red swamp crayfish, *Procambarus clarkii*. *J. Chem. Ecol.* **25(4)**: 781–794.

Methionine-Enkephalin Induces Hyperglycemia Through Eyestalk Hormones in the Estuarine Crab *Scylla serrata*

P. SREENIVASULA REDDY* AND B. KISHORI

Department of Biotechnology, Sri Venkateswara University, TIRUPATI - 517 502, India

Abstract. The hypothesis is tested that methionine-enkephalin, a hormone produced in and released from eyestalk of crustaceans, produces hyperglycemia indirectly by stimulating the release of hyperglycemic hormone from the eyestalks. Injection of methionine-enkephalin leads to hyperglycemia and hyperglucosemia in the estuarine crab *Scylla serrata* in a dose-dependent manner. Decreases in total carbohydrate (TCHO) and glycogen levels of hepatopancreas and muscle with an increase in phosphorylase activity were also observed in intact crabs after methionine-enkephalin injection. Eyestalk ablation depressed hemolymph glucose (19%) and TCHO levels (22%), with an elevation of levels of TCHO and glycogen of hepatopancreas and muscle. Tissue phosphorylase activity decreased significantly during bilateral eyestalk ablation. Administration of methionine-enkephalin into eyestalkless crabs caused no significant alterations in these parameters when compared to eyestalk ablated crabs. These results support the hypothesis that methionine-enkephalin produces hyperglycemia in crustaceans by triggering release of hyperglycemic hormone from the eyestalks.

Introduction

In decapod crustaceans, hemolymph sugar level is regulated by hyperglycemic hormone. Abramowitz *et al.* (1944) were the first to demonstrate that injection of eyestalk extract induced hyperglycemia in *Callinectes*. Since then, hyperglycemia as a response to injection of eyestalk extract

has been observed in almost all groups of crustaceans (see review by Keller, 1992). This neurohormone is stored in and released from the sinus gland. The chemical nature, mode, and site of action of hyperglycemic hormone has been extensively studied in a number of crustaceans (see reviews by Keller *et al.*, 1985; Sedlmeier, 1985). The amino acid sequence of hyperglycemic hormones has been determined from a large number of crustaceans (see La Combe *et al.*, 1999, for review). The gene for hyperglycemic hormone was also cloned from crabs (Kegel *et al.*, 1989), lobster (Tensen *et al.*, 1991), prawn (Ohira *et al.*, 1997), isopod (Martin *et al.*, 1993), and crayfish (Kegel *et al.*, 1991; Huberman *et al.*, 1993; Yasuda *et al.*, 1994). Recently, we reported the expression of hyperglycemic hormone gene at different molt stages in *Homarus americanus*, the American lobster (Reddy *et al.*, 1997).

Since the discovery of opioid peptides in decapod crustaceans by Mancillas *et al.* (1981), several workers have attempted to determine the physiological function of these peptides, but the results are fragmentary. Sarojini *et al.* (1995, 1996, 1997) provided evidence that methionine-enkephalin slowed ovarian maturation in the fiddler crab *Uca pugilator* and the crayfish *Procambarus clarkii*, and suggested that methionine-enkephalin produces this effect indirectly by stimulating the release of gonad-inhibiting hormone from eyestalks. In *Uca pugilator*, methionine-enkephalin appears to stimulate release of the concentrating hormones for black and red pigment cells (Quackenbush and Fingerman, 1984) and the dark-adapting hormone for distal retinal pigment cells (Kulkarni and Fingerman, 1987). We reported a neurotransmitter role for methionine-enkephalin in regulating the hemolymph sugar level of the freshwater crab *Oziotelphusa senex senex*, and hypothesized that methionine-enkephalin produces hyperglycemia indi-

Received 14 July 2000; accepted 6 March 2001.

* To whom correspondence should be addressed. E-mail: psreddy@vsnl.com

rectly by stimulating release of hyperglycemic hormone (Reddy, 1999).

The objectives of the present study were threefold: (a) by extending our studies to the estuarine crab *Scylla serrata*, to test our hypothesis, generated by the study of *Ozietelphusa senex senex*, that methionine-enkephalin produces hyperglycemia in decapod crustaceans; (b) to determine the changes in levels of tissue carbohydrates and phosphorylase activity during methionine-enkephalin treatment; and (c) to provide evidence that supports the triggering of release of hyperglycemic hormone during methionine-enkephalin treatment.

Materials and Methods

Individuals of *Scylla serrata* (15 ± 2 cm in carapace width; 110 ± 5 g wet weight) were collected from the Chennai coast, India. They were kept in large aquaria with continuous aeration and acclimatized to laboratory conditions for one week under constant salinity (25 ± 1 ppt), pH (7.2 ± 0.1), and temperature ($23 \pm 2^\circ\text{C}$). During this period the crabs were fed fish flesh. Feeding was stopped 24 h before the beginning of the experiments, and no food was given during experimentation. Only intermolt (Stage C₄), intact, male crabs were used in the present study.

Methionine-enkephalin (Sigma Chemical Co.) was dissolved in physiological saline (Pantin, 1934). In these experiments, each of the 10 groups of crabs used consisted of 10 individuals. The first group served as normal and received no treatment. A second group served as control, with each crab in this group receiving an injection of 10 μl of physiological saline (Pantin, 1934) through the base of the coxa of the 3rd pair of the walking legs. In groups 3–5 respectively, each crab received an injection of 10^{-7} , 10^{-8} , and 10^{-9} mole methionine-enkephalin in 10 μl volume. Both eyestalks were ablated from all the crabs in groups 6–10. The eyestalks were extirpated by cutting them off at the base, without prior ligation but with cautery of the wound after operation. Twenty-four hours after eyestalk ablation, these groups were used for experimentation. Crabs in group 6 served simply as eyestalkless animals, and crabs in group 7 received 10 μl crustacean Ringer solution and served as eyestalkless controls. In groups 8–10 respectively, each crab was injected with 10^{-7} , 10^{-8} , and 10^{-9} mole methionine-enkephalin in 10 μl volume. Based on preliminary kinetic studies, the crabs were sacrificed for analysis 2 h after injection (Figs. 1, 2).

Hemolymph (500 μl) was aspirated by syringe, through the arthroal membrane of the coxa of the 4th pair of walking legs. The other tissues (hepatopancreas

and muscle from chela propodus) were then quickly dissected out, weighed, and analyzed by the procedures outlined below.

Hemolymph total carbohydrate level. Hemolymph total carbohydrate (TCHO) levels were estimated in trichloroacetic acid supernatant (10% TCA w/v) according to the method of Carroll *et al.* (1956).

Hemolymph glucose level. For measurement of glucose, 100 μl of hemolymph was mixed with 300 μl of 95% ethanol. After deproteinization (4°C , $14,000 \times g$, 10 min), the sample was combined with a mixture of glucose enzyme reagent (glucose-6-phosphate dehydrogenase and NADP) and color reagents (phenazine methosulfate and iodinitrotetrazolium chloride) (kit from Sigma). After 30 min, the intensity of the color was measured at 490 nm and quantified with standards.

Tissue TCHO and glycogen levels. TCHO levels in the tissues (hepatopancreas and muscle) were estimated in the 10% TCA supernatant (5% w/v), and glycogen was estimated in the ethanolic precipitate of TCA supernatant, according to the method of Carroll *et al.* (1956).

To 0.5 ml of clear supernatant was added 5.0 ml of anthrone reagent, and the combination was boiled for 10 min in a water bath. The samples were then immediately cooled. A standard sample containing a known quantity of glucose solution was always tested along with the experimental samples. Absorbance was measured at 620 nm against a reagent blank.

Tissue phosphorylase activity. Phosphorylase activity was assayed in hepatopancreas and muscle by colorimetric determination of inorganic phosphate released from glucose-1-phosphate by the method of Cori *et al.* (1955). First, 0.4 ml of the enzyme was incubated with 2.0 mg of glycogen for 20 min at 35°C , then the reaction was initiated by the addition of 0.2 ml of 0.016 M glucose-1-phosphate (G-1-P) to one tube (phosphorylase *a*) and a mixture of 0.2 ml of G-1-P and 0.004 M adenosine-5-monophosphate (phosphorylase *ab*) to another tube.

The reaction was incubated for 15 min for determining total phosphorylase and for 30 min for active phosphorylase. The reaction was terminated by the addition of 5.0 ml of 5 N sulfuric acid. Released inorganic phosphate was estimated by the method of Taussky and Shorr (1953).

Protein determination. Total protein levels in the enzyme source were estimated following the method of Lowry *et al.* (1951) using bovine serum albumin as standard.

Table 1

Effect of eyestalk ablation (ESX) (24-h post-ablation) and injection of methionine-enkephalin into intact and ablated crabs on hemolymph total sugar and glucose levels in *Scylla serrata*

	No treatment	Ringer injection	10 ⁻⁷ mol/crab	10 ⁻⁸ mol/crab	10 ⁻⁹ mol/crab	Dunnet's comparison test
Total Sugar (mg/100 ml)						
Intact (Group 1)	12.11 ± 1.01	12.73 ± 1.84 ^a (5.12)	28.8 ± 2.18 ^b (126.23)	19.64 ± 1.41 ^b (54.28)	16.52 ± 1.94 ^b (29.77)	$F_{(4,45)} = 137.160$
ESX (Group 2)	9.41 ± 1.13 ^b (-22.22)	9.34 ± 1.03 ^{b,c} (-0.74)	9.41 ± 1.13 ^{b,c} (0.74)	9.43 ± 1.01 ^{b,c} (0.96)	9.21 ± 1.08 ^{b,c} (-1.39)	$F_{(4,45)} = 0.099$
Two-way ANOVA: $F_{1,90}$ (Between groups) = 772.002, $P < 0.001$; $F_{4,90}$ (Among treatments) = 98.747, $P < 0.001$; $F_{4,90}$ (Interaction) = 94.552, $P < 0.001$.						
Glucose (mg/100 ml)						
Intact (Group 1)	6.41 ± 0.62	6.55 ± 0.76 ^a (2.16)	12.07 ± 1.34 ^b (84.27)	11.44 ± 1.28 ^b (74.65)	9.13 ± 0.78 ^b (39.38)	$F_{(4,45)} = 75.613$
ESX (Group 2)	5.19 ± 1.01 ^b (-19.03)	5.52 ± 0.81 ^{b,c} (6.35)	5.19 ± 1.01 ^{b,c} (-5.97)	5.21 ± 0.91 ^{b,c} (-5.61)	5.44 ± 0.77 ^{b,c} (-1.44)	$F_{(4,45)} = 0.387$
Two-way ANOVA: $F_{1,90}$ (Between groups) = 440.810, $P < 0.001$; $F_{4,90}$ (Among treatments) = 40.092, $P < 0.001$; $F_{4,90}$ (Interaction) = 44.753, $P < 0.001$.						

Values are mean ± SD of 10 individual crabs. Values in parentheses are percent change from control. For calculation of percent change for eyestalk-ablated (ESX) crabs and Ringer-injected intact crabs, intact crabs served as control; for met-injected crabs, Ringer-injected crabs served as control.

^a Not significant compared with intact crabs.

^b $P < 0.001$ compared to intact crabs.

^c Not significant compared to eyestalkless crabs.

Statistical analysis. Statistical analysis of the results was made using a two-way ANOVA test followed by Dunnet's multiple range test (preceded by one-way ANOVA), using SPSS version 10.0 (SPSS Inc., Chicago, IL).

Results

Effects of methionine-enkephalin on carbohydrate metabolism of intact crabs

Injection of methionine-enkephalin into intact crabs resulted in significant hyperglycemia and hyperglucosemia in a dose-dependent manner (Table 1), whereas injection of physiological saline had no effect on hemolymph carbohydrate levels. At doses between 10⁻⁹ mol/crab (36.41%) and 10⁻⁶ mol/crab (147.81%), the effect of methionine-enkephalin was statistically significant. For doses lower than 10⁻⁹ mol/crab, however, methionine-enkephalin did not elicit a hyperglycemic response (Fig. 1). A time course for methionine-enkephalin-induced hyperglycemia is shown in Figure 2 for a 10⁻⁷ mol/crab dose, which is a nearly saturating dose. The hemolymph glucose level increased significantly within 30 min of methionine-enkephalin injection, reached a peak at 2 h, then declined gradually.

Hepatopancreas glycogen and TCHO levels in crabs that received methionine-enkephalin were significantly lower than those of control crabs (Table 2). Decreases in muscle glycogen and TCHO levels were also significant after the injection of methionine-enkephalin (Table 3), suggesting

the possible mobilization of glucose molecules from hepatopancreas and muscle to hemolymph.

Phosphorylase (both total and active) activity levels were significantly increased in both hepatopancreas and muscle

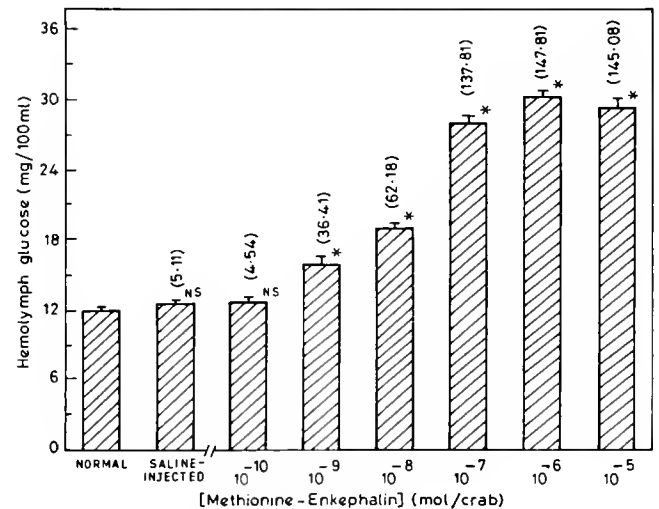


Figure 1. Dose-dependent effect of methionine-enkephalin on the hemolymph glucose levels in intact *Scylla serrata*. Two hours after injection of saline (10 μ l/animal) or methionine-enkephalin at the doses indicated, hemolymph was withdrawn from crabs for glucose determination. Each bar represents a mean ± SD ($n = 10$). Numbers in parentheses indicates the percent increase from the normal values. * Significant difference from normal crabs at $P < 0.001$. NS Not significant.

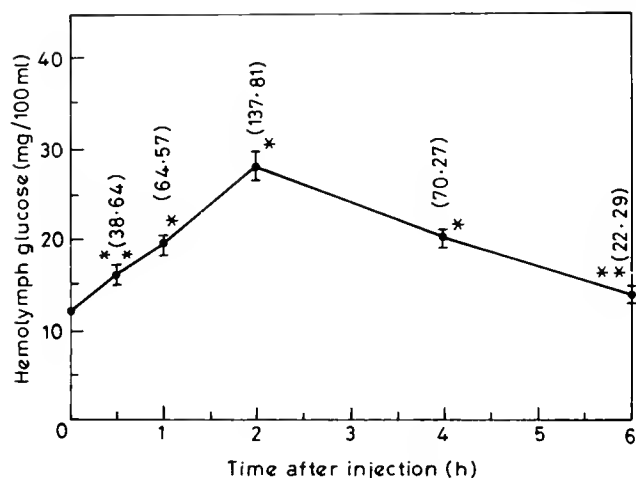


Figure 2. Time course of methionine-enkephalin-induced hyperglycemia. After injection of methionine-enkephalin (10^{-7} mol/crab), hemolymph was withdrawn from intact crabs at the time points indicated for glucose determination. Each point represents a mean \pm SD ($n = 10$). Numbers in parentheses represent percent change from zero time controls. * Significant difference from zero time control at $P < 0.001$. ** Significant difference from zero time control at $P < 0.001$. ^{NS} Not significant from zero time control.

after the injection of methionine-enkephalin (Tables 4, 5). The ratio of active to total phosphorylase also increased in the tissues of crabs after the injection of methionine-en-

kephalin, indicating conversion of inactive to active phosphorylase.

Effects of bilateral eyestalk ablation and injection of methionine-enkephalin into ablated crabs on carbohydrate metabolism

Bilateral eyestalk removal caused a significant decrease in hemolymph carbohydrate level (Table 1). Enhancement of TCHO level of hepatopancreas and muscle was also significant in eyestalk-ablated crabs (Tables 2, 3). The increase was greater in muscle. Glycogen level in hepatopancreas increased significantly in eyestalkless crabs. A similar pattern was observed in muscle. Tissue phosphorylase activity levels decreased significantly in eyestalk-ablated crabs (Tables 4, 5).

Injection of methionine-enkephalin into eyestalkless crabs did not significantly change hemolymph carbohydrate levels compared to Ringer-injected eyestalkless crabs (Table 1). The levels of tissue TCHO and glycogen and activity levels of total and active phosphorylase were also not significantly altered in eyestalkless crabs after methionine-enkephalin injection (Tables 2–5).

Discussion

The effect of eyestalk hormones on tissue carbohydrate levels and phosphorylase activity has been extensively stud-

Table 2

Effect of eyestalk ablation (ESX) (24-h post-ablation) and injection of methionine-enkephalin into intact and ablated crabs on hepatopancreas total carbohydrate (TCHO) and glycogen levels in Scylla serrata

	No treatment	Ringer injection	10^{-7} mol/crab	10^{-8} mol/crab	10^{-9} mol/crab	Dunnet's comparison test
TCHO (mg/g)						
Intact	13.66 \pm 1.54	13.84 \pm 1.61 ^a	8.47 \pm 0.97 ^b	9.01 \pm 1.51 ^b	9.47 \pm 1.49 ^b	$F_{(4,45)} = 38.033$
(Group 1)		(1.32)	(-38.80)	(-34.89)	(-31.57)	$P < 0.001$
ESX	17.87 \pm 1.94 ^b	18.01 \pm 1.97 ^{b,c}	17.44 \pm 1.43 ^{b,c}	17.81 \pm 1.62 ^{b,c}	17.93 \pm 1.59 ^{b,c}	$F_{(4,45)} = 0.229$
(Group 2)	(30.96)	(0.67)	(-0.74)	(-0.96)	(-1.39)	
Two-way ANOVA: $F_{1,90}$ (Between groups) = 566.317, $P < 0.001$; $F_{4,90}$ (Among treatments) = 19.027, $P < 0.001$; $F_{4,90}$ (Interaction) = 14.896, $P < 0.001$.						
Glycogen (mg/g)						
Intact	1.22 \pm 0.10	1.23 \pm 0.09 ^a	0.58 \pm 0.14 ^b	0.61 \pm 0.13 ^b	0.64 \pm 0.21 ^b	$F_{(4,45)} = 148.477$
(Group 1)		(0.82)	(-52.84)	(-50.40)	(-47.96)	$P < 0.001$
ESX	2.04 \pm 0.29 ^b	2.06 \pm 0.31 ^{b,c}	2.11 \pm 1.18 ^{b,c}	2.09 \pm 0.21 ^{b,c}	2.07 \pm 0.28 ^{b,c}	$F_{(4,45)} = 0.230$
(Group 2)	(67.21)	(0.98)	(2.42)	(1.45)	(0.48)	
Two-way ANOVA: $F_{1,90}$ (Between groups) = 1658.593, $P < 0.001$; $F_{4,90}$ (Among treatments) = 24.964, $P < 0.001$; $F_{4,90}$ (Interaction) = 27.016, $P < 0.001$.						

Values are mean \pm SD of 10 individual crabs. Values in parentheses are percent change from control. For calculation of percent change for ESX crabs and Ringer-injected intact crabs, intact crabs served as control; for met-injected crabs, Ringer-injected crabs served as control.

^a Not significant compared with intact crabs.

^b $P < 0.001$ compared to intact crabs.

^c Not significant compared to eyestalkless crabs.

Table 3

Effect of eyestalk ablation (ESX) (24 h post-ablation) and injection of methionine-enkephalin into intact and ablated crabs on muscle total carbohydrate (TCHO) and glycogen levels in *Scylla serrata*

	No treatment	Ringer injection	10 ⁻⁷ mol/crab	10 ⁻⁸ mol/crab	10 ⁻⁹ mol/crab	Dunnet's comparison test
TCHO (mg/g)						
Intact (Group 1)	4.39 ± 0.53	4.41 ± 0.49 ^a (0.46)	2.94 ± 0.31 ^b (-33.33)	3.01 ± 0.37 ^b (-31.74)	3.12 ± 0.92 ^b (-29.25)	$F_{(4,45)} = 30.829$ $P < 0.001$
ESX (Group 2)	6.26 ± 0.71 ^b (42.59)	6.31 ± 0.81 ^{b,c} (0.80)	6.31 ± 0.76 ^{b,c} (0)	6.25 ± 0.84 ^{b,c} (-0.95)	6.33 ± 0.92 ^{b,c} (0.31)	$F_{(4,45)} = 0.045$
Two-way ANOVA: $F_{1,90}$ (Between groups) = 579.612, $P < 0.001$; $F_{4,90}$ (Among treatments) = 8.707, $P < 0.001$; $F_{4,90}$ (Interaction) = 9.114, $P < 0.001$.						
Glycogen (mg/g)						
Intact (Group 1)	0.66 ± 0.06	0.64 ± 0.09 ^a (-3.03)	0.34 ± 0.09 ^b (-46.87)	0.37 ± 0.06 ^b (-42.18)	0.41 ± 0.08 ^b (-35.31)	$F_{(4,45)} = 45.114$ $P < 0.001$
ESX (Group 2)	1.01 ± 0.09 ^b (53.03)	1.02 ± 0.11 ^{b,c} (0.99)	0.99 ± 0.14 ^{b,c} (-2.94)	1.07 ± 0.33 ^{b,c} (4.90)	1.03 ± 0.21 ^{b,c} (0.98)	$F_{(4,45)} = 0.188$
Two-way ANOVA: $F_{1,90}$ (Between groups) = 422.031, $P < 0.001$; $F_{4,90}$ (Among treatments) = 6.391, $P < 0.001$; $F_{4,90}$ (Interaction) = 6.713, $P < 0.001$.						

Values are mean (mg glucose/g tissue) ± SD of 10 individual crabs. Values in parentheses are percent change from control. For calculation of percent change for ESX crabs and Ringer-injected intact crabs, intact crabs served as control; for met-injected crabs, Ringer-injected crabs served as control.

^a Not significant compared with intact crabs.

^b $P < 0.001$ compared to intact crabs.

^c Not significant compared to eyestalkless crabs.

ied (Keller, 1965; Ramamurthi *et al.*, 1968; Sagardia, 1969). Eyestalk removal inactivates the phosphorylase system and activates uridine-diphosphate-glucose glycogen transglucosylase (glycogen synthetase) (Keller, 1965; Ramamurthi *et al.*, 1968). Ramamurthi *et al.* (1968) also observed stimulation of uptake and incorporation of glucose ¹⁴C into the glycogen fraction of muscle tissue after eyestalk removal; this stimulation was accompanied by a decrease in hemolymph sugar level. Injection of eyestalk extract reversed these changes. The hyperglycemic hormone of eyestalks of the crab *Oziotelphusa senex senex* and the prawn *Penaeus monodon* enhances the activity of the phosphorylase system (Reddy *et al.*, 1982, 1984; Reddy, 1992).

An increase in phosphorylase activity and a decrease in glycogen and TCHO levels in hepatopancreas and muscle of *Scylla serrata*, followed by hyperglycemia after the injection of methionine-enkephalin, indicate glycogenolysis and mobilization of sugar molecules from tissues to hemolymph. This is in agreement with other findings (see review by Reddy and Ramamurthi, 1999). Though the hormone that elevates hemolymph sugar is conventionally called crustacean hyperglycemic hormone (CHH), Hohnke and Scheer (1970) suggested that the primary function of the CHH is not to elevate hemolymph sugar level, but to elevate intracellular glucose through the degradation of glycogen by activating the enzyme phosphorylase. The conversion of phosphorylase from its inactive to active form results in

glycogenolysis, and the resultant glucose molecules leak into the hemolymph, causing hyperglycemia. This view has been supported by Telford (1975).

Our results clearly demonstrate that methionine-enkephalin is involved in the regulation of carbohydrate metabolism in the crab *Scylla serrata*. In the present study, we show that methionine-enkephalin elicited a hyperglycemic response in *S. serrata* in a dose-dependent manner (Fig. 1). Methionine-enkephalin-induced hyperglycemia has been similarly demonstrated in the freshwater crab *Oziotelphusa senex senex* (Reddy, 1999) and the brackish-water prawns *Penaeus indicus* and *Metapenaeus monocerus* (Kishori *et al.*, 2001). The doses of methionine-enkephalin that induced hyperglycemia ranged from 10⁻⁹ to 10⁻⁶ mol/animal (Fig. 1), which is comparable to those reported for *O. senex senex* (Reddy, 1999). Our observation that methionine-enkephalin was ineffective in inducing hyperglycemia in eyestalk-ablated *S. serrata* (Table 1) is also consistent with those obtained in crabs (Reddy, 1999) and prawns (Kishori *et al.*, 2001) and suggests that the hyperglycemic effect of methionine-enkephalin results from an enhanced release of CHH (Keller, 1992; Soye, 1997).

Injection of methionine-enkephalin into intact *S. serrata* also has two other effects. It activates the phosphorylase system, which causes degradation of glycogen. It also results in accumulation of sugar molecules in the tissues; these molecules are ultimately mobilized to hemolymph,

Table 4

Effect of eyestalk ablation (ESX) (24 h post-ablation) and injection of methionine-enkephalin into intact and ablated crabs on hepatopancreas phosphorylase activity levels in *Scylla serrata*

	No treatment	Ringer injection	10 ⁻⁷ mol/crab	10 ⁻⁸ mol/crab	10 ⁻⁹ mol/crab	Dunnet's comparison test
Phosphorylase a						
Intact (Group 1)	2.62 ± 0.29	2.67 ± 0.33 ^a (1.91)	3.87 ± 0.46 ^b (44.94)	3.63 ± 0.34 ^b (35.95)	3.60 ± 0.42 ^b (34.83)	$F_{(4,45)} = 28.430$ $P < 0.001$
ESX (Group 2)	1.72 ± 0.31 ^b (-34.35)	1.67 ± 0.29 ^{b,c} (-2.33)	1.69 ± 0.11 ^{b,c} (1.19)	1.81 ± 0.22 ^{b,c} (8.38)	1.84 ± 0.31 ^{b,c} (10.17)	$F_{(4,45)} = 1.473$
Two-way ANOVA: $F_{1,90}$ (Between groups) = 716.848, $P < 0.001$; $F_{4,90}$ (Among treatments) = 23.852, $P < 0.001$; $F_{4,90}$ (Interaction) = 18.208, $P < 0.001$.						
Phosphorylase ab						
Intact (Group 1)	4.52 ± 0.41	4.56 ± 0.44 ^a (0.89)	5.81 ± 0.67 ^b (27.41)	5.69 ± 0.52 ^b (24.78)	5.56 ± 0.73 ^b (21.92)	$F_{(4,45)} = 15.846$ $P < 0.001$
ESX (Group 2)	4.06 ± 0.44 ^b (-10.18)	4.08 ± 0.41 ^{b,c} (0.49)	4.10 ± 0.39 ^{b,c} (0.49)	4.12 ± 0.34 ^{b,c} (0.98)	4.09 ± 0.51 ^{b,c} (0.24)	$F_{(4,45)} = 0.044$
Two-way ANOVA: $F_{1,90}$ (Between groups) = 169.103, $P < 0.001$; $F_{4,90}$ (Among treatments) = 11.291, $P < 0.001$; $F_{4,90}$ (Interaction) = 9.985, $P < 0.001$.						

Values are mean (iP released/mg protein/h) ± SD of 10 individual crabs. Values in parentheses are percent change from control. For calculation of percent change for ESX crabs and Ringer-injected intact crabs, intact crabs served as control; for met-injected crabs, Ringer-injected crabs served as control.

^a Not significant compared with intact crabs.

^b $P < 0.001$ compared to intact crabs.

^c Not significant compared to eyestalkless crabs.

causing hyperglycemia. Methionine-enkephalin might have elevated the phosphorylase system in intact crabs in several different ways—for example, by triggering release of hyperglycemic hormone or by mimicking the action of this hormone. However, because methionine-enkephalin was not able to produce these changes in eyestalkless crabs, it seems most likely that methionine-enkephalin exerted its hyperglycemic effect by triggering release of hyperglycemic hormone from the sinus gland of eyestalks. This supports our earlier results that sinus glands in the eyestalks of crabs are the main release site for hyperglycemic hormone (Reddy and Ramamurthi, 1982).

The mechanisms whereby methionine-enkephalin causes release of neurohormones are still uncertain. In mammals, endogenous opioid peptides are involved in regulating the release of neurohypophysial peptides (Bicknell *et al.*, 1988; Yamada *et al.*, 1988; Sasaki *et al.*, 2000). In crustaceans, opioid-peptide-like (methionine-enkephalin-like, leucine-enkephalin-like and *b*-endorphin-like) hormones were isolated and characterized from X-organ sinus gland complexes of eyestalks (Fingerman *et al.*, 1983, 1985). However, there is little information about the effect of opioid peptides on release of neurohormones in crustaceans. Sarojini *et al.* (1995, 1996), using highly selective opioid antagonists, provided evidence that methionine-enkephalin exerts its effect by acting through delta-type opioid receptors in regulating ovarian maturation in *Procambarus*

clarkii. *In vivo* studies with tissues of *P. clarkii* showed that methionine-enkephalin exerted its effect by at least modulating the release of eyestalk peptide hormone (Sarojini *et al.*, 1997). Recently, we provided evidence for a neurotransmitter role for methionine-enkephalin in causing hyperglycemia in the crab *O. senex senex* (Reddy, 1999). Methionine-enkephalin also triggers the release of red-pigment-concentrating hormone, black-pigment-dispersing hormone (Quackenbush and Fingerman, 1984), and dark-pigment-adapting hormone (Kulkarni and Fingerman, 1987). Three facts make it seem likely that this hyperglycemic action of methionine-enkephalin in the present study on *S. serrata* is also indirect and involves stimulation of release of CHH. Methionine-enkephalin-like material is present in the neuroendocrine complex of the eyestalk of crustaceans (Fingerman *et al.*, 1983, 1985). Methionine-enkephalin mediation of release of neurohormones has been demonstrated (Reddy, 1999). In cases where methionine-enkephalin has been found to stimulate neurohormone release, it does not act in the absence of neuroendocrine organs. As further support for the conclusion, eyestalk extract from methionine-enkephalin injected prawns showed significantly less activity than the normal eyestalk extract in inducing hyperglycemia (Kishori *et al.*, 2001).

Although the mechanisms that trigger release of CHH are still unknown, it is noteworthy that 5-hydroxytryptamine (5-HT), or serotonin, triggers CHH release in the crayfish

Table 5

Effect of eyestalk ablation (ESX) (24 h post-ablation) and injection of methionine-enkephalin into intact and ablated crabs on muscle phosphorylase activity levels in *Scylla serrata*

	No treatment	Ringer injection	10 ⁻⁷ mol/crab	10 ⁻⁸ mol/crab	10 ⁻⁹ mol/crab	Dunnet's comparison test
Phosphorylase <i>a</i>						
Intact (Group 1)	1.92 ± 0.09	1.94 ± 0.14 ^a (1.04)	3.26 ± 0.36 ^b (68.04)	3.01 ± 0.12 ^b (55.15)	3.02 ± 0.26 ^b (55.67)	$F_{(4,45)} = 84.853$ $P < 0.001$
ESX (Group 2)	0.99 ± 0.08 ^b (-48.44)	1.02 ± 0.11 ^{b,c} (3.03)	1.01 ± 0.09 ^{b,c} (-0.74)	1.04 ± 0.13 ^{b,c} (1.96)	1.06 ± 0.21 ^{b,c} (3.92)	$F_{(4,45)} = 0.368$
Two-way ANOVA: $F_{1,90}$ (Between groups) = 1711.188, $P < 0.001$; $F_{4,90}$ (Among treatments) = 58.745, $P < 0.001$; $F_{4,90}$ (Interaction) = 52.927, $P < 0.001$.						
Phosphorylase <i>ab</i>						
Intact (Group 1)	2.49 ± 0.45	2.52 ± 0.49 ^a (1.21)	3.49 ± 0.41 ^b (38.49)	3.46 ± 0.44 ^b (37.30)	3.44 ± 0.51 ^b (36.50)	$F_{(4,45)} = 16.086$ $P < 0.001$
ESX (Group 2)	2.22 ± 0.32 ^b (-11.65)	2.18 ± 0.31 ^{b,c} (-0.91)	2.22 ± 0.34 ^{b,c} (1.83)	2.24 ± 0.42 ^{b,c} (2.75)	2.25 ± 0.41 ^{b,c} (3.21)	$F_{(4,45)} = 0.061$
Two-way ANOVA: $F_{1,90}$ (Between groups) = 136.048, $P < 0.001$; $F_{4,90}$ (Among treatments) = 10.259, $P < 0.001$; $F_{4,90}$ (Interaction) = 8.734, $P < 0.001$.						

Values are mean (iP released/mg protein/h) ± SD of 10 individual crabs. Values in parentheses are percent change from control. For calculation of percent change for ESX crabs and Ringer-injected intact crabs, intact crabs served as control; for met-injected crabs, Ringer-injected crabs served as control.

^a Not significant compared with intact crabs.

^b $P < 0.001$ compared to intact crabs.

^c Not significant compared to eyestalkless crabs.

Orconectes limosus (Keller and Bayer, 1968), *Astacus leptodactylus* (Strolenberg and Van Herp, 1977), and *Procambarus clarkii* (Lee *et al.*, 2000). Strolenberg and Van Herp (1977), working with *A. leptodactylus*, and Martin (1978), working with *Porcellio dilatatus*, found that the sinus glands of specimens injected with 5-HT show increased numbers of exocytotic profiles, suggestive of increased CHH release. Exocytosis in *A. leptodactylus* was maximal 2 h after 5-HT was injected, and the hemolymph glucose concentration peaked 4 h after the injection (Strolenberg and Van Herp, 1977). In *P. dilatatus*, hyperglycemia induced by 5-HT is mediated by 5-HT₁- and 5-HT₂-like receptors in triggering release of CHH (Lee *et al.*, 2000).

In summary, we have shown that methionine-enkephalin is a potent hyperglycemic regulator in the crab *Scylla serrata*. The most likely site of action of methionine-enkephalin is the eyestalks, where the X-organ-sinus glands may respond to methionine-enkephalin stimulation by releasing CHH. Based on these results, experiments are being conducted to determine whether methionine-enkephalin enhances the release of CHH in crustaceans.

Acknowledgments

We thank Prof. Armugam, University of Madras, Chennai, for supplying *Scylla serrata* and providing necessary laboratory facilities, and Dr. K. V. S. Sharma, Professor,

Department of Statistics, Sri Venkateswara University, for analyzing the data. We also thank the anonymous reviewers whose comments improved our manuscript. We are grateful to Prof. R. Ramamurthi, Department of Zoology, for his encouragement. Mr. S. Umasankar and Miss B. Prema Sheela provided skilled technical assistance. This work was carried out with the financial assistance from Department of Science and Technology research grant (SP/SO/CO4/96) to Dr. PSR. We also thank the staff, Department of Biotechnology, Sri Venkateswara University, for their invaluable assistance.

Literature Cited

- Abramowitz, A. A., F. L. Hisaw, and D. N. Papandrea. 1944. The occurrence of a diabetogenic factor in the eyestalks of crustaceans. *Biol. Bull.* **86**: 1-5.
- Bicknell, R. J., G. Leng, J. A. Russell, R. G. Dyer, S. Mansfield, and B. G. Zhao. 1988. Hypothalamic opioid mechanisms controlling oxytocin neurons during parturition. *Brain Res. Bull.* **20**: 743-749.
- Carroll, N. V., N. N. Longley, and J. G. Roe. 1956. Glycogen determination in liver and muscle by use of anthrone reagent. *J. Biol. Chem.* **220**: 583-593.
- Cori, G. T., B. Illingworth, and P. G. Keller. 1955. Muscle phosphorylase. Pp. 200-207 in *Methods in Enzymology*, Vol. 1, S. P. Colowick and N. O. Kaplan, eds. Academic Press, New York.
- Fingerman, M., M. M. Hanumante, and L. L. Vacca. 1983. Enkephalin-like and substance P-like immunoreactivity in the eyestalk neuroen-

- ocrine complex of the fiddler crab, *Uca pugilator*. *Soc. Neurosci. Abstr.* **9**: 439.
- Fingerman, M., M. M. Hanumante, G. K. Kulkarni, R. Ikeda, and L. L. Vacca. 1985.** Localization of substance P-like, leucine-enkephalin-like, methionine-enkephalin-like, and FMFR amide-like immunoreactivity in the eyestalk of the fiddler crab, *Uca pugilator*. *Cell Tissue Res.* **241**: 473–477.
- Hohnke, L., and B. T. Scheer. 1970.** Carbohydrate metabolism in crustaceans. Pp. 147–166 in *Chemical Zoology*, Vol. 5, M. Florin and B. T. Scheer, eds. Academic Press, New York.
- Huberman, A., M. B. Aguilar, K. Brew, J. Shahanowitz, and D. F. Hunt. 1993.** Primary structure of the major isomorph of the crustacean hyperglycemic hormone (CHH-1) from the sinus gland of Mexican crayfish *Procambarus bowyeri* (Ortmann): interspecies comparison. *Peptides* **14**: 7–16.
- Kegel, G., B. Reichwein, S. Weese, G. Gaus, J. Peter-Katalinic, and R. Keller. 1989.** Amino acid sequence of the crustacean hyperglycemic hormone (CHH) from the shore crab, *Carcinus maenas*. *FEBS Lett.* **255**: 10–14.
- Kegel, G., B. Reichwein, C. P. Tensen, and R. Keller. 1991.** Amino acid sequence of crustacean hyperglycemic hormone (CHH) from the crayfish *Orconectes limosus*. Emergence of a novel neuropeptide family. *Peptides* **12**: 909–913.
- Keller, R. 1965.** Über eine hormonale Kontrolle des Polysaccharidstoffwechsels beim Flusskrebs *Cambarus maenas*. *Z. Vgl. Physiol.* **51**: 49–59.
- Keller, R. 1992.** Crustacean neuropeptides: structures, functions and comparative aspects. *Experientia* **48**: 439–448.
- Keller, R., and J. Beyer. 1968.** Zur hyperglykamischen Wirkung von Serotonin und Augestiel-extrakt beim Flusskrebs *Orconectes limosus*. *Z. Vgl. Physiol.* **59**: 78–85.
- Keller, R., P. Jaros, and G. Kegel. 1985.** Crustacean hyperglycemic neuropeptides. *Am. Zool.* **25**: 207–221.
- Kishori, B., B. Premasheela, R. Ramamurthi, and P. S. Reddy. 2001.** Evidence for hyperglycemic effect of methionine-enkephalin in prawns *Penaeus indicus* and *Metapenaeus monocerus*. *Gen. Comp. Endocrinol.* (in press).
- Kulkarni, G. K., and M. Fingerman. 1987.** Distal retinal pigment of the fiddler crab, *Uca pugilator*. Release of the dark-adapting hormone by methionine-enkephalin and FMRF-amide. *Pigm. Cell Res.* **1**: 51–56.
- Lacombe, C., P. Greve, and G. Martin. 1999.** Overview on the sub-grouping of the crustacean hyperglycemic hormone family. *Neuropeptides* **33**: 71–80.
- Lee, C. Y., S. M. Yau, C. S. Liao, and W. J. Huang. 2000.** Serotogenic regulation of blood glucose levels in the crayfish, *Procambarus clarkii*: site of action and receptor characterization. *J. Exp. Zool.* **286**: 596–605.
- Lowry, O. H., N. J. Rosebrough, A. L. Farr, and R. J. Randall. 1951.** Protein measurement with Folin phenol reagent. *J. Biol. Chem.* **193**: 265–275.
- Mancillas, J. R., J. F. McGinty, A. I. Selverston, H. Karten, and F. E. Bloom. 1981.** Immunocytochemical localization of enkephalin and substance P in retina and eyestalk neurones of lobster. *Nature* **293**: 576–578.
- Martin, G. 1978.** Action de la sérotonine sur la glycémie et sur la libération des neurosecretions contenues dans la glande du sinus de *Porcellio dilatatus* Bradt (Crustacé, Isopode, Oniscoïde). *C. R. Seances Soc. Biol. Fil.* **172**: 304–307.
- Martin, G., O. Sorokine, and A. Van Dorselaer. 1993.** Isolation and molecular characterization of hyperglycemic neuropeptide from the sinus gland of the terrestrial isopod *Armadillidium vulgare* (Crustacea). *Eur. J. Biochem.* **211**: 601–607.
- Ohira, T., T. Watanabe, H. Nagasawa, and K. Aida. 1997.** Cloning and sequence analysis of a cDNA encoding a crustacean hyperglycemic hormone from the Kuruma prawn *Penaeus japonicus*. *Mol. Mar. Biol. Biotechnol.* **6**: 59–63.
- Pantin, C. F. A. 1934.** The excitation of crustacean muscle. *J. Exp. Biol.* **11**: 11–27.
- Quackenbush, L. S., and M. Fingerman. 1984.** Regulation of neurohormone release in the fiddler crab, *Uca pugilator*: Effects of gamma-aminobutyric acid, octopamine, met-enkephalin and beta-endorphin. *Comp. Biochem. Physiol.* **79C**: 77–84.
- Ramamurthi, R., M. W. Mumbach, and B. T. Scheer. 1968.** Endocrine control of glycogen synthesis in crabs. *Comp. Biochem. Physiol.* **67B**: 437–445.
- Reddy, P. S. 1992.** Changes in carbohydrate metabolism of *Palaemonetes* in response to crustacean hyperglycemic hormone. *Arch. Int. Physiol. Biochim. Biophys.* **100**: 281–283.
- Reddy, P. S. 1999.** A neurotransmitter role for methionine-enkephalin in causing hyperglycemia in the fresh water crab *Oziotelphusa senex senex*. *Curr. Sci.* **76**: 1126–1128.
- Reddy, P. S., and R. Ramamurthi. 1982.** Neuroendocrine control of carbohydrate metabolism in the rice field crab (*Oziotelphusa senex senex*). *J. Reprod. Biol. Comp. Endocrinol.* **2**: 49–57.
- Reddy, P. S., and R. Ramamurthi. 1999.** Recent trends in crustacean endocrine research. *Proc. Indian Natl. Sci. Acad.* **B65**: 15–32.
- Reddy, P. S., A. Bhagyalakshmi, V. Chandrasekharam, and R. Ramamurthi. 1982.** Hyperglycemic activity of crab and scorpion hormones in grasshopper, *Poeciloceris pictus*. *Experientia* **38**: 811–812.
- Reddy, P. S., A. Bhagyalakshmi, V. Chandrasekharam, and R. Ramamurthi. 1984.** Differential responsiveness of phosphorylase system and fat body carbohydrates of *Poeciloceris pictus* (Insecta) to hyperglycemic factors of crab (Crustacea) and scorpion (Arachnida). *Gen. Comp. Endocrinol.* **54**: 43–45.
- Reddy, P. S., G. D. Prestwich, and E. S. Chang. 1997.** Crustacean hyperglycemic hormone gene expression in the lobster *Homarus americanus*. Pp. 51–5 in *Advances in Comparative Endocrinology*, Vol. 1, S. Kawashima and S. Kikuyama, eds. Monduzzi Editore, Bologna, Italy.
- Sagardia, F. 1969.** The glycogen phosphorylase system from the muscle of the blue crab, *Callinectes danae*. *Comp. Biochem. Physiol.* **28**: 1377–1385.
- Sarojini, R., R. Nagabhushanam, and M. Fingerman. 1995.** Evidence for opioid involvement in the regulation of ovarian maturation of the fiddler crab, *Uca pugilator*. *Comp. Biochem. Physiol.* **111A**: 279–282.
- Sarojini, R., R. Nagabhushanam, and M. Fingerman. 1996.** *In vivo* assessment of opioid agonists and antagonists on ovarian maturation in the red swamp crayfish, *Procambarus clarkii*. *Comp. Biochem. Physiol.* **115C**: 149–153.
- Sarojini, R., R. Nagabhushanam, and M. Fingerman. 1997.** An *in vitro* study of the inhibitory action of methionine enkephalin on ovarian maturation in the red swamp crayfish, *Procambarus clarkii*. *Comp. Biochem. Physiol.* **117C**: 207–210.
- Sasaki, T., K. Shimada, and N. Saito. 2000.** Regulation of opioid peptides on the release of arginine vasotocin in the hen. *J. Exp. Zool.* **286**: 481–486.
- Sedlmeier, D. 1985.** Mode of action of the crustacean hyperglycemic hormone. *Am. Zool.* **25**: 223–232.
- Soyez, D. 1997.** Occurrence and diversity of neuropeptides from the crustacean hyperglycemic hormone family in arthropods. *Ann. NY Acad. Sci.* **814**: 319–323.

- Strolenberg, G. E. C., and F. Van Herp. 1977.** Mise en évidence du phénomène d'exocytose dans la glande du sinus d'*Astacus leptodactylus* (Nordmann) sous l'influence d'injection de sérotonine. *C. R. Acad. Sci. Ser. III Sci. Vie* **284D**: 57–59.
- Taussky, H. M., and E. Shorr. 1953.** A micro colorimetric method for determination of inorganic phosphate. *J. Biol. Chem.* **202**: 675–682.
- Telford, M. 1975.** Blood glucose in crayfish—III. The sources of glucose and role of eyestalk factor in hyperglycemia of *Cambarus robustus*. *Comp. Biochem. Physiol.* **51**: 69–73.
- Tensen, C. P., D. P. V. De Kleijn, and F. Van Herp. 1991.** Cloning and sequence analysis of cDNA encoding two crustacean hyperglycemic hormones from the lobster *Homarus americanus*. *Eur. J. Biochem.* **200**: 103–106.
- Yamada, T., K. Nakao, H. Itoh, N. Morii, S. Shiono, M. Sakamoto, A. Sugawara, Y. Saito, M. Mukoyama, H. Arai, M. Eigyo, A. Matushita, and H. Imura. 1988.** Inhibitory action of leuromorphin on vasopressin secretion in conscious rats. *Endocrinology* **122**: 985–990.
- Yasuda, A., Y. Yasuda, T. Fujita, and Y. Naya. 1994.** Characterization of crustacean hyperglycemic hormone from the crayfish (*Procambarus clarkii*): multiplicity of molecular forms by stereoinversion and diversion functions. *Gen. Comp. Endocrinol.* **95**: 387–398.

Theoretical and Experimental Dissection of Gravity-Dependent Mechanical Orientation in Gravitactic Microorganisms

YOSHIHIRO MOGAMI,* JUNKO ISHII,† AND SHOJI A. BABA

Department of Biology, Ochanomizu University, Otsuka, Tokyo 112-8610, Japan

Abstract. Mechanisms of gravitactic behaviors of aquatic microorganisms were investigated in terms of their mechanical basis of gravity-dependent orientation. Two mechanical mechanisms have been considered as possible sources of the orientation torque generated on the inert body. One results from the differential density within an organism (the gravity-buoyancy model) and the other from the geometrical asymmetry of an organism (the drag-gravity model). We first introduced a simple theory that distinguishes between these models by measuring sedimentation of immobilized organisms in a medium of higher density than that of the organisms. Ni²⁺-immobilized cells of *Paramecium caudatum* oriented downwards while floating upwards in the Percoll-containing hyper-density medium but oriented upwards while sinking in the hypo-density control medium. This means that the orientation of *Paramecium* is mechanically biased by the torque generated mainly due to the anterior location of the reaction center of hydrodynamic stress relative to those of buoyancy and gravity; thus the torque results from the geometrical fore-aft asymmetry and is described by the drag-gravity model. The same mechanical property was demonstrated in gastrula larvae of the sea urchin by observing the orientation during sedimentation of the KCN-immobilized larvae in media of different density: like the paramecia, the gastrulae oriented upwards in hypo-density medium and downwards in hyper-density medium. Immobilized pluteus larvae, however, oriented upwards regardless of the density of the medium. This indicates that the orientation of the pluteus is biased by the torque generated mainly due to the posterior location of the reaction center of gravity relative to those of buoyancy and hydro-

dynamic stress; thus the torque results from the fore-aft asymmetry of the density distribution and is described by the gravity-buoyancy model. These observations indicate that, during development, sea urchin larvae change the mechanical mechanism for the gravitactic orientation. Evidence presented in the present paper demonstrates a definite relationship between the morphology and the gravitactic behavior of microorganisms.

Introduction

Many swimming microorganisms, including ciliate and flagellate protozoa and the planktonic larvae of some invertebrates, are negatively gravitactic; that is, they tend to swim preferentially upwards in water columns despite being heavier than water. This behavior requires the organism to orient upwards in relation to the gravity vector. Several mechanisms have been postulated for the gravitactic orientation of aquatic microorganisms (Chia *et al.*, 1983; Bean, 1984; Machemer and Bräucker, 1992). From a physical point of view and taking account of the mechanical properties of these microorganisms, it has been postulated that the interaction of gravitational and hydrodynamic forces may cause them to orient with fore end upward. In addition to the mechanical basis, gravitactic orientation might also be explained on the physiological basis of gravity perception. To modulate the propulsive activity, some mechanosensitive devices that sense gravity (for example, statocysts) might be needed. Although functional statocysts have been found in some unicellular organisms (Fenchel and Finlay, 1984, 1986), a line of evidence for gravity-dependent modulation of propulsion has been accumulated for *Paramecium* (Machemer *et al.*, 1991; Ooya *et al.*, 1992) and *Englena* (Machemer-Röhnisch *et al.*, 1999), which have no statocyst-like structure.

The present paper focuses on the mechanical properties of

Received 14 July 2000; accepted 30 March 2001.

* To whom correspondence should be addressed. E-mail: mogami@cc.ocha.ac.jp

† Died on 1 March 1999.

microorganisms, which, irrespective of propulsion, generate the torque to orient the organisms either upwards or downwards. This mechanical torque should bias the gravitactic orientation, even if the organisms have active physiological mechanisms of gravitaxis. According to Roberts (1970), two mechanical mechanisms have been considered as possible sources of the orientation torque. These are reconsidered, in the present paper, as two mechanical models, the gravity-buoyancy model and the drag-gravity model.

The gravity-buoyancy model was first postulated by Verworn (1889, cited in Machemer and Bräucker, 1992) for the negative gravitaxis of *Paramecium*. This model is based on the differential density within an organism. If the internal density of the organism is not homogeneous, the center of mass (the center of gravity) does not necessarily coincide with the centroid (the center of buoyancy). Posterior accumulation of the mass would result in the upward orientation of the organisms, and anterior accumulation would result in the downward orientation.

The drag-gravity model was postulated by Roberts (1970) on the basis of the low Reynolds number hydrodynamics of the swimming of microorganisms that have a geometrical fore-aft asymmetry. This model is characterized by a dumbbell with two spheres of unequal diameter but homogeneous density, which could mimic the fore-aft asymmetry of the microorganisms. According to Stokes' drag formula, the larger sphere of the dumbbell can sink faster than the smaller, at the rate of the square of the ratio of diameters. The applicability of this model has been confirmed by scale-model experiments (Roberts, 1970).

Organisms, in general, possess some asymmetry both in internal density and in external geometry. It is therefore possible that these two mechanical models operate independently to generate the gravity-induced orientation torque. Since the mechanical properties for gravitactic orientation are independent of propulsive thrust, we can assess the mechanical influence by measuring the orientation of immobilized organisms sinking under gravity. Both models predict that, when immobilized, an organism orients upwards when sinking in a medium with a density lower than its own.

In the present paper, we show that the above two models can be distinguished by observing what happens to an organism placed in a medium whose density is higher than its own. We show the results of the experiments on the gravitactic orientation of *Paramecium* and sea urchin larvae, both of which are known to perform typical negative gravitaxis (Mogami *et al.*, 1988; Ooya *et al.*, 1992).

Theory

The external forces acting on the body of an aquatic microorganism due to gravity acceleration are gravitational (F_G) and buoyant forces (F_B), each of which is generated as the product of the volume and density of the body or of the external fluid. The vector sum of the forces encounters the hydrodynamic

force (F_H). Since the Reynolds number of an aquatic microorganism in translational motion is significantly less than unity (of the order of 10^{-2}), F_H is generated in proportion to the velocity (Happel and Brenner, 1973; Vogel, 1994). F_G , F_B , and F_H act on the center of mass (G), the centroid (B), and the reaction center of hydrodynamic stress (H), respectively. For an immobilized microorganism sinking in the fluid, these three forces are balanced as

$$F_G + F_B + F_H = 0. \quad (1)$$

Each term in the equation (positive in upward direction) is described as

$$F_G = -V\rho_i g, \quad (2)$$

$$F_B = V\rho g, \text{ and} \quad (3)$$

$$F_H = -Ks, \quad (4)$$

where V and ρ_i are the total volume and the average density of the organism, ρ and g the density of the external fluid and the acceleration due to gravity, and K and s the coefficient of hydrodynamic drag and the sinking velocity.

We assume in the present paper that a microorganism has a body of rotating symmetry on its fore-aft axis. The simplest case of this approximation is that the body has fore-aft symmetry, such as a prolate spheroid. When a prolate spheroid with uniform density is sinking in the fluid, the three forces act on the same point and therefore do not generate any torque to rotate the body (Fig. 1a).

If, however, the body of a prolate spheroid has a region of higher density in the rear half of the body, as postulated in the gravity-buoyancy model, G is located posterior to B and H (Fig. 1b). This generates the torque (T_V ; subscript V is after Verworn) which is given by

$$T_V = F_G L_G \sin \theta, \quad (5)$$

where L_G is the distance between G and B (and/or H), and θ is the orientation angle of the fore-aft axis of the body to the vertical.

The fore-aft asymmetry of the external geometry, as postulated in the drag-gravity model, also separates the reaction centers of the forces. If a microorganism of homogeneous density has a larger radius of revolution around the fore-aft axis in the posterior part (Fig. 1c), H is located anterior to B and G , according to the analogy of a fore-aft asymmetrical dumbbell of homogeneous density (Happel and Brenner, 1973). The torque (T_R ; subscript R is after Roberts) by the anterior shift of the center of hydrodynamic force is given by

$$T_R = -F_H L_H \sin \theta = (F_G + F_B) L_H \sin \theta, \quad (6)$$

where L_H is the distance between H and G (and/or B).

Provided that the Reynolds number of rotational motion is sufficiently small, all torques should be proportional to

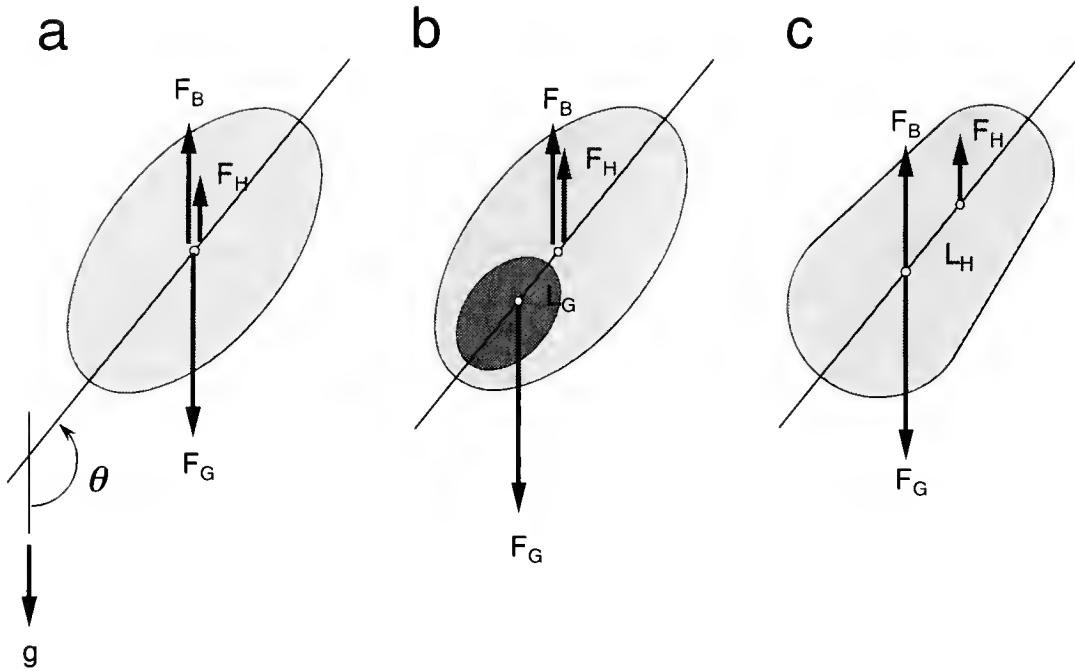


Figure 1. Schematic drawings illustrating the mechanical (physical) basis for the generation of gravity-dependent orientation torque. Gravity (F_G), buoyancy (F_B), and hydrodynamic force (F_H) are balanced in sinking microorganisms; these forces act at the center of mass (G), the centroid (B), and the reaction center of hydrodynamic stress (H), respectively. (a) Three forces act at the same point in the body of prolate spheroid with uniform density. (b) The center of mass is deviated to the rear end of the body of prolate spheroid, which generates the torque in proportion to F_G and the sine of the orientation angle to the gravity vector (θ). (c) The reaction center of hydrodynamic stress is deviated to the front end of the body with fore-aft asymmetry but with uniform density, which generates the torque in proportion to the vector sum of F_G and F_B and the sine of the orientation angle.

the first power of rotational velocity ($d\theta/dt$). In such cases equations of rotational motion are given by

$$-R\eta \frac{d\theta}{dt} = T_V \text{ or } T_R, \quad (7)$$

where R is the coefficient of resistance for rotational motion and η is the viscosity of the external fluid. From these equations the rotational velocity of each model is given as a common form of

$$\frac{d\theta}{dt} = \beta \sin \theta, \quad (8)$$

where the proportional factor is the instantaneous rate at $\theta = 90$ degrees, and given by

$$\beta = \beta_V = \frac{V\rho_i g L_G}{R\eta} \text{ and} \quad (9)$$

$$\beta = \beta_R = \frac{V(\rho_i - \rho) g L_H}{R\eta}, \quad (10)$$

for the gravity-buoyancy and drag-gravity models, respectively.

Equations 9 and 10 indicate that β_V is insensitive to

changes in the density of the external medium (ρ), whereas β_R reverses the sign as ρ exceeds the density of organisms (ρ_i). This means that the two models can be distinguished by increasing ρ greater than ρ_i . When immobilized organisms are immersed in the hyper-density medium ($\rho > \rho_i$), they would orient upwards during floating upwards if they obeyed the gravity-buoyancy model, whereas they would orient downwards if they obeyed the drag-gravity model.

The gravity-buoyancy and drag-gravity models are the two extremes of these conditions that can generate the orientation torque depending on the different physical mechanisms. Passive orientation of the organisms (Eq. 8), in fact, would be explained as a result of combining the two models, because none of three forces would necessarily have a common reaction center. In order to extract the origin of the mechanical bias of the orientation, Equation 8 should be examined by measuring β by the sedimentation experiment using media of different ρ . If β is constant independent of ρ , the gravity-buoyancy model is the only mechanism for generating the orientation torque. Otherwise, the drag-gravity model may play a part in the generation of the torque. A negative value of β in the hyper-density medium indicates

that the drag-gravity model is the major mechanism in passive gravitactic orientation.

Materials and Methods

Microorganisms and experimental solutions

Paramecium caudatum was grown at 24 °C in a hay infusion in Dryl's solution (2 mM sodium citrate, 1.2 mM Na₂HPO₄, 1.0 mM NaH₂PO₄, 1.5 mM CaCl₂, pH 7.2). Cells grown to the early stationary phase (14–20 d after incubation) were collected and adapted in the experimental solution (KCM: 1.0 mM KCl, 1.0 mM CaCl₂, 1.0 mM MOPS, pH 7.2). After the adaptation, cells gravitactically accumulating beneath the water surface were collected and immobilized in the KCM containing 5 mM NiCl₂. Hyper-density KCM (P-KCM) was prepared by substituting a colloidal solution of Percoll (Sigma) for water up to 60% (v/v) in KCM. At 24 °C, the specific gravity and relative viscosity of KCM were 1.00 and 1.02, respectively; those of P-KCM were 1.06 and 1.57. Specific gravity of the experimental solutions was determined by weighing the known volume, and viscosity was measured by means of an Ostwald viscometer.

Larvae of the sea urchin *Hemicentrotus pulcherrimus* were grown in the laboratory at 17 °C (Degawa *et al.*, 1986). Larvae at the mid- to late gastrula stage and the early pluteus stage (*ca.* 24 and 48 h after insemination, respectively) were collected by hand centrifuge and washed once with artificial seawater (ASW; 450 mM NaCl, 10 mM KCl, 10 mM CaCl₂, 25 mM MgCl₂, 28 mM MgSO₄, 10 mM Tris-HCl, pH 8.0). For immobilization, larvae were immersed in ASW containing 2 mM KCN. Hyper-density ASW (P-ASW) was prepared by substituting Percoll for water up to 22% (v/v) in ASW. At 25 °C, the specific gravity and relative viscosity of ASW were 1.01 and 1.07, respectively; those of P-ASW were 1.04 and 1.14.

Recordings and analyses of gravity-dependent orientation

Ni²⁺-immobilized *Paramecium* cells and KCN-immobilized sea urchin larvae were transferred, with experimental solutions to be tested, into a chamber made of a slide and coverslip and silicone rubber spacer (inner dimension 12 × 24 × 1 mm for *Paramecium* and 16 × 16 × 1 mm for sea urchin larvae) and kept air bubble-free without any particular sealant. The chamber was set on a horizontal microscope equipped with a rotating stage. After trapping immobilized specimens at the bottom or the top of the chamber (depending on the density of the medium), the chamber was rotated upside down, and the orientation motion during vertical movement due to gravity was recorded with a video camera (XC-77, Sony, Tokyo) and a videotape recorder. To avoid the hydrodynamic interactions between nearby moving objects, we chose organisms moving down (or up) far from neighbors (>1 mm, about 5 body lengths, apart). For

measuring the orientation angle, we selected recordings in which the orientation motion was observed in a single focal plane.

The orientation angle as a function of time (θ , t) was measured directly on the video monitor. The rotational velocity as a function of orientation angle ($d\theta/dt$, θ) was obtained as an average velocity $((\theta_{i+1} - \theta_i)/\Delta t)$ at the angle of geometrical average $((\theta_i + \theta_{i+1})/2)$ between every successive datum of inclination angle *versus* time. β in Equation 8 was obtained by nonlinear least-squares regression of the velocity data ($d\theta/dt$, θ) to the equation

$$\frac{d\theta}{dt} = \beta \sin(\theta + \alpha), \quad (11)$$

where α is a factor to adjust the angle between the morphologically defined fore-aft axis and the mechanically defined axis.

Results

The drag-gravity model is the major mechanism of Paramecium

When *Paramecium* was immobilized by Ni²⁺, it maintained an anterior-thinner cell shape. This shape was preserved in P-KCM as well as in KCM: cells showed no significant changes in axial length ($162 \pm 17 \mu\text{m}$ [$n = 30$] and $163 \pm 16 \mu\text{m}$ [$n = 21$], $P = 0.64$, for cells in KCM and P-KCM, respectively) or in maximum width ($47.2 \pm 6.9 \mu\text{m}$ and $46.5 \pm 4.7 \mu\text{m}$, $P = 0.69$). Thus it is highly likely that rotational motion of the immobilized cell occurs with the same coefficient of resistance in both media.

Typical recordings of gravity-dependent orientation of immobilized paramecia in the hypo- and hyper-density media are shown in Figure 2a and b. In KCM ($\rho < \rho_i$), paramecia oriented upwards during sinking due to gravity, whereas in P-KCM ($\rho > \rho_i$) they oriented downwards during floating up. As shown in Figure 2c, plots of orientation rates ($d\theta/dt$) against orientation angle (θ) fit well to the sinusoidal function of Equation 11. Values for β obtained by least-square regression were positive in the control hypo-density medium and negative in the hyper-density medium (Table 1). Negative values of β in the hyper-density medium indicate that the drag-gravity model is the major mechanism of mechanical gravitactic orientation in *Paramecium*.

Sea urchin larvae change the mechanical mechanism of gravitactic orientation during development

When sea urchin larvae were treated with KCN, their cilia ceased beating and stood nearly perpendicular to the larval surface. The outer morphology of the larvae was observed to be well preserved in P-ASW as well as in ASW: for gastrulae, axial length was $151 \pm 7.6 \mu\text{m}$ ($n = 16$) and $145 \pm 6.1 \mu\text{m}$ ($n = 13$), $P = 0.19$, in ASW and P-ASW,

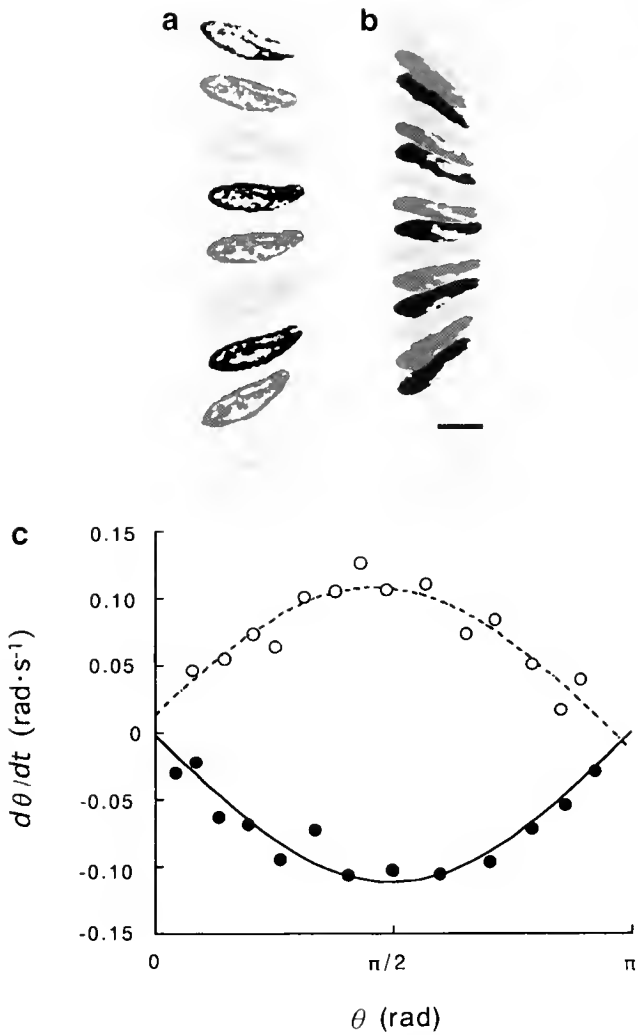


Figure 2. Typical examples of gravity-dependent orientation of Ni^{2+} -immobilized *Paramecium caudatum*. (a, b) Sequential images of gravity-dependent orientation of a cell in KCM (a) and of another in P-KCM (b), in which recorded images are superimposed at 1-s intervals and the time sequence of the motion is illustrated by cyclic change in tone (dark \rightarrow medium \rightarrow light). In each figure the anterior end of the cell is located to the right, and the gravity vector is towards the bottom of the figure. Scale bar, 0.1 mm. (c) Orientation rates ($d\theta/dt$) as a function of the inclination angle (θ). Data from the cells shown in a (KCM) and b (P-KCM) are plotted with open and closed circles, respectively. Sinusoidal curves were obtained by the least-squares fitting to Equation 11.

respectively, and the maximum width was $135 \pm 3.7 \mu\text{m}$ and $132 \pm 5.7 \mu\text{m}$, $P = 0.06$; for plutei, axial length was $235 \pm 19 \mu\text{m}$ ($n = 26$) and $240 \pm 13 \mu\text{m}$ ($n = 18$), $P = 0.29$, in ASW and P-ASW, respectively, and the maximum width was $175 \pm 13 \mu\text{m}$ and $175 \pm 12 \mu\text{m}$, $P = 0.98$. This may justify the common basis for drag coefficients in rotation in the different density media, as in *Paramecium*.

The gravity-dependent orientation of immobilized larvae is shown in Figure 3a to d, which demonstrates the clear difference between gastrula and pluteus. In ASW ($\rho < \rho_l$), both gastrula and pluteus oriented upwards while sinking; in

hyper-density P-ASW, however, gastrula oriented downwards but pluteus upwards while floating up. As shown in Figure 3e and f, the orientation rate appears to be a sinusoidal function of the orientation angle; although data from larvae fitted less closely to Equation 11 than did those from *Paramecium*, this was probably due to the uncertainty in measuring the orientation angle of the larvae. We sometimes observed that larvae rotated slowly around the fore-aft axis during sedimentation. This slow axial rotation made it difficult to determine the fore-aft axis of the larvae.

As shown in Table 1, values of β obtained from gastrula larvae were positive in the control medium and negative in the hyper-density medium. Thus, in gastrulae as in *Paramecium*, the drag-gravity model is the major mechanism of passive gravitactic orientation. However, pluteus larvae have positive values of β both in the control and in the hyper-density medium (Table 1). The relatively weak dependency of β of plutei on the density of the external medium indicates that the gravity-buoyancy model is the major mechanism of passive gravitactic orientation in these larvae. These results indicate that sea urchin larvae change the mechanical mechanism of gravitactic orientation during development.

Discussion

Estimation of the contribution of the mechanical models in the gravitactic orientation

The Reynolds number of rotational motion (Re_r) of the microorganisms is defined as

$$\text{Re}_r = \frac{l^2 \omega \rho}{\eta}, \quad (12)$$

where l is a characteristic body length and ω is the angular velocity of rotation (Happel and Brenner, 1973). From the maximum velocity of rotation (*ca.* $0.2 \text{ rad} \cdot \text{s}^{-1}$, Table 1), Re_r of *Paramecium* or sea urchin larvae is calculated to be about 2×10^{-3} , which is sufficiently smaller than unity. This means that the linear assumption of Equation 7 (see the *Theory* section) is valid to formulate the rotational motion of these microorganisms.

The orientation torque generated as a result of the combination of the torque originating from different mechanical sources causes the passive orientation of the immobilized organisms. It is difficult to formulate the combination, because we know little about the density distribution within an organism and its geometrical asymmetry. The simplest assumption for the combination of the rotational torque is that G , B , and H are located on the geometrical fore-aft axis of the organisms. This gives a sinusoidal function as a linear summation of the sinusoidal equations, each of which is deduced from the gravity-buoyancy and drag-gravity model, respectively. As a result, the orientation rate is given as

Table 1

Orientation rate (β), in $\text{rad} \cdot \text{s}^{-1}$, measured in different density media

Organism	Normal medium			Percoll-containing medium		
	Mean \pm SD	Range	<i>n</i>	Mean \pm SD	Range	<i>n</i>
<i>Paramecium</i>	0.090 \pm 0.033	0.043 – 0.183	23	-0.104 \pm 0.058	-0.257 – -0.041	14
Sea urchin larvae						
Gastrula	0.140 \pm 0.032	0.107 – 0.197	8	-0.120 \pm 0.020	-0.150 – -0.090	7
Pluteus	0.157 \pm 0.031	0.105 – 0.190	9	0.110 \pm 0.013	0.097 – 0.137	7

$$\frac{d\theta}{dt} = (\beta_V + \beta_R) \sin \theta. \quad (13)$$

This simple linear assumption seems to be supported by the fact that α in Equation 11 was calculated on average as nearly zero ($0.00 \pm 0.26 \text{ rad}$ ($n = 37$) for *Paramecium*, 0.03 ± 0.18 ($n = 15$) for gastrula, and 0.06 ± 0.21 ($n = 16$) for pluteus). Therefore, it is likely that the morphologically defined fore-aft axis almost coincides with the mechanically defined axis. According to the assumption above, β_S obtained in the different density media are given by

$$\beta_N = \frac{V\rho_i g L_G}{R\eta_N} + \frac{V(\rho_i - \rho_N) g L_H}{R\eta_N} \text{ and} \quad (14)$$

$$\beta_P = \frac{V\rho_i g L_G}{R\eta_P} + \frac{V(\rho_i - \rho_P) g L_H}{R\eta_P}, \quad (15)$$

where β_N is the maximum orientation velocity measured in the normal density (ρ_N) medium (KCM or ASW) of the viscosity of η_N , and β_P is that measured in the hyper-density (ρ_P) medium (P-KCM or P-ASW) of the viscosity of η_P . Equations 14 and 15 give L_H , the distance from B to H, as

$$L_H = \frac{\eta_N \beta_N - \eta_P \beta_P}{\rho_P - \rho_N} \cdot \frac{R}{Vg}, \quad (16)$$

and, thus, β_R and β_V are given by:

$$\beta_R = \frac{\rho_i - \rho_N}{\rho_P - \rho_N} \left(\beta_N - \frac{\eta_P}{\eta_N} \beta_P \right) \text{ and} \quad (17)$$

$$\beta_V = \beta_N - \beta_R. \quad (18)$$

For *Paramecium*, $\rho_N = 1.00$, $\rho_P = 1.06$ and $\rho_i = 1.03 \text{ g} \cdot \text{cm}^{-3}$ (Ooya *et al.*, 1992), and $\eta_P/\eta_N = 1.53$. For sea urchin larvae, $\rho_N = 1.01$, $\rho_P = 1.04$, and $\rho_i = 1.03$ and $1.03 \text{ g} \cdot \text{cm}^{-3}$, for gastrula and pluteus, respectively (values were obtained by sedimentation equilibrium experiments; data not shown), and $\eta_P/\eta_N = 1.07$. Using these values and β_N and β_P in Table 1, Equations 17 and 18 can be used to obtain values for the contribution of the two mechanisms to negative gravitaxis in normal-density medium. The upward orientation of *Paramecium* in KCM, corresponding to $\beta_N = 0.09 \text{ rad} \cdot \text{s}^{-1}$, is the result of an upward drag-gravity

component ($\beta_R = 0.12 \text{ rad} \cdot \text{s}^{-1}$) combined with a smaller downward gravity-buoyancy component ($\beta_V = -0.03 \text{ rad} \cdot \text{s}^{-1}$). The situation is similar for sea urchin gastrulae. The upward orientation with $\beta_N = 0.14 \text{ rad} \cdot \text{s}^{-1}$ results from an upward drag-gravity component ($\beta_R = 0.18 \text{ rad} \cdot \text{s}^{-1}$) combined with a small downward gravity-buoyancy component ($\beta_V = -0.04 \text{ rad} \cdot \text{s}^{-1}$). However, the upward orientation of pluteus larvae with $\beta_N = 0.16 \text{ rad} \cdot \text{s}^{-1}$ reflects a very different situation. The gravity-buoyancy component has reversed direction from downward to upward, and has increased to $\beta_V = 0.13 \text{ rad} \cdot \text{s}^{-1}$. The upward drag-gravity component has diminished greatly, to $\beta_R = 0.03 \text{ rad} \cdot \text{s}^{-1}$, so that it now makes only a small contribution to the upward orientation.

The mechanical property of *Paramecium*

There have been several investigations on the mechanical basis of the passive upward orientation of *Paramecium*. Most of them favored the gravity-buoyancy model as a major mechanism of gravitactic orientation. Fukui and Asai (1980) reported that Triton-treated immobilized cells oriented mostly upwards at the sedimentation equilibrium in sucrose density gradient. This upward orientation was evident in well-fed cells but not in starved cells. The upward-orienting posture was found under centrifugal forces in Ni^{2+} -immobilized cells in the isodensity medium (Taneda *et al.*, 1987) and also in the cells swimming at isopycnic level in the density gradient with Ficoll or Percoll (Kuroda and Kamiya, 1989). It was also reported that upward orientation was induced by centrifugal force effectively in the cells at the early culture phase but not in those at the late phase, which showed little or no gravitaxis. These results appear to conform with the conclusion that the upward orientation of *Paramecium* is strongly biased by the torque resulting from the higher density of the posterior part of the organism; the increased density is mainly due to the accumulation of food vacuoles (Fukui and Asai, 1985).

It should be noted, however, that the results of the sedimentation equilibrium experiments were ascribed only to the function of the gravity-buoyancy model and not to the contribution of the drag-gravity model, since $F_H = 0$ with buoyancy artificially balanced with gravity. Furthermore, it

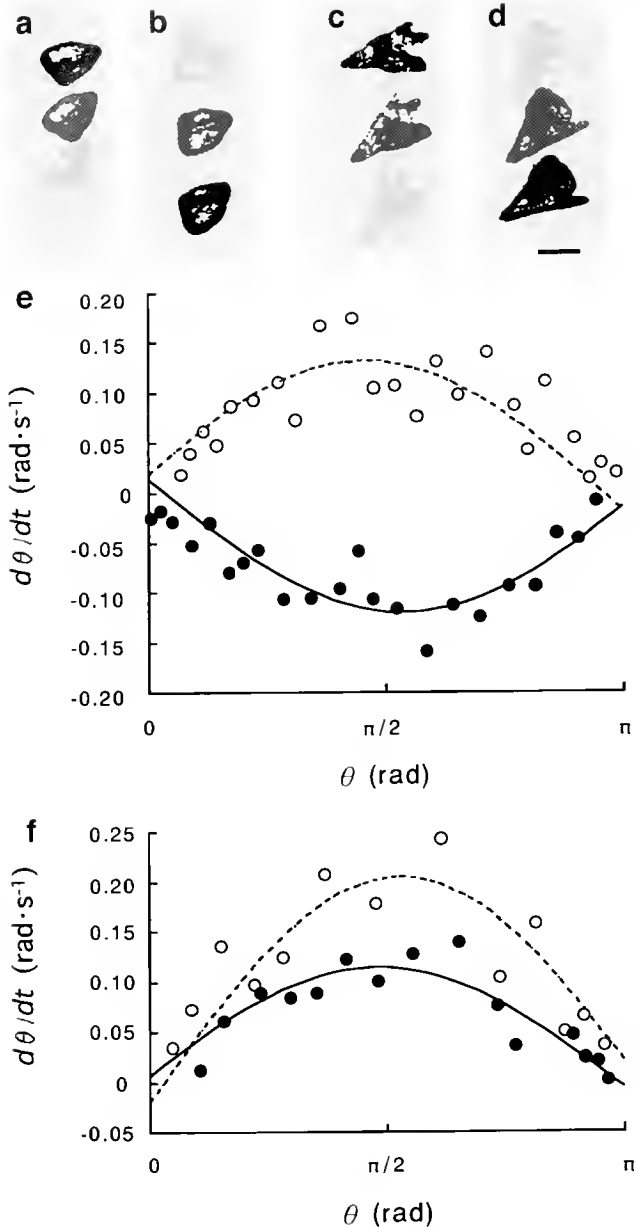


Figure 3. Typical examples of gravity-dependent orientation of KCN-immobilized sea urchin (*Hemicentrotus pulcherrimus*) larvae. (a–d) Sequential images of gravity-dependent orientation of the single different larvae at the gastrula (a and b) and the pluteus (c and d) stages. Movements of a larva in ASW (a and c) and of another in P-ASW (b and d) are shown at 3-s intervals in the same way as in Fig. 2a and b. In each figure the animal pole of the larva (leading end in forward swimming) is located to the right, and the gravity vector is towards the bottom of the figure. Scale bar, 0.1 mm (e, f) orientation rates ($d\theta/dt$) as a function of the inclination angle (θ), measured from gastrula (e) and pluteus (f). In e, data from the gastrulae shown in a (ASW) and b (P-ASW) are plotted with open and closed circles, respectively. In f, data from the pluteus shown in c (ASW) and d (P-ASW) are plotted with open and closed circles, respectively. Sinusoidal curves were obtained by the least-squares fitting to Equation 11.

seems likely that the gravity-buoyancy component of the orientation torque might be enhanced in these experiments. Since the center of gravity would shift in relation to the

content and the distribution of organelles such as food vacuoles, it is probable that in the sedimentation equilibrium experiments, the intracellular distribution of the organelle was reorganized by gravity during long-lasting sedimentation of Triton-permeabilized cells through the sucrose density gradient (Fukui and Asai, 1980), or by a large centrifugal acceleration ($100 \times g$, Taneda *et al.*, 1987; $300\text{--}400 \times g$, Kuroda and Kamiya, 1989). This may result in accumulation of organelles in the rear part of the cell, and may cause upward orientation, even if the cells originally have a slightly top-heavy organelle distribution that gives a negative β_V , as estimated above. These facts suggest that the results of previous experiments are still equivocal for the contribution of the drag-gravity model in the gravitactic orientation of *Paramecium*.

The evidence presented in the *Results*, on the contrary, indicate that the drag-gravity model makes a major contribution to generating a torque for the gravitactic orientation. Although the possibility of a minimal contribution cannot be ruled out, it is clear that the gravity-buoyancy model cannot solely explain the alteration of the sign of the rotational torque in the hyper-density medium. In addition, paramecia were observed in P-KCM to swim mostly downwards (data not shown). Swimming cells changed the net direction of their helical swimming trajectory gradually downwards and accumulated at the bottom of the chamber against the strong floating bias. Positive gravitaxis of *Paramecium* in the hyper-density medium can be explained by the drag-gravity model, not by the gravity-buoyancy model.

Developmental changes in the mechanical property in sea urchin larvae

In the present paper we demonstrated a change in the mechanical basis for gravitactic orientation during the development of sea urchin larvae: from the drag-gravity model in gastrulae to the gravity-buoyancy model in plutei. Gastrulae have a thicker posterior part, similar to that of *Paramecium*, which is required for the drag-gravity model to function. Plutei, on the other hand, have a thicker anterior part. Therefore they may orient the rear end upwards if the rotational torque is generated according to the drag-gravity model. This was not the case for plutei. Regardless of the remarkable fore-aft asymmetry in morphology, plutei obeyed the gravity-buoyancy model. Gravitactic orientation by different mechanisms was also revealed in the gravitactic swimming behavior of the larvae in P-ASW. In spite of the strong floating bias, gastrulae swam preferentially downwards (positive gravitaxis) and accumulated at the bottom of the chamber, whereas plutei swam upwards (negative gravitaxis) and accumulated at the top of the chamber (data not shown).

Mogami *et al.* (1988) found that sea urchin larvae change their gravitactic behavior during development. Larvae at the blastula stage to the early gastrula stage swim preferentially

upwards. This may be explained by a major upward drag-gravity component of orientation torque. The negative gravitactic behavior becomes less remarkable in prism larvae: they tend to swim in random directions independent of the gravity vector. This transient disappearance of gravitaxis may correspond to the alteration of the orientation mechanism revealed in the present paper. At the pluteus stage, larvae again show negative gravitaxis as they acquire the orientation mechanism with a major upward gravity-buoyancy component. A strong separation between the centers of gravity and buoyancy may develop in association with the growth of skeletal structures. Rudiments of spicules initiated in the early gastrula fully extend to give rise to the specific shape of the pluteus larva. The spicule is made of magnesian calcite with a density about three times higher than the average density (Okazaki and Inoué, 1976). As spicules grow, they may change the density distribution to shift the center of gravity toward the rear of the cell. If plutei hereafter maintained the rear-end-heavy mass distribution, they could maintain negative gravitactic behavior irrespective of pronounced morphological changes during the late larval stages.

Although the functional role of the drag-gravity model has been accepted in theory, it was not experimentally demonstrated in the orientation movement of organisms. In the present paper we present the first evidence that external geometry is actually important to the gravitactic behavior of aquatic microorganisms. The morphology-dependent interaction of the organisms with the external fluid seems to be more complicated than hypothesized in the *Theory* section of this paper. The slow axial rotation observed in sedimenting sea urchin larvae indicates a hydrodynamic coupling between translational and rotational motion (Happel and Brenner, 1973). Therefore, it is probable that the hydrodynamic coupling secondarily functions to drift the swimming direction upwards, as argued in previous researches (Winet and Jahn, 1974; Nowakowska and Grebecki, 1977).

In conclusion, the present study on the mechanical properties of gravitactic orientation in the gravity field demonstrates a relation between the morphology of microorganisms and their gravitactic behavior. This relationship might be instructive in researching cases of microbial gravitaxis whose mechanism is still disputed.

Acknowledgments

This study was carried out as a part of "Ground Research Announcement for Space Utilization" promoted by Japan Space Forum.

Literature Cited

- Bean, B.** 1984. Microbial geotaxis. Pp. 163–198 in *Membrane and Sensory Transduction*, G. Colombetti and F. Lenzi, eds. Plenum Press, New York.
- Chia, F.-S., J. Buckland-Nicks, and C. M. Young.** 1983. Locomotion of marine invertebrate larvae: a review. *Can. J. Zool.* **62**: 1205–1222.
- Degawa, M., Y. Mogami, and S. A. Baba.** 1986. Developmental changes in Ca^{2+} sensitivity of sea-urchin embryo cilia. *Comp. Biochem. Physiol.* **82A**: 83–90.
- Fenchel, T., and B. Finlay.** 1984. Geotaxis in the ciliated protozoan *Loxodes*. *J. Exp. Biol.* **110**: 17–33.
- Fenchel, T., and B. Finlay.** 1986. The structure and function of Muller vesicles in loxodid ciliates. *J. Protozool.* **33**: 68–76.
- Fukui, K., and H. Asai.** 1980. The most probable mechanism of the negative geotaxis of *Paramecium caudatum*. *Proc. Jpn. Acad.* **56(B)**: 172–177.
- Fukui, K., and H. Asai.** 1985. Negative geotactic behavior of *Paramecium caudatum* is completely described by the mechanism of buoyancy-oriented upward swimming. *Biophys. J.* **47**: 479–482.
- Happel, J., and H. Brenner.** 1973. *Low Reynolds Number Hydrodynamics*. Noordhoff International Publishing, Leyden.
- Kuroda, K., and N. Kamiya.** 1989. Propulsive force of *Paramecium* as revealed by the video centrifuge microscope. *Exp. Cell Res.* **184**: 268–272.
- Machemer, H., and R. Bräucker.** 1992. Gravireception and gravireponses in ciliates. *Acta Protozool.* **31**: 185–214.
- Machemer, H., S. Machemer-Röhnisch, R. Bräucker, and K. Takahashi.** 1991. Gravitaxis in *Paramecium*: theory and isolation of a physiological response to the natural gravity vector. *J. Comp. Physiol. A* **168**: 1–12.
- Machemer-Röhnisch, S., U. Nagel, and H. Machemer.** 1999. A gravity-induced regulation of swimming speed in *Euglena gracilis*. *J. Comp. Physiol.* **185**: 517–522.
- Mogami, Y., C. Oohayashi, T. Yamaguchi, Y. Ogiso, and S. A. Baba.** 1988. Negative geotaxis in sea urchin larvae: a possible role of mechanoreception in the late stages of development. *J. Exp. Biol.* **137**: 141–156.
- Nowakowska, G., and A. Grebecki.** 1977. On the mechanism of orientation of *Paramecium caudatum* in the gravity field. II. Contributions to a hydrodynamic model of geotaxis. *Acta Protozool.* **16**: 359–370.
- Okazaki, K., and S. Inoué.** 1976. Crystal property of the larval sea urchin spicule. *Dev. Growth Differ.* **18**: 413–434.
- Ooya, M., Y. Mogami, A. Izumi-Kurofani, and S. A. Baba.** 1992. Gravity-induced changes in propulsion of *Paramecium caudatum*: a possible role of gravireception in protozoan behaviour. *J. Exp. Biol.* **163**: 153–167.
- Roberts, A. M.** 1970. Geotaxis in motile micro-organisms. *J. Exp. Biol.* **53**: 687–699.
- Taneda, K., S. Miyata, and A. Shiota.** 1987. Geotactic behavior in *Paramecium caudatum* II. Geotaxis assay in a population of the specimens. *Zool. Sci.* **4**: 789–795.
- Verworn, M.** 1889. *Psychophysiologische Protistenstudien*. Gustav Fischer, Jena. (Cited by Machemer and Bräucker, 1992.)
- Vogel, S.** 1994. *Life in Moving Fluids; The Physical Biology of Flow*, 2nd ed. Princeton University Press, Princeton, NJ.
- Winet, H., and T. L. Jahn.** 1974. Geotaxis in protozoa. I. A propulsion gravity model for *Tetrahymena* (Ciliata). *J. Theor. Biol.* **46**: 449–465.

Synthesis of Several Light-Harvesting Complex I Polypeptides Is Blocked by Cycloheximide in Symbiotic Chloroplasts in the Sea Slug, *Elysia chlorotica* (Gould): A Case for Horizontal Gene Transfer Between Alga and Animal?

JEFFREY J. HANTEN^{1,2} AND SIDNEY K. PIERCE^{2,*}

¹ *Department of Biology, University of Maryland, College Park, Maryland 20742; and*

² *Department of Biology, University of South Florida, Tampa, Florida 33620*

Abstract. The chloroplast symbiosis between the ascoglossan (=Sacoglossa) sea slug *Elysia chlorotica* and plastids from the chromophytic alga *Vaucheria litorea* is the longest-lived relationship of its kind known, lasting up to 9 months. During this time, the plastids continue to photosynthesize in the absence of the algal nucleus at rates sufficient to meet the nutritional needs of the slugs. We have previously demonstrated that the synthesis of photosynthetic proteins occurs while the plastids reside within the diverticular cells of the slug. Here, we have identified several of these synthesized proteins as belonging to the nuclear-encoded family of polypeptides known as light-harvesting complex I (LHCI). The synthesis of LHCI is blocked by the cytosolic ribosomal inhibitor cycloheximide and proceeds in the presence of chloramphenicol, a plastid ribosome inhibitor, indicating that the gene encoding LHCI resides in the nuclear DNA of the slug. These results suggest that a horizontal transfer of the LHCI gene from the alga to the slug has taken place.

Introduction

Most alga-animal symbioses are extracellular associations between two genetically distinct organisms. The alga is usually located extracellularly or enclosed within vacu-

oles inside the animal's cells. Rarer, but not uncommon, are intracellular symbioses occurring with intact algal chloroplasts that are captured by specialized cells within the animal. In particular, several species of ascoglossan (=Sacoglossa) (Opisthobranchia) sea slugs capture intact, functional plastids from their algal food source and retain them within specialized cells lining the mollusc's digestive diverticula. This phenomenon has been termed chloroplast symbiosis (Taylor, 1970) or kleptoplasty (Clark *et al.*, 1990). The sequestered plastids continue to photosynthesize for periods ranging from a few days to a few months, depending on the species (Greene, 1970; Hinde and Smith, 1974; Graves *et al.*, 1979; Clark *et al.*, 1990).

The longest such association, lasting as long as 9 months, is found in *Elysia chlorotica* (Gould), which obtains symbiotic plastids from the chromophytic alga *Vaucheria litorea* (C. Agardh) (West, 1979; Pierce *et al.*, 1996). The association begins at metamorphosis of the slug from planktonic veliger to juvenile. In laboratory cultures, filaments of *V. litorea* must be present for metamorphosis to take place (West *et al.*, 1984). Veligers home in, attach to the filaments, and metamorphose into juvenile slugs over the next 24 h. The juveniles eat the algal filaments and sequester the chloroplasts within one of at least two morphologically distinct types of epithelial cells lining the walls of the digestive diverticula (West *et al.*, 1984). Once the plastids are sequestered, the slugs can sustain photosynthesis at rates sufficient to satisfy the nutritional needs for the complete life cycle of the slug, when provided with direct light and carbon dioxide (Mujer *et al.*, 1996; Pierce *et al.*, 1996).

Received 22 September 2000; accepted 19 April 2001.

* To whom correspondence should be addressed. E-mail: pierce@chumal.cas.usf.edu

Abbreviations: CAP, chloramphenicol; CHX, cycloheximide; FCPC, fucoxanthin chlorophyll *a/c* binding proteins; LHC, light-harvesting complex; PSI, photosystem I.

Even in nature the slugs obtain most of their energy from photosynthesis (West, 1979).

The longevity of this relationship in *E. chlorotica* makes it especially interesting. Photosynthesis requires the continuous synthesis of a variety of chloroplast proteins because many of them, including those used in light harvesting, are rapidly degraded and must be replaced (Greenberg *et al.*, 1989; Mattoo *et al.*, 1989; Barber and Andersson, 1992; Wollman *et al.*, 1999). Furthermore, photosynthesis requires the interaction of as many as 1000 proteins, only about 13% of which are coded in the plastid genome (Martin and Herrmann, 1998). In the plant cell, substantial nuclear input is required to sustain photosynthetic function, in the form of direct coding of the proteins as well as providing the means for their intracellular transport and regulation (Berry-Lowe and Schmidt, 1991; Wollman *et al.*, 1999). Considering the level of nuclear and extra-plastid input required, it is not surprising that the longevity of the plastids in most kleptoplastic slugs is relatively short. However, several photosynthetic proteins are synthesized in the sequestered plastids of *E. chlorotica* (Pierce *et al.*, 1996), including the large subunit of RuBisCO, D1, D2, CP43, *cyt f* and others (Pierce *et al.*, 1996; Mujer *et al.*, 1996; Green *et al.*, 2000). Although all of the synthesized plastid proteins identified to date are plastid encoded (Mujer *et al.*, 1996; Pierce *et al.*, 1996; Green *et al.*, 2000), two groups of synthesized plastid proteins can be distinguished pharmacologically: those inhibited by cycloheximide (CHX), an 80S cytosolic ribosome inhibitor (Obrig *et al.*, 1971), and those inhibited by chloramphenicol (CAP), which inhibits protein synthesis on 70S plastid and mitochondrial ribosomes (Lamb *et al.*, 1968; Stone and Wilke, 1975).

Because the inhibition by CHX suggests that the genes for several plastid proteins must reside in the nuclear DNA, we have done some experiments to identify these proteins and test that possibility. Our present study reports the identification of several of the CHX-blocked proteins as members of the light-harvesting complex I (LHCI), a family of pigment-binding proteins responsible for collecting radiation energy from sunlight and transferring it to photosystem I (PSI). LHCI proteins are encoded by the *Lhca* genes in the nuclear genome of all the plants and algae whose genomes have been examined (Jansson, 1994, 1999; Green and Durnford, 1996; Durnford *et al.*, 1999; Wollman *et al.*, 1999). This result suggests that the LHCI genes have been somehow transferred from the algal nucleus to the slug's DNA.

Materials and Methods

Animals and alga

Specimens of *Elysia chlorotica* were collected in both the spring and fall from an intertidal marsh near Menemsha Pond on the island of Martha's Vineyard, Massachusetts. The slugs were maintained in 10-gallon aquaria at 10 °C in

aerated, artificial seawater (ASW; Instant Ocean, 925-1000 mosm) on a 16/8-h light/dark cycle (GE cool-white fluorescent tubes, 15 W).

Sterile cultures of *Vaucheria litorea* were maintained in enriched ASW (400 mosm) [modified from the F/2 medium (Bidwell and Spotte, 1985)]. The alga was grown at 20 °C on a 16/8-h light/dark cycle (GE cool-white fluorescent tubes; 40 W), and the medium was changed weekly.

Inhibitor treatments and plastid protein labeling

All reagents used were molecular bio-grade (DNase-, RNase-, and protease-free) purchased from Sigma unless otherwise noted. Effective concentrations of CHX and CAP were determined empirically with initial dose-response curves (Pierce *et al.*, 1996). CHX (2 mg ml⁻¹) was used to inhibit protein synthesis on 80S cytosolic ribosomes; CAP (160 µg ml⁻¹; stock concentration 50 mg ml⁻¹ in absolute ethanol) was used to inhibit translation on 70S plastid and mitochondrial ribosomes. Two to four slugs, total wet weight about 1.25 g, were placed into glass scintillation vials containing ASW (1000 mosm) and the appropriate inhibitor, and incubated under intense light (150 W, GE Cool Beam incandescent indoor flood lamp) at 20 °C in a gently agitating water bath. After 1 h, 20 µCi ml⁻¹ [³⁵S]-methionine (0.7 MBq ml⁻¹, trans-[³⁵S]-methionine, ICN) was added, and the slugs were incubated for an additional 6 h, previously demonstrated to provide ample time to incorporate radioactive label into the plastid proteins (Pierce *et al.*, 1996). Additional slugs were incubated in 0.025% ethanol/ASW (v/v) solution plus [³⁵S]-methionine to serve as a control for the carrier in CAP treatments.

Chloroplast isolation and protein separation

Chloroplasts were isolated from slugs by using a centrifugation protocol. The slugs were homogenized in the presence of the mucolytic agent N-acetyl-cysteine (500 mM), and the homogenate was filtered successively through cheesecloth, Miracloth (Calbiochem), and then nylon mesh (60 µm to 10 µm) to remove large debris and the copious amount of mucus the animals produce. The plastids were purified on a pre-formed, 25% Percoll (v/v) gradient, which provides a very pure fraction containing large numbers of intact plastids (Pierce *et al.*, 1996). In this experiment, the lowest green band containing labeled plastids was isolated from the gradient by using a flamed Pasteur pipette, and residual Percoll was removed by centrifugation. The purified chloroplast pellets were resuspended, lysed by freeze-thawing, and stored at -20°C until use. The incorporation of radioactive label was determined by a liquid scintillation counter (Beckman LS6000IC), and the protein content was determined using the modified Lowry assay (Peterson, 1977). The resulting specific activity was calculated as counts per minute (cpm) (µg protein)⁻¹. Chlorophyll con-

tent was determined by extracting the pigment in 80% acetone, then measuring the extract absorbance spectrophotometrically at 652 nm. The results were calculated as micrograms per microliter according to standard equations (Joyard *et al.*, 1987).

Sodium dodecyl sulfate–polyacrylamide gel electrophoresis (SDS-PAGE) autoradiography was used to assess the effects of CHX and CAP on the pattern of protein synthesis. The plastid lysates obtained from the above procedure were boiled for 2 min in Tris-HCl (pH 6.8)–10% SDS (w/v) buffer containing 5% β -mercaptoethanol (β -ME) (v/v). The solubilized proteins were loaded in equal amounts onto 15% SDS-polyacrylamide gels and separated by electrophoresis (Laemlli, 1970). The gels were stained with Coomassie brilliant blue, dried, and exposed to film (Kodak Biomax MR) for 2 to 30 days at -80°C , depending on the level of radioactive label present. Approximate molecular masses of the proteins were determined by comparison to the migration distances of known molecular weight standards (BioRad, broad-range kaleidoscope) run in adjacent lanes on each gel.

Immunoblot identification of plastid proteins

After the plastid isolation and protein separation *via* SDS-PAGE as described above, the proteins were electrophoretically transferred (30 V, 4 $^{\circ}\text{C}$, overnight) to PVDF membranes (Immobilon-P; Millipore) (Towbin *et al.*, 1979). As additional controls, *V. litorea* chloroplasts [isolated and purified using a 30% to 75% Percoll step gradient as previously described (Pierce *et al.*, 1996)] and thylakoids from the red alga *Porphyridium cruentum* (generously donated by Professor Elisabeth Gantt, University of Maryland), were lysed, and the proteins were separated electrophoretically and transferred to membranes as above. The membranes were blocked with 5% (w/v) dehydrated milk dissolved in Tris-buffered saline (TBS) (Tris-base 50 mM, NaCl 0.9%, pH 7.5) for 1 h at room temperature, washed twice in TBS for 10 min, and treated with primary antibody for 1 h. In this case, the primary antibody was a polyclonal antibody to LHCl which was produced in a rabbit using a 22-kDa, recombinant LHCl polypeptide produced from a clone of the *LhcaRI* gene of *P. cruentum* (Grabowski *et al.*, 2000) (also provided by Professor Gantt) [*"RI"* indicating it is a rhodophyte gene (Tan *et al.*, 1997a)] as the antigen combined with Freund's adjuvant in a standard immunization procedure. After binding of the primary antibody, the membranes were washed twice as above and incubated with secondary antibody, anti-rabbit conjugated hydrogen peroxidase, for 1 h. After washing, the bands were visualized with a 4-chloro-1-naphthol and hydrogen peroxide reaction according to manufacturer's instructions. The immunolabeled western blots were exposed to film as described above to

identify the coincidence of antibody binding and radioactive incorporation in the presence of each inhibitor.

As a control to confirm that the CAP was blocking plastid-directed protein synthesis and that CHX was not, parallel measurements were run to monitor cytochrome *f* (cyt *f*) synthesis. Earlier experiments conducted on *E. chlorotica* have demonstrated that cyt *f* is synthesized in the slugs and is encoded in the plastid DNA (Green *et al.*, 2000). Thus, if CHX and CAP are working as expected, their effect on cyt *f* and any nuclear-encoded proteins should be opposite. Anti-cyt *f*, raised to *P. cruentum* cyt *f*, was also a gift of Professor Gantt.

Immunoprecipitations

Immunoprecipitations were conducted to confirm the identity of the radioactive immunolabeled bands on the western blots, using a modified version of the protocol previously used to precipitate proteins from isolated *E. chlorotica* plastids (Pierce *et al.*, 1996). Plastid proteins were solubilized in lysing buffer (10 mM Tris-HCl, 10 mM EDTA, 150 mM NaCl, 1 mM PMSF, 1% (v/v) Nonidet P-40, pH 8.0), using equal amounts of chlorophyll per sample, mixed with a small amount of Protein-A Sepharose beads to eliminate nonspecific binding, and incubated on ice with occasional agitation. The beads were removed by centrifugation and discarded, the supernatant was saved, and the appropriate antibody was added to the lysate and rotated overnight (4 $^{\circ}\text{C}$). Protein-A beads, swelled in washing buffer (50 mM Tris-HCl, 5 mM EDTA, 150 mM NaCl, 1 mM PMSF, 0.1% (v/v) Nonidet P-40, pH 8.0), were added the following morning and rotated (3 h, room temperature). The antigen–antibody–protein-A Sepharose bead complexes were washed several times in washing buffer and removed by centrifugation. In the case of cyt *f*, the antigen–antibody–protein-A Sepharose bead complexes were resuspended in 10.0 M urea, 10% SDS (w/v), 5% β -ME (v/v), pH 12.5, and boiled for 10 min to liberate the cyt *f* antigen. The solution was centrifuged, the supernatant was removed, and the beads were discarded. The supernatant proteins were separated by SDS-PAGE as described above, and the gel was autoradiographed.

The LHCl antibody-antigen complex could not be broken efficiently with any treatment, which prevented the visualization of the labeled LHCl proteins *via* SDS-PAGE. Although this was unexpected, it is not unusual and may have been caused by a number of factors. The presence of several different LHCl polypeptides with varying isoelectric points, ranging between 4.5 and 9.5 (De Martino *et al.*, 2000), makes it very difficult to create optimal reaction conditions for each one. The polyclonal antibody molecules bind to all the LHCl polypeptides as well as to each other, creating a large antigen-antibody complex with a core inaccessible to the chemicals necessary to liberate the antigen. Very few

researchers have attempted LHC immunoprecipitations because of the pitfalls involved in precipitating inner-membrane proteins (Anderson and Blobel, 1983). Instead, other protocols have been designed using mild detergents to extract intact photosystem holocomplexes from the thylakoids, followed by protein separation on sucrose density gradients (Fawley and Grossman, 1986; Buchel and Wilhelm, 1993; Wolfe *et al.*, 1994; Schmid *et al.*, 1997). These isolations require large amounts of starting material (Schmid *et al.*, 1997) that greatly exceed what is available to us in the slugs. So, instead, we used the LHCI antibody to demonstrate that LHCI had incorporated radioactivity.

Following the procedure described above, the protein A Sepharose beads were reacted with anti-LHCI and then with a radiolabeled plastid protein extract. The antigen-antibody-protein-A Sepharose bead complexes were repeatedly washed by centrifugation until the radioactivity in the supernatant was reduced to background. The washed antigen-antibody-protein-A Sepharose bead complexes were resuspended in optifluor (Packard), and radioactivity was determined by a scintillation counter. Controls for nonspecific binding to protein-A Sepharose beads were conducted with the same procedure, but without the addition of the LHCI antibody. Counts per minute resulting from nonspecific binding were subtracted from experimental values for each inhibitor treatment and controls, and the final data were converted to $\text{cpm} (\mu\text{g chlorophyll})^{-1} (\mu\text{g protein})^{-1}$. The normalized data were averaged and expressed in terms of percent of control for each inhibitor.

Results

Plastid protein synthesis and identification

The Coomassie-stained SDS-PAGE gels of protein extracts from isolated slug plastids were similar to controls regardless of the inhibitor present, either CHX or CAP, indicating no difference in the protein composition of the plastids after treatment (Fig. 1). However, autoradiograms of SDS-PAGE gels of plastid proteins extracted from slugs incubated in the presence of [^{35}S]-methionine indicate that very different patterns of protein synthesis occur in the slugs between controls and inhibitors as well as between inhibitors (Fig. 2). CHX has a profound effect on protein synthesis, preventing synthesis of the majority of the protein bands labeled in the absence of inhibitor (Fig. 2, CON), whereas the synthesis of many more labeled bands occurs in the presence of CAP. Furthermore, these protein bands differ from those visualized in the CHX treatments (Fig. 2).

Verification of inhibitor effects

Cyt *f* antibodies reacted with a protein band synthesized in the presence of CHX on western blots at approximately 36 kDa (Fig. 3). Immunoprecipitations using anti-cyt *f*

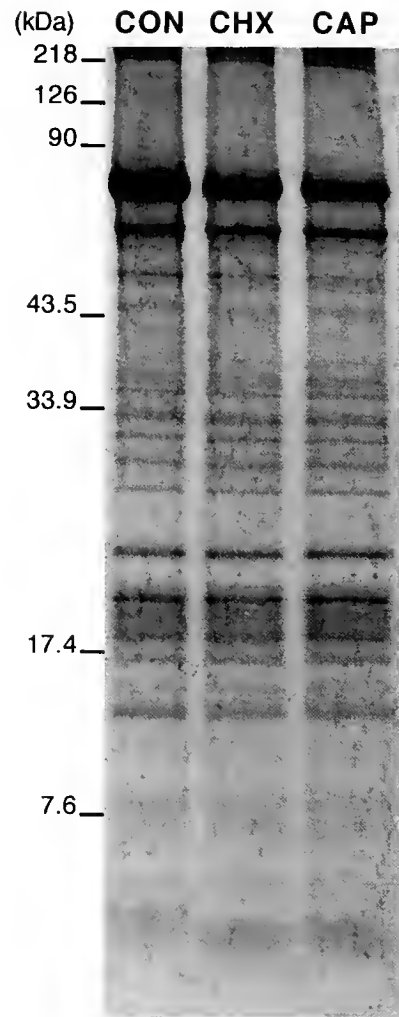


Figure 1. Coomassie brilliant blue-stained 15% SDS-PAGE gel of proteins extracted from isolated *Elysia* chloroplasts. The protein bands visualized are identical regardless of the inhibitor treatment, CHX or CAP (CON refers to control). Approximate molecular weights are indicated to the left.

identify a band with a molecular weight corresponding to cyt *f*, confirming its identity (Fig. 4). Autoradiograms of the same gels show [^{35}S]-methionine incorporation into cyt *f* in the presence of CHX, but not in the presence of CAP (Fig. 5).

The anti-LHCI we made to *Porphyridium cruentum* recombinant LHCI recognized both the recombinant LHCI antigen (Fig. 5A, lane 1) and the LHCI polypeptides from *P. cruentum* thylakoids (Fig. 5B, lane 2). Six polypeptide bands were identified in *P. cruentum*, ranging in approximate molecular weights from 19 to 24 kDa (Fig. 5B, lane 2), sizes consistent with those previously described for the LHCI polypeptides in this species (Tan *et al.*, 1995). The antibody bound onto western blots of plastid proteins from *Vaucheria litorea* and *Elysia chlorotica*, with or without the CHX and CAP treatments (Fig. 5C, lanes *V. lit.*, CON,

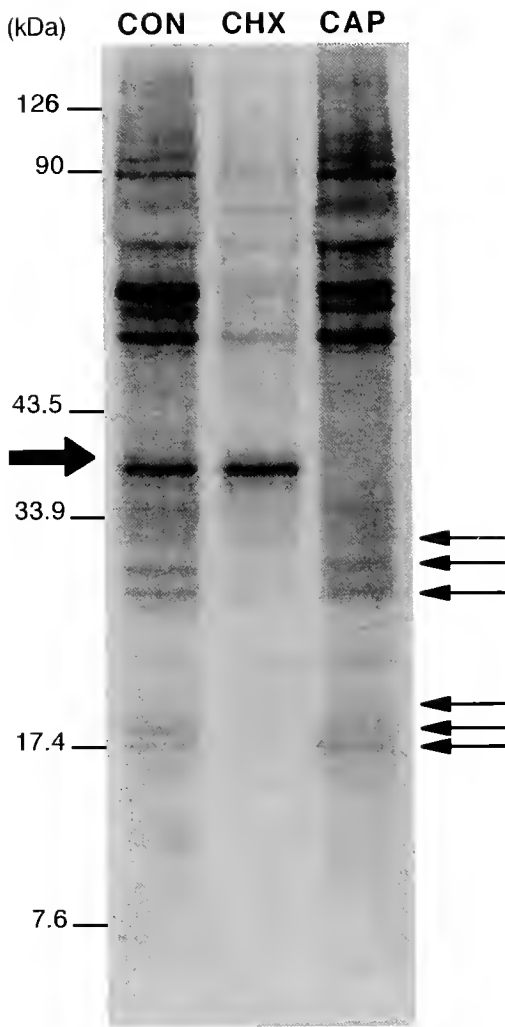


Figure 2. Autoradiograph of plastid proteins separated by SDS-PAGE gel run under the same conditions as those depicted in Figure 2. The plastid proteins incorporating [35 S]-methionine label differ following treatment with CHX or CAP. The control (CON) represents chloroplast proteins isolated from slugs without inhibitor treatment. Arrows identify the approximate positions of *cyt f* (large arrow) and the LHCI (small arrows) proteins.

CHX, CAP). As expected, the six polypeptide bands bound by the anti-LHCI in *V. litorea* and *E. chlorotica* plastids have a slightly greater size range—18 to 32 kDa—than those identified in *P. cruentum*. These same antibody-labeled bands from *E. chlorotica* plastid proteins incorporate radioactive label in the presence of CAP, but incorporation is blocked by the presence of CHX (Fig. 6).

The amount of radiolabel precipitated by anti-LHCI from the slug plastid extracts following CHX treatment is only 2% of the control level, indicating a reduction in LHCI synthesis (Fig. 7). In contrast, the LHCI proteins in CAP-treated slugs incorporated [35 S]-methionine at 92% of control rates, more than 40-fold higher than the level found in CHX treated animals (Fig. 7).

Discussion

LHCI, a family of plastid polypeptides essential for photosynthesis, is synthesized while *Vaucheria litorea* chloroplasts reside within the cells of the digestive diverticula of *Elysia chlorotica*. In addition, our data indicate the LHCI polypeptides are probably the products of genes located in the host-cell nuclear genome because their synthesis is inhibited by the cytosolic ribosome inhibitor, CHX, but not by the presence of the plastid ribosome inhibitor, CAP. This remarkable result would not be surprising in a plant or algal species since the LHCI polypeptide family's genes, *Lhca1-Lhca6*, reside in the nuclear DNA of all plants and algae examined to date (Jansson, 1994; Green and Durnford,

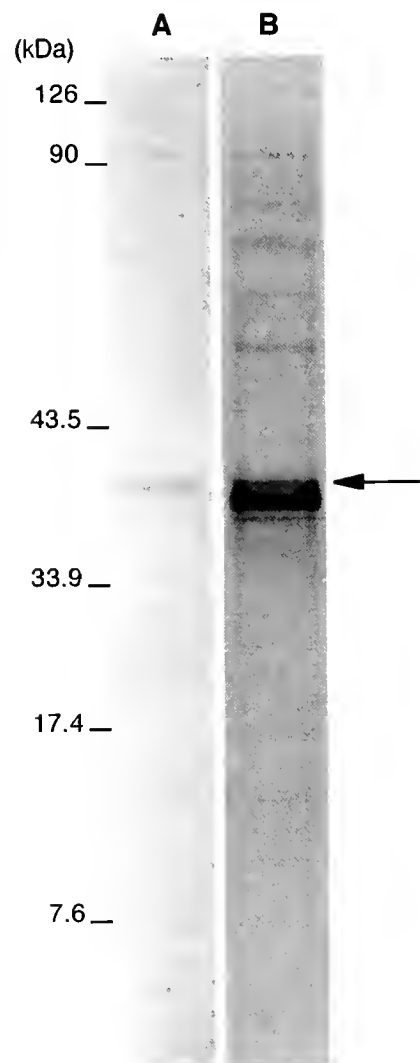


Figure 3. Immunoblot labeled with antibody to *cyt f* (A), and its corresponding autoradiograph (B). The slugs were exposed to CHX and the proteins were labeled as described in the methods. Anti-*cyt f* binds at approximately 36 kDa, coincident with a radiolabeled protein. The arrow indicates the autoradiograph band corresponding to the position of *cyt f*.

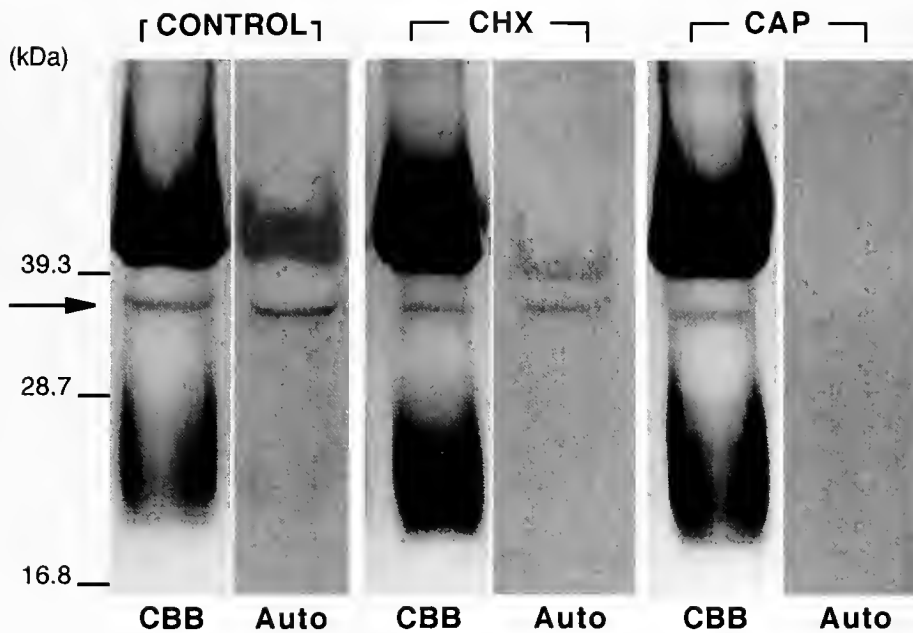


Figure 4. Immunoprecipitation of *cyt f*. Coomassie brilliant blue (CBB)-stained gels of proteins precipitated with anti-*cyt f* from chloroplast extracts from slugs subjected to no inhibitor (Control), to CHX, or to CAP, and their corresponding autoradiographs (Auto). The arrow indicates the position of *cyt f*. Large bands above and below *cyt f* are the heavy and light chains of the antibody, respectively. The radioactivity corresponding to the antibody bands in control and CHX is probably undissociated *cyt f*.

1996; Durnford *et al.*, 1999; Jansson, 1999; Wollman *et al.*, 1999). However, the synthesis of LHCI directed by an animal's genome indicates that genes have been transferred into the slug DNA.

Although surprising, the site of synthesis and the identification of LHCI seem to be without question as long as inhibitor and antibody specificity are not problems. Both CHX and CAP have been used in a wide array of studies, and their sites of action are well established. In fact, they have been used, exactly as we have done here, to establish that the site of synthesis of the "light harvesting chlorophyll protein" (=LHCI) occurs on 80s cytoplasmic ribosomes in *Phaeodactylum tricoratum* (Fawley and Grossman, 1986).

There are several reasons to conclude that our antibody is specific. We raised the antibody against the red alga LHCI not only because it was available, but also because the chromophytes, the taxonomic group of *V. litorea*, probably arose through a secondary symbiosis from a red alga (Rieth, 1995; Green and Durnford, 1996; Palmer and Delwiche, 1996; Martin and Herrmann, 1998; Delwiche, 1999). Furthermore, *Porphyridium cruentum* LHCI possesses both sequence homologies and immunological relatedness to the chromophytic light-harvesting proteins (Wolfe *et al.*, 1994; Rieth, 1995; Tan *et al.*, 1997b). Thus, a polyclonal antibody raised to a rhodophyte LHCI should have a good chance of specifically recognizing the LHCI polypeptides in *V. litorea*. Our results indicate that the anti-LHCI binds the *P. cruentum* recombinant LHCI, the antigenic source for the

antibody, as well as all six of the native *P. cruentum* LHCI proteins (Tan *et al.*, 1995; Grabowski *et al.*, 2000) in control immunoblots of extracted thylakoids. The anti-LHCI immunoblots of *E. chlorotica* and *V. litorea* also identified six protein bands with a greater size range than the LHCI proteins identified in *P. cruentum*. Those bands are consistent with the sizes of LHCI polypeptides from many species (Gantt, 1996; Jansson, 1999; Wollman *et al.*, 1999), and no other bands were labeled by the antibody. Seeing six LHCI proteins is not surprising, because LHCI is typically found in multiple homologs in algae, ranging from two in one species of Xanthophyceae (Buchel and Wilhelm, 1993) to at least six paralogs in some rhodophytes (Tan *et al.*, 1995), and as many as eight in the chromophyte *Heterosigma carterae* (Durnford and Green, 1994). With few exceptions [such as in *Euglena gracilis* (Jansson, 1994)], each is encoded by a separate, nuclear gene belonging to the *Lhc* super-gene family (Jansson, 1999). Thus, location of the gene aside, the presence of six LHCI proteins in the endosymbiotic plastids in *E. chlorotica* is not surprising.

It seems clear that each of the bands immunodecorated by anti-LHCI corresponds to a single LHCI polypeptide and not a dimer. LHCI dimers can result from their association with other LHC proteins and their respective photosystems *in situ*, and they do not always readily dissociate under the denaturing conditions of SDS-PAGE (Tan *et al.*, 1995). If LHCI dimers were present here, they should have minimum molecular weights of about 36 kDa, corresponding to dou-

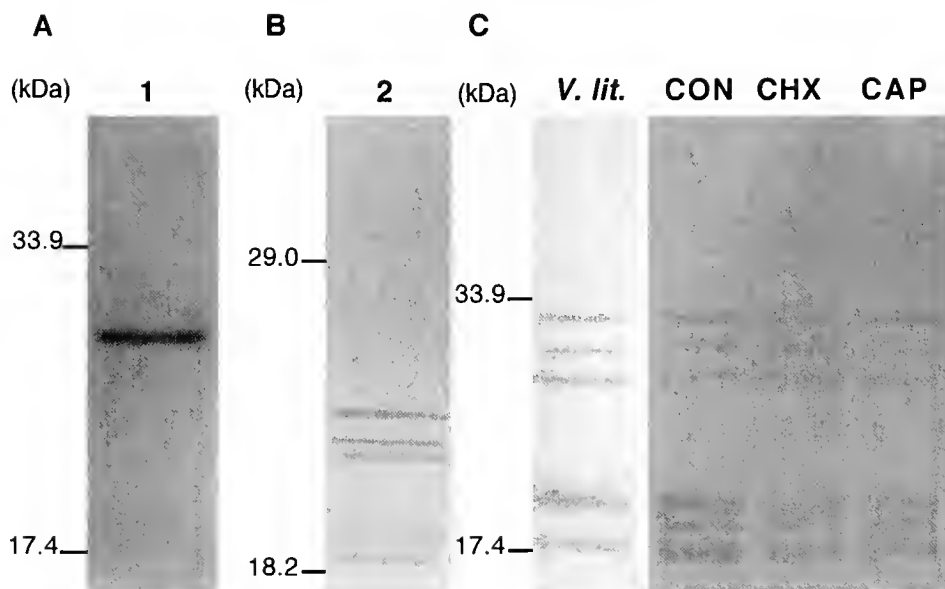


Figure 5. Immunoblots testing the antibody raised to *Porphyridium cruentum* LHCI. (A) Anti-LHCI binds the recombinant 22 kDa *Lhca* R1 product from *P. cruentum* (lane 1). Its appearance as a 28–30 kDa protein in SDS-PAGE and subsequent immunoblots results from the addition of a 33 amino acid N-terminal fusion in the recombinant protein (Grabowski *et al.*, 2000). (B) Anti-LHCI binds LHCI polypeptides extracted from *P. cruentum* thylakoids (lane 2). (C) *Vaucheria litorea* (lane *V. lit.*) and *Elysia chlorotica* plastid proteins have six bands binding the anti-LHCI identical in size to each other. All six proteins are present in the slugs regardless of the inhibitor treatment [lanes CON (control), CHX and CAP]. Molecular weights are indicated to the left of (A), (B), and (C).

ble the molecular weight of the smallest immunolabeled band. However, the largest of the six immunolabeled bands present in the gels is about 32 kDa, seemingly too small to be an LHCI dimer.

Other dimers might form with a number of photosystem I (PSI) proteins due to the close association of LHCI with the PSI subunits that compose the PSI-LHCI holocomplex (Wollman *et al.*, 1999; Jansson, 1999). This also does not seem to be the case here. Anti-PSI, raised against the cyanobacteria PSI holocomplex (again, courtesy of Professor Gantt), binds a single 10-kDa protein band on western blots of *E. chlorotica* plastid proteins (data not shown). The combination of this PSI polypeptide with any of the three smaller bands (18–20 kDa) that react with the anti-LHCI could form a dimer with molecular weights comparable to each of the three larger polypeptides (28–32 kDa). However, since anti-PSI and anti-LHCI do not co-label any bands, an LHCI-PSI dimer is unlikely.

An additional possibility might be that one of the bands could be another LHC-type protein possessing immunological similarities to LHCI, such as the fucoxanthin chlorophyll *alc* binding proteins (FCPC) found in chromophytes or light-harvesting complex II (LHCII) proteins. In fact, our previous work has demonstrated the presence of FCPC in plastids of both *E. chlorotica* and *V. litorea*. However, the size of the FCPC protein identified there does not correspond to the weights of the proteins bound by the anti-LHCI

used here (Pierce *et al.*, 1996; Green *et al.*, 2000). Furthermore, previous attempts to demonstrate FCPC synthesis with radioactive labels in the slugs have not yielded positive results (Pierce *et al.*, 1996).

The LHCII family of polypeptides is closely related to LHCI, performing similar functions in photosystem II to those performed by LHCI in PSI. The LHC II genes are in the same nuclear-encoded *Lhc* super-gene family (Jansson, 1999) and share sequence homologies with those genes encoding LHCI (Durnford *et al.*, 1999; Jansson, 1999; Wollman *et al.*, 1999). There is, however, a clear separation in the phylogenies of LHCI and LHCII (Durnford *et al.*, 1999), indicating some degree of dissimilarity between the two proteins. Nevertheless, the possibility seems to remain that the proteins bound by our antibody could be from LHCII.

Of the LHCII components, CP24, CP26, and CP29 contain the most sequence similarities to the LHCIs (Green and Durnford, 1996) and have molecular weights, 25–30 kDa (Wollman *et al.*, 1999), that roughly correspond to those of the three largest polypeptides identified in our anti-LHCI immunoblots of *E. chlorotica* and *V. litorea* plastid proteins (28–32 kDa), which appear to be slightly larger than most LHC proteins in chromophytes (Green and Durnford, 1996). An LHCII antibody derived from pea (generously donated by Dr. Kenneth Cline, University of Florida) was unreactive in our immunoblotting protocol (data not shown). This

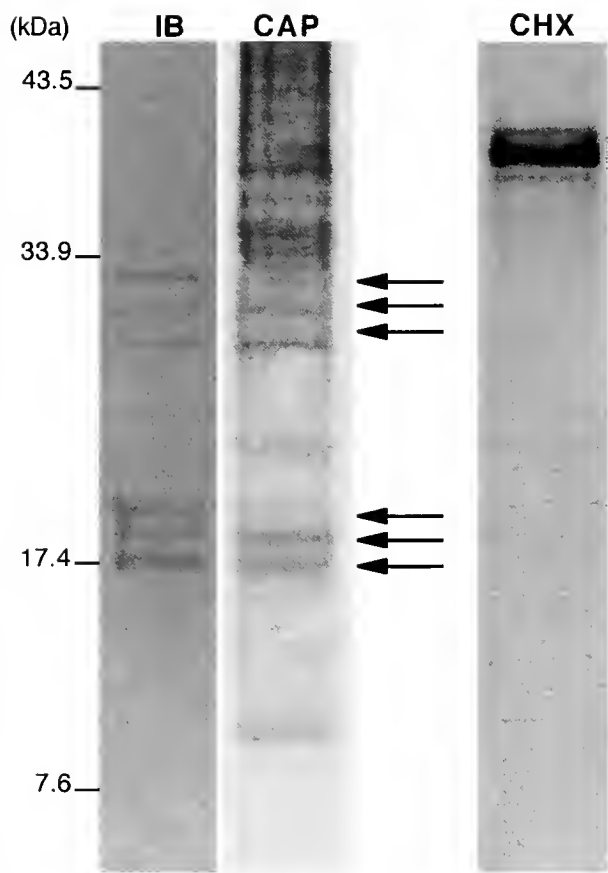


Figure 6. Immunoblot (IB) of LHCI synthesized in the presence of CAP and ^{35}S -methionine, and its corresponding autoradiograph (CAP). The arrows indicate radiolabeled bands coinciding to LHCI immunolabeled bands shown in (IB). The bands in (CAP) are not labeled in the presence of CHX (CHX).

result seems to indicate that the polypeptides are not LHCI, but since the similarity between the green plant and chromophyte LHC proteins is relatively low (Green and Durnford, 1996; Durnford *et al.*, 1999), we probably cannot completely eliminate the possibility that the anti-LHCI is binding LHCI polypeptides. However, just like LHCI, all of the LHCI genes are nuclear encoded in the plants and algae where they have been found (Jansson, 1994, 1999; Wollman *et al.*, 1999), and even if we have identified LHCI, the conclusion is still the same: that an algal LHC gene has been transferred to the DNA of the slug.

The immunoprecipitations provide additional evidence that the LHCI polypeptides are being synthesized on the cytoplasmic ribosomes in the slug. The high amount of radioactivity precipitated by the antibody in the presence of CAP compared to that precipitated in the presence of CHX demonstrates that the proteins recognized by the anti-LHCI are indeed synthesized in the slugs. Since the amount of radioactivity incorporated varied from slug to slug and from experiment to experiment, we had to normalize the immunoprecipitation data as percent of control in order to com-

pare them. However, in a typical experiment, the values for the amount of radioactive material incorporated into the precipitate in the presence of CAP ranged from 5000 to 25,000 cpm, whereas those in the presence of CHX ran from 150 to 400 cpm, which may give a clearer picture of the level of material bound by the antibody.

The results of the pharmacological experiments, the immunoblots, and the immunoprecipitations, taken together, provide substantial evidence that LHCI is the identity of some of the plastid proteins that are synthesized in the presence of CAP. The inhibition of LHCI synthesis by CHX suggests that the algal *Lhca* genes have somehow been transferred to the slug.

To be certain that a gene transfer has occurred, direct evidence of the gene in the genomic DNA of the slug must be found, and we are pursuing this confirmation. However, in addition to the results presented here, other circumstantial evidence for the transfer of the LHCI genes between alga and slug is available in several characteristics of the association. First, although the turnover rate of LHCI in *E. chlorotica* is unknown, the fact that it is synthesized indicates that it is not an unusually robust protein—LHCI replacement is necessary for plastid function to proceed. Second, *Lhca* genes have not been found in the plastid genomes of any organism (Durnford *et al.*, 1999), including other *Vaucheria* species (Linne von Berg and Kowallik, 1992). Of course, if LHCI were present in the plastid genome, it would be synthesized with CHX present, as is the case with the *cyt f* controls; but it is not. Third, the *V. litorea* plastid genome is 119.1 kb (Green *et al.*, 2000), which is similar in size to those of other algae, including *V.*

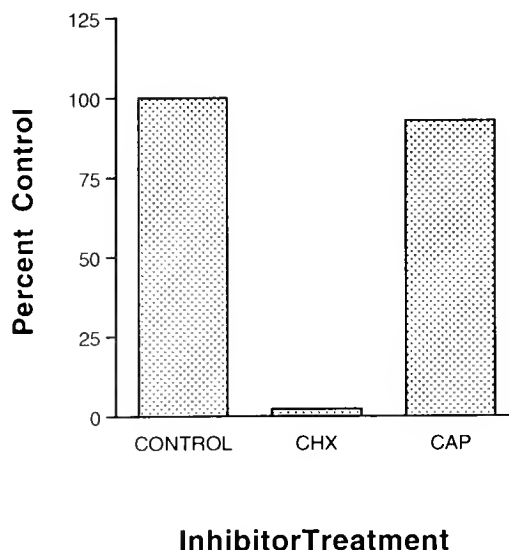


Figure 7. CHX inhibits synthesis of LHCI. In the presence of CHX, anti-LHCI precipitated only 2% of control radioactivity incorporated into LHCI compared to 92% of control in the presence of CAP. Control rates were defined as 100%, and inhibitor rates were calculated as a mean percent of control ($n = 6$).

sessilis and *V. bursata* (Linne von Berg and Kowallik, 1988, 1992), but small relative to those of other plants (Martin and Herrmann, 1998). Even though the plastid genomes of chromophytic algae have a greater coding capacity, relative to their size, than other algae because of fewer introns and inverted repeats (Reith, 1995), they are too small to carry sufficient genetic information to encode all of the enzymes required for photosynthesis and plastid protein targeting. Fourth, transfer of algal DNA remnants or a nucleomorph-type structure during plastid capture seems unlikely. To date, nucleomorphs have been found only in the Cryptophyta and Chlorarachniophyta (Delwiche, 1999; Zauner *et al.*, 2000) and have not been identified in any chromophyte (Maier *et al.*, 1991; Delwiche, 1999). Although DNA of this type would probably be transcribed on nucleomorph 80S ribosomes (Douglas *et al.*, 1991) and blocked by CHX, neither substantial electron microscopy (Kawaguti and Yamasu, 1965; Graves *et al.*, 1979; Mujer *et al.*, 1996) nor molecular testing (Green *et al.*, 2000) has so far produced evidence for either nucleomorphs or algal nuclear remnants in *E. chlorotica*. Furthermore, if algal DNA remnants were present somewhere in the slug cells, the likelihood is remote of their containing the correct genes and being present in all of the plastid-containing cells in all of the slugs in the populations year after year. Finally, others have suggested that some of the proteins necessary to maintain photosynthesis may be encoded in the mitochondrial genome and are redirected to the chloroplast (Rumpho *et al.*, 2000). Although dual targeting of proteins has been demonstrated in *Arabidopsis* (Chow *et al.*, 1997; Menand *et al.*, 1998), it seems highly unlikely with LHCl. LHCl has never been found associated with mitochondria in any organism; and CAP, which inhibits the mitochondrial ribosomes in addition to those associated with the plastids, would prevent its synthesis anyway.

The horizontal transfer of DNA from the endosymbiont to the nucleus of the host cell provides the basis for the theory of the endosymbiotic origin of eukaryotic organelles. This movement of the symbiont's genes to the host enabled the host to incorporate the organelle's function into its own biochemistry and to faithfully replicate it in subsequent generations. The remnants of eubacterial genes in the mitochondrial and plastid genomes of modern eukaryotes probably resulted from such events (Martin and Herrmann, 1998). Most of the discussions regarding the evolution of plastids focus on the horizontal gene transfer resulting from the primary endosymbiotic event in which a primitive prokaryote engulfed a cyanobacteria (Palmer, 1993; Reith, 1995; Palmer and Delwiche, 1996; Martin *et al.*, 1998; Tengs *et al.*, 2000). Other hypotheses propose a secondary endosymbiosis, probably involving a eukaryote that engulfed a red or green alga (Gibbs, 1981; Palmer and Delwiche, 1996; Martin *et al.*, 1998; Zhang *et al.*, 1999; Delwiche, 1999; Tengs *et al.*, 2000), that produced the plastids

of the chromophytic algae and their relatives. In many of these cases, the identity of the initial host, symbiont, or both is unknown. In the case of *E. chlorotica* and *V. litorea*, the origin of LHCl is known; if the gene has been transferred, the transfer occurred between two multicellular eukaryotes and represents a case of tertiary endosymbiosis.

Finally, the mechanism by which such a gene transfer could occur may be found in the viruses that appear in each generation of the slugs at the end of their life cycle. The viruses have several features in common with Retroviridae and seem to be endogenous (Pierce *et al.*, 1999). Retroviruses are capable of transferring genes between organisms; if they are incorporated in the germ cells, they are transferred to the subsequent generations as Mendelian genes (Scharfman *et al.*, 1991). Thus, resolving the relationships between the slugs, alga, plastids, and viruses may have profound implications for both cell and evolutionary biology.

Acknowledgments

Research support was provided by a National Science Foundation award (IBN-9604679) to SKP. We thank Elisabeth Gantt and Beatrice Grabowski for their helpful suggestions.

Literature Cited

- Anderson, D. J., and G. Blobel. 1983. Immunoprecipitations of proteins from cell-free translations. *Methods Enzymol.* **96**: 111–120.
- Barber, J., and B. Andersson. 1992. Too much of a good thing: Light can be bad for photosynthesis. *Trends Biochem. Sci.* **17**: 61–66.
- Berry-Lowe, S. L., and G. W. Schmidt. 1991. Chloroplast protein transport. Pp. 257–302 in *The Molecular Biology of Plastids: Cell Culture and Somatic Cell Genetics of Plants*, Vol. 7A, L. Bogorad and I. K. Vasil, eds. Academic Press, New York.
- Bidwell, J. P., and S. Spotte. 1985. *Artificial Seawaters: Formulas and Methods*. Jones and Bartlett, Boston. Pp. 305–306.
- Buchel, C., and C. Wilhelm. 1993. Isolation and characterization of a photosystem I-associated antenna (LHCl) and a photosystem I-core complex from the chlorophyll *c*-containing alga *Pleurochloris meiringensis* (Xanthophyceae). *J. Photochem. Photobiol. B Biol.* **20**: 87–93.
- Chow, K.-S., D. P. Singh, J. M. Roper, and A. G. Smith. 1997. A single precursor protein for ferredoxin-NADP+ reductase from *Arabidopsis* is imported *in vitro* into both chloroplasts and mitochondria. *J. Biol. Chem.* **272**: 27565–27571.
- Clark, K. B., K. R. Jensen, and H. M. Strits. 1990. Survey of functional kleptoplasty among West Atlantic Ascoglossa (=Sacoglossa) (Mollusca: Opisthobranchia). *Veliger* **33**: 339–345.
- Delwiche, C. F. 1999. Tracing the thread of plastid diversity through the tapestry of life. *Am. Nat.* **154**: S164–S177.
- De Martino, A., D. Douady, M. Quinet-Szely, B. Rousseau, F. Crepineau, K. Apt, and L. Caron. 2000. The light-harvesting antenna of brown alga: highly homologous proteins encoded by a multigene family. *Eur. J. Biochem.* **267**: 5540–5549.
- Douglas, S. E., C. A. Murphy, D. F. Spencer, and M. W. Gray. 1991. Cryptomonad algae are evolutionary chimaeras of two phylogenetically distinct unicellular eukaryotes. *Nature* **350**: 148–151.
- Durnford, D. G., and B. R. Green. 1994. Characterization of the

- light-harvesting proteins of the chromophytic alga, *Olisthodiscus luteus* (*Heterosigma carterae*). *Biochim. Biophys. Acta* **1184**: 118–126.
- Durnford, D. G., J. A. Deane, S. Tan, G. I. McFadden, E. Gantt, and B. R. Green. 1999. A phylogenetic assessment of the eukaryotic light-harvesting antenna proteins, with implications for plastid evolution. *J. Mol. Evol.* **48**: 59–68.
- Fawley, M. W., and A. R. Grossman. 1986. Polypeptides of a light-harvesting complex of the diatom, *Phaeodactylum tricornutum* are synthesized in the cytoplasm of the cell as precursors. *Plant Physiol.* **81**: 149–155.
- Gantt, E. 1996. Pigment protein complexes and the concept of the photosynthetic unit: chlorophyll complexes and phycobilisomes. *Photosyn. Res.* **48**: 47–53.
- Gibbs, S. P. 1981. The chloroplasts of some algal groups may have evolved from endosymbiotic eukaryotic algae. *Ann. NY Acad. Sci.* **361**: 193–207.
- Grabowski, B., S. Tan, F. X. Cunningham, Jr., and E. Gantt. 2000. Characterization of the *Porphyridium cruentum* chl *a*-binding LHC by *in vitro* reconstitution: *LhcaR1* binds 8 chl *a* molecules and proportionately more carotenoids than CAB proteins. *Photosyn. Res.* **63**: 85–96.
- Graves, D. A., M. A. Gibson, and J. S. Bleakney. 1979. The digestive diverticula of *Alderia modesta* and *Elysia chloronca*. *Veliger* **21**: 415–422.
- Green, B. J., W.-Y. Li, J. R. Manhart, T. C. Fox, E. L. Summer, R. A. Kennedy, S. K. Pierce, and M. E. Rumpho. 2000. Mollusc-algal chloroplast endosymbiosis. Photosynthesis, thylakoid protein maintenance, and chloroplast gene expression continue for many months in the absence of the algal nucleus. *Plant Physiol.* **124**: 331–342.
- Green, B. R., and D. G. Durnford. 1996. The chlorophyll carotenoid proteins of oxygenic photosynthesis. *Annu. Rev. Plant. Physiol. Plant. Mol. Biol.* **47**: 685–714.
- Greenberg, B. M., V. Gaba, O. Cananni, S. Malkin, A. K. Mattoo, and M. Edelman. 1989. Separate photosensitizers mediate degradation of the 32 kDa photosystem II reaction center protein in the visible and UV spectral regions. *Proc. Natl. Acad. Sci. USA* **86**: 6617–6620.
- Greene, R. W. 1970. Symbiosis in sacoglossan opisthobranchs: functional capacity of symbiotic chloroplasts. *Mar. Biol.* **7**: 138–142.
- Hinde, R., and D. C. Smith. 1974. "Chloroplast symbiosis" and the extent to which it occurs in Sacoglossa (Gastropoda: mollusca). *Biol. J. Linn. Soc.* **6**: 349–356.
- Jansson, S. 1994. The light-harvesting chlorophyll *alb*-binding proteins. *Biochim. Biophys. Acta* **1184**: 1–19.
- Jansson, S. 1999. A guide to the Lhc genes and their relatives in *Arabidopsis*. *Trends Plant Sci.* **4**: 236–240.
- Joyard, J., A.-J. Dorne, and R. Douce. 1987. Use of thermolysin to probe the cytosolic surface of the outer envelope membranes from plastids. Pp. 195–206 in *Methods in Enzymology*, Vol. 148, L. Packer and R. Douce, eds. Academic Press, San Diego, CA.
- Kawaguti, S., and T. Yamasu. 1965. Electron microscopy on the symbiosis between an elysoid gastropod and chloroplasts of a green alga. *Biol. J. Okayama Univ.* **11**: 57–65.
- Laemmli, U. K. 1970. Cleavage of structural proteins during assembly of the head of bacteriophage T4. *Nature* **227**: 608–685.
- Lamh, A. J., G. D. Clark-Walker, and A. W. Linnane. 1968. The biogenesis of mitochondria: the differentiation of mitochondrial and cytoplasmic protein synthesizing systems *in vitro* by antibiotics. *Biochim. Biophys. Acta* **161**: 415–427.
- Linne von Berg, K.-H., and K. V. Kowallik. 1988. Structural organization and evolution of the plastid genome of *Vaucheria sessilis* (Xanthophyceae). *Biosystems* **21**: 239–247.
- Linne von Berg, K.-H., and K. V. Kowallik. 1992. Structural organization of the chloroplast genome of the chromophytic alga *Vaucheria bursata*. *Plant Mol. Biol.* **18**: 83–95.
- Maier, U.-G., C. J. B. Hoffman, E. Eschbach, J. Wolters, and G. L. Igloi. 1991. Demonstration of nucleomorph-encoded eukaryotic small subunit ribosomal RNA in cryptomonads. *Mol. Gen. Genet.* **230**: 155–160.
- Martin, W., and R. G. Herrmann. 1998. Gene transfer from organelles to nucleus: How much, what happens and why? *Plant Physiol.* **118**: 9–17.
- Martin, W., B. Stoebe, V. Goremykin, S. Hansmann, M. Hasegawa, and K. V. Kowallik. 1998. Gene transfer to the nucleus and the evolution of chloroplasts. *Nature* **393**: 162–165.
- Mattoo, A. K., J. B. Marder, and M. Edelman. 1989. Dynamics of the photosystem II reactions center. *Cell* **5**: 241–246.
- Menand, B., L. Marechal-Drouard, W. Sakamoto, A. Dietrich, and H. Wintz. 1998. A single gene of chloroplast origin codes for mitochondrial and chloroplastic methionyl-tRNA synthetase in *Arabidopsis thaliana*. *Proc. Natl. Acad. Sci. USA* **95**: 11014–11019.
- Mujer, C. V., D. L. Andrews, J. R. Manhart, S. K. Pierce, and M. E. Rumpho. 1996. Chloroplast genes are expressed during intracellular symbiotic association of *Vaucheria litorea* plastids with the sea slug *Elysia chlorotica*. *Proc. Natl. Acad. Sci. USA* **93**: 12333–12338.
- Obrig, T. G., W. J. Culp, W. L. McKeehan, and B. Hardesty. 1971. The mechanism by which cycloheximide and related glutarimide antibiotics inhibit peptide synthesis on reticulocyte ribosomes. *J. Biol. Chem.* **246**: 174–181.
- Palmer, J. D. 1993. A genetic rainbow of plastids. *Nature* **364**: 762–763.
- Palmer, J. D., and C. F. Delwiche. 1996. Second-hand chloroplasts and the case of the disappearing nucleus. *Proc. Natl. Acad. Sci. USA* **93**: 7432–7435.
- Peterson, G. L. 1977. A modification of the protein assay method of Lowry *et al.* which is more generally applicable. *Anal. Biochem.* **83**: 346–356.
- Pierce, S. K., R. W. Biron, and M. E. Rumpho. 1996. Endosymbiotic chloroplasts in molluscan cells contain proteins synthesized after plastid capture. *J. Exp. Biol.* **199**: 2323–2330.
- Pierce, S. K., T. K. Maugel, M. E. Rumpho, J. J. Hanten, and W. L. Mondy. 1999. Annual viral expression in a sea slug population: life cycle control and symbiotic chloroplast maintenance. *Biol. Bull.* **197**: 1–6.
- Rieth, M. 1995. Molecular biology of rhodophyte and chromophyte plastids. *Annu. Rev. Plant Physiol. Plant Mol. Biol.* **46**: 549–575.
- Rumpho, M. E., E. J. Summer, and J. R. Manhart. 2000. Solar-powered sea slugs. Mollusc/algal chloroplast symbiosis. *Plant Physiol.* **123**: 29–38.
- Scharfmann, R., J. H. Alexrod, and I. M. Verma. 1991. Long-term *in vivo* expression of retrovirus-mediated gene transfer in mouse fibroblast implants. *Proc. Natl. Acad. Sci. USA* **88**: 4626–4630.
- Schmid, V. H. R., K. V. Cammarata, B. U. Bruns, and G. W. Schmidt. 1997. *In vitro* reconstitution of the photosystem I light-harvesting complex LHCl-730: Heterodimerization is required for antenna pigment organization. *Proc. Natl. Acad. Sci. USA* **94**: 7667–7672.
- Stone, A. B., and D. Wilkie. 1975. Loss of cytochrome oxidase in *Saccharomyces cerevisiae* during inhibition of mitochondrial proteins synthesis by erythromycin and chloramphenicol. *J. Gen. Microbiol.* **91**: 150–156.
- Tan, S., G. R. Wolfe, F. X. Cunningham, Jr., and E. Gantt. 1995. Decrease in the PSI antenna complex with increasing growth irradiance in the red alga *Porphyridium cruentum*. *Photosyn. Res.* **45**: 1–10.
- Tan, S., F. X. Cunningham, Jr., and E. Gantt. 1997a. *LhcaR1* of the red alga *Porphyridium cruentum* encodes a polypeptide of the LHC I complex with seven potential chlorophyll *a*-binding residues that are conserved in most LHCs. *Plant Mol. Biol.* **33**: 157–167.

- Tan, S., A. Ducret, R. Aebersold, and E. Gantt. 1997b. Red algal LHC I genes have similarities with both Chl *alc*- and *alc*-binding proteins: A 21 kDa polypeptide encoded by *LhcaR2* is one of the six LHC I polypeptides. *Photosyn. Res.* **53**: 129–140.
- Taylor, D. L. 1970. Chloroplasts as symbiotic organelles. *Int. Rev. Cytol.* **27**: 29–64.
- Tengs, T., O. J. Dahlberg, K. Shalchian-Tabrizi, D. Klaveness, K. Rudi, C. F. Delwiche, and K. S. Jakobson. 2000. Phylogenetic analyses indicate that the 19' hexanoloxy-fucoanthin-containing dinoflagellates have tertiary plastids of haptophyte origin. *Mol. Biol. Evol.* **17**: 718–729.
- Towbin, H., T. Staehelin, and J. Gordon. 1979. Electrophoretic transfer of proteins from polyacrylamide gels to nitrocellulose sheets: procedure and some applications. *Proc. Natl. Acad. Sci. USA* **76**: 4350–4354.
- West, H. H. 1979. Chloroplast symbiosis and the development of the ascoglossan opisthobranch *Elysia chlorotica*. Ph.D. dissertation. Northeastern University, Boston, MA.
- West, H. H., J. Harrigan, and S. K. Pierce. 1984. Hybridization of two populations of marine opisthobranch with different developmental patterns. *Veliger* **26**(3): 199–206.
- Wolfe, G. R., F. X. Cunningham, D. Durnford, B. R. Green, and E. Gantt. 1994. Evidence for a common origin of chloroplasts with light-harvesting complexes of different pigmentation. *Nature* **367**: 566–568.
- Wollman, F.-A., L. Minai, and R. Nechushtai. 1999. The biogenesis and assembly of photosynthetic proteins in thylakoid membranes. *Biochim. Biophys. Acta* **1411**: 21–85.
- Zauner, S., M. Fraunholz, J. Wastl, S. Penny, M. Beaton, T. Cavalier-Smith, U.-G. Maier, and S. Douglas. 2000. Chloroplast protein and centrosomal genes, a tRNA intron, and odd telomeres in an unusually compact eukaryotic genome, the cryptomonad nucleomorph. *Proc. Natl. Acad. Sci. USA* **97**: 200–205.
- Zhang, Z., B. R. Green, and T. Cavalier-Smith. 1999. Single gene circles in dinoflagellate chloroplast genomes. *Nature* **400**: 155–159.

Asexual Reproduction in *Pygospio elegans* Claparède (Annelida, Polychaeta) in Relation to Parasitism by *Lepocreadium setiferoides* (Miller and Northup) (Platyhelminthes, Trematoda)

DEAN G. McCURDY*

Coastal Studies Center, 6775 College Station, Bowdoin College, Brunswick, Maine 04011-8465

Abstract. Life-history theory predicts that parasitized hosts should alter their investment in reproduction in ways that maximize host reproductive success. I examined the timing of asexual reproduction (fragmentation and regeneration) in the polychaete annelid *Pygospio elegans* experimentally exposed to cercariae of the trematode *Lepocreadium setiferoides*. Consistent with adaptive host response, polychaetes that became infected by metacercariae of trematodes fragmented sooner than unexposed controls. Parasites were not directly associated with fission in that exposed polychaetes that did not become infected also fragmented earlier than controls. For specimens of *P. elegans* that were not exposed to trematodes, new fragments that contained original heads were larger than those that contained original tails, whereas original head and tail fragments did not differ in size for infected polychaetes. In infected specimens, metacercariae were equally represented in original head and tail fragments and were more likely to be found in whichever fragment was larger. Despite early reproduction, parasitism was still costly because populations of *P. elegans* exposed to parasites were smaller than controls when measured 8 weeks later and because exposure to cercariae reduced survivorship of newly divided polychaetes. Taken together, my results suggest that early fragmentation is a host response to minimize costs associated with parasitism.

Introduction

Hosts respond to parasitism in a number of ways, which include avoidance of parasites in space or time (*e.g.*, mi-

gration; Folstad *et al.*, 1991), removal of parasites before they cause damage (*e.g.*, grooming; Léonard *et al.*, 1999), and immunological defense (*e.g.*, encapsulation; Kraaijeveld and Godfray, 1997). There is increasing evidence that hosts may also exhibit life-history adaptations to minimize the impacts of parasites on reproductive success (Minchella and LoVerde, 1981; Polak and Starmer, 1998; McCurdy *et al.*, 1999, 2000a). Life-history responses of hosts after exposure to parasites represent reallocations of energy in ways that increase reproductive success relative to non-responses. This type of reaction has been termed an adaptive host response (Minchella, 1985; Forbes, 1993). Unlike avoidance or resistance to parasites, life-history responses pose little or no maintenance costs to hosts (*i.e.*, no cost when parasites are absent) because the hosts do not alter their life histories until they come into contact with parasites (Minchella, 1985). Specifically, in systems where parasites pose greater costs to host energy budgets over time (decreasing future reproductive potential to a greater extent than current reproduction), hosts are expected to respond to infections by hastening their onset of reproduction. This response occurs, for example, in intertidal amphipods infected by trematodes (McCurdy *et al.*, 1999, 2000a). Although the reproductive success of hosts that respond through life-history variation is lower than that of hosts not exposed to parasites, it is greater than that of infected hosts that fail to respond (McCurdy *et al.*, 2001).

To date, tests of the hypothesis of the adaptive host response have been confined to hosts that reproduce sexually (Minchella and LoVerde, 1981; Polak and Starmer, 1998; McCurdy *et al.*, 1999, 2000a). However, the responses of sexual hosts can be difficult to interpret because selection may act differently on males and females to max-

Received 19 October 2000; accepted 10 April 2001.

* Current address: Department of Biology, Albion College, Albion, Michigan 49224.

E-mail: dmccurdy@albion.edu

imize reproductive success (Zuk, 1990), and because of factors specific to sexual mating systems (e.g., mate availability and choice; McCurdy *et al.*, 2000b; but see Minchella and LoVerde, 1981, for an exception). As a result, host investment in reproduction (reproductive effort) is assessed, but the actual consequences of this investment (reproductive success) are difficult to quantify (Perrin *et al.*, 1996; McCurdy *et al.*, 2000a).

I tested for adaptive host response in an asexual spionid polychaete, *Pygospio elegans*. This species is common in intertidal mudflats and sandflats throughout the Northern Hemisphere (Anger, 1984). Adults of this species construct tubes in the sediment and feed on detritus and phytoplankton (Anger *et al.*, 1986). Asexual reproduction in *P. elegans* is accomplished through transverse fragmentation, followed by rapid regeneration of missing components (Rasmussen, 1953; Hobson and Green, 1968; Gibson and Harvey, 2000). Wilson (1985) found that asexual reproduction in *P. elegans* is density- and resource-dependent in that populations grew larger when polychaetes were housed at low densities or provided with augmented levels of food. The impacts of parasitism on asexual reproduction and regeneration, however, have not been investigated in this or other species of polychaetes.

I investigated life-history responses of *P. elegans* to parasitism by exposing polychaetes to cercariae of the trematode *Lepocreadium setiferoides*. During the spring and summer, cercariae emerge from mud snails, *Ilyanassa obsoleta*, and infect spionid polychaetes as second-intermediate hosts; winter flounder, *Pseudopleuronectes americanus*, serve as final hosts of the parasite (Martin, 1938; McCurdy *et al.*, 2000c). In their polychaete host, trematodes do not reproduce. However, unlike many species of trematodes that emerge from *I. obsoleta*, metacercariae of *L. setiferoides* do not simply encyst within their second-intermediate hosts, but continue to grow and develop for several weeks (Martin, 1938; McCurdy, pers. obs.). Thus, the costs of parasitism to the energy budgets of polychaete hosts are expected to increase over time after infection.

Predictions

If *Pygospio elegans* responds to parasitism through life-history variation, I predicted that polychaetes would fragment soon after infection, before parasitism becomes costly. *P. elegans* also exhibits flexibility in asexual reproduction, as individual polychaetes may fragment into more than five pieces (Rasmussen, 1953; Gibson and Harvey, 2000). In light of this fact, I also expected that newly infected polychaetes might minimize the impacts of parasitism by isolating infection in small fragments or even lose infections by dividing across infected segments. In addition, *P. elegans* may also reproduce sexually (including poecilogonous development, with planktotrophic and adelophagic

larvae; Morgan *et al.*, 1999), so I examined polychaetes for evidence of sexual reproduction as a possible response to parasitism. For infected polychaetes, the advantages of sexual reproduction might include enhanced dispersal of offspring (Chia *et al.*, 1996)—possibly away from infected snails—and increased genetic variation (Lively, 1996). In fact, the evolution and maintenance of sexual reproduction have been explained as a host response to parasitism because sex is more likely to produce individuals that are able to escape parasitism over evolutionary timescales (reviewed by Hurst and Peck, 1996).

In addition to investigating host responses to parasitism, I assessed the impact of parasitism by *Lepocreadium setiferoides* on the asexual reproductive success of *P. elegans* over an 8-week period. I also assessed the costs of parasitism to survivorship and regeneration of polychaetes that had previously been cut into two fragments, mimicking the fragmentation that results from asexual reproduction or sublethal predation (Woodin, 1982; Zajac, 1995). In all cases, I considered two additional possibilities, other than adaptive host response, to explain observed changes in host behavior and development in relation to parasitism. First, such changes might have been due to adaptations of parasites to increase transmission rates (parasite manipulation; Poulin *et al.*, 1994). This possibility is particularly relevant to the parasite-host system I studied because there is evidence for parasite manipulation by cercariae and metacercariae of another trematode that parasitizes *Ilyanassa obsoleta* (Curtis, 1987; McCurdy *et al.*, 1999, 2000a). Second, observed changes in behavior might have been due to side effects of infection that are not adaptive for the host or parasite (Poulin, 1995).

Materials and Methods

Collections and infection protocols

I collected specimens of *Pygospio elegans* from a mudflat between Wyer and Orr's Islands, Harpswell, Maine (43°47'N, 69°58'W). This mudflat is located in Casco Bay, Gulf of Maine, and has semidiurnal tides that range from 2 to 4 m (Born, 1999). I chose to sample at the Wyer-Orr's mudflat because densities of *P. elegans* were high there ($>20,000 \text{ m}^{-2}$), but *Ilyanassa obsoleta* and its associated cercarial parasites were rare ($<0.25 \text{ snails m}^{-2}$), minimizing the likelihood that polychaetes used in experiments were already infected. I collected polychaete tubes in the mid-intertidal zone by sieving the top 5 cm of mud (500- μm mesh) and transported tubes to the nearby running-seawater laboratory at the Coastal Studies Center of Bowdoin College for sorting. I retained only undamaged, entire adult polychaetes ($>2 \text{ mm}$) that were not about to fragment (detectable because *P. elegans* constricts just prior to fission; Gibson and Harvey, 2000).

To obtain cercarial trematodes for experiments, I col-

lected specimens of *I. obsoleta* from throughout the intertidal zone at Strawberry Creek, Great Island, Maine (43°49'N, 69°58'W). This mudflat is located 2.5 km from the Wyer-Orr's mudflat and supports high densities of *I. obsoleta* ($>10 \text{ m}^{-2}$). In the laboratory, I housed 550 mud snails in separate 9-oz plastic cups with 125 ml of filtered seawater (55 μm , 31 ppt, 23 °C). I retained only large snails ($>15 \text{ mm}$, tip of apex to lip of siphonal canal) because previous studies have shown that the prevalence of *Leporecreadium setiferoides* increases with shell height of snails (Curtis, 1997; McCurdy *et al.*, 2000c). After 30 h, I examined each cup for cercariae of *L. setiferoides* (identified using McDermott, 1951), combined cercarial-infested seawater from cups of six snails that had shed cercariae, and pipetted 20 ml of the solution into each dish that contained a polychaete that was to be exposed. Unexposed polychaetes each received 20 ml of seawater from six cups that contained snails that did not shed cercariae (confirmed by dissection, as cercarial release is a poor indicator of infection status; Curtis and Hubbard, 1990).

Experiments

To investigate the impact of parasites on the timing of asexual reproduction, I individually housed 52 adult specimens of *P. elegans* in 150-ml custard dishes filled with unfiltered seawater with or without cercariae (18 °C, 16 h light day⁻¹). After 24 h, I transferred each polychaete to a new dish filled with seawater and lined with defaunated mud (prepared by passing mud through a 425- μm sieve and heating it to 70 °C). Every 24 h, I suspended each dish from a harness and determined the status of each polychaete by observing its tube (or tubes) through the bottom of its dish with the aid of a fiber-optic illuminator and 10 \times magnifying loupe. Polychaetes could easily be observed because they constructed tubes that opened against the bottoms of their dishes. Polychaetes were fed the pea-flower-based supplement Liquifry Marine (Interpet Inc.; Brown *et al.*, 1999) every 3 days (concentration = 1 drop l⁻¹) following a complete change of water. I removed polychaetes from the experiment when they died or fragmented, and I measured the relaxed length of all fragments with an ocular micrometer (nearest 0.1 mm; Gudmundsson, 1985). I then dissected each fragment to determine if it was infected by trematode metacercariae and compared median time-to-fragmentation among exposed but uninfected, exposed and infected, and unexposed polychaetes. In making this comparison, I separated exposed but uninfected polychaetes from unexposed ones because of the possibility that host response might be associated with indirect cues associated with parasitism (*i.e.*, response might not require an actual infection to occur). To compare time-to-fragmentation, I applied a non-parametric Kruskal-Wallis ANOVA because the residuals

for all groups were non-normal. I then applied Dunn's method to compare differences among medians (Zar, 1996).

To investigate how exposure to parasites affected the reproductive success of *P. elegans*, I randomly housed 18 sets of 10 polychaetes (hereafter referred to as populations of polychaetes) in separate dishes and exposed half of the sets to cercariae of trematodes (housing conditions for polychaetes were as described above). Because the infection status of polychaetes that died during this experiment could not be determined without disturbing surviving polychaetes, I assessed rates of experimental and background infection by randomly removing two sentinel populations after 3 days: a population of polychaetes that had been exposed to cercariae, and a population of unexposed polychaetes. Rates of infection at that time represented maximum levels that could occur because cercariae of *L. setiferoides* survive for less than 48 h outside a host (Stunkard, 1972). After 8 weeks, I removed the remaining dishes and processed each population by counting the number of polychaetes retained after sieving (425- μm mesh) and dissecting each polychaete to determine its infection status.

To assess survivorship and regenerative ability of newly divided polychaetes in relation to parasitism, I cut 59 polychaetes into two fragments and exposed 30 pairs of fragments to cercariae. Cutting each polychaete resulted in a smooth, clean blastema similar to that resulting from sublethal predation or asexual fragmentation (Gibson and Harvey, 2000; pers. obs.). To mimic conditions in nature, where newly fragmented polychaetes generally remain in the same burrow during regeneration (Gudmundsson, 1985; Gibson and Harvey, 2000), I individually housed original head and tail fragments together in a dish with seawater and mud (housing conditions as described above). To avoid disturbing fragments (as above), I assessed initial rates of infection at 3 days after exposure or non-exposure by removing and dissecting randomly chosen sentinel pairs of exposed fragments ($n = 10$ polychaetes) and unexposed fragments ($n = 10$ polychaetes). At 10 days after exposure or non-exposure, I removed all remaining fragments, measured their lengths, and determined their infection status.

Results

Parasitism and host fragmentation

In the experiment investigating the impact of trematodes on the timing of asexual reproduction in *Pygospio elegans*, parasite prevalence was low (42.3% of polychaetes exposed became infected; $n = 26$). Asexual fragmentation always yielded two fragments; one containing the original head and thorax and a second containing the original tail (see Gibson and Harvey, 2000, for a description of body components). In all cases, polychaetes fragmented within 24 h of observable constrictions. Time-to-fragmentation differed between exposed and infected, exposed but uninfected, and unexposed

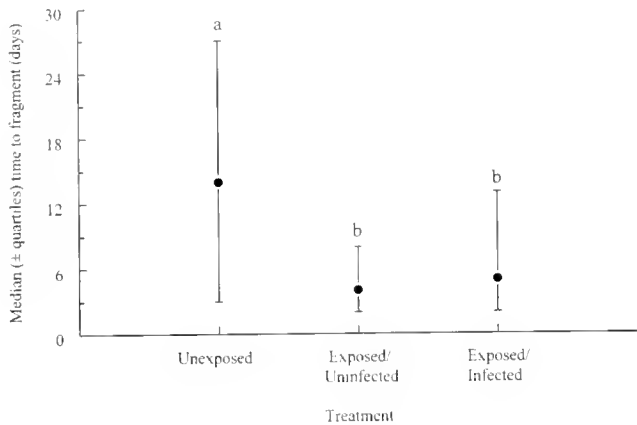


Figure 1. Median (\pm quartiles) numbers of days for asexual reproduction to occur in individuals of *Pygospio elegans* that were experimentally infected, exposed but not infected, and not exposed to cercariae of the trematode *Lepocreadium setiferoides*. Polychaetes and parasites were collected from mudflats in Harpswell, Maine, and housed in the laboratory. Medians with the same letter do not differ significantly from each other.

polychaetes ($H_{(2,52)} = 10.56$, $P < 0.01$; Fig. 1). Specifically, polychaetes that were exposed to cercariae but did not become infected fragmented earlier than unexposed polychaetes ($Q = 2.99$, $P < 0.005$), as did polychaetes that were exposed and became infected ($Q = 2.16$, $P < 0.05$). Of all polychaetes that were exposed to cercariae, however, infection status did not affect time-to-fragmentation ($Q = 0.49$, NS).

For unexposed polychaetes and exposed polychaetes that remained uninfected, fragments that contained original heads were larger than those that contained original tails, whereas lengths of original head and tail fragments did not differ for infected polychaetes (Table 1). In infected polychaetes, parasites were just as likely to be found in fragments that contained original heads ($n = 5$) as those that contained original tails ($n = 5$) (an additional polychaete harbored a metacercaria in each new fragment). For infected polychaetes, infected fragments were significantly larger than uninfected fragments (infected fragments: $\bar{x} \pm s = 2.0 \pm 0.2$ mm; uninfected fragments: $\bar{x} \pm s = 1.4 \pm 0.2$ mm; paired $t_{(9)} = 2.28$, $P < 0.05$), and in 9 of 10 cases, metacercariae were found in the larger fragment ($X^2_{(1)} = 6.4$, $P = 0.01$). Cercariae were not observed to penetrate segments that comprised, or were adjacent to, planes of fission.

Parasitism and host asexual reproductive success

At 3 days post exposure, 17 of 20 fragments (8.5 of the original 10 polychaetes) were alive in the sentinel population that was exposed to cercariae. Only one fragment in this population was infected by trematodes—a living tail fragment infected with a single metacercaria. In the sentinel population that was not exposed to cercariae, 18 of 20

fragments were alive after 3 days and no parasites were found (one fragment, containing an original head, was lost during processing). At 8 weeks after exposure or non-exposure, I saw no evidence of recent fission in polychaetes as all fragments had complete or nearly complete heads and tails. Therefore, I considered all fragments equally when measuring population sizes at that time. Populations of polychaetes that were exposed to cercariae were smaller than those that were not exposed (exposed populations: $\bar{x} \pm s = 17.3 \pm 2.4$ polychaetes; unexposed populations: $\bar{x} \pm s = 29.8 \pm 3.7$ polychaetes; $t_{(14)} = 2.84$, $P = 0.01$). When dissected, only seven polychaetes in exposed populations were infected (one polychaete in each of three populations and two polychaetes in each of two populations), and none of the polychaetes in any of the unexposed populations was infected.

Considering sentinel polychaetes that had been cut into two pieces, 2 of 10 polychaetes exposed to cercariae were infected at 3 days post-exposure. In each case, the infection was in the original head fragment and by a single metacercaria. None of the 10 unexposed polychaetes was infected. When examining the remaining polychaetes 7 days later, I found that both head and tail fragments of exposed polychaetes were less likely to be alive than the respective fragments of unexposed polychaetes (head fragments: $X^2_{(1)} = 8.07$, $P < 0.005$; tail fragments: $X^2_{(1)} = 12.22$, $P < 0.001$; Fig. 2). Only two exposed polychaetes were infected by metacercariae (one polychaete had an infected tail fragment and another an infected head fragment; $n = 20$), and no unexposed polychaetes were infected ($n = 19$). In all cases, regeneration of "lost" components was nearly complete by 10 days, and lengths of original head and tail fragments did not differ in relation to exposure (unexposed heads: $\bar{x} \pm SE = 2.65 \pm 0.15$; exposed heads: $\bar{x} \pm SE = 2.56 \pm 0.26$; $t_{(26)} = 0.32$, NS; unexposed tails: $\bar{x} \pm SE =$

Table 1

Sizes of fragments produced by asexual fission of *Pygospio elegans* in relation to parasitism

	Fragment length (mm)		Paired t test
	Heads	Tails	
Unexposed	2.1 ± 0.2	1.57 ± 0.1	$t_{(23)} = 2.7$, $P = 0.01$
Exposed but uninfected	2.4 ± 0.2	1.57 ± 0.2	$t_{(14)} = 2.3$, $P = 0.04$
Exposed and infected	1.9 ± 0.2	1.71 ± 0.2	$t_{(10)} = 0.8$, $P = 0.44$

Data are means and standard errors for lengths of fragments containing original heads and those containing original tails of polychaetes that were experimentally infected, exposed but not infected, and not exposed to cercariae of the trematode *Lepocreadium setiferoides*. The last column shows results from paired t tests for lengths of original head versus tail fragments.

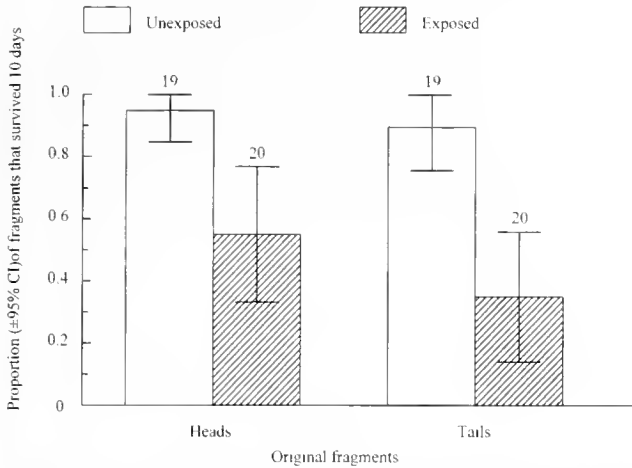


Figure 2. Proportions ($\pm 95\%$ confidence intervals) of original head and tail fragments of individuals of *Pygospio elegans* that survived for 10 days in the laboratory following exposure or non-exposure to cercariae of the trematode *Lepocreadium setiferoides*. Sample sizes are shown above the bars.

2.71 ± 0.19 ; exposed tails: $\bar{x} \pm SE = 2.49 \pm 0.28$; $t_{(22)} = 0.63$, NS).

Discussion

Parasitism and host fragmentation

In support of the hypothesis of adaptive host response I found that specimens of *Pygospio elegans* infected by metacercariae of *Lepocreadium setiferoides* hastened their onset of asexual reproduction relative to unexposed controls. By doing so, polychaetes may be expected to achieve greater reproductive success than if they had failed to respond because of increasing costs associated with parasitism over time (Forbes, 1993). However, my observation that early fragmentation also occurred in exposed polychaetes that remained uninfected complicates this interpretation. In a study that separated hosts by exposure and infection status, Minchella and Loverde (1981) found that freshwater snails of the species *Biomphalaria glabrata* increased their rates of early egg laying when infected by *Schistosoma mansoni*, but that the rates for exposed but uninfected individuals and unexposed controls did not differ. These authors argued that only infected snails responded because successful parasitism was associated with a high cost to future reproduction (castration).

For individuals of *P. elegans* exposed to, but not infected by, cercariae, early reproduction could still be an adaptive host response if exposure to cercariae in nature is a reliable indicator that costly infections will soon result (Minchella, 1985). Support for this idea comes from the observation that *Ilyanassa obsoleta* infected by *L. setiferoides*, although uncommon across mudflats, can remain for several months in small patches where some *P. elegans* are found (Mc-

Curdy *et al.*, 2000c). As a result, thousands of cercariae are shed in areas where infections are most likely to occur. Additional information on the infection process of *L. setiferoides* is necessary to determine whether polychaetes detect cercariae, and whether the exposure-related response resulted from the presence of cercariae or from failed attempts at penetration. There is evidence from other parasite-host systems that invertebrates can detect and exhibit anti-parasite behaviors to minimize the likelihood of infection (*e.g.*, Léonard *et al.*, 1999).

Early fragmentation of *P. elegans* is unlikely to be a parasite adaptation, because it apparently does not increase transmission rates for cercariae or metacercariae. Specifically, fragmentation was not associated with increased susceptibility to parasitism: most polychaetes fragmented after free-living cercariae would have (≥ 48 h; Stunkard, 1972). For metacercariae, residing in small fragments would not appear to benefit transmission to final hosts, because flounder select prey at larger sizes relative to conspecifics, and even small differences in prey size preference can profoundly influence the energy budgets of predators foraging on mudflats (MacDonald and Green, 1986; Boates and Smith, 1989; Keats, 1990). To assess whether early fragmentation is actually adaptive for parasites or hosts, the consequences of early fragmentation could be further explored by constructing a model derived from empirical observations of parasites, their intermediate hosts, and the predators that are their final hosts. This approach was used recently to show that the early onset of receptivity to mating observed in females of the amphipod *Corophium volutator* infected by the trematode *Gynaecotyla adunca* resulted in greater reproductive success for the amphipods than if they had waited to become receptive at the optimal time for uninfected females (McCurdy *et al.*, 2001).

I found no evidence that fragmentation of *P. elegans* served to isolate or remove metacercariae, in that fission produced only two fragments, the smaller of which almost never contained metacercariae. It is unclear whether the greater presence of metacercariae in larger fragments is adaptive for the parasite or its host or whether larger fragments merely represent larger targets for parasites. Metacercariae might benefit from residing in larger fragments because of the availability of additional resources for parasite development or the possibility of a greater transmission rate to final hosts (as stated above, flounder tend to select larger prey). If residing in larger fragments is parasite-mediated, the observation that metacercariae develop near the site of initial penetration (Stunkard, 1972; pers. obs) indicates that the mechanism does not involve movements by metacercariae through the host coelom and into larger fragments. Fragmentation could also be interpreted as a host response: If larger fragments are better able to tolerate stresses associated with parasitism, the result would be a net reproductive benefit to hosts. In fact, host response need not

be exclusive of benefits to parasites, depending on the timing of altered behavior of infected hosts (McCurdy *et al.*, 1999). Simulated parasites such as Sephadex beads (Suwan-chaichinda and Paskewitz, 1998) could be used to help separate effects mediated by the parasite from those mediated by the host. Experiments with simulated parasites would provide cues to the host that it has become infected while removing the possibility of parasite manipulation.

Across all experiments, I found no evidence for onset of sexual reproduction, observing neither eggs nor spermatozoa. Seasonal constraints may have precluded sexual reproduction, which usually occurs only during the winter in *P. elegans* (Rasmussen, 1953; Gudmundsson, 1985; Wilson, 1985). However, even if the polychaetes had shown evidence of sexual reproduction, this tactic might be expected to increase reproductive success only if mates were available; an unlikely event given the rarity of parasites in natural populations of *P. elegans* (above).

Parasitism and host asexual reproductive success

I found that even a low level of exposure to cercariae (on average, 8% of cercariae that a single snail sheds in 30 h) reduced the asexual reproductive success of *P. elegans* (45%, measured in populations 8 weeks after exposure). In a related finding from another experiment, both head and tail fragments were less likely to survive to complete regeneration than were unexposed fragments. Direct effects of parasitism are not sufficient to account for these results given that few exposed polychaetes actually became infected in either experiment. One possibility is to explain the reduced reproductive success of exposed but uninfected hosts as the result of a trade-off between host reproductive effort and costly activities associated with defenses against parasites. Recent work has shown that hosts exposed to parasites may trade off energy used in reproduction for behaviors or immune responses to resist parasites (Sheldon and Verhulst, 1996; Léonard *et al.*, 1999).

Regardless of the underlying causes, the dramatic reduction in reproductive success of *P. elegans* after exposure to cercariae has implications for natural populations of this species and for soft-bottom intertidal communities. *Pygospio elegans* often dominates such communities, and thus can directly affect the distribution and abundance of other infauna (Wilson, 1983; Brey, 1991; Kube and Powilleit, 1997). In addition, it is possible that parasitism of *P. elegans* may influence the structure of intertidal communities by altering or creating engineering functions in hosts. Engineering functions are those that produce new habitat as a result of changes in behaviors or life history associated with parasitism (Thomas *et al.*, 1999). Clearly, researchers should consider the impacts of parasites on the ecology and evolution of the reproductive strategies of marine invertebrates and on the structure of infaunal communities.

Acknowledgments

I thank Glenys Gibson for her suggestions on experimental design and Mark Forbes for our many discussions about life-history theory. Funding was provided by postdoctoral fellowships from the Natural Sciences and Engineering Research Council of Canada and the Coastal Studies Center, Bowdoin College.

Literature Cited

- Anger, V. 1984. Reproduction in *Pygospio elegans* (Spionidae) in relation to its geographical origin and to environmental conditions: a preliminary report. *Fortschr. Zool.* **29**: 45–51.
- Anger, K., V. Anger, and E. Hagmeier. 1986. Laboratory studies on larval growth of *Polydora ligni*, *Polydora ciliata*, and *Pygospio elegans* (Polychaeta: Spionidae). *Helgol. Meeresunters.* **40**: 377–395.
- Boates, J. S., and P. C. Smith. 1989. Crawling behaviour of the amphipod, *Corophium volutator* and foraging by semipalmated sandpipers, *Calidris pusilla*. *Can. J. Zool.* **67**: 457–462.
- Born, M. A. 1999. *Tidelog: Northern New England Edition*. Pacific Publishers, Bolinas, CA.
- Brey, T. 1991. Interactions in soft bottom benthic communities: quantitative aspects of behaviour in the surface deposit feeders *Pygospio elegans* (Polychaeta) and *Macoma balthica* (Bivalvia). *Helgol. Meeresunters.* **45**: 301–316.
- Brown, R. J., M. Conradi, and M. H. Depledge. 1999. Long-term exposure to 4-nonylphenol affects sexual differentiation and growth of the amphipod *Corophium volutator* (Pallas, 1766). *Sci. Total Environ.* **233**: 77–88.
- Chia, F. S., G. Gibson, and P. Y. Qian. 1996. Poecilogony as a reproductive strategy of marine invertebrates. *Oceanol. Acta* **19**: 203–208.
- Curtis, L. A. 1987. Vertical distribution of an estuarine snail altered by a parasite. *Science* **235**: 1509–1511.
- Curtis, L. A. 1997. *Ilyanassa obsoleta* (Gastropoda) as a host for trematodes in Delaware estuaries. *J. Parasitol.* **83**: 793–803.
- Curtis, L. A., and K. M. K. Hubbard. 1990. Trematode infections in a gastropod host misrepresented by observing shed cercariae. *J. Exp. Mar. Biol. Ecol.* **143**: 131–137.
- Folstad, I., A. C. Nilssen, O. Halvorsen, and J. Andersen. 1991. Parasite avoidance: the cause of post-calving migrations in Rangifer? *Can. J. Zool.* **69**: 2423–2429.
- Forbes, M. R. L. 1993. Parasitism and host reproductive effort. *Oikos* **67**: 444–450.
- Gibson, G. D., and J. M. L. Harvey. 2000. Morphogenesis during asexual reproduction in *Pygospio elegans* Claparede (Annelida, Polychaeta). *Biol. Bull.* **199**: 41–49.
- Gudmundsson, H. 1985. Life history patterns of polychaete species of the Family Spionidae. *J. Mar. Biol. Assoc. UK* **65**: 93–111.
- Hobson, K. D., and R. H. Green. 1968. Asexual and sexual reproduction of *Pygospio elegans* (Polychaeta) in Barnstable Harbor, Massachusetts. *Biol. Bull.* **135**: 410 (abstract).
- Hurst, L. D., and J. R. Peck. 1996. Recent advances in understanding of the evolution and maintenance of sex. *Trends Ecol. Evol.* **11**: 46–52.
- Keats, D. W. 1990. Food of winter flounder *Pseudopleuronectes americanus* in a sea urchin dominated community in eastern Newfoundland (Canada). *Mar. Ecol. Prog. Ser.* **60**: 13–22.
- Kraaijeveld, A. R., and C. J. Godfray. 1997. Trade-off between parasitoid resistance and larval competitive ability in *Drosophila melanogaster*. *Nature* **389**: 278–280.
- Kube, J., and M. Powilleit. 1997. Factors controlling the distribution of *Marenzelleria cf. viridis*, *Pygospio elegans* and *Streblospio shrubsolii*

- (Polychaeta: Spionidae) in the southern Baltic Sea, with special attention for the response to an event of hypoxia. *Aquat. Ecol.* **31**: 187–198.
- Léonard, N., M. R. Forbes, and R. L. Baker. 1999.** Effects of *Limnochares americana* (Hydrachnidia: Limnocharidae) mites on life history traits and grooming behaviour of its damselfly host, *Enallagma ebrium* (Odonata: Coenagrionidae). *Can. J. Zool.* **77**: 1615–1622.
- Lively, C. M. 1996.** Host-parasite coevolution and sex: Do interactions between biological enemies maintain genetic variation and cross-fertilization? *Bioscience* **46**: 107–114.
- Macdonald, J. S., and R. H. Green. 1986.** Food resource utilization by five benthic feeding fish in Passamaquoddy Bay, New Brunswick (Canada). *Can. J. Fish. Aquat. Sci.* **43**: 1534–1546.
- Martin, W. E. 1938.** Studies on trematodes of Woods Hole: the life cycle of *Lepocreadium setiferoides* (Miller and Northup), *Allocreadidae*, and the description of *Cercaria cumingiae* N. Sp. *Biol. Bull.* **75**: 463–474.
- McCurdy, D. G., M. R. Forbes, and J. S. Boates. 1999.** Testing alternative hypotheses for variation in amphipod behaviour and life history in relation to parasitism. *Int. J. Parasitol.* **29**: 1001–1009.
- McCurdy, D. G., M. R. Forbes, and J. S. Boates. 2000a.** Male amphipods increase their mating effort before behavioural manipulation by trematodes. *Can. J. Zool.* **78**: 606–612.
- McCurdy, D. G., J. S. Boates, and M. R. Forbes. 2000b.** Reproductive synchrony in the intertidal amphipod *Corophium volutator*. *Oikos* **88**: 301–308.
- McCurdy, D. G., J. S. Boates, and M. R. Forbes. 2000c.** Spatial distribution of the intertidal snail *Ilyanassa obsoleta* in relation to parasitism by two species of trematodes. *Can. J. Zool.* **78**: 1137–1143.
- McCurdy, D. G., J. S. Boates, and M. R. Forbes. 2001.** An empirical model of the optimal timing of reproduction for female amphipods infected by trematodes. *J. Parasitol.* **87**: 24–31.
- McDermott, J. J. 1951.** Larval trematode infection in *Nassa obsoleta* (Say), from New Jersey waters. Ph.D. dissertation, Rutgers University, Newark, NJ.
- Minchella, D. J. 1985.** Host life-history variation in response to parasitism. *Parasitology* **90**: 205–216.
- Minchella, D. J., and C. M. LaVerde. 1981.** A cost of increased early reproductive effort in the snail *Biomphalaria glabrata*. *Am. Nat.* **118**: 876–881.
- Morgan, T. S., A. D. Rogers, G. L. J. Paterson, L. E. Hawkins, and M. Sheader. 1999.** Evidence for poecilogony in *Pygospio elegans* (Polychaeta: Spionidae). *Mar. Ecol. Prog. Ser.* **178**: 121–132.
- Perrin, N., P. Christie, and H. Richner. 1996.** On host life-history response to parasitism. *Oikos* **75**: 317–210.
- Polak, M., and W. T. Starmer. 1998.** Parasite-induced risk of mortality elevates reproductive effort in *Drosophila*. *Proc. R. Soc. Lond. B* **265**: 2197–2201.
- Poulin, R. 1995.** “Adaptive” changes in behaviour of parasitized animals: a critical review. *Int. J. Parasitol.* **25**: 1371–1383.
- Poulin, R., J. Brodeur, and J. Moore. 1994.** Parasite manipulation of behaviour: should hosts always lose? *Oikos* **70**: 479–484.
- Rasmussen, E. 1953.** Asexual reproduction in *Pygospio elegans* Claparède (Polychaeta sedentaria). *Nature* **171**: 1161–1162.
- Sheldon, B. C., and S. Verhulst. 1996.** Ecological immunology: costly parasite defenses and trade-offs in evolutionary ecology. *Trends Ecol. Evol.* **11**: 317–321.
- Stunkard, H. W. 1972.** Observations on the morphology and life-history of the digenetic trematode, *Lepocreadium setiferoides* (Miller and Northup, 1926) Martin, 1938. *Biol. Bull.* **142**: 326–334.
- Suwanchaichinda, C., and S. M. Paskewitz. 1998.** Effects of larval nutrition, adult body size, and adult temperature on the ability of *Anopheles gambiae* (Diptera: Culicidae) to melanize Sephadex® beads. *J. Med. Entomol.* **35**: 157–161.
- Thomas, F., R. Poulin, T. de Meccüs, J. Guégan, and F. Renaud. 1999.** Parasites and ecosystem engineering: what roles could they play? *Oikos* **84**: 167–171.
- Wilson, W. H., Jr. 1983.** The role of density dependence in a marine infaunal community. *Ecology* **64**: 295–306.
- Wilson, W. H., Jr. 1985.** Food limitation of asexual reproduction in a spionid polychaete. *Int. J. Invertebr. Reprod. Dev.* **8**: 61–65.
- Woodin, S. A. 1982.** Browsing: important in marine sedimentary environments? Spionid polychaete examples. *J. Mar. Biol. Assoc. UK* **60**: 35–45.
- Zajac, R. N. 1995.** Sublethal predation on *Polydora cornuta* (Polychaeta: Spionidae): patterns of tissue loss in a field population, predator functional response and potential demographic impacts. *Mar. Biol.* **123**: 531–541.
- Zar, J. H. 1996.** *Biostatistical Analysis*. Prentice-Hall, Upper Saddle River, NJ.
- Zuk, M. 1990.** Reproductive strategies and disease susceptibility: an evolutionary viewpoint. *Parasitol. Today* **6**: 231–233.

Delayed Insemination Results in Embryo Mortality in a Brooding Ascidian

J. STEWART-SAVAGE^{1,*}, AIMEE PHILLIPPI², AND PHILIP O. YUND²

¹*Department of Biological Sciences, University of New Orleans, New Orleans, Louisiana 70148; and*

²*Darling Marine Center, School of Marine Sciences, University of Maine, Walpole, Maine 04573*

Abstract. We explored the effects of temporal variation in sperm availability on fertilization and subsequent larval development in the colonial ascidian *Botryllus schlosseri*, a brooding hermaphrodite that has a sexual cycle linked to an asexual zooid replacement cycle. We developed a method to quantify the timing of events early in this cycle, and then isolated colonies before the start of the cycle and inseminated them at various times. Colony-wide fertilization levels (assayed by early cleavage) increased from zero to 100% during the period when the siphons of a new generation of zooids were first opening, and remained high for 24 h before slowly declining over the next 48 h. Because embryos are brooded until just before the zooids degenerate at the end of a cycle, delayed fertilization might also affect whether embryos can complete development within the cycle. Consequently, we also determined the effect of delayed insemination on successful embryo development through larval release and metamorphosis. When fertilization was delayed beyond the completion of siphon opening, there was an exponential decline in the percentage of eggs that ultimately produced a metamorphosed larva at the end of the cycle. Thus, even though the majority of oocytes can be fertilized when insemination is delayed for up to 48 h, the resulting embryos cannot complete development before the brooding zooids degenerate.

Introduction

Field experiments have contributed greatly to current understanding of fertilization processes in free-spawning marine invertebrates (reviewed by Levitan and Petersen, 1995; Yund, 2000). In response to the evidence of potential

sperm limitation reported in some field studies, many laboratory studies have started to explore diverse related aspects of invertebrate reproductive biology such as gamete viscosity (Thomas, 1994a,b), egg size and sperm swimming speed (Levitan, 1998), egg longevity (Meidel and Yund, 2001), sperm morphology (Eckelbarger *et al.*, 1989a,b), and the kinetics of fertilization (Young, 1994; Levitan, 1998; Powell *et al.*, 2001). However, results from laboratory studies have in turn led some authors to question the extent to which simple field fertilization experiments adequately mimic the details of fertilization processes in nature (*e.g.*, Thomas, 1994a,b; Meidel and Yund, 2001). Field experiments may often circumvent aspects of reproductive strategies that have evolved to mitigate sperm limitation (Yund, 2000). Hence laboratory experiments still play a vital role in understanding reproductive strategies, and field fertilization studies should endeavor to incorporate the details of the fertilization process gleaned from laboratory work.

Performing realistic field experiments with marine invertebrates that brood embryos presents challenges that are very different from those faced when dealing with broadcast spawners. The biggest challenge with field fertilization studies of broadcasters is interpreting results obtained by artificially holding eggs in a concentrated group (*e.g.*, Levitan and Young, 1995; Wahle and Peckham, 1999) or by removing them from the water column after only a brief interval (Levitan, 1991; Coma and Lasker, 1997). This issue is moot with brooders, who by definition retain eggs and have internal fertilization. However, a different set of problems merits further consideration. The precise timing of egg viability, sperm release, and fertilization itself is often less well understood than in broadcasters. Sperm function may be regulated by the female through sperm chemotaxis (Miller, 1985), activation (Bolton and Havenhand, 1996), or storage (Bishop and Ryland, 1991). In the latter case, the

Received 20 October 2000; accepted 8 March 2001.

* To whom correspondence should be addressed. E-mail: jssavage@uno.edu

temporal pattern of fertilization within a female may be uncoupled from the pattern of sperm release by males. In hermaphrodites, the potential for self-fertilization is a concern, and genetic analyses of paternity may be required to conclusively exclude selfing in some taxa (Yund and McCartney, 1994). For some brooders, the actual path of sperm access to eggs is poorly understood. Information on all of these topics is critical both to the design of more realistic field fertilization studies and to the interpretation of existing studies.

The colonial ascidian *Botryllus schlosseri* is a useful model for field fertilization studies (Grosberg, 1991; Yund and McCartney, 1994; Yund, 1995, 1998). Fertilization is internal, and embryos are brooded until released as tadpole larvae (Milkman, 1967). When colonies are grown on glass surfaces, egg production can be quantified non-destructively (Yund *et al.*, 1997), thus permitting estimation of fertilization levels by comparing egg and embryo counts (Yund, 1995, 1998). Although the general time of fertilization within the life cycle (*i.e.*, temporal resolution on the order of a day) has long been known (Milkman, 1967), the finer-scale timing (temporal resolution on the order of hours) has not been explored. Many authors have assumed that the apparent temporal separation of fertilization and sperm release prevents self-fertilization (*e.g.*, Milkman, 1967; Grosberg, 1987; Yund and McCartney, 1994), but we have recently shown (Stewart-Savage and Yund, 1997) that sperm release commences several days earlier than previously thought. Although sperm storage has been demonstrated in another colonial ascidian (Bishop and Ryland, 1991; Bishop and Sommerfeldt, 1996), past workers have implicitly assumed that storage is unlikely in *B. schlosseri* (Milkman, 1967; Grosberg, 1991; Yund, 1995, 1998). To the best of our knowledge, this assumption has never been explicitly tested. To address this interrelated set of issues, this paper explores the effect of variation in the timing of fertilization on fertilization levels and subsequent larval development in *B. schlosseri*, and compares those results with published information on the timing of sperm release.

Materials and Methods

Study organism

Colonies of *Botryllus schlosseri* are composed of asexually produced zooids arranged in clusters, or systems, with all zooids in a system sharing a common exhalant siphon. Throughout the life of a colony, all zooids periodically undergo a synchronous asexual zooid replacement cycle in which a new generation of zooids, termed buds, forms between the existing zooids (Berrill, 1941; Izzard, 1973). At the end of the life span of adult zooids (about 8 days at 16 °C; cycle length is temperature dependent), the buds expand, take over the function of the previous generation of zooids (which are quickly resorbed), and then commence

their sexual reproductive cycle. The sexual cycle includes the internal fertilization of the mature eggs soon after the inhalant siphons open (Milkman, 1967); the continuous release of sperm starting 16 h later (Stewart-Savage and Yund, 1997); and the brooding of developing embryos, which are released just before the zooids degenerate at the end of the cycle (Milkman, 1967).

Standard methods

The colonies of *B. schlosseri* that were employed in this study were collected from the Damariscotta River, Maine. Animals were grown on glass microscope slides in the flowing seawater system at the University of Maine's Darling Marine Center. Field-collected colonies that had been established in laboratory culture were divided to provide clonal replicates (ramets) of genotypes. Colonies employed in all experiments were monitored for the approach of takeover (the transition between zooid generations). When colonies were about to commence takeover (late stage 5 through early stage 6 by the criteria of Milkman, 1967), they were isolated in 50 ml of sperm-free (aged >24 h) seawater. Isolated colonies were housed in an incubator at 16 °C (range: 14–18 °C) and fed phytoplankton (*Dunaliella* sp.) at densities of approximately 10⁵ cells/ml. Water and food were changed twice daily. Colonies were monitored for siphon opening and then isolated in individual 250-ml containers with algae (water and food were changed daily) until exposed to sperm. Sperm exposure was accomplished by placing colonies in a flowing seawater tank in proximity to numerous male-phase colonies (>24 h after siphon opening; Stewart-Savage and Yund, 1997) for 1 h. After insemination, colonies were rinsed with aged seawater and returned to isolation.

Experimental protocols

To standardize insemination times, we first had to accurately quantify the start of the reproductive cycle (*i.e.*, the functional opening of siphons). Inhalant siphons are formed early in the takeover process, but the common exhalant siphon of a system generally does not form until near the end. However, it is difficult to ascertain functional siphon opening on morphological criteria alone. In the course of other work, we observed that the consumption of green algae immediately turned the digestive systems of actively feeding zooids (*i.e.*, those that must have open siphons) green. Consequently, we used algal uptake as an assay for siphon opening. To establish the temporal pattern of siphon opening, we isolated 14 colonies and briefly exposed them to algae three to four times during the process of takeover. At each sample interval we recorded the percentage of siphons that were open (% of zooids with green digestive systems). From these data we calculated an average rate of siphon opening. This approach subsequently allowed us to

make single observations of the percentage of siphons that were open and back-calculate the time of the first siphon opening. Both of our other experiments use this approach to estimate the time of initial siphon opening, and the timing of insemination is expressed relative to this event.

To examine the effect of the timing of fertilization on fertilization levels, we exposed colonies to sperm through a range of different times after siphon opening (0.5 to 96 h; $n = 79$). Colonies with about 20 eggs (mean of $20.0 \pm$ standard error of 11.6) were utilized throughout, and all eggs and embryos in a colony were surgically removed 10–18 h after insemination and scored for successful development. Initial studies indicated that embryos should be in the 8-cell to the 32-cell stages during this time range. Uncleaved eggs were scored as unfertilized, as were embryos with an abnormal cleavage pattern (arrested cleavage, abnormal cell number or shape). A few embryos at advanced developmental stages (e.g., gastrula) were excluded from the data set since fertilization was by either contaminating or self sperm.

To examine the effect of timing of fertilization on subsequent development and metamorphosis, colonies were initially fertilized in sets of multiple ramets per genotype. For each genotype, one ramet was left unfertilized (to assess the level of sperm contamination or self-fertilization), one ramet was fertilized about 22 (± 2) h after the beginning of siphon opening (when results from the previous experiment indicated that all siphons should be open), and remaining ramets (2–3) were fertilized at various times up to 85 h after initial siphon opening. Because fertilization was consistently minimal in unfertilized controls and the availability of genotypes with multiple egg-bearing ramets was often limited, later trials were conducted without the control treatment. Before takeover, we counted the number of eggs produced by each colony (minimum egg production was set at 25 eggs). After insemination, colonies were returned to isolation until all ramets of a genotype had been fertilized and at least 24 h had elapsed since the last insemination. Colonies were subsequently housed in a flowing seawater table with an independent seawater supply while embryonic development proceeded; they were re-isolated at stage four (Milkman, 1967). After each isolated colony had started the next reproductive cycle, all metamorphosed juveniles in the isolation container were counted. Data from colonies that died or became visibly unhealthy during the experiment were discarded.

Results

Timing of siphon opening

Feeding did not begin until after the organization of zooids into new systems and formation of the common exhalant siphon. Although the rate of siphon opening varied among colonies (Fig. 1; range of 3.0%/h–17.8%/h), the

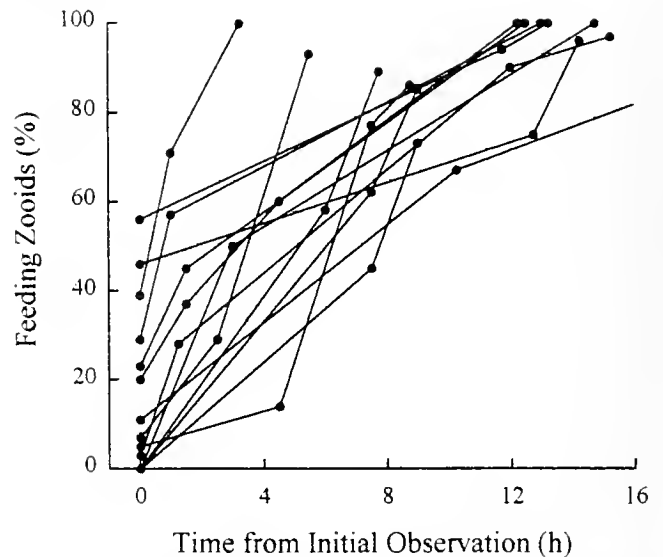


Figure 1. Rate of siphon opening in colonies of *Botryllus schlosseri* as assayed by the presence of algae in the digestive system. Colonies were isolated in 50 ml aged seawater with 2×10^5 algae/ml and monitored at intervals of from 1 to 12 h. Zero time is the first observation of algae in the gut. Temporal patterns for 14 individual colonies are shown. Differences in the y-intercept simply reflect how far the takeover process had proceeded when colonies were first observed; slopes indicate the rate of siphon opening.

average rate of siphon opening of the colonies was 7.8%/h \pm 4.5%/h ($\bar{X} \pm$ SD). We used the average rate of siphon opening to normalize the time of sperm exposure to the start of siphon opening for colonies in the other two experiments.

Effect of timing of insemination on fertilization levels

To determine the time frame during which eggs can be fertilized within the female, we exposed virgin females to a 1-h pulse of sperm at various times after the beginning of siphon opening and assayed successful fertilization by the percentage of normally cleaved embryos present (Fig. 2). When virgin females were exposed to sperm during the period in which their siphons were opening (first 24 h), the level of fertilization increased with time (Fig. 2B). In colonies fertilized during siphon opening, there was no spatial relationship between fertilized and unfertilized eggs either within or among systems; it was common to find both in the same zooid. Because the rate of increasing fertilization (5.4%/h) is similar to the rate of siphon opening (7.8%/h \pm 4.5%/h), we conclude that fertilization of the eggs within a zooid occurs shortly after the opening of the siphon.

After the completion of siphon opening, fertilization success remained high (>90%) for 24 h and then declined over the next 48 h with a $T_{50\%}$ of 72 h (Fig. 2B). In a subset of genotypes where multiple ramets were inseminated at different times in the same reproductive cycle, thus controlling for potential genotype and cycle effects, the effect of

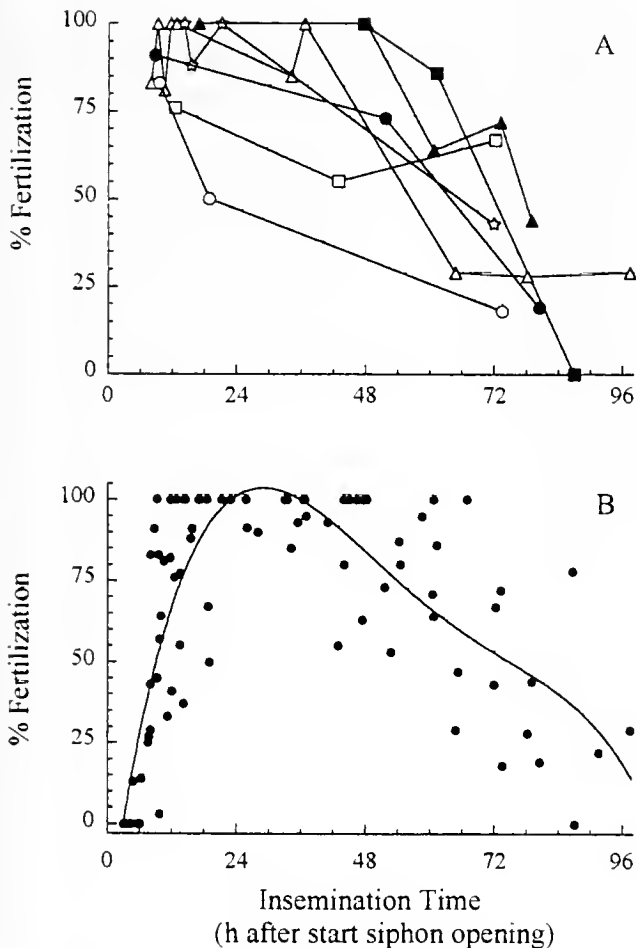


Figure 2. Effect of insemination pulse timing on fertilization levels. Colonies were isolated before the start of siphon opening, monitored for the timing of siphon opening, and exposed to sperm for 1 h; the number of cleaving embryos was determined 10–18 h later. (A) Fertilization levels in different ramets of seven genotypes fertilized at different points in the same reproductive cycle. (B) Overall effect of insemination time on fertilization success in ramets from 25 genotypes. The line represents a polynomial regression of the data ($R^2 = 0.580$).

delayed insemination on fertilization varied by genotype (Fig. 2A). Of the seven genotypes in which different ramets were inseminated at different times, five genotypes had a decline in fertilization that mirrored the population data. In the other two genotypes, fertilization levels declined rapidly in one, but remained relatively stable over 60 h in the other. Excluding the genotype that exhibited little decline in fertilization, the average $T_{50\%}$ for the reduction of fertilization was 62 ± 15 h, a value similar to the population-wide regression.

Effect of timing of insemination on embryo development and metamorphosis

The maximum duration of gestation is fixed by the length of the asexual zooid replacement cycle. Since eggs could be

fertilized well after siphon opening, but the time of embryo release is fixed, we examined the effect of delayed insemination on reproductive success. Successful embryo metamorphosis was selected as an assay of reproductive success because it integrates possible effects on fertilization, development, larval behavior, and settlement. In five trials that included unfertilized (low control), insemination at 22 h (high control), and ramets inseminated at different times after siphon opening, the percentage of eggs that successfully developed through metamorphosis consistently decreased with the time of insemination (Fig. 3A). The unfertilized controls resulted in either zero or very low (<5%) levels of larval metamorphosis (Fig. 3A). However, the percent of eggs developing through metamorphosis varied substantially among 22-h insemination controls (Fig. 3A). Because of the low levels of successful metamorphosis in two genotypes fertilized at 22 h, we calculated the $T_{50\%}$ relative to the maximum value for each genotype. The relative $T_{50\%}$ for the reduction of metamorphosis success was 41 ± 6 h after the start of siphon opening (about 19 h after the completion of siphon opening). When data from all 12 trials were combined (Fig. 3B), larval metamorphosis exhibited an exponential decline with fertilization time beyond 22 h. No larval metamorphosis occurred when colonies were fertilized more than 78 h after the start of siphon opening.

Two outliers (both ramets of the same genotype) had disproportionately high levels of metamorphosis when fertilized about 48 h after siphon opening (Fig. 3B, open squares). Independent evidence (*i.e.*, observations of successful embryo development in isolated colonies) suggested that this genotype may sometimes be able to self-fertilize. Alternatively, the high fertilization levels in these two colonies may be the result of sperm contamination. Because these inconsistent values are limited to one genotype, we have excluded these values from the regression in Figure 3B. Inclusion of the two points in the regression has little effect on the equation parameters, but it substantially reduces the coefficient of determination. Note that many other ramets of this genotype were employed in this experiment (Fig. 3B, open squares) and produced results consistent with those of the other genotypes.

Discussion

Although more than 50% of *Botryllus schlosseri* eggs can be fertilized 38 to 48 h after the completion of siphon opening (Fig. 2), few viable larvae are produced unless fertilization occurs within the first 19 h (Fig. 3). The decrease in embryo production after delayed fertilization could be caused by either egg aging or limitations on the duration of brooding. As in most invertebrates, the time required to complete development is a function of temperature in *B. schlosseri*. Since the asexual zooid replacement

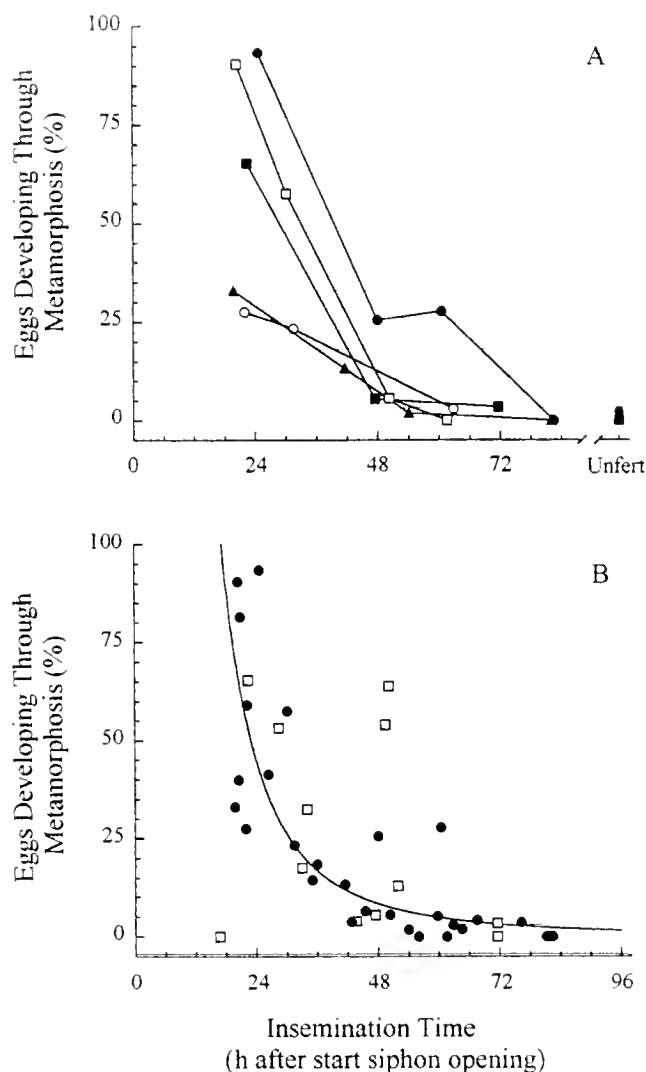


Figure 3. Effect of insemination pulse timing on embryo development and larval metamorphosis. Colonies with quantified egg production were isolated before the start of siphon opening, monitored for the timing of siphon opening, and exposed to sperm for 1 h; the number of settled juveniles was determined 5–7 days later. (A) Developmental success of different ramets from five genets. In three of the genets, one ramet was never exposed to sperm (unfertilized, solid symbols). (B) Overall effect of insemination time on successful development. The open squares are the ramets from the putative self-fertilizing genotype; closed symbols represent the other 11 genotypes. The line is an exponential regression of the data except for two outliers at 48 h ($R^2 = 0.713$).

cycle is also a function of temperature (Grosberg, 1982), delayed fertilization could cause the brooding zooids to degenerate before the embryos have become competent to undergo metamorphosis. The deleterious effects of egg aging have been demonstrated in mammals (Juetten and Bavister, 1983; Xu *et al.*, 1997), but such effects are usually manifested early in development. Since early development was normal in all but one colony with delayed fertilization (pers. obs.), the decreased gestational duration caused by

delayed fertilization is more likely to be responsible. Nevertheless, additional work on the mechanism by which delayed fertilization decreases larval production could more fully resolve this issue.

In spite of the narrow temporal window in which both fertilization and development are likely to be successful (Figs. 2 and 3), field experiments indicate that colonies of *B. schlosseri* are very adept at acquiring sperm. A single male-phase colony can fertilize most eggs of a nearby female-phase colony with very few sperm (Yund, 1998). If several males are present, they compete to fertilize eggs (Yund, 1995, 1998), and closer males can be successful at the expense of more distant males (Yund and McCartney, 1994). Although sperm transfer usually occurs among nearby colonies (Yund, 1995), sperm can also be obtained from very distant locations when insufficient local sperm are available (Yund, 1998). Even eggs of colonies isolated from the nearest natural populations by tens of meters can be fertilized at appreciable levels (Yund and McCartney, 1994). The apparent ease of fertilization under field conditions, in spite of a very limited temporal window for successful fertilization and development, suggests that the process of sperm capture by colonies must be extremely efficient. Nevertheless, in low-density populations where sperm may be in short supply (Yund, 1998), or in marginal habitats in which sperm production is suppressed (Stewart-Savage *et al.*, 2001), our work suggests that reproductive failure may occur in spite of successful fertilization if fertilization occurs too late in the reproductive cycle. Recent field sampling has demonstrated this phenomenon in natural populations near the end of the annual reproductive season (Yund and Phillippi, unpubl. data).

Unlike the colonial ascidian *Diplosoma listerianum*, in which fertilization can be temporally disassociated from sperm exposure and colonies can store sperm for up to one month (Bishop and Ryland, 1991; Bishop and Sommerfeldt, 1996), *B. schlosseri* colonies apparently cannot store sperm. The evidence for this conclusion is, first, that colonies isolated in sperm-free seawater were not fertilized until we experimentally supplied a sperm pulse, indicating that sperm are not stored and transferred from one asexual generation of zooids to the next. The apparently complete resorption of all zooid tissue at the end of the cycle further suggests that transmission between cycles is unlikely. Second, the tight temporal relationship between siphon opening and fertilization (Fig. 2B) suggests that sperm cannot enter until the new generation of zooids opens its siphons and starts to feed. Third, the narrow window of time in which fertilization is both possible (Fig. 2) and results in viable offspring (Fig. 3) eliminates any apparent fitness advantage to sperm storage within a single asexual generation.

The route of sperm access to eggs in *B. schlosseri* is unknown, but there are at least two possible points of entry (Ryland and Bishop, 1993): sperm enter through the

inhalant siphon and cross the pharyngeal basket to reach the eggs, or sperm enter through the exhalant siphon and then swim to the eggs. During takeover in *B. schlosseri*, the exhalant siphon of each system is formed before the inhalant siphons of all of the component zooids open, and the precise timing of exhalant siphon formation varies among systems (pers. obs.). If sperm enter *via* the exhalant siphon, fertilization levels in the early time intervals of our fertilization timing experiment should have varied among systems, but should not have varied within a system. However, we routinely found mixtures of fertilized and unfertilized eggs within the same system, suggesting that sperm entry to each zooid required an open inhalant as well as exhalant siphon. Although further work is required to determine the route of sperm entry into *Botryllus* colonies, we think it is unlikely that sperm enter *via* the exhalant siphon.

Hermaphroditism creates another challenge for successful reproduction in *B. schlosseri*. Inbreeding depression (Sabbadin, 1971) is likely to exert selective pressure to prevent self-fertilization, even though selfing would be a possible mechanism to assure fertilization in the narrow time window in which fertilization can produce functional embryos. When the data in this paper are combined with previous data on the timing of sperm release (Stewart-Savage and Yund, 1997), it is apparent that the male and female phases of the reproductive cycle overlap in *B. schlosseri* (Fig. 4). Sperm release overlaps for about 48 h with the window for successful fertilization, but there is substantially less overlap with the narrower window in which fertilization results in viable embryos (Fig. 4). Consequently, *B. schlosseri* is not a true sequential hermaphrodite (Milkman, 1967), but the male and female phases are functionally separated in time. This functional segregation of the reproductive phases probably plays some role in

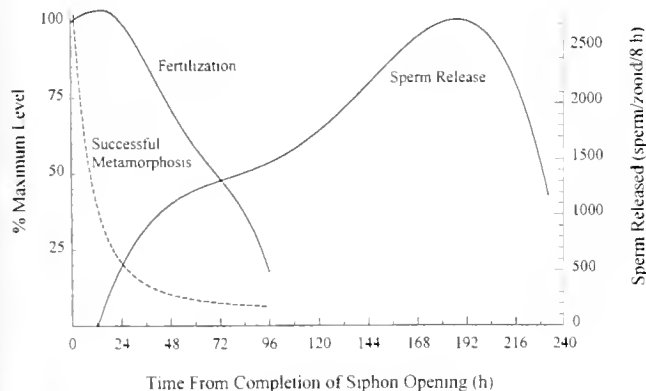


Figure 4. Relationship between male and female reproductive phases in *Botryllus schlosseri*. Data collected at different temperatures have been normalized to a 10-day cycle length. The zero time point is the completion, rather than the initiation (as in Figs. 2 and 3), of siphon opening. The sperm release curve is redrawn from Stewart-Savage and Yund (1997) with permission.

ensuring that few metamorphosing embryos result from self-fertilization. However, the very success of our experimental protocols indicates that one or more additional mechanisms to prevent self-fertilization must exist. Eggs of colonies isolated in small volumes of water until points in the reproductive cycle at which substantial self-sperm should have been present (Fig. 4) nevertheless remained unfertilized until we introduced a pulse of sperm (with the possible exception of the two outliers in Fig. 3B). Consequently, some form of self-incompatibility, as described in other colonial and solitary ascidians (Rosati and De Santis, 1978; Bishop, 1996), appears likely in *B. schlosseri* (see also Scofield *et al.*, 1982).

Acknowledgments

Financial support was provided by the National Science Foundation (OCE-97-30354). This is contribution number 366 from the Darling Marine Center.

Literature Cited

- Berrill, N. J. 1941. The development of the bud in *Botryllus*. *Biol. Bull.* 80: 169–184.
- Bishop, J. D. D. 1996. Female control of paternity in the internally fertilizing compound ascidian *Diplosoma listerianum*. I. Autoradiograph investigation of sperm movements in the female reproductive tract. *Proc. R. Soc. Lond. B* 263: 369–376.
- Bishop, J. D. D., and J. S. Ryland. 1991. Storage of exogenous sperm by the compound ascidian *Diplosoma listerianum*. *Mar. Biol.* 108: 111–118.
- Bishop, J. D. D., and A. D. Sommerfeldt. 1996. Autoradiographic investigation of uptake and storage of exogenous sperm by the ovary of the compound ascidian *Diplosoma listerianum*. *Mar. Biol.* 125: 663–670.
- Bolton, T. F., and J. N. Havenhand. 1996. Chemical mediation of sperm activity and longevity in the solitary ascidians *Ciona intestinalis* and *Asciella aspersa*. *Biol. Bull.* 190: 329–335.
- Coma, R., and H. R. Lasker. 1997. Effects of spatial distribution and reproductive biology on *in situ* fertilization rates of a broadcast-spawning invertebrate. *Biol. Bull.* 193: 20–29.
- Eckelbarger, K. J., C. M. Young, and J. L. Cameron. 1989a. Modified sperm ultrastructure in four species of soft-bodied echinoderms (Echinodermata: Echinothuriidae) from the bathyal zone of the deep sea. *Biol. Bull.* 177: 230–236.
- Eckelbarger, K. J., C. M. Young, and J. L. Cameron. 1989b. Ultrastructure and development of dimorphic sperm in the abyssal echinoid *Phrissocystis multispina* (Echinodermata: Echinoidea): implications for deep sea reproductive biology. *Biol. Bull.* 176: 257–271.
- Grosberg, R. K. 1982. Ecological, genetical, and developmental factors regulating life history variation within a population of the colonial ascidian *Botryllus schlosseri* (Pallas) Savigny. Ph.D. dissertation, Yale University, New Haven, CT.
- Grosberg, R. K. 1987. Limited dispersal and proximity-dependent mating success in the colonial ascidian *Botryllus schlosseri*. *Evolution* 41: 372–384.
- Grosberg, R. K. 1991. Sperm-mediated gene flow and the genetic structure of a population of the colonial ascidian *Botryllus schlosseri*. *Evolution* 45: 130–142.
- Izzard, C. S. 1973. Development of polarity and bilateral asymmetry in the palaeal bud of *Botryllus schlosseri* (Pallas). *J. Morphol.* 139: 1–26.

- Juettner, J., and B. D. Bavister. 1983. Effects of egg aging on *in vitro* fertilization and first cleavage division in the hamster. *Gamete Res.* **8**: 219–230.
- Levitan, D. R. 1991. Influence of body size and population density on fertilization success and reproductive output in a free-spawning invertebrate. *Biol. Bull.* **181**: 261–268.
- Levitan, D. R. 1998. Does Bateman's principle apply to broadcast-spawning organisms? Egg traits influence *in situ* fertilization rates among congeneric sea urchins. *Evolution* **52**: 1043–1056.
- Levitan, D. R., and C. Petersen. 1995. Sperm limitation in the sea. *Trends Ecol. Evol.* **10**: 228–231.
- Levitan, D. R., and C. M. Young. 1995. Reproductive success in large populations: experimental measures and theoretical predictions of fertilization in the sea biscuit *Clypeaster rosaceus*. *J. Exp. Mar. Biol. Ecol.* **190**: 221–241.
- Meidel, S. K., and P. O. Yund. 2001. Egg longevity and time-integrated fertilization in a temperate sea urchin (*Strongylocentrotus droebachiensis*). *Biol. Bull.* **201**: 000–000.
- Milkman, R. 1967. Genetic and developmental studies on *Botryllus schlosseri*. *Biol. Bull.* **132**: 229–243.
- Miller, R. L. 1985. Sperm chemo-orientation in the metazoa. Pp. 275–337 in *Biology of Fertilization*, Vol. 2, C. B. Metz and A. Monroy, eds. Academic Press, Orlando, FL.
- Powell, D. K., P. A. Tyler, and L. S. Peck. 2001. Effect of sperm concentration and sperm ageing on fertilization success in the Antarctic soft-shelled clam *Laternula elliptica* and the Antarctic limpet *Nacella concinna*. *Mar. Ecol. Prog. Ser.* **215**: 191–200.
- Rosati, F., and R. De Santis. 1978. Studies on fertilization in the ascidians. I. Self-sterility and specific recognition between gametes of *Ciona intestinalis*. *Exp. Cell Res.* **112**: 111–119.
- Ryland, J. S., and J. D. D. Bishop. 1993. Internal fertilization in hermaphroditic colonial invertebrates. *Oceanogr. Mar. Biol. Annu. Rev.* **31**: 445–477.
- Sabbadin, A. 1971. Self- and cross-fertilization in the compound ascidian *Botryllus schlosseri*. *Dev. Biol.* **24**: 379–391.
- Scofield, V. L., J. M. Schlumberger, and I. L. Weissman. 1982. Colony specificity in the colonial tunicate *Botryllus* and the origins of vertebrate immunity. *Am. Zool.* **22**: 783–794.
- Stewart-Savage, J., and P. O. Yund. 1997. Temporal pattern of sperm release from the colonial ascidian, *Botryllus schlosseri*. *J. Exp. Zool.* **279**: 620–625.
- Stewart-Savage, J., A. Stires, and P. O. Yund. 2001. Environmental effect on the reproductive effort of *Botryllus schlosseri*. Pp. 311–314 in *Biology of Ascidians*, H. Sawada, H. Yokosawa, and C. C. Lambert, eds. Springer-Verlag, Tokyo, Japan.
- Thomas, F. I. M. 1994a. Physical properties of gametes in three sea urchin species. *J. Exp. Biol.* **194**: 263–284.
- Thomas, F. I. M. 1994b. Transport and mixing of gametes in three free-spawning polychaete annelids, *Phragmatopoma californica* (Fewkes), *Sabellaria cementarium* (Moore), and *Schizobranchia insignis* (Bush). *J. Exp. Mar. Biol. Ecol.* **179**: 11–27.
- Wable, R. A., and S. H. Peckham. 1999. Density-related reproductive trade-offs in the green sea urchin, *Strongylocentrotus droebachiensis*. *Mar. Biol.* **134**: 127–137.
- Xu, Z., A. Abbott, G. S. Kopf, R. M. Schultz, and T. Ducibella. 1997. Spontaneous activation of ovulated mouse eggs: time dependent effects on M-phase exit, cortical granule exocytosis, maternal messenger ribonucleic acid recruitment and inositol 1,4,5-trisphosphate sensitivity. *Biol. Reprod.* **57**: 743–750.
- Young, C. M. 1994. The biology of external fertilization in deep-sea echinoderms. Pp. 179–200 in *Reproduction, Larval Biology and Recruitment of the Deep-sea Benthos*, C. M. Young and K. J. Eckelbarger, eds. Columbia University Press, New York.
- Yund, P. O. 1995. Gene flow via the dispersal of fertilizing sperm in a colonial ascidian (*Botryllus schlosseri*): the effect of male density. *Mar. Biol.* **122**: 649–654.
- Yund, P. O. 1998. The effect of sperm competition on male gain curves in a colonial marine invertebrate. *Ecology* **79**: 328–339.
- Yund, P. O. 2000. How severe is sperm limitation in natural populations of marine free-spawners? *Trends Ecol. Evol.* **15**: 10–13.
- Yund, P. O., and M. A. McCartney. 1994. Male reproductive success in sessile invertebrates: competition for fertilizations. *Ecology* **75**: 2151–2167.
- Yund, P. O., Y. Marcum, and J. Stewart-Savage. 1997. Life-history variation in a colonial ascidian: broad-sense heritabilities and tradeoffs in allocation to asexual growth and male and female reproduction. *Biol. Bull.* **192**: 290–299.

Morula Cells as the Major Immunomodulatory Hemocytes in Ascidians: Evidences From the Colonial Species *Botryllus schlosseri*

LORIANO BALLARIN^{1,*}, ANTONELLA FRANCHINI², ENZO OTTAVIANI², AND ARMANDO SABBADIN¹

¹*Department of Biology, University of Padova, via U. Bassi 58/B, 35100 Padova, Italy; and*

²*Department of Biology, University of Modena and Reggio Emilia, via Campi 213/D, 41100 Modena, Italy*

Abstract. Immunocytochemical methods were used to study the presence and distribution of IL-1- α - and TNF- α -like molecules in the hemocytes of the colonial ascidian *Botryllus schlosseri*. Only a few unstimulated hemocytes were positive to both the antibodies used. When the hemocytes were stimulated with either mannan or phorbol 12-mono-myristate, the phagocytes were not significantly changed in their number, staining intensity, or cell morphology. In contrast, stimulated morula cells were intensely labeled, indicating that these cells play an important immunomodulatory role.

Introduction

Phagocytes and morula cells are two types of circulating hemocytes that play a key role in ascidian immunobiology. Phagocytes can easily recognize and ingest non-self cells and particles (Smith, 1970; Anderson, 1971; Fuke and Fukumoto, 1993; Ballarin *et al.*, 1994; Ohtake *et al.*, 1994; Dan-Sohkawa *et al.*, 1995; Cima *et al.*, 1996) and are able to synthesize and release opsonic agglutinins (Coombe *et al.*, 1984; Kelly *et al.*, 1992; Ballarin *et al.*, 1999). Morula cells, a ubiquitous hemocyte type among ascidians, take part in a variety of biological functions of immunological relevance, such as hemolymph clotting, tunic synthesis, and

encapsulation of foreign bodies (Endean, 1955b; Smith, 1970; Anderson, 1971; Chaga, 1980; Wright, 1981; Zaniolo, 1981). They are by far the most frequent circulating ascidian cell-type (Endean, 1955a; Andrew, 1961; Smith, 1970; Kustin *et al.*, 1976; Ballarin *et al.*, 1995), and their abundance suggests direct involvement in other important defense reactions. Although most of their roles in ascidian immune responses still remain unclear, morula cells can induce cytotoxicity after recognition of foreign molecules or cells (Parrinello, 1996; Cammarata *et al.*, 1997; Ballarin *et al.*, 1998), and they are also required for phagocytosis (Smith and Peddie, 1992).

Cytokines are soluble molecules that mediate communication among various immunocyte types in vertebrate immune systems. In the last decade, much evidence has accumulated indicating that cytokine-like molecules are also involved in invertebrate immune responses, and their presence has been demonstrated in hemocytes of molluscs, annelids, arthropods, echinoderms, and tunicates (Beck and Habicht, 1991; Ottaviani *et al.*, 1995a,b, 1996; Franchini *et al.*, 1996). Cytokine-like molecules stimulate cell proliferation, increase hemocyte motility and phagocytic activity, and induce nitric oxide synthase (Raftos *et al.*, 1991; Ottaviani *et al.*, 1995b). As regards ascidians, the activities of interleukin-1 (IL-1)- and IL-2- but not tumor necrosis factor (TNF)-like molecules have been revealed in various species, either solitary or colonial (Beck *et al.*, 1989). Tunicate IL-1-like molecules modulate immune responses and are secreted by hemocytes in response to exogenous stimuli (Raftos *et al.*, 1991, 1992, 1998; Beck *et al.*, 1993; Kelly *et al.*, 1993).

Received 18 July 2000; accepted 10 May 2001.

* To whom correspondence should be addressed. E-mail: ballarin@civ.bio.unipd.it

Abbreviations: FSW, filtered seawater; HA, hyaline amoebocytes; IL, interleukin; MLC, macrophage-like cells; PMM, phorbol 12-mono-myristate; TNF, tumor necrosis factor.

We have studied—in hemocytes of the colonial ascidian *Botryllus schlosseri*—the presence and distribution of molecules that are immunoreactive to antibodies raised to human IL-1- α and TNF- α . The results indicate that these immunoreactive molecules are mainly detectable in stimulated morula cells, suggesting that these cells have a role in immunomodulation. Moreover, previous results in other ascidian species are supported (Smith and Peddie, 1992).

Materials and Methods

Animals

Wild colonies of *Botryllus schlosseri* from the lagoon of Venice, Italy, were used. They were kept in aerated aquaria, attached to glass slides, and fed with Liquifry Marine (Liquifry Co., England) and algae.

Hemocyte monolayers

Colonies were rinsed in filtered seawater (FSW), pH 7.5, containing 10 mM L-cysteine as anticoagulant. The tunic marginal vessels were then punctured with a fine tungsten needle, and hemolymph was collected with a glass micropipette. Hemolymph was centrifuged at $780 \times g$ for 10 min, and pellets were resuspended in FSW to a final hemocyte concentration of $8\text{--}10 \times 10^6$ cells/ml. Samples of the hemocyte suspension (50–100 μ l) were cytocentrifuged onto slides with a Shandon Instrument Cytospin II running at 500 rpm for 2 min. Hemocytes were then stained with May Grünwald-Giemsa for morphological examination with a Leitz Dialux 22 light microscope.

Hemocyte stimulation

Cell suspensions were placed in 1-ml tubes on a revolving mixer, and hemocytes were stimulated by incubation for 5, 15, 30, and 60 min with mannan at 5 mg/ml or phorbol 12-mono-myristate (PMM) at 20 nM in FSW containing 10 mM L-cysteine to prevent cell clotting. Mannan, a quite common microbial polysaccharide, is easily recognized by mannose receptors, the presence of which has been indirectly inferred on the surface of *Botryllus* phagocytes (Ballarin *et al.*, 1994). PMM is a well-known activator of protein kinase C that mimics the action of diacylglycerol (Wolfe, 1993). The above-reported concentrations of the two compounds were previously demonstrated as the most effective in stimulating *Botryllus* phagocytes and the related respiratory burst (Ballarin *et al.*, 1994; Cima *et al.*, 1996). FSW

was used for controls. The viability of hemocytes, after the incubation, was assessed by the trypan blue exclusion assay (Gorman *et al.*, 1996).

Immunocytochemistry

The immunocytochemical procedure described by Ottaviani *et al.* (1990) was performed. The following two primary antibodies were used: polyclonal anti-human IL-1- α (1:250, 1:500, 1:1000) (Santa Cruz Biotech., USA) and monoclonal anti-human TNF- α (1:25, 1:50, 1:100) (NeoMarkers, USA). Cells were incubated with primary antibodies overnight at 4°C, and reactivity was revealed by immunoperoxidase staining using avidin-biotin-peroxidase complex (Hsu *et al.*, 1981). The best results were obtained with anti-IL-1- α and anti-TNF- α diluted 1:500 and 1:25, respectively. In control preparations, the primary antibodies were either substituted with non-immune sera or absorbed with homologous antigen (*i.e.*, human IL-1- α and TNF- α) before addition to hemocyte monolayers. Moreover, a polyclonal antibody raised against *Botryllus* agglutinin (BA) (Ballarin *et al.*, 2000) was also assayed as a control for specificity. Nuclei were counterstained with hematoxylin. The frequency of positive hemocytes, phagocytes, and morula cells was reported as the percentage of the total hemocyte number, which was determined by counting at least 600 cells in 10 fields under the light microscope.

Statistical analysis

All experiments were repeated in triplicate, and statistical analysis was performed using the chi-square test (χ^2).

Results

Morphology of cytocentrifuged *Botryllus* hemocytes

The main hemocyte types present in *B. schlosseri* hemolymph were identifiable under the light microscope after cytocentrifugation. Lymphocyte-like cells, representing 2%–4% of circulating hemocytes, contain a large round nucleus surrounded by a thin layer of basophilic cytoplasm. Phagocytes, which include hyaline amoebocytes (HA; actively phagocytosing cells) and macrophage-like cells (MLC) (Ballarin *et al.*, 1994), have roundish nuclei and neutrophilic cytoplasm which, in the case of MLC, surrounds one or more vacuoles containing ingested material (Fig. 1a, b). Phagocytes constitute 30%–40% of circulating blood cells. Morula cells, the frequency of which is 30%–50% of total hemocytes, are characterized by the presence of several yellowish-green vacuoles (Fig. 2a, c). Nephro-

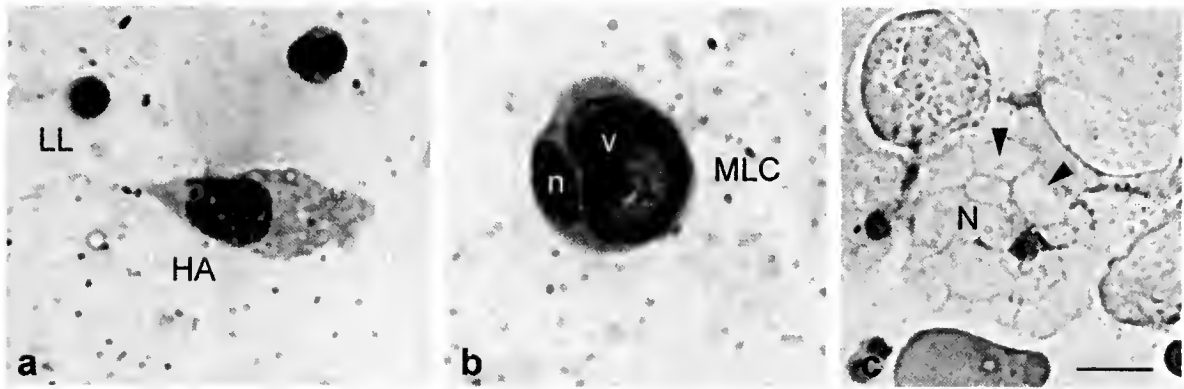


Figure 1. Cyto-centrifuged *Botryllus schlosseri* hemocytes stained with May Grünwald-Giemsa solution. (a) Lymphocyte-like cell (LL) and hyaline amoebocyte (HA); (b) macrophage-like cell (MLC; n: nucleus; v: vacuole); (c) nephrocyte (N) with several empty vacuoles (arrowheads). Bar = 10 μ m.

cytes and pigment cells (6%–10% of circulating hemocytes) were not well preserved after cyto-centrifugation; they appeared as giant cells with empty vacuoles (Fig. 1c).

Response of unstimulated hemocytes to anti-cytokine antibodies

Using anti-IL-1- α and anti-TNF- α , only some phagocytes and a few morula cells were labeled after immunoperoxidase staining (Table 1). Thus, most HA, MLC, and morula cells were not immunoreactive with either antibody (Fig. 3). Moreover, no other cell-types stained positively for

the two cytokines. No labeling was observed when non-immune sera were used.

Response of stimulated hemocytes to anti-cytokine antibodies

When monolayers of hemocytes were activated with either mannan or PMM, the number of immunoreactive morula cells and the intensity of their immunoreactivity were progressively augmented with increasing incubation times (Figs. 2, 4). The difference in the number of unstimulated and stimulated reactive morula cells was always significant ($P < 0.001$). In contrast, no significant changes with respect to unstimulated hemocytes were observed in the number, morphology, or stain intensity of positive phagocytes for all the incubation times. In each preparation, more than 95% of hemocytes were viable. Unstimulated and stimulated hemocytes always showed negative results with either non-immune sera or absorbed antibodies. The anti-BA antibody, as previously reported (Ballarin *et al.*, 2000), only recognized amoebocytic phagocytes and no morula cells (Fig. 3), supporting the specificity of the anti-cytokine antibodies used.

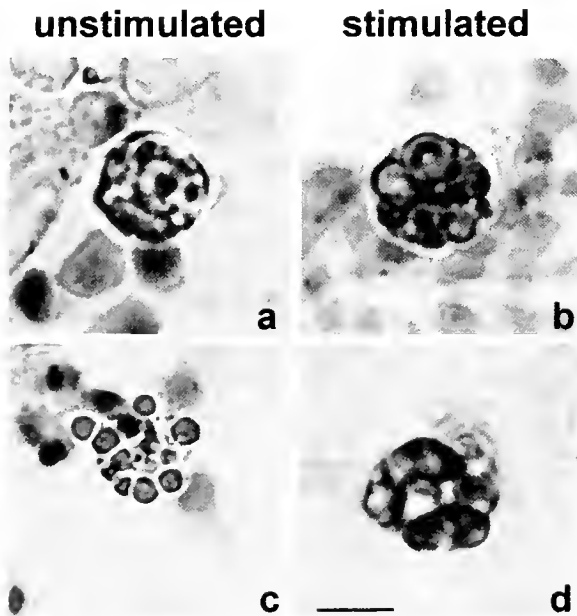


Figure 2. Unstimulated (a, c) and stimulated (b, d) morula cells after immunoperoxidase staining with anti-cytokine antibodies. (a, b) Incubation with anti-IL-1- α antibody; (c, d) treatment with the TNF- α antibody. Bar = 15 μ m.

Table 1

Immunoreactivity of unstimulated Botryllus hemocytes to antibodies raised to human cytokines

Cell type	Antibodies ^a	
	Anti-IL-1- α	Anti-TNF- α
Phagocytes ^b	0.4 \pm 0.3	0.9 \pm 0.4
Morula cells	1.1 \pm 0.9	4.5 \pm 1.2

^a Values are percentage of total hemocytes plus or minus the standard deviation.

^b Phagocytes include hyaline amoebocytes and macrophage-like cells.

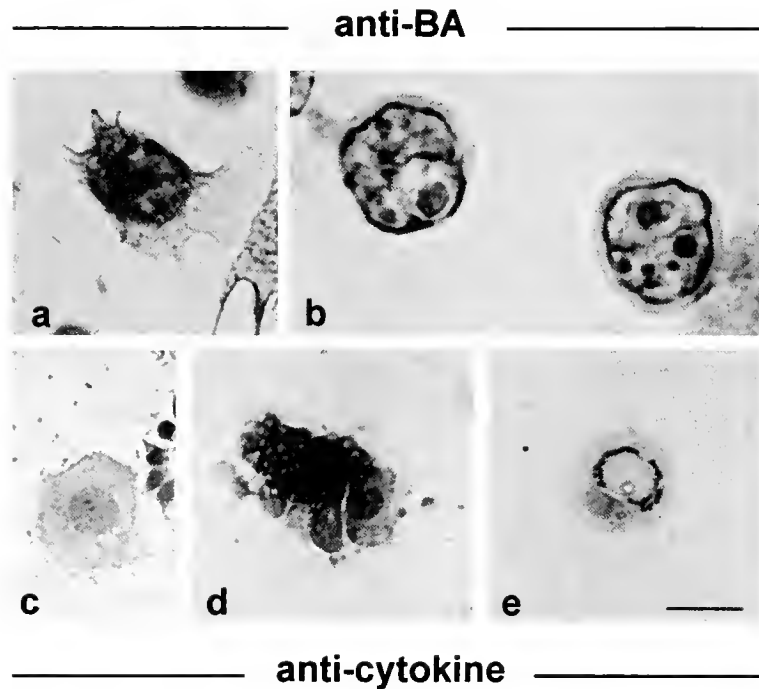


Figure 3. Immunocytochemistry on *Botryllus schlosseri* hemocytes with anti-BA (a, b), and anti-cytokine (c–e) antibodies. (a) Positive HA; (b) negative morula cells; (c) unlabeled, unstimulated HA; (d) stimulated HA positive for IL-1- α ; (e) stimulated MLC positive for TNF- α . Bar = 15 μ m.

Discussion

In the present work, we demonstrate that molecules recognized by antibodies raised to human IL-1- α and TNF- α are present in immunocytes of the compound ascidian *Botryllus schlosseri*. After stimulation, only morula cells, among all hemocytes, show a marked and significant increase in immunoreactivity. The increase in the number of immunoreactive cells depends on the length of the time of hemocyte incubation with the stimulating agents. In contrast, among unstimulated hemocytes, only some morula cells and a few phagocytes are immunoreactive. Therefore, although the ligands recognized by the antibodies used are unknown and notwithstanding that serological cross-reactivity is not sufficient proof of evolutionary homology between those ligands and vertebrate cytokines, still our data indicate that the morula cells have an important immunomodulatory role in ascidian blood.

We hypothesize that morula cells are the main source of cytokine-like molecules in *Botryllus* hemolymph, which can better explain their abundance in the circulation. Indeed, these cells are able to encapsulate foreign bodies (Anderson, 1971; Wright, 1981; De Leo *et al.*, 1996) and are involved in clotting after blood vessel damage (Vallee, reported by Wright, 1981). In many ascidian species, they can also induce cytotoxicity after recognition of foreign molecules or cells (Parrinello, 1996; Cammarata *et al.*, 1997; Ballarin *et al.*, 1998). All these events can be modulated by cytokine-

like molecules produced by activated cells. In agreement with this view, TNF- α -like molecules are involved in insect encapsulation (Franchini *et al.*, 1996), and IL-1-like molecules have been shown to stimulate echinoderm coelomocyte aggregation, which occurs in encapsulation (Beck and Habicht, 1991). Moreover, in vertebrates, both TNF- α and IL-1- α stimulate immune and inflammatory responses, and TNF- α is required for blood coagulation (Abbas *et al.*, 1991).

The induction of cytokine-like molecules in hemocytes after stimulation has already been reported in bivalve molluscs and insects: in all these cases, phagocytes are the immunoreactive cells (Hughes *et al.*, 1990; Franchini *et al.*, 1996). Analogously, in vertebrates, mononuclear phagocytes are the main source of both IL-1- α and TNF- α (Abbas *et al.*, 1991). Nevertheless, the situation in *Botryllus* appears peculiar in that positivity to anti-cytokine antibodies is absent from the majority of phagocytes without significant differences in its distribution between unstimulated and stimulated cells.

Although morula cells have no phagocytic activity, they are reported to promote phagocytosis by ascidian phagocytes (Smith and Peddie, 1992). Thus, the stimulatory effect on phagocytes and the enhancement of phagocytosis by morula cell lysates (Smith and Peddie, 1992) may easily be explained by the immunomodulatory role of the cytokines they produce. This idea is strongly supported by the obser-

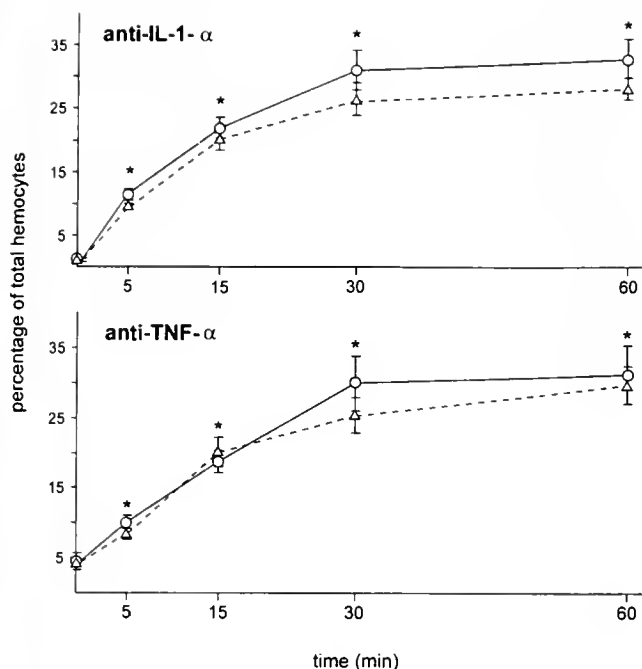


Figure 4. Morula cells positive to anti-IL-1- α and anti-TNF- α , expressed as percentage of total hemocytes, after stimulation with either mannan at 5 mg/ml (circles) or PMM at 20 nM (triangles) for 5, 15, 30, and 60 min. * $P < 0.001$ vs. control (unstimulated hemocytes, $t = 0$).

vation that the time-dependent increase of immunoreactive morula cells closely resembles the time-dependent increase in the frequency of phagocytizing hemocytes in *in vitro* assays (Ballarin *et al.*, 1997). The opsonic role of tunicate IL-1-like molecules reported by Kelly *et al.* (1993) is in agreement with this view.

Acknowledgments

The authors wish to thank Mr. M. Del Favero, Mr. R. Mazzaro, and Mr. C. Friso for their technical assistance. This work was supported by a grant from the University of Padova to one of us (L.B.).

Literature Cited

- Abbas, A. K., A. H. Lichtman, and J. S. Pober. 1991. *Cellular and Molecular Immunology*. W. B. Saunders, Philadelphia.
- Anderson, R. S. 1971. Cellular responses to foreign bodies in the tunicate *Molgula manhattensis* (DeKay). *Biol. Bull.* **141**: 91–98.
- Andrew, W. 1961. Phase microscope studies of living blood-cells of the tunicates under normal and experimental conditions, with a description of a new type of motile cell appendage. *Q. J. Microsc. Sci.* **102**: 89–105.
- Ballarin, L., F. Cima, and A. Sabbadin. 1994. Phagocytosis in the colonial ascidian *Botryllus schlosseri*. *Dev. Comp. Immunol.* **18**: 467–481.
- Ballarin, L., F. Cima, and A. Sabbadin. 1995. Morula cells and histocompatibility in the colonial ascidian *Botryllus schlosseri*. *Zool. Sci.* **12**: 757–764.
- Ballarin, L., F. Cima, and A. Sabbadin. 1997. Calcium homeostasis and yeast phagocytosis in the compound ascidian *Botryllus schlosseri*. *Comp. Biochem. Physiol.* **118A**: 153–158.
- Ballarin, L., F. Cima, and A. Sabbadin. 1998. Phenoloxidase and cytotoxicity in the compound ascidian *Botryllus schlosseri*. *Dev. Comp. Immunol.* **22**: 479–492.
- Ballarin, L., C. Tonello, L. Guidolin, and A. Sabbadin. 1999. Purification and characterization of a humoral opsonin, with specificity for D-galactose, in the colonial ascidian *Botryllus schlosseri*. *Comp. Biochem. Physiol.* **123B**: 115–123.
- Ballarin, L., C. Tonello, and A. Sabbadin. 2000. Humoral opsonin from the colonial ascidian *Botryllus schlosseri* as a member of the galectin family. *Mar. Biol.* **136**: 823–827.
- Beck, G., and G. S. Habicht. 1991. Primitive cytokines: harbingers of vertebrate defense. *Immunol. Today* **12**: 180–183.
- Beck, G., G. R. Vasta, J. J. Marchalonis, and G. S. Habicht. 1989. Characterization of interleukin-1 activity in tunicates. *Comp. Biochem. Physiol.* **92B**: 93–98.
- Beck, G., R. F. O'Brien, G. S. Habicht, D. L. Stillman, E. L. Cooper, and D. A. Raftos. 1993. Invertebrate cytokines III: Invertebrate interleukin-1-like molecules stimulate phagocytosis by tunicate and echinoderm cells. *Cell. Immunol.* **146**: 284–299.
- Cammarata, M., V. Arizza, N. Parrinello, G. Candore, and C. Caruso. 1997. Phenoloxidase dependent cytotoxic mechanism in ascidian (*Styela plicata*) hemocytes against erythrocyte and K562 tumor cells. *Eur. J. Cell. Biol.* **74**: 302–307.
- Chaga, O. Y. 1980. Ortho-diphenoloxidase system of ascidians. *Tsitologiya* **22**: 619–625 (in Russian).
- Cima, F., L. Ballarin, and A. Sabbadin. 1996. New data on phagocytes and phagocytosis in the compound ascidian *Botryllus schlosseri* (Tunicata: Ascidiacea). *Ital. J. Zool.* **63**: 357–364.
- Coombe, D. R., P. L. Ey, and C. R. Jenkin. 1984. Particle recognition by haemocytes from the colonial ascidian *Botrylloides leachi*: evidence that the *B. leachi* HA-2 agglutinin is opsonic. *J. Comp. Physiol.* **154**: 509–521.
- Dan-Sohkawa, M., M. Morimoto, and H. Kaneko. 1995. *In vitro* reactions of coelomocytes against sheep red blood cells in the solitary ascidian *Halocynthia roretzi*. *Zool. Sci.* **12**: 411–417.
- De Leo, G., N. Parrinello, D. Parrinello, G. Cassara, and M. A. Di Bella. 1996. Encapsulation response of *Ciona intestinalis* (Ascidiacea) to intratunicular erythrocyte injection. I. The inner capsular architecture. *J. Invertebr. Pathol.* **67**: 205–212.
- Endean, R. 1955a. Studies of the blood and tests of some Australian ascidians. I. The blood of *Pyura stolonifera* (Heller). *Aust. J. Mar. Freshwater Res.* **6**: 35–59.
- Endean, R. 1955b. Studies of the blood and tests of some Australian ascidians. III. The formation of the test of *Pyura stolonifera* (Heller). *Aust. J. Mar. Freshwater Res.* **6**: 157–164.
- Franchini, A., J. A. Miyan, and E. Ottaviani. 1996. Induction of ACTH- and TNF- α -like molecules in the hemocytes of *Calliphora vomitoria* (Insecta, Diptera). *Tissue Cell* **28**: 587–592.
- Fuke, M., and M. Fukumoto. 1993. Correlative fine structural, behavioral, and histochemical analysis of ascidian blood cells. *Acta Zool. (Stockh.)* **74**: 61–71.
- Gorman, A., J. McCarthy, D. Finucane, W. Reville, and T. Cotter. 1996. Morphological assessment of apoptosis. Pp. 1–20 in *Techniques in Apoptosis: A User's Guide*, T. G. Cotter and S. J. Martin, eds. Portland Press, London.
- Hsu, S. M., L. Raine, and H. Fanger. 1981. Use of avidin-biotin-peroxidase complex (ABC) immunoperoxidase techniques: a comparison between ABC and unlabeled antibody (PAP) procedures. *J. Histochem. Cytochem.* **29**: 577–580.

- Hughes, T. K., E. M. Smith, R. Chin, P. Cadet, J. Sinisterra, M. K. Leung, M. A. Shipp, B. Scharrer, and G. B. Stefano. 1990. Interactions of immunoreactive monokines (interleukin-1 and tumor necrosis factor) in the bivalve mollusc *Mytilus edulis*. *Proc. Natl. Acad. Sci. USA* **87**: 4426-4429.
- Kelly, K. L., E. L. Cooper, and D. A. Raftos. 1992. Purification and characterization of a humoral opsonin from the solitary urochordate *Styela clava*. *Comp. Biochem. Physiol.* **103B**: 749-753.
- Kelly, K. L., E. L. Cooper, and D. A. Raftos. 1993. Cytokine-like activity of a humoral opsonin from the solitary urochordate *Styela clava*. *Zool. Sci.* **10**: 57-64.
- Kustin, K., D. S. Levine, G. C. McLeod, and W. A. Curby. 1976. The blood of *Ascidia nigra*: blood cell frequency distribution, morphology, and the distribution and valence of vanadium in living blood cells. *Biol. Bull.* **150**: 426-441.
- Ohtake, S.-I., T. Abe, F. Shishikura, and K. Tanaka. 1994. The phagocytes in hemolymph of *Halocynthia roretzi* and their phagocytic activity. *Zool. Sci.* **11**: 681-691.
- Ottaviani, E., F. Petraglia, G. Montagnani, A. Cossarizza, D. Monti, and C. Franceschi. 1990. Presence of ACTH and β -endorphin immunoreactive molecules in the freshwater snail *Planorbium corneus* (L.) (Gastropoda, Pulmonata) and their possible role in phagocytosis. *Regul. Pept.* **27**: 1-9.
- Ottaviani, E., E. Caselgrandi, and C. Franceschi. 1995a. Cytokines and evolution: *in vitro* effects of IL-1 α , IL-1 β , TNF- α and TNF- β on an ancestral type of stress response. *Biochem. Biophys. Res. Commun.* **207**: 288-292.
- Ottaviani, E., A. Franchini, S. Cassanelli, and S. Genedani. 1995b. Cytokines and invertebrate immune responses. *Biol. Cell.* **85**: 87-91.
- Ottaviani, E., A. Franchini, D. Kletsas, and C. Franceschi. 1996. Presence and role of cytokines and growth factors in invertebrates. *Ital. J. Zool.* **63**: 317-323.
- Parrinello, N. 1996. Cytotoxic activity of tunicate hemocytes. Pp. 190-217 in *Invertebrate Immunology*, B. Rinkevich and W. E. G. Müller, eds. Springer-Verlag, Berlin.
- Raftos, D. A., E. L. Cooper, G. S. Habicht, and G. Beck. 1991. Invertebrate cytokines: tunicate cell proliferation stimulated by an interleukin 1-like molecule. *Proc. Natl. Acad. Sci. USA* **88**: 9518-9522.
- Raftos, D. A., E. L. Cooper, D. L. Stillman, G. S. Habicht, and G. Beck. 1992. Invertebrate cytokines II: release of interleukin-1-like molecules from tunicate hemocytes stimulated with zymosan. *Lymphokine Cytokine Res.* **11**: 235-240.
- Raftos, D. A., D. L. Stillman, and E. L. Cooper. 1998. Chemotactic responses of tunicate (Urochordata, Ascidiacea) hemocytes *in vitro*. *J. Invertebr. Pathol.* **72**: 44-49.
- Smith, M. J. 1970. The blood cells and tunic of the ascidian *Halocynthia aurantium* (Pallas). I. Hematology, tunic morphology, and partition of cells between blood and tunic. *Biol. Bull.* **138**: 354-378.
- Smith, V. J., and C. M. Peddie. 1992. Cell cooperation during host defense in the solitary tunicate *Ciona intestinalis* (L.). *Biol. Bull.* **183**: 211-219.
- Wolfe, S. L. 1993. *Molecular and Cellular Biology*. Wadsworth, Belmont, CA.
- Wright, R. K. 1981. Urochordates. Pp. 565-626 in *Invertebrate Blood Cells*, Vol. 2. N. A. Ratcliffe and A. F. Rowley, eds. Academic Press, London.
- Zaniolo, G. 1981. Histology of the ascidian *Botryllus schlosseri* tunic: in particular, the test cells. *Boll. Zool.* **48**: 169-178.

Molecular Evidence that *Sclerolinum brattstromi* Is Closely Related to Vestimentiferans, not to Frenulate Pogonophorans (Siboglinidae, Annelida)

KENNETH M. HALANYCH^{1,*}, ROBERT A. FELDMAN², AND ROBERT C. VRIJENHOEK³

¹ *Biology Department MS 33, Woods Hole Oceanographic Institution, Woods Hole, Massachusetts 02543*; ² *Molecular Dynamics, Inc., part of Amersham Pharmacia Biotech, 928 East Arques Ave., Sunnyvale, California 94086-4250*; and ³ *Monterey Bay Aquarium Research Institute, 7700 Sandholdt Road, Moss Landing, California 95039*

Abstract. Siboglinids, previously referred to as pogonophorans, have typically been divided into two groups, frenulates and vestimentiferans. Adults of these marine protostome worms lack a functional gut and harbor endosymbiotic bacteria. Frenulates usually live in deep, sedimented reducing environments, and vestimentiferans inhabit hydrothermal vents and sulfide-rich hydrocarbon seeps. Taxonomic literature has often treated frenulates and vestimentiferans as sister taxa. *Sclerolinum* has traditionally been thought to be a basal siboglinid that was originally regarded as a frenulate and later as a third lineage of siboglinids, Monilifera. Evidence from the 18S nuclear rDNA gene and the 16S mitochondrial rDNA gene presented here shows that *Sclerolinum* is the sister clade to vestimentiferans although it lacks the characteristic morphology (*i.e.*, a vestimentum). The rDNA data confirm the contention that *Sclerolinum* is different from frenulates, and further supports the idea that siboglinid evolution has been driven by a trend toward increased habitat specialization. The evidence now available indicates that vestimentiferans lack the molecular diversity expected of a group that has been argued to have Silurian or possibly Cambrian origins.

Introduction

Siboglinids were formerly called pogonophorans and include two groups of marine protostomes, frenulates and vestimentiferans, that are commonly referred to as beard-

worms and tubeworms, respectively. Both groups lack a functional gut as adults and rely on endosymbiotic bacteria for nutrition. They have a closed circulatory system and possess a metamerized tail region called the opisthosoma. Vestimentiferans are distinguished from frenulates by the presence of a vestimentum, a winged region near the anterior of the organism. Both taxa occur in reducing environments and typically are found at depths below several hundred meters. Due to the limited availability of samples and the difficulty of retrieving live specimens, several aspects of their biology (*e.g.*, reproduction, physiology) are still poorly understood. Vestimentiferans, in general, have been better studied than frenulates because they are keystone species in eastern Pacific hydrothermal vent habitats and in Pacific and Caribbean seeps.

The taxonomic literature concerning frenulate and vestimentiferan siboglinids has a colorful and confusing history. One taxonomic scheme recognizes frenulates (*aka* pogonophorans *sensu stricto*) and vestimentiferans as distinct phyla (Jones, 1985). Alternatively, vestimentiferans have also been recognized as a class within the phylum Pogonophora (Jones, 1981; Ivanov, 1994). Others place frenulates and vestimentiferans within the phylum Annelida (Land and Nørrevang, 1977; Kojima *et al.*, 1993; Bartolomaeus, 1995; McHugh, 1997; Rouse and Fauchald, 1997; also see Southward, 1988). The latter hypothesis has been supported by recent morphological (Rouse and Fauchald, 1995, 1997), embryological (Young *et al.*, 1996; Southward, 1999), and molecular analyses (Kojima *et al.*, 1993; McHugh, 1997; Black *et al.*, 1997; Kojima, 1998; Halanych *et al.*, 1998). To further complicate matters, a ranked classification scheme has produced different names for the same clade of organ-

Received 22 November 2000; accepted 11 April 2001.

* To whom correspondence should be addressed. E-mail: khalanych@whoi.edu

isms. Vestimentiferans have been called Vestimentifera (Jones, 1981), Obturata (Jones, 1981; Southward, 1988; Southward and Galkin, 1997), and Afrenulata (Webb, 1969). Frenulates have been called Pogonophora (Jones, 1985), Frenulata (Webb, 1969), Perviata (Southward, 1988), and originally Siboglinidae (Caullery, 1914).

Hereafter we apply the following nomenclature: (1) Vestimentifera are equated with Obturata and Afrenulata; (2) Frenulata are equated with Perviata and Pogonophora (*sensu* Jones, 1985); (3) Monilifera is a third monogeneric clade that includes *Sclerolimum*; and (4) Siboglinidae refers to the clade that includes Vestimentifera, Frenulata, and Monilifera. We recognize that the term "Pogonophora" is more commonly used and that rules of priority for nomenclature do not apply to higher taxa. However, we have opted to use the term "Siboglinidae" throughout this manuscript to emphasize that this group of organisms represents derived annelids (McHugh, 1997; Rouse and Fauchald, 1997). We restrict the term "pogonophoran" to common usage.

Even among siboglinids, there has been one group, *Sclerolimum*, that has been particularly problematic in terms of phylogenetic position. Unlike most frenulates that live in the mud, *Sclerolimum* species can live on decaying organic material like wood or rope made from natural fibers (Webb, 1964a; Southward, 1972). This taxon was originally considered a member of the frenulate family Polybrachiidae (Southward, 1961), but Webb (1964b), mainly citing differences in the postannular region, argued that *Sclerolimum* could not be ascribed to either of the two orders (Thecanephria and Athecanephria) of siboglinids recognized at the time (vestimentiferans had not been discovered yet). He erected a new family, Sclerolinidae, that he states should "have order rank." Ivanov (1991) more formally recognized the unique nature of *Sclerolimum*, and in 1994 he proposed that Frenulata (= Perviata), Monilifera (= Sclerolinidae), and the Vestimentifera be regarded as three taxa with equal rank (*i.e.*, classes within the phylum Pogonophora). Additionally, Ivanov (1994) further suggested that Monilifera are allied to the Vestimentifera on the basis of the common absence of several characters (*e.g.*, spermatophores, telosomal diaphragm, metasoma preannular and postannular regions) relative to the Frenulata. Southward (1999) suggested that Monilifera might be similar to the ancestral siboglinid form, thus predicting that it should occupy a basal position in siboglinid phylogeny. Distinguishing between these hypotheses on the placement of *Sclerolimum* will allow us to test the notion of Black *et al.* (1997) that habitat preference or specificity may be an important factor in siboglinid evolution. If Black *et al.* are correct, *Sclerolimum* is expected to occupy a position between frenulates and vestimentiferans (which may be consistent with Ivanov's ideas), and not a position basal to the frenulate-vestimentiferan clade.

To date, molecular studies that include siboglinids have either focused on vestimentiferans (Williams *et al.*, 1993; Black *et al.*, 1997; Kojima *et al.*, 1997; Halanych *et al.*, 1998) or have addressed siboglinid origins (Winnepenninckx *et al.*, 1995a; Kojima *et al.*, 1993; Kojima, 1998; McHugh, 1997). Most studies have included only one frenulate representative. Although Black *et al.* (1997) included two "frenulate" siboglinids, one of these, the Loihi worm, was undescribed. Additionally, several 18S sequences were reported in a symposium contribution (Halanych *et al.*, 1998) for which page limitations did not permit detailed analyses or explanation. Herein we extend these previous analyses by increasing the sampling of frenulates, including *Sclerolimum*, and using novel 18S rDNA and 16S rDNA data. The present findings support the notion that habitat requirements have been important in siboglinid evolution. Additionally, frenulates are sister to a *Sclerolimum*-vestimentiferan clade, the latter of which showed limited diversity suggestive of a recent radiation within the clade.

Materials and Methods

Taxa employed

Table 1 lists the species analyzed and GenBank accession numbers for the rDNA sequences used in this study. The frenulate and vestimentiferan operational taxonomic units (OTUs) included in this study represent all of the currently recognized genera available to the authors. The addition of closely related species within a genus would have increased OTUs without increasing the phylogenetic signal for the issues under examination and were therefore excluded. For example, there are no nucleotide differences observed in the 18S rDNA of *Escarpija spicata* (Guaymas Basin) and *E. laminata* (Florida Escarpment). Limiting the number of OTUs also reduced computation time, allowing for more thorough analyses. Unless otherwise noted, collection localities correspond to those given in Black *et al.* (1997). *Siboglinum ekmani*, *S. fiordicum*, and *Sclerolimum brattstromi* were collected near Bergen, Norway, and identified by Eve Southward, Marine Biological Association of the United Kingdom. Identification of the frenulates *Spirobrachia* and *Polybrachia* were made by Eve Southward on the basis of animal and tube morphology. Both specimens were collected by TVGrab from the Aleutian Trench (57°27.394'N, 148°00.013'W) at a depth of 4890 m on the German research vessel *Sonne*.

The non-siboglinid annelid OTUs for the 18S data were chosen to represent a diversity of lineages for which sequences were available. The arthropod (*Artemia*) sequence was designated as the most distant outgroup for rooting purposes. Based on both morphology (*e.g.*, Eernisse *et al.*, 1992) and molecular studies (*e.g.*, Halanych *et al.*, 1995; Winnepenninckx *et al.*, 1995a; Aguinaldo *et al.*, 1997; Eernisse, 1997), arthropods are clearly outside of the proto-

TABLE 1

Taxa used in rDNA analyses

Organism	GenBank Accession ^a		Organism	GenBank Accession ^a	
	18S rDNA	16S rDNA		18S rDNA	16S rDNA
Pogonophora			Chaetoptera		
Frenulata			<i>Chaetopterus variopedatus</i>	U67324 ^c	
<i>Galathealinum brachiosum</i>	AF168738	AF315040	Hirudinea		
<i>Polybrachia</i> sp.	AF168739	AF315037	<i>Haemopsis sanguisuga</i>	X91401 ^d	
<i>Siboglinum fiordicum</i> GB	X79876 ^b		<i>Hirudo medicinalis</i>		AF315058
<i>Siboglinum fiordicum</i>	AF315060	AF315039	Oligochaetae		
<i>Siboglinum ekmani</i>	AF315062	AF315038	<i>Enchytraeus</i> sp.	Z83750 ^d	
<i>Spirobrachia</i> sp.	AF168740	AF315036	Phyllodocida		
Vestimentifera			<i>Glycera americana</i>	U19519 ^e	
<i>Escarpia spicata</i>	AF168741	AF315041	Polynoidea		
Escarpiid n. sp.		AF315053	<i>Lepidonotopodium fimbriatum</i>		AF315056
<i>Lamellibrachia barhami</i>	AF168742	AF315043	<i>Branchiopolynoë symmytilida</i>		AF315055
		AF315044	Sabellida		
		AF315045	<i>Sabella pavonina</i>	U67144 ^c	
		AF315047	Tubificidae		
<i>Oasisia alvinae</i>	AF168743	AF315052	<i>Tubifex</i> sp.		AF315057
<i>Ridgeia piscesae</i>	AF168744	AF315048	Echiura		
		AF315051	<i>Ochetostoma erythrogrammon</i>	X79875 ^b	
		AF315054	<i>Urechis</i> sp.		AF315059
<i>Ridgeia piscesae</i> GB	X79877 ^b		Sipuncula		
<i>Riftia pachyptila</i>	AF168745	AF315049	<i>Phascolosoma granulatum</i>	X79874 ^b	
		AF315050	Nemertea		
<i>Tevnia jerichonana</i>	AF168746	AF315042	<i>Lineus</i> sp.	X79878 ^b	
Monilifera			Mollusc		
<i>Sclerolinum brattstromi</i>	AF315061	AF315046	<i>Scutopus ventrolineatus</i>	X91977 ^f	
Annelida			Priapulida		
Alvinellidae			<i>Priapulys caudatus</i>	X80234 ^g	
<i>Paralvinella palmiformis</i>	AF168747		Arthropod		
			<i>Artemia salina</i>	X01723 ^h	

^a Unless otherwise noted, sequences were obtained in this study.^b Sequence from Winnepeninckx *et al.* (1995a).^c Sequence from Nadot and Grant (unpublished).^d Sequence from Kim *et al.* (1996).^e Sequence from Halanych *et al.* (1995).^f Sequence from Winnepeninckx *et al.* (1996).^g Sequence from Winnepeninckx *et al.* (1995b).^h Sequence from Nelles *et al.* (1984).

stone worm radiation. Because siboglinids are not closely related to molluscs and because of rate heterogeneity problems within the Mollusca, only a single representative (the aplacophoran *Scutopus*) was used. Due to alignment limitations, outgroups employed in the 16S analyses—a leech, an oligochaete, two polynoid polychaetes, and an echiurid—were more limited (see Table 1). Because different investigators collected the data at different times, there was not a 1:1 correspondence in OTUs between data sets. We felt it more important to present all the relevant data rather than trim taxa from the data sets. The aligned data sets are available at the journal's Supplement's page (<http://www.mbl.edu/BiologicalBulletin/VIDEO/BB.video.html>) and at TREEBASE (<http://phylogeny.harvard.edu/treebase>).

Data collection

Total genomic DNA was extracted using a modified hexadecyl-trimethyl-ammonium bromide (CTAB) protocol (Doyle and Dickson, 1987). The entire 18S nuclear rDNA gene was amplified *via* PCR (polymerase chain reaction), using the universal metazoan oligonucleotide primers 18e and 18P (Halanych *et al.*, 1998). A region of the 16S mitochondrial rDNA was amplified using 16Sar-5' and 16Sbr-3' primers (Palumbi, 1996). Each 50 μ l reaction consisted of about 50 ng of template DNA, 0.5 μ M of each primer, 2.5 mM MgCl₂, 200 μ M dNTPs, 5 μ l of manufacturer's 10 \times reaction buffer, and 1.5 U *Taq* polymerase (Promega Inc., Wisconsin). Cycling profiles were as fol-

lows: 18S—initial denaturation at 95 °C for 3 min, 35 cycles of amplification (denaturation at 95 °C for 1 min, annealing at 50 °C for 2 min, extension at 72 °C for 2 min 30 s), and a final extension at 72 °C for 5 min; 16S—initial denaturation at 94 °C for 2 min, 40 cycles of amplification (denaturation at 94 °C for 30 s, annealing at 46 °C for 30 s, extension at 72 °C for 1 min), and a final extension at 72 °C for 7 min. PCR products were purified using the QIAEX II gel extraction kit (Qiagen Inc., California). Approximately 60 ng of purified PCR product was used in sequencing reactions according to the manufacturer's instructions (FS Dye Termination Mix or Big Dye, Applied Biosystems Inc., California). The reaction profile was 25 repetitions of denaturation at 94 °C for 30 s, annealing at 50 °C for 15 s, and extension at 64 °C for 4 min. Dye-labeled fragments were separated by electrophoresis on a Perkin Elmer ABI 373A or 377 DNA sequencer. Both strands of the PCR product were sequenced. In addition to the PCR primers, the oligonucleotide primers used for sequencing are given in Halanych *et al.* (1998) or Hillis and Dixon (1991). The sequences were assembled and verified using the AutoAssembler and Sequence Navigator programs (Applied Biosystems Inc., California). The terminal primer regions were not included in the sequences submitted to GenBank or in the phylogenetic analyses.

Phylogenetic analyses

Sequence alignment was produced with a Clustal W program (Thompson *et al.*, 1994) and subsequently corrected by hand using the protostome secondary structure models available through the Ribosomal Database project (<http://rdp.cme.msu.edu/html/>). Regions that could not be unambiguously aligned (*e.g.*, divergent loop domains) were excluded from analyses. Tree reconstructions were implemented with the PAUP* 4.0b4b2 program (Swofford, 2000), and MacClade 3.06 (Maddison and Maddison, 1992) was used for character and tree analyses. Neighbor-joining (NJ), parsimony, and maximum likelihood (ML) analyses were performed and yielded similar results. In the interest of brevity, results and discussion will focus on ML analyses.

NJ trees were reconstructed under Jukes-Cantor, Kimura-2-parameter, Tamura-Nei, general-time-reversible, and log/det models. All except log/det were examined under equal rates of among-site rate variation using the empirically derived gamma shape parameter, α , of 0.3 (see Swofford *et al.*, 1996, for summary of different assumptions used in these models). A Kishino-Hasegawa (1989) likelihood evaluation of the resulting topologies revealed no significant differences between models for either the 16S or the 18S data. Kishino-Hasegawa evaluations estimated a six-substitution-type rate matrix for which nucleotide base frequencies were set to empirical values and α was estimated. NJ bootstraps consisted of a log/det correction (model was

arbitrarily chosen) with 1000 iterations. Parsimony analyses consisted of heuristic searches with 100 random sequence additions and tree-bisection-reconnection (TBR) branch swapping. Transitions (Ti) and transversions (Tv) were given equal weighting. ML evaluation of parsimony topologies was the same as for NJ topologies. One thousand iterations were used for parsimony bootstrap analyses. When using likelihood to search for the "best" tree (as opposed to evaluating given trees), computation time was limiting. Therefore, we used a nucleotide model with two substitution types where the Ti/Tv ratio was set to the value estimated for the best parsimony tree (empirical base frequencies were used). ML searches were heuristic with 10 random sequence-addition replicates. ML bootstraps employed the "Faststep" option with 100 iterations.

Results

The 18S rDNA data set consisted of 26 OTUs and 1935 nucleotide positions. Of the 1614 nucleotide positions that could be unambiguously aligned, 34.6% (559 positions) were variable and 18.7% (303 positions) were parsimony informative. Figure 1 shows the single best likelihood tree (Ln likelihood = -8260.55148) recovered. All search methods in all analyses found a monophyletic siboglinid clade (bootstrap support was $\geq 98\%$ for all methods). Resolution within the vestimentiferan clade, as well as between annelid groups, was poor, however. The moniliferan *Sclerolimum brattstromi* falls out with the vestimentiferan taxa in all analyses (bootstrap $\geq 98\%$). The remaining frenulates form a distinct sister-clade to the *Sclerolimum*-vestimentiferan clade with $\geq 99\%$ bootstrap support.

Resolution among annelid taxa and within the vestimentiferans was poor due to the lack of phylogenetic signal. Because this paper does not focus on the annelid radiation, we did not try to enhance resolution among all annelid taxa. However, we did attempt to boost the signal within the vestimentiferan clade by employing a less inclusive taxonomic alignment. For metazoan 18S sequences, inclusion of broader taxonomic diversity can often create larger regions of ambiguous alignment that should not be included in analyses, due to poor assumptions about positional homology. Thus by reducing the taxonomic breadth examined, the phylogenetic signal can potentially be increased by a "better" alignment (Halanych, 1998). Unfortunately, even when just the siboglinids were aligned, little genetic diversity was observed, and the vestimentiferan taxa were still poorly resolved (not shown). The exception was *Lamellibrachia barhami*, which was consistently placed as the most basal vestimentiferan. Table 2 shows the logdet/paralinear distances (below diagonal) and absolute distances (above diagonal) for this less-inclusive, siboglinid-only alignment (in which most divergent domains could be unambiguously aligned). Even though the distance values for the siboglinid-

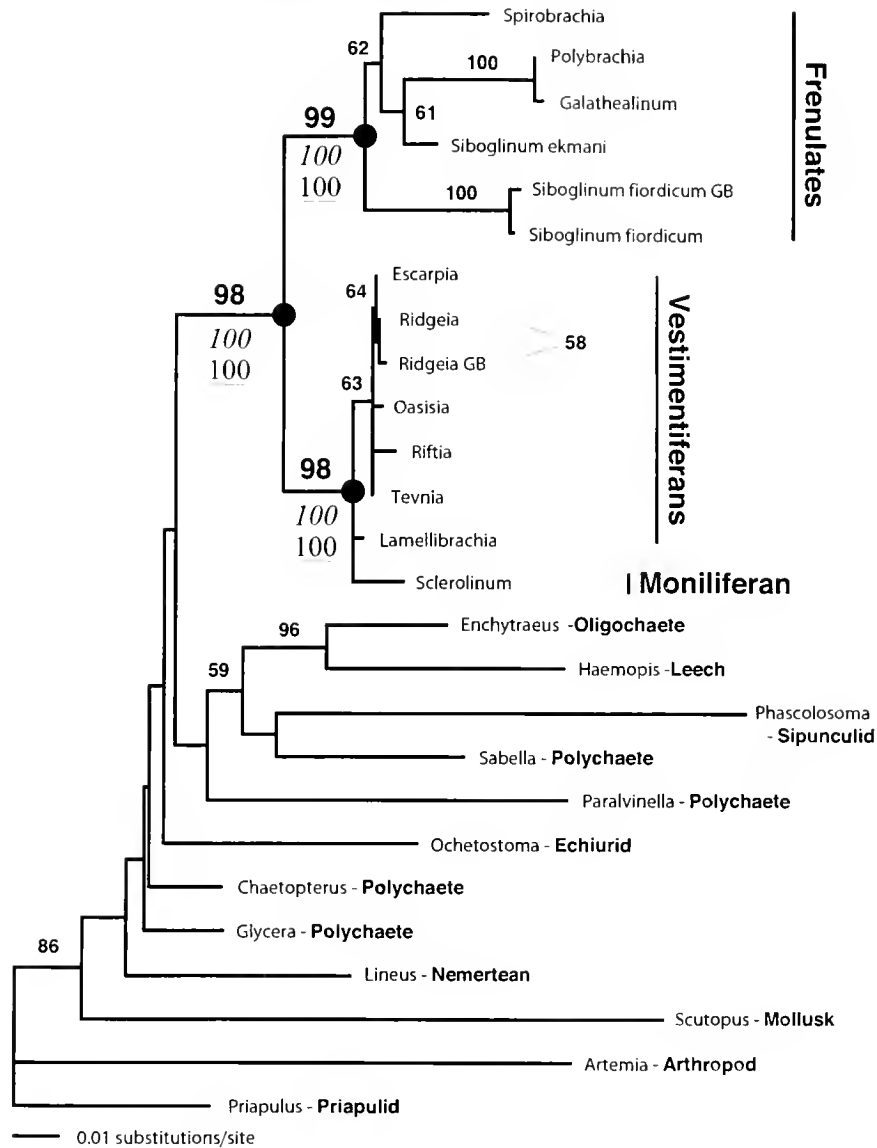


Figure 1. Results of 18S rDNA phylogenetic analyses. The single best likelihood tree (\ln likelihood = -8260.55148) found. Analysis details are given in the text. Maximum likelihood bootstrap values of $\geq 50\%$ are given in bold. Parsimony (italic) and neighbor joining (underlined) values are also given for the major nodes of interest (values for other nodes were omitted in the interest of space). Branch lengths are drawn proportional to the inferred amount of change along the branch (scale shown).

only alignment are only slightly greater than the full alignment values, the greatest distance within vestimentiferans was only 0.02 (with a maximum of 25 nucleotide differences), revealing that there was very little 18S genetic diversity within this group.

The 16S rDNA data set consisted of 24 OTUs, each with 497 nucleotide positions. Of the 465 nucleotide positions that could be unambiguously aligned, 60.4% (281 positions) were variable and 47.7% (222 positions) were parsimony informative. The reconstructed topology (\ln likelihood = -3967.21062), Figure 2, was qualitatively similar to the 18S topology. Siboglinids are divided into two major lin-

eages: vestimentiferans plus the moniliferan *Sclerolinum brattstromi* (bootstrap support 83% for ML and 100% for NJ and parsimony) and a frenulate sister-clade (bootstrap support $\geq 94\%$ in all analyses). Again, *S. brattstromi* was basal to the vestimentiferans. In a departure from the 18S analyses, *Riftia pachyptila*, not *Lamellibrachia barhami*, often fell out as the most basal vestimentiferan. However, this was never supported by $>54\%$ bootstrap support; ML analyses that excluded the non-siboglinid outgroups revealed that the base of the Vestimentifera was poorly resolved with 16S data. A comparison of genetic divergence values (Table 3) indicates that there was limited genetic

TABLE 2

Pairwise distances for the siboglinid-only 18S rDNA data set; absolute distances above diagonal and log/det distances below diagonal

	1	2	3	4	5	6	7	8	9	10	11	12	13	14
1 <i>Spirobrachia</i>	—	109	113	87	132	131	124	122	125	124	131	125	121	120
2 <i>Polybrachia</i>	0.07	—	9	104	138	137	139	140	140	140	147	142	140	136
3 <i>Galathealinum</i>	0.07	0.01	—	106	142	141	142	143	143	143	150	145	143	139
4 <i>Siboglinum ekmani</i>	0.05	0.06	0.06	—	116	117	113	110	113	110	121	112	107	112
5 <i>Siboglinum fiordicum</i>	0.08	0.09	0.09	0.07	—	5	140	136	136	140	143	138	134	139
6 <i>Siboglinum fiordicum</i> GB	0.08	0.08	0.09	0.07	0.00	—	143	139	139	143	146	141	137	140
7 <i>Escarpia</i>	0.08	0.09	0.09	0.07	0.09	0.09	—	7	14	10	19	6	13	31
8 <i>Ridgeia</i>	0.08	0.09	0.09	0.07	0.09	0.09	0.00	—	8	7	17	4	12	32
9 <i>Ridgeia</i> GB	0.08	0.09	0.09	0.07	0.09	0.09	0.01	0.00	—	14	21	11	19	38
10 <i>Oasisia</i>	0.08	0.09	0.09	0.07	0.09	0.09	0.01	0.00	0.01	—	20	7	14	32
11 <i>Riftia</i>	0.08	0.09	0.09	0.07	0.09	0.09	0.01	0.01	0.01	0.01	—	16	25	39
12 <i>Tevnia</i>	0.08	0.09	0.09	0.07	0.09	0.09	0.00	0.00	0.01	0.00	0.01	—	11	30
13 <i>Lamellibrachia</i>	0.07	0.09	0.09	0.07	0.08	0.09	0.01	0.01	0.01	0.01	0.01	0.01	—	28
14 <i>Sclerolinum</i>	0.08	0.09	0.09	0.07	0.09	0.09	0.02	0.02	0.02	0.02	0.02	0.02	0.02	—

variation within vestimentiferans (≤ 0.11 log/det distance; a maximum of 47 nucleotide differences).

As for the frenulate clade, neither 18S or 16S supported a monophyletic *Siboglinum*; but because only two *Siboglinum* species were examined, additional taxa are needed to verify the status of this frenulate taxon. Additionally, we performed Kishino-Hasegawa (1989) likelihood evaluation for both genes to test the monophyly of the frenulate and vestimentiferan-*Sclerolinum* clades. To this end, we used the constraints option in PAUP* 4.0b4b2 to conduct parsimony heuristic searches (specifics same as above) to find the best trees that were consistent and inconsistent with the monophyly of these clades. Both the 16S and the 18S data significantly support the monophyly of both groups (18S frenulates—average ML score supporting monophyly = -8244.69 , non-monophyly score = -8278.135 , P value < 0.01 ; 16S frenulates—monophyly = -3894.889 , non-monophyly = -3927.49 , P value < 0.005 ; 18S vestimentiferan-*Sclerolinum*—monophyly = -8244.69 , non-monophyly = -8271.922 , P value < 0.05 ; 16S vestimentiferan-*Sclerolinum*—monophyly = -3894.889 , non-monophyly = -3911.802 , P value < 0.05).

Discussion

The monophyly of siboglinids (aka, Pogonophora *sensu lato*) is supported by morphological (Southward, 1988, 1993; Rouse and Fauchald, 1995; Rouse, 2001), embryological (Southward, 1999), and molecular (Winnepeninckx *et al.*, 1995a; Black *et al.*, 1997; McHugh, 1997; Halanych *et al.*, 1998, this study) evidence. Thus, in agreement with others (Southward, 1988, 1999; Ivanov, 1994; McHugh, 1997), we see no support for the recognition of vestimentiferans and frenulates as having fundamentally different body plans (*i.e.*, "phyla" *sensu* Jones, 1985). The assertion made by Webb (1964b) and later by Ivanov (1991, 1994) that *Sclerolinum* was notably different from frenulates is

validated by the present data. Moreover, we found that *Sclerolinum brattstromi* is closely allied to the vestimentiferans, and does not occupy a position basal to a frenulate-vestimentiferan clade, confirming Ivanov's (1991; 1994; Ivanov and Selivanova, 1992) ideas that moniliferans occupy a position intermediate between vestimentiferans and frenulates.

Southward (1993) also suggested a possible evolutionary link between *Sclerolinum* and vestimentiferans. This contention is confirmed by the present analysis, as well as a recent morphological cladistic analysis (Rouse, 2001). Using 44 morphological characters coded for all recognized siboglinid genera, Rouse found support for the monophyly of Frenulata, Vestimentifera, and the *Sclerolinum*-vestimentiferan clade. However, our use of nomenclature differs from Rouse with regard to the term Monilifera, which he applies to the *Sclerolinum*-vestimentiferan clade. Because this term was originally (Ivanov and Selivanova, 1992) applied to only *Sclerolinum*, and because of the morphological differences from vestimentiferans, Rouse's use of the term will inject confusion into the literature. Although we acknowledge that Monilifera, as defined here, is redundant with the generic name *Sclerolinum*, several aspects of siboglinid evolution and taxonomy are in need of additional study. Thus, we have chosen not to name this clade until more is understood about siboglinid evolution.

The placement of *Sclerolinum* was especially interesting in the context of the evolution of habitat preference. Previous studies of vestimentiferans (Black *et al.*, 1997), clams (Peck *et al.*, 1997), mussels (Craddock *et al.*, 1995), and shrimp (Shank *et al.*, 1999) reveal that vent-endemic organisms are related to, and possibly derived from, species associated with hydrocarbon seeps that occur near subduction zones and continental margins. Furthermore, recent observations (Feldman *et al.*, 1998; Baco *et al.*, 1999; Distel

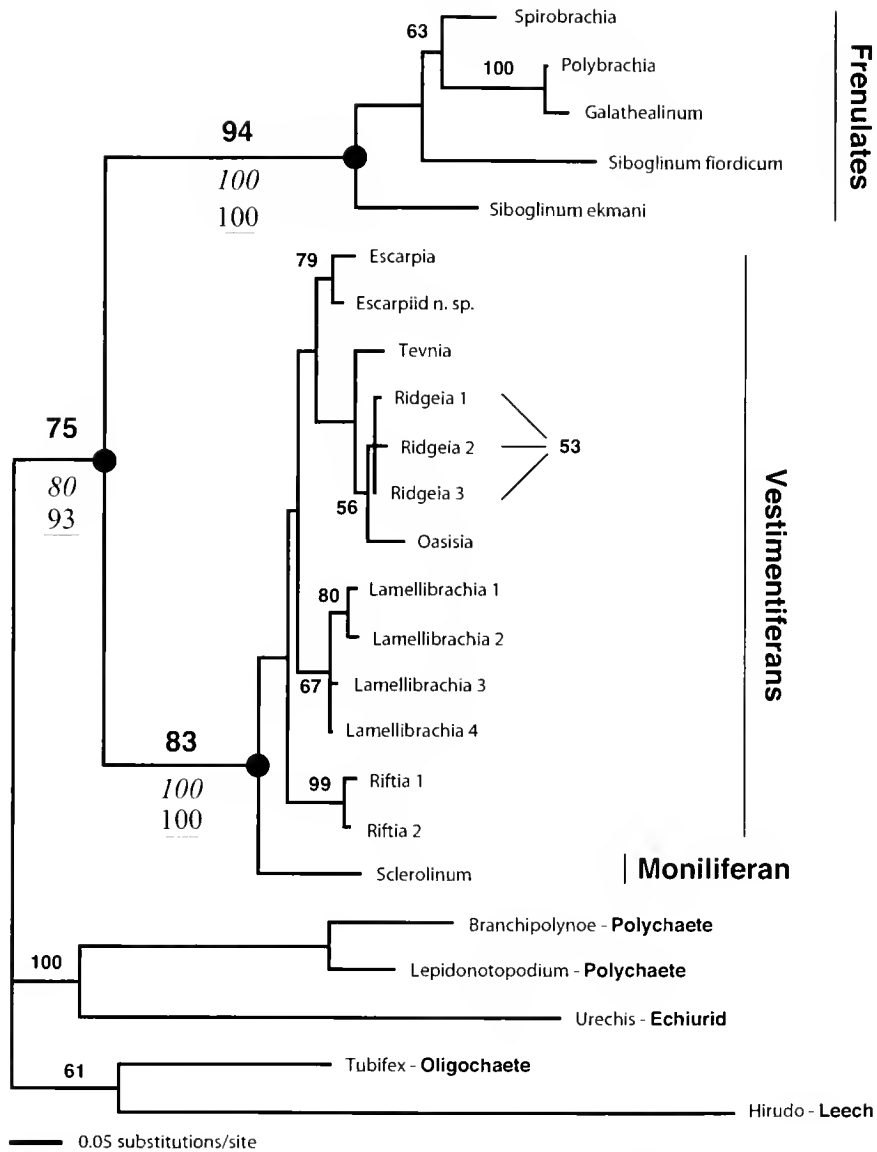


Figure 2. Results of 16S rDNA phylogenetic analyses. The best likelihood tree (Ln likelihood = -3967.21062) found. Another tree with a Ln likelihood score of -3967.25739 was found in the same search. The trees differed in relationships within the *Ridgeia* clade. Analysis details are given in the text. Maximum likelihood (ML) bootstrap values of $\geq 50\%$ are given in bold. Parsimony (italic) and neighbor joining (underlines) values are also given for the major nodes of interest (values for other nodes were omitted in the interest of space). In the ML bootstrap analysis, *Lamellibrachia* and *Sclerolinum* formed a clade in 55% of the iterations. That is not shown above because it is incompatible with the "best" ML tree. Branch lengths are drawn proportional to the inferred amount of change along the branch (scale shown).

et al., 2000) reveal that several symbiont-bearing clams, vestimentiferan tubeworms, and mussels can survive on rotting organic material, such as wood or a whale carcass. The moniliferan *S. brattstromi* and related species (*e.g.*, *S. javanicum*, *S. minor*, and *S. major*) are typically found growing on decaying organic material such as wood or rope (Webb, 1964a, b; Southward, 1972; Ivanov and Selivanova, 1992). Other members of the genus, (*e.g.*, *S. sibogae* and *S. magdalenae*) lived buried in mud (Southward, 1972). These

habitat preferences suggest that affinity for a mud or silt habitat was ancestral in siboglinids, allowing us to speculate that a pattern of evolution from low-oxygen, sedimented habitats to decaying organic material to hydrocarbon seeps to hydrothermal vents has occurred within the *Sclerolinum*-vestimentiferan clade.

Although neither the 18S nor the 16S data clearly resolve relationships within the Vestimentifera, the cytochrome *c* oxidase subunit I (COI) data of Black *et al.* (1997) show

TABLE 3

Pairwise distances for 16S rDNA data set; absolute distances above diagonal and log/det distances below diagonal

	1	2	3	4	5	6	7	8	9	10	11	12	13	14	15	16	17	18	19	20	21	22	23	24
1 <i>Spirobrachia</i>	—	41	52	65	65	119	116	114	112	116	111	114	119	121	121	117	118	122	120	129	125	141	123	141
2 <i>Polybrachia</i>	0.09	—	8	68	67	113	111	108	108	108	106	113	114	111	113	109	106	106	117	126	114	129	121	134
3 <i>Gadathelminum</i>	0.12	0.02	—	81	79	118	117	113	107	115	114	118	119	118	119	117	107	112	122	134	125	134	133	146
4 <i>Siboglinum fiordicum</i>	0.16	0.17	0.21	—	90	129	125	120	116	121	116	117	128	130	129	125	117	122	127	128	129	142	121	142
5 <i>Siboglinum ekmani</i>	0.15	0.16	0.19	0.23	—	121	117	120	116	119	115	117	123	125	123	119	115	120	126	129	140	116	133	144
6 <i>Escarpia</i>	0.30	0.30	0.31	0.35	0.33	—	12	29	32	35	34	36	32	36	31	31	35	37	58	126	119	130	117	144
7 <i>Escarpid</i> n. sp.	0.29	0.29	0.30	0.34	0.31	0.03	—	30	29	32	27	34	30	31	29	27	35	39	52	124	114	126	112	139
8 <i>Tevnia</i>	0.30	0.28	0.29	0.33	0.32	0.07	0.07	—	16	17	17	26	43	43	40	39	35	37	70	122	109	133	119	139
9 <i>Ridgeia</i> 1	0.30	0.29	0.28	0.33	0.33	0.08	0.07	0.04	—	2	2	17	35	33	32	33	38	37	70	123	106	127	115	138
10 <i>Ridgeia</i> 2	0.30	0.29	0.30	0.33	0.32	0.08	0.08	0.04	0.00	—	5	21	37	40	34	36	40	38	73	127	109	134	120	142
11 <i>Ridgeia</i> 3	0.28	0.28	0.30	0.31	0.31	0.08	0.06	0.04	0.00	0.01	—	16	35	36	34	32	40	43	68	124	107	131	116	138
12 <i>Oasisia</i>	0.30	0.30	0.31	0.32	0.32	0.09	0.08	0.06	0.04	0.05	0.04	—	38	39	41	41	43	47	69	123	108	128	114	139
13 <i>Lamellibrachia</i> 1	0.31	0.30	0.32	0.35	0.34	0.08	0.08	0.10	0.09	0.09	0.08	0.09	—	7	11	11	38	42	51	127	115	128	116	146
14 <i>Lamellibrachia</i> 2	0.32	0.29	0.31	0.36	0.34	0.09	0.08	0.10	0.08	0.10	0.08	0.09	0.02	—	14	12	36	43	53	127	116	125	118	148
15 <i>Lamellibrachia</i> 3	0.32	0.30	0.31	0.35	0.33	0.08	0.07	0.09	0.08	0.08	0.08	0.10	0.03	0.03	—	4	34	35	52	130	118	131	118	150
16 <i>Lamellibrachia</i> 4	0.30	0.28	0.31	0.34	0.32	0.08	0.07	0.09	0.08	0.09	0.07	0.10	0.03	0.03	0.01	—	31	35	50	128	116	129	116	148
17 <i>Riftia</i> 1	0.32	0.28	0.27	0.32	0.32	0.08	0.08	0.08	0.09	0.10	0.10	0.10	0.09	0.09	0.08	0.07	—	6	58	122	112	125	116	149
18 <i>Riftia</i> 2	0.32	0.28	0.29	0.33	0.32	0.09	0.09	0.08	0.09	0.09	0.10	0.11	0.10	0.10	0.08	0.08	0.02	—	62	129	117	133	121	154
19 <i>Sclerolinum</i>	0.31	0.31	0.32	0.34	0.32	0.15	0.13	0.18	0.19	0.19	0.17	0.18	0.13	0.13	0.13	0.13	0.12	0.15	—	120	120	129	119	143
20 <i>Branchiopolyne</i>	0.38	0.39	0.41	0.38	0.38	0.39	0.38	0.37	0.40	0.39	0.38	0.38	0.39	0.38	0.40	0.39	0.38	0.39	0.36	—	52	126	114	139
21 <i>Lepidionotopodium</i>	0.37	0.34	0.38	0.39	0.39	0.35	0.33	0.31	0.32	0.32	0.30	0.32	0.34	0.34	0.35	0.34	0.34	0.35	0.36	0.13	—	126	118	136
22 <i>Urechis</i>	0.42	0.38	0.40	0.42	0.43	0.41	0.39	0.42	0.43	0.43	0.41	0.40	0.40	0.38	0.41	0.40	0.40	0.40	0.42	0.40	0.38	—	119	150
23 <i>Tubifex</i>	0.35	0.35	0.40	0.34	0.34	0.35	0.34	0.36	0.37	0.37	0.35	0.34	0.35	0.36	0.36	0.35	0.36	0.36	0.36	0.36	0.34	0.35	0.36	—
24 <i>Hirudo</i>	0.43	0.42	0.46	0.44	0.40	0.44	0.42	0.43	0.45	0.44	0.42	0.43	0.45	0.45	0.46	0.45	0.47	0.48	0.43	0.43	0.42	0.46	0.36	—

TABLE 4

Percent of significant tests when comparing relative substitution rates between the two major siboglinid clades

Test type*	Number of tests	Significant results	Percent significant
Between frenulates and vestimentiferan- <i>Sclerolimum</i> clade			
18S rDNA	480	331	69.0
16S rDNA	350	47	13.4
Within frenulates			
18S rDNA	150	53	35.3
16S rDNA	50	1	2.0
Within vestimentiferan- <i>Sclerolimum</i> clade			
18S rDNA	280	80	28.6
16S rDNA	455	13	2.9

Results of relative rates tests based on an HKY plus gamma model in the HyPhy program. The program is distributed by S. Muse, Department of Statistics, North Carolina State University.

* The 18S comparisons employed all Lophotrochozoan outgroups.

seep tubeworms to be basal to vent tubeworms (but see Williams *et al.*, 1993). This pattern in the evolution of habitat preference roughly proceeds from less reducing to more reducing (greater sulfide and methane availability) environments. A similar evolutionary trend was observed in bathymodiolid mussels (Craddock *et al.*, 1995; Distel *et al.*, 2000). Examination of additional taxa is needed to verify whether this is a general trend in the evolution of vent and seep taxa.

All molecular studies to date (Williams *et al.*, 1993; Black *et al.*, 1997; and Tables 2 and 3) reveal that vestimentiferans exhibit very limited molecular diversity for a group suggested to be several hundred million years old. This lack of diversity may be due to a slowdown in the rate of molecular change (*i.e.*, nucleotide substitution) in vestimentiferans, a recent common origin for extant vestimentiferans, or possibly both. For the present 18S rDNA sequences, vestimentiferans appear to have experienced a significant molecular slowdown relative to the frenulates or other protostome taxa (Table 4; as judged using an HKY plus gamma correction model in the HyPhy software package distributed by S. Muse, Department of Statistics, North Carolina State University). With 16S data, only 13.4% of tests between frenulates and members of the vestimentiferan-*Sclerolimum* clade were significant. Although this value is not statistically significant, it is a greater percentage than is found within either group (~3%), suggesting that a limited rate discrepancy may exist. Similar rate disparities were not observed for COI data (Black *et al.*, 1997), but only one frenulate was used in the comparison. Nonetheless, we concluded that present-day vestimentiferans constitute a young evolutionary group.

In contrast, previous interpretation of Silurian tubeworm fossils (Little *et al.*, 1997) as vestimentiferans suggested that these worms constitute an ancient animal lineage. It is possible that the Silurian tubeworm fossils represent an earlier offshoot from an ancient siboglinid lineage, but this will be impossible to test as the fossils lack the necessary soft-tissue preservation. Additionally, we note that many wormlike invertebrates make tubes. For example, some alvinellid polychaetes observed during our recent expedition to vents along the Southern Eastern Pacific Rise (32°S, 100°W) occupied tubes with diameters comparable to the tubes of mature *Riftia pachyptila*. Many of the alvinellid tubes were partially overgrown by sulfide chimneys, and thus were effectively "fossilized." Although we are not convinced of the interpretation of Silurian fossils as representative of an extant lineage of vestimentiferans, we should point out that specimens from the Cretaceous are convincing (Little *et al.*, 1999). In contrast, all the hydrothermal vent-endemic taxa that have been examined with appropriate molecular tools appear to be from relatively recent radiations (*i.e.*, <100 MY; Black *et al.*, 1997; Peek *et al.*, 1997; Shank *et al.*, 1999; McArthur and Koop, 1999; but see McArthur and Tunnicliffe, 1998, for possible exceptions).

Acknowledgments

We appreciate thoughtful interactions and support of our colleagues at Rutgers University. We wish to thank the crews and staff of the R/V *Altantis/Alvin*, the German research vessel *Sonne*, and the Bergen Marine Station in Espregren for their help in obtaining organisms. Samples of the *Spirobrachia* and *Polybrachia* were provided by R. Lutz (with help from Gyöngyvér Lévai) and identified by Eve Southward, who has been especially generous with information and guidance. The Escarpiid n. sp. was kindly made available by Verena Tunnicliffe and Eve Southward. Material from Norway was collected with aid from the Training and Mobility of Researchers Programme of the European Union, through Contract NO. ERBFMGECT950013 to Eve Southward. Research was supported by an NSF grant, OCE96-33131 to RCV and R. Lutz. The Richard B. Sellars Endowed Research Fund and The Andrew W. Mellon Foundation Endowed Fund for Innovative Research provided partial support to KMH. This is WHOI contribution number 10443.

Literature Cited

- Aguinaldo, A. M. A., J. M. Turbeville, L. S. Linford, M. C. Rivera, J. R. Garey, R. A. Raff, and J. A. Lake. 1997. Evidence for a clade of nematodes, arthropods and other moulting animals. *Nature* 387: 489-493.
- Baco, A. R., C. R. Smith, G. K. Roderick, A. S. Peek, and R. C. Vrijenhoek. 1999. Molecular identification of vesicomyid clams associated with whale-falls on the California Slope. *Mar. Ecol. Prog. Ser.* 182: 137-147.

- Bartolomeaus, T. 1995. Structure and formation of the uncini in *Pectinaria koreni*, *Pectinaria auricoma* (Terebellida) and *Spirorbis spirorbis* (Sabellida): implications for annelid phylogeny and the position of the Pogonophora. *Zoomorphology* **115**: 161–177.
- Black, M. B., K. M. Halanych, P. A. Y. Maas, W. R. Hoeh, J. Hashimoto, D. Desbruyeres, R. A. Lutz, and R. C. Vrijenhoek. 1997. Molecular systematics of vestimentiferan tubeworms from hydrothermal vents and cold-water seeps. *Mar. Biol.* **130**: 141–149.
- Caulley, M. 1914. Sur les Siboglinidae, type nouveau d'invertébrés recueilli par l'expédition du Siboga. *C. R. Acad. Sci.* **158**: 2014–2017.
- Craddock, C., W. R. Hoeh, R. G. Gustafson, R. A. Lutz, J. Hashimoto, and R. C. Vrijenhoek. 1995. Evolutionary relationships among deep-sea mytilids (Bivalvia: Mytilidae) from hydrothermal vents and cold-water methane/sulfide seeps. *Mar. Biol.* **121**: 477–485.
- Distel, D. L., A. R. Baco, E. Chuang, W. Morrill, C. Cavanaugh, and C. R. Smith. 2000. Marine ecology: Do mussels take wooden steps to deep-sea vents? *Nature* **403**: 725.
- Doyle, J. J., and E. Dickson. 1987. Preservation of plant samples for DNA restriction endonuclease analysis. *Taxon* **36**: 715–722.
- Eernisse, D. J. 1997. Arthropod and annelid relationships re-examined. Pp. 43–56 in *Arthropod Relationships*, R. A. Fortey and R. H. Thomas, eds. Chapman and Hall, London.
- Eernisse, D. J., J. S. Albert, and F. E. Anderson. 1992. Annelida and Arthropoda are not sister taxa: a phylogenetic analysis of spiralian metazoan phylogeny. *Syst. Biol.* **41**: 305–330.
- Feldman, R. A., T. M. Shank, M. B. Black, A. R. Baco, C. R. Smith, and R. C. Vrijenhoek. 1998. Vestimentiferan on a whale fall. *Biol. Bull.* **194**: 116–119.
- Halanych, K. 1998. Considerations for reconstructing metazoan history: signal, resolution and hypothesis testing. *Am. Zool.* **38**: 929–941.
- Halanych, K. M., J. D. Bacheller, A. M. A. Aguinaldo, S. M. Liva, D. M. Hillis, and J. A. Lake. 1995. Evidence from 18S ribosomal DNA that the lophophorates are protostome animals. *Science* **267**: 1641–1643.
- Halanych, K. M., R. A. Lutz, and R. C. Vrijenhoek. 1998. Evolutionary origins and age of vestimentiferan tube-worms. *Cah. Biol. Mar.* **39**: 355–358.
- Hillis, D. M., and M. T. Dixon. 1991. Ribosomal DNA: molecular evolution and phylogenetic inference. *Q. Rev. Biol.* **66**: 411–453.
- Ivanov, A. V. 1991. Monilifera—a new subclass of Pogonophora. *Dokl. Akad. Nauk. S.S.S.R.* **319**: 505–507.
- Ivanov, A. V. 1994. On the systematic position of Vestimentifera. *Zool. Jahrb. Abt. Syst. Ökol. Geogr. Tiere* **121**: 409–456.
- Ivanov, A. V., and R. V. Selivanova. 1992. *Sclerolinum javanicum* sp. n., a new pogonophoran living on rotten wood. A contribution to the classification of Pogonophora. *Biol. Morva (Vladivost.)* **1–2**: 27–33.
- Jones, M. L. 1981. *Riftia pachyptila*, new genus, new species, the vestimentiferan worm from the Galapagos rift geothermal vents (Pogonophora). *Proc. Biol. Soc. Wash.* **93**: 1295–1313.
- Jones, M. L. 1985. On the Vestimentifera, new phylum: six new species, and other taxa, from hydrothermal vents and elsewhere. *Bull. Biol. Soc. Wash.* **6**: 117–158.
- Kim, C. B., S. Y. Moon, S. R. Gelder, and W. Kim. 1996. Phylogenetic relationships of annelids, molluscs, and arthropods evidenced from molecules and morphology. *J. Mol. Evol.* **43**: 207–215.
- Kishino, H., and M. Hasegawa. 1989. Evaluation of the maximum likelihood estimate of the evolutionary tree topologies from DNA sequence data, and the branching order in Hominoidea. *J. Mol. Evol.* **29**: 170–179.
- Kojima, S. 1998. Paraphyletic status of Polychaeta suggested by phylogenetic analysis based on the amino acid sequences of elongation factor-1-alpha. *Mol. Phylogenet. Evol.* **9**: 255–261.
- Kojima, S., T. Hashimoto, M. Hasegawa, S. Murata, S. Ohta, H. Seki, and N. Okada. 1993. Close phylogenetic relationship between Vestimentifera (tube worms) and Annelida revealed by amino acid sequence of elongation factor-1a. *J. Mol. Evol.* **37**: 66–70.
- Kojima, S., R. Segawa, J. Hashimoto, and S. Ohta. 1997. Molecular phylogeny of vestimentiferans collected around Japan, revealed by the nucleotide sequences of mitochondrial DNA. *Mar. Biol.* **127**: 507–513.
- Land, J. v. d., and A. Nørrevang. 1977. The systematic position of *Lamellibrachia* (Annelida, Vestimentifera). *Z. Zool. Syst. Evolutionsforsch.* **1975**: 85–101.
- Little, C. T. S., R. J. Herrington, V. V. Maslennikov, N. J. Morris, and V. V. Zaykov. 1997. Silurian hydrothermal-vent community from the southern Urals, Russia. *Nature* **385**: 146–148.
- Little, C., J. Cann, R. Herrington, and M. Morrisseau. 1999. Late Cretaceous hydrothermal vent communities from the Troodos ophiolite, Cyprus. *Geology* **27**: 1027–1030.
- Maddison, W. P., and D. R. Maddison. 1992. *MacClade: Analysis of Phylogeny and Character Evolution*. Sinauer Associates, Sunderland, MA.
- McArthur, A. G., and B. F. Koop. 1999. Partial 28S rDNA sequences and the antiquity of hydrothermal vent endemic gastropods. *Mol. Phylogenet. Evol.* **13**: 255–274.
- McArthur, A. G., and V. Tunnicliffe. 1998. Relics and antiquity revisited in modern vent fauna. Pp. 271–291 in *Modern Ocean Floor Processes and the Geological Record*, R. A. Mills and K. Harrison, eds. Geological Society, London.
- McHugh, D. 1997. Molecular evidence that echiurans and pogonophorans are derived annelids. *Proc. Natl. Acad. Sci. USA* **94**: 8006–8009.
- Nelles, L., B. L. Fang, G. Volckaert, A. Vandenberghe, and R. De Wachter. 1984. Nucleotide sequence of a crustacean 18S ribosomal RNA gene and secondary structure of eukaryotic small subunit ribosomal RNAs. *Nucleic Acids Res.* **12**: 8749–8768.
- Palumbi, S. R. 1996. Nucleic acids II: the polymerase chain reaction. Pp. 205–248 in *Molecular Systematics*, D. M. Hillis, C. Mortiz, and B. K. Mable, eds. Sinauer Associates, Sunderland, MA.
- Peek, A. S., R. G. Gustafson, R. A. Lutz, and R. C. Vrijenhoek. 1997. Evolutionary relationships of deep-sea hydrothermal vent and cold-water seep clams (Bivalvia: Vesicomidae): results from mitochondrial cytochrome oxidase subunit I. *Mar. Biol.* **130**: 151–161.
- Rouse, G. 2001. A cladistic analysis of Siboglinidae Caullery, 1914 (Polychaeta, Annelida): formerly the phyla Pogonophora and Vestimentifera. *Zool. J. Linn. Soc.* **132**: 55–80.
- Rouse, G. W., and K. Fauchald. 1995. The articulation of annelids. *Zool. Scr.* **24**: 269–301.
- Rouse, G. W., and K. Fauchald. 1997. Cladistics and polychaetes. *Zool. Scr.* **26**: 139–204.
- Shank, T. M., M. B. Black, K. M. Halanych, R. A. Lutz, and R. C. Vrijenhoek. 1999. Miocene radiation of deep-sea hydrothermal vent shrimp (Caridea: Bresiliidae): evidence from mitochondrial cytochrome oxidase subunit I. *Mol. Phylogenet. Evol.* **13**: 244–254.
- Southward, E. C. 1961. *Siboga-Expeditie Pogonophora*. Siboga-Expeditie series, vol. 25. E. J. Brill, Leiden.
- Southward, E. C. 1972. On some Pogonophora from the Caribbean and the Gulf of Mexico. *Bull. Mar. Sci.* **22**: 739–776.
- Southward, E. C. 1988. Development of the gut and segmentation of newly settled stages of *Ridgeia* (Vestimentifera): implications for relationship between Vestimentifera and Pogonophora. *J. Mar. Biol. Assoc. UK* **68**: 465–487.
- Southward, E. C. 1993. Pogonophora. Pp. 327–369 in *Microscopic Anatomy of Invertebrates*. Wiley-Liss, New York.
- Southward, E. C. 1999. Development of Perviata and Vestimentifera (Pogonophora). *Hydrobiologia* **402**: 185–202.
- Southward, E. C., and S. V. Galkin. 1997. A new vestimentiferan

- (Pogonophora: Obturata) from hydrothermal vent fields in the Manus Back-Arc Basin (Bismarck Sea, Papua New Guinea, southwest Pacific Ocean). *J. Nat. Hist.* **31**: 43–55.
- Swofford, D. L. 2000.** *PAUP* 4.0 (Phylogenetic Analysis Using Parsimony)*. Sinauer Associates, Sunderland, MA.
- Swofford, D. L., G. J. Olsen, P. J. Waddell, and D. M. Hillis. 1996.** Phylogenetic inference. Pp. 407–514 in *Molecular Systematics*, D. M. Hillis, C. Mortiz, and B. K. Mable, eds. Sinauer Associates, Sunderland, MA.
- Thompson, J. D., D. G. Higgins, and T. J. Gibson. 1994.** CLUSTAL W: improving the sensitivity of progressive multiple sequence alignment through sequence weighting, position specific gap penalties and weight matrix choice. *Nucleic Acids Res.* **22**: 4673–4680.
- Webb, M. 1964a.** A new bidentaculate pogonophoran from Hardangerfjorden, Norway. *Sarsia* **15**: 49–55.
- Webb, M. 1964b.** Additional notes on *Sclerolinum brattstromi* (Pogonophora) and the establishment of a new family, Sclerolinidae. *Sarsia* **16**: 47–58.
- Webb, M. 1969.** *Lamellibrachia barhami*, gen. nov. sp. nov. (Pogonophora), from the northeast Pacific. *Bull. Mar. Sci.* **19**: 18–47.
- Williams, N. A., D. R. Dixon, E. C. Southward, and P. W. H. Holland. 1993.** Molecular evolution and diversification of the vestimentiferan tube worms. *J. Mar. Biol. Assoc. U.K.* **73**: 437–452.
- Winnepenninckx, B., T. Backeljau, and R. De Wachter. 1995a.** Phylogeny of protostome worms derived from 18S rRNA sequences. *Mol. Biol. Evol.* **12**: 641–649.
- Winnepenninckx, B., T. Backeljau, L. Y. Mackey, J. M. Brooks, R. De Wachter, S. Kumar, and J. R. Garey. 1995b.** 18S rRNA data indicate that Aschelminthes are polyphyletic in origin and consist of at least three distinct clades. *Mol. Biol. Evol.* **12**: 1132–1137.
- Winnepenninckx, B., T. Backeljau, and R. De Wachter. 1996.** Investigation of molluscan phylogeny on the basis of 18S rRNA sequences. *Mol. Biol. Evol.* **13**: 1306–1317.
- Young, C. M., E. Vázquez, A. Metaxas, and P. A. Tyler. 1996.** Embryology of vestimentiferan tube worms from deep-sea methane/sulphide seeps. *Nature* **381**: 514–516.

Effect of Cloning Rate on Fitness-Related Traits in Two Marine Hydroids

LAWRENCE M. PONCZEK* AND NEIL W. BLACKSTONE

Department of Biological Sciences, Northern Illinois University, DeKalb, Illinois 60115

Abstract. *Hydractinia symbiolongicarpus* and *Podocoryna carnea* are colonial marine hydroids capable of reproducing both sexually and asexually. Asexual reproduction, by colony fragmentation, produces a genetic clone of the parent colony. This study examines the effect of very different cloning rates on colony growth rate, oxygen uptake rate, and colony morphology. Colonies of one clone of each species were maintained for an extended time in two treatments: in a state of constant vegetative growth by repeated cloning, and in a state restricted from vegetative growth (no cloning). For both species, tissue explants taken from the growing colonies grew more slowly than similar explants taken from the restricted colonies. For one species, tissue explants from the growing colonies used oxygen at a higher rate than similar explants from restricted colonies; for the other species, no difference was detected, although the sample size was small. For both species, tissue explants from restricted colonies formed more circular, "sheet-like" shapes, whereas those from their growing counterparts formed more irregular, "runner-like" shapes. After these experiments, in the third winter of treatment, all colonies experienced a severe tissue regression. Within 6 months after this event, the colonies had regrown to their former sizes. A growth assay at this point revealed no difference in growth rate, possibly suggesting an epigenetic basis for these results. Changes in clonal growth rates and morphology correlated with variation in fragmentation rate might affect the ecology of these and other clonal organisms.

Introduction

Clonal (or "modular") organisms differ from unitary, sexually reproducing ones in that asexual reproduction pro-

duces identical genetic copies of the parent rather than genetically unique offspring. In many organisms, episodes of clonal reproduction may be intercalated with periods of gamete production. This clonal life cycle has obviously been successful; two-thirds of metazoan phyla contain clonal species (Bell, 1982), and most of the earth's sessile biotic covering is composed of clonal life forms (Jackson *et al.*, 1985). During the past few decades, studies in evolutionary biology have delineated various differences between clonal and unitary organisms. In terms of ecology, for instance, clonal organisms typically outcompete asexual ones in marine hard substratum environments, where space is commonly a limiting resource (Jackson, 1977; Larwood and Rosen, 1979). Because its modules are functionally independent, a colony has great regenerative powers and can recover from a substantial colony mortality (Hughes and Cancino, 1985). In addition, a comparison of life histories between the two reproductive modes reveals some inherent and fundamental differences. Fecundity of clones or colonies is indeterminate, because iteration of vegetatively produced modules can yield an indefinite number of reproductive units. This contrasts with unitary organisms, whose fecundity typically levels off or declines with age (Hall and Hughes, 1996). Consequently senescence, a derived property of the unitary soma (Medawar, 1952), may be negligible in clonal genets (Hughes, 1989), which may be very large and comprise a number of unconnected ramets (genetically identical but physiologically separate units).

Despite this considerable attention, one attribute of clonal organisms that has not been studied is the effect on fitness-related traits of the rate of cloning—that is, the number of episodes of asexual reproduction prior to the sexual phase of the life cycle. The rates might differ, for example, between corals inhabiting a turbulent shallow-water habitat and those occupying a deeper, more physically stable environment (*e.g.*, Wulff, 1985). How might

Received 10 July 2000; accepted 26 March 2001.

* To whom correspondence should be addressed. E-mail: plankton9@prodigy.net

variability in this attribute affect the functioning and fitness of an organism?

This question was addressed experimentally using marine hydroids as a model system. This is an appropriate use, since hydractiniid hydroids are colonial organisms commonly used in laboratory manipulations. The species used here, *Hydractinia symbiolongicarpus* and *Podocoryna* (= *Podocoryne carnea*), reproduce both asexually (by colony fragmentation) and sexually (Brusca and Brusca, 1990). The rate of cloning can be precisely controlled in the laboratory, since a colony fragment can be surgically excised from a parent colony and cultured as an independent, yet genetically identical, colony. For a genotype of each of these species, rate of cloning was varied, and growth rate and colony morphology were measured. These are fitness-related traits (Larwood and Rosen, 1979; McFadden *et al.*, 1984; Jackson *et al.*, 1985; Yund, 1991; Brazeau and Lasker, 1992). Fitness has been defined as the expected contribution of a phenotype, genotype, or allele to future generations, relative to other organisms and genes in the environment; and thus it may be measured as numerical dominance over time (Stearns, 1992). For hydroids, which typically inhabit space-limited habitats, the fitness advantage of a high relative growth rate is manifest. Colony morphology is another factor that may affect competitive ability, and therefore it also is important to the success of a clone in a particular environment (Larwood and Rosen, 1979; Jackson *et al.*, 1985). Although laboratory experiments such as these cannot measure actual fitness in nature, we attempt to gain insight into what might happen when similar colony fragments, one from a rapidly fragmenting clone and one from a relatively unfragmented clone, meet in the same natural environment. Do such fragments grow at different rates and thus have different fitnesses? A difference in growth rate could be correlated with a difference in metabolic efficiency. After finding a difference in colony growth rate between these treatments, we measured oxygen consumption rate as an indicator of overall metabolic rate. The implications of these results are discussed in the general context of clonal biology.

Materials and Methods

Study species

Hydractiniid hydroids (phylum Cnidaria) are marine animals that live as encrusting colonies consisting of repeated modular units (polyps) specialized for feeding or reproduction. The polyps are interconnected by tubular stolons that house gastrovascular canals, forming a net-like structure. Each colony thus comprises a single integrated physiological unit. A colony grows onto suitable available substratum by extending peripheral stolons and developing erect feeding polyps at intervals along them. Colony growth ceases when space is no longer available; for instance, in *H.*

symbiolongicarpus, which typically encrusts the shells of hermit crabs, colony growth is limited by the size of the shell. *P. carnea* also grows on hermit crab shells, but is found on other hard substrata as well (Edwards, 1972). The two species differ further in that *H. symbiolongicarpus* forms a relatively dense mat of stolonial tissue as the colony enlarges, but *P. carnea* does not—its stolons are separated by areas free of tissue. Clonal reproduction occurs when a fragment that is separated from a parent colony (*e.g.*, by physical abrasion) is situated on a surface suitable for attachment and growth (Jackson *et al.*, 1985). An entire new colony, genetically identical to the parent colony, can grow, limited in size by available space. Sexual reproduction is accomplished by gamete formation and release into the surrounding seawater where syngamy may occur, leading to the development of a motile planula larva. (*H. symbiolongicarpus* produces gametes directly from specialized reproductive polyps; the life cycle of *P. carnea* includes a motile gametogenic medusa stage.) The planula larva may then attach to a hermit crab shell or other hard substratum suitable for growth, where a genetically novel colony develops.

Culture methods

Colonies of both *H. symbiolongicarpus* and *P. carnea* were collected from the shells of hermit crabs near the Yale Peabody Museum Field Station in Connecticut in 1994. Explants, consisting of a small portion of a colony made up of a few feeding polyps along with interconnecting stolons, were surgically removed from the field-collected colonies and secured with nylon thread to rectangular (3 in × 1 in) glass microscope slides to create stock colonies from which samples could be removed. The slides were then suspended from floating racks in 120-l aquaria filled with Reef Crystals artificial seawater (salinity 35‰), and maintained at a temperature of 20.5° ± 0.5°C. The aquaria used undergravel filtration, and 50% of the water was changed each week. Ammonia, nitrites, and nitrates were maintained below detectable levels (Aquarium Systems test kits). The colonies were fed brine shrimp nauplii 3 times per week. No attempt was made to control the amount of food ingested; observation indicates that generally all polyps in all colonies feed to repletion. Thus, colonies with more or larger polyps are capable of consuming more food. An artificial light cycle of 14:10, L:D, was provided, supplemented by natural light coming in through windows. The colonies were allowed to grow over the slides until large enough to permit removal of a sufficient number of small explants for use as experimental replicates. All replicates used in the experiment were maintained in the same conditions as the stock colonies.

Experimental manipulations

For each hydroid species, 25 clonal replicates from a single parent colony were created on 12-mm round glass

coverslips by surgical explanting from the stock colonies. New explants were secured to the coverslips with nylon thread. Within about one day, the colony attaches itself to the glass of the coverslip. Five of these (for each species) were treated in the following way: a colony was allowed to grow until it had either nearly covered the coverslip or until it began to produce reproductive polyps (in preparation for gamete production). Then a small piece of the colony, consisting of two feeding polyps together with the interconnecting stolon, was explanted onto a fresh coverslip. The new colony was cultured as before, and the old colony was discarded. In this way, the growing replicates were maintained in a state of constant growth and purely clonal reproduction; these colonies are herein referred to as "growing." The remaining 20 replicates (for each species) were allowed to grow completely over the 12-mm cover slips and to produce gametes or medusae in an unrestricted manner. They were left undisturbed for the duration of the experiment, except for removal of explants for the purpose of the various assays. These colonies are referred to as "restricted." The restricted replicates were maintained in higher numbers because of the impossibility of regenerating them (without cloning) in the event of colony mortality. The number of colonies produced ensured that sufficient colony tissue was available for the assays.

Measures of growth rate

Explants consisting of exactly two intermediate-sized feeding polyps and a minimal amount of interconnecting stolon were taken from the experimental colonies, with multiple explants from the same replicate kept to a minimum; that is, an effort was made to take suitably sized fragments from all of the 5 growing replicate colonies and as many of the 20 restricted colonies as possible to obtain the 12 replicates of each treatment for the growth assays. These were then attached synchronously to fresh 12-mm coverslips. Although 12 replicates per treatment per species were initiated, some explants failed to attach to the coverslips, so actual sample sizes per treatment were smaller. Explants were allowed to grow for a period of 3 weeks; none exhausted the available space during the assays. None of the colonies assayed entered a gamete- or medusa-producing phase, so all polyps present during the assays were feeding polyps. Colony size was measured as number of polyps produced and, in two of the three growth assays performed, by total protein content of the colony. For the 3-week polyp counts and total protein measures, between-treatment comparisons were made for each species using analysis of variance.

To ensure that the experimental colonies did not inadvertently get replaced by any vagrant colonies (of different genotype) that might have found their way into the aquarium, clonal identity was tested. This was also done to

support the assumption that significant genetic divergence was not occurring in the colonies during the experiments. To test clonal identity, explants were made from all five of the growing colonies for each species onto clean microscope slides (one slide per explant). One explant from a randomly selected restricted colony was then placed on each slide, and the pair of colonies was allowed to grow until stolonal contact was made. When meeting in this way, colonies from the same clone will merge to produce a single physiological entity having interconnected stolons (Hughes, 1989; Mokady and Buss, 1996). When unrelated clones meet, tissue rejection rather than fusion occurs.

Measures of total protein

Subsequent to polyp counts, the colony to be measured was first macerated in ultrapure water (200–450 μ l, depending on colony size) using a Teflon pestle driven by an electric drill. Then a small sample of the resulting fluid was assayed with the Bio-Rad protein assay kit #500-001, which uses a bovine gamma globulin protein standard and the Bradford method of protein staining (with Coomassie brilliant blue G-250 dye). Binding of the dye to proteins causes a maximum absorbance shift from 465 nm to 595 nm. Absorbance at this wavelength was measured in a Beckman DU-64 spectrophotometer and compared to a standard curve to determine protein amounts. Although questions arise in using a bovine standard for assays of cnidarians (Zamer *et al.*, 1989), these concerns are mitigated in this case because the same genotypes are being compared, and thus relative, not absolute, comparisons are sufficient.

Measures of oxygen uptake rate

Colonies to be assayed were obtained by explanting two-polyp fragments from all five growing colonies and several restricted colonies onto fresh coverslips. These were allowed to grow until they nearly reached the edge of the coverslip. All assays were performed 24 h after feeding: at that time polyps are generally not contracting (Dudgeon *et al.*, 1999), and the colonies could be considered to be in a resting state. Measures of oxygen uptake made at these times can be used as an indication of standard metabolic rate (Schmidt-Nielsen, 1997; Lowell and Spiegelman, 2000). For each assay, a colony of each treatment type was selected, matched as closely as possible in size to minimize any size effects. The two colonies were then assayed sequentially. The assays were done in this pairwise fashion so that any ambient conditions that might affect oxygen uptake rate (variation in atmospheric pressure, *etc.*) would not introduce a sampling bias into the data for either treatment.

Colonies were assayed for rate of oxygen uptake with a Strathkelvin Instruments oxygen meter, model 781. The temperature of the oxygen measurement chamber was controlled with a Neslab Instruments model RTE-100D exter-

nal circulation waterbath at $20.5^{\circ} \pm 0.02^{\circ}\text{C}$. The colony was attached, with a small amount of grease, to a 12-mm glass coverslip to which a small stir bar had been affixed. After instrument calibration, the measurement chamber was loaded with 1.0 ml of seawater filtered to $0.2 \mu\text{m}$ and saturated with oxygen by stirring. Oxygen uptake was measured every 3 min for a period of at least 30 min with stirring. Shortly after each individual assay was begun, the rate of oxygen uptake by the sample colony stabilized and remained linear for the entire 30-min period. The rate thus obtained from each sample provided an observation to be used in the data analysis. Data from the oxygen uptake rate assays were analyzed using analysis of covariance, beginning initially with a test of heterogeneity of slopes. When the slopes were found to not differ, between-treatment differences in elevation were compared.

Characterization of colony morphology

A hydroid colony can be described as tending towards having a more "sheet-like" or "runner-like" morphology (McFadden *et al.*, 1984). Sheet-like colonies, typical of *H. symbiolongicarpus*, are characterized by a relatively circular central stolon area whose periphery has few projecting stolons with free ends. Runner-like colonies, characteristic of *P. carnea*, have a relatively large number of projecting free-ended stolons and a small enclosed central stolon area. A size-free shape measure that may be used to compare colony morphologies is given by (colony perimeter)/ $\sqrt{\text{colony area}}$ (Blackstone and Buss, 1991). A minimum value of $2\sqrt{\pi}$ describes a circular colony with no projecting peripheral stolons; this is the quintessential sheet. As the value of the metric increases, the colony appears more runner-like. Using this shape metric, colonies of both species were tested for a treatment effect. Colonies to be analyzed were explanted onto fresh 12-mm glass coverslips and allowed to grow until a stolon reached the edge of the coverslip, at which time shape analysis was begun. Colony perimeters and areas were quantified by first imaging the colony, then performing image analysis with OPTIMAS 5.0 software (Media Cybernetics) for the Windows operating system. Data gathered in this way were analyzed using analysis of variance, the *F* statistic being computed to compare treatments for each species.

Time course of experiments

The initial experimental explants were made at the beginning of August 1996 (*H. symbiolongicarpus*) and in mid-September 1996 (*P. carnea*). The first growth assays were performed 12 months later. Shape analyses were done in December 1997. The second growth assays for *H. symbiolongicarpus* were performed in July 1998, nearly 24 months after initial explants. At this same time, oxygen uptake assays of *P. carnea* were done. In November 1998,

oxygen uptake assays of *H. symbiolongicarpus* were begun. Shortly after this time, when six pairs of *H. symbiolongicarpus* colonies had been assayed for oxygen uptake, all of the colonies in the experiment underwent a severe tissue regression. This event truncated the *H. symbiolongicarpus* oxygen uptake assays and precluded a planned second growth assay for *P. carnea*. Similar midwinter regressions generally occur in field-collected hydroid colonies exposed to natural light (*pers. obs.*). In the case of the manipulated colonies, this regression was especially severe, with all colonies experiencing almost complete tissue death. However, enough living tissue remained in the colonies so that within 6 months they had regained their previous size. A final growth assay was done for *P. carnea* after 32 months from the initiation of the experiment (beginning of May), and for *H. symbiolongicarpus* after 35 months (beginning of July). Also after 35 months, fusion tests between restricted and growing colonies of each species were begun.

Results

Measures of growth rate

The first growth-rate assay was performed about 12 months after the initial explants of the experimental colonies were made. For both species, the growing colonies grew more slowly than the restricted ones (Fig. 1; ANOVA of log-transformed 3-week polyp counts; *H. symbiolongicarpus*, $F = 9.27$, $df = 1, 20$, $P < 0.007$; *P. carnea*, $F = 13.21$, $df = 1, 22$, $P < 0.002$). A second growth assay was begun for *H. symbiolongicarpus* after 24 months, entailing polyp counts as well as measures of total protein. Again, the restricted colonies grew at a faster rate than their growing counterparts, this time to a more pronounced degree (Fig. 2; ANOVA of log-transformed polyp counts, $F = 65.02$, $df = 1, 17$, $P \ll 0.001$; ANOVA of log-transformed total pro-

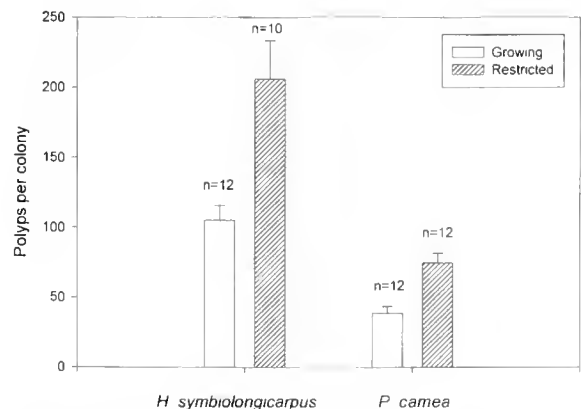


Figure 1. Growth rate comparisons of growing and restricted *Hydractinia symbiolongicarpus* and *Podocoryna carnea* colonies from the assay performed after 12 months of experimental treatment. Means and standard errors of the number of polyps in a colony are represented.

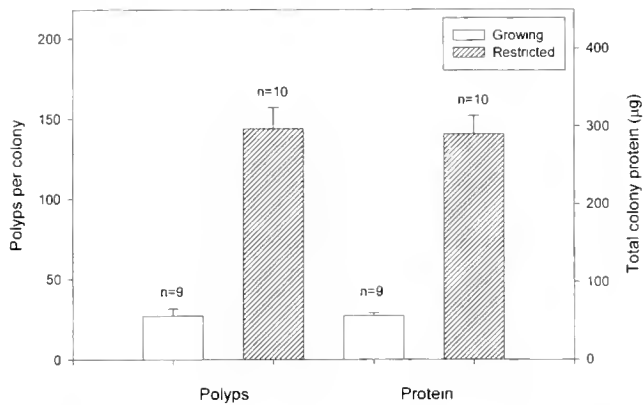


Figure 2. Growth rate comparison of growing and restricted *Hydractinia symbiolongicarpus* colonies from the assay performed after 24 months of experimental treatment. The left y-axis shows the number of polyps in a colony; the right y-axis shows total colony protein. Means and standard errors are represented.

tein, $F = 227.70$, $df = 1, 17$, $P \ll 0.001$). Note that colony size, measured as number of polyps, and total colony protein are highly correlated (Fig. 3). A second growth assay for the *P. carnea* colonies was precluded by the widespread midwinter tissue regression that occurred in early 1999.

The fusion tests resulted in the colonies fusing, suggesting that significant genetic divergence, at least at histocompatibility loci, had not occurred. This result also strongly supports the assumption that experimental colonies were not replaced by other genotypes during the experiments.

Measures of oxygen uptake rate

At all sizes, growing colonies of *P. carnea* consumed oxygen at a higher rate than did restricted colonies (Fig. 4a).

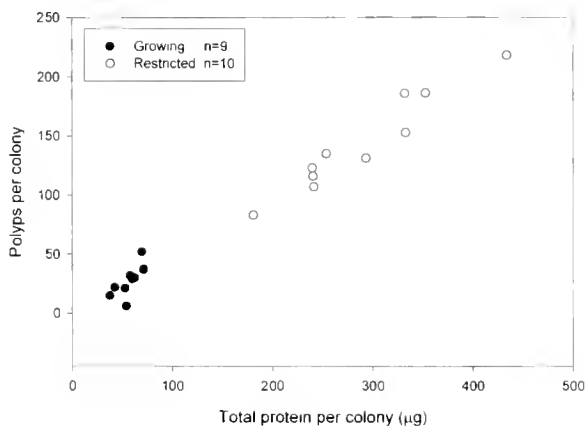


Figure 3. Bivariate scatter plots of the number of polyps in a colony and its total protein content. Linear regression using combined data from both treatments yields the equation $y = 0.507x - 2.44$ (R -squared = 0.98). This intercept is not significantly different from zero ($T = -0.568$, $P > 0.58$). Regression lines for growing and restricted colonies do not differ in slope (ANCOVA, $F = 0.84$, $df = 1, 15$, $P > 0.37$) or elevation ($F = 0.97$, $df = 1, 16$, $P > 0.34$).

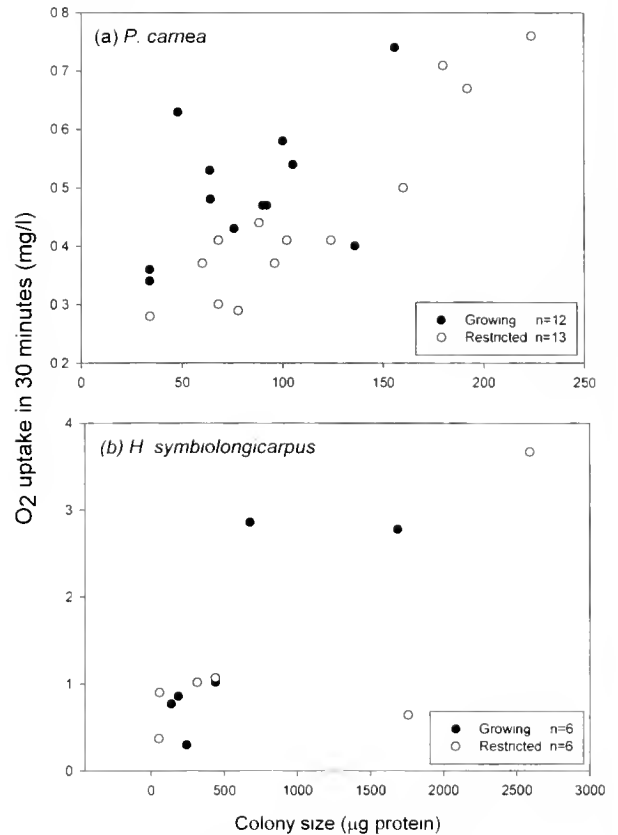


Figure 4. Bivariate scatter plots of oxygen uptake rate of growing and restricted colonies. (a) Data for *Podocoryna carnea*. The slopes of the regression lines for the growing and restricted treatments do not differ (ANCOVA, $F = 1.75$, $df = 1, 21$, $P > 0.20$), but an elevation difference was found ($F = 20.54$, $df = 1, 22$, $P < 0.0002$). These relationships were strengthened by omission of a single outlying data point from the growing data set (slope: $F = 0.10$, $df = 1, 20$, $P > 0.76$; intercept: $F = 41.06$, $df = 1, 21$, $P < 0.0001$). (b) Data for *Hydractinia symbiolongicarpus*. The slopes of the regression lines for the two treatments were not significantly different (ANCOVA, $F = 0.83$, $df = 1, 8$, $P > 0.39$), and neither were the intercepts ($F = 0.98$, $df = 1, 9$, $P > 0.35$).

Although no significant difference in oxygen consumption rate was found between treatments for *H. symbiolongicarpus* (Fig. 4b), a trend may be discerned in the data that would indicate agreement with the result found for *P. carnea*. The sample size is too small to render this trend statistically significant, however.

Characterization of colony morphology

Growing colonies of both species had a more runner-like morphology than their restricted counterparts (Fig. 5; *H. symbiolongicarpus*, $F = 12.56$, $df = 1, 20$, $P < 0.002$; *P. carnea*, $F = 6.16$, $df = 1, 22$, $P < 0.0212$).

Growth rate after regression

A growth assay was performed 4 to 6 months after the pronounced winter regression. At this time, no significant

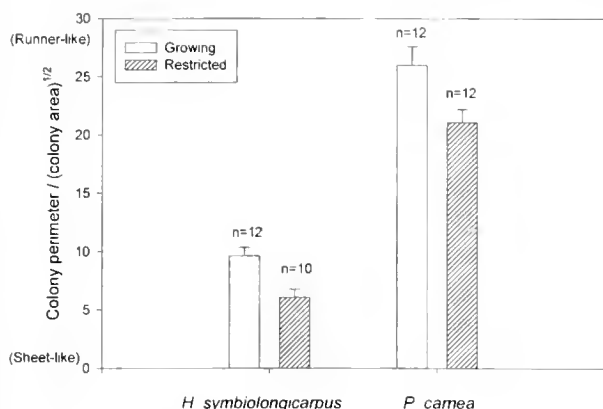


Figure 5. Comparison of growing and restricted colonies after 18 months of experimental treatment in terms of colony morphology as given by the shape metric (colony perimeter) $^{1/2}$ /(colony area). Means and standard errors are represented.

difference was detected between treatments in either species for growth as measured by total colony polyp counts (Fig. 6a; *H. symbiolongicarpus*, $F = 0.06$, $df = 1, 16$, $P > 0.806$; *P. carnea*, $F = 0.44$, $df = 1, 18$, $P > 0.516$, data for both analyses log-transformed) or by total colony protein (Fig. 6b; *H. symbiolongicarpus*, $F = 0.17$, $df = 1, 16$, $P > 0.689$; *P. carnea*, $F = 1.04$, $df = 1, 18$, $P > 0.321$; data for both analyses log-transformed).

Discussion

Two experimental treatments were used in this study of hydroid colonies. One group of replicates was allowed to completely overgrow and remain undisturbed on 12-mm coverslips ("restricted" colonies); a second group was repeatedly cloned as vegetative growth continued, without being allowed to enter into a gamete-producing sexual phase ("growing" colonies). A clear difference in growth rate was found between treatments in both species studied, with restricted colonies exceeding growing colonies in growth rate during controlled assays. Since only one clone was used per species, this result is not replicated at the level of the species. Nevertheless, at a higher level (*i.e.*, species within family), the two clones provide replication of this primary result.

Assays of the oxygen uptake rate between treatments revealed that the growing colonies of *Podocoryna carnea* exceeded the restricted ones in oxygen consumption. Although no significant statistical difference was found for *Hydractinia symbiolongicarpus*, the sample size was small, and a trend seems to be discernible in the data that would suggest agreement with the result for *P. carnea*. Such a result may seem counterintuitive; the colony that uses more oxygen might also be expected to grow faster. On the other hand, higher oxygen uptake may be correlated with lower growth rate if the former indicates greater metabolic expen-

diture on, for instance, somatic maintenance. Such a hypothesis is not entirely implausible. These hydroid colonies are ecologically space-limited, typically inhabiting small hermit crab shells. It is likely that selection favors rapid sequestration of available space to prevent the settlement of competitors; colonies may maximally allocate energy resources to growth until the available space is covered. Under such conditions of intense metabolic demand, cellular metabolism may generate high levels of reactive oxygen species (Allen, 1996; Chiueh, 2000). These reactive species can cause various defects in macromolecules, so continuously growing colonies might experience defects in the mechanisms of oxidative phosphorylation or allocate greater resources to production of anti-oxidant enzymes (*e.g.*, Blackstone, 2001). Thus the data are consistent with the hypothesis that growing colonies expend more energy on functions other than somatic growth, although further study of this issue is needed. Our interpretation of these results is that the restricted colonies are metabolically more efficient and so can allocate more energy to growth (Lowell and Spiegelman, 2000).

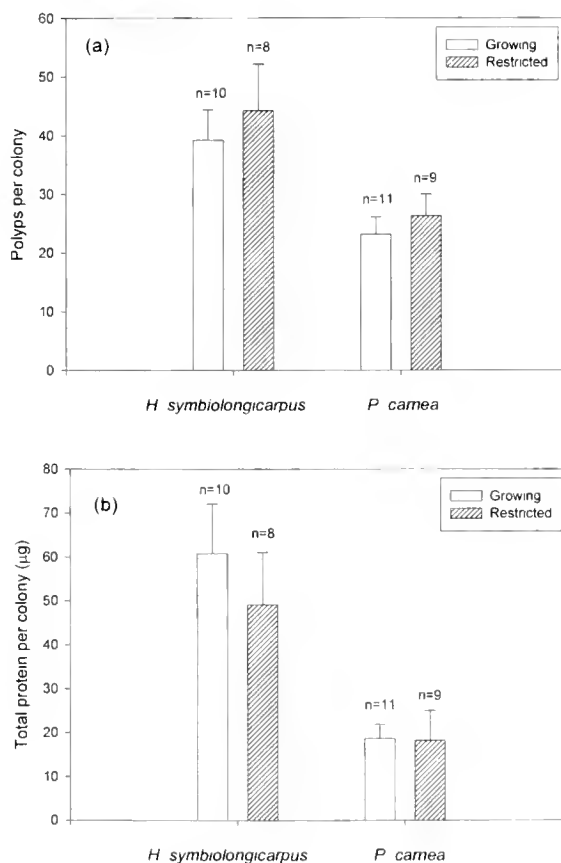


Figure 6. Growth rate comparisons of growing and restricted *Hydractinia symbiolongicarpus* and *Podocoryna carnea* colonies from the assay performed after 32–35 months of experimental treatment. Means and standard errors are represented. (a) Number of polyps per colony (b) Total colony protein content.

The widespread tissue regression that occurred apparently reset to zero the growth rate difference that had been entrained by the experimental treatments. By this view, the physiological basis of the difference prior to regression was transmitted to the clonal fragments of the growing colonies, becoming enhanced over time as shown by the decreasing colony growth rate. This may suggest an epigenetic basis for the phenomenon, wherein a particular state of gene activity underlies the increased rate of oxygen consumption coupled with the reduced growth rate. During the regression event, all colonies lost most of their living tissue, effecting a cell population bottleneck. The elimination of the growth rate difference could perhaps be due to sampling error in the cells that escaped death during the regression, or to some dedifferentiation process involving a return to a metabolic ground state. In any case, cells of similar condition and gene activity seem to have survived the regression. Periodic regressions of this kind have been observed in some clonal taxa and are possibly related to senescence (Bayer and Todd, 1997; Gardner and Mangel, 1997). The life span of the modules (polyps) that make up a colony may be extended through cycles of degeneration and regeneration (Hughes, 1989).

Comparing absolute growth rates of colonies undergoing both treatments early in the experiment (Fig. 1) with those measured some two years later (Fig. 3) reveals a consistent decline. Furthermore, the growth rate equalization after regression occurred not by the growing colonies recovering a rapid growth rate but by the faster growing restricted ones assuming a similarly diminished rate. This reduction in growth rate over time may be considered to be a manifestation of colony senescence (Bell, 1988). By this criterion, growing colonies senesced more rapidly than restricted ones prior to the tissue regression event, suggesting that a high cloning rate accelerates colony senescence relative to uncloned colonies. After regression, the degree of clonal senescence (measured by growth rate) became equalized.

Hydractiniid hydroid colonies fragment to produce potentially viable clonal modules, thus enlarging and dispersing the genet asexually (Cerrano *et al.*, 1998). The colony fragmentation rate (equivalent to the cloning rate considered in this study) presumably could vary with the physical environment in which the hydroids are found. In aquaria, Cerrano *et al.* (1998) found that clonal colonies arising from fragments of *Podocoryna exigua* colonies can grow on a sandy-bottom substratum and that hermit crabs with naked shells placed into this environment were colonized within a few days. If such a process occurs naturally in *P. exigua* and other hydractiniid hydroids, such as the species used in this study, a genet might extend itself naturally by fragmentation. Clonal lineages may vary in fragmentation rate and growth rate of colonial ramets. This study shows that cloning rate could

possibly affect the growth rate of a ramet within a lineage through negative feedback, since variation in growth rate may be passed on through some epigenetic mechanism such as cytosine methylation (but see Tweedie and Bird, 2000; and Amedeo *et al.*, 2000). Nevertheless, histocompatibility data (Grosberg *et al.*, 1996; Mokady and Buss, 1996) suggest that in at least some populations of *H. symbiolongicarpus* the rate of fragmentation is low relative to the rate of sexual recruitment.

The alteration in morphology with variation in cloning rate might have a bearing on the ecological functioning of a hydroid colony (McFadden *et al.*, 1984; Yund, 1991; Brazeau and Lasker, 1992). Intraspecific competition is common between *Hydractinia* colonies (Buss and Blackstone, 1991). The present study has shown that a high cloning rate can produce a more runner-like colony morphology, thus tending towards a form associated with a "guerrilla" ecological strategy (Jackson *et al.*, 1985). Such a clone might have more limited direct competitive ability, but might also be dispersed to more locations due to its greater rate of fragmentation.

Asexual reproduction is an essential part of the life history of all clonal organisms and is thus an important factor in their evolution and ecology. In some taxa, fragmentation rate depends on morphological characters, which are at least in part genetic and thus subject to selection. The fragmentation rate of clones of branching coral reef demosponges was found to depend on branch thickness (Wulff, 1985). A coral of the genus *Plexaura* has evidently evolved morphological characters that make fragmentation more common in this species than in its congeners and produce some populations in which more than 90% of the individuals are clonemates (Lasker, 1990). A possible difference in growth rate dependent on cloning rate would have to be taken into account when considering the demographic impact of fragmentation.

The effects of the two experimental treatments on the clonal replicates of both hydroid species indicate that frequently fragmenting colonies exhibit reduced colony growth rates, hence diminished reproductive potential and compromised competitive ability in the space-limited habitats in which they are typically found. Moreover, a within-species difference in colony morphology was found between unfragmented colonies and those maintained in a constant state of vegetative growth by repeated cloning (fragmenting); this difference could affect the ecological functioning of the colonies in nature. However, these discrepancies may disappear if a large-scale regression of colony tissue occurs. Regardless of the specific physiological mechanisms producing these differential effects, fragmentation rate can be important to various aspects of the biology of clonal organisms.

Acknowledgments

Comments were provided by K. Gasser, B. Johnson-Wint, and P. Meserve. The National Science Foundation (IBN-94-07049 and IBN-00-90580) provided support.

Literature Cited

- Allen, J. F. 1996. Separate sexes and the mitochondrial theory of aging. *J. Theor. Biol.* **180**: 135–140.
- Amedeo, P., Y. Habu, K. AlSar, O. Mittelstein Scheid, and J. Paszkowski. 2000. Disruption of the plant gene MOM releases transcriptional silencing of methylated genes. *Nature* **405**: 203–206.
- Bayer, M., and C. D. Todd. 1997. Evidence for zooid senescence in the marine bryozoan *Electra pilosa*. *Invertebr. Biol.* **116**: 331–340.
- Bell, G. 1982. *The Masterpiece of Nature: The Evolution and Genetics of Sexuality*. Croom Helm, London and Canberra.
- Bell, G. 1988. *Sex and Death in Protozoa: The History of an Obsession*. Cambridge University Press, Cambridge.
- Blackstone, N. W. 2001. Redox state, reactive oxygen species, and adaptive growth in colonial hydroids. *J. Exp. Biol.* **204**: 1845–1853.
- Blackstone, N. W., and L. W. Buss. 1991. Shape variation in hydractiniid hydroids. *Biol. Bull.* **180**: 394–405.
- Brazeau, D. A., and H. R. Lasker. 1992. Growth rates and growth strategy in a clonal marine invertebrate, the Caribbean octocoral *Briareum asbestinum*. *Biol. Bull.* **183**: 269–277.
- Brusca, R., and G. Brusca. 1990. *Invertebrate Biology*. Sinauer Associates, Sunderland, MA. 922 pp.
- Buss, L. W., and N. W. Blackstone. 1991. An experimental exploration of Waddington's epigenetic landscape. *Philos. Trans. R. Soc. Lond.* **332**: 49–58.
- Cerrano, C., G. Bavestrello, S. Puce, and M. Sara. 1998. Biological cycle of *Podocoryna exigua* (Cnidaria: Hydrozoa) from a sandy bottom of the Ligurian sea. *J. Mar. Biol. Assoc. U.K.* **78**: 1101–1111.
- Chineh, C. C., ed. 2000. *Reactive Oxygen Species*. *Ann. N. Y. Acad. Sci.* **899**: 425 pp.
- Dudgeon, S., A. Wagner, J. R. Vaisnys, and L. W. Buss. 1999. Dynamics of gastrovascular circulation in the hydrozoan *Podocoryne carnea*: the one-polyp case. *Biol. Bull.* **196**: 1–17.
- Edwards, C. 1972. The hydroids and the medusae *Podocoryne areolata*, *P. borealis*, and *P. carnea*. *J. Mar. Biol. Assoc. U. K.* **52**: 97–144.
- Gardner, S. N., and M. Mangel. 1997. When can a clonal organism escape senescence? *Am. Nat.* **150**: 462–490.
- Grosberg, R. K., D. R. Levitan, and B. B. Cameron. 1996. Evolutionary genetics of allorecognition in the colonial hydroid *Hydractinia symbiolongicarpus*. *Evolution* **50**: 2221–2240.
- Hall, V. R., and T. P. Hughes. 1996. Reproductive strategies of modular organisms: comparative studies of reef-building corals. *Ecology* **77**: 950–963.
- Hughes, R. N. 1989. *A Functional Biology of Clonal Animals*. Chapman and Hall, New York.
- Hughes, R. N., and J. M. Cancino. 1985. Ecological overview of cloning in metazoa. Pp. 153–186 in *Population Biology and Evolution of Clonal Organisms*, J. B. C. Jackson, L. W. Buss, and R. E. Cook, eds. Yale University Press, New Haven.
- Jackson, J. B. C. 1977. Competition on marine hard substrata: the adaptive significance of solitary and colonial strategies. *Am. Nat.* **111**: 743–767.
- Jackson, J. B. C., L. W. Buss, and R. E. Cook, eds. 1985. *Population Biology and Evolution of Clonal Organisms*. Yale University Press, New Haven.
- Larwood, G., and B. Rosen, eds. 1979. *Biology and Systematics of Colonial Organisms*. Academic Press, London.
- Lasker, H. R. 1990. Clonal propagation and population dynamics of a gorgonian coral. *Ecology* **71**: 1578–1589.
- Lowell, B. B., and B. M. Spiegelman. 2000. Towards a molecular understanding of adaptive thermogenesis. *Nature* **404**: 652–660.
- McFadden, C. S., M. J. McFarland, and L. W. Buss. 1984. Biology of hydractiniid hydroids. 1. Colony ontogeny in *Hydractinia echinata* (Flemming). *Biol. Bull.* **166**: 54–67.
- Medawar, P. B. 1952. *An Unsolved Problem of Biology*. H. K. Lewis, London.
- Mokady, O., and L. W. Buss. 1996. Transmission genetics of allorecognition in *Hydractinia symbiolongicarpus* (Cnidaria: Hydrozoa). *Genetics* **143**: 823–827.
- Schmidt-Nielsen, K. 1997. *Animal Physiology: Adaptation and Environment*. Cambridge University Press, Cambridge.
- Stearns, S. C. 1992. *The Evolution of Life Histories*. Oxford University Press, Oxford.
- Tweedie, S., and A. Bird. 2000. Mutant weed breaks silence. *Nature* **405**: 137–138.
- Wulff, J. L. 1985. Variation in clone structure of fragmenting coral reef sponges. *Biol. J. Linn. Soc.* **27**: 311–330.
- Yund, P. O. 1991. Natural selection on hydroid colony morphology by intraspecific competition. *Evolution* **45**: 1564–1573.
- Zamer, W. E., J. M. Shick, and D. W. Tapley. 1989. Protein measurement and energetic considerations: comparisons of biochemical and stoichiometric methods using bovine serum albumin and protein isolated from sea anemones. *Limnol. Oceanogr.* **34**: 256–263.

Egg Longevity and Time-Integrated Fertilization in a Temperate Sea Urchin (*Strongylocentrotus droebachiensis*)

SUSANNE K. MEIDEL* AND PHILIP O. YUND

School of Marine Sciences, Darling Marine Center, University of Maine, Walpole, Maine 04573

Abstract. Recent field experiments have suggested that fertilization levels in sea urchins (and other broadcast spawners that release their gametes into the water column) may often be far below 100%. However, past experiments have not considered the potentially positive combined effects of an extended period of egg longevity and the release of gametes in viscous fluids (which reduces dilution rates). In a laboratory experiment, we found that eggs of the sea urchin *Strongylocentrotus droebachiensis* had high viability for 2 to 3 d. Fertilization levels of eggs held in sperm-permeable egg baskets in the field and exposed to sperm slowly diffusing off a spawning male increased significantly with exposure from 15 min to 3 h. In a field survey of time-integrated fertilizations (over 24, 48, and 72 h) during natural sperm release events, eggs held in baskets accrued fertilizations over as much as 48 h and attained fairly high fertilization levels. Our results suggest that an extended period of egg longevity and the release of gametes in viscous fluids may result in higher natural fertilization levels than currently expected from short-term field experiments.

Introduction

Recent work has started to explore the fertilization dynamics of free-spawning marine organisms that release one or both gametes into the water column (*e.g.*, algae: Pearson and Brawley, 1996; corals: Lasker *et al.*, 1996; starfish: Babcock *et al.*, 1994; sea urchins: Levitan *et al.*, 1992; ascidians: Yund, 1998; fish: Petersen *et al.*, 1992). Although the details of scientific approaches vary, studies can be

broadly grouped into experiments in which a limited number of manipulated organisms are induced to spawn, and surveys of natural spawning events (Levitan, 1995; Yund, 2000). Experimental studies that control spawning synchrony and spatial relationships to test specific mechanistic hypotheses generally suggest that fertilization levels may be limited by sperm availability unless males and females spawn simultaneously, at close range, or under nearly ideal flow conditions (see Levitan and Petersen, 1995; and Yund, 2000, for reviews). In contrast, many surveys of natural spawns report fairly high fertilization levels, at least at the times and places in which most members of a population spawn (Yund, 2000). However, comparisons between existing experiments and surveys are complicated by two major factors. First, results from experimental studies can successfully predict fertilization levels in natural spawns only if experimental conditions (both biotic and abiotic) accurately mimic natural spawning conditions; however, experiments often circumvent reproductive strategies that may have evolved to enhance fertilization (Yund, 2000). Second, experiments and surveys are rarely conducted with the same species, so it is virtually impossible to distinguish between taxonomic and methodological effects in existing studies.

Echinoderms have proven to be a particularly valuable model system for short-term field experiments, and experimental fertilization data from echinoderms generally support the paradigm of severe sperm limitation under a wide range of flow and population conditions (*e.g.*, Pennington, 1985; Levitan, 1991; Levitan *et al.*, 1992; Wahle and Peckham, 1999; but see Babcock *et al.*, 1994). However, there are no published surveys of fertilization levels in natural spawns of echinoderms. The absence of survey data is probably due in part to a lack of information on temporal spawning patterns and the proximate environmental cues that initiate spawning (though multiple cues have been

Received 22 September 2000; accepted 26 April 2001.

* To whom correspondence should be addressed. E-mail: meidel@maine.edu

proposed and investigated: Himmelman, 1975; Starr *et al.*, 1990, 1992, 1993).

Two interrelated adaptations that have been largely bypassed in previous experimental studies may have considerable effects on fertilization levels in natural spawns of temperate echinoderms. The first is an extended period of egg viability, which potentially allows fertilizations to accrue over time. Short-term experiments make one or both of the following assumptions: that most eggs are fertilized within the first few seconds of release (Denny and Shibata, 1989; Levitan *et al.*, 1991) and that gametes are quickly diluted to concentrations below which fertilization can occur. Consequently, extended egg viability has implicitly been presumed to have little influence on fertilization levels in the field. Meanwhile, recent estimates of egg longevity have steadily extended what was presumed to be a relatively short period of viability. Pennington (1985) reported a minimum viability period of 24 h for eggs of the temperate sea urchin *Strongylocentrotus droebachiensis* (Müller), and eggs of a West coast sea urchin are now known to be viable for up to 2 wk when stored under axenic conditions (Epel *et al.*, 1998). If eggs can be fertilized for a long period of time, extended or repeated exposure of eggs to sperm during long-duration spawning events (or events in which multiple males spawn successively) could result in high time-integrated levels of fertilization, even if sperm are limiting in the short term.

A second adaptation that may interact with extended egg longevity to increase fertilization levels is the release of gametes in viscous fluids, which reduces gamete dilution rates and potentially increases the duration of egg exposure to sperm. Thomas (1994) has shown that three species of sea urchins (*Tripneustes gratilla*, *Echinometra mathaei*, and *Colobocentrotus atratus*) release gametes in such viscous fluids that eggs and sperm remain on the test and spines at current speeds less than $0.13 \text{ m} \cdot \text{s}^{-1}$. When the current speed increases, gametes are transported away from this reservoir in long (3–4 cm) strings or clumps, which led Thomas (1994) to hypothesize that sea urchins may achieve high fertilization levels if gametes encounter each other in these structures. Sperm concentrated in clumps presumably also have greater longevity because of a reduction in the respiratory dilution effect (Chia and Bickell, 1983). In contrast to natural sperm release, fertilization experiments often mimic "males" with syringes from which diluted gametes are extruded at a fixed (and fast) rate, thus circumventing the potentially beneficial effect of "sticky" sperm that cling to the test and spines and slowly diffuse away.

In this study, we investigate the effects of these two aspects of sea urchin reproductive biology on fertilization levels in *Strongylocentrotus droebachiensis*. We initially determine the duration of egg viability at two points during the reproductive season. We then explore whether extended (3 h) exposure of eggs to sperm diffusing off a male sea

urchin enhances fertilization levels relative to short-term (15 min) contact at various downstream distances. Finally, we use the full period of egg viability to assay time-integrated fertilization levels during natural sperm release events in small populations and use the distribution of developmental stages in these field samples to evaluate the temporal distribution of fertilization events.

Materials and Methods

General procedures

To obtain fresh eggs and sperm for use in experiments and field sampling, sea urchins (*Strongylocentrotus droebachiensis*) were injected through the peristomial membrane with 0.2–2.0 ml of 0.5 M KCl. Females spawned into 50-ml glass beakers containing chilled seawater that had been aged (~15–20 h; hereafter referred to as aged seawater) to eliminate ambient sperm. Female spawn was checked to confirm the absence of immature oocytes (as indicated by the presence of a large nucleus and nucleolus) and then washed three times with aged seawater. Dry sperm was pipetted directly from the aboral surface of spawning males and kept refrigerated until use (maximum 2 h).

To assay fertilization levels in the field, unfertilized eggs were deployed in sperm-permeable containers. These egg baskets consisted of a 0.1-m-long frame of PVC pipe (internal diameter 0.05 m) with the sides (~90% of circumference) cut away, covered with 35- μm Nitex mesh (after Wahle and Peckham, 1999, as modified from Levitan *et al.*, 1992), and two Styrofoam floats attached for positive buoyancy. Baskets were suspended from the surface or deployed on the bottom in different spatial arrangements as described in the following sections.

Egg longevity

To determine the viability period of eggs of *Strongylocentrotus droebachiensis*, we performed laboratory experiments at the beginning (experiment 1: February 28 to March 2, 2000) and in the middle (experiment 2: March 28 to April 1, 2000) of the spawning season along the coast of Maine (March to May, Cocanour and Allen, 1967). In each experiment, 120 μl of freshly spawned eggs (mean \pm SE of 1651 ± 69 eggs) from each of four females were added to 10 ml aged seawater (aerated for 1 h prior to use) in 20-ml glass scintillation vials. At the start of each experiment (0 h) and after 24, 48, 72, and 96 h (experiment 2 only), eggs in each of four replicate vials per female (only one replicate per female at 0 h in experiment 1) were fertilized with 20 μl of a 10-fold sperm dilution (10 μl fresh dry sperm from 3 males, 90 μl aged seawater). Vials were gently agitated three times during a 15-min period, following which the fertilization process was stopped with the addition of 2.5 ml 37% formaldehyde. At each time point, one additional vial

per female was fixed without fertilization, as a control for false fertilization envelopes (from causes such as egg damage or low egg quality). Vials were kept at ambient seawater temperature (1° – 3° C) during both experiments. Fertilization levels were calculated as the percentage of a random subsample of 300 eggs with a fertilization envelope.

Two-way analyses of variance (ANOVA) with the fixed factors Female (four levels) and Time (three levels in experiment 1; five in experiment 2) were used to analyze variation in fertilization levels (% fertilization). To achieve homogeneity of variances, percent fertilization values were arcsine transformed for experiment 1 (O'Brien's test, $F = 1.20$, $P > 0.32$) but not transformed for experiment 2 (O'Brien's test, $F = 1.35$, $P > 0.19$). The Student-Newman-Keuls (SNK) test was used for *post-hoc* comparisons of levels within main effects in the absence of a significant interaction effect.

Cumulative fertilization in the field: 15 min vs 3 h

In this experiment, we determined whether extended (3 h) exposure of eggs in baskets to sperm from a spawning male enhanced fertilization levels relative to short-term (15 min) exposure. We constructed a fertilization platform that was mounted on a concrete block (L \times W \times H: 0.36 m \times 0.33 m \times 0.14 m) deployed by a rope. The platform consisted of a pine board (1.59 m \times 0.24 m \times 0.02 m) bolted to the concrete block so that it extended 0.31 m upstream of the block and 0.92 m downstream. The board housed one male and two female stations. The male station was simply a surface-mounted PVC plate (0.08 m \times 0.12 m \times 0.003 m), located 0.30 m from the upstream end of the board, to which a spawning male could be fastened. Female stations consisted of eyebolts anchoring ropes that extended to the surface and were located 0.3 and 1.0 m downstream of the male station.

Experiments were performed on a sandy substratum below the dock of the University of Maine's Darling Marine Center in the Damariscotta River estuary (ME, $43^{\circ}50'N$, $69^{\circ}33'W$) at a depth of 4.30 m at mean low water (MLW). For each trial ($n = 8$), four egg baskets (two side by side \sim 0.05 m above the platform at each of two female stations) containing 500 μ l freshly spawned eggs (mean \pm SE: 7613 ± 455 eggs) from one female were attached to the eyebolts. A male was induced to spawn by injection of 2.5–4.5 ml 0.5 M KCl and then attached to the male station with rubber bands. The fertilization platform was then immediately deployed. In addition to the platform, two mobile female stations (baskets on weighted lines with the lower basket 0.35 m above the substratum) were deployed 2 m upstream (control for ambient sperm: one basket) and \sim 2.60 m downstream (two baskets spaced 0.1 m apart vertically, omitted from trial 1) from the male station. After 15 min, one egg basket from each of the three downstream

female stations was retrieved without disturbing the remainder of the array, by pulling it to the surface on its own line. The remaining baskets were retrieved after 3 h, and the presence or absence of sperm on the aboral surface of the male was recorded. Eggs were immediately collected and fixed with formaldehyde. To determine fertilization levels, 300 eggs per vial (200–300 in five cases, 154 in one case) were randomly sampled and scored for the presence or absence of a fertilization envelope. Where sufficient numbers of eggs were retrieved (82% of baskets), small subsamples were taken before fixation and scored after about 15–20 h for the presence or absence of later developmental stages.

During trials 2 through 8, current velocity was recorded with a 3D-ACM acoustic-doppler current meter (Falmouth Scientific). Each trial took place around mid-tide (*i.e.*, commenced \sim 1.5 h after high [or low] water and ended \sim 1.5 h before low [or high] water) to minimize variation in the flow regime.

Three laboratory controls (held at \sim 3°C), consisting of 200 μ l freshly spawned eggs in 10 ml aged seawater, were assayed for (1) fertilization at the start of each trial; (2) fertilization at the end of each trial; and (3) the presence of false fertilization envelopes, scored twice (after retrieval of 15 min and 3 h samples). Laboratory controls were scored in the same manner as field samples.

A two-way ANOVA with the fixed factors Time (two levels) and Distance (three levels) was used to determine differences in fertilization levels (%) in field samples. Percent fertilization values were arcsine transformed prior to analysis to achieve homogeneity of variances (O'Brien's test, $F = 0.94$, $P > 0.47$).

Sperm availability in nature

We measured cumulative (over 24, 48, or 72 h) fertilization levels of eggs retained in baskets during natural spawning events of *Strongylocentrotus droebachiensis*. This sampling design is a hybrid between an experiment and a true survey of natural spawns, because any sperm present were naturally released, but egg locations were under experimental control. Sampling started in mid-February and ended in early April in 1999 and 2000 but varied in intensity (both spatial and temporal) during the two years. In 1999, samples were collected at a single station at Christmas Cove (ChC, mouth of the Damariscotta River estuary); in 2000, samples were collected from three stations at ChC and four stations at Clarks Cove (CIC, 1 km seaward of the Darling Marine Center and \sim 9 km from the ChC site). Both sites were relatively sheltered with a sandy substratum, and surveys of the immediate surroundings indicated the absence of sea urchin populations other than those sampled (*pers. obs.*). A small population of *S. droebachiensis* (\sim 150 animals in 1999, \sim 60 in 2000) occurred naturally at ChC. At CIC, we

released about 350 sea urchins on a rock ledge around the lower low water line on January 29, 2000, but this population appeared to have declined to about 30 animals by April 7, 2000.

At each site, multiple stations were positioned to provide samples at different nominal distances from the sea urchins. At ChC, station 1 was within 1 m of a rock wall that was inhabited by sea urchins during the autumn months; station 2 was on the shoreward end of a floating dock, 5 m straight offshore of the wall; and station 3 was on the seaward end of the same dock, about 13 m from the wall. The shallow depth of station 1 (1.4 m at MLW) allowed sampling at only one depth (0.15 to 0.35 m above the substratum). At stations 2 and 3, we sampled the surface waters during each interval (1.4 to 6.2 m above the substratum, depending on the tidally variable water depth): at times of anticipated sperm presence (based on 1999 results) we also sampled the bottom water 0.15 to 0.35 m above the substratum. During 1999, only station 3 was sampled, and egg baskets were deployed only near the surface. Because the sea urchins were free to move, the positions of our stations relative to spawning males could not be known precisely. However, likely locations can be inferred from sea urchin movement patterns. In 1999, sea urchins mainly remained on the rock wall or wandered between stations 1 and 2, whereas in 2000 many animals spent the spawning season on a piling adjacent to station 2.

We employed a similar sampling scheme at CIC, with minor modifications to accommodate local dock structures. Station 1 was within 1 m of the rock ledge to which sea urchins were transplanted; station 2 was 1 m straight offshore of station 1 (along a fixed wooden dock); and stations 3 and 4 were on floating docks about 12 m from station 1, at 45° angles to either side of the transect from stations 1 to 2. Because of minimal water depth (1.0 to 1.4 m at MLW), all stations were sampled at only a single depth (stations 1 and 2: 0.15 to 0.35 m above the substratum; stations 3 and 4: 0.4 to 3.5 m above the substratum, depending on the tidally variable water depth). Stations 3 and 4 were sampled only when sperm were expected to be present.

At each site, sets of three replicate egg baskets (spaced ~0.1 m apart vertically) were deployed at each station and depth and retrieved 24 h (1999 only), 48 h, or (on only three occasions) 72 h later. In 1999, baskets contained 500 μ l of eggs (~7600 eggs) from one female, and in 2000 they contained 800 μ l of eggs (mean number \pm SE: 11216 \pm 787 eggs) pooled from two to three females. Laboratory controls (200 μ l of eggs in 10 ml aged seawater) were used to determine the incidence of fertilization membranes prior to basket deployment (presumably reflecting sperm contamination) and at the time of retrieval (presumably reflecting false membranes). To determine fertilization levels, 300 eggs per basket or vial were randomly subsampled and scored in three categories: unfertilized, presence of a fertil-

ization envelope, or development through a later stage (2–64 cells, unhatched/hatched blastula, gastrula). Eggs with fertilization envelopes present were judged to have been fertilized only if the sample also contained later developmental stages. From 41% of baskets (181 out of 441), fewer than 300 eggs were retrieved; in these cases, all retrieved eggs were scored. For the calculation of mean fertilization levels, only baskets with more than 50 retrieved eggs were used, resulting in a loss of replicates at some sites and times.

We estimated the approximate distribution of fertilization events during a sample interval from the distribution of developmental stages in a sample and the known rate of development to each stage. We used Stephens' (1972) developmental times for *S. droebachiensis* at 4°C from fertilization to 32-cell stage (2-cell: 5 h; 4-cell: 8 h; 8-cell: 10.5 h; 16-cell: 14 h; 32-cell: 18 h). From the 64-cell stage to gastrulation, we used our own observations of developmental times (64-cell: 21 h; blastula: 24 h; hatching: 40 h; early gastrula: 48 h). We calculated the distribution of fertilizations (%) in time as the percent at each stage (*i.e.*, of a certain age, in h) of all embryos detected (pooled from three replicate baskets).

To establish the extent to which spawning had occurred during the 2000 sampling period, we collected sea urchins for analysis of gonad index (wet weight of gonads as a percentage of total wet body weight) from ChC ($n = 10$) and CIC ($n = 11$) on April 7 and 11, 2000, respectively.

Results

Egg longevity

Egg viability in aged seawater in the laboratory (as assayed by fertilization with fresh sperm) varied significantly among time intervals and females in both experiments (Fig. 1). In experiment 1 (February 28 to March 2, 2000), the effects of both Female ($F_{3,36} = 5.68$, $P = 0.003$) and Time ($F_{2,36} = 8.94$, $P < 0.001$) were significant, but the interaction between the two main factors was not ($F_{6,36} = 1.74$, $P = 0.14$). *Post-hoc* comparisons revealed that fertilization levels were significantly lower for female 2, but similar for females 1, 3, and 4 (SNK-test, $P < 0.05$; Fig. 1A). Fertilization levels were highest at 0 h, similar at 24 and 48 h (SNK, $P > 0.05$), and significantly lower by 72 h (SNK, $P < 0.05$). In experiment 2 (March 28 to April 1, 2000), there were again significant Female ($F_{3,60} = 18.0$, $P < 0.001$) and Time ($F_{4,60} = 273$, $P < 0.001$) effects, as well as a significant interaction between the two main factors ($F_{12,60} = 32.9$, $P < 0.001$). Fertilization of eggs from females 1 and 4 remained relatively high at 72 h, while levels declined markedly for females 2 and 3 (Fig. 1B). For females 1 and 2, fertilizations dropped to very low levels by 96 h, while fertilizations for females 3 and 4 were higher at 96 h than at 72 h (Fig. 1B). Of a total of 36 control sample-

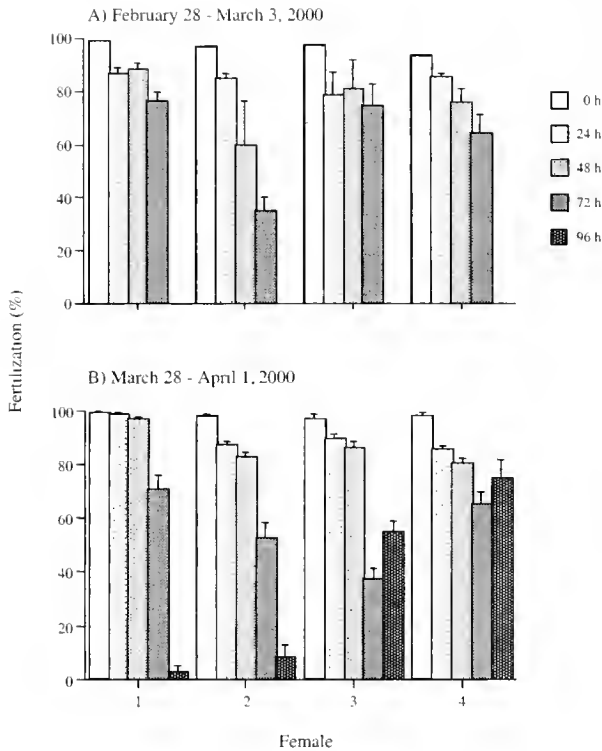


Figure 1. Mean (+SE) fertilization levels (%) over time of eggs from four female sea urchins (A) at the beginning (experiment 1) and (B) in the middle (experiment 2) of the spawning season. Replication is four vials for each female/time combination (except experiment 1 at 0 h; replication = 1).

(16 and 20 in experiments 1 and 2, respectively). 5 had 0.3% false fertilization envelopes and 1 had 0.7%.

In spite of the significant variation among sample times and females in both experiments, egg viability was basically quite high for 48 to 72 h (Fig. 1). With the exception of female 2 in experiment 1, more than 75% of eggs held in aged seawater in the laboratory were viable for 48 h (Fig. 1). At 72 h, viability was in the 50%–75% range for eggs from 6 of the 8 females (Fig. 1).

Cumulative fertilization level (15 min vs 3 h)

When eggs in baskets were exposed to a continuous sperm supply from a spawning male, fertilization levels increased from 15 min to 3 h at distances of 0.3 and 1.0 m downstream from the male, but remained similar over time at 2.6 m (Fig. 2). In the 15-min samples, fertilization decreased with distance from 0.3 to 1.0 m, but remained similar between 1 and 2.6 m (Fig. 2). In the 3-h samples, fertilization decreased monotonically with distance. The two-way ANOVA indicated significant Time ($F_{1,39} = 31.3$, $P < 0.001$) and Distance ($F_{2,39} = 40.1$, $P < 0.001$) effects, as well as a significant interaction between the two main factors ($F_{2,39} = 4.87$, $P = 0.013$). In 5 out

of 8 trials, the male still had sperm on its test at the end of the 3-h deployment, suggesting that fertilization would have continued well beyond the end of our sample interval.

Upstream controls for ambient sperm levels (Fig. 2) generally had $\leq 0.3\%$ fertilization except in trials 1, 6, and 7 when fertilization levels reached 5.3%, 9.0%, and 2.0%, respectively. We attribute fertilizations in trial 6 to a large boat wake that probably created oscillatory water motion and transported sperm towards the upstream control sample immediately before retrieval of the 15-min samples, and we attribute fertilizations in trial 7 to false envelopes (see below). Fertilizations in trial 1 could not be attributed to any obvious cause, and the recorded value was subtracted from the fertilization levels recorded in experimental baskets for that trial.

The apparent absence of a decline in fertilization between the 1- and 2.6-m samples at 15 min and the lack of an increase in fertilization between the 15-min and 3-h samples at 2.6 m are both attributable to one exceptional sample. During trial 5, we recorded a fertilization level of 48% at 2.6 m at 15 min, while values in other trials ranged only from 0.0% to 3.3% (mean \pm SE %: $1.4\% \pm 0.5\%$; $n = 6$) at 15 min and from 3.7% to 15.3% ($6.9\% \pm 1.8\%$; $n = 6$) at 3 h. If this outlier is excluded, fertilization declines from 1 to 2.6 m at 15 min and increases from 15 min to 3 h at 2.6 m.

In laboratory controls, fertilization levels were always very high at the beginning (mean \pm SE: $94.6\% \pm 1.7\%$; $n = 8$) and the end ($94.8\% \pm 1.6\%$; $n = 8$) of a trial. Controls for sperm contamination or false fertilization envelopes mostly indicated 0% envelopes (15 min, $0.3\% \pm 0.2\%$; 3 h, $0.5\% \pm 0.4\%$; $n = 8$) except in trial 7 where

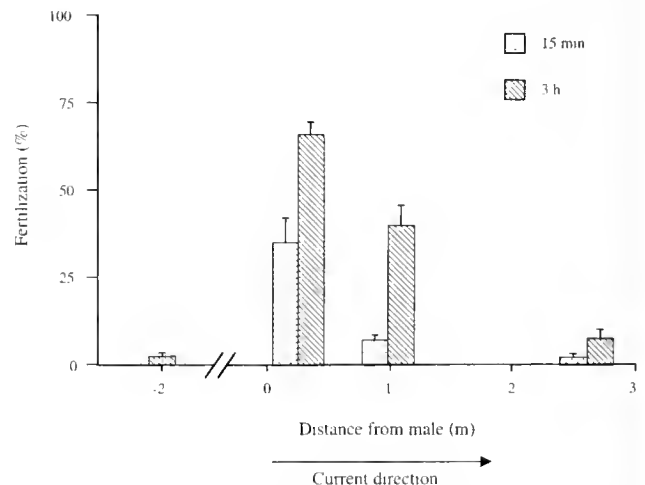


Figure 2. Fertilization as a function of distance and duration of sperm exposure in the field experiment. Mean (+SE) fertilization levels (%) are reported for each time/distance combination. Spawning male is located at 0.0 m mark. Upstream basket was retrieved after 3 h (hatched bar); downstream baskets after 15 min (stippled bars) or 3 h. Replication is 8 trials, except 7 trials for 2.6 m after 15 min, and 6 trials for 2.6 m after 3 h.

1.7% and 3.3% envelopes were found after 15 min and 3 h, respectively. These percentages were subtracted from the fertilization levels recorded in the field for that trial.

Current velocities varied widely during trials 2 through 7 and ranged mainly from 0.08 to 0.20 $\text{m} \cdot \text{s}^{-1}$ (Fig. 3). Mean velocities varied 5-fold among trials during the initial 15-min period (from 0.026 to 0.130 $\text{m} \cdot \text{s}^{-1}$) but were quite similar over 3 h (from 0.121 to 0.155 $\text{m} \cdot \text{s}^{-1}$).

Sperm availability in nature

In both years of the survey (1999, 2000) and at both sites (ChC, CIC), no fertilizations were recorded during most of the sample intervals. However, in both years several sperm-release events of variable magnitude were detected. In 1999 at ChC (only station 3 surface was sampled), fertilizations occurred on March 5 (mean time-integrated fertilization level 4.7%), March 23 (57.3%), March 31 (6.6%), and April 1 (24.6%). In 2000 at ChC, fertilizations occurred on February 19 (station 1 only, 39.5%), March 10 (station 1, 10.3%; station 2, 9.3% surface; no bottom samples were deployed and no fertilization was detected at station 3), March 19 (station 1, 62.3%; station 2, 34.3% surface and 11.3% bottom; station 3, 30.4% surface and 5.3% bottom), and March 29 (station 1, 3.4%; station 2, 4.6% surface; station 3, 4.5% surface; no bottom samples were deployed). At CIC (sampled only in 2000), fertilizations were detected on March 10 (station 1, 24.1%; no fertilization was detected

at station 2; stations 3 and 4 were not sampled), March 17 (station 1, 27.7%; station 2, 10.4%; station 3, 26.2%; station 4, 3.7%), and April 3 (station 1, 6.9%; station 2, 3.3%; stations 3 and 4 were not sampled).

In laboratory controls, fertilization levels were always very high at the start of each sample interval (mean \pm SE %: 1999, 96.7% \pm 0.7%, $n = 19$; 2000, 93.8% \pm 0.9%, $n = 20$). Controls for false fertilization envelopes (stored in the laboratory and fixed upon retrieval of the corresponding field sample) had very low levels of false envelopes (1999, 0.8% \pm 0.5%, $n = 16$; 2000, 0.2% \pm 0.1%, $n = 20$).

Based on the distribution of developmental stages (two-cell to early gastrula) at the time of collection, we estimated that the temporal fertilization pattern varied markedly among the major sperm release events that we detected (Figs. 4–6). Because the discrete developmental stages that we scored are separated by longer time intervals later in development, the 24-h sample interval utilized in 1999 at ChC produced far better resolution of the time of fertilization (~ 3 h) than did the 48- to 72-h intervals employed in 2000 (~ 3 -h resolution for the 24 h immediately preceding sample collection, but ~ 10 h for the portion of the interval > 24 h prior to collection). In 1999, fertilizations occurred in fairly continuous trickles over about 48 h (March 3–5; Fig. 4A) or 24 h (March 22–24; Fig. 4B) or in two distinct pulses of similar magnitude about 24 h apart (March 30–April 1;

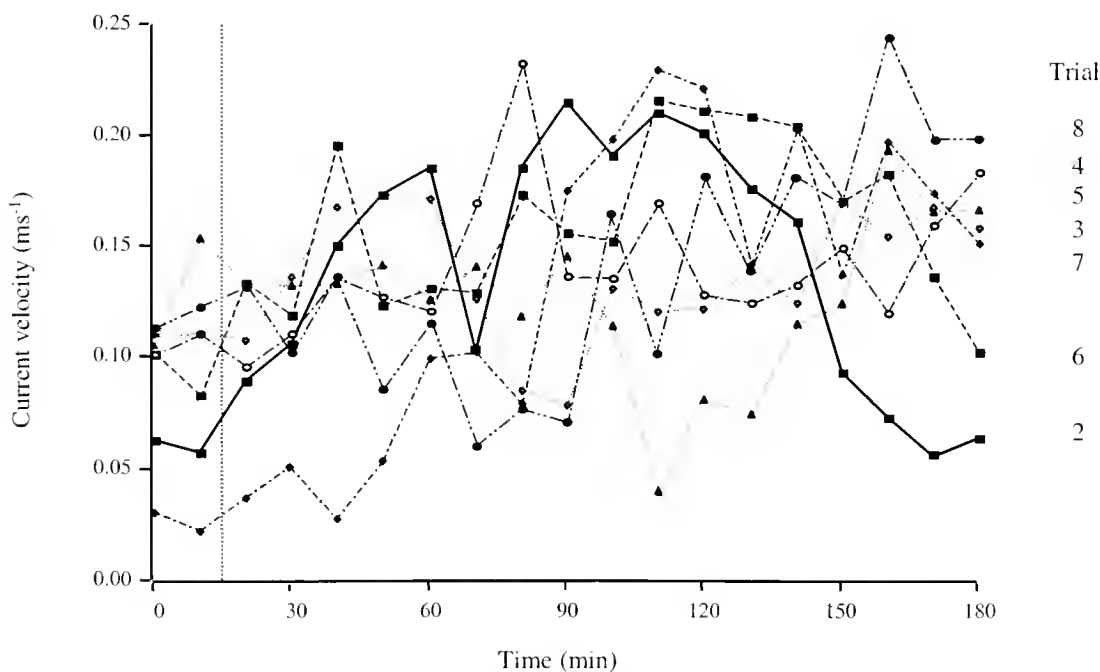


Figure 3. Current velocity ($\text{m} \cdot \text{s}^{-1}$) during seven trials of the field fertilization experiment. Vertical dashed line indicates 15-min interval. Trial 2: each point is one measurement; trials 3–8: each point is mean of 8 measurements collected as two sets of 4 measurements at 15-s intervals 5 min apart. Standard errors are omitted for clarity.

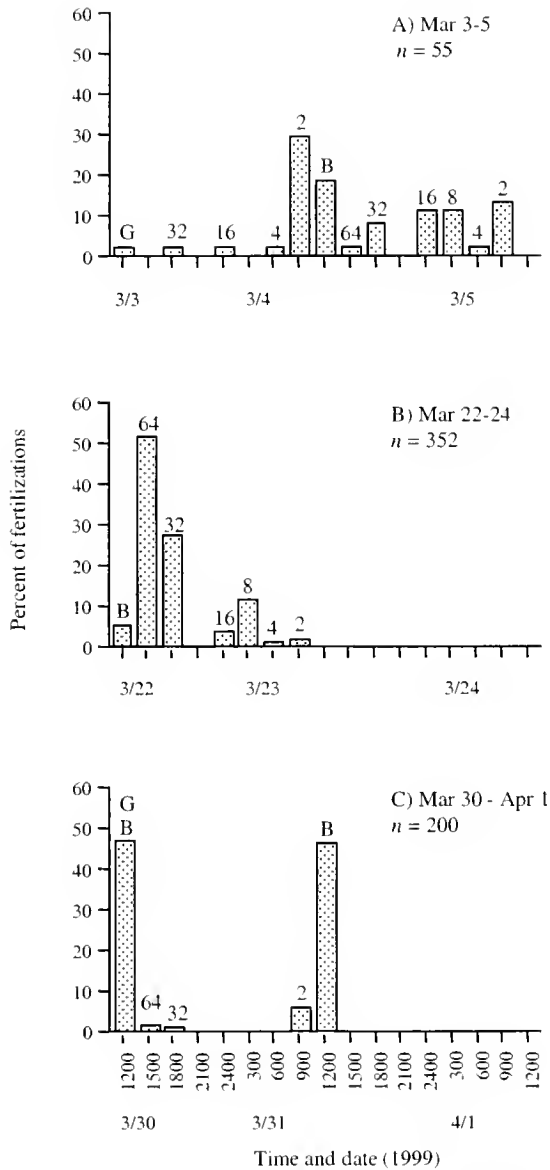


Figure 4. Temporal distribution of fertilizations at Christmas Cove station 3 (surface) during 1999 sample intervals. (A) March 3–5. (B) March 22–24. (C) March 30–April 1. *n*, total number of embryos counted per station (pooled from two to three baskets). Developmental stage corresponding to each inferred fertilization time is indicated above the bar (2, 4, 8, 16, 32, and 64, number of cells; B, unhatched blastula; G, gastrula). When sperm availability extended through two sample intervals (A, C), fertilization times are inferred from both samples.

Fig. 4C). During the most widespread sperm release event in 2000 (March 17–19), fertilizations at 4 of the 5 ChC station/depth combinations were fairly evenly spread over about 24 h (Fig. 5A, B, D, E), but at the fifth station/depth combination virtually all sperm arrived during a much shorter time interval (Fig. 5C). Although the distribution of fertilizations in three apparent pulses at the four stations and depths (Fig. 5A, B, D, E) is an artifact of lower temporal resolution later in development, resolution was nevertheless

sufficient to distinguish fairly consistent sperm availability from a single, shorter pulse (Fig. 5C). During the corresponding fertilization event at CIC (March 15–17, 2000), fertilizations at stations 1 to 3 were also distributed over about 24 h (Fig. 6B–D). At CIC, fertilizations in the March 8–10, 2000 event at station 1 occurred in two major and one minor pulse spread over about 27 h (Fig. 6A).

Sea urchins collected at the end of the field survey at ChC and CIC had intermediate to high gonad indices relative to levels previously recorded for *S. droebachiensis* off the Maine coast (Cocanour and Allen, 1967). Mean gonad indices (\pm SE) were as follows: ChC females, 19.9% \pm 4.7% (*n* = 3), males, 12.3% \pm 2.5% (*n* = 7); CIC females, 14.2% \pm 8.8% (*n* = 5), males, 9.1% \pm 7.0% (*n* = 6). Consequently, additional spawning is likely to have taken place later in the season, after sampling ceased.

Discussion

More than 75% of eggs of the temperate sea urchin *Strongylocentrotus droebachiensis* were generally viable for 48 h when kept in the laboratory in aged (but otherwise untreated) seawater, and viability through 72 h ranged from 50% to 75% in most females (Fig. 1). Subsamples from later time intervals that were isolated prior to formaldehyde addition continued to develop normally through gastrulation (unpub. data). Consequently, fertilization appears to be a reasonable assay of true egg longevity, and does not merely indicate a prolonged ability to elevate a fertilization envelope. Overall, our egg longevity values are greater than earlier estimates of 8 h in sterilized seawater (Wahle and Peckham, 1999) and 24 h in filtered seawater (Pennington, 1985), but shorter than the 1–2 weeks for sea urchin eggs kept under axenic conditions (Epel *et al.*, 1998). Variation both within and among studies, coupled with observations of egg damage in our field surveys, suggests that egg viability is not static but is instead affected by a combination of endogenous and exogenous factors. Variation in egg longevity among the different females in our laboratory experiment (Fig. 1) illustrates the presence of endogenous individual variation. Epel *et al.* (1998) attribute the extreme egg longevity in their study to the removal of bacterial contaminants that can cause the lysis of eggs under laboratory conditions. We observed another form of exogenous damage to eggs in some field samples subject to rough weather (pers. obs.), especially when sediment particles became trapped in the egg baskets. Although damage from sediment abrasion may simply represent a basket artifact, it may also be indicative of a type of egg damage that occurs in nature. Factors controlling egg longevity may ultimately prove to play a significant role in determining fertilization levels in natural spawns.

When we exposed eggs to sperm slowly diffusing from a spawning male's spines and tests (which functionally pro-

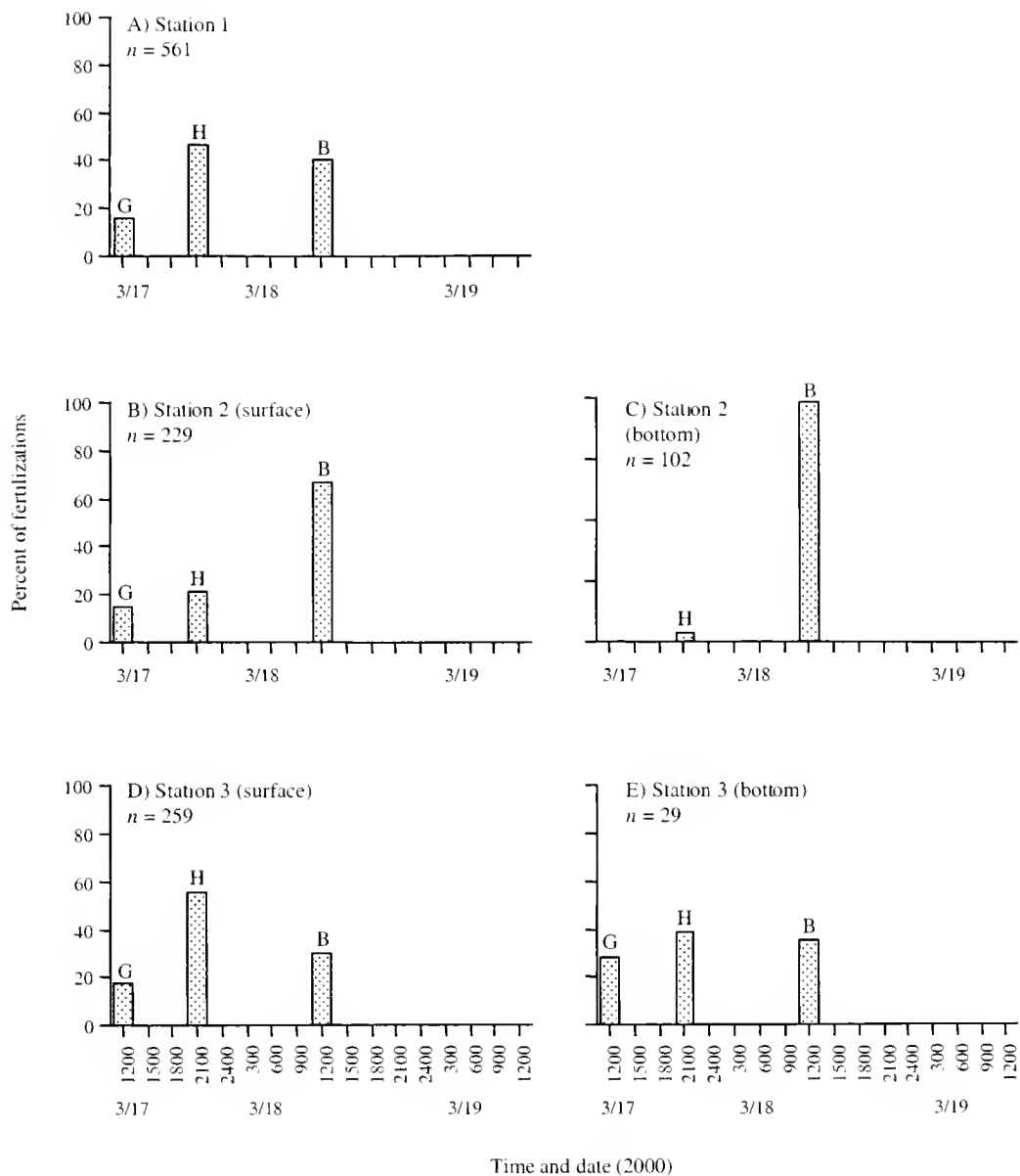


Figure 5. Temporal distribution of fertilizations at Christmas Cove during sample interval March 17–19, 2000. (A) Station 1. (B) Station 2 (surface). (C) Station 2 (bottom). (D) Station 3 (surface). (E) Station 3 (bottom). n , total number of embryos counted per station (pooled from three baskets). Developmental stage corresponding to each inferred fertilization time is indicated above the bar (B, unhatched blastula; H, hatched blastula; G, gastrula).

longs male spawning duration, even though sperm release *per se* may have been short in duration), we recorded higher fertilization levels with time at most downstream locations (Fig. 2). Even though current velocities at our experimental site were often considerable and always exceeded the $0.13 \text{ m} \cdot \text{s}^{-1}$ sperm diffusion threshold suggested by Thomas (1994) during at least some portion of each trial (Fig. 3), 62% of our males still had substantial sperm clinging to their spines and tests when retrieved at the end of the 3-h period (similar observations are reported in Pearse *et al.*,

1988, for a female *S. droebachiensis*). Hence even our 3-h experiment probably underestimates the total time-integrated fertilization levels of fixed-position eggs downstream of a spawning male. Short-term fertilization experiments that use sperm-filled syringes to mimic males (Pennington, 1985; Levitan, 1991; Levitan *et al.*, 1992; Wahle and Peckham, 1999) completely bypass this effect.

The relatively long period of egg viability in *S. droebachiensis* makes it feasible to use sperm-permeable baskets of eggs to assess spatial and temporal patterns of sperm

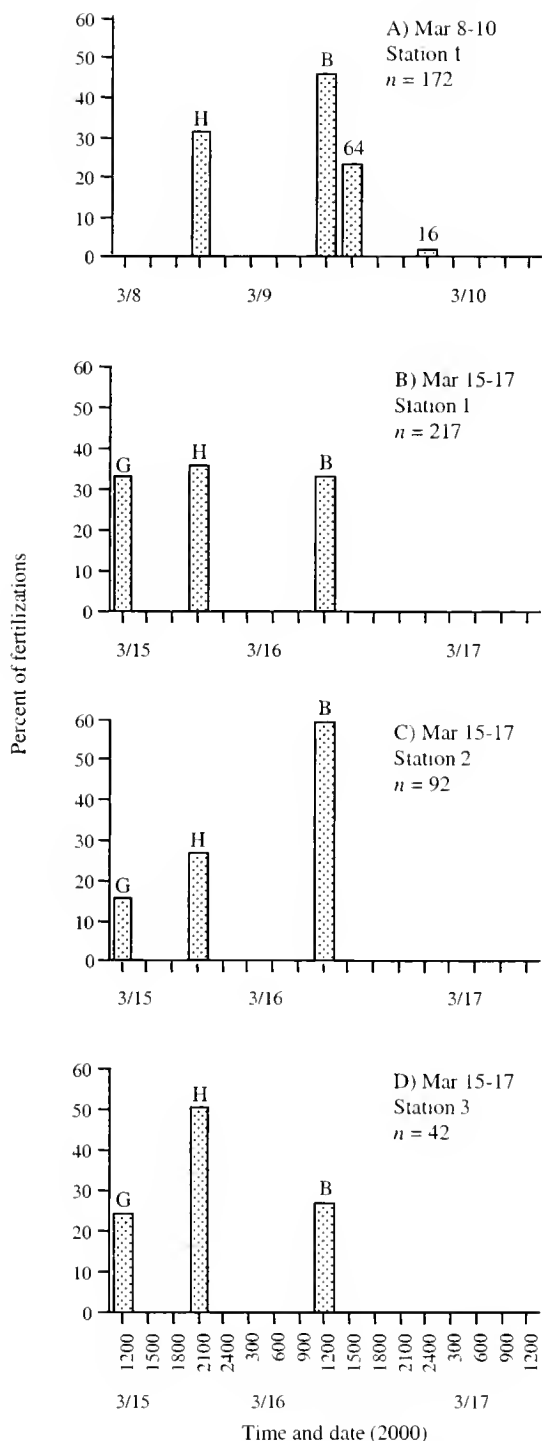


Figure 6. Temporal distribution of fertilizations at Clarks Cove during sample intervals March 8-10 (A) and March 15-17, 2000 (B-D). (A) Station 1. (B) Station 1. (C) Station 2. (D) Station 3. *n*, total number of embryos counted per station (pooled from three baskets). Developmental stage corresponding to each inferred fertilization time is indicated above the bar (32 and 64, number of cells; B, unhatched blastula; H, hatched blastula; G, gastrula).

availability in nature. Our preliminary application of this method detected several sperm-release events in two small populations, one occurring naturally (ChC) and one estab-

lished experimentally (CIC). Several features of the detected sperm-release events are noteworthy. First, total time-integrated fertilization levels were highly variable, ranging from 3.3% to 62% fertilization (when sperm were detected). We emphasize that our experimental design is a hybrid between an experiment and a true survey, because egg position was under experimental control but sperm release occurred naturally. Furthermore, we do not know the actual location of the male or males that spawned, though repeated observations of the distribution of sea urchins during the survey suggest that spawners were likely to be near stations 1 or 2 at both sites (animals were never present at station 3 at ChC, or stations 3 or 4 at CIC). Given these considerations, great care should be exercised when interpreting the absolute fertilization levels reported here. Variation in fertilization levels among sample dates probably reflects the number and proximity of spawning males, but it may be erroneous to conclude that either the higher or lower levels assayed truly represent fertilization levels in natural spawns.

Second, the spatial sampling scheme adopted during 2000 permits some inferences about the spatial scale of sperm availability. Some sperm-release events appear to be highly localized (*e.g.*, ChC, February 19, 2000, station 1 only; CIC, March 10, 2000, station 1 only), with eggs at one station fertilized while eggs a few meters away were not. These sperm distributions are consistent with a pattern of localized sperm availability as indicated by field fertilization experiments conducted with sea urchins (Pennington, 1985; Levitan, 1991; Levitan *et al.*, 1992; Wahle and Peckham, 1999). At other times sperm were present throughout much larger areas (*e.g.*, March 19, 2000, at ChC, March 17, 2000, at CIC). During these widespread sperm-availability events, fertilization levels were often appreciable in much of the site (along a 12-m linear transect at ChC, and within an $\sim 72\text{-m}^2$ triangle at CIC). Regardless of the actual location or number of males spawning, the spatial distribution of fertilizations is more extensive than predicted by simple field fertilization experiments (though more consistent with predictions from a whole-population spawning model; Levitan and Young, 1995).

Third, the single sample that provides fertilization levels at different depths at multiple stations (ChC stations 2 and 3, March 19, 2000) indicated higher fertilization levels near the surface than near the bottom. At least close to shore in shallow water, spawned sperm may tend to be concentrated near the surface rather than near the bottom. The distribution is particularly interesting because eggs are negatively buoyant and hence generally assumed to remain near the bottom.

The distribution of developmental stages in retrieved samples during our 1999 field survey indicated that fertilizations during natural sperm release events may accrue over as much as 48 h (Fig. 4). The decreased temporal resolution

in our 2000 survey nevertheless produced temporal patterns that were consistent with fertilization over about 24 h in most samples (Figs. 5, 6). Fertilizations that occur over extended time periods could be the result of continuous extrusion of sperm from a single male's gonopores, the diffusion of sperm from a gamete reservoir that has accumulated on a male's test, or spawning by multiple males at different times.

Our approach of using egg baskets in field experiments and surveys can potentially be criticized because eggs were held stationary at relatively high concentrations instead of being allowed to move and disperse with the currents. If eggs are rapidly transported away from the female during natural spawns, and thus quickly diluted, egg longevity would be less important in determining cumulative fertilization levels than suggested by our results. But because eggs are spawned in a viscous mass that tends to remain on the test (Thomas, 1994), restraining eggs in baskets may adequately approximate natural spawns and provide a good estimator of fertilization levels under a range of flow conditions. Future work should address the outstanding question of where eggs are actually fertilized: in the egg mass on a female's test (*i.e.*, a fixed location), as they transition from that mass into the water column (still essentially a fixed location), or in the mainstream of flow. The answer to this question is likely to vary with habitat and flow regime.

Our study suggests that details of the reproductive biology of sea urchins can potentially have considerable effects on fertilization levels in the field and that caution should be used when extrapolating fertilization levels in natural spawns from experiments that circumvent these apparent adaptations. We suggest that successful fertilization in sea urchins may result not only from short-term exposure to highly concentrated sperm from a nearby male, but also from long-term exposure to more dilute sperm from a number of more distant males. This proposed scenario is similar to our understanding of fertilization in brooding invertebrates with mechanisms to capture dilute sperm (*e.g.*, Yund, 1998; Bishop, 1998), and has also been suggested for tube-dwelling broadcasters that can move sperm-containing water past spawned eggs (M. E. Williams and M. G. Bentley, University of St. Andrews, Scotland, unpub. obs.). We suggest that fertilization in other broadcast-spawning invertebrates may not be fundamentally all that different.

Acknowledgments

We thank Tim Miller and the staff of the Darling Marine Center for their assistance. Many thanks also go to Matt Babineau and Amy Gilbert whose help in the lab and field was invaluable. We are also grateful to Rick Wahle for many useful discussions throughout this study, to Ed Myers

for access to his dock at the CIC site, and to two anonymous reviewers for helpful comments on an earlier version of this manuscript. Funding was provided by the National Science Foundation (OCE-97-30354). This is contribution no. 364 from the Darling Marine Center.

Literature Cited

- Babcock, R. C., C. N. Mundy, and D. Whitehead. 1994. Sperm diffusion models and *in situ* confirmation of long-distance fertilization in the free-spawning asteroid *Acanthaster planci*. *Biol. Bull.* **186**: 17–28.
- Bishop, J. D. D. 1998. Fertilization in the sea: Are the hazards of broadcast spawning avoided when free-spawned sperm fertilize retained eggs? *Proc. R. Soc. Lond. B* **265**: 725–731.
- Chia, F.-S., and L. R. Bickell. 1983. Echinodermata. Pp. 545–620 in *Reproductive Biology of Invertebrates, Vol. II: Spermatogenesis and Sperm Function*. K. G. Adiyodi and R. G. Adiyodi, eds. John Wiley, New York.
- Cocanour, B., and K. Allen. 1967. The breeding cycles of a sand dollar and a sea urchin. *Comp. Biochem. Physiol.* **20**: 327–331.
- Denny, M. W., and M. F. Shibata. 1989. Consequences of surf-zone turbulence for settlement and external fertilization. *Am. Nat.* **134**: 859–889.
- Epel, D., M. Kaufman, L. Xiao, H. Kibak, and C. Patton. 1998. Enhancing use of sea urchin eggs and embryos for cell and developmental studies: method for storing spawned eggs for extended periods. *Mol. Biol. Cell.* **9**: 182a.
- Himmelman, J. H. 1975. Phytoplankton as a stimulus for spawning in three marine invertebrates. *J. Exp. Mar. Biol. Ecol.* **20**: 199–214.
- Lasker, H. R., D. A. Brazeau, J. Calderon, M. A. Coffroth, R. Coma, and K. Kim. 1996. *In situ* rates of fertilization among broadcast spawning gorgonian corals. *Biol. Bull.* **190**: 45–55.
- Levitán, D. R. 1991. Influence of body size and population density on fertilization success and reproductive output in a free-spawning invertebrate. *Biol. Bull.* **181**: 261–268.
- Levitán, D. R. 1995. The ecology of fertilization in free-spawning invertebrates. Pp. 123–156 in *Ecology of Marine Invertebrate Larvae*, L. R. McEdward, ed. CRC Press, Boca Raton, FL.
- Levitán, D. R., and C. Petersen. 1995. Sperm limitation in the sea. *Trends Ecol. Evol.* **10**: 228–231.
- Levitán, D. R., and C. M. Young. 1995. Reproductive success in large populations: empirical measures and theoretical predictions of fertilization in the sea biscuit *Clypeaster rosaceus*. *J. Exp. Mar. Biol. Ecol.* **190**: 221–241.
- Levitán, D. R., M. A. Sewell, and F.-S. Chia. 1991. Kinetics of fertilization in the sea urchin *Strongylocentrotus franciscanus*: interaction of gamete dilution, age, and contact time. *Biol. Bull.* **181**: 371–378.
- Levitán, D. R., M. A. Sewell, and F.-S. Chia. 1992. How distribution and abundance influence fertilization success in the sea urchin *Strongylocentrotus franciscanus*. *Ecology* **73**: 248–254.
- Pearse, J. S., D. J. McClary, M. A. Sewell, W. C. Austin, A. Perez-Ruzafa, and M. Byrne. 1988. Simultaneous spawning of six species of echinoderms in Barkley Sound, BC. *Invertebr. Reprod. Dev.* **14**: 279–288.
- Pearson, G. A., and S. H. Brawley. 1996. Reproductive ecology of *Fucus distichus* (Phaeophyceae): an intertidal alga with successful external fertilization. *Mar. Ecol. Prog. Ser.* **143**: 211–223.
- Pennington, J. T. 1985. The ecology of fertilization of echinoid eggs:

- the consequences of sperm dilution, adult aggregation, and synchronous spawning. *Biol. Bull.* **169**: 417-430.
- Petersen, C. W., R. R. Warner, S. Cohen, H. C. Hess, and A. T. Sewell. 1992.** Variable pelagic fertilization success: implications for mate choice and spatial patterns of mating. *Ecology* **73**: 391-401.
- Starr, M., J. H. Himmelman, and J.-C. Therriault. 1990.** Direct coupling of marine invertebrate spawning with phytoplankton blooms. *Science* **247**: 1071-1074.
- Starr, M., J. H. Himmelman, and J.-C. Therriault. 1992.** Isolation and properties of a substance from the diatom *Phaeodactylum tricorutum* which induces spawning in the sea urchin *Strongylocentrotus droebachiensis*. *Mar. Ecol. Prog. Ser.* **79**: 275-287.
- Starr, M., J. H. Himmelman, and J.-C. Therriault. 1993.** Environmental control of green sea urchin, *Strongylocentrotus droebachiensis*, spawning in the St. Lawrence estuary. *Can. J. Fish. Aquat. Sci.* **50**: 894-901.
- Stephens, R. E. 1972.** Studies on the development of the sea urchin *Strongylocentrotus droebachiensis*. I. Ecology and normal development. *Biol. Bull.* **142**: 132-144.
- Thomas, F. I. M. 1994.** Physical properties of gametes in three sea urchin species. *J. Exp. Biol.* **194**: 263-284.
- Wable, R. A., and H. Peckham. 1999.** Density-related reproductive trade-offs in the green sea urchin *Strongylocentrotus droebachiensis*. *Mar. Biol.* **134**: 127-137.
- Yund, P. O. 1998.** The effect of sperm competition on male gain curves in a colonial marine invertebrate. *Ecology* **79**: 328-339.
- Yund, P. O. 2000.** How severe is sperm limitation in natural populations of marine free-spawners? *Trends Ecol. Evol.* **15**: 10-13.

Biogeography of *Asterias*: North Atlantic Climate Change and Speciation

JOHN P. WARES

Duke University Zoology, Box 90325, Durham, North Carolina 27708

Abstract. Fossil evidence suggests that the seastar genus *Asterias* arrived in the North Atlantic during the trans-Arctic interchange around 3.5 Ma. Previous genetic and morphological studies of the two species found in the Atlantic today suggested two possible scenarios for the speciation of *A. rubens* and *A. forbesi*. Through phylogenetic and population genetic analysis of data from a portion of the cytochrome oxidase I mitochondrial gene and a fragment of the ribosomal internal transcribed spacer region, I show that the formation of the Labrador Current 3.0 Ma was probably responsible for the initial vicariance of North Atlantic *Asterias* populations. Subsequent adaptive evolution in *A. forbesi* was then possible in isolation from the European species *A. rubens*. The contact zone between these two species formed recently, possibly due to a Holocene founding event of *A. rubens* in New England and the Canadian Maritimes.

Introduction

The North Atlantic Ocean is populated by hundreds of taxa which invaded from the North Pacific following the opening of the Bering Strait about 3.5 million years ago (Ma; Durham and MacNeil, 1967; Vermeij, 1991). Some of these species have maintained genetic contact with source populations in the Pacific until recently (Palumbi and Kessling, 1991; van Oppen *et al.*, 1995), but many of them have subsequently differentiated from the source populations and are now recognized as distinct species (*e.g.*, Gosling, 1992; Reid *et al.*, 1996; Collins *et al.*, 1996). Circumstantial evidence suggests strongly that the seastar genus *Asterias* (Echinodermata: Asteroidea: Asteroiidae: Asteroiinae) participated in the trans-Arctic interchange (Worley and Franz,

1983; Vermeij, 1991). Today, two species are recognized in the North Atlantic: *A. forbesi* on the North American coast, primarily from Cape Hatteras to Cape Cod (Franz *et al.*, 1981), and *A. rubens* on the American coast primarily from Cape Cod northward (Franz *et al.*, 1981), and on the European coast from Iceland to western France (Clark and Downey, 1992; Hayward and Ryland, 1995). American populations of *A. rubens* have been previously described as *A. vulgaris*, a junior synonymy (Clark and Downey, 1992). These species co-occur over a broad range of the North American continental shelf centered on Cape Cod (Gosner, 1978; Menge, 1979; Franz *et al.*, 1981).

Two current hypotheses attempt to explain the recent speciation between *A. forbesi* and *A. rubens*. Schopf and Murphy (1973) suggested that they were a germinate species pair formed by a late Pleistocene (0.02–2.5 Ma) vicariance event (*i.e.*, a separation of populations) at Cape Cod, possibly due to lower sea levels during glacial maxima. There is some evidence for hybridization between these seastars, but the separation could be maintained by localized adaptation to the different thermal regimes north and south of Cape Cod (Franz *et al.*, 1981). However, this thermal boundary was latitudinally unstable throughout the Pleistocene (Cronin, 1988) and only in the past 20,000 years (Holocene) has it returned to its current state. If the geographical isolation between these taxa was recent, as proposed in Schopf and Murphy (1973), then strong natural selection within each region has prevented widespread hybridization.

The second hypothesis, based on morphological and paleoceanographic evidence, suggested a late Pliocene (approximately 2.5–5 Ma) separation of *Asterias* into distinct North American and European species, followed by a Holocene recolonization of North America by the European species *A. rubens* (Worley and Franz, 1983). This hypothesis would therefore suggest that the differentiation between

Received 28 September 2000; accepted 10 May 2001.

Current address: Dept. of Biology, University of New Mexico, Castetter Hall, Albuquerque, NM 87131. E-mail: jpwares@unm.edu

Table 1

Collection sites for individuals of each species in this study

Species [Population]	Location	Sample size
<i>A. rubens</i> [North America]	Maine (44°N, 69°W)	12
	Nova Scotia (46°N, 62°W)	6
	Newfoundland (50°N, 55°W)	5
<i>A. rubens</i> [Europe]	Iceland (64°N, 22°W)	2
	Norway (63°N, 10°E)	8
	Ireland (53°N, 10°E)	10
	France (48°N, 3°E)	5
<i>A. forbesi</i>	North Carolina (34°N, 76°W)	5
	Cape Cod (41°N, 70°W)	3
<i>A. amurensis</i>	Sea of Japan (43°N, 131°E)	4
<i>Leptasterias</i> sp.	Iceland (64°N, 22°W)	1

Voucher specimens are being maintained in the marine invertebrate collections of C. W. Cunningham at Duke University.

the two Atlantic species is entirely due to long-term isolation. Thus, subsequent physiological adaptations to warmer water in *A. forbesi* (Franz *et al.*, 1981) are independent of the speciation event. Essentially, the distinction between these species reflects either primary divergence due to selection or secondary contact following vicariance (Endler, 1977).

In this study, mitochondrial and nuclear sequence data were collected from populations of *A. forbesi* and *A. rubens* throughout North America and Europe, as well as from populations of the Pacific sister taxon *A. amurensis* (Clark and Downey, 1992). Phylogenetic and population genetic assays were used to test the hypotheses described above. It appears that Worley and Franz (1983) were remarkably accurate in suggesting a Pliocene speciation followed by a recent invasion of *A. rubens* from Europe, even in their prediction of details of timing, mechanisms, and effects. Although selection may have driven some of the divergence, it now seems clear that the initial separation of *A. rubens* and *A. forbesi* is due to late Pliocene changes in climate and ocean current flow, whereas North American populations of *A. rubens* are very recent arrivals.

Materials and Methods

Asterias specimens were collected from intertidal sites listed in Table 1. Tube feet were immediately placed in 95% ethanol or DMSO buffer (0.25 M EDTA pH 8.0, 20% DMSO, saturated NaCl; Seutin *et al.*, 1991). Species were identified on the basis of key morphological characters described in Clark and Downey (1992) and Hayward and Ryland (1995).

DNA extraction and amplification

DNA was phenol-extracted from each specimen following the protocol in Hillis *et al.* (1996). These extractions

were stored at -80°C . PCR amplification of an approximately 700-bp portion of the mitochondrial cytochrome *c* oxidase I (COI) protein-encoding gene was performed using the primers LCO1490 and HCO 2198 from Folmer *et al.* (1994). Amplification was performed in 50- μl reactions containing 10–100 ng DNA, 0.02 mM each primer, 5 μl Promega 10 \times polymerase buffer, 0.8 mM dNTPs (Pharmacia Biotech), and 1 unit *Taq* polymerase (Promega). Reactions took place in a Perkin-Elmer 480 thermal cycler with a cycling profile of 94 $^{\circ}$ (60 s) – 40 $^{\circ}$ (90 s) – 72 $^{\circ}$ (150 s) for 40 cycles. The internal transcribed spacer (ITS) region was amplified under similar conditions, with an annealing temperature of 50 $^{\circ}\text{C}$ and with primers ITS4 and ITS5 (White *et al.*, 1990). For each individual, sequences were obtained for three to four clones, and the consensus sequence was obtained to eliminate *Taq* error.

PCR products were prepared for sequencing and were cycle-sequenced as in Wares (2001) using both PCR primers. COI sequences representing each individual in this study have been deposited with GenBank (AF240022–240081); ITS sequences were only obtained for 10 individuals, representing each species and region, and are also accessible in GenBank (AF346608–AF346617). Sequences were aligned and edited for ambiguities using complementary fragments in Sequencher 3.0 (Genecodes Corp., Cambridge, MA). No gaps or poorly aligned regions occurred in the COI alignment, but missing characters were trimmed from the ends of the alignment to produce equal sequence lengths for all individuals. In the ITS alignment, all missing or ambiguous characters, including gaps, were removed. Consensus sequences were exported as a NEXUS file for subsequent analysis in PAUP*4.0b4a (Swofford, 1998).

Phylogenetic analysis

A heuristic search for the set of most-parsimonious trees based on the COI data was performed using PAUP*4.0b4a (Swofford, 1998). Trees were rooted using *Leptasterias polaris* (Asteriinae) and individuals of *A. amurensis*. Starting trees were obtained *via* stepwise addition, with simple addition sequence. Tree-bisection-reconnection was used for branch swapping, and branches were collapsed if the maximum branch length was zero.

Maximum-likelihood (ML) phylogenies were also generated in PAUP*. The best-fit model for all likelihood analyses (HKY with Γ -distributed rate variation; Hasegawa *et al.*, 1985; Yang, 1994) was determined by adding parameters until the likelihood description of the neighbor-joining tree did not significantly improve (Goldman, 1993; Cunningham *et al.*, 1998), using the likelihood-ratio test of ModelTest (Posada and Crandall, 1998). A series of bootstrap replicates (100 ML replicates, heuristic search) using PAUP* were performed to determine support for interspecific relationships in the clade. Estimates of the transition-

transversion ratio for the HKY model, along with the gamma-distributed parameter for among-site rate heterogeneity, were held constant for bootstrap replicates. A maximum likelihood phylogeny of the ITS sequence data was also generated using the appropriate best-fit model (F81: equal rates among sites, unequal base frequencies).

Estimates of speciation time within the North Atlantic require an estimate of the mutation rate (μ). Because paleontological evidence suggests that *Asterias* arrived in the North Atlantic during the trans-Arctic interchange about 3.5 Ma (Worley and Franz, 1983; Vermeij, 1991), and because climatic changes shortly thereafter would have prevented additional trans-Arctic migration, this date was used to calibrate the divergence between the Pacific species *A. amurensis* and the North Atlantic taxa. Other species, including the echinoderm *Strongylocentrotus pallidus*, have clearly maintained more recent connections across the Arctic (Palumbi and Kessing, 1991). However, *S. pallidus* appears to be more tolerant of Arctic conditions than *Asterias* (Worley and Franz, 1983; Palumbi and Kessing, 1991).

The ML estimate of the internal branch length separating the sister taxa (representing net nucleotide divergence d , Nei and Li, 1979) was used to estimate the appropriate mutation rate μ (Edwards and Beerli, 2000), where $\mu = 0.5 d / (3.5 \text{ Ma})$. Estimates were obtained for the full COI data set (first, second, and third codon positions), as well as third position only. Use of the third-position estimate circumvents problems with branch length estimation when there is strong rate variation (Wares and Cunningham, in press), as well as problems with the potential influences of non-neutral evolution.

Haplotype networks may be more appropriate representations of genealogical relationships within species than are outgroup-rooted phylogenetic trees, because ancestral haplotypes are still present in the population (Crandall and Templeton, 1996). Methods associated with haplotype networks were used to determine the root haplotype for *A. rubens*. Determination of the root haplotype prevents spurious conclusions about ancestry among populations. Networks were created using a parsimony criterion in the program TCS (alpha version 1.01, Clement *et al.*, 2000); at the same time, a Bayesian analysis of the likelihood that parsimony is violated (Templeton *et al.*, 1992) was performed to ensure that the data set was unlikely to be complicated by homoplasy.

The ML root was determined using GeneTree (Griffiths and Tavaré, 1994); the likelihood of each possible rooted gene tree was determined under an infinite-alleles model. This model assumes that there are no multiply substituted nucleotide sites. The method allows for recoding of characters so that independent substitutions are analyzed separately, but this was not an issue with the *A. rubens* COI data. The relative likelihood of each tree in comparison with all

other possible rooted trees was calculated using 10^7 simulations in GeneTree.

Tests of rate constancy

Likelihood-ratio tests (Felsenstein, 1988; Goldman, 1993) were used to test the hypothesis that the data collected were consistent with a constant-rate Poisson-distributed process of substitution (molecular clock). This procedure ensures that the data can be used to estimate the time of divergence between *A. rubens* and *A. forbesi*. The ML phylogeny was estimated using the best-fit model, and then the likelihood of this phylogeny was recalculated while constraining the estimate to fit the molecular clock model. These likelihood (L) estimates were used to calculate the χ^2 -distributed test statistic $\delta = 2[\ln(L_0) - \ln(L_1)]$, with $(n - 2)$ degrees of freedom where n is the number of taxa in the tree.

Neutrality tests

Because adaptive selection may have played a role in the divergence between *A. rubens* and *A. forbesi* (given a short divergence time; Schopf and Murphy, 1973), polymorphism data for each species were input to DNAsp v.3.5 (Rozas and Rozas, 1999) to test for patterns of non-neutral evolution. Within each species, Tajima's (1989) test generates a beta-distributed parameter indicating the difference in two estimates (polymorphic sites and number of alleles) of diversity. Significantly low statistics can indicate non-neutral evolution (Tajima, 1989). Additionally, a McDonald-Kreitman test (McDonald and Kreitman, 1991) was performed on each pairwise set of species polymorphism data to determine whether selection has played a role in the divergence between *A. rubens* and *A. forbesi*. Also, DNAsp was used to calculate haplotype diversity (H , see eqn. 8.4 in Nei, 1987) and sampling variance for each species or population.

Results

The COI data set (60 individuals) includes 627 characters, of which 484 are constant, 49 are parsimony-uninformative, and 94 are parsimony-informative. Base frequencies are 33.7% A, 19.6% C, 21.6% G, and 25.1% T for this fragment. Most of the substitutions (92.3%) are at third-position sites; overall, 63% of all third-position characters are polymorphic. These third-position sites are heavily AT-biased (39.0% A, 15.1% C, 11.8% G, and 33.9% T).

The best-fit model (HKY + Γ) was used to estimate distances among individuals to determine whether there is any evidence for saturation at third-position characters in the COI coding region. A plot of pairwise genetic distances versus number of third-position substitutions does not indicate any pattern of saturation (data not shown); in fact, all of the information within each species is based on third-posi-

tion substitutions. Additionally, the best-fit model was re-estimated for this character partition; likelihood-ratio tests indicate that the HKY model with invariant sites ($I = 0.213$) and no rate variation describes the third-position data effectively. The *Asterias* data sets do not reject the molecular clock model, whether all positions are considered ($P = 0.163$), or only third positions ($P = 0.231$).

Maximum-likelihood analysis was used to determine the interspecific gene tree, using all codon positions and the HKY + Γ model (Tr:Tv 8.256, $\alpha = 0.0608$, four rate classes). The ML tree ($L = 1472.87$) is presented in Figure 1A, including all individuals sampled within *A. amurensis*, *A. rubens*, and *A. forbesi*. Bootstrap support is indicated on the tree, with each species being fully resolved in 100% of replicates. The Pacific species *A. amurensis* is basal to a strongly supported clade of Atlantic species in this phylogeny.

Following exclusion of missing and ambiguous characters in the ITS data set (length of fragment varies from 413 to 482 bases when gaps included), these data include 368 characters of which 343 are constant, 1 is parsimony-uninformative, and 24 are parsimony-informative. Indels did not vary within species and were removed (analysis with gapped characters included produced nearly identical results). Parsimony analysis produced a single most-parsimonious tree of 25 steps, and the ML phylogeny (best-fit model F81, no rate variation) is shown in Figure 1B. Under a variety of mutational models, this phylogeny is statistically indistinct from the COI phylogeny in Figure 1A. Likelihood-ratio tests indicate that, in addition to a similar interspecific topology, branch lengths on the COI and ITS phylogenies are proportional ($P > 0.10$), though the substitution rate is significantly different ($P < 0.05$). Bootstrap replicates of the ITS data also indicate strong support for differentiation among these species. The ITS data do not reject a molecular clock model.

Divergence among these species is indicated in Table 2. HKY + Γ distances in the COI fragment indicate that *A. amurensis*, *A. forbesi*, and *A. rubens* have been isolated from each other for a similar amount of time; assuming trans-Arctic isolation around 3.5 Ma, *A. rubens* and *A. forbesi* have been separated for at least 3.0 Ma. Although the estimated divergence date is higher when all codon positions are included (Table 2), and these data do not reject a molecular clock, neutrality tests (see below) suggest that some second-position substitutions may be under selection. Therefore, third-position sites may be more appropriate for the divergence estimate. The estimated divergence time is also higher when the ITS data are used; however, there is no reason to believe that speciation predated the appearance of *Asterias* in the North Atlantic, and the long branch leading to *A. forbesi* is not easily explained since it appears in both phylogenies (one using a protein-coding gene, one using untranslated spacer region data). This longer branch appears

to influence the age estimates of the COI (all positions) and ITS data sets strongly.

A McDonald-Kreitman test (McDonald and Kreitman, 1991) rejects a pattern of neutral substitution between *A. rubens* and *A. forbesi* ($P < 0.01$, Table 3). Despite branch lengths that do not reject the molecular clock model, there is an excess of amino acid replacement substitutions between the Atlantic species. The replacement substitutions between *A. rubens* and *A. forbesi* do not include any first-position substitutions. Half (8/16) of the amino acid substitutions do not involve a change in charge or polarity, whereas almost half (7/16) of the changes substitute a basic residue for an uncharged or nonpolar residue. However, there does not seem to be an obvious pattern to these changes between *A. rubens* and *A. forbesi*. Other species comparisons do not reject the neutral model of substitution (Table 3). Within each species, Tajima's (1989) test is nonsignificant (*A. amurensis*, $D = 0.837$, $P > 0.10$; *A. forbesi*, $D = -0.705$, $P > 0.10$; *A. rubens*, $D = -1.482$, $P > 0.10$), indicating that there is no reason to suspect non-neutral evolution in the intraspecific comparisons.

Additionally, Bayesian analysis (Templeton *et al.*, 1992; Clement *et al.*, 2000) of the COI data within *A. rubens* indicates greater than 95% confidence that the intraspecific gene tree is parsimonious. The ML root haplotype is found on both coasts of the Atlantic (Fig. 1A, Haplotype B), and this haplotype is at least an order of magnitude more likely to be the ancestral haplotype than any other haplotype of *A. rubens* (likelihood index = 0.857). All North American haplotypes are also found in Europe; the unique haplotypes found in Europe contribute to a significantly higher allelic diversity ($P < 0.01$, Table 4). The ITS data are consistent with the COI data in that there is no allelic diversity among North American and European individuals of *A. rubens* ($n = 6$).

Discussion

Understanding the mechanisms that are responsible for the divergence of *Asterias rubens* and *A. forbesi* first requires that the timing of their divergence be estimated. Estimates based on the molecular calibrations reported here suggest that these species last shared a common ancestor at least 3.0 Ma (Table 2), not long after the genus first arrived in the North Atlantic (around 3.5 Ma; Worley and Franz, 1983; Vermeij, 1991). Note, however, that asterozoan skeletons are rarely preserved in the fossil record, because they lack rigidly articulated skeletons and rapidly disintegrate (Barker and Zullo, 1980); indeed, fossils of *A. forbesi* have been reported only twice, each time in Pleistocene interglacial sediments. Thus, little direct evidence points to the first appearance of *Asterias* in the North Atlantic (Durham and MacNeil, 1967; Worley and Franz, 1983), and the biogeographic data used in this paper is therefore based on con-

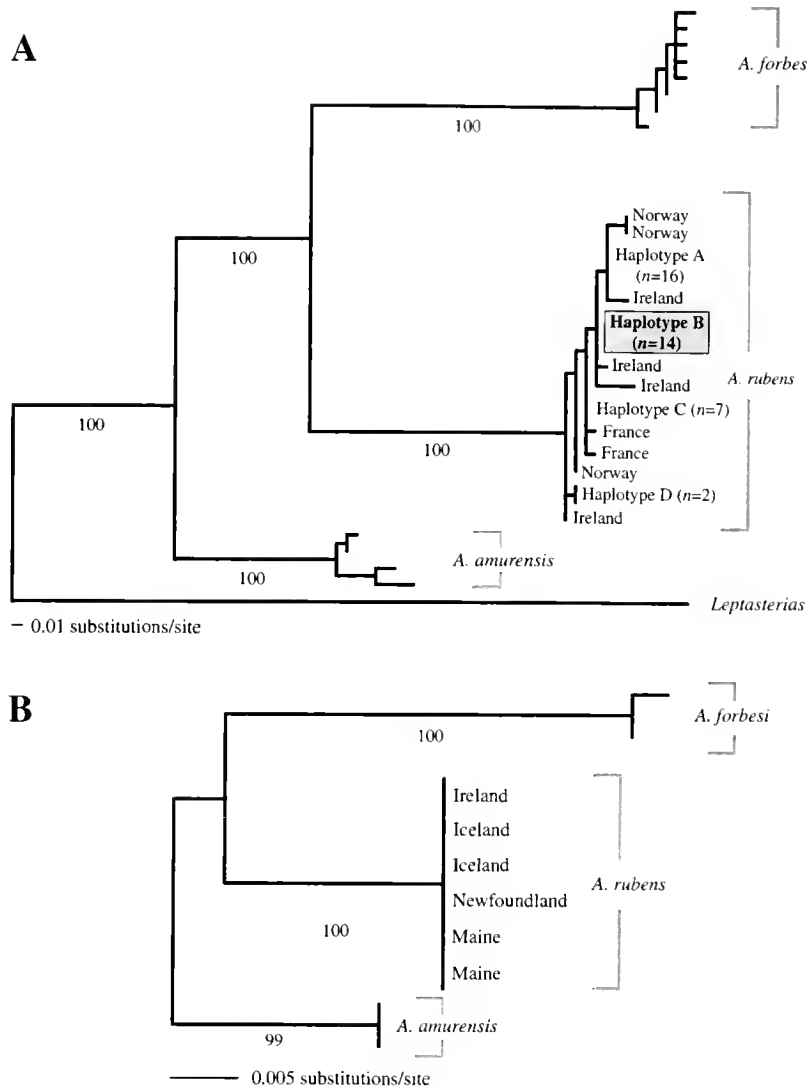


Figure 1. Phylogenetic trees for *Asterias* generated using the best-fit maximum likelihood model in each data set (COI: HKY + Γ ; ITS: F81). (A) Cytochrome *c* oxidase I phylogeny of inter- and intraspecific *Asterias* relationships. Here all characters (first, second, and third position) are included; an identical topology is found using parsimony or distance methods, or looking at third-position characters alone. Bootstrap support for each species is indicated by the numbers below each branch. These data do not reject a molecular clock model. The divergence across the Arctic (between *A. amurensis* and the Atlantic species) is considered to be 3.5 Ma; this generates an estimate of about 3.0 Ma for the divergence between *A. rubens* and *A. amurensis* (see Table 2 and Discussion). Haplotypes A–D of *A. rubens* are found on both the North American and European coasts (A: Maine ($n = 8$), Nova Scotia ($n = 2$), Newfoundland ($n = 2$), Iceland ($n = 1$), Norway ($n = 2$), Ireland ($n = 1$); B: Maine ($n = 2$), Nova Scotia ($n = 4$), Newfoundland ($n = 3$), Iceland ($n = 1$), Ireland ($n = 2$), France ($n = 2$); C: Maine ($n = 1$), Norway ($n = 3$), Ireland ($n = 2$), and France ($n = 1$); D: Ireland ($n = 1$), and Maine ($n = 1$)). Amphi-Atlantic haplotype B is the maximum likelihood root (index = 0.857). (B) Internal transcribed spacer (ITS) phylogeny of inter- and intraspecific *Asterias* relationships. Likelihood ratio tests do not reject a hypothesis of proportional branch lengths ($P > 0.10$) suggesting that, aside from substantial differences in substitution rate, the two phylogenies are equivalent representations of interspecific differentiation. A nearly identical phylogeny is reconstructed when indels are included in the ITS data.

sistent fossil evidence from other cold temperate species that participated in the trans-Arctic exchange. Nevertheless, there is reason to believe that *Asterias* also spread from the Pacific to the Atlantic at about 3.5 Ma (Worley and Franz, 1983). Miocene and early Pliocene temperatures were

around 5°–6°C warmer in the North Atlantic and Arctic, permitting the initial trans-Arctic passage of temperate species (Berggren and Hollister, 1974; Vermeij, 1991), but then two dramatic changes were initiated around 3.0 Ma that appear to play a role in speciation within the North Atlantic.

Table 2

Internal branch lengths (based on best-fit likelihood model) separating *Asterias* species (lower triangle*, all 3 matrices)

All characters	<i>A. amurensis</i>	<i>A. rubens</i>	<i>A. forbesi</i>
<i>A. amurensis</i>		$\mu = 1.954 \times 10^{-8} \pm 8.63 \times 10^{-9}$	$\mu = 2.665 \times 10^{-8} \pm 9.59 \times 10^{-9}$
<i>A. rubens</i>	0.13678 \pm 0.06044		3.59 Ma
<i>A. forbesi</i>	0.18658 \pm 0.06715	0.16576 \pm 0.04595	

3rd position only	<i>A. amurensis</i>	<i>A. rubens</i>	<i>A. forbesi</i>
<i>A. amurensis</i>		$\mu = 6.689 \times 10^{-8} \pm 3.36 \times 10^{-8}$	$\mu = 9.751 \times 10^{-8} \pm 3.74 \times 10^{-8}$
<i>A. rubens</i>	0.48084 \pm 0.2352		2.96 Ma
<i>A. forbesi</i>	0.68254 \pm 0.26168	0.49270 \pm 0.15661	

ITS-1	<i>A. amurensis</i>	<i>A. rubens</i>	<i>A. forbesi</i>
<i>A. amurensis</i>		$\mu = 5.142 \times 10^{-9} \pm 2.04 \times 10^{-9}$	$\mu = 7.188 \times 10^{-9} \pm 2.40 \times 10^{-9}$
<i>A. rubens</i>	0.0361 \pm 0.0143		3.84 Ma
<i>A. forbesi</i>	0.0500 \pm 0.0168	0.0470 \pm 0.0163	

The calibration date of 3.5 Ma is used to obtain the mutation rate μ for comparisons between *A. amurensis* and the Atlantic species. The estimated divergence time between *A. rubens* and *A. forbesi* is based on the mean of this calibrated mutation rate (cytochrome *c* oxidase I [COI] all positions, top; COI 3rd position only, middle; internal transcribed spacer (ITS) 1, bottom).

* In each matrix, the lower triangle containing the internal branch lengths is made up of the matrix cells below the diagonal line of empty cells representing comparisons within the same value. The upper triangle contains the estimated mutation rates and estimated divergence data.

At that time, warm North Atlantic currents were displaced by the formation of the cold-water Labrador Current. This event created a significant thermal gradient in the North Atlantic, and tropical-temperate faunas were abruptly replaced with polar and subpolar faunas on the continental

shelf off Nova Scotia and the rest of New England (Berggren and Hollister, 1974; Worley and Franz, 1983; Cronin, 1988). As Northern Hemisphere glaciation began, the present-day latitudinally controlled faunal provincialization was established as well (Berggren and Hollister, 1974). This dramatic cooling of the northwestern North Atlantic probably initiated the separation of North Atlantic *Asterias* into European and North American populations with very little genetic contact (Worley and Franz, 1983). Subsequent Pleistocene glaciation would have prevented the long-term

Table 3

McDonald-Kreitman tests on each *Asterias* species pair using cytochrome *c* oxidase I (COI) translated data

Species pair	Fixed differences	Polymorphisms
<i>A. rubens</i> - <i>A. forbesi</i>		
Synonymous	39	19
Nonsynonymous	16	0
		$P < 0.001$
<i>A. rubens</i> - <i>A. amurensis</i>		
Synonymous	36	21
Nonsynonymous	12	1
		$P > 0.05$
<i>A. forbesi</i> - <i>A. amurensis</i>		
Synonymous	44	15
Nonsynonymous	14	1
		$P > 0.15$

Only the comparison between *A. rubens* and *A. forbesi* indicates a significant departure from neutral evolution. A two-tailed Fisher's exact test was used for each set of comparisons.

Table 4

Comparisons of haplotype diversity (H , see eqn. 8.4 in Nei 1987, calculated in DNAsp 3.50, Rozas and Rozas 1999) for the cytochrome *c* oxidase I fragment in each species and population of *A. rubens*

Species/Population	Haplotype diversity (H)	σ^2
<i>Asterias rubens</i>	0.793	0.00138
North America	0.597	0.00395
Europe	0.893	0.00143
<i>Asterias forbesi</i>	0.964	0.00596
<i>Asterias amurensis</i>	0.999	0.03125

European populations of *A. rubens* have significantly higher allelic diversity than North American populations ($P < 0.01$); this finding is supported by nonparametric haplotype sampling in Wares (2000).

establishment of populations in New England, as most of the North American coast from Long Island Sound northward was covered by a kilometer of ice during glacial maxima (Kelley *et al.*, 1995).

Pacific and Atlantic populations of other species appear to have had more recent trans-Arctic genetic contact than the estimates above would suggest for *Asterias* (Palumbi and Kessing, 1991; van Oppen *et al.*, 1995). Moreover, rapid climatic fluctuations (Cronin, 1988; Roy *et al.*, 1996) during the Pleistocene could have permitted large-scale changes in the geographic range of cold temperate species. However, both the sea urchin *Strongylocentrotus pallidus* (Palumbi and Kessing, 1991) and the red alga *Phycodrys rubens* (van Oppen *et al.*, 1995) appear to have greater tolerance for Arctic waters than *Asterias* does. Worley and Franz (1983) report that expansion of *Asterias* populations into habitats as far north as Greenland only occurs periodically, and that these populations cannot tolerate colder waters (Franz *et al.*, 1981). However, the indirect morphological and paleontological evidence is bolstered by the molecular evidence, which strongly suggests that *A. rubens* and *A. forbesi* diverged shortly after their ancestral lineage separated from the Pacific *A. amurensis*. The estimates of mutation rate presented here are very similar to other estimates for both the COI fragment (Knowlton and Weigt, 1998; Schubart *et al.*, 1998; Wares, 2001; Wares and Cunningham, in press) and the ITS fragment (Schlötterer *et al.*, 1994; van Oppen *et al.*, 1995). Thus these data strongly support earlier inferences of a late Pliocene trans-Arctic passage and subsequent speciation within the Atlantic.

An analysis of genealogical patterns within *A. rubens* confirms that the North American populations of this species are descendants of a recent colonization from Europe that probably followed the most recent glacial maximum (about 20,000 BP, Holder *et al.*, 1999). The genealogical data presented here fit several important patterns that suggest a recent range expansion (Wares, 2000). All North American haplotypes are identical to the most-common European haplotypes (Fig. 1A). Generally, invading haplotypes are the most deeply nested haplotype in the European (putative source) population. This is to be expected, because deeply nested ancestral haplotypes are often the most common (Castelloe and Templeton, 1994), and therefore have a higher probability of participating in long-distance dispersal events. Haplotype B (Fig. 1A) is a good illustration of this expectation—it is closely related to each other haplotype and has a high copy number in both European and American populations. These observations contribute to the high likelihood (85.7%, more than an order of magnitude greater likelihood than any other haplotype) that this is the ancestral allele in *A. rubens*.

Additionally, allelic diversity is significantly lower in North American *A. rubens* than in Europe (Table 4), a signal of recent range expansion (Hewitt, 1996; Austerlitz *et al.*,

1997). However, the North American colonization is difficult to date because there are no unique haplotypes in North America; ancestral allelic polymorphism tends to inflate indirect estimates of population size and age (Kuhner *et al.*, 1998; Edwards and Beerli, 2000). The lack of unique diversity in North America also prevents the meaningful use of other phylogeographic methods; for instance, statistics of the geographic dispersion of haplotypes (for review see Templeton, 1998) are uninformative (Wares, unpubl. data). This is primarily because even closely related individuals (identical haplotypes) are distributed across the entire geographic range of *A. rubens*. It is possible that the multiple shared alleles between Europe and North America represent a multiple-invasion history; *Asterias* larvae are planktotrophic and disperse in the water column for 6 or more weeks (Clark and Downey, 1992).

There is evidence that natural selection has played some role in the overall divergence between these species. A significant number of amino acid replacement substitutions distinguish *A. rubens* from *A. forbesi* (Table 3), all of them reflecting second- or third-position nucleotide substitutions. There is no obvious pattern to the amino acid replacements, as most of them involve substitutions among uncharged or nonpolar amino acids. Two of the three species in the genus *Asterias* are found in cold-temperate waters, while *A. forbesi* is found in the warmer mid-Atlantic region (Schopf and Murphy, 1973; Franz *et al.*, 1981). Many of the physiological differences between *A. rubens* and *A. forbesi* (Franz *et al.*, 1981) reflect this latitudinal distribution. However, the possibility that these amino acid substitutions are related to physiological differences in the warm-temperate *A. forbesi* has never been tested. The difference in temperature between the habitats of *A. rubens* and *A. forbesi* is unlikely to contribute to differences in metabolic rate that could accelerate the mutation rate (for review see Rand, 1994). Nevertheless, this hypothesis is worth examination, because *A. forbesi* is supported by relatively long branches in both the COI and the non-coding ITS region (Table 2, Fig. 1B). If natural selection is playing a role in the amino acid divergences of the mitochondrial COI gene between *A. rubens* and *A. forbesi*, there is no reason why a noncoding nuclear sequence should reflect the same increase in divergence rate.

In conclusion, the biogeographic response of *Asterias* to late Pliocene climatic and oceanographic change fits a pattern predicted by Worley and Franz (1983). Following the arrival of *Asterias* in the North Atlantic around 3.5 Ma (Worley and Franz, 1983; Verneij, 1991), populations were established on both the European and North American coasts during a period when the North Atlantic was as much as 5–6°C warmer (Berggren and Hollister, 1974). The formation of the Labrador Current 3.0 Ma rapidly changed the faunal composition of the intertidal Canadian Maritimes and New England coast, and *Asterias* populations in this region

probably went extinct. An American population survived under the conditions of the mid-Atlantic coast and Gulf Stream waters (*A. forbesi*), and the European population (*A. rubens*) has recently recolonized the cold-temperate shores of New England and the Canadian Maritimes. Thus, the zone of sympatry between these two species appears to be a zone of secondary contact. Hybridization is considered rare between these species (Schopf and Murphy, 1973; Worley and Franz, 1983), but whether behavioral mechanisms (Franz *et al.*, 1981) or gametic recognition mechanisms (Hellberg and Vacquier, 1999; Pernet, 1999) are responsible is unclear.

The genetic data presented here illustrate a strong concordance between paleoceanographic changes and indirect estimates of speciation between the North Atlantic *Asterias* species. The species boundaries are phylogenetically quite distinct, and the divergence estimates based on these genetic data appear to support a late Pliocene, rather than late Pleistocene or Holocene, separation. A better understanding of the balance between oceanographic and climatic changes in the late Pliocene and Pleistocene, and of the response of species based on varying life-history characters to these changes, will enable us to predict the responses of other taxa (Cunningham and Collins, 1998; Wares and Cunningham, in press).

Acknowledgments

I thank G. Manchenko, A. Ingólfsson, J. Maunder, B. O'Connor, D. Garbary, D. M. Rand, and C. Damiani for assistance in the field collecting seastars. The manuscript was greatly improved thanks to discussions with T. Turner and the suggestions of two anonymous reviewers. These analyses were done in the laboratory of C. W. Cunningham, whose aid during this and other projects was invaluable. A National Science Foundation Dissertation Improvement Grant (NSF DEB-99-72707) to J. P. W. funded this study.

Literature Cited

- Austerlitz, F., B. Jung-Muller, B. Godelle, and P.-H. Gouyon. 1997. Evolution of coalescence times, genetic diversity and structure during colonization. *Theor. Popul. Biol.* 51: 148–164.
- Barker, L., and V. A. Zullo. 1980. *Asterias forbesi* (Desor) (Asterozoa, Asteroidea) from the Pleistocene "Coquina" at Fort Fisher, New Hanover County, North Carolina. *J. Elisha Mitchell Sci. Soc.* 96: 39–44.
- Berggren, W. A., and C. D. Hollister. 1974. Paleogeography, paleobiogeography, and the history of circulation in the Atlantic Ocean. *Soc. Econ. Paleontol. Mineral.* 20: 126–186.
- Castelloe, J., and A. R. Templeton. 1994. Root probabilities for intraspecific gene trees under neutral coalescent theory. *Mol. Phylogenet. Evol.* 3: 102–113.
- Clark, A. M., and M. E. Downey. 1992. *Starfishes of the Atlantic*. Chapman & Hall, London.
- Clement, M., D. Posada, and K. A. Crandall. 2000. TCS: a computer program to estimate gene genealogies. *Mol. Ecol.* 9: 1657–1660.
- Collins, T. M., K. Frazer, A. R. Palmer, G. J. Vermeij, and W. M. Brown. 1996. Evolutionary history of northern hemisphere *Nucella* (Gastropoda, Muricidae): molecular, morphological, ecological, and paleontological evidence. *Evolution* 50: 2287–2304.
- Crandall, K. A., and A. R. Templeton. 1996. Applications of intraspecific phylogenetics. Pp. 81–99 in *New Uses for New Phylogenies*, P. H. Harvey, A. J. Brown, J. Maynard Smith, and S. Nee, eds. Oxford University Press, Oxford.
- Cronin, T. M. 1988. Evolution of marine climates of the U. S. Atlantic coast during the past four million years. *Philos. Trans. R. Soc. Lond. B* 318: 661–678.
- Cunningham, C. W., and T. M. Collins. 1998. Beyond area relationships: extinction and recolonization in molecular marine biogeography. Pp. 297–321 in *Molecular Ecology and Evolution: Approaches and Applications*, B. Schierwater, B. Streit, G. Wagner, and R. DeSalle, eds. Birkhauser Verlag, Basel.
- Cunningham, C. W., H. Zhu, and D. M. Hillis. 1998. Best-fit maximum-likelihood models for phylogenetic inference: Empirical tests with known phylogenies. *Evolution* 52: 978–987.
- Durham, J. W., and F. S. MacNeil. 1967. Cenozoic migrations of marine invertebrates through the Bering Strait region. Pp. 326–349 in *The Bering Land Bridge*, D. M. Hopkins, ed. Stanford University Press, Stanford.
- Edwards, S. V., and P. Beerli. 2000. Perspective: Gene divergence, population divergence, and the variance in coalescence time in phylogeographic studies. *Evolution* 54: 1839–1854.
- Ender, J. A. 1977. *Geographic Variation, Speciation, and Clines*. Princeton University Press, Princeton, NJ.
- Felsenstein, J. 1988. Phylogenies from molecular sequences: inference and reliability. *Annu. Rev. Genet.* 22: 521–565.
- Folmer, O., M. Black, W. Hoeh, R. Lutz, and R. Vrijenhoek. 1994. DNA primers for amplification of mitochondrial cytochrome *c* oxidase subunit I from diverse metazoan invertebrates. *Mol. Mar. Biol. Biotechnol.* 3: 294–299.
- Franz, D. R., E. K. Worley, and A. S. Merrill. 1981. Distribution patterns of common seastars of the middle Atlantic continental shelf of the northwest Atlantic (Gulf of Maine to Cape Hatteras). *Biol. Bull.* 160: 394–418.
- Goldman, N. 1993. Statistical tests of models of DNA substitution. *J. Mol. Evol.* 36: 182–198.
- Gosling, E. M. 1992. Systematics and geographical distribution of *Mytilus*. Pp. 1–20 in *The Mussel Mytilus: Ecology, Physiology, Genetics, and Culture*, E. M. Gosling, ed. Elsevier, Amsterdam.
- Gosner, K. L. 1978. *A Field Guide to the Atlantic Seashore From the Bay of Fundy to Cape Hatteras*. Houghton Mifflin, Boston.
- Griffiths, R. C., and S. Tavaré. 1994. Sampling theory for neutral alleles in a varying environment. *Philos. Trans. R. Soc. Lond. B* 344: 403–410.
- Hasegawa, M., H. Kishino, and T. Yano. 1985. Dating of the human-ape splitting by a molecular clock of mitochondrial DNA. *J. Mol. Evol.* 21: 160–174.
- Hayward, P. J., and J. S. Ryland. 1995. *Handbook of the Marine Fauna of North-West Europe*. Oxford University Press, Oxford.
- Hellberg, M. E., and V. D. Vacquier. 1999. Rapid evolution of fertilization selectivity and lysin cDNA sequences in teguline gastropods. *Mol. Biol. Evol.* 16: 839–848.
- Hewitt, G. M. 1996. Some genetic consequences of ice ages, and their role in divergence and speciation. *Biol. J. Linn. Soc.* 58: 247–276.
- Hillis, D. M., B. K. Mable, A. Larson, S. K. Davis, and E. A. Zimmer. 1996. Nucleic acids IV: Sequencing and cloning. Pp. 321–384 in *Molecular Systematics*, D. M. Hillis, C. Moritz, and B. K. Mable, eds. Sinauer, Sunderland, MA.
- Holder, K., R. Montgomerie, and V. L. Friesen. 1999. A test of the glacial refugium hypothesis using patterns of mitochondrial and nu-

- clear DNA sequence variation in rock ptarmigan (*Lagopus mutus*). *Evolution* **53**: 1936–1950.
- Kelley, J. T., A. R. Kelley, and S. Appollonio. 1995.** Landforms of the Gulf of Maine. Pp. 19–38 in *From Cape Cod to the Bay of Fundy: an Environmental Atlas of the Gulf of Maine*, P. W. Conkling, ed. MIT Press, Cambridge, MA.
- Knowlton, N., and L. A. Weigt. 1998.** New dates and new rates for divergence across the Isthmus of Panama. *Proc. R. Soc. Lond. B* **265**: 2257–2263.
- Kuhner, M. K., J. Yamato, and J. Felsenstein. 1998.** Maximum likelihood estimation of population growth rates based on the coalescent. *Genetics* **149**: 429–434.
- McDonald, J. H., and M. Kreitman. 1991.** Adaptive protein evolution at the *Adh* locus in *Drosophila*. *Nature* **351**: 652–654.
- Menge, B. A. 1979.** Coexistence between the seastars *Asterias vulgaris* and *A. forbesi* in a heterogeneous environment: a non-equilibrium explanation. *Oecologia* **41**: 245–272.
- Nei, M. 1987.** *Molecular Evolutionary Genetics*. Columbia University Press, New York.
- Nei, M., and W.-H. Li. 1979.** Mathematical model for studying genetic variation in terms of restriction endonucleases. *Proc. Natl. Acad. Sci. USA* **76**: 5269–5273.
- Palumbi, S. R., and B. D. Kessing. 1991.** Population biology of the trans-Arctic exchange: mtDNA sequence similarity between Pacific and Atlantic sea urchins. *Evolution* **45**: 1790–1805.
- Pernet, B. 1999.** Gamete interactions and genetic differentiation among three sympatric polychaetes. *Evolution* **53**: 435–446.
- Posada, D., and K. A. Crandall. 1998.** Modeltest: testing the model of DNA substitution. *Bioinformatics* **14**: 817–818.
- Rand, D. 1994.** Thermal habitat, metabolic rate, and the evolution of mtDNA. *Trends Ecol. Evol.* **9**: 125–131.
- Reid, D. G., E. Rumbak, and R. H. Thomas. 1996.** DNA, morphology and fossils: phylogeny and evolutionary rates of the gastropod genus *Littorina*. *Philos. Trans. R. Soc. Lond. B* **351**: 877–895.
- Roy, K., J. W. Valentine, D. Jablonski, and S. M. Kidwell. 1996.** Scales of climatic variability and time averaging in Pleistocene biotas: implications for ecology and evolution. *Trends Ecol. Evol.* **11**: 458–463.
- Rozas, J., and R. Rozas. 1999.** DnaSP version 3: an integrated program for molecular population genetics and molecular evolution analysis. *Bioinformatics* **15**: 174–175.
- Schlötterer, C., M. Hauser, A. von Haeseler, and D. Tautz. 1994.** Comparative evolutionary analysis of rDNA ITS regions in *Drosophila*. *Mol. Biol. Evol.* **11**: 513–522.
- Schopf, T. J. M., and L. S. Murphy. 1973.** Protein polymorphism of the hybridizing seastars *Asterias forbesi* and *Asterias vulgaris* and implications for their evolution. *Biol. Bull.* **145**: 589–597.
- Schubart, C. D., R. Diesel, and S. B. Hedges. 1998.** Rapid evolution to terrestrial life in Jamaican crabs. *Nature* **393**: 363–365.
- Seutin, G., B. N. White, and P. T. Boag. 1991.** Preservation of avian blood and tissue samples for DNA analyses. *Can. J. Zool.* **69**: 82–90.
- Swofford, D. L. 1998.** *PAUP*. Phylogenetic Analysis Using Parsimony (* and Other Methods)*. Version 4. Sinauer Associates, Sunderland, MA.
- Tajima, F. 1989.** Statistical method for testing the neutral mutation hypothesis by DNA polymorphism. *Genetics* **123**: 585–595.
- Templeton, A. R. 1998.** Nested clade analyses of phylogeographic data: testing hypotheses about gene flow and population history. *Mol. Ecol.* **7**: 381–397.
- Templeton, A. R., K. A. Crandall, and C. F. Sing. 1992.** A cladistic analysis of phenotypic associations with haplotypes inferred from restriction endonuclease mapping and DNA sequence data. III. Cladogram estimation. *Genetics* **132**: 619–633.
- van Oppen, M. J. H., S. G. A. Draisma, J. L. Olsen, and W. T. Stam. 1995.** Multiple trans-Arctic passages in the red alga *Phycodrys rubens*: evidence from nuclear rDNA ITS sequences. *Mar. Biol.* **123**: 179–188.
- Vermeij, G. 1991.** Anatomy of an invasion: the trans-Arctic interchange. *Paleobiology* **17**: 281–307.
- Wares, J. P. 2000.** Abiotic influences on the population dynamics of marine invertebrates. Ph.D. dissertation, Duke University, Durham, NC.
- Wares, J. P. 2001.** Patterns of speciation inferred from mitochondrial DNA in North American *Chthamalus* (Cirripedia: Balanomorpha: Chthamaloidea). *Mol. Phylogenet. Evol.* **18**: 104–116.
- Wares, J. P., and C. W. Cunningham. 1999.** Phylogeography and historical ecology of the North Atlantic intertidal. *Evolution* (in press).
- White, T. J., T. Bruns, S. Lee, and J. Taylor. 1990.** Amplification and direct sequencing of fungal ribosomal RNA genes for phylogenetics. Pp. 315–322 in *PCR Protocols: A Guide to Methods and Applications*, M. A. Innis, D. H. Gelfand, J. J. Sninsky, and T. J. White, eds. Academic Press, San Diego.
- Worley, E. K., and D. R. Franz. 1983.** A comparative study of selected skeletal structures in the seastars *Asterias forbesi*, *A. vulgaris*, and *A. rubens* with a discussion of possible relationships. *Proc. Biol. Soc. Wash.* **96**: 524–547.
- Yang, Z. 1994.** Maximum likelihood phylogenetic estimation from DNA sequences with variable rates over sites: Approximate methods. *J. Mol. Evol.* **39**: 306–314.

Systematics and Biogeography of the Jellyfish *Aurelia labiata* (Cnidaria: Scyphozoa)

LISA-ANN GERSHWIN

Cabrillo Marine Aquarium, San Pedro, California 90731 and CSU Northridge, California 91330

Abstract. The hypothesis that the common eastern North Pacific *Aurelia* is *A. aurita* is falsified with morphological analysis. The name *Aurelia labiata* is resurrected, and the species is redescribed, to refer to medusae differing from *A. aurita* by a suite of characters related to a broad and elongated manubrium. Specifically, the oral arms are short, separated by and arising from the *base* of the fleshy manubrium, and the planulae are brooded upon the manubrium itself, rather than on the oral arms. *Aurelia aurita* possesses no corresponding enlarged structure. Furthermore, the number of radial canals is typically much greater in *A. labiata*, and thus the canals often appear more anastomosed than in *A. aurita*. Finally, most *A. labiata* medusae possess a 16-scalloped bell margin, whereas the margin is 8-scalloped in most *A. aurita*. Separation of the two forms has previously been noted on the basis of allozyme and isozyme analyses and on the histology of the neuromuscular system. Partial 18S rDNA sequencing corroborates these findings. Three distinct morphotypes of *A. labiata*, corresponding to separate marine bioprovinces, have been identified among 17 populations from San Diego, California, to Prince William Sound, Alaska. The long-undisputed species *A. limbata* may be simply a color morph of *A. labiata*, or a species within a yet-unelaborated *A. labiata* species complex. The first known introduction of *Aurelia cf. aurita* into southern California waters is documented. Although traditional jellyfish taxonomy tends to recognize many species as cosmopolitan or nearly so, these results indicate that coastal species, such as *A. labiata*, may experience rapid divergence among isolated populations, and that the taxonomy of such species should therefore be scrutinized with special care.

Introduction

Perhaps had Darwin not been afflicted with seasickness, he might have noticed the bewildering array of geographically varying jellyfish morphologies. Some of his contemporaries documented species separated by only short distances but differing greatly in appearance (Eschscholtz, 1829; Brandt, 1835, 1838; Agassiz, 1862; Haeckel, 1879, 1880). Morphological distinctions have since been reported for populations of *Cassiopea* from separate islands of the Caribbean (Hummelinck, 1968), *Mastigias* in different lakes of Palau (Hamner and Hauri, 1981), and *Aurelia* scyphistomae from various parts of the Thames estuary (Lambert, 1935). In his studies of the genus *Cyanea*, Brewer (1991) reported distinct morphotypes that could be correlated with isolated locations in Long Island Sound, USA; these observations resurrected a long-standing argument about species distribution and recognition criteria of North Atlantic *Cyanea*. Nineteenth-century taxonomists recognized different species, corresponding to a latitudinal gradation, on both sides of the Atlantic. *Cyanea arctica* Peron and Lesueur, 1810, was known as the boreal species from Europe to North America. In the western Atlantic, *C. fulva* L. Agassiz, 1862, was found along the mid-Atlantic states, while the form south of the Carolinas was recognized as *C. versicolor* L. Agassiz, 1862. In the eastern Atlantic, *C. capillata* (Linnaeus, 1746) was established as the northern European species, while *C. lamarckii* Haeckel, 1880, was identified in warmer southern European waters. This pattern of biodiversity was largely overlooked by twentieth-century taxonomists, who often lumped the forms and recognized only *C. capillata* (Mayer, 1910; Bigelow, 1914; Stiasny and van der Maaden, 1943; Kramp, 1961; Calder, 1971; Larson, 1976).

The scarcity of biogeographic studies of jellyfishes may be, in part, attributable to the unclear systematics of these

Received 16 December 1998; accepted 5 April 2001.

Current address: Dept. of Integrative Biology, University of California, Berkeley, CA 94720. E-mail: gershwin@socrates.berkeley.edu

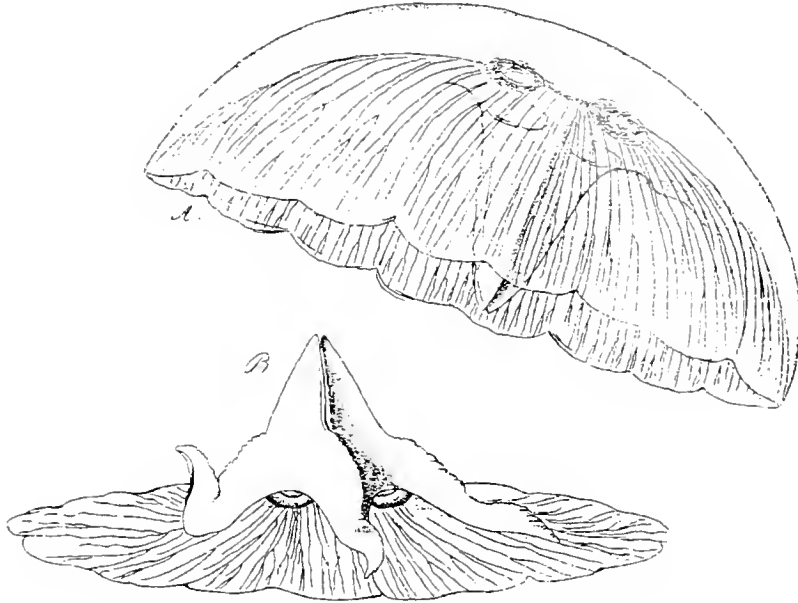


Figure 1. Original illustrations of *Aurelia labiata*, showing greatly enlarged manubrium: (A) lateral view of medusa; (B) oblique view of subumbrella. (Reprinted from Chamisso and Eysenhardt, 1821).

animals. Color differences, patterns of pigmentation, and anatomical variation led to the description of many nominal species during the expeditions of the nineteenth century (see Mayer, 1910; Kramp, 1961). The range of variation in jellyfishes is not well understood, and species definitions are often vague, focusing only on the few most obvious characters. For example, if one sees a flat, whitish medusa with four horseshoe-shaped gonads, most tend to think it must be *Aurelia aurita*. The details of anatomy have not been scrutinized closely. Therefore, significant morphological differences have not been detected, and inappropriate identifications and erroneous conclusions regarding biogeography have been made. The systematic tangle and biogeographic mistakes are common throughout the medusan taxa, though I focus herein on *Aurelia*.

Mayer (1910) recognized 13 unique forms of *Aurellia* (the spelling was later formally changed back to *Aurelia* by Rees, 1957), and sorted these forms into three morphological groups:

1. *A. aurita* (Linnaeus, 1746) sensu Lamarck, 1816, and its seven varieties, described as *A. cruciata* Haeckel, 1880, *A. colpota* Brandt, 1835 [sensu Götte, 1886] (as =*A. coerulea* von Lendenfeld, 1884), *A. flavidula* Peron and Lesueur, 1810 [incorrectly listed as 1809] (as =*A. habanensis* Mayer, 1900), *A. hyalina* Brandt, 1835, *A. dubia* Vanhöffen, 1888, *A. vitiana* Agassiz and Mayer, 1899, and *A. marginalis* L. Agassiz, 1862
2. *A. labiata* Chamisso and Eysenhardt, 1821 [incorrectly listed as 1820], with three varieties, described as

A. clausa Lesson, 1829, *A. limbata* (Brandt, 1835) [incorrectly listed as 1838], and *A. maldivensis* Bigelow, 1904

3. *A. solida* Browne, 1905

Mayer distinguished *A. labiata* and its varieties from the other two groups based primarily on the degree of scalloping of the bell margin, being 16-notched in the former and 8-notched in the latter. He subsequently found a specimen of *A. aurita* at Tortugas, Florida, closely resembling *A. labiata*, leading him to conclude that *A. labiata* was probably derived as a mutation from *A. aurita* (Mayer, 1917). Kramp also wavered on the validity of *A. labiata*, first recognizing the species in his 1961 synopsis, then later regarding it as doubtful (1965, 1968). Most recently, authors such as Russell (1970), Larson (1990), and Arai (1997) have recognized two valid species: *A. limbata*, which is primarily arctic and has a conspicuous brown bell margin, and *A. aurita*, whose name has been treated as the senior synonym of all others. Russell (1970) followed Kramp (1965, 1968) in regarding all other species as varieties, whereas Larson (1990) and Arai (1997) simply did not mention any other species.

The source of this confusion is unclear, as the original description of *A. labiata* was quite specific. Translated from Latin, "It differs from *A. aurita* by its very long oral lips. Marginal tentacles were not observed, but are without a doubt present. Arms appressed to the bell. Diameter of the bell nearly a foot" (Chamisso and Eysenhardt, 1821). The focus of the description and its accompanying illustrations is the strikingly unique elongated manubrium (Figs. 1, 2).

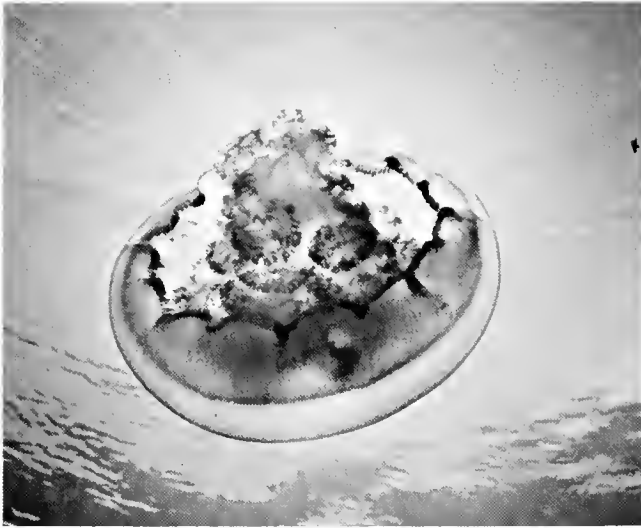


Figure 2. *Aurelia labiata*, adult medusa, from Monterey Bay, California.

although this character is rarely mentioned in later revisions. Furthermore, the characteristically short oral arms arising from the base of the manubrium were mentioned as being held close to the bell, a trait that is readily apparent in live specimens. Ironically, the commonly accepted character of 16 marginal scallops is not mentioned, although it is subtly illustrated. It is unclear why certain key characters of the original description have been ignored by later workers.

Disorder in the nomenclature of *Aurelia* worldwide has caused confusion about the identity of the species in the eastern North Pacific. Depending on the author, one to three species have been recognized. Most authors have applied the name *A. aurita* to all forms. Some distinguish *A. limbata*, although this appears to have been occasionally confused with *A. labiata* (Zubkoff and Lin, 1975; Greenberg *et al.*, 1996). When *A. labiata* has been recognized, it has been separated from *A. aurita* only by the doubling of marginal scallops (Hand, 1975; Kozloff, 1974). Although *A. labiata* was originally described from California, most reports of the species (apparently incorrectly) are from regions outside the eastern North Pacific.

Throughout all the confusion, several studies have reported differences between the eastern North Pacific *Aurelia* and those of other regions, yet failed to elaborate the systematics. Chia *et al.* (1984) found that the muscle system in Puget Sound polyps is distinct from that of polyps from Plymouth, England. Zubkoff and Lin (1975) observed peculiar banding in the isozyme patterns of *Aurelia* scyphistomae from Puget Sound, Washington, that caused them to wonder whether this population may belong to a species other than *A. aurita*. Similarly, Greenberg *et al.* (1996) could distinguish two groups on their allozyme patterns: one group consisted of two populations of *A. "aurita"* from Japan (one from Tokyo Bay, and one aquarium-raised) plus

a population that was apparently introduced to San Francisco Bay; and the second group consisted of wild medusae from Monterey Bay, California, and Vancouver, British Columbia. They further distinguished the two groups on the basis of morphology, using manubrium length and the highly anastomosed condition of the radial canals.

To test the hypothesis that the common eastern North Pacific *Aurelia* is *A. aurita*, I compared the morphology of 17 populations of *Aurelia* from San Diego, California, to Prince William Sound, Alaska, to the morphology of *A. aurita* from Europe, and *A. flavidula* from the eastern United States, as described and figured by Agassiz (1862), Mayer (1910), Kramp (1961), Russell (1970), and many of the references therein. The conclusions that I have drawn on morphological characters are consistent with those emerging from the enzyme analyses of Zubkoff and Lin (1975) and Greenberg *et al.* (1996), the neuromuscular study of Chia *et al.* (1984), and the DNA sequencing results of J. Lowrie of the Cnidarian Research Institute (pers. comm., June 2000)—that is, that the common eastern North Pacific *Aurelia* is not *A. aurita*. However, it does match the description of the species previously described as *Aurelia labiata* Chamisso and Eysenhardt, 1821. Thus, I propose a revalidation of *A. labiata*, and herein offer a redescription and designate a neotype. In scrutinizing the morphology of *A. labiata*, I further found that each population possesses unique characters that cluster into three morphotypes corresponding to well-demarcated biogeographic provinces. The purposes of this paper are to describe the morphological and geographical variation in *A. labiata* and to stabilize the nomenclature for the species. This is necessary as a basis for further systematic investigation, for ongoing biodiversity studies, and for proper management of species introductions.

Materials and Methods

Aurelia aurita and other forms

Literature-based comparisons were made using the European form, *Aurelia aurita*, and are denoted traditionally (*e.g.*, *Aurelia aurita*). The full breadth of literature used for comparison is too massive to list here, but can be found in the synonymies of Mayer (1910), Kramp (1961), and Russell (1970).

Literature-based comparisons were made with *A. flavidula* from the eastern United States, primarily following Agassiz (1862) and the references in the synonymy of Mayer (1910).

Literature-based comparisons were made to the boreal *A. limbata* using Brandt (1835, 1838), Vanhöffen (1906), Kishinouye (1910), Bigelow (1913, 1920), Uchida (1934), Bigelow (1938), Kramp (1942), Stiasny and van der Maaden (1943), Naumov (1961), Uchida and Nagao (1963), and Faulkner (1974).

Comparisons were made using live, captive medusae descended from a Japanese population (cultured at Cabrillo Marine Aquarium); although the phylogenetic relationship between the European and Japanese forms is still in question, they are structurally similar—that is, they both lack the enlarged manubrium characteristic of *A. labiata*.

Comparisons were also made on some live, wild medusae from Spinnaker Bay, Long Beach, California, which possessed the *A. aurita* body form, and on the descriptions of Greenberg *et al.* (1996) for the introduced San Francisco Bay form. Live representatives of Greenberg's population at Foster City could not be found. References made to forms that possess the *A. aurita* body type but are of uncertain taxonomic affiliation are denoted non-traditionally (*e.g.*, *Aurelia* "aurita" or *Aurelia cf. aurita*). This includes the captive Japanese form, as well as introduced forms.

Systematics of Aurelia labiata

Attempts were made to locate the holotype at the following institutions: The California Academy of Sciences (San Francisco) (CAS), Institut Royal des Sciences Naturelles de Belgique (Brussels), Museum für Naturkunde (Berlin), Muséum National D'Histoire Naturelle (Paris), Museum of Comparative Zoology (Harvard), Nationaal Natuurhistorisch Museum (Leiden), National Museum of Natural History (Washington), Natural History Museum (London), Zoological Institute (St. Petersburg), Zoological Museum (Copenhagen), and the Zoological Museum (Moscow University). All would have been reasonable depositories or recipients of a transfer of a holotype of a California species found by European explorers on a Russian expedition of that time. However, none had *A. labiata* type material nor knew where it might be kept; indeed, it appears doubtful that specimens were originally collected and deposited. Thus, my observations were made on animals from near the type locality and from many other regions along the Pacific Coast of North America.

A neotype was designated in order to stabilize the taxonomy of the species, and is deposited in the California Academy of Sciences in San Francisco. The original type locality could not be identified. Chamisso and Eysenhardt (1821) recorded the species from "New California," and a map in Schweizer (1973) indicates only somewhere near San Francisco Bay. However, specimens that I collected near San Francisco Bay were in poor shape, so the most intact representative specimen from the available material was selected from Monterey Bay (*ca.* 100 miles to the south). Morphological differences were not apparent between specimens from San Francisco and Monterey, excepting those attributable to collection.

I preferentially examined live medusae in the wild to avoid artifacts of captivity and preservation; however, cultured and captive medusae were observed supplementally.

In the wild, mature and immature medusae were collected from July 1995 to March 2000 by hand and by dip nets from nine locations in California (Coronado Island, San Diego; Newport Beach; Spinnaker Bay, Long Beach; Catalina Island; Marina del Rey; Santa Barbara; Monterey Bay; Sausalito, San Francisco Bay; Tomales Bay), and from Newport, Oregon; Poulsbo, Washington; Friday Harbor, San Juan Island, Washington; and Brentwood Bay, Saanich Inlet, British Columbia. Cultured and captive medusae were examined at the Birch Aquarium at Scripps, San Diego, California (San Diego *A. labiata*); Cabrillo Marine Aquarium, San Pedro, California (both Japanese *Aurelia* "aurita" and Long Beach *A. labiata*); Monterey Bay Aquarium, Monterey, California (Japanese *A. "aurita"* and Monterey *A. labiata*); Oregon Coast Aquarium, Newport, Oregon (Japanese *A. "aurita"* and Newport *A. labiata*); Point Defiance Zoo and Aquarium, Tacoma, Washington (*A. labiata* from Poulsbo, Washington); and the Seattle Aquarium, Seattle, Washington (*A. labiata* from Poulsbo, Washington). In addition to the above observations, characters were assessed as much as possible from a videotape taken in July 1996 of medusae from Prince William Sound, Alaska; from photographs of *A. labiata* from Steamer Bay, Alaska (Barr and Barr, 1983) and *A. limbata* from Amchitka Island, Alaska (Faulkner, 1974); and from preserved specimens from the Farallon Islands, California.

Measurements were taken on 7–20 live medusae from each of the following locations: Coronado Island, Newport Beach, Spinnaker Bay, Marina del Rey, Monterey Bay, Tomales Bay, Newport (OR), Poulsbo, and Brentwood Bay. Each medusa was individually dipped out of the water with a bucket and measured immediately with a vernier caliper or ruler to the nearest millimeter. Bell diameter (BD) was typically measured with the specimen lying flat on its exumbrellar surface. Manubrium length (ML) was usually measured with the animal in the water with the manubrium projecting upward, but captive medusae from Newport (OR) were measured with the manubrium hanging downward in the water. Since the manubrium is stiff and cartilaginous, its position did not appear to bias the measurements. To account for the difference in size at maturity of medusae from different populations, manubrium lengths were normalized as a percentage of bell diameter.

In addition to the measurements described above, about 200 medusae from each population were cursorily examined for the following characters, then released: manubrium shape, number of marginal scallops, oral arm length, number of radial canals emanating from each gastro-genital sinus, bell shape and color, and if female, the location and pattern of larval brood.

German papers were translated with Power Translator 6.02 for Windows (Globalink).

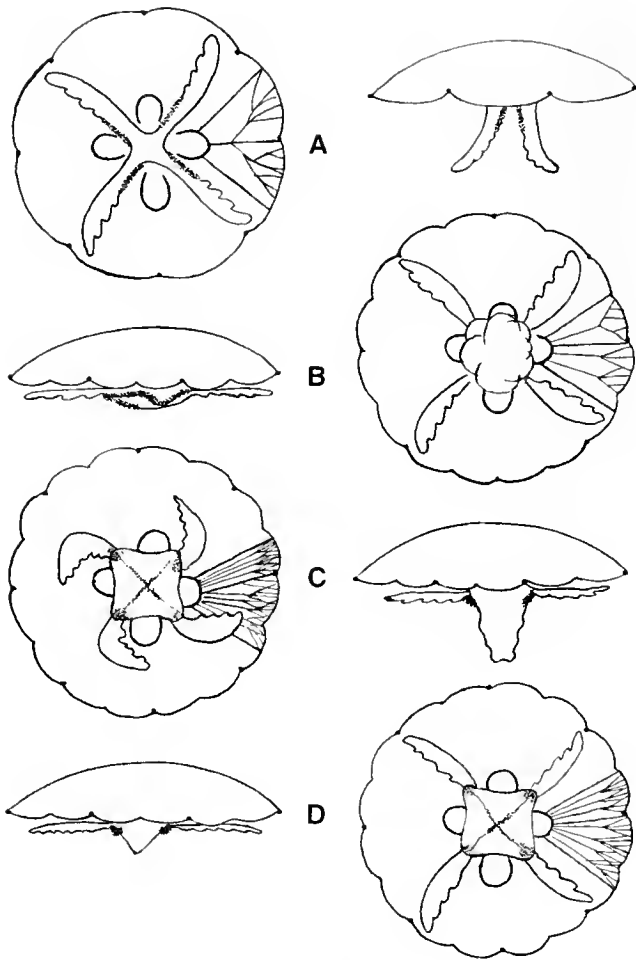


FIG. 3. Comparative diagram of three morphotypes of *Aurelia labiata* with *A. aurita*, subumbrellar and lateral views. (A) *Aurelia aurita*. (B) Southern morph, from Southern California Bight. (C) Central morph, from Santa Barbara, California, to Oregon. (D) Northern morph, from Puget Sound, Washington, to Alaska. In *A. aurita*, manubrium is inconspicuous, oral arms meet in the middle, the radial canals are few, and the margin has 8 scallops. In *A. labiata*, the manubrium protrudes below the bell margin, which has 16 scallops, there are many radial canals, and the oral arms do not meet. Darkened areas along oral arms (*A. aurita*) and manubrium (*A. labiata*) indicate position of larval brood.

Results

Comparison with European Aurelia aurita (Fig. 3)

Medusae from every population that I studied in the eastern North Pacific differed from published descriptions of the European *A. aurita* but closely matched the original description of *A. labiata*. Specifically, the *A. labiata* body form is characterized by an enlarged, fleshy manubrium; oral arms arising from the base of the manubrium; planulae brooding upon the manubrium; up to 15 radial canals arising from each gastro-genital sinus, and typically anastomosing in older individuals; and secondary scalloping of the bell margin between rhopalia (Fig. 3B-D). In contrast, the *A.*

aurita body type possesses no such enlarged manubrium structure; the oral arms meet in the middle of the animal; planulae are brooded upon the oral arms; typically only 3-5, sometimes 7, radial canals arise from each gastro-genital sinus; and secondary scalloping is rarely observed (Fig. 3A).

Comparison with western Atlantic Aurelia "flavidula"

The nominal species *Aurelia flavidula* is another taxonomic tangle that was somewhat resolved by Kramp (1942). Kramp concluded that the yellow Greenlandic form seen by Fabricius (1780) and named by Peron and Lesueur (1810) was identical to *A. limbata*, later named by Brandt (1835), and that calling the northern Atlantic American form *A. flavidula* was a mistake by Agassiz (1862). Agassiz had differentiated the western Atlantic *A. "flavidula"* from the European *A. aurita* on the former having a marginal network of anastomoses, the gonadal pouches closer together and occupying fully 1/3 of the bell diameter, and differences in the mouth fringes. Kramp further cautioned that using the name *A. flavidula* would be confusing, so he gave the common American Atlantic form the name *A. occidentalis*, distinguishing it from *A. aurita* on the heavier anastomosing of the radial canals; he later lumped it into *A. aurita* without comment (Kramp, 1961).

Proper phylogenetic placement of both the Greenlandic form and the common American Atlantic form must await a revision of the genus *Aurelia* based on live material. For the Greenlandic form, being yellow and having anastomosed canals seem insufficient for concluding conspecificity with the Alaskan *A. limbata*. Ideally, conspecificity should be based on numerous characters inherited by common descent, not by shared color. The importance of anastomosed canals is discussed below. The American Atlantic form, regardless of its identity, does not possess the enlarged manubrium and related characters of *A. labiata*; whether it is present along the Pacific coast of North America has not yet been determined.

Systematics of Aurelia labiata

The common moon jellyfish found in 17 populations from San Diego, California, to Prince William Sound, Alaska, is characterized by the body form described by Chamisso and Eysendardt (1821) for *A. labiata*. Many of the references to *Aurelia* of the eastern North Pacific do not contain illustrations or photographs; those that do are most often based on the European morphology. In at least one example, the same photograph is used in both West coast and East coast American field guides (Audubon Society, 1981). A large body of literature has thus been responsible for perpetuating the misidentification. The synonymy below contains only the references that have figures or descriptions positively referable to *A. labiata sensu* Chamisso and

Eysenhardt, 1821; thus, even references to *A. labiata* are not included below if they do not include the enlarged manubrium. The remainder of references to eastern North Pacific *Aurelia* are dealt with below in appropriate sections.

***Aurelia labiata* Chamisso and Eysenhardt, 1821
(Figs. 2; 3B-D)**

Aurelia labiata Chamisso and Eysenhardt, 1821: 358, pl. 28, fig. 1A. B.—Mayer, 1910: 622, 628, in part, eastern North Pacific records only.

Medusa labiata.—Eschscholtz, 1829: 64.

Aurelia labiata.—de Blainville, 1834: 294, pl. 42, figs. 1, 2 (Cham. & Eysen. illustrations).—Lesson, 1843: 377.—L. Agassiz, 1862: 160.—A. Agassiz, 1865: 43.—Haeckel, 1880: 557 (monograph).—Fewkes, 1889a: 593 (Point Conception, Monterey; manubrium).—Torrey, 1909: 11 (coll. by Cham. & Eysen.).—Barr and Barr, 1983: 80, text fig. 28 (Field Guide (= FG): AK).—Wrobel and Mills, 1998: 55 (FG: Pacific coast).—Gershwin, 1999: 993-1000, in part (symmetry variation).

Aurelia aurita non Linnaeus 1758.—Hauser and Evans, 1978: 21 text photo, 81 (commensal crab).—Snively, 1978: 152 text fig., pl. 77 (FG: BC, WA, OR).—Gotshall, 1994: 24, fig. 40 (FG).

Aurelia sp.—Campbell, 1992: 12, 13, Back cover (photographs).—Greenberg *et al.*, 1996: 401-409, in part, text fig 3, 4 (allozymes).

Moon jellyfish.—Malign, 1985: 40 (photograph).—Steffoff, 1997: 9 (photograph).

Holotype. Apparently not extant.

Neotype. CASIZ 111024, Monterey Bay, CA, coll. 19 April 1997 by D. Wrobel; gravid female, preserved 25-cm bell diameter (BD), 12-cm manubrium length (ML).

Additional preserved material. CAS 20, Farallon Islands, East Landing, coll. 14 Sep 1975 by D.R. Lindberg. CAS 95506, same data as CAS 20. CAS 95507, same data as CAS 20. CAS 81306, Monterey Bay, Pacific Grove, coll. 13 Nov 1990 by N. Greenberg, *ca.* 15-cm BD, manubr. 6.5 cm. CAS 81307, Monterey Bay, Pacific Grove, coll. 13 Nov 1990 by N. Greenberg, BD *ca.* 15 cm, ML *ca.* 6 cm. CAS 86767, 2 specimens, Vancouver Island, Sooke Basin, Roche Cove, coll. 11 Sep. 1990 by N. Greenberg, 14.5-cm BD, 6 cm ML. CAS 81304, Monterey Bay, Pacific Grove, coll. 13 Nov 1990 by N. Greenberg, *ca.* 13-cm BD, *ca.* 4-cm ML. CAS 81306, Monterey Bay, Pacific Grove, coll. 13 Nov 1990 by N. Greenberg. CAS 107800, 2 specimens, Monterey (CA), coll. 30 July 1966 by Rofen. CAS 111016 and 111020, Brentwood Bay, Saanich Inlet, coll. 24 June 1996 by LG. CAS 111017, Point Defiance, Puget Sound, coll. 5 April 1996 by LG. CAS 111021-111022, numerous specs, Santa Barbara, coll. 30 Nov 1996 by S. Anderson. CAS 111023, numerous specs, Marshall dock, Tomales Bay (CA), coll. 30 June 1996 by LG. CAS 111227, Spinnaker Bay, Long Beach (CA), coll. Sep 1995–Jan 1997 by L. Gershwin. In addition, preserved, unregistered specimens were examined from collections at Bodega Marine Laboratory, Cabrillo Marine Aquarium, Friday Harbor Laboratory, and Santa Barbara Museum of Natural History.

Diagnosis. *Aurelia* with manubrium elongated, wide, protruding below the bell margin when viewed laterally. Oral arms shorter than bell radius, attached to base of manu-

brium, extending outward to bell margin or bent at 90° angle typically counterclockwise. Bell margin 16-scalloped, with a primary indentation at each of 8 rhopalia and a secondary indentation midway between rhopalia. Older individuals typically with many radial canals arising from each gastro-genital sinus; in some, the outer branches are greatly anastomosed. Embryos and larvae brooded on the manubrium or on stiff, shelf-like manubrial extensions, rarely on the oral arms.

Redescription.

Medusa. (Based on mature tetramerous individuals.) Bell typically quite flat at rest, in some subhemispherical; older individuals may have raised hump over gonadal region. Diameter at maturity ranging from 100 mm to 450 mm, depending on population. Manubrium fleshy, rigid; rectangular, pyramidal, or rounded in side view; variably ruffled at 4 corners; width approximately 1/3 of bell diameter; with stiffened, whorled, perradial mesogleal extensions. Index of manubrium length to bell diameter varying geographically, longest in Oregon ($x = 37.2\% \pm 3.6\%$; $n = 10$, Newport), shortest in southern California ($x = 16.7\% \pm 2.6\%$; $n = 7$, Spinnaker Bay, Long Beach). Oral arms 4, perradial, straight or curved at 90° angles typically counterclockwise (but occasionally variable), arising from base of manubrium; length short, reaching approximately to bell margin (thus only $\pm 1/3$ bell diameter); extending laterally outward against subumbrellar surface of bell. In older cultured individuals, oral arms may hang downward. Size of subgenital ostia varying, encircled by raised mesoglea in some individuals. Interradial and adradial canals typically unbranched; perradial canals branched once, or in large individuals the gastro-genital sinus may overgrow the trifurcation causing the perradial canal to appear unbranched. Eradial canals branched, 4-12 arising from each gastro-genital sinus. Some large specimens have conspicuous anastomoses of canals on outer third of bell. Gastro-genital sinuses interradian, 4, but varying from 1 to 8 (perhaps more), in rounded to flattened horseshoe-shaped or heart-shaped rings, with adaxially-pointing free ends. Bell with 16 marginal scallops produced by 8 primary indentations at rhopalia located along the perradial and interradian axes, with secondary indentations between adjacent rhopalia. Bell transparent and colorless in juveniles and young adults, becoming milky white, or tinted pinkish, purple, peach, or bluish in older medusae. Color of gonad pale pinkish or brownish in mature females, dark purple in mature males, but often appearing white in males ready to spawn.

Planula. Elliptical to elongated; ciliated. Color most often white, but other colors found in certain populations: lavender (Monterey), peach (Saanich Inlet), or yellow-ochre (Spinnaker Bay). Planktonic or benthic locomotion by ciliary movement. Brooded on manubrium or its whorls.

Scyphistoma. Polyps 2-3 mm in height, with oral disk 1-2

mm diameter. Manubrium short, cruciform. Septal funnels conspicuous. Typically with 16 tentacles, alternating shorter and longer; number of tentacles highly varied, often corresponding to symmetry of parent medusae, parent polyp, or offspring ephyrae. At Friday Harbor, Washington, and Santa Cruz Island, California, scyphistomae typically with 20 tentacles. Color whitish to pale pinkish-orange. Habit benthic, usually hanging downwards from underside of docks, mussel shells, or rocks. Asexual proliferation by side budding, stolon budding, or podocyst formation. See Chia *et al.* (1984) for a histological study of the neuromuscular system.

Strobila. Ranging from monodisk to polydisk with more than 20 developing ephyrae. Color varying with locality: cinnamon in southern California, buff in Monterey. Polyp remaining flesh-colored or whitish. Strobilation time about 7 days; easily induced with periods of chilling.

Ephyra. Diameter 2-3 mm at release. With 8 marginal arms, each with a terminal rhopalium flanked by 2 lappets. Nematocysts scattered over the exumbrellar surface. Number of arms and rhopalia highly varied, not always in correspondence with each other or within a clone. Color same as the strobila: cinnamon or pale buff.

Type locality. Monterey Bay, California.

Distribution. I have collected *A. labiata* from Saanich Inlet, British Columbia, to San Diego, California. To the north, I was able to confirm its presence in Prince William Sound, Alaska, from a videotape; the species has also been photographed at Steamer Bay, in southeast Alaska (Barr and Barr, 1983). Its range may extend southward into the waters off Baja California, Mexico. The species generally occurs in bays and harbors where it is easily collected from jetties and boat slips, but medusae have been observed drifting in open waters off Santa Barbara, California (S. Anderson, Univ. California Santa Barbara, pers. comm., Nov. 1996), near Monterey Bay, California (D. Wrobel, Monterey Bay Aquarium, pers. comm., Oct. 1996; D. Powell, Monterey Bay Aquarium, pers. comm., May 1997), off Newport, Oregon (D. Compton, Oregon Coast Aquarium, pers. comm., June 1996), and in Puget Sound (LG, pers. obs., June 1996). The polyps generally strobilate in early spring, and the medusae quickly mature, spawn, and die by mid-summer or early fall. In some years and in some localities, the population of medusae is present throughout the year (Spinnaker Bay, LG, pers. obs.; Monterey, D. Wrobel, pers. comm.).

Biogeography

Observations of 17 populations from San Diego, California to Prince William Sound, Alaska have shown that the species can be reliably subdivided into three easily distin-

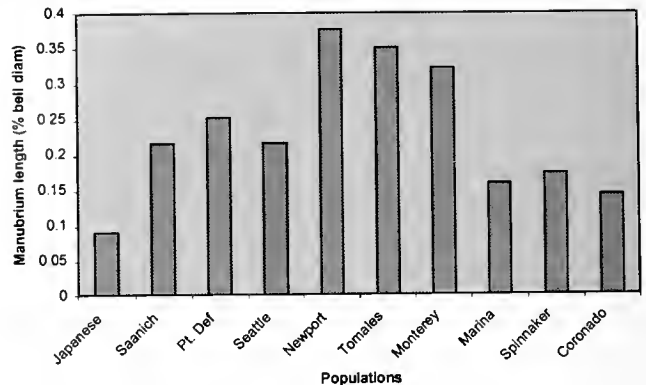


Figure 4. Average manubrium lengths of Japanese *Aurelia cf. aurita* and nine populations of *A. labiata*. Japanese = *Aurelia cf. aurita*, cultured at Cabrillo Marine Aquarium. Northern morph: Saanich = Saanich Inlet, British Columbia; Pt. Def. = Poulsbo, Washington (cultured at Pt. Defiance Aquarium); Seattle = Poulsbo, Washington (cultured at Seattle Aquarium). Central morph: Newport = Newport, Oregon (captive at Oregon Coast Aquarium); Tomales = Tomales Bay, California; Monterey = Monterey, California. Southern morph: Marina = Marina del Rey, California; Spinnaker = Spinnaker Bay, California; Coronado = Coronado Island, California. Between morphotype comparison. ANOVA; $F = 42.595$, $df = 3,5$, $P = 0.001$.

guishable geographical morphotypes. Though bell diameter is highly variable with environmental conditions, even among nearby populations (Lucas and Lawes, 1998), manubrium length, expressed as a percentage of bell diameter, differs significantly among the three forms (Fig. 4, ANOVA; $F = 42.595$, $df = 3,5$, $P = 0.001$). These three forms are easily distinguished as follows (summary in Table 1). Following the synopsis of each form is a list of literature that pertains to *Aurelia* from the region, but contains insufficient information for positive determination.

Southernmost form (Fig. 3B). Manubrium a wide, rounded frilly mound, not distinctly pyramidal. Radial canals few to many, possibly dependent on age; adradials particularly wide in San Diego medusae. Oral arms typically straight, not curved. Planulae ranging in color from white to ochre to bright orange, brooded in a reticulating pattern on frills of manubrium. Bell colorless to milky whitish; some individuals with dark purple tentacles. Male gonads dark purple, female gonads pale pink. Typical maximum size, 35 cm. Marina del Rey medusae with pronounced rhopalial hoods set up off the margin.

Known range. California, from San Diego to Marina del Rey, possibly extending north to Ventura and south into Baja California. Populations are apparently isolated and discontinuous; not observed at Oceanside, Dana Point, Los Angeles Harbor, or Malibu. Reported at Catalina Island. Local residents at Ventura Harbor and Channel Islands Harbor tell of seeing an occasional medusa or two; it is currently unclear if they are this form. Typically occurring until late spring, occasionally into autumn.

Table 1

Comparison of morphotype characters, *Aurelia labiata*

Character	Northern morph	Central morph	Southern morph
Manubrium length (\bar{x}) (as % bell diam)	22.98%	37.15%	16.73%
SD	$\pm 0.04\%$	$\pm 0.04\%$	$\pm 0.03\%$
<i>n</i>	26	10	7
site	Poulsbo/Saanich	Newport	Spinnaker Bay
Manubrium shape	pyramidal	long and tapered	rounded
Oral arm length	1/3 bell diam	1/3+ bell diam	1/3 bell diam
Oral arm shape	\pm straight	counterclockwise	straight
# canals per sinus	7-9	7-15	5-7
Anastomosing	heavy	very heavy	moderate
Bell size	to 12 cm	to 45 cm	to 25 cm
Bell color	whitish or peach	purple, pink, or white	whitish
Planula color	white or peach	white or purple	white, ochre, or orange

Literature.

Aurelia aurita.—MacGinitie and MacGinitie, 1949: 131, text fig. 32 (growth, strobilation, Newport Bay).—MacGinitie and MacGinitie, 1968: 131, text fig. 32 (growth, strobilation, Newport Bay).—Reish, 1972: 25, text fig. 26 (FG: Southern CA).—Allen, 1976: 22, 75 (FG: Southern CA).—Reish, 1995: 38, fig. 31 (FG: Southern CA).

Central form (Fig. 3C). Manubrium extremely elongated, rectangular and tapering. Canals numerous, typically heavily anastomosed in largest individuals. Oral arms straight or bent counterclockwise. Planulae distinctly lavender, brooded in teardrop-shaped clumps on the base of manubrium or on shelves. Scyphistomae pale buff colored. Medusae from Monterey, California tending to be distinctly purple; Santa Barbara, California, medusae often pale pink. Gonads dark purple in males, pale brown in females. Diameter of captive medusae from Newport, Oregon, recorded to 45 cm, with longest manubrium being 17 cm!

Known range. Santa Barbara (including Channel Islands), California to Newport, Oregon. Likely occurring, but unconfirmed, along the outer coast of southern Washington state. Abundant in late summer.

Literature.

Aurelia labiata.—Fewkes, 1889b: 122 (Santa Barbara Channel; pink).—Boyd, 1972 (fouling organism; Bodega Harbor, CA).—Pearcy, 1972: 354 (Oregon).—Hand, 1975: 95 (FG: Central CA).

Aurelia aurita.—?Galigher, 1925: 94 (scyphistomae; Monterey, CA).—Hamner and Jenssen, 1974: 833-848, text fig. 1 (growth and degrowth, Tomales Bay, CA).—Shenker, 1984: 619-630 (abundance; OR).—Abbott, 1987: 28 (morphology; Monterey).—Keen and Gong, 1989: 735-744 (scyphistoma clonal growth; Tomales Bay, CA).—Niesen, 1997: 43 (FG: Northern CA).—Rigsby, 1997: 207 (Monterey Bay).

Aurelia labiata.—Light *et al.*, 1954: 41 (FG: central CA).

Aurelia aurita.—Hedgpeth, 1962: 52, text fig. B (FG: Northern CA).

Aurelia sp.—Gottshall *et al.*, 1965: 149 (prey of blue rockfish; Bodega, Monterey, Morro Bay).—Pereyra and Alton, 1972: 448 (near Columbia River, OR).

Northernmost form (Fig. 3D). Manubrium low, pyramidal. Many parallel radial canals in mature individuals, giving a lacy appearance to the bell. Oral arms more or less straight, but may be variable in the same individual in

Departure Bay specimens (M. Arai, Pacific Biological Station, Nanaimo, BC, pers. comm. 2000). Planulae variably colored; brooded at the base of the manubrium and on manubrial shelves. Overall coloration peach or whitish, with gonads dark purple in males, pale brown in females. At Poulsbo, Washington, maximum diameter approximately 12 cm; brooded planulae white, appearing as a wash or haze rather than in discrete bundles. At Saanich Inlet, British Columbia, medusae larger, to approximately 15-cm diameter during my study, but reported to range from 14-29-cm (Hamner *et al.*, 1994); brooded planulae peach-colored.

Known range. Puget Sound, Washington, to Prince William Sound, Alaska; mainly occurring in late spring.

Literature.

Aurelia labiata.—Carl, 1963: 101 (FG: BC).—Kozloff, 1974: 22, in part (FG: WA).

Aurelia limbata.—?Stiasny, 1922: 522 (Vancouver).—?van der Maaden, 1939: 33 (rhopalial folds; Vancouver).

Aurelia aurita.—Bigelow, 1913: 98 (marginal scallops; Puget Sound).—Clemens, 1933: 16 (Canada).—Kozloff, 1973: 62, text photo 10 (FG: WA).—Arai and Jacobs, 1980: 120 (medusivory; BC).—Mills, 1981: 22 (seasonality; Puget Sound).—Kozloff, 1983: 56, text photo 13 (FG: WA).—Chia *et al.*, 1984: 69-79 (scyphistoma structure; Puget Sound).—Larson, 1986: 107-120 (chemical composition; Saanich Inlet).—Kozloff, 1987: 65 (FG: Pacific Northwest).—Larson, 1987: 93-100 (carbon cycling; Saanich Inlet).—Strathmann, 1987: 76 (development; Puget Sound).—Strand and Hamner, 1988: 409-414 (prey of *Phacellophora*, Saanich Inlet).—Norris, 1989: 381-393 (fossilization).—Arai, 1991: 363 (chemical predation cues; BC).—Keen, 1991: 1-176 (scyphistoma biology; Tomales Bay).—Fantin and Lowenstein, 1992: 13 (polyp and medusa proteins).—Hamner *et al.*, 1994: 347-356 (sun migration; Saanich Inlet).

Aurelia sp.—MacGinitie, 1955: 120 (color range; Pt. Barrow, AK).—Zubkoff and Lin, 1975: 915 (isozymes).

In addition to the literature apparently attributable to each form above, a large body of literature exists which pertains to *Aurelia* of the eastern North Pacific but cannot be attributed to a single region as described above. Many of these references do not illustrate the species, or in some cases, use general drawings or photographs from other locations.

Aurelia aurita.—Johnson and Snook, 1927: 82, text fig 62 (FG).—Guberlet, 1936: 45, text photo (FG; Northwest).—Guberlet, 1949: 45, text photo (FG; Northwest).—Hartman and Emery, 1956: 307 (CA).—Guberlet, 1962: 45, text photo (FG; Northwest).—Flora and Fairbanks, 1966: 50, Fig. 42: (FG; BC, WA, OR).—Johnson and Snook, 1967: 82, text fig 62 (FG).—Brusca and Brusca, 1978: 52, text fig. 22 (FG; CA).—McLachlan and Ayres, 1979: 47, text photo (FG; Pacific Northwest).—Gotshall and Laurent, 1980: 40, text photo 40 (FG, Pac. coast).—Haderlie *et al.*, 1980: 52, pl. 3.22 (FG; CA).—Audubon Society, 1981: 363, in part, pl. 502 (photo is of *A. aurita*, possibly outside NE Pacific).—Austin, 1985: 71 (Alaska to southern California).—McConnaughey and McConnaughey, 1985: 466, pl. 384 (photo is of *A. aurita*, but may have been taken elsewhere).—Ricketts *et al.*, 1985: 303, text fig. 316 (FG).—Farmer, 1986: 111 (FG; AK to so. CA).—Parsons, 1986: 18 (sting treatment).—Connor and Baxter, 1989: 53 (in kelp forest).—Amos, 1990: 36, in part, Alaska to southern California (photo is of *Aequorea* sp. (Cnidaria: Hydrozoa) but attributed to *A. aurita*).—Larson, 1990: 546-556 (distribution).—Larson and Arneson, 1990: 130-136 (California).—Niesen, 1994: 48, text fig. 4-33 (FG; CA).—Thuesen and Childress, 1994: 84-96 (enzyme activity; southern and central CA).

Aurelia (and *Aurelia* sp.).—Ricketts and Calvin, 1939: 244, text fig. 109 (FG).—Wells, 1942: 146, text fig. (FG).—Ricketts and Calvin, 1948: 144, 244, text fig. 109 (FG).—Ricketts and Calvin, 1952: 328, text fig. 109 (FG).—Smith, 1962: 13, text fig. 10 (FG; Pac. Northwest).

Aurelia aurita.—Light, 1941: 19 (invert. manual).—Ricketts and Calvin, 1968: 264, text fig. 266 (FG).

Aurelia (and *Aurelia* sp.).—Tierney *et al.*, 1967: 26, text fig. (FG).
Jellyfish.—Ulmer, 1968 (children's book).

Aurelia labiata.—North, 1976: 153 (FG; CA).—Austin, 1985: 71 (Alaska to central CA).

A second *Aurelia aurita* introduction

A second population of *Aurelia aurita*, apparently introduced, has recently been found at Spinnaker Bay, Long Beach, California (the first was found at South San Francisco Bay, California, by Greenberg *et al.*, 1996). It is impossible to know exactly when it first appeared; however, I have been working closely with the Spinnaker Bay population since 1995, and have only observed this other form since 1997. Morphologically, it is allied to the European and Japanese forms. However, preliminary 18S rDNA partial sequence analyses indicate that it is similar to a population from Fort Lauderdale, Florida (J. Lowrie, Cnidarian Research Institute, pers. comm., June 2000). Lowrie has further found that the Spinnaker Bay population clusters into at least four genetic subpopulations, one closely related to island populations, one as described above, and two apparent hybrid forms. This pattern is evident in the morphology as well. Since 1997, both *A. labiata* and *A. aurita* medusae have been observed side by side, as well as some that possess characters of both.

Comparison with Japanese *Aurelia aurita*

The Japanese form of *A. aurita* closely matches the descriptions of the European form (*e.g.*, Russell, 1970), and thus differs morphologically from *A. labiata* in a similar manner. Kishinouye (1891) described a form from Tokyo Bay, Japan, named *Aurelia japonica*; it was said to differ

from *A. aurita* in having prominent subgenital cavities and in having broad and folded lobes on the proximal halves of the oral arms (Kirkpatrick, 1903). Whether this form is identical to the European form or to *A. flavidula*, or to the Japanese material presently raised in American public aquariums, has not yet been determined and is beyond the scope of this paper.

Notes on *Aurelia limbata*

Upon casual inspection, *A. limbata* appears to be unmistakable because of its chocolate-brown marginal pigment band (see Audubon Magazine, Jan. 1974 cover, for an excellent photograph). It also appears to be distinctive in having relatively few tentacles and in the extreme anastomosing of the radial canals in all growth stages. However, closer examination may show *A. limbata* of the Arctic to be a fourth morph of *A. labiata*, or possibly even a color variant of the northern form. Mayer (1910) regarded *A. limbata* as a variety of *A. labiata*, apparently based on its having 16 marginal scallops. I have not had the opportunity to examine specimens of *A. limbata*, but written descriptions, drawings, and photographs reveal additional similarities. Like the northern form of *A. labiata*, *A. limbata* has a triangular protruding manubrium and many radial canals emanating from each gastro-genital sinus (Kishinouye, 1910; Faulkner, 1974; but the former character is not apparent in Mertens's illustrations published by Brandt in 1838). In addition, *A. limbata* shares with the Marina del Rey, California, population of *A. labiata* the peculiar character of large and conspicuous rhopalial hoods that are well above the bell margin. There has been some debate about the phylogenetic meaning of wrinkles in the rhopalial pits (see Uchida, 1934; van der Maaden, 1939); this character has not been checked in *A. labiata*. Furthermore, the anastomosing of the radial canals is far more developed in *A. limbata*. If the two nominal species are eventually regarded as conspecific, the name *A. labiata* would have chronological priority. More logically, *A. limbata* may be a separate species in an undefined species complex currently known as *A. labiata*.

Discussion

Biogeographical and systematic implications

Most twentieth century authors regard *Aurelia aurita* as cosmopolitan, occurring abundantly the world over, and some recognize *Aurelia limbata* of the Arctic Ocean as the only other species in the genus. These notions are dispelled by the present results. Not only is *A. aurita* replaced along the American Pacific coastline by *A. labiata*, but the latter is also divided into three morphologically distinctive forms coincident with established bioprovinces. Furthermore, there is some evidence that *A. limbata* may be a color morph

or possibly even a separate species within the clade currently known as *A. labiata*. Thus, the *Aurelia* group may actually consist of numerous local species, as was indicated by Lambert (1935), Hummelinck (1968), Hamner and Hauri (1981), and Brewer (1991) for other taxa, or possibly even more than one genus. Future molecular analysis of the morphotypes may elucidate the degree of differentiation.

One of the predictions of this hypothesis is that additional populations of *Aurelia* found along the Pacific coast of North America may be assignable among the three morphotypes, according to morphology and latitude. The eastern North Pacific flow patterns are consistent with the morphological differences of the jellyfishes, with both currents and morphologies diverging in the vicinity of Point Conception, California, and Puget Sound, Washington. The three regions corresponding to the morphotype ranges are coincident with the Californian, Oregonian, and Aleutian bioprovinces of molluscs (Hall, 1964: fig. 5; see also Valentine, 1966: fig. 1). Although molluscan provinces appear to be determined by sustained reproductive water temperatures (Hall, 1964), the cause of similar distribution in *Aurelia* is currently without explanation. Logically, temperature could play a role, but *Aurelia* is able to grow and reproduce continually in the laboratory in a wide range of temperatures, both cooler and warmer than the ambient ocean temperature (unpubl. notes). It is well documented that the distributions of benthic groups such as molluscs (Campbell and Valentine, 1977; Roy *et al.*, 1998) and algae (Abbot and Hollenberg, 1976) conform to biogeographical provinces. In contrast, the ranges of pelagic taxa are typically thought to be ill-defined at the fine scale, being confined primarily by the great gyres, if not cosmopolitan (Lalli and Parsons, 1993; Nybakken, 1993). For a nearshore pelagic invertebrate such as *A. labiata*, this generalization does not hold true. Further studies should examine *Aurelia* and other widespread coastal medusae in regions with similar latitudinal gradients, that is, eastern and western continental shores in both hemispheres.

Several recent studies may become important in our understanding of nearshore medusa distribution. First, Hellberg (1996) examined differential gene flow between one coral species that brooded its larvae and another with pelagic, feeding larvae; he found greater genetic subdivision in the brooding species. Likewise, *Aurelia* spp. and *Cyanea* spp. are planula brooders, and thus may have less gene flow among populations than previously assumed. Second, Cowen *et al.* (2000) found that simulated larvae do not disperse as readily as generally thought. Indeed, it appears that dispersal in some cases may be overestimated by nine orders of magnitude. Medusae, like larvae, are not passive particles. Rather, their dispersal ability is subject to their own behaviors as well as to diffusion and mortality. Many medusae swim actively against a gentle current, or drop lower in the water column to avoid currents (pers. obs.);

these behaviors may serve as anti-dispersal mechanisms. Finally, Barber *et al.* (2000) found a sharp genetic break in nearby populations of the mantis shrimp *Haptosquilla pulchella* in Indonesia, and suggested the presence of a sort of "marine Wallace's line." Even though the stomatopod larvae are planktonic, and thus have the means to disperse over great distances, it appears that they do not. Whether the same explanation can be applied to *Aurelia* remains to be shown.

Because so much of the coastline is hospitable to *A. labiata*, it is helpful to ask whether other similar species may be present as well. Currently there is no evidence of endemic species other than *A. labiata*, excepting the unresolved nomenclatural questions relating to *A. limbata*. However, it is easy to imagine that other forms may have been overlooked in a similar way as *A. labiata*, or that within the species I herein recognize as *A. labiata*, numerous cryptic species exist. The recent scientific literature abounds with discoveries of cryptic species, such as one recent startling example, wherein the fungal *Gibberella fujikuroi* species complex was found to comprise 45 phylogenetic species (O'Donnell *et al.*, 1998)! Given that many of the populations of *A. labiata* along the eastern North Pacific coast are uniquely diagnosable, and that these diagnosable forms partition into the three latitudinal morphotypes, the possibility of cryptic species seems high. Indeed, Greenberg *et al.* (1996) hypothesized restricted gene flow between eastern Pacific populations, based on significant allele frequency differences. Thus, the biogeographic pattern in *A. labiata* may represent cladogenesis in action, or possibly even a splitting event of the recent past. I hesitate at this time to recognize the three forms as distinct species, or for that matter to assign the eastern North Pacific forms to a new genus, although it is clear that the three forms are quite different from one another and from *A. aurita*. Although scyphozoan population genetics have not yet been studied in depth, some cnidarians have surprisingly low rates of genetic divergence (see Knowlton, 2000), so species conclusions should be made cautiously. Thus, until the clade currently known as *A. aurita* is resolved, it is difficult to comment with confidence on the internal and external relationships of the morphotypes of *A. labiata*. However, this does beg the questions of species concept and species recognition criteria.

Taxonomic characters

Throughout most of the twentieth century, it was customary to recognize medusan taxa based on certain key characters, regardless of distribution and discrete forms of variation; that is, all populations possessing a small number of given characters were thought to be one species. For example, in the Pelagiidae, the character of tentacle number has been so highly regarded that a large and conspicuous spe-

cies was incorrectly classified, favoring a tentacle number over all other characters combined (Gershwin and Collins, 2001). The same reasoning seems to have applied to *Aurelia*, favoring the "essence" of *A. aurita* over all other characters. This appears to have resulted in excessive lumping for many taxa. In contrast, I have employed a phylogenetic perspective, bringing together data from morphology, geography, and genetics to evaluate a lineage's history. However, some characters are still worthy of further comment, as they have led to confusion in the past.

Perhaps the most ignored character is the best key in separating *A. labiata* from *A. aurita*. Greenberg *et al.* (1996) used manubrium length in distinguishing the American form from the Japanese form, but failed to notice the associated changes in the relationship of the oral arms to each other and the altered brooding habits (Figs. 1, 2, 3B-D). To summarize, in *A. labiata* the oral arms are relatively short, about one-third the bell diameter, and project outward from the base of the fleshy manubrium. In addition, the larvae are brooded on the manubrium or on the rigid manubrial shelves. In contrast, *A. aurita* lacks the fleshy manubrium; consequently, the oral arms meet at the mouth and are about one-half the bell diameter. Furthermore, the brood pouches for the larvae line the upper portions of the oral arms. Thus, the large manubrium of *A. labiata* relates to a suite of morphological and functional differences from *A. aurita*.

Kramp (1913) considered the anastomosed canals to be a distinctive character in separating the Greenlandic form of *A. aurita* (as *A. flavidula*) from the typical form, and most descriptions of *A. limbata* include this character. However, the canals of some captive medusae of both *A. labiata* and *A. "aurita"* eventually become heavily anastomosed (F. Sommer, Monterey Bay Aquarium, pers. comm., and my own unpublished observations), possibly attributable to the phenomenon of growth and degrowth (Hamner and Jenssen, 1974). This was not taken into consideration by Greenberg *et al.* (1996), in claiming that the anastomoses could be used as a reliable character for distinguishing eastern Pacific *Aurelia* from western Pacific *Aurelia*. Indeed, their North American medusae were held captive nearly a year, whereas their Asian medusae were held only for 2 months. Although this character does seem more conspicuous in large specimens of *A. labiata* than in *A. "aurita"*, this may be due to the increased number of canals in *A. labiata*; that is, many canals anastomosing may give the appearance of a finer mesh than one would expect in an individual with fewer canals. This too (extra canals) was not taken into account by Greenberg *et al.* (1996). A closer study of anastomosis of canals might be helpful in future taxonomic studies.

Some authors have reported that the number of canals arising from the gastro-gonadal sinuses is taxonomically unreliable because it is associated with size and rate of growth (Stiasny, 1922; Bigelow, 1938; Kramp, 1942, 1965; Russell, 1970). Indeed, I have observed that older, larger

individuals do tend to have more canals than smaller, younger individuals. However, old, large *A. aurita* typically have 1 or 2 radial canals arising in each space between interradial and adradial canals (for a total of 5-7 canals arising from each gonad), whereas old, large *A. labiata* typically have 3-6 radials per side (for a total of 9-15 total per gonad). However, in the closely related *A. limbata*, Stiasny (1922) and Bigelow (1938) argued that the number of radial canals and the degree of branching are both useful characters. Curiously, medusae of the northern and central forms tend to possess greater numbers of radial canals than do medusae of the southern form.

The taxonomic significance of the 16-scalloped bell margin is currently unclear. Medusae from all endemic eastern North Pacific populations that I have observed possess this scalloping, in some cases quite conspicuously so. However, use of this character to distinguish species has been criticized by Kramp (1965), citing that in *A. limbata* the secondary scalloping is lost in preservation, and agreeing with Bigelow (1913) that the degree of scalloping is merely due to contraction of the bell. Because of its occasional occurrence in *A. aurita*, the secondary scalloping should not be used as the distinguishing taxonomic character of *A. labiata* as has been done in the past. However, it remains one of several useful field characters for *A. labiata* and may prove useful in similarly distinguishing other species worldwide.

Confusion has arisen regarding certain specimens from Nanaimo, British Columbia. Stiasny (1922) and van der Maaden (1939) assigned them to *A. limbata*; whereas Kramp (1942) identified them as a variety of *A. aurita* based on the width of their radial canals. I have not yet examined these specimens. However, Stiasny's (1922) description is consistent with *A. labiata*, namely, the 16-scalloped margin and the 5-9 radial canals issuing from each gastrovascular sinus.

At present, *A. labiata* appears to be a temperate endemic restricted to the eastern North Pacific. However, this leaves a series of references to medusae with 16 marginal scallops as *A. labiata*, although their morphological characteristics and geographic locations suggest that they are not. Available drawings and a photograph all clearly show 16 scallops of the margin, but do not show a protruding manubrium or numerous radial canals (Mayer, 1910, 1917; Uchida, 1928). Since the illustrations of Chamisso and Eysenhardt (1821) indicate a large manubrium, I exclude medusae that lack this character from this classification. However, I have not examined specimens from the following sources for complete diagnostic characteristics.

Aurelia labiata.—Mayer 1910: 628, fig. 398 (*A. limbata* as var. of *A. labiata*; Philippines).—Light, 1914a: 294 (harmless); Philippines).—Lie, 1914b: 200 (Philippines).—Mayer, 1915: 160, 182 (*A. labiata* derived from *A. aurita*).—Mayer, 1917: 205, text fig. 11 (Philippines and Tortugas, Florida).—Light, 1921: 31 (Philippines).—Bigelow, 1938: 167 (synonymous with *A. aurita*).

Aurelia labiata.—Stiasny, 1919: 93 (Malay Archipelago).—Stiasny,

1926: 244 (Philippines; *A. labiata* is a variety of *A. aurita*).—Uchida 1928: 373-376 (pentamerous, Pafau).—Stiasny, 1931: 140 (specimen at British Museum).—Stiasny, 1935: 34 (Aroe Islands).—Stiasny, 1937: 207 (East Indies).—Ranson, 1945: 60, 61 (review of genus).—Kramp 1961: 340 (taxonomy).—Kramp, 1965: 262-263, plate I fig. 1 (*A. labiata* same as *A. aurita*).—Kramp 1968: 68 (discusses *A. labiata*).—Russell 1970: 140 (discussion of synonymy). Powell, 1975: 6 (New Zealand).

Two reports of *A. labiata* in Hawaii (Chu and Cutress, 1954: 9; Devaney and Eldredge, 1977: 111) are worthy of attention. Drawings I made in 1993 from live animals in the Waikiki Aquarium appear to be of *A. labiata*. However, preserved specimens from the same location examined in 1997 lacked the enlarged manubrium. At this time, I provisionally include Hawaiian *Aurelia* with *A. labiata*, but firm determination must wait until additional live and preserved material can be examined. The Oahuan form appears to be introduced, as it was not reported until 1954, but the origin of the introduction is not yet known (J. T. Carlton, Mystic Seaport, Mystic, CT, and L. G. Eldredge, B. P. Bishop Museum, Honolulu, HI, pers. comm.).

Thus far, little consensus exists over what characters are taxonomically reliable for jellyfishes over a wide range of populations. To further confound the problem, immature specimens of closely related species often bear a striking resemblance. However, recent rearing of Japanese *Aurelia* "*aurita*" and Monterey *A. labiata* in the same aquarium yielded distinctive morphs consistent with the two species (M. Schaadt, Cabrillo Marine Aquarium, San Pedro, CA, pers. comm., Oct. 1999). Although I have herein distinguished only the northern, central, and southern morphs, medusae from each of the 11 locations were easily identifiable. The ability to distinguish morphological characteristics associated with particular populations of *Aurelia* spp. will not only help to resolve the phylogeny of the group, but may also help in identifying the origins of introductions such as those in Spinnaker Bay, California; San Francisco Bay, California (Greenberg *et al.*, 1996); and Oahu, Hawaii (J.T. Carlton and L.G. Eldredge, pers. comm., 1998).

Field key to the eastern North Pacific forms of *Aurelia*

1. Bell lacking secondary notches between adjacent rhopalia, margin 8-scalloped. Lacking broad and/or elongated manubrium. Currently known only from South San Francisco Bay and Spinnaker Bay *cf. A. aurita*
 - 1'. Bell with secondary notches between adjacent rhopalia, appearing 16-scalloped. Possessing conspicuously broad and/or elongated manubrium 2
 2. Bell with conspicuous chocolate-brown margin. Primarily Arctic *A. limbata*
 - 2'. Bell lacking brown margin 3
 3. Manubrium greatly elongated, tapering rectangular in shape. Generally found Pt. Conception, CA, to northern Oregon. Color variable from white to purple to pink. Often very large, to 45-cm or more . . . *A. labiata*, central morph

3'. With manubrium protruding in lateral view, but much less than one-third bell diameter 4

4. Manubrium pyramidal. Generally found in and north of Puget Sound. Color variable from white to peach. Typically small, 12-15 cm *A. labiata*, northern morph

4'. Manubrium rounded. Generally found south of Pt. Conception. Color typically milky white, occasionally with dark tentacles *A. labiata*, southern morph

Acknowledgments

I thank the staff and volunteers of the Cabrillo Marine Aquarium for unwavering encouragement, Susan Gershwin and Norma Kobzina for tracking down obscure references, Richard Harbison for translation of Chamisso and Eysenhardt (1821), Eric Hochberg for valuable museum and manuscript assistance, Claudia Mills and Allen Collins for stimulating discussions and help in a multitude of ways, Freya Sommer for sharing her knowledge and passion for jellyfishes, Gary Williams for his artwork and taxonomic guidance, Dave Wrobel for the beautiful photograph reproduced in Figure 2, the countless friends and colleagues who provided valuable suggestions on previous versions of the manuscript. Sincerest thanks to Mary Arai for providing assistance beyond the normal standard for review, and to an anonymous reviewer for additional helpful comments. In addition, I am indebted to the following people and institutions for help in obtaining specimens and information (in alphabetical order): Leslee Yasukochi and Eric Johnson at Birch Aquarium at Scripps; Jim Ulcickas at the Bluewater Grill, Newport Beach, California; Cadet Hand and staff at Bodega Marine Lab; Chris Mah at California Academy of Sciences; researchers and students at Friday Harbor Labs; Freya Sommer, Dave Wrobel, Dave Powell, and Ed Seidel at Monterey Bay Aquarium; Dave Compton and Polly Delle at Oregon Coast Aquarium; researchers and staff at Oregon Institute of Marine Biology; John Carlyle at Point Defiance Zoo and Aquarium; Yogi and Kathy Carolsfeld at Saanich Inlet; Erin Johnston and Shaun Larson at Seattle Aquarium; Spinnaker Bay and Spinnaker Cove homeowners; Thomas Shirley and Jennifer Boldt at University of Alaska; Shane Anderson at UC Santa Barbara; Rossi Marx at University of Victoria; and Joyce and Stuart Welch at Tomales Bay. I am thankful for financial support from the Friends of Cabrillo Marine Aquarium, the Howard Hughes Medical Institute Undergraduate Research in Biological Sciences Program, and the University of California, Berkeley, UCMP Contribution #1727.

Literature Cited

- Abbott, D. P. 1987. *Observing Marine Invertebrates*. Stanford University Press, Stanford, CA.
- Abbott, I. A., and G. J. Hollenberg. 1976. *Marine Algae of California*. Stanford University Press, Stanford, California.

- Agassiz, L. 1862. *Contributions to the Natural History of the United States of America*. Little, Brown, Boston.
- Agassiz, A. 1865. North American Acalephae. *Mem. Mus. Comp. Zool. Harvard College* 1(2): 1–234.
- Agassiz, A. and A. G. Mayer. 1899. Acalephs from the Fiji Islands. *Bull. Mus. Comp. Zool. Harvard* 32(9): 157–189.
- Allen, R. K. 1976. *Common Intertidal Invertebrates of Southern California*. Rev. ed. Peek Publications, Palo Alto, CA.
- Amos, S. H. 1990. *Familiar Seashore Creatures. The Audubon Society Pocketguide*. Alfred A. Knopf, New York.
- Arai, M. N. 1991. Attraction of *Aurelia* and *Aequorea* to prey. *Hydrobiologia* 216/217: 363–366.
- Arai, M. N. 1997. *A Functional Biology of Scyphozoa*. Chapman and Hall, London.
- Arai, M. N., and J. R. Jacobs. 1980. Interspecific predation of common Strait of Georgia planktonic coelenterates: laboratory evidence. *Can. J. Fish. Aquat. Sci.* 37: 120–123.
- Audubon Society. 1981. *The Audubon Society Field Guide to North American Seashore Creatures*. Alfred A. Knopf, New York.
- Austin, W. C. 1985. *An Annotated Checklist of Marine Invertebrates in the Cold Temperate Northeast Pacific*. Khoyatan Marine Laboratory, Cowichan Bay, BC, Canada.
- Barber, P. H., S. R. Palumbi, M. V. Erdmann, and M. K. Moosa. 2000. A marine Wallace's line? *Nature* 406: 692–693.
- Barr, N., and L. Barr. 1983. *Under Alaskan Seas*. Alaska Northwest Publishing Company, Anchorage.
- Bigelow, H. B. 1904. Medusae from the Maldive Islands. *Bull. Mus. Comp. Zool. Harvard* 39: 245–269.
- Bigelow, H. B. 1913. Medusae and Siphonophorae collected by the U.S. Fisheries Steamer "Albatross" in the north-western Pacific, 1906. *U.S. Nat. Mus. Proc. Wash.*, 1913. 44: 1–119.
- Bigelow, H. B. 1914. Fauna of New England. 12. List of the medusae craspedotae, siphonophorae, scyphomedusae, ctenophorae. *Boston Soc. Nat. Hist. Occas. Pap.* 7(part 12): 1–37.
- Bigelow, H. B. 1920. Medusae and Ctenophores from the Canadian Arctic Expedition. 1913–1918. Part H. Medusae and Ctenophora. *Rep. Canadian Arctic Exped.* 8: 19 pp.
- Bigelow, H. B. 1938. Plankton of the Bermuda Oceanographic Expeditions. VIII. Medusae taken during the years 1929 and 1930. *Zoologica, N.Y.* 23 (part 2): 99–189.
- Boyd, M. J. 1972. Fouling community structure and development in Bodega Harbor, California. Ph.D. dissertation, University of California, Davis.
- Brandt, J. F. 1835. *Prodromus descriptionis animalium ob H. Mertensio in orbis terrarum circumnavigatione observatorum. Fascic. I. Polypos, Acalephas Discophoras et Siphonophoras, nec non Echinodermata continens*. Sumptibus Academiae. Petropoli.
- Brandt, J. F. 1838. Ausführliche Beschreibung der von C.H. Mertens auf seiner Weltumsegelung beobachteten Schirmquallen. *Mem. Acad. Sci. St.-Petersb. Sci. Nat. Series 6.* 2: 237–411.
- Brewer, R. H. 1991. Morphological differences between, and reproductive isolation of, two populations of the jellyfish *Cyanea* in Long Island Sound, USA. *Hydrobiologia* 216/217: 471–477.
- Browne, E. T. 1905. Scyphomedusae. *Fauna Geogr. Maldive & Laccadive Archipelagos* 2(suppl. 1): 958–971.
- Brusca, G. J., and R. C. Brusca. 1978. *A Naturalist's Seashore Guide*. Mad River Press, Eureka, CA.
- Calder, D. R. 1971. Nematocysts of polyps of *Aurelia*, *Chrysaora* and *Cyanea* and their utility in identification. *Trans. Am. Microsc. Soc.* 90: 269–274.
- Campbell, C. A., and J. W. Valentine. 1977. Comparability of modern and ancient marine faunal provinces. *Paleobiology* 3: 49–57.
- Campbell, E. 1992. *A Guide to the World of the Jellyfish*. Monterey Bay Aquarium Foundation, Monterey, CA.
- Carl, G. C. 1963. *Guide to Marine Life of British Columbia*. British Columbia Provincial Museum, Victoria, BC, Canada.
- Chamisso, A., and C. G. Eysenhardt. 1821. De animalibus quibusdam e classe Vermium Linneana, in circumnavigatione terrae, auspicate Comite N. Romanzoff duce Ottone de Kotzebue, annis 1815–1818 per acta, observatis. *Nova Acta Acad. Caesar. Leop. Carol.* 10: 345–374, pl. 24–33.
- Chia, F.-S., H. M. Amerongen, and D. G. Petaya. 1984. Ultrastructure of the neuromuscular system of the polyp of *Aurelia aurita* L., 1758 (Cnidaria, Scyphozoa). *J. Morphol.* 180: 69–79.
- Chu, G. W. T. C., and C. E. Cutress. 1954. Human dermatitis caused by marine organisms in Hawaii. *Proc. Hawaii. Acad. Sci.* 29th Annual Meeting: 9.
- Clemens, W. A. 1933. *A Checklist of the Marine Fauna and Flora of the Canadian Pacific Coast*. National Research Council of Canada, Ottawa.
- Connor, J., and C. Baxter. 1989. *Kelp Forests*. Monterey Bay Aquarium, Monterey, CA.
- Cowen, R. K., M. M. L. Kamazima, S. Sponaugle, C. B. Paris, and D. B. Olson. 2000. Connectivity of marine populations: Open or closed? *Science* 287: 857–859.
- de Blainville, H. M. D. 1834. Manuel d'Actinologie, ou de Zoophytologie. F. G. Levrault, Paris.
- Devaney, D. M. and L. G. Eldredge. 1977. Class Scyphozoa. Pp. 108–118 in *Reef and Shore Fauna of Hawaii, Section 1: Protozoa through Ctenophora*, D. M. Devaney and L. G. Eldredge, eds. Bishop Museum Press, Honolulu, HI.
- Eschscholtz, F. 1829. *System der Acalephen. Eine ausführliche Beschreibung aller medusenartigen Strahlthiere*. F. Dummlert Berlin.
- Fabricius, O. 1780. *Fauna Groenlandica*. Impensis Ioannis Gottlob Rothe, Hafniae et Lipsiae.
- Farmer, W. M. 1986. *Seashore Discoveries*. Farmer, Santee, CA.
- Faulkner, D. 1974. (Cover Photograph). *Audubon* January 1974.
- Fautin, D. G., and J. M. Löwenstein. 1992. Scyphomedusae and their polyps are the same immunologically: implications for systematics. *Comp. Biochem. Physiol. B* 102(1): 13–14.
- Fewkes, J. W. 1889a. On a few Californian medusae. *Am. Nat.* 23: 591–602.
- Fewkes, J. W. 1889b. New invertebrata from the coast of California. *Bull. Essex Inst.* 21: 99–146.
- Flora, C. J., and E. Fairbanks. 1966. *The Sound and the Sea*, 2nd ed. Pioneer Printing, Bellingham, WA.
- Galigher, A. E. 1925. Occurrence of larval stages of Scyphozoa in the Elkhorn Slough, Monterey Bay, Calif. *Am. Nat.* 59: 94–96.
- Gershwin, L. 1999. Clonal and population variation in jellyfish symmetry. *J. Mar. Biol. Assoc. UK* 79: 993–1000.
- Gershwin, L., and A. G. Collins. 2001. A preliminary phylogeny of Pelagiidae (Cnidaria, Scyphozoa), with new observations of *Chrysaora colorata* comb. nov. *J. Nat. Hist.* (in press).
- Gotshall, D. W. 1994. *Guide to Marine Invertebrates Alaska to Baja California*. Sea Challengers, Monterey, CA.
- Gotshall, D. W., and L. L. Laurent. 1980. *Pacific Coast Subtidal Marine Invertebrates*. Sea Challengers, Los Osos, CA.
- Gotshall, D. W., J. G. Smith, and A. Holbert. 1965. Food of the blue rockfish, *Sebastes mystinus*. *Calif. Fish Game* 51(3): 147–162.
- Greenberg, N., R. L. Garthwaite, and D. C. Potts. 1996. Allozyme and morphological evidence for a newly introduced species of *Aurelia* in San Francisco Bay, California. *Mar. Biol.* 125: 401–410.
- Guberlet, M. L. 1936. *Animals of the Seashore*. Binforde & Mort, Portland, OR.
- Guberlet, M. L. 1949. *Animals of the Seashore*, rev. ed. Binforde & Mort, Portland, OR.
- Guberlet, M. L. 1962. *Animals of the Seashore*, 3rd ed. Binforde & Mort, Portland, OR.

- Haderlie, E. C., C. Hand, and W. B. Gladfelter. 1980. Cnidaria (Coelenterata): The Sea Anemones and Their Allies. Pp. 40–75 in *Intertidal Invertebrates of California*, R. H. Morris, D. P. Abbott, and E. C. Haderlie, eds. Stanford University Press, Stanford, CA.
- Haeckel, E. 1879. *Das System der Medusen: Erster Theil einer Monographie der Medusen*. G. Fischer, Jena.
- Haeckel, E. 1880. *System der Acraspeden: Zweite Hälfte des System der Medusen*. Denkschriften, Jena.
- Hall, C. A. Jr. 1964. Shallow-water marine climates and molluscan provinces. *Ecology* **45**: 226–234.
- Hamner, W. M., and I. R. Hauri. 1981. Long-distance horizontal migrations of zooplankton (Scyphomedusae: *Mastigias*). *Limnol. Oceanogr.* **26**: 414–423.
- Hamner, W. M., and R. M. Jensen. 1974. Growth, degrowth, and irreversible cell differentiation in *Aurelia aurita*. *Am. Zool.* **14**: 833–849.
- Hamner, W. M., P. P. Hamner, and S. W. Strand. 1994. Sun-compass migration by *Aurelia aurita* (Scyphozoa): population retention and reproduction in Saanich Inlet, British Columbia. *Mar. Biol.* **119**: 347–356.
- Hand, C. 1975. Scyphozoa. Pp. 94–96 in *Light's Manual: Intertidal Invertebrates of the Central California Coast*, 3rd ed. R. I. Smith and J. T. Carlton, eds. University of California Press, Berkeley.
- Hartman, O., and K. O. Emery. 1956. Bathypelagic coelenterates. *Limnol. Oceanogr.* **1**: 304–312.
- Hausser, H., and B. Evans. 1978. *The Living World of the Reef*. Walker, New York.
- Hedgpeth, J. W. 1962. *Introduction to Seashore Life of the San Francisco Bay Region and the Coast of Northern California*. University of California Press, Berkeley.
- Hellberg, M. E. 1996. Dependence of gene flow on geographic distance in two solitary corals with different larval dispersal capabilities. *Evolution* **50**(3): 1167–1175.
- Hummelinck, P. W. 1968. Caribbean scyphomedusae of the genus *Casiopea*. *Studies of the Fauna of Curacao and other Caribbean Islands*, No. 97. **25**: 1–57.
- Johnson, M. E., and H. J. Snook. 1927. *Seashore Animals of the Pacific Coast*. Macmillan, New York.
- Johnson, M. E., and H. J. Snook. 1967. *Seashore Animals of the Pacific Coast*. Dover Publications, New York.
- Keen, S. L. 1991. Clonal dynamics and life history evolution in the jellyfish *Aurelia aurita*. Ph.D. dissertation. University of California, Davis.
- Keen, S. L., and A. J. Gong. 1989. Genotype and feeding frequency affect clone formation in a marine cnidarian. *Funct. Ecol.* **3**: 735–745.
- Kirkpatrick, F. Z. S. 1903. Notes on some medusae from Japan. *Annu. Mag. Nat. Hist., Ser. 7* **12**: 615–621.
- Kishinouye, K. 1891. *Aurelia japonica*. *Zool. Mag. (Tokyo)* **3**(33): 289, pl. 7.
- Kishinouye, K. 1910. Some medusae of Japanese waters. *J. Coll. Sci. Tokyo.* **27**: 1–35.
- Knowlton, N. 2000. Molecular genetic analyses of species boundaries in the sea. *Hydrobiologia* **420**: 73–90.
- Kozloff, E. N. 1973. *Seashore Life of Puget Sound, the Strait of Georgia, and the San Juan Archipelago*. University of Washington Press, Seattle.
- Kozloff, E. N. 1974. *Keys to the Marine Invertebrates of Puget Sound, the San Juan Archipelago, and Adjacent Regions*. University of Washington Press, Seattle.
- Kozloff, E. N. 1983. *Seashore Life of the Northern Pacific Coast. An Illustrated Guide to Northern California, Oregon, Washington, and British Columbia*. University of Washington Press, Seattle.
- Kozloff, E. N. 1987. *Marine Invertebrates of the Pacific Northwest*. University of Washington Press, Seattle.
- Kramp, P. L. 1913. Medusae collected by the "Tjalfe" Expedition. *Vidensk. Medd. Dan. Naturhist. Foren.* **65**: 257–286.
- Kramp, P. L. 1942. Medusae: The 'Godthaab' Expedition 1928. *Medd. Gronl. Bd.* **81**(1): 1–168.
- Kramp, P. L. 1961. Synopsis of the medusae of the world. *J. Mar. Biol. Assoc. UK* **40**: 1–469.
- Kramp, P. L. 1965. Some medusae (mainly Scyphomedusae) from Australian coastal waters. *Trans. R. Soc. S. Aust.* **89**: 257–278.
- Kramp, P. L. 1968. The Scyphomedusae collected by the Galathea Expedition 1950–52. *Vidensk. Medd. Dan. Naturhist. Foren.* **131**: 67–98.
- Lalli, C. M., and T. R. Parsons. 1993. *Biological Oceanography: An Introduction*. Butterworth-Heinemann, Oxford.
- Lamarck, 1816. *Histoire naturelle des Animaux sans Vertèbres*. Verdrière, Paris.
- Lambert, F. J. 1935. Observations on the scyphomedusae of the Thames Estuary and their metamorphoses. *Trav. Stat. Zool. Winereux.* **12**: 281–307.
- Larson, R. J. 1976. Marine flora and fauna of the Northeastern United States. Cnidaria: Scyphozoa. *NOAA Tech. Rep. NMFS Circ.* **397**: 1–18.
- Larson, R. J. 1986. Water content, organic content, and carbon and nitrogen composition of medusae from the northeast Pacific. *J. Exp. Mar. Biol. Ecol.* **99**: 107–120.
- Larson, R. J. 1987. Respiration and carbon turnover rates of medusae from the NE Pacific. *Comp. Biochem. Physiol.* **87A**: 93–100.
- Larson, R. J. 1990. Scyphomedusae and cubomedusae from the Eastern Pacific. *Bull. Mar. Sci.* **47**: 546–556.
- Larson, R. J., and A. C. Arneson. 1990. Two medusae new to the coast of California: *Carybdea marsupialis* (Linnaeus, 1758), a cubomedusa and *Phyllorhiza punctata* von Lendenfeld, 1884, a rhizostome scyphomedusa. *Bull. South. Calif. Acad. Sci.* **89**(3): 130–136.
- Lesson, R. P. 1829. *Voyage medical autour du monde execute sur la corvette La Coquille pendant les annees 1822–25*. Zoologie, Paris.
- Lesson, R. P. 1843. *Histoire Naturelle des Zoophytes, Acalèphes*. Librairie encyclopédique de Roret, Paris.
- Light, S. F. 1914a. Another dangerous jellyfish in Philippine waters. *Philipp. J. Sci.* **B9**(3): 291–295.
- Light, S. F. 1914b. Some Philippine Scyphomedusae, including two new genera, five new species, and one new variety. *Philipp. J. Sci.* **9**: 195–231.
- Light, S. F. 1921. Further notes on Philippine scyphomedusan jellyfishes. *Philipp. J. Sci.* **18**: 25–32.
- Light, S. F. 1941. *Laboratory and Field Text in Invertebrate Zoology*. Associated Students Store, University of California, Berkeley.
- Light, S. F., R. I. Smith, F. A. Pitelka, D. P. Abbott, and F. M. Weesner. 1954. *Intertidal Invertebrates of the Central California Coast*. University of California Press, Berkeley.
- Linnaeus, C. 1746. *Fauna svecica, sistens animalia Sveciae regni: Quadrupedia, Aves, Amphibia, Pisces, Insecta, Vernes, distributa per classes & ordines, genera & species, cum differentiis specierum, synonymis autorum, nominibus incolarum, locis habitationum, descriptionibus insectorum*. Sumtu & literis L. Salvii, Stockholm.
- Linnaeus, C. 1758. *Systema Naturae*, 10th ed. Impensis L. Salvii, Holmiae.
- Lucas, C. H., and S. Lawes. 1998. Sexual reproduction of the scyphomedusa *Aurelia aurita* in relation to temperature and variable food supply. *Mar. Biol.* **131**(4): 629–638.
- MacGinitie, G. E. 1955. Distribution and ecology of the marine invertebrates of Point Barrow, Alaska. *Smithson. Misc. Collect.* **128**: 1–201.
- MacGinitie, G. E., and N. MacGinitie. 1949. *Natural History of Marine Animals*. McGraw-Hill, New York.

- MacGinitie, G. E., and N. MacGinitie.** 1968. *Natural History of Marine Animals*, 2nd ed. McGraw-Hill, New York.
- Malmig, A.** 1985. *Where the Waves Break: Life at the Edge of the Sea*. Carolrhoda Books, Minneapolis.
- Mayer, A. G.** 1900. Some medusae from Tortugas, Florida. *Bull. Mus. Comp. Zool. Harvard College* 37(2): 13–82.
- Mayer, A. G.** 1910. *Medusae of the World. Vols. I and II, the Hydromedusae. Vol. 3: The Scyphomedusae*. Carnegie Institution, Washington, DC.
- Mayer, A. G.** 1915. Medusae of the Philippines and of Torres Straits. Being a report on the Scyphomedusae collected by the U.S. Fisheries Bureau steamer 'Albatross' in the Philippine Islands and Malay Archipelago, 1907–1910, and upon the medusae collected by the expedition of the Carnegie Institution of Washington to Torres Straits, Australia, in 1913. *Pap. Tortugas Lab.* 8: 157–202.
- Mayer, A. G.** 1917. Report upon the Scyphomedusae collected by the United States Bureau of Fisheries steamer "Albatross" in the Philippine Islands and Malay Archipelago. *Bull. U. S. Nat. Mus.* 100(1): 175–233.
- McConnaughey, B., and E. McConnaughey.** 1985. *The Audubon Society Guides: Pacific Coast*. Alfred A. Knopf, New York.
- McLachlan, D. H., and J. Ayres.** 1979. *Fieldbook of Pacific Northwest Sea Creatures*. Naturegraph, Happy Camp, CA.
- Mills, C. E.** 1981. Seasonal occurrence of planktonic medusae and ctenophores in the San Juan Archipelago (NE Pacific). *Wasmann J. Biol.* 39: 6–29.
- Naumov, D. V.** 1961. Stsifoidnye meduzy morei S.S.S.R. [Scyphomedusae of the seas of the USSR.] (In Russian). *Opredeliteli po Faune SSSR* 75: 1–98.
- Niesen, T. M.** 1994. *Beachcomber's Guide to California Marine Life*. Gulf Publishing, Houston, TX.
- Niesen, T. M.** 1997. *Beachcomber's Guide to Marine Life of the Pacific Northwest*. Gulf Publishing, Houston, TX.
- Norris, R. D.** 1989. Cnidarian taphonomy and affinities of the Ediacara biota. *Lethaia*, 22: 381–393.
- North, W. J.** 1976. *Underwater California*. University of California Press, Berkeley.
- Nybakken, J. W.** 1993. *Marine Biology: an Ecological Approach*, 3rd ed. HarperCollins, New York.
- O'Donnell, K., E. Cigelnik, and H. I. Nirenburg.** 1998. Molecular systematics and phylogeography of the *Gibberella fujikuroi* species complex. *Mycologia* 90(3): 465–493.
- Parsons, C.** 1986. *Dangerous Marine Animals of the Pacific Coast*. Helm Publishing, San Luis Obispo, CA.
- Pearcy, W. G.** 1972. Distribution and ecology of oceanic animals off Oregon. Pp. 351–377 in *The Columbia River Estuary and Adjacent Ocean Waters*. A. T. Pruter and D. L. Alverson, eds. University of Washington Press, Seattle.
- Pereyra, W. T., and M. S. Alton.** 1972. Distribution and relative abundance of invertebrates off the Northern Oregon Coast. Pp. 444–474 in *The Columbia River Estuary and Adjacent Ocean Waters*. A. T. Pruter and D. L. Alverson, eds. University of Washington Press, Seattle.
- Peron, F., and C. A. Lesueur.** 1810. Tableau des caractères généraux et spécifiques de toutes les espèces de méduses connues jusqu'à ce jour. *Ann. Mus. Hist. Nat. Paris* 14: 325–366.
- Powell, A. W. B.** 1975. *Native Animals of New Zealand*. Auckland Institute and Museum, Auckland.
- Ranson, G.** 1945. Scyphoméduses provenant des Campagnes du Prince Albert Ier de Monaco. *Séries Résultats des campagnes scientifiques. Monaco* 106: 1–92.
- Rees, W. J.** 1957. Proposed validation under the plenary powers of the generic name 'Aurelia' Lamarck 1816 (class Scyphozoa). *Bull. Zool. Nomencl.* 13(1957–1958): 26–28.
- Reish, D. J.** 1972. *Marine Life of Southern California*. Forty-Niner Shops, Long Beach, CA.
- Reish, D. J.** 1995. *Marine Life of Southern California*, 2nd ed. Kendall/Hunt Publishing, Dubuque, IA.
- Ricketts, E. F., and J. Calvin.** 1939. *Between Pacific Tides*. Stanford University Press, Stanford, CA.
- Ricketts, E. F., and J. Calvin.** 1948. *Between Pacific Tides*, rev. ed. Stanford University Press, Stanford, CA.
- Ricketts, E. F., and J. Calvin.** 1952. *Between Pacific Tides*, 3rd ed., revised by Joel W. Hedgpeth. Stanford University Press, Stanford, CA.
- Ricketts, E. F. and J. Calvin.** 1968. *Between Pacific Tides*, 4th ed., revised by Joel W. Hedgpeth. Stanford University Press, Stanford, CA.
- Ricketts, E. F., J. Calvin, and J. Hedgpeth.** 1985. *Between Pacific Tides*, 5th ed., revised by D.W. Phillips. Stanford University Press, Stanford, CA.
- Rigsby, M.** 1997. Open waters. Pp. 178–207 in *Natural History of the Monterey Bay National Marine Sanctuary*. Monterey Bay Aquarium and NOAA, Monterey, CA.
- Roy, K., D. Jablonski, J. W. Valentine, and G. Rosenberg.** 1998. Marine latitudinal diversity gradients: Tests of causal hypotheses. *Proc. Nat. Acad. Sci. USA* 95: 3699–3702.
- Russell, F. S.** 1970. *Medusae of the British Isles. II. Pelagic Scyphozoa with a Supplement to the First Volume on Hydromedusae*. Cambridge University Press, Cambridge.
- Schweizer, N. R.** 1973. *A Poet among Explorers: Chamisso in the South Seas*. Verlag Herbert Lang, Bern.
- Shenker, J. M.** 1984. Scyphomedusae in surface waters near the Oregon coast, May–August, 1981. *Estuarine Coastal Shelf Sci.* 19: 619–632.
- Smith, L.** 1962. *Common Seashore Life of the Pacific Northwest*. Naturegraph, Healdsburg, CA.
- Snively, G.** 1978. *Exploring the Seashore in British Columbia, Washington and Oregon*. Gordon Soules Book Publishers, Vancouver, BC, Canada.
- Steffoff, R.** 1997. *Jellyfish*. Benchmark Books, Tarrytown, NY.
- Stiasny, G.** 1919. Die Scyphomedusen-Sammlung des Naturhistorischen Reichsmuseums in Leiden. II. Stauromedusen. Coronatae, Semaestomae. *Zool. Meded.* 5: 66–98.
- Stiasny, G.** 1922. Papers from Dr. Th. Mortensen's Pacific Expedition 1914–1916. XII. Die Scyphomedusen-sammlung von Dr. Th. Mortensen nebst anderen Medusen aus dem Zoologischen Museum der Universität in Kobenhagen. *Vidensk. Medd. Naturhist. Foren.* 73: 513–558.
- Stiasny, G.** 1926. Über Einige Scyphomedusen von Puerto Galera, Mindoro (Philippinen). *Zool. Meded.* 9: 239–248.
- Stiasny, G.** 1931. Die Rhizostomeen-Sammlung des British Museum (Natural History) in London. *Zool. Meded.* 14: 137–78.
- Stiasny, G.** 1935. Die Scyphomedusen der Snellius expedition. *Verh. K. Akad. Wet. Amst., Sect. 2.* 34(6): 1–44.
- Stiasny, G.** 1937. Biological results of the Snellus Expedition. III. Die fundorte der Scyphomedusen und Tornarien. *Temminckia* 2: 203–210.
- Stiasny, G., and H. van der Maaden.** 1943. Über Scyphomedusen aus dem Ochotskischen und Kamtschatka Meer nebst einer Kritik der Genera *Cyanea* und *Desmonema*. *Zool. Jahrb. (Syst.)* 76(3): 227–266.
- Strand, S. W., and W. M. Hamner.** 1988. Predatory behavior of *Phacellophora camtschatica* and size-selective predation upon *Aurelia aurita* (Scyphozoa: Cnidaria) in Saanich Inlet, British Columbia. *Mar. Biol.* 99: 409–414.
- Strathmann, M. F.** 1987. *Reproduction and Development of Marine Invertebrates of the Northern Pacific Coast*. University of Washington Press, Seattle.
- Thuesen, E. V., and J. J. Childress.** 1994. Oxygen consumption rates and metabolic enzyme activities of oceanic California medusae in relation to body size and habitat depth. *Biol. Bull.* 187: 84–98.
- Tierney, R. J., J. W. Ulmer, L. J. Waxdeck, H. N. Fenster, and J. R. Eckenrood.** 1967. *Exploring Tidal Life Along the Pacific Coast*. Tidepool Associates, Oakland, CA.

- Torrey, H. B. 1909.** The Leptomedusae of the San Diego region. *Univ. Calif. Publ. Zool.* **6**: 11–31.
- Uchida, T. 1928.** Short notes on medusae. I. Medusae with abnormal symmetry. *Annot. Zool. Jpn.* **2**: 373–376.
- Uchida, T. 1934.** A saemostome medusa with some characters of rhizostomae. *Proc. Imp. Acad.* **10**: 698–700.
- Uchida, T., and Z. Nagao. 1963.** The metamorphosis of the Scyphomedusa, *Aurelia limbata* (Brandt). *Annot. Zool. Jpn.* **36**: 83–91.
- Ulmer, J. W. 1968.** *Exploring Our Coast (Seashore Discovery Book 1)*. Oecologica, Tomales, CA.
- Valentine, J. W. 1966.** Numerical analysis of marine molluscan ranges of the extratropical northeastern Pacific shelf. *Limnol. Oceanogr.* **11**: 198–211.
- van der Maaden, H. 1939.** Über das Sinnesgrübchen von *Aurelia aurita* Linné. *Zool. Anz.* **125**: 29–35.
- Vanhöffen, E. 1888.** Untersuchungen ueber Semaestome und Rhizostome Medusen. *Bibl. Zool.* **1**(3): 1–52.
- Vanhöffen, E. 1906.** Acraspedae. *Nordisches Plankton* **6**(11): 40–64.
- von Lendenfeld, R. 1884.** The scyphomedusae of the southern hemisphere. Part III.—Conclusion. IV. Ordo—Discomedusae. *Proc. Linn. Soc. N.S.W.* **9**: 259–306.
- Wells, H. 1942.** *Seashore Life*. California State Department of Education, Sacramento.
- Wrobel, D., and C. Mills. 1998.** *Pacific Coast Pelagic Invertebrates: A Guide to the Common Gelatinous Animals*. Sea Challengers and Monterey Bay Aquarium, Monterey, CA.
- Zubkoff, P. L., and A. L. Lin. 1975.** Isozymes of *Aurelia aurita* scyphistomae obtained from different geographical locations. Pp. 915–930 in *Isozymes. IV. Genetics and Evolution*. C. L. Markert, ed. Academic Press, New York.



**Marine
Biological
Laboratory
Woods Hole
Massachusetts**

One Hundred and Third Report
for the Year 2000
One Hundred and Twelfth Year

Officers of the Corporation

Sheldon J. Segal, *Chairman of the Board of Trustees*
Frederick Bay, *Co-Vice Chair*
Mary J. Greer, *Co-Vice Chair*
John E. Dowling, *President of the Corporation*
John E. Burris, *Director and Chief Executive Officer*
William T. Speck, *Interim Director and Chief Executive Officer*
Mary B. Conrad, *Treasurer*
Robert E. Mainer, *Clerk of the Corporation*

Contents

Report of the Director and CEO	R1
Report of the Treasurer	R6
Financial Statements	R7
Report of the Library Director	R18
Educational Programs	
Summer Courses	R20
Special Topics Courses	R24
Other Programs	R32
Summer Research Programs	
Principal Investigators	R35
Other Research Personnel	R36
Library Readers	R37
Institutions Represented	R38
Year-Round Research Programs	R43
Honors	R57
Board of Trustees and Committees	R64
Administrative Support Staff	R68
Members of the Corporation	
Life Members	R71
Members	R72
Associate Members	R83
Certificate of Organization	R86
Articles of Amendment	R86
Bylaws	R86
Publications	R91

Photo credits:

E. Armstrong—R3 (bottom), R4 (top), R20, R21, R24, R27, R35, R47, R55
K. Begos—R38
D. Buffam—R2 (bottom)
M. Dornblaser—R68
J. Dowling—R30
L. Golder—R64
Gray Museum of the Marine Biological Laboratory—R57
R. Hanlon—R43
R. Howard—R4 (bottom), R18
A. Kuzirian—R6
B. Liles—R71
H. Luther—R23, R46
J. Montgomery—R2 (top)
P. Presley—R1
A. Rader—R86



Report of the Director and Chief Executive Officer

It is with great pleasure that I write this report as the Marine Biological Laboratory's newest Director and Chief Executive Officer. My relationship with the MBL has grown and expanded in rewarding and exciting ways during the past twenty-five years. I am now pleased to have the opportunity to serve as Director of this esteemed Laboratory. I first came to the MBL as a student and then returned as an investigator for several summers. My role expanded when I was elected to the Laboratory's Board of Trustees in 1994, and again when I joined the Discovery Campaign Steering Committee. In 1999, I succeeded Mel Cunningham as Chair of the Development Committee. Since being appointed Interim Director upon John Burris's departure in the summer of 2000, I've had a wonderful opportunity to view the inner workings of this remarkable institution.

I think it's fair to say that the Marine Biological Laboratory is stronger and healthier both financially and programmatically than it has ever been in its history. In this report, I'll review what has led us to this point, share with you some highlights from the year 2000, and discuss where the Trustees and I see the Laboratory going in the next few years.

The Discovery Campaign

The Marine Biological Laboratory concluded its first comprehensive fundraising campaign—Discovery: The Campaign for Science at the Marine Biological Laboratory—in December 2000. Our goal was to raise \$25 million for a variety of initiatives at the MBL. When we began planning for the campaign, some felt that this goal was a stretch for the institution. Thanks to the generosity of thousands of Trustees, Corporation Members, Associates, Alumni, Staff Members, Foundations, and Friends of the Laboratory, the MBL far surpassed that goal, raising more than \$41 million by the end of the year 2000 in support of research, education, the library and physical plant, and the annual fund.

Funds raised through the Discovery Campaign have

already had a major impact on the Laboratory's educational and research programs. One of the most obvious achievements of the Campaign is the construction of the C. V. Starr Environmental Sciences Building, which will become the new home of The Ecosystems Center in 2001. Thanks to the Campaign we also established the Josephine Bay Paul Center for Comparative Molecular Biology and Evolution and hired two new assistant scientists there (Michael Cummings and Jennifer Wernegreen); added five new summer courses and the Semester in Environmental Sciences Program for undergraduates to our education roster; created more than a dozen endowed scholarships for students and endowed fellowships for young researchers; established a program in scientific aquaculture in the Marine Resources Center; endowed the director's chair of the Marine Resources Center; and expanded our public outreach efforts through the creation of the Robert W. Pierce Visitors Center.

In addition, we raised funds to support endowed lectureships for the summer courses and an annual lecture in Bioethics starting in the summer of 2001, and to help shore up the Laboratory's aging physical plant. Moreover, we received gifts to permanently endow the maintenance of the Waterfront Park and the Pierce Visitors Center. Finally, thanks to gifts to the Discovery Campaign, the Library has been air-conditioned and the Crane House on Millfield Street has been refurbished and added to our year-round housing inventory.

Physical Plant

We've also been able to tackle some other long-overdue maintenance projects on campus. For example, the crumbling section of seawall near the Lillie Building has been reconstructed. By the summer of 2001, the Brick Dormitory will have been renovated and furnished for year-round use. Cottages at Memorial Circle have been updated and de-lead, and we have begun renovations at Devils Lane. The research laboratories in the Lillie Building are being renovated to accommodate expanding



year-round research programs in the Bay Paul Center, BioCurrents Research Center, and Architectural Dynamics in Living Cells Program. We've also added fresh paint and carpeting to the Meigs Room, and have begun painting and replacing lighting and other fixtures throughout the Swope Building.

Our plans also include renovating summer research laboratories in the Whitman Building. We expect to begin modestly renovating the Homestead building, which, once vacated by the staff of The Ecosystems Center, will eventually become home to the administrative offices of Financial Services, Education, Human Resources, and *The Biological Bulletin*.

The Biological Bulletin

The Marine Biological Laboratory's journal, *The Biological Bulletin*, celebrated a major milestone in 2000. Edited by Michael J. Greenberg of the University of Florida's Whitney Laboratory, the journal has been publishing peer-reviewed articles of general biological interest for more than 100 years. During the summer of 2001 the journal will launch a new initiative by publishing articles electronically with HighWire Press of Stanford University.

Education

During the summer of 2000, the MBL's Educational Program offered a record 22 summer and special topics courses. Three hundred and thirty-five course directors and faculty members taught 490 advanced graduate and postdoctoral students in the courses last summer. An additional 315 guest lecturers and instructors participated in the courses as well. From all accounts, the quality of our students improves every year.

We offered a symposium on the history of biology and a workshop in microbial diversity designed for middle

and high school teachers. Last summer brought quite a few undergraduates to the MBL as well, through a variety of Research Experience for Undergraduate Programs. One program focused on Marine Models, another was coordinated by the Boston University Marine Program, and others were offered by the Marine Resources and Ecosystems Centers. I'm pleased to report that funding has been allocated for two additional research programs for undergraduates beginning in summer 2001.

The MBL's own semester-long undergraduate program, The Semester in Environmental Sciences, offered by the staff of The Ecosystems Center, completed its 3rd year in 2000 with 15 students participating. The consortium of colleges whose students come for the fall semester continues to grow, currently numbering more than 40 members.

Research

The summer research program ran at full capacity during the summer of 2000. One hundred and thirty-two investigators used all of our available lab space. In fact, one applicant had to set up his research in a dark room. The majority of the investigators (60%) were professors/ chief scientists, followed by associate professors (20%) and postdoctoral fellows (10%). The balance was comprised of assistant scientists and graduate students.

I'm proud to report that for the second year in a row an MBL Summer Scientist—Avram Hershko of the Technion in Israel—has won the prestigious Lasker Award (Clay Armstrong won this award in 1999). This award is second only to the Nobel Prize in significance in science. Dr. Hershko will deliver a Friday Evening Lecture during the summer of 2001. I'm also pleased to be able to count two of the year 2000's Nobel Prize winners as members of the MBL family: Paul Greengard of Rockefeller University, an alumnus of the Embryology Course and a former faculty member of the Neurobiology Course, and Eric Kandel of Columbia, a past MBL





investigator and Corporation Member. These awards validate the tremendous significance and impact the MBL's research and educational programs have on the biology community at large.

The MBL's research fellowship program hosted 21 investigators during the summer of 2000. The range of the research being undertaken by these scientists was remarkable, and the caliber of their backgrounds scored high by the Fellowship Committee and our external advisors. The Science Writing Fellowship Program also continued to figure prominently among print and broadcast journalists for the outstanding opportunity it affords them to work alongside scientists to learn about the process of doing science.

The Ecosystems Center

Research is and will always be a key mission of the MBL. We have seen a continued growth in our resident research programs. The Ecosystems Center, directed by Jerry Melillo and John Hobbie, now numbers more than 60 staff, and its funding base has more than doubled during the past 5 years. It is now in excess of \$7 million. Thirty research projects are underway around the globe, from Siberia to Martha's Vineyard. In 2000 The Ecosystems Center celebrated its 25th anniversary with a weekend-long celebration. The festivities included an open house, a one-day symposium complete with a visit by Rep. William Delahunt of the Massachusetts 10th District, and a reunion clambake at the Swope Center. More than 50 Ecosystems Center alumni from all over the world traveled to Woods Hole to celebrate the success of the Center's first 25 years and to discuss the future of ecosystems science.

The Josephine Bay Paul Center

The Bay Paul Center for Comparative Molecular Biology and Evolution, under Mitch Sogin's direction,

currently has 33 scientists and support staff. The Center's project to sequence the genome of the parasite *Giardia* is nearly complete.

For the first time, the MBL has received a prestigious gift from the Keck Foundation. This \$1 million award will establish the W. M. Keck Ecological and Evolutionary Genetics Facility at the Bay Paul Center. Microbial ecologists, molecular evolutionists, and genome scientists from the Bay Paul Center, The Ecosystems Center, and other scientific groups within the Woods Hole community will form a coalition to study how the genes of millions of microbes work together to influence biogeochemical processes within ecosystems.

The BioCurrents Research Center

The NIH BioCurrents Research Center, directed by Peter Smith, has increased in size and now numbers 11 scientists, thanks to the recent addition of Drs. Orian Shirihai and Stefan McDonough to the scientific staff. Among their many research projects, Smith and his colleagues continue to collaborate with Dr. Barbara Corkey of Boston Medical Center on the study of how cells process insulin. They are currently fine tuning instruments that will enable them to monitor the movement and release of glucose, insulin, and calcium within pancreatic beta cells, the goal being to learn more about how diabetes type II works at a cellular level. Another exciting collaboration is underway between the BioCurrents Research Center and the Bay Paul Center to study the evolution, diversity, and physiology of organisms living in extreme environments—like the hot vents of the deep oceans and extremely acidic (battery acid-like) ecosystems.

The Marine Resources Center

Research using DNA fingerprinting to assess paternity and reproductive patterns and population structure in the





local squid fishery—valued at \$33 million annually—continues in the Marine Resources Center (MRC), under the direction of Roger Hanlon. Work on how polarized vision is used by the squid to help detect prey is also a focal point. During the Campaign, a landmark gift from Honorary Trustee Ellen Grass established the first endowed Directorship at the MBL. This gift, the grant from the Schooner Foundation to establish the Program in Scientific Aquaculture, and a recent anonymous grant of \$500,000 ensures future vitality for the MRC. The MRC is also currently in the process of hiring three faculty-level scientists and a scientific aquaculturist.

I've only touched on a few of the MBL's resident research initiatives. In addition to these research centers, the MBL is home to a score of investigators' research programs that focus on a range of topics including infertility, microscopy, learning and memory, and the effects of lead poisoning on children.

The Library

The MBL/WHOI Library continues to expand both its print and electronic serial collections. More than 2000 full-text electronic journals are now available on our scientists' desktops through the Library's web site. The entire collection has grown to more than 200,000 volumes, occupying all the space the Library has available in Woods Hole. Storage issues are currently being addressed by providing more electronic access to journals and by sending some volumes off campus to the Harvard Depository.

Looking Ahead

It's an exciting time for the Marine Biological Laboratory. Now more than ever, the Trustees are committed to building and strengthening the MBL's year-round research program. Within the next year, the

Trustees will start developing a 5- to 10-year strategic plan—a map charting the direction that the Laboratory will take in both research and education in the coming years. This plan will further strengthen and position the Laboratory to serve science and society.

As we continue to build the year-round research programs, plans have been developed to add a new year-round research program in Global Infectious Diseases and Parasitism. Parasites cause debilitating and often lethal diseases in billions of people around the world. The World Health Organization estimates that one in ten are infected by one or more of the five major parasitic diseases: schistosomiasis, filariasis, malaria, trypanosomiasis, and leishmaniasis. The MBL is already a leader in the field of parasitology and infectious disease, hosting two major international parasitology meetings and offering a world-renowned course in the Biology of Parasitism each summer. This new program will build on the Laboratory's existing strengths in this field and take advantage of the high throughput technologies and scientific expertise available in the Bay Paul Center, creating a one-of-a-kind research environment that fosters interactions between parasitologists and experts in molecular biology, phylogenetics, and environmental microbiology. The Trustees agree that this is a strong and important addition to the MBL's year-round research portfolio.

On the education side, Mitch Sogin and Clare Fraser, one of our newest Trustees, are planning to offer an exciting and novel course in genomics. This course will premiere in Fall 2002. We hope to offer more and more cutting-edge courses throughout the year in the future.

Trustees

The Trustees elected four new Board members and reappointed one Trustee to the Class of 2005 at their November 4, 2000 meeting. Dr. Porter W. Anderson, who completed his first term on the Board this year, was



appointed to a second term. He is joined by Dr. Claire M. Fraser, President and Director of The Institute for Genomic Research in Maryland; Mr. George Logan, Chairman of the Board and Organizer of the Valley Financial Corporation as well as Principal of the Wood Park Capital Corporation in Roanoke, VA; Robert A. Prendergast, Professor of Ophthalmology and Associate Professor of Pathology at The Wilmer Institute at The Johns Hopkins University School of Medicine, Baltimore, MD; and John W. Rowe, M.D., President and CEO of Aetna Inc. Thomas S. Crane, Coordinator of Mintz Levin Cohn Ferris Glovsky and Popeo's Health Care Fraud and Abuse and Corporate Compliance practice group serving the firm's Boston and Washington, DC, offices, was elected Clerk of the Corporation.

Sheldon Segal, John Dowling, and Mary B. Conrad were reelected to serve as Chairman of the Board, President of the Corporation, and Treasurer, respectively. Trustee Al Zeien was elected Vice Chair of the Board. The Board also thanked retiring members Fred Bay, Marty Cox, Mary Greer, William Steere, and Gerald Weissmann for their tireless efforts on behalf of the Laboratory.

In Memoriam

As this report was going to press, we were saddened to learn of the tragic deaths of Jim and Alma Ebert, who were killed on May 22, 2001, in a car accident while traveling from Baltimore to Woods Hole for the summer. Jim was President of the MBL Corporation from 1970 to 1978 and again from 1990 to 1998. He was Director of the Laboratory from 1970 to 1978, a Trustee from 1964 to 1968, and was named Director Emeritus in 2000. Alma was active in the MBL Associates, volunteering her time and energy on behalf of the Laboratory, and supporting Jim during his tenure as Director.

For five decades the MBL has benefited from Jim's considerable knowledge and experience. He was instrumental in bringing significant funding to the Laboratory, and his guidance and insight were key to the MBL's success. The loss of these dear friends will be deeply felt by the MBL family for many years.

—William T. Speck



Report of the Treasurer

The Marine Biological Laboratory had another impressive operating year in 2000 that was partially offset by weak near-term investment portfolio returns. Auspicious growth in Operating Support and the decline in the Equity Markets were the major contributors to the mixed results.

Three areas of Operating Support showed double-digit increases. The growth in Government Grants accelerated to 14.7% over 1999 results and represented an all-time high of 45.2% of Total Operating Support. Fees for Conferences and Services grew even faster, up 17.1%. Short-term Investment Income also grew by 13.1% as a result of stronger interest rate returns on a larger portfolio of Cash & Cash Equivalents, Short-Term Investments, and the Assets Held by the Bond Trustee. This had a very favorable impact, particularly on the Change in Unrestricted Net Assets from Operations. It increased from only \$138 thousand in 1999 to \$1.3 million in 2000. This represented a very strong 9.5% Operating Margin.

Reviewing our Non-Operating Activities, we expanded our Investment in Plant to \$4.64 million, more than doubling what was done in 1999. Total Contributions, again, exceeded \$10 million in the final year of our Discovery Campaign with almost 45% going toward Plant improvements. On the other hand, MBL experienced \$2.1 million, or 3.9%, in realized and unrealized investment losses. We also utilized \$1.4 million from our standard spending rate draw. This impacted our Long-term Investment portfolio, which fell slightly in value for the first time since 1994.

Even with this, MBL reported a \$3.2 million Total Change in Net Assets. This represented the sixth year of positive change, but represented only a 4.3% Return on Average Net Assets.

MBL's 2000 Balance Sheet experienced some significant changes from 1999. Assets grew by over \$11 million due to double-digit growth of 16.4% in Net Plant Assets, increased liquidity, and added Assets held by the Bond Trustee, which was a result of the \$10.2 million Variable Rate Revenue Bonds issued March 8, 2000. The Bond refinanced \$2.3 million of higher cost debt, with the balance of the proceeds being used to make capital improvements to MBL's educational, research, and housing facilities. Even with this increased debt, MBL has a sound Leverage Ratio (Unrestricted and Temporarily Restricted Net Assets-to-Debt) of 5.26 \times at year-end 2000. Also note our strong operational returns resulted in an improved Debt Coverage Ratio of 11.6 \times over previous years. One last positive sign to note is a \$3 million increase in the Laboratory's Unrestricted Net Assets.

In summary, the Laboratory completed an effective leverage of its financial strength, closed a very successful fundraising campaign, and demonstrated strong operational returns. This more than offset the marginal decline in portfolio performance, and we remain well poised to continue our capital improvement efforts.

—Mary B. Conrad



PricewaterhouseCoopers LLP
One International Place
Boston, MA 02110
Telephone (617) 478 5000
Facsimile (617) 478 3900

REPORT OF INDEPENDENT ACCOUNTANTS

To the Board of Trustees of
Marine Biological Laboratory:

In our opinion, the accompanying balance sheet of Marine Biological Laboratory (the "Laboratory") at December 31, 2000 and the related statements of activities and of cash flows for the year then ended present fairly, in all material respects, the financial position of the Laboratory as of December 31, 2000, and the changes in its net assets and its cash flows for the year then ended in conformity with accounting principles generally accepted in the United States of America. These financial statements are the responsibility of the Laboratory's management; our responsibility is to express an opinion on these financial statements based on our audit. The prior year summarized comparative information has been derived from the Laboratory's 1999 financial statements, and in our report dated April 7, 2000, we expressed an unqualified opinion on those financial statements. We conducted our audit in accordance with auditing standards generally accepted in the United States of America. Those standards require that we plan and perform the audit to obtain reasonable assurance about whether the financial statements are free of material misstatement. An audit includes examining, on a test basis, evidence supporting the amounts and disclosures in the financial statements. An audit also includes assessing the accounting principles used and significant estimates made by management, as well as evaluating the overall financial statement presentation. We believe that our audit provides a reasonable basis for our opinion.

Our audit was conducted for the purpose of forming an opinion on the basic financial statements taken as a whole. The supplemental schedule of functional expenses as of December 31, 2000 is presented for the purpose of additional analysis and is not a required part of the basic financial statements. Such information has been subjected to the auditing procedures applied in the audit of the basic financial statements and, in our opinion, is fairly stated, in all material respects, in relation to the basic financial statements taken as a whole.

April 6, 2001

MARINE BIOLOGICAL LABORATORY

BALANCE SHEET

As of December 31, 2000

(With Comparative Totals as of December 31, 1999)

ASSETS	<u>2000</u>	<u>1999</u>
Cash and cash equivalents	\$ 3,583,033	\$ 1,942,285
Short-term investments, at market	3,599,833	3,182,537
Accounts receivable, net of allowance for doubtful accounts of \$47,222 in 2000 and \$59,978 in 1999	1,109,706	1,158,073
Current portion of pledges receivable	5,026,750	3,974,385
Receivables due for costs incurred on grants and contracts	2,036,734	1,380,766
Other current assets	<u>352,983</u>	<u>306,518</u>
Total current assets	<u>15,709,039</u>	<u>11,944,564</u>
Assets held by bond trustee	5,423,615	—
Long-term investments, at market	44,494,649	45,001,493
Pledges receivable, net of current portion	2,433,292	3,498,787
Plant assets, net	23,423,156	20,118,725
Other assets	<u>206,280</u>	<u>—</u>
Total long-term assets	<u>76,180,922</u>	<u>68,619,005</u>
Total assets	<u>\$ 91,690,031</u>	<u>\$ 80,563,569</u>
LIABILITIES AND NET ASSETS		
Current portion of long-term debt	\$ —	\$ 267,404
Accounts payable and accrued expenses	2,073,375	1,957,508
Deferred income and advances on contracts	<u>1,016,060</u>	<u>656,745</u>
Total current liabilities	<u>3,089,435</u>	<u>2,881,657</u>
Annuities and unitrusts payable	1,393,735	1,460,948
Long-term debt, net of current portion	10,200,000	2,056,692
Advances on contracts	<u>1,230,743</u>	<u>1,574,758</u>
Total long-term liabilities	<u>12,824,478</u>	<u>5,092,398</u>
Total liabilities	<u>15,913,913</u>	<u>7,974,055</u>
Commitments and contingencies		
Net assets:		
Unrestricted	22,903,287	19,887,437
Temporarily restricted	30,752,413	33,349,244
Permanently restricted	<u>22,120,418</u>	<u>19,352,833</u>
Total net assets	<u>75,776,118</u>	<u>72,589,514</u>
Total liabilities and net assets	<u>\$ 91,690,031</u>	<u>\$ 80,563,569</u>

The accompanying notes are an integral part of the financial statements.

MARINE BIOLOGICAL LABORATORY

STATEMENT OF ACTIVITIES

For the Year Ended December 31, 2000

(With Comparative Totals for the Year Ended December 31, 1999)

	<u>Unrestricted</u>	<u>Temporarily Restricted</u>	<u>Permanently Restricted</u>	<u>2000</u>	<u>1999</u>
Operating support and revenues:					
Government grants	\$14,048,464	\$ —	\$ —	\$14,048,464	\$12,248,442
Private contracts	1,697,062	—	—	1,697,062	1,819,240
Laboratory rental income	1,598,373	—	—	1,598,373	1,548,168
Tuition, net	543,305	—	—	543,305	537,835
Fees for conferences and services	4,407,311	—	—	4,407,311	3,765,039
Contributions	1,693,185	2,347,731	1,908,528	5,949,444	8,620,519
Investment income	1,736,186	594,530	—	2,330,716	2,060,478
Miscellaneous revenue	468,482	—	—	468,482	466,903
Present value adjustment to annuities	—	55,176	—	55,176	(30,533)
Net assets released from restrictions	4,144,547	(4,249,547)	105,000	—	—
Total operating support and revenues	<u>30,336,915</u>	<u>(1,252,110)</u>	<u>2,013,528</u>	<u>31,098,333</u>	<u>31,036,091</u>
Expenses:					
Research	17,799,627	—	—	17,799,627	14,147,645
Instruction	5,626,223	—	—	5,626,223	4,742,287
Conferences and services	1,307,458	—	—	1,307,458	2,252,842
Other programs (Note 2)	4,261,327	—	—	4,261,327	5,297,773
Total expenses	<u>28,994,635</u>	<u>—</u>	<u>—</u>	<u>28,994,635</u>	<u>26,440,547</u>
Change in net assets before nonoperating activity	<u>1,342,280</u>	<u>(1,252,110)</u>	<u>2,013,528</u>	<u>2,103,698</u>	<u>4,595,544</u>
Nonoperating revenue:					
Contribution to Plant:					
Private	404,018	4,109,597	125,000	4,638,615	1,757,319
Government	—	—	—	—	198,443
Release from restriction	1,615,142	(1,615,142)	—	—	—
Invested in Plant	<u>2,019,160</u>	<u>2,494,455</u>	<u>125,000</u>	<u>4,638,615</u>	<u>1,955,762</u>
Total investment income and gains/losses	(284,514)	(2,484,381)	629,057	(2,139,838)	5,938,476
Less: investment earnings used for operations	(61,076)	(1,354,795)	—	(1,415,871)	(1,262,020)
Reinvested (utilized) investment income and gains/losses	<u>(345,590)</u>	<u>(3,839,176)</u>	<u>629,057</u>	<u>(3,555,709)</u>	<u>4,676,456</u>
Total change in net assets	<u>3,015,850</u>	<u>(2,596,831)</u>	<u>2,767,585</u>	<u>3,186,604</u>	<u>11,227,762</u>
Net assets, beginning of year	<u>19,887,437</u>	<u>33,349,244</u>	<u>19,352,833</u>	<u>72,589,514</u>	<u>61,361,752</u>
Net assets, end of year	<u>\$22,903,287</u>	<u>\$30,752,413</u>	<u>\$22,120,418</u>	<u>\$75,776,118</u>	<u>\$72,589,514</u>

The accompanying notes are an integral part of the financial statements.

MARINE BIOLOGICAL LABORATORY

STATEMENT OF CASH FLOWS

For the Year Ended December 31, 2000

(With Comparative Totals for the Year Ended December 31, 1999)

	<u>2000</u>	<u>1999</u>
Cash flows from operating activities:		
Change in net assets	\$3,186,604	\$11,227,762
Adjustments to reconcile change in net assets to net cash provided by (used in) operating activities:		
Depreciation and amortization	1,791,975	1,562,487
Unrealized (appreciation) depreciation on investments	6,700,396	(3,544,380)
Realized gain on investments	(3,886,669)	(1,639,795)
Present value adjustment to annuities and unitrusts payable	(55,176)	30,533
Contributions restricted for long-term investment and annuities	(2,033,528)	(2,485,624)
Provision for bad debt	—	36,968
Provision for uncollectible pledges	423,982	—
Change in certain balance sheet accounts:		
Accounts receivable	48,367	47,489
Pledges receivable	(410,852)	(3,010,156)
Grants and contracts receivable	(655,968)	150,317
Other current assets and other assets	(252,745)	251,390
Accounts payable and accrued expenses	115,867	(100,233)
Deferred income	359,315	193,872
Annuities and unitrusts payable	(73,167)	68,112
Advances on contracts	(344,015)	302,368
Net cash provided by operating activities	<u>4,914,386</u>	<u>3,091,110</u>
Cash flows from investing activities:		
Purchase of property and equipment	(5,096,406)	(2,145,041)
Proceeds from sale of investments	68,837,634	63,101,047
Purchase of investments	(76,930,252)	(65,485,238)
Net cash used in investing activities	<u>(13,189,024)</u>	<u>(4,529,232)</u>
Cash flows from financing activities:		
Payments on annuities and unitrusts payable	(96,316)	(49,897)
Receipt of permanently restricted gifts	2,033,528	2,438,148
Annuity and unitrusts donations received	102,270	47,476
Bond issuance	10,200,000	—
Payments on long-term debt	(2,324,096)	(243,274)
Net cash provided by financing activities	<u>9,915,386</u>	<u>2,192,453</u>
Net increase in cash and cash equivalents	1,640,748	754,331
Cash and cash equivalents at beginning of year	<u>1,942,285</u>	<u>1,187,954</u>
Cash and cash equivalents at end of year	<u>\$3,583,033</u>	<u>\$1,942,285</u>

The accompanying notes are an integral part of the financial statements.

Marine Biological Laboratory

Notes to Financial Statements

1. Background

The Marine Biological Laboratory (the "Laboratory") is a private, independent not-for-profit research and educational institution dedicated to establishing and maintaining a laboratory and station for scientific study and investigation, and a school for instruction in biology and natural history. The Laboratory was founded in 1888 and is located in Woods Hole, Massachusetts.

2. Significant Accounting Policies

Basis of Presentation

The accompanying financial statements have been prepared on the accrual basis of accounting and in accordance with the principles outlined in the American Institute of Certified Public Accountants' Audit Guide, "Not-For-Profit Organizations." The financial statements include certain prior-year summarized comparative information in total but not by net asset class. Such information does not include sufficient detail to constitute a presentation in conformity with generally accepted accounting principles. Accordingly, such information should be read in conjunction with the Laboratory's financial statements for the year ended December 31, 1999, from which the summarized information was derived.

The Laboratory classifies net assets, revenues, and realized and unrealized gains and losses based on the existence or absence of donor-imposed restrictions and legal restrictions imposed under Massachusetts State law. Accordingly, net assets and changes therein are classified as follows:

Unrestricted

Unrestricted net assets are not subject to donor-imposed restrictions of a more specific nature than the furtherance of the Laboratory's mission. Revenues from sources other than contributions are generally reported as increases in unrestricted net assets. Expenses are reported as decreases in unrestricted net assets. Gains and losses on investments and other assets or liabilities are reported as increases or decreases in unrestricted net assets unless their use is restricted by explicit donor stipulations or law. Expirations of temporary restrictions on net assets, that is, the donor-imposed stipulated purpose has been accomplished and/or the stipulated time period has elapsed, are reported as reclassifications between the applicable classes of net assets and titled "Net assets released from restrictions."

Temporarily Restricted

Temporarily restricted net assets are subject to legal or donor-imposed stipulations that will be satisfied either by the actions of the Laboratory, the passage of time, or both. These assets include contributions for which the specific, donor-imposed restrictions have not been met and pledges, annuities, and unitrusts for which the ultimate purpose of the proceeds is not permanently restricted. As the restrictions are met, the assets are released to unrestricted net assets. Also, realized/unrealized gains/losses associated with permanently restricted gifts which are not required to be added to principal by the donor are classified as temporarily restricted and maintain the donor requirements for expenditure.

Permanently Restricted

Permanently restricted net assets are subject to donor-imposed stipulations that they be invested to provide a permanent source of income to the Laboratory. These assets include contributions, pledges and trusts which require that the corpus be invested in perpetuity and only the income be made available for program operations in accordance with donor restrictions.

Performance Indicator

Nonoperating revenues include realized and unrealized gains on investments during the year as well as investment income on the master pooled investments and revenues that are specifically for the acquisition or construction of plant assets. Investment income from short-term investments and investments held in trust by others are included in operating support and revenues. To the extent that nonoperating investment income and gains are used for operations as determined by the Laboratory's total return utilization policy (see below), they are reclassified from nonoperating as "Investment earnings used for operations" to operating as "Investment income" on the statement of activities. All other activity is classified as operating revenue.

Cash and Cash Equivalents

Cash equivalents consist of resources invested in overnight repurchase agreements and other highly liquid investments with original maturities of three months or less.

Financial instruments which potentially subject the Laboratory to concentrations of risk consist primarily of cash and investments. The Laboratory maintains cash accounts with one banking institution.

Investments

Investments purchased by the Laboratory are carried at market value. Donated investments are recorded at fair market value at the date of the gift. For closely held non-publicly traded investments, management determines the fair value based upon the most recent information available from the limited partnership. For determination of gain or loss upon disposal of investments, cost is determined based on the first-in, first-out method.

Investments with an original maturity of three months to one year, or those that are available for operations within the next fiscal year, are classified as short-term. All other investments are considered long-term. Investments are maintained primarily with three institutions.

In 1924, the Laboratory became the beneficiary of certain investments, included in permanently restricted net assets, which are held in trust by others. The Laboratory has the continuing rights to the income produced by these funds in perpetuity, subject to the contractual restrictions on the use of such funds. Accordingly, the trust has established a process to conduct a review every ten years by an independent committee to ensure the Laboratory continues to perform valuable services in biological research in accordance with the restrictions placed on the funds by the agreement. The committee met in 1994 and determined that the Laboratory has continued to meet the contractual requirements. The market values of such investments are \$7,904,545 and \$7,275,488 at December 31, 2000 and 1999, respectively. The dividend and interest income on these investments, included in unrestricted support and revenues, totaled \$201,407 and \$221,882 in 2000 and 1999, respectively.

Investment Income and Distribution

For the master pooled investments, the Laboratory employs a total return utilization policy that establishes the amount of the investment return made available for spending each year. The Finance Committee of the Board of Trustees has approved a spending policy that the withdrawal will be based on a percentage of the 12 quarter average ending market values of the funds. The market value includes the principal plus reinvested income, realized and unrealized gains and losses. Spending rates in excess of 5%, but not exceeding 7%, can be utilized if approved in advance by the Finance Committee of the Board of Trustees. For fiscal 2000 and 1999, the Laboratory obtained approval to expend 6% of the latest 12 quarter average ending market values of the investments.

The net appreciation on permanently and temporarily restricted net assets is reported together with temporarily restricted net assets until such time as all or a portion of the appreciation is distributed for spending in accordance with the total return utilization policy and applicable state law.

Investment income on the pooled investment account is allocated to the participating funds using the market value unit method (Note 4).

Assets Held by Bond Trustee

Assets held by bond trustee relate to assets held by an outside trustee under the March 1, 2000 loan and trust agreement. Per the prospectus, these funds may be used solely for capital projects as determined by the Laboratory's Board of Directors. At December 31, 2000, these assets were invested in a qualified GIC under a funding agreement with an insurance company.

Plant Assets

Buildings and equipment are recorded at cost. Donated facility assets are recorded at fair market value at the date of the gift. Depreciation is computed using the straight-line method over the asset's estimated useful life. Estimated useful lives are generally three to five years for equipment and 20 to 40 years for buildings and improvements. Depreciation is not recorded for those assets classified as construction-in-process as they have not yet been placed into service. Depreciation expense for the years ended December 31, 2000 and 1999 amounted to \$1,791,975 and \$1,562,487, respectively, and has been recorded in the statement of activities in the appropriate functionalized categories. When assets are sold or retired, the cost and accumulated depreciation are removed from the accounts and any resulting gain or loss is included in unrestricted income for the period.

Annuities and Unitrusts Payable

Amounts due to donors in connection with gift annuities and unitrusts are determined based on remainder value calculations, with varied assumptions of rates of return and payout terms.

Deferred Income and Advances on Contracts

Deferred income includes prepayments received on Laboratory publications and advances on contracts to be spent within the next year. Advances on contracts includes funding received for grants and contracts before it is earned. Long-term advances are invested in the master pooled account until they are expended.

Revenue Recognition

Sources of revenue include grant payments from governmental agencies, contracts from private organizations, and income from the rental of laboratories and classrooms for research and educational programs. The Laboratory recognizes revenue associated with grants and contracts at the time the related direct costs are incurred or expended. Recovery of related indirect costs is recorded at predetermined fixed rates negotiated with the government. Revenue related to conferences and services is recognized at the time the service is provided, while tuition revenue is recognized as classes are offered. The tuition income is net of student financial aid of \$579,790 and \$527,258 in 2000 and 1999, respectively. Fees for conferences and other services include the following activities: housing, dining, library, scientific journals, aquatic resources and research services.

Contributions

Contribution revenue includes gifts and pledges. Gifts are recognized as revenue upon receipt. Pledges are recognized as temporarily or permanently restricted revenue in the year pledged and are recorded at the present value of expected future cash flows, net of allowance for unfulfilled pledges. Gifts and pledges, other than cash, are recorded at fair market value at the date of contribution.

Expenses

Expenses are recognized when incurred and charged to the functions to which they are directly related. Expenses that relate to more than one function are allocated among functions based upon either modified total direct cost or square footage allocations.

Other programs expense consists primarily of fundraising, year-round labs and library room rentals, costs associated with aquatic resource sales and scientific journals. Total fundraising expense for 2000 and 1999 is \$1,156,656 and \$1,008,920, respectively.

Use of Estimates

The preparation of financial statements in conformity with generally accepted accounting principles requires management to make estimates and assumptions that affect the reported amounts of assets and liabilities and disclosure of contingent assets and liabilities at the date of financial statements and the reported amounts of revenues and expenses during the reporting period. Actual results could differ from those estimates.

Tax-Exempt Status

The Laboratory is exempt from federal income tax under Section 501(c)(3) of the Internal Revenue Code.

Reclassification

Certain prior year balances have been reclassified to conform with the current year presentation.

3. *Investments*

The following is a summary of the cost and market value of investments at December 31, 2000 and 1999:

	<u>Market</u>		<u>Cost</u>	
	<u>2000</u>	<u>1999</u>	<u>2000</u>	<u>1999</u>
Certificates of deposit	\$ 40,000	\$ 40,000	\$ 40,000	\$ 40,000
Money market securities	764,969	1,781,128	764,969	1,781,128
U.S. Government securities	2,300,738	69,125	2,165,197	69,951
Corporate fixed income	2,412,548	2,364,068	2,537,913	2,536,808
Common stocks	16,144,089	15,665,205	16,318,538	10,608,588
Mutual funds	19,909,549	26,664,204	19,306,250	23,851,004
Limited partnerships	6,522,589	1,600,300	5,324,442	958,982
Total investments	<u>\$ 48,094,482</u>	<u>\$ 48,184,030</u>	<u>\$ 46,457,309</u>	<u>\$ 39,846,461</u>

Investment portfolios for the years ended December 31, 2000 and 1999 are as follows:

	<u>Market</u>		<u>Cost</u>	
	<u>2000</u>	<u>1999</u>	<u>2000</u>	<u>1999</u>
<i>Short-Term Investments</i>				
Certificates of deposit	\$ 40,000	\$ 40,000	\$ 40,000	\$ 40,000
Money market	377,654	233,938	377,654	233,938
Mutual funds	3,102,515	2,875,480	3,085,445	2,965,273
Common stocks in transit	79,664	33,119	79,664	33,119
Total short term	\$3,599,833	\$3,182,537	\$3,648,491	\$3,272,330
<i>Long-Term Investments</i>				
Pooled investments:				
Master pooled investments	\$34,116,704	\$35,354,938	\$33,153,390	\$27,514,505
Separately invested:				
General Chase Trust	6,204,107	5,717,108	5,654,623	5,335,721
Library Chase Trust	1,700,438	1,558,380	1,543,691	1,448,569
Annuity and unitrusts investments	2,473,400	2,371,067	2,522,842	2,275,336
Total long term	<u>44,494,649</u>	<u>45,001,493</u>	<u>42,874,546</u>	<u>36,574,131</u>
Total investments	<u>\$48,094,482</u>	<u>\$48,184,030</u>	<u>\$46,457,309</u>	<u>\$39,846,461</u>

R14 Annual Report

For the years ended December 31, 2000 and 1999, the Laboratory recorded net realized gains of \$3,886,669 and \$1,639,795; net unrealized losses (gains) of \$6,700,396 and \$(3,544,380); and dividend and interest income of \$1,588,734 and \$1,533,579, respectively.

4. Accounting for Pooled Investments

Certain net assets are pooled for investment purposes. Investment income from the pooled investment account is allocated on the market value unit basis, and each fund subscribes to or disposes of units on the basis of the market value per unit at the beginning of the calendar quarter within which the transaction takes place. The unit participation of the funds at December 31, 2000 and 1999 is as follows:

	<u>2000</u>	<u>1999</u>
Unrestricted	11,290	8,573
Temporarily restricted	40,042	42,351
Permanently restricted	73,724	65,789
Advances on contracts	5,396	5,557
	<u>130,452</u>	<u>122,270</u>

Pooled investment activity on a per-unit basis was as follows:

	<u>2000</u>	<u>1999</u>
Unit value at beginning of year	\$ 283.37	\$ 225.51
Unit value at end of year	<u>261.53</u>	<u>283.37</u>
Total return on pooled investments	<u>\$ (21.84)</u>	<u>\$ 57.86</u>

5. Long-Term Debt

Long-term debt consisted of the following at December 31:

	<u>2000</u>	<u>1999</u>
Variable rate (6.3% at December 31, 1999) Massachusetts Industrial Finance Authority Series 1992A Bonds payable in annual installments through 2012	\$ —	\$ 890,000
6.63% Massachusetts Industrial Finance Authority Series 1992B Bonds, payable in annual installments through 2012	—	1,175,000
5.8% The University Financing Foundation, Inc. payable in monthly installments through 2000	—	120,929
5.8% The University Financing Foundation, Inc. payable in monthly installments through 2002	—	138,167
Variable rate (4.75%) Massachusetts Development Finance Agency Bonds payable in annual installments from 2006 through 2030	10,200,000	—
	<u>\$ 10,200,000</u>	<u>\$ 2,324,096</u>

In March 2000, the Massachusetts Development Finance Agency issued on behalf of the Laboratory a series of Variable Rate Revenue Bonds (the "Bonds") in the amount of \$10,200,000. The initial interest rate on the issue was 3.65% and is reset weekly. At December 31, 2000, the rate was 4.75%. The bonds are scheduled to mature on February 1, 2030. The Laboratory is required to make interest payments only for the first five years. The first principal payment is due February 1, 2006 with incremental increases through maturity. The proceeds of these bonds were used to finance the capital improvements of the Laboratory's educational, research, and administrative facilities, specifically the construction and equipping of the Environmental Sciences building. A portion of the proceeds was also used to extinguish all of the Laboratory's prior debt obligations.

As collateral for the bonds, the Laboratory has entered into a Letter of Credit Reimbursement Agreement which is set to expire on March 15, 2007. The Letter of Credit is in an amount sufficient to pay the aggregate principal amount of the bonds and up to 46 days' interest.

The agreements related to these bonds subject the Laboratory to certain covenants and restrictions. Under the most restrictive covenant of this debt, the Laboratory is required to maintain a debt service coverage ratio.

In 1992, the Laboratory issued \$1,100,000 Massachusetts Industrial Finance Authority (MIFA) Series 1992A Bonds with a variable interest rate and \$1,500,000 MIFA Series 1992B with an interest rate of 6.63%. Interest expense totaled \$33,201 for the year ended December 31, 2000. The Series 1992 A and B Bonds were scheduled to mature in December 2012, but were retired on March 8, 2000 with the new bond proceeds.

On March 17, 1998, the Laboratory entered into a ten-year interest rate swap contract in connection with the Series 1992A Bonds. This contract was canceled as part of the extinguishment of old debt and new debt issuance on March 8, 2000.

In 1996, the Laboratory borrowed \$500,000 with an interest rate of 5.8% per annum from the University Financing Foundation, Inc. The interest expense for the year ended December 31, 2000 was \$1,950. The loan was paid off in March 2000 with the new bond proceeds.

In 1997, the MBL borrowed \$250,000 with an interest rate of 5.8% per annum from the University Financing Foundation, Inc. The interest expense for the year ended December 31, 2000 was \$2,140. This loan was scheduled to mature in 2002 but was paid off in connection with the new debt issued in March of 2000.

The Laboratory has a line of credit agreement with a commercial bank from which it may draw up to \$1,000,000. The line of credit has an interest rate of prime plus 1/2 percent. The line expires May 29, 2001. No amounts were outstanding under this agreement at December 31, 2000 and 1999.

6. Plant Assets

Plant assets consist of the following at December 31:

	<u>2000</u>	<u>1999</u>
Land	\$ 702,908	\$ 702,908
Buildings	35,236,087	33,702,485
Equipment	5,059,022	4,667,026
Construction in process	<u>4,681,629</u>	<u>1,510,821</u>
 Total	 45,679,646	 40,583,240
Less: Accumulated depreciation	<u>(22,256,490)</u>	<u>(20,464,515)</u>
 Plant assets, net	 <u>\$23,423,156</u>	 <u>\$20,118,725</u>

7. Retirement Plan

The Laboratory participates in the defined contribution pension plan of TIAA-CREF (the "Plan"). The Plan is available to permanent employees who have completed two years of service. Under the Plan, the Laboratory contributes 10% of total compensation for each participant. Contributions amounted to \$862,850 and \$785,509 for the years ended December 31, 2000 and 1999, respectively.

8. Pledges

Unconditional promises to give are included in the financial statements as pledges receivable and the related revenue is recorded in the appropriate net asset category. Unconditional promises to give are expected to be realized in the following periods:

	<u>2000</u>	<u>1999</u>
In one year or less	\$ 5,026,750	\$ 3,974,385
Between one year and five years	3,021,752	3,632,683
After five years	<u>—</u>	<u>202,948</u>
 Total	 8,048,502	 7,810,016
Less: discount of \$168,460 in 2000 and \$236,844 in 1999 and allowance of \$420,000 in 2000 and \$100,000 in 1999	<u>(588,460)</u>	<u>(336,844)</u>
	<u>\$ 7,460,042</u>	<u>\$ 7,473,172</u>

9. Postretirement Benefits

The Laboratory accounts for its postretirement benefits under Statement No. 106, "Employers' Accounting for Postretirement Benefits Other than Pensions," which requires employers to accrue, during the years that the employee renders the necessary service, the expected cost of benefits to be provided during retirement. As permitted, the Laboratory has elected to amortize the transition obligation over 20 years commencing on January 1, 1994.

The Laboratory's policy is that all current retirees and certain eligible employees who retired prior to June 1, 1994 will continue to receive postretirement health benefits. The remaining current employees will receive benefits; however, those benefits will be limited as defined by the Plan. Employees hired on or after January 1, 1995 will not be eligible to participate in the postretirement medical benefit plan.

R16 Annual Report

The following tables set forth the Plan's funded status as of December 31:

	<u>2000</u>	<u>1999</u>
Change in benefit obligation		
Postretirement benefit obligation at beginning of year	\$ 2,043,659	\$ 2,171,119
Service cost	23,020	28,231
Interest cost	149,574	134,533
Actuarial gain	(87,740)	(174,966)
Benefits paid	<u>(136,844)</u>	<u>(115,258)</u>
Postretirement benefit obligation at end of year	<u>1,991,669</u>	<u>2,043,659</u>
Change in plan assets		
Fair value of plan assets at beginning of year	936,149	820,645
Employer contribution	182,776	192,082
Actual return on plan assets	56,465	38,680
Benefits paid	<u>(136,844)</u>	<u>(115,258)</u>
Fair value of plan assets at end of year	<u>1,038,546</u>	<u>936,149</u>
Funded status	(953,123)	(1,107,510)
Unrecognized actuarial gain	(185,377)	(125,351)
Unrecognized net obligation at transaction	<u>1,128,691</u>	<u>1,215,513</u>
Accrued postretirement benefit cost	(9,809)	(17,348)
Less estimated amount payable within one year and classified as a current liability	<u>—</u>	<u>—</u>
Accrued postretirement benefit cost, net of current portion	<u>\$ (9,809)</u>	<u>\$ (17,348)</u>
Weighted-average assumptions as of December 31		
Discount rate	7.50%	8.00%

For purposes of measuring the benefit obligation, an 8.0% annual rate of increase in the per capita cost of covered health benefits was assumed for 2000. The rate was assumed to decrease gradually to 5% in 2005 and remain at that level thereafter.

	<u>2000</u>	<u>1999</u>
Components of net periodic benefit cost		
Service cost	\$ 23,020	\$ 28,231
Interest cost	149,574	134,533
Expected return on assets	(69,524)	(61,425)
Amortization of net obligation at transition	86,822	86,822
Recognized net actuarial loss	<u>(14,655)</u>	<u>(5,385)</u>
Net periodic benefit cost	<u>\$ 175,237</u>	<u>\$ 182,776</u>
Impact of 1% increase in health care cost trend:		
on interest cost plus service cost during past year	\$ 14,271	\$ (71,626)
on accumulated postretirement benefit obligation	41,263	(456,863)
Impact of 1% decrease in health care cost trend:		
on interest cost plus service cost during past year	(11,946)	(10,559)
on accumulated postretirement benefit obligation	(233,324)	(235,728)

Pension plan assets consist of investments in a money market fund.

MARINE BIOLOGICAL LABORATORY

SUPPLEMENTAL SCHEDULE OF FUNCTIONAL EXPENSES

For the Year Ended December 31, 2000

(With Comparative Totals for the Year Ended December 31, 1999)

	Research	Instruction	Conferences	Other	Facilities Maintenance	Administration	Library Services	Research Services	Aquatic Research Services	2000 Total	1999 Total
Salaries	\$ 4,404,934	\$ 447,259	\$ 552,998	\$ 626,728	\$ 1,303,126	\$ 1,909,060	\$ 373,101	\$ 382,174	\$ 259,136	\$ 10,258,516	\$ 9,854,375
Fringe benefits	1,242,196	127,469	157,605	178,618	371,391	759,395	106,334	108,860	73,854	3,125,722	3,046,751
Professional services	187,605	431,349	80	25,070	14,555	205,047	6,920	10,000	—	940,626	713,843
Subcontracts	1,948,041	—	1,656,795	—	—	—	—	—	—	3,604,836	2,936,708
Equipment	718,775	53,308	14,673	3,265	(289)	(15,578)	—	14,426	—	788,580	507,695
Supplies	1,143,432	445,593	100,547	142,269	330,665	150,680	26,674	370,430	57,562	2,767,852	2,471,122
Travel	522,561	363,399	6,737	60,260	2,015	50,903	8,662	7,124	—	1,021,661	871,625
Serials	2,454	8,789	—	4,518	3,305	2,506	638,040	80	—	659,692	528,925
Utilities	4,170	1,079	220,849	1,853	672,381	124,140	10	548	1,863	1,026,893	993,310
Depreciation	—	—	2,809	—	1,789,166	—	—	—	—	1,791,975	1,562,487
Other	305,964	390,302	296,346	178,230	911,716	415,290	176,580	259,092	74,762	3,008,282	2,953,706
*Internal direct charges, net	1,478,052	1,332,532	(1,979,367)	(6,841)	(258,542)	(44,351)	328,556	(747,050)	(102,989)	—	—
Total	11,958,184	3,601,079	1,030,072	1,213,970	5,139,489	3,617,092	1,664,877	405,684	364,188	28,994,635	26,440,547
**Overhead expense allocations	5,841,443	2,025,144	277,386	3,047,357	(5,139,489)	(3,617,092)	(1,664,877)	(405,684)	(364,188)	—	—
Total expenses	\$ 17,799,627	\$ 5,626,223	\$ 1,307,458	\$ 4,261,327	\$ —	\$ —	\$ —	\$ —	\$ —	\$ 28,994,635	\$ 26,440,547

*Internal direct charges are net expenses from one functional area to another based upon the actual use of goods and services.

**Overhead expense allocations include the costs allocated from the Laboratory's functional areas to the final cost objectives.

The accompanying notes are an integral part of the financial statements.

Report of the Library Director

During the past several years a major paradigm shift has clearly taken place in the MBL/WHOI Library. We now have more than 2000 full-text electronic journals available on the network. The library web site is the starting point for content rich information that is being delivered to the much heralded "scientists' desktop."

The simple act of checking in a journal and placing it on the shelf or requesting an Interlibrary Loan now requires the use of various pieces of software like Prospero, CLIO, OCLC Microenhancer, OCLC Passport, Ariel, Microsoft Office, EDI, ABLE, URSA, and various modules of Mariner, as well as online delivery service software for statewide courier services: FedEx, UPS, CISTI, NTIS, and ISI. The inauguration of information delivery *via* our web site also employs the use of SQUID, Geobrowser, LUCID, MySQL, Ultra Edit, Adobe GoLive, Adobe Premiere, Adobe Acrobat, Omni Page, Web Star, Fetch, Quid Pro Quo, Microsoft Office, Portfolio, Graphics Converter, Home Page, SSH, FileMaker, BB Edit, Illustrator, Photoshop, PageMaker, and Apache, and languages such as PHP3, Perl, and SQL. Obviously, "instant" delivery of information requires many hours of staff time implementing major software and hardware infrastructure installations to support this effort.

This instant information drive is powerful, but intellectual ownership and archival requirements are elusive in the world of ePublishers and libraries. Print subscriptions still arrive daily, and electronic journals seem to disappear from a web site at whim. We are making choices in an age of disruptive technologies and value-changing economies. Still, much was



accomplished in 2000 in the library. The emphasis this year was on expanding the serial collection, both print and electronic. The collection has grown to more than 200,000 volumes—occupying all the physical space we have available in Woods Hole.

Space and Renovations

Providing space for library resources is a constant concern for library patrons and staff. Some of the storage problems have been addressed by providing more electronic access to journals and sending some volumes off campus to the Harvard Depository. A Feasibility Study performed by Jay Lucker, Library Consultant, and Stephen Hale, Architect, presented several design ideas to the Trustees. Along with the major recommendation for additional space, the study resulted in a redesign of the equipment and furniture in the catalog room, which allowed more computer terminals for patrons, and the installation of a "window" to the reference desk for easy access to "live" reference information. In addition, the WHOI Archives finished a compact shelving project that encompasses 2130 square feet and resulted in 11,200 linear feet; it will allow for more aggressive record management and 15 years' added growth in archival space projections.

The major improvement to the current library space in the Lillie building was the installation of a new HVAC system that supplies heat in the winter and cooling in the summer to the stack area, the library office, and the reading rooms. This joint venture, financially supported

by both MBL and WHOI, is preventing the wild temperature swings that can be so damaging to the collections. This is a key improvement and the basis for any conservation and preservation program.

Special Collection and Rare Books

Dr. Garland Allen and Carol Winn identified nearly 2500 volumes in the open stacks, dating from the early 19th century, that require preservation and increased security to protect their plates and illustrations. Our Rare Books Room is filled to capacity, so we must find additional space for these materials in the coming years.

The Mary Sears collection, which included individual pieces of the *Challenger* and *Siboga* expeditions, was cataloged and indexed this year. Dr. Arthur Humes' collection was also processed; it included a collection of exotic shells. Also acquired and added to the Florence Gould Collection in the Rare Books was Guillaume Rondelet's *Libri de Piscibus Marinis* (1554). This volume is now the oldest book in the collection and one of the first books to describe marine organisms and fishes.

Electronic Access

As access to information becomes more interactive and information retrieval moves at breakneck speed, the importance of web design and accessibility heightens. The library's web page will continue to be in "re-design" mode with the addition of new resources and services. A new staff member, Amy Stout, Digital Systems and Services Coordinator, is in charge of posting and monitoring the use of this integral part of the library's services. Major upgrades to the library's software took place this year, which resulted in a new look and feel to the web interface, allowing more flexibility in customizing displays for patrons.

Electronic access to the *Oxford English Dictionary* and web versions of Zoo Record and PsycINFO were new additions to the library holdings this year. The library joined JSTOR, a project that provides digital archives of classic serials in the general sciences, ecology, and botany. JSTOR gives us access, for example, to the entire run of *The Philosophical Transactions of the Royal Society of London* from Volume 1, Number 1 in 1665.

Cooperating Libraries

The Boston Library Consortium (BLC) received grant funding from the Massachusetts Board of Library Commissioners for the implementation of a virtual catalog and interlibrary loan (ILL) direct distance borrowing project (VirCat). This grant has made it possible for a growing number of libraries in the consortium to allow patron initiated borrowing from each other's collections without going through the ILL librarians. A group of BLC libraries, including MBL/

WHOI, purchased ScienceDirect from Elsevier. This increased our full-text electronic coverage of Elsevier titles from 111 to 850, which represents the combined holdings of Elsevier titles by the BLC members along with an additional 400 Springer-Verlag full-text eJournals.

Volunteers and Staff

Judy Ashmore, the Assistant Director for MBL Library Operations, Marguerite (Peg) Costa, Cataloger, and Margot Garritt, WHOI Archivist, together representing more than 50 years of experience in the Library, retired this year. Their work has been greatly appreciated by the entire Woods Hole scientific community.

Eleanor Uhlinger, former Director of the Pell Marine Science Library, joined the library as Assistant Director in January 2001. Sha Li (Lisa), Director of Information Services Center and Library for the South China Sea Institute of Oceanology, Chinese Academy of Sciences in Guangzhou, China, spent two months in the library on a study visit learning new technology.

The volunteers in the Rare Books Room and Archives in the Main library, as well as the volunteers in the Data library, have provided invaluable assistance in helping to organize and make these collections available for future scientists. The oral history project at WHOI has been a great success and will be of inestimable value as the 75th anniversary of that institution approaches. Peg Costa joined the ranks of volunteers and helps Carol Winn with the original cataloging project in the rare books.

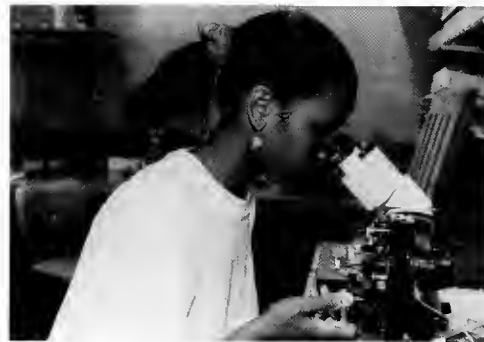
It is with extreme sorrow that I report that Dr. Robert Huettner died in March 2001. He will be remembered as someone who had a very real element of the spirit of discovery and learning, a teacher who exuded enthusiasm as well as knowledge. Bob and his wife, Millie, have been volunteers in the Rare Books room for more than 10 years.

The MBL/WHOI Library hosted the Information Futures Institute at the Jonsson Center in May and welcomed leaders in the field of library science. Participation in these meetings is important not only for the national recognition it affords, but for the leadership these groups exercise in shaping the future of research libraries.

The library has embraced the era of informatics. Funded by the Jewett Foundation, extensive research is underway creating an electronic Key system in taxonomy and a taxonomic name server that will serve the academic enterprise over the web. The library committee has finished its strategic plan, which continues to support the library's mission, and looks forward to a future providing a collaborative and collegial environment, with access to information essential to scientific research, preservation of materials for future generations, and teaching in the Woods Hole scientific institutions.

—Catherine Norton

Educational Programs



Summer Courses

Biology of Parasitism: Modern Approaches (June 8–August 11, 2000)

Directors

Pearce, Edward, Cornell University
Tschudi, Christian, Yale University School of Medicine

Faculty

Phillips, Meg, University of Texas Southwestern Medical Center
Russell, David, Washington University School of Medicine
Scott, Phillip, University of Pennsylvania
Selkirk, Murray, Imperial College of Science, Technology & Medicine, United Kingdom
Sibley, David, Washington University School of Medicine
Ullu, Elisabetta, Yale University School of Medicine
Waters, Andrew P., Leiden University Medical Centre

Lecturers

Allen, Judith, University of Edinburgh
Artis, David, University of Pennsylvania
Bangs, Jay, University of Wisconsin-Madison
Beckers, Cornelis, University of Alabama, Birmingham
Beverley, Stephen, Washington University School of Medicine
Borst, Piet, Netherlands Cancer Institute
Burleigh, Barbara, Harvard School of Public Health
Cully, Doris, Merck & Co.
Dunne, David, Cambridge University
Fidock, David, Albert Einstein College of Medicine
Goldberg, Daniel, Washington University School of Medicine
Grencis, Richard, University of Manchester, United Kingdom
Guiliano, David
Gull, Keith, University of Manchester, United Kingdom
Hajduk, Steve, University of Alabama, Birmingham
Hoffman, Steve
Hunter, Christopher, University of Pennsylvania
Komuniecki, Richard, University of Toledo
Kopf, Manfred, Basel Institute for Immunology, Switzerland
Landfear, Scott, Oregon Health Sciences University
Langhorne, Jean, Medical Research Council
McKerrow, James
Mottram, Jeremy, University of Glasgow
O'Neill, Scott, Yale University School of Medicine
Parsons, Marilyn, Seattle Biomedical Research Institute
Preiser, Peter, Medical Research Council
Rathod, Pradip, Catholic University of America
Sacks, David, National Institutes of Health
Scherf, Artur, Institut Pasteur, France
Sher, Alan, National Institutes of Health

Sinnis, Photini, New York University School of Medicine
Tarleton, Rick, University of Georgia
Turco, Sam, University of Kentucky Medical Center
Wang, Ching Chung, University of California, San Francisco
Wirth, Dyann, Harvard School of Public Health

Teaching Assistants

Beatty, Wandy, Washington University School of Medicine
Djikeng, Appolinaire, Yale University School of Medicine
Hussein, Ayman, Imperial College of Science, Technology & Medicine, United Kingdom
Jackson, Laurie, University of Texas Southwestern
Kissinger, Jessica, University of Pennsylvania
Lovett, Jennie, Washington University School of Medicine
MacDonald, Andrew, Cornell University
Morrisette, Naomi, Washington University School of Medicine
Reiner, Steven
van der Wel, Annemarie, Biomedical Primate Research Centre, The Netherlands

Course Assistants

Chipperfield, Caitlin Nadine, Cornell University
Johnson, Ben, Cornell University

Students

Andersson, John, Karolinska Institut
D'Angelo, Maximiliano, University of Buenos Aires
Dolezal, Pavel, Charles University, Prague
Ferreira, Ludmila, Universidade Federal de Minas Gerais
Figueiredo, Luisa, Institut Pasteur
Gilk, Stacey, University of Vermont
Lamb, Tracey, University of Edinburgh
Lowell, Joanna, Rockefeller University
Martins, Gislaine, University of Sao Paulo
Murta, Silvana, Centro de Pesquisas "René Rachou," Brazil
O'Donnell, Rebecca, University of Melbourne
Ralph, Stuart, University of Melbourne
Sehgal, Alfica, Tata Institute of Fundamental Research India
Tangle, Laura, *U.S. News & World Report*, Science Writer
Triggs, Veronica, University of Wisconsin, Madison
Ulbert, Sebastian, Netherlands Cancer Institute
Villarino, Alejandro, University of Pennsylvania

Embryology: Concepts and Techniques in Modern Developmental Biology (June 18–July 29, 2000)

Directors

Bronner-Fraser, Marianne, California Institute of Technology
Fraser, Scott, California Institute of Technology

Faculty

Adoutte, Andre, University of Paris-Sud, France
 Blair, Seth S., University of Wisconsin, Madison
 Carroll, Sean, University of Wisconsin, Madison
 Collazo, Andres, House Ear Institute
 Ettensohn, Charles, Carnegie Mellon University
 Harland, Richard, University of California, Berkeley
 Henry, Jonathan, University of Illinois, Urbana
 Krumlauf, Robb, National Institute for Medical Research
 Levine, Michael, University of California, Berkeley
 Martindale, Mark, Kewalo Marine Laboratory
 Niswander, Lee, Memorial Sloan-Kettering Cancer Center
 Rothman, Joel, University of California, Santa Barbara
 Saunders, John, Jr., Marine Biological Laboratory
 Schupbach, Trudi, Princeton University
 Shankland, Martin, University of Texas, Austin
 Soriano, Philippe, Fred Hutchinson Cancer Research Center
 Wieschaus, Eric, Princeton University
 Wray, Gregory, Duke University
 Zeller, Robert, University of California, San Diego

Lecturers

Davidson, Eric, California Institute of Technology
 Holland, Linda, University of California, San Diego
 Hopkins, Nancy, Massachusetts Institute of Technology
 Joyner, Alexandra, New York University School of Medicine
 Rosenthal, Nadia, Massachusetts General Hospital, East
 Smith, William, University of California, Santa Barbara
 Stern, Claudio, Columbia University

Teaching Assistants

Allison, Toby, Howard Hughes Medical Institute
 Atit, Radhika, Memorial Sloan-Kettering Cancer Center
 Baker, Clare, California Institute of Technology
 Garcia-Castro, Martin, California Institute of Technology
 Gendreau, Steve, Exelixis, Inc.
 Kuhlman, Julie, University of Oregon
 Lane, Mary Ellen, University of Massachusetts Medical Center
 Lartillot, Nicolas, University of Paris-Sud, France
 Liu, Karen, University of California, Berkeley
 Maduro, Morris, University of California, Santa Barbara
 Mariani, Francesca, University of California, Berkeley
 Micchelli, Craig, University of Wisconsin, Madison
 Ober, Elke, University of California, San Francisco
 Seaver, Elaine, University of Hawaii
 Tabin, Clifford, Harvard Medical School
 Tobey, Allison, Memorial Sloan-Kettering Cancer Center
 Trainor, Paul, Medical Research Council, United Kingdom
 Wallingford, John, University of California, Berkeley
 Walsh, Emily, University of California, San Francisco
 Williams, Terri A., Yale University
 Wilson, Valerie, University of Edinburgh

Course Assistants

Hurwitz, Mark, Marine Biological Laboratory
 Stringer, Kristen, Marine Biological Laboratory
 Wylie, Matthew, Marine Biological Laboratory

Students

Aspöck, Gudrun, University of Basel
 Ballard, Victoria, University of Surrey, United Kingdom
 Bates, Damien, Murdoch Childrens Research Institute



Beckhelling, Clare, Marine Biology Station, France
 Bellipanni, Gianfranco, University of Pennsylvania
 Cheeks, Rebecca, University of North Carolina, Chapel Hill
 Dichmann, Darwin, Hagedorn Research Institute
 Dorman, Jennie, University of Washington
 Ellertsdóttir, Elín, University of Freiburg
 Espinoza, Nora, Louisiana State University
 Ezin, Max, University of Virginia
 Field, Holly, University of California, San Francisco
 Gong, Ying, California Institute of Technology
 Gross, Jeffrey, Duke University
 Huber, Jennifer, University of Hawaii
 Imai, Kazushi, Columbia University
 Javaherian, Ashkan, Cold Spring Harbor Lab
 Jiang, Di, National Institutes of Health
 Khokha, Mustafa, University of California, Berkeley
 Kyrkjebø, Vibeke, Sars Centre
 Lee, Vivian, Oregon Health Sciences University
 Mansfield, Jennifer, Columbia University
 Marx, Vivien, Freelance Science Journalist
 Nasevicius, Aidan, University of Minnesota
 Prud'homme, Benjamin, CNRS
 Skromne, Isaac, Princeton University
 Warkman, Andrew, University of Western Ontario

*Microbial Diversity (June 11–July 27, 2000)**Directors*

Harwood, Caroline, University of Iowa
 Spormann, Alfred, Stanford University

Faculty

Overmann, Jorg, University of Oldenburg
 Schmidt, Thomas, Michigan State University

Lecturers

DeLong, Edward, Monterey Bay Aquarium Research Institute
 Gaasterland, Terry, Rockefeller University
 Greenberg, E. Peter, University of Iowa
 Groisman, Eduardo A., Washington University School of Medicine
 McFall-Ngai, Margaret, University of Hawaii
 Ormston, Nicholas, Yale University
 Parsek, Matthew, Northwestern University
 Rainey, Paul, Oxford University
 Schoolnik, Gary, NIH/NIAID

Stemmer, Pim, Maxygen, Inc.
Visscher, Pieter, University of Connecticut
Walker, Graham, Massachusetts Institute of Technology
Weinstock, George, University of Texas, Houston

Teaching Assistants

Johnson, Hope, Stanford University
Leadbetter, Jared, University of Iowa
Lepp, Paul, Stanford University
Schaefer, Amy, University of Iowa

Course Coordinator

Hawkins, Andrew, University of Iowa

Course Assistant

Ament, Nell, Marine Biological Laboratory

Students

Barak, Yoram, Hebrew University
Begos, Kevin, *Winston-Salem Journal*, Science Writer
Blake, Ruth, Yale University
Buckley, Daniel, Michigan State University
Callaghan, Amy, Rutgers University
Goldman, Robert, University of Houston
Hansel, Colleen, Stanford University
Kadavy, Dana, University of Nebraska, Lincoln
Kirisits, Mary Jo, University of Illinois, Urbana-Champaign
Lester, Kristin, Stanford University
Lin, Li-hung, Princeton University
MacRae, Jean, University of Maine
McCance, James, Leicester University, England
McMullin, Erin, Penn State University
Neretin, Lev, Shirshov Institute of Oceanography
Powell, Sabrina, University of North Carolina, Chapel Hill
Scott, Bart, SoundVision Productions Science Writer
Simpson, Joyce, University of Illinois, Urbana
Singh, Brajesh, Imperial College
Stevenson, Bradley, Michigan State University
Ward, Dawn, University of Delaware
Zaar, Annette, Universität Freiburg

Neural Systems and Behavior

(June 11–August 4, 2000)

Directors

Carr, Catherine, University of Maryland
Levine, Richard, University of Arizona, Tucson

Faculty

Broduehrer, Peter, Bryn Mawr College
Dudchenko, Paul, University of Stirling
Ferrari, Michael, University of Arkansas
French, Kathleen, University of California, San Diego
Glanzman, David, University of California, Los Angeles
Kelley, Darcy, Columbia University
Knerim, James, University of Texas Medical School
Kristan, William, University of California, San Diego
Nadim, Farzan, Rutgers University
Nusbaum, Michael, University of Pennsylvania School of Medicine
Prusky, Glen, The University of Lethbridge, Canada
Roberts, William, University of Oregon

Szczupak, Lidia, Universidad de Buenos Aires
Weeks, Janis, University of Oregon
Wood, Emma, University of Edinburgh
Zakon, Harold, University of Texas, Austin

Lecturers

Angustine, George, Duke University
Korn, Henri, Pasteur Institut
Maler, Leonard, University of Ottawa
Pflueger, Hans-Joachim, Freie Universität Berlin
Ribera, Angela, University of Colorado Health Science Center
Schwartz, Andrew, The Neuroscience Institute
Walters, Edgar T., University of Texas Medical School

Teaching Assistants

Armstrong, Cecilia, University of Washington
Beenhakker, Mark, University of Pennsylvania
Blitz, Dawn Marie, University of Chicago
Bower, Mark, University of Arizona, Tucson
Chen, Shanning, House Ear Institute
Chitwood, Raymond, Baylor College of Medicine
Coleman, Melissa, St. Joseph's Hospital
Duch, Carsten, University of Arizona, Tucson
Gamkrelidze, Georgi, Lucent Technology
Gerrard, Jason, University of Arizona, Tucson
Goodman, Miriam B., Columbia University
Hill, Andrew, Emory University
Masino, Mark, Emory University
McAnelly, Lynne, University of Texas, Austin
Otis, Thomas, University of California, Los Angeles
Parameshwaran, Suchitra, University of Maryland
Philpot, Benjamin, Brown University
Soares, Daphne, University of Maryland
Stell, Brandon, University of California, Los Angeles
Villareal, Greg, University of California, Los Angeles
Yong, Rocio, University of California, Los Angeles
Zee, M. Jade, University of Oregon

Course Assistants

Almers, Lucy, Marine Biological Laboratory
Psujek, Sean, Marine Biological Laboratory

Students

Akay, Turgay, University of Cologne
Archie, Kevin, University of Southern California
Billimoria, Cyrus, Brandeis University
Black, Michael, Arizona State University
Boyden, Edward, Stanford University
Bradford, Yvonne, University of Oregon
Cardin, Jessica, University of Pennsylvania
Dasika, Vasant, Boston University
Ding, Long, University of Pennsylvania
Froemke, Robert, University of California, Berkeley
Grammer, Michael, University of Southern California
Hubbard, Aida, University of Texas, San Antonio
Hurt, Barbekka, University of Colorado, Boulder
Karmarkar, Uma, University of California, Los Angeles
Konur, Sila, Columbia University
Oestreich, Joerg, University of Texas, Austin
Rela, Lorena, University of Buenos Aires
Sinha, Shiva, University of Maryland
Siuda, Edward, Michigan State University
Tobin, Anne-Elise, Emory University



Neurobiology (June 11–August 12, 2000)

Directors

Faber, Donald, Albert Einstein College of Medicine
Lichtman, Jeff W., Washington University School of Medicine

Section Director

Greenberg, Michael, Children's Hospital

Faculty

Denk, Winfried, Max-Planck Institute for Medical Research
Gan, Wenbiao, New York University School of Medicine
Griffith, Leslie, Brandeis University
Harris, Kristen, Boston University
Hart, Anne, Massachusetts General Hospital
Heuser, John E., Washington University School of Medicine
Howell, Brian, National Institutes of Health
Khodakhah, Kamran, University of Colorado School of Medicine
Lambert, Nevin, Medical College of Georgia
Lin, Jen-Wei, Boston University
Nedivi, Elly, Massachusetts Institute of Technology
Nowak, Linda, Cornell University
Reese, Thomas, National Institutes of Health
Sanes, Joshua, Washington University Medical School
Schweizer, Felix, University of California, Los Angeles
Shamah, Steven, Children's Hospital

Smith, Carolyn, National Institutes of Health
Terasaki, Mark, University of Connecticut Health Center
Thompson, Wesley J., University of Texas
Van Vactor, David, Harvard Medical School
Wong, Rachel, Washington University School of Medicine

Lecturers

Barres, Ben A., Stanford University School of Medicine
Bean, Bruce, Harvard University
Conchello, Jose-Angel, Washington University
Ghosh, Anirvan, Johns Hopkins University School of Medicine
Linden, David, Johns Hopkins University
McCleskey, Edwin, Oregon Health Sciences University
McMahan, Uel, Stanford University School of Medicine
Miller, Chris, Brandeis University
Sigworth, Fred, Yale University
Smith, Stephen, Stanford University School of Medicine
Tsien, Roger, University of California, San Diego
Turrigiano, Gina

Teaching Assistants

Pereda, Alberto, Albert Einstein College of Medicine
Petersen, Jennifer, National Institutes of Health
Turney, Stephen, Washington University
Walsh, Mark, Washington University School of Medicine

Course Assistants

Chiu, Delia, Marine Biological Laboratory
Nover, Harris, Marine Biological Laboratory

Students

Ang, Eugenius, Yale University
Kettunen, Petronella, Karolinska Institutet
Khabbaz, Anton, Princeton University/Lucent Technologies
Livet, Jean, IBDM, Marseille
Long, Michael, Brown University
McKellar, Claire, Harvard University
Misgeld, Thomas, Max-Planck-Institute of Neurobiology, Martinsried, Germany
Nelson, Laura, National Institute for Medical Research, United Kingdom
Ruta, Vanessa, The Rockefeller University
Weissman, Tamily, Columbia University
Yasuda, Ryohei, Teiko University Biotech Research Center
Zhong, Haining, Johns Hopkins University

Physiology: The Biochemical and Molecular Basis of Cell Signaling (June 11–July 22, 2000)

Directors

Garbers, David, University of Texas Southwestern Medical Center
Reed, Randall, Johns Hopkins University School of Medicine

Faculty

Furlow, John, University of California, Davis
Lockless, Steve, University of Texas Southwestern Medical Center
Noel, Joseph, Salk Institute
Prasad, Brinda, Johns Hopkins School of Medicine
Quill, Timothy, University of Texas Southwestern Medical Center
Ranganathan, Rama, University of Texas Southwestern Medical Center



Verdecia, Mark, Salk Institute
Wedel, Barbara, University of Texas Southwestern Medical Center
Zhao, Haiqing, Johns Hopkins School of Medicine
Zielinski, Raymond, University of Illinois, Urbana

Isenberg Lecturer

Hudspeth, A., James, Rockefeller University

Lecturers

Armstrong, Clay, University of Pennsylvania
Buck, Linda, Harvard Medical School
Clapham, David, Harvard Medical School
Devreotes, Peter, Johns Hopkins University School of Medicine
Dixon, Jack, University of Michigan Medical School
Ehrlich, Barbara, Yale University
Fraser, Scott, California Institute of Technology
Freedman, Leonard, Memorial Sloan-Kettering Cancer Center
Hilgemann, Donald W., University of Texas Southwestern Medical Center
Huganir, Richard, Johns Hopkins University School of Medicine
Jaffe, Lionel, Marine Biological Laboratory
MacKinnon, Roderick, Rockefeller University
Mangelsdorf, David, University of Texas Southwestern Medical Center
Oprian, Daniel, Brandeis University
Stamler, Jonathan S., Duke University Medical Center
Wilkie, Thomas, University of Texas Southwestern Medical Center

Course Coordinator

Lenme, Scott, University of Texas Southwestern Medical Center
Rossi, Kristen, University of Texas Southwestern Medical Center

Students

Brelidze, Tinatin, University of Miami School of Medicine
Carroll, Michael, University of Newcastle upon Tyne, United Kingdom
Colón-Ramos, Daniel, Duke University
Cordeiro, Maria, Sofia Instituto Gulbenkian de Ciência, Portugal
Costa, Patricia, University of Rio de Janeiro
Cotrufo, Tiziana, Scuola Normale Superiore
Crespo-Barreto, Juan, University of Puerto Rico
Cruz, Georgina, University of South Florida
Dayel, Mark, University of California, San Francisco
Fleegal, Melissa, University of Florida
Fleischer, Jörg, University of Hohenheim
Glater, Elizabeth, Brown University

Jhaveri, Dhanisha, Tata Institute of Fundamental Research
Johansson, Viktoria, Göteborg University
Mah, Silvia, Scripps Institution of Oceanography
Marrari, Yannick, Villefranche Sur Mer
Meister, Jean-Jacques, Swiss Federal Institute of Technology
Menna, Elisabetta, Institute of Neurophysiology, Pisa
Nguyen, Anh, University of Kansas
Petrie, Ryan, University of Calgary
Rankin, Kathleen, Oberlin College
Rodeheffer, Carey, Emory University
Rodgers, Erin, University of Alabama, Birmingham
Seipel, Susan, Rutgers University
Sen, Subhojit, Tata Institute of Fundamental Research
Shatkin-Margolis, Seth, Duke University
Shilkrut, Mark, Technion-Israel Institute of Technology
Takai, Erica, Columbia University
Zeidner, Gil, Weizmann Institute of Science

Special Topics Courses

Analytical and Quantitative Light Microscopy *(May 4–May 12, 2000)*

Directors

Sluder, Greenfield, University of Massachusetts Medical School
Wolf, David, BioHybrid Technologies Inc.

Faculty

Amos, William B., Medical Research Council, United Kingdom
Cardullo, Richard, University of California, Riverside
Gelles, Jeff, Brandeis University
Inoué, Shinya, Marine Biological Laboratory
Oldenbourg, Rudolf, Marine Biological Laboratory
Salmon, Edward, University of North Carolina, Chapel Hill
Silver, Randi, Cornell University Medical College
Spring, Kenneth, National Institutes of Health
Straight, Aaron, Harvard Medical School
Swedlow, Jason, University of Dundee

Lecturer

McCrone, Walter, McCrone Research Institute

Teaching Assistants

Grego, Sonia, University of North Carolina, Chapel Hill
Hinchcliffe, Edward, University of Massachusetts Medical School
Pollard, Angela, BioHybrid Technologies

Course Coordinator

Miller, Rick, University of Massachusetts Medical School

Students

Abraham, Clara, University of Chicago
Alvarez, Xavier, N.E. Regional Primate Research Center, Harvard Medical School
Andrews, Paul, University of Dundee
Bonnet, Gregoire, Rockefeller University
Bravo-Zanoguera, Miguel, University of California, San Diego
Cohen, David, Cornell University Medical College
Connett, Marie, Westvaco Forest Sciences Lab
Crittenden, Sarah, University of Wisconsin, Madison

D'Onofrio, Terrence, Pennsylvania State University
 Faruki, Shamsa, Wadsworth Center
 Gasser, Susan, Swiss Cancer Institute
 Handwerker, Korie, Carnegie Institution of Washington
 Hunter, Edward, Q3DM
 Jansma, Patricia, University of Arizona
 Kraft, Catherine, University of Pittsburgh
 Lee, Michelle, Harvard Medical School
 Lowe, Christopher, University of California, Berkeley
 Lu, Bai, National Institutes of Health/NICHD
 Maldonado, Héctor, Universidad Central del Caribe
 Matsumoto, Yutaka, University of Colorado
 McKinney, Leslie, Uniformed Services University
 Morelock, Maurice, Boehringer Ingelheim Pharmaceuticals
 Mundigl, Olaf, Roche Diagnostics
 Mycek, Mary-Ann, Dartmouth College
 Provencal, Bob, Los Alamos National Laboratory
 Sanabria, Priscila, Universidad Central del Caribe
 Sedwick, Caitlin, University of Chicago
 Tang, Jay, Indiana University
 Tirnauer, Jennifer, Harvard Medical School
 Xu, Fang, The Hospital for Special Surgery

Frontiers in Reproduction: Molecular and Cellular Concepts and Applications (May 21–July 1, 2000)

Directors

Hunt, Joan, University of Kansas Medical Center
 Mayo, Kelly, Northwestern University
 Schatten, Gerald, Oregon Health Sciences University

Faculty

Ascoli, Mario, University of Iowa College of Medicine
 Campbell, Keith, PPL Therapeutics
 Camper, Sally, University of Michigan Medical School
 Chan, Anthony, Oregon Health Sciences University
 Croy, Barbara Anne, University of Guelph, Canada
 Dominko, Tanja, Oregon Regional Primate Research Center
 Gibori, Geula, University of Illinois
 Hunt, Patricia A., Case Western Reserve University
 Jaffe, Laurinda, University of Connecticut Health Center
 Moore, Karen, University of Florida
 Morris, Patricia, The Rockefeller University
 Mukherjee, Abir, Northwestern University
 Nilson, John, Case Western Reserve Medical School
 Page, Ray, PPL Therapeutics Inc.
 Pedersen, Roger, University of California, San Francisco
 Shupnik, Margaret, University of Virginia Medical Center
 Smith, Lawrence, University of Montreal
 Terasaki, Mark, University of Connecticut Health Center
 Wakayama, Teruhiko, Rockefeller University
 Weigel, Nancy, Baylor College of Medicine

Lecturers

Balczon, Ronald, University of South Alabama
 Behringer, Richard, University of Texas
 Charo, Alta, University of Wisconsin, Madison
 Compton, Duane, Dartmouth Medical School
 Crowley, William, Massachusetts General Hospital
 De Sousa, Paul, Alexandre Roslin Institute
 Fazleabas, Asgerally, University of Illinois

Hennighausen, Lothar, National Institutes of Health, NIDDK
 Mitchison, Timothy, Harvard Medical School
 Myles, Diana, University of California
 Ober, Carole, University of Chicago
 Orth, Joanne, Temple University School of Medicine
 Palazzo, Robert, University of Kansas
 Piedrahita, Jorge, Texas A&M University
 Reijo Pera, Renee, University of California
 Richards, Jo-Anne, Baylor College of Medicine
 Ruderman, Joan, Harvard Medical School
 Shenker, Andrew, Children's Memorial Hospital, CMIER
 Sluder, Greenfield, University of Massachusetts Medical School
 Stearns, Tim
 Strauss, Jerome, University of Pennsylvania Medical Center
 Tilly, Jonathan L., Massachusetts General Hospital
 Wall, Robert, U.S. Department of Agriculture
 Wessel, Gary, Brown University
 Woodruff, Teresa, Northwestern University

Teaching Assistants

Berard, Mark, University of Michigan
 Carroll, David, Florida Institute of Technology
 Giusti, Andrew, University of Connecticut Health Center
 Gray, Heather, University of Chicago
 Greenwood, Janice, University of Guelph
 Hinkle, Beth, University of Connecticut Health Center
 Hodges, Craig, Case Western Reserve University
 Jaquette, Julie, University of Iowa
 Malik, Nusrat, Baylor College of Medicine
 Miller, Michelle, Oregon Health Sciences University
 Payne, Christopher, Oregon Regional Primate Research Center
 Runft, Linda, University of Connecticut Health Center
 Saunders, Thomas, University of Michigan
 Takahashi, Diana, Oregon Regional Primate Research Center
 Voronina, Ekaterina, Brown University
 Weck, Jennifer, Northwestern University

Course Coordinators

Burnett, Tim, University of Kansas Medical Center
 Marin Bivens, Carrie, University of Massachusetts
 McMullen, Michelle, Northwestern University
 Petroff, Margaret, University of Kansas Medical Center
 Simerly, Calvin, Oregon Regional Primate Research Center

Students

Alberio, Ramiro, Ludwig-Maximilian University, Germany
 Allegrucci, Cinzia, Perugia University, Italy
 Ashkar, Ali, University of Guelph
 Berkowitz, Karen, University of Pennsylvania
 Chong, Kowit-Yu, Oregon Regional Primate Research Center
 Diaz, Lorenza, INNSZ
 Graham, Kathryn, Oregon Health Sciences University
 Greenlee, Anne, Marshfield Medical Research Foundation
 Heifetz, Yael, Cornell University
 Keller, Dominique, Texas A&M University
 Lavoie, Holly, University of South Carolina
 Majumdar, Subeer, National Institute of Immunology
 Powell, Jacqueline, Morehouse School of Medicine
 Richard, Craig, Magee-Women's Research Institute
 Sahgal, Namita, Kansas University Medical Center
 Zhang, Gongqiao, University of Virginia



Fundamental Issues in Vision Research
(August 13–25, 2000)

Directors

Masur, Sandra K., Mount Sinai School of Medicine
Papermaster, David, University of Connecticut Health Center

Faculty

Barlow, Robert, Syracuse University
Barres, Ben A., Stanford University School of Medicine
Beebe, David C., Washington University School of Medicine
Berson, Eliot L., Harvard Medical School
Bok, Dean, University of California, Los Angeles
Dickersin, Kay, Brown University
Dowling, John E., Harvard University
Fisher, Richard, National Institutes of Health
Gordon, Marion, Rutgers College of Pharmacy
Hamm, Heidi E., Northwestern University Medical School
Horton, Jonathan, University of California
Horwitz, Joseph, University of California, Los Angeles
Lang, Richard A., New York University School of Medicine
LaVail, Jennifer, University of California, San Francisco
Lavker, Robert, University of Pennsylvania
Lehrer, Robert, University of California, Los Angeles
Leske, M. Cristina, State University of New York, Stony Brook
Lieberman, Ellen, National Institutes of Health
Malchow, Robert, University of Illinois, Chicago

Masland, Richard, Massachusetts General Hospital
Nathans, Jeremy, Johns Hopkins University School of Medicine
Niederkmorn, Jerry Y., University of Texas Southwestern Medical Center
Overbeek, Paul A., Baylor College of Medicine
Piatigorsky, Joram, National Institutes of Health
Raviola, Elio, Harvard Medical School
Shatz, Carla, Harvard Medical School
Stambolian, Dwight, University of Pennsylvania
Sugrue, Stephen P., University of Florida College of Medicine
Wasson, Paul, Harvard Medical School

Lecturers

Assad, John, Harvard Medical School
Hernandez, M. Rosario, Washington University School of Medicine
Moses, Marsha, Children's Hospital, Boston
Russell, Paul, National Institutes of Health

Students

Al-Khatib, Khalidun, University of Illinois, Chicago
Bernstein, Audrey, Mount Sinai Medical School
Birnbau, Andrea, University of Illinois, Chicago
Camelo, Serge, Institut Pasteur
Cronin, Carolyn, University of Virginia
Gaudio, Paul, Yale University
Goh, Meilan Stephanie, University of Illinois, Chicago
Hartford, April, University of Louisville
Jessani, Nadim, Scripps Research Institute
Jiang, Shunai, Emory University
Kenyon, Kristy, Massachusetts Eye and Ear Infirmary
Libby, Richard, Medical Research Council, United Kingdom
Liu, Xiaorong, University of Virginia
Mahajan, Vinit, University of California, Irvine
Pennesi, Mark, Baylor College of Medicine
Pittman, Kristi, North Carolina State University
Rose, Linda, University of Maryland
Ruttan, Gregory, University of Miami, Florida
Sagdullaev, Botir, University of Louisville
Shestopalov, Valery, Washington University

Medical Informatics (May 28–June 3, 2000)

Director

Masys, Daniel, University of California, San Diego

Faculty

Canese, Kathi, National Library of Medicine
Cimino, James, Columbia University
Friedman, Charles, University of Pittsburgh
Giuse, Nunzia, Vanderbilt University Medical Center
Hightower, Allen, Centers for Disease Control and Prevention
Kingsland, Lawrence, National Library of Medicine
Lindberg, Donald, National Library of Medicine
McDonald, Clement, Regenstrief Institute
Miller, Randolph, Vanderbilt University Medical Center
Nahin, Annette, National Library of Medicine
Ozholt, Judy, Vanderbilt University Medical Center
Stead, William, Vanderbilt University Medical Center
Wheeler, David, National Library of Medicine

Students

Athreya, Balu, DuPont Hospital for Children
Barnes, Judith, Ingham Regional Medical Center

Betts, Eugene, Medical College of Georgia
 Blatt, Jody, Health Care Financing Administration
 Brill, Peter, Trover Foundation
 Brown, Janis, University of Southern California
 Clintworth, William, University of Southern California
 Cohn, Wendy, University of Virginia
 Cowper, Diane, Hines VA Hospital
 Cooper, Natasha, Penn State College of Medicine
 Desai, Sundeep, Northwestern Medical Faculty Foundation
 Ebbeling, Kelly, University of Wisconsin, Madison
 Fulda, Pauline, Louisiana State University
 Halsted, Deborah, Houston Academy of Medicine
 Harris, Anthony, University of Maryland
 Levine, Alan, University of Texas, Houston
 Jenson, James, University of New Mexico
 Klingen, Donald, Riverside Regional Medical Center
 Kubal, Joseph, VA Information Resource Center
 McKnight, Michelynn, Norman Regional Hospital
 Obijiofor, Chioma, Bioresources Development and Conservation Program
 Schwartz, Marilyn, Naval Medical Center, San Diego
 Smith, John, University of Alabama, Birmingham
 Sooho, Alan, Battle Creek Veterans Administration
 Stocking, John, University of Louisville
 Strachan, Dina, King/Drew Medical Center
 Thibodeau, Patricia, Duke University
 Vaidya, Vinay, University of Maryland
 Woeltje, Keith, Medical College of Georgia
 Yamamoto, David, University of California, Los Angeles
 Zick, Laura, Clarian Health

Medical Informatics (October 1–7, 2000)

Director

Cimino, James, Columbia University

Faculty

Bakken, Suzanne, Columbia University
 Cimino, Chris, Albert Einstein College of Medicine
 Friedman, Charles, University of Pittsburgh
 Jenders, Robert, Columbia University
 Kingsland, Lawrence, National Library of Medicine
 Lindberg, Donald, National Library of Medicine
 Masys, Daniel, University of California, San Diego
 McCray, Alexa, National Library of Medicine
 Nahin, Annette, National Library of Medicine
 Perednia, Douglas, Association of Telehealth Providers
 Starren, Justin, Columbia University
 Wheeler, David, National Library of Medicine

Students

Amend, Clifford, Care First Blue Cross Blue Shield
 Babu, Ajit, St. Louis VA Medical Center
 Baer, Michael, Lebanon Veterans Admin. Medical Center
 Barclay, Allan, Indiana University School of Medicine
 Burke, Cynthia, Hampton University
 Byrd, Vetrica, University of Alabama, Birmingham
 Dam, Steven, University of Western Ontario
 Davis, Wayne, University of Michigan Medical School
 DiPro, Joseph, University of Georgia
 Fernandes, John, Chicago College Osteopathic Medicine
 Frank, Christine, Rush-Presbyterian-St. Luke's Medical Center



Gallardo, Gladys, Universidad Central del Caribe
 Gamble, James, Manila Health Center
 Gill, Jagjit, Mayo Clinic and Foundation
 Goodwin, Cheryl, Swedish Medical Center
 Guarcello, Catherine, St. Elizabeth's Medical Center
 Jones, Dixie, LSU Health Science Center
 Kelly, Catherine, Massachusetts General Hospital
 Mackowiak, Leslie, Duke University Health System
 McKoy, Karen, Lahey Clinic
 Moser, Stephen, University of Alabama, Birmingham
 Murray, Kathleen, University of Alaska Anchorage
 Pepper, David, University Medical Center
 Riesenber, Lee, Ann Guthrie Healthcare System
 Sath, Nila, Vanderbilt University Medical Center
 Sullivan, Eileen, University of New Mexico
 Taylor, Vera, Morehouse School of Medicine
 Wellik, Kay, Mayo Clinic Scottsdale
 Wiedermann, Bernhard, Children's National Medical Center, Washington

Methods in Computational Neuroscience (July 30–August 26, 2000)

Directors

Bialek, William, NEC Research Institute
 de Ruyter, Rob, NEC Research Institute

Faculty

Abbott, Lawrence, Brandeis University
 Colby, Carol, University of Pittsburgh
 Collett, Thomas, University of Sussex
 Dan, Yang, University of California, Berkeley
 Delaney, Kerry, Simon Fraser University, Canada
 Doupe, Allison, University of California, San Francisco
 Ermentrout, Bard, University of Pittsburgh
 Ferster, David, Northwestern University
 Gelperin, Alan, Bell Laboratories
 Hopfield, John, Princeton University
 Johnston, Daniel, Baylor College of Medicine
 Kelley, Darcy, Columbia University
 Kleinfeld, David, University of California, San Diego
 Kopell, Nancy, Boston University
 Marder, Eve, Brandeis University
 Markram, H., University of California
 Miller, K. D., University of California, San Francisco

Mitra, Partha, AT&T Bell Laboratories
Nemenman, Ilya, NEC Research Institute
Rieke, Fred, University of Washington
Seung, H. Sebastian, Massachusetts Institute of Technology
Sigvardt, Karen, University of California, Davis
Solla, Sara A., Northwestern University Medical School
Sompolinsky, Haim, The Hebrew University, Israel
Tank, David, AT&T Bell Laboratories
Tishby, Naftali, The Hebrew University, Israel
Tsodyks, Mikhail, Weizmann Institute of Science
Zucker, Steven, Yale University

Lab Instructor

Jensen, Roderick, Wesleyan University

Lecturers

Baylor, Denis, Stanford University Medical Center
Berry, Michael, Princeton University
Koberle, Roland, Universidade de Sao Paulo, Brasil
Laughlin, Simon Barry, Cambridge University, United Kingdom
Logothetis, Nikos, Max-Planck-Institute for Biological Cybernetics
Srinivasan, Mandyam V., Australian National University, Australia

Teaching Assistants

Aguera y Arcas, B., Princeton University
Lewen, Geoffrey David, NEC Research Institute
White, John, Boston University

Course Assistants

Jensen, Kate, Marine Biological Laboratory
Purpura, Keith, Marine Biological Laboratory

Students

Aharonov-Barki, Ranit, Hebrew University
Bartlett, Edward, University of Wisconsin, Madison
Bodelón, Clara, Boston University
Boudreau, Christen (Beth), Baylor College of Medicine
Feinerman, Ofer, Weizmann Institute of Science
Felsen, Gidon, University of California, Berkeley
Globerson, Amir, Hebrew University
Gütig, Robert, University of Freiburg
Jin, Dezhe, University of California, San Diego
Kang, Kukjin, Hebrew University
Krishna, B. Suresh, New York University
Lauritzen, Thomas, University of California, San Francisco
Parthasarathy, Hemai, Nature America
Paz, Ron, Hebrew University
Petereit, Christian, Universität Bielefeld
Pierce, John, Vibration & Sound Sol, Ltd.
Rokni, Uri, Hebrew University
Schreiber, Susanne, Humboldt Universität Berlin
Shi, Songhai, Cold Spring Harbor Laboratory
Sirota, Anton, Rutgers University
Szalicszyo, Krisztina, Hungarian Academy of Science
Taylor, Dawn, Arizona State University
Ulanovsky, Nachum, Hebrew University
Werfel, Justin, Massachusetts Institute of Technology

Microinjection Techniques in Cell Biology

(May 16–23, 2000)

Director

Silver, Robert, Marine Biological Laboratory

Faculty

Klaessig, Suzanne, Cornell University
Kline, Douglas, Kent State University
Shelden, Eric, University of Michigan
Wilson, Susan, Cornell University

Teaching Assistant

Miller, Roy Andrew, Kent State University

Students

Cabot, Ryan, University of Missouri
Caswell, Wayne, Labey Clinic
Combelles, Catherine, Tufts University
Davies, Daryl, University of Southern California
Dong, Lily, UT Health Science Center, San Antonio
Geraci, Fabiana, University of Palermo
Gilbert, Joanna, Harvard Medical School
Gundersen-Rindal, Dawn, U.S. Department of Agriculture
Harwood, Claire, University of Pennsylvania
Hawash, Ibrahim, Purdue University
Howe, Charles, Stanford University
Kay, EunDuck, Doheny Eye Institute
Kline-Smith, Susan, Indiana University
Macdonald, Jennifer, Medical University of South Carolina
Nguyen, Hong-Ngan, University of Louisiana of Lafayette
Okusu, Akiko, Harvard University
von Dassow, Peter, Scripps Institute of Oceanography
Webb, Bradley, Queen's University
Widelitz, Randall, University of Southern California
Yang, Jin, Duke University, HHMI

Modeling of Biological Systems

(March 25–May 4, 2000)

Director

Silver, Robert, Marine Biological Laboratory

Faculty

Boston, Raymond C., University of Pennsylvania
Cheatham, Thomas E., University of Utah
Herzfeld, Judith, Brandeis University
Hummel, John, Argonne National Laboratory
Kollman, Peter, University of California, San Francisco
Moate, Peter, University of Pennsylvania
Pearson, John, Los Alamos National Laboratory
Petsko, Greg A., Brandeis University
Ponce Dawson, Silvina, Ciudad Universitaria, Argentina

Students

Genick, Ulrich, The Salk Institute
Ginsberg, Tara, University of Texas, Houston
Hershberg, Uri, Hebrew University
Immerstrand, Charlotte, Linköping University, Sweden
Jiang, Yi, Los Alamos National Laboratory

Mosavi, Leila, University of Connecticut Health Center
 Quinteiro, Guillermo, University of Buenos Aires
 Teng, Ching-Ling, University of Virginia
 Uppal, Hirdesh, Punjab Veterinary Vaccine Institute, India

Molecular Biology of Aging (August 12–18, 2000)

Directors

Guarente, Leonard P., Massachusetts Institute of Technology
 Wallace, Douglas, Emory University School of Medicine

Faculty

Austad, Steven, University of Idaho
 Beal, M. Flint, Cornell University
 Bohr, Vilhelm A., National Institutes of Health
 Campisi, Judith, Lawrence Berkeley National Laboratory
 Culotta, Valeria L., Johns Hopkins University
 de Lange, Titia, The Rockefeller University
 Hanawalt, Philip, Stanford University
 Johnson, Thomas, University of Colorado
 Jones, Dean P., Emory University
 Kenyon, Cynthia, University of California, San Francisco
 Kim, Stuart, Stanford, University School of Medicine
 Lithgow, Gordon J., University of Manchester
 Martin, George, University of Washington School of Medicine
 McChesney, Patricia, University of Texas Southwestern
 Medical Center
 Price, Donald L., Johns Hopkins University School of Medicine
 Richardson, Arlan, University of Texas Health Science Center,
 San Antonio
 Ruvkun, Gary, Massachusetts General Hospital
 Tanzi, Rudolph E., Harvard Medical School
 Tower, John, University of Southern California
 Van Voorhies, Wayne, University of Arizona, Tucson
 Wright, Woodring E., University of Texas Southwestern
 Medical Center

Lecturers

Finch, Celeb, University of Southern California
 Hekimi, Siegfried, McGill University
 Weindruch, Richard H., Veterans Administration Hospital

Teaching Assistants

Coskun, Elif Pinar, Emory University School of Medicine
 Ford, Ethan, Massachusetts Institute of Technology
 Kerstann, Keith, Emory University School of Medicine
 Kokoszka, Jason, Emory University
 Levy, Shawn, Vanderbilt-Ingram Cancer Center
 Marciniak, Robert, Massachusetts Institute of Technology
 McVey, Mitch, Massachusetts Institute of Technology
 Murdock, Deborah, Emory University

Course Coordinator

Burke, Rhonda E., Emory University School of Medicine

Course Assistant

Ament, Nell, Marine Biological Laboratory

Students

Bailey, Adina, University of California, Berkeley
 Baur, Joe, UT Southwestern Medical Center, Dallas

Bordone, Laura, University of Minnesota
 Cui, Wei, Roslin Institute, Edinburgh
 Cypser, James, University of Colorado
 Filosa, Stefania, IIGB-CNR
 Furfaro, Joyce, Pennsylvania State University
 Harper, James, University of Idaho
 Huang, Xudong, Massachusetts General Hospital
 Johnson, Kristen, Purdue University
 Konigsberg, Mina, Universidad Autonoma Metropolitana
 Kostrominova, Tatiana, University of Michigan
 Luo, Yuan, University of Southern Mississippi
 Muñoz, Denise, University of Buenos Aires/UC Berkeley
 Peel, Alyson, The Buck Center for Research in Aging
 Podlutzky, Andrej, National Institute on Aging
 Radulescu, Andreea, Albert Einstein College of Medicine
 Srivivsan, Chandra, University of California, Los Angeles
 Tong, Jiayuan (James), Cold Spring Harbor
 Zaid, Ahmed, Stockholm University

Molecular Mycology: Current Approaches to Fungal Pathogenesis (August 7–25, 2000)

Directors

Edwards, John, Jr., Harbor-UCLA Medical Center
 Magee, Paul T., University of Minnesota
 Mitchell, Aaron P., Columbia University

Faculty

Filler, Scott, Harbor-UCLA Medical Center
 Heitman, Joseph, Duke University Medical Center
 Rhodes, Judith, University of Cincinnati Medical Center
 White, Theodore, Seattle Biomedical Research Institute

Lecturers

Cushion, Melanie, University of Cincinnati
 Doering, Tamara, Washington University School of Medicine
 Fink, Gerald, Whitehead Institute
 Kozel, Thomas, University of Nevada School of Medicine
 Kwon-Chung, June, National Institutes of Health
 Levitz, Stuart, Boston University
 Magee, Beatrice, University of Minnesota
 Puziss, John, Proteome, Inc.
 Quinn, Cheryl, Pharmacia & Upjohn
 Scherer, Stewart, Rosetta Inpharmatics

Teaching Assistants

Flenniken, Michelle, Montana State University
 Johnston, Douglas, Harbor-UCLA Medical Center
 Lengeler, Klaus B., Duke University Medical Center

Course Assistant

Martin, Sam, Marine Biological Laboratory

Students

Askew, David, University of Cincinnati
 Austin, W. Lena, Howard University
 Blankenship, Jill, Duke University
 Burr, Ian, Pfizer Central Research
 Francis, Susan, University of Washington
 Hochstenbach, Frans, University of Amsterdam
 Ibrahim, Ashraf, Harbor-UCLA Medical Center



Lo, Hsiu-Jung, National Health Research Institutes
Mol, Pietermella, University of Amsterdam
Munro, Carol, University of Aberdeen
Perea, Sofia, University of Texas
Spellberg, Brad, Harbor-UCLA Medical Center
Spreghini, Elisabetta, Yale University
Toenjes, Kurt, University of Vermont
Wasylnka, Julie, Simon Fraser University

Neural Development and Genetics of Zebrafish ***(August 13–26, 2000)***

Directors

Dowling, John E., Harvard University
Hopkins, Nancy, Massachusetts Institute of Technology

Faculty

Chien, Chi-Bin, University of Utah Medical Center
Collazo, Andres, House Ear Institute
Eisen, Judith S., University of Oregon
Fetcho, Joseph, State University of New York, Stony Brook
Hanlon, Roger, Marine Biological Laboratory
Houart, Corrine, University College London, United Kingdom
Kimmel, Charles, University of Oregon
Lin, Shuo, Medical College of Georgia
Neuhauss, Stephan, Max-Planck-Institut für Entwicklungsbiologie,
Germany
Talbot, William S., Stanford University School of Medicine
Wilson, Stephen, University College London, United Kingdom

Lecturers

Astrosky, Keith, Massachusetts Institute of Technology
Fraser, Scott, California Institute of Technology

Teaching Assistants

Amacher, Sharon, University of California, Berkeley
Clarke, Jon, University College London, United Kingdom
Fadool, James, Florida State University
Granato, Michael, University of Pennsylvania
Lyons, David, University College London
Mazanec, April, University of Oregon
Mullins, Mary, University of Pennsylvania
Perkins, Brian, Harvard University
Pomrehn, Andrea, Stanford University
Wagner, Daniel, University of Pennsylvania Medical School

Walker-Durchanck, Charline, University of Oregon
Waterbury, Julie, University of Pennsylvania

Course Coordinator

Schmitt, Ellen, Harvard University

Facility Technician

Linnon, Beth, Marine Biological Laboratory

Course Assistant

Bradley, Margaret, Marine Biological Laboratory

Students

Challa, Anil Kumar, Ohio State University
Croall, Dorothy, University of Maine
Darimont, Beatrice, University of Oregon
Kaneko, Maki, University of Houston
Leung, Fung Ping, Hong Kong University
Levkowitz, Gil, Weizmann Institute of Science
Lupo, Giuseppe, University of Pisa
Maldonado, Ernesto, Massachusetts Institute of Technology
Mangoli, Maryam, University College London, United Kingdom
Meyer, Martin, Stanford University
Naco, Grace, Johns Hopkins School of Medicine
Nelson, Ralph, National Institutes of Health
Niell, Cristopher, Stanford University
Schneider, Valerie, Harvard Medical School
Starr, Catherine, The Rockefeller University
Yvon, Anne-Marie, University of Massachusetts, Amherst

Neurobiology & Development of the Leech ***(August 13–September 1, 2000)***

Directors

Calabrese, Ronald L., Emory University
Sahley, Christine, Purdue University
Shankland, Martin, University of Texas, Austin

Faculty

Ali, Declan, Hospital for Sick Children
Baader, Andreas, Universität Bern, Switzerland
Bissen, Shirley, University of Missouri
Blackshaw, Susanna, University of Oxford, United Kingdom
Brodfehrer, Peter, Bryn Mawr College
Carbonetto, Salvatore, Montreal General Hospital, Canada
Drapeau, Pierre, McGill University, Canada
Fernandez de Miguel, Francisco, Universidad Nacional Autonoma
de Mexico
Masino, Mark, Emory University
Modney, Barbara, Cleveland State University
Muller, Kenneth, University of Miami School of Medicine
Nicholls, John, SISSA, Italy
Weisblat, David, University of California, Berkeley

Lecturer

Macagno, Eduardo, Columbia University

Course Assistant

Johnson, Ben, Marine Biological Laboratory

Students

Carrasco, Rosa, Purdue University
 Duan, Yuanli, University of Miami
 Kuo, Dian-Han, University of Texas, Austin
 Kwon, Hyung-wook, University of Arizona
 Reka, Lorena, University of Buenos Aires
 Scimemi, Annalisa, SISSA, Italy
 Song, Mi Hye, University of California, Berkeley
 Trueta, Citlali, UNAM
 Weber, Douglas, Arizona State University
 West, Morris, University of Florida
 Yashina, Irene, University of Illinois at Chicago
 Zoccolan, Davide, SISSA, Italy

***Optical Microscopy and Imaging in the
 Biomedical Sciences (October 11–19, 2000)***

Director

Izzard, Colin, State University of New York, Albany

Faculty

DePasquale, Joseph, New York State Department of Health
 Hard, Robert, State University of New York, Buffalo
 Inoué, Shinya, Marine Biological Laboratory
 Maxfield, Frederick, Cornell University Medical College
 Murray, John, University of Pennsylvania School of Medicine
 Piston, David M., Vanderbilt University
 Spring, Kenneth, National Institutes of Health
 Swedlow, Jason, University of Dundee, UK

Lecturers

Hirsch, Jan, Leica, Inc.
 Keller, H. Ernst, Zeiss Optical Systems
 Oldenbourg, Rudolf, Marine Biological Laboratory

Teaching Assistant

Sigurdson, Wade, State University of New York, Buffalo

Course Associate

Snyder, Kenneth, State University of New York, Buffalo

Course Assistant

Pierini, Lynda, Weill Medical College of Cornell University

Students

Arudechandran, Ramachandran, National Institutes of Health
 Christensen, Trace, Mayo Clinic
 Diez, Stefan, Max-Planck-Institute
 Dohrunz, Lynn, University of Alabama, Birmingham
 Flett, Alexander, University of Dundee
 Furie, Bruce, Harvard Medical School
 Garcia-Mata, Rafael, University of Alabama, Birmingham
 Gaspar, Claudia, Montreal General Hospital
 Goldsworthy, Michael, Memorial University of Newfoundland
 Gross, Peter, Beth Israel Deaconess Medical Center
 Hagting, Anja, Wellcome/CRC Institute
 Holtom, Gary, Pacific Northwest National Laboratory
 Hu, Ke, University of Pennsylvania
 Islam, Mohammad, University of Pennsylvania
 Karlsson, Christina, Karolinska Institute

Linser, Paul, Whitney Lab, University of Florida
 Martinez, Angie, Harvard Medical School
 Martins, Gabriel, State University of New York, Buffalo
 North, Alison, Rockefeller University
 Ono, Yasuko, University of Arizona
 Praetorius, Jeppe, National Institutes of Health
 Qiao, Jizeng, Massachusetts General Hospital
 Rice, Marian, Mount Holyoke College
 Schmidtke, David, University of Oklahoma

***Rapid Electrochemical Measurements
 (May 11–15, 2000)***

Director

Gerhardt, Greg, University of Kentucky

Faculty

Cass, Wayne, University of Kentucky
 Carrier, Theresa, University of Kentucky
 Gratton, Alain, McGill University
 Hoffman, Alex, National Institutes of Health
 Huettl, Peter, University of Kentucky
 Palmer, Michael, University of Colorado Health Science Center
 Porterfield, David, University of Missouri-Rolla
 Purdom, Matt, University of Kentucky
 Stanford, John, University of Kentucky
 Sulzer, David, Columbia University
 Surgener, Stewart, University of Kentucky

Teaching Assistants

Burmeister, Jason, University of Kentucky
 Pomerleau, Francois, McGill University

Course Coordinator

Lindsay, Robin, University of Kentucky

Students

Ahmad, Laura, Eli Lilly & Company
 Bruno, John, The Ohio State University
 Byrd, Kenneth, Indiana University School of Medicine
 Cho, Sunyoung, Kyunghee University, Korea
 Espey, Michael, National Institutes of Health
 Fadel, Jim, Vanderbilt University
 Grinevich, Vladimir, University of Kentucky
 Hull, Elaine, State University of New York, Buffalo
 Jackson, Mark, Yale University
 Jow, Brian, Wyeth-Ayerst Research
 Judy, Jack, University of California, Los Angeles
 Kusano, Kiyoshi, National Institutes of Health
 Lan, Esther, University of California, Los Angeles
 Lee, Irwin, Harvard Medical School
 Maidment, Nigel, University of California, Los Angeles
 Montañez, Sylvia, University of Texas Health Science Center
 Olazabal, Daniel, Rutgers University
 Perry, Kenneth, Lilly Research Labs
 Phillips, Janice, University of St. Andrews
 Reid, Stephen, University of Saskatchewan
 Salvatore, Michael, Louisiana State University Health Sciences Center
 Siapas, Athanassios, Massachusetts Institute of Technology
 Walker, Eric, University of California, Los Angeles
 Wilbrecht, Linda, Rockefeller University

Workshop on Molecular Evolution
July 30–August 11, 2000

Director

Cummings, Michael, Marine Biological Laboratory

Faculty

Beerli, Peter, University of Washington
Edwards, Scott, University of Washington
Eisen, Jonathan, Institute for Genomic Research
Felsenstein, Joseph, University of Washington
Fraser, Claire M., Institute for Genomic Research
Huelsenbeck, John P., University of Rochester
Kuhner, Mary, University of Washington
Lewis, Paul O., University of Connecticut
Maddison, Wayne P., University of Arizona
Meyer, Axel, University of Konstanz, Germany
Patel, Nipam, University of Chicago
Pearson, William, University of Virginia Health Sciences Center
Rand, David, Brown University
Rice, Ken, Bioinformatics
Riley, Margaret A., Yale University
Swofford, David, Smithsonian Institution
Thompson, Steven, BioInfo 4U
Voytas, Daniel F., Iowa State University
Yokoyama, Shozo, Syracuse University

Lecturer

Yoder, Anne D., Northwestern University Medical School

Teaching Assistants

Amaral-Zettler, Linda, Marine Biological Laboratory
Babin, Josephine, Louisiana State University
Church, Sheri A., University of Virginia
Dennis, Paige M., University of Massachusetts
Frantz/Dale, Ben
McArthur, Andrew, Marine Biological Laboratory
Medina, Monica, Marine Biological Laboratory
Myers, Daniel, Marine Biological Laboratory
Pritham, Ellen, University of Massachusetts
Reed, David, Louisiana State University
Waring, Molly E., Marine Biological Laboratory

Students

Allender, Charlotte, Southampton University
Ardell, David, Uppsala University
Barbour, Jason, University of California, San Francisco
Barić, Sanja, University of Innsbruck
Bedard, Donna, Rensselaer Polytechnic Institute
Birungi, Josephine, Yale School of Medicine
Borenstein, Seth, Knight Ridder Newspapers
Boykin, Laura, University of New Mexico
Calcagnotto, Daniela, America Museum of Natural History
Cipriano, Frank, San Francisco State University
Drozdowicz, Yolanda, University of Pennsylvania
Eick, Brigitte, University of Cape Town
Epenbeck, Dirk, University of Amsterdam
Ganter, Philip, Tennessee State University
García Sáez, Alberto, Alfred Wegener Institute
García, Martín, UNAM
Gurgel, Carlos, University of Louisiana, Lafayette
Handley, Scott, Centers for Disease Control and Prevention

Hanel, Reinhold, University of Innsbruck
Held, Christoph, Universität Bielefeld
Holland, Brenden, University of Hawaii
Johns, Susan, University of California, San Francisco
Joseph, Leo, Academy of Natural Sciences
Kalia, Awdhesh, Yale University
Kim, Hygyung, Smithsonian Institution
Kulathinal, Rob, McMaster University
Liu, Ji, University of Georgia
Longnecker, Krista, Oregon State University
Lundholm, Nina, University of Copenhagen
Mark Welch, David, Harvard University
McLaughlin, Ian, PE Biosystems
McMahon, Katherine, University of California, Berkeley
Moncayo, Abelardo, University of Texas
Munroe, Stephen, Marquette University
Nepokroeff, Molly, Smithsonian Institution
Newman, Lucy, University of Maryland
Nilsen, Frank, Institute of Marine Research
O'Connor, Daniel, University of California, San Diego
Olson, Julie, Harbor Branch Oceanographic Institution
Pannacciulli, Federica, University of Genoa
Pellegrino, Katia, Brigham Young University
Perez, Ernesto, Université Libre de Bruxelles
Perez-Losada, Marcos, Brigham Young University
Phillips, Louise, University of Melbourne
Regnery, Russell, Centers for Disease Control & Prevention
Rhoads, Allen, Howard University
Richardson, Paul, Joint Genome Institute
Rokas, Antonis, University of Edinburgh
Salzburger, Walter, University of Innsbruck
Sankalé, Jean-Louis, Harvard School of Public Health
Stone, Karen, University of Alaska, Fairbanks
Tiffin, Peter, University of California, Irvine
Utiger, Urs, Zoologisches Museum Zürich
Vasilio, Vasilis, University of Colorado Health Sciences Center
Vincent, Martin, Centers for Disease Control and Prevention
Watson, Linda, Miami University
Westneat, Mark, Field Museum of Natural History
Wilgenbusch, James, Smithsonian Institution
Wilmotte, Annick, University of Liege
Won, Yong-Jin, Rutgers University
Xie, Gang (Gary), Los Alamos National Laboratory

Other Programs

Marine Models in Biological Research
Undergraduate Program
(June 13–August 11, 2001)

Directors

Browne, Carole L., Wake Forest University
Tytell, Michael, Wake Forest University School of Medicine

Faculty

Allen, Nina S., North Carolina State University
Browne, Carole, Wake Forest University
Furie, Barbara, Harvard School of Medicine
Furie, Bruce, Harvard School of Medicine
Gould, Robert, New York State Institute for Basic Research
Hanlon, Roger, Marine Biological Laboratory



Malchow, R. Paul, University of Illinois, Chicago
 Mensinger, Allen, University of Minnesota, Duluth
 Palazzo, Robert, University of Kansas
 Rome, Lawrence, University of Pennsylvania
 Tytell, Michael, Wake Forest University School of Medicine
 Wainwright, Norman, Marine Biological Laboratory

Seminar Speakers

Augustine, George, Duke University Medical Center
 Ehrlich, Barbara, Yale University School of Medicine
 Gallant, Paul, National Institutes of Health
 Hill, Susan, Michigan State University
 Oldenbourg, Rudolf, Marine Biological Laboratory
 Sloboda, Roger, Dartmouth College

Students

Fornwalt, Brandon, University of South Carolina
 Gilles, Nicole, University of Minnesota
 Gupton, Stephanie, North Carolina State University
 Hembree, Chad, Wake Forest University
 Kingston, Margaret, Wake Forest University
 Lee, Tony, Duke University
 Levin, Tracy, Smith College
 Mangiamela, Lisa, Colgate University
 Rosenkranz, Naomi, Yeshiva University
 Szucsik, Amanda, Rutgers University
 Zerbe, Jamie, University of Kansas

NASA Planetary Biology Internship ***(June–September 2000)***

Directors

Dolan, Michael E., University of Massachusetts
 Margulis, Lynn, University of Massachusetts

Interns

Amponsah-Manager, Kwabena, University of Ghana
 Clarkson, William, Oxford University
 Delaye, Luis, National Autonomous University of Mexico
 Finarelli, John, University of New Hampshire
 Lamb, David, University of North Dakota
 Lawson, Jennifer, University of Illinois, Chicago

Lloret y Sánchez, Lourdes, National Autonomous University of Mexico
 Mikuki, Jill A., Portland State University
 O'Donnell, Vicki, National University of Ireland, Maynooth
 Richards, Thomas, Southampton University

Sponsors

Arrhenius, Gustaf, Scripps Institution of Oceanography
 Cady, Sherry, Portland State University
 Des Marais, David, NASA Ames Research Center
 Gogarten, Peter, University of Connecticut
 Hinkle, C. Ross, Kennedy Space Center
 Nierzwicki-Bauer, Sandra, RPI
 Pohorille, Andrew, NASA Ames Research Center
 Priscu, John, Montana State University
 Roberts, Michael S., Kennedy Space Center
 Rothschild, Lynn, NASA Ames Research Center

Semester in Environmental Science ***(September 4–December 15, 2000)***

Administration

Hobbie, John E., Director
 Foreman, Kenneth H., Associate Director
 Moniz, Polly C., Administrative Assistant

Faculty

Deegan, Linda A.
 Foreman, Kenneth H.
 Giblin, Anne E.
 Hobbie, John E.
 Hopkinson, Charles S., Jr.
 Hughes, Jeffrey
 Melillo, Jerry M.
 Nadelhoffer, Knute J.
 Neill, Christopher
 Peterson, Bruce J.
 Rastetter, Edward B.
 Shaver, Gaius R.
 Vallino, Joseph J.
 Williams, Mathew

Research and Teaching Assistants

Eldridge, Cynthia
 Gay, Marcus
 Kwiatkowski, Bonnie
 Micks, Patricia
 Morrisseau, Sarah
 Tholke, Kris

SES Students

Angeloni, Catherine A., Wheaton College
 Bandstra, Leah M., Beloit College
 Businski, Tara N., Bates College
 Chiarelli, Robyn N., Brandeis University
 Creswell, Joel E., Macalester College
 Dalsimer, Heather S., Dickinson College
 Hayes, Alison B., Lawrence University
 Johnson, Rebecca T., Oberlin College
 Karasack, Rebecca D., Dickinson College
 Krumholz, Jason S., Lawrence University

Lawrence, Corey R., Clarkson University
Schwartz, Jessica C., Connecticut College
Shayler, Hannah A., Connecticut College
Taylor, Catherine A., Brandeis University
Teeters, Kelsa E., Brandeis University

Villareal, Greg, University of California, Los Angeles
Whittle, Chris, University of Alaska, Fairbanks

***SPINES—Summer Program in Neuroscience,
Ethics and Survival (June 10–July 8, 2000)***

Directors

Martinez, Joe, University of Texas, San Antonio
Townsel, James G., Meharry Medical College

Faculty

Augustine, George, Duke University
Berger-Sweeney, Joanne E., Wellesley College
Escalona de Motta, Gladys, University of Puerto Rico
Etgen, Anne, Albert Einstein College of Medicine
Fox, Thomas O., Harvard University Medical School
Gonzalez-Lima, Francisco, University of Texas
Maynard, Kenneth I., Massachusetts General Hospital
Zukin, R. Suzanne, Albert Einstein College

Lecturers

Kravitz, Edward, Harvard Medical School
Wyche, James, Brown University

Teaching Assistant

Hohmann, Christine, Morgan State University

Course Coordinator

Garcia, Elizabeth, University of Texas, San Antonio

Students

Boomer, Akilah, Johns Hopkins University
Colón, Wanda, University of Puerto Rico
Davis, Kamisha, University of Utah
Kamendi, Harriet, Howard University
Lorge, Greta, University of Michigan
Mercado, Eduardo, Rutgers University
Reyes, Rosario, University of Oregon
Rodríguez, Gustavo, Purdue University
Vidal, Luis, University of Puerto Rico

***Teachers' Workshop: Living in the Microbial
World (August 13–19, 2000)***

Directors

Dugas, Jeff, University of Connecticut, Storrs
Olendzenski, Lorraine, University of Connecticut, Storrs

Faculty

Dorritie, Barbara, Cambridge Rindge and Latin School, Cambridge, MA
Wier, Andrew, University of Massachusetts, Amherst

Presenters

Amils, Ricardo, Autonomous University of Madrid, Spain
Edgcomb, Virginia, Marine Biological Laboratory
Margulis, Lynn, University of Massachusetts, Amherst
Stolz, John, Duquesne University
Wainwright, Norm, Marine Biological Laboratory

Teacher Participants

Barker, Jean, Pleasant Lea Junior High School, Lee's Summit, MO
Brothers, Chris, Falmouth High School, MA
Campbell, LeeAnne, Mashpee High School, MA
Demetriou, Christina, Astor School, Dover, United Kingdom
Dugan, Maureen, Nashoba Regional High School, Bolton, MA
Ebberly, Stuart, Astor School, Dover, United Kingdom
Estabrooks, Gordon, Boston Latin School, MA
Fenske, Sue, Bernard J. Campbell Junior High School, Lee's Summit, MO
Jaye, Robert, Solomon Schecter Day School, MA
Johnson, Linda, Nauset Regional Middle School, Orleans, MA
Kamborian, Kimberly, Fenway High School, Boston, MA
Kuhn, Gale, Amherst Regional High School, MA
Panico, Suzanne, Fenway High School, Boston, MA
Soracco, Marlene, Bourne High School, MA
Stupples, Eileen, Sir Roger Manwood School, Kent, United Kingdom
Trask, Janet, Mashpee High School, MA
Trimarchi, Ruth, Amherst Regional High School, MA
Tunte, Deb, Nauset Regional Middle School, Orleans, MA
Veneman, Val, Amherst Regional High School, MA
Virchick, Garret, Fenway High School, Boston, MA
Watts, Ngaire, Sir Roger Manwood School, Kent, United Kingdom



Summer Research Programs

Principal Investigators

Antic, Srdjan, Yale University School of Medicine
Armstrong, Clay, University of Pennsylvania
Armstrong, Peter B., University of California, Davis
Augustine, George J., Duke University Medical Center

Baker, Robert, New York University Medical Center
Barlow, Robert B., Jr., State University of New York Health
Science Center

Beaugé, Luis, Instituto de Investigacion Medica "Mercedes y Martin
Ferreyra," Argentina

Belluscio, Leonardo, Duke University Medical Center
Ben-Jonathan, Nira, University of Cincinnati
Bennett, Michael V. L., Albert Einstein College of Medicine
Bodznick, David, Wesleyan University
Boron, Walter, Yale University Medical School
Boyer, Barbara, Union College
Boyle, Richard, Oregon Health Sciences University
Brady, Scott T., The University of Texas Southwestern Medical
Center, Dallas

Brown, Joel, Albert Einstein College of Medicine
Browne, Carole, Wake Forest University School of Medicine
Bruzzone, Roberto, Institut Pasteur, France
Burger, Max M., Friedrich Miescher Institut, Switzerland
Burgess, David, Boston College
Burgos, Mario, Universidad Nacional de Cuyo, Argentina

Changeux, Jean-Pierre, Institut Pasteur, France
Chappell, Richard L., Hunter College, City University of New York
Chiao, Chuan-Chin, University of Maryland
Clay, John, National Institutes of Health
Cohen, Lawrence B., Yale University School of Medicine
Cohen, William D., Hunter College, City University of New York

De Weer, Paul, University of Pennsylvania School of Medicine
Devlin, C. Leah, Penn State University
DiPolo, Reinaldo, Instituto Venezolano Investigaciones Cientificas,
Venezuela
Dodge, Frederick, State University of New York Upstate Medical
University

Edds-Walton, Peggy, University of California, Riverside
Ehrlich, Barbara, Yale University School of Medicine

Fadool, Debra Ann, Florida State University
Fay, Richard, Loyola University of Chicago

Field, Christine, Harvard University Medical School
Fishman, Harvey M., University of Texas Medical Branch, Galveston

Gadsby, David, Rockefeller University
Garcia-Blanco, Mariano, Duke University Medical Center
Gerhart, John, University of California, Berkeley
Giuditta, Antonio, University of Naples, Italy
Goldman, Robert D., Northwestern University Medical School
Gould, Robert, New York State Institute for Basic Research
Groden, Joanna, University of Cincinnati

Haimo, Leah, University of California, Riverside
Hale, Melina, State University of New York, Stony Brook
Haydon, Philip, Iowa State University
Heck, Diane, Rutgers University
Hershko, Avram, Technion-Israel Institute of Technology, Israel
Highstein, Steven M., Washington University School of Medicine
Hill, Susan Douglas, Michigan State University
Hines, Michael, Yale University School of Medicine
Hofmann, Johann, Stanford University
Holmgren, Miguel, Harvard University Medical School
Holz, George, New York University School of Medicine

Johnston, Daniel, Baylor College of Medicine
Jones, Teresa, National Institutes of Health

Kaczmarek, Leonard, Yale University School of Medicine
Kaminer, Benjamin, Boston University School of Medicine
Kaplan, Barry, National Institutes of Mental Health
Kaplan, Ilene M., Union College
Kaupp, U.B., Institut für Biologische Informationsverarbeitung,
Germany

Khan, Shahid, Albert Einstein College of Medicine
Kier, William, University of North Carolina, Chapel Hill
Kirschner, Marc, Harvard University Medical School
Koulen, Peter, Yale University School of Medicine
Kuhns, William, The Hospital for Sick Children, Canada
Kuner, Thomas, Duke University Medical Center

Lafer, Eileen M., University of Texas Health Science Center
Landowne, David, University of Miami School of Medicine
Langford, George, Dartmouth College
Laskin, Jeffrey, University of Medicine and Dentistry of New Jersey
Laufer, Hans, University of Connecticut
LaVail, Jennifer, University of California, San Francisco
LeBaron, Richard, University of Texas, San Antonio
Lenzi, David, University of Virginia School of Medicine
Levitan, Irwin, University of Pennsylvania Medical Center
Link, Brian, Harvard University

Lipicky, Raymond J., Food and Drug Administration
Llinás, Rodolfo R., New York University Medical Center

Magee, Jeff, Louisiana State University Medical Center
Malchow, Robert Paul, University of Illinois, Chicago
Margaroli, Antonio, University of Milan, Italy
Martinez, Joe, University of Texas, San Antonio
McFarlane, Matthew, New York University Medical Center
McNeil, Paul, Medical College of Georgia
Mensing, Allen, University of Minnesota, Duluth
Messerli, Mark, Purdue University
Mitchison, Timothy, Harvard University Medical School
Moore, John W., Duke University Medical Center
Mooseker, Mark, Yale University

Nasi, Enrico, Boston University School of Medicine

Ogden, David, National Institute for Medical Research
Ogunseitan, Oladele A., University of California, Irvine

Palazzo, Robert, University of Kansas
Pant, Harish, National Institutes of Health
Parysek, Linda, University of Cincinnati
Paydarfar, David, University of Massachusetts Medical School

Rakowski, Robert F., Finch University of Health Sciences/The Chicago
Medical School
Ratner, Nancy, University of Cincinnati
Reese, Thomas S., National Institutes of Health
Rieder, Conly, Wadsworth Center
Ripps, Harris, University of Illinois College of Medicine
Rome, Larry, University of Pennsylvania
Rosenbaum, Joel, Yale University
Russell, John M., Syracuse University

Saggau, Peter, Baylor College of Medicine
Salmon, Edward, University of North Carolina, Chapel Hill
Schmolsky, Matthew, University of Utah
Sloboda, Roger D., Dartmouth College
Spiegel, Evelyn, Dartmouth College
Spiegel, Melvin, Dartmouth College
Srinivas, Miduturu, Albert Einstein College of Medicine
Steinacker, Antoinette, University of Puerto Rico
Sugimori, Mutsuyuki, New York University Medical Center

Telzer, Bruce, Pomona College
Tilney, Lewis, University of Pennsylvania
Trinkaus, John P., Yale University
Tytell, Michael, Wake Forest University School of Medicine

Udvardia, Ava, Duke University Medical Center

Wadsworth, Pat, University of Massachusetts
Wang, Jing, Lucent Technologies
Weidner, Earl, Louisiana State University
White, Thomas, Harvard University Medical School
Whittaker, J. Richard, University of New Brunswick, Canada
Wills, Zachary, Harvard University Medical School

Yamoah, Ebenezer, University of California, Davis
Young, Iain, University of Pennsylvania

Zecevic, Dejan P., Yale University School of Medicine
Zimmerberg, Joshua, National Institutes of Health

Zottoli, Steven, Williams College
Zukin, R. Suzanne, Albert Einstein College of Medicine

Other Research Personnel

Abe, Teruo, Niigata University Brain Research Institute, Japan
Ahmed, Tanweer, University of Leeds, United Kingdom
Allen, Nina, North Carolina State University
Altamirano, Anibal, Instituto de Investigacion Medica "Mercedes y
Martin Ferreyra," Argentina
Angarita, Benjamin, Williams College
Artigas, Pablo, Rockefeller University
Asokan, Rengasamy, University of California, Davis
Atherton, Jill, Allegheny College

Basanei, Gorka, National Institutes of Health
Bauer, Sharon, Hunter College
Bendiksby, Michael, Duke University Medical Center
Berberian, Graciela, Instituto de Investigacion Medica "Mercedes y
Martin Ferreyra," Argentina
Bergamaschi, Andrea, University S. Raffaele, Italy
Bertetto, Lisa, Wesleyan University
Bingham, Eula, University of Cincinnati Medical School
Bonacci, Lisa, Hunter College
Bornstein, Gil, Technion—Israel Institute of Technology, Israel
Boudko, Dmitri, University of Florida
Boyle, Richard, Oregon Health Sciences University
Breitwieser, Gerda, Johns Hopkins University School of Medicine
Bucior, Iwona, Friedrich Miescher Institute, Switzerland

Callender, Delon, Hunter College
Chou, Ying-Hao, Northwestern University
Clarkson, Melissa, University of Kansas
Clegg, Janet, University of California, Riverside
Clegg, Michael, University of California, Riverside
Colvin, Robert, Ohio University

Desai, Arshad, European Molecular Biology Laboratory, Germany
Djurisic, Maja, Yale University School of Medicine
Doussau, Frederic, Duke University Medical Center
Dunham, Philip, Syracuse University

Easter, Joshua, Williams College
Eddleman, Christopher, Texas Tech Medical School
Escalada, Arthur, University of Barcelona Medical School, Spain
Eyman, Maria, University of Naples, Italy

Faas, Guido, Baylor College of Medicine
Forger, Daniel, Courant Institute

Gace, Arian, Louisiana State University
Gainer, Harold, National Institutes of Health
Galbraith, James A., National Institutes of Health
Gallant, Paul E., National Institutes of Health
George, Paul, Brown University
Gerosa-Erni, Daniela, Friedrich Miescher Institute, Switzerland
Gilles, Nicole, University of Minnesota
Gioio, Anthony, National Institutes of Health
Goda, Makoto, Kyoto University, Japan
Goldman, Anne E., Northwestern University Medical School
Gomez, Maria del Pilar, Boston University School of Medicine
Grant, Philip, National Institutes of Health

Gupton, Stephanie, North Carolina State University
Gyoeva, Fatima K., Institute of Protein Research, Russia

Hardin, Robert, Brigham and Women's Hospital
Harper, Claudia, Massachusetts Institute of Technology
Harrington, John, University of South Alabama, Mobile
Harrow, Faith, Hunter College
Harwood, Claire, University of Pennsylvania
Hembree, Walter, Wake Forest University
Hernandez, Carlos, New York University School of Medicine
Hernandez, Ruben, University of Texas, San Antonio
Hitt, James, State University of New York Health Science Center
Hiza, Nicholas, Williams College
Hogan, Emilia, Yale University Medical School
Hussain, Mohammad, Albert Einstein College of Medicine
Hutchins, Heidi, National Institutes of Health

Innocenti, Barbara, Iowa State University

Janowitz, Tobias, Yale University
Johanning, Friedrich, Yale University
Jonas, Elizabeth, Yale University
Jones, Kendrick, Brown University

Kamino, Kohtaro, Tokyo University School of Medical and
Dental, Japan
Kang, Guoxin, New York University School of Medicine
Kapoor, Tarun, Harvard University Medical School
Karson, Miranda, Michigan State University
Kingston, Margaret, Wake Forest University
Klimov, Andrei, University of Pennsylvania
Kopacek, Petr, Institute of Parasitology ASCR, The Czech Republic
Koroleva, Zoya, Hunter College
Kreitzer, Mathew, University of Illinois, Chicago
Kumar, Mukesh, National Institutes of Health
Kuner, Thomas, Duke University Medical Center

Lambert, Justin, University of Arizona
Lee, Kyeng Gea, Hunter College
Lee, Licheng, Duke University
Levin, Tracy, Smith College
Levitan, Edwin, University of Pittsburgh School of Medicine
Liu, Vincent, New York University Medical Center
Loboda, Andrey, University of Pennsylvania
Lovell, Peter, Whitney Laboratory
Lowe, Christopher, University of California, Berkeley

Maddox, Paul, University of North Carolina, Chapel Hill
Marder, Eve, Brandeis University
Marshall, Wallace, Yale University
McIntyre, Charmian, Brandeis University
McQuiston, Rory, Baylor College of Medicine
Miller, Todd, Hunter College
Molina, Anthony, University of Illinois, Chicago
Morgan, Jennifer, Duke University Medical Center
Moroz, Leonid, University of Florida
Mutyambizi, Kudakwashe, Williams College

Naitoh, Yutaka, University of Hawaii
Nguyen, Michael P., University of Texas Medical Branch
Nierman, Jennifer, Williams College

Noble, Peter, University of South Carolina

Oegema, Karen, European Molecular Biology Laboratory, Germany

Petersen, Jennifer, National Institutes of Health
Prasad, Kondury, University of Texas Health Science Center
Price, Nichole, Connecticut College

Qian, Haohua, University of Illinois, Chicago

Ramsey, David, Harvard University
Rapoport, Scott, University of California, San Diego
Rhodes, Paul, New York University Medical School
Ringel, Israel, Hebrew University, Israel
Rosenkranz, Naomi, Yeshiva University
Russell, James, National Institute of Health

Saidel, William, Rutgers University
Salzberg, Brian, University of Pennsylvania
Sandberg, Leslie, Dartmouth College
Schneider, Eric, Brown University
Schwartz, Lawrence, University of Massachusetts
Scotto, Lavina, National Institutes of Health
Shuster, Charles, Boston College
Simpson, Tracy, University of Hartford
Solzin, Johannes, Institut für Biologische Informationsverarbeitung,
Germany
Stafford, Phillip, Dartmouth College
Stephens, Natalie, Williams College
Stockbridge, Norman, U.S. Department of Agriculture
Sul, Jai-Yoon, Iowa State University
Szucsik, Amanda, Rutgers University

Takahashi, Joseph, Northwestern University
Tani, Tomomi, Tokyo Metropolitan Institute of Medical Science, Japan
Taylor, Kevin, Wake Forest University
Thrower, Edwin, Yale University
Tokumaru, Hiroshi, Duke University Medical Center
Tokumaru, Keiko, Duke University Medical Center
Tran, Phong, Columbia University
Twersky, Laura, Saint Peter's College
Tyson, Cortni, Williams College

Viitanen, Liisa, Boston College

Wachowiak, Matt, Yale University School of Medicine
Wassersug, Richard, Dalhousie
Weyand, Ingo, Institut für Biologische Informationsverarbeitung,
Germany

Yamaguchi, Ayako, Columbia University
Yoo, Soonmoon, University of Texas Medical Branch

Zakevicius, Jane M., University of Illinois College of Medicine
Zerbe, Jamie, University of Kansas
Zhou, Yuehan, Yale University
Zochowski, Michal, Yale University

Library Readers

Abbott, Jayne, Marine Research
Ahmadjian, Vernon, Clark University
Allen, Garland, Washington University



Alliegro, Mark, Louisiana State University Health Sciences Center
 Alsop, Peggy, Tennessee Department of Health
 Anderson, Everett, Harvard Medical School

Baccetti, Baccio, Institute of General Biology
 Barry, Susan, Mount Holyoke College
 Baylor, Martha, Marine Biological Laboratory
 Benjamin, Thomas, Harvard Medical School
 Bernhard, Jeffery, University of Massachusetts Medical Center
 Bernheimer, Alan, New York University School of Medicine
 Borgese, Thomas, Lehman College-CUNY
 Boyer, John, Union College

Candelas, Graciela, University of Puerto Rico
 Changeux, JeanPierre, Rand Fellowship
 Child, Frank, Trinity College
 Clarkson, Kenneth, Lucent Technologies
 Cobb, Jewel P., California State University
 Cohen, Seymour, American Cancer Society
 Cooperstein, Sherwin J., University of Connecticut Health Center
 Copeland, Donald, Marine Biological Laboratory
 Corwin, Jeffrey, University of Virginia
 Cowling, Vincent, Palm Beach, FL

De Toledo-Morrell, Leyla, Rush University

Epstein, Herman, Brandeis University

Fraenkel, Dan, Harvard Medical School
 Frenkel, Krystyna, New York University School of Medicine

Galatzer-Levy, Robert, University of Chicago
 German, James, Cornell University Medical College
 Grossman, Albert, New York University Medical School
 Gruner, John, Cephalon, Inc.

Harrington, John, University of South Alabama
 Haubrich, Robert, Denison University
 Haugaard, Niels, HUP Philadelphia
 Herskovits, Zara, Belfer Educational Center
 Herskovits, Theodore, Fordham University
 Hitchcock-DeGregorii, Sarah, Robert Wood Johnson Medical School
 Hunter, Robert, Gartnaval Royal Hospital

Inoue, Sadayuki, McGill University
 Issodorides, Marietta, Athens, Greece

Jacobson, Allan, University of Massachusetts Medical School
 Jaye, Robert, Solomon Schechter Day School
 Josephson, Robert K., University of California, Irvine

Kaltenbach, Jane, Mount Holyoke College
 Karlin, Arthur, Columbia University
 Kelly, Robert, University of Illinois
 King, Kenneth, Falmouth, MA
 Kornberg, Hans, Boston University
 Krane, Stephen, Harvard Medical School

Laster, Leonard, University of Massachusetts Medical Center
 Lee, John, City College of New York
 Lesser, Carolyn, University of Wisconsin
 Linck, Richard, University of Minnesota
 Lorand, Laszlo, Northwestern University Medical School
 Luckenbill, Louise, Ohio University

Mauzerall, David, Rockefeller University
 Mitchell, Ralph, Harvard University
 Mizell, Merle, Tulane University
 Mizoguchi, Hazime, Johns Hopkins University

Nagel, Ronald, AECOM NYC
 Naugle, John, National Aeronautics and Space Administration
 Nickerson, Peter, SUNY Buffalo

Pappas, George D., University of Illinois, Chicago
 Prendergast, Robert, John Hopkins University

Schippers, Jay, Resource Foundation
 Shepro, David, Boston University
 Siwicki, Kathleen, Swarthmore College
 Spector, Abraham, Columbia University
 Spotte, Stephen, University of Connecticut
 Sundquist, Eric, USGS
 Sweet, Frederick, Washington University

Trager, William, The Rockefeller University
 Tweedell, Kenyon, University of Notre Dame
 Tykocinski, Mark, University of Pennsylvania

Van Holde, Kensal, Oregon State University

Walton, Alan, Cavendish Lab
 Warren, Leonard, University of Pennsylvania

Yevick, George, Stevens Institute of Technology

Domestic Institutions Represented

Academy of Natural Sciences
 Alabama, University of, Birmingham
 Alaska, University of, Anchorage
 Alaska, University of, Fairbanks
 Albert Einstein College of Medicine
 Allegheny College
 American Cancer Society
 American Museum of Natural History
 Argonne National Laboratory
 Arizona State University
 Arizona, University of, Tucson
 Arkansas, University of

2000 Library Room Readers

Lucio Cariello
Stazione Zoologica A. Dohrn

Michael Clegg

Giuseppe D'Alessio
University of Naples

Robert Goldman
Northwestern University Medical School

Harlyn Halvorson
Marine Biological Laboratory

Michael Hines
Yale University School of Medicine

Alex Keynan
Israel Academy of Science

John Moore
Duke Medical Center

Michael Rabinowitz
Marine Biological Laboratory

George Reynolds
Princeton University

Ann Stuart
UNC Chapel Hill

Gerry Weissmann
NYU School of Medicine

Association of Telehealth Providers
AT&T Bell Laboratories

Battle Creek Veterans Administration
Baylor College of Medicine
Bell Laboratories
BioHybrid Technologies, Inc.
BioInfo 4U
Bioinformatics
Bioresources Development and Conservation Programme
Blue Cross Blue Shield of Maryland
Boston College
Boston University
Boston University School of Medicine
Bowdoin College
Brandeis University
Brigham and Women's Hospital
Brigham Young University
Brown University
Bryn Mawr College
Buck Center for Research in Aging

California Institute of Technology
California, University of, Berkeley
California, University of, Davis
California, University of, Irvine
California, University of, Los Angeles
California, University of, Riverside
California, University of, San Diego
California, University of, San Francisco
California, University of, Santa Barbara
Care First Blue Cross Blue Shield
Carnegie Institution of Washington
Carnegie Mellon University
Case Western Reserve Medical School
Case Western Reserve University
Catholic University of America
Centers for Disease Control and Prevention
Cephalon, Inc.
Chicago College of Osteopathic Medicine
Chicago, University of
Children's Hospital, Boston
Children's Memorial Hospital—CMIER
Children's National Medical Center
Cincinnati University Medical Center
Cincinnati, University of
City College of New York
Clarian Health
Cleveland State University
Cold Spring Harbor Laboratory
Colorado University Health Science Center
Colorado, University of, Boulder
Colorado University School of Medicine
Columbia University
Connecticut College
Connecticut University Health Center
Connecticut, University of
Cornell University
Cornell University Medical College
Courant Institute

Dartmouth College
Dartmouth Medical School
Deaconess Medical Center

Delaware, University of
Denison University
Doheny Eye Institute
Duke University
Duke University Medical Center
DuPont Hospital for Children

Eli Lilly & Company
Emory University
Emory University School of Medicine
Exelixis, Inc.

Field Museum of Natural History
Finch University of Health Sciences
Florida Institute of Technology
Florida State University
Florida University Brain Institute
Florida University College of Medicine
Florida, University of
Food and Drug Administration
Fordham University
Fred Hutchinson Cancer Research Center

Georgia, University of
Guthrie Healthcare System

Hampton University
Harbor Branch Oceanographic Institution
Harbor-UCLA Medical Center
Hartford, University of
Harvard Medical School
Harvard School of Public Health
Harvard University
Hawaii, University of
Health Care Financing Administration
Hines VA Hospital
Hospital for Special Surgery
Hospital of the University of Pennsylvania
House Ear Institute
Houston Academy of Medicine
Houston, University of
Howard Hughes Medical Institute
Howard University
Howard University School of Medicine
Hunter College

Idaho, University of
Illinois, University of, Chicago
Illinois, University of, Urbana-Champaign
Indiana University
Indiana University School of Medicine
Ingham Regional Medical Center
Institute for Genomic Research
Iowa University College of Medicine
Iowa State University
Iowa, University of

Johns Hopkins University
Johns Hopkins University School of Medicine
Joint Genome Institute

Kansas University Medical Center
Kansas, University of
Kent State University

R40 Annual Report

Kentucky University Medical Center
Kentucky, University of
Kewalo Marine Laboratory
King/Drew Medical Center
Knight Ridder Newspapers

Lahey Clinic
Lawrence Berkeley National Laboratory
Lehman College, CUNY
Leica, Inc.
Lilly Research Labs
Los Alamos National Laboratory
Louisiana State University
Louisiana State University Health Sciences Center
Louisiana, University of, Lafayette
Louisville, University of
Loyola University of Chicago
Lucent Technologies

Magee-Women's Research Institute
Maine, University of
Mani'iaq Health Center
Marine Biological Laboratory
Marquette University
Marshfield Medical Research Foundation
Maryland, University of, Baltimore County
Massachusetts Eye and Ear Infirmary
Massachusetts General Hospital
Massachusetts Institute of Technology
Massachusetts, University of, Amherst
Massachusetts, University of, Medical School
Maxygen, Inc.
Mayo Clinic and Foundation
McCrone Research Institute
Medical College of Georgia
Medical University of South Carolina
Meharry Medical College
Memorial Sloan-Kettering Cancer Center
Merck & Co.
Miami, University of
Miami University School of Medicine
Michigan State University
Michigan University Medical School
Michigan, University of
Midwestern University
Minnesota University Medical School
Minnesota, University of
Missouri, University of, Rolla
Montana State University
Monterey Bay Aquarium Research Institute
Morehouse School of Medicine
Morgan State University
Mount Holyoke College
Mount Sinai School of Medicine
Murdoch Institute

National Aeronautics and Space Administration
National Institute of Mental Health
National Institute on Aging, NIH
National Institutes of Health
National Library of Medicine
Nature America
Naval Medical Center, San Diego
Nebraska, University of, Lincoln

NEC Research Institute
Neuroscience Institute
Nevada University School of Medicine
New England Regional Primate Research Center
New Mexico, University of
New York Health Science Center, State University of
New York State Department of Health
New York State Institute for Basic Research
New York, State University of, Albany
New York, State University of, Buffalo
New York, State University of, Stony Brook
New York University
New York University Medical Center
New York University School of Medicine
Norman Regional Hospital
North Carolina State University
North Carolina, University of, Chapel Hill
Northwestern Medical Faculty Foundation
Northwestern University
Northwestern University Medical School
Notre Dame, University of

Oberlin College
Ohio State University
Ohio University
Oregon Health Sciences University
Oregon Regional Primate Research Center
Oregon State University
Oregon, University of

PE Biosystems
Penn State University
Pennsylvania State University College of Medicine
Pennsylvania University Medical Center
Pennsylvania, University of
Pennsylvania University School of Medicine
Pfizer Central Research
Pharmacia & Upjohn
Pittsburgh, University of
Pomona College
Princeton University
Proteome, Inc.
Puerto Rico, University of
Purdue University
Purdue University Cancer Center

Q3DM, Inc.

Regenstrief Institute
Rensselaer Polytechnic Institute
Riverside Regional Medical Center
Robert Wood Johnson Medical School
Roche Diagnostics
Rochester, University of
Rockefeller University, The
Rosetta Inpharmatics
Rush-Presbyterian-St. Luke's Medical Center
Rutgers College of Pharmacy
Rutgers University

Saint Peter's College
Salk Institute
San Francisco State University
Scripps Institution of Oceanography

Scripps Research Institute
 Seattle Biomedical Research Institute
 Smith College
 Smithsonian Institution
 Solomon Schechter Day School
 SoundVision Productions
 South Alabama, University of
 South Carolina, University of
 South Florida, University of
 Southampton University
 Southern California, University of
 Southern Mississippi, University of
 St. Elizabeth's Medical Center
 St. Joseph's Hospital
 St. Louis VA Medical Center
 St. Mary's College of Maryland
 Stanford University
 Stanford University Medical Center
 Stanford University School of Medicine
 Stevens Institute of Technology
 Swarthmore College
 Swedish Medical Center
 Syracuse University

Temple University School of Medicine
 Tennessee Department of Health
 Tennessee State University
 Texas A&M University
 Texas Tech Medical School
 Texas University Health Science Center
 Texas University Medical School
 Texas, University of, Austin
 Texas, University of, Houston
 Texas, University of, San Antonio
 Texas University Southwestern Medical Center
 Toledo, University of
 Trover Foundation
 Tufts University
 Tufts University School of Medicine
 Tulane University

U.S. Department of Agriculture
U.S. News & World Report
 Uniformed Services University
 Union College
 University of Medicine and Dentistry of New Jersey
 Utah University Medical Center
 Utah, University of

VA Information Research Center
 VA Maryland Health Care System
 Vanderbilt University
 Vanderbilt University Medical Center
 Vanderbilt-Ingram Cancer Center
 Vermont, University of
 Veterans Administration Hospital
 Veterans Affairs Medical Center
 Virginia University Health Sciences Center
 Virginia University Medical Center
 Virginia, University of

Wadsworth Center
 Wake Forest University
 Wake Forest University School of Medicine

Washington University
 Washington, University of
 Washington University School of Medicine
 Weill Medical College of Cornell University
 Wellesley College
 Wesleyan University
 Western Reserve Medical School
 Westvaco Forest Sciences Lab
 Whitehead Institute
 Whitney Laboratory, University of Florida
 Williams College
Winston-Salem Journal
 Wisconsin, University of, Madison
 Woods Hole Oceanographic Institution
 Wyeth-Ayerst Research

Yale University
 Yale University School of Medicine
 Yeshiva University

Zeiss Optical Systems

Foreign Institutions Represented

Aberdeen, University of, Scotland
 Albert-Ludwigs-Universität Freiburg, Germany
 Alfred Wegener Institute, Germany
 Amsterdam, University of, The Netherlands
 Australian National University, Australia

Basel Institute for Immunology, Switzerland
 Basel, University of, Switzerland
 Bern, University of, Switzerland
 Bielefeld, University of, Germany
 Biomedical Primate Research Centre, The Netherlands
 Boehringer Ingelheim Pharmaceuticals, Inc., Germany
 Buenos Aires, University of, Argentina

Calgary, University of, Canada
 Cambridge University, United Kingdom
 Cape Town, University of, South Africa
 Centre de Genetique Moleculaire, France
 Centre National de la Recherche Scientifique—CNRS, France
 Centro de Pesquisas "René Rachou," Brazil
 Charles University, Prague, Czech Republic
 Comision Nacional de Energia Atomica, Argentina
 Copenhagen, University of, Denmark

Dalhousie University, Canada
 Dundee, University of, Scotland

Edinburgh, University of, Scotland
 European Molecular Biology Laboratory, Germany

Friedrich Miescher Institute, Switzerland
 Freie Universität, Berlin, Germany

Gartnavel Royal Hospital, Scotland
 Genoa, University of, Italy
 Glasgow, University of, Scotland
 Göteborg University, Sweden
 Guelph, University of, Canada

- Hagedorn Research Institute, Denmark
Hebrew University, Israel
Hebrew University Medical School, Israel
Hohenheim, University of, Germany
Hong Kong, University of
Hong Kong University of Science and Technology
Hospital for Sick Children, Canada
Humboldt Universität Berlin, Germany
Hungarian Academy of Sciences, Hungary
- IBDM, Marseille, France
Imperial College of Science, Technology and Medicine, United Kingdom
Innsbruck, University of, Austria
Institut für Biologische Informationsverarbeitung, Germany
Institut Pasteur, France
Institute of Cell, Animal, and Population Biology, Scotland
Institute of Neurophysiology, Pisa, Italy
Institute of Parasitology ASCR, The Czech Republic
Institute of Protein Research, Russia
Instituto de Investigacion Medica "Mercedes y Martin Ferreyra," Argentina
Instituto de Investigaciones Biomedicas, Spain
Instituto Gulbenkian de Ciencia, Portugal
Instituto Nacional de la Nutricion, Mexico
Instituto Venezolano Investigaciones Cientificas, Venezuela
Istituto Internazionale di Genetica e Biofisica, Italy
- Karolinska Institute, Sweden
Köln, University of, Germany
Konstanz, University of, Germany
Kyoto University, Japan
Kyunghee University, Korea
- Leeds, University of, United Kingdom
Leicester, University of, United Kingdom
Leiden University Medical Centre, The Netherlands
Lethbridge, University of, Canada
Liege, University of, Belgium
Linköping University, Sweden
Ludwig-Maximilian University, Germany
- Manchester, University of, United Kingdom
Marine Biology Station, France
Max-Planck-Institute for Biological Cybernetics, Germany
Max-Planck-Institute for Medical Research, Germany
McGill University, Canada
McMaster University, Canada
Medical Research Council, United Kingdom
Melbourne, University of, Australia
Montreal General Hospital, Canada
Montreal, University of, Canada
- Naples, University of, Italy
National Institute for Medical Research, United Kingdom
Netherlands Cancer Institute
- New Brunswick, University of, Canada
Newcastle-upon-Tyne, University of, United Kingdom
Niigata University Brain Research Institute, Japan
Nobel Institute for Neurophysiology, Sweden
- Oldenburg, University of, Germany
Ottawa, University of, Canada
Oxford University, United Kingdom
- Palermo, University of, Italy
Perugia, University of, Italy
Pisa, University of, Italy
Porto, University of, Portugal
PPL Therapeutics Inc., Scotland
Punjab Agricultural University, India
- Rayne Institute, United Kingdom
Rio de Janeiro, University of, Brazil
Roslin Institute, Edinburgh, Scotland
- Sao Paulo, University of, Brazil
Sars Centre, Norway
Saskatchewan, University of, Canada
Scuola Internazionale Superiore di Studi Avanzati (SISSA), Italy
Scuola Normale Superiore, Italy
Shirshov Institute of Oceanology, Russia
Simon Fraser University, Canada
Sofia Instituto Gulbenkian de Ciência, Portugal
St. Andrews, University of, Scotland
Stirling, University of, Scotland
Stockholm University, Sweden
Surrey, University of, United Kingdom
Sussex, University of, United Kingdom
Swiss Federal Institute of Technology, Switzerland
Swiss Institute for Experimental Cancer Research, Switzerland
Sydney, University of, Australia
- Tata Institute of Fundamental Research, India
Technion-Israel Institute of Technology, Israel
Teikyo University Biotechnology Research Center, Japan
Tokyo University School of Medical and Dental, Japan
- Universidad Autonoma Metropolitana, Mexico
Universidad Nacional Autonoma de Mexico
Universidad Nacional de Cuyo, Argentina
Universidade Federal de Minas Gerais, Brazil
Universität Freiburg, Germany
Université Libre de Bruxelles, Belgium
Université Paris-Sud, France
Uppsala University, Sweden
- Veterinary Vaccine Institute, India
- Weizmann Institute of Science, Israel
Western Ontario, University of, Canada
- Zurich, University of, Switzerland



Year-Round Research Programs

Architectural Dynamics in Living Cells Program

Established in 1992, this program focuses on architectural dynamics in living cells—the timely and coordinated assembly and disassembly of macromolecular structures essential for the proper functioning, division, motility, and differentiation of cells; the spatial and temporal organization of these structures; and their physiological and genetic control. The program is also devoted to the development and application of powerful new imaging and manipulation devices that permit such studies directly in living cells and functional cell-free extracts. The Architectural Dynamics in Living Cells Program promotes interdisciplinary research carried out by resident core and visiting investigators.

Resident Core Investigators

Inoué, Shinya, Distinguished Scientist
Oldenbourg, Rudolf, Associate Scientist
Shribak, Michael, Staff Scientist

Staff

Knudson, Robert, Instrumental Development Engineer
Baraby, Diane, Laboratory Assistant
MacNeil, Jane, Executive Assistant

Visiting Investigators

Desai, Arshad, EMBL, Heidelberg, Germany
Fukui, Yoshio, Northwestern University Medical School
Goda, Makoto, Kyoto University, Japan
Keefe, David, Rhode Island Women and Infants Hospital
Liu, Lin, Rhode Island Women and Infants Hospital
Maddox, Paul, University of North Carolina—Chapel Hill
Mitchison, Timothy J., Harvard Medical School
Salmon, Edward D., University of North Carolina—Chapel Hill
Tran, Phong, Columbia University

The Josephine Bay Paul Center for Comparative Molecular Biology and Evolution

This Center employs the latest advances in phylogenetic theory, computational biology, and high-throughput genome sciences to study evolutionary processes that trace back to the first life forms on earth. Through the application of high-powered statistical techniques, scientists in the Josephine Bay Paul Center investigate how the evolution of genes and genomes has driven phenotypic change at all levels of biological

organization. This holistic approach provides tools to quantify and assess biodiversity and to identify genes and genetic mechanisms of biomedical and environmental importance. We study all kinds of microbes, their evolutionary history, their interactions with each other and macroscopic forms of life, and how members of diverse microbial communities contribute and respond to environmental change. Examples of current research include: 1) a project supported by the National Science Foundation to study the co-evolution of genomes for symbiotic bacteria and their hosts; 2) investigations supported by the National Institutes of Health to study expression and the complete genome sequence of *Giardia lamblia*, a water-borne human pathogen that attacks the intestinal tract and exacts a terrible toll on public health worldwide; 3) a computational biology program funded by the NIH, NASA, and private corporations to integrate evolutionary theory with the functional annotation of protein coding regions in bacterial genomes; and 4) an interdisciplinary study supported by NASA and NSF to study life in extreme environments on the planet earth in search of general principles that can guide the quest for living forms elsewhere in the universe. The Center encourages studies of genotypic diversity across all phyla and promotes the use of modern molecular genetics and phylogeny to gain insights into the evolution of molecular structure and function.

Our research activities are complemented by an active education program. In addition to training postdoctoral fellows, the Josephine Bay Paul Center offers the internationally recognized Workshop in Molecular Evolution at the Marine Biological Laboratory, a workshop for secondary educators titled Living in the Molecular World, and several comprehensive web sites: 1) a description of research and education associated with our membership in the Astrobiology Institute at the Marine Biological Laboratory; 2) the interactive EcoCyc Project (an interactive program that describes the metabolism of *E. coli* as well as the identity and location of functional genes in the *E. coli* genome); 3) the *Giardia lamblia* genome page (which provides annotated analyses and current progress summaries from the MBL's *Giardia lamblia* genome project); and 4) the Workshop in Molecular Evolution site (which offers descriptions, information, and advice about sophisticated software packages for phylogenetic inferences and analyses of population biology data).

A generous gift from the Bay Paul Foundation and continuing annual support from the G. Unger Vettesen Foundation provided initial funding in 1997 to form The Josephine Bay Paul Center for Comparative Molecular Biology and Evolution. The Center has excellent resources for studies of molecular biology and evolution, including well-equipped research laboratories and a powerful computational facility. With a grant from the W.M. Keck Foundation in 2000, the center established a technology-rich Ecological and Evolutionary Genetics Facility. This advanced laboratory provides a full range of high-throughput, DNA-sequencing equipment, a DNA microarray facility and high-performance computers. Several adjunct appointments and collaborative projects strengthen research activities in the center. These activities include interdisciplinary investigations of microbial diversity with scientists at the Woods Hole Oceanographic Institution, molecular ecology studies at the MBL Ecosystem Center's Plum Island LTER site, physiology

R44 Annual Report

studies of acidophilic protists with the MBL BioCurrents Research Center, and collaborative efforts to study mechanisms and patterns of evolution with faculty of Harvard University, the Harvard School of Public Health, and the University of Sydney, Australia. Future expansion in the Josephine Bay Paul Center will focus upon molecular evolution of global infectious disease and genome sciences.

Resident Core Investigators

Sogin, Mitchell, Director and Senior Scientist
Cornell, Neal, Senior Scientist
Cummings, Michael, Assistant Scientist
McArthur, Andrew, Staff Scientist II
Morrison, Hilary, Staff Scientist II
Riley, Monica, Senior Scientist
Wernegreen, Jennifer, Assistant Scientist

Adjunct Scientists

Halanych, Ken, Woods Hole Oceanographic Institution
Meselson, Matthew, Harvard University
Patterson, David, University of Sydney
Teske, Andreas, Woods Hole Oceanographic Institution

Laboratory of Neal Cornell

Dr. Neal Cornell, a senior scientist at the Marine Biological Laboratory, played a key role in designing and attracting new faculty to the Josephine Bay Paul Center for Comparative Molecular Biology and Evolution. Dr. Cornell passed away in 2000, but all of us who knew him cherish fond memories and harbor a deep gratitude for his contributions to science and the MBL community. Research in Dr. Cornell's laboratory, which continued to pursue his research goals through the end of 2000, was concerned with the comparative molecular biology of genes that encode the enzymes for heme biosynthesis. These efforts placed particular emphasis on 5-aminolevulinic synthase, the first enzyme in the pathway. Because the ability to produce heme from common metabolic materials is a near universal requirement for living organisms, these genes provide useful indicators of molecular aspects of evolution. For example, 5-aminolevulinic synthase in vertebrate animals and simple eukaryotes such as yeast and *Plasmodium falciparum* have high sequence similarity to the enzyme from the alpha-purple subgroup of eubacteria. This supports the suggestion that alpha-purple bacteria are the closest contemporary relatives of the ancestor of eukaryotic mitochondria. The analysis also raises the possibility that plant and animal mitochondria had different origins. Aminolevulinic synthase genes in mitochondria-containing protists are currently being analyzed to obtain additional insight into endosymbiotic events. Also, genes of primitive chordates are being sequenced to gain information about the large-scale gene duplication that played a very important role in the evolution of higher vertebrates. Other studies in the laboratory have been concerned with the effects of environmental pollutants on heme biosynthesis in marine fish, and it has been shown that polychlorinated biphenyls (PCBs) enhance the expression of the gene for aminolevulinic synthase.

Staff

Cornell, Neal W., Senior Scientist
Faggart, Maura A., Research Assistant



Laboratory of Michael P. Cummings

Our research is in the area of molecular evolution and genetics and includes examination of patterns and processes of sequence evolution. We use methods from molecular biology, population genetics, systematics, statistics, and computer science. The basis for much of the research is comparative; it includes several levels of biological organization, and involves both computer-based and empirical studies. A major research focus is analysis genotype-phenotype relationships using tree-based statistical models (decision trees) and extension of this methodology. Current investigations in this area examine how gene sequence data can be used to understand and predict drug resistance in tuberculosis, variation in color vision, and basic immune system functions at the molecular level. For example, using drug resistance in *Mycobacterium tuberculosis* as a model system, we are investigating how well phenotype (level of drug resistance) can be predicted with genotype information (DNA sequence data). Understanding evolution of drug resistance, and developing accurate methods for its prediction using DNA sequence data, can help in assessing potential resistance in a more timely fashion and circumvent the need for culturing bacteria. More generally, the relationship of genotype to phenotype is a fundamental problem in genetics, and through these investigations we hope to gain insight. The primary empirical work in the laboratory involves examination of opsins, proteins involved in color vision, from local species of Odonata (dragonflies and damselflies). Other projects include a review of genetic diversity in plants using coalescence-based analyses and the genetic consequences of reserve designs in conservation.

Staff

Cummings, Michael P., Assistant Scientist
McInerney, Laura A., Research Assistant II

Visiting Investigators

Clegg, Michael T., University of California, Riverside
 Clegg, Janet, University of California, Riverside
 Neel, Maile C., University of California, Riverside

Visiting Graduate Students

Church, Sheri A., University of Virginia
 Garcia-Verela, Martín, Universidad Nacional Autónoma de México

Undergraduates

Myers, Daniel S., Pomona College
 Waring, Molly E., Harvey Mudd College

Laboratory of Monica Riley

The genome of the bacterium *Escherichia coli* contains all of the information required for a free-living chemoautotrophic organism to live, adapt, and multiply. The information content of the genome can be dissected from the point of view of understanding the role of each gene and gene product in achieving these ends. The many functions of *E. coli* have been organized in a hierarchical system representing the complex physiology and structure of the cell. In collaboration with Dr. Peter Karp of SRI International, an electronic encyclopedia of information has been constructed on the genes, enzymes, metabolism, transport processes, regulation, and cell structure of *E. coli*. The interactive EcoCyc program has graphical hypertext displays, including literature citations, on nearly all of *E. coli* metabolism, all genes and their locations, a hierarchical system of cell functions and some regulation and transport processes.

In addition, the *E. coli* genome contains valuable information on molecular evolution. We are analyzing the sequences of proteins of *E. coli* in terms of their evolutionary origins. By grouping like sequences and tracing back to their common ancestors, we learn not only about the paths of evolution for all contemporary *E. coli* proteins, but we extend even further back before *E. coli*, traversing millennia to the earliest evolutionary times when a relatively few ancestral proteins served as ancestors to all contemporary proteins of all living organisms. The complete genome sequence of *E. coli* and sophisticated sequence analysis programs permit us to identify evolutionarily related protein families, determining ultimately what kinds of unique ancestral sequences generated all of present-day proteins. The data developed in the work has proven to be valuable to the community of scientists sequencing other genomes. *E. coli* data serve as needed reference points.

Staff

Riley, Monica, Senior Scientist
 Liang, Ping, Staff Scientist I
 McConnack, Tom, Postdoctoral Scientist
 Nahum, Laila, Postdoctoral Scientist
 Pelegrini-Toole, Alida, Research Assistant II
 Serres, Margerethe, Postdoctoral Scientist

Laboratory of Mitchell L. Sogin

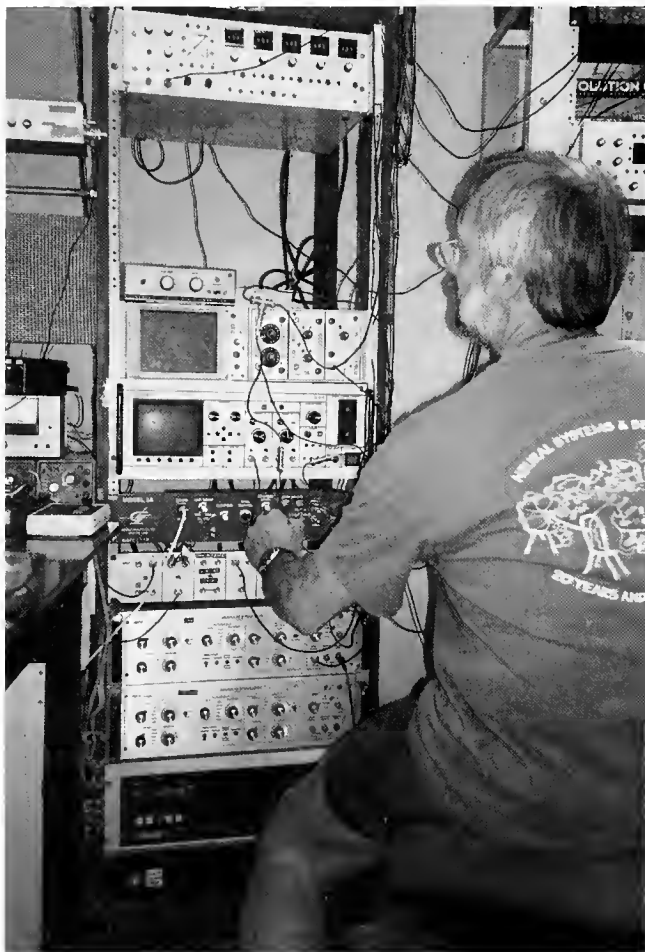
This laboratory employs comparative phylogenetic studies of genes and genomes to define patterns of evolution that gave rise to contemporary biodiversity on the planet earth. The laboratory is especially interested in discerning how the eukaryotic cell was invented as well as the identity of microbial groups that were ancestral to animals, plants, and fungi. The laboratory takes advantage of the extraordinary conservation of ribosomal RNAs to define phylogenetic

relationships that span the largest of evolutionary distances. These studies have overhauled traditional eukaryotic microbial classifications systems. The laboratory has discovered new evolutionary assemblages that are as genetically diverse and complex as plants, fungi, and animals. The nearly simultaneous separation of these eukaryotic groups (described as the eukaryotic "Crown") occurred approximately one billion years ago and was preceded by a succession of earlier diverging protist lineages, some as ancient as the separation of the prokaryotic domains. Many of these early branching life forms are represented by parasitic protists including *Giardia lamblia*, which is a significant human parasite. Because of its medical importance and relevance to understanding the evolutionary history of eukaryotes, we have initiated a project to determine the entire genome sequence of *Giardia lamblia*. In addition to identifying other genes that will be of value for unraveling sudden evolutionary radiations that cannot be resolved by rRNA comparisons, this project will provide insights into the presence or absence of important biochemical properties in the earliest ancestors common to all eukaryotic species. Finally, this project has revealed important features of genome architecture that require a reconsideration of available mechanisms for controlling gene expression in eukaryotes.

A second research theme is the study of microbial life in extreme environments and molecular-based investigations of diversity and gene expression in microbial communities. Using the ribosomal RNA database and nucleic acid-based probe technology, it is possible to detect and monitor microorganisms, including those that cannot be cultivated in the laboratory. This strategy has uncovered new habitats and major revelations about geographical distribution of microorganisms. We are particularly interested in protists that thrive in acid mine drainages and the characterization of physiological mechanisms that allow their growth at extraordinarily low (<2.0) pH levels. Our investigations of gene expression in microbial communities is based upon the premise that microorganisms are the primary engines of our biosphere. They orchestrate all key processes in geochemical cycling, biodegradation, and in the protection of entire ecosystems from environmental insults. They are responsible for most of the primary production in the oceans. Microbial creatures of untold diversity have complex chemistries, physiologies, developmental cycles, and behaviors. With the powerful tools of high-throughput DNA sequencing and DNA microarrays for massive parallel expression studies, we can directly measure how microbial gene expression patterns in an entire ecosystem respond to changing chemical and physical parameters. We will employ an experimental paradigm that links biogeochemical processes with ever-changing temporal and spatial distributions of microbial populations and their metabolic properties. The concurrent measurement of biogeochemical parameters, community-wide gene expression patterns, and spatial descriptions of microbial populations offers a means to understand the structure and function of biogeochemical machinery at different levels of biological organization. We seek to discover the links between biological diversity and the resilience and stability of biogeochemical transformations.

Staff

Sogin, Mitchell L., Director and Senior Scientist
 Amaral Zettler, Linda, Postdoctoral Scientist
 Beaudoin, David, Research Assistant
 Bressoud, Scott, Laboratory Technician
 Eakin, Nora, Research Assistant
 Edcomb, Virginia, Postdoctoral Scientist
 Farr, Rebecca, Research Assistant
 Gao, Lingqiu, Research Assistant II
 Kim, Ulandt, Research Assistant
 Kysela, David, Research Assistant
 Laan, Maris, Research Assistant II



Lim, Pauline, Executive Assistant
 Luders, Bruce, Research Assistant
 McArthur, Andrew, Postdoctoral Scientist
 Medina, Monica, Postdoctoral Scientist
 Morrison, Hilary G., Postdoctoral Scientist
 Nixon, Julie, Postdoctoral Scientist
 Sansone, Rebecca, Executive Assistant
 Schlichter, Mimi, Executive Assistant
 Shulman, Laura, Senior Research Assistant
 Shakir, Muhammed Afaq, Postdoctoral Scientist

Visiting Investigators

Bahr, Michele, The Ecosystems Center
 Campbell, Robert, Serono Laboratories, Inc.
 Crump, Byron, The Ecosystems Center

Laboratory of Jennifer Wernegreen

The work in this lab focuses on the evolution of bacteria that complete their life cycles within or closely related with eukaryotic host cells. These symbiotic prokaryotes include well-known parasites as well as obligately mutualistic bacteria that provide nutritional or other benefits to their hosts. By virtue of their host associations, endosymbionts may have smaller population sizes and experience different selective forces than their free-living bacterial relatives. These changes in population size and selection may each contribute to the features shared by many endosymbiont genomes, such as low genomic

G + C (guanine + cytosine) contents, small genome sizes, and elevated rates of DNA sequence evolution. Our research explores the molecular and evolutionary mechanisms that shape these characteristics of endosymbiont genomes, with a focus on mutualistic endosymbionts of insects and obligate pathogens of animals.

One aim of this lab is to differentiate the effects of genetic drift, directional mutation pressure, and natural selection on molecular evolution of symbiotic and free-living bacteria. Our primary approach has been to compare patterns of DNA sequence divergence at homologous loci across symbiotic and related free-living bacterial species. These comparisons have revealed a strong effect of genetic drift and directional mutational pressure on sequence evolution in *Buchnera aphidicola*, the vertically transmitted endosymbiont of aphids, compared to its close free-living relative, *Escherichia coli*. Recently, our molecular phylogenetic analyses have shown that *Buchnera* lacks horizontal gene transfer that is typical of many free-living bacterial groups. On-going and future work will explore the molecular evolution of other insect endosymbionts in the gamma-3 Proteobacteria, including the obligate bacterial associates of carpenter ants (*Camponotus*). We also employ full genome comparisons to identify genes that have been lost in small endosymbiont genomes, and to compare patterns of genome reduction in mutualistic and pathogenic lineages. Of particular interest is the substantial loss of proof-reading and DNA repair loci from several symbiont genomes, which may elevate mutational rates and biases in these species.

Staff

Wernegreen, Jennifer, Assistant Scientist

BioCurrents Research Center

The BioCurrents Research Center (BRC) is a national resource of the National Institutes of Health, part of the Biomedical Technology Resource Program of the NCTR. As with all such resources it has two main goals: 1) to research and develop new biomedical technologies, and 2) to make specialized technologies available to visiting biomedical investigators. The emphasis of the BRC is on the physiology of cellular transport mechanisms, particularly as they influence the boundary conditions in the media adjacent to the plasma membrane. To this end we develop new microsensor technologies that operate in a self-referencing mode. We offer access to ion-selective, electrochemical, and biosensor devices, coupled to advanced imaging techniques and electrophysiological approaches—combinations unique to the BRC.

The BRC has seen a marked expansion in year 2000 after a successful competitive renewal in December of 1999. This resulted in an increase in staff, which included the appointment of two Assistant Scientists: Stefan McDonough and Orian Shirihai. Two new postdoctoral researchers also joined the group in 2000: Sung-Kwon Jung and Andreas Hengstenberg, as did Laurel Moore and Robert Lewis in support roles. Towards the end of 2000 we added Mark Messerli, who works with both the BRC and Bay Paul Center.

The current structure of the resource comprises the core support facility and three independent laboratories, as well as a number of affiliate endeavors where the members of the Center work closely with colleagues in the MBL and the regional medical schools. In particular, we have strong links with the MBL program in Architectural Dynamics in Living Cells, the Laboratory for Reproductive Medicine, and the Bay Paul Center. Our involvement with regional hospitals includes Boston Medical Center (diabetes), Massachusetts General Hospital (protein trafficking), and Women and Infants (reproductive biology). In summary, the core in-house research emphasis is on biophysics of calcium transport and regulation (S. McDonough), the molecular biology

of transport processes (O. Shirihai), and sensor development and the biology of transport mechanisms (P.J.S. Smith).

In addition, the BRC is developing an online database of pharmacological compounds. The database has made considerable progress over the past year and should be openly available by the summer of 2001. It will be accessible through our web page at (www.mbl.edu/BioCurrents).

The Center supports an extensive outreach program to regional and national universities, medical schools, and hospitals, and publishes extensively in the field of cellular transport. Over the past year we have continued to host a diverse group of visiting investigators whose studies have ranged from ion transport and metabolic studies at the single cell level to mapping ion flux associated with the olfactory sensilla of the intact blue crab. Overall our emphasis remains on biomedical studies using the specialized microsensors available, particularly those designed to measure flux of calcium, potassium, hydrogen, oxygen, nitric oxide, and ascorbate. Under development are the newer biosensors and electro-optical probes.

The Center also maintains other core support facilities, such as a fully equipped cell culture facility, electrode manufacture, and microinjection systems which, as available, we also open to the general scientific community.

Staff

Smith, Peter J.S., Director and Senior Scientist
 Hammar, Kasia, Research Assistant III
 Hengstenberg, Andreas, Visiting Postdoctoral Fellow
 Jung, Sung-Kwon, Postdoctoral Researcher
 Lewis, Robert, Electronic Support
 McDonough, Stefan, MBL Assistant Scientist
 McLaughlin, Jane A., Research Assistant III
 Messerli, Mark, NASA Research Fellow
 Moore, Laurel, Database Development
 Sanger, Richard H., Research Assistant III
 Shirihai, Orian, MBL Assistant Scientist

Laboratory of Stefan McDonough

Calcium ions trigger many cellular functions including neurotransmission, muscle contraction, regulation of cell membrane excitability, and the activation of enzymatic cascades. A major route of calcium entry into a cell is through voltage-gated calcium ion channels, proteins found in the plasma membrane of every excitable cell and many nonexcitable cells. These proteins form channels that open to allow a selective influx of calcium ions into the cell when the cell fires an electrical spike. Calcium channels are current or potential targets for clinical drugs treating cardiac arrhythmia, epilepsy, hypertension, pain, diabetes, and brain damage after stroke.

Research in this laboratory focuses on the channels that conduct calcium entry, the mechanisms controlling calcium levels within the cell, and the tools to distinguish among different types of calcium channels. Experiments are carried out using patch-clamp electrophysiology on mammalian neurons, mammalian cardiac myocytes, or cloned calcium channels expressed in nonexcitable cells. One effort, in collaboration with the laboratories of Bruce and Barbara Furie and of Alan Rigby, is to identify and characterize conotoxins that target voltage-gated ion channels. Other experiments use the self-referencing ion-selective and oxygen sensors of the BioCurrents Center, in collaboration with the Laboratory of Peter Smith. Current areas of research include the effects of zinc ions on calcium channels, a possible cause of ischemic neuronal damage; calcium channel biophysics during the cardiac ventricular action potential; the metabolic cost to the heart of maintaining calcium homeostasis during resting and excited states; and the mechanisms of



activation of alternatively spliced forms of neuronal N-type calcium channels.

Laboratory of Orian Shirihai

Erythroid differentiation involves expression of a set of unique transport and enzymatic systems to support a robust induction of hemoglobin synthesis. Active communication between the mitochondrial matrix and cytosol is essential for heme biosynthesis. The first step, production of aminolevulinic acid (ALA), occurs in the inner matrix. ALA is transported to the cytosol and eventually converted to coproporphyrinogen III, which reenters the mitochondrion and, upon further modifications, is joined with iron to form heme. This product is then transported out of the inner matrix for assembly of cytochromes or hemoglobin. Thus, at least four mitochondrial transport steps are required. Although the enzymatic steps in heme synthesis are well characterized, little is known about how biosynthetic intermediates are shuttled across mitochondrial membranes. While malfunctioning of these transporters most probably underlie hematologic and neurologic diseases, their substrates are photoactivated toxic molecules used in photo-dynamic therapy for cancer; the mechanism of transport into the target organelle is of major interest.

A novel mitochondrial transporter, discovered by Dr. Shirihai, has been the focus of research in the lab. This protein, named ABC-me (for ATP-binding cassette-mitochondrial erythroid), localizes to the mitochondrial inner membrane and is expressed at particularly high levels in erythroid tissues of embryos and adults. ABC-me is induced during erythroid maturation in cell lines and primary hematopoietic cells, and its over-expression enhances hemoglobin synthesis in erythroleukemia cells. Members of the ABC transporter superfamily have been implicated in numerous human diseases, including cystic fibrosis (CFTR), adrenoleukodystrophy (ALDP), Zellweger's syndrome

(PMP70), progressive familial intrahepatic cholestasis (SPGP), and Stargardt macular dystrophy (ABCR). To explore the functional role of this transporter, the lab is generating a knockout mouse and cell line, which would serve as a tool to study the biophysics and biochemistry of this transporter as well as the phenotype appearing in the absence of this gene. ABC-me represents a novel member of the ABC superfamily with a potentially important role in erythroid development. In collaboration with Dr. Weiss from the University of Pennsylvania and Dr. Orkin from Harvard, we have recently cloned and sequenced the human homologue of ABC-me and started screening multiple samples from candidate patients sent to us by physicians from the United States, Italy, and England.

Laboratory of Peter J.S. Smith

The activities of this laboratory center on instrument development, providing new insights into cellular transport mechanisms, and applying these devices to biomedical problems. Much of the biological work is done in collaboration with visiting investigators to the BRC. Over the past year an increasing body of work has been undertaken using the new amperometric microsensors capable of measuring single cell movement of gases such as oxygen and nitric oxide. We continue to investigate the metabolic cost of ion regulation in single cultured neurons.

In collaboration with Mitch Sogin of the Bay Paul Center, a new research area was launched, investigating the transport physiology of extremophilic organisms. The emphasis is to understand how membrane-borne transport proteins continue to regulate a near neutral cytosol while being exposed to acidic conditions of pH 1 or 2. This project is funded through the NSF LEXEN program, attracting Mark Messerli to the group, first as an MBL summer fellow but now on a full-time basis funded by a NASA Fellowship.

In sensor design, we have made great progress with the new generation of amperometric sensors, incorporating an immobilized enzyme. Our attempts have focused on glucose and, thanks to the efforts of Sung-Kwon Jung, our first single cell glucose flux measurements have been achieved. Hybrid, electro-optical sensors have also been a focus over the past year, where, working with visiting fellow Andreas Hengstenberg, we have successfully built a micro-oxygen sensor on the surface of a single mode fiber optic capable of stimulating a preloaded cellular reporter molecule. In collaboration with Stefan McDonough, this technology has been successful in imaging calcium activity while recording oxygen uptake from a single cardiac myocyte.

Boston University Marine Program

Faculty

Atema, Jelle, Professor of Biology, Director
Dionne, Vincent, Professor of Biology
Golubic, Stjepko, Professor of Biology
Kaufman, Les, Associate Professor of Biology
Lobel, Phillip, Associate Professor of Biology
Voigt, Rainer, Research Associate Professor
Ward, Nathalie, Lecturer

Staff

Decarie, Linette, Senior Staff Coordinator
DiNunno, Paul, Research Assistant, Dionne Lab
Hall, Sheri, Program Manager
McCafferty, Michelle, Administrative Assistant
Gilbert, Niki, Program Assistant

Postdoctoral Investigators

Grasso, Frank, Atema Laboratory
Kaatz, Ingrid, Lobel Laboratory
Trott, Thomas, Atema Laboratory

Visiting Faculty and Investigators

Hanlon, Roger, Marine Biological Laboratory
Hecker, Barbara, Hecker Consulting
Moore, Michael, Woods Hole Oceanographic Institution
Simmons, Bill, Sandia National Laboratory
Wainwright, Norman, Marine Biological Laboratory

Graduate Students

PhD Students

Existing

Cole, Marci
Dale, Jonathon
Dooley, Brad
Hauxwell, Jennifer
Herrold, Ruth
Kroeger, Kevin
Ma, Diana
Miller, Carolyn
Oliver, Steven
Stieve, Erica
Tomasky, Gabrielle
York, Joanna
Zettler, Erik

New

Frenz, Christopher
Skomal, Gregory

Masters Students

Existing

Allen, Christel
Atkinson, Abby
Bentis, Christopher
Bowen, Jennifer
Casper, Brandon
Cavanaugh, Joseph
Chichester, Heather
D'Ambrosio, Alison
Errigo, Michael
Evgendou, Angeliki
Fredland, Inga
Frenz, Christopher
Grable, Melissa
Grebner, Dawn
Kollaros, Maria
Konkle, Anne
Lamb, Amy
Lawrence, David
Lever, Mark
Levine, Michael
Malley, Vanessa
Martel, David
Nevtackas, Justin
Oweke, Ojwang William
Perez, Edmundo
Pugh, Tracy

Ramon, Marina
 Ripley, Jennifer
 Roycroft, Karen
 Smith, Spence
 Stueckle, Todd
 Sweeny, Melissa
 Tuohy-Sheen, Elizabeth
 Watson, Elise
 Weiss, Erica
 Wright, Dana

New

Bogomolni, Andrea
 Bonacci, Lisa
 deHart, Pieter
 Estrada, James
 Rice, Aaron
 Rutecki, Deborah
 Shriver, Andrea
 Summers, Erin
 Wittenmyer, Robert

Undergraduate Students

Spring 00

Kwong, Grace
 Loewensteiner, David

Fall 00

Batson, Melissa
 Bergan, Michael
 Boynton, Seth
 Burke, Alexandra
 Buynevitch, Artem
 Christie, Mark
 Combellick, Lindsay
 Darrell, Andrea
 De Falco, Tomaso
 Dewey, Hollis
 Faloon, Kristine
 Feeney, Brett
 Hendricks, Amber
 Hunt, Tamah
 Kavountzis, Erol
 Kim, Joanne
 Kowalchuk, Lynn
 Linehan, Candace
 Lynch, Michael
 Mattei, Bethany
 McKay, Breda
 McOwen, Micah
 Miller, Jessica
 Morano, Janelle
 Newville, Melinda
 Nichols, Dominica
 Nguyen, Jean
 O'Neil, Diane
 Rohrbaugh, Lynne
 Sorocco, Debra
 Tubbs, Mollie
 Wezensky, Eryn
 Yopak, Kara
 Zink, Rachel



Summer 2000 Interns

O'Connell, Timmy

Laboratory of Jelle Atema

Many organisms and cellular processes use chemical signals as their main channel of information about the environment. All environments are noisy and require some form of filtering to detect important signals. Chemical signals are transported by turbulent currents, viscous flow, and molecular diffusion. Receptor cells extract chemical signals from the environment through various filtering processes. In our laboratory, fish, marine snails, and crustacea have been investigated for their ability to use chemical signals under water. Currently, we use the lobster and its exquisite senses of smell and taste as our major model to study the signal-filtering capabilities of the whole animal and its narrowly tuned chemoreceptor cells.

Research in our laboratory focuses on amino acids, which represent important food signals for the lobster, and on the function and chemistry of pheromones used in lobster courtship. We examine animal behavior in the sea and in the lab. This includes social interactions and chemotaxis. To understand the role of chemical signals in the sea we use real lobsters and untethered small robots. Our research includes measuring and computer modeling odor plumes and the water currents lobsters generate to send and receive chemical signals. Other research interests include neurophysiology of receptor cells and anatomical studies of receptor organs and pheromone glands.

Laboratory of Vincent Dionne

Odors are powerful stimuli. They can focus the attention, elicit behaviors (or misbehaviors), and even resurrect forgotten memories. These actions are directed by the central nervous system, but they depend upon the initial transduction of chemical signals by olfactory receptor neurons in the nasal passages. More than just a single process appears to underlie odor transduction, and the intracellular pathways that are used are far more diverse than once thought. Hundreds of putative odor receptor molecules have been identified that work through several different second messengers to modulate the activity of various types of membrane ion channels.

Our studies are being conducted with aquatic salamanders using amino acids and other soluble chemical stimuli that these animals perceive as odors. Using electrophysiological and molecular approaches, the research examines how these cellular components produce odor detection, and how odors are identified and discriminated.

Laboratory of Les Kaufman

Current research projects in the laboratory deal with speciation and extinction dynamics of haplochromine fishes in Lake Victoria. We are studying the systematics, evolution, and conservation genetics of a species flock encompassing approximately 700 very recently evolved taxa in the dynamic and heavily impacted landscape of northern East Africa. In the lab we are studying evolutionary morphology, behavior, and systematics of these small, brightly colored cichlid fishes.

Another area of study is developmental and skeletal plasticity in fishes. We are studying the diversity of bone tissue types in fishes, differential response to mineral and mechanical challenge, and matrophilic *versus* environmental effects in the development of coral reef fishes.

We also study the biological basis for marine reserves in the New England fisheries. We are involved in collaborative research with NURC, NMFS, and others studying the relative impact on groundfish stocks of juvenile habitat destruction *versus* fishing pressure.

Laboratory of Phillip Lobel

Fishes are the most diverse vertebrate group and provide opportunities to study many aspects of behavior, ecology, and evolution. We primarily study 1) how fish are adapted to different habitats, and 2) behavioral ecology of species interactions. Current research focuses on fish acoustic communications.

We are also conducting a long-term study of the marine biology of Johnston Atoll, Central Pacific Ocean. Johnston Atoll has been occupied continuously by the military since the 1930s and has proven to be a unique opportunity for assessing the biological impacts of island industrialization and its effects on reefs. Johnston Atoll is the site of the U.S. Army's chemical weapons demilitarization facility, JACADS.

Laboratory of Ivan Valiela

A focus of our work is the link between land use on watersheds and consequences in the receiving estuarine ecosystems. The work examines how landscape use and urbanization increase nutrient loading to groundwater and streams. Nutrients in groundwater are transported to the sea, and, after biogeochemical transformation, enter coastal waters. There, increased nutrients bring about a series of changes on the ecological components. To understand the coupling of land use and consequences to receiving waters, we study the processes involved, assess ecological consequences, and define opportunities for coastal management.

A second long-term research topic is the structure and function of salt marsh ecosystems, including the processes of predation, herbivory, decomposition, and nutrient cycles.

Center for Advanced Studies in the Space Life Sciences

In 1995, the NASA Life Sciences Division and the Marine Biological Laboratory established a cooperative agreement with the formation of the Center for Advanced Studies in the Space Life Sciences (CASSLS at MBL). The Center's overall goals are to increase awareness of the NASA Life Sciences Program within the basic science community and to examine and discuss potential uses of microgravity and other aspects of spaceflight as probes to provide new insights to fundamental processes important to basic biology and medicine.

Through symposia, workshops and seminars, CASSLS advises NASA and the biological science community on a wide variety of topics.

Through fellowships, CASSLS supports summer research for investigators in areas pertinent to the aims of NASA life sciences.

Since the Center began its operations in July 1995, more than 400 people have attended eight CASSLS workshops. Typically these workshops last for two to four days and feature an international array of scientists and NASA/International space agency staff. In many cases, workshop chairs have a long-time association with the MBL. Workshop schedules incorporate many opportunities for interaction and discussion. A major outcome for workshops is the publication of proceedings in a peer-reviewed journal. Moreover, our meetings introduce outstanding biologists to research questions and prominent scientists involved in gravitational biology and the NASA Life Sciences Program.

The Center sponsored one workshop in 2000: "Invertebrate Sensory Information Processing: Implications for Biologically Inspired Autonomous Systems," chaired by Dr. Frank Grasso. The Center sponsored one Fellow during the summer of 2000: Dr. Mark Messerli, Biology Department, Purdue University. He conducted research in regulation of cytoplasmic pH in eucaryotic acidophiles in collaboration with Dr. Peter J.S. Smith and Dr. Mitchell Sogin of the Marine Biological Laboratory. In addition, two scholars-in-residence worked with the Center in 2000: Dr. Richard Wassersug of Dalhousie University and Dr. Lawrence Schwartz of the University of Massachusetts, Amherst. Finally, the Center worked with colleagues in Astrobiology and the Josephine Bay Paul Center to offer a stimulating lecture series.

Staff

Blazis, Diana E.J., Director

Oldham, Pamela A., Administrative Assistant

Scholars-in-residence

Schwartz, Lawrence

Wassersug, Richard

The Ecosystems Center

The Ecosystems Center carries out research and education in ecosystems ecology. Terrestrial and aquatic scientists work in a wide variety of ecosystems ranging from the streams, lakes and tundra of the Alaskan Arctic (limits on plant primary production) to sediments of Massachusetts Bay (controls of nitrogen cycling), to forests in New England (effects of soil warming on carbon and nitrogen cycling), and South America (effects on greenhouse gas fluxes of conversion of rain forest to pasture) and to large estuaries in the Gulf of Maine (effects on plankton and benthos of nutrients and organic matter in stream runoff). Many projects, such as those dealing with carbon and nitrogen cycling in forests, streams, and estuaries, use the stable isotopes ¹³C and ¹⁵N to investigate natural processes. A mass spectrometer facility is available. Data from field and laboratory research are used to construct mathematical models of whole-system responses to change. Some of these models are combined with geographically referenced data to produce estimates of how environmental changes affect key ecosystem indexes, such as net primary productivity and carbon storage, throughout the world's terrestrial biosphere.

The results of the Center's research are applied, wherever possible, to the questions of the successful management of the natural resources of the earth. In addition, the ecological expertise of the staff is made available to public affairs groups and governmental agencies who deal with problems such as acid rain, coastal eutrophication, and possible carbon dioxide-caused climate change.

The Semester in Environmental Science was offered again in Fall

2000. Fifteen students from seven colleges participated in the program. The center also offers opportunities for postdoctoral fellows.

Administrative Staff

Hobbie, John E., Co-Director
 Melillo, Jerry M., Co-Director
 Foreman, Kenneth H., Associate Director, Semester in Environmental Studies
 Berthel, Dorothy J., Administrative Assistant
 Donovan, Suzanne J., Executive Assistant
 Moniz, Priscilla C., Administrative Assistant, Semester in Environmental Studies
 Nuñez, Guillermo, Research Administrator
 Scanlon, Deborah G., Executive Assistant
 Seifert, Mary Ann, Administrative Assistant

Scientific Staff

Hobbie, John E., Senior Scientist
 Melillo, Jerry M., Senior Scientist
 Deegan, Linda A., Associate Scientist
 Giblin, Anne E., Associate Scientist
 Herbert, Darrell A., Staff Scientist
 Holmes, Robert M., Staff Scientist
 Hopkinson, Charles S., Senior Scientist
 Hughes, Jeffrey E., Staff Scientist
 Nadelhoffer, Knute J., Senior Scientist
 Neill, Christopher, Assistant Scientist
 Peterson, Bruce J., Senior Scientist
 Rastetter, Edward B., Associate Scientist
 Shaver, Gaius R., Senior Scientist
 Stuedler, Paul A., Senior Research Specialist
 Tian, Hanqin, Staff Scientist
 Vallino, Joseph J., Assistant Scientist
 Williams, Mathew, Assistant Scientist

Educational Staff Appointments

Buzby, Karen, Postdoctoral Scientist
 Cieri, Matthew D., Postdoctoral Scientist
 Crump, Byron, Postdoctoral Scientist
 García-Montiel, Diana C., Postdoctoral Scientist
 LeDizès-Maurel, Séverine, Postdoctoral Scientist
 Kappel-Schmidt, Inger, Postdoctoral Scientist
 Nordin, Annika, Postdoctoral Scientist
 Raymond, Peter, Postdoctoral Scientist
 Sommerkorn, Martin, Postdoctoral Scientist
 Tobias, Craig R., Postdoctoral Scientist
 Williams, Michael R., Postdoctoral Scientist

Technical Staff

Ahrens, Toby, Research Assistant
 Bahr, Michele P., Research Assistant
 Bettez, Neil D., Research Assistant
 Burnette, Donald W., Research Assistant
 Claessens, Lodevicus H.J.M., Research Assistant
 Colman, Benjamin P., Research Assistant
 Eldridge, Cynthia, Research Assistant
 Fox, MaryKay, Research Assistant
 Garritt, Robert H., Senior Research Assistant
 Gay, Marcus O., Research Assistant
 Goldstein, Joshua H., Research Assistant

Jablonski, Sarah A., Research Assistant
 Jillson, Tracy A., Research Assistant
 Kelsey, Samuel, Research Assistant
 Kicklighter, David W., Senior Research Assistant
 Kwiatkowski, Bonnie L., Research Assistant
 Laundre, James A., Senior Research Assistant
 Lezberg, Ann, Research Assistant
 Lux, Heidi, Research Assistant
 Merson, Rebekah, Research Assistant
 Micks, Patricia, Research Assistant
 Morriseau, Sara, Research Assistant
 Nolin, Amy L., Research Assistant
 Nowicki, Genevieve, Research Assistant
 O'Brien, Katherine A., Research Assistant
 Otter, Marshall L., Research Assistant
 Pan, Shufen, Research Assistant
 Peterson, G. Gregory, Research Assistant
 Regan, Kathleen M., Research Assistant
 Ricca, Andrea, Research Assistant
 Schwamb, Carol, Laboratory Assistant
 Slavik, Karie A., Research Assistant
 Thielier, Kama K., Research Assistant
 Tholke, Kristin S., Research Assistant
 Thomas, Suzanne M., Research Assistant
 Tucker, Jane, Senior Research Assistant
 Vasiliou, David S., Research Assistant
 Weston, Nathaniel B., Research Assistant
 Wright, Amos, Research Assistant
 Wyda, Jason C., Research Assistant

Consultants

Bowles, Francis P., Research Systems Consultant
 Bowles, Margaret C., Administrative Consultant

Visiting Scientists and Scholars

DeStasio, Bart, SES Faculty Fellow, Lawrence College
 Koba, Keisuke, Graduate School of Informatics, Kyoto University, Japan

Laboratory of Aquatic Biomedicine

Our laboratory has developed the *Spisula solidissima* embryo model to study mechanisms of neurotoxicology. We have shown that polychlorinated biphenyls (PCBs) selectively target the nervous system during development. We are now linking up and down regulation of the p53 family of genes with neuronal cell development using new probes developed by this laboratory.

In the second line of research, we are using the clam leukemia model to investigate how environmental chemicals influence the progression of leukemia. Further, we are studying whether mutations in p53 alter the pathogenesis of leukemia in populations of *Mya arenaria*. Field work to Nova Scotia showed that leukemia in *Mya* was also detected in Sydney, N.S., which is heavily polluted with a variety of industrial chemicals.

Staff

Reinisch, Carol L., Senior Scientist
 Cox, Rachel, Postdoctoral Scientist
 Jessen-Eller, Kathryn, Postdoctoral Scientist
 Kreiling, Jill, Postdoctoral Scientist
 Stephens, Ray, Adjunct Scientist

Visiting Scientists

Shohet, Stephen, University of California, San Francisco
Walker, Charles, University of New Hampshire

Student

Miller, Jessica, Boston University

Laboratory of Cell Communication

Established in 1994, this laboratory is devoted to the study of intercellular communication. The research focuses on the cell-to-cell channel, a membrane channel built into the junctions between cells. This channel provides one of the most basic forms of intercellular communication in organs and tissues. The work is aimed at the molecular physiology of this channel, in particular, at the mechanisms that regulate the communication. The channel is the conduit of growth-regulating signals. It is instrumental in a basic feedback loop whereby cells in organs and tissues control their number; in a variety of cancer forms it is crippled.

This laboratory has shown that transformed cells lacking communication channels lost the characteristics of cancer cells, such as unregulated growth and tumorigenicity, when their communication was restored by insertion of a gene that codes for the channel protein. Work is now in progress to track the channel protein within the cells from its point of synthesis, the endoplasmic reticulum, to its functional destination in the plasma membrane, the cell-to-cell junction, by expressing a fluorescent variant of the channel protein in the cells. Knowledge about the cellular regulation of this process will aid our understanding of what goes awry when a cell loses the ability to form cell-to-cell channels and thus to communicate with its neighbors, thereby taking the path towards becoming cancerous.

Another line of work is taking the first steps at applying information theory to the biology of cell communication. Here, the intercellular information spoor is tracked to its source: the macromolecular intracellular information core. The outlines of a coherent information network inside and between the cells are beginning to emerge.

Staff

Loewenstein, Werner, Senior Scientist
Rose, Birgit, Senior Scientist
Jillson, Tracy, Research Assistant

Laboratory of Paul Colinvaux

We have shown that accumulated pollen data now leave little doubt that the Amazon lowlands remained forested without fragmentation throughout glacial cycles. Changes in relative abundance of trees within the highly diverse forests can be seen in the pollen record, however, particularly in response to changing temperature. The pollen vocabulary for the Amazon on which this conclusion is based has been codified in our *Amazon Pollen Manual and Atlas* with text in Portuguese as well as English for the benefit of Brazilian researchers. We show that the Amazon ecosystems yield two kinds of pollen signals: what might be called the "classical" signal by wind-blown pollen, which allows separation of biomes and many edaphically constrained facies of Amazon forests such as *varzea* or *igapo*; and a species-rich signal from animal-pollinated trees washed from the immediate watershed or catchment of the sedimentary basin.

With our collaborators in Brazil and the University of Florida we

completed pollen and stratigraphic analyses, now being prepared for publication, of the first transglacial lake core from a forested site (Maicuru Inselberg) in the eastern Amazon lowlands. Our collaborators at the Florida Institute of Technology and the University of Cincinnati identified chemical changes in the early sedimentary history of Lake Pata in the western Amazon lowlands that show a strong synchronicity with insolation changes associated with the precessional component of astronomical climate forcing back to marine oxygen isotope stage 7, this being the first such signal from the equatorial lowlands. In 2000 we also concluded a paleoenvironmental reconnaissance of the Lake Nicaragua region and are developing plans for raising a long core from the lake.

Staff

Colinvaux, Paul, Adjunct Scientist

Laboratory of Ayse Dosemeci

The laboratory investigates molecular processes that underlie synaptic modification. The main project is to clarify how the frequency of activation at a synapse can determine whether the synapse will be potentiated (strengthened) or depressed (weakened) through the participation of an enzyme called CaM kinase II. This enzyme is regulated by autophosphorylation on distinct sites in the presence and absence of calcium. Biochemical studies with isolated postsynaptic density fractions are conducted to clarify functional consequences of CaMKII autophosphorylation in response to sequential exposure to calcium-containing and calcium-free media at different temporal patterns.

In a related project, a new affinity-based method is being developed for the preparation of postsynaptic density fractions of high purity. In collaboration with Dr. Lucas Pozzo-Miller (University of Alabama, Birmingham), we are studying changes in the activity of CaMKII in hippocampal slices following high-frequency and low-frequency electrical stimulation to generate long-term potentiation and long-term depression, respectively. Related projects in collaboration with Dr. Thomas Reese (NIH, NINDS) include studies on the redistribution of CaMKII and structural changes in the post-synaptic density in response to excitatory stimuli.

Staff

Dosemeci, Ayse, Adjunct Scientist

Visiting Investigator

Pozzo-Miller, Lucas, University of Alabama

Laboratory of Barbara Furie and Bruce Furie

γ -Carboxyglutamic acid is a calcium-binding amino acid that is found in the conopeptides of the predatory marine cone snail, *Conus*. This laboratory has been investigating the biosynthesis of this amino acid in *Conus* and the structural role of γ -carboxyglutamic acid in the conopeptides. This satellite laboratory relates closely to the main laboratory, the Center for Hemostasis and Thrombosis Research, on the Harvard Medical School campus in Boston; the main focus of the primary laboratory is the synthesis and function of γ -carboxyglutamic acid in blood-clotting proteins and the role of vitamin K.

Cone snails are obtained from the South Pacific and maintained in the Marine Resources Center. Until recently, the marine cone snail had been the sole invertebrate known to synthesize γ -carboxyglutamic acid (Gla).

The venomous cone snail produces neurotoxic conopeptides, some rich in Gla, which it injects into its prey to immobilize it. To examine the biosynthetic pathway for Gla, we have studied the *Conus* carboxylase which converts glutamic acid to γ -carboxyglutamic acid. This activity has an absolute requirement for vitamin K. The *Conus* carboxylase substrates contain a carboxylation recognition site on the conotoxin precursor. Given the functional similarity of mammalian vitamin K-dependent carboxylases and the vitamin K-dependent carboxylase from *Conus textile*, we hypothesized that structurally conserved regions would identify sequences critical to this common functionality.

Furthermore, we examined the diversity of animal species that maintain vitamin K-dependent carboxylation to generate γ -carboxyglutamic acid. We have cloned full-length carboxylase homologs from the beluga whale (*Delphinapterus leucas*) and toadfish (*Opsanus tau*). In addition, we have partially cloned the carboxylase gene from chicken (*Gallus gallus*), hagfish (*Myxine glutinosa*), horseshoe crab (*Limulus polyphemus*), and cone snail (*Conus textile*) in order to compare these structures to the known bovine, human, rat, and mouse cDNA sequences. Comparison of the predicted amino acid sequences identified a highly conserved 32-amino acid residue region in all of these putative carboxylases. In addition, this amino acid motif is also present in the *Drosophila* genome and identified a *Drosophila* homolog of the γ -carboxylase. Assay of hagfish liver and *Drosophila* demonstrated carboxylase activity in these non-vertebrates. More recently, we have cloned the entire vitamin K-dependent carboxylase gene from the cone snail, *Conus textile*. The predicted amino acid sequence shows most regions are similar to the mammalian sequence, and that there is about 40% sequence identity overall. These results demonstrate the broad distribution of the vitamin K-dependent carboxylase gene, including a highly conserved motif that is likely critical for enzyme function. The vitamin K-dependent biosynthesis of γ -carboxyglutamic acid appears to be a highly conserved function in the animal kingdom.

Novel γ -carboxyglutamic acid-containing conopeptides have been isolated from the venom of *Conus textile*. The amino acid sequence, amino acid composition, and molecular weights of these peptides have been determined. For several peptides, the cDNA encoding the precursor conotoxin has been cloned. The three-dimensional structure of some of these Gla-containing conopeptides are being determined by 2D NMR spectroscopy. Complete resonance assignments of conotoxin P14.1 were made from 2D ^1H NMR spectra via identification of intraresidue spin systems using ^1H - ^1H through-bond connectivities. NOESY spectra provided d_{N} , d_{N} , and d_{N} NOE connectivities and vicinal spin-spin coupling constants $^3J_{\text{HN}_\alpha}$ were used to calculate ϕ torsion angles. Structure determination is nearing completion. The goal of this project is to determine the structural role of γ -carboxyglutamic acid in the Gla-containing conotoxins and other γ -carboxyglutamic acid-containing proteins.

Staff

Furie, Barbara C., Adjunct Scientist
 Furie, Bruce, Adjunct Scientist
 Begley, Gail, Scientist I
 Czerwiec, Eva, Postdoctoral Fellow
 Rigby, Alan, Adjunct Scientist
 Stenflo, Johan, Visiting Scientist

Laboratory of Shinya Inoué

Scientists in this laboratory study the molecular mechanism and control of mitosis, cell division, cell motility, and cell morphogenesis, with emphasis on biophysical studies made directly on single living cells, especially developing eggs in marine invertebrates. Development of biophysical instrumentation and methodology, such as the centrifuge polarizing microscope, high-extinction polarization optical and video

microscopy, digital image processing techniques including dynamic stereoscopic imaging, and exploration of their underlying optical theory are an integral part of the laboratory's efforts.

Staff

Inoué, Shinya, Distinguished Scientist
 Burgos, Mario, Visiting Scientist
 Goda, Makoto, Visiting Scientist
 Baraby, Diane, Laboratory Assistant
 Knudson, Robert, Instrument Development Engineer
 MacNeil, Jane, Executive Assistant

Laboratory of Rudolf Oldenbourg

The laboratory investigates the molecular architecture of living cells and of biological model systems using optical methods for imaging and manipulating these structures. For imaging cell architecture non-invasively and non-destructively, dynamically and at high resolution, we have developed a new polarized light microscope (Pol-Scope). The Pol-Scope combines microscope optics with new electro-optical components, video, and digital image processing for fast analysis of specimen birefringence over the entire viewing field. Examples of biological systems currently investigated with the Pol-Scope are microtubule-based structures (asters, mitotic spindles, single microtubules); actin-based structures (acroosomal process, stress fibers, nerve growth cones); zona pellucida of vertebrate oocytes; and biopolymer liquid crystals.

Staff

Oldenbourg, Rudolf, Associate Scientist
 Shribak, Michael, Staff Scientist
 Knudson, Robert, Instrument Development Engineer
 Baraby, Diane, Laboratory Assistant

Laboratory of Michael Rabinowitz

This laboratory investigates environmental geochemistry and epidemiology. Areas of recent activity include modeling lead bioavailability, writing a history of lead biokinetic models, performing a case control survey of tea drinking and oral cancer in Taiwan, quantifying the transport and fate of various sources of residential lead exposure, and serving on several advisory boards of Superfund research projects in Boston and New York.

Current activity focuses on characterizing lead paints and pigments. Hundreds of lead poisoning lawsuits are filed every year against landlords, but no compensation has ever been paid by the half dozen companies that made lead pigments, because it has not been possible to identify the specific manufacturer. This research has been funded by the Eagle Picher Trust. Other activity, sponsored by HUD, involves using stable isotopes of lead to determine the relative importance of various household surfaces (doors, floors, windows, walls) as sources of indoor dust lead levels. Dust lead is the major predictor of childhood lead exposure and poisoning. This would allow for more focused deleading.

Another effort has been using historical fire insurance maps to locate and identify unrecognized hazardous waste sites.

Staff

Rabinowitz, Michael, Associate Scientist

Laboratory for Reproductive Medicine, Brown University and Women and Infants Hospital, Providence

Work in this laboratory centers on investigating cellular mechanisms underlying female infertility. Particular emphasis is placed on the physiology of the oocyte and early embryo, with the aim of assessing developmental potential and mitochondria dysfunction arising from mtDNA deletions. The studies taking place at the MBL branch of the Brown Laboratory use some of the unique instrumentation available through the resident programs directed by Rudolf Oldenbourg and Peter J.S. Smith. Most particularly, non-invasive methods for oocyte and embryo study are being sought. Of several specific aims, one is to use the Pol-Scope to analyze the dynamic birefringence of meiotic spindles. An additional aim is to study transmembrane ion transport using non-invasive electro-physiological techniques available at the BioCurrents Research Center. The newly developed oxygen probe offers the possibility of looking directly at abnormalities in the mitochondria arising from accumulated mtDNA damage. Our laboratory has also focused on studying the mechanism underlying age-associated infertility in terms of oocyte quality and has attempted to rescue developmentally compromised oocytes or embryos through nuclear-cytoplasmic transfer technology. We have characterized oxidative stress-induced mitochondrial dysfunctions, developmental arrest, and cell death in early embryos using animal models. Ultimately, this laboratory aims to produce clinical methods for assessing preimplantation embryo viability, an advance that will significantly contribute to the health of women and children.

Staff

Keefe, David, Director
Liu, Lin, Adjunct Scientist
Trimarchi, James, Adjunct Scientist

Laboratory of Osamu Shimomura

Aequorin, from the jellyfish *Aequorea aequorea*, was the first calcium-sensitive photoprotein discovered by us in 1961. Because of its high sensitivity to Ca^{2+} and biological harmlessness, the protein has been widely used as a probe to monitor intracellular free calcium levels. Aequorin is a unique protein that contains a high level of energy for light emission in the molecule, and its structure has been the target of many studies in the past. The complete 3-dimensional structure of aequorin was finally obtained by X-ray crystallography 38 years after its discovery, in collaboration with three other laboratories. Aequorin is found to be a globular molecule having four helix-loop-helix "EF-hand" domains, of which three can bind Ca^{2+} . The molecule contains coelenterazine-2-hydroperoxide in its hydrophobic core cavity, as the chromophoric ligand which decomposes into coelenteramide and carbon dioxide accompanied by the emission of blue light.

Staff

Shimomura, Osamu, Senior Scientist, MBL, and Boston University School of Medicine
Shimomura, Akemi, Research Assistant

Laboratory of Robert B. Silver

The members of this laboratory study how living cells make decisions. The focus of the research, typically using marine models, is on two main areas: the role of calcium in the regulation of mitotic cell division (sea urchins, sand dollars, etc.) and structure and function relationships of hair cell stereociliary movements in vestibular physiology (oyster toadfish). Other related areas of study, *i.e.* synaptic transmission (squid), are also, at times, pursued. Tools include video light microscopy, multispectral, subwavelength, and very high-speed (sub-millisecond frame rate) photon counting video light microscopy, telemanipulation of living cells and tissues, and modeling of decision processes. A cornerstone of the laboratory's analytical efforts is high performance computational processing and analysis of video light microscopy images and modeling. With luminescent, fluorescent, and absorptive probes, both empirical observation and computational modeling of cellular, biochemical, and biophysical processes permit interpretation and mapping of space-time patterns of intracellular chemical reactions and calcium signaling in living cells. A variety of *in vitro* biochemical, biophysical, and immunological methods are used. In addition to fundamental biological studies, the staff designs and fabricates optical hardware, and designs software for large video image data processing, analysis, and modeling.

Staff

Silver, Robert, Associate Scientist

Visiting Investigators

Hummel, John, Argonne National Laboratory
Jiang, Yi, Los Alamos National Laboratory
Keller, Bruce, SUNY Upstate Medical University
Kriebel, Mahlon, SUNY Upstate Medical University
Pappas, George, University of Illinois School of Medicine
Pearson, John, Los Alamos National Laboratory

Laboratory of Norman Wainwright

The mission of the laboratory is to understand the molecular defense mechanisms exhibited by marine invertebrates in response to invasion by bacteria, fungi, and viruses. The primitive immune systems demonstrate unique and powerful strategies for survival in diverse marine environments. The key model has been the horseshoe crab *Limulus polyphemus*. *Limulus* hemocytes exhibit a very sensitive LPS-triggered protease cascade which results in blood coagulation. Several proteins found in the hemocyte and hemolymph display microbial binding proteins that contribute to antimicrobial defense. Commensal or symbiotic microorganisms may also augment the antimicrobial mechanisms of macroscopic marine species. Secondary metabolites are being isolated from diverse marine microbial strains in an attempt to understand their role. Microbial participation in oxidation of the toxic gas hydrogen sulfide is also being studied.

Staff

Wainwright, Norman, Senior Scientist
Child, Alice, Research Assistant
Williams, Kendra, Research Assistant

Visiting Investigator

Anderson, Porter, University of Rochester



Laboratory of Seymour Zigman

This laboratory is investigating basic mechanisms of photooxidative stress to the ocular lens due to environmentally compatible UVA radiation. This type of oxidative stress contributes to human cataract formation. Other studies are the search for and use of chemical antioxidants to retard the damage that occurs. Cultured mammalian lens epithelial cells and whole lenses *in vitro* are exposed to environmentally compatible UVA radiation with or without previous antioxidant feeding. The following parameters of lens damage are examined: molecular excitation to singlet states *via* NADPH (the absorber); cell growth inhibition and cell death; catalase inactivation; cytoskeletal description (of actin, tubulin, integrins); and cell membrane damage (lipid oxidation, loss of gap junction integrity and intercellular chemical communications). Thus far, the most successful antioxidant to reduce these deficiencies is alpha-tocopherol (10 $\mu\text{g}/\text{ml}$) and tea polyphenols (especially from green tea). The preliminary phases of the research are usually carried out using marine animal eyes (*i.e.*, smooth dogfish) as models. Our goal is to provide information that will suggest means to retard human cataract formation.

Staff

Zigman, Seymour, Laboratory Director, Professor of Ophthalmology, Boston University Medical School
 Rafferty, Keen, Research Associate, Boston University Medical School
 Rafferty, Nancy S., Research Associate, Boston University Medical School
 Zigman, Bunnie R., Laboratory Manager, Boston University Medical School

The Marine Resources Center

The Marine Resources Center (MRC)—a modern, 32,000-square-foot structure—features advanced facilities for maintaining and culturing aquatic organisms essential to advanced biological, biomedical, and ecological research. In addition to research, the MRC provides a variety of important, complementary services to the MBL community through its Aquatic Resources Division, its Aquaculture and Engineering Division, and its administrative division.

The MRC and its life support systems have increased the ability of MBL scientists to conduct research and have inspired new concepts in scientific experiments. Vigorous research programs focusing on basic biological and biomedical aquatic models are currently being developed at the Center, including the Program in Scientific Aquaculture and the Program in Sensory Biology and Neuroethology.

Research and educational opportunities for established investigators, postdoctoral fellows, and graduate and undergraduate students are

available at the MRC. Investigators and students find that the MRC's unique life support and seawater engineering systems make this a favorable environment in which to conduct research using a variety of aquatic organisms and flexible tank space for customized experimentation on live animals.

Staff

Hanlon, Roger, Director and Senior Scientist
 Carroll, James, Life Support Technical Assistant
 Enos, Edward, Aquatic Resources Division Superintendent
 Gilland, Edwin, Research Associate
 Grossman, William, Marine Specimen Collector/Diving Safety Officer
 Hanley, Janice, Water Quality and Animal Health Technician
 Klimm, William, Licensed Boat Captain—R/V Gemma
 Kuzirian, Alan, Associate Scientist
 Linnon, Beth, Special Projects Coordinator
 Mebane, William, Aquaculture and Engineering Division Superintendent
 Santore, Gabrielle, Executive Assistant
 Sexton, Andrew, Marine Organism Shipper
 Smolowitz, Roxanna, MBL Veterinarian
 Sullivan, Daniel, Boat Captain
 Tassinari, Eugene, Senior Biological Collector
 Whelan, Sean, Diver/Marine Specimen Collector

Summer and Fall Employees and Volunteers

Buynovich, Artem, Work-study Student, Boston University
 Carroll, Amanda, Volunteer
 Dimond, Jay, Diver/Collector
 Douton, Kate, AmeriCorps Assistant
 Faloon, Kristine, Work-study Student, Boston University
 Gudas, Chris, Diver/Collector
 Kavountzis, Erol, Work-study Student, Boston University
 Miraglia, Valentina, Volunteer, Universita di Napoli "Federico II," Italy
 Potter, Chris, Diver/Collector
 Reynolds, Justin, Diver/Collector
 Robbins, Gillian, Volunteer
 Rohrbough, Lynne, Work-study Student, Boston University
 Tubbs, Mollie, Work-study Student, Boston University
 Zucchini, Massimo, Volunteer, Universita di Napoli "Federico II," Italy

Laboratory of Roger Hanlon

This laboratory investigates the behavior of cephalopods and other marine organisms with an integrative biology approach focused at the organismal level. Molecular, cellular, and ecological approaches are used to complement this organismal approach, and there is emphasis on sensory biology and behavioral ecology.

Laboratory studies on the mechanisms and functions of polarized light sensitivity in cephalopods are underway. Olfactory sensing by *Nautilus* (which functions in food detection and location as well as mate choice) is being studied in the laboratory. Visual features that octopuses use for maze learning are also being investigated. Lab experiments in large indoor seawater tanks are being conducted to determine how male squids, *Loligo pealeii*, use visual, then contact, chemical cues in egg capsules to initiate highly robust agonistic behavior.

The functional morphology and neurobiology of the chromatophore system of cephalopods are studied on a variety of cephalopod species, and image analysis techniques are being developed to study crypsis and the mechanisms that enable cryptic body patterns to be neurally regulated by visual input. Various aspects of predation, antipredator defenses, and reproduction are conducted in field sites worldwide.

Sexual selection theory is being tested using squid and cuttlefish. Field and laboratory studies focus on mechanisms of agonistic behavior.

female mate choice, and sperm competition. The latter studies involve DNA fingerprinting to determine paternity and help assess alternative mating tactics.

Population structure and reproductive success in several highly valuable squid fisheries (*Loligo vulgaris reynaudii* in South Africa, *Loligo pealeii* in the N.E. United States, *Loligo opalescens* in California) are being assessed for fishery management and conservation. We also culture species of commercial and biomedical importance. For example, the toadfish *Opsanus beta* is used in vestibular research related to human medicine, yet the species is difficult to obtain from nature. Thus, we are performing the first mariculture experiments to culture toadfish through the life cycle to provide the biomedical community with high-quality experimental animals. Such an approach lightens the impact of collecting toadfish from the natural environment.

Staff

Hanlon, Roger, Senior Scientist
Ament, Seth, Summer Research Assistant, Harvard University
Boal, Jean, Adjunct Scientist
Buresch, Kendra, Research Assistant
Conroy, Lou-Anne, Summer Research Assistant, Dartmouth College
Gilles, Nicole, REU Intern, University of Minnesota, Duluth
Lee, Tony, REU Intern, Duke University
Richmond, Hazel, Research Assistant
Shashar, Nadav, Adjunct Scientist
Sussman, Raquel, Investigator
Vaughan, Katrina, Summer Research Assistant, University of Wales, Swansea

Visiting Investigators

Baddeley, Roland, University of Sussex, England
Baker, Robert, New York University
Cavanaugh, Joseph, Boston University Marine Program
Chiao, Chuan-Chin, Grass Fellow, University of Maryland, Baltimore County
Cronin, Thomas, University of Maryland, Baltimore County
Grable, Melissa, Boston University Marine Program
Hall, Karina, University of Adelaide, Australia
Hatfield, Emma, FRS Marine Laboratory, Aberdeen, Scotland
Karson, Miranda, Michigan State University
Kier, William, University of North Carolina
Mensinger, Allen, University of Minnesota, Duluth
Messenger, John, University of Cambridge, England
Osorio, Daniel, Investigator, University of Sussex, England
Saidel, William, Rutgers University
Schmolecky, Matthew, Grass Fellow, University of Utah

Laboratory of Alan M. Kuzirian

Research in the laboratory explores the functional morphology and ultrastructure of various organ systems in molluscs. The program includes mariculture of the nudibranch, *Hemissenda crassicornis*, with emphasis on developing reliable culture methods for rearing and maintaining the animal as a research resource. The process of metamorphic induction by natural and artificial inducers is being explored in an effort to understand the processes involved and as a means to increase the yield of cultured animals. Morphologic studies stress the ontogeny of neural and sensory structures associated with the photic and vestibular systems which have been the focus of learning and memory studies, as well as the spatial and temporal occurrence of regulatory and transmitter neurochemicals. Concurrent studies detailing the toxic effects of lead on *Hemissenda* learning and memory,

feeding, and the physiology of cultured neurons are also being conducted. New studies include cytochemical investigations of the Ca²⁺/GTP binding protein, calcexitin, and its modulation with learning and lead exposure.

Collaborative research includes histochemical investigations on strontium's role in initiating calcification in molluscan embryos (shell and statoliths), immunocytochemical labelling of cell-surface antigens, neurosecretory products, second messenger proteins involved with learning and memory, as well as intracellular transport organelles using mono- and polyclonal antibodies on squid (*Loligo pealeii*) giant axons and *Hemissenda* sensory and neurosecretory neurons. Additional collaborations involve studying neuronal development of myelin, myelination defects, as well as nerve regeneration and repair in phylogenetically conserved nervous systems.

Additional collaborative research includes DNA fingerprinting using RAPD-PCR techniques in preparation for isogenic strain development of laboratory-reared *Hemissenda* and hatchery produced bay scallops (*Argopectin irradians*) with distinct phenotypic markers for rapid field identification and stock assessments. Recently obtained funding will expand this research to perform population genetic analyses of currently designated yellowtail flounder (*Limanda ferruginea*) stocks occurring in the Northeast Fisheries Region.

Systematic and taxonomic studies of nudibranch molluscs, to include molecular phylogenetics, are also of interest.

Staff

Kuzirian, Alan M., Associate Scientist
Kozlowski, Robbin, Research Technician

Visiting Investigators

Chikarmane, Hemant, Investigator
Clay, John R., NINDS/NIH
Gould, Robert, NYS Institute of Basic Research

Summer Interns

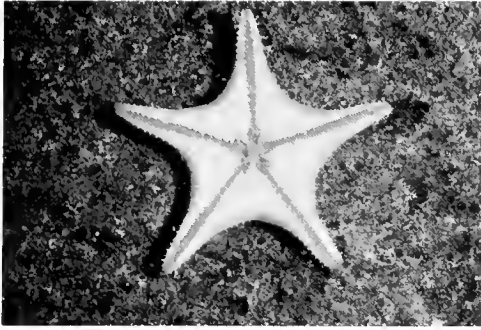
Kingston, Margaret, REU Intern, Wake Forest University
Kuzirian, Mark, REU Intern, University of Rhode Island
Lee, Tony, REU Intern, Duke University

Laboratory of Roxanna Smolowitz

This laboratory investigated the pathogenesis of aquatic animal diseases using traditional pathological methods combined with *in situ* molecular methods. Research conducted during 2000 included 1) examination of hard-clam-strain susceptibility to a protistan disease agent named Quahog Parasite Unknown, and the methods of transmission of that organism between infected and uninfected animals; 2) detection of disease-causing, protozoan organisms (MSX and SSO) in eastern oysters using PCR and *in situ* hybridization techniques; and 3) evaluation of inbred strains of oysters for resistance to disease vs. productivity as commercial aquaculture stock. Work began on the determination of possible causes of lobster shell disease in the northeast.

Staff

Smolowitz, Roxanna, MBL Veterinarian
Brothers, Christine, Laboratory Assistant
Cavanaugh, Joseph, Laboratory Assistant
Marks, Ernie, AmeriCorps member
Stukey, Jetley, Laboratory Assistant
Summers, Erin, Laboratory Assistant
Tirrell, Kerri-Ann, AmeriCorps member



Honors

Friday Evening Lectures

June 16	Edward Pearce, Cornell University "Life-long Enemies—The Relationship Between Schistosomes and Their Hosts"
June 23	Stephen Farrand, University of Illinois at Champaign-Urbana "Agrobacterium tumefaciens: Nature's Own Genetic Engineer"
June 30	Judith Eisen, University of Oregon "From Lobster to Zebrafish: Development of Identified Neurons" (Lang Lecture)
July 7	David Anderson, California Institute of Technology "Stem Cells from the Mammalian Nervous System: Basic Biology and Implications for Tissue Repair"
July 14	Sallie Chisholm (Penny), Massachusetts Institute of Technology "The Invisible Forest: Marine Phytoplankton and Climate"
July 20-21	Eve Marder, Brandeis University 1) "Activity-dependent Tuning of Neurons and Synapses in Adult and Developing Circuits" 2) "Neurotransmitter Modulation of Neural Networks" (Forbes Lectures)
July 28	Jean-Pierre Changeux, Institut Pasteur "Chemical Communications in the Brain: Nicotine, Receptors, and Learning" (Glassman Lecture)
August 4	Susan Middleton/David Liittschwager "Paradise Up Close: Hawaii—Endangered Eden"
August 11	Titia de Lange, The Rockefeller University "At the Ends of Our Chromosomes: the Key to Immortality"

Fellowships and Scholarships

In 2000, the MBL awarded research fellowships to 22 scientists from around the world. The MBL awarded scholarships to 77 students in the MBL's summer courses as well as 4 post-course research awards. Donors provided gifts for endowed and expendable funds amounting to \$256,090 in support of the research fellowships program and an additional \$738,107 to provide scholarships to students in MBL courses. Those funds that received donations in 2000 are listed below. The individuals who received fellowships and scholarships are listed beginning on p. R58.

Robert Day Allen Fellowship Fund

Drs. Joseph and Jean Sanger

Jean and Katsuma Dan Fellowship Fund

Drs. Joseph and Jean Sanger
Mrs. Eleanor Steinbach

Thomas B. Grave and Elizabeth F. Grave Scholarship

Estate of Elizabeth F. Grave

The American Society for Cell Biology Scholarships

The American Society for Cell Biology

Bernard Davis Fellowship Fund

Mrs. Elizabeth M. Davis

Daniel S. and Edith T. Grosch Scholarship Fund

Mr. Gustav Grosch
Ms. Laura Grosch and Mr. Herb Jackson

Frederik B. Bang Fellowship Fund

Mrs. Betsy G. Bang

The Mac V. Edds, Jr. Endowed Scholarship Fund

Dr. and Mrs. James D.
Dr. and Mrs. Kenneth T. Edds
Dr. Louise M. Luckenbill-Edds

Aline D. Gross Scholarship Fund

Dr. and Mrs. Paul R. Gross
Dr. and Mrs. Benjamin Kaminer
Technic, Inc.

Max Burger Endowed Scholarship for the Embryology Course

Dr. Max M. Burger

Gerald D. and Ruth L. Fischbach Endowed Scholarship Fund

Drs. Gerald and Ruth Fischbach

E. E. Just Endowed Research Fellowship Fund

The Cole Memorial Family Fund

Fred Karush Endowed Library Readership

Dr. and Mrs. Laszlo Lorand
Dr. and Mrs. Arthur M. Silverstein

Keffer Hartline Fellowship Fund

Mrs. Elizabeth K. Hartline
Dr. and Mrs. Edward F. MacNichol, Jr.
Dr. William H. Miller
Dr. Torsten Wiesel and Ms. Jean Stein
Dr. and Mrs. Stephen Yeandle

Kuffler Fellowship Fund

Dr. and Mrs. Edward A. Kravitz

MBL Associates Endowed Scholarship Fund

MBL Associates
Mrs. Anne L. Meigs-Brown

James A. and Faith Miller Fellowship Fund

Drs. David and Virginia Miller

Frank Morrell Endowed Memorial Scholarship

Dr. Leyla deToledo-Morrell

Mountain Memorial Fund

Dr. and Mrs. Dean C. Allard, Jr.
Ms. Brenda J. Bodian
Dr. and Mrs. Benjamin Kaminer
Mr. and Mrs. Thomas H. Roberts
Dr. and Mrs. R. Walter Schlesinger

Neural Systems and Behavior Scholarship Fund

Anonymous (1)
Mr. Srdjan D. Antic
Drs. Mary Atkisson and Joel White
Bristol-Myers Squibb Corporation
Dr. and Mrs. John Byrne
Ms. Lu Chen
Dr. Warren M. Grill
Dr. Anya C. Hurlbert
Dr. Eve Marder
Dr. Mark W. Miller

Mr. Rex R. Robison
Ms. M. Jade Zee

Nikon Fellowship

Nikon Instruments, Inc.

The Plum Foundation John E. Dowling Fellowship Fund

The Plum Foundation

William Townsend Porter Scholarship Fund for Minority Students

William Townsend Porter Foundation

Phillip H. Presley Scholarship Fund

Carl Zeiss, Inc.

Science Writing Fellowships Program Support

American Society for Biochemistry and Molecular Biology
American Society for Cell Biology
American Society for Photobiology
FASEB
NASA (Astrobiology Institute)
National Institutes of Health—Office of Science Education
National Institutes of Health—National Cancer Institute
National Science Foundation—Biological Sciences
National Science Foundation—Office of Polar Programs
Society for Integrative and Comparative Biology
Times Mirror Foundation
Waksman Foundation for Microbiology
The Washington Post Company

The Catherine Filene Shouse SES Scholarship Fund

The Catherine Filene Shouse Foundation

The Catherine Filene Shouse Scholarship Fund

The Catherine Filene Shouse Foundation

The Catherine Filene Shouse Fellowship Fund

The Catherine Filene Shouse Foundation

The Evelyn and Melvin Spiegel Fellowship Fund

The Sprague Foundation
Drs. Joseph and Jean Sanger

H. B. Steinbach Fellowship Fund

Mrs. Eleanor Steinbach

Eva Szent-Gyorgyi Scholarship Fund

Dr. and Mrs. Laszlo Lorand
Drs. Joseph and Jean Sanger
Dr. Andrew and Ms. Ursula Szent-Gyorgyi

Universal Imaging Fellowship Fund

Universal Imaging Corporation

The Irving Weinstein Endowed Scholarship

The Irving Weinstein Foundation, Inc.

Walter L. Wilson Endowed Scholarship

Dr. Paul N. Chervin
Dr. Jean R. Wilson
Mr. and Mrs. Ross A. Wilson

Young Scholars/Fellows Program

Drs. Harriet and Alan Bernheimer
Dr. and Mrs. Francis P. Bowles
Dr. and Mrs. Sherwin J. Cooperstein
Mrs. Elizabeth M. Davis
Mrs. James R. Glazebrook
Ms. Jeannie Leonard
Mrs. Barbara C. Little
Dr. and Mrs. Anthony Linzzi
Drs. Luigi and Elaine Mastroianni
Drs. Matthew and Jeanne Meselson
Dr. and Mrs. Philip Person
Drs. Dorothy Skinner and John Cook
Drs. Ann Stuart and John Moore
Mr. and Mrs. Richard Yoder

Fellowships Awarded

MBL Summer Research Fellows

• Srdjan Antic, M.D., is a post-doctoral fellow in the Department of Cellular and Molecular Physiology at Yale University School of

Medicine, New Haven, CT. The title of his project is "Selective modulation of the dendritic membrane potential." Dr. Antic is funded by the *Baxter Postdoctoral Fellowship*, the *Charles R. Crane Fellowship Fund*, the *MBL Associates Fellowship Fund*, and the *James A. and Faith Miller Memorial Fund*.

• Roberto Bruzzone, Ph.D., is an Associate Professor at the Institut Pasteur in Paris, France. The title of this research is "Molecular analysis of the biophysical properties of connexin channels that mediate cell-cell communication between neurons of the vertebrate retina and CNS." Dr. Bruzzone is funded by the *Erik B. Fries Endowed Fellowship*, the *MBL Associates Fellowship Fund*, and the *H. B. Steinbach Fellowship Fund*.

• Mario H. Burgos, M.D., is an Emeritus Professor of the Medical School at the Universidad Nacional de Cuyo and Director of the Instituto de Histología y Embriología, National Council of Research (CONICET), Argentina. His research project is titled, "Mechanism of release of spermatozoa from the *Sertoli* cells." He is also collaborating with Dr. Shinya Inoué in the identification of the birefringent zones in *Arbacia* eggs after centrifuge polarizing microscopy. Dr. Burgos is funded by the *Chairman's Fellowship*.

• Jean-Pierre Changeux is a Professor at the Collège de France and Director of the Unit of Molecular Neurobiology at the Institut Pasteur in Paris. He is the author of *Neuronal Man: The Biology of Mind* (1990). Dr. Changeux has been awarded a *Herbert W. Rand Fellowship* for his research.

• Debra Ann Fadool, Ph.D., is an Associate Professor in the Biomedical Research Facility at Florida State University, Tallahassee, FL. The title of her research project is "Chemosensory transduction in the vomero-nasal organ." Dr. Fadool is funded by the *Frederik B. Bang Fellowship Fund*, the *Ann E. Kammer Memorial Fellowship Fund*, and the *MBL Associates Fellowship Fund*.

• Mariano A. Garcia-Blanco, M.D., Ph.D., is Associate Professor of Genetics, Microbiology, and Medicine at Duke University Medical Center, Durham, NC. He is a Raymond and Beverly Sackler Scholar and is a member of the Biochemistry Study Section of the National Institutes of Health. The *Josiah Macy, Jr. Foundation* is funding his research.

• George G. Holz, Ph.D., has been appointed Associate Professor at New York University School of Medicine to establish a Diabetes Research Laboratory at New York University Medical Center. His summer research project is "Spatial distribution of second messengers in pancreatic β -cells." Dr. Holz is funded by the *Erik B. Fries Endowed Fellowship*, the *Frank R. Lillie Fellowship Fund*, and the *MBL Associates Fellowship Fund*.

• Peter Koulen, Ph.D., is a postdoctoral associate in the Department of Pharmacology at Yale University School of Medicine, New Haven, CT. The title of his research project is "Calcium signaling in zebrafish neurons mediated by differentially distributed intracellular calcium channels." Dr. Koulen has received funding from the *Erik B. Fries Endowed Fellowship* and the *Lucy B. Lemann Fellowship Fund*.

• George Langford, Ph.D., is the Ernest Everett Just Professor of Natural Sciences and Professor of Biological Sciences at Dartmouth College, Hanover, NH. His research project is titled "Actin-based vesicle transport in the squid giant axon." Dr. Langford is funded by the *Josiah Macy, Jr. Foundation*.

• Jennifer LaVail, Ph.D., is Professor of Anatomy/Ophthalmology at the University of California, San Francisco. She is spending her second summer at the MBL. Her research project is titled "HSV tegument proteins in axonal transport and microtubule architecture." Dr. LaVail is funded by an *MBL Research Fellowship* and the *Evelyn and Melvin Spiegel Fellowship Fund*.

• Carolyn Lesser has published eight children's books and numerous articles. She has also served as a consultant and lecturer. Ms. Lesser was awarded a Science Writing Fellowship in 1999, and is a Desk Reader at the MBL/WHOI Library in 2000. Ms. Lesser is funded by the *Fred Karnish Endowed Library Readership*.

• Jeffrey Magee, Ph.D., is an Assistant Professor in the Neuroscience Center at Louisiana State University Medical Center, New Orleans, Louisiana. The title of his research is "Mechanisms of

Ca^{2+} entry into hippocampal neurons." Dr. Magee is funded by the *MBL Associates Fellowship Fund* and the *Lucy B. Lemann Fellowship Fund*.

• Antonio Malgaroli, Ph.D., is a Professor in the Unit of Neurobiology of Learning at the University of San Raffaele, Milan, Italy. The title of his summer research is "Presynaptically silent synapses in the hippocampus." Dr. Malgaroli is funded by the *Herbert W. Rand Fellowship* and the *Frank R. Lillie Fellowship Fund*.

• Mark Messerli, Ph.D., is a Research Associate in the Department of Biological Sciences at Purdue University, West Lafayette, IN. The title of his research project is "Regulation of cytoplasmic pH in eucaryotic acidophiles." Dr. Messerli is funded by a *NASA Life Sciences Program Fellowship*.

• Timothy Mitchison, M.D., is a Professor in the Department of Cell Biology at Harvard Medical School, Boston, MA. His research project is titled "Optical Approaches to Cell Division." *The Universal Imaging Corporation* is funding Dr. Mitchison.

• David Ogden, Ph.D., is a Principal Investigator at the National Institute for Medical Research in London, England. The title of his research is "Central electrosensory processing in the skate." Dr. Ogden is funded by an *MBL Associates Fellowship*.

• Oladele A. Ogunseitan, Ph.D., is an Associate Professor in the Department of Environmental Analysis and Design at the University of California, Irvine. Dr. Ogunseitan returns to the MBL to study "Toxic metal resistance, swarming phenotype, and enzyme polymorphism in *Vibrio alginolyticus*." Dr. Ogunseitan is funded by the *Josiah Macy, Jr. Foundation*.

• David Paydarfar, Ph.D., is an Associate Professor at the Department of Neurobiology at the University of Massachusetts Medical School in Worcester. The title of his research project is "Can noise regulate oscillatory state? *In numero* and *in vitro* analysis of squid axon membrane." Dr. Paydarfar is funded by the *Frederick B. Bang Fellowship Fund*, the *M. G. F. Fuortes Memorial Fellowship Fund*, the *MBL Associates Fellowship Fund*, and the *John O. Crane Fellowship Fund*.

• Peter Saggau, Ph.D., is an Associate Professor in the Division of Neuroscience at Baylor College of Medicine, Houston, Texas. The title of his summer research project is "Transmission and plasticity at single hippocampal synapses." Dr. Saggau received the *Nikon Fellowship*.

• Miduturu Srinivas, Ph.D., is a Research Associate at the Albert Einstein College of Medicine, Bronx, New York. His research project for the summer is titled "Biophysical properties of gap junctions in retinal neurons." Dr. Srinivas is funded by the *Erik B. Fries Endowed Fellowship* and the *H. Keffer Hartline Fellowship Fund*.

• Thomas W. White, Ph.D., is an Instructor in the Department of Neurobiology at Harvard Medical School, Boston, MA. His research title is "Gap junctional communication in the retina." Dr. White is funded by the *H. Keffer Hartline Fellowship Fund*, the *Stephen W. Kuffler Fellowship Fund*, and the *Frank R. Lillie Fellowship Fund*.

• Iain Stuart Young, Ph.D., is a Research Associate in the Department of Biology at the University of Pennsylvania, Philadelphia. The title of Dr. Young's summer research is "The molecular mechanisms of relaxation in superfast muscles." Dr. Young is funded by the *Robert Day Allen Fellowship Fund*, the *MBL Research Fellowship Fund*, the *H. Burr Steinbach Memorial Fellowship Fund*, and the *Lucy B. Lemann Fellowship Fund*.

Grass Fellows

• Leonardo Belluscio, Ph.D., Duke University Medical Center. Project: "The role of spontaneous activity in the olfactory system."

• Chuan-Chin Chao, University of Maryland, Baltimore County.

R60 Annual Report

Project: "Camouflage in cephalopods: visual control and effectiveness when viewed by predators."

- Melina Hale, Ph.D., State University of New York at Stony Brook. Project: "The neural basis of startle behavior and its development in the toadfish (*Opsanus tau*)."

Project: "The neural basis of startle behavior and its development in the toadfish (*Opsanus tau*)."

• Johann Hofmann, Ph.D., Stanford University. Project: "The consequences of socially induced differential growth on the retina."

- Thomas Kuner, M.D., Duke University Medical Center.

Project: "The timing of NSF action in neurotransmitter release probed with photolysis of caged peptides."

• Brian Link, Ph.D., Harvard University. Project: "Time-lapse analysis of zebrafish retinal cells during development: investigation of lamination mutants."

• Matthew B. McFarlane, Ph.D., New York University Medical Center. Project: "Central pathways mediating the horizontal vestibulo-ocular reflex in an elasmobranch, *Scyliorhinus canicula*."

• Matthew T. Schmolesky, University of Utah. Project: "Visual stimulus encoding in the optic lobe of squid *Loligo pealei*."

- Ava J. Udvadia, Ph.D., Duke University Medical Center.

Project: "Investigation of signaling pathways that activate axon growth-associated gene expression in regenerating spinal neurons."

• Jing W. Wang, Ph.D., Lucent Technologies. Project: "Optical imaging and electrophysiological recording of *Drosophila* central nervous system: A search for the significance of synchrony."

• Zachary P. Willis, Harvard Medical School. Project: "The function of dAbl pathway components in neuronal outgrowth and growth cone turning *in vitro*."

MBL Science Writing Fellowships Program

Fellows

Begos, Kevin, *Winston-Salem Journal*

Ben-Ari, Elia, *BioScience*

Scholarships Awarded

The Bruce and Betty Alberts Endowed Scholarship in Physiology

Fleegal, Melissa, University of Florida

American Society for Cell Biology

Colón-Ramos, Daniel, Duke University

Bradford, Yvonne, University of Oregon

Crespo-Barreto, Juan, University of Puerto Rico

Espinoza, Nora, University of Chicago

Glater, Elizabeth, Brown University

Greenlee, Anne, Marshfield Medical Research Foundation

Hubbard, Aida, University of Texas, San Antonio

Mah, Silvia, Scripps Institution of Oceanography

Powell, Jacqueline, Morehouse School of Medicine

Triggs, Veronica, University of Wisconsin, Madison

Biology Club of the College of the City of New York

Konur, Sila, Columbia University

Berger, Cynthia, Finger Lakes Productions

Borenstein, Seth, Knight Ridder Newspapers

Enright, Leo, BBC

Fagin, Dan, *Newsday*

Garber, Ken, Freelance

Gorman, Jessica, *Discover* magazine

Hathaway, William, *Hartford Courant*

Helmuth, Laura, *Science* magazine

Mansur, Mike, *Kansas City Star*

Martin, Roger, University of Kansas

Marx, Vivien, Freelance

Milano, Gianna, Mondadori Publishing Company

Nemecek, Sasha, *Scientific American*

Poulson, David, Booth Newspapers

Senkowsky, Sonya, *Anchorage Daily News*

Scott, Bari, SoundVision Productions

Tangley, Laura, *U.S. News and World Report*

Program Staff

Goldman, Robert D., Northwestern University, Co-Director

Hinkle, Pamela Clapp, Marine Biological Laboratory, Administrative Director

Rensberger, Boyce, Knight Science Journalism Program, Co-Director

Hands-On Laboratory Faculty

Chisholm, Rex, Northwestern University, Biomedical Hands-On

Laboratory Director

Hobbie, John E., Marine Biological Laboratory, Environment Hands-On

Laboratory Co-Director

Melillo, Jerry, Marine Biological Laboratory, Environment Hands-On

Laboratory Co-Director

Palazzo, Robert, University of Kansas, Biomedical Hands-On

Laboratory Associate Director

C. Lalor-Burdick Scholarship

Powell, Jacqueline, Morehouse School of Medicine

Burroughs Wellcome Fund Biology of Parasitism Course

Andersson, John, Karolinska Institute

D'Angelo, Maximiliano, University of Buenos Aires

Dolezal, Pavel, Charles University

Ferreira, Ludmila, Universidade Federal de Minas Gerais

Figueiredo, Luisa, University of Porto

Gilk, Stacey, University of Vermont

Lowell, Joanna, Rockefeller University

Martins, Gislaine, Faculdade de Medicina de Ribeirao Preto

Murta, Silvana, Centro e Pesquisas René Rachou-FIOCRUZ

Sehgal, Alfica, Tata Institute of Fundamental Research

Ulbert, Sebastian, Netherlands Cancer Institute

Villarino, Alejandro, University of Pennsylvania

Burroughs Wellcome Fund Frontiers in Reproduction Course

Alberio, Ramiro, Ludwig-Maximilian University

Allegrucci, Cinzia, Università degli Studi di Perugia

Ashkar, Ali, University of Guelph
 Chong, Kowit-Yu, Oregon Regional Primate Research Center
 Heifetz, Yael, Cornell University
 Lavoie, Holly, University of South Carolina
 Majumdar, Subeer, Primate Research Center
 Powell, Jacqueline, Morehouse School of Medicine
 Richard, Craig, University of Pittsburgh
 Sahgal, Namita, Kansas University Medical Center
 Zhang, Gongqiao, University of Virginia

**Burroughs Wellcome Fund
 Modeling of Biological Systems Course**

Ginsberg, Tara, University of Texas Medical School
 Immerstrand, Charlotte, Linköping University
 Quinteiro, Guillermo, Comisión Nacional de Energía Atómica
 Teng, Ching-Ling, University of Virginia
 Uppal, Hirdesh, Punjab Agricultural University
 Genick, Ulrich, The Salk Institute for Biological Studies
 Hershberg, Uri, Hebrew University
 Mosavi, Leila, University of Connecticut Health Center

**Burroughs Wellcome Fund
 Molecular Mycology Course**

Austin, W. Lena, Howard University School of Medicine
 Ibrahim, Ashraf, Harbor-UCLA Medical Center
 Mol, Pieternella, University of Amsterdam
 Munro, Carol, University of Aberdeen
 Perea, Sofia, The University of Texas Health Science Center
 Spellberg, Brad, Harbor-UCLA Medical Center
 Spreghini, Elisabetta, Yale University School of Medicine
 Toenjes, Kurt, University of Vermont
 Wasylnka, Julie, Simon Fraser University

Gary N. Calkins Memorial Scholarship Fund

Ellertsdóttir, Elin, University of Freiburg

Edwin Grant Conklin Memorial Fund

Jhaveri, Dhanisha, Tata Institute of Fundamental Research

**William F. and Irene C. Diller
 Memorial Scholarship Fund**

Jhaveri, Dhanisha, Tata Institute of Fundamental Research
 Menna, Elisabetta, Institute of Neurophysiology, Pisa

**The Ellison Medical Foundation
 Biology of Parasitism Course**

Gilk, Stacey, University of Vermont
 Lowell, Joanna, Rockefeller University
 O'Donnell, Rebecca, University of Melbourne
 Ralph, Stuart, University of Melbourne
 Triggs, Veronica, University of Wisconsin, Madison
 Villarino, Alejandro, University of Pennsylvania

**The Ellison Medical Foundation
 Molecular Biology of Aging Course**

Bailey, Adina, University of California, Berkeley
 Baur, Joe, University of Texas Southwestern
 Bordone, Laura, University of Minnesota Medical School
 Cui, Wei, Roslin Institute
 Cypser, James, University of Colorado
 Filosa, Stefania, IIGB-CNR
 Furfaro, Joyce, Pennsylvania State University College of Medicine
 Harper, James, University of Idaho
 Huang, Xudong, Massachusetts General Hospital-East
 Johnson, Kristen, Purdue University
 Konigsberg, Mina, Universidad Autónoma
 Kostrominova, Tatiana, University of Michigan
 Luo, Yuan, University of Southern Mississippi
 Muñoz, Denise, University of California
 Peel, Alyson, The Buck Center for Research in Aging
 Podlutzky, Andrej, National Institute on Aging, NIH
 Radulescu, Andreea, Albert Einstein College of Medicine
 Srivivsan, Chandra, University of California, Los Angeles
 Tong, Jiayuan (James), Cold Spring Harbor Laboratory
 Zaid, Ahmed, Stockholm University

Caswell Grave Scholarship Fund

Bates, Damien, Murdoch Institute
 Brelidze, Tinatin, University of Miami School of Medicine
 Cordeiro, Maria Sofia, Instituto Gulbenkian de Ciencia
 Gong, Ying, California Institute of Technology
 Menna, Elisabetta, Institute of Neurophysiology, Pisa
 Prud'homme, Benjamin, Centre de Genetique Moleculaire

Daniel S. Grosch Scholarship Fund

Neretin, Lev, Shirshov Institute of Oceanography

Aline D. Gross Scholarship Fund

Cordeiro, Maria Sofia, Instituto Gulbenkian de Ciencia
 Johansson, Viktoria, Göteborgs Universitet

William Randolph Hearst Foundation Scholarship

Rankin, Kathleen, Oberlin College
 Rodeheffer, Carey, Emory University
 Rodgers, Erin, University of Alabama, Birmingham
 Shatkin-Margolis, Seth, Duke University
 Takai, Erica, Columbia University

Howard Hughes Medical Institute

Akay, Turgay, Köln University
 Barak, Yoram, Hebrew University
 Ding, Long, University of Pennsylvania
 Globerson, Amir, Hebrew University
 Imai, Kazushi, Columbia University P&S
 Konur, Sila, Columbia University
 Krishna, B. Suresh, New York University
 Kyrkjebo, Vibeke, Sars International Centre
 Lauritzen, Thomas, University of California, San Francisco
 Lin, Li-hung, Princeton University
 McCance, James, University of Leicester
 Menna, Elisabetta, Institute of Neurophysiology, Pisa

Nasevicius, Aidan, University of Minnesota
Paz, Ron, Hebrew University Medical School
Petereit, Christian, Universität Bielefeld
Prud'homme, Benjamin, Centre de Genetique Moleculaire
Rela, Lorena, Universidad de Buenos Aires
Rokni, Uri, Hebrew University of Jerusalem
Schreiber, Susanne, Humboldt Universität Berlin
Shi, Songhai, Cold Spring Harbor Laboratory
Singh, Brajesh, Imperial College at Silwood Park
Skromne, Isaac, Princeton University
Szalicszyo, Krisztina, Hungarian Academy of Sciences
Warkman, Andrew, University of Western Ontario
Zaar, Annette, Universität Freiburg

International Brain Research Organization

Challa, Anil Kumar, Ohio State University
Leung, Fung Ping, Hong Kong University of Science and Technology
Lupo, Giuseppe, University of Pisa
Maldonado, Ernesto, Massachusetts Institute of Technology

Arthur Klorfein Scholarship and Fellowship Fund

Aspöck, Gudrun, University of Basel
Gong, Ying, California Institute of Technology
Imai, Kazushi, Columbia University P&S
Kyrkjebo, Vibeke, Sars International Centre
Lee, Vivian, Oregon Health Sciences University
Prud'homme, Benjamin, Centre de Genetique Moleculaire
Skromne, Isaac, Princeton University

Frank R. Lillie Fellowship and Scholarship Fund

Carroll, Michael, University of Newcastle
Costa, Patricia, Universidad Federal do Rio de Janeiro
Cotrufo, Tiziana, Institute of Neurophysiology
Dayel, Mark, University of California, San Francisco
Fleegal, Melissa, University of Florida
Marrari, Yannick, Observatoire Océanographique
Petrie, Ryan, University of Calgary
Rankin, Kathleen, Oberlin College
Shatkin-Margolis, Seth, Duke University
Takai, Erica, Columbia University

Jacques Loeb Founders' Scholarship Fund

Fleegal, Melissa, University of Florida
Petrie, Ryan, University of Calgary
Shilkrut, Mark, Technion-Israel Institute of Technology

Massachusetts Space Grant Consortium

Barbour, Jason, University of California, San Francisco
Handley, Scott, Centers for Disease Control and Prevention
Holland, Brenden, University of Hawaii
Longnecker, Krista, Oregon State University
McMahon, Katherine, University of California, Berkeley
Munroe, Stephen, Marquette University
Nepokroeff, Molly, Smithsonian Institution
Stone, Karen, University of Alaska Museum, Fairbanks
Xie, Gary, Los Alamos National Lab

S.O. Mast Memorial Fund

Marrari, Yannick, Observatoire Océanographique
Zhong, Haining, Johns Hopkins University

MBL Associates Endowed Scholarship Fund

Rela, Lorena, Universidad de Buenos Aires

MBL Pioneers Scholarship Fund

Ballard, Victoria, Weill Medical College
Bates, Damien, Murdoch Institute
Beckhelling, Clare, Laboratoire de Biologie-Cellulaire
Lee, Vivian, Oregon Health Sciences University
Warkman, Andrew, University of Western Ontario

Merck & Company, Inc. Scholarships

Gilk, Stacey, University of Vermont
Lamb, Tracey, ICAPB
Lowell, Joanna, Rockefeller University
Martins, Gislaïne, Faculdade de Medicina de Ribeirao Preto
Murta, Silvana, Centro e Pesquisas René Rachou-FIOCRUZ
O'Donnell, Rebecca, University of Melbourne
Ralph, Stuart, University of Melbourne
Villarino, Alejandro, University of Pennsylvania

Charles Baker Metz and William Metz Scholarship Fund in Reproductive Biology

Keller, Dominique, Texas A&M University
Richard, Craig, University of Pittsburgh

Frank Morrell Endowed Memorial Scholarship

Kettunen, Petronella, Novel Institute for Neurophysiology

Mountain Memorial Fund Scholarship

Carroll, Michael, University of Newcastle
Cordeiro, Maria Sofia, Instituto Gulbenkian de Ciencia
Cotrufo, Tiziana, Institute of Neurophysiology
Sen, Subhojit, Tata Institute of Fundamental Research
Shilkrut, Mark, Technion-Israel Institute of Technology
Zeidner, Gil, The Weizmann Institute of Science

Pfizer Inc Endowed Scholarship

Dayel, Mark, University of California, San Francisco
Lin, Li-hung, Princeton University

Planetary Biology Internship Awards

Kadavy, Dana, University of Nebraska, Lincoln
Ward, Dawn, University of Delaware

William Townsend Porter Fellowship and Scholarship Fund

Bradford, Yvonne, University of Oregon
Colón-Ramos, Daniel, Duke University
Crespo-Barreto, Juan, University of Puerto Rico
Espinoza, Nora, University of Chicago

Glater, Elizabeth, Brown University
 Hubbard, Aida, University of Texas, San Antonio
 Triggs, Veronica, University of Wisconsin, Madison

**Phillip H. Presley Scholarship Award
 Funded by Carl Zeiss, Inc.**

Neretin, Lev, Shirshov Institute of Oceanography
 Zaar, Annette, Universität Freiburg
 Livet, Jean, INSERM U.382
 McKellar, Claire, Harvard Medical School
 Misgeld, Thomas, Institute for Clinical Neuroimmunology
 Nelson, Laura, National Institute for Medical Research
 Yasuda, Ryohei, Teikyo University Biotech. Research Center
 Aspöck, Gudrun, University of Basel
 Beckhelling, Clare, Laboratoire de Biologie-Cellulaire
 Nasevicius, Aidas, University of Minnesota

Herbert W. Rand Fellowship and Scholarship Fund

Bodelón, Clara, Boston University
 Costa, Patricia, Universidad Federal do Rio de Janeiro
 Cotrufo, Tiziana, Institute of Neurophysiology
 Cruz, Georgina, University of South Florida
 Dayel, Mark, University of California, San Francisco
 Feinerman, Ofer, Weizmann Institute of Science
 Jhaveri, Dhanisha, Tata Institute of Fundamental Research
 Johansson, Viktoria, Göteborgs Universitet
 Kang, Kukjin, Hebrew University of Jerusalem
 Marrari, Yannick, Observatoire Océanographique
 Menna, Elisabetta, Institute of Neurophysiology, Pisa
 Sen, Subhojit, Tata Institute of Fundamental Research
 Shilkrut, Mark, Technion-Israel Institute of Technology
 Ulanovsky, Nachum, Hebrew University
 Zeidner, Gil, Weizmann Institute of Science

Ruth Sager Memorial Scholarship

Cheeks, Rebecca, University of North Carolina, Chapel Hill

Howard A. Schneiderman Endowed Scholarship

Misgeld, Thomas, Institute for Clinical Neuroimmunology
 Nelson, Laura, National Institute for Medical Research
 Zhong, Haining, Johns Hopkins University

Moshe Shilo Memorial Scholarship Fund

Barak, Yoram, Hebrew University

Post-Course Research Awards

Colon-Ramos, Daniel, Duke University (Physiology)
 Costa, Patricia, University of Rio de Janeiro (Physiology)

Society of General Physiologists' Scholarship

Ballard, Victoria, Weill Medical College
 McKellar, Claire, Harvard Medical School
 Menna, Elisabetta, Institute of Neurophysiology, Pisa
 Rela, Lorena, Universidad de Buenos Aires

Marjorie W. Stetten Scholarship Fund

Ballard, Victoria, Weill Medical College
 Ellertsdóttir, Elin, University of Freiburg

Horace W. Stunkard Scholarship Fund

Berkowitz, Karen, Hospital of the University of Pennsylvania
 Sahgal, Namita, Kansas University Medical Center

Surdna Foundation Scholarship

Brelidze, Tinatin, University of Miami School of Medicine
 Cotrufo, Tiziana, Institute of Neurophysiology
 Ding, Long, University of Pennsylvania
 Johansson, Viktoria, Göteborgs Universitet
 Kettunen, Petronella, Nobel Institute for Neurophysiology
 Livet, Jean, INSERM U.382
 Marrari, Yannick, Observatoire Océanographique
 McKellar, Claire, Harvard Medical School
 Misgeld, Thomas, Institute for Clinical Neuroimmunology
 Nelson, Laura, National Institute for Medical Research
 Sen, Subhojit, Tata Institute of Fundamental Research
 Yasuda, Ryohei, Teikyo University Biotech. Research Center
 Zeidner, Gil, Weizmann Institute of Science

**William Morton Wheeler Family Founders'
 Scholarship**

Zhong, Haining, Johns Hopkins University

Walter L. Wilson Endowed Scholarship Fund

Brelidze, Tinatin, University of Miami School of Medicine
 Cotrufo, Tiziana, Institute of Neurophysiology

**World Academy of Arts and Sciences
 Emily Mudd Scholarship**

Greenlee, Anne, Marshfield Medical Research Foundation
 Powell, Jacqueline, Morehouse School of Medicine

World Health Organization

Diaz, Lorenza, Instituto Nacional de la Nutricion

Dayel, Mark, University of California, San Francisco (Physiology)
 Siuda, Eduard, Michigan State University (Neural Systems and Behavior)



Board of Trustees and Committees

Corporation Officers and Trustees

Chairman of the Board of Trustees, Sheldon J. Segal, The Population Council
Co-Vice Chair of the Board of Trustees, Frederick Bay, Josephine Bay Paul and C. Michael Paul Foundation
Co-Vice Chair of the Board of Trustees, Mary J. Greer, New York, NY
President of the Corporation, John E. Dowling, Harvard University
Director and Chief Executive Officer, John E. Barris, Marine Biological Laboratory*
Interim Director and Chief Executive Officer, William T. Speck, Marine Biological Laboratory*
Treasurer of the Corporation, Mary B. Conrad, Fiduciary Trust International*
Clerk of the Corporation, Robert E. Mainer, The Boston Company
Chair of the Science Council, Robert B. Barlow, SUNY Health Science Center*
Chair of the Science Council, Kerry S. Bloom, University of North Carolina*

Class of 2001

Anderson, Porter W., North Miami Beach, FL
Bay, Frederick, Josephine Bay Paul and C. Michael Paul Foundation, Inc.
Cox, Martha W., Hobe Sound, FL
Greer, Mary J., New York, NY
Steere, William C. Jr., Pfizer Inc
Weissmann, Gerald, New York University School of Medicine

Class of 2002

Lakian, John R., The Fort Hill Group, Inc.
Ruderman, Joan V., Harvard Medical School
Segal, Sheldon J., The Population Council
Speck, William T., Marine Biological Laboratory
Zeien, Alfred M., The Gillette Company

Class of 2003

Kelley, Darcy Brisbane, Columbia University
Landeau, Laurie J., Marinetics, Inc.
Lee, Burton J. III, Vero Beach, FL
O'Hanley, Ronald P., Mellon Institutional Asset Management
Pierce, Jean, Boca Grande, FL
Ryan, Vincent J., Schooner Capital LLC

* *Ex officio*

Class of 2004

Jacobson, M. Howard, Bankers Trust
Langford, George M., Dartmouth College
Miller, G. William, G. William Miller & Co., Inc.
Press, Frank, The Washington Advisory Group
Weld, Christopher M., Sullivan and Worcester, Boston
Wiesel, Torsten N., The Rockefeller University

Honorary Trustees

Cunningham, Mary Ellen, Grosse Pointe Farms, MI
Ebert, James D., Baltimore, MD
Golden, William T., New York, NY
Grass, Ellen R., The Grass Foundation

Trustees Emeriti

Adelberg, Edward A., Yale University, New Haven, CT
Buck, John B., Sykesville, MD
Cohen, Seymour S., Woods Hole, MA
Colwin, Arthur L., Key Biscayne, FL
Colwin, Laura Hunter, Key Biscayne, FL
Copeland, Donald Eugene, Woods Hole, MA
Crowell, Sears Jr., Indiana University, Bloomington, IN
Hayashi, Teru, Woods Hole, MA
Hubbard, Ruth, Cambridge, MA
Kleinholz, Lewis, Reed College, Portland, OR
Krahl, Maurice, Tucson, AZ
Prosser, C. Ladd, University of Illinois, Urbana, IL
Russell-Hunter, W. D., Syracuse University, Syracuse, NY
Saunders, John W., Waquoit, MA
Shepro, David, Boston, MA
Trigg, D. Thomas, Wellesley, MA
Vincent, Walter S., Woods Hole, MA

Directors Emeriti

Ebert, James D., Baltimore, MD
Gross, Paul, Falmouth, MA
Halvorson, Harlyn O., Woods Hole, MA

Executive Committee of the Board of Trustees

Segal, Sheldon J., Chair
 Bay, Frederick, Co-Vice Chair
 Greer, Mary J., Co-Vice Chair
 Anderson, Porter W.
 Barlow, Robert B.
 Bloom, Kerry S.
 Burris, John E.
 Conrad, Mary B., Treasurer
 Mainer, Robert E.
 O'Hanley, Ronald P.
 Speck, William T.
 Weissmann, Gerald

Science Council

Barlow, Robert B., Chair (2001)
 Bloom, Kerry S., Chair (2000)
 Armstrong, Clay M. (2002)
 Armstrong, Peter (2002)
 Atema, Jelle (2001)
 Burris, John E.*
 Dawidowicz, E. A.*
 Haimo, Leah (2001)
 Hopkinson, Charles (2002)
 Jaffe, Laurinda (2001)
 Smith, Peter J. S. (2001)
 Sogin, Mitchell (2002)
 Speck, William T.*
 Weeks, Janis C. (2002)

Standing Committees of the Board of Trustees

Development

Speck, William, Chair
 Anderson, Porter W.
 Barlow, Robert W.
 Bay, Frederick
 Conrad, Mary B.
 Cox, Martha W.
 Dowling, John
 Ebert, James D.
 Grant, Philip
 Lakian, John R.
 Langford, George
 Lee, Burton J.
 Miller, G. William
 Pierce, Jean
 Steere, William C.
 Weld, Christopher M.
 Wiesel, Torsten

Facilities and Capital Equipment

Anderson, Porter W., Chair
 Bay, Frederick
 Boyer, Barbara
 Langford, George
 Press, Frank
 Ruderman, Joan
 Weld, Christopher M.
 Wiesel, Torsten

* *Ex officio*

Investment

Conrad, Mary B., Chair
 Jacobson, M. Howard
 Lakian, John R.
 Mainer, Robert E.
 Miller, G. William
 O'Hanley, Ronald P.
 Ryan, Vincent J.
 Segal, Sheldon J.
 Zeien, Alfred M.

Finance

O'Hanley, Ronald, Chair
 Conrad, Mary B.
 DeHart, Donald
 Jacobson, M. Howard
 Kelley, Darcy Brisbane
 Lakian, John R.
 Landeau, Laurie J.
 Loewenstein, Werner
 Mainer, Robert E.
 Manz, Robert
 Miller, G. William
 Ryan, Vincent J.
 Zeien, Alfred M.

Nominating

Weissmann, Gerald, Chair
 Barlow, Robert B.
 Bloom, Kerry S.
 Cox, Martha W.
 Greer, Mary J.
 Pierce, Jean
 Segal, Sheldon J.
 Speck, William T.

Standing Committees of the Corporation and Science Council

Buildings and Grounds

Boyer, Barbara C., Chair
Cutler, Richard*
Eckberg, Bill
Fleet, Barry*
Hayes, Joe*
McArthur, Andrew
Peterson, Bruce J.
Tweedell, Kenyon S.
Valiela, Ivan

Beckwith, Mary*
Bloom, Kerry S.*
Browne, Robert*
Cutler, Richard*
Goux, Susan*
Hinkle, Pamela Clapp*
Malchow, Robert P.
McDonough, Stefan
Rastetter, Edward
Stuart, Ann E.
Weeks, Janis C.

Education Committee

Barlow, Robert B.*
Bloom, Kerry S.*
Dawidowicz, E. A.*
Dionne, Vincent, Chair
Dunlap, Paul
Fink, Rachel
Hanlon, Roger
Kiehart, Dan
Madison, Dan
Venuti, Judith
Wadsworth, Patricia
Zottoli, Steve

MBL/WHOI Library Joint Advisory Committee

Shepro, David, Chair, MBL
Ashmore, Judy, MBL*
Dow, David, NMFS
Harbison, G. Richard, WHOI
Hobbie, John, MBL
Hurter, Colleen, WHOI*
Norton, Cathy, MBL*
Robb, James, USGS
Smith, Peter J. S., MBL
Smolowitz, Roxanna, MBL
Tucholke, Brian, WHOI
Warren, Bruce, WHOI

Fellowships

Pederson, Thoru, Chair
Dawidowicz, E. A.*
Deegan, Linda
Ehrlich, Barbara
Kaufmann, Sandra* (Recording Secretary)
Lemos, Jose
Pipscombe, Diane
Sluder, Greenfield
Smith, Peter J. S.
Treistman, Steven (Guest Member)

Research Services and Space

Laufer, Hans, Chair
Armstrong, Peter B.
Cutler, Richard*
Dawidowicz, E. A.*
Foreman, Kenneth
Kerr, Louis M.*
Landowne, David
Mattox, Andrew*
Melillo, Jerry
Mizell, Merle
Smith, Peter J. S.
Stuedler, Paul
Valiela, Ivan

Housing, Food Service and Child Care

Browne, Carol, Chair
Barlow, Robert B.*

Discovery: The Campaign for Science at the Marine Biological Laboratory Steering Committee

Bay, Frederick, Campaign Chair
Golden, William T., Honorary Chair
Grass, Ellen R., Honorary Chair
Clowes, Alexander W., Vice-Chair
Cox, Martha W., Vice-Chair
Miller, G. William, Vice-Chair
Weissmann, Gerald, Vice-Chair
Anderson, Porter

Barlow, Robert B., Jr.
Bernstein, Norman
Cobb, Jewell Plummer
Conrad, Mary B.
Cunningham, Mary-Ellen
Dowling, John E.
Ebert, James D.
Fischbach, Gerald D.
Goldman, Robert D.
Greer, Mary J.
Jacobson, M. Howard

* *Ex officio*

Landeau, Laurie J.
Langford, George M.
Lee, Burton J. III
Pierce, JeJe
Prendergast, Robert A.
Shepro, David
Speck, William T.
Steere, William C. Jr.
Swope, John F.
Weld, Christopher M.
Zeien, Alfred M.

Council of Visitors

Norman B. Asher, Esq., Hale and Dorr, Counsellors at Law,
Boston, MA

Mr. Robert W. Ashton, Bay Foundation, New York, NY

Mr. Donald J. Bainton, Continental Can Co., Boca Raton, FL
Mr. David Bakalar, Chestnut Hill, MA
Mr. Charles A. Baker, The Liposome Company, Inc., Princeton, NJ
Dr. George P. Baker, Mass General Hospital, Boston, MA
Dr. Sumner A. Barenberg, Bernard Technologies, Chicago, IL
Mr. Mel Barkan, The Barkan Companies, Boston, MA
Mr. Bruce A. Beal, The Beal Companies, Boston, MA
Mr. Robert P. Beech, Component Software International, Inc.,
Mason, OH
Mr. George Berkowitz, Legal Sea Foods, Allston, MA
Jewelle and Nathaniel Bickford, New York, NY
Dr. Elkan R. Blout, Harvard Medical School, Boston, MA
Mr. and Mrs. Philip Bogdanovitch, Lake Clear, NY
Mr. Malcolm K. Brachman, Northwest Oil Company, Dallas, TX
Dr. Goodwin M. Breinin, NY University Medical Center,
New York, NY

Mr. John Callahan, Carpenter, Sheperd & Warden, New London, NH
Mrs. Elizabeth Campanella, West Falmouth, MA
Thomas S. Crane, Esq., Mintz Levin Cohen Ferris Glovsky & Popeo,
PC, Boston, MA
Dr. Stephen D. Crocker, Cyber Cash Inc., Reston, VA
Mrs. Lynn W. Piasecki Cunningham, Piasecki Productions,
Brookline, MA
Dr. Anthony J. Cutaia, Anheuser-Busch, Inc., St. Louis, MO

Dr. Georges de M n il, DM Foundation, New York, NY
Mrs. Sara Greer Dent, Chevy Chase, MD
Mr. D. H. Douglas-Hamilton, Hamilton Thorne Research, Beverly, MA
Mr. Benjamin F. du Pont, Du Pont Company, Deepwater, NJ

Dr. Sylvia A. Earle, Deep Ocean Engineering, Oakland, CA
Mr. and Mrs. Hoyt Ecker, Vero Beach, FL
Mr. Anthony B. Evnin, Venrock Associates, New York, NY

Stuart Feiner, Esq., Inco Limited, Toronto, Ontario, Canada
Mrs. Hadley Mack French, Edsel and Eleanor Ford House, Grosse
Pointe Farms, MI

Mr. and Mrs. Huib Geerlings, Boston, MA
Mr. William J. Gilbane, Jr., Gilbane Building Company, Providence, RI
Dr. Michael J. Goldblatt, Defense Sciences Office, Arlington, VA
Mr. Maynard Goldman, Maynard Goldman & Associates, Boston, MA

Ms. Charlotte I. Hall, Edgartown, MA
Dr. Thomas R. Hedges, Jr., Neurological Institute, PA Hospital,
Philadelphia, PA
Drs. Linda Hirshman and David Forkosh, Brandeis University & FMH
Foundation, Waltham, MA
Mr. Thomas J. Hynes, Jr., Meredith & Grew, Inc., Boston, MA

Mrs. Elizabeth Ford Kontulis, New Canaan, CT

Mr. and Mrs. Robert Lambrecht, Boca Grande, FL
Dr. Catherine C. Lastavica, Tufts University School of Medicine,
Boston, MA
Mr. Joel A. Leavitt, Boston, MA
Mr. Stephen W. Leibholz, TechLabs, Inc., Huntingdon, PA
Mrs. Margaret Lilly, West Falmouth, MA
Mr. Richard Lipkin, Laird & Co., LLC, New York, NY
Mr. George W. Logan, Valley Financial Corp., Roanoke, VA

Mr. Michael T. Martin, SportsMark, Inc., New York, NY
Dr. Walter E. Massey, President, Morehouse College, Atlanta, GA
Mrs. Christy Swift Maxwell, Grosse Pointe Farms, MI
Mr. Ambrose Monell, G. Unger Vetlesen Foundation, Palm Beach, FL

Dr. Mark Novitch, Washington, DC

Mr. David R. Palmer, David Ross Palmer & Associates, Waquoit, MA
Dr. Roderic B. Park, Richmond, CA
Mr. Santo P. Pasqualucci, Falmouth Co-Operative Bank, Falmouth, MA
Mr. Robert Pierce, Jr., Pierce Aluminum Co., Canton, MA

Mr. Richard Reston, *Vineyard Gazette*, Edgartown, MA
Mr. Marius A. Robinson, Fundamental Investors Ltd., Biscayne, FL
John W. Rowe, M.D., Mt. Sinai School of Medicine & Mt. Sinai
Medical Center, New York, NY
Mr. Edward Rowland, Tucker, Anthony, Inc., Boston, MA

Mr. Gregory A. Sandomirsky, Mintz Levin Cohen Ferris Glovsky &
Popeo, PC, Boston, MA
Mrs. Mary Schmidek, Marion, MA
Dr. Cecily C. Selby, New York, NY
Mr. Robert S. Shifman, St. Simon's Island, GA
Mr. and Mrs. Gregory Skau, Grosse Pointe Farms, MI
Mr. Malcolm B. Smith, General American Investors Co.,
New York, NY
Mr. John C. Stegeman, Campus Rentals, Ann Arbor, MI
Mr. Joseph T. Stewart, Jr., Skillman, NJ
Mr. John W. Stroh, III, The Stroh Brewery Company, Detroit, MI
Mr. Gerard L. Swope, Washington, DC
Mr. John F. Swope, Concord, NH

Mr. and Mrs. Stephen E. Taylor, Milton, MA

Mrs. Donna Vanden Bosch-Flynn, Spring Lake, NJ
Mrs. Carolyn W. Verbeck, Vineyard Haven, MA

Mr. Benjamin S. Warren III, Grosse Pointe Farms, MI
Nancy B. Weinstein, R.N., The Hospice, Inc., Glen Ridge, NJ
Stephen S. Weinstein, Esq., Morristown, NJ
Mr. Frederick J. Weyerhaeuser, Beverly, MA
Mrs. Robin Wheeler, West Falmouth, MA
Mr. Tony L. White, The Perkin Elmer Corporation, Norwalk, CT



Administrative Support Staff¹

Biological Bulletin

Greenberg, Michael J., Editor-in-Chief
Hinkle, Pamela Clapp, Managing Editor
Burns, Patricia
Gibson, Victoria R.
Marrama, Carol
Schachinger, Carol H.

Director's Office

Burris, John E., Director and Chief Executive Officer
Speck, William T., Interim Director and Chief Executive Officer
Donovan, Marcia H.

Equal Employment Opportunity

MacNeil, Jane L.

Veterinarian Services

Dushman, Beth²
O'Shea, Erin²
Smolowitz, Roxanna
St. Pierre, Aimee²
Stukey, Jetley
Watmough, Elizabeth²
Weiss, Erica²

Ecosystems Center Administrative Staff

Berthel, Dorothy J.
Donovan, Suzanne J.
Nunez, Guillermo
Seifert, Mary Ann

External Affairs

Carotenuto, Frank C., Director
Butcher, Valerie
Faxon, Wendy P.
Johnson, A. Kristine
Martin, Theresa H.
Patch-Wing, Dolores
Quigley, Barbara A.
Shaw, Kathleen L.

Associates Program

Bohr, Kendall B.
Sgarzi, Dorothy J.²

Communications Office

Hinkle, Pamela Clapp, Director
Flynn, Bridget
Hartmann, Kelley²
Joslin, Susan
Kent, Elizabeth F.²
Langill, Christine²
Liles, Beth R.
Mossman, Beverly
Sloboda, Lara N.²

Financial Services Office

Lane, Jr., Homer W., Chief Financial Officer
Bowman, Richard, Controller
Mullen, Richard J., Manager, Research Administration
Afonso, Janis
Aguiar, Deborah
Bliss, Casey M.
Crosby, Kenneth
Lancaster, Cindy
Livingstone, Suzanne
McLaughlin, Rebecca Jill
Ranzinger, Laura
Stellrecht, Lynette

Stock Room

Schorer, Timothy M., Supervisor
Burnette, Donald
Olive, Charles W., Jr.
Treisman, Ethan²

Purchasing

Hall, Lionel E., Jr., Supervisor
Barkley, Rachel A.²
Hunt, Lisa M.

Housing and Conferences

Beckwith, Mary M., Director
King, LouAnn D., Director
Adams, Jessica²
Campbell, Anne T.
Grasso, Deborah

¹ Including persons who joined or left the staff during 2000.

² Summer or temporary.

Hanlon, Arlene K.²
 Johnson-Horman, Frances N.
 Kruger, Sally J.
 Masse, Todd C.
 Perito, Diana

Human Resources

Goux, Susan P., Director
 Houser, Carmen

Josephine Bay Paul Center for Comparative Molecular
 Biology and Evolution Administrative Staff

Harris, Marian
 Lim, Pauline
 Sansone, Rebecca
 Schlichter, Mimi

Journal of Membrane Biology

Loewenstein, Werner R., Editor
 Fay, Catherine H.
 Howard Isenberg, Linda L.
 Lynch, Kathleen F.

Marine Resources Center

Hanlon, Roger T., Director
 Santore, Gabrielle

Aquatic Resources Department

Enos, Edward G., Jr., Superintendent
 Dimond, James L.²
 Grossman, William M.
 Gudas, Christopher N.²
 Klimm, Henry W., III
 Potter, Benjamin²
 Reynolds, Justin M.²
 Sexton, Andrew W.
 Sullivan, Daniel A.
 Tassinari, Eugene
 Whelan, Sean P.

MRC Life Support System

Mebane, William N., Systems Operator
 Carroll, James
 Hanley, Janice S.
 Kuzirian, Alan

MBL/WHOI Library

Norton, Catherine N., Director
 Ashmore, Judith A.
 Costa, Marguerite E.
 Deveer, Joseph M.
 Farrar, Stephen R. L.
 Lavoie, Amy²
 Martel, David²
 Monahan, A. Jean
 Moniz, Kimberly L.
 Moore, Laurel E.
 Nelson, Heidi
 Person, Matthew

Riley, Jacqueline
 Walton, Jennifer

Copy Center

Mountford, Rebecca J., Supervisor
 Brissenden, Roberta²
 Clark, Sarah²
 Clark, Tamara L.
 Cosgrove, Nancy
 Douglas, Valerie M.²
 Eldridge, Myles²
 Jenkins, Sarah²
 Mancini, Mary E.
 Reuter, Laura

Information Systems Division

Inzina, Barbara, Network Manager
 Borst, Douglas T.²
 Campbell, David J., Jr.
 Cohen, Alex²
 Douglas, Valerie²
 Houser, Clarissa²
 Jones, Patricia L.
 Kokmeyer, Remmert²
 Lowell, Gregory
 Mountford, Rebecca J.
 Moynihan, James V.
 Purdy, Heather²
 Remsen, David P.
 Renna, Denis J.
 Space, David B.
 Wheeler, Patrick
 Williams, Shelly R.²

NASA Center for Advanced Studies in the Space Life Sciences

Blazis, Diana, Administrator
 Golden, Catherine
 Oldham, Pamela

Research Administration and Educational Programs

Dawidowicz, Eliezar A., Director
 Brooks, Marilyn²
 Hamel, Carol C.
 Holzworth, Kelly
 Kaufmann, Sandra J.
 Mebane, Dorianne C.
 White, Laurie

Central Microscopy Facility and General Use Rooms

Kerr, Louis M., Supervisor
 Bennett-Stamper, Christina²
 Luther, Herbert
 Peterson, Martha B.

Safety Services

Mattox, Andrew H., Environmental, Health, and Safety Manager
 Normand, Danielle²

Satellite/Periwinkle Children's Programs

Robinson, Paulina H.²
Audran, Chantal²
Beaudoin, Cynthia²
Bothner, Katharine²
Brown, Shannon²
Duncan, Brett M.²
Fitzelle, Annie²
Gallant, Carolyn²
Gallant, Cynthia²
Guiffrida, Beth²
Halter, Sarah²
Karalekas, Nina²
Noonan, Brendan²
Noonan, Ryan²
Pascavage, Leigh²
Shanley, Jennifer²
Shwartz, Cortney²

Service, Projects and Facilities

Cutler, Richard D., Director
Enos, Joyce B.
Guarente, Jeffrey²

Apparatus

Baptiste, Michael G.
Barnes, Franklin D.
Haskins, William A.
Pratt, Barry

Building Services and Grounds

Hayes, Joseph H., Superintendent
Anderson, Lewis B.
Atwood, Paul R.
Baker, Harrison S.
Barnes, Susan M.
Berrios, Jessica
Berube, Douglas T.²
Berthel, Frederick
Billings, Julia²
Boucher, Richard L.
Brereton, Richard S.²
Cameron, Lawrence M.²
Chen, Zhi Xin
Clayton, Daniel
Collins, Paul J.
Cutillo, David
Djelidi, Meriam J.²
Doherty, Garrett²
Fernandez, Peter R.²
Ficher, Jason
Frisk, Maria²
Gibbons, Roberto G.
Gore, Simon J.²
Hannigan, Catherine
Heede, Kelly²
Houle, Michael E.²

Illgen, Robert F.
Kaczmarek, Konrad²
Keefe, Edward C.
Kijowski, Wojciech²
Ledwell, L. Patrick²
MacDonald, Cynthia C.
Massi, Christopher²
McGee, Melissa
McHugh, Mary²
McNamara, Noreen M.
McQuillan, Jeffrey²
McVey, Brienna²
Mendoza, Duke R.²
O'Brien, William P.²
Peros, Kristina²
Pratt, Barry
Rana, Saoud²
Robinson, Marva
Ryan, Nicholas P.²
Santiago, Crystal²
Schlemmermeyer, Jaan²
Shum, Mei Wah
Sizelove, Robert²
Ullian, Adam²
Wagner, Paul²
Ware, Lynn M.
Waterbury, Matthew²

Plant Operations and Maintenance

Fleet, Barry M., Manager
Cadose, James W., Maintenance Supervisor
Barnes, John S.
Blunt, Hugh F.
Bourgoin, Lee E.
Callahan, John J.
Carroll, James R.
Duncan, Brett²
Elias, Michael
Fish, David L., Jr.
Fuglister, Charles K.
Goehl, George
Gonsalves, Walter W., Jr.
Hathaway, Peter J.
Henderson, Jon R.
Kelley, Kevin
Langill, Richard
Lochhead, William M.
McAdams, Herbert M., III
McHugh, Michael O.
Mills, Stephen A.
Olive, Charles W., Jr.
Rattacasa, Frank²
Rozum, John
Scanlan, Melanie
Settlemyre, Donald
Shepherd, Denise M.
Toner, Michael
Wetzel, Ernest D.²



Members of the Corporation

Life Members

Acheson, George H., 25 Quissett Avenue, Woods Hole, MA 02543
(deceased 2000)

Adelberg, Edward A., 204 Prospect Street, New Haven, CT 06511-2107

Afzelius, Bjorn, University of Stockholm, Wenner-Gren Institute,
Department of Ultrastructure Research, Stockholm, SWEDEN

Amatniek, Ernest, (address unknown)

Arnold, John M., 329 Sippewissett Road, Falmouth, MA 02540

Bang, Betsy G., 76 F. R. Lillie Road, Woods Hole, MA 02543

Bartlett, James H., University of Alabama, Department of Physics, Box
870324, Tuscaloosa, AL 35487-0324 (deceased 2000)

Berne, Robert M., 19 Gardiner Road, Woods Hole, MA 02543

Bernheimer, Alan W., New York University Medical Center,
Department of Microbiology, 550 First Avenue, New York, NY
10016

Bertholf, Lloyd M., Westminster Village, #2114, 2025 East Lincoln
Street, Bloomington, IL 61701-5995

Bosch, Herman F., 163 Elm Road, Falmouth, MA 02540-2430

Brinley, F. J., National Institutes of Health, NINCDS, Neurological
Disorders Program, Room 812 Federal Building, Bethesda, MD 20892

Buck, John B., Fairhaven C-020, 7200 Third Avenue, Sykesville, MD
21784

Burhanck, Madeline P., P.O. Box 15134, Atlanta, GA 30333

Burhanck, William D., P.O. Box 15134, Atlanta, GA 30333

Clark, Arnold M., 53 Wilson Road, Woods Hole, MA 02543

Clark, James M., 258 Wells Road, Palm Beach, FL 33480-3625

Cohen, Seymour S., 10 Carrot Hill Road, Woods Hole, MA
02543-1206

Colwin, Arthur L., 320 Woodcrest Road, Key Biscayne, FL
33149-1322

Colwin, Laura Hunter, 320 Woodcrest Road, Key Biscayne, FL
33149-1322

Cooperstein, Sherwin J., University of Connecticut, School of
Medicine, Department of Anatomy, Farmington, CT 06030-3405

Copeland, D. Eugene, Marine Biological Laboratory, Woods Hole, MA
02543

Corliss, John O., P.O. Box 2729, Bala Cynwyd, PA 19004-2116

Costello, Helen M., 137 Carolina Meadows, Chapel Hill, NC
27514-8512

Crouse, Helen, Rte. 3, Box 213, Hayesville, NC 28904

DeHaan, Robert L., Emory University School of Medicine, Department
of Anatomy & Cell Biology, 1648 Pierce Drive, Room 108, Atlanta,
GA 30322

Dudley, Patricia L., 3200 Alki Avenue SW, #401, Seattle, WA 98116

Edwards, Charles, 3429 Winding Oaks Drive, Longboat Key, FL
34228

Elliott, Gerald F., The Open University Research Unit, Foxcombe Hall,
Berkeley Road, Boars Hill, Oxford OX1 5HR, UK

Failla, Patricia M., 2149 Loblolly Lane, Johns Island, SC 29455

Frazier, Donald T., University of Kentucky Medical Center,
Department of Physiology and Biophysics, MS501 Chandler Medical
Center, Lexington, KY 40536

Gabriel, Mordecai L., Brooklyn College, Department of Biology, 2900
Bedford Avenue, Brooklyn, NY 11210

Glusman, Murray, New York State Psychiatric Institute, 722 W. 168th
St., Unit #70, New York, NY 10032

Graham, Herbert, 36 Wilson Road, Woods Hole, MA 02543

Hamburger, Viktor, Washington University, Department of Biology,
740 Trinity Avenue, St. Louis, MO 63130 (deceased 2001)

Hamilton, Howard L., University of Virginia, Department of Biology,
238 Gilmer Hall, Charlottesville, VA 22901

Harding, Clifford V., Jr., 100 Saconesnet Road, Falmouth, MA 02540

Haschemeyer, Audrey E. V., 21 Glendon Road, Woods Hole, MA
02543-1406

Hayashi, Teru, 15 Gardiner Road, Woods Hole, MA 02543-1113

Hisaw, Frederick L., (address unknown)

Huskin, Francis C. G., c/o Dr. John E. Walker, U.S. Army Natick
RD&E Center, SAT NC-YSM, Kansas Street, Natick, MA 01760-
5020

- Hubbard, Ruth**, Harvard University, Biological Laboratories, Cambridge, MA 02138
- Hunter, W. Bruce**, 305 Old Sharon Road, Peterborough, NH 03458-1736
- Hurwitz, Charles**, Stratton VA Medical Center, Research Service, Albany, NY 12208
- Katz, George**, 1636 Brookhouse Drive, Apt. BR131, Sarasota, FL 34731
- Kingsbury, John M.**, Cornell University, Department of Plant Biology, Plant Science Building, Ithaca, NY 14853
- Kleinholz, Lewis**, Reed College, Department of Biology, 3203 SE Woodstock Boulevard, Portland, OR 97202
- Kusano, Kiyoshi**, National Institutes of Health, Building 36, Room 4D-20, Bethesda, MD 20892
- Laderman, Ezra**, Yale University, New Haven, CT 06520
- LaMarche, Paul H.**, Eastern Maine Medical Center, 489 State Street, Bangor, ME 04401
- Lauffer, Max A.**, Penn State University Medical Center, Department of Biophysics & Physiology, Hershey, PA 17033
- Leviton, Herbert**, National Science Foundation, 4201 Wilson Boulevard, Room 835, Arlington, VA 22230
- Lochhead, John H.**, 49 Woodlawn Road, London SW6 6PS, UK
- Loewus, Frank A.**, Washington State University, Institute of Biological Chemistry, Pullman, WA 99164
- Lofffield, Robert B.**, University of New Mexico, School of Medicine, 915 Stanford Drive, Albuquerque, NM 87131
- Lorand, Laszlo**, Northwestern University Medical School, CMS Biology, Searle 4-555, 303 East Chicago Avenue, Chicago, IL 60611-3008
- Mainer, Robert E.**, The Boston Company, Inc., One Boston Place, OBP-15-D, Boston, MA 02108
- Malkiel, Saul**, 174 Queen Street, #9A, Falmouth, MA 02540
- Marsh, Julian B.**, 9 Eliot Street, Chestnut Hill, MA 02467-1407
- Martin, Lowell V.**, 10 Buzzards Bay Avenue, Woods Hole, MA 02543
- Mathews, Rita W.**, East Hill Road, P.O. Box 237, Southfield, MA 01259-0237
- Metuzals, Janis**, University of Ottawa Faculty of Medicine, Department of Pathology, 451 Smyth Road, Ottawa, ON K1H 8M5, Canada
- Moore, John A.**, University of California, Department of Biology, Riverside, CA 92521
- Moore, John W.**, Duke University Medical Center, Department of Neurobiology, Box 3209, Durham, NC 27710
- Moscona, Aron A.**, 221 West 82nd Street, #8C, New York, NY 10024
- Musacchia, X. J.**, P.O. Box 5054, Bella Vista, AR 72714-0054
- Nasatir, Maimon**, P.O. Box 379, Ojai, CA 93024
- Passano, Leonard M.**, University of Wisconsin, Department of Zoology, Birge Hall, Madison, WI 53706
- Price, Carl A.**, 20 Maker Lane, Falmouth, MA 02540
- Prosser, C. Ladd**, University of Illinois, Department of Physiology, 524 Burrill Hall, Urbana, IL 61801
- Prytz, Margaret McDonald**, (Address unknown)
- Renn, Charles E.**, (Address unknown)
- Reynolds, George T.**, Princeton University, Department of Physics, Jadwin Hall, Princeton, NJ 08544
- Rice, Robert V.**, 30 Burnham Drive, Falmouth, MA 02540
- Rockstein, Morris**, 600 Biltmore Way, Apt. 805, Coral Gables, FL 33134
- Roth, Jay S.**, 26 Huettner Road, P.O. Box 692, Woods Hole, MA 02543-0692
- Ronkin, Raphael R.**, 3212 McKinley Street, NW, Washington, DC 20015-1635
- Roslansky, John D.**, 57 Buzzards Bay Avenue, Woods Hole, MA 02543
- Roslansky, Priscilla F.**, Associates of Cape Cod, Inc., P.O. Box 224, Woods Hole, MA 02543-0224
- Sanders, Howard L.**, Woods Hole Oceanographic Institution, Woods Hole, MA 02543 (deceased 2001)
- Sato, Hidemi**, Nagoya University, 3-24-101, Oakinishi Machi, Toba Mie 517-0023, JAPAN
- Schlesinger, R. Walter**, 7 Langley Road, Falmouth, MA 02540-1809
- Scott, Allan C.**, Colby College, Waterville, ME 04901
- Silverstein, Arthur M.**, Johns Hopkins University, Institute of the History of Medicine, 1900 E. Monument Street, Baltimore, MD 21205
- Sjodin, Raymond A.**, 3900 N. Charles Street, Apt. #1301, Baltimore, MD 21218-1719
- Smith, Paul F.**, P.O. Box 264, Woods Hole, MA 02543-0264
- Speer, John W.**, 293 West Main Road, Portsmouth, RI 02871
- Spereklakis, Nicholas**, University of Cincinnati, Department of Physiology/Biophysics, 231 Bethesda Avenue, Cincinnati, OH 45267-0576
- Spiegel, Evelyn**, Dartmouth College, Department of Biological Sciences, 204 Gilman, Hanover, NH 03755
- Spiegel, Melvin**, Dartmouth College, Department of Biological Sciences, 204 Gilman, Hanover, NH 03755
- Stephens, Grover C.**, University of California, School of Biological Sciences, Department of Ecology and Evolution/Biology, Irvine, CA 92717
- Strehler, Bernard L.**, 31561 Crystal Sands Drive, Laguna Niguel, CA 92677
- Sussman, Maurice**, 72 Carey Lane, Falmouth, MA 02540
- Sussman, Raquel B.**, Marine Biological Laboratory, Woods Hole, MA 02543
- Szent-Gyorgyi, Gwen P.**, 45 Nobska Road, Woods Hole, MA 02543
- Thorndike, W. Nicholas**, Wellington Management Company, 200 State Street, Boston, MA 02109
- Trager, William**, The Rockefeller University, 1230 York Avenue, New York, NY 10021-6399
- Trinkaus, J. Philip**, Yale University, Department of Molecular, Cellular and Developmental Biology, Osborne Memorial Laboratory, New Haven, CT 06520
- Villee, Claude A., Jr.**, Harvard Medical School, Carrel L, Countway Library, 10 Shattuck Street, Boston, MA 02115
- Vincent, Walter S.**, 16 F.R. Lillie Road, Woods Hole, MA 02543
- Waterman, Talbot H.**, Yale University, Box 208103, 912 KBT Biology Department, New Haven, CT 06520-8103
- Wigley, Roland L.**, 35 Wilson Road, Woods Hole, MA 02543
- Witkovsky, Paul**, NYU Medical Center, Department of Ophthalmology, 550 First Avenue, New York, NY 10016

Members

- Abt, Donald A.**, Aquavet, University of Pennsylvania, School of Veterinary Medicine, 230 Main Street, Falmouth, MA 02540

- Adams, James A.**, 3481 Paces Ferry Road, Tallahassee, FL 32308
- Adelman, William J.**, 160 Locust Street, Falmouth, MA 02540
- Alkon, Daniel L.**, National Institutes of Health, Laboratory of Adaptive Systems, 36 Convent Drive, MSC 4124, 36/4A21, Bethesda, MD 20892-4124
- Allen, Garland E.**, Washington University, Department of Biology, Box 1137, One Brookings Drive, St. Louis, MO 63130-4899
- Allen, Nina S.**, North Carolina State University, Department of Botany, Box 7612, Raleigh, NC 27695
- Alliegro, Mark C.**, Louisiana State University Medical Center, Department of Cell Biology and Anatomy, 1901 Perdido Street, New Orleans, LA 70112
- Anderson, Everett**, Harvard Medical School, Department of Cell Biology, 240 Longwood Avenue, Boston, MA 02115-6092
- Anderson, John M.**, 110 Roat Street, Ithaca, NY 14850
- Anderson, Porter W.**, 914 Grande Avenue, Key Largo, FL 33037
- Arnett-Kibel, Christine**, University of Massachusetts, Dean of Science Faculty, Boston, MA 02125
- Armstrong, Clay M.**, University of Pennsylvania School of Medicine, B701 Richards Building, Department of Physiology, 3700 Hamilton Walk, Philadelphia, PA 19104-6085
- Armstrong, Ellen Prosser**, 57 Millfield Street, Woods Hole, MA 02543
- Armstrong, Peter B.**, University of California, Section of Molecular and Cell Biology, 149 Briggs Hall, Davis, CA 95616-8755
- Arnold, William A.**, Oak Ridge National Laboratory, Biology Division, 102 Balsalm Road, Oak Ridge, TN 37830
- Ashton, Robert W.**, Bay Foundation, 17 West 94th Street, New York, NY 10025
- Atema, Jelle**, Boston University Marine Program, Marine Biological Laboratory, Woods Hole, MA 02543
- Baccetti, Baccio**, University of Sienna, Institute of Zoology, 53100 Siena, Italy
- Baker, Robert G.**, New York University Medical Center, Department of Physiology and Biophysics, 550 First Avenue, New York, NY 10016
- Baldwin, Thomas O.**, University of Arizona, Department of Biochemistry, P.O. Box 210088, Tucson, AZ 85721-0088
- Baltimore, David**, California Institute of Technology, 1200 East California Boulevard, Pasadena, CA 91125
- Barlow, Robert B.**, SUNY Upstate Medical University, Center for Vision Research, 750 East Adams Street, Syracuse, NY 13210
- Barry, Daniel T.**, National Aeronautics and Space Administration, Lyn B. Johnson Space Center, 2101 NASA Road 1, Houston, TX 77058
- Barry, Susan R.**, Mount Holyoke College, Department of Biological Sciences, South Hadley, MA 01075
- Bass, Andrew H.**, Cornell University, Department of Neurobiology and Behavior, Seely Mudd Hall, Ithaca, NY 14853
- Battelle, Barbara-Anne**, University of Florida, Whitney Laboratory, 9505 Ocean Shore Boulevard, St. Augustine, FL 32086
- Bay, Frederick**, Bay Foundation, 17 W. 94th Street, First Floor, New York, NY 10025-7116
- Baylor, Martha B.**, P.O. Box 93, Woods Hole, MA 02543
- Bearer, Elaine L.**, Brown University, Division of Biology and Medicine, Department of Pathology, BMC 518, Providence, RI 02912
- Beatty, John M.**, University of Minnesota, Department of Ecology and Behavioral Biology, 1987 Gortner, Street Paul, MN 55108
- Beaugè, Luis Alberto**, Instituto de Investigacion Medica, Department of Biophysics, Casilla de Correo 389, Cordoba 5000, Argentina
- Begenisich, Ted**, University of Rochester, Medical Center, Box 642, 601 Elmwood Avenue, Rochester, NY 14642
- Begg, David A.**, University of Alberta, Faculty of Medicine, Department of Cell Biology and Anatomy, Edmonton, Alberta T6G 2H7, Canada
- Bell, Eugene**, 305 Commonwealth Avenue, Boston, MA 02115
- Benjamin, Thomas L.**, Harvard Medical School, Pathology, D2-230, 200 Longwood Avenue, Boston, MA 02115
- Bennett, Michael V. L.**, Albert Einstein College of Medicine, Department of Neuroscience, 1300 Morris Park Avenue, Bronx, NY 10461
- Bennett, Miriam F.**, Colby College, Department of Biology, Waterville, ME 04901
- Bennett, R. Suzanne**, Albert Einstein College of Medicine, Department of Neuroscience, 1410 Pelham Parkway South, Bronx, NY 10461
- Berg, Carl J. Jr.**, P.O. Box 681, Kilauea, Kauai, HI 96754-0681
- Berlin, Suzanne T.**, 87 Payneton Hill Road, York, ME 03909-5401
- Bernstein, Norman**, Columbia Realty Venture, 5301 Wisconsin Avenue, NW, #600, Washington, DC 20015-2015
- Bezanilla, Francisco**, Health Science Center, Department of Physiology, 405 Hilgard Avenue, Los Angeles, CA 90024
- Biggers, John D.**, Harvard Medical School, Department of Physiology, Boston, MA 02115
- Bishop, Stephen H.**, 2609 Eisenhower, Ames, IA 50010
- Blaustein, Mordecai P.**, University of Maryland, School of Medicine, Department of Physiology, Baltimore, MD 21201
- Blazis, Diana E. J.**, Marine Biological Laboratory, Center for Advanced Studies in the Space Life Sciences, Woods Hole, MA 02543
- Blennemann, Dieter**, 1117 East Putnam Avenue, Apt. #174, Riverside, CT 06878-1333
- Bloom, George S.**, The University of Texas Southwestern Medical Center, Department of Cell Biology and Neuroscience, 5323 Harry Hines Boulevard, Dallas, TX 75235-9039
- Bloom, Kerry S.**, University of North Carolina, Department of Biology, 623 Fordham Hall CB#3280, Chapel Hill, NC 27599-3280
- Bodznick, David A.**, Wesleyan University, Department of Biology, Lawn Avenue, Middletown, CT 06497-0170
- Boettiger, Edward G.**, P.O. Box 48, Rochester, VT 05767-0048
- Booolootian, Richard A.**, Science Software Systems, Inc., 3576 Woodcliff Road, Sherman Oaks, CA 91403
- Borgese, Thomas A.**, Lehman College, CUNY, Department of Biology, Bedford Park Boulevard, West, Bronx, NY 10468
- Borst, David W., Jr.**, Illinois State University, Department of Biological Sciences, Normal, IL 61790-4120
- Bowles, Francis P.**, Marine Biological Laboratory, Ecosystems Center, Woods Hole, MA 02543
- Boyer, Barbara C.**, Union College, Biology Department, Schenectady, NY 12308
- Brandhorst, Bruce P.**, Simon Fraser University, Institute of Molecular Biology/Biochemistry, Barnaby, B.C. V5A 1S6, Canada
- Brinley, F. J., Jr.**, NINCDS/NIH, Neurological Disorders Program, Room 812 Federal Building, Bethesda, MD 20892
- Bronner-Fraser, Marianne**, California Institute of Technology, Beckman Institute Division of Biology, 139-74, Pasadena, CA 91125
- Brown, Stephen C.**, SUNY, Department of Biological Sciences, Albany, NY 12222
- Brown, William L.**, 80 Black Oak Road, Weston, MA 02193
- Browne, Carole L.**, Wake Forest University, Department of Biology, Box 7325 Reynolda Station, Winston-Salem, NC 27109
- Browne, Robert A.**, Wake Forest University, Department of Biology, Box 7325, Winston-Salem, NC 27109
- Bucklin, Anne C.**, University of New Hampshire, Ocean Process Analysis Laboratory, 142 Morse Hall, Durham, NH 03824
- Bullis, Robert A.**, Oceanic Institute of Applied Aquaculture, 41-202 Kalaniana'ole Highway, Waimanalo, HI 96795
- Burger, Max M.**, Friedrich Miescher-Institute, P.O. Box 2543, CH-4002 Basel, Switzerland

- Burgess, David R.**, Boston College, Department of Biology, Higgins Hall, 140 Commonwealth Avenue, Chestnut Hill, MA 02167
- Burgos, Mario H.**, IHEM Medical School, UNC Conicet, Casilla de Correo 56, 5500 Mendoza, Argentina
- Burky, Albert**, University of Dayton, Department of Biology, Dayton, OH 45469
- Burris, John E.**, Beloit College, 700 College Street, Beloit, WI 53511
- Burstyn, Harold Lewis**, Air Force Research Laboratory (IFOJ), Office of the Staff Judge Advocate, 26 Electronic Parkway, Rome, NY 13441-4514
- Bursztajn, Sherry**, LSU Medical Center, 1501 Kings Highway, Building BRIF 6-13, Shreveport, LA 71130
- Calabrese, Ronald L.**, Emory University, Department of Biology, 1510 Clifton Road, Atlanta, GA 30322
- Cameron, R. Andrew**, California Institute of Technology, Division of Biology 156-29, Pasadena, CA 91125
- Campbell, Richard H.**, Bang-Campbell Associates, Eel Pond Place, Box 402, Woods Hole, MA 02543
- Candelas, Graciela C.**, University of Puerto Rico, Department of Biology, P.O. Box 23360, UPR Station, San Juan, PR 00931-3360
- Cariello, Lucio**, Stazione Zoologica "A. Dohrn," Villa Comunale, 80121 Naples, Italy
- Case, James F.**, University of California, Marine Science Institute, Santa Barbara, CA 93106
- Cassidy, Father Joseph D.**, Providence College, Priory of St. Thomas Aquinas, Providence, RI 02918-0001
- Cavanaugh, Colleen M.**, Harvard University, Biological Laboratories, 16 Divinity Avenue, Cambridge, MA 02138
- Chaet, Alfred B.**, University of West Florida, Department of Cell and Molecular Biology, 11000 University Parkway, Pensacola, FL 32514
- Chambers, Edward L.**, University of Miami School of Medicine, Department of Physiology and Biophysics P.O. Box 016430, Miami, FL 33101
- Chang, Donald C.**, Hong Kong University, Science and Technology, Department of Biology, Clear Water Bay, Kowloon, Hong Kong
- Chappell, Richard L.**, Hunter College, CUNY, Department of Biological Sciences, 695 Park Avenue, New York, NY 10021
- Child, Frank M.**, 28 Lawrence Farm Road, Woods Hole, MA 02543-1416
- Chisholm, Rex Leslie**, Northwestern University, Medical School, Department of Cell Biology, Chicago, IL 60611
- Citkowitz, Elena**, Hospital of St. Raphael, Lipid Disorders Clinic, 1450 Chapel Street, New Haven, CT 06511
- Clark, Eloise E.**, Bowling Green State University, Biological Sciences Department, Bowling Green, OH 43403
- Clark, Hays**, 150 Gomez Road, Hobe Sound, FL 33455
- Clark, Wallis H., Jr.**, 12705 NW 112th Avenue, Alachua, FL 32615
- Claude, Philippa**, University of Wisconsin, Department of Zoology, Zoology Research Building 125, 1117 W Johnson Street, Madison, WI 53706
- Clay, John R.**, National Institutes of Health, NINDS, Building 36, Room 2-CO2, Bethesda, MD 20892
- Clowes, Alexander W.**, University of Washington, School of Medicine, Department of Surgery, Box 356410, Seattle, WA 98195-6410
- Cobb, Jewel Plummer**, California State University, 5151 University Drive, Health Center 205, Los Angeles, CA 90032-8500
- Cohen, Carolyn**, Brandeis University, Rosenstiel Basic Medical, Sciences Research Center, Waltham, MA 02254
- Cohen, Lawrence B.**, Yale University School of Medicine, Department of Physiology, 333 Cedar Street, New Haven, CT 06520
- Cohen, Maynard M.**, Rush Medical College, Department of Neurological Sciences, 600 South Paulina, Chicago, IL 60612
- Cohen, William D.**, Hunter College, Department Biological Sciences, 695 Park Avenue, New York, NY 10021
- Coleman, Annette W.**, Brown University, Division of Biology and Medicine, Providence, RI 02912
- Colinvaux, Paul**, Marine Biological Laboratory, Woods Hole, MA 02543
- Collier, Jack R.**, 3431 Highway, #107, P.O. Box 139, Effie, LA 71331
- Collier, Marjorie McCann**, 3431 Highway 107, P.O. Box 139, Effie, LA 71331
- Collier, R. John**, Harvard Medical School, Department of Microbiology and Molecular Genetics, 200 Longwood Avenue, Room 356, Boston, MA 02115
- Cook, Joseph A.**, Edna McConnell Clark Foundation, 250 Park Avenue, New York, NY 10177-0026
- Cornwall, Melvin C., Jr.**, Boston University School of Medicine, Department of Physiology L714, Boston, MA 02118
- Corson, D. Wesley, Jr.**, Storm Eye Institute, Room 537, 171 Ashley Avenue, Charleston, SC 29425
- Corwin, Jeffrey T.**, University of Virginia, School of Medicine, Department Otolaryngology and Neuroscience, Box 396, Charlottesville, VA 22908
- Couch, Ernest F.**, Texas Christian University, Department of Biology, TCU Box 298930, Fort Worth, TX 76129
- Cox, Rachel Llanelly**, Woods Hole Oceanographic Institute, Biology Department, Woods Hole, MA 02543
- Crane, Sylvia E.**, c/o Mr. Thomas Crane, 40 Chestnut Street, Weston, MA 02493
- Cremer-Bartels, Gertrud**, Horstmarer Landweg 142, 48149 Muenster, Germany
- Crow, Terry J.**, University of Texas Medical School, Department of Neurobiology and Anatomy, Houston, TX 77225
- Crowell, Sears**, Indiana University, Department of Biology, Bloomington, IN 47405
- Crowth, Robert J.**, Shriners Hospitals for Children, 51 Blossom Street, Boston, MA 02114
- Cummings, Michael P.**, Marine Biological Laboratory, Bay Paul Center, Woods Hole, MA 02543
- Cunningham, Mary-Ellen**, 62 Cloverly Road, Grosse Pointe Farms, MI 48236-3313 (deceased 2000)
- Cutler, Richard D.**, Marine Biological Laboratory, Woods Hole, MA 02543
- Davidson, Eric H.**, California Institute of Technology, Division of Biology 156-29, 391 South Holliston, Pasadena, CA 91125
- Davison, Daniel B.**, Bristol-Myers Squibb PRI, Bioinformatics Department, 5 Research Parkway, Wallingford, CT 06492
- Daw, Nigel W.**, 5 Old Pawson Road, Branford, CT 06405
- Dawidowicz, Eliezar A.**, Marine Biological Laboratory, Office of Research Administration and Education, Woods Hole, MA 02543
- De Weer, Paul J.**, University of Pennsylvania, B400 Richards Building, Department of Physiology, 3700 Hamilton Walk, Philadelphia, PA 19104-6085
- Deegan, Linda A.**, Marine Biological Laboratory, The Ecosystems Center, Woods Hole, MA 02543
- DeGroof, Robert C.**, 145 Water Crest Drive, Doylestown, PA 18901-3267
- Denckla, Martha Bridge**, Johns Hopkins University, School of Medicine, Kennedy-Krieger Institute, 707 North Broadway, Baltimore, MD 21205
- DePhillips, Henry A.**, Trinity College, Department of Chemistry, 300 Summit Street, Hartford, CT 06106

- DeSimone, Douglas W.**, University of Virginia, Department of Cell Biology, Box 439, Health Sciences Center, Charlottesville, VA 22908
- Dettbarn, Wolf-Dietrich**, 4422 Wayland Drive, Nashville, TN 37215
- Dionne, Vincent E.**, Boston University Marine Program, Marine Biological Laboratory, Woods Hole, MA 02543
- Dowling, John E.**, Harvard University, Biological Laboratories, 16 Divinity Street, Cambridge, MA 02138
- Drapeau, Pierre**, Montreal General Hospital, Department of Neurology, 1650 Cedar Avenue, Montreal, Quebec H3G 1A4, Canada
- DuBois, Arthur Brooks**, John B. Pierce Foundation Laboratory, 290 Congress Avenue, New Haven, CT 06519
- Duncan, Thomas K.**, Nichols College, Environmental Sciences Department, Dudley, MA 01571
- Dunham, Philip B.**, Syracuse University, Department of Biology, 130 College Place, Syracuse, NY 13244-1220
- Dunlap, Paul V.**, University of Michigan, Department of Biology, 830 North University Avenue, Ann Arbor, MI 48109-1048
- Ebert, James D.**, The Johns Hopkins University, Department of Biology, Homewood, 3400 North Charles Street, Baltimore, MD 21218-2685 (deceased 2001)
- Eckberg, William R.**, Howard University, Department of Biology, P.O. Box 887, Administration Building, Washington, DC 20059
- Edds, Kenneth T.**, R & D Systems, Inc., Hematology Division, 614 McKinley Place, NE, Minneapolis, MN 55413
- Eder, Howard A.**, Albert Einstein College of Medicine, 1300 Morris Park Avenue, Bronx, NY 10461
- Edstrom, Joan**, 53 Two Ponds Road, Falmouth, MA 02540
- Egyud, Laszlo G.**, Cell Research Corporation, P.O. Box 67209, Chestnut Hill, MA 02167-0209
- Ehrlich, Barbara E.**, Yale University Medical School, Department of Pharmacology, Sterling Hall of Medicine, B207, 333 Cedar Street, New Haven, CT 06520-8066
- Eisen, Arthur Z.**, Washington University, Division of Dermatology, St. Louis, MO 63110
- Eisen, Herman N.**, Massachusetts Institute of Technology, Center for Cancer Research, E17-128, 77 Massachusetts Avenue, Cambridge, MA 02139-4307
- Elder, Hugh Young**, University of Glasgow, Institute of Physiology, Glasgow G12 8QQ, Scotland
- Englund, Paul T.**, Johns Hopkins Medical School, Department of Biological Chemistry, 725 North Wolfe Street, Baltimore, MD 21205
- Epel, David**, Stanford University, Hopkins Marine Station, Ocean View Boulevard, Pacific Grove, CA 93950
- Epstein, Herman T.**, 18 Lawrence Farm Road, Woods Hole, MA 02543
- Epstein, Ray L.**, 701 Winthrop Street, #311, Taunton, MA 02780-2187
- Farb, David H.**, Boston University School of Medicine, Department of Pharmacology L603, 80 East Concord Street, Boston, MA 02118
- Farmanfarmaian, A. Verdi**, Rutgers University, Department of Biological Sciences, Nelson Biology Laboratory POB 1059, Piscataway, NJ 08855
- Feldman, Susan C.**, University of Medicine and Dentistry, New Jersey Medical School, 100 Bergen Street, Newark, NJ 07103
- Festoff, Barry William**, VA Medical Center, Neurology Service (151), 4801 Linwood Boulevard, Kansas City, MO 64128
- Fink, Rachel D.**, Mount Holyoke College, Department of Biological Sciences, Clapp Laboratories, Room 215, South Hadley, MA 01075
- Finkelstein, Alan**, Albert Einstein College of Medicine, 1300 Morris Park Avenue, Bronx, NY 10461
- Fischbach, Gerald D.**, Columbia College of Physicians and Surgeons, 630 West 168th Street, R 2-401, New York, NY 10032
- Fishman, Harvey M.**, University of Texas Medical Branch, Department of Physiology and Biophysics, 301 University Boulevard, Galveston, TX 77555-0641
- Flanagan, Dennis**, 12 Gay Street, New York, NY 10014
- Fluck, Richard Allen**, Franklin and Marshall College, Department of Biology, Box 3003, Lancaster, PA 17604-3003
- Foreman, Kenneth H.**, Marine Biological Laboratory, Woods Hole, MA 02543
- Fox, Thomas Oren**, Harvard Medical School, Division of Medical Sciences, MEC 435, 260 Longwood Avenue, Boston, MA 02115
- Franzini-Armstrong, Clara**, University of Pennsylvania, School of Medicine, 330 South 46th Street, Philadelphia, PA 19143
- Fraser, Scott**, California Institute of Technology, Beckman Institute 139-74, 1201 East California Boulevard, Pasadena, CA 91125
- Frazier, Donald T.**, University of Kentucky Medical Center, Department of Physiology and Biophysics, MS501 Chandler Medical Center, Lexington, KY 40536
- French, Robert J.**, University of Calgary, Health Sciences Centre, Alberta, T2N 4N1, CANADA
- Fulton, Chandler M.**, Brandeis University, Department of Biology, MS 008, Waltham, MA 02454-9110
- Furie, Barbara C.**, Beth Israel Deaconess Medical Center, BIDMC Cancer Center, Kirstein 1, 330 Brookline Avenue, Boston, MA 02215
- Furie, Bruce**, Beth Israel Deaconess Medical Center, BIDMC Cancer Center, Kirstein 1, 330 Brookline Avenue, Boston, MA 02215
- Furshpan, Edwin J.**, Harvard Medical School, Department of Neurobiology, 220 Longwood Avenue, Boston, MA 02115
- Futrelle, Robert P.**, Northeastern University, College of Computer Science, 360 Huntington Avenue, Boston, MA 02115
- Gabr, Howaida**, Suez Canal University, Department of Marine Science, Faculty of Science, Ismailia, Egypt
- Gadsby, David C.**, The Rockefeller University, Laboratory of Cardiac Physiology, 1230 York Avenue, New York, NY 10021-6399
- Gainer, Harold**, National Institutes of Health, NINDS.BNP.DIR, Neurochemistry, Building 36, Room 4D20, Bethesda, MD 20892-4130
- Galatzer-Levy, Robert M.**, 534 Judson Avenue, Evanston, IL 60202
- Gall, Joseph G.**, Carnegie Institution, 115 West University Parkway, Baltimore, MD 21210
- Gallo, Michael A.**, UMDNJ-Robert Wood Johnson Medical School, EOHSI, Room 408, 170 Frelinghuysen Road, Piscataway, NJ 08854-8020
- Garber, Sarah S.**, Allegheny University of the Health Sciences, Department of Physiology, 2900 Queen Lane, Philadelphia, PA 19129
- Gelperin, Alan**, Bell Labs Lucent, Department Biology Comp., Rm 1C464, 600 Mountain Avenue, Murray Hill, NJ 07974
- German, James L., III**, Weill Medical College of Cornell University, 1300 York Avenue, New York, NY 10021
- Gihbs, Martin**, Brandeis University, Institute for Photobiology of Cells and Organelles, Waltham, MA 02254
- Giblin, Anne E.**, Marine Biological Laboratory, The Ecosystems Center, Woods Hole, MA 02543
- Gibson, A. Jane**, Cornell University, Department of Biochemistry, Biotech Building, Ithaca, NY 14850
- Gifford, Prosser**, Library of Congress, Madison Building LM605, Washington DC 20540
- Gilbert, Daniel L.**, National Institutes of Health, Biophysics Sec., BNP, Building 36, Room 5A-27, Bethesda, MD 20892

- Giudice, Giovanni**, Universita di Palermo, Dipartimento di Biologia, Cellulare e Dello Sviluppo, I-90123 Palermo, Italy
- Giuditta, Antonio**, University of Naples, Department of General Physiology, Via Mezzocannone 8, Naples, 80134, Italy
- Glynn, Paul**, P.O. Box 369, Hampton Falls, NH 03844
- Golden, William T.**, Chairman Emeritus, American Museum of Natural History, 500 Fifth Avenue, 50th Floor, New York, NY 10110
- Goldman, Robert D.**, Northwestern University Medical School, Department of Cell and Molecular Biology, 303 E. Chicago Avenue, Chicago, IL 60611-3008
- Goldsmith, Paul K.**, National Institutes of Health, 9000 Rockville Pike, Building 10, Room 8C206, Bethesda, MD 20892
- Goldsmith, Timothy H.**, Yale University, Department of Biology, New Haven, CT 06510
- Goldstein, Moise H., Jr.**, The Johns Hopkins University, ECE Department, Barton Hall, Baltimore, MD 21218
- Gould, Robert Michael**, NYS Institute of Basic Research, Department of Pharmacology, 1050 Forest Hill Road, Staten Island, NY 10314-6399
- Govind, C. K.**, Scarborough College, Life Sciences Division, 1265 Military Trail, West Hill, Ontario M1C 1A4, Canada
- Grace, Dick**, Doreen Grace Fund, The Brain Center, Promontory Point, New Seabury, MA 02649
- Graf, Werner M.**, College of France, 11 Place Marcelin Berthelot, 75231 Paris Cedex 05, France
- Grant, Philip**, National Institutes of Health, NINDS\BN\DIR-Neurochemistry, Building 36, Room 4D20, Bethesda, MD 20892-4130
- Grass, Ellen R.**, The Grass Foundation, 77 Reservoir Road, Quincy, MA 02170-3610 (deceased 2001)
- Grassle, Judith P.**, Rutgers University, Institute of Marine and Coastal Studies, 71 Dudley Road, New Brnmswick, NJ 08901-8521
- Graubard, Katherine G.**, University of Washington, Department of Zoology, NJ-15, Box 351800, Seattle, WA 98195-1800
- Greenberg, Everett Peter**, University of Iowa, College of Medicine, Department of Microbiology, Iowa City, IA 52242
- Greenberg, Michael J.**, University of Florida, The Whitney Laboratory, 9505 Ocean Shore Boulevard, St. Augustine, FL 32080-8610
- Greer, Mary J.**, 176 West 87th Street, #12A, New York, NY 10024-2902
- Griffin, Donald R.**, Harvard University, Concord Field Station, Old Causeway Road, Bedford, MA 01730
- Gross, Paul R.**, 123 Perkins Street, Jamaica Plain, MA 02130
- Grossman, Albert**, New York University Medical Center, 550 First Avenue, New York, NY 10016
- Grossman, Lawrence**, The Johns Hopkins University, Hygien Building, Room W8306, Baltimore, MD 21205
- Gruner, John A.**, Cephalon, Inc., 145 Brandywine Parkway, West Chester, PA 19380-4245
- Gunning, A. Robert**, P. O. Box 165, Falmouth, MA 02541
- Gwilliam, G. Francis**, Reed College, Department of Biology, Portland, OR 97202
- Haimo, Leah T.**, University of California, Department of Biology, Riverside, CA 92521
- Hajduk, Stephen L.**, University of Alabama, School of Medicine/Dentistry, Department of Biochemistry/Molecular Genetics, University Station, Birmingham, AL 35294
- Hall, Linda M.**, Shriners Hospital for Children, 2425 Stockton Boulevard, Sacramento, CA 95817
- Halvorson, Harlyn O.**, University of Massachusetts, Policy Center for Marine Biosciences and Technology, 100 Morrissey Boulevard, Boston, MA 02125-3393
- Haneji, Tatsuji**, The University of Tokushima, Department of Histology & Oral Histology, School of Dentistry, 18-15, 3 Kuramoto-cho, Tokushima 770-8504, Japan
- Hanlon, Roger T.**, Marine Biological Laboratory, Woods Hole, MA 02543
- Harosi, Ferenc**, New College of the USF, Division of Natural Sciences, 5700 North Tamiami Trail, Sarasota, FL 34243-2197
- Harrigan, June F.**, 7415 Makaa Place, Honolulu, HI 96825
- Harrington, Glenn W.**, Weber State University, Department of Microbiology, Ogden, UT 84408
- Harrington, John P.**, University of South Alabama, Department of Chemistry, Mobil, AL 36688
- Harrison, Stephen C.**, Harvard University, Department of Molecular and Cell Biology, 7 Divinity Avenue, Cambridge, MA 02138
- Haselkorn, Robert**, University of Chicago, Department of Molecular Genetics and Cell Biology, Chicago, IL 60637
- Hastings, J. Woodland**, Harvard University, The Biological Laboratories, 16 Divinity Avenue, Cambridge, MA 02138-2020
- Hayes, Raymond L., Jr.**, Howard University, College of Medicine, 520 W Street, NW, Washington, DC 20059
- Heck, Diane E.**, Rutgers University, Department of Pharmacology/Toxicology, 681 Frelinghuysen Road, Piscataway, NJ 08855
- Henry, Jonathan Joseph**, University of Illinois, Department of Cell and Structural Biology, 601 South Goodwin Avenue #B107, Urbana, IL 61801-3709
- Hepler, Peter K.**, University of Massachusetts, Department of Biology, Morrill III, Amherst, MA 01003
- Herndon, Walter R.**, University of Tennessee, Department of Botany, Knoxville, TN 37996-1100
- Hershko, Avram**, Technion-Israel Institute of Technology, Unit of Biochemistry, The Bruce Rappaport Faculty of Medicine, Haifa 31096, Israel
- Herskovits, Theodore T.**, Fordham University, Department of Chemistry, John Mulcahy Hall, Room 638, Bronx, NY 10458
- Hiatt, Howard H.**, Brigham and Women's Hospital, Department of Medicine, 75 Francis Street, Boston, MA 02115
- Highstein, Stephen M.**, Washington University, Department of Otolaryngology, Box 8115, 4566 Scott Avenue, St. Louis, MO 63110
- Hildebrand, John G.**, University of Arizona, ARL Division of Neurobiology, P.O. Box 210077, Tucson, AZ 85721-0077
- Hill, Richard W.**, Michigan State University, Department of Zoology, East Lansing, MI 48824
- Hill, Susan D.**, Michigan State University, Department of Zoology, East Lansing, MI 48824
- Hillis, Llewellya W.**, Marine Biological Laboratory, Woods Hole, MA 02543
- Hineblcliff, Edward H.**, University of Massachusetts Medical School, Department of Cell Biology, 377 Plantation Street, Worcester, MA 01605
- Hinkle, Gregory J.**, Bioinformatics Group, Cereon Genomics, 45 Sidney St., Cambridge, MA 02139
- Hinsch, Gertrude W.**, University of South Florida, Department of Biology, Tampa, FL 33620
- Hinsch, Jan**, Leica, Inc., 110 Commerce Drive, Allendale, NJ 07401
- Hobbie, John E.**, Marine Biological Laboratory, The Ecosystems Center, Woods Hole, MA 02543
- Hodge, Alan J.**, 3843 Mount Blackburn Avenue, San Diego, CA 92111
- Hoffman, Joseph F.**, Yale University School of Medicine, Cellular and Molecular Physiology, 333 Cedar Street, New Haven, CT 06520-8026
- Hollyfield, Joe G.**, The Cleveland Clinic, Ophthalmic Research, 9500 Euclid Avenue, Cleveland, OH 44195

- Holz, George G., IV**, New York University Medical Center, Department of Physiology and Neuroscience, Medical Sciences Building, Room 442, 550 First Avenue, New York, NY 10016
- Hopkinson, Charles S., Jr.**, Marine Biological Laboratory, Woods Hole, MA 02543
- Houk, James C.**, Northwestern University Medical School, 303 East Chicago Avenue, Ward 5-315, Chicago, IL 60611-3008
- Hoy, Ronald R.**, Cornell University, Section of Neurobiology and Behavior, 215 Mudd Hall, Ithaca, NY 14853
- Huang, Alice S.**, California Institute of Technology, Mail Code 1-9, Pasadena, CA 91125
- Hufnagel-Zackroff, Linda A.**, University of Rhode Island, Department of Microbiology, Kingston, RI 02881
- Hummon, William D.**, Ohio University, Department of Biological Sciences, Athens, OH 45701
- Humphreys, Susie H.**, Food and Drug Administration, HFS-308, 200 C Street, SW, Washington, DC 20204-0001
- Humphreys, Tom**, University of Hawaii, Kewalo Marine Laboratory, 41 Ahui Street, Honolulu, HI 96813
- Hunt, Richard T.**, ICRF, Clare Hall Laboratories, South Mimms Potter's Bar, Herts EN6-3LD, England
- Hunter, Robert D.**, Oakland University, Department of Biological Sciences, Rochester, MI 48309-4401
- Huxley, Hugh E.**, Brandeis University, Rosenstiel Center, Biology Department, Waltham, MA 02154
- Ilan, Joseph**, Case Western Reserve University, School of Medicine, Department of Anatomy, Cleveland, OH 44106
- Ingoglia, Nicholas A.**, New Jersey Medical School, Department of Pharmacology/Physiology, 185 South Orange Avenue, Newark, NJ 07103
- Inoué, Saduyki**, McGill University, Department of Anatomy, 3640 University Street, Montreal, PQ H3A 2B2, Canada
- Inoué, Shinya**, Marine Biological Laboratory, Woods Hole, MA 02543
- Isselbacher, Kurt J.**, Massachusetts General Hospital Cancer Center, Charlestown, MA 02129
- Issidorides, Marietta Radovic**, National and Capodistrian University of Athens, Department of Psychiatry, Eginition Hospital, 74, Vas. Sophias Avenue, 115 28 Athens, Greece
- Izzard, Colin S.**, SUNY-Albany, Department of Biological Sciences, 1400 Washington Avenue, Albany, NY 12222
- Jacobs, Neil**, Hale and Dorr, 60 State Street, Boston, MA 02109
- Jaffe, Laurinda A.**, University of Connecticut Health Center, Department of Physiology, Farmington Avenue, Farmington, CT 06032
- Jaffe, Lionel**, Marine Biological Laboratory, Woods Hole, MA 02543
- Jeffery, William R.**, University of Maryland, Department of Biology, College Park, MD 20742
- Johnston, Daniel**, Baylor College of Medicine, Division of Neuroscience, One Baylor Plaza, Room S740, Houston, TX 77030
- Josephson, Robert K.**, University of California, School of Biological Science, Department of Psychobiology, Irvine, CA 92697
- Kaczmarek, Leonard K.**, Yale University School of Medicine, Department of Pharmacology, 333 Cedar Street, New Haven, CT 06520
- Kaley, Gabor**, New York Medical College, Department of Physiology, Basic Sciences Building, Valhalla, NY 10595
- Kaltenbach, Jane**, Mount Holyoke College, Department Biological Sciences, South Hadley, MA 01075
- Kaminer, Benjamin**, Boston University Medical School, Physiology Department, 80 East Concord Street, Boston, MA 02118
- Kaneshiro, Edna S.**, University of Cincinnati, Biological Sciences Department, JL 006, Cincinnati, OH 45221-0006
- Kaplan, Ehud**, Mount Sinai School of Medicine, I Gustave Levy Place, Box 1183, New York, NY 10029
- Karakashian, Stephen J.**, Apartment 16-F, 165 West 91st Street, New York, NY 10024
- Karlin, Arthur**, Columbia University, Center for Molecular Recognition, 630 West 168th Street, Room 11-401, New York, NY 10032
- Karnovsky, Morris John**, Harvard Medical School, Department of Pathology, 200 Longwood Avenue, Boston, MA 02115
- Keller, Hartmut Ernst**, Carl Zeiss, Inc., One Zeiss Drive, Thornwood, NY 10594
- Kelley, Darcy B.**, Columbia University, Department of Biological Sciences, 911 Fairchild, Mailcode 2432, New York, NY 10027
- Kelly, Robert E.**, 5 Little Harbor Road, Woods Hole, MA 02543
- Kemp, Norman E.**, University of Michigan, Department of Biology, Ann Arbor, MI 48109
- Kendall, John P.**, Faneuil Hall Associates, 176 Federal Street, 2nd Floor, Boston, MA 02110
- Kerr, Louis M.**, Marine Biological Laboratory, Woods Hole, MA 02543
- Keynan, Alexander**, Israel Academy of Science and Humanity, P.O. Box 4040, Jerusalem, Israel
- Khan, Shahid M. M.**, Albert Einstein College of Medicine, Department of Physiology and Biophysics, 1300 Morris Park Avenue, Room U273, Bronx, NY 10461
- Khodakhah, Kamran**, University of Colorado School of Medicine, Department of Physiology and Biophysics, 4200 East 9th Avenue, C-240, Denver, CO 80262
- Kiehart, Daniel P.**, Duke University Medical Center, Department of Cell Biology, Box 3709, 308 Nanaline Duke Building, Durham, NC 27710
- Kleinfeld, David**, University of California, Department of Physics, 0319 9500 Gilman Drive, La Jolla, CA 92093
- Klessen, Rainer**, (address unknown)
- Klotz, Irving M.**, Northwestern University, Department of Chemistry, Evanston, IL 60201
- Knudson, Robert A.**, Marine Biological Laboratory, Woods Hole, MA 02543
- Koide, Samuel S.**, The Rockefeller University, The Population Council, 1230 York Avenue, New York, NY 10021
- Kornberg, Hans**, Boston University, The University Professors, 745 Commonwealth Avenue, Boston, MA 02215
- Kosower, Edward M.**, Tel-Aviv University, Department of Chemistry, Ramat-Aviv, Tel Aviv, 69978, Israel
- Krahl, Maurice E.**, 2783 West Casas Circle, Tucson, AZ 85741 (deceased 2000)
- Krane, Stephen M.**, Massachusetts General Hospital, 55 Fruit Street, Bulf-165, Boston, MA 02114
- Krauss, Robert**, P.O. Box 291, Denton, MD 21629
- Kravitz, Edward A.**, Harvard Medical School, Department of Neurobiology, 220 Longwood Avenue, Boston, MA 02115
- Kriebel, Mahlon E.**, SUNY Health Science Center, Department of Physiology, Syracuse, NY 13210
- Kristan, William B., Jr.**, University of California, Department of Biology 0357, 9500 Gilman Drive, La Jolla, CA 92093-0357
- Kropinski, Andrew M.**, Queen's University, Department of Microbiology/Immunology, Botterell Hall, Room 74, Kingston, Ontario K7L 3N6, CANADA

- Kuffler, Damien P.**, Institute of Neurobiology, 201 Boulevard del Valle, San Juan 00901, PR
- Kuhns, William J.**, Hospital for Sick Children, Biochemistry Research, 555 University Avenue, Toronto, Ontario M5G 1X8, Canada
- Kunkel, Joseph G.**, University of Massachusetts, Department of Biology, Amherst, MA 01003
- Kuzirian, Alan M.**, Marine Biological Laboratory, Woods Hole, MA 02543-1015
- Laderman, Aimlee D.**, Yale University, School of Forestry and Environmental Studies, 370 Prospect Street, New Haven, CT 06511
- Landeau, Laurie J.**, Listowel, Inc., 2 Park Avenue, Suite 1525, New York, NY 10016
- Landis, Dennis M. D.**, University Hospital of Cleveland, Department Neurology, 11100 Euclid Avenue, Cleveland, OH 44106
- Landis, Story C.**, National Institutes of Health, Building 36, Room 5A05, 36 Convent Drive, Bethesda, MD 20892-4150
- Landowne, David**, University of Miami Medical School, Department of Physiology and Biophysics, PO Box 016430, Miami, FL 33101
- Langford, George M.**, Dartmouth College, Department of Biological Sciences, 6044 Gilman Laboratory, Hanover, NH 03755
- Laskin, Jeffrey**, University of Medical and Dentistry of New Jersey, Robert Wood Johnson Medical School, 675 Hoes Lane, Piscataway, NJ 08854
- Lasser-Ross, Nechama**, New York Medical College, Department of Physiology, Valhalla, NY 10595
- Laster, Leonard**, University of Massachusetts Medical School, 55 Lake Avenue, North, Worcester, MA 01655
- Laties, Alan**, Scheie Eye Institute, Myrin Circle, 51 North 39th Street, Philadelphia, PA 19104
- Lauffer, Hans**, University of Connecticut, Department of Molecular and Cell Biology, U-125, 75 North Eagleville Road Storrs, CT 06269-3125
- Lazarow, Paul B.**, Mount Sinai School of Medicine, Department of Cell Biology and Anatomy, 1190 Fifth Avenue, Box 1007, New York, NY 10029-6574
- Lazarus, Maurice**, Federated Department Stores, Sears Crescent, City Hall Plaza, Boston, MA 02108
- Leadbetter, Edward R.**, University of Connecticut, Department of Molecular and Cell Biology, U-131, Beach Hall, Room 249, 354 Mansfield Road, Storrs, CT 06269-2131
- Lederberg, Joshua**, The Rockefeller University, Suite 400 (Founders Hall), 1230 York Avenue, New York, NY 10021
- Lee, John J.**, City College of CUNY, Department of Biology, Convent Avenue and 138th Street, New York, NY 10031
- Lehy, Donald B.**, 35 Willow Field Drive, North Falmouth, MA 02556
- Leighton, Stephen B.**, Beecher Instruments, P.O. Box 8704, Silver Spring, MD 20910
- Lerner, Aaron B.**, Yale University School of Medicine, Department of Dermatology, P.O. Box 3333, New Haven, CT 06510
- Levin, Jack**, Veterans Administration, Medical Center, 111 H2, 4150 Clement Street, San Francisco, CA 94121
- Levine, Michael**, University of California, Department MCB, 401 Barker Hall, Berkeley, CA 94720
- Levine, Richard B.**, University of Arizona, Division of Neurobiology, Room 611, Gould Simpson Building, PO Box 210077, Tucson, AZ 85721-0077
- Levinthal, Francoise**, Columbia University, Department of Biological Sciences, Broadway and 116th Street, New York, NY 10026
- Levitan, Irwin B.**, University of Pennsylvania, School of Medicine, 218 Stemmler Hall, 3450 Hamilton Walk, Philadelphia, PA 19104-6074
- Linck, Richard W.**, University of Minnesota School of Medicine, Cell Biology and Neuroanatomy Department, 4-135 Jackson Hall, 321 Church Street, Minneapolis, MN 55455
- Lipicky, Raymond J.**, Food and Drug Administration, CDER/ODEI/HFD-110, 5600 Fishers Lane, Rockville, MD 20857
- Lisman, John E.**, Brandeis University, Molecular and Cell Biology, 415 South Street, Waltham, MA 02454-9110
- Liuzzi, Anthony**, 180 Beacon Street, #8G, Boston, MA 02116
- Llinas, Rodolfo R.**, New York University Medical Center, Department of Physiology/Biophysics, 550 First Avenue, Room 442, New York, NY 10016
- Lobel, Phillip S.**, Boston University Marine Program, Marine Biological Laboratory, Woods Hole, MA 02543
- Loew, Franklin M.**, Becker College, 61 Sever Street, Worcester, MA 01615-0071
- Loewenstein, Birgit Rose**, 102 Ransom Rd., Falmouth, MA 02540
- Loewenstein, Werner R.**, 102 Ransom Rd., Falmouth, MA 02540
- London, Irving M.**, Harvard-MIT, Division, E-25-551, Cambridge, MA 02139
- Longo, Frank J.**, University of Iowa, Department of Anatomy, Iowa City, IA 52442
- Luckenbill, Louise M.**, 430 Sippiwissett Road, Falmouth, MA 02540
- Macagno, Eduardo R.**, Columbia University, 109 Low Memorial Library, Mail Code 4306, New York, NY 10027
- MacNichol Edward R., Jr.**, Boston University School of Medicine, Department of Physiology, 80 East Concord Street, Boston, MA 02118
- Maglott-Duffield, Donna R.**, American Type Culture Collection, 12301 Parklawn Drive, Rockville, MD 20852-1776
- Maienschein, Jane Ann**, Arizona State University, Department of Physiology, P.O. Box 872004, Tempe, AZ 85287-2004
- Malhon, Craig C.**, SUNY, University Medical Center, Pharmacology-HSC, Stony Brook, NY 11794-8651
- Malchow, Robert P.**, University of Illinois, Department of Biology, M/C 066, 845 West Taylor Street, Chicago, IL 60607
- Manalis, Richard S.**, Indiana-Purdue University, Department of Biological Science, 2101 Coliseum Boulevard East, Fort Wayne, IN 46805
- Manz, Robert D.**, P.O. Box 428, Glen Mills, PA 19342
- Margulis, Lynn**, University of Massachusetts, Department of Geosciences, Morrill Science Center, Box 35820, Amherst, MA 01003-5820
- Marinucci, Andrew C.**, 102 Nancy Drive, Mercerville, NJ 08619
- Martinez, Joe L., Jr.**, The University of Texas, Division of Life Sciences, 6900 North Loop 1604 West, San Antonio, TX 78249-0662
- Martinez-Palomo, Adolfo**, CINVESTAV-IPN, Sec. de Patologia Experimental, 07000 Mexico, D.F.A.P. 140740, Mexico
- Mastroianni, Luigi, Jr.**, Hospital of University of Pennsylvania, 106 Dulles, 3400 Spruce Street, Philadelphia, PA 19104-4283
- Mauzerall, David**, Rockefeller University, 1230 York Avenue, New York, NY 10021
- McAnelly, M. Lynne**, University of Texas, Section of Neurobiology, School of Life Sciences, Austin, TX 78712
- McCann, Frances V.**, Dartmouth Medical School, Department of Physiology, Lebanon, NH 03756
- McLaughlin, Jane A.**, Marine Biological Laboratory, Woods Hole, MA 022543
- McMahon, Robert F.**, University of Texas, Arlington, Department of Biology, Box 19498, Arlington, TX 76019
- Meedel, Thomas**, Rhode Island College, Biology Department, 600 Mount Pleasant Avenue, Providence, RI 02908

- Meinertzhagen, Ian A.**, Dalhousie University, Department of Psychology, Halifax, NS B3H 4J1, Canada
- Meiss, Dennis E.**, Immunodiagnostic Laboratories, 488 McCormick Street, San Leandro, CA 94577
- Melillo, Jerry M.**, Marine Biological Laboratory, Ecosystems Center, Woods Hole, MA 02543
- Mellon, DeForest, Jr.**, University of Virginia, Department of Biology, Gilmer Hall, Charlottesville, VA 22903
- Mellon, Richard P.**, P.O. Box 187, Laughlintown, PA 15655-0187
- Mendelsohn, Michael E.**, New England Medical Center, Molecular Cardiology Laboratory, NEMC Box 80, 750 Washington Street, Boston, MA 02111
- Mensingher, Allen F.**, University of Minnesota, Biology Department, LSC1 211, Duluth, MN 55812
- Merriman, Melanie Pratt**, 7511 Beach View Drive, North Bay Village, FL 33141
- Meselson, Matthew**, Harvard University, Fairchild Biochemistry Building, 7 Divinity Avenue, Cambridge, MA 02138
- Miledi, Ricardo**, University of California, Irvine, Department of Psychobiology, 2205 Biology Science II, Irvine, CA 92697-4550
- Milkman, Roger D.**, University of Iowa, Department of Biological Sciences, Biology Building, Room 318, Iowa City, IA 52242-1324
- Miller, Andrew L.**, Flat 2A, Block 2, Greon Park, Razor Hill, Clearwater Bay, Kowloon, Hong Kong
- Miller, Thomas J.**, Analogic, 8 Centennial Drive, Peabody, MA 01960
- Mills, Robert**, 6410 21st Avenue W, #311, Brandon, FL 34210 (deceased 2001)
- Misevic, Gradimir**, University Hospital of Basel, Department of Research, Mebelstr. 20, CH-4031 Basel, Switzerland
- Mitchell, Ralph**, Harvard University, Division of Applied Sciences, 29 Oxford Street, Cambridge, MA 02138
- Miyakawa, Hiroyoshi**, Tokyo College of Pharmacy, Laboratory of Cellular Neurobiology, 1432-1 Horinouchi, Hachioji, Tokyo 192-03, Japan
- Miyamoto, David M.**, Drew University, Department of Biology, Madison, NJ 07940
- Mizell, Merle**, Tulane University, Department of Cell and Molecular Biology, New Orleans, LA 70118
- Moreira, Jorge E.**, National Institutes of Health, NICHD, Department of Cell and Molecular Biol., Bethesda, MD 20852
- Morin, James G.**, Cornell University, Department of Ecology and Evolutionary Biology, G14 Stimson Hall, Ithaca, NY 14853-2801
- Morrell, Leyla deToledo**, Rush-Presbyterian St. Luke's Medical Center, 1653 West Congress Parkway, Chicago, IL 60612
- Morse, Stephen S.**, 275 Central Park West, New York, NY 10024
- Mote, Michael I.**, Temple University, Department of Biology, Philadelphia, PA 19122
- Muller, Kenneth J.**, University of Miami School of Medicine, Department of Physiology and Biophysics, 1600 NW 10th Avenue, R-430, Miami, FL 33136
- Murray, Andrew W.**, University of California, Department of Physiology, Box 0444, 513 Parnassus Avenue, San Francisco, CA 94143-0444
- Nabrit, Samuel M.**, 686 Beckwith Street, SW, Atlanta, GA 30314
- Nadelhoffer, Knute J.**, Marine Biological Laboratory, 7 MBL Street, Woods Hole, MA 02543
- Nagel, Ronald L.**, Albert Einstein College of Medicine, 1300 Morris Park Avenue, Bronx, NY 10461
- Naka, Ken-ichi**, 2-9-2 Tatumi Higashi, Okazaki, 444, Japan
- Nakajima, Yasuko**, University of Illinois, College of Medicine, Anatomy and Cell Biology Department, M/C 512, Chicago, IL 60612
- Narahashi, Toshio**, Northwestern University Medical School, Department of Pharmacology, 303 East Chicago Avenue, Chicago, IL 60611
- Nasi, Enrico**, Boston University School of Medical, Department of Physiology, R-406, 80 East Concord Street, Boston, MA 02118
- Neill, Christopher**, Marine Biological Laboratory, 7 MBL Street, Woods Hole, MA 02543
- Nelson, Margaret C.**, Cornell University, Section of Neurobiology and Behavior, Ithaca, NY 14850
- Nicholls, John G.**, SISSA, Via Beirut 2, 1-34014 Trieste, Italy
- Nickerson, Peter A.**, SUNY at Buffalo, Department of Pathology, Buffalo, NY 14214
- Nicosia, Santu V.**, University of South Florida, College of Medicine, Box 11, Department of Pathology, Tampa, FL 33612
- Noe, Bryan D.**, Emory University School of Medicine, Department of Anatomy and Cell Biology, Atlanta, GA 30322
- Norton, Catherine N.**, Marine Biological Laboratory, 7 MBL Street, Woods Hole, MA 02543
- Nusbaum, Michael P.**, University of Pennsylvania School of Medicine, Department of Neuroscience, 215 Stemmler Hall, Philadelphia, PA 19104-6074
- O'Herron, Jonathan**, Lazard Freres and Company, 30 Rockefeller Plaza, 59th Floor, New York, NY 10020-1900
- Obaid, Ana Lia**, University of Pennsylvania School of Medicine, Neuroscience Department, 234 Stemmler Hall, Philadelphia, PA 19104-6074
- Ohki, Shinpei**, SUNY at Buffalo, Department of Biophysical Sciences, 224 Cary Hall, Buffalo, NY 14214
- Oldenbourg, Rudolf**, Marine Biological Laboratory, 7 MBL Street, Woods Hole, MA 02543
- Olds, James L.**, George Mason University, Krasnow Institute for Advanced Studies, Mail Stop 2A1, Fairfax, VA 22030-4444
- Olins, Ada L.**, Foundation for Blood, 69 U.S. Route One, P.O. Box 190, Scarborough, ME 04070-0190
- Olins, Donald E.**, Foundation for Blood, 69 U.S. Route One, P.O. Box 190, Scarborough, ME 04070-0190
- Oschman, James L.**, 827 Central Avenue, Dover, NH 03820
- Palazzo, Robert E.**, University of Kansas, Department of Physiology and Cell Biology, Lawrence, KS 66045
- Palmer, John D.**, University of Massachusetts, Department of Zoology, 221 Morrill Science Center, Amherst, MA 01003
- Pant, Harish C.**, National Institutes of Health, NINCDS, Laboratory of Neurochemistry, Building 36, Room 4D20, Bethesda, MD 20892
- Pappas, George D.**, University of Illinois, Psychiatric Institute, 1601 W. Taylor Street, MC 912, Chicago, IL 60612
- Pardee, Arthur B.**, Dana-Farber Cancer Institute, D810, 44 Binney Street, Boston, MA 02115
- Pardy, Roosevelt L.**, University of Nebraska, School of Life Sciences, Lincoln, NE 68588
- Parmentier, James L.**, Massachusetts General Hospital, Partners/Fenway/Shattuck Center for Aids Research, 149 13th Street, Room 5219, Charlestown, MA 02129
- Pederson, Thoru**, University of Massachusetts Medical Center, Worcester Foundation Campus, 222 Maple Avenue, Shrewsbury, MA 01545
- Perkins, Courtland D.**, 400 Hilltop Terrace, Alexandria, VA 22301
- Persin, Philip**, 137-87 75th Road, Flushing, NY 11367
- Peterson, Bruce J.**, Marine Biological Laboratory, 7 MBL Street, Woods Hole, MA 02543

- Pethig, Ronald**, University College of North Wales, School of Electronic Engineering, Bangor, Gwynedd, LL 57 IUT, United Kingdom
- Pfohl, Ronald J.**, Miami University, Department of Zoology, Oxford, OH 45056
- Pierce, Sidney K., Jr.**, University of South Florida, Department of Biology, SCA 110, 4202 East Fowler Avenue, Tampa, FL 33620
- Pleasure, David E.**, Children's Hospital, Neurology Research, 5th Floor, Ambramson Building, Philadelphia, PA 19104
- Poindexter, Jeanne S.**, Barnard College, Columbia University, 3009 Broadway, New York, NY 10027-6598
- Pollard, Harvey B.**, U.S.U.H.S., 4301 Jones Bridge Road, Bethesda, MD 20814
- Pollard, Thomas D.**, Salk Institute for Biological Studies, 10010 N. Torrey Pines Road, La Jolla, CA 92037
- Porter, Beverly H.**, 5542 Windysun Court, Columbia, MD 21045
- Porter, Mary E.**, University of Minnesota, Department of Cell Biology and Neuroanatomy, 4-135 Jackson Hall, 321 Church Street SE, Minneapolis, MN 55455
- Potter, David D.**, Harvard Medical School, Department of Neurobiology, 25 Shattuck Street, Boston, MA 02115
- Potts, William T.**, University of Lancaster, Department of Biology, Lancaster, England
- Powers, Maureen K.**, University of California, Department of Molecular & Cellular Biology, Life Sciences Addition, Berkeley, CA 94720
- Prendergast, Robert A.**, 29 Pondlet Place, Falmouth, MA 02540
- Prior, David J.**, Northern Arizona University, Arts and Sciences Dean's Office, Box 5621, Flagstaff, AZ 86011
- Prusch, Robert D.**, Gonzaga University, Department of Life Sciences, Spokane, WA 99258
- Purves, Dale**, Duke University Medical Center, Department of Neurobiology, Box 3209, 101-I Bryan Research Building, Durham, NC 27710
- Quigley, James P.**, The Scripps Research Institute, Department of Vascular Biology, 10550 N. Torrey Pines Road VB-1, La Jolla, CA 92037
- Rabb, Irving W.**, 1010 Memorial Drive, #20A, Cambridge, MA 02138
- Rabin, Harvey**, 1102 Ralston Road, Rockville, MD 20852
- Rabinowitz, Michael B.**, Marine Biological Laboratory, 7 MBL Street, Woods Hole, MA 02543
- Rafferty, Nancy S.**, Marine Biological Laboratory, 7 MBL Street, Woods Hole, MA 02543
- Rakowski, Robert F.**, Finch University of Health Sciences, The Chicago Medical School, Department of Physiology and Biophysics, 3333 Greenbay Road, N. Chicago, IL 60064
- Ramon, Fidel**, Universidad Nacional Autonoma de Mexico, Division EStreet Posgrado E Invest., Facultad de Medicina, 04510, D.F., Mexico
- Rastetter, Edward B.**, Marine Biological Laboratory, The Ecosystems Center, Woods Hole, MA 02543
- Rebhun, Lionel I.**, University of Virginia, Department of Biology, Gilmer Hall 45, Charlottesville, VA 22901
- Reddan, John R.**, Oakland University, Department of Biological Sciences, Rochester, MI 48309-4401
- Reese, Thomas S.**, National Institutes of Health, NINDS, Department of Neurobiology, Building 36, Room 2A-21, 36 Convent Drive, Bethesda, MD 20892
- Reinisch, Carol L.**, Marine Biological Laboratory, 7 MBL Street, Woods Hole, MA 02543
- Rickles, Frederick R.**, 3910 Highwood Court, N.W., Washington, DC 20007
- Rieder, Conly L.**, Wadsworth Center, Division of Molecular Medicine, P.O. Box 509, Albany, NY 12201-0509
- Riley, Monica**, Marine Biological Laboratory, 7 MBL Street, Woods Hole, MA 02543
- Ripps, Harris**, University of Illinois at Chicago, Department of Ophthalmology/Visual Sciences, 1855 West Taylor Street, Chicago, IL 60612
- Ritchie, J. Murdoch**, Yale University School of Medicine, Department of Pharmacology, 333 Cedar Street, New Haven, CT 06510
- Rome, Lawrence C.**, University of Pennsylvania, Department of Biology, Leidy Labs, Philadelphia, PA 19104
- Rosenbluth, Jack**, New York University School of Medical, Department of Physiology and Biophysics, RR 714, 400 East 34th Street, New York, NY 10016
- Rosenbluth, Raja**, Simon Fraser University, Institute of Molecular Biology and Biochemistry, Burnaby, BC V5A 1S6, Canada
- Rosenfield, Allan**, Columbia University School of Public Health, 600 West 168th Street, New York, NY 10032-3702
- Rosenkranz, Herbert S.**, 130 Desoto Street, Pittsburgh, PA 15213-2535
- Ross, William N.**, New York Medical College, Department of Physiology, Valhalla, NY 10595
- Rottenfusser, Rudi**, Marine Biological Laboratory, 7 MBL Street, Woods Hole, MA 02543
- Rowland, Lewis P.**, Neurological Institute, 710 West 168th Street, New York, NY 10032
- Ruderman, Joan V.**, Harvard Medical School, Department of Cell Biology, C2-428, 240 Longwood Avenue, Boston, MA 02115
- Rummel, John D.**, NASA Headquarters, Office of Space Science, Washington, DC 20546
- Rushforth, Norman B.**, Case Western Reserve University, Department of Biology, Cleveland, OH 44106
- Russell-Hunter, William D.**, 711 Howard Street, Easton, MD 21601-3934
- Saffo, Mary Beth**, Harvard University, MCZ Labs 408, 26 Oxford Street, Cambridge, MA 02138
- Salama, Guy**, University of Pittsburgh, Department of Physiology, Pittsburgh, PA 15261
- Salmon, Edward D.**, University of North Carolina, Department of Biology, CB 3280, Chapel Hill, NC 27514
- Salyers, Abigail**, University of Illinois, Department of Microbiology, B-103, 601 South Goodwin Avenue, Urbana, IL 61801
- Salzberg, Brian M.**, University of Pennsylvania School of Medicine, Department of Neuroscience, 215 Stemmler Hall, Philadelphia, PA 19104-6074
- Sanger, Jean M.**, University of Pennsylvania School of Medicine, Department of Anatomy, 36th and Hamilton Walk, Philadelphia, PA 19104
- Sanger, Joseph W.**, University of Pennsylvania Medical Center, Department of Cell and Developmental Biology, 36th and Hamilton Walk, Philadelphia, PA 19104-6058
- Saunders, John W., Jr.**, 118 Metoxit Road, P.O. Box 3381, Waquoit, MA 02536
- Schachman, Howard K.**, University of California, Molecular and Cell Biology Department, 229 Stanley Hall, #3206, Berkeley, CA 94720-3206
- Schatten, Gerald P.**, Oregon Health Sciences University, Oregon Regional Primate Research Center, 505 N.W. 185th Avenue, Beaverton, OR 97006

- Schmeer, Arlene C.**, Merceene Cancer Research Institute, 790 Prospect Street, New Haven, CT 06511
- Schuel, Herbert**, SUNY at Buffalo, Department of Anatomy/Cell Biology, Buffalo, NY 14214
- Schwartz, Lawrence**, University of Massachusetts, Department of Biology, Morrill Science Center, Amherst, MA 01003
- Schweitzer, A. Nicola**, Brigham and Women's Hospital, Immunology Division, Department of Pathology, 221 Longwood Avenue, LMRC 521, Boston, MA 02115
- Segal, Sheldon J.**, The Population Council, One Dag Hammarskjold Plaza, New York, NY 10036
- Senft, Stephen Lamont**, Yale University, Neuroengineering/Neuroscience Center, P.O. Box 208205, New Haven, CT 06520-8205
- Shanklin, Douglas R.**, University of Tennessee, Department of Pathology, Room 576, 800 Madison Avenue, Memphis, TN 38117
- Shashar, Nadav**, The Interuniversity Institute of Eilat, P.O. Box 469, Eilat 88103, Israel
- Shashoua, Victor E.**, Harvard Medical School, Ralph Lowell Labs, McLean Hospital, 115 Mill Street, Belmont, MA 02178
- Shaver, Gaius R.**, Marine Biological Laboratory, The Ecosystems Center, Woods Hole, MA 02543
- Shaver, John R.**, Michigan State University, Department of Zoology, East Lansing, MI 48824
- Sheetz, Michael P.**, Duke University Medical Center, Department of Cell Biology, Bx 3709, 388 Nanaline Duke Building, Durham, NC 27710
- Shepro, David**, Boston University, CAS Biology, 5 Cummington Street, Boston, MA 02215
- Shimomura, Osamu**, Marine Biological Laboratory, 7 MBL Street, Woods Hole, MA 02543
- Shipley, Alan M.**, P.O. Box 943, Forestdale, MA 02644
- Silver, Robert B.**, Marine Biological Laboratory, 7 MBL Street, Woods Hole, MA 02543
- Siwicki, Kathleen K.**, Swarthmore College, Biology Department, 500 College Avenue, Swarthmore, PA 19081-1397
- Skinner, Dorothy M.**, 24 Gray Lane, Falmouth, MA 02540
- Sloboda, Roger D.**, Dartmouth College, Department of Biological Science, 6044 Gilman, Hanover, NH 03755-1893
- Sluder, Greenfield**, University of Massachusetts Medical School, Room 324, 377 Plantation Street, Worcester, MA 01605
- Smith, Peter J. S.**, Marine Biological Laboratory, 7 MBL Street, Woods Hole, MA 02543
- Smith, Stephen J.**, Stanford University School of Medicine, Department of Molecular and Cellular Physiology, Beckman Center, Stanford, CA 94305
- Smolowitz, Roxanna S.**, Marine Biological Laboratory, 7 MBL Street, Woods Hole, MA 02543
- Sogin, Mitchell L.**, Marine Biological Laboratory, 7 MBL Street, Woods Hole, MA 02543
- Sorenson, Martha M.**, Cidade Universitaria-UFRJ, Department Bioquimica Medica-ICB, 21941-590 Rio de Janeiro, Brazil
- Speck, William T.**, Marine Biological Laboratory, 7 MBL Street, Woods Hole, MA 02543
- Spector, Abraham**, Columbia University, Department of Ophthalmology, 630 West 168th Street, New York, NY 10032
- Speksnijder, Johanna E.**, DeMeent 12, 3984JJ Odijk, The Netherlands
- Spray, David C.**, Albert Einstein College of Medicine, Department of Neuroscience, 1300 Morris Park Avenue, Bronx, NY 10461
- Spring, Kenneth R.**, National Institutes of Health, 10 Center Drive, MSC 1598, Building 10, Room 6N260, Bethesda, MD 20892-1603
- Steele, John H.**, Woods Hole Oceanographic Institution, Woods Hole, MA 02543
- Steinacker, Antoinette**, University of Puerto Rico, Institute of Neurobiology, 201 Boulevard Del Valle, San Juan, PR 00901
- Steinberg, Malcolm**, Princeton University, Department of Molecular Biology, M-18 Moffett Laboratory, Princeton, NJ 08544-1014
- Stemmer, Andreas C.**, Institut für Robotik, ETH-Center, 8092 Zurich, Switzerland
- Stenflo, Johan**, University of Lund, Department of Clinical Chemistry, Malmö General Hospital, S-205 02 Malmö, Sweden
- Stetten, Jane Lazarow**, 4701 Willard Avenue, #1413, Chevy Chase, MD 20815-4627
- Stuedler, Paul A.**, Marine Biological Laboratory, The Ecosystems Center, Woods Hole, MA 02543
- Stokes, Darrell R.**, Emory University, Department of Biology, 1510 Clifton Road NE, Atlanta, GA 30322-1100
- Stommel, Elijah W.**, Dartmouth Hitchcock Medical Center, Neurology Department, 1 Medical Drive, Lebanon, NH 03756
- Stracher, Alfred**, SUNY Health Science Center, Department of Biochemistry, 450 Clarkson Avenue, Brooklyn, NY 11203
- Strumwasser, Felix**, P.O. Box 923, East Falmouth, MA 02536-2278
- Stuart, Ann E.**, 1818 North Lakeshore Drive, Chapel Hill, NC 27514
- Sugimori, Mutsuyuki**, New York University Medical Center, Department of Physiology and Neuroscience, Room 442, 550 First Avenue, New York, NY 10016
- Summers, William C.**, Western Washington University, Huxley College of Environmental Studies, Bellingham, WA 982259181
- Suprenant, Kathy A.**, University of Kansas, Department of Physiology and Cell Biology, 4010 Haworth Hall, Lawrence, KS 66045
- Sydlík, Mary Anne**, Hope College, Peale Science Center, 35 East 12th St./PO Box 9000, Holland, MI 49422
- Szent-Gyorgyi, Andrew G.**, Brandeis University, Molecular and Cell Biology, 415 South Street, Waltham, MA 02454-9110
- Tamm, Sidney L.**, Boston University, CAS Biology, 5 Cummington Street, Boston, MA 02215
- Tanzer, Marvin L.**, University of Connecticut School of Dental Medicine, Department of Biostructure and Function, Farmington, CT 06030-3705
- Tasaki, Ichiji**, National Institutes of Health, NIMH, Laboratory of Neurobiology, Building 36, Room 2B-16, Bethesda, MD 20892
- Taylor, D. Lansing**, Cellomics, Inc., 635 William Pitt Way, Pittsburgh, PA 15238
- Taylor, Edwin W.**, University of Chicago, Department of Molecular Genetics, 920 E. 58th Street, Chicago, IL 60637
- Teal, John M.**, 567 New Bedford Lane, Rochester, MA 02770
- Telfer, William H.**, University of Pennsylvania, Department of Biology, Philadelphia, PA 19104
- Telzer, Bruce**, Pomona College, Department of Biology, Thille Building, 175 West 6th Street, Claremont, CA 91711
- Terasaki, Mark**, University of Connecticut Health Center, Department of Physiology, 263 Farmington Avenue, Farmington, CT 06032
- Townsel, James G.**, Meharry Medical College, Department of Anatomy and Physiology, 1005 DB Todd Boulevard, Nashville, TN 37208
- Travis, David M.**, 19 High Street, Woods Hole, MA 02543-1221
- Treisman, Steven N.**, University of Massachusetts Medical Center, Department of Pharmacology, 55 Lake Avenue North, Worcester, MA 01655
- Trigg, D. Thomas**, One Federal Street, 9th Floor, Boston, MA 02211
- Troll, Walter**, NYU Medical Center, Department of Environmental Medicine, 550 First Avenue, New York, NY 10016
- Troxler, Robert F.**, Boston University School of Medicine, Department of Biochemistry, 80 East Concord Street, Boston, MA 02118
- Tucker, Edward B.**, Baruch College, CUNY, Department of Natural Sciences, 17 Lexington Avenue, New York, NY 10010

- Turner, Ruth D.**, Harvard University, Museum of Comparative Zoology, Mollusk Department, Cambridge, MA 02138 (deceased 2000)
- Tweedell, Kenyon S.**, University of Notre Dame, Department of Biological Sciences, Notre Dame, IN 46556-0369
- Tykocinski, Mark L.**, Case Western Reserve University, Institute of Pathology, 2085 Adelbert Road, Cleveland, OH 44106
- Tytell, Michael**, Wake Forest University, Bowman Gray School of Medicine, Department of Anatomy and Neurobiology, Winston-Salem, NC 27157
- Ueno, Hiroshi**, Kyoto University, AGR Chemistry, Faculty of Agriculture, Sakyo, Kyoto 606-8502, Japan
- Valiela, Ivan**, Boston University Marine Program, Marine Biological Laboratory, Woods Hole, MA 02543
- Vallee, Richard**, University of Massachusetts Medical Center, Worcester Foundation Campus, 222 Maple Avenue, Shrewsbury, MA 01545
- Valois, John J.**, 420 Woods Hole Road, Woods Hole, MA 02543
- Van Dover, Cindy Lee**, The College of William and Mary, Biology Department, 328 Millington Hall, Williamsburg, VA 23187
- Van Holde, Kensal E.**, Oregon State University, Biochemistry and Biophysics Department, Corvallis, OR 97331-7503
- Vogl, Thomas P.**, Environmental Research Institute of Michigan, 1101 Wilson Boulevard, Arlington, VA 22209
- Wainwright, Norman R.**, Marine Biological Laboratory, 7 MBL Street, Woods Hole, MA 02543
- Waksman, Byron H.**, New York University Medical Center, Department of Pathology, 550 First Avenue, New York, NY 10016
- Wall, Betty**, 9 George Street, Woods Hole, MA 02543
- Wangh, Lawrence J.**, Brandeis University, Department of Biology, 415 South Street, Waltham, MA 02254
- Warner, Robert C.**, 1609 Temple Hills Drive, Laguna Beach, CA 92651
- Warren, Leonard**, Wistar Institute, 36th and Spruce Streets, Philadelphia, PA 19104
- Waterbury, John B.**, Woods Hole Oceanographic Institution, Department of Biology, Woods Hole, MA 02543
- Waxman, Stephen G.**, Yale Medical School, Neurology Department, 333 Cedar Street, P.O. Box 208018, New Haven, CT 06510
- Weber, Annemarie**, University of Pennsylvania School of Medicine, Department of Biochemistry and Biophysics, Philadelphia, PA 19066
- Weeks, Janis C.**, University of Oregon, Institute of Neuroscience, Eugene, OR 97403-1254
- Weidner, Earl**, Louisiana State University, Department of Biological Sciences, 502 Life Sciences Building, Baton Rouge, LA 70803
- Weiss, Alice Sara**, 105 University Boulevard West, Silver Spring, MD 20901
- Weiss, Dieter G.**, University of Rostock, Institute of Zoology, D-18051 Rostock, Germany
- Weiss, Leon P.**, University of Pennsylvania School of Veterinary Medicine, Department of Animal Biology, Philadelphia, PA 19104
- Weiss, Marisa C.**, Paoli Memorial Hospital, Department of Radiation Oncology, 255 W. Lancaster Avenue, Paoli, PA 19301
- Weissmann, Gerald**, New York University Medical Center, Department of Medicine/Division Rheumatology, 550 First Avenue, New York, NY 10016
- Westerfield, Monte**, University of Oregon, Institute of Neuroscience, Eugene, OR 97403
- Whittaker, J. Richard**, University of New Brunswick, Department of Biology, BS 4511, Fredericton, NB E3B 6E1, Canada
- Wiesel, Torsten N.**, Rockefeller University, 1230 York Avenue, New York, NY 10021
- Wilkens, Lon A.**, University of Missouri, Department of Biology, 8001 Natural Bridge Road, St. Louis, MO 63121-4499
- Wilson, Darcy B.**, Torrey Pines Institute, 3550 General Atomics Court, Building 2, Room 138, San Diego, CA 92121
- Wilson, T. Hastings**, Harvard Medical School, Department of Physiology, 25 Shattuck Street, Boston, MA 02115
- Witkovsky, Paul**, NYU Medical Center, Department of Ophthalmology, 550 First Avenue, New York, NY 10016
- Wittenberg, Beatrice**, Albert Einstein College of Medicine, Department of Physiology and Biophysics, Bronx, NY 10461
- Wittenberg, Jonathan B.**, Albert Einstein College of Medicine, Department of Physiology and Biophysics, Bronx, NY 10461
- Wonderlin, William F.**, West Virginia University, Pharmacology and Toxicology Department, Morgantown, WV 26506
- Worden, Mary Kate**, University of Virginia, Department of Neuroscience, McKim Hall Box 230, Charlottesville, VA 22908
- Worgul, Basil V.**, Columbia University, Department of Ophthalmology, 630 West 168 Street, New York, NY 10032
- Wu, Chau Hsiung**, Northwestern University Medical School, Department of Pharmacology (S215), 303 East Chicago Avenue, Chicago, IL 60611-3008
- Wytenbach, Charles R.**, University of Kansas, Biological Sciences Department, 2045 Haworth Hall, Lawrence, KS 66045-2106
- Zakon, Harold H.**, University of Texas, Section of Neurobiology, School of Life Science, Austin, TX 78712
- Zigman, Seymour**, Marine Park Condominiums, 174 Queen Street, Unit 10-F, Falmouth, MA 02540
- Zigmond, Michael J.**, University of Pittsburgh, S-526 Biomedical Science Tower, 3500 Terrace Street, Pittsburgh, PA 15213
- Zimmerberg, Joshua J.**, National Institutes of Health, LCMB, NICHD, Building 10, Room 10D14, 10 Center Drive, Bethesda, MD 20892
- Zottoli, Steven J.**, Williams College, Department of Biology, Williamstown, MA 01267
- Zucker, Robert S.**, University of California, Neurobiology Division, Molecular and Cellular Biology Department, Berkeley, CA 94720

MBL Associates*Executive Board*

Ruth Ann Laster, President
 Jack Pearce, Vice President
 Kitty Brown, Treasurer
 Molly N. Cornell, Secretary
 Duncan Aspinwall, Membership Chair
 Tammy Smith Amon
 Barbara Atwood
 Julie Child
 Seymour Cohen
 Elizabeth Farnham
 Michael Feulon
 Pat Ferguson
 Sallie A. Giffen
 Alice Knowles
 Rebecca Lash
 Cornelia Hanna McMurtrie
 Joan Pearlman
 Virginia Reynolds
 Volker Ulbrich

*Associates Liaison/Gift Shop
Coordinator*

Kendall B. Bohr

Patron

Judge and Mrs. John S. Langford

Sustaining Associate

Mr. and Mrs. G. Nathan Calkins, Jr.
 Mrs. Janet F. Gillette
 Dr. and Mrs. Edward F. MacNichol, Jr.

Supporting Associate

Mr. and Mrs. William O. Burwell
 Mr. and Mrs. Thomas Claffin
 Mrs. George H. A. Clowes
 Dr. and Mrs. James D. Ebert
 Mr. and Mrs. David Fausch
 Mr. Mike Feulon and Ms. Linda Sallop
 Dr. and Mrs. James J. Ferguson, Jr.
 Mrs. Janet F. Gillette
 Mrs. Mary L. Goldman
 Mr. and Mrs. Lon Hocker
 Mr. and Mrs. Arthur King
 Dr. and Mrs. Leonard Laster
 Drs. Luigi and Elaine Mastroianni
 Mr. and Mrs. Walter J. Salmon
 Mrs. Anne W. Sawyer
 Dr. John Tochko and Mrs. Christina Myles-Tochko
 Mr. and Mrs. John J. Valois
 Mr. and Mrs. Leslie J. Wilson

Family Membership

Dr. and Mrs. Edward A. Adelberg
 Mr. and Mrs. David C. Ahearn
 Dr. and Mrs. Dean C. Allard, Jr.
 Drs. James and Helene Anderson
 Dr. and Mrs. Samuel C. Armstrong
 Mr. and Mrs. Duncan P. Aspinwall
 Mr. and Mrs. Donald R. Aukamp
 Mr. and Mrs. John M. Baitzell
 Mr. and Mrs. David Bakalar
 Dr. and Mrs. Robert B. Barlow, Jr.
 Mr. and Mrs. John E. Barnes
 Dr. and Mrs. Robert M. Berne
 Drs. Harriet and Alan Bernheimer
 Mr. and Mrs. Robert O. Bigelow
 Dr. and Mrs. Edward G. Boettiger
 Mr. and Mrs. Kendall B. Bohr
 Dr. and Mrs. Thomas A. Borge
 Dr. and Mrs. Francis P. Bowles
 Dr. and Mrs. John B. Buck
 Dr. and Mrs. John E. Burriss
 Mr. and Mrs. D. Bret Carlson
 Dr. and Mrs. Richard L. Chappell
 Dr. and Mrs. Frank M. Child
 Dr. and Mrs. Arnold M. Clark
 Mr. and Mrs. James M. Cleary
 Dr. and Mrs. Laurence P. Cloud
 Drs. Harry Conner and Carol Scott-Conner
 Mrs. Neal Cornell
 Mr. and Mrs. Norman C. Cross
 Dr. and Mrs. John M. Cummings
 Mr. and Mrs. Joel P. Davis
 Mr. and Mrs. F. Gerald Douglass
 Dr. and Mrs. John E. Dowling
 Dr. and Mrs. Arthur Brooks DuBois
 Dr. and Mrs. Michael J. Fishbein
 Mr. and Mrs. Harold Frank
 Mr. and Mrs. Howard G. Freeman
 Dr. and Mrs. Robert A. Frosch
 Dr. and Mrs. John J. Funkhouser
 Dr. and Mrs. Mordecai L. Gabriel
 Dr. and Mrs. Sydney Gellis
 Dr. and Mrs. James L. German, III
 Dr. and Mrs. Harold S. Ginsberg
 Dr. and Mrs. Murray Glusman
 Drs. Alfred and Joan Goldberg
 Mr. and Mrs. Charles Goodwin, III
 Mr. and Mrs. Anthony D. Green
 Dr. and Mrs. Thomas C. Gregg
 Dr. and Mrs. Newton H. Gresser
 Mr. and Mrs. Peter A. Hall
 Dr. and Mrs. Harlyn O. Halvorson
 Dr. and Mrs. Richard Bennet Harvey
 Dr. and Mrs. J. Woodland Hastings
 Dr. Robert R. Haubrich
 Mr. and Mrs. Gary G. Hayward
 Dr. and Mrs. Howard H. Hiatt
 Mr. and Mrs. David Hibbitt
 Dr. and Mrs. John E. Hobbie
 Mr. and Mrs. Gerald J. Holtz
 Drs. Francis Hoskin and Elizabeth Farnham

Dr. and Mrs. Robert J. Huettner
 Dr. and Mrs. Shinya Inoué
 Dr. and Mrs. Kurt J. Isseibacher
 Mrs. Mary D. Janney
 Dr. and Mrs. Benjamin Kaminer
 Mr. and Mrs. Paul W. Knaplund
 Mr. and Mrs. A. Sidney Knowles, Jr.
 Mr. and Mrs. Walter E. Knox
 Sir and Lady Hans Kornberg
 Dr. and Mrs. S. Andrew Kulin
 Mr. Ezra and Dr. Aimee Laderman
 Mr. and Mrs. Trevor Lambert
 Dr. and Mrs. George M. Langford
 Dr. and Mrs. Hans Laufer
 Dr. and Mrs. Berton J. Leach
 Dr. and Mrs. John J. Lee
 Mr. and Mrs. Stephen R. Levy
 Mr. and Mrs. Robert Livingstone, Jr.
 Dr. and Mrs. Laszlo Lorand
 Mr. and Mrs. Francis C. Lowell, Jr.
 Dr. Isabelle and Mr. Bernard Manuel
 Mr. and Mrs. Joseph C. Martyna
 Mr. and Mrs. Frank J. Mather, III
 Dr. and Mrs. Robert T. McCluskey
 Dr. and Mrs. William M. McDermott
 Dr. and Mrs. Jerry M. Melillo
 Mr. and Mrs. Wesley J. Merritt
 Mr. and Mrs. Richard Meyers
 Mr. and Mrs. Charles A. Mitchell
 Dr. and Mrs. Merle Mizell
 Dr. and Mrs. Charles H. Montgomery
 Mr. and Mrs. Stephen A. Moore
 Dr. and Mrs. John E. Naugle
 Dr. Pamela Nelson and Mr. Christopher Olmsted
 Mr. and Mrs. Frank L. Nickerson
 Dr. and Mrs. Clifford T. O'Connell
 Mr. and Mrs. James J. O'Connor
 Mr. and Mrs. David R. Palmer
 Mr. and Mrs. Robert Parkinson
 Mr. and Mrs. Richard M. Paulson, Jr.
 Dr. and Mrs. John B. Pearce
 Mr. and Mrs. William J. Pechilis
 Mrs. Nancy Pendleton
 Mr. and Mrs. John B. Peri
 Dr. and Mrs. Courtland D. Perkins
 Dr. and Mrs. Philip Person
 Mr. and Mrs. Frederick S. Peters
 Mr. and Mrs. E. Joel Peterson
 Mr. and Mrs. Harold Piiskaln
 Mr. and Mrs. George H. Plough
 Dr. and Mrs. Aubrey Pothier, Jr.
 Mr. and Mrs. Allan Putnam
 Dr. and Mrs. Lionel J. Rebbun
 Dr. and Mrs. George T. Reynolds
 Dr. and Mrs. Harris Ripps
 Dr. Paul B. Rizzoli
 Ms. Jean Roberts
 Drs. Priscilla and John Roslansky
 Mr. and Mrs. John D. Ross
 Dr. and Mrs. John W. Saunders, Jr.
 Dr. and Mrs. R. Walter Schlesinger

Mr. and Mrs. Harold H. Sears
Dr. and Mrs. Sheldon J. Segal
Mr. and Mrs. Daniel Shearer
Dr. and Mrs. David Shepro
Mr. and Mrs. Bertram R. Silver
Mr. and Mrs. Jonathan O. Simonds
Drs. Frederick and Marguerite Smith
Dr. and Mrs. Alan B. Steinbach
Dr. and Mrs. William K. Stephenson
Mr. and Mrs. E. Kent Swift, Jr.
Mr. and Mrs. Gerard L. Swope, III
Mr. Norman N. Tolkan
Dr. and Mrs. Walter Troll
Prof. and Mrs. Michael Tytell
Mr. and Mrs. Volker Ulbrich
Dr. and Mrs. Gerald Weissmann
Dr. and Mrs. Paul S. Wheeler
Dr. and Mrs. Martin Keister White
Mr. and Mrs. Geoffrey G. Whitney, Jr.
Mr. and Mrs. Lynn H. Wilke
Dr. and Mrs. T. Hastings Wilson
Mrs. Sumner Zacks
Dr. Linda and Mr. Erik Zettler
Dr. and Mrs. Seymour Zigman

Individual Membership

Drs. Fred and Peggy Alsup
Mrs. Tammy Smith Amon
Mr. Dean N. Arden
Mrs. Ellen Prosser Armstrong
Mrs. Kimball C. Atwood, III
Mr. Everett E. Bagley
Dr. Millicent Bell
Mr. C. John Berg
Dr. Thomas P. Bleck
Ms. Avis Blomberg
Mr. Theodore A. Bonn
Mr. James V. Bracchitta
Mrs. Jennie P. Brown
Mrs. M. Kathryn S. Brown
Dr. Robert H. Broyles
Mrs. Barbara Gates Burwell
Dr. Graciela C. Candelas
Mr. Frank C. Carotenuto
Dr. Robert H. Carrier
Mrs. Patricia A. Case
Ms. Mia D. Champion
Dr. Sallie Chisholm
Mrs. Octavia C. Clement
Mr. Allen W. Clowes
Dr. Jewel Plummer Cobb
Mrs. Margaret H. Coburn
Dr. Seymour S. Cohen
Dr. Alan Robert Cole
Ms. Anne S. Concannon
Prof. D. Eugene Copeland
Dr. Vincent Cowling
Mrs. Marilyn E. Crandall
Ms. Dorothy Crossley
Ms. Helen M. Crossley
Mrs. Villa B. Crowell
Mrs. Alexander T. Daignault
Dr. Morton Davidson

Mrs. Elizabeth M. Davis
Ms. Maureen Davis
Ms. Carol Reimann DeYoung
Ms. Shirley Dierolf
Mrs. Juliette G. Dively
Mr. David L. Donovan
Ms. Suzanne Droban
Mr. Roy A. Duffus
Ms. Maureen J. Dugan
Mrs. Charles Eastman
Dr. Frank Egloff
Ms. Judy Ernst
Dr. Stephen L. Estabrooks
Mrs. Eleanor B. Faithorn
Mrs. Ruth Alice Fitz
Ms. Sylvia M. Flanagan
Mr. John W. Folino, Jr.
Mrs. Kathryn W. Foster
Dr. Krystyna Frenkel
Mr. Paul J. Freyheit
Mrs. Ruth E. Fye
Mrs. Lois E. Galvin
Miss Eleanor Garfield
Mrs. Ruth H. Garland
Mr. John Garnett
Ms. Sallie A. Giffen
Mrs. James R. Glazebrook
Mr. Michael P. Goldring
Mrs. Phyllis Goldstein
Mrs. DeWitt S. Goodman
Ms. Muriel Gould
Mrs. Rose Grant
Ms. Janet M. Gregg
Mrs. Jeanne B. Griffith
Mrs. Barbara Grossman
Mrs. Valerie A. Hall
Ms. Mary Elizabeth Hamstrom
Dr. Carol W. Hannenberg
Ms. Elizabeth E. Hathaway
Mrs. Elizabeth Heald
Mrs. Jane G. Heald
Mrs. Betty G. Hubbell
Miss Elizabeth B. Jackson
Mr. Raymond L. Jewett
Mrs. Barbara W. Jones
Mrs. Joan T. Kanwisher
Mrs. Sally Karush
Ms. Patricia E. Keoughan
Dr. Peter N. Kivy
Dr. Aimlee D. Laderman
Mrs. Janet W. Larcum
Ms. Rebecca Lash
Mr. William Lawrence
Dr. Marian E. LeFevre
Mr. Edwin M. Libbin
Mr. Lennart Lindberg
Mrs. Barbara C. Little
Mrs. Sarah J. Loessel
Mr. Richard C. Lovering
Mrs. Margaret M. MacLeish
Ms. Anne Camille Maher
Mrs. Nancy R. Malkiel
Ms. Diane Maranchie
Dr. Miriam Jacob Mauzerall

Mrs. Mary Hartwell Mavor
Mr. Paul McGonigle
Dr. Susan Gerbi McIlwain
Ms. Mary W. McKoan
Ms. Jane A. McLaughlin
Ms. Louise McManus
Ms. Cornelia Hanna McMurtrie
Mrs. Anne L. Meigs-Brown
Mr. Ted Melillo
Dr. Martin Mendelson
Ms. Carmen Merryman
Mrs. Grace S. Metz
Mrs. Mary G. Miles
Mrs. Florence E. Mixer
Mr. Lawrence A. Monte
Mrs. Mary E. Montgomery
Ms. Cynthia Moor
Mr. James V. Moynihan
Mrs. Eleanor M. Nace
Mrs. Anne Nelson
Ms. C. Marie Newman
Dr. Eliot H. Nierman
Mr. Edmund F. Nolan
Ms. Catherine N. Norton
Dr. Renee Bennett O'Sullivan
Dr. Arthur B. Pardee
Ms. Carolyn L. Parmenter
Ms. Joan Pearlman
Mr. Raymond W. Peterson
Ms. Elizabeth T. Price
Ms. Dianne Purves
Mrs. Julia S. Rankin
Dr. Margaret M. Rappaport
Mr. Fred J. Ravens, Jr.
Ms. Mary W. Rianhard
Dr. Mary Elizabeth Rice
Dr. Monica Riley
Mrs. Lola E. Robertson
Mrs. Arlene Rogers
Ms. Jean Rogers
Mrs. Wendy E. Rose
Mrs. Atholie K. Rosett
Dr. Virginia F. Ross
Dr. John D. Rummel
Mr. Raymond A. Sanborn
Mr. Claude Schoepf
Ms. Elaine Schott
Ms. Emily Schwartz-Clark
Mrs. Elsie M. Scott
Dr. Cecily C. Selby
Mrs. Deborah G. Senft
Ms. Dorothy Sgarzi
Mrs. Charlotte Shemin
Ms. Enid K. Sichel
Dr. Jeffrey D. Silberman
Mrs. Cynthia C. Smith
Mr. Sean W. Smith
Mrs. Louise M. Specht
Dr. Guy L. Steele, Sr.
Dr. Robert E. Steele
Mrs. Eleanor Steinbach
Mrs. Judith G. Stetson
Mrs. Jane Lazarow Stetten
Mrs. Elizabeth Stommel

Mr. Albert H. Swain
 Mrs. Belle K. Taylor
 Mr. James K. Taylor
 Mr. Emil D. Tietje, Jr.
 Mrs. Alice Todd
 Mr. Arthur D. Traub
 Mr. D. Thomas Trigg
 Ms. Natalie Trousof
 Ms. Ciona Ulbrich
 Ms. Sylvia Vatuk
 Ms. Susan Veeder
 Mr. Lee D. Vincent
 Mr. Arthur D. Voorhis
 Mrs. Eve Warren
 Mr. John T. Weeks
 Mr. Michael S. Weinstein
 Ms. Lillian Wendorff
 Ms. Mabel Y. Whelpley
 Mrs. Barbara Whitehead
 Mrs. Ava Whittemore
 Mrs. Joan R. Wickersham
 Mrs. Clare M. Wilber
 Mrs. Helen Wilson
 Ms. Nancy Woitkoski
 Ms. Marion K. Wright
 Mrs. Dorothy M. York
 Mrs. Margery P. Zinn

Elisabeth Buck
 Jewel Cobb
 Janet Daniels
 Carol DeYoung
 Fran Eastman
 Alma Ebert
 Jane Foster
 Becky Glazebrook
 Muriel Gould
 Barbara Grossman
 Jean Halvorson
 Hanna Hastings
 Sally Karush
 Marcella Katz
 Alice Knowles
 Donna Kornberg
 Evelyn Laufer
 Barbara Little
 Winnie Mackey
 Diane Maranchie
 Miriam Mauzerall
 Mary Mavor
 Jane McCormack
 Louise McManus
 Mary Miles
 Florence Mixer
 Lorraine Mizell
 Helen Murphy
 Bertha Person
 Margareta Pothier
 Liz Price
 Julie Rankin
 Arlene Rogers
 Lil Saunders
 Cynthia Smith
 Peggy Smith
 Louise Specht
 Jane Stetten

Barbara Thomson
 Alice Todd
 Elaine Troll
 Natalie Trousof
 Barbara Van Holde
 Doris Van Keuren
 Susan Veeder
 Carol Ann Wagner
 Mabel Whelpley
 Clare Wilber
 Betty Wilson
 Grace Wittzell
 Bunnie Rose Zigman

MBL Summer Tour Guides

Gloria Borgese
 Nancy Campana
 Frank Child
 Julie Child
 Nancy Fraser
 Sallie Giffen
 Nichole Graham
 Lois Harvey
 Lincoln Kraeuter
 Barbara Little
 Jennifer Machado
 Charles Mahoney
 Francis X. Mahoney
 Julie Rankin
 Howard Redpath
 Arlene Rogers
 Pucky Roslansky
 Suzanne Thomas
 Mary Ulbrich
 John Valois
 Margery Zinn

MBL Gift Shop Volunteers

Marion Adelberg
 Barbara Atwood
 Beth Berne
 Harriet Bernheimer
 Avis Blomberg
 Gloria Borgese
 Kitty Brown

Certificate of Organization Articles of Amendment Bylaws



Certificate of Organization

(On File in the Office of the Secretary of the Commonwealth)

No. 3170

We, Alpheus Hyatt, President, William Stanford Stevens, Treasurer, and William T. Sedgwick, Edward G. Gardiner, Susan Mims and Charles Sedgwick Minot being a majority of the Trustees of the Marine Biological Laboratory in compliance with the requirements of the fourth section of chapter one hundred and fifteen of the Public Statutes do hereby certify that the following is a true copy of the agreement of association to constitute said Corporation, with the names of the subscribers thereto:

We, whose names are hereto subscribed, do, by this agreement, associate ourselves with the intention to constitute a Corporation according to the provisions of the one hundred and fifteenth chapter of the Public Statutes of the Commonwealth of Massachusetts, and the Acts in amendment thereof and in addition thereto.

The name by which the Corporation shall be known is
THE MARINE BIOLOGICAL LABORATORY.

The purpose for which the Corporation is constituted is to establish and maintain a laboratory or station for scientific study and investigations, and a school for instruction in biology and natural history.

The place within which the Corporation is established or located is the city of Boston within said Commonwealth.

The amount of its capital stock is none.

In Witness Whereof, we have hereunto set our hands, this twenty seventh day of February in the year eighteen hundred and eighty-eight, Alpheus Hyatt, Samuel Mills, William T. Sedgwick, Edward G. Gardiner, Charles Sedgwick Minot, William G. Farlow, William Stanford Stevens, Anna D. Phillips, Susan Mims, B. H. Van Vleck. That the first meeting of the subscribers to said agreement was held on the thirteenth day of March in the year eighteen hundred and eighty-eight.

In Witness Whereof, we have hereunto signed our names, this thirteenth day of March in the year eighteen hundred and eighty-eight, Alpheus Hyatt, President, William Stanford Stevens, Treasurer, Edward G. Gardiner, William T. Sedgwick, Susan Mims, Charles Sedgwick Minot.

(Approved on March 20, 1888 as follows:

I hereby certify that it appears upon an examination of the within written certificate and the records of the corporation duly submitted to my inspection, that the requirements of sections one, two and three of chapter one hundred and fifteen, and sections eighteen, twenty and twenty-one of chapter one hundred and six, of the Public Statutes, have been complied with and I hereby approve said certificate this twentieth day of March A.D. eighteen hundred and eighty-eight.

Charles Endicott
Commissioner of Corporations)

Articles of Amendment

(On File in the Office of the Secretary of the Commonwealth)

We, James D. Ebert, President, and David Shepro, Clerk of the Marne Biological Laboratory, located at Woods Hole, Massachusetts 02543, do hereby certify that the following amendment to the Articles of Organization of the Corporation was duly adopted at a meeting held on August 15, 1975, as adjourned to August 29, 1975, by vote of 444 members, being at least two-thirds of its members legally qualified to vote in the meeting of the corporation:

Voted: That the Certificate of Organization of this corporation be and it hereby is amended by the addition of the following provisions:

"No Officer, Trustee or Corporate Member of the corporation shall be personally liable for the payment or satisfaction of any obligation or liabilities incurred as a result of, or otherwise in connection with, any commitments, agreements, activities or affairs of the corporation.

"Except as otherwise specifically provided by the Bylaws of the corporation, meetings of the Corporate Members of the corporation may be held anywhere in the United States.

"The Trustees of the corporation may make, amend or repeal the Bylaws of the corporation in whole or in part, except with respect to any provisions thereof which shall by law, this Certificate or the bylaws of the corporation, require action by the Corporate Members."

The foregoing amendment will become effective when these articles of amendment are filed in accordance with Chapter 180, Section 7 of the General Laws unless these articles specify, in accordance with the vote adopting the amendment, a later effective date not more than thirty days after such filing, in which event the amendment will become effective on such later date.

In Witness whereof and Under the Penalties of Perjury, we have hereto signed our names this 2nd day of September, in the year 1975, James D. Ebert, President; David Shepro, Clerk

(Approved on October 24, 1975, as follows:

I hereby approve the within articles of amendment and, the filing fee in the amount of \$10 having been paid, said articles are deemed to have been filed with me this 24th day of October, 1975.

Paul Guzzi
Secretary of the Commonwealth)

Bylaws

(Revised August 7, 1992 and December 10, 1992)

ARTICLE I—THE CORPORATION

A Name and Purpose The name of the Corporation shall be The Marne Biological Laboratory. The Corporation's purpose shall be to establish and maintain a

laboratory or station for scientific study and investigation and a school for instruction in biology and natural history.

B. *Nondiscrimination.* The Corporation shall not discriminate on the basis of age, religion, color, race, national or ethnic origin, sex or sexual preference in its policies on employment and administration or in its educational and other programs.

ARTICLE II—MEMBERSHIP

A. *Members.* The Members of the Corporation ("Members") shall consist of persons elected by the Board of Trustees (the "Board"), upon such terms and conditions and in accordance with such procedures, not inconsistent with law or these Bylaws, as may be determined by the Board. At any regular or special meeting of the Board, the Board may elect new Members. Members shall have no voting or other rights with respect to the Corporation or its activities except as specified in these Bylaws, and any Member may vote at any meeting of the Members in person only and not by proxy. Members shall serve until their death or resignation unless earlier removed with or without cause by the affirmative vote of two-thirds of the Trustees then in office. Any Member who has retired from his or her home institution may, upon written request to the Corporation, be designated a Life Member. Life Members shall not have the right to vote and shall not be assessed for dues.

B. *Meetings.* The annual meeting of the Members shall be held on the Friday following the first Tuesday in August of each year, at the Laboratory of the Corporation in Woods Hole, Massachusetts, at 9:30 a.m. The Chairperson of the Board shall preside at meetings of the Corporation. If no annual meeting is held in accordance with the foregoing provision, a special meeting may be held in lieu thereof with the same effect as the annual meeting, and in such case all references in these Bylaws, except in this Article II.B., to the annual meeting of the Members shall be deemed to refer to such special meeting. Members shall transact business as may properly come before the meeting. Special meetings of the Members may be called by the Chairperson or the Trustees, and shall be called by the Clerk, or in the case of the death, absence, incapacity or refusal by the Clerk, by any other officer, upon written application of Members representing at least ten percent of the smallest quorum of Members required for a vote upon any matter at the annual meeting of the Members, to be held at such time and place as may be designated.

C. *Quorum.* One hundred (100) Members shall constitute a quorum at any meeting. Except as otherwise required by law or these Bylaws, the affirmative vote of a majority of the Members voting in person at a meeting attended by a quorum shall constitute action on behalf of the Members.

D. *Notice of Meetings.* Notice of any annual meeting or special meeting of Members, if necessary, shall be given by the Clerk by mailing notice of the time and place and purpose of such meeting at least 15 days before such meeting to each Member at his or her address as shown on the records of the Corporation.

E. *Waiver of Notice.* Whenever notice of a meeting is required to be given a Member, under any provision of the Articles or Organization or Bylaws of the Corporation, a written waiver thereof, executed before or after the Meeting by such Member, or his or her duly authorized attorney, shall be deemed equivalent to such notice.

F. *Adjournments.* Any meeting of the Members may be adjourned to any other time and place by the vote of a majority of those Members present at the meeting, whether or not such Members constitute a quorum, or by any officer entitled to preside at or to act as Clerk of such meeting, if no Member is present or represented. It shall not be necessary to notify any Members of any adjournment unless no Member is present or represented at the meeting which is adjourned, in which case, notice of the adjournment shall be given in accordance with Article II.D. Any business which could have been transacted at any meeting of the Members as originally called may be transacted at an adjournment thereof.

ARTICLE III—ASSOCIATES OF THE CORPORATION

Associates of the Corporation. The Associates of the Marine Biological Laboratory shall be an unincorporated group of persons (including associations and corporations) interested in the Laboratory and shall be organized and operated under the general supervision and authority of the Trustees. The Associates of the Marine Biological Laboratory shall have no voting rights.

ARTICLE IV—BOARD OF TRUSTEES

A. *Powers.* The Board of Trustees shall have the control and management of the affairs of the Corporation. The Trustees shall elect a Chairperson of the Board who shall serve until his or her successor is elected and qualified. They shall annually elect a President of the Corporation. They shall annually elect a Vice Chairperson of the Board who shall be Vice Chairperson of the meetings of the Corporation. They shall

annually elect a Treasurer. They shall annually elect a Clerk, who shall be a resident of Massachusetts. They shall elect Trustees-at-Large as specified in this Article IV. They shall appoint a Director of the Laboratory for a term not to exceed five years, provided the term shall not exceed one year if the candidate has attained the age of 65 years prior to the date of the appointment. They shall choose such other officers and agents as they shall think best. They may fix the compensation of all officers and agents of the Corporation and may remove them at any time. They may fill vacancies occurring in any of the offices. The Board shall have the power to choose an Executive Committee from their own number as provided in Article V, and to delegate to such Committee such of their own powers as they may deem expedient in addition to those powers conferred by Article V. They shall, from time to time, elect Members to the Corporation upon such terms and conditions as they shall have determined, not inconsistent with law or these Bylaws.

B. *Composition and Election.*

(1) The Board shall include 24 Trustees elected by the Board as provided below:

(a) At least six Trustees ("Corporate Trustees") shall be Members who are scientists, and the other Trustees ("Trustees-at-Large") shall be individuals who need not be Members or otherwise affiliated with the Corporation.

(b) The 24 elected Trustees shall be divided into four classes of six Trustees each, with one class to be elected each year to serve for a term of four years, and with each such class to include at least one Corporate Trustee. Such classes of Trustees shall be designated by the year of expiration of their respective terms.

(2) The Board shall also include the Chief Executive Officer, Treasurer and the Chairperson of the Science Council, who shall be *ex officio* voting members of the Board.

(3) Although Members or Trustees may recommend individuals for nomination as Trustees, nominations for Trustee elections shall be made by the Nominating Committee in its sole discretion. The Board may also elect Trustees who have not been nominated by the Nominating Committee.

C. *Eligibility.* A Corporate Trustee or a Trustee-at-Large who has been elected to an initial four-year term or remaining portion thereof, of which he/she has served at least two years, shall be eligible for re-election to a second four-year term, but shall be ineligible for re-election to any subsequent term until one year has elapsed after he/she has last served as a Trustee.

D. *Removal.* Any Trustee may be removed from office at any time with or without cause, by vote of a majority of the Members entitled to vote in the election of Trustees; or for cause, by vote of two-thirds of the Trustees then in office. A Trustee may be removed for cause only if notice of such action shall have been given to all of the Trustees or Members entitled to vote, as the case may be, prior to the meeting at which such action is to be taken and if the Trustee to be so removed shall have been given reasonable notice and opportunity to be heard before the body proposing to remove him or her.

E. *Vacancies.* Any vacancy in the Board may be filled by vote of a majority of the remaining Trustees present at a meeting of Trustees at which a quorum is present. Any vacancy in the Board resulting from the resignation or removal of a Corporate Trustee shall be filled by a Member who is a scientist.

F. *Meetings.* Meetings of the Board shall be held from time to time, not less frequently than twice annually, as determined by the Board. Special meetings of Trustees may be called by the Chairperson, or by any seven Trustees, to be held at such time and place as may be designated. The Chairperson of the Board, when present, shall preside over all meetings of the Trustees. Written notice shall be sent to a Trustee's usual or last known place of residence at least two weeks before the meeting. Notice of a meeting need not be given to any Trustee if a written waiver of notice executed by such Trustee before or after the meeting is filed with the records of the meeting, or if such Trustee shall attend the meeting without protesting prior thereto or at its commencement the lack of notice given to him or her.

G. *Quorum and Action by Trustees.* A majority of all Trustees then in office shall constitute a quorum. Any meeting of Trustees may be adjourned by vote of a majority of Trustees present, whether or not a quorum is present, and the meeting may be held as adjourned without further notice. When a quorum is present at any meeting of the Trustees, a majority of the Trustees present and voting (excluding abstentions) shall decide any question, including the election of officers, unless otherwise required by law, the Articles of Organization or these Bylaws.

H. *Transfers of Interests in Land.* There shall be no transfer of title nor long-term lease of real property held by the Corporation without prior approval of not less than two-thirds of the Trustees. Such real property transactions shall be finally acted upon at a meeting of the Board only if presented and discussed at a prior meeting of the Board. Either meeting may be a special meeting and no less than four weeks shall elapse between the two meetings. Any property acquired by the Corporation after December 1, 1989 may be sold, any mortgage or pledge of real property (regardless

of when acquired) to secure borrowings by the Corporation may be granted, and any transfer of title or interest in real property pursuant to the foreclosure or endorsement of any such mortgage or pledge of real property may be effected by any holder of a mortgage or pledge of real property of the Corporation, with the prior approval of not less than two-thirds of the Trustees (other than any Trustee or Trustees with a direct or indirect financial interest in the transaction being considered for approval) who are present at a regular or special meeting of the Board at which there is a quorum.

ARTICLE V—COMMITTEES

A. *Executive Committee.* There shall be an Executive Committee of the Board of Trustees which shall consist of not more than eleven (11) Trustees, including *ex officio* Trustees, elected by the Board.

The Chairperson of the Board shall act as Chairperson of the Executive Committee and the Vice Chairperson as Vice Chairperson. The Executive Committee shall meet at such times and places and upon such notice and appoint such subcommittees as the Committee shall determine.

The Executive Committee shall have and may exercise all the powers of the Board during the intervals between meetings of the Board except those powers specifically withheld, from time to time, by vote of the Board or by law. The Executive Committee may also appoint such committees, including persons who are not Trustees, as it may, from time to time, approve to make recommendations with respect to matters to be acted upon by the Executive Committee or the Board.

The Executive Committee shall keep appropriate minutes of its meetings, which shall be reported to the Board. Any actions taken by the Executive Committee shall also be reported to the Board.

B. *Nominating Committee.* There shall be a Nominating Committee which shall consist of not fewer than four nor more than six Trustees appointed by the Board in a manner which shall reflect the balance between Corporate Trustees and Trustees-at-Large on the Board. The Nominating Committee shall nominate persons for election as Corporate Trustees and Trustees-at-Large, Chairperson of the Board, Vice Chairperson of the Board, President, Treasurer, Clerk, Director of the Laboratory and such other officers, if any, as needed, in accordance with the requirements of these Bylaws. The Nominating Committee shall also be responsible for overseeing the training of new Trustees. The Chairperson of the Board of Trustees shall appoint the Chairperson of the Nominating Committee. The Chairperson of the Science Council shall be an *ex officio* voting member of the Nominating Committee.

C. *Science Council.* There shall be a Science Council (the "Council") which shall consist of Members of the Corporation elected to the Council by vote of the Members of the Corporation, and which shall advise the Board with respect to matters concerning the Corporation's mission, its scientific and instructional endeavors, and the appointment and promotions of persons or committees with responsibility for matters requiring scientific expertise. Unless otherwise approved by a majority of the members of the Council, the Chairperson of the Council shall be elected annually by the Council. The chief executive officer of the Corporation shall be an *ex officio* voting member of the Council.

D. *Board of Overseers.* There shall be a Board of Overseers which shall consist of not fewer than five nor more than eight scientists who have expertise concerning matters with which the Corporation is involved. Members of the Board of Overseers may or may not be Members of the Corporation and may be appointed by the Board of Trustees on the basis of recommendations submitted from scientists and scientific organizations or societies. The Board of Overseers shall be available to review and offer recommendations to the officers, Trustees and Science Council regarding scientific activities conducted or proposed by the Corporation and shall meet from time to time, not less frequently than annually, as determined by the Board of Trustees.

E. *Board Committees Generally.* The Trustees may elect or appoint one or more other committees (including, but not limited to, an Investment Committee, a Development Committee, an Audit Committee, a Facilities and Capital Equipment Committee and a Long-Range Planning Committee) and may delegate to any such committee or committees any or all of their powers, except those which by law, the Articles of Organization or these Bylaws the Trustees are prohibited from delegating; provided that any committee to which the powers of the Trustees are delegated shall consist solely of Trustees. The members of any such committee shall have such tenure and duties as the Trustees shall determine. The Investment Committee, which shall oversee the management of the Corporation's endowment funds and marketable securities shall include as *ex officio* members, the Chairperson of the Board, the Treasurer and the Chairperson of the Audit Committee, together with such Trustees as may be required for not less than two-thirds of the Investment Committee to consist of Trustees. Except as otherwise provided by these Bylaws or determined by the Trustees, any such committee may make rules for the conduct of its business, but,

unless otherwise provided by the Trustees or in such rules, its business shall be conducted as nearly as possible in the same manner as is provided by these Bylaws for the Trustees.

F. *Actions Without a Meeting.* Any action required or permitted to be taken at any meeting of the Executive Committee or any other committee elected by the Trustees may be taken without a meeting if all members of such committees consent to the action in writing and such written consents are filed with the records of meetings. Members of the Executive Committee or any other committee elected by the Trustees may also participate in any meeting by means of a telephone conference call, or otherwise take action in such a manner as may, from time to time, be permitted by law.

G. *Manual of Procedures.* The Board of Trustees, on the recommendation of the Executive Committee, shall establish guidelines and modifications thereof to be recorded in a Manual of Procedures. Guidelines shall establish procedures for: (1) Nomination and election of members of the Corporation, Board of Trustees and Executive Committee; (2) Election of Officers; (3) Formation and Function of Standing Committees.

ARTICLE VI—OFFICERS

A. *Enumeration.* The officers of the Corporation shall consist of a President, a Treasurer and a Clerk, and such other officers having the powers of President, Treasurer and Clerk as the Board may determine, and a Director of the Laboratory. The Corporation may have such other officers and assistant officers as the Board may determine, including (without limitation) a Chairperson of the Board, Vice Chairperson and one or more Vice Presidents, Assistant Treasurers or Assistant Clerks. Any two or more offices may be held by the same person. The Chairperson and Vice Chairperson of the Board shall be elected by and from the Trustees, but other officers of the Corporation need not be Trustees or Members. If required by the Trustees, any officer shall give the Corporation a bond for the faithful performance of his or her duties in such amount and with such surety or sureties as shall be satisfactory to the Trustees.

B. *Tenure.* Except as otherwise provided by law, by the Articles of Organization or by these Bylaws, the President, Treasurer, and all other officers shall hold office until the first meeting of the Board following the annual meeting of Members and thereafter, until his or her successor is chosen and qualified.

C. *Resignation.* Any officer may resign by delivering his or her written resignation to the Corporation at its principal office or to the President or Clerk and such resignation shall be effective upon receipt unless it is specified to be effective at some other time or upon the happening of some other event.

D. *Removal.* The Board may remove any officer with or without cause by a vote of a majority of the entire number of Trustees then in office, at a meeting of the Board called for that purpose and for which notice of the purpose thereof has been given, provided that an officer may be removed for cause only after having an opportunity to be heard by the Board at a meeting of the Board at which a quorum is personally present and voting.

E. *Vacancy.* A vacancy in any office may be filled for the unexpired balance of the term by vote of a majority of the Trustees present at any meeting of Trustees at which a quorum is present or by written consent of all of the Trustees, if less than a quorum of Trustees shall remain in office.

F. *Chairperson.* The Chairperson shall have such powers and duties as may be determined by the Board and, unless otherwise determined by the Board, shall serve in that capacity for a term coterminous with his or her term as Trustee.

G. *Vice Chairperson.* The Vice Chairperson shall perform the duties and exercise the powers of the Chairperson in the absence or disability of the Chairperson, and shall perform such other duties and possess such other powers as may be determined by the Board. Unless otherwise determined by the Board, the Vice Chairperson shall serve for a one-year term.

H. *Director.* The Director shall be the chief operating officer and, unless otherwise voted by the Trustees, the chief executive officer of the Corporation. The Director shall, subject to the direction of the Trustees, have general supervision of the Laboratory and control of the business of the Corporation. At the annual meeting, the Director shall submit a report of the operations of the Corporation for such year and a statement of its affairs, and shall, from time to time, report to the Board all matters within his or her knowledge which the interests of the Corporation may require to be brought to its notice.

I. *Deputy Director.* The Deputy Director, if any, or if there shall be more than one, the Deputy Directors in the order determined by the Trustees, shall, in the absence or disability of the Director, perform the duties and exercise the powers of the Director and shall perform such other duties and shall have such other powers as the Trustees may, from time to time, prescribe.

J. *President.* The President shall have the powers and duties as may be vested in him or her by the Board.

K. *Treasurer and Assistant Treasurer.* The Treasurer shall, subject to the direction of the Trustees, have general charge of the financial affairs of the Corporation, including its long-range financial planning, and shall cause to be kept accurate books of account. The Treasurer shall prepare a yearly report on the financial status of the Corporation to be delivered at the annual meeting. The Treasurer shall also prepare or oversee all filings required by the Commonwealth of Massachusetts, the Internal Revenue Service, or other Federal and State Agencies. The account of the Treasurer shall be audited annually by a certified public accountant.

The Assistant Treasurer, if any, or if there shall be more than one, the Assistant Treasurers in the order determined by the Trustees, shall, in the absence or disability of the Treasurer, perform the duties and exercise the powers of the Treasurer, shall perform such other duties and shall have such other powers as the Trustees may, from time to time, prescribe.

L. *Clerk and Assistant Clerk.* The Clerk shall be a resident of the Commonwealth of Massachusetts, unless the Corporation has designated a resident agent in the manner provided by law. The minutes or records of all meetings of the Trustees and Members shall be kept by the Clerk who shall record, upon the record books of the Corporation, minutes of the proceedings at such meetings. He or she shall have custody of the record books of the Corporation and shall have such other powers and shall perform such other duties as the Trustees may, from time to time, prescribe.

The Assistant Clerk, if any, or if there shall be more than one, the Assistant Clerks in the order determined by the Trustees, shall, in the absence or disability of the Clerk, perform the duties and exercise the powers of the Clerk and shall perform such other duties and shall have such other powers as the Trustees may, from time to time, prescribe.

In the absence of the Clerk and an Assistant Clerk from any meeting, a temporary Clerk shall be appointed at the meeting.

M. *Other Powers and Duties.* Each officer shall have in addition to the duties and powers specifically set forth in these Bylaws, such duties and powers as are customarily incident to his or her office, and such duties and powers as the Trustees may, from time to time, designate.

ARTICLE VII—AMENDMENTS

These Bylaws may be amended by the affirmative vote of the Members at any meeting, provided that notice of the substance of the proposed amendment is stated in the notice of such meeting. As authorized by the Articles of Organization, the Trustees, by a majority of their number then in office, may also make, amend or repeal these Bylaws, in whole or in part, except with respect to (a) the provisions of these Bylaws governing (i) the removal of Trustees and (ii) the amendment of these Bylaws and (b) any provisions of these Bylaws which by law, the Articles of Organization or these Bylaws, requires action by the Members.

No later than the time of giving notice of meeting of Members next following the making, amending or repealing by the Trustees of any Bylaw, notice thereof stating the substance of such change shall be given to all Members entitled to vote on amending the Bylaws.

Any Bylaw adopted by the Trustees may be amended or repealed by the Members entitled to vote on amending the Bylaws.

ARTICLE VIII—INDEMNITY

Except as otherwise provided below, the Corporation shall, to the extent legally permissible, indemnify each person who is, or shall have been, a Trustee, director or officer of the Corporation or who is serving, or shall have served at the request of the Corporation as a Trustee, director or officer of another organization in which the Corporation directly or indirectly has any interest as a shareholder, creditor or otherwise, against all liabilities and expenses (including judgments, fines, penalties, and reasonable attorneys' fees and all amounts paid, other than to the Corporation or such other organization, in compromise or settlement) imposed upon or incurred by any such person in connection with, or arising out of, the defense or disposition of any action, suit or other proceeding, whether civil or criminal, in which he or she may be a defendant or with which he or she may be threatened or otherwise involved, directly or indirectly, by reason of his or her being or having been such a Trustee, director or officer.

The Corporation shall provide no indemnification with respect to any matter as to which any such Trustee, director or officer shall be finally adjudicated in such action, suit or proceeding not to have acted in good faith in the reasonable belief that his or her action was in the best interests of the Corporation. The Corporation shall provide no indemnification with respect to any matter settled or comprised unless such matter

shall have been approved as in the best interests of the Corporation, after notice that indemnification is involved, by (i) a disinterested majority of the Board of the Executive Committee, or (ii) a majority of the Members.

Indemnification may include payment by the Corporation of expenses in defending a civil or criminal action or proceeding in advance of the final disposition of such action or proceeding upon receipt of an undertaking by the person indemnified to repay such payment if it is ultimately determined that such person is not entitled to indemnification under the provisions of this Article VIII, or under any applicable law.

As used in the Article VIII, the terms "Trustee," "director," and "officer" include their respective heirs, executors, administrators and legal representatives, and an "interested" Trustee, director or officer is one against whom in such capacity the proceeding in question or another proceeding on the same or similar grounds is then pending.

To assure indemnification under this Article VIII of all persons who are determined by the Corporation or otherwise to be or to have been "fiduciaries" of any employee benefits plan of the Corporation which may exist, from time to time, this Article VIII shall be interpreted as follows: (i) "another organization" shall be deemed to include such an employee benefit plan, including without limitation, any plan of the Corporation which is governed by the Act of Congress entitled "Employee Retirement Income Security Act of 1974," as amended, from time to time, ("ERISA"); (ii) "Trustee" shall be deemed to include any person requested by the Corporation to serve as such for an employee benefit plan where the performance by such person of his or her duties to the Corporation also imposes duties on, or otherwise involves services by, such person to the plan or participants or beneficiaries of the plan; (iii) "fines" shall be deemed to include any excise tax plan pursuant to ERISA; and (iv) actions taken or omitted by a person with respect to an employee benefit plan in the performance of such person's duties for a purpose reasonably believed by such person to be in the interest of the participants and beneficiaries of the plan shall be deemed to be for a purpose which is in the best interests of the Corporation.

The right of indemnification provided in this Article VIII shall not be exclusive of or affect any other rights to which any Trustee, director or officer may be entitled under any agreement, statute, vote of Members or otherwise. The Corporation's obligation to provide indemnification under this Article VIII shall be offset to the extent of any other source of indemnification of any otherwise applicable insurance coverage under a policy maintained by the Corporation or any other person. Nothing contained in the Article shall affect any rights to which employees and corporate personnel other than Trustees, directors or officers may be entitled by contract, by vote of the Board or of the Executive Committee or otherwise.

ARTICLE IX—DISSOLUTION

The consent of every Trustee shall be necessary to effect a dissolution of the Marine Biological Laboratory. In case of dissolution, the property shall be disposed of in such a manner and upon such terms as shall be determined by the affirmative vote of two-thirds of the Trustees then in office in accordance with the laws of the Commonwealth of Massachusetts.

ARTICLE X—MISCELLANEOUS PROVISIONS

A. *Fiscal Year.* Except as otherwise determined by the Trustees, the fiscal year of the Corporation shall end on December 31st of each year.

B. *Seal.* Unless otherwise determined by the Trustees, the Corporation may have a seal in such form as the Trustees may determine, from time to time.

C. *Execution of Instruments.* All checks, deeds, leases, transfers, contracts, bonds, notes and other obligations authorized to be executed by an officer of the Corporation in its behalf shall be signed by the Director or the Treasurer except as the Trustees may generally or in particular cases otherwise determine. A certificate by the Clerk or an Assistant Clerk, or a temporary Clerk, as to any action taken by the Members, Board of Trustees or any officer or representative of the Corporation shall as to all persons who rely thereon in good faith be conclusive evidence of such action.

D. *Corporate Records.* The original, or attested copies, of the Articles of Organization, Bylaws and records of all meetings of the Members shall be kept in Massachusetts at the principal office of the Corporation, or at an office of the Corporation's Clerk or resident agent. Said copies and records need not all be kept in the same office. They shall be available at all reasonable times for inspection by any Member for any proper purpose, but not to secure a list of Members for a purpose other than in the interest of the applicant, as a Member, relative to the affairs of the Corporation.

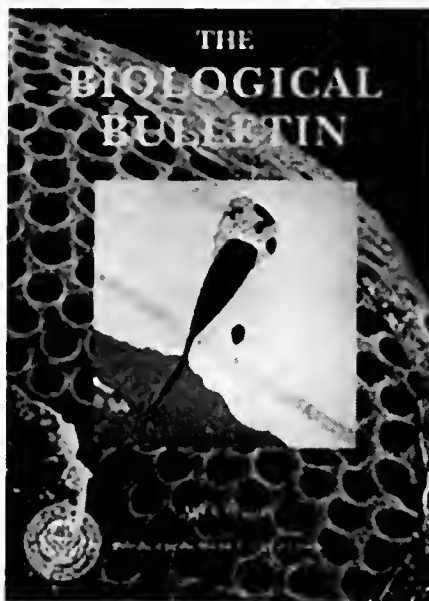
E. *Articles of Organization.* All references in these Bylaws to the Articles of Organization shall be deemed to refer to the Articles of Organization of the Corporation, as amended and in effect, from time to time.

F. *Transactions with Interested Parties.* In the absence of fraud, no contract or other

R90 Annual Report

transaction between this Corporation and any other corporation or any firm, association, partnership or person shall be affected or invalidated by the fact that any Trustee or officer of this Corporation is pecuniarily or otherwise interested in or is a director, member or officer of such other corporation or of such firm, association or partnership or in a party to or is pecuniarily or otherwise interested in such contract or other transaction or is in any way connected with any person or person, firm, association, partnership, or corporation pecuniarily or otherwise interested therein; provided that the fact that he or she individually or as a director, member or officer of such corporation, firm, association or partnership in such a party or is so interested shall be disclosed to or shall have been

known by the Board of Trustees or a majority of such Members thereof as shall be present at a meeting of the Board of Trustees at which action upon any such contract or transaction shall be taken; any Trustee may be counted in determining the existence of a quorum and may vote at any meeting of the Board of Trustees for the purpose of authorizing any such contract or transaction with like force and effect as if he/she were not so interested, or were not a director, member or officer of such other corporation, firm, association or partnership, provided that any vote with respect to such contract or transaction must be adopted by a majority of the Trustees then in office who have no interest in such contract or transaction.



Publications

- Abenavoli A., L. Forti, and A. Malgaroli. 2000. Mechanisms of spontaneous miniature activity at CA3-CA1 synapses: evidence for a divergence from a random Poisson process. *Biol. Bull.* **199**: 184–186.
- Ahrens, T. D., and P. A. Siver. 2000. Trophic condition and water chemistry of lakes on Cape Cod, Massachusetts, USA. *Lake Reservoir Manage.* **16**(4): 268–280.
- Alvarez, J., A. Giuditta, and E. Koenig. 2000. Protein synthesis in axons and terminals: significance for maintenance, plasticity and regulation of phenotype. With a critique of slow transport theory. *Progr. Neurobiol.* **62**: 1–62.
- Amaral Zettler, L. A., T. A. Nerad, C. J. O'Kelly, M. T. Peglar, P. M. Gillevet, J. D. Silberman, and M. L. Sogin. 2000. A molecular reassessment of the Leptomyxid amoebae. *Protist* **151**: 275–282.
- Armstrong, P. B., and R. Asokan. 2000. A Ca^{+2} -independent cytolitic system from the blood of the marine snail, *Busycon canaliculum*. *Biol. Bull.* **199**: 194–195.
- Asokan, R., M. T. Armstrong, and P. B. Armstrong. 2000. Association of α_2 -macroglobulin with the coagulin clot in the American horseshoe crab, *Limulus polyphemus*: A potential role in stabilization from proteolysis. *Biol. Bull.* **199**: 190–192.
- Atkins, M. S., A. G. McArthur, and A. P. Teske. 2000. *Ancyromonadida*: A new phylogenetic lineage among the protozoa closely related to the common ancestor of metazoans, fungi, and choanoflagellates (Opisthokonta). *J. Mol. Evol.* **51**: 278–285.
- Basil, J. A., R. T. Hanlon, S. I. Sheikh, and J. Atema. 2000. Three-dimensional odor tracking by *Nautilus pompilius*. *J. Exp. Biol.* **203**(9): 1409–1414.
- Bearer, E. L., X. O. Breakefield, D. Schuback, T. S. Reese, and J. H. LaVail. 2000. Retrograde axonal transport of herpes simplex virus: Evidence for a single mechanism and a role for tegument. *Proc. Natl. Acad. Sci. USA* **97**(14): 8146–8150.
- Begley, G. S., B. C. Furie, E. Czerwicz, K. L. Taylor, G. L. Furie, L. Bronstein, J. Stenflo, and B. Furie. 2000. A conserved motif within the vitamin K-dependent carboxylase gene is widely distributed across animal phyla. *J. Biol. Chem.* **275**: 36245–36249.
- Bittner, G. D., and H. M. Fishman. 2000. Axonal sealing following injury. Pp. 337–370 in *Nerve Regeneration*, N. Ingoglia and M. Murray, eds. Marcel Dekker, New York.
- Blazquez, P., A. Partsalis, N. Gerrits, and S. M. Highstein. 2000. Input of the anterior and posterior semicircular canals via interneurons carrying head velocity information to the dorsal Y group of the vestibular nuclei. *J. Neurophysiol.* **83**: 2891–2904.
- Boal, J. G., A. W. Dunham, K. T. Williams, and R. T. Hanlon. 2000. Experimental evidence for spatial learning in octopuses (*Octopus bimaculoides*). *J. Comp. Psychol.* **114**(3): 246–252.
- Böse, C. M., D. Qiu, A. Bergamaschi, B. Gravante, M. Bossi, A. Villa, F. Rupp, and A. Malgaroli. 2000. Agrin controls synaptic differentiation in hippocampal neurons. *J. Neurosci.* **20**: 9086–9095.
- Bouzat, J. L., L. K. McNeil, H. M. Robertson, L. F. Solter, J. Nixon, J. E. Beever, H. R. Gaskins, G. Olsen, S. Subramaniam, M. L. Sogin, and H. A. Lewin. 2000. Phylogenomic analysis of a proteasome gene family from early-diverging eukaryotes. *J. Mol. Evol.* **51**: 532–543.
- Breton, S., N. N. Nsumu, T. Galli, I. Sabolic, P. J. S. Smith, and D. Brown. 2000. Tetanus toxin-mediated cleavage of cellubrevin inhibits proton secretion in the male reproductive tract. *Am. J. Physiol. Renal Physiol.* **278**: F717–725.
- Brothers, C., E. Marks, and R. Smolowitz. 2000. Conditions affecting growth and zoosporulation of protistan parasite QPX in culture. *Biol. Bull.* **199**: 200–201.
- Burgos, M. H., M. Goda, and S. Inoué. 2000. Fertilization-induced changes in the fine structure of stratified *Arbacia* eggs. II. Observations with electron microscopy. *Biol. Bull.* **199**: 213–214.
- Bush, M. B., M. C. Miller, P. E. De Oliveira, and P. A. Colinvaux. 2000. Two histories of environmental change and human disturbance in eastern lowland Amazonia. *The Holocene* **10**: 543–554.
- Buzby, K. M., and L. A. Deegan. 2000. Inter-annual fidelity to summer feeding sites in Arctic grayling. *Environ. Biol. Fishes* **59**: 319–327.
- Buzby, K. M., and S. A. Perry. 2000. Modeling the potential effects of climate change on leaf pack processing in central Appalachian streams. *Can. J. Fish. Aquat. Sci.* **57**: 1773–1783.
- Canadell, J. G., H. A. Mooney, D. D. Baldocchi, J. A. Berry, J. R. Ehleringer, C. B. Field, S. T. Gower, D. Y. Hollinger, J. E. Hunt, R. B. Jackson, S. W. Running, G. R. Shaver, W. Steffen, S. E. Trumbore, R. Valentini, and B. Y. Bond. 2000. Carbon metabolism of the terrestrial biosphere: A multi-technique approach for improved understanding. *Ecosystems* **3**: 115–130.
- Chatterjee, A., D. M. Porterfield, P. J. S. Smith, and S. J. Roux. 2000. Gravity-directed calcium current in germinating spores of *Ceratopseris richardii*. *Planta* **210**: 607–610.
- Chikarmane, H. M., A. M. Kuzirian, R. Kozłowski, M. Kuzirian, and T. Lee. 2000. Population genetic structure of the goosefish, *Lophius americanus*. *Biol. Bull.* **199**: 227–228.
- Clark, M. A., N. A. Moran, P. Baumann, and J. J. Wernegreen. 2000.

- Cospeciation between bacterial endosymbionts (*Buchnera*) and a recent radiation of aphids (*Uroleucon*) and pitfalls of testing for phylogenetic congruence. *Evolution* **54**: 517–525.
- Clay, J. R., and A. M. Kuzirian. 2000. Localization of voltage-gated K^+ channels in squid giant axons. *J. Neurobiol.* **45**: 172–184.
- Clein, J. S., B. L. Kwiatkowski, A. D. McGuire, J. E. Hobbie, E. B. Rastetter, J. M. Melillo, and D. W. Kicklighter. 2000. Modeling carbon responses of tundra ecosystems to historical and project climate: A comparison of a plot- and a global-scale ecosystem model to identify process-based uncertainties. *Global Change Biol.* **6**(Suppl. 1): 127–140.
- Colinvaux, P. A., and P. E. De Oliveira. 2000. Paleocology and climate of the Amazon basin during the last glacial cycle. *J. Quat. Sci.* **15**: 347–356.
- Colinvaux, P. A., P. E. De Oliveira, and M. B. Bush. 2000. Amazon and neotropical plant communities on glacial time scales: The failure of the aridity and refuge hypotheses. *Quat. Sci. Rev.* **19**: 141–169.
- Creton, R., J. A. Kreiling, and L. F. Jaffe. 2000. Presence and roles of calcium gradients along the dorsal-ventral axis in *Drosophila* embryos. *Dev. Biol.* **217**: 375–385.
- Crump, B. C., and J. A. Baross. 2000. Archaeaplankton in the Columbia River, its estuary and the adjacent coastal ocean, USA. *FEMS Microbiol. Ecol.* **31**: 231–239.
- Danuser, G., and R. Oldenbourg. 2000. Probing f-actin flow by tracking shape fluctuations of radial bundles in lamellipodia of motile cells. *Biophys. J.* **79**: 191–201.
- Danuser, G., P. T. Tran, and E. D. Salmon. 2000. Tracking differential interference contrast diffraction line images with nanometer sensitivity. *J. Microsc.* **198**(1): 34–53.
- Deegan, L. A., J. E. Hughes, and R. A. Rountree. 2000. Salt marsh ecosystem support of marine transient species. Pp. 333–365 in *Concepts and Controversies in Tidal Marsh Ecology*. M. P. Weinstein and D. A. Kreeger, eds. Kluwer Academic, Boston, MA. 864 pp.
- Delgado-Viscogliosi, P., E. Viscogliosi, D. Gerbod, J. Kulda, M. L. Sogin, and V. P. Edgcomb. 2000. Molecular phylogeny of parabasalids based on small subunit rRNA sequences, with emphasis on the Trichomonadinae subfamily. *J. Eukaryot. Microbiol.* **47**: 70–75.
- Detrait, E., C. S. Eddleman, S. M. Yoo, M. Fukuda, M. P. Nguyen, G. D. Bittner, and H. M. Fishman. 2000. Axolemmal repair requires proteins that mediate synaptic vesicle fusion. *J. Neurobiol.* **44**: 382–391.
- Detrait, E. R., S. Yoo, C. S. Eddleman, M. Fukuda, G. D. Bittner, and H. M. Fishman. 2000. Plasmalemmal repair of severed neurites of PC12 cells requires Ca^{2+} and synaptotagmin. *J. Neurosci. Res.* **62**: 566–573.
- De Weer, P., D. C. Gadsby, and R. F. Rakowski. 2000. The Na/K-ATPase: A current-generating enzyme. Pp. 27–34 in *Na/K ATPase and Related ATPases*, K. Taniguchi and S. Kaya, eds. Excerpta Medica International Congress Series 1207. Elsevier, Amsterdam.
- DiPolo, R., G. Berberian, and L. Beaugé. 2000. In squid nerves intracellular Mg^{2+} promotes deactivation of the ATP-upregulated Na^+/Ca^{2+} exchanger. *Am. J. Physiol. Cell Physiol.* **279**: C1631–C1639.
- Dosemeci, A., T. S. Reese, J. Petersen, and J-H. Tao-Cheng. 2000. A novel particulate form of $Ca^{2+}/CaMKII$ -dependent protein kinase II in neurons. *J. Neurosci.* **20**: 3076–3084.
- Doussau, F., and G. J. Augustine. 2000. The actin cytoskeleton and neurotransmitter release: An overview. *Biochimie* **82**: 353–363.
- Eddleman, C. S., G. D. Bittner, and H. M. Fishman. 2000. Barrier permeability at cut axonal ends progressively decreases until an ionic seal is formed. *Biophys. J.* **79**: 1883–1890.
- Epstein, D. A., H. T. Epstein, F. M. Child, and A. M. Kuzirian. 2000. Memory consolidation in *Hermisenda crassicornis*. *Biol. Bull.* **199**: 182–183.
- Fadool, D. A., K. Tucker, J. J. Phillips, and J. A. Simmen. 2000. Brain insulin receptor causes activity-dependent current suppression in the olfactory bulb through multiple phosphorylation of Kv1.3. *J. Neurophysiol.* **83**: 2332–2348.
- Filoso, S., and M. R. Williams. 2000. The hydrochemical influence of the Branco River on the Negro River and Anavilhanas archipelago, Amazonas, Brazil. *Arch. Hydrobiol.* **148**: 563–585.
- Fisher, T. R., D. Correll, R. Costanza, J. T. Hollibaugh, C. S. Hopkinson, Jr., R. W. Howarth, N. N. Rabalais, J. E. Richey, C. J. Vörösmarty, and R. Wiegert. 2000. Synthesizing drainage basin inputs to coastal systems. Pp. 81–105 in *Estuarine Science: A Synthetic Approach to Research and Practice*, J. Hobbie, ed. Island Press, Washington, D.C.
- Förster, H., M. P. Cummings, and M. D. Coffey. 2000. Phylogenetic relationships of *Phytophthora* species based on ribosomal ITS 1 DNA sequence analysis with emphasis on Waterhouse groups V and VI. *Mycol. Res.* **104**: 1055–1061.
- Fukui, Y., T. Q. P. Uyeda, C. Kitayama, and S. Inoué. 2000. How well can an amoeba climb? *Proc. Natl. Acad. Sci. USA* **97**: 10020–10025.
- Funk, D. J., L. Helbling, J. J. Wernegreen, and N. A. Moran. 2000. Perfect evolutionary congruence among multiple symbiont genomes in an aphid species. *Proc. R. Soc. Lond. B* **657**: 2517–2521.
- Garcia-Montiel, D., C. Neill, J. M. Melillo, S. M. Thomas, P. A. Stuedler, and C. C. Cerri. 2000. Soil phosphorus transformations after forest clearing for pasture in the Brazilian Amazon. *Soil Sci. Soc. Am. J.* **64**: 1792–1804.
- García-Verela, M., G. Pérez-Ponce de León, P. de la Torre, M. P. Cummings, S. S. S. Sarma, and J. P. Lacleste. 2000. Phylogenetic analysis of *Acanthocephala* based on 18S ribosomal gene sequences. *J. Mol. Evol.* **50**: 532–540.
- Gerbod, D., V. P. Edgcomb, C. Noël, P. Delgado-Viscogliosi, and E. Viscogliosi. 2000. Phylogenetic position of parabasalid symbionts from the termite *Kaloterms flavicollis* based on small subunit rRNA sequences. *Int. Microbiol.* **3**: 165–172.
- Gleeson, R. A., K. Hammar, and P. J. S. Smith. 2000. Sustaining olfaction at low salinities: Mapping ion flux associated with the olfactory sensilla of the blue crab *Callinectes sapidus*. *J. Exp. Biol.* **203**: 3145–3152.
- Gleeson, R. A., L. M. McDowell, H. C. Aldrich, K. Hammar, and P. J. S. Smith. 2000. Sustaining olfaction at low salinities: Evidence for a paracellular route of ion movement from the hemolymph to the sensillar lymph in the olfactory sensillar of the blue crab. *Callinectes sapidus*. *Cell Tissue Res.* **301**: 423–431.
- Goda, M., M. H. Burgos, and S. Inoué. 2000. Fertilization-induced changes in the fine structure of stratified *Arbacia* eggs. I. Observations on live cells with the centrifuge polarizing microscope. *Biol. Bull.* **199**: 212–213.
- Gough, L., G. R. Shaver, J. Carroll, D. Royer, and J. A. Laundre. 2000. Vascular plant species richness in Alaskan arctic tundra: The importance of soil pH. *J. Ecol.* **88**: 54–66.
- Gould, R. M., C. M. Freund, J. Engler, and H. G. Morrison. 2000. Optimization of homogenization conditions used to isolate mRNAs in processes of myelinating oligodendrocytes. *Biol. Bull.* **199**: 215–217.
- Hanselmann, R., R. Smolowitz, and D. Gibson. 2000. Identification of proliferating cells in hard clams. *Biol. Bull.* **199**: 199–200.
- Harasewych, M. G., and A. G. McArthur. 2000. A molecular phylogeny of the Patellogastropoda (Mollusca: Gastropoda). *Mar. Biol.* **137**: 183–194.
- Harrington, J. M., and P. B. Armstrong. 2000. Initial characterization of a potential anti-fouling system in the American horseshoe crab, *Limulus polyphemus*. *Biol. Bull.* **199**: 189–190.
- Head, J. F., S. Inouye, K. Teranishi, and O. Shimomura. 2000. The crystal structure of the photoprotein aequorin at 2.3 Å resolution. *Nature* **405**: 372–376.
- Hendricks, J. J., J. D. Aber, K. J. Nadelhoffer, and R. D. Hallett. 2000.

- Nitrogen controls on fine root substrate quality in temperate forest ecosystems. *Ecosystems* **3**: 57–69.
- Henry, J. Q., M. Q. Martindale, and B. C. Boyer. 2000. The unique developmental program of the acoel flatworm *Neochildia fusca*. *Dev. Biol.* **220**: 285–295.
- Herak-Kramberger, C., I. Sabolic, M. Blanus, P. J. S. Smith, D. Brown, and S. Breton. 2000. Cadmium inhibits vacuolar H⁺ ATPase-mediated acidification in rat epididymis. *Biol. Reprod.* **63**: 599–606.
- Hobbie, E. A., S. A. Macko, and M. Williams. 2000. Correlations between foliar delta 15N and nitrogen concentrations may indicate plant-mycorrhizal interactions. *Oecologia* **122**: 273–283.
- Hobbie, J. E., ed. 2000. *Estuarine Science: A Synthetic Approach to Research and Practice*. Island Press, Washington, D.C. 539 pp.
- Holmes, R. M. 2000. The importance of ground water to stream ecosystem function. Pp. 137–148 in *Streams and Ground Waters*, J. B. Jones and P. J. Mulholland, eds. Academic Press, San Diego, CA.
- Holmes, R. M., B. J. Peterson, L. Deegan, J. Hughes, and B. Fry. 2000. Nitrogen biogeochemistry in the oligohaline zone of a New England estuary. *Ecology* **81**: 416–432.
- Holmes, R. M., B. J. Peterson, V. V. Gordeev, A. V. Zhulidov, M. Meybeck, R. B. Lammers, and C. J. Vörösmarty. 2000. Flux of nutrients from Russian rivers to the Arctic Ocean: Can we establish a baseline against which to judge future changes? *Water Resources Res.* **36**: 2309–2320.
- Holmgren, M., J. Wagg, F. Bezanilla, R. F. Rakowski, P. De Weer, and D. C. Gadsby. 2000. Three distinct sequential steps in extracellular release of three Na⁺ ions by the Na,K-ATPase. *Nature* **403**: 898–901.
- Hughes, J. E., L. A. Deegan, B. J. Peterson, R. M. Holmes, and B. Fry. 2000. Nitrogen flow through the food web in the oligohaline zone of a New England estuary. *Ecology* **81**: 433–452.
- Inouye, S., K. Watanabe, H. Nakamura, and O. Shimomura. 2000. Secretional luciferase of the luminous shrimp *Oplophorus gracilirostris*: cDNA cloning of a novel imidazopyrazinone luciferase. *FEBS Lett.* **481**: 19–25.
- Jackson, R. B., H. J. Schenk, E. G. Jobbagy, J. Canadell, G. D. Colello, R. E. Dickinson, C. B. Field, P. Friedlingstein, M. Heimann, K. Hibbard, D. W. Kicklighter, A. Kleidon, R. P. Neilson, W. J. Parton, O. E. Sala, and M. T. Sykes. 2000. Belowground consequences of vegetation change and their treatment in models. *Ecol. Appl.* **10**: 470–483.
- Johnson, L. C., G. R. Shaver, D. H. Cades, E. Rastetter, K. Nadelhoffer, A. Giblin, J. Laundre, and A. Stanley. 2000. Plant carbon-nutrient interactions control CO₂ exchange in Alaskan wet sedge tundra ecosystems. *Ecology* **81**: 453–469.
- Jonasson, S., T. V. Callaghan, G. R. Shaver, and L. A. Nielsen. 2000. Arctic terrestrial ecosystems and ecosystem function. Pp. 275–313 in *The Arctic: Environment, People, Policy*, M. Nuttall and T. V. Callaghan, eds. Harwood Academic Publishers, Amsterdam.
- Jung, S.-K., K. Hammar, and P. J. S. Smith. 2000. Development of self-referencing oxygen microsensor and its application to single pancreatic HIT cells: Effects of adenylate cyclase activator forskolin on oxygen consumption. *Biol. Bull.* **199**: 197–198.
- Kalume, D. E., J. Stenflo, E. Czerwicz, B. Hambe, B. C. Furie, B. Furie, and P. Rnepstorff. 2000. Determination of the covalent structure of two conotoxins from *Conus textile* by MALDI-TOF and ESI MS. *J. Mass Spectrom.* **35**: 145–156.
- Kaplan, I. M., and H. Kite-Powell. 2000. Safety at sea and fisheries management: Fishermen's attitudes and the need for co-management. *Mar. Policy* **24**: 493–497.
- Kreiling, J. A., R. E. Stephens, A. M. Kuzirian, K. Jessen-Eller, and C. L. Reinisch. 2000. Polychlorinated biphenyls are selectively neurotoxic in the developing *Spisula solidissima* embryo. *J. Toxicol. Environ. Health A* **61**: 101–119.
- Kremer, J. N., W. M. Kemp, A. E. Giblin, I. Valiela, S. P. Seitzinger, and E. E. Hofmann. 2000. Linking biogeochemical processes to higher trophic levels. Pp. 299–341 in *Estuarine Science: A Synthetic Approach to Research and Practice*, J. Hobbie, ed. Island Press, Washington, D.C.
- Kuhns, W. J., M. M. Burger, M. Sarkar, X. Fernandez-Busquets, and T. Simpson. 2000. Enzymatic biosynthesis of N-linked glycan by the marine sponge *Microciona prolifera*. *Biol. Bull.* **199**: 192–194.
- Kuner, T., and G. J. Augustine. 2000. A genetically encoded ratiometric indicator for chloride: Capturing chloride transients in cultured hippocampal neurons. *Neuron* **27**: 447–459.
- Lam, Y.-w., L. B. Cohen, M. Wachowiak, and M. R. Zochowski. 2000. Odors elicit three different oscillations in the turtle olfactory bulb. *J. Neurosci.* **20**: 749–762.
- Landowne, D. 2000. Heavy water (D₂O) alters the sodium channel gating current in squid giant axons. *Biol. Bull.* **199**: 164–165.
- Langford, G. M. 2000. Video-enhanced microscopy for analysis of cytoskeleton structure and function. Pp. 31–43 in *Methods in Molecular Biology, Vol. 161: Cytoskeleton Methods and Protocols*, Ray H. Gavin, ed. Humana Press, Totowa, NJ.
- Lichstein, J. W., M. L. Ballinger, A. R. Blanchette, H. M. Fishman, and G. D. Bittner. 2000. Structural changes at cut ends of earthworm giant axons in the interval between dye barrier formation and neuritic outgrowth. *J. Comp. Neurol.* **416**: 143–157.
- Liu, L., R. Oldenbourg, J. R. Trimarchi, and D. L. Keefe. 2000. A reliable, noninvasive technique for spindle imaging and enucleation of mammalian oocytes. *Nature Biotechnol.* **18**: 223–225.
- Liu, L., J. R. Trimarchi, and D. L. Keefe. 2000. Involvement of mitochondria in oxidative stress-induced cell death in mouse zygotes. *Biol. Reprod.* **62**: 1745–1753.
- Liu, L., J. R. Trimarchi, R. Oldenbourg, and D. L. Keefe. 2000. Increased birefringence in the meiotic spindle provides a new marker for the onset of activation in living oocytes. *Biol. Reprod.* **63**: 251–258.
- MacKenzie, R., D. Newman, M. M. Burger, R. Roy, and W. J. Kuhns. 2000. Adhesion of a viral envelope protein to a non-self-binding domain of the aggregation factor in the marine sponge *Microciona prolifera*. *Biol. Bull.* **199**: 209–211.
- Magill, A. H., J. D. Aber, G. M. Berntson, W. H. McDowell, K. J. Nadelhoffer, J. M. Melillo, and P. Steudler. 2000. Long-term additions and nitrogen saturation in two temperate forests. *Ecosystems* **3**: 238–253.
- Mandile, P., S. Vescia, P. Montagnese, S. Piscopo, M. Cotugno, and A. Giuditta. 2000. Post-trial sleep sequences including transition sleep are involved in avoidance learning of adult rats. *Behav. Brain Res.* **112**: 23–31.
- Maxwell, M. R., and R. T. Hanlon. 2000. Female reproductive output in the squid *Loligo pealeii*: Multiple egg clutches and implications for a spawning strategy. *Mar. Ecol. Prog. Ser.* **199**: 159–170.
- Maxwell, M. R., K. M. Buresch, and R. T. Hanlon. 2000. Pattern of inheritance of microsatellite loci in the squid *Loligo pealeii* (Mollusca: Cephalopoda). *Mar. Biotechnol.* **2**: 517–521.
- McArthur, A. G., H. G. Morrison, J. E. J. Nixon, N. Q. E. Passama-neck, U. Kim, G. Hinkle, M. K. Crocker, M. E. Holder, R. Farr, C. J. Reich, G. J. Olsen, S. B. Aley, R. D. Adam, F. D. Gillin, and M. L. Sogin. 2000. The *Giardia* genome project database. *FEMS Microbiol. Lett.* **189**: 271–273.
- McCulloch, D. H., P. I. Ivinnet, D. Landowne, and E. L. Chambers. 2000. Calcium influx mediates the voltage-dependence of sperm entry into sea urchin eggs. *Dev. Biol.* **223**: 449–462.
- McGuire, A. D., J. M. Melillo, J. T. Randerson, W. J. Parton, M. Heimann, R. A. Meier, J. S. Clein, D. W. Kicklighter, and S. Sauf. 2000. Modeling the effects of snowpack on heterotrophic respiration across northern temperate and high latitude regions: Comparison with

- measurements of atmospheric carbon dioxide in high latitudes. *Biogeochemistry* **48**: 94–114.
- McGuire, A. D., J. S. Clein, J. M. Melillo, D. W. Kicklighter, R. A. Meier, C. J. Vörösmarty, and M. C. Serreze. 2000. Modelling carbon responses of tundra ecosystems to historical and projected climate: Sensitivity of pan-Arctic carbon storage to temporal and spatial variation in climate. *Global Change Biol.* **6**: 141–159.
- McNeil, P. L., S. S. Vogel, K. Miyake, and M. Terasaki. 2000. Patching plasma membrane disruptions with cytoplasmic membrane. *J. Cell Sci.* **113**: 1891–1902.
- Mensingher, A. F., D. J. Anderson, C. J. Buchko, M. A. Johnson, D. C. Martin, P. A. Tresco, R. B. Silver, and S. M. Highstein. 2000. Chronic recording of regenerating VIIIth nerve axons with a sieve electrode. *J. Neurophysiol.* **83**(1): 611–615.
- Messerli, M. A., R. Creton, L. F. Jaffe, and K. R. Robinson. 2000. Periodic increases in elongation rate precede periodic increases in cytosolic Ca^{2+} during tip growth of *Lilium longiflorum* pollen tubes. *Dev. Biol.* **222**: 84–98.
- Molina, A. J. A., P. J. S. Smith, and R. P. Malchow. 2000. Hydrogen ion fluxes from isolated retinal horizontal cells: Modulation by glutamate. *Biol. Bull.* **199**: 168–170.
- Molyneux, B. J., M. K. Mulcahey, P. Stafford, and G. M. Langford. 2000. Sequence and phylogenetic analysis of squid myosin V: a vesicle motor in nerve cells. *Cell Motil. Cytoskeleton* **46**: 108–115.
- Moran, N. A., and J. J. Wernegreen. 2000. Are mutualism and parasitism irreversible evolutionary alternatives for endosymbiotic bacteria? Insights from molecular phylogenetics and genomics. *Trends Ecol. Evol.* **15**: 321–326.
- Morgan, J. R., K. Prasad, W. Hao, G. J. Augustine, and E. Lafer. 2000. A conserved clathrin assembly motif essential for synaptic vesicle endocytosis. *J. Neurosci.* **20**: 8667–8676.
- Mulholland, P. J., J. L. Tank, D. M. Sanzone, W. M. Wollheim, B. J. Peterson, J. R. Webster, and J. L. Meyer. 2000. Food resources of stream macroinvertebrates determined by natural-abundance stable C and N isotopes and a super (15)N tracer addition. *J. North Am. Benthol. Soc.* **19**(1): 145–157.
- Nadelhoffer, K. J. 2000. The potential effects of nitrogen deposition on fine root production in forest ecosystems. *New Phytol.* **137**: 131–139.
- Nadelhoffer, K. J., R. D. Bowden, R. D. Boone, and K. Lajtha. 2000. Controls on forest soil organic matter development and dynamics: Chronic litter manipulation as a potential international LTER activity. Pp. 3–9 in *Cooperation in Long Term Ecological Research in Central and Eastern Europe: Proceedings of the ILTER Regional Workshop*, 22–25 June, Budapest, Hungary. K. Lajtha and K. Vanderbilt, eds. Oregon State University, Corvallis, OR.
- Neill, C., and E. A. Davidson. 2000. Soil carbon accumulation or loss following deforestation for pasture in the Brazilian Amazon. Pp. 197–211 in *Global Climate Change and Tropical Ecosystems*, R. Lal, J. M. Kimble, and B. A. Stewart, eds. CRC Press, New York.
- Ng, W. V., P. Liang, M. Riley, L. Hood, and S. DasSarma. 2000. Genome sequence of *Halobacterium* species NRC-1. *Proc. Natl. Acad. Sci. USA* **97**: 12176–12181.
- Ogunseitan, O. A., S. Yang, and J. Ericson. 2000. Microbial delta-aminolevulinic acid dehydratase as a biosensor for lead (Pb) bioavailability in contaminated environments. *Soil Biol. Biochem.* **32**: 1899–1906.
- Ohara, P. T., M. S. Chin, and J. H. LaVail. 2000. The spread of herpes simplex virus type 1 from trigeminal neurons to the murine cornea: an immunoelectron microscopy study. *J. Virol.* **74**(10): 4776–4786.
- Oldenbourg, R., and P. Török. 2000. Point spread functions of a polarizing microscope equipped with high numerical aperture lenses. *Appl. Optics* **39**: 6325–6331.
- Oldenbourg, R., K. Katoh, and G. Danuser. 2000. Mechanism of lateral movement of filopodia and radial actin bundles across neuronal growth cones. *Biophys. J.* **78**: 1176–1182.
- Palazzo, R. E., and B. J. Schnackenberg. 2000. Centrosome maturation. *Curr. Top. Dev. Biol.* **49**: 449–470.
- Pan, Y., J. M. Melillo, D. W. Kicklighter, X. Xiao, and A. D. McGuire. 2000. Modeling structural and functional responses of terrestrial ecosystems in China to changes in climate and atmospheric CO_2 . *Acta Phytocol. Sinica* **24**(4): 513–526.
- Pollock, D. D., J. A. Eisen, N. A. Doggett, and M. P. Cummings. 2000. A case for evolutionary genomics and the comprehensive examination of sequence biodiversity. *Mol. Biol. Evol.* **17**: 1776–1788.
- Porterfield, D. M., and P. J. S. Smith. 2000. Single-cell, real-time measurements of extracellular oxygen and proton fluxes from *Spirogyra grevilleana*. *Protoplasma* **212**: 80–88.
- Porterfield, D. M., R. F. Corkey, R. H. Sanger, K. Tornheim, P. J. S. Smith, and B. E. Corkey. 2000. Oxygen consumption oscillates in single clonal pancreatic beta-cells (HIT). *Diabetes* **49**: 1511–1516.
- Prahlad, V., B. T. Helfand, G. M. Langford, R. D. Vale, and R. D. Goldman. 2000. Fast transport of neurofilament protein along microtubules in squid axoplasm. *J. Cell Sci.* **113**: 3939–3946.
- Raymond, P. A., and J. E. Bauer. 2000. Bacterial consumption of DOC during transport through a temperate estuary. *Aquat. Microb. Ecol.* **22**: 1–12.
- Raymond, P. A., J. E. Bauer, and J. J. Cole. 2000. Atmospheric CO_2 evasion, dissolved inorganic carbon production, and net heterotrophy in the York River estuary. *Limnol. Oceanogr.* **45**: 1707–1717.
- Riley, M., and M. Serres. 2000. *Escherichia coli*. In *The Prokaryotes: An Evolving Electronic Resource for the Microbiological Community*. [Online]. Springer-Verlag, New York. Available: <http://www.prokaryotes.com>.
- Riley, M., and M. Serres. 2000. Interim report on genomics of *E. coli*. *Annu. Rev. Microbiol.* **54**: 341–411.
- Sagar, S., B. Pazdur, E. Indyk, and R. F. Rakowski. 2000. The beta subunit of the Na^+, K^+ -ATPase in *Xenopus laevis*. Pp. 261–264 in *Na/K ATPase and Related ATPases*, K. Taniguchi and S. Kaya, eds. Excerpta Medica International Congress Series 1207. Elsevier, Amsterdam.
- Sandberg, L., P. Stafford, and G. M. Langford. 2000. Effects of myosin-II antibody on actin-dependent vesicle transport in extracts of clam oocytes. *Biol. Bull.* **199**: 202–203.
- Schimmel, D., J. Melillo, H. Tian, A. D. McGuire, D. Kicklighter, T. Kittel, N. Rosenbloom, S. Running, P. Thorton, D. Ojima, W. Parton, R. Kelly, M. Sykes, R. Neilson, and B. Rizzo. 2000. Contribution of increasing CO_2 and climate to carbon storage by ecosystems in the United States. *Science* **287**: 2004–2006.
- Schmidt, I. K., L. Ruess, E. Bááth, A. Michelsen, F. Ekelund, and S. Jonasson. 2000. Long-term manipulation of the microbes and microfauna of two subarctic heaths by addition of fungicide, bactericide, carbon and fertilizer. *Soil Biol. Biochem.* **32**: 707–720.
- Schmolesky, M. T., Y.-C. Wang, D. J. Creel, and A. G. Leventhal. 2000. Abnormal retinotopic organization of the dorsal lateral geniculate nucleus of the tyrosinase negative albino cat. *J. Comp. Neurol.* **427**: 209–219.
- Schmolesky, M. T., Y.-C. Wang, M. Pu, and A. G. Leventhal. 2000. Degradation of stimulus selectivity of visual cortical cells in senescent rhesus monkeys. *Nat. Neurosci.* **3**(4): 384–390.
- Schnackenberg, B. J., D. R. Hull, R. D. Balczon, and R. E. Palazzo. 2000. Reconstitution of microtubule nucleation potential in centrosomes isolated from *Spisula solidissima* oocytes. *J. Cell Sci.* **113**: 943–953.
- Serikawa, K. A., D. M. Porterfield, P. J. S. Smith, and D. F. Mandoli. 2000. Calcification and measurements of net proton and oxygen flux reveal subcellular domains in *Acetabularia acetabulum*. *Planta* **211**(4): 474–483.
- Shashar, N., R. Hagan, J. G. Boal, and R. T. Hanlon. 2000. Cuttlefish

- use polarization sensitivity in predation on silvery fish. *Vision Res.* **40**(1): 71–75.
- Shaver, G. R., J. Canadell, F. S. Chapin, III, J. Gurevitch, J. Harte, G. Henry, P. Ineson, S. Jonasson, J. Melillo, L. Pitelka, and L. Rustad. 2000. Global warming and terrestrial ecosystems: a conceptual framework for analysis. *BioScience* **50**: 871–882.
- Shimomura, O., and K. Teranishi. 2000. Light-emitters involved in the luminescence of coelenterazine. *Luminescence* **15**: 51–58.
- Simenstad, C., S. Brandt, A. Chalmers, R. Dame, L. Deegan, R. Hodson, and E. Houde. 2000. Habitat-biotic interactions. Pp. 427–455 in *Estuarine Science: A Synthetic Approach to Research and Practice*, J. Hobbie, ed. Island Press, Washington, D.C.
- Stafford, P., J. Brown, and G. M. Langford. 2000. Interaction of actin- and microtubule-based motors in squid axoplasm probed with antibodies to myosin V and kinesin. *Biol. Bull.* **199**: 203–205.
- Stieglitz, M., A. Giblin, J. Hobbie, M. Williams, and G. Kling. 2000. Simulating the effects of climate change and climate variability on carbon dynamics in Arctic tundra. *Global Biogeochem. Cycles* **14**(Part 4): 1123–1136.
- Suddith, A. W., E. A. Vaisberg, S. A. Kuznetsov, W. Steffen, C. L. Rieder, and R. E. Palazzo. 2000. Centriole duplication, centrosome maturation and spindle assembly in lysates of *Spisula solidissima* oocytes. Pp. 215–228 in *Methods in Molecular Biology*, Vol. 161: *Cytoskeleton Methods and Protocols*, R. Gavin, ed. Humana Press, Totowa, NJ.
- Swarnakar, S., R. Asnkan, J. P. Quigley, and P. B. Armstrong. 2000. Binding of alpha 2-macroglobulin and limulin: Regulation of the plasma hemolytic system of the American horseshoe crab, *Limulus*. *Biochem. J.* **347**: 679–685.
- Tank, J. L., J. L. Meyer, D. M. Sanzone, P. J. Mulholland, J. R. Webster, B. J. Peterson, W. M. Wollheim, and N. E. Leonard. 2000. Analysis of nitrogen cycling in a forest stream during autumn using a ¹⁵N-tracer addition. *Limnol. Oceanogr.* **45**(5): 1013–1029.
- Tian, H., J. M. Melillo, D. W. Kicklighter, A. D. McGuire, J. Helfrich, III, B. Moore, III, and C. J. Vörösmarty. 2000. Climatic and biotic controls on annual carbon storage in Amazonian ecosystems. *Global Ecol. Biogeography* **9**: 315–336.
- Trimarchi, J. R., L. Liu, D. M. Porterfield, P. J. S. Smith, and D. L. Keefe. 2000. A non-invasive method for measuring pre-implantation embryo physiology. *Zygote* **8**: 15–24.
- Trimarchi, J. R., L. Liu, D. M. Porterfield, P. J. S. Smith, and D. L. Keefe. 2000. Oxidative phosphorylation-dependent and -independent oxygen consumption by individual preimplantation mouse embryos. *Biol. Reprod.* **62**: 1866–1874.
- Trimarchi, J. R., L. Liu, P. J. S. Smith, and D. L. Keefe. 2000. Non-invasive measurement of potassium efflux as an early indicator of cell death in mouse embryos. *Biol. Reprod.* **63**: 851–857.
- Vallinn, J. J. 2000. Improving marine ecosystem models: Use of data assimilation and mesocosm experiments. *J. Mar. Res.* **58**: 117–164.
- Vallino, J. J., and G. Stephanopoulos. 2000. Metabolic flux distributions in *Corynebacterium glutamicum* during growth and lysine overproduction. *Biotechnol. Bioeng.* **67**: 872–885.
- Vinade, L., and A. Dosemeci. 2000. Regulation of the phosphorylation state of the AMPA receptor GluR1 subunit in the postsynaptic density. *Cell Mol. Neurobiol.* **20**: 451–463.
- Vincent, W. F., and J. E. Hobbie. 2000. Ecology of Arctic lakes and rivers. Pp. 197–232 in *The Arctic: Environment, People, Policies*, M. Nuttall and T. V. Callaghan, eds. Harwood Academic Publishers, Amsterdam.
- Vörösmarty, C. J., and B. J. Peterson. 2000. Macro-scale models of water and nutrient flux to the coastal zone. Pp. 43–79 in *Estuarine Science: A Synthetic Approach to Research and Practice*, J. Hobbie, ed. Island Press, Washington, D.C.
- Wachowiak, M., M. Zochowski, L. B. Cohen, and C. X. Falk. 2000. The spatial representation of odors by olfactory receptor neuron input to the olfactory bulb is concentration invariant. *Biol. Bull.* **199**: 162–163.
- Werngreen, J. J., and N. A. Moran. 2000. Decay of mutualistic potential in aphid endosymbionts through silencing of biosynthetic loci: *Buchnera* of *Diuraphis*. *Proc. R. Soc. Lond. B* **267**: 1423–1431.
- Werngreen, J. J., H. Ochman, I. B. Jones, and N. A. Moran. 2000. The decoupling of genome size and sequence divergence in a symbiotic bacterium. *J. Bacteriol.* **182**: 3867–3869.
- White, T. W., H. Ripps, M. Srinivas, and R. Bruzzone. 2000. Voltage gating properties of channels formed by a skate retinal connexin. *Biol. Bull.* **199**: 165–168.
- Williams, M., W. Eugster, E. B. Rastetter, J. P. McFadden, and F. S. Chapin, III. 2000. The controls on net ecosystem productivity along an arctic transect: A model comparison with flux measurements. *Global Change Biol.* **6**(Suppl. 1): 116–126.
- Wollmuth, L. P., T. Kuner, C. Jatzke, P. H. Seeburg, N. Heintz, and J. Zuo. 2000. The Lurcher mutation identifies $\delta 2$ as an AMPA/kainate receptor-like channel that is potentiated by Ca^{2+} . *J. Neurosci.* **20**: 5973–5980.
- Wu, G., A. G. McArthur, A. Fiser, A. Sali, M. L. Sogin, and M. Muller. 2000. Core histones of the amitochondriate protist *Giardia lamblia*. *Mol. Biol. Evol.* **17**: 1156–1163.
- Zochowski, M., L. B. Cohen, G. Fuhrmann, and D. Kleinfeld. 2000. Distributed and partially separate pools of neurons are correlated with two different components of the gill withdrawal reflex in *Aplysia*. *J. Neurosci.* **20**: 8485–8492.
- Zottoli, S. J., and D. S. Faber. 2000. The Mauthner cell: What has it taught us? *The Neuroscientist* **6**: 25–37.





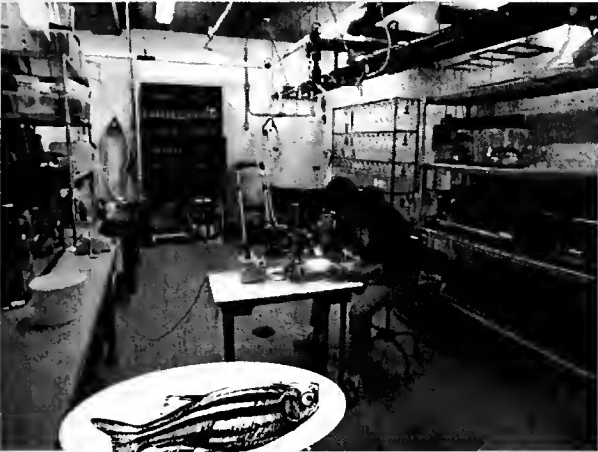
MARINE RESOURCES CENTER

MARINE BIOLOGICAL LABORATORY • WOODS HOLE, MA 02543 • (508)289-7700

WWW.MBL.EDU/SERVICES/MRC/INDEX.HTML

Animal and Tissue Supply for Education & Research

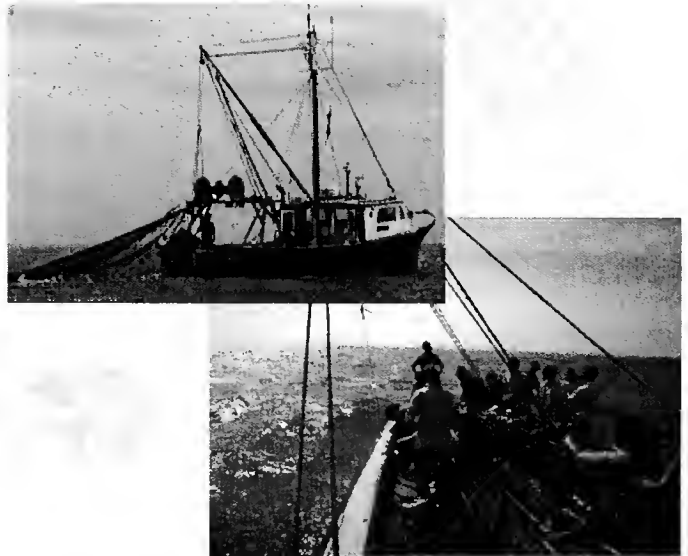
- 150 aquatic species available for shipment via online catalog: <<http://www.mbl.edu/animals/index.html>>; phone: (508)289-7375; or e-mail: specimens@mbl.edu
- zebrafish colony containing limited mutant strains
- custom dissection and furnishing of specific organ and tissue samples



zebrafish facilities

MRC Services Available

- basic water quality analysis
- veterinary services (clinical, histopathologic, microbial services, health certificates, etc.)
- aquatic systems design (mechanical, biological, engineering, etc.)
- educational tours and collecting trips aboard the R/V Gemma

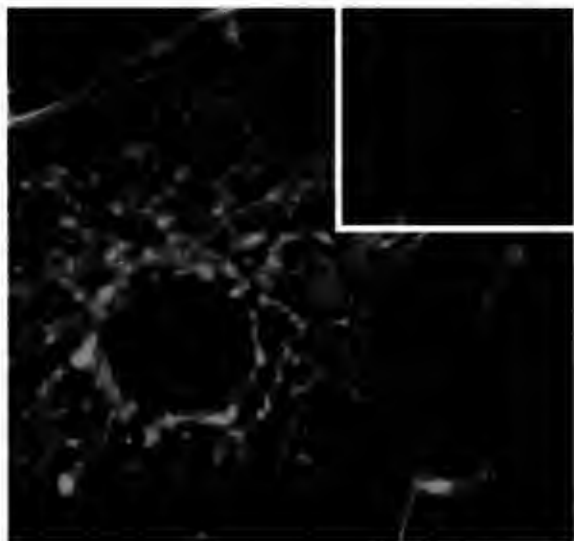


Using the MRC for Your Research

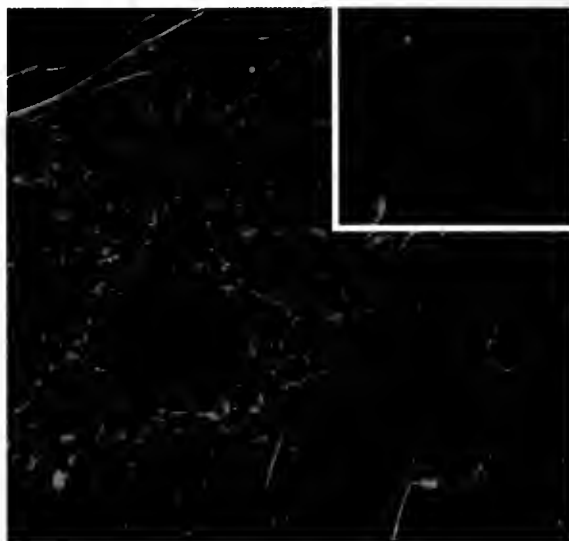
- capability for advanced animal husbandry (temperature, light control, etc.)
- availability of year-round, developmental life stages
- adaptability of tank system design for live marine animal experimentation



The Ultimate Deconvolution Machine.



Original Widefield Image.



*Iterative DCV (measured PSF);
Maximum Likelihood; 15 CG Iterations; Regularized.*

When image quality is essential and capturing lost information is a must, Carl Zeiss 3D Deconvolution system is the answer.

Our fast, intuitive software allows reassignment of non-focal haze, noise and blur to provide image restoration to its brilliant best. Choose between theoretically calculated or measured PSF, iterative or non-iterative method, and the Zeiss 3D Deconvolution will do the rest.

Whether conventional widefield or confocal fluorescence imaging, your own 3D deconvolution system from Zeiss takes you to new heights of image fidelity.

Let us show you how!

For immediate demonstration, call **800-233-2343**.

Carl Zeiss, Inc.
Microscopy & Imaging Systems
One Zeiss Drive
Thornwood, NY 10594

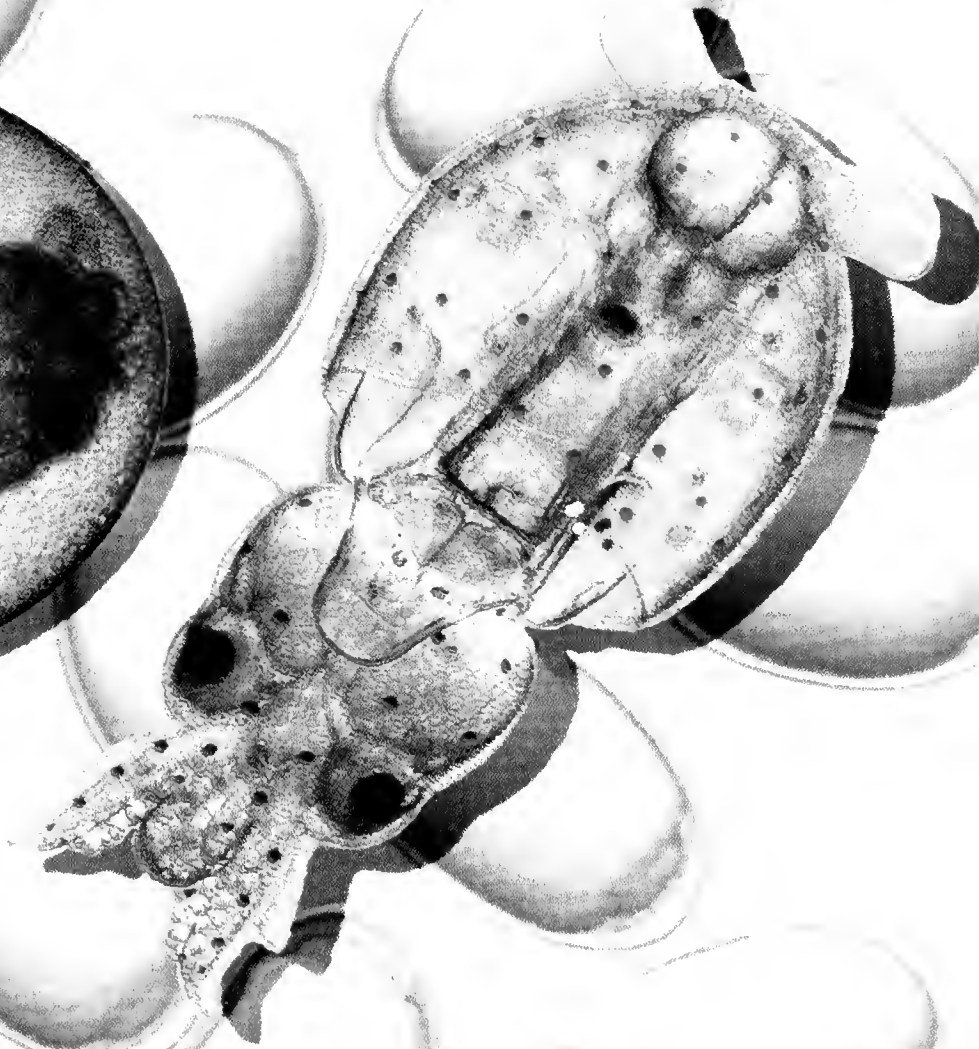
800.233.2343
Fax 914.681.7446
micro@zeiss.com
www.zeiss.com/micro



Volume 201

Number 2

THE BIOLOGICAL BULLETIN



OCTOBER 2001

Published by the Marine Biological Laboratory

<http://www.biolbull.org>





THE BIOLOGICAL BULLETIN ONLINE

The Marine Biological Laboratory is pleased to announce that the full text of *The Biological Bulletin* is available online at

<http://www.biolbull.org>

The Biological Bulletin publishes outstanding experimental research on the full range of biological topics and organisms, from the fields of Neurobiology, Behavior, Physiology, Ecology, Evolution, Development and Reproduction, Cell Biology, Biomechanics, Symbiosis, and Systematics.

Published since 1897 by the Marine Biological Laboratory (MBL) in Woods Hole, Massachusetts, *The Biological Bulletin* is one of America's oldest peer-reviewed scientific journals.

The journal is aimed at a general readership, and especially invites articles about those novel phenomena and contexts characteristic of intersecting fields.

The Biological Bulletin Online contains the full content of each issue of the journal, including all figures and tables, beginning with the February 2001 issue (Volume 200, Number 1). The full text is searchable by keyword, and the cited references include hyperlinks to Medline. PDF files are available beginning in February 2000 (Volume 198,

Number 1), some abstracts are available beginning with the October 1976 issue (Volume 151, Number 2), and some Tables of Contents are online beginning with the October 1965 issue (Volume 129, Number 2).

Each issue will be placed online approximately on the date it is mailed to subscribers; therefore the online site will be available prior to receipt of your paper copy. Online readers may want to sign up for the eTOC (electronic Table of Contents) service, which will deliver each new issue's table of contents *via* e-mail. The web site also provides access to information about the journal (such as Instructions to Authors, the Editorial Board, and subscription information), as well as access to the Marine Biological Laboratory's web site and other publications.

There is currently a free trial period for access to *The Biological Bulletin*. Once the free trial period ends on January 31, 2002, individuals and institutions who are subscribers to the journal in print or are members of the Marine Biological Laboratory Corporation will be able to activate an online subscription. All other access (*e.g.*, to Abstracts, eTOCs, searching, Instructions to Authors) will remain freely available. Online access will be included in the print subscription price.

<http://www.biolbull.org>

Made to my exact specifications.



Here's how the BX2's modular design came through for me. First, the 8 position universal condenser offers the flexibility to choose from brightfield, darkfield and phase. Next, it's assortment of DIC prisms makes it possible to match the optical image shear to the specimen, achieving the optimal balance of contrast and resolution. Finally, the motorized nosepiece, Z-drive, condenser, illuminator and filter wheels are fully integrated through the user-friendly software package. So digital images can now be acquired, processed and analyzed faster than before. Now let's move on.

And yours. And y



Picture yourself sitting here, looking into your Olympus BX2 research microscope, your fluorescence requirements having been met. Specifically: The aspherical collector lens produces a fluorescence intensity that's twice as bright as others. The unique excitation balancers improve visualization of multiple labels. The six-position filter turret makes single and multiband imaging faster and simpler. And the rectangular field stop, another Olympus exclusive, protects the specimen by exposing only the precise area being imaged. With all this modularity and flexibility, my BX2 microscope is also your BX2 microscope.



Now modularity re
Olympus FLUOVIEW
laser scanning mic
5 imaging channels
intuitive operation
productivity is grea
the BX2 is the only
a Metal Matrix Con
static and thermal r
use of 3D microscop
time-lapse observat
high-end digital ima
resulting in a comp
confocal system. It
optimal solution.

BX²

Research Microscope Series

OLYMPUS
FOCUS ON LIFE

Visit us at www.olympus-america.com or call 1-800-455-6238.

Cover

The composite image on the cover shows, in the background, a scattering of ovoid embryos of the squid *Loligo pealeii*; each is encased in a chorionic membrane (about 25 μm thick all around; 45–50 μm at the micropyle, where sperm enter). The size of these early embryos is 1.6×1.0 mm, and they have been developing for about 24 hours since their fertilization. The mature eggs from which they developed were fertilized in a petri dish and, shortly thereafter, the egg cytoplasm streamed toward the animal pole and formed a clear lenticular cap called the blastodisc, which underwent meroblastic cleavage, as in birds. The blastodisc is clearly visible as a low, flat projection at the end of the embryo under the micropyle. Also shown on the cover, in the foreground, are two mature 21-day embryos, or hatchlings, one still in its chorion. In life, the hatchlings (in or out of the chorion) would be about the same size (2 mm); the chorion swells to accommodate the growing embryo. [The cover images were produced by Karen Crawford, St. Mary's College of Maryland.]

The embryos on the cover are unusual in that they were cultured *in vitro*; that is why they are all separate and clean. In nature, squid eggs are released from the female's oviduct in batches of about 180, packaged in elongated, jellylike capsules, or egg strings. Fertilization and development occur within the egg string, which is deposited, with those of other females, in a communal egg mass attached to a suitable benthic surface. The reproduction, reproductive behavior, and development of *Loligo pealeii* are set out, online, at <http://www.mbl.edu/publications/Loligo/squid>.

Embryos within egg strings are readily cultured; moreover, they can be snipped out of their matrix periodically and examined, providing a means of following and describing squid development. But

the development of embryos that are removed from the egg string soon fails, so the ability to manipulate an early embryo and then to culture it through to hatching is precluded. Thus, many methods of experimental and comparative embryology become difficult or impossible with squid: *e.g.*, the effect on later stages of manipulating earlier ones; classical chemical treatments that perturb axis formation; isolation of large numbers of specific stages of embryos for molecular analysis; and even time-lapse microscopy. The result is that squid embryos, being difficult to work with, have been neglected.

In the summer of 1984, at the General Scientific Meetings of the Marine Biological Laboratory, Karen Crawford (Klein) and Laurinda A. Jaffe described a method of fertilizing squid eggs *in vitro* and culturing them through organogenesis to chorionated hatchlings. Now, 17 years later and at the same venue, Crawford shows us that the embryos can be made to hatch on their own. More important, she reports (p. 251) that treatment of fertilized eggs of *Loligo pealeii* with colchicine, but not cytochalasin D, interferes with ooplasmic segregation and blastodisc formation, suggesting that microtubules participate in these processes—in contrast to the process as it is known in zebrafish.

This short report is signaling that squid embryogenesis is now accessible and may be applicable and informing to other aspects of physiology currently being studied with hatchlings or adult animals. Some of these aspects are represented in this issue: *e.g.*, neuronal development (J. P. H. Burbach *et al.*, p. 252); morphological and functional ontogeny of squid mantle (J. T. Thompson and W. M. Kier, p. 136; p. 154); polarization patterns in squid and cuttlefish skin (N. Shashar *et al.*, p. 267); vesicle transport in giant axon (J. R. Brown *et al.* [p. 240] and J. R. Clay and A. M. Kuzirian [p. 243]); and excitability (J. R. Clay and A. Shrier, p. 186).

THE BIOLOGICAL BULLETIN

OCTOBER 2001

Editor	MICHAEL J. GREENBERG	The Whitney Laboratory, University of Florida
Associate Editors	LOUIS E. BURNETT R. ANDREW CAMERON CHARLES D. DERBY MICHAEL LABARBERA	Grice Marine Biological Laboratory, College of Charleston California Institute of Technology Georgia State University University of Chicago
Section Editor	SHINYA INOUÉ, <i>Imaging and Microscopy</i>	Marine Biological Laboratory
Online Editors	JAMES A. BLAKE, <i>Keys to Marine Invertebrates of the Woods Hole Region</i> WILLIAM D. COHEN, <i>Marine Models Electronic Record and Compendia</i>	ENSR Marine & Coastal Center, Woods Hole Hunter College, City University of New York
Editorial Board	PETER B. ARMSTRONG ERNEST S. CHANG THOMAS H. DIETZ RICHARD B. EMILET DAVID EPEL GREGORY HINKLE MAKOTO KOBAYASHI ESTHER M. LEISE DONAL T. MANAHAN MARGARET MCFALL-NGAI MARK W. MILLER TATSUO MOTOKAWA YOSHITAKA NAGAHAMA SHERPY D. PAINTER J. HERBERT WAITE RICHARD K. ZIMMER	University of California, Davis Bodega Marine Lab., University of California, Davis Louisiana State University Oregon Institute of Marine Biology, Univ. of Oregon Hopkins Marine Station, Stanford University Cereon Genomics, Cambridge, Massachusetts Hiroshima University of Economics, Japan University of North Carolina Greensboro University of Southern California Kewalo Marine Laboratory, University of Hawaii Institute of Neurobiology, University of Puerto Rico Tokyo Institute of Technology, Japan National Institute for Basic Biology, Japan Marine Biomed. Inst., Univ. of Texas Medical Branch University of California, Santa Barbara University of California, Los Angeles
Editorial Office	PAMELA CLAPP HINKLE VICTORIA R. GIBSON CAROL SCHACHINGER WENDY CHILD	Managing Editor Staff Editor Editorial Associate Subscription & Advertising Secretary

Published by
MARINE BIOLOGICAL LABORATORY
WOODS HOLE, MASSACHUSETTS

OCT 30 2001

<http://www.biolbull.org>

Genomic Research Leaders Choose Microway® Scalable Clusters

Eos Biotechnology, Marine Biological Laboratory, Millennium Pharmaceuticals, Mount Sinai Medical School, NIH, Pfizer, and Rockefeller University All Choose Microway Custom Clusters and Workstations for Reliability, Superior Technical Support and Great Pricing.

- 1.4 GHz Dual Athlon, 1.7 GHz Pentium 4, or 1 GHz Dual Pentium III in 1U or 2U Clusters
- Dual Alpha 833 MHz Clusters and Towers
For maximum price/performance choose our Alpha 1U 833 MHz, 4 MB DDR Cache CS20, 4U UP2000+ or 4U 264DP RuggedRack™
- Myrinet, Gigabit Ethernet or Dolphin Wulffit High Speed Low Latency Interconnects
- RAID and Fibre Channel Storage Solutions



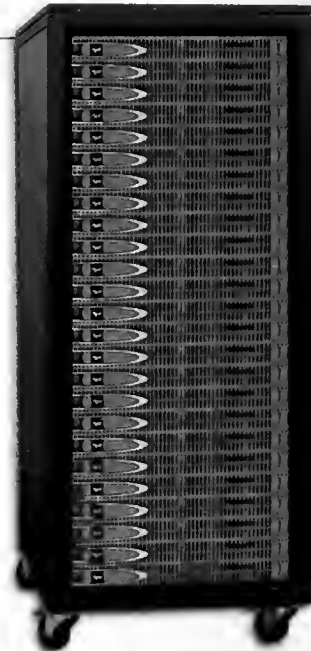
Microway® Screamer™
Dual Alpha UP2000+
833 MHz, 4MB Cache in
RuggedRack™ Chassis
with RRR™ Redundant
Power Supply

Microway has earned an excellent reputation since 1982. If you need a quality product that is fine tuned and built to last, from a company that will be around to support you for years to come, Microway is The Number One Choice.

Microway has delivered high-performance computing products since 1982, when our pioneering software made it possible to use an 8087 in the IBM-PC. In 1987 we created the world's first PC parallel processing systems. Since then, our QuadPuter™ architecture has migrated from Transputers to i860s and finally to Alphas in 1995. Over the past three years, we engineered and delivered over 300 clusters that utilized MPI running on Linux. As a software developer and hardware manufacturer, we know the value of extensive testing and validation. We are experts at configuring and validating the low latency interconnects we employ in our clusters. Our technical support is legendary — the systems we sell arrive at your site and WORK! Los Alamos chose Microway to maintain and upgrade its 144 node Alpha Avalon Cluster because of our reputation. Large clusters we have sold include 400+ nodes at the University of Wisconsin and 250+ nodes at Rockefeller University.

Microway offers three Athlon/Pentium enclosures—1U, 2U and tower, plus five Alpha configurations—1U, 3U, 4U RuggedRack™, QuadPuter™ and full tower. Our 264DP includes two 21264's with up to 4 GB of memory in our custom 4U RuggedRack, which features front accessible redundant power supplies and hard disks. This rugged configuration was chosen by the U.S. Navy for onboard use. We also offer a dual Alpha UP2000+ running at 833MHz with 2GB of memory. Our QuadPuter chassis holds 4 Alpha processors and up to 4GB memory. The 1U CS20 dual Alpha (at right) is the highest density computational platform available.

Microway is API-Networks' Top North American Channel Partner.



"Most Powerful, Highest Density Computational Platform On the Planet"

Microway Scalable 25 Node
50 Processor Cluster Using CS20 Dual
833 MHz Alphas and Myrinet Interconnect
Yielding Peak Throughput of 82.5 GigaFlo

"I have ordered numerous Alpha and Intel-based servers and workstations from Microway running both Tru64 UNIX and Linux. We have been very happy with both the performance and great value of Microway's products. The major UNIX vendors don't come close to Microway in this regard, and we have also found that Microway provides better value than other Linux hardware vendors. I have also used Microway's tech support and was pleased with their response. We've been using their systems for over a year and have had only a couple of minor incidents which were dealt with promptly."

— David Kristofferson, Ph.D., MBA,
Director of Information Systems, Eos Biotechnology, Inc.

Find out why over 75% of Microway's sales come from repeat customers.

Please call 508-746-7341 for a technical salesperson who speaks your language!

Visit us at www.microway.com



Microway
Technology you can count on™

Research Park Box 79, Kingston, MA 02364 • 508-746-7341 • info@microway.com

CONTENTS

VOLUME 201, No. 2: OCTOBER 2001

RESEARCH NOTE

- Maier, Ingo, Christian Hertweck, and Wilhelm Boland**
Stereochemical specificity of lamoxirene, the sperm-releasing pheromone in kelp (Laminariales, Phaeophyceae) 121

PHYSIOLOGY AND BIOMECHANICS

- Johnson, Amy S.**
Drag, drafting, and mechanical interactions in canopies of the red alga *Chondrus crispus* 126
- Thompson, Joseph T., and William M. Kier**
Ontogenetic changes in fibrous connective tissue organization in the oval squid, *Sepioteuthis lessoniana* Lesson, 1830 136
- Thompson, Joseph T., and William M. Kier**
Ontogenetic changes in mantle kinematics during escape jet locomotion in the oval squid, *Sepioteuthis lessoniana* Lesson, 1830 154
- Martinez, Anne-Sophie, Jean-Yves Toullec, Bruce Shillito, Mireille Charmantier-Daures, and Guy Charmantier**
Hydromineral regulation in the hydrothermal vent crab *Bythograea thermydron* 167

NEUROBIOLOGY AND BEHAVIOR

- Campbell, A. C., S. Coppard, C. D'Abreo, and R. Tudor-Thomas**
Escape and aggregation responses of three echinoderms to conspecific stimuli 175
- Clay, John R., and Alvin Shrier**
Action potentials occur spontaneously in squid giant axons with moderately alkaline intracellular pH 186

SYSTEMATICS

- Dahlgren, Thomas G., Bertil Åkesson, Christoffer Schander, Kenneth M. Halanych, and Per Sundberg**
Molecular phylogeny of the model annelid *Ophryotrocha* 193

ECOLOGY AND EVOLUTION

- Rondeau, Amélie, and Bernard Sainte-Marie**
Variable mate-guarding time and sperm allocation by male snow crabs (*Chionoecetes opilio*) in response to sexual competition, and their impact on the mating success of females 204

BIOGRAPHY

- Zottoli, Steven J.**
The origins of The Grass Foundation 218

SHORT REPORTS FROM THE 2001 GENERAL SCIENTIFIC MEETINGS OF THE MARINE BIOLOGICAL LABORATORY

FEATURED REPORT

- The Editors**
Introduction to the featured report, green fluorescent protein: enhanced optical signals from native crystals 231
- Inoué, Shinya, and Makoto Goda**
Fluorescence polarization ratio of GFP crystals 231

CELL BIOLOGY

- Knudson, Robert A., Shinya Inoué, and Makoto Goda**
Centrifuge polarizing microscope with dual specimen chambers and injection ports 234
- Tran, P. T., and Fred Chang**
Transmitted light fluorescence microscopy revisited. 235
- Hernandez, R. V., J. M. Garza, M. E. Graves, J. L. Martinez, Jr., and R. G. LeBaron**
The process of reducing CA1 long-term potentiation by the integrin binding peptide, GRGDSP, occurs within the first few minutes following theta-burst stimulation. 236
- Kuhns, William J., Dario Rusciano, Jane Kaltenbach, Michael Ho, Max Burger, and Xavier Fernandez-Busquets**
Up-regulation of integrins $\alpha_3\beta_1$ in sulfate-starved marine sponge cells: functional correlates 238

Brown, Jeremiah R., Kyle R. Simonetta, Leslie A. Sandberg, Phillip Stafford, and George M. Langford	
Recombinant globular tail fragment of myosin-V blocks vesicle transport in squid nerve cell extracts	240
Wöllert, Torsten, Ana S. DePina, Leslie A. Sandberg, and George M. Langford	
Reconstitution of active pseudo-contractile rings and myosin-II-mediated vesicle transport in extracts of clam oocytes	241
Clay, John R., and Alan M. Kuzirian	
A novel, kinesin-rich preparation derived from squid giant axons	243
Weidner, Earl	
Microsporidian spore/sporoplasm dynactin in <i>Spraguea</i>	245
Conrad, Mara L., R. L. Parady, and Peter B. Armstrong	
Response of the blood cell of the American horseshoe crab, <i>Limulus polyphemus</i> , to a lipopolysaccharide-like molecule from the green alga <i>Chlorella</i>	246
Silver, Robert	
LT _B ₄ evokes the calcium signal that initiates nuclear envelope breakdown through a multi-enzyme network in sand dollar (<i>Echinarcus parma</i>) cells	248

DEVELOPMENTAL BIOLOGY

Crawford, Karen	
Ooplasm segregation in the squid embryo, <i>Loligo pealeii</i>	251
Burbach, J. Peter H., Anita J. C. G. M. Hellemons, Marco Hoekman, Philip Grant, and Harish C. Pant	
The stellate ganglion of the squid <i>Loligo pealeii</i> as a model for neuronal development: expression of a POU Class VI homeodomain gene, <i>Rpf-1</i>	252
Link, Brian A.	
Evidence for directed mitotic cleavage plane reorientations during retinal development within the zebrafish	254
Smith, Ryan, Emma Kavanagh, Hilary G. Morrison, and Robert M. Gould	
Messenger RNAs located in spiny dogfish oligodendrocyte processes	255
Hill, Susan D., and Barbara C. Boyer	
Phalloidin labeling of developing muscle in embryos of the polychaete <i>Capitella</i> sp. 1.	257
Rice, Aaron N., David S. Portnoy, Ingrid M. Kaatz, and Phillip S. Lobel	
Differentiation of pharyngeal muscles on the basis of enzyme activities in the cichlid <i>Tramitichromis intermedium</i>	258

NEUROBIOLOGY

Twig, Gilad, Sung-Kwon Jung, Mark A. Messerli, Peter J. S. Smith, and Orian S. Shirihai	
Real-time detection of reactive oxygen intermediates from single microglial cells	261

Silver, Robert B., Mahlon E. Kriebel, Bruce Keller, and George D. Pappas	
Porocytosis: Quantal synaptic secretion of neurotransmitter at the neuromuscular junction through arrayed vesicles	263
Chappell, Richard L., and Stephen Redenti	
Endogenous zinc as a neuromodulator in vertebrate retina: evidence from the retinal slice	265
Shashar, Nadav, Douglas Borst, Seth A. Ament, William M. Saidel, Roxanna M. Smolowitz, and Roger T. Hanlon	
Polarization reflecting iridophores in the arms of the squid <i>Loligo pealeii</i>	267
Chiao, Chuan-Chin, and Roger T. Hanlon	
Cuttlefish cue visually on area—not shape or aspect ratio—of light objects in the substrate to produce disruptive body patterns for camouflage	269
Errigo, M., C. McGuinness, S. Meadors, B. Mittmann, F. Dodge, and R. Barlow	
Visually guided behavior of juvenile horseshoe crabs	271
Meadors, S., C. McGuinness, F. A. Dodge, and R. B. Barlow	
Growth, visual field, and resolution in the juvenile <i>Limulus</i> lateral eye	272
Kozlowski, Corinne, Kara Yopak, Rainer Voigt, and Jelle Atema	
An initial study on the effects of signal intermittency on the odor plume tracking behavior of the American lobster, <i>Homarus americanus</i>	274
Hall, Benjamin, and Kerry Delaney	
Cholinergic modulation of odor-evoked oscillations in the frog olfactory bulb	276
Zottoli, S. J., D. E. W. Arnolds, N. O. Asamoah, C. Chevez, S. N. Fuller, N. A. Hiza, J. E. Nierman, and L. A. Taboada	
Dye coupling evidence for gap junctions between supramedullary/dorsal neurons of the cunner, <i>Tautoglabrus adspersus</i>	277
Kaatz, Ingrid M., and Phillip S. Lobel	
A comparison of sounds recorded from a catfish (<i>Orinocodoras eigenmanni</i> , Doradidae) in an aquarium and in the field	278
Fay, R. R., and P. L. Edds-Walton	
Bimodal units in the torus semicircularis units of the toadfish (<i>Opsanus tau</i>)	280

MARICULTURE

Mensing, Allen F., Katherine A. Stephenson, Sarah L. Pollema, Hazel E. Richmond, Nichole Price, and Roger T. Hanlon	
Mariculture of the toadfish <i>Opsanus tau</i>	282
Rieder, Leila E., and Allen F. Mensinger	
Strategies for increasing growth of juvenile toadfish	283
Chikarmane, Hemant M., Alan M. Kuzirian, Ian Carroll, and Robbin Dengler	
Development of genetically tagged bay scallops for evaluation of seeding programs	285

Williams, Libby, G. Carl Noblitt IV, and Robert Buchsbaum		
The effects of salt marsh haying on benthic algal biomass	287	
Hinckley, Eve-Lyn S., Christopher Neill, Richard McHorney, and Ann Lezberg		
Dissolved nitrogen dynamics in groundwater under a coastal Massachusetts forest.	288	
Hauxwell, Alyson M., Christopher Neill, Ivan Valiela, and Kevin D. Kroeger		
Small-scale heterogeneity of nitrogen concentrations in groundwater at the seepage face of Edgartown Great Pond	290	
Novak, Melissa, Mark Lever, and Ivan Valiela		
Top down <i>vs.</i> bottom-up controls of microphytobenthic standing crop: role of mud snails and nitrogen supply in the littoral of Waquoit Bay estuaries	292	
		Fila, Laurie, Ruth Herrold Carmichael, Andrea Shriver, and Ivan Valiela
		Stable N isotopic signatures in bay scallop tissue, feces, and pseudofeces in Cape Code estuaries subject to different N loads
		Grady, Sara P., Deborah Rutecki, Ruth Carmichael, and Ivan Valiela
		Age structure of the Pleasant Bay population of <i>Crepidula fornicata</i> : a possible tool for estimating horse-shoe crab age
		Kuzirian, Alan M., Eleanor C. S. Terry, Deanna L. Bechtel, and Patrick I. James
		Hydrogen peroxide: an effective treatment for ballast water
		<i>ORAL PRESENTATIONS</i>
		Published by title only

ANNOUNCEMENT

The Marine Biological Laboratory is pleased to announce that it has entered into an agreement with HighWire Press of Stanford University to publish *The Biological Bulletin* electronically. The online journal was launched on 23 August 2001. It will be available free of charge to subscribers and the general public for six months after that date. Subsequently, subscribers to *The Biological Bulletin* will receive both the print and electronic versions of the journal.

We invite you to visit *The Biological Bulletin* online at
<http://www.biolbull.org>

THE BIOLOGICAL BULLETIN

THE BIOLOGICAL BULLETIN is published six times a year by the Marine Biological Laboratory, 7 MBL Street, Woods Hole, Massachusetts 02543.

Subscriptions and similar matter should be addressed to Subscription Manager, THE BIOLOGICAL BULLETIN, Marine Biological Laboratory, 7 MBL Street, Woods Hole, Massachusetts 02543. Subscription per year (six issues, two volumes): \$235 for libraries; \$95 for individuals. Subscription per volume (three issues): \$117.50 for libraries; \$47.50 for individuals. Back and single issues (subject to availability): \$40 for libraries; \$20 for individuals.

Communications relative to manuscripts should be sent to Michael J. Greenberg, Editor-in-Chief, or Pamela Clapp Hinkle, Managing Editor, at the Marine Biological Laboratory, 7 MBL Street, Woods Hole, Massachusetts 02543. Telephone: (508) 289-7428. FAX: 508-289-7922. E-mail: pclapp@mbi.edu.

<http://www.biobull.org>

THE BIOLOGICAL BULLETIN is indexed in bibliographic services including *Index Medicus* and MEDLINE, *Chemical Abstracts*, *Current Contents*, *Elsevier BIOBASE/Current Awareness in Biological Sciences*, and *Geo Abstracts*.

Printed on acid free paper,
effective with Volume 180, Issue 1, 1991.

POSTMASTER: Send address changes to THE BIOLOGICAL BULLETIN, Marine Biological Laboratory, 7 MBL Street, Woods Hole, MA 02543.

Copyright © 2001, by the Marine Biological Laboratory

Periodicals postage paid at Woods Hole, MA, and additional mailing offices.

ISSN 0006-3185

INSTRUCTIONS TO AUTHORS

The Biological Bulletin accepts outstanding original research reports of general interest to biologists throughout the world. Papers are usually of intermediate length (10–40 manuscript pages). A limited number of solicited review papers may be accepted after formal review. A paper will usually appear within four months after its acceptance.

Very short, especially topical papers (less than 9 manuscript pages including tables, figures, and bibliography) will be published in a separate section entitled "Research Notes." A Research Note in *The Biological Bulletin* follows the format of similar notes in *Nature*. It should open with a summary paragraph of 150 to 200 words comprising the introduction and the conclusions. The rest of the text should continue on without subheadings, and there should be no more than 30 references. References should be referred to in the text by number, and listed in the Literature Cited section in the order that they appear in the text. Unlike references in *Nature*, references in the Research Notes section should conform in punctuation and arrangement to the style of recent issues of *The Biological Bulletin*. Materials and Methods should be incorporated into appropriate figure legends. See the article by Lohmann *et al.* (October 1990, Vol. **179**: 214–218) for sample style. A Research Note will usually appear within two months after its acceptance.

The Editorial Board requests that regular manuscripts conform to the requirements set below; those manuscripts that do not conform will be returned to authors for correction before review.

1. **Manuscripts.** Manuscripts, including figures, should be submitted in quadruplicate, with the originals clearly marked. (Xerox copies of photographs are not acceptable for review purposes.) The submission letter accompanying the manuscript should include a telephone number, a FAX number, and (if possible) an E-mail address for the corresponding author. The original manuscript must be typed in no smaller than 12 pitch or 10 point, using double spacing (*including* figure legends, footnotes, bibliography, etc.) on one side of 16- or 20-lb. bond paper, 8 by 11 inches. Please, no right justification. Manuscripts should be proofread carefully and errors corrected legibly in black ink. Pages should be numbered consecutively. Margins on all sides should be at least 1 inch (2.5 cm). Manuscripts should conform to the *Council of Biology Editors Style Manual*, 5th Edition (Council of Biology Editors, 1983) and to American spelling. Unusual abbreviations should be kept to a minimum and should be spelled out on first reference as well as defined in a footnote on the title page. Manuscripts should be divided into the following components: Title page, Abstract (of no more than 200 words), Introduction, Materials and Methods, Results, Discussion, Acknowledgments, Literature Cited, Tables, and Figure Legends. In addition, authors should supply a list of words and phrases under which the article should be indexed.

2. **Title page.** The title page consists of a condensed title or running head of no more than 35 letters and spaces, the manuscript title, authors' names and appropriate addresses, and footnotes

listing present addresses, acknowledgments or contribution numbers, and explanation of unusual abbreviations.

3. **Figures.** The dimensions of the printed page, 7 by 9 inches, should be kept in mind in preparing figures for publication. We recommend that figures be about 1 times the linear dimensions of the final printing desired, and that the ratio of the largest to the smallest letter or number and of the thickest to the thinnest line not exceed 1:1.5. Explanatory matter generally should be included in legends, although axes should always be identified on the illustration itself. Figures should be prepared for reproduction as either line cuts or halftones. Figures to be reproduced as line cuts should be unmounted glossy photographic reproductions or drawn in black ink on white paper, good-quality tracing cloth or plastic, or blue-lined coordinate paper. Those to be reproduced as halftones should be mounted on board, with both designating numbers or letters and scale bars affixed directly to the figures. All figures should be numbered in consecutive order, with no distinction between text and plate figures and cited, in order, in the text. The author's name and an arrow indicating orientation should appear on the reverse side of all figures.

Digital art: *The Biological Bulletin* will accept figures submitted in electronic form; however, digital art must conform to the following guidelines. Authors who create digital images are wholly responsible for the quality of their material, including color and halftone accuracy.

Format. Acceptable graphic formats are TIFF and EPS. Color submissions must be in EPS format, saved in CMKY mode.

Software. Preferred software is Adobe Illustrator or Adobe Photoshop for the Mac and Adobe Photoshop for Windows. Specific instructions for artwork created with various software programs are available on the Web at the Digital Art Information Site maintained by Cadmus Professional Communications at <http://cpc.cadmus.com/da/>

Resolution. The minimum requirements for resolution are 1200 DPI for line art and 300 for halftones.

Size. All digital artwork must be submitted at its actual printed size so that no scaling is necessary.

Multipanel figures. Figures consisting of individual parts (e.g., panels A, B, C) must be assembled into final format and submitted as one file.

Hard copy. Files must be accompanied by hard copy for use in case the electronic version is unusable.

Disk identification. Disks must be clearly labeled with the following information: author name and manuscript number; format (PC or Macintosh); name and version of software used.

Color: *The Biological Bulletin* will publish color figures and plates, but must bill authors for the actual additional cost of printing in color. The process is expensive, so authors with more than one color image should—consistent with editorial concerns, especially citation of figures in order—combine them into a single plate to reduce the expense. On request, when supplied with a copy of a color illustration, the editorial staff will provide a pre-publication estimate of the printing cost.

4. **Tables, footnotes, figure legends, etc.** Authors should follow the style in a recent issue of *The Biological Bulletin* in

preparing table headings, figure legends, and the like. Because of the high cost of setting tabular material in type, authors are asked to limit such material as much as possible. Tables, with their headings and footnotes, should be typed on separate sheets, numbered with consecutive Roman numerals, and placed after the Literature Cited. Figure legends should contain enough information to make the figure intelligible separate from the text. Legends should be typed double spaced, with consecutive Arabic numbers, on a separate sheet at the end of the paper. Footnotes should be limited to authors' current addresses, acknowledgments or contribution numbers, and explanation of unusual abbreviations. All such footnotes should appear on the title page. Footnotes are not normally permitted in the body of the text.

5. **Literature cited.** In the text, literature should be cited by the Harvard system, with papers by more than two authors cited as Jones *et al.*, 1980. Personal communications and material in preparation or in press should be cited in the text only, with author's initials and institutions, unless the material has been formally accepted and a volume number can be supplied. The list of references following the text should be headed Literature Cited, and must be typed double spaced on separate pages, conforming in punctuation and arrangement to the style of recent issues of *The Biological Bulletin*. Citations should include complete titles and inclusive pagination. Journal abbreviations should normally follow those of the U. S. A. Standards Institute (USASI), as adopted by BIOLOGICAL ABSTRACTS and CHEMICAL ABSTRACTS, with the minor differences set out below. The most generally useful list of biological journal titles is that published each year by BIOLOGICAL ABSTRACTS (BIOSIS List of Serials; the most recent issue). Foreign authors, and others who are accustomed to using THE WORLD LIST OF SCIENTIFIC PERIODICALS, may find a booklet published by the Biological Council of the U.K. (obtainable from the Institute of Biology, 41 Queen's Gate, London, S.W.7, England, U.K.) useful, since it sets out the WORLD LIST abbreviations for most biological journals with notes of the USASI abbreviations where these differ. CHEMICAL ABSTRACTS publishes quarterly supplements of additional abbreviations. The following points of reference style for THE BIOLOGICAL BULLETIN differ from USASI (or modified WORLD LIST) usage:

A. Journal abbreviations, and book titles, all underlined (for italics)

B. All components of abbreviations with initial capitals (not as European usage in WORLD LIST e.g., *J. Cell. Comp. Physiol.* NOT *J. cell. comp. Physiol.*)

C. All abbreviated components must be followed by a period, whole word components *must not* (i.e., *J. Cancer Res.*)

D. Space between all components (e.g., *J. Cell. Comp. Physiol.*, not *J.Cell.Comp.Physiol.*)

E. Unusual words in journal titles should be spelled out in full, rather than employing new abbreviations invented by the author. For example, use *Rit Visindafjélagss Íslendinga* without abbreviation.

F. All single word journal titles in full (e.g., *Veliger, Ecology, Brain*).

G. The order of abbreviated components should be the same as the word order of the complete title (*i.e.*, *Proc.* and *Trans.* placed where they appear, not transposed as in some BIOLOGICAL ABSTRACTS listings).

H. A few well-known international journals in their preferred forms rather than WORLD LIST or USASI usage (*e.g.*, *Nature*, *Science*, *Evolution* NOT *Nature, Lond.*, *Science, N.Y.*; *Evolution, Lancaster, Pa.*)

6. **Reprints, page proofs, and charges.** Authors may purchase reprints in lots of 100. Forms for placing reprint orders are sent with page proofs. Reprints normally will be delivered about 2 to 3 months after the issue date. Authors (or delegates for foreign authors) will receive page proofs of articles shortly before publication. They will be charged the current cost of printers' time for corrections to these (other than corrections of printers' or editors' errors). Other than these charges for authors' alterations, *The Biological Bulletin* does not have page charges.

Stereochemical Specificity of Lamoxirene, the Sperm-Releasing Pheromone in Kelp (Laminariales, Phaeophyceae)

INGO MAIER^{1,*}, CHRISTIAN HERTWECK², AND WILHELM BOLAND²

¹Fachbereich Biologie, Universität Konstanz, 78457 Konstanz, Germany; and ²Max-Planck-Institute for Chemical Ecology, Carl-Zeiss-Promenade 10, 07745 Jena, Germany

Sexual reproduction in the large brown seaweeds of the Laminariales, commonly called kelp, involves signaling chemicals, or "pheromones," that induce sperm release from antheridia and subsequent chemotactic orientation of sperm towards the luring eggs. Lamoxirene (cis-2-cyclohepta-2',5'-dienyl-3-vinyloxirane) has been identified as the sperm-releasing pheromone in the largest and most advanced group of the Laminariales, comprising the Laminariaceae, Alariaceae, and Lessoniaceae. Recently, a stereoselective synthesis of lamoxirene has yielded pure substances for biological studies. Here, we used closed-loop stripping and chiral gas chromatography to establish which of the four possible stereoisomers of lamoxirene functions as the naturally occurring sperm-releasing pheromone in Undaria pinnatifida. In addition, the relationship between absolute configuration and sperm-releasing bioactivity in Laminaria, Alaria, Undaria, and Macrocystis was clarified in bioassays with lamoxirene stereoisomers. Our experiments established (1'R,2S,3R)-lamoxirene as the most bioactive compound in all species tested and as the main component in egg secretions. Thus no species specificity in the stereochemistry of the sperm-releasing pheromone of the Laminariales has yet been found.

Sexuality in the Laminariales is strictly controlled by environmental cues and is coordinated by chemical interaction. Pheromones secreted by eggs produced on microscopic female gametophytes (Fig. 1) induce the release of sperm from antheridia on nearby male gametophytes and subsequently attract the sperm to the eggs (1–4). The species in the Laminariales belonging to the Laminariaceae,

Alariaceae, and Lessoniaceae are characterized by the exclusive possession of lamoxirene (*cis*-2-cyclohepta-2',5'-dienyl-3-vinyloxirane, Fig. 2) as the sperm-releasing pheromone (3, 5, 6). Lamoxirene may exist in four spatial variations (stereoisomers: enantiomers and diastereomers, Fig. 2), which may or may not occur in nature or function as pheromones, respectively. Supernatant taken from mature female cultures induces sperm release in many, if not all, interspecific combinations within this group (Maier, unpublished). These observations support the idea that pheromonal cross-reaction and even competition between kelp gametes may also occur in the field. In particular, this holds for sympatric species with overlapping reproductive periods, as exemplified by the four European *Laminaria* species listed in Table 1. However, experiments using culture supernatants or racemic synthetic pheromone do not rule out the possibility that kelps use specific mixtures of stereoisomers for differentiation of sympatric species (4, 7). Similar strategies, with different enantiomers or diastereomers used by different species, or specific mixtures being more active than single components, are well-known in insects (8). It was shown that two of the lamoxirenes, compound **1** and its diastereomer **3** (Fig. 2), are secreted in a ratio of 2.45:1 by eggs of *Laminaria digitata*, and preliminary bioassays revealed the highest biological activity in pheromone samples enriched in lamoxirene **1** (9).

Recently, an effective stereoselective synthesis of lamoxirene has become available (10), offering for the first time the chance of quantitative bioassays with pure stereoisomers of lamoxirene. Unfortunately, bioassay results on lamoxirene **1** and **3** were exchanged in the previous publication (10). In the present paper, we report the results of bioassays that correct this mistake and broaden the original data on *Laminaria* spp. to a number of other genera and families in

Received 18 December 2000; accepted 28 June 2001.

* To whom correspondence should be addressed. E-mail: Ingo.Maier@uni-konstanz.de

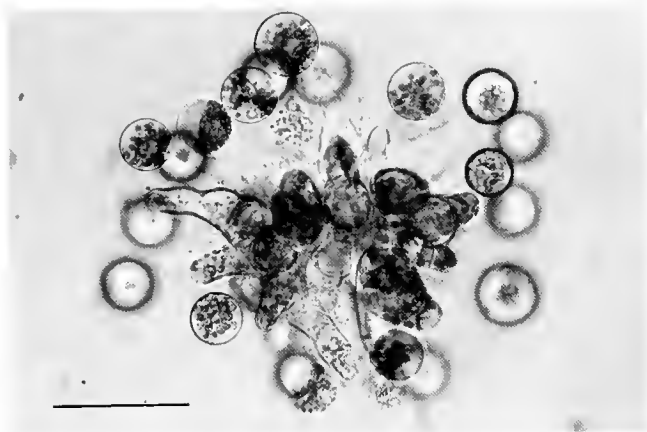


Figure 1. Female gametophyte of *Laminaria hyperborea* with several released eggs secreting pheromone. Scale bar = 50 μm .

the Laminariales. In addition to bioassays, the absolute configuration of naturally occurring lamoxirene **1** in *Undaria pinnatifida* is confirmed by chiral gas chromatography.

Clonal male gametophytes of several species of Laminariales (Table 1) were kept vegetatively in red fluorescent light (about $15 \mu\text{mol m}^{-2} \text{s}^{-1}$, 16:8 h light/dark cycle) at 10°C with ASM-1 (11) as a culture medium. For the induction of gametogenesis, they were fragmented using a tissue homogenizer and transferred into white fluorescent light ($30 \mu\text{mol m}^{-2} \text{s}^{-1}$, 16 h light cycle) at 10°C . The gametophytes were used in sperm-release assays 12 days later, when numerous mature antheridia had been formed.

Lamoxirene stereoisomers **1**–**4** (Fig. 2) with high configurational purity (enantiomeric excess, e.e.) were available in dimethylsulfoxide (DMSO, puriss. p.a., FLUKA): lamox-

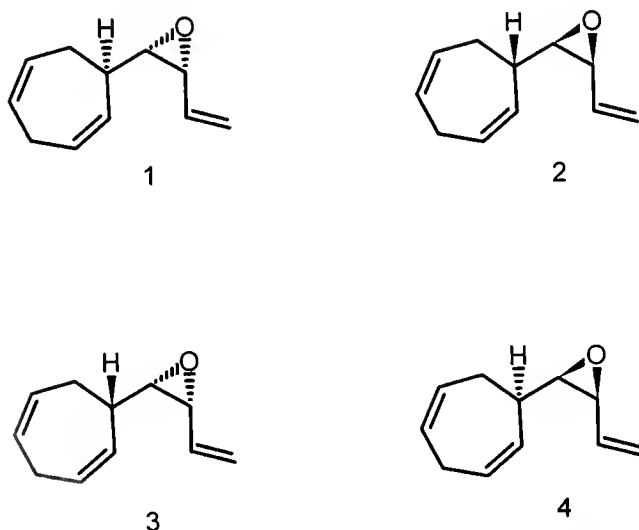


Figure 2. The four stereoisomers of lamoxirene: **1** = (1R,2'S,3'R); **2** = (1S,2'R,3'S); **3** = (1S,2'S,3'R); **4** = (1R,2'R,3'S).

Table 1

Classification and geographic origin of species used in bioassays

Classification	Origin
Family Laminariaceae	
<i>Laminaria digitata</i> (Huds.) Lamour.	Helgoland, German Bight, North Sea
<i>L. hyperborea</i> (Gunn.) Fosl.	Helgoland
<i>L. saccharina</i> (L.) Lamour.	Helgoland
<i>L. ochroleuca</i> Pyl.	Roscoff, Brittany, France
Family Alariaceae	
<i>Alaria esculenta</i> (L.) Grev.	Tjörnes, Iceland
<i>A. esculenta</i> (L.) Grev.	St. John's, Newfoundland, Canada
<i>Undaria pinnatifida</i> (Harv.) Suringar	Hokkaido, Japan
Family Lessoniaceae	
<i>Macrocystis pyrifera</i> (L.) C. Ag.	Santa Barbara, California

irene **1**: 97% e.e.; lamoxirene **2**: 90% e.e.; lamoxirene **3**: 95% e.e.; lamoxirene **4**: 96% e.e. (10). The solutions were serially diluted (1×10^{-3} to 1×10^{-11} M, 5×10^{-4} M to 5×10^{-11} M, 2×10^{-4} M to 2×10^{-11} M) in DMSO. In addition, an equimolar mixture of lamoxirenes **1** and **3** was prepared and diluted accordingly.

For the stereochemical analysis of natural lamoxirene, female gametophytes of *Undaria pinnatifida* from Hokkaido, Japan, were cultivated as described above for the male gametophytes. Upon massive egg release, volatile egg secretions from the gametophyte suspension were adsorbed onto a bed of 1.5 mg activated carbon by closed loop stripping (2, 3), followed by elution with 20 μl diethylether. Chiral capillary gas chromatography (FS-Lipodex E, Macherey-Nagel, Düren, Germany; 25 m \times 0.32 mm, carrier H_2) revealed a single lamoxirene peak (e.e. > 97%), identified as lamoxirene **1** by comparison with synthetic samples (12).

To compare the biological activity of the different stereoisomers in the induction of sperm release, a new semi-quantitative assay was employed. Instead of preparing aqueous pheromone solutions by distribution from a water-immiscible fluorocarbon phase as in the original assay (13), lamoxirene was directly diluted from stock solutions in DMSO into seawater. 0.5% of a lamoxirene solution was added to culture medium in 3-ml or 5-ml glass vials, carefully mixed, equilibrated to 12°C , and used immediately. All experiments were carried out in a climate-controlled culture room at 12°C . In the bioassay, 100 μl of a suspension of male gametophytes were mixed with 100 μl of an aqueous pheromone solution in a concavity slide. The final concentration of DMSO in all assays was 0.25%. DMSO alone did not induce sperm release, except in *Alaria esculenta* from Iceland (Table 1). This strain was thus excluded from all further experiments. The reaction to DMSO was not observed in *A. esculenta* from Newfoundland, which was used instead. Release of sperm was observed in a stereomicroscope at $40\times$ magnification under dark-field

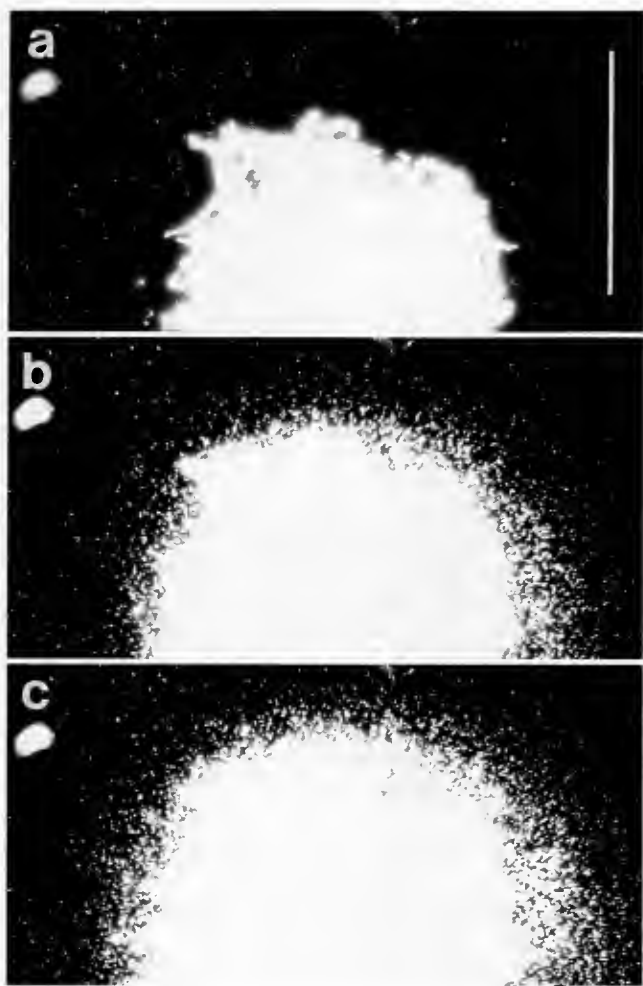


Figure 3. A male gametophyte of *Alaria esculenta* in the bioassay before (a) and with massive sperm release 60 s (b) and 90 s (c) after the addition of lamoxirene (dark-field illumination, microflash exposure). Scale bar = 1 mm.

illumination (Fig. 3). At saturating concentrations, release of an estimated several hundred sperm occurred within 7–15 s. A pheromone solution was considered inactive when no release occurred within 1 min. At the threshold, several spermatozooids were reliably released within 1 min, and stronger release occurred at the next higher concentration step. Assays were performed at least in triplicate and repeated in an independent experimental series. The results of bioassays on lamoxirene-induced sperm release in *Laminaria digitata* are shown in Table 2, and threshold concentrations for all species investigated are summarized in Table 3.

The response of the algae to pheromone was very reproducible (Table 2), and threshold concentrations were sharply defined. They were somewhat higher than those reported earlier (0.01 nM with racemic lamoxirene in *L. digitata*, *L. hyperborea*, and *Macrocystis pyrifera* (6); 0.002 nM in *L. digitata* with lamoxirene **1** (9)). The bioassay used here is simple and avoids inaccuracies introduced by solvent/water-distribution, but is probably more prone to pheromone loss by adsorption and volatilization than the original assay. The given thresholds should thus be regarded as conservative approximations.

In the species tested, lamoxirene **1** was generally the most active stereoisomer, followed by lamoxirene **3**. *L. saccharina* was the only exception, with compounds **1** and **3** being equally effective. The relative biological activity of lamoxirene stereoisomers matches the composition of egg secretions, with lamoxirene **1** being the main or the only stereoisomer produced in *L. digitata* (9) and *U. pinnatifida* (this study), respectively. Lamoxirene **3** occurs as a by-product in *L. digitata*, while lamoxirene **2** and **4** have not yet been identified as natural products. Lamoxirene **4** is virtually inactive, which underlines the central importance of the spatial orientation of the epoxy group in relation to the terminal double bond in the side chain and the ring system. This has already been indicated in earlier studies on receptor specificity (13). In *L. digitata*, *L. hyperborea*, and *L. och-*

Table 2

Results of bioassays on pheromone-induced sperm release in *Laminaria digitata*

Lamoxirene	Pheromone concentration (nM)							
	0.025	0.05	0.1	0.25	0.5	1	2.5	10
1	0, 0, 0	+ , 0 , +	+, +, +	++, +, ++	+++, +++	—	—	—
2	—	—	0, 0, 0	0, 0, 0	0, 0, 0	0, 0, 0	+, +, +	++, ++
3	—	0, 0, 0	0, 0, 0	+ , + , 0	+, +, +	+, +, +	++, ++	+++, +++
4	—	—	—	—	—	0, 0, 0	0, 0, 0	+, +, +
						0, 0, 0	0, +, 0	0 , + , +

The thresholds are printed in bold.

—: not tested; 0, +, ++, +++: no or max. 2, 3–20, 20–100, several hundred sperm released, respectively.

Table 3

Threshold concentrations in seawater for the induction of spermatozoid release by lamoxirene stereoisomers

Species	Threshold concentrations (nM)			
	Lamoxirene 1	Lamoxirene 2	Lamoxirene 3	Lamoxirene 4
<i>Laminaria digitata</i>	0.05	2.5	0.25	10
<i>L. hyperborea</i>	0.01	0.1	0.02	2.5
<i>L. saccharina</i>	1	2.5	1	>20*
<i>L. ochroleuca</i>	0.02	1	0.25	10
<i>Alaria esculenta</i>	0.1	1	0.25	10
<i>Undaria pinnatifida</i>	0.1	1	1	>20*
<i>Macrocystis pyrifera</i>	0.1	1	1	20

* Highest test concentration available.

roleuca, the diastereomer mixture of lamoxirenes 1 and 3 had no higher biological activity in sperm release than lamoxirene 1 alone (Table 4, A compared with B and C). On the contrary, weak competitive effects indicated by slightly increased thresholds were observed in *L. digitata* and *L. hyperborea* (Table 4, A compared with B).

In conclusion, the stereochemical specificity of lamoxirene action in pheromone-induced sperm release is conserved among all species tested. This holds not only for the sympatric European *Laminaria* and *Alaria*, but also for *Undaria* and *Macrocystis* from the North Pacific and thus probably for all species belonging to the Laminariaceae, Alariaceae, and Lessoniaceae. These families comprise the monophyletic "core group" of the most advanced Laminariales (14, 15). The origin of their pheromone system and its stereochemistry reaches back to at least the divergence of the group from a common ancestor, which dates to between 16 and 40 million years ago based on molecular clock estimations and various other considerations, including biogeography and paleoceanography (3, 14, 16–18).

Species specificity in gamete interaction in the Laminariales is thus not achieved by pheromone specificity in the induction of sperm release, but must be mediated by subsequent mechanisms. These may include differential sperm attraction to the egg, which is also under pheromonal con-

trol, and gamete surface recognition. In *L. digitata*, it was previously shown that different pheromone receptors are involved in sperm release and chemotaxis, and that desmarestene (6-(*cis*-1',3'-butadienyl)-cyclohepta-1,4-diene), not lamoxirene, is the most potent chemoattractant in this species (19). The possibility thus exists that a species-specific diversification of complex egg secretions and pheromone receptors is operative on the chemoattraction level.

Literature Cited

1. Maier, I. 1987. Environmental and pheromonal control of sexual reproduction in *Laminaria*. Pp. 66–74 in *Algal Development—Molecular and Cellular Aspects*, W. Wiessner, D. G. Robinson, and R. C. Starr, eds. Springer-Verlag, Berlin.
2. Maier, I., and D. G. Müller. 1986. Sexual pheromones in algae. *Biol. Bull.* **170**: 145–175.
3. Maier, I., D. G. Müller, G. Gassmann, W. Boland, and L. Jaenicke. 1987. Sexual pheromones and related egg secretions in Laminariales (Phaeophyta). *Z. Naturforsch. Sect. C* **42**: 948–954.
4. Maier, I. 1995. Brown algal pheromones. *Prog. Phycol. Res.* **11**: 51–102.
5. Marner, F.-J., B. Müller, and L. Jaenicke. 1984. Lamoxirene. Structural proof of the spermatozoid releasing and attracting pheromone of Laminariales. *Z. Naturforsch. Sect. C* **39**: 689–691.
6. Müller, D. G., I. Maier, and G. Gassmann. 1985. Survey on sexual pheromone specificity in Laminariales (Phaeophyceae). *Phycologia* **24**: 475–477.
7. Boland, W., U. Flegel, G. Jorndt, and D. G. Müller. 1987. Absolute configuration and enantiomer composition of hormosirene. *Naturwissenschaften* **74**: 448–449.
8. Mori, K. 1997. Pheromones: synthesis and bioactivity. *Chem. Commun.* **1997**: 1153–1158.
9. Maier, I., G. Pohnert, S. Pantke-Böcker, and W. Boland. 1996. Solid-phase microextraction and determination of the absolute configuration of the *Laminaria digitata* (Laminariales, Phaeophyceae) spermatozoid-releasing pheromone. *Naturwissenschaften* **83**: 378–379.
10. Hertweck, C., and W. Boland. 2000. Tandem reduction-chloroallylboration of esters: asymmetric synthesis of lamoxirene, the spermatozoid releasing and attracting pheromone of the Laminariales (Phaeophyceae). *J. Org. Chem.* **65**: 2458–2463.

Table 4

Threshold concentrations of total lamoxirene (M) in sperm release

Experiment	A	B	C
<i>Laminaria digitata</i>	2.3×10^{-10}	1.1×10^{-10}	1.2×10^{-10}
<i>L. hyperborea</i>	1.1×10^{-10}	5.7×10^{-11}	2.5×10^{-11}
<i>L. ochroleuca</i>	1.1×10^{-10}	1.1×10^{-10}	1.2×10^{-10}

Experiment A: equimolar combination of lamoxirenes 1 and 3, B: same concentration of lamoxirene 1, lamoxirene 3 replaced by pure DMSO; C: lamoxirene 1 only, but total lamoxirene as in A. The total solvent concentration was identical in all tests.

11. **Maier, I., and M. Calenberg. 1994.** Effect of extracellular Ca^{2+} and Ca^{2+} -antagonists on the movement and chemoorientation of male gametes of *Ectocarpus siliculosus* (Phaeophyceae). *Bot. Acta* **107**: 451–460.
12. **Hertweck, C. 1999.** *Funktionalisierte Vinyloxirane durch Reduktive Allylierung von Estern: Stereoselektive Synthesen von Lamoxiren und Splüingoidbasen*. Dissertation, University of Bonn, Germany.
13. **Maier, I., D. G. Müller, C. Schmid, W. Boland, and L. Jaenicke. 1988.** Pheromone receptor specificity and threshold concentrations for spermatozoid release in *Laminaria digitata*. *Naturwissenschaften* **75**: 260–263.
14. **Maier, I. 1984.** *Sexualität bei Braunalgen aus der Ordnung Laminariales und die Phylogenie der Ordnung*. Dissertation, University of Konstanz, Germany.
15. **Boo, S. M., W. J. Lee, H. S. Yoon, A. Kato, and H. Kawai. 1999.** Molecular phylogeny of Laminariales (Phaeophyceae) inferred from small subunit ribosomal DNA sequences. *Phycol. Res.* **47**: 109–114.
16. **Estes, J. A., and P. D. Steinberg. 1988.** Predation, herbivory, and kelp evolution. *Paleobiology* **14**: 19–36.
17. **Lüning, K., and I. tom Dieck. 1990.** The distribution and evolution of the Laminariales: North Pacific-Atlantic relationships. Pp. 187–204 in *Evolutionary Biogeography of the Marine Algae of the North Atlantic*, D. J. Garbary, and G. R. South, eds. Springer-Verlag, Berlin.
18. **Saunders, G. W., and L. D. Druehl. 1992.** Nucleotide sequences of the small-subunit ribosomal RNA genes from selected Laminariales (Phaeophyta): implications for kelp evolution. *J. Phycol.* **28**: 544–549.
19. **Maier, I., D. G. Müller, and W. Boland. 1994.** Spermatozoid chemotaxis in *Laminaria digitata* (Phaeophyceae). III. Pheromone receptor specificity and threshold concentrations. *Z. Naturforsch. Sect. C* **49**: 601–606.

Drag, Drafting, and Mechanical Interactions in Canopies of the Red Alga *Chondrus crispus*

AMY S. JOHNSON

Department of Biology, Bowdoin College, Brunswick, Maine 04011

Abstract. Dense algal canopies, which are common in the lower intertidal and shallow subtidal along rocky coastlines, can alter flow-induced forces in their vicinity. Alteration of flow-induced forces on algal thalli may ameliorate risk of dislodgement and will affect important physiological processes, such as rates of photosynthesis. This study found that the force experienced by a thallus of the red alga *Chondrus crispus* (Stackhouse) at a given flow speed within a flow tank depended upon (1) the density of the canopy surrounding the thallus, (2) the position of the thallus within the canopy, and (3) the length of the stipe of the thallus relative to the height of the canopy. At all flow speeds, a solitary thallus experienced higher forces than a thallus with neighbors. A greater than 65% reduction in force occurred when the thallus drafted in the region of slower velocities that occurs in the wake region of even a single upstream neighbor, similar to the way racing bicyclists draft one behind the other. Mechanical interactions between thalli were important to forces experienced within canopies. A thallus on the upstream edge of a canopy experienced 6% less force than it did when solitary, because the canopy physically supported it. A thallus in the middle of a canopy experienced up to 83% less force than a solitary thallus, and forces decreased with increasing canopy density. Thus, a bushy morphology that increases drag on a solitary thallus may function to decrease forces experienced by that thallus when it is surrounded by a canopy, because that morphology increases physical support provided by neighbors.

Introduction

Algal canopies dominate space in the intertidal and shallow subtidal along rocky coastlines and provide secondary habitat for encrusting organisms as diverse as bryozoans,

hydroids, sponges, and tunicates. Algal canopies alter flow in their vicinity (Koehl and Alberte, 1988; Eckman *et al.*, 1989) in ways that determine such important phenomena as algal production and physiology (Taylor and Hay, 1984; reviewed by Hurd, 2000), the recruitment of algal propagules (Johnson and Brawley, 1998) and invertebrate larvae (Duggins *et al.*, 1990), the flux of gases and nutrients to the surface of algal thalli (Koehl and Alberte, 1988), and the potential for breakage of thalli due to flow-induced forces (Koehl and Wainwright, 1977; Dudgeon and Johnson, 1992; Gaylord *et al.*, 1994; Johnson and Koehl, 1994; Blanchette, 1997; Koehl, 1999; Gaylord, 2000).

Flow forces may limit the size of some algae (Carrington, 1990; Gaylord *et al.*, 1994; Denny, 1999; Gaylord, 2000), either by dislodgment of entire thalli or by pruning (Blanchette, 1997; Dudgeon *et al.*, 1999). However, most measurements of flow-induced forces on algal thalli have examined thalli only in isolation from their canopy (Charters *et al.*, 1969; Gerard, 1987; Koehl and Alberte, 1988; Sheath and Hambrook, 1988; Armstrong, 1989; Dudgeon and Johnson, 1992; Johnson and Koehl, 1994; Gaylord *et al.*, 1994; Shaughnessy *et al.*, 1996; but see Carrington, 1990; Holbrook *et al.*, 1991). A surrounding canopy, however, is likely to mediate flow-induced forces experienced by constituent thalli. For example, a canopy probably slows flow within (Koehl and Alberte, 1988; Eckman *et al.*, 1989), thus decreasing forces experienced by constituent algal thalli. Total force on an individual thallus, however, will be due both to direct fluid dynamic forces, such as drag, and to forces resulting from mechanical interactions with neighboring thalli (Holbrook *et al.*, 1991). This paper quantifies the dynamics of the interactions among adjacent thalli due to flow forces on individual thalli and on a canopy of the red alga *Chondrus crispus*.

C. crispus occurs in dense canopies (up to 4 stipes per cm²; S. Dudgeon, unpubl. data) on intertidal and shallow

Received 16 January 2001; accepted 18 June 2001.

E-mail: ajohnson@bowdoin.edu

subtidal rocky shores along the northeast coast of the United States and Canada. In the Gulf of Maine, *C. crispus* can be found from about 1 m above mean low water to about 15 m below mean low water (Mathieson and Burns, 1971; Dudgeon *et al.*, 1999). It occurs in distributions that range from intermittent patches of thalli arising from a single holdfast to areas where the substratum is covered with a dense, uniform canopy (as tall as ~ 0.07 m in height when emersed at low tide; S. Dudgeon, California State University at Northridge, unpubl. data). A large specimen of *C. crispus* generally consists of a relatively long, narrow stipe topped by a bushy, bifurcated thallus (Fig. 1). Multiple stipes arise

from a persistent encrusting holdfast; thalli seldom occur in isolation from neighboring thalli.

Flow-induced dislodgment of subtidal *C. crispus* thalli has not been quantified. However, winter dislodgment of thalli from tall intertidal canopies (>4 cm tall) can be as great as 30% (Dudgeon and Johnson, 1992); and the seasonal decrease in biomass of the largest thalli in an intertidal population (which ranged in size from 2.5 cm² to 250 cm² in planform area) can be as great as 75% (M. Pratt and A. Johnson, unpubl. data). Because thalli regenerate quickly from persistent encrusting holdfasts, dislodgment is not typically a selective death for the genet. New thalli of *C.*

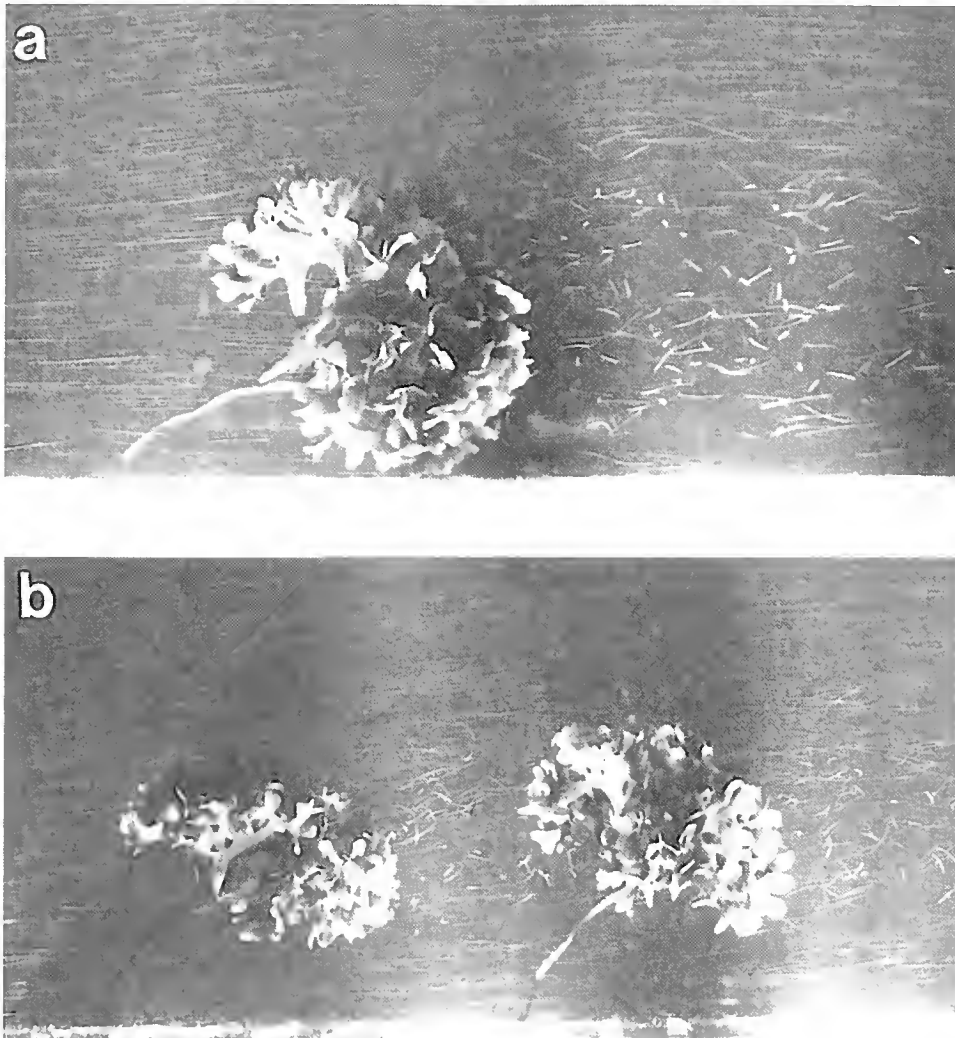


Figure 1. Long-exposure photographs of *Chondrus crispus* taken at an ambient flow speed of 0.10 m s⁻¹ showing (a) a solitary thallus and (b) a pair of thalli, where the thallus shown in (a) is in the downstream position. Flow direction is from left to right. For scale, the distance between stipes was 0.09 m. Only the middle section of the tank is illuminated by a narrow slit of light. Longer streaks indicate faster components of velocities in the downstream direction. Streaks at the top of the photograph are uniform in length, indicating freestream flow. Flow was slowed in the wake of thalli; drag was consequently less on the thallus shown in (a) when it drafted (b) within the wake of an upstream thallus. The lower drag is reflected by the decrease in bend of the stipe in (b) relative to (a).

crispus grow rapidly, outcompeting other species in the lower rocky intertidal of New England (Lubchenco, 1980; Dudgeon and Johnson, 1992; Dudgeon *et al.*, 1999).

In this study I examine how flow-induced forces on algal thalli depend on both the individual morphology of the thalli and on the density and morphology of the surrounding canopy. I specifically determine how flow-induced forces experienced by a thallus are influenced by (1) the density of the canopy, (2) the position of the thallus within the canopy, and (3) the length of stipe of a thallus relative to the height of the canopy.

Materials and Methods

Collection and maintenance of algae

Thalli of *Chondrus crispus* were collected at a shallow subtidal site at 9 m in depth located 0.2 km northeast of Canoe Beach, East Point, Nahant, Massachusetts (42° 25'N; 70° 54'W). Horizontal surfaces in the collection area, which was protected from extreme wave action, were dominated by *C. crispus*. Individual thalli, still attached to the holdfast at the base of the stipe, were maintained within circulating seawater tables at 15°C and were used in experiments within 2 weeks after their removal. Thalli remained healthy for the duration of experiments.

Quantification of flow and force

The downstream forces exerted by the stipe of a thallus on the substratum were measured by attaching the end of the stipe that was originally attached to the holdfast onto a force beam. That beam protruded downward through a hole in a flat, horizontally oriented, clear acrylic plastic plate located 0.2 m above the floor of a recirculating seawater flow tank (two flow tanks were used, each 0.2 m wide by 2 m long, similar to that described in Vogel and LaBarbera, 1978). There was freestream flow adjacent to the fronds of the canopy, as is evident in Figure 1, thus indicating that boundary effects from the bottom of the flow tank were negligible. Forces measured represented those due to drag but not due to acceleration; this is reasonable, as Gaylord (2000) found that forces due to acceleration contribute negligibly to wave-induced forces measured on algal thalli.

Experimental flow speeds were constrained by the maximum flow speeds attainable within each flow tank (0.21 m s⁻¹ in the flow tank used for the quantification of the C_D and E of solitary thalli; 0.45 m s⁻¹ in the flow tank used for canopy experiments), but were similar to monthly maxima measured over the period of a year at the collection site by an Interocean S4 recording electromagnetic flow meter. The mean flow speed each month was between 0.023 and 0.042 m s⁻¹, and the maximum flow speed each month was between 0.28 and 0.61 m s⁻¹ measured at 0.5 m off the substratum (K. Sebens, University of Maryland, unpubl.

data). Thalli used in these experiments were from this subtidal habitat. Maximum flow speeds experienced by intertidal specimens of *C. crispus* in breaking waves will be faster.

Experimental flow speeds (U) were calculated from the measured drag on a flat, circular disk (diameter = 3.62×10^{-2} m) oriented perpendicular to flow, using the standard empirical drag equation

$$D = \frac{1}{2} \rho U^2 C_D S \quad (1)$$

where D = drag, ρ = fluid density, U = flow speed, C_D = coefficient of drag, and S = projected area of the disk. The disk was attached to a force beam that projected 0.05 m below the water surface in the working section of the tank. The drag on the beam alone was subtracted from each measurement. Disks have a constant coefficient of drag, $C_D = 1.17$, over the range of Reynolds numbers used in this study (Hoerner, 1965); therefore the standard empirical drag equation (Eqn. 1) applies (Vogel, 1994).

In all treatments described below, total force on a thallus was quantified as the force that the thallus exerted on the force beam. Drag accounts for the total force acting on an individual thallus only when that thallus is not mechanically interacting with other thalli within the canopy. Therefore, I call the force exerted on the beam "drag" when there were no mechanical interactions between thalli, and "total force" when there were also mechanical interactions between thalli.

Coefficient of drag

Drag measurements (at $U = 0.21$ m s⁻¹) were used to calculate the coefficient of drag (C_D) for eight solitary thalli using Eqn. 1, where S = planform area of the thallus. The planform area of each thallus was measured to the nearest 0.01 cm² by digitizing the outlines of a photograph of a thallus that had been pressed flat between two plates of glass, such that the branches of each thallus did not overlap. This measurement of planform area is equivalent to the "planform area" (Carrington, 1990), the "actual planform area" (Johnson and Koehl, 1994), the "maximal projected blade area" (Gaylord *et al.*, 1994), the "total projected blade area" (Gaylord and Denny, 1997), the "maximum projected blade area" (Denny *et al.*, 1997), and the "real area" (Koehl, 2000) quantified by other researchers. For *C. crispus*, which has a complex three-dimensional morphology, this measurement of planform area represents the most reliable and repeatable measure of S . The change in frontal area that occurs as a function of flow speed is accounted for by changes in the C_D . The eight solitary thalli used for these measurements ranged in mass from 2.6 to 7.2 g (mean = 4.5 g, SE = 0.6) and in planform area from 0.0031 to 0.0092 m² (mean = 0.0061 m², SE = 0.0008).

Reconfiguration in flow

Flexible structures such as algae reconfigure in flow as velocity increases such that their relative drag is reduced at higher flow speeds. For solitary thalli, a useful measure of velocity-dependent relative drag reduction is the E -value (Vogel, 1984), which quantifies this relative reduction in drag (*i.e.*, the decrease in C_D with increase in velocity).

$$\frac{D}{U^2} = K_E U^E \quad (2)$$

where D = drag at a particular flow speed (U). A value for E is determined as the slope of a linear regression of $\log(D/U^2)$ versus $\log U$ for regions of this graph without inflection points; K_E is the antilog of the intercept of this line. The magnitude of E is zero for a structure, such as a rigid sphere, that does not reconfigure in flow. The steeper the negative slope (*i.e.*, the greater the absolute value of the negative slope), the greater the *relative* drag reduction experienced with an increase in velocity as a consequence of reconfiguration.

E and K_E were determined for the same eight solitary thalli of *C. crispus* for which the C_D was quantified (described above).

Canopy experiments

For all treatments in the canopy experiments, force exerted by one thallus (mass = 7.9 g, planform area = 0.01 m²) on the force beam was determined at flow speeds of 0.09, 0.18, 0.27, 0.36, and 0.45 m s⁻¹. All measurements were repeated three times (sufficient sampling given the low variance observed). All statistical comparisons between treatments, using ANOVA, are for force determined at the

highest experimental flow speed (0.45 m s⁻¹). Scheffé F -tests were used for *a posteriori* comparisons between treatments.

At all experimental velocities and for all treatments, forces on the stipe of the experimental thallus were quantified when it was 0.05 m long (*i.e.*, only half the length of the stipe protruded into flow, which was the same as the length of the stipes of the rest of the canopy), and 0.10 m long (*i.e.*, the full length of the stipe protruded into flow, which was twice the length of the stipes of the rest of the canopy). Forces on the experimental thallus were quantified for the following treatments: (1) in isolation (Fig. 1a); (2) in the presence of one other thallus (of approximately the same size and shape as the experimental thallus) located 0.09 m upstream (Fig. 1b); (3) on the upstream edge, middle, and downstream edge of a lower density canopy (0.08 thalli per cm²; Fig. 2); and (4) in the middle of a higher density canopy (0.16 thalli per cm²).

The lower density experimental canopy, which consisted of 32 thalli, mimicked the observed maximum density of the bushy tops of *C. crispus* in a typical shallow subtidal zone where they were collected (0.08 thalli per cm²; determined by counting the bushy tops within 20, 100 cm² quadrats). For experimental simplicity, the higher density experimental canopy, which consisted of 64 thalli, was chosen to double that of the lower density experimental canopy. That density is similar to that of large thalli (those with more than five branches) that occurred in a low intertidal habitat (number of 5 × 5 cm quadrats = 5; mean density = 0.2 thallus per cm², SE = 0.07; S. Dudgeon, unpubl. data).

Canopies were created by fastening individual thalli to a flat plate and suspending the plate upside down in the flow tank. Canopy thalli were positioned into regularly spaced,



Figure 2. Sketch from a long-exposure photograph of a low-density canopy of *Chondrus crispus* (0.08 thalli per cm²) at an ambient flow speed of 0.1 m s⁻¹. Flow direction is from left to right. For scale, the distance from the stipe at the leading edge to the stipe on the trailing edge was 0.2 m. Streaks between the thalli of the canopy were shorter, indicating that flow was slowed within the canopy. Forces were less on thalli associated with a canopy not only because flow was slowed (*i.e.*, drag was reduced), but also because the canopy provides mechanical support: thalli were most bent over at the upstream edge of the canopy but were more erect than the more isolated thalli shown in Figure 1.

staggered arrays by inserting the narrow end of the stipe through 1-mm holes in the plate and holding the stipes in place by means of soft modeling clay. Every other row of thalli was offset from the one before it so that any given thallus within the canopy was directly downstream of another thallus two rows in front of it. The length of the stipes of the thalli within the canopy was always 0.05 m from the surface of the plate.

Results

Thalli reorient in flow

When exposed to flow, a solitary thallus of *Chondrus crispus* immediately flopped over close to the substratum with the stipe reoriented parallel to flow (Fig. 1a). A thallus also reoriented when downstream of a single other thallus but bent over less than when solitary at the same ambient flow speed (Fig. 1b). In contrast, thalli within the canopies bent over less than did solitary thalli (Fig. 2).

Coefficient of drag and E of solitary thalli

The C_D of eight solitary thalli (measured at 0.21 m s^{-1} ; range = 0.46 to 0.83, mean = 0.60, SE = 0.046) was independent of thallus size; linear regression analysis: (1) C_D by mass (g): $F_{(1,7)} = 1.8$, $P = 0.22$, (2) C_D by planform area (m^2): $F_{(1,7)} = 2.6$, $P = 0.18$.

The E of those eight thalli (range = -0.46 to -0.92 , mean = -0.64 , SE = 0.06) was independent of thallus size (linear regression analysis: $F_{(1,7)} = 2.1$, $P = 0.19$ [E by thallus mass]; $F_{(1,7)} = 1.2$, $P = 0.31$ [E by thallus area]). The magnitude of K_E increased with increasing thallus mass (linear regression analysis: $F_{(1,7)} = 6.8$, $P = 0.04$, $r^2 = 0.53$):

$$K_E = 0.132 M^{1.04}, \quad (3)$$

where the units for the coefficient were $\text{kg}^{-0.04} \text{ m}^{-0.36} \text{ s}^{-0.64}$. By substituting the values for E and K_E into Eqn. 2, it can be seen that drag for these thalli can be modeled as:

$$D = 0.132 M^{1.04} U^{1.36} \quad (4)$$

Drafting behind upstream thalli

The drag on the solitary experimental thallus of *C. crispus* used in the canopy experiments was 0.16 N (SE = 0.0015 N; measured at a flow speed of 0.45 m s^{-1} ; Fig. 3). Doubling the length of the stipe on this thallus increased drag by only 6% (mean force_(0.45 ms⁻¹) = 0.16 N (short); 0.17 N (SE = 0.00017 N, long); $t_{(4)} = 3.2$, $P = 0.03$). The $C_{D@0.45 \text{ ms}^{-1}}$ of the thallus used in the canopy experiments was 0.16.

At 0.45 m s^{-1} , drag on the experimental thallus decreased by more than 65% (ANOVA: $F_{(2,8)} = 2360$, $P \ll 0.0001$; Fig. 3) whether it was downstream of only a single thallus

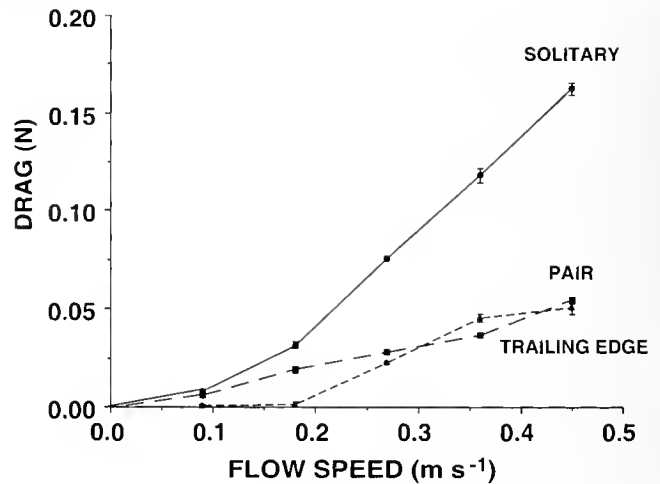


Figure 3. Drag (N) as a function of flow speed (m s^{-1}) for an experimental thallus of *Chondrus crispus* when solitary (circles, solid line), 0.09 m downstream of a single other thallus (squares, long dashed line) and on the trailing edge of a low-density canopy (triangles, short dashed line). Bars represent two standard errors about the mean; where not visible, these bars were smaller than the symbols.

(mean force_(0.45 ms⁻¹) = 0.055 N, SE = 0.00087 N) or of an entire canopy of thalli (mean force_(0.45 ms⁻¹) = 0.051 N, SE = 0.0014 N). Drag on the thallus at this flow speed was independent of whether there was only a single thallus or an entire canopy of thalli upstream (Scheffé F -test). Doubling the length of the stipe on this thallus when it was located on the downstream edge of a canopy increased the drag it experienced by 19% (mean force_(0.45 ms⁻¹) = 0.051 N [short]; 0.063 N [SE = 0.0026 N, long]; $t_{(4)} = 4.3$, $P = 0.01$).

Mechanical interactions between thalli

Total force on the experimental thallus decreased when the thallus was placed in the middle of an algal canopy (ANOVA: $F_{(2,8)} = 561$, $P \ll 0.0001$; Fig. 4) and decreased more with increasing density of the canopy (Scheffé F -tests; mean force_(0.45 ms⁻¹) = 0.089 N [SE = 0.0046 N, low density]; 0.028 N [SE = 0.00054, high density]). Thus, there was an 83% decrease in total force for this thallus in the middle of a dense canopy. Surprisingly, total force on the thallus when surrounded by a low density of neighboring thalli was greater than when it drafted in the wake of a single upstream neighbor (Scheffé F -tests; compare Fig. 3 "Pair" with Fig. 4 "Low density"). Doubling the length of the stipe did not significantly alter the total force the thallus experienced in the mid-canopy position (mean force_(0.45 ms⁻¹) = 0.089 N [short]; 0.079 N [SE = 0.0071 N, long]; $t_{(4)} = -1.2$, $P = 0.31$).

Forces on the experimental thallus varied with position in the canopy (ANOVA_(0.45 ms⁻¹); $F_{(3,11)} = 244$, $P \ll 0.0001$; Fig. 5), decreasing with increasing distance down-

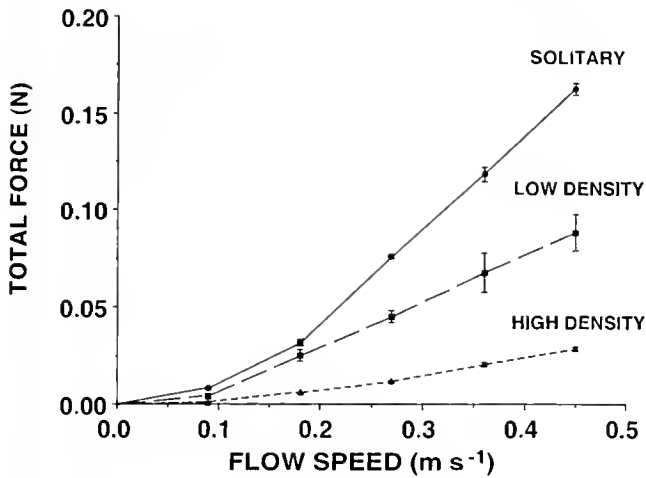


Figure 4. Force (N) as a function of flow speed (m s^{-1}) for an experimental thallus of *Chondrus crispus* when solitary (circles, solid line), in the middle of a low-density canopy (squares, long dashed line) and in the middle of a higher density canopy (triangles, short dashed line). Bars represent two standard errors about the mean; where not visible, these bars were smaller than the symbols.

stream of the upstream edge (Scheffé *F*-tests). When the experimental thallus was placed at the upstream edge of the low density canopy it experienced only 6% lower total force than when solitary (Scheffé *F*-test; mean force_(0.45 ms⁻¹) = 0.16 N [solitary]; 0.15 N [SE = 0.0042 N, upstream edge]; Fig. 5). Doubling the length of the stipe of this thallus in this upstream position increased the total force experienced by the thallus by 6% (mean force_(0.45 ms⁻¹) = 0.15 N [short]; 0.16 N [SE = 0.0028 N, long]; $t_{(4)} = 3.65$, $P = 0.02$).

Discussion

Understanding the consequences of flow to organisms entails not only examining their flow-related characteristics in isolation, but also, where appropriate, in the presence of surrounding neighbors. In marine environments, interactions among closely spaced neighbors can alter feeding currents around suspension-feeders such as sea anemones (Koehl, 1976), sabellid polychaetes (Merz, 1984), bryozoans (Okamura, 1988), and phoronids (Johnson, 1990, 1997), and can influence the productivity of algae (Taylor and Hay, 1984; Holbrook *et al.*, 1991; Dudgeon *et al.*, 1999) and seagrass (Koch, 1994). Effects on feeding and productivity occur, in part, because the presence of a canopy can alter turbulent mixing (reviewed in Worcester, 1995) and slow flow in seagrass (Fonseca *et al.*, 1982; Eckman, 1987; Gambi *et al.*, 1990; Worcester, 1995; Koch and Gust, 1999), kelp (Koehl and Alberte, 1988; Eckman *et al.*, 1989; Duggins *et al.*, 1990; Jackson, 1998), and intertidal macroalgae (this study, see Fig. 2). Alteration of flow within canopies also influences recruitment of planktonic larvae (Eckman,

1983, 1987; Jackson, 1986; Duggins *et al.*, 1990), algal propagules (Johnson and Brawley, 1998), and surfgrass seeds (Blanchette *et al.*, 1999). Canopies can also influence the subsequent growth of both invertebrates (Eckman, 1987; Eckman and Duggins, 1991) and plants (Holbrook *et al.*, 1991; Johnson and Brawley, 1998; Koch, 1999); and the risk of flow-induced dislodgment can be altered by living in dense conspecific populations as diverse as mussels (Harger and Landenberger, 1971; Bell and Gosline, 1997) and kelp (Koehl and Wainwright, 1977).

Experiments presented here show that flow-induced forces on thalli of the red alga *Chondrus crispus* must be considered in the context of interactions with neighboring thalli. The following discussion first examines how a solitary thallus of *C. crispus* orients in flow as velocity increases, and then goes on to examine the consequences of canopies to the reorientation of, and forces experienced by, a thallus.

Drag in isolation: How much do thalli reconfigure in flow?

Drag reduction is the most common mechanism considered when examining force reduction in flow. The *E* for solitary thalli of *C. crispus* (mean = -0.64) indicates that flexibility of the thalli resulted in a lower drag than the thalli would have experienced had they not reconfigured as velocity increased. Although this *E* is less negative (*i.e.*, represents a more shallow slope) than that of many other species of large macroalgae (*e.g.*, *Sargassum filipendula*: -1.06 to -1.47, Pentcheff, value given in Vogel, 1984; *Hedophyllum sessile*: -0.57 to -1.2, Armstrong, 1989; *Nereocystis luetkeana*: -0.75 to -1.2, Johnson and Koehl,

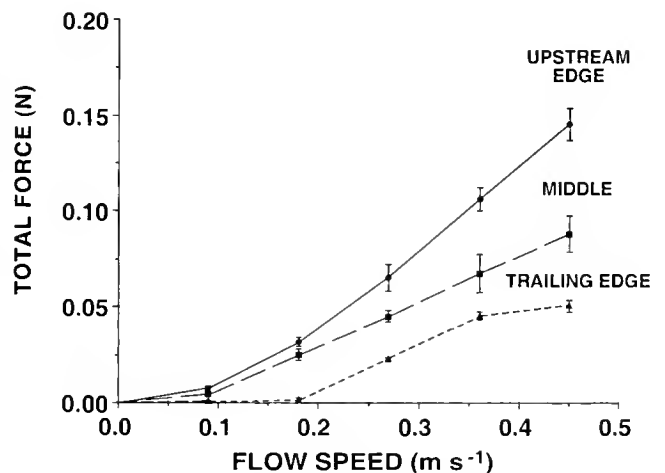


Figure 5. Force (N) as a function of flow speed (m s^{-1}) for an experimental thallus of *Chondrus crispus* when on the upstream edge (circles, solid line), middle (squares, long dashed line) and trailing edge (triangles, short dashed line) of a low-density canopy. Bars represent two standard errors about the mean; where not visible, these bars were smaller than the symbols.

1994), it is within the range of that determined for freshwater red algae (-0.33 to -1.27 ; Sheath and Hambrook, 1988), as well as for seven other species of intertidal macroalgae that are more similar in size to *C. crispus* (-0.28 to -0.76 , Carrington, 1990).

A small absolute value for a negative E can occur for thalli that are initially well-streamlined (low C_D over all flow speeds) such that additional rearrangement of the thallus has little effect on relative drag reduction with increasing flow speed (Armstrong, 1989; Johnson and Koehl, 1994). This is not the case for *C. crispus*: the coefficient of drag for *C. crispus* is relatively high at low flow speeds (this study: mean $C_D = 0.60$ at 0.21 m s^{-1} ; Dudgeon and Johnson, 1992: mean $C_D = 0.48$ at 0.21 m s^{-1} , $n = 33$) even for a small intertidal macroalga (Carrington, 1990). Thus, drag reduction, either by built-in streamlining (low C_D over all velocities, small absolute value of E) or by rearrangement into a more streamlined shape (high C_D at low velocities, but large absolute value of E), appears to be relatively unimportant to *C. crispus*. Perhaps drag reduction is a relatively unimportant source of force reduction when thalli are within a dense canopy of surrounding thalli.

Reduction of forces in canopies: The role of drafting and mechanical interactions between thalli

The response of the experimental thallus of *C. crispus* to flow differed dramatically between the solitary, paired, and within-canopy treatments. Differences in response were reflected in the degree to which thalli reoriented and by the magnitude of the forces experienced by the stipe in a given flow. The solitary experimental thallus, which experienced the greatest reorientation, also experienced the greatest forces; the presence of even a single upstream neighbor decreased the reorientation of, as well as the force on, that thallus. These changes occurred because the downstream (experimental) thallus was within the area of slowed water movement in the wake of the upstream thalli (Fig. 1b). I call this phenomenon "drafting" by analogy to the strategy racing bicyclists use, whereby a bicyclist rides in the wake of the bicycle in front. Thus, the higher drag on a downstream thallus with a longer stipe probably occurred because the longer stipe placed that thallus into a faster region of the wake of the upstream thallus.

Since flow speed within the canopy is expected to decrease with increasing canopy density (Gambi *et al.*, 1990), it is tempting to conclude that the decrease in force experienced by the thallus within a canopy was also due to a concomitant decrease in its drag. Just drafting in the wake of a single upstream neighbor, however, reduced force on the experimental thallus more than being surrounded by the lower density canopy. Why might the presence of a surrounding canopy result in a *higher* force than just a single neighbor?

The experimental thallus in the middle of a canopy could not collapse and reorient in the same way as a solitary thallus (compare Fig. 1 with Fig. 2). It was mechanically supported by the surrounding canopy, as well as being physically pushed and pulled by its surrounding neighbors. Thus, forces within algal canopies are due not only to hydrodynamic drag on specific individual thalli, but are also a result of physical interactions within the surrounding canopy. Upstream thalli were also mechanically supported by the canopy (Fig. 2), as seen by the reduced force on a thallus in this position when compared with that on the solitary thallus.

Similarly, Holbrook *et al.* (1991) found that dense stands of the sea palm *Postelsia palmaeformis* provided mechanical support for central members, which drooped over when the surrounding neighbors were removed. In contrast, Koehl and Wainwright (1977) suggested that mechanical entanglements between thalli of the giant kelp *Nereocystis luetkeana* increase loads on unbroken stipes in a tangled group of broken and unbroken thalli, thereby increasing the probability of breakage of the unbroken stipes within the canopy. A critical difference between these two species is that *P. palmaeformis* resists gravitational forces in air with short, wide stipes, whereas *N. luetkeana* resists hydrodynamic forces in pure tension by means of long, slender stipes. *C. crispus* is more similar to *N. luetkeana* in that the stipes resist hydrodynamic forces in tension, but is dissimilar in that downstream individuals of *C. crispus* can provide mechanical support to upstream thalli and in that the smaller size of *C. crispus* is likely to make any specific entanglements between thalli easier to untangle and less likely to promote dislodgement.

My results are in contrast to those of Carrington (1990), who found only minor drag reduction among groups of up to six thalli of *Mastocarpus papillatus*, a similar species of intertidal red alga (both species are in the order Gigartinales). There are several reasons for the differences in our results. Firstly, there were methodological differences between the studies. The canopies that I mimicked, which consisted of 32 and 64 thalli, were larger than that of Carrington (1990). The more extensive canopies used in my study better mimic those in which *C. crispus* naturally occurs. Furthermore, Carrington (1990) measured drag on the entire group of thalli (not on an individual thallus within the group) and then divided the total drag for that group by the sum of the drags measured for each individual thallus. While this method will give an estimate of drag reduction experienced by the entire group (*e.g.*, Vogel, 1989), it will fail to reveal much about forces experienced by individual thalli in different positions within the group. The latter is more important because it is the individual stipes of the thalli that typically break, not the holdfasts (which can be shared by multiple thalli).

Secondly, the differences between the results of our stud-

ies could be due to differences in the morphology of the species we studied. For example, unlike the majority of intertidal seaweeds, including *M. papillatus*, large *C. crispus* thalli do not lay flattened on the substratum when emersed during low tides but instead are supported by the three-dimensional branches of their thalli. Furthermore, comparisons of C_D between these studies indicate that *C. crispus* (this study: subtidal $C_{D(0.21\text{ m s}^{-1})} = 0.46\text{--}0.83$; mean $C_{D(0.21\text{ m s}^{-1})} = 0.60$; Dudgeon and Johnson [1992]: intertidal $C_{D(0.21\text{ m s}^{-1})} = 0.19\text{--}1.1$, mean $C_{D(0.21\text{ m s}^{-1})} = 0.48$, $n = 33$; M. Pratt and A. Johnson [unpubl. data]: intertidal $C_{D(0.55\text{ m s}^{-1})} = 0.14\text{--}0.91$, mean $C_{D(0.55\text{ m s}^{-1})} = 0.39$, $n = 149$) has an overall higher drag morphology than *M. papillatus* ($C_{D(1\text{ m s}^{-1})} = 0.02\text{--}0.27$; predicted $C_{D(0.21\text{ m s}^{-1})} = 0.28$; Carrington, 1990). These results suggest that intertidal *M. papillatus* is a more streamlined alga (relatively low C_D over all velocities) than *C. crispus* and would therefore be less subject to mechanical interlocking of thalli within a canopy.

A streamlined or streamlining morphology typically reduces the drag on macroalgae (Vogel, 1984; Johnson and Koehl, 1994; Koehl, 1986; Gerard, 1987; Koehl and Alberte, 1988; Armstrong, 1989). However, for smaller macroalgae that live in dense canopies, a morphology that enhances mechanical interactions between thalli (small absolute value for a negative E , high C_D) may be more important than a low-drag morphology to the mediation of forces ultimately experienced at the stipe. Furthermore, increases in density of the canopy cause decreases in the forces experienced, which may be important to dislodgment.

Thus, the density of a canopy of *C. crispus* as well as the bushiness and morphology of constituent thalli are important ecophysiological variables in the population dynamics of *C. crispus*. There is considerable morphological variation in *C. crispus* (Chopin and Floch, 1992), which is associated with differences in flow habitat and tidal height (*e.g.*, more dichotomies per unit length at less exposed, high intertidal sites; Gutierrez and Fernandez, 1992), and with differences in water temperature (*e.g.*, faster growth rates and more branches per unit length produced at higher temperatures; Kübler and Dudgeon, 1996). The increased photosynthetic area associated with greater branching is likely to increase productivity of those thalli (Kübler and Dudgeon, 1996). An increase in photosynthetic area, as well as decreased shading from neighbors (which might be associated with a more bushy morphology), could be particularly important to subtidal populations where light is often limiting. Increased size and more extensive branching will also increase the drag of individual thalli, but might, *via* mechanical interactions with adjacent thalli, increase the protection conferred by canopies.

Do canopies reduce risk of dislodgment?

For *C. crispus*, the presence of a canopy clearly decreases the forces on, and increases the upright orientation of, constituent thalli. If such forces were an important source of thallus loss, one might reasonably conclude that canopies reduce risk of dislodgment of thalli within the canopy. However, for *C. crispus* thalli growing subtidally, the drag determined on the solitary thallus in this study (0.16 N measured at 0.45 m s^{-1}) was more than an order of magnitude less than that required to break healthy, undamaged stipes of *C. crispus* (breaking force = 3 to 12 N; Dudgeon and Johnson, 1992). An order of magnitude difference persists even if the standard drag equation (Eqn. 1) is used to overestimate the force on a stipe at the highest flow speed measured in the field in the subtidal habitat where *C. crispus* was collected for this study (0.3 N; 0.61 m s^{-1}). This result indicates that subtidal thalli of *C. crispus* have an environmental stress factor (ESF; calculated as the ratio of breaking force to the force due to drag) of at least 10. ESF is a safety factor calculated over a specific time period (*e.g.*, a season) or a life-history stage rather than over a lifetime; *sensu* Johnson and Koehl, 1994. High values of ESF imply relative safety, whereas low values of ESF imply higher risk of dislodgement. Thus, only thalli otherwise compromised by damage are likely to break in this subtidal habitat (see Biedka *et al.*, 1987, and Denny *et al.*, 1989, for a discussion of the contribution of cracks to the fracture mechanics of macroalgae).

In contrast, the largest thalli of intertidal *C. crispus* from the summer populations are typically dislodged during fall and winter storms (Dudgeon and Johnson, 1992; M. Pratt and A. Johnson, unpubl. data). So, intertidal canopies do not prevent thallus dislodgment. They probably do, however, increase the flow speed at which a thallus of a given size can persist in the intertidal. An example calculation will illustrate this point. Although subtidal thalli can sometimes have longer stipes, larger size, and greater branching than do intertidal thalli (*pers. obs.*), thalli similar in size (m^2) and shape (C_D) to those used in the present experiments occur at intertidal sites: the experimental thalli used in the present study overlap in terms of both C_D (t -test, $P_{1,46} = 0.41$) and planform area (t -test, $P_{1,46} = 0.79$) with the largest thalli found in two dense intertidal canopies in Maine in the autumn (M. Pratt and A. Johnson, unpubl. data). Because of the similarity in size and shape of the subtidal and intertidal thalli from these two studies, the E -value from this study (Eqn. 4) can be used to estimate the drag of the intertidal thalli, and thereby their ESF, at the site-relevant maximum flow speeds for these intertidal sites in the autumn (M. Pratt and A. Johnson, unpubl. data). This method might still overestimate drag (underestimate ESF) if the E of intertidal thalli were more negative than those of the subtidal thalli (*i.e.*, the intertidal thalli were more flexible). Counterbal-

ancing this possibility is that this method of estimation (as used by Gaylord *et al.*, 1994; Denny, 1995; Bell, 1999) tends to underestimate drag (overestimate ESF) because E tends to get less negative at higher flow speeds as thalli reach their maximum ability to reconfigure (Bell, 1999). Even though this method tends to underestimate drag at higher flow speeds, 83% of the largest thalli found at these intertidal sites in the autumn are predicted to have a maximum drag greater than the maximum breaking force for their stipes. Thus, 83% of thalli have an $ESF < 1$ (mean $ESF = 0.62$ [SE = 0.06], t -test: $P_{(1,39)} < 0.001$ that the mean ESF is equal to 1; range $ESF = 0.1$ – 1.5).

The unexpected presence of these thalli in the autumn intertidal could result in part from differences in local flow microhabitat; however, this seems unlikely as the flow measurements were made in the middle of the algal canopy. Thalli might also persist if their C_D values at these high flow speeds were lower than those predicted from the E -value used; however, this is also unlikely as the method used already tends to give a low estimate for the C_D (Bell, 1999). Instead, thalli may persist at higher flows than predicted from estimates on individual thalli because of the mediation of those forces by the surrounding canopies.

Canopies matter

Measurements of drag, C_D , and E of isolated thalli must be considered in the context of the forces that thalli experience within canopies. This is because the morphology of thalli may influence breakage not only because of their individual drag characteristics, but also because of the way that morphology influences the forces that they experience within canopies. Even in the absence of breakage, canopy-induced changes in forces on thalli are important. The consequent reorientation and reconfiguration of thalli are likely to affect important processes, such as rates of photosynthesis (Greene and Gerard, 1990; Norton, 1991; Wing and Patterson, 1993; Kübler and Raven, 1994) or the probability of fertilization (Brawley and Johnson, 1992). For algae that live in canopies, an understanding of the consequences of the interaction of their morphology with flow requires information not just in isolation, but also within the canopies they compose.

Acknowledgments

Thanks to T. Joseph Bradley, S. Dudgeon, O. Ellers, J. Gosline, M. Koehl, J. Miles, and D. Ritchie for helpful discussions and assistance and to B. Lindsay for the drawing of the canopy. Thanks also to S. Dudgeon, M. Pratt, and K. Sebens for use of unpublished data and to two anonymous reviewers.

Literature Cited

- Armstrong, S. L. 1989. The behavior in flow of the morphologically variable seaweed *Hedophyllum sessile* (CAG) Setchell. *Hydrobiologia* **183**: 115–122.
- Bell, E. C. 1999. Applying flow tank measurements to the surf zone: predicting dislodgment of the Gigartinales. *Phycol. Res.* **47**: 159–166.
- Bell, E. C., and J. M. Gosline. 1997. Strategies for life in flow: tenacity, morphometry, and probability of dislodgment of two *Mytilus* species. *Mar. Ecol. Prog. Ser.* **159**: 197–208.
- Biedka, R. F., J. M. Gosline, and R. E. De Wreede. 1987. Biomechanical analysis of wave-induced mortality in the marine alga *Pterygophora californica*. *Mar. Ecol. Prog. Ser.* **36**: 163–170.
- Blanchette, C. A. 1997. Size and survival of intertidal plants in response to wave action: a case study with *Fucus gardneri*. *Ecology* **78**: 1563–1578.
- Blanchette, C. A., S. E. Worcester, D. Reed, and S. J. Holbrook. 1999. Algal morphology, flow, and spatially variable recruitment of surfgrass *Phyllospadix torreyi*. *Mar. Ecol. Prog. Ser.* **184**: 119–128.
- Brawley, S. H., and L. Johnson. 1992. Gametogenesis, gametes and zygotes: an ecological perspective on sexual reproduction in the algae. *Br. Phycol. J.* **27**: 233–252.
- Carrington, E. 1990. Drag and dislodgment of an intertidal macroalga: consequences of morphological variation in *Mastocarpus papillatus* Kutzing. *J. Exp. Mar. Biol. Ecol.* **139**: 185–200.
- Charters, A. C., M. Neushul, and C. Barilotti. 1969. The functional morphology of *Eisenia arborea*. *Proc. Int. Seaweed Symp.* **6**: 89–105.
- Chopin, T., and J.-Y. Floch. 1992. Eco-physiological and biochemical study of two of the most contrasting forms of *Chondrus crispus* (Rhodophyta, Gigartinales). *Mar. Ecol. Prog. Ser.* **81**: 185–195.
- Denny, M. W. 1995. Predicting physical disturbance: mechanistic approaches to the study of survivorship on wave-swept shores. *Ecol. Monogr.* **65**: 371–418.
- Denny, M. W. 1999. Are there mechanical limits to size in wave-swept organisms? *J. Exp. Biol.* **202**: 3463–3467.
- Denny, M. W., V. Brown, E. Carrington, G. Kraemer, and G. Miller. 1989. Fracture mechanics and the survival of wave-swept macroalgae. *J. Exp. Mar. Biol. Ecol.* **127**: 211–228.
- Denny, M. W., B. P. Gaylord, and E. A. Cowen. 1997. Flow and flexibility. II. The roles of size and shape in determining wave forces on the bull kelp *Nereocystis luetkeana*. *J. Exp. Biol.* **200**: 3165–3183.
- Dudgeon, S. R., and A. S. Johnson. 1992. Thick versus thin: thallus morphology and tissue mechanics influence differential drag and dislodgment of two co-dominant seaweeds. *J. Exp. Mar. Biol. Ecol.* **165**: 23–43.
- Dudgeon, S. R., R. S. Steneck, J. R. Davison, and R. L. Vadas. 1999. Coexistence of similar species in a space-limited intertidal zone. *Ecol. Monogr.* **69**: 331–352.
- Duggins, D. O., J. E. Eckman, and A. T. Sewell. 1990. Ecology of understory kelp environments. II. Effects of kelps on recruitment of benthic invertebrates. *J. Exp. Mar. Biol. Ecol.* **143**: 27–45.
- Eckman, J. E. 1983. Hydrodynamic processes affecting benthic recruitment. *Limnol. Oceanogr.* **28**: 241–257.
- Eckman, J. E. 1987. The role of hydrodynamics in recruitment, growth, and survival of *Argopecten irradians* (L.) and *Anomia simplex* (D'Orbigny) within eelgrass meadows. *J. Exp. Mar. Biol. Ecol.* **106**: 165–191.
- Eckman, J. E., and D. O. Duggins. 1991. Life and death beneath macrophyte canopies: effects of understory kelps on growth rates and survival of marine, benthic suspension feeders. *Oecologia* **87**: 473–487.
- Eckman, J. E., D. O. Duggins, and A. T. Sewell. 1989. Ecology of understory kelp environments. I. Effects of kelps on flow and particle transport near the bottom. *J. Exp. Mar. Biol. Ecol.* **129**: 173–187.

- Fonseca, M. S., J. S. Fisher, J. C. Zieman, and G. W. Thayer. 1982. Influence of the seagrass, *Zostera marina* L., on current flow. *Estuar. Coast. Shelf Sci.* **15**: 351–364.
- Gambi, M. C., A. R. M. Nowell, and P. A. Jumars. 1990. Flume observations on flow dynamics in *Zostera marina* (eelgrass) beds. *Mar. Ecol. Prog. Ser.* **61**: 159–169.
- Gaylord, B. 2000. Biological implications of surf-zone flow complexity. *Limnol. Oceanogr.* **45**: 174–188.
- Gaylord, B., and M. W. Denny. 1997. Flow and flexibility. I. Effects of size, shape and stiffness in determining wave forces on the stipitate kelps *Eisenia arborea* and *Pterygophora californica*. *J. Exp. Biol.* **200**: 3141–3164.
- Gaylord, B., C. Blanchette, and M. W. Denny. 1994. Mechanical consequences of size in wave-swept algae. *Ecol. Monogr.* **64**: 287–313.
- Gerard, V. A. 1987. Hydrodynamic streamlining of *Laminaria saccharina* Lamour. in response to mechanical stress. *J. Exp. Mar. Biol. Ecol.* **107**: 237–244.
- Greene, R. M., and V. A. Gerard. 1990. Effects of high-frequency light fluctuations on growth and photoacclimation of the red alga *Chondrus crispus*. *Mar. Biol.* **105**: 337–344.
- Gutierrez, L. M., and C. Fernandez. 1992. Water motion and morphology in *Chondrus crispus* (Rhodophyta). *J. Phycol.* **28**: 156–162.
- Harger, J. R. E., and D. E. Landenberger. 1971. The effect of storms as a density dependent mortality factor on populations of sea mussels. *Veliger* **14**: 195–201.
- Hoerner, S. F. 1965. *Fluid Dynamic Drag*. Hoerner Fluid Dynamics, Bricktown, NJ.
- Holbrook, N. M., M. W. Denny, and M. A. R. Koehl. 1991. Intertidal "trees": consequences of aggregation on the mechanical and photosynthetic properties of sea palms *Postelsia palmaeformis* Ruprecht. *J. Exp. Mar. Biol. Ecol.* **146**: 39–67.
- Hurd, C. L. 2000. Water motion, marine macroalgal physiology, and production. *J. Phycol.* **36**: 453–472.
- Jackson, G. A. 1986. Interaction of physical and biological processes in the settlement of planktonic larvae. *Bull. Mar. Sci.* **39**: 202–212.
- Jackson, G. A. 1998. Currents in the high drag environment of a coastal kelp stand off California. *Cont. Shelf Res.* **17**: 1913–1928.
- Johnson, A. S. 1990. Flow around phoronids: consequences of a neighbor to suspension feeders. *Limnol. Oceanogr.* **35**: 1395–1401.
- Johnson, A. S. 1997. Flow is genet and ramet blind: consequences of individual, group and colony morphology on filter feeding and flow. *Proceedings of the 8th International Coral Reef Symposium* **2**: 1093–1096.
- Johnson, A. S., and M. A. R. Koehl. 1994. Maintenance of dynamic strain similarity and environmental stress factor in different flow habitats: thallus allometry and material properties of a giant kelp. *J. Exp. Biol.* **195**: 381–410.
- Johnson, L. E., and S. H. Brawley. 1998. Dispersal and recruitment of a canopy-forming intertidal alga: the relative roles of propagule availability and post-settlement processes. *Oecologia* **117**: 517–526.
- Koch, E. W. 1994. Hydrodynamics, diffusion-boundary layers and photosynthesis of the seagrasses *Thalassia testudinum* and *Cymodocea nodosa*. *Mar. Biol.* **118**: 767–776.
- Koch, E. W. 1999. Preliminary evidence on the interdependent effect of currents and porewater geochemistry on *Thalassia testudinum* Banks ex König seedlings. *Aquat. Bot.* **63**: 95–102.
- Koch, E. W., and G. Gust. 1999. Water flow in tide- and wave-dominated beds of the seagrass *Thalassia testudinum*. *Mar. Ecol. Prog. Ser.* **184**: 63–72.
- Koehl, M. A. R. 1976. Mechanical design in sea anemones. Pp. 23–31 in *Coelenterate Ecology and Behavior*, G. O. Mackie, ed. Plenum Publishing, NY.
- Koehl, M. A. R. 1986. Seaweeds in moving water: form and mechanical function. Pp. 603–734 in *On the Economy of Plant Form and Function*, T. J. Givnish, ed. Cambridge University Press, Cambridge.
- Koehl, M. A. R. 1999. Ecological biomechanics of benthic organisms: life history, mechanical design, and temporal patterns of mechanical stress. *J. Exp. Biol.* **202**: 3469–3476.
- Koehl, M. A. R. 2000. Mechanical design and hydrodynamics of blade-like algae: *Chondracanthus exasperatus*. Pp. 295–308 in *Proceedings of the Third International Plant Biomechanics Conference*, H. C. Spatz and T. Speck, eds. Thieme Verlag, Stuttgart.
- Koehl, M. A. R., and R. S. Alberte. 1988. Flow, flapping and photosynthesis of *Nereocystis luetkeana*: a functional comparison of undulate and flat blade morphologies. *Mar. Biol.* **99**: 435–444.
- Koehl, M. A. R., and S. A. Wainwright. 1977. Mechanical adaptations of a giant kelp. *Limnol. Oceanogr.* **22**: 1067–1071.
- Kübler, J. E., and S. R. Dudgeon. 1996. Temperature dependent change in the complexity of form of *Chondrus crispus* fronds. *J. Exp. Mar. Biol. Ecol.* **207**: 15–24.
- Kübler, J. E., and J. A. Raven. 1994. Consequences of light limitation for carbon acquisition in three rhodophytes. *Mar. Ecol. Prog. Ser.* **110**: 203–209.
- Luhchenco, J. 1980. Algal zonation in the New England rocky intertidal community: an experimental analysis. *Ecology* **61**: 333–344.
- Mathieson, A. C., and R. L. Burns. 1971. Ecological studies of economic red algae. I. Photosynthesis and respiration of *Chondrus crispus* Stackhouse and *Gigartina stellata* (Stackhouse) Batters. *J. Exp. Mar. Biol. Ecol.* **7**: 197–206.
- Merz, R. A. 1984. Self-generated versus environmentally produced feeding currents: a comparison for the sabellid polychaete *Eudistylia vancoveri*. *Biol. Bull.* **167**: 200–209.
- Norton, T. A. 1991. Conflicting constraints on the form of intertidal algae. *Br. Phycol. J.* **26**: 203–218.
- Okamura, B. 1988. The influence of neighbors on the feeding of an epifaunal bryozoan. *J. Exp. Mar. Biol. Ecol.* **120**: 105–123.
- Shaughnessy, F. J., R. E. De Wreede, and E. C. Bell. 1996. Consequences of morphology and tissue strength to blade survivorship of two closely related Rhodophyta species. *Mar. Ecol. Prog. Ser.* **136**: 257–266.
- Sheath, R. G., and J. A. Hambrink. 1988. Mechanical adaptations to flow in freshwater red algae. *J. Phycol.* **24**: 107–111.
- Taylor, P. R., and M. E. Hay. 1984. Functional morphology of intertidal seaweeds: adaptive significance of aggregate vs. solitary forms. *Mar. Ecol. Prog. Ser.* **18**: 295–302.
- Vogel, S. 1984. Drag and flexibility in sessile organisms. *Am. Zool.* **24**: 37–44.
- Vogel, S. 1989. Drag and reconfiguration of broad leaves in high winds. *J. Exp. Botany* **40**: 941–948.
- Vogel, S. 1994. *Life in Moving Fluids*. Princeton University Press, Princeton.
- Vogel, S., and M. LaBarbera. 1978. Simple flow tanks for research and teaching. *BioScience* **28**: 638–643.
- Wing, S. R., and M. R. Patterson. 1993. Effects of wave-induced light flecks in the intertidal zone on the photosynthesis in the macroalgae *Postelsia palmaeformis* and *Hedophyllum sessile* (Phaeophyceae). *Mar. Biol.* **116**: 519–525.
- Worcester, S. E. 1995. Effects of eelgrass beds on advection and turbulent mixing in low current and low shoot density environments. *Mar. Ecol. Prog. Ser.* **126**: 223–232.

Ontogenetic Changes in Fibrous Connective Tissue Organization in the Oval Squid, *Sepioteuthis lessoniana* Lesson, 1830

JOSEPH T. THOMPSON* AND WILLIAM M. KIER

Department of Biology, CB#3280 Coker Hall, University of North Carolina, Chapel Hill, North Carolina 27599-3280

Abstract. Ontogenetic changes in the organization and volume fraction of collagenous connective tissues were examined in the mantle of *Sepioteuthis lessoniana*, the oval squid. Outer tunic fiber angle (the angle of a tunic collagen fiber relative to the long axis of the squid) decreased from 33.5° in newly hatched animals to 17.7° in the largest animals studied. The arrangement of intramuscular collagen fiber systems 1 (IM-1) and 2 (IM-2) also changed significantly during ontogeny. Because of the oblique trajectory of the IM-1 collagen fibers, two fiber angles were needed to describe their organization: (1) IM-1_{SAG}, the angle of an IM-1 collagen fiber relative to the squid's long axis when viewed from a sagittal plane and (2) IM-1_{TAN}, the angle of an IM-1 collagen fiber relative to the squid's long axis when viewed from a plane tangential to the outer curvature of the mantle. The sagittal component (IM-1_{SAG}) of the IM-1 collagen fiber angle was lowest in hatchling squid (32.7°) and increased exponentially during growth to 43° in squid with a dorsal mantle length (DML) of 15 mm. In squid larger than 15 mm DML, IM-1_{SAG} fiber angle did not change. The tangential component (IM-1_{TAN}) of IM-1 collagen fiber angle was highest in hatchling squid (39°) and decreased to 32° in the largest squid examined. IM-2 collagen fiber angle (the angle of an IM-2 collagen fiber relative to the outer surface of the mantle) was lowest in hatchling squid (34.6°) and increased exponentially to about 50° in 15-mm DML animals. In squid larger than 15 mm

DML, IM-2 fiber angle increased slightly with size. The volume fraction of collagen in IM-1 and IM-2 increased 68 and 36 times, respectively, during growth. The ontogenetic changes in the organization of collagen fibers in the outer tunic, IM-1, and IM-2 may lead to ontogenetic differences in the kinematics of mantle movement and in elastic energy storage during jet locomotion.

Introduction

In the hydrostatic skeletons of soft-bodied invertebrates, the organization of connective tissue fibers is crucial for providing structural reinforcement, controlling shape, transmitting stresses, and storing elastic energy (*e.g.*, Harris and Crofton, 1957; Chapman, 1958; Clark and Cowey, 1958; Clark, 1964; Wainwright, 1970; Wainwright *et al.*, 1976; Wainwright and Koehl, 1976; Koehl, 1977; Gosline and Shadwick, 1983a). Though not particularly well documented for invertebrates, the organization of connective tissue fibers can change substantially during ontogeny (Cassada and Russell, 1975; Cox *et al.*, 1981). Such ontogenetic changes in the arrangement of connective tissue fibers may alter the functions and properties of the hydrostatic skeleton. The goal of this study is to examine the functional implications of ontogenetic changes in connective tissue fiber organization in a soft-bodied invertebrate.

Squid mantle morphology

Squid are soft-bodied molluscs that combine a hydrostatic skeleton with an uncalcified, chitinous gladius (= pen) to provide shape and structural support for the mantle. The mantle lacks the large, fluid-filled spaces characteristic of the hydrostatic skeleton of many worms and polyps. Instead, the muscle fibers and connective tissue fibers of the

Received 13 December 2000; accepted 8 May 2001.

*To whom correspondence should be addressed. E-mail: joethomp@email.unc.edu

Abbreviations: DML, dorsal mantle length; IM-1, intramuscular fiber system 1; IM-1_{SAG}, sagittal component of IM-1 fiber angle; IM-1_{TAN}, tangential component of IM-1 fiber angle; IM-2, intramuscular fiber system 2.

mantle are packed into a dense, three-dimensional array. Water contained within the muscle fibers and the connective tissue fibers themselves serves as the incompressible fluid. In such a system of structural support, termed a "muscular hydrostat" by Kier and Smith (1985), the volume of the mantle remains constant, such that a change in one dimension must result in a change in at least one of the other dimensions of the mantle.

The mechanical support for the mantle arises from a complex, three-dimensional arrangement of muscle fibers, connective tissue fibers, and the gladius. The muscle fibers in squid mantle are arranged primarily in two orientations: circumferentially and radially. Contraction of the circumferential muscles decreases mantle circumference and expels water from the mantle cavity through the funnel during the exhalant phase of jet locomotion (Young, 1938). Contraction of the radial muscle fibers thins the mantle wall and increases the mantle circumference, filling the mantle cavity during the inhalant phase of jet locomotion (Young, 1938).

The fibrous connective tissues of the squid mantle are arranged into five networks (Fig. 1): the inner and outer tunics, which sandwich the circumferential and radial muscles, plus three networks of intramuscular collagen fibers (Ward and Wainwright, 1972; Bone *et al.*, 1981). Intramuscular fiber system 1 (IM-1) consists of collagen fibers (Gosline and Shadwick, 1983b; MacGillivray *et al.*, 1999) that originate and insert on the inner and outer tunics (Ward and Wainwright, 1972). Viewed in sagittal section, the IM-1 collagen fibers are arranged at a low angle (28° in *Loliguncula brevis*) relative to the long axis of the mantle (Ward and Wainwright, 1972) (Fig. 1). In sections tangential to the surface of the mantle, the collagen fibers in IM-1 are also arranged at low angles (10° to 15° in *Alloteuthis subulata*) relative to the long axis of the mantle (Bone *et al.*, 1981) (Fig. 1). Thus, the IM-1 fibers actually follow an oblique path through the mantle wall, relative to both tangential and sagittal planes.

Intramuscular fiber system 2 (IM-2) is composed of collagen fibers (MacGillivray *et al.*, 1999) localized to the radial muscle bands (Bone *et al.*, 1981) (Fig. 1). Collagen fibers in IM-2 originate and insert on the inner and outer tunics and are arranged at an angle of about 55° to the mantle surface in *Alloteuthis subulata* (Bone *et al.*, 1981).

The final connective tissue fiber system in squid mantle is intramuscular fiber system 3 (IM-3). Collagen fibers (MacGillivray *et al.*, 1999) in IM-3 are arranged parallel to the circumferential muscle fibers and are not attached to the tunics (Bone *et al.*, 1981).

Mantle connective tissue function

The tunics and intramuscular collagen fibers serve important roles in controlling shape change in the mantle. The low fiber angles reported for tunic and IM-1 fibers in *Lol-*

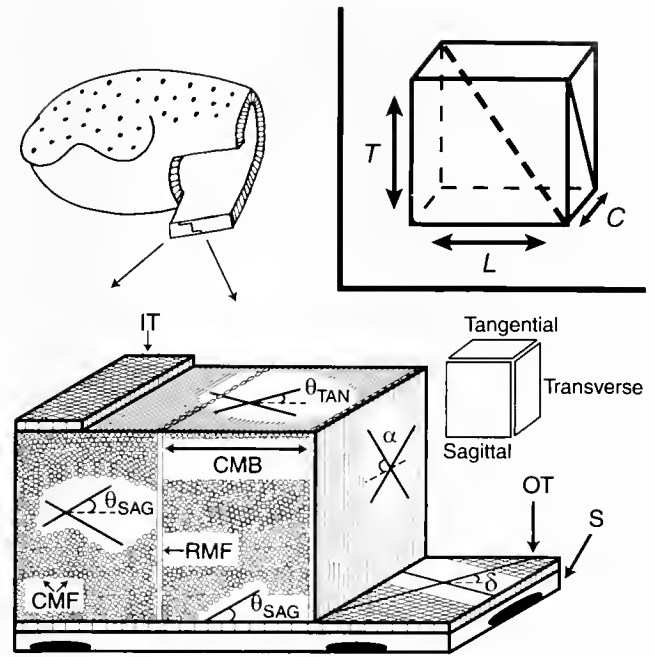


Figure 1. A schematic diagram illustrating mantle organization. The block of mantle tissue at the bottom left is from the ventral portion of the squid mantle at the upper left. The section planes are indicated immediately to the right of the block of tissue. Note that the IM-1 collagen fibers follow an oblique trajectory through the mantle. Thus, the fibers are seen in both the sagittal and tangential planes. IM-2 collagen fibers are restricted to radial muscle bands in the transverse plane. α , IM-2 fiber angle; δ , outer tunic fiber angle; θ_{SAG} , sagittal component of the IM-1 fiber angle; θ_{TAN} , tangential component of the IM-1 fiber angle; CMB, circumferential muscle band; CMF, circumferential muscle fibers; IT, inner tunic; OT, outer tunic; RMF, radial muscle fibers; S, skin. INSET. The inset at the top right of the figure is the polygon used to model the effect of ontogenetic changes in collagen fiber orientation on mantle kinematics and fiber strain. The solid gray line denotes an IM-2 collagen fiber, and the dashed gray line represents a single IM-1 collagen fiber. C, L, and T represent the circumferential direction, longitudinal direction, and thickness of the mantle wall, respectively. The circumference of the model (side C) was varied to simulate jet locomotion. See Discussion for additional details.

liguncula brevis suggest strongly that the tunics and IM-1 help prevent mantle elongation during contraction of the circumferential muscles (Ward and Wainwright, 1972). This putative role is corroborated by Ward's (1972) observation that mantle length in *L. brevis* does not change measurably during jetting, though Packard and Trueman (1974) report small (*i.e.*, $<5\%$) increases in *Loligo vulgaris* and *Sepia officinalis*.

The collagen fibers in IM-1 and IM-2 may resist the substantial increase in mantle thickness that occurs during circumferential muscle contraction. In addition, these collagen fibers are thought to store elastic energy during the exhalant phase of the jet and return that energy to help restore mantle shape and refill the mantle cavity (Ward and Wainwright, 1972; Bone *et al.*, 1981; Gosline *et al.*, 1983; Gosline and Shadwick, 1983a, b; Shadwick and Gosline,

1985; MacGillivray *et al.*, 1999; Curtin *et al.*, 2000). The IM-1 and IM-2 collagen fibers may also help restore mantle shape during the low-amplitude movements that occur during respiration (Gosline *et al.*, 1983).

Specific problem addressed

Virtually all the published work on squid mantle morphology and function is on adult loliginid squid. The few studies of hatchling or juvenile loliginid squid reveal dramatic changes in mantle function during ontogeny. For example, the morphology and physiology of the mantle musculature in *Photololigo* sp. and *Loligo opalescens* (Moltchanivskyj, 1994; Preuss *et al.*, 1997) and the neuromuscular physiology underlying the escape response in *L. opalescens* (Gilly *et al.*, 1991) change significantly during growth from hatchlings to adults. Importantly for this study, the range of mantle movement during jet locomotion in newly hatched *L. opalescens* and *Loligo vulgaris* is greater than in adult animals (Packard, 1969; Gilly *et al.*, 1991; Preuss *et al.*, 1997). Given the link between the mantle connective tissue arrangement and mantle kinematics, it is likely that the orientation, the mechanical properties, or both the orientation and mechanical properties of squid mantle collagen change during ontogeny. Here, we examine ontogenetic changes in the arrangement and amount of connective tissue in the mantle in the oval squid, *Sepioteuthis lessoniana* (Cephalopoda: Loliginidae). The effect of ontogenetic changes in the collagen fiber arrangement of the outer tunic, IM-1, and IM-2 on mantle kinematics and elastic energy storage during jet locomotion is also analyzed.

Materials and Methods

Animals

We obtained an ontogenetic series of *Sepioteuthis lessoniana* Lesson, 1830. Wild embryos collected from three locations (Gulf of Thailand; Okinawa Island, Japan; Tokyo region, East Central Japan) over a 2-year period were reared (Lee *et al.*, 1994) by the National Resource Center for Cephalopods (NRCC) at the University of Texas Medical Branch (Galveston, TX). Each of the three cohorts consisted of thousands of embryos from six to eight different egg mops. Thus, it is likely that the sample populations were not the offspring of a few closely related individuals, but were representative of the natural population at each collection site.

Commencing at hatching, and at weekly intervals thereafter, live squid were sent *via* overnight express shipping from the NRCC to the University of North Carolina. The squid, which ranged from 5 mm to 70 mm in dorsal mantle length (DML), were killed by over-anesthesia in a solution of 7.5% MgCl₂ mixed 1:1 with artificial seawater (Messen-

ger *et al.*, 1985). The MgCl₂ solution relaxed the mantle musculature of nearly all of the squid. Animals in which the mantle musculature was contracted noticeably were not used for the histological study. The MgCl₂ solution did not distort the shape of the mantle. The resting mantle diameter of an anesthetized squid was always 80% to 90% of the peak mantle diameter measured during jet locomotion in the same, unanesthetized animal (for details of the kinematics measurements, see Thompson and Kier, 2001).

Histology

The mantle tissue was examined using standard histological methods. Immediately after death, the squid were fixed whole in 10% formalin in seawater for 48 to 96 h at 20° to 23 °C. In the larger animals (>25 mm DML), the animal was decapitated to permit unrestricted flow of fixative into the mantle cavity. The mantles were fixed whole, rather than dissected into smaller blocks of tissue, to help minimize shape changes (*e.g.*, curling or bending of the tissue block) that could affect connective tissue fiber angle.

Following fixation, the tissue was dehydrated in a graded series of ethanol and cleared in HistoClear (National Diagnostics, Atlanta, GA) or Hemo-D (Fisher Scientific, Pittsburgh, PA). There was no discernible scale-related distortion of the mantle during dehydration and clearing. After clearing, the mantle was dissected into smaller pieces and embedded in paraffin (Paraplast Plus, Oxford Labware, St. Louis, MO; melting point 56 °C). To minimize shrinkage artifacts, infiltration with molten paraffin was limited to a total of 90 min (30-min baths × 3 changes) instead of the 180 min (60-min baths × 3 changes) recommended by Kier (1992).

Following clearing, most of the squid smaller than 30 mm DML were sliced in half along the sagittal plane using a fine razor blade. One half of the animal was oriented in the embedding mold to permit the cutting of sagittal sections; the other half was oriented for cutting of transverse sections. Many of the smaller squid were sliced in half along the frontal plane. The dorsal and ventral halves were oriented in the embedding molds to allow grazing sections to be cut. For the squid larger than 30 mm DML, large blocks of tissue of about 5 mm by 3 mm by the thickness of the mantle were dissected from several locations along the length and around the circumference of the mantle. These tissue blocks were oriented in the embedding molds to permit the cutting of sagittal, transverse, and tangential sections.

The tissue blocks were sectioned using a rotary microtome. The sections were mounted on slides coated with Mayer's albumin and stained with picrosirius stain (Sweet *et al.*, 1964; protocol adapted from López-DeLeón and Rojkind, 1985). Other connective tissue stains were used successfully (*e.g.*, Milligan trichrome, picro-ponceau, and van Gieson's stain) but picrosirius stain provided the best

contrast between the collagenous and non-collagenous components of the tissue sections and made identification of intramuscular collagen fibers straightforward.

Several additional attributes made picrosirius an excellent choice for this study. First, the sirius red F3B dye molecules attach with their long axes parallel to the long axes of the collagen fibrils, enhancing the natural birefringence of collagen fibers (Montes and Junqueira, 1988). Second, picrosirius is an outstanding stain for resolving the smallest collagen fibers and fibrils. The stain has been used previously to visualize the fine reticular collagen fibers present in embryonic mammalian skin and organs, the thin type-II collagen fibrils present in mammalian cartilage, and the extremely fine type-IV collagen fibrils present in mammalian basal laminae (Montes and Junqueira, 1988). Third, there is a strong correlation between the collagen volume fraction estimated from paraffin-embedded human liver sections using the picrosirius stain and the collagen volume fraction from the same tissue sections measured by hydroxyproline content analysis (López-DeLeón and Rojkind, 1985). Thus, picrosirius stain is ideal for both visualizing collagen fibers and making precise estimates of collagen volume fraction.

The stained sections were viewed using brightfield and polarized light microscopy. Fiber angles were measured from digital photomicrographic images using image analysis software (SigmaScan Pro, SPSS Science, Chicago, IL).

Initial survey

We made an initial survey of the mantle intramuscular fiber (IM) networks 1 and 2 in five squid (25 mm to 70 mm DML) to help develop a protocol for measuring IM fiber angles. In this survey, IM-1 and IM-2 fiber angles from different regions along the length and around the circumference of the mantle were examined. IM-1 and IM-2 fiber angles were measured at four positions along the length of the mantle (1/10, 1/4, 1/2, and 3/4 DML) and at three positions around the circumference of the mantle (ventral, lateral, dorsal). Given the potential for regional differences in IM fiber angle (see Results for details), all the comparisons among the squid were made at the same location: the ventral portion of the mantle between 1/3 and 2/3 DML.

IM-1 fiber angle measurements

IM-1 collagen fibers are arranged obliquely to the sagittal plane (Fig. 1). Therefore, to describe accurately the trajectory of these fibers, two fiber angles must be measured. The first angle, called IM-1_{SAG} here, is the angle of IM-1 collagen fibers relative to the long axis of the mantle in the sagittal plane (Fig. 1). The second angle, which we call IM-1_{TAN}, is the IM-1 fiber angle relative to the long axis of the mantle in a plane tangential to the outer surface of the mantle and perpendicular to the sagittal plane (Fig. 1).

IM-1_{SAG} fiber angle measurements

IM-1_{SAG} fiber angles were measured from sagittal sections (thickness 10–15 μm) of the mantle. Criteria were developed to ensure consistency across all squid in the ontogenetic series. First, all measurements of fiber angles were made from the ventral portion of the mantle between 1/3 and 2/3 DML. This eliminated errors due to variation in fiber angle along the length and around the circumference of the mantle.

Second, because the apparent fiber angle depends on the viewer's perspective, IM-1_{SAG} fiber angles were measured only from tissue sections in which the circumferential muscle fibers of the mantle were cut in nearly perfect cross section. This restriction ensured that the perspective was similar for all the squid examined. Adjusting the orientation of the tissue block relative to the microtome knife made it possible, through trial and error, to meet this criterion, and conformance was determined by examining test sections 20 μm thick.

Third, sagittal tissue sections contained IM-1 fibers of varying lengths. It was difficult to obtain accurate angle measurements of the shortest fibers in each section. Therefore, IM-1_{SAG} fiber angle measurements were made only on IM-1 fibers longer than the width of one circumferential muscle band. A circumferential muscle band was defined as a region of circumferential muscle fibers bounded by radial muscle fibers (Fig. 1).

Fourth, in all animals larger than about 15 mm DML, IM-1_{SAG} fiber angles were measured only from crossed IM-1 fibers. The angle between the two fibers was measured and the half angle reported as the IM-1_{SAG} fiber angle (Fig. 1). In squid smaller than 15 mm DML, IM-1 fibers were so scarce that there were few instances of crossed fibers. In these small squid, IM-1_{SAG} fiber angles were measured relative to the outer or the inner tunic (Fig. 1). In areas where the tunics were folded due to histological artifact, IM-1_{SAG} fiber angles were not measured.

Finally, the fiber angle of every IM-1_{SAG} fiber in a given microscope field that conformed to the criteria was measured. A minimum of 20 measurements was made from each squid larger than about 15 mm DML. Because IM-1 fibers were sparse in animals smaller than 15 mm DML, the minimum number of fiber angle measurements was eight in these animals.

IM-1_{TAN} fiber angle measurements

IM-1_{TAN} fiber angles were measured from relatively thick (10 to 15 μm) tangential sections of the mantle. To ensure consistency in fiber angle measurements among all squid, the criteria listed previously were used with two exceptions. First, IM-1_{TAN} fiber angles were measured only in those sections in which the radial muscle fibers were cut in nearly perfect cross section (determined from 20- μm ;

thick test sections). Second, for squid larger than about 15 mm DML, fiber angles were measured only from crossed IM-1 fibers. In the smallest squid (<15 mm DML), there were few IM-1 fibers and virtually no crossed fibers. In these squid, IM-1_{TAN} fiber angles were measured relative to a band of radial muscle fibers. Subtracting the measured angle from 90° gave the angle of the IM-1_{TAN} fiber relative to the long axis of the squid.

IM-2 fiber angle measurements

IM-2 fiber angles were measured from 5 μm thick transverse sections of the mantle. As with the IM-1 measurements, IM-2 fiber angles were measured only from the ventral portion of the mantle between 1/3 and 2/3 DML. Fiber angles were measured only from sections that were nearly perfect transverse sections of the mantle. Sections oblique to the transverse plane show circumferential muscle fibers in closely spaced bands separated by a few radial muscle fibers. Nearly perfect transverse sections exhibited uninterrupted circumferential muscle fibers. IM-2 fiber angle was measured only from crossed fibers (Fig. 1). Given the scarcity of IM-2 fibers in squid smaller than about 15 mm DML, it was not always possible to measure crossed fibers. In these small squid, IM-2 fiber angle was also measured relative to nearby radial muscle fibers. Finally, the fiber angle of every IM-2 fiber in the microscope field was measured. No fewer than 20 fiber angle measurements were made from each squid longer than about 15 mm DML. The relative paucity of IM-2 fibers in squid smaller than 15 mm DML reduced the minimum number of fiber angle measurements to eight per squid.

Outer tunic fiber angle measurements

Outer tunic fiber angles were measured from 5-μm-thick grazing sections of the mantle. Tunic fiber angles were measured only from the ventral portion of the mantle between 1/3 and 2/3 DML and only from crossed fibers. The half angle between the crossed tunic fibers, relative to the long axis of the squid, was reported as the fiber angle (Fig. 1). A minimum of 20 fiber angle measurements was made from each squid.

Stereology

Stereological methods were used to estimate the volume fraction of IM-1 and IM-2 collagen fibers relative to the volume of the mantle musculature. To obtain an accurate estimate of the volume fraction of a particular tissue component, stereology requires that the tissue of interest be sectioned in randomly oriented planes (Weibel, 1979). Because it is difficult to positively identify a collagen fiber in a random section plane as an IM-1 or IM-2 fiber, it was not possible to use random section planes. IM-1 collagen fiber

volume fraction was therefore determined from sagittal sections of the ventral mantle in which fiber identity could be verified. Likewise, IM-2 collagen fiber volume fraction was measured from transverse sections of the ventral mantle. Although this violates an assumption of stereology, it allows accurate comparison of the relative volume fraction of collagen fibers among squid in the ontogenetic series. However, this method is inappropriate for estimation of the absolute volume fraction of collagen fibers in the mantle (Weibel, 1979).

The procedure for collagen volume fraction determination was similar for both IM-1 and IM-2. The ventral portion of the mantle between 1/3 and 2/3 DML was examined. A slide containing either sagittal (IM-1) or transverse (IM-2) 10-μm-thick tissue sections was placed on the stage of a compound microscope, and the tissue positioned under a 40× objective lens without observation through the oculars. The tissue section was brought into focus, and an image of the section was captured by a digital camera. The image was expanded to fill the screen of the monitor, and a transparent plastic overlay with a grid of 24 lines × 24 lines (Weibel, 1979) was taped to the screen. The intersection of a collagen fiber in IM-1 (sagittal sections only) or IM-2 (transverse sections only) with the junction of two lines (= a point; there were 24 lines × 24 lines = 576 points on the grid) was counted as a "hit." After the image was sampled, the microscope stage was moved haphazardly without observing the image through the microscope. In all cases, the stage was moved sufficiently far to ensure that the same portion of the mantle tissue was not examined twice. Another digital image was then captured, and the procedure was repeated at 2 or 3 different locations within the same tissue section and on between 3 and 10 different tissue sections per squid. The average volume fraction of collagen in IM-1 and IM-2 relative to the average volume of the mantle musculature was calculated by dividing the total number of hits by the total number of points counted for each squid (Weibel, 1979).

In stereology, both the acceptable standard error of the volume fraction estimate and the volume fraction of the item of interest determine the total number of points that must be counted (Weibel, 1979). The total number of points (P_C) was determined by

$$P_C = (t_\alpha^2/m_i d^2) * (1 - V_v/V_v) \quad (\text{Weibel, 1979}) \quad (1)$$

where m_i is the number of tissue sections examined per squid, d is the confidence interval, t_α is the acceptable error probability (the chance that the true volume fraction will be outside the confidence interval), and V_v is the volume fraction of the item of interest. To determine P_C , the volume fraction (V_v) of collagen in both IM-1 and IM-2 was estimated for four squid of various sizes (5 mm, 15 mm, 27 mm, and 69 mm DML) using the procedure outlined in the

Table 1

Comparison of the relative volume fraction of collagen in IM-1 and IM-2 among squid divided into the life-history stages of Segawa (1987)

Life-history stage	IM-1 points counted	IM-1 volume fraction	IM-2 points counted	IM-2 volume fraction
Hatchling ($n = 4$)	14,985 (14,265)	0.00095 \pm 0.0002	10,414 (9,504)	0.0027 \pm 0.0018
Juvenile 1 ($n = 4$)	6,516 (616)	0.015 \pm 0.0036	5,340 (647)	0.027 \pm 0.024
Juvenile 2 ($n = 4$)	4,344 (606)	0.032 \pm 0.012	3,258 (436)	0.057 \pm 0.021
Young 2 ($n = 4$)	3,801 (975)	0.065 \pm 0.036	3,258 (746)	0.097 \pm 0.024

The mean volume fraction of collagen is listed in boldface type \pm the standard deviation of the mean. The total number of points counted for each individual squid is listed. The adjacent numbers in parentheses indicate the number of points that need to be counted ($=P_C$, see equation 1) to obtain an error probability of 5% and a confidence interval of $\pm 10\%$. Within IM-1 and within IM-2, the volume fraction of collagen differed significantly among all life-history stages (one-way ANOVA on ranks, $P < 0.05$).

previous paragraph. Using the initial estimate of V_V , an error probability of 5%, and a confidence interval of $\pm 10\%$, the total number of points to be counted (P_C) was calculated (Table 1). The V_V of collagen was strongly correlated with squid size. Thus, the total number of points counted per squid varied with size. Note that the actual number of points counted per squid was much greater than the minimum required to obtain an error probability of 5% and a confidence interval of $\pm 10\%$. Thus, the actual error probability and confidence interval were smaller than the predicted values.

Statistical analysis

The sample population used in this study was subdivided into the life-history stages described by Segawa (1987). The life-history stages were selected as an independent organization scheme upon which to base the statistical analysis. Segawa (1987) studied the life cycle of *S. lessoniana* from embryo to adult and divided the life cycle into seven stages on the basis of morphological and ecological characters. These seven stages are hatchling (up to 10 mm DML), juvenile 1 (11–25 mm DML), juvenile 2 (26–40 mm DML), young 1 (41–60 mm DML), young 2 (61–100 mm DML), subadult (100–150 mm DML), and adult (>150 mm DML). The sample population of *S. lessoniana* used in the current investigation included the hatchling, juvenile 1, juvenile 2, and young 2 stages.

Nonparametric statistics were used for most of the analyses because the sample population was not normally distributed. For comparisons among the life-history stages, Kruskal-Wallis one-way analysis of variance on ranks was used with Dunn's method of pairwise multiple comparisons (Zar, 1996). All statistical analyses were completed using SigmaStat 1.01 (SPSS Science).

Results

General description of mantle morphology

The mantle of *Sepioteuthis lessoniana* is similar to that described for other loliginid squid (Young, 1938; Ward and

Wainwright, 1972; Bone *et al.*, 1981). The outer tunic is located underneath the collagen-rich skin. The fibers within the outer tunic are robust and closely packed. The outer tunic serves as the insertion for the radial muscle fibers, the IM-1 collagen fibers, and the IM-2 collagen fibers. The fairly low-resolution microscopic methods used in this study did not permit a detailed examination of the connections between the outer tunic and the IM collagen fibers or the radial musculature.

The majority of the mantle is composed of circumferential muscle fibers. These muscle fibers are bordered by the outer and inner tunics and are partitioned by regularly spaced bands of radial muscle fibers. Consistent with the trend for *Photololigo* sp. (Moltschanivskyj, 1994), the circumferential muscle fibers increased in diameter during ontogeny from $2.5 \mu\text{m} \pm 0.49 \mu\text{m}$ (mean \pm standard deviation, $n = 46$ from four specimens) in newly hatched squid to $3.9 \mu\text{m} \pm 0.66 \mu\text{m}$ ($n = 43$ from four individuals) in the largest animals examined. In addition, the ratio of mitochondria-rich to mitochondria-poor (Bone *et al.*, 1981; Mommsen *et al.*, 1981) circumferential muscle fibers decreased from 1:5 in newly hatched squid to 1:7 in young 2 stage squid. The number of mitochondria-rich fibers adjacent to the inner tunic is twice that of the mitochondria-rich muscle fibers adjacent to the outer tunic in *S. lessoniana*.

The inner tunic is adjacent to the mantle musculature and to the thin epithelial lining of the mantle cavity. The radial muscle fibers and the collagen fibers in IM-1 and IM-2 insert on the inner tunic.

Initial survey

An initial survey of the mantle revealed that IM-1 fiber angle and IM-2 fiber angle differ both along the length and around the circumference of the mantle in an individual squid. In the ventral portion of the mantle, there were no significant differences in IM-1 fiber angle or in IM-2 fiber angle between 1/4 and 3/4 DML. However, IM-1 fiber angle was about 10° higher at 1/10 DML and about 10° lower between 3/4 DML and the posterior tip of the mantle. Similar differences in IM-1 fiber angle along the length of

the mantle were also noted in the lateral and dorsal regions. There was no correlation between mantle thickness at either 1/10 or 3/4 DML and the fiber angle at that location.

Between 1/4 and 3/4 DML, both IM-1 fiber angle and IM-2 fiber angle were about 10° lower in the dorsal region of the mantle than in either the lateral or ventral portions. Within an individual squid, there were no significant differences between the average IM-1 fiber angles or IM-2 fiber angles in the lateral or ventral portion of the mantle between 1/4 and 3/4 DML. Again, there was no apparent correlation between mantle thickness and fiber angle at a particular location around the circumference of the mantle.

The implications of these differences in collagen fiber arrangement are unclear. It is interesting, however, that MacGillivray *et al.* (1999) did not report significant differences in mantle mechanical properties either along the length or around the circumference of the mantle in *Loligo pealei*. It is possible that the differences in IM-1 and IM-2 fiber angle reported here for *S. lessoniana* are not present in *L. pealei*. Alternatively, such differences, if present, may not translate into significant differences in mantle mechanical properties.

IM-1 fiber ontogeny

IM-1 collagen fibers were scarce in newly hatched squid relative to older, larger animals (Fig. 2). Dozens of sagittal tissue sections from a hatchling squid could be searched without encountering a single IM-1 fiber. As the squid grew during ontogeny, IM-1 collagen fibers became increasingly numerous and robust (Fig. 2). The diameter of IM-1 fibers increased during ontogeny from $0.58 \mu\text{m} \pm 0.060 \mu\text{m}$ standard deviation (SD; $n = 24$ from four individuals) in newly hatched squid to $0.68 \mu\text{m} \pm 0.052 \mu\text{m}$ SD ($n = 37$ from three animals) in the young 2 stage squid.

IM-1 fiber angle changed dramatically during ontogeny (Fig. 2). IM-1_{SAG} fiber angle was between 26° and 33° in newly hatched animals and increased exponentially during growth from hatching to about 15 mm DML (Fig. 3A). IM-1_{SAG} fiber angle remained fairly constant (about 43°) in squid larger than 15 mm DML (Fig. 3A). A one-way ANOVA on ranks showed that while hatchling stage IM-1_{SAG} fiber angle was significantly lower than the fiber angle of squid in the other life-history stages examined ($P < 0.05$, Table 2), there were no significant differences in fiber angle among the juvenile 1, juvenile 2, and young 2 stage animals (Table 2).

IM-1_{TAN} fiber angle also changed substantially during ontogeny. IM-1_{TAN} fiber angle was highest in newly hatched animals (between 35° and 46°) and declined to about 28° in the largest squid examined (Fig. 3B). A one-way ANOVA on ranks indicated that hatchling stage IM-1_{TAN} fiber angle was significantly higher than the fiber angle in all older, larger animals ($P < 0.05$, Table 2).

There were no significant differences in IM-1_{TAN} fiber angle among the squid in the juvenile 1, juvenile 2, and young 2 life-history stages (Table 2).

IM-2 fiber ontogeny

IM-2 collagen fibers were scarce in newly hatched animals when compared to the older, larger squid in the study (Fig. 4). As with IM-1 fibers, many mantle tissue sections could be observed without locating a single IM-2 collagen fiber. However, IM-2 fibers increased in abundance and diameter as the squid grew during ontogeny (Fig. 4). The diameter of IM-2 collagen fibers increased from an average of $0.54 \mu\text{m} \pm 0.080 \mu\text{m}$ SD ($n = 28$ from four animals) in newly hatched squid to an average of $0.71 \mu\text{m} \pm 0.087 \mu\text{m}$ SD ($n = 31$ from three specimens) in the young 2 stage animals.

IM-2 fiber angle changed significantly during ontogeny (Fig. 4). IM-2 fiber angle was between 27° and 36° in newly hatched squid and rose exponentially until the squid grew to 15 mm DML (Fig. 3C). In squid larger than 15 mm DML, IM-2 fiber angle ranged between 48° and 58° (Fig. 3C). A one-way ANOVA on ranks showed that IM-2 fiber angle was lower in hatchling stage squid than in all older, larger animals ($P < 0.05$, Table 2). The one-way ANOVA on ranks also revealed that the IM-2 fiber angle in the juvenile 2 stage squid was marginally higher than in the juvenile 1 stage animals ($P = 0.05$, Table 2). There were no significant differences in IM-2 fiber angle between juvenile 1 and young 2 stage animals.

Outer tunic fiber ontogeny

Regardless of size, all the squid possessed a robust outer tunic (Fig. 5). The collagen fibers constituting the outer tunic changed in orientation during ontogeny. The outer tunic fiber angle was highest in newly hatched animals (between 27° and 36°) and declined during ontogeny (Fig. 3D). In squid larger than about 15 mm DML, outer tunic fiber angle decreased slightly with size from about 26° to 16° (Fig. 3D). A one-way ANOVA on ranks showed that the outer tunic fiber angle was higher in hatchling stage animals than in all older, larger squid ($P < 0.05$, Table 2). In addition, outer tunic fiber angle was slightly higher in juvenile 2 stage animals than in either juvenile 1 or young 2 stage animals ($P = 0.05$, Table 2). There were no significant differences in outer tunic fiber angle between juvenile 1 and young 2 stage squid.

Volume fraction of collagen in IM-1 and IM-2

Relative to the volume of mantle musculature, the volume fraction (V_V) of collagen in both IM-1 and IM-2 increased nearly 2 orders of magnitude during ontogeny (Fig. 6, Table 1). The volume fraction of collagen in IM-1

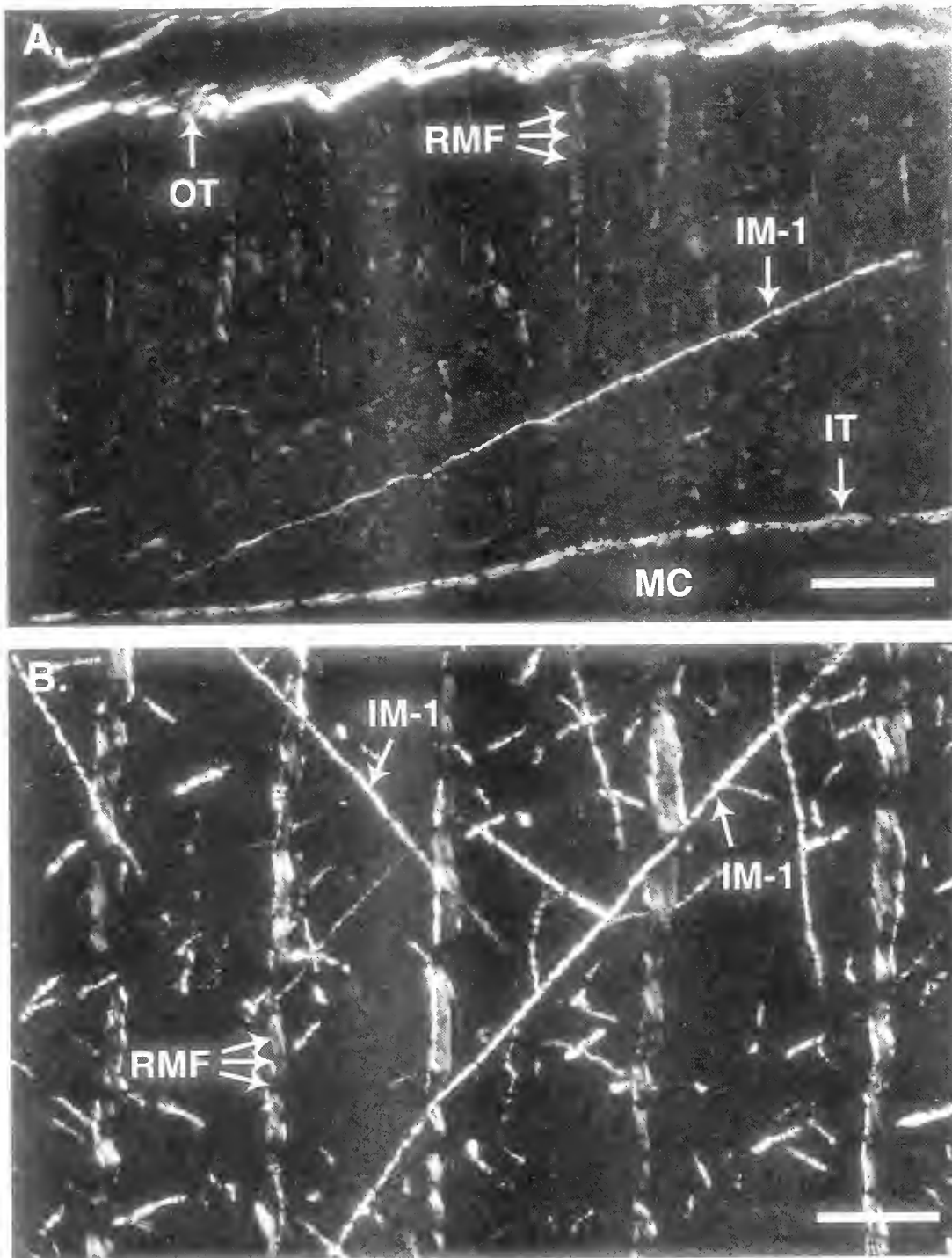


Figure 2. Photomicrographs (polarized light microscopy) of 5- μ m-thick sagittal sections of the ventral mantle that illustrate ontogenetic differences in IM-1 collagen fibers. Sections were stained with picrosirius. The orientation of the mantle in both panels is identical. IM-1, intramuscular fiber system 1 collagen fiber, IT, inner tunic, MC, mantle cavity, OT, outer tunic, RMF, radial muscle band. Scale bar in A and B, 20 μ m. (A) The ventral mantle of a newly hatched squid (DMI, 5.5 mm) with a single IM-1 collagen fiber. The section is oblique to the sagittal plane. (B) The ventral mantle of a young 2 stage squid (DMI, 65 mm). Note the low IM-1 collagen fiber angle and the absence of other IM-1 collagen fibers in the field of view in the hatching squid. In the larger squid, IM-1 fiber angles are higher, and IM-1 collagen fibers are abundant.

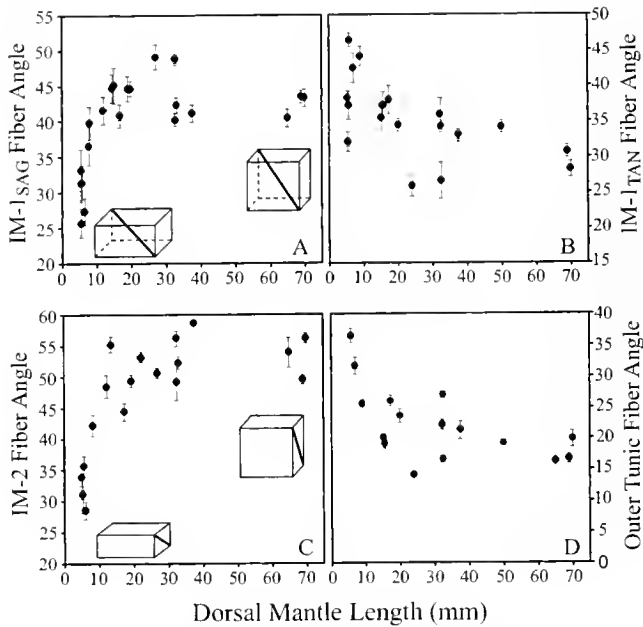


Figure 3. Ontogenetic changes in organization of mantle connective tissue. In all panels, each data point represents the mean of between 8 and 20 fiber angle measurements for one squid. The bars indicate the standard error of the mean. (A) Sagittal component of the IM-1 fiber angle *versus* dorsal mantle length (DML). IM-1_{SAG} is lowest in newly hatched squid and rises exponentially during growth up to 15 mm DML. In squid larger than 15 mm DML, IM-1_{SAG} does not change significantly. The block at the lower left illustrates the lower IM-1_{SAG} and higher IM-1_{TAN} fiber angles of a hatchling (see inset in Fig. 1 for orientation). The block at upper right illustrates the higher IM-1_{SAG} and lower IM-1_{TAN} fiber angles of an older, larger squid. (B) Tangential component of IM-1 fiber angle *versus* DML. IM-1_{TAN} is highest in newly hatched squid and declines during growth. (C) IM-2 fiber angle *versus* DML. IM-2 fiber angle is lowest in hatchlings and rises exponentially during growth up to 15 mm DML. In squid larger than 15 mm DML, IM-2 fiber angle increases slightly. The block at the lower left illustrates the lower IM-2 fiber angle in hatchlings. The block at the upper right illustrates the higher IM-2 fiber angle of larger squid. (D) Outer tunic fiber angle *versus* DML. Outer tunic fiber angle is highest in hatchlings and declines during ontogeny.

increased 68 times, from an average of 0.00095 in newly hatched squid to an average of 0.065 in the largest animals examined in this study (Table 1). A one-way ANOVA on ranks indicated that the volume fraction of collagen in IM-1 was significantly different among all the life history stages ($P < 0.05$, Table 1).

The volume fraction of collagen in IM-2 increased 36 times, from an average of 0.0027 in newly hatched animals to an average of 0.097 in the largest squid studied (Fig. 6, Table 1). A one-way ANOVA on ranks showed that the volume fraction of collagen was significantly different among all the life history stages examined ($P < 0.05$, Table 1).

Discussion

Connective tissue fibers limit the range of movement in many soft-bodied, cylindrical animals that rely upon a hydrostatic skeleton for support (*e.g.*, Harris and Crofton, 1957; Chapman, 1958; Clark and Cowey, 1958; Clark, 1964). The collagen fibers in the outer tunic, IM-1, and IM-2 may also affect the limits of mantle movement during jet locomotion. Because the fiber angles in all of the connective tissue fiber networks examined here change significantly during ontogeny, the kinematics of mantle movement probably change significantly as well.

The outer tunic

The tunics of squid are hypothesized to restrict mantle lengthening during jet locomotion (Ward and Wainwright, 1972). This important function ensures that the mechanical work performed by the circumferential musculature is used to decrease mantle cavity volume, thereby forcing water out of the funnel and producing thrust, instead of lengthening the mantle. The average outer tunic fiber angle of 17.7° from young 2 stage *Sepioteuthis lessoniana* was substantially

Table 2

Comparison of mantle collagen fiber organization among squid divided into the life-history stages of Segawa (1987)

Life-history stage	IM-1 _{SAG} fiber angle	IM-1 _{TAN} fiber angle	IM-2 fiber angle	Tunic fiber angle
Hatchling	32.7 ± 9.22 (6)	39.0 ± 6.37 (5)	34.6 ± 6.76 (5)	33.5 ± 6.37 (3)
Juvenile 1	43.7 ± 7.33 (7)	33.2 ± 6.74 (5)	49.7 ± 6.52 (5)*	20.6 ± 6.74 (5)
Juvenile 2	43.2 ± 6.29 (5)	32.8 ± 6.59 (4)	53.9 ± 6.00 (5)*	22.4 ± 6.59 (5)*
Young 2	42.3 ± 6.50 (3)	31.9 ± 3.65 (3)	53.3 ± 5.40 (3)	17.7 ± 3.65 (3)*

The mean fiber angle is listed in boldface type in each column ± the standard deviation of the mean. The number of squid in the sample is in parentheses. Each mean fiber angle was calculated from between 8 and 25 measurements of fiber angle for each squid in the sample. All the fiber angle measurements for each squid in a life-history stage were pooled to calculate the mean and the standard deviation. In each column, the mean fiber angle for the hatchling stage squid was significantly different from the mean fiber angle for the juvenile 1, juvenile 2, and young 2 life-history stages (one-way ANOVA on ranks, $P < 0.05$). The asterisks in the IM-2 fiber angle column indicate significant differences in mean fiber angle between the juvenile 1 and juvenile 2 life-history stages (one-way ANOVA on ranks, $P = 0.05$). The asterisks in the tunic fiber angle column indicate a significant difference in mean fiber angle between the juvenile 2 and young 2 life-history stages (one-way ANOVA on ranks, $P = 0.05$). Other within-column comparisons of fiber angle were not significantly different.

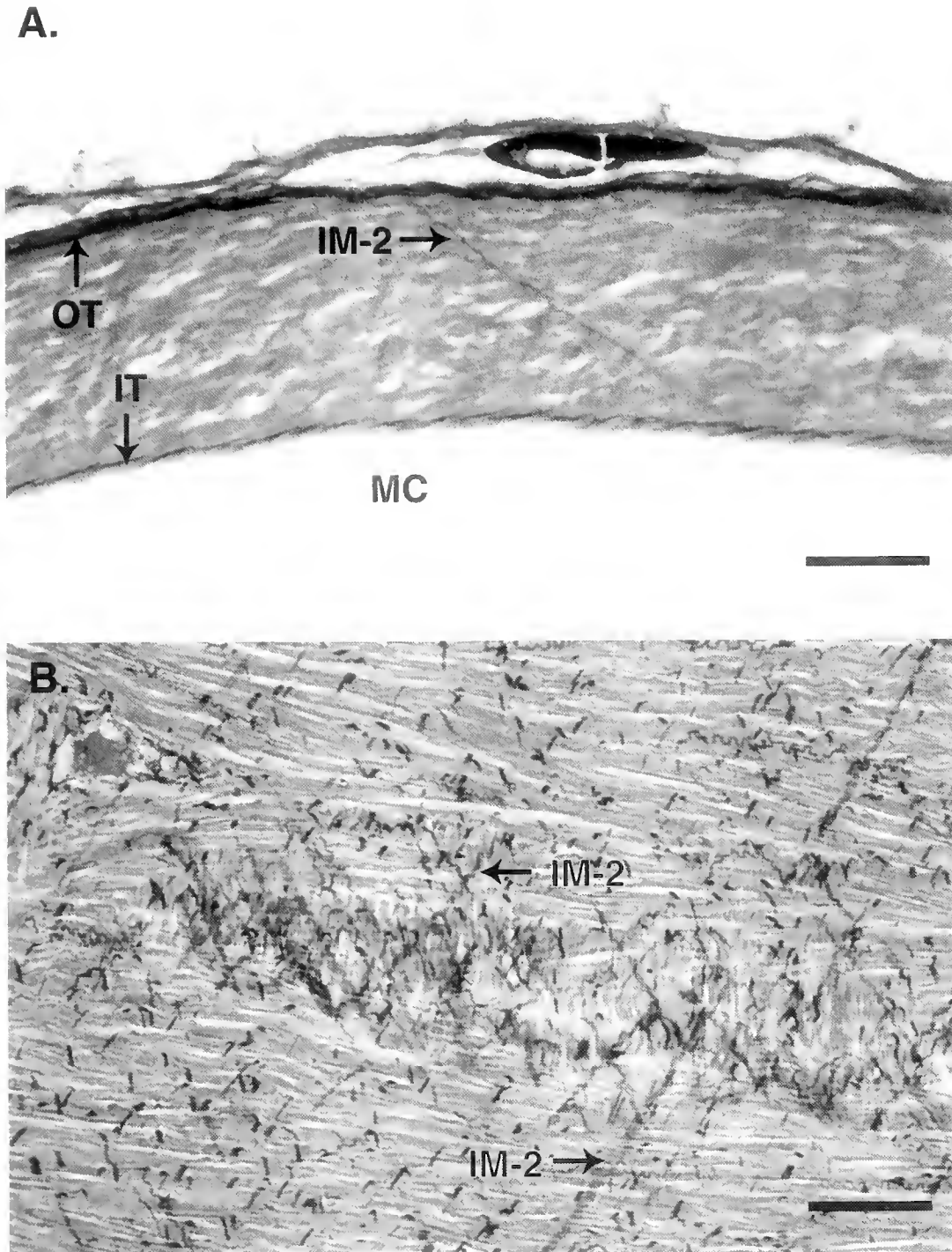


Figure 4. Photomicrographs (brightfield microscopy) of 10- μm -thick transverse sections of the ventral mantle that illustrate ontogenetic differences in IM-2 collagen fibers. Sections were stained with picrosirius. The orientation of the mantle is identical in both images. IM-2, intramuscular fiber system 2 collagen fiber; IT, inner tunic; MC, mantle cavity; OT, outer tunic. Scale bar in A and B, 60 μm . (A) A single IM-2 collagen fiber in a newly hatched squid (DML, 5 mm). Note the low IM-2 fiber angle and the scarcity of other IM-2 collagen fibers in the field of view. (B) IM-2 collagen fibers in the ventral mantle of a young 2 stage squid (DML, 69 mm). The faint vertical fibers near the center of the image are radial muscle fibers. Note that the IM-2 fiber angle is higher and IM-2 collagen fibers are abundant.

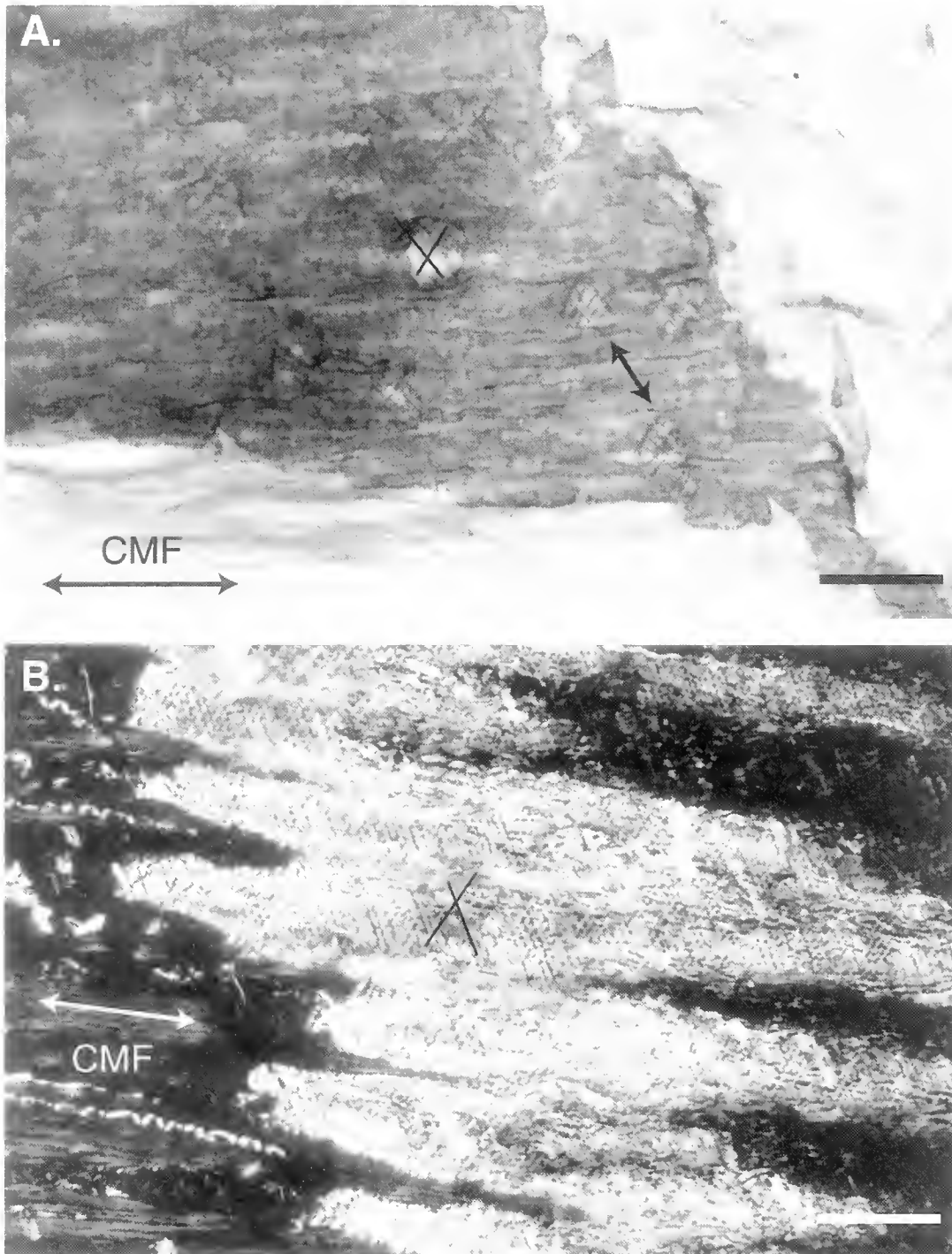


Figure 5. Photomicrographs of 5- μm -thick grazing sections of ventral squid mantle that illustrate the ontogenetic change in outer tunic collagen fiber angle. Black lines overlay a pair of collagen fibers in A and B to help illustrate the fiber angle. CMF, circumferential muscle fibers. Scale bars, 20 μm . (A) Outer tunic collagen fibers in a newly hatched squid (DML, 6 mm). Brightfield microscopy with picrosirius stain. The small arrow indicates additional outer tunic collagen fibers. (B) Outer tunic collagen fibers in a juvenile 2 stage squid (DML, 38 mm). Polarized light microscopy with picrosirius stain. Note the higher fiber angle in the hatchling animal.

lower than the 27° average outer tunic fiber angle reported for *Lolliguncula brevis* and *Loligo pealei* by Ward and Wainwright (1972). Indeed, the outer tunic fiber angle mea-

sured for mature *L. brevis* and *L. pealei* by Ward and Wainwright (1972) is much closer to the hatchling stage outer tunic fiber angle of 33.5° in *S. lessoniana*.

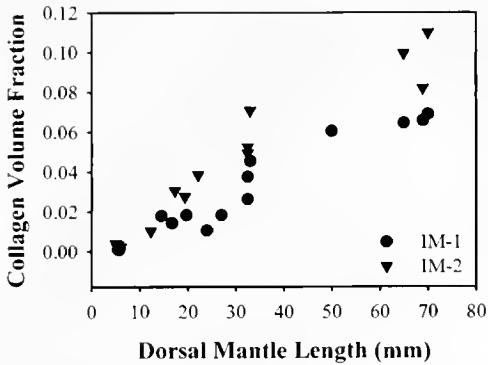


Figure 6. Collagen volume fraction in the ventral mantle *versus* dorsal mantle length. Each point represents the volume fraction of collagen for one squid. Circles indicate the volume fraction of collagen in IM-1, and triangles indicate the volume fraction of collagen in IM-2. The IM-2 data points obscure the IM-1 data for the hatchling stage squid.

The outer tunic fibers of all the *S. lessoniana* studied are oriented appropriately to resist lengthening of the mantle during jet locomotion (see Chapman, 1958, and Clark and Cowey, 1958). Both the mechanical properties and fiber angle of outer tunic collagen fibers affect mantle lengthening during jet locomotion. If the mechanical properties of the outer tunic collagen fibers do not change during ontogeny, the ability of the outer tunic to resist increases in mantle length during jet locomotion will depend on fiber angle. For example, if the maximum extensibility of an outer tunic collagen fiber is 0.13, a realistic assumption based on mechanical tests of squid mantle collagen (Gosline and Shadwick, 1983b), the mantle length of a hatchling stage squid may increase up to 23% during a jet whereas the mantle length of a young 2 stage animal may increase up to 17%. Thus, the ontogenetic variation in outer tunic fiber angle may allow greater mantle length increases during jet locomotion in newly hatched squid than in older, larger squid.

The possible increases in mantle length calculated above for *S. lessoniana* probably represent maximal values. The force balance between the outer tunic collagen fibers, other networks of connective tissue fibers, the chitinous gladius, and perhaps, the collagen-rich skin may all serve to limit changes in mantle length. The purpose of the calculation is simply to highlight the influence of outer tunic fiber angle on the *potential* for increases in mantle length during jet locomotion. Indeed, Ward (1972) did not observe increases in mantle length during jet locomotion in *L. brevis*. Packard and Trueman (1974), however, did notice small increases (~5%) in the ventral mantle length of subadult *Loligo vulgaris* and adult *Sepia officinalis*. As the next section illustrates, small increases in mantle length during the jet may facilitate elastic energy storage in the IM-1 collagen fibers of newly hatched *S. lessoniana*.

IM-1

Previous reports of IM-1_{SAG} fiber angle from *Lolliguncula brevis* and *Loligo pealei* are about 15° lower than the fiber angle reported here for the young 2 stage *S. lessoniana* (Ward and Wainwright, 1972). The discrepancy may be due to species differences or to the histological methods selected for the analysis. It is also possible that age or size differences may account for the disparity because mature squid were analyzed in the previous study. It is not possible to compare the IM-1_{SAG} hatchling fiber angle because, to our knowledge, there are no published values for newly hatched squid.

Bone *et al.* (1981) reported IM-1_{TAN} fiber angle data for *Alloteuthis subulata* and *Loligo forbesi*. In both species, the IM-1_{TAN} fiber angle was 15° to 20° lower than the angle measured here for young 2 stage *S. lessoniana*. The fiber angle reported by Bone *et al.*, however, was measured in partially contracted specimens. Contraction of the mantle results in a decrease of the IM-1_{TAN} fiber angle. Histological methodology, species differences, or age/size differences may also account for the disparity between the published fiber angle data and this study.

The significant ontogenetic change in IM-1_{SAG} and IM-1_{TAN} fiber angle may affect the kinematics of mantle movement during jet locomotion. To explore this idea, we developed a three-dimensional geometric model to evaluate the influence of changes in fiber angle on mantle kinematics. The model consists of a right rectangular polygon of mantle tissue (inset in Fig. 1). A single IM-1 collagen fiber extends from the front lower right corner to the rear upper left corner of the polygon (the gray dashed line in Fig. 1). The long axis of the polygon is parallel to the long axis of the mantle, and the short axis (side *C*) is parallel to the circumferential muscle fibers. The height of the polygon (side *T*) represents the thickness of a portion of the mantle wall. The dimensions of the polygon are in arbitrary units.

The polygon is assumed to have constant volume, and the IM-1 fiber is free to reorient as the polygon changes in dimensions. The short axis (side *C*, Fig. 1) of the polygon was decreased to simulate circumferential muscle contraction during jet locomotion. IM-1_{SAG} and IM-1_{TAN} average fiber angles from hatchling and young 2 stage *S. lessoniana* (see Table 2) were used as the initial condition (*i.e.*, “resting” mantle circumference) in which strain in the IM-1 fiber was assumed to be zero. Initially, the mantle length was held constant during the simulations. The strain on the IM-1 fiber and the IM-1_{SAG} and IM-1_{TAN} fiber angles were then calculated for a range of mantle circumference changes (see Appendix for a sample calculation).

The model predicts the effects of changes in IM-1 fiber angle on mantle kinematics. If mantle length is held constant during the jet cycle and if an IM-1 collagen fiber extensibility of 0.13 is assumed (Gosline and Shadwick,

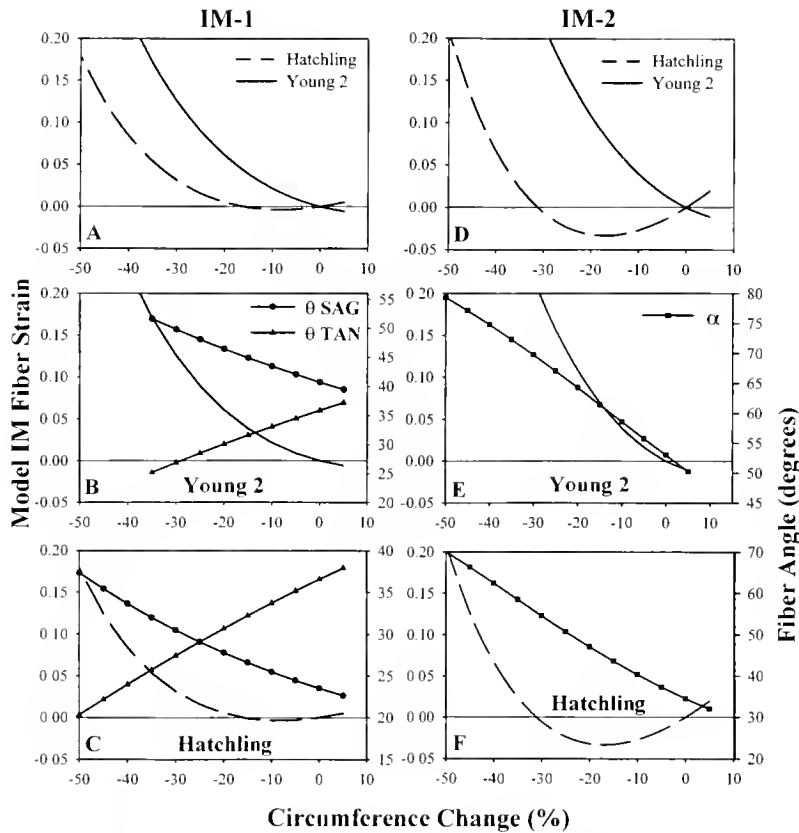


Figure 7. Predicted ontogenetic differences in collagen fiber strain and fiber angle during jet locomotion. The plots in the left column are for model IM-1 collagen fibers; the plots in the right column are for model IM-2 collagen fibers. The horizontal axis in each plot is the mantle circumference change that occurs during a simulated jet. Zero indicates the resting mantle circumference in an anesthetized squid. Negative numbers indicate mantle contraction, and positive numbers denote expansion of the mantle. The left vertical axis in each plot indicates strain on the model collagen fiber. The positive strain values above the horizontal zero line indicate lengthening of the model collagen fiber; the negative values below the zero line indicate compression. The right vertical axis in plots B, C, E, and F indicate the fiber angle of the model collagen fiber. The dashed lines represent strain data for the hatchling stage model and solid lines represent strain data for the young 2 stage model. Lines with symbols indicate the fiber angle predictions. (A and D) IM-1 fiber strain and IM-2 fiber strain, respectively, during a simulated jet. Mantle length was held constant during the simulated jet. Strain is lower at a given mantle circumference in the IM-1 and IM-2 hatchling stage model collagen fibers during the simulated jet than in the young 2 stage collagen fibers. In both A and D, if the maximum extensibility of the model collagen fibers remains unchanged during ontogeny, hatchling stage squid will experience much greater mantle contraction during the simulated jet than the young 2 squid. The hatchling fiber is compressed during the initial 17% of the mantle contraction in the IM-1 model and during the initial 32% of mantle contraction in the IM-2 model. Consequently, storage of strain energy in the model IM-1 and IM-2 collagen fibers is not possible unless the mantle contracts more than 17% and 32%, respectively. (B and C) Predicted changes in the sagittal (θ_{SAG}) and tangential (θ_{TAN}) components of the IM-1 fiber angle for a young 2 and a hatchling stage squid, respectively. In each case, note that θ_{SAG} increases while θ_{TAN} decreases during the simulated jet. (E and F) Predicted changes in the IM-2 fiber angle (α) for a young 2 and a hatchling stage squid, respectively. The fiber angle increases during the simulated jet in both cases.

1983b), the range of possible mantle movements changes substantially during ontogeny. In the model of the hatchling stage *S. lessoniana*, mantle circumference may decrease about 45% (Fig. 7A) during jet locomotion, whereas the mantle circumference of a young 2 stage animal may decrease only about 30% (Fig. 7A). In both hatchling and young 2 stage squid, the models show that IM-1_{SAG} fiber

angle increases during the jet, while IM-1_{TAN} fiber angle decreases (Fig. 7B, 7C). It is also interesting to note that the low initial IM-1_{SAG} fiber angle and the high initial IM-1_{TAN} fiber angle in hatchling stage squid result in IM-1 fiber compression during the initial -17% mantle circumference change (Fig. 7A). If mantle length is constant during the jet, low-amplitude movements (*i.e.*, less than a 17% decrease in

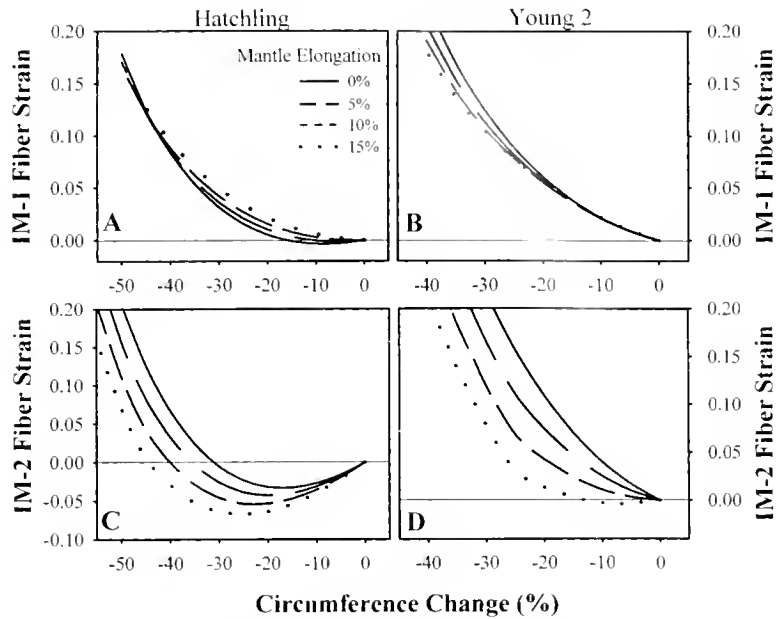


Figure 8. The effect on collagen fiber strain of an increase in mantle length during simulated jet locomotion. The plots in the left column are for the hatchling stage models; plots in the right column are for the young 2 stage models. The horizontal axis in each plot is the change in mantle circumference that occurs during a simulated jet. Zero indicates the resting mantle circumference in an anesthetized squid. Negative numbers indicate mantle contraction. The vertical axis in each plot indicates strain on the model collagen fiber. The positive strain values above the horizontal zero line indicate elongation of the model collagen fiber; the negative values below the zero line indicate compression. The amount of mantle elongation during the simulated jet in each graph is indicated in the legend for graph A. (A) Predicted IM-1 fiber strain in a hatchling stage squid. Increases in mantle length result in higher strain on the model collagen fiber early in the simulated jet stroke but do not greatly influence the possible range of mantle kinematics. (B) Predicted IM-1 fiber strain in a young 2 stage squid. Increases in mantle length do not affect strain on the model collagen fiber early in the simulated jet but do increase the possible range of mantle kinematics. (C and D) Predicted IM-2 fiber strain in a hatchling stage and a young 2 stage squid, respectively. Increases in mantle length during the simulated jet stroke substantially affect the possible range of mantle kinematics and the strain of the model IM-2 collagen fibers.

mantle circumference) of the mantle will not store strain energy in IM-1 collagen fibers in newly hatched squid.

We also examined the effect of mantle length increase during jet locomotion on mantle kinematics using the model. For both the hatchling and young 2 stage models, mantle length was allowed to increase 5%, 10%, and 15% during the jet cycle. In the hatchling stage model, mantle length was increased steadily until a mantle circumference change of -45% was reached (*i.e.*, the point in the previous IM-1 hatchling model where strain on the IM-1 collagen fiber was 0.13). In the young 2 stage model, mantle length was increased gradually until a mantle circumference change of -30% was reached (*i.e.*, the point in the previous IM-1 young 2 model where the strain on the IM-1 collagen fiber was 0.13). After mantle circumference changes of -45% for the hatchling stage model and -30% for the young 2 stage model were reached, mantle length was held constant. Note that incorporating the increases in mantle length earlier in the jetting cycle (*e.g.*, up to a mantle circumference change of -20% , then holding mantle length constant) does not affect the predicted maximum range of

mantle contraction, though it does result in higher strain in the hatchling stage model IM-1 collagen fiber early in the jetting cycle. In all the simulations, the strain on the IM-1 fiber was calculated for a range of mantle circumference changes.

Incorporating mantle length increase during jet locomotion into the model results in several interesting predictions. In hatchling stage *S. lessoniana*, modest increases in mantle length during the jet did not substantially affect the maximum possible amplitude of mantle contraction, but they did result in an increase in IM-1 collagen fiber strain during low-amplitude mantle movements (Fig. 8A). The potentially important consequence of small increases in mantle length during jetting for newly hatched squid is that strain energy storage in IM-1 collagen fibers is possible during low-amplitude movements of the mantle (*e.g.*, respiration and slow jet locomotion). In the young 2 stage squid, only the 15% increase in mantle length during jet locomotion had any noticeable effect on IM-1 collagen fiber strain (Fig. 8B). The maximum possible mantle circumference change during the jet, however, increased slightly with modest in-

creases in mantle length (Fig. 8B). Thus, the model predicts that small increases in mantle length during low-amplitude mantle movements (*e.g.*, slow jetting or respiration) in newly hatched *S. lessoniana* may result in increased energy storage in IM-1 collagen fibers; small increases in mantle length in older, larger squid do not. The predicted increase in elastic energy storage comes at the expense of a decrease in thrust. For slow jetting or respiration, this cost may not outweigh the benefits of elastic energy storage.

IM-2

The average IM-2 fiber angle of young 2 stage *S. lessoniana* was about the same as the 55° reported for *Alloteuthis subulata* and *Loligo forbesi* by Bone *et al.* (1981). It is not possible to compare the average IM-2 fiber angle of the hatchling stage *S. lessoniana* with the literature because we are not aware of any published IM-2 fiber angles in newly hatched squid.

The significant change in IM-2 fiber angle during ontogeny may contribute to substantial ontogenetic changes in mantle kinematics during jet locomotion. We examined the implications of a fiber angle change on mantle kinematics using a model similar to the one used to predict the effect of IM-1 collagen fiber angle on mantle kinematics. The IM-2 model consists of the same polygon mentioned above, except there is a single IM-2 fiber running from the lower right corner to the upper left corner of plane *CT* (solid gray fiber in plane *CT*, Fig. 1). The assumptions are the same for both the IM-1 and IM-2 models.

The model predicts the potential effects of an ontogenetic change in IM-2 fiber angle on mantle kinematics. If the extensibility of the IM-2 collagen fiber in the model is limited to 0.13 (Gosline and Shadwick, 1983b), a mantle circumference change of about -45% is possible in hatchling stage *S. lessoniana* during jet locomotion (Fig. 7D). During mantle contraction, the hatchling IM-2 fiber angle will increase from about 35° to about 67° (Fig. 7F). Due to the low initial fiber angle, the IM-2 collagen fiber is compressed during the first -32% change in mantle circumference (Fig. 7D). The model predicts that strain energy storage in the IM-2 collagen fibers will occur only during vigorous jet locomotion that results in large decreases ($>32\%$) in mantle circumference. Interestingly, this suggests that if hatchling stage *S. lessoniana* use elastic mechanisms to restore mantle shape during respiratory movements of the mantle, as hypothesized for mature *Loligo opalescens* by Gosline *et al.* (1983), strain energy storage can only take place in the IM-1 collagen fibers.

The model predicts substantially different mantle kinematics for young 2 stage *S. lessoniana*. Again, if IM-2 collagen fiber extensibility is assumed to be 0.13, mantle circumference changes during jet locomotion of up to about -25% are possible (Fig. 7D). The fiber angle will increase

from the initial value of 53° to about 65° at the end of the jet (Fig. 7E). Given the high initial fiber angle, the strain experienced by the IM-2 collagen fibers will increase rapidly during the jet (Fig. 7D).

Because the mantle tissue is probably constant in volume over the brief period of a single mantle contraction (Ward, 1972), increases in mantle length during jet locomotion will influence the strain experienced by the IM-2 collagen fibers. Therefore, we also examined the effect of mantle length increase during jet locomotion on mantle kinematics. Mantle length in both the hatchling and young 2 stage models was allowed to increase 5%, 10%, and 15% during the jet cycle. In the hatchling stage model, mantle length was increased gradually until a mantle circumference change of -45% was reached (*i.e.*, the point in the previous hatchling IM-2 model where strain on the IM-2 collagen fiber was 0.13). In the young 2 stage model, mantle length was increased progressively until a mantle circumference change of -25% was reached (*i.e.*, the point in the previous young 2 IM-2 model where strain on the IM-2 collagen fiber was 0.13). Mantle length was held constant after mantle circumference changes of -45% and -25% , for the hatchling and young 2 stage models respectively, were reached. The strain on the IM-2 fiber was calculated for a range of changes in mantle circumference.

The models predict substantial effects on both mantle kinematics and elastic energy storage when mantle length increases during jet locomotion. The hatchling stage model predicts that modest 5% or 10% increases in mantle length during jetting increase proportionately the range of possible mantle circumference changes (Fig. 8C). Increases in the maximum amplitude of mantle movements during jet loco-

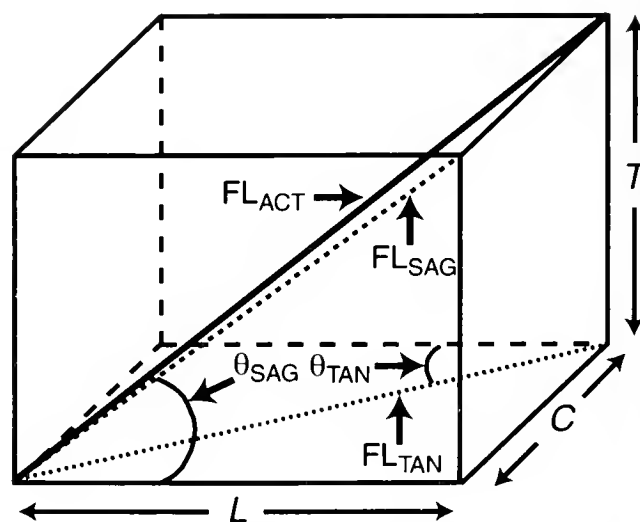


Figure 9. The imaginary polygon used to calculate strain on the model IM-1 and IM-2 collagen fibers during simulated jet locomotion. Only the model IM-1 collagen fiber (solid gray line) is shown. See the Appendix for more detail.

motion, however, result in the compression of IM-2 collagen fibers for a longer portion of the jet cycle (Fig. 8C). Thus, if the mantle of a hatchling stage squid lengthens even a small amount, the IM-2 collagen fibers will store elastic energy only during vigorous jet locomotion.

The young 2 model predicts similar increases in the range of possible changes in mantle circumference with increases in mantle length during jetting (Fig. 8D). In contrast to the hatchling stage model, the young 2 stage model predicts that only increases in mantle length greater than 10% will result in compression of the IM-2 collagen fiber during jet locomotion (Fig. 8D). Thus, modest increases in mantle length will permit elastic energy storage in IM-2 collagen fibers during low-amplitude movements of the mantle.

Can IM-1 and IM-2 fiber angles predict mantle kinematics?

The models for IM-1 and IM-2 described above both suggest that a much greater range of mantle circumference change is possible during jet locomotion in newly hatched *S. lessoniana* than in older, larger squid. The models predict that mantle circumference changes up to -45% are possible in hatchling stage squid compared with -25% and -30% in young 2 stage squid. The few published accounts of mantle kinematics support these predictions. In *Loligo opalescens* the range of circumference change during vigorous jet locomotion is at least 10% greater in hatchling animals than in older, larger squid (Gilly *et al.*, 1991). Maximum mantle circumference changes are about -40% to -42% in hatchlings and about -30% in mature animals (Gilly *et al.*, 1991). In *Loligo vulgaris*, the maximum mantle circumference changes are about -45% and -30% in hatchling and adult animals, respectively, during escape-jet locomotion (calculated from Packard, 1969). During escape-jet locomotion in *S. lessoniana*, mantle circumference changes -45% and -33% in hatchling stage and young 2 stage squid, respectively (Thompson, 2000; Thompson and Kier, 2001). Even during less vigorous jet locomotion and respiratory mantle movements, the range of mantle circumference change is considerably greater in newly hatched *L. opalescens* (Preuss *et al.*, 1997). Given the assumptions of the geometric models, the measurement errors inherent in the histological methods, the cross-species comparisons, and the lack of consideration for the role of circumferential muscle mechanics in mantle contraction, it is striking that the models accurately predict the maximum amplitude of actual mantle kinematics. Thus, we hypothesize that the arrangement of intramuscular collagen fibers likely plays a crucial role in determining the mechanical properties of squid mantle.

Predictions of elastic energy storage from the IM collagen fiber models

The mathematical models of IM-1 and IM-2 predict ontogenetic changes in the potential of the intramuscular collagen fibers to store elastic energy. During low-amplitude mantle contraction in hatchling stage *S. lessoniana*, the models predict that IM-1 and IM-2 collagen fibers are compressed and, thus, are unable to store elastic energy. This prediction holds if mantle length remains constant during the simulated jet or if mantle length increases (only up to 10% for IM-1 fibers) during the jet. Only during large-amplitude mantle movements (*e.g.*, during vigorous jet locomotion) do the hatchling stage models predict that IM-1 and IM-2 collagen fibers are stretched and, thus, able to store elastic energy. Conversely, the models predict that IM-1 and IM-2 collagen fibers in young 2 stage *S. lessoniana* are stretched as the mantle contracts and, thus, can store elastic energy during jet locomotion.

The hatchling stage models also predict a difference in the relative elongation of IM-1 and IM-2 collagen fibers during jet locomotion. If mantle length remains constant during the jet, a mantle circumference decrease of 18% is required to elongate an IM-1 collagen fiber, whereas a mantle circumference decrease of 33% is necessary to extend an IM-2 collagen fiber. Thus, the hatchling stage models predict that IM-2 collagen fibers may not contribute to elastic energy storage in the mantle except during vigorous jet locomotion.

Volume fraction of collagen

Isolated portions of squid and cuttlefish mantle store elastic energy in experiments that simulate mantle movement during the exhalant phase of jet locomotion (Gosline and Shadwick, 1983a, b; MacGillivray *et al.*, 1999; Curtin *et al.*, 2000). The amount of elastic energy stored in the mantle depends on the volume of collagen in the tissue, the strain experienced by the collagen fibers, and the mechanical properties of the mantle collagen fibers. The volume fraction of collagen in IM-1 and IM-2 increased 68 times and 36 times, respectively, during ontogeny. If IM-1 and IM-2 collagen fibers are strained comparably during locomotion in squid of all ages, and if the mechanical properties of collagen do not change with growth, the elastic energy storage capacity of the mantle is likely to increase dramatically during ontogeny.

Future directions

We have described ontogenetic changes in IM-1 and IM-2 fiber angle and in mantle collagen volume fraction. To analyze these changes further, and to begin testing the predictions of the models, accurate measurement of mantle length during jet locomotion is needed. In addition, the

predictions of the models assume that the mechanical properties of squid mantle collagen do not change during ontogeny. This important assumption needs to be tested, particularly because the mechanical properties of collagen change during the growth of many animals (e.g., Parry and Craig, 1988). Therefore, mechanical tests of intact portions of squid mantle, in combination with data on mantle length during jet locomotion, are necessary to test the predictions of the models and to understand better the ecological and evolutionary implications of ontogenetic changes in the morphology of mantle connective tissue.

Acknowledgments

This research was supported by NSF grants to W.M.K. (IBN-9728707 and IBN-9219495). Grants and fellowships to J.T.T. from the Wilson Fund, the American Malacological Association, and Sigma Xi helped defray research expenses. We thank L. Walsh at the NRCC for her expertise in shipping squid cross-country and E. Burgin for his help in sectioning and staining. We are grateful to the Duke-UNC biomechanics group for discussion of several of the ideas in this paper and to D. Pfennig for statistical advice. Finally, we thank S. A. Wainwright, J. Taylor, and two anonymous reviewers for constructive comments and suggestions on an earlier version of the paper.

Literature Cited

- Bone, Q., A. Pulsford, and A. D. Chubb. 1981. Squid mantle muscle. *J. Mar. Biol. Assoc. U.K.* **61**: 327-342.
- Cassada, R. C., and R. L. Russell. 1975. The dauerlarva, a post-embryonic developmental variant of the nematode *Caenorhabditis elegans*. *Dev. Biol.* **46**: 326-342.
- Chapman, G. 1958. The hydrostatic skeleton in the invertebrates. *Biol. Rev. Camb. Philos. Soc.* **33**: 338-371.
- Clark, R. B. 1964. *Dynamics in Metazoan Evolution*. Clarendon Press, Oxford.
- Clark, R. B., and J. B. Cowey. 1958. Factors controlling the change of shape of certain nemertean and turbellarian worms. *J. Exp. Biol.* **35**: 731-748.
- Cox, G. N., S. Staprans, and R. S. Edgar. 1981. The cuticle of *Caenorhabditis elegans*. II. Stage-specific changes in ultrastructure and protein composition during postembryonic development. *Dev. Biol.* **86**: 456-470.
- Curtin, N. A., R. C. Woledge, and Q. Bone. 2000. Energy storage by passive elastic structures in the mantle of *Sepia officinalis*. *J. Exp. Biol.* **203**: 869-878.
- Gilly, W. F., B. Hopkins, and G. O. Mackie. 1991. Development of giant motor axons and neural control of escape responses in squid embryos and hatchlings. *Biol. Bull.* **180**: 209-220.
- Gosline, J. M., and R. E. Shadwick. 1983a. The role of elastic energy storage mechanisms in swimming: an analysis of mantle elasticity in escape jetting in the squid, *Loligo opalescens*. *Can. J. Zool.* **61**: 1421-1431.
- Gosline, J. M., and R. E. Shadwick. 1983b. Molluscan collagen and its mechanical organization in squid mantle. Pp. 371-398 in *The Mollusca. Vol. I: Metabolic Biochemistry and Molecular Biomechanics*, P. W. Hochachka, ed. Academic Press, New York.
- Gosline, J. M., J. D. Steeves, A. D. Harman, and M. E. DeMont. 1983. Patterns of circular and radial mantle muscle activity in respiration and jetting of the squid *Loligo opalescens*. *J. Exp. Biol.* **104**: 97-109.
- Harris, J. E., and H. D. Crofton. 1957. Structure and function in the nematodes: Internal pressure and cuticular structure in *Ascaris*. *J. Exp. Biol.* **34**: 116-130.
- Kier, W. M. 1992. Hydrostatic skeletons and muscular hydrostats. Pp. 205-231 in *Biomechanics: Structures and Systems. A Practical Approach*, A. A. Biewener, ed. IRL Press at Oxford University Press, New York.
- Kier, W. M., and K. K. Smith. 1985. Tongues, tentacles, and trunks: The biomechanics of movement in muscular hydrostats. *Zool. J. Linn. Soc.* **83**: 307-324.
- Koehl, M. A. R. 1977. Mechanical diversity of connective tissue of the body wall of sea anemones. *J. Exp. Biol.* **69**: 107-125.
- Lee, P. G., P. E. Turk, W. T. Yang, and R. T. Hanlon. 1994. Biological characteristics and biomedical applications of the squid *Sepioteuthis lessoniana* cultured through multiple generations. *Biol. Bull.* **186**: 328-341.
- López-DeLeón, A., and M. Rojkind. 1985. A simple micromethod for collagen and total protein determination in formalin-fixed paraffin-embedded sections. *J. Histochem. Cytochem.* **33(8)**: 737-743.
- MacGillivray, P. S., E. J. Anderson, G. M. Wright, and M. E. DeMont. 1999. Structure and mechanics of the squid mantle. *J. Exp. Biol.* **202**: 683-695.
- Messenger, J. B., M. Nixon, and K. P. Ryan. 1985. Magnesium chloride as an anaesthetic for cephalopods. *Comp. Biochem. Physiol.* **82C**: 203-205.
- Moltschanivskyj, N. A. 1994. Muscle tissue growth and muscle fibre dynamics in the tropical loliginid squid *Photololigo* sp. (Cephalopoda: Loliginidae). *Can. J. Fish. Aquat. Sci.* **51**: 830-835.
- Mommsen, T. P., J. Ballantyne, D. MacDonald, J. Gosline, and P. W. Hochachka. 1981. Analogues of red and white muscle in squid mantle. *Proc. Nat. Acad. Sci. USA* **78(5)**: 3274-3278.
- Montes, G. S., and Junqueira, L. C. U. 1988. Histochemical localization of collagen and of proteoglycans in tissues. Pp. 41-72 in *Collagen. Vol. II: Biochemistry and Biomechanics*, M. E. Nimni, ed. CRC Press, Boca Raton, FL.
- Packard, A. 1969. Jet propulsion and the giant fibre response of *Loligo*. *Nature* **221**: 875-877.
- Packard, A., and E. R. Trueman. 1974. Muscular activity of the mantle of *Sepia* and *Loligo* (Cephalopoda) during respiratory movements and jetting, and its physiological interpretation. *J. Exp. Biol.* **61**: 411-419.
- Parry, D. A. D., and A. S. Craig. 1988. Collagen fibrils during development and maturation and their contribution to the mechanical attributes of connective tissue. Pp. 1-23 in *Collagen. Vol. II: Biochemistry and Biomechanics*, M. E. Nimni, ed. CRC Press, Boca Raton, FL.
- Preuss, T., Z. N. Lebaric, and W. F. Gilly. 1997. Post-hatching development of circular mantle muscles in the squid *Loligo opalescens*. *Biol. Bull.* **192**: 375-387.
- Segawa, S. 1987. Life history of the oval squid, *Sepioteuthis lessoniana* in Kominato and adjacent waters central Honshu, Japan. *J. Tokyo Univ. Fish.* **74(2)**: 67-105.
- Shadwick, R. E., and J. M. Gosline. 1985. The role of collagen in the mechanical design of squid mantle. Pp. 299-304 in *Biology of Invertebrate and Lower Vertebrate Collagens*, A. Bairati and R. Garrone, eds. Plenum Press, New York.
- Sweat, F., H. Puchler, and S. I. Rosenthal. 1964. Sirius red F3BA as a stain for connective tissue. *Arch. Pathol.* **78**: 69-72.
- Thompson, J. T. 2000. The ontogeny of mantle structure and function in the oval squid, *Sepioteuthis lessoniana* (Cephalopoda: Loliginidae). Ph.D. dissertation, University of North Carolina at Chapel Hill.

- Thompson, J. T., and W. M. Kier. 2001.** Ontogenetic changes in mantle kinematics during escape-jet locomotion in the oval squid, *Sepioteuthis lessoniana* Lesson, 1830. *Biol. Bull.* **201**: 154–166.
- Wainwright, S. A. 1970.** Design in hydraulic organisms. *Naturwissenschaften* **57**: 321–326.
- Wainwright, S. A., and M. A. R. Koehl. 1976.** The nature of flow and the reaction of benthic cnidaria to it. Pp. 5–21 in *Coelenterate Ecology and Behavior*, G. O. Mackie, ed. Plenum Press, New York.
- Wainwright, S. A., W. D. Biggs, J. D. Currey, and J. M. Gosline. 1976.** *Mechanical Design in Organisms*. Princeton University Press, Princeton.
- Ward, D. V. 1972.** Locomotory function of the squid mantle. *J. Zool. (Lond)* **167**: 487–499.
- Ward, D. V., and S. A. Wainwright. 1972.** Locomotory aspects of squid mantle structure. *J. Zool. (Lond)* **167**: 437–449.
- Weibel, E. R. 1979.** *Stereological Methods. Vol. 1: Practical Methods for Biological Morphometry*. Academic Press, New York.
- Young, J. Z. 1938.** The functioning of the giant nerve fibres of the squid. *J. Exp. Biol.* **15**: 170–185.
- Zar, J. H. 1996.** *Biostatistical Analysis*. Prentice Hall, Upper Saddle River, NJ.

Appendix

The following is a brief summary of the variables, assumptions, and steps used in the calculation of strain on the IM-1 model collagen fiber. The procedure for calculating strain on the model IM-2 collagen fiber is similar to that outlined below and is not shown. The only difference between the two calculations is that the model IM-2 collagen fiber is restricted to plane CT (Fig. 1). That simplifies the calculation, in that the IM-2 projected fiber length is the same as the actual fiber length.

Variables (see Fig. 9 in text)

θ_{SAG} = IM-1_{SAG} fiber angle

θ_{TAN} = IM-1_{TAN} fiber angle

L = Polygon length (parallel to mantle length)

C = Polygon width (parallel to mantle circumference)

T = Polygon thickness (parallel to mantle wall thickness)

FL_{SAG} = Projected fiber length of the IM-1 collagen fiber in the sagittal plane

FL_{TAN} = Projected fiber length of the IM-1 collagen fiber in the tangential plane

FL_{ACT} = Actual length of IM-1 collagen fiber

Initial conditions

$\theta_{SAG\ Hatch} = 32^\circ$ $\theta_{SAG\ Young2} = 43^\circ$

$\theta_{TAN\ Hatch} = 39^\circ$ $\theta_{TAN\ Young2} = 32^\circ$

$FL_{SAG} = 1.0$ (arbitrary units)

$L = FL_{SAG} \cos \theta_{SAG}$

$T = FL_{SAG} \sin \theta_{SAG}$

Steps

(1). Calculate polygon width, C :

$$C = L \tan \theta_{TAN}$$

(2). Calculate polygon volume:

$$\text{Volume} = LTC$$

Note, the volume of the model polygon was assumed to remain constant during the simulation.

(3). Keeping volume constant, vary side C (from $1.0C$ to $0.5C$) to mimic circumferential muscle contraction during jet locomotion. Solve for polygon thickness, T :

$$T = \text{Volume} \div LC$$

Note, for the calculations in which mantle length was constant, side L was held constant as side C was varied. For the calculations in which mantle length was allowed to increase, side L was increased 5%, 10%, or 15% in length as side C was varied.

(4). Calculate the projected fiber length of the IM-1_{TAN} collagen fiber, FL_{TAN} :

$$FL_{TAN} = \sqrt{C^2 + L^2}$$

(5). Calculate the actual length of the IM-1 collagen fiber, FL_{ACT} :

$$FL_{ACT} = \sqrt{T^2 + FL_{TAN}^2}$$

(6). Calculate θ_{SAG} and θ_{TAN} :

$$\tan \theta_{SAG} = T \div L$$

$$\tan \theta_{TAN} = C \div L$$

Ontogenetic Changes in Mantle Kinematics During Escape-Jet Locomotion in the Oval Squid, *Sepioteuthis lessoniana* Lesson, 1830

JOSEPH T. THOMPSON* AND WILLIAM M. KIER

Department of Biology, CB#3280 Coker Hall, University of North Carolina, Chapel Hill, North Carolina 27599-3280

Abstract. We investigated the kinematics of mantle movement during escape jet behavior in an ontogenetic series of *Sepioteuthis lessoniana*, the oval squid. Changes in mantle diameter during the jet were measured from digitized S-VHS video fields of tethered animals that ranged in age from hatchlings to 9 weeks. The amplitude of both mantle contraction and mantle hyperinflation (expressed as percent change from the resting mantle diameter) during an escape jet was significantly greater in hatchlings than in older, larger squid ($P < 0.05$). The maximum amplitude of mantle contraction during the escape jet decreased from an average of -40% in hatchlings to -30% in the largest animals studied. The maximum amplitude of mantle hyperinflation decreased from an average of 18% in hatchlings to 9% in the largest squid examined. In addition, the maximum rate of mantle contraction decreased significantly during ontogeny ($P < 0.05$), from a maximum of 8.6 mantle circumference lengths per second (L/s) in hatchlings to 3.8 L/s in the largest animals studied. The ontogenetic changes in the mantle kinematics of the escape jet occurred concomitantly with changes in the organization of collagenous connective tissue fiber networks in the mantle. The alteration in mantle kinematics during growth may result in proportionately greater mass flux during the escape jet in newly hatched squid than in larger animals.

Introduction

Post-embryonic change in morphology is a common feature of most organisms (*e.g.*, Werner, 1988). Such ontogenetic modifications may affect the ecology of the organism (Calder, 1984; Werner, 1988; Stearns, 1992) and may provide insight into the evolution of form and function, yet they are often neglected in studies of functional morphology and comparative biomechanics. Significant effects on the life cycle of an organism need not involve dramatic alterations of morphology during ontogeny. For example, at hatching, cephalopod molluscs are broadly similar in form to adults (Boletzky, 1974; Sweeney *et al.*, 1992). Yet these tiny hatchlings grow several orders of magnitude in size, shift from the neuston or plankton to the benthos or nekton (Marliave, 1980; Hanlon *et al.*, 1985), and may use different mechanisms to capture prey (O'Dor *et al.*, 1985; Chen *et al.*, 1996; Kier, 1996) and to locomote (Villanueva *et al.*, 1995). In many cases, these life-cycle changes are correlated with morphological alterations that, while not always as drastic as the wholesale changes that occur during the metamorphosis of some other marine molluscs, may be equally important in their effect on the performance or ecology of the animal.

Cephalopods depend upon a hydrostatic skeleton for support during locomotion and movement. In the mantle of loliginid squid, skeletal support for locomotion is provided by a complex arrangement of fibers of muscle and of collagenous connective tissue (Ward and Wainwright, 1972; Bone *et al.*, 1981). The connective tissue fibers are arranged in five highly organized networks: the inner and outer tunics, and three distinct systems of intramuscular fibers (Ward and Wainwright, 1972; Bone *et al.*, 1981; for review, see Gosline and DeMont, 1985). These networks of colla-

Received 13 December 2000; accepted 8 May 2001.

* To whom correspondence should be addressed. E-mail: joethomp@email.unc.edu

Abbreviations: DML, dorsal mantle length; IM-1, intramuscular fiber system 1; IM-2, intramuscular fiber system 2; IM-3, intramuscular fiber system 3.

gen fibers help control changes in mantle shape during contraction of the muscles that power locomotion. In addition, the intramuscular collagen fibers store elastic energy during the exhalant phase of the jet and return the energy to help restore mantle shape and refill the mantle cavity (Ward and Wainwright, 1972; Bone *et al.*, 1981; Gosline *et al.*, 1983; Gosline and Shadwick, 1983a; Shadwick and Gosline, 1985; MacGillivray *et al.*, 1999).

The organization of mantle connective tissue changes significantly during ontogeny in *Sepioteuthis lessoniana*, the oval squid. In hatchlings, the arrangement of outer tunic and intramuscular collagen fibers is hypothesized to permit large-amplitude movements of the mantle (Thompson, 2000; Thompson and Kier, 2001). In early ontogeny, the fiber angle of the collagen fiber networks changes exponentially, potentially limiting the amplitude of movement as the squid grow (Thompson, 2000; Thompson and Kier, 2001). Although these changes in connective tissue organization do not constitute a discrete metamorphosis, their influence on the mechanical properties of the mantle and the mechanics of jet locomotion may be considerable.

To explore the implications of changes in the organization of mantle connective tissue for the mechanics of jet locomotion, we studied the kinematics of the escape jet in an ontogenetic series of *S. lessoniana*. The escape jet is a distinct form of locomotion that typically involves a brief initial hyperinflation of the mantle (*i.e.*, the mantle is expanded radially beyond its resting diameter; see Gosline *et al.*, 1983) followed by a rapid contraction that expels water from the mantle cavity *via* the muscular funnel. In tethered *S. lessoniana*, we measured ontogenetic changes in the following kinematic parameters during the escape jet: the amplitude of mantle hyperinflation and mantle contraction, the rate of mantle contraction, and the frequency of escape jetting. In addition, we used measurements of mantle radius, mantle wall thickness, and mantle cavity volume to calculate the relative mass flux produced during the escape jet. Finally, we examined the relationship between mantle connective tissue morphology and mantle kinematics during the escape jet.

Materials and Methods

Animals

We obtained an ontogenetic series of *Sepioteuthis lessoniana* Lesson, 1830. We chose *S. lessoniana* for the experiments because members of this species hatch at a large size relative to other squid (5–7 mm dorsal mantle length and 0.01–0.03 g body weight) and, like other squid in the family Loliginidae, they are capable of escape-jet locomotion immediately upon hatching (Fields, 1965; Choe, 1966; Packard, 1969; Moynihan and Rodaniche, 1982; Segawa, 1987; Gilly *et al.*, 1991).

We used *S. lessoniana* embryos that were collected from

three locations (Gulf of Thailand; Okinawa Island, Japan; Tokyo Region, East Central Japan) over a 2-year period and reared (Lee *et al.*, 1994) by the National Resource Center for Cephalopods (NRCC) at the University of Texas Medical Branch (Galveston, TX). Each of the three cohorts consisted of thousands of embryos from six to eight different egg mops. Thus, it is likely that the sample populations were not the offspring of a few closely related individuals, but were representative of the natural population at each collection site.

Commencing at hatching, and at weekly intervals thereafter, live squid were sent *via* overnight express shipping from the NRCC to the University of North Carolina. Animals from each of the following eight age classes were used in the experiments: newly hatched and 1, 2, 3, 4, 5, 6, and 9 weeks after hatching. These age classes correspond to the early life history stages defined by Segawa (1987), in which the squid achieve external adult morphology at a dorsal mantle length (DML) of about 40 mm (age ~6 week) and begin to mature sexually at 150 mm DML (age >9 weeks).

Prior to the start of the experiments, the animals were allowed about 30 min to equilibrate in an 80-l circular holding tank. The temperature (23 °C) and salinity (35 ppt) of the water in the holding tanks matched the temperature and salinity of the water in which the squid were raised. Circular water flow in the tank helped keep the squid swimming parallel to the sides of the tank to prevent injury. There were never more than seven squid in the holding tank at one time, and the maximum time an individual spent in the tank was 4 h.

Tethering

Initially, we attempted to measure mantle kinematics in free-swimming squid. The small size of the hatchling squid, combined with their inability to maintain position in flow, made it difficult to videotape at high magnification and thus obtain adequate spatial resolution for the kinematic measurements. To allow videotaping at high magnification and to increase the spatial resolution of the edges of the mantle, and thus the accuracy of the kinematic measurements, the squid were tethered.

Individual squid were removed from the holding tank with a glass beaker and anesthetized lightly in a 1:1 solution of 7.5% MgCl₂; artificial seawater (Messenger *et al.*, 1985). Anesthesia durations varied with the size of the animal (longer times for larger animals) but were never longer than 2 min. While anesthetized, the squid were tethered (Fig. 1). A needle (0.3-mm-diameter insect pin for smaller animals or 0.7-mm-diameter hypodermic needle for larger animals) was inserted through the brachial web of the squid, anterior to the brain cartilage and posterior to the buccal mass. The needle was positioned between these two rigid structures to prevent it from tearing the soft tissue of the squid. The

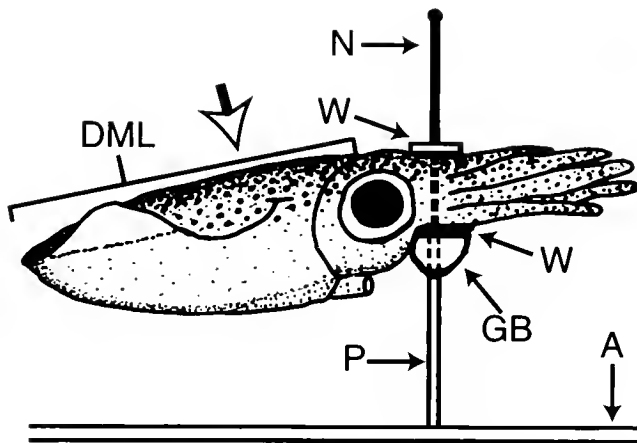


Figure 1. The tethering apparatus. A, acrylic plastic base; GB, glue bead; N, needle; P, post; W, plastic washer. DML indicates dorsal mantle length; white arrow points at $\frac{1}{3}$ DML.

needle was inserted into a hollow stainless steel post (hypodermic tubing) attached to a sheet of acrylic plastic. The needle fit tightly in the hollow post to prevent movement. Flat, polyethylene washers on the post and needle were positioned above and below the head to prevent vertical movement.

Insertion of the needle through the anesthetized squid was rapid and required minimal handling of the animal. Individuals of this species become nearly transparent under anesthesia, making the buccal mass and the brain cartilage readily visible. Needle placement was verified after the experiment by examination of the location of the needle entrance and exit wounds.

Tethered squid were transferred to the video arena (0.4 m long by 0.2 m wide by 0.15 m deep) filled with aerated 23 °C artificial seawater and were allowed to recover. Tethered squid remained alive and in apparent good health for up to several hours, though most squid were tethered for fewer than 15 min.

Critique of tethering

Although tethering is an invasive technique, there were several indications that it was not unduly traumatic to the squid. First, tethered squid behaved similarly to the animals in the holding tank. Both the tethered and free-swimming squid spent most of the time hovering using the fins and low-amplitude jets. Second, unlike squid that are in distress or startled, more than 90% of the tethered animals did not eject ink. Third, the chromatophore patterns of tethered squid did not differ qualitatively from the patterns exhibited by the free-swimming squid in the holding tank. Finally, squid that were untethered and returned to the holding tank swam normally and could survive for several hours. It is not known how long these animals could have survived, be-

cause all the animals were killed for histological analysis after the day's experiments were completed.

Tethering did, however, affect two aspects of swimming behavior. Tethered squid (1) performed escape jets with higher frequency and (2) performed more consecutive escape jets than the free-swimming squid in the holding tank. It is possible that the tethering apparatus may have affected mantle kinematics by restricting the flow of water out of the funnel. This is unlikely because the post was between 30% and 50% of the minimum funnel aperture in hatchlings and less than 20% of the minimum funnel diameter in the largest animals studied. In addition, the tethering apparatus did not contact the funnel during the experiments.

Mantle kinematics

Escape-jet behavior was recorded from above with a Panasonic AG-450 S-VHS professional video camera. The camera was adjusted so that the squid filled as much of the field of view as possible. To maximize the measurement resolution, the animal was oriented with the long axis of the mantle vertical in the video field (*i.e.*, perpendicular to the video scan lines). Though the animals were free to rotate around the tether during the experiments, most remained near the original orientation. The frame rate of the camera (60 video fields per second) was more than 10 times faster than the observed frequency of the mantle jetting cycle. To reduce image blur, the high-speed shutter of the camera was set at 1/1000 s. Illumination was adjusted by means of a variac to the minimum level necessary to provide good contrast between the squid and the background.

Videotapes were analyzed using a Panasonic AG-1980P professional S-VHS videocassette recorder to identify escape-jet sequences suitable for digitizing. Only those sequences in which the mantle remained in the same orientation (*i.e.*, the mantle remained nearly horizontal and did not twist relative to the head) were digitized. Individual video fields were digitized using an Imagenation (Beaverton, OR) PXC200 frame-grabber card in a microcomputer.

Mantle diameter changes during vigorous escape jets were measured from digitized video fields using morphometrics software (SigmaScan Pro 4.0, SPSS Science, Chicago, IL). Diameter at $\frac{1}{3}$ of the dorsal mantle length (DML) was measured in each video field prior to the start of and throughout the duration of an escape jet. The mantle diameter at $\frac{1}{3}$ DML (from dorsal mantle edge, Fig. 1) was selected because the greatest amplitude mantle movements occurred at that location in all squid examined. We normalized the data by dividing the mantle diameter measured in each video field by the resting diameter (=diameter of the anesthetized squid at $\frac{1}{3}$ DML) of the squid. Normalization by the resting mantle diameter standardized the analysis of mantle hyperinflation and mantle contraction data among the squid and allowed for comparisons between animals of

different size. More than five escape-jet sequences were analyzed from each animal. Only the sequences that yielded the greatest mantle hyperinflation and the greatest mantle contraction were reported.

For many of the escape-jet sequences, the mantle diameter data were plotted against time. Time was estimated from the video camera frame rate (approximately 0.017 s per video field). To correct for differences in animal size, the diameter change between consecutive video fields was divided by the resting mantle diameter. The rate of mantle contraction was determined by dividing the mantle diameter change between successive video fields by 0.017 s. This calculation yielded a set of incremental rates of mantle contraction. The highest incremental rate was reported as the maximum rate of mantle contraction for that animal.

The frequency of escape jets was calculated by dividing the number of complete escape-jet cycles (the exhalant plus the inhalant phases) by the time required to perform the behavior. Time was estimated from the frame rate of the video camera as above. Measurements were made only from video sequences of squid that performed two or more escape jets in rapid succession. Multiple measurements were made for each squid, but only the highest calculated escape-jet frequency was reported.

Morphometrics

The dorsal mantle length of anesthetized squid was measured to the nearest 0.1 mm using calipers. We chose dorsal mantle length as a measure of squid size because it is simple to measure accurately and it correlates strongly with squid wet weight (Segawa, 1987).

The volume of the mantle cavity was measured for most animals after videotaping. Each squid was anesthetized (Messenger *et al.*, 1985) at 20 °C for 15 min to relax the mantle musculature. The animal was then lifted from the anesthetic by the arms so that the mantle cavity remained filled with water. The exterior of the squid was gently blotted dry and the animal weighed on an electronic balance to the nearest 0.0001 g. The squid was returned to the water and then lifted by the tip of the mantle so that water emptied from the mantle cavity. The mantle was squeezed gently, in the posterior to anterior direction, to aid draining of the mantle cavity. The outside of the squid was blotted dry and the animal weighed again. We calculated the volume of the mantle cavity by dividing the difference in weight between the two measurements by the density of seawater at 20 °C ($1.024 \times 10^3 \text{ kg m}^{-3}$). This procedure was repeated three to five times for each squid, and the average mantle cavity volume was recorded. We normalized the volume measurements by dividing the mantle cavity volume by the wet weight of the squid.

Mantle radius was measured in all the squid. Resting mantle diameter was measured from digitized video frames

of the dorsal mantle of anesthetized animals. The mantle was assumed to be cylindrical, and the diameter was measured at $\frac{1}{3}$ DML. Mantle radius was then calculated from the diameter data.

The thickness of the mantle wall was measured in 21 specimens. Anesthetized animals were decapitated and a transverse slice of the mantle was made at one-third DML. A digital image of the slice was captured using a dissecting microscope, and the thickness of the mantle wall at the ventral midline was measured using morphometrics software.

The mantle wall thickness and radius were used to calculate mantle circumferential strain during the escape jet. The circumferential strain experienced during jet locomotion at the midpoint in the thickness of the mantle wall was calculated using the following equation from MacGillivray *et al.* (1999):

$$\epsilon_c = 1 - [(R_f - \frac{1}{2}t_f)/(R_i - \frac{1}{2}t_i)] \quad (1)$$

ϵ_c is the circumferential strain, R_i is the initial ("resting") outer radius of the mantle, R_f is the final outer radius of the contracted mantle, t_i is the initial thickness of the mantle wall, and t_f is the thickness of the contracted mantle wall. The resting outer radius and mantle wall thickness, R_i and t_i , were measured from the digital images. The final outer radius of the contracted mantle, R_f , was measured from the videotapes, and t_f was then calculated using the following equation from MacGillivray *et al.* (1999):

$$t_f = R_f - [R_f^2 - t_i(2R_i - t_i)]^{0.5} \quad (2)$$

By convention, negative circumferential strain values indicate contraction of the mantle, and positive values indicate hyperinflation of the mantle.

Statistics

All correlations were made using the Spearman rank order correlation (Sokal and Rohlf, 1981). This nonparametric statistical test was used because the data for dorsal mantle length were not distributed normally (Kolmogorov-Smirnov goodness of fit test, $P < 0.01$; Zar, 1996) due to a sample bias toward smaller squid.

The mantle kinematics data were subdivided into the life-history stages identified by Segawa (1987). This scheme separates *S. lessoniana* into seven size classes based on morphological and ecological characteristics. The squid used in the experiments include four of Segawa's (1987) life-history stages: hatchling (5 mm to 10 mm DML), juvenile 1 (11 mm to 25 mm DML), juvenile 2 (26 mm to 40 mm DML), and young 2 (60 mm to 100 mm DML). After subdivision into the appropriate life-history stage, the data in each stage were compared with a one-way ANOVA. Pairwise comparisons were made using the Student-Newman-Keuls method of comparison (Zar, 1996). This analysis

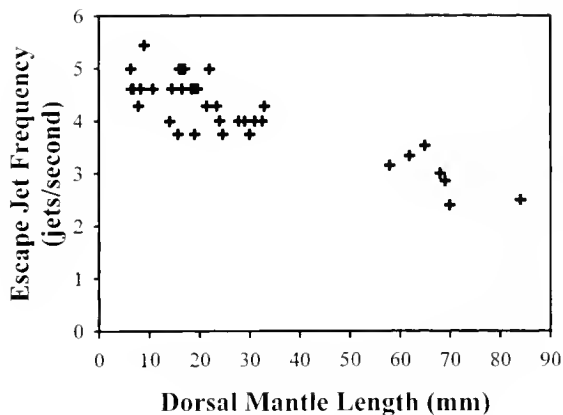


Figure 2. Ontogenetic change in escape-jet frequency. Each point represents the average frequency of at least two consecutive escape jets. Escape-jet frequency was inversely correlated with squid size (Spearman rank order correlation coefficient, -0.75 , $P < 0.0001$, $n = 38$).

was appropriate because the data in each stage were distributed normally (Kolmogorov-Smirnov goodness of fit test, $P > 0.4$ for each stage; Zar, 1996).

The mantle wall thickness and mantle radius data were log transformed and regressed against dorsal mantle length using a least-squares technique (Zar, 1996). Student's t distribution was used to test the slopes against the null hypothesis slope of 1.0 (Zar, 1996).

Results

Escape-jet behavior

Tethered specimens of *Sepioteuthis lessoniana* escape jetted spontaneously upon recovery from the anesthesia and in response to visual stimuli outside the aquarium. Squid escape jetted periodically during the experimental trials and frequently jetted multiple times in succession. The number of escape jets performed consecutively seemed to vary with the size and age of the animal, with smaller, younger squid performing more consecutive escape jets than larger, older squid. Hatchling-stage squid (5 mm to 10 mm DML) often jetted five times in rapid succession, paused briefly, and then repeated the series of five jets two or three additional times. Such behavior was never observed in squid larger than about 25 mm DML (the juvenile 2 life history stage of Segawa, 1987). The escape-jet frequency of smaller, younger squid was higher than that of older and larger squid (Fig. 2; correlation coefficient, -0.75 , $P < 0.0001$, $n = 38$). For example, newly hatched squid performed four to five escape-jet cycles per second, whereas two to three escape-jet cycles per second were recorded for the largest squid.

Mantle kinematics

The mantle kinematics during escape-jet behavior varied both in an individual squid over time and among all the

squid studied. There were two distinct modes of mantle movement immediately prior to the start of an escape jet. In one mode, there was little mantle hyperinflation and the mantle cavity was ventilated, presumably by contraction of the circumferential musculature (Fig. 3A; see Gosline *et al.*, 1983). In the other mode, the mantle cavity was ventilated primarily by mantle hyperinflation, presumably by contraction of the radial musculature (Fig. 3B; see Gosline *et al.*, 1983). There was no correlation between squid size and the mode of mantle kinematics prior to the start of an escape jet. Many of the squid studied exhibited both modes of mantle kinematics, but the second mode (hyperinflation) was the most common.

Regardless of age or size, the escape jet was stereotyped. At the start, the mantle hyperinflated, filling the mantle cavity with water (Fig. 4A). Next, the collar flaps closed and the anteriormost edge of the mantle began to contract (analogous to a drawstring closing a bag) (Fig. 4B). The contraction of the anterior mantle edge was most noticeable in

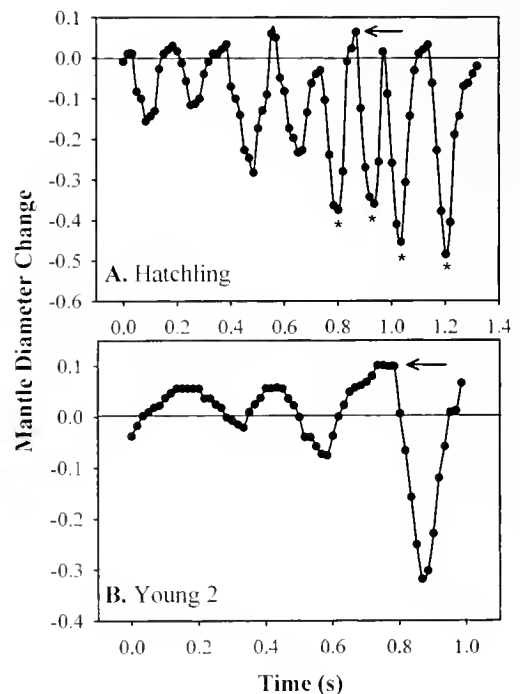


Figure 3. Mantle diameter change over time. The horizontal line at 0.0 indicates the resting mantle diameter of the anesthetized squid. The negative numbers indicate mantle contraction, and positive values denote mantle hyperinflation. (A) A hatchling stage squid (5.5 mm dorsal mantle length, DML) that performed four consecutive escape jets (indicated by asterisks). The arrow indicates a mantle hyperinflation immediately prior to an escape jet. Note that the low-amplitude mantle movements prior to the escape jets do not involve substantial mantle hyperinflation. (B) A single escape jet from a young 2 stage squid (65 mm DML). The arrow indicates the mantle hyperinflation prior to the start of the escape jet. Note that the lower amplitude mantle movements prior to the escape jet consist almost entirely of mantle hyperinflation and do not involve substantial mantle contraction.

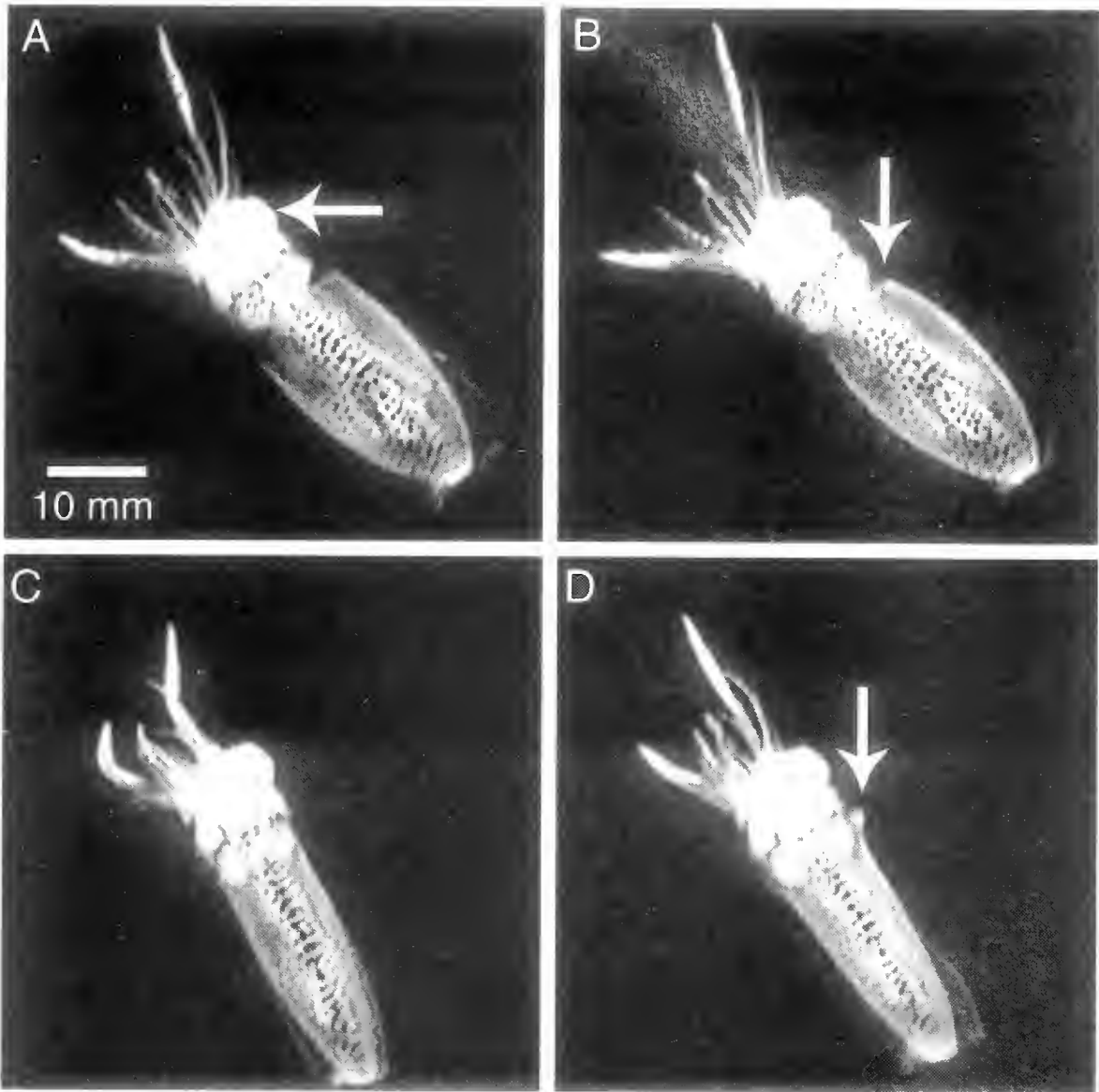


Figure 4. Nonconsecutive digitized video frames from an escape jet by a 3-week-old specimen of *Sepioteuthis lessonana* (25-mm DML). (A) The squid immediately before the start of mantle contraction. The mantle is fully expanded, and the mantle cavity is full of water. The bright region of reflection on the head (arrow) is the plastic washer of the tethering apparatus. (B) The squid just after the start of the escape jet. The anterior edge of the mantle (arrow) has contracted, and the remainder of the mantle is just beginning to contract. (C) The mantle near its maximum contraction for the escape jet. The head is drawn back into the mantle cavity, and the fins are folded along the body. (D) The end of the exhalant phase and the start of the inhalant phase of the escape jet. The fins (barely visible on right side) are unfolding and beginning to undulate. The head is maximally withdrawn into the mantle cavity, and the anterior edge of the mantle is starting to flare (arrow) away from the head.

squid larger than 40 mm DML (about 5 to 6 weeks post hatching). One video field (about 17 ms) after the start of anterior mantle-edge contraction, two events occurred: (1) the fins were folded against the ventral side of the mantle, and (2) the remainder of the mantle began to contract rapidly, expelling water from the mantle cavity through the funnel (Figs. 4B, C). Nearly simultaneous with folding of

the fins, the head was drawn back into the mantle cavity, presumably by the activation of the head retractor muscles. Maximal head retraction was completed within two video fields (about 34 ms) and was maintained until the end of the exhalant phase of the jet (Fig. 4C). At the end of the exhalant phase of the jet, the fins unfolded and began undulating immediately. Concurrent with fin unfolding, the

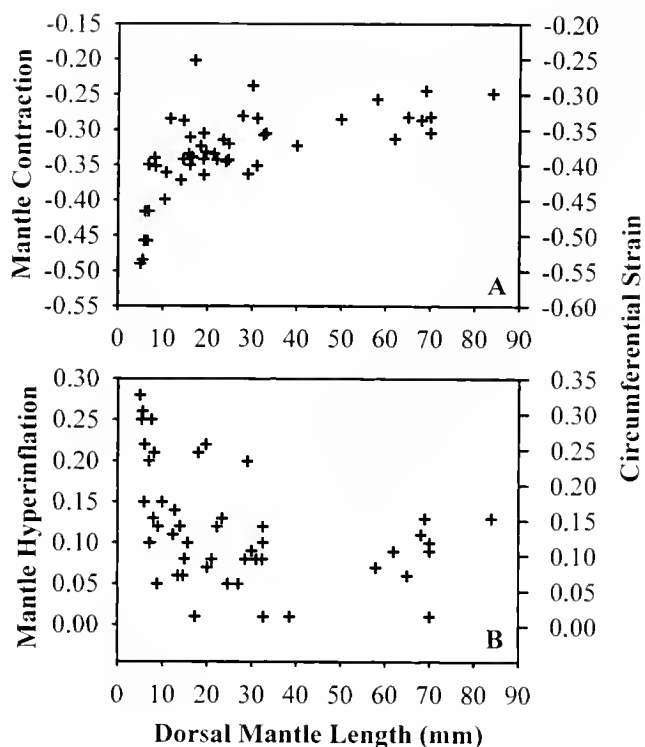


Figure 5. Ontogenetic changes in mantle contraction and mantle hyperinflation during the escape jet. Each point represents the maximum mantle diameter change (contraction or hyperinflation) for an individual squid during an escape jet. (A) Mantle contraction and circumferential strain *versus* dorsal mantle length. The plot shows a significant decrease in the maximum mantle contraction of the escape jet during ontogeny (Spearman rank order correlation coefficient, 0.70, $P < 0.0001$, $n = 55$). (B) Mantle hyperinflation prior to the start of an escape jet *versus* dorsal mantle length. The plot shows a significant ontogenetic decrease in maximum mantle hyperinflation prior to an escape jet (Spearman rank order correlation coefficient, -0.49 , $P < 0.0001$, $n = 49$). For A and B, the mantle contraction and hyperinflation scales differ from the circumferential strain scales because both mantle contraction and hyperinflation are measures of the outer circumference of the mantle, whereas circumferential strain is a measure of changes in mantle wall circumference at the midpoint of the thickness of the mantle wall, and mantle thickness increases during contraction (because the mantle wall is isovolumetric).

anterior margin of the mantle flared outward (Fig. 4D). In animals smaller than 20 mm DML, this flaring was usually accompanied by even greater contraction of the mantle in the anterior $\frac{1}{3}$ of the mantle.

Ontogeny of mantle kinematics

A significant ontogenetic change in the amplitude of mantle movement during escape-jet behavior was observed in *S. lessoniana*. In smaller and younger animals there was a greater change in mantle diameter than in larger, older squid (Fig. 5A; Spearman rank order correlation coefficient, 0.7, $P \ll 0.001$, $n = 55$). In newly hatched squid, the mantle contracted 41% to 49% during the escape jet, but it contracted by only 25% to 32% in larger animals (Fig. 5A; see Table 1 for descriptive statistics based on life history stage). After dividing the data into the life-history stages described by Segawa (1987), the average mantle contraction during the escape jet of the hatchling stage (5 mm to 10 mm DML) squid was significantly greater than in any other life history-stage measured (one-way ANOVA, Student-Newman-Keuls test, $P < 0.05$; Table 1). In addition, the average mantle contraction of squid in the juvenile 1 stage (11 mm to 25 mm DML) was significantly larger than squid in the young 2 stage (60 mm to 100 mm DML) (one-way ANOVA, Student-Newman-Keuls test, $P = 0.05$; Table 1).

There was a significant ontogenetic decrease in the amplitude of mantle hyperinflation prior to the start of the escape jet (Spearman rank order correlation coefficient, -0.49 , $P \ll 0.001$, $n = 49$). In newly hatched *S. lessoniana*, the mantle hyperinflated between 15% and 27%, but it hyperinflated only 1% to 15% in older, larger animals (Fig. 5B; see Table 1 for descriptive statistics). After dividing the data into the life-history stages of Segawa (1987), the average mantle hyperinflation prior to the start of the escape jet was significantly greater in the hatchling stage squid than in all the other stages (one-

Table 1

Comparison of mantle kinematics during the escape jet among squid divided into the life-history stages defined by Segawa (1987)

Life-history stage	Maximum contraction	Maximum hyperinflation	Maximum contraction rate (lengths/s)
Hatchling	-0.40 ± 0.057 (13)	0.18 ± 0.072 (14)	8.6 ± 2.1 (14)
Juvenile 1	-0.32 ± 0.037 (23)*	0.11 ± 0.015 (15)	4.8 ± 1.2 (16)
Juvenile 2	-0.31 ± 0.040 (8)	0.086 ± 0.054 (11)	3.8 ± 1.7 (10)
Young 2	-0.28 ± 0.024 (9)*	0.088 ± 0.038 (9)	3.8 ± 0.55 (9)

Values represent mean maximum mantle contraction, mantle hyperinflation, and mantle contraction rate during the escape jet plus or minus the standard deviation of the mean. The number of squid in the sample is in parentheses. Maximum values for mantle contraction amplitude, mantle hyperinflation amplitude, or mantle contraction rate for all squid in a life-history stage were pooled to calculate the mean and the standard deviation. In each column, the mean value for the hatchling stage squid was significantly different from the mean for the juvenile 1, juvenile 2, and young 2 life-history stages (one-way ANOVA on ranks, $P < 0.05$). The asterisks in the Maximum contraction column denote a significant difference in mantle contraction between the juvenile 1 and young 2 life-history stages (one-way ANOVA on ranks, $P = 0.05$). Other within-column comparisons of mantle kinematics were not significantly different.

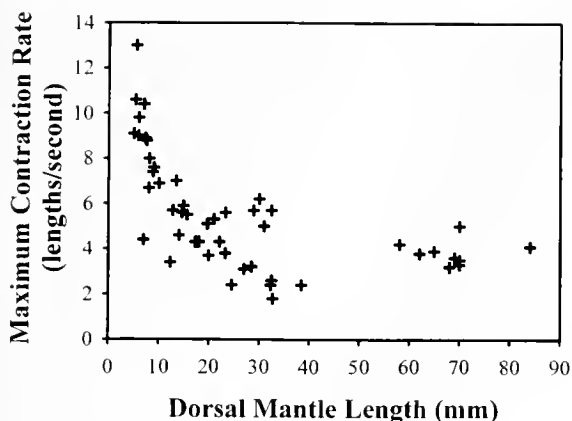


Figure 6. Ontogenetic change in the maximum rate of mantle contraction. Each point represents the maximum rate of mantle contraction during the escape jet for one individual. The maximum mantle contraction rate of the escape jet decreased significantly during ontogeny (Spearman rank order correlation coefficient, -0.76 , $P < 0.0001$, $n = 49$).

way ANOVA, Student-Newman-Keuls test, $P < 0.05$; Table 1).

The maximum rate of mantle contraction during the escape jet was highest in newly hatched squid and declined during ontogeny (Fig. 6; Spearman rank order correlation coefficient, -0.76 , $P \ll 0.001$, $n = 49$). The maximum rate of mantle contraction varied from 7 to 13 mantle circumference lengths per second in newly hatched squid and from 3 to 5 lengths per second in the largest squid (Fig. 6). A one-way ANOVA among the life-history stages (Segawa, 1987) indicated that hatchling stage *S. lessoniana* had a significantly greater maximum rate of mantle contraction during the escape jet than all other life history stages (Student-Newman-Keuls test, $P < 0.05$; Table 1).

Morphometrics

Mass-specific mantle cavity volume decreased during ontogeny (Fig. 7A). Despite the variation among squid of similar size, there was a significant negative correlation between mass-specific mantle cavity volume and dorsal mantle length (Spearman rank order correlation coefficient, -0.50 , $P = 0.002$, $n = 36$).

The thickness of the mantle wall increased during ontogeny (Fig. 7B). The slope of the regression, 1.29, was significantly greater than 1 (Student's *t* test, $P < 0.01$).

Mantle radius also increased during ontogeny (Fig. 7C). The slope of the regression, 0.85, was significantly less than 1 (Student's *t* test, $P < 0.01$).

Discussion

The escape-jet sequence

The general pattern of the escape jet did not vary with squid age or size. However, the mantle kinematics during

an escape jet did change as the squid grew. These ontogenetic changes in escape-jet kinematics may arise from alterations in the neurophysiology (Gilly *et al.*, 1991), muscle physiology (Preuss *et al.*, 1997), morphology (Moltschaniwskyj, 1995), or mechanical properties of the mantle. Furthermore, the changes may have implications

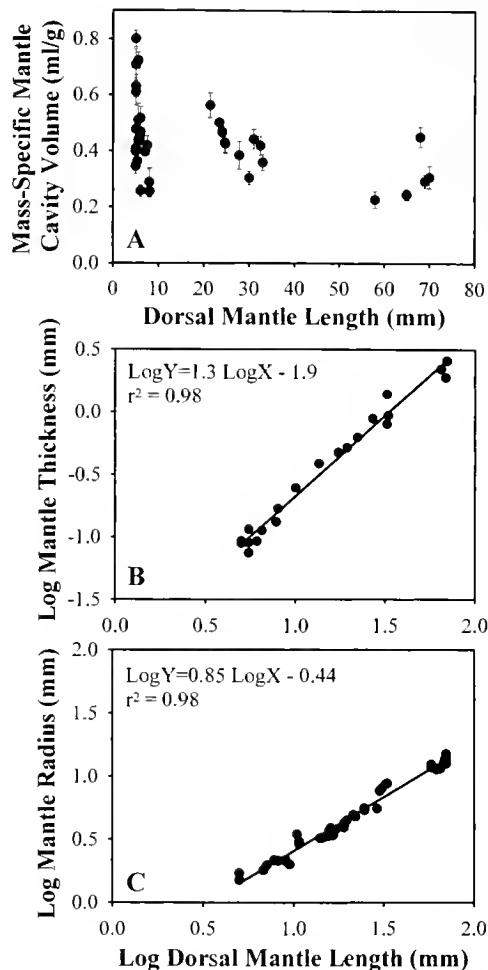


Figure 7. Ontogenetic changes in mantle morphometrics. (A) Mass-specific mantle cavity volume *versus* dorsal mantle length. Each point represents the average of between three and five measurements of mantle cavity volume for each squid \pm the standard error of the mean. Dividing the average mantle cavity volume for one squid by the wet weight of the same animal normalized the data for the volume of the mantle cavity. Mass-specific mantle cavity volume decreased significantly during ontogeny (Spearman rank order correlation coefficient, -0.50 , $P = 0.002$, $n = 36$). (B) Log mantle wall thickness *versus* log dorsal mantle length. The equation for the least-squares regression and the corrected r^2 value are listed at the upper left. The slope of the regression (1.29) was significantly greater than 1.0 (Student's *t* test, $P < 0.01$), indicating a positive allometric relationship between mantle wall thickness and mantle length. (C) Log mantle radius *versus* log dorsal mantle length. The equation for the least-squares regression and the corrected r^2 value are listed at the upper left. The slope of the regression (0.85) was significantly less than 1.0 (Student's *t* test, $P < 0.01$), indicating a negative allometric relationship between mantle radius and mantle length.

for the mechanics of escape-jet locomotion during growth.

Fatigue

The relative proportions of circumferential muscle fiber types in the mantle of *S. lessoniana* change during ontogeny (Thompson, 2000; Thompson and Kier, 2001). Newly hatched individuals of *S. lessoniana* have a larger proportion of mitochondria-rich circumferential muscle fibers (analogous to vertebrate red muscle fibers, see Bone *et al.*, 1981, and Mommsen *et al.*, 1981) than older, larger squid. Preuss *et al.* (1997) reported a similar change during growth in the relative proportion of circumferential muscle fiber types in the mantle of another loliginid squid, *Loligo opalescens*. Preuss *et al.* (1997) suggested that the greater proportion of mitochondria-rich circumferential mantle muscle fibers made the hatchling squid more resistant to fatigue than older, larger animals. The data from the present study support their hypothesis. Small, young specimens of *S. lessoniana* were able to perform more consecutive escape jets and seemed to tire much less readily than their larger, older counterparts. However, motivational differences between small and large squid may also affect jetting behavior.

Newly hatched squid seem to rely more heavily on frequent jet locomotion than do larger squid (Fields, 1965; Hoar *et al.*, 1994; Preuss *et al.*, 1997). Two reasons have been suggested for this tendency. First, the fins of newly hatched squid are rudimentary relative to the adult fins (Boletzky, 1974; Okutani, 1987; Hoar *et al.*, 1994), and it has been proposed that these diminutive fins may not generate sufficient thrust for locomotion or hovering (Boletzky, 1987; Hoar *et al.*, 1994). Second, most newly hatched squid live in a fluid regime that is characterized by an intermediate Reynolds number (estimated from data in Packard, 1969, and O'Dor *et al.*, 1986; see Jordan, 1992, and Daniel *et al.*, 1992, for further discussion of intermediate Re) and in which the near parity of viscous and inertial forces inhibits coasting after a jet. Unlike large squid that can perform a single jet and then coast for a considerable distance, small squid must jet continuously to locomote. Hence, there may be an advantage in having a large proportion of the locomotor musculature specialized for fatigue resistance, particularly if jetting is the primary mode of locomotion. The price for such specialization, however, may be a reduction in the peak force produced by the mantle musculature during contraction.

Mantle kinematics

The mantle cavity of a hatchling of *S. lessoniana* holds a proportionately greater volume of water than the mantle cavity of a larger squid (Fig. 7A). In addition, a larger proportion of this volume is ejected from a hatchling during

an escape jet (Fig. 5A). Finally, the maximum rate of mantle contraction during an escape jet is highest in a newly hatched squid (Fig. 6). Taken together, these data imply that mass flux (*i.e.*, the product of the density of water in the mantle cavity and the volume rate of water flow out of the mantle cavity) during the escape jet is proportionately greater in hatchling than in larger, older individuals of *S. lessoniana*.

We used the mantle kinematics and morphometric data to calculate the relative mass flux during the escape jet in two life stages of *S. lessoniana*: a 5.5-mm-DML hatchling stage and a 65-mm-DML young 2 stage. We modeled the mantle as a cylinder with the "resting" wall thickness and radius calculated from the regressions of the mantle wall thickness (Fig. 7B) and mantle radius (Fig. 7C) data. To simplify the calculations, we based them on a transverse slice of the cylinder at $\frac{1}{3}$ DML. We assumed that both the length of the cylinder and the volume of the cylinder wall were constant; thus, the cylinder-wall area of the slice was held constant during the calculations. The initial mass-specific mantle cavity volume for each squid was obtained from the data in Figure 7A. We used the data for average mantle contraction and the maximum rate of mantle contraction from Table 1 to calculate the amplitude and rate of changes in mantle radius. We used equation (2) to calculate the increase in mantle wall thickness during the simulated jet. Finally, we calculated the relative mass (*i.e.*, mass of water divided by mass of squid) of water remaining in the mantle cavity during the simulated jet at 25-ms intervals.

The calculations predict greater relative mass flux during the escape jet in the hatchling stage squid than in the young 2 stage (Fig. 8A). The average mass flux over the duration of the exhalant phase of the escape jet in a hatchling stage squid is about 2 times greater than that of an animal in the young 2 stage (Fig. 8A).

We calculated the average mass flux over the entire duration of the exhalant phase of the escape jet for the 55 squid from Figure 5A. We modeled the mantle as a cylinder of constant length with a mantle cavity volume determined from Figure 7A. Using the mantle contraction data from Figure 5A, and calculating changes in the thickness of the mantle wall during the jet using equation (2), we calculated the normalized mass of water in the mantle cavity (*i.e.*, mass of water divided by mass of squid) at the start and at the end of an escape jet. The change in normalized mass was divided by the duration of the exhalant phase of the jet to give the average mass flux. The calculations show an ontogenetic decrease in the normalized average mass flux of the escape jet (Fig. 8B). Mass flux is proportionately highest in hatchling squid and decreases rapidly during growth (Fig. 8B; correlation coefficient, -0.81 , $P < 0.0001$, $n = 55$).

Does the predicted ontogenetic decline in relative mass flux imply that the mass-specific thrust produced the escape jet is highest early in ontogeny? Mass flux constitutes only

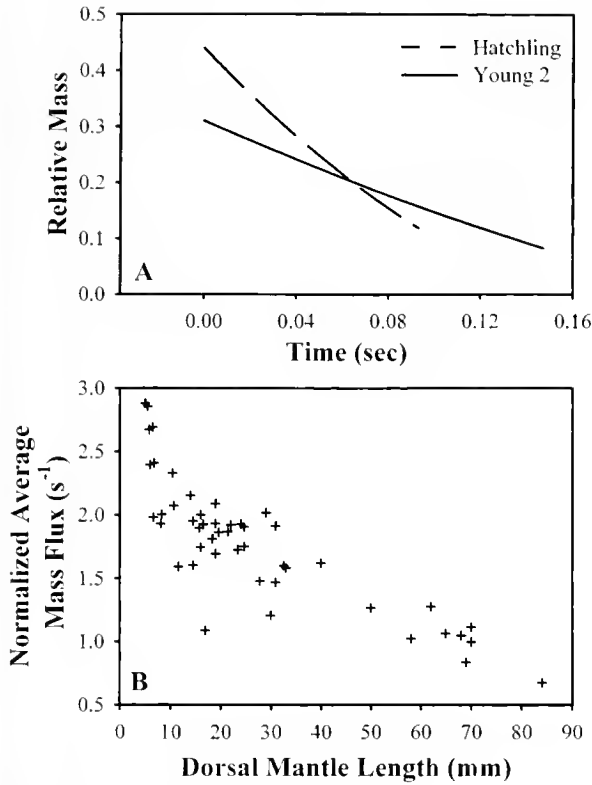


Figure 8. Ontogenetic differences in the mass flux of the escape jet. (A) Calculation of the relative mass of water remaining in the mantle cavity versus the time course of the exhalant phase of one escape jet. The dashed line represents a hatchling stage squid (5.5 mm dorsal mantle length) and the solid line a young 2 stage animal (65 mm dorsal mantle length). For each squid, the relative mass of water in the mantle cavity at 0.025-s intervals during the escape jet was calculated using morphometric and mantle kinematics data. See the Discussion for more details. The data for each animal were fitted with a polynomial equation. The equations are, $Y = 1.7X^2 - 1.8X + 0.31$ ($r^2 = 0.99$) for the young 2 squid and $Y = 9.3X^2 - 4.3X + 0.44$ ($r^2 = 0.99$) for the hatchling squid. The derivative of each equation yields the average mass flux during the escape jet. The average mass flux of the hatchling animal is approximately 2 times greater than that for the larger animal. Note that mass flux is highest early in the escape jet and diminishes at the end of the escape jet. (B) Calculation of the average mass flux of the escape jet versus dorsal mantle length. Each point represents the average mass flux of the exhalant phase of the escape jet normalized by the wet weight of the squid. Normalized average mass flux decreased significantly during ontogeny (Spearman rank order correlation coefficient, -0.81 , $P < 0.0001$, $n = 55$). See the Discussion for more details.

a portion of the total jet thrust. Under steady-state conditions, the instantaneous thrust produced during a jet is proportional to the product of the instantaneous mass flux and the instantaneous velocity of the water exiting the funnel (averaged over the funnel aperture; Vogel, 1994). Because it is likely that unsteady effects are important in jet locomotion (Anderson and DeMont, 2000), an unsteady term must also be included in an equation used to calculate jet thrust (see Anderson and DeMont, 2000).

Under both steady-state and unsteady conditions, the velocity of water exiting the funnel depends, in large part, on the diameter of the funnel aperture. The funnel complex is largest in newly hatched squid and decreases in relative size during ontogeny (Boletzky, 1974; unpubl. obs. of *S. lessoniana* and *Loligo pealei*). Unfortunately, funnel aperture cannot be determined simply from the size of the funnel of an anesthetized squid because it is a muscular structure that changes shape during a single jet (Zuev, 1966; O'Dor, 1988; Anderson and DeMont, 2000). Furthermore, measuring funnel aperture accurately during escape-jet locomotion in small hatchling and juvenile squid is not currently feasible. Without data on the scaling of the funnel aperture and dynamic changes in the aperture during a jet cycle, it is not possible to make precise predictions about the mass-specific thrust produced during the escape jet.

Whether jet thrust is generated by means of steady or unsteady mechanisms, the greater relative mass flux predicted for hatchling-stage individuals of *S. lessoniana* could allow a given thrust to be achieved with a relatively low jet velocity. This may result in a hatchling stage squid having a higher propulsion efficiency than an older, larger squid. Anderson and DeMont (2000) calculated the hydrodynamic propulsion efficiency (η) of the exhalant phase of the jet stroke using the following equation of rocket motor propulsion efficiency:

$$\eta = (2VV_j)/(V^2 + V_j^2), \quad (3)$$

where V is the velocity of flow past the squid and V_j is the velocity of the jet relative to the squid. According to equation (3), the highest propulsion efficiency is achieved when V_j approximates V . Because V_j must be greater than V for a squid to accelerate, relatively lower jet velocity increases propulsion efficiency. Anderson and DeMont (2000) emphasize, however, that the overall propulsion efficiency of the jet includes both the efficiency of the jet stroke and the efficiency of refilling the mantle cavity. A thorough ontogenetic comparison of total hydrodynamic propulsion efficiency must, therefore, also consider the efficiency of mantle cavity refilling.

In the intermediate Reynolds number fluid regime of the newly hatched and juvenile squid, the generation of jet thrust may not be represented accurately by existing equations. Previous theoretical treatments consider jet propulsion at high Reynolds numbers. In the absence of a mathematical model of jet locomotion at these intermediate Reynolds numbers, measurements of the actual thrust produced are required. Therefore, direct measurements of the thrust produced during an escape jet are needed to understand how the ontogenetic changes in mantle kinematics affect thrust.

Skeletal support and mantle kinematics

In many vermiform animals, the arrangement of connective tissue fibers in the body wall helps to control the shape of the animal during locomotion and movement (e.g., Harris and Crofton, 1957; Clark and Cowey, 1958). Similarly, the ontogenetic changes in mantle kinematics during escape-jet locomotion may result from ontogenetic alterations in the organization and the mechanical properties of the skeletal support system of the squid mantle.

In the mantle, skeletal support for locomotion is provided by a complex arrangement of fibers of muscle and connective tissue (Ward and Wainwright, 1972; Bone *et al.*, 1981). As described earlier, the connective tissue fibers are arranged in distinct networks: the inner tunic, the outer tunic, and three distinct systems of intramuscular (IM) fibers—IM-1, IM-2, and IM-3 (Ward and Wainwright, 1972; Bone *et al.*, 1981; for review, see Gosline and DeMont, 1985). The fibers in all the IM systems are collagenous (Ward and Wainwright, 1972; Gosline and Shadwick, 1983a; MacGillivray *et al.*, 1999), and the collagen fibers in IM-1 and IM-2 are hypothesized to antagonize the circumferential muscles that provide power for locomotion.

The organization of collagen fibers in the outer tunic and IM fiber networks of the mantle changes dramatically during the ontogeny of *S. lessoniana* (Thompson, 2000; Thompson and Kier, 2001). The IM-1 collagen fiber angle (*i.e.*, the angle of the collagen fiber relative to the long axis of the mantle) is lowest in newly hatched squid and increases exponentially during growth in squid up to 15 mm DML. In squid larger than about 15 mm DML, IM-1 fiber angle does not change substantially. IM-2 collagen fiber angle (*i.e.*, the angle of the collagen fiber relative to the outer curvature of the mantle) is lowest in hatchlings and rises exponentially until the squid reach 15 mm DML. In animals larger than 15 mm DML, IM-2 fiber angle increases only slightly with size. The correlation between these ontogenetic alterations in connective tissue organization and the mantle kinematics measured in this study is striking (Fig. 9). Maximum mantle contraction (Fig. 5A), maximum mantle hyperinflation (Fig. 5B), and maximum mantle contraction rate (Fig. 6) all change exponentially up to a dorsal mantle length of about 15 mm.

It is possible that the allometric changes in mantle thickness and mantle radius (Fig. 7B, C) might, at least in part, underlie the ontogenetic change in IM-1 and IM-2 fiber angle. We were unable, however, to detect a clear relationship between the scaling of mantle thickness or radius and IM-1 or IM-2 fiber angle.

Simple mathematical models (Thompson, 2000; Thompson and Kier, 2001) of the ontogenetic changes in IM-1 and IM-2 fiber angle predict significantly greater amplitude of mantle movements during escape-jet locomotion in newly hatched squid than in older, larger animals. The models,

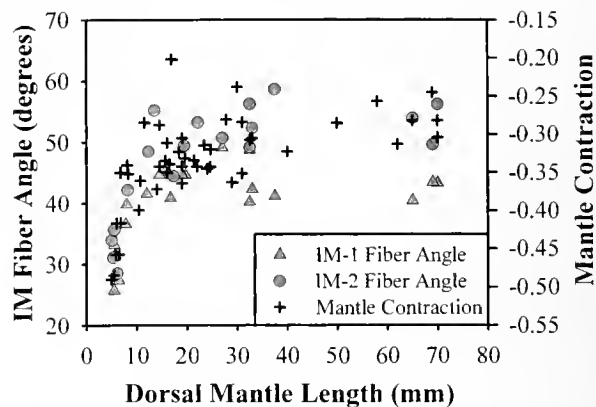


Figure 9. Correlation between ontogenetic changes in intramuscular collagen fiber angle and the mantle kinematics of the escape jet. The maximum mantle contraction during an escape jet (data from Fig. 5A) is indicated by the black crosses, and the scale is on the right side of the plot. The gray triangles indicate the average fiber angle of intramuscular fiber system 1 (IM-1) collagen fibers, and the gray circles denote the average fiber angle of IM-2 collagen fibers. Note the correlation between IM-1 and IM-2 average fiber angles and the mantle kinematics of the escape jet.

which consider only the fiber angle and probable mechanical properties of the IM collagen fibers (see Gosline and Shadwick, 1983b), predict that mantle circumference changes up to -45% are possible in hatchling stage squid, whereas changes of only -25% to -30% are possible in squid at the young 2 stage (Thompson, 2000; Thompson and Kier, 2001). The present study supports the predictions of the models. Maximum mantle contraction during the escape jet in hatchlings of *S. lessoniana* ranged from -41% to -49% and from -27% to -32% in animals at the young 2 stage. Additional work on the ontogeny of the mechanical properties of squid mantle collagen is necessary to understand better the relationship among connective tissue organization, mantle mechanical properties, and mantle function.

Muscle mechanics

The maximum rate of mantle contraction was significantly higher in newly hatched individuals of *S. lessoniana* than in the larger animals (Fig. 6; Table 1). The shortening velocity of muscle fibers depends on the load of the muscle, the length of the thick filaments and sarcomeres, and the rate of cross-bridge cycling (Schmidt-Nielsen, 1997). The loading of the muscle fibers during jet propulsion is difficult to measure. It should be possible, however, to measure the contractile properties and myofibril dimensions of the circumferential muscle from an ontogenetic series of squid to examine the possibility of a change in performance of the muscle during ontogeny.

Comparison of the shortening speed of the circumferential muscles calculated here for *S. lessoniana* with previous

measurements in adults of *Alloteuthis subulata* and *Sepia officinalis* are complicated by differences in temperature. The unloaded shortening speed at 11 °C of the circumferential musculature in *A. subulata* and *S. officinalis* was measured to be 2.0 lengths per second and 1.5 lengths per second, respectively (Milligan *et al.*, 1997). In *S. lessoniana*, the maximum rate of mantle contraction at 23 °C ranged from a high of 13 lengths per second in the hatchlings to 4 in the young 2 stage squid.

Although the Q_{10} for cephalopod muscles has not been measured, previous work on type 1 and type 2 iliofibularis muscle fibers from *Xenopus laevis* (Lännergren *et al.*, 1982) revealed a Q_{10} of approximately 2 over this temperature range. Thus, although the difference in measured shortening velocity between the young 2 stage of *S. lessoniana* and the adult of *A. subulata* may be due to temperature, it is unlikely that the much higher velocities measured in the hatchlings are simply an effect of temperature. In addition, the circumferential muscles are contracting against a load during an escape jet, and thus the unloaded shortening velocity of circumferential muscle in *S. lessoniana* will be higher than the values reported here.

In conclusion, we have described significant ontogenetic changes in the mantle kinematics of the escape jet in tethered squid. These kinematic changes are correlated strongly with alterations in the organization of the connective tissue fibers in the mantle; furthermore, they may affect the mass flux of the escape jet. An analysis of the mechanics of escape-jet locomotion in an ontogenetic series of squid is needed to better comprehend the implications of growth-related changes in mantle kinematics. Such an analysis will help us to understand the functional consequences of ontogenetic changes in morphology and will provide insight into the evolution of the form and function of hydrostatic skeletons.

Acknowledgments

This research was supported by NSF grants to W.M.K. (IBN-9728707 and IBN-9219495). Grants and fellowships to J.T.T. from the Wilson Fund, the American Malacological Society, and Sigma Xi helped defray research expenses. We thank L. Walsh at the NRCC for her expertise in shipping squid cross-country. We thank J. M. Gosline, S. Johnsen, J. Taylor, T. Uyeno, and two anonymous reviewers for constructive comments and suggestions on an earlier version of the paper.

Literature Cited

- Anderson, E. J., and M. E. DeMont. 2000. The mechanics of locomotion in the squid *Loligo pealei*: locomotory function and unsteady hydrodynamics of the jet and intramantle pressure. *J. Exp. Biol.* **203**: 2851–2863.
- Boletzky, S. v. 1974. The "larvae" of Cephalopoda: A review. *Thalassia Jugosl.* **10**(1/2): 45–76.
- Boletzky, S. v. 1987. Juvenile behaviour. Pp. 45–60 in *Cephalopod Life Cycles. Vol. II: Comparative Reviews*, P. R. Boyle, ed. Academic Press, New York.
- Bone, Q., A. Pulsford, and A. D. Chubb. 1981. Squid mantle muscle. *J. Mar. Biol. Assoc. UK* **61**: 327–342.
- Calder, W. A. 1984. *Size, Function, and Life History*. Harvard University Press, Cambridge.
- Chen, D. S., G. v. Dykhuizen, J. Hodge, and W. F. Gilly. 1996. Ontogeny of copepod predation in juvenile squid (*Loligo opalescens*). *Biol. Bull.* **190**: 69–81.
- Choe, S. 1966. On the eggs, rearing, habits of the fry, and growth of some Cephalopoda. *Bull. Mar. Sci.* **16**: 330–348.
- Clark, R. B., and J. B. Cowey. 1958. Factors controlling the change of shape of certain nemertean and turbellarian worms. *J. Exp. Biol.* **35**: 731–748.
- Daniel, T. L., C. Jordan, and D. Grunbaum. 1992. Hydromechanics of swimming. Pp. 17–49 in *Advances in Comparative and Environmental Physiology. Vol. 11. Mechanics of Animal Locomotion*, R. M. Alexander, ed. Springer-Verlag, New York.
- Fields, W. G. 1965. The structure, development, food relations, reproduction and life history of the squid *Loligo opalescens* Berry. *Fish Bull.* **131**: 1–108.
- Gilly, W. F., B. Hopkins, and G. O. Mackie. 1991. Development of giant motor axons and neural control of escape responses in squid embryos and hatchlings. *Biol. Bull.* **180**: 209–220.
- Gosline, J. M., and M. E. DeMont. 1985. Jet-propelled swimming in squids. *Sci. Am.* **252**(1): 96–103.
- Gosline, J. M., and R. E. Shadwick. 1983a. The role of elastic energy storage mechanisms in swimming: an analysis of mantle elasticity in escape jetting in the squid, *Loligo opalescens*. *Can. J. Zool.* **61**: 1421–1431.
- Gosline, J. M., and R. E. Shadwick. 1983b. Molluscan collagen and its mechanical organization in squid mantle. Pp. 371–398 in *The Mollusca. Vol. 1: Metabolic Biochemistry and Molecular Biomechanics*, P. W. Hochachka, ed. Academic Press, New York.
- Gosline, J. M., J. D. Steeves, A. D. Harman, and M. E. DeMont. 1983. Patterns of circular and radial mantle muscle activity in respiration and jetting of the squid *Loligo opalescens*. *J. Exp. Biol.* **104**: 97–109.
- Hanlon, R. T., J. W. Forsythe, and S. v. Boletzky. 1985. Field and laboratory behavior of "Macrotritopus larvae" reared to *Octopus defilippi* Verany, 1851 (Mollusca: Cephalopoda). *Vie Milieu* **35**(3/4): 237–242.
- Harris, J. E., and H. D. Crofton. 1957. Structure and function in the nematodes: internal pressure and cuticular structure in *Ascaris*. *J. Exp. Biol.* **34**: 116–130.
- Hoar, J. A., E. Sim, D. M. Webber, and R. K. O'Dor. 1994. The role of fins in the competition between squid and fish. Pp. 27–43 in *Mechanics and Physiology of Animal Swimming*, L. Maddock, Q. Bone, and J. M. Rayner, eds. Cambridge University Press, Cambridge.
- Jordan, C. E. 1992. A model of rapid-start swimming at intermediate Reynolds number: undulatory locomotion in the chaetognath *Sagitta elegans*. *J. Exp. Biol.* **163**: 119–137.
- Kier, W. M. 1996. Muscle development in squid: ultrastructural differentiation of a specialized muscle fiber type. *J. Morphol.* **229**: 271–288.
- Lännergren, J., P. Lindblom, and B. Johansson. 1982. Contractile properties of two varieties of twitch fibres in *Xenopus laevis*. *Acta Physiol. Scand.* **114**: 523–535.
- Lee, P. G., P. E. Turk, W. T. Yang, and R. T. Hanlon. 1994. Biological characteristics and biomedical applications of the squid *Sepioteuthis lessoniana* cultured through multiple generations. *Biol. Bull.* **186**: 328–341.
- MacGillivray, P. S., E. J. Anderson, G. M. Wright, and M. E. DeMont. 1999. Structure and mechanics of the squid mantle. *J. Exp. Biol.* **202**: 683–695.

- Marliave, J. B.** 1980. Neustonic feeding in early larvae of *Octopus dofleini* (Wülker). *Veliger* **23**(4): 350–351.
- Messinger, J. B., M. Nixon, and K. P. Ryan.** 1985. Magnesium chloride as an anaesthetic for cephalopods. *Comp. Biochem. Physiol.* **82C**: 203–205.
- Milligan, B. J., N. A. Curtin, and Q. Bune.** 1997. Contractile properties of obliquely striated muscle from the mantle of squid (*Alloteuthis subulata*) and cuttlefish (*Sepia officinalis*). *J. Exp. Biol.* **200**: 2425–2436.
- Moltchanivskyj, N. A.** 1995. Changes in shape associated with growth in the loligid squid *Photololigo* sp.: a morphometric approach. *Can. J. Zool.* **73**: 1335–1343.
- Mommsen, T. P., J. Ballantyne, D. MacDonald, J. Gosline, and P. W. Hochachka.** 1981. Analogues of red and white muscle in squid mantle. *Proc. Nat. Acad. Sci. USA* **78**: 3274–3278.
- Moyriban, M., and A. E. Rodaniche.** 1982. The behavior and natural history of the Caribbean reef squid *Sepioteuthis sepioidea*. *Fortschr. Verhaltensforsch.* Supplement 25. Verlag-Parey, Berlin. 151 pp.
- O'Dor, R. K.** 1988. The forces acting on swimming squid. *J. Exp. Biol.* **137**: 421–442.
- O'Dor, R. K., P. Helm, and N. Balch.** 1985. Can rhynchoteuthions suspension feed? (Mollusca: Cephalopoda). *Vie Milieu* **35**(3/4): 267–271.
- O'Dor, R. K., E. A. Foy, P. L. Helm, and N. Balch.** 1986. The locomotion and energetics of hatching squid, *Illex illecebrosus*. *Am. Malac. Bull.* **4**(1): 55–60.
- Okutani, T.** 1987. Juvenile morphology. Pp. 33–44 in *Cephalopod Life Cycles, Vol. II: Comparative Reviews*, P. R. Boyle, ed. Academic Press, New York.
- Packard, A.** 1969. Jet propulsion and the giant fibre response of *Loligo*. *Nature* **221**: 875–877.
- Preuss, T., Z. N. Lebaric, and W. F. Gilly.** 1997. Post-hatching development of circular mantle muscles in the squid *Loligo opalescens*. *Biol. Bull.* **192**: 375–387.
- Schmidt-Nielsen, K.** 1997. *Animal Physiology*, 5th ed. Cambridge University Press, Cambridge.
- Segawa, S.** 1987. Life history of the oval squid, *Sepioteuthis lessoniana* in Kominato and adjacent waters central Honshu, Japan. *J. Tokyo Univ. Fish.* **74**(2): 67–105.
- Shadwick, R. E., and J. M. Gosline.** 1985. The role of collagen in the mechanical design of squid mantle. Pp. 299–304 in *Biology of Invertebrate and Lower Vertebrate Collagens*, A. Bairati and R. Garrone, eds. Plenum Press, New York.
- Sokal, R. R., and F. J. Rohlf.** 1981. *Biometry*, 2nd ed. W. H. Freeman, New York.
- Stearns, S. C.** 1992. *The Evolution of Life Histories*. Oxford University Press, Oxford.
- Sweeney, M. J., C. F. E. Roper, K. M. Mangold, M. R. Clarke, and S. v. Boletzky (eds.).** 1992. *Larval and Juvenile Cephalopods: A Manual For Their Identification*. Smithsonian Contributions to Zoology, No. 513.
- Thompson, J. T.** 2000. The ontogeny of mantle structure and function in the oval squid, *Sepioteuthis lessoniana* (Cephalopoda: Loliginidae). Ph.D. dissertation, University of North Carolina at Chapel Hill.
- Thompson, J. T., and W. M. Kier.** 2001. Ontogenetic changes in fibrous connective tissue organization in the oval squid, *Sepioteuthis lessoniana* Lesson, 1830. *Biol. Bull.* **201**: 136–153.
- Villanueva, R., C. Nozais, and S. v. Boletzky.** 1995. The planktonic life of octopuses. *Nature* **377**: 107.
- Vogel, S.** 1994. *Life in Moving Fluids*, 2nd ed. Princeton University Press, Princeton.
- Ward, D. V., and S. A. Wainwright.** 1972. Locomotory aspects of squid mantle structure. *J. Zool. (Lond.)* **167**: 437–449.
- Werner, E. E.** 1988. Size, scaling, and the evolution of complex life cycles. Pp. 60–81 in *Size-Structured Populations*, B. Ebenman and L. Persson, eds. Springer-Verlag, New York.
- Zar, J. H.** 1996. *Biostatistical Analysis*. Prentice Hall, Upper Saddle River, NJ.
- Zuev, G. V.** 1966. Characteristic features of the structure of cephalopod molluscs associated with controlled movements. *Ekologo-Morfologicheskije Issledovaniya Nektomnykh Zhivotnykh*. Kiev, Special Publication. (Canadian Fisheries and Marine Services Translation Series 1011, 1968).

Hydromineral Regulation in the Hydrothermal Vent Crab *Bythograea thermydron*

ANNE-SOPHIE MARTINEZ¹, JEAN-YVES TOULLEC², BRUCE SHILLITO³,
MIREILLE CHARMANTIER-DAURES¹, AND GUY CHARMANTIER^{1,*}

¹Laboratoire d'Ecophysiologie des Invertébrés, EA 3009 Adaptation Ecophysiologique au cours de l'Ontogénèse, Université Montpellier II, Pl E. Bataillon, 34095 Montpellier cedex 05, France;

²Laboratoire Biogénèse des Peptides Isomères, UMR Physiologie et Physiopathologie, Université P. et M. Curie, 7 Quai Saint-Bernard, 75252 Paris cedex 05, France; and ³Laboratoire de Biologie Cellulaire et Moléculaire du Développement, UMR 7622, Groupe Biologie Marine, UPMC, 7 Quai Saint-Bernard, 75252 Paris cedex 05, France

Abstract. This study investigates the salinity tolerance and the pattern of osmotic and ionic regulation of *Bythograea thermydron* Williams, 1980, a brachyuran crab endemic to the deep-sea hydrothermal vent habitat. Salinities of 33‰–35‰ were measured in the seawater surrounding the captured specimens. *B. thermydron* is a marine stenohaline osmoconformer, which tolerates salinities ranging between about 31‰ and 42‰. The time of osmotic adaptation after a sudden decrease in external salinity is about 15–24 h, which is relatively short for a brachyuran crab. In the range of tolerable salinities, it exhibits an iso-osmotic regulation, which is not affected by changes in hydrostatic pressure, and an iso-ionic regulation for Na⁺ and Cl⁻. The hemolymph Ca²⁺ concentration is slightly hyper-regulated, K⁺ concentration is slightly hyper-hypo-regulated, and Mg²⁺ concentration is strongly hypo-regulated. These findings probably reflect a high permeability of the teguments to water and ions. In addition to limited information about salinity around hydrothermal vents, these results lead to the hypothesis that *B. thermydron* lives in a habitat of stable seawater salinity. The osmoconformity of this species is briefly discussed in relation to its potential phylogeny.

Introduction

Hydrothermal vents, first discovered in 1977 on the Galapagos Ridge, are unique deep-sea habitats. They are char-

acterized by variable and extreme conditions of some physicochemical parameters, in particular by high temperature, high sulfide and metal content, high level of carbon dioxide, low level of oxygen and low pH (Truchot and Lallier, 1998; Sarradin *et al.*, 1998, 1999). To live in this environment, biological communities associated with the vents have developed behavioral, physiological, morphological, and reproductive adaptations such as symbiosis (Fisher, 1990), physiological and biochemical systems for sulfide detoxification (Powell and Somero, 1986; Cosson and Vivier, 1997; Geret *et al.*, 1998; Truchet *et al.*, 1998), behavioral and molecular responses to high temperature (Dahlhoff *et al.*, 1991; Dixon *et al.*, 1992; Segonzac *et al.*, 1993; Desbruyères *et al.*, 1998; Fisher, 1998), and specialized sensory organs to locate hot chimneys (Jinks *et al.*, 1998).

Among this vent fauna live endemic brachyuran decapod crustaceans (superfamily: *Bythograeoidea* Williams, 1980; family: *Bythograeidae* Williams, 1980; genera: *Bythograea* Williams, 1980; *Cyanagraea* de Saint Laurent, 1984; *Segonzacia* Guinot, 1989; *Austinograea* Hessler and Martin, 1989) (Tudge *et al.*, 1998). They have been found in all the known hydrothermal vents—*Bythograea* and *Cyanagraea* in the East Pacific, *Austinograea* in the West Pacific, *Segonzacia* in the mid-Atlantic (Tunnicliffe *et al.*, 1998). Information published on these brachyurans includes studies on their biogeography and evolution (Hessler and Wilson, 1983; Newman, 1985; Tunnicliffe, 1988), reproductive biology and larval development (Van Dover *et al.*, 1984, 1985; Epifanio *et al.*, 1999), and ecology and distribution (Van Dover, 1995; Guinot and Segonzac, 1997). Probably

Received 2 January 2001; accepted 9 June 2001.

* To whom correspondence should be addressed. E-mail: charmantier@univ-montp2.fr

due to the difficulty of getting live specimens, physiological studies are scarcer and have addressed aspects of respiration (Lallier *et al.*, 1998), sulfide detoxification (Vetter *et al.*, 1987), and temperature or pressure effects on the mitochondria, heart rate, or oxygen consumption rate (Mickel and Childress, 1982a,b; Dahlhoff *et al.*, 1991) of these crabs.

To our knowledge, no information is available on the hydromineral metabolism of the hydrothermal vent animals and particularly of the brachyuran crustaceans. Salinity is one of the main environmental factors exerting a selection pressure on aquatic organisms, and the successful establishment of a species in a given habitat depends on the ability of the organisms to adapt to, among other factors, the typical level and variations in salinity (Charmantier, 1998). This major adaptive process is achieved through different behavioral or physiological mechanisms. Osmoregulation is one of the most important of these mechanisms in some animal groups, including crustaceans. It has been explored in the adults of numerous crustacean species (reviews in Mantel and Farmer, 1983; Péqueux, 1995).

The present study has been conducted with one species of bythograeid crab from hydrothermal vents, *Bythograea thermydron* Williams, 1980. This crab is the most frequently observed [density about 20 individuals per m² (Guinot and Segonzac, 1997)] and captured species among brachyuran crustaceans on the East Pacific sites (Guinot, 1989). It is found predominantly in the warm water (>20°C) surrounding mussels and vestimentiferans on which it feeds, and also at the periphery of the vent areas where temperature is about 2°C (Grassle, 1986, cited by Epifanio *et al.*, 1999). These habitats, influenced by the spatially and temporally variable input of hydrothermal fluid, are greatly variable over short time and distance. Information on their salinity does not exist or is unpublished. It is thus unclear whether the salinity of the water surrounding the vents is as stable as the deep-sea water environment or is variable under the influence of the hydrothermal fluid. Physiological studies have indicated that adults of *B. thermydron* are tolerant of wide variations in temperature, dissolved oxygen, and hydrogen sulfide (Mickel and Childress, 1982a,b; Vetter *et al.*, 1987; Airries and Childress, 1994), but their ability to tolerate salinity variation and to osmoregulate is not known. The objectives of the present study were thus to evaluate the salinity tolerance and the pattern of osmoregulation of *B. thermydron*. The salinity of the natural habitat of the crab was also measured. As the hemolymph osmolality of crustaceans is mostly established by inorganic ions (essentially Na⁺ and Cl⁻) (Péqueux, 1995), the ionic regulation of this crab was also studied.

Materials and Methods

Animals

Adults of *Bythograea thermydron* were collected by the submarine *Nautile*, using resin watertight containers (about

1 × 0.5 × 0.5 m), on the East Pacific Rise (EPR) on the 13°N and 9°N sites [12°46–50'N, 103°57'W and 9°50'N, 104°17'W (Tunnicliffe *et al.*, 1998)], at a depth of about 2500 m, during the HOPE 99 mission in May 1999. Only a small number of crabs were available, which resulted in 3 to 10 individuals for each experimental condition. As this species seems incapable of long-term survival outside the high-pressure environment of the deep sea (Mickel and Childress, 1982a; Airries and Childress, 1994), most of the crabs were transferred into aquaria with running aerated Pacific surface seawater as soon as they reached the ship *Atalante*, and they were used in the following hours for experiments conducted on board, at atmospheric pressure, at a water temperature of 13°C. Some of them were also exposed to high pressure (see below). Crab cephalothoracic widths were 6–8 cm. Their molt stages (Drach, 1939) were not checked, but soft (post-molt) crabs were not used in experiments.

Ambient salinity

Water samples from the depth of the *Riftia pachypila* ring on the 13°N and 9°N EPR sites were collected in 750-ml titanium syringes manipulated by the *Nautile*. The water osmolality in mosm/kg was measured on an automatic micro-osmometer (Wescor Varro 5520). The corresponding values of salinity in parts per thousand were calculated by interpolation of data according to Weast (1969).

Preparation of media

Dilute media were prepared by adding fresh water to Pacific surface seawater (1002 ± 2 mosm/kg; approximately 34.6‰), and high-salinity media were prepared by adding ocean salts (Wimex, Germany) to seawater. Salinities were expressed as osmolality (in mosm/kg) and salt concentration (in parts per thousand). The osmolality of the media was measured with a Wescor Varro 5520 micro-osmometer. Media with the following osmolalities and corresponding salinities were prepared: 740 mosm/kg (25.4‰), 800 (27.5), 900 (31.0), 1002 (34.6), 1100 (38.2), 1200 (41.9), 1300 (45.7). Experiments were conducted at 13°C in 40-l aerated aquaria that were kept in the dark except at the time of sampling, when light was briefly necessary.

Salinity tolerance

The objective of the experiment was to estimate the survival time of the crabs at different salinities. The crabs were transferred directly from seawater to the experimental media. Observations were made and dead individuals were removed 1, 2, 3, 5, 6, 12, 15, and 24 h after the beginning of the tests. The absence of body movement after repeated touches with a probe was considered as a proof of death.

Hydromineral regulation

Acclimation time. To estimate the time necessary for hemolymph osmolality stabilization following a decrease in salinity, the crabs were first transferred from seawater (1002 mosm/kg), into a 740-mosm/kg medium. Hemolymph samples were taken from surviving animals after 0, 2.45, 5, and 15 h in the dilute medium. As 75% of the animals were dead at 15 h and 100% shortly afterward, a second experiment was conducted in an 800-mosm/kg medium. Survival was 60% at 12 h and 17% at 24 h. Hemolymph samples were taken from the surviving crabs after 0, 1, 2, 3, 6, 12, 24, and 48 h.

Osmotic regulation. The hemolymph osmolality of some crabs was measured as soon as they were brought on board. The crabs were then transferred to the different media, and their hemolymph osmolality was remeasured after a period of osmotic stabilization in each medium; the length of this period was determined from the results on adaptation time. A similar experiment was conducted under high pressure, at 15°C. The crabs were immersed in an 800-mosm/kg medium, in individual 400-ml containers set in a 19-l pressurized tank called "Incubateur Pressurisé pour l'Observation en Culture d'Animaux Marins Profonds" (IPOCAMP) (Shillito, unpub.). The crabs were subjected for 13 h to a pressure of 260 bars, which approximates the pressure at the site of capture. The hemolymph was then sampled and its osmolality was measured.

For sampling, the crabs were rinsed with deionized water and dried with absorbent paper. Hemolymph was sampled with a hypodermic needle mounted on a syringe and inserted at the basis of a posterior pereopod. The osmolality

of a 10- μ l sample of hemolymph was immediately measured on the Wescor Varro 5520 micro-osmometer.

Ionic regulation. Hemolymph from the same samples was quickly diluted to 25% in deionized water, stored in Eppendorf tubes, and kept at -80°C . After transport to the Montpellier laboratory in liquid nitrogen, the hemolymph and media samples were dissolved in deionized water to the appropriate volume, and their ionic contents were determined using an amperometric Aminco-Cotlove chloridimeter for the titration of Cl^{-} , an Eppendorf flame photometer for Na^{+} , K^{+} , Ca^{2+} , and a Varian AA-1275 atomic absorption photometer for Mg^{2+} .

Statistical analysis

Statistical comparisons of experimental data were performed by one-way analysis of variance (ANOVA) (Sokal and Rohlf, 1981) by using the software StatView 4.02 (Abacus Concept, Inc.).

Results

Ambient salinity

The salinity measured from bottom seawater samples was 996–1007 mosm/kg at the 13°N EPR site, and 950 mosm/kg at the 9°N EPR site.

Salinity tolerance

The survival rates of adults of *Bythograea thomydron* in Figure 1 were different according to salinity and decreased

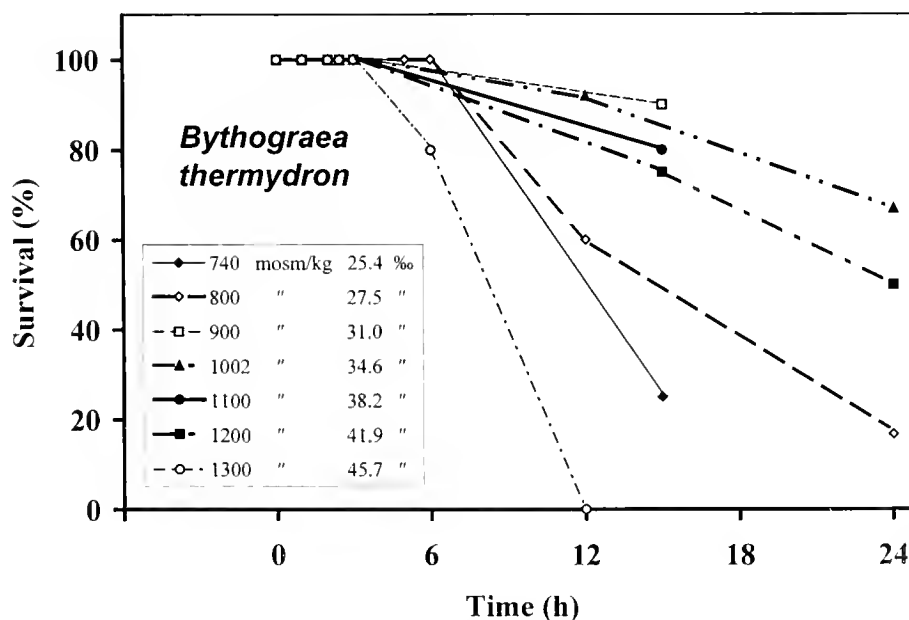


Figure 1. *Bythograea thomydron*. Survival rate (in %) at different salinities according to the time of exposure. Number of crabs per condition at the start of the experiment: 3 to 10.

with the time of exposure (Fig. 1). They decreased sharply to less than 25% within 15–24 h at the highest (1300 mosm/kg) and lowest (740, 800 mosm/kg) salinities. Survival was higher in seawater (1002 mosm/kg) and in salinities ranging from 900 to 1200 mosm/kg.

Hydromineral regulation

Acclimation time. The time of adaptation after a sudden change in salinity was evaluated at two low salinities (Fig. 2). In both media, the hemolymph osmolality decreased sharply within 12 h. After 15 h in the 740-mosm/kg medium, hemolymph osmolality had decreased to 805 mosm/kg—that is, to about 65 mosm/kg above the medium osmolality. As all crabs had died before 24 h, it was not possible to determine whether hemolymph osmolality had entirely stabilized at 15 h. After a transfer to the 800-mosm/kg medium, the hemolymph osmolality stabilized within 24 h. Its mean values were respectively 817 and 808 mosm/kg (no significant difference) after 24 h and 48 h in this medium. In subsequent experiments, the time of exposure to different media was based on these results and was kept in general at 15–24 h.

Osmotic regulation. Upon the arrival of the crabs on board the ship following their transfer from the bottom, their hemolymph osmolality was 1025 ± 4 mosm/kg ($n = 18$) and 984 ± 12 mosm/kg ($n = 29$) at the 13°N EPR and 9°N EPR sites respectively. The ability of the crabs to osmoregulate was then evaluated in the range of tolerable salinities between 900 mosm/kg and 1200 mosm/kg. The crabs osmoconformed in the whole range of tested salinities (Fig.

3A). The hemolymph osmotic concentration was close to that of the medium, different from it by only 9 to 22 mosm/kg, 15 mosm/kg on average.

The hemolymph osmolality was also measured in crabs maintained in the 800-mosm/kg medium, under a pressure of 260 bars. The mean value of hemolymph osmolality following this treatment for 13 h was 860 ± 9 mosm/kg ($n = 3$), not significantly different from the value of 856 ± 6 mosm/kg ($n = 3$) in control crabs kept in the same medium for 13 h under atmospheric pressure.

Ionic regulation. The results concerning hemolymph ion concentrations in the different media are given in Figure 3B–F. In seawater, Na^+ and Cl^- were the main osmoeffectors in hemolymph since they accounted for about 95% of the total hemolymph osmolality, and this trend was retained in all media. The hemolymph Cl^- concentration followed that of the medium in the whole range of tolerable salinities. It tended to be slightly hypo-regulated in most media (Fig. 3B). Na^+ regulation was iso-ionic; hemolymph Na^+ concentration constantly remained slightly above that of the medium, by 8 to 23 mEq $\text{Na}^+/\text{l}^{-1}$ (Fig. 3C). K^+ was slightly hypo-regulated (by approximately 2.5 mEq K^+/l^{-1}) in the media in which concentrations were above 10.5 mEq K^+/l^{-1} (900 mosm/kg), and it was slightly hyper-regulated (by approximately 3.5 mEq K^+/l^{-1}) in the lowest salinity (800 mosm/kg, 9.3 mEq K^+/l^{-1}) (Fig. 3D). Hemolymph Ca^{2+} concentration was slightly hyper-regulated (by 1.2 to 3.6 mEq $\text{Ca}^{2+}/\text{l}^{-1}$) at most tested salinities (Fig. 3E). Hemolymph Mg^{2+} concentration was strongly hypo-regulated (by about 33 to 57 mEq $\text{Mg}^{2+}/\text{l}^{-1}$) over the entire range of salinities (Fig. 3F).

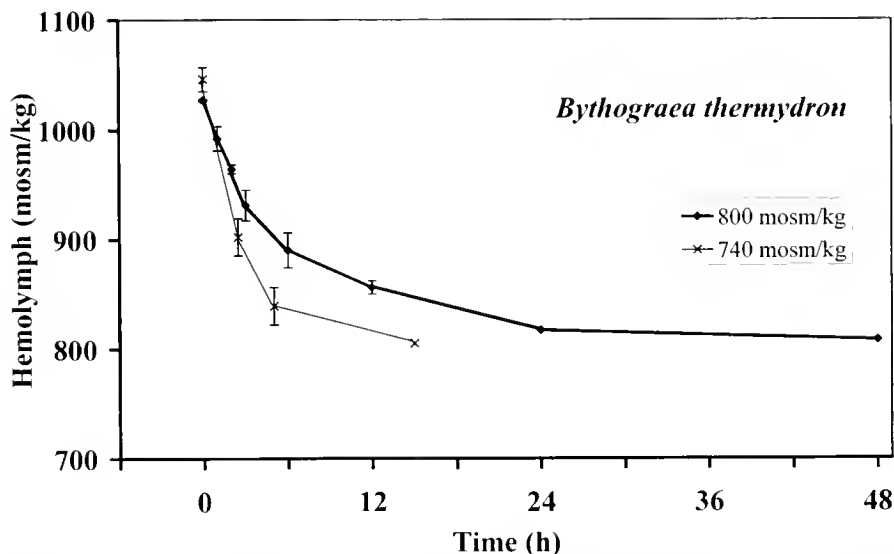


Figure 2. *Bythograea thermydron*. Change in hemolymph osmolality according to the time after rapid transfer from Pacific surface seawater (1002 ± 2 mosm/kg) to dilute media at 740 mosm/kg and 800 mosm/kg. Error bars: mean \pm SD; n : 4 to 6 individuals.

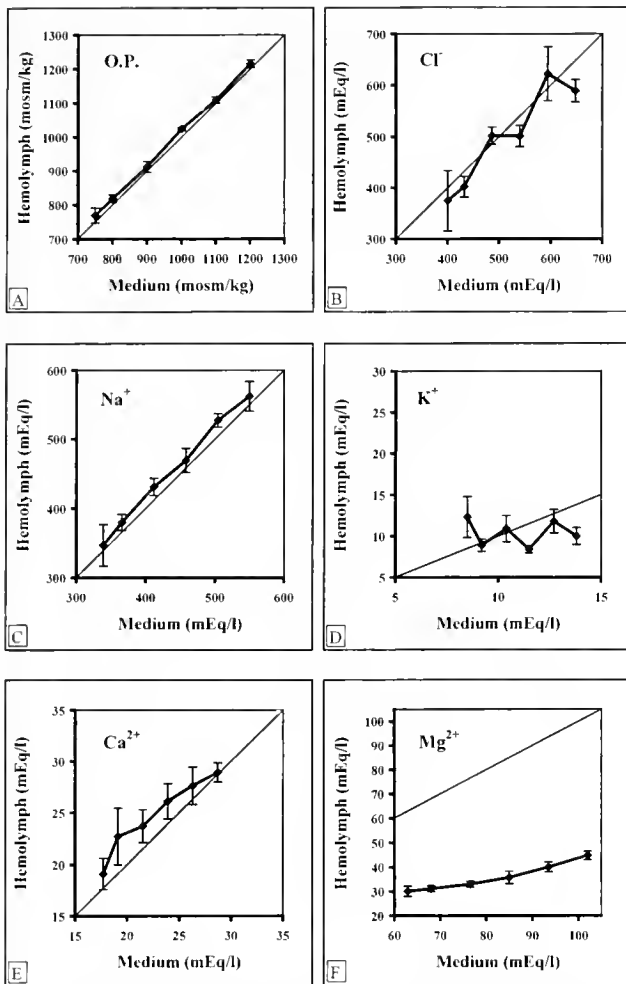


Figure 3. *Bythograea therymydron*. Variations in hemolymph osmolality (A: O.P.) (osmotic pressure in mosm/kg) and ionic concentrations (B to F) (in $\text{mEq} \cdot \text{l}^{-1}$) after hemolymph osmolality stabilization (about 15–24 h), in relation to the osmolality or ionic concentration of the medium. Time of exposure to the different media was 24 h (A) or 15–24 h (B to F). Error bars: mean \pm SD; n : 3 to 12 individuals; isoconcentration lines are drawn.

Discussion

Salinity tolerance

The limited number of available animals and lack of time and space on board the ship prevented long-term tolerance experiments. Specimens of *Bythograea therymydron* survived for 24 h in a narrow range of salinities ranging from about 31‰ to 42‰. These crabs, unable to withstand a great extent of salinity fluctuations, are thus stenohaline animals. They share this feature with other species of decapods whose habitat is most often restricted to seawater, for example, the Majidae, the Cancridae, and the Calappidae (review in Mantel and Farmer, 1983; Péqueux, 1995).

Acclimation time

In *B. therymydron*, the time required to reach an osmotic steady-state after a sudden decrease in external salinity was

about 15 to 24 h. This is short for a brachyuran crab, similar to the 15 h required for osmotic equilibration in osmoconformers such as the Majidae *Maja* sp. and *Hyas* sp. transferred to 75‰ seawater (Prosser and Brown, 1965). Osmotic adaptation requires longer times in strongly osmoregulating species, such as 48 h in osmoregulating crabs (Charmantier, 1998) and up to 96 h in crayfish (Susanto and Charmantier, 2000). The short acclimation time found in *B. therymydron* probably indicates a relatively high exchange of water and ions between the organism and the external medium and a high permeability of the body surface in this species; it also reflects the weak salinity stress applied.

Hydromineral regulation

B. therymydron osmoconformed over the narrow range of tolerable salinities. When salinity varied, the hemolymph osmolality tended to follow the external osmolality, with a slight positive difference of only about 15 mosm/kg. This is probably due to the colloid osmotic pressure of plasma proteins. *B. therymydron* is therefore an osmoconformer like the Majidae *Libinia emarginata*, *Pugettia producta* (Mantel and Farmer, 1983), *Maja* sp. (Potts and Parry, 1963), and *Chionoecetes* sp. (Mantel and Farmer, 1983; Hardy *et al.*, 1994); the Cancridae *Cancer antennarius* (Jones, 1941; Gross, 1964) and *C. pagurus* (Péqueux, 1995); and the Calappidae *Calappa hepatica* (Kamemoto and Kato, 1969). As already noted by different authors (reviewed in Mantel and Farmer, 1983; Péqueux, 1995), osmoconformity does not permit survival at salinities widely different from seawater, and these osmoconformers are marine stenohaline species. As in other crustaceans, the osmolality of the hemolymph of *B. therymydron* was mostly due to inorganic ions, essentially Na^+ and Cl^- (Péqueux, 1995), which accounted for about 95% of the total hemolymph osmolality. The regulation of these ions was almost iso-ionic. In these crabs, hemolymph Cl^- and Na^+ concentrations respectively represented about 93% and 102% of the same ion concentrations in the medium. There is thus a slight excess of Na^+ and a slight deficit of Cl^- in the hemolymph compared to the medium, as is noted in other osmoconformers such as the Majidae *Libinia emarginata* (Gilles, 1970), *Maja* sp. (Potts and Parry, 1963), and *Chionoecetes opilio* (Hardy *et al.*, 1994); the Cancridae *Cancer antennarius* (Gross, 1964); and the Calappidae *Calappa hepatica* (Spencer *et al.*, 1979).

In *B. therymydron*, the hemolymph Ca^{2+} concentration was slightly hyper-regulated, as noted by Prosser (1973) in marine crustaceans. K^+ concentration was slightly hyper-hypo-regulated. However, among crustaceans, K^+ is often found in higher concentration in the hemolymph than in the medium (Mantel and Farmer, 1983).

In *B. therymydron*, Mg^{2+} concentration was strongly hypo-regulated. The concentration of this ion was about 44% of that found in the medium, a percentage included in the

standard range of hemolymph Mg^{2+} concentration for brachyurans, that is, between 20% and 80% of the medium concentration (Prosser, 1973). As in several species of crabs, Mg^{2+} might be excreted through the antennal glands (Morritt and Spicer, 1998). Other osmoconformers such as *Maja squinado* or *Hyas sp.*, which are relatively "unresponsive" (slow-moving) species, have higher hemolymph Mg^{2+} concentration (about 80% of that of seawater) (Robertson, 1960; Frederich *et al.*, 2000). *B. thermydron* exhibits a hemolymph Mg^{2+} concentration closer to that of more "active" crabs such as *Carcinus maenas* and *Pachygrapsus marmoratus*, in which the ion concentration is below 50% of that found in the medium (Robertson, 1960; Frederich *et al.*, 2000). This fact can be related to the active locomotor behavior of *B. thermydron* (Williams, 1980; Guinot, 1988; Guinot and Segonzac, 1997), which is evident in visual observations and video monitoring (Jean-Yves Toullec, pers. obs.) that show the crabs frequently moving on chimneys, in and out of the warm areas, and among the vestimentiferans or mussels on which they feed. In addition, these results show that the crabs had retained a strong ability to hypo-regulate Mg^{2+} in their hemolymph after their transfer to the surface and one or two days of exposure to different media. Thus, their osmoconformity and their Na^+ and Cl^- iso-regulation most probably result from a specific pattern and not from damage to the integument or serious stress due to the pressure change associated with bringing the crabs to the surface.

Exposure to high pressure did not affect the hemolymph osmolality of *B. thermydron* exposed to low salinity, when compared to crabs kept at atmospheric pressure. In these deep-sea hydrothermal crabs, osmoconformity thus appears to be unaffected by a change in hydrostatic pressure. This contrasts with the few tested epibenthic crabs in which osmotic and ionic regulation may vary in relation to pressure. For instance, short-term exposure (1–3 h) to pressure of 50–100 bars significantly affected the concentration of the inorganic ions (Na^+ , K^+ , Cl^- , Ca^{2+} , Mg^{2+}) in hemolymph of *Carcinus maenas* (Péqueux and Gilles, 1984), but changed only the Ca^{2+} content of the hemolymph in *Eriochel sinensis* (Sébert *et al.*, 1997).

Ecological implications

Because *B. thermydron* is a marine stenohaline osmoconformer, we may hypothesize that this species occupies a deep hydrothermal habitat where salinity is stable and close to that of seawater. This hypothesis has been verified in the present study through direct measurements of the ambient salinity. The salinity of the hydrothermal water directly measured on samples taken on the 9°N and 13°N EPR was approximately 32.7‰ to 34.3‰–34.7‰. These values are close to the salinity of standard Pacific seawater, 34.62‰ (Ivanoff, 1972). The osmoregulation pattern of *B. thermy-*

dron confirms that these crabs live in an environment where salinity is stable and close to 33‰–35‰. In addition, these values of salinity add to the knowledge of the ambient parameters of the deep-sea hydrothermal environment (Mid-Atlantic Ridge or East Pacific Rise) where Ca^{2+} , Mg^{2+} , Cl^- , PO_4^{3-} , NO_2^- , NH_4^+ , NO_3^- , and NO_2^- concentrations have been measured (Truchot and Lallier, 1998; Sarradin *et al.*, 1998, 1999).

Phylogeny and osmoregulatory adaptation

The phylogenetic origin of the Bythograeidae is disputed (Delamare Deboutteville and Guinot, 1981; Guinot, 1988, 1990). According to Williams (1980), Tudge *et al.* (1998), and Sternberg *et al.* (1999), *Bythograea thermydron* exhibits some similarities to Potamoidea (Potamidae), Portunoidea (Portunidae), and Xanthoidea (Goneplacidae; Xanthidae; Trapeziidae). The marine stenohaline osmoconformer *B. thermydron* may thus have derived from families consisting mainly of crab species that are able to strongly osmoregulate (Jones, 1941; Shaw, 1959; Robertson, 1960; Ballard and Abbott, 1969; Kamemoto and Kato, 1969; Harris and Micallef, 1971; Taylor *et al.*, 1977; Birchard *et al.*, 1982; Blasco and Forward, 1988; review in Mantel and Farmer, 1983). During its evolution, *B. thermydron* would have lost its ancestor's osmoregulatory ability, which had become superfluous in an environment where salinity is stable. A similar, if not identical, pattern of evolution has been reported in some freshwater caridean shrimps—for example, *Palaemonetes paludosus* (Dobkin and Manning, 1964) and *P. argentinus* (Charmantier and Anger, 1999). These species, which live in fresh water or in low-salinity habitats, have lost the useless function of hypo-regulation usually present in osmoregulatory caridean shrimps and have retained only the capacity to hyper-regulate.

Acknowledgments

The authors warmly thank Prof. Danièle Guinot, who provided useful ideas on crab phylogeny and reviewed a draft of the manuscript. They also thank Dr. F. Lallier, the chief scientist of the HOPE 99 cruise, Dr. P.-M. Sarradin for the supply of bottom seawater, and Dr. L. Nonnotte for the loan of the osmometer used aboard ship.

Literature Cited

- Airries, C. N., and J. J. Childress. 1994. Homeoviscous properties implicated by the interactive effects of pressure and temperature on the hydrothermal vent crab *Bythograea thermydron*. *Biol. Bull.* **187**: 208–214.
- Ballard, B. S., and W. Abbott. 1969. Osmotic accommodation in *Calinectes sapidus* Rathbun. *Comp. Biochem. Physiol.* **29**: 671–687.
- Birchard, G. F., L. Drolet, and L. H. Mantel. 1982. The effect of reduced salinity on osmoregulation and oxygen consumption in the lady crab, *Ovalipes ocellatus* (Herbst). *Comp. Biochem. Physiol.* **71A**: 321–324.

- Blasco, E., and R. B. Forward, Jr. 1988. Osmoregulation of the xanthid crab, *Panopeus herbstii*. *Comp. Biochem. Physiol.* **90A**: 135–139.
- Charmantier, G. 1998. Ontogeny of osmoregulation in crustaceans: a review. *Invertebr. Reprod. Dev.* **33**: 177–190.
- Charmantier, G., and K. Anger. 1999. Ontogeny of osmoregulation in the palaemonid shrimp *Palaemonetes argentinus* (Crustacea: Decapoda). *Mar. Ecol. Prog. Ser.* **181**: 125–129.
- Cosson, R. P., and J.-P. Vivier. 1997. Interactions of metallic elements and organisms within hydrothermal vents. *Cah. Biol. Mar.* **38**: 43–50.
- Dahlhoff, E., J. O'Brien, G. N. Somero, and R. D. Vetter. 1991. Temperature effects on mitochondria from hydrothermal vent invertebrates: evidence for adaptation to elevated and variable habitat temperatures. *Physiol. Zool.* **64**: 1490–1508.
- Delamare Deboutteville, C., and D. Guinot. 1981. Considérations sur les Bythograeoidea Williams, nouvelle superfamille de crabes de la dorsale Pacifique Est. *Ville Réunion des Carcinologistes de Langue Française*, Banyuls-sur-Mer, France, 1–6 June 1981 (Abstract).
- Deshruyères, D., P. Chevalloné, A.-M. Alayse, D. Jollivet, F. H. Lallier, C. Jouin-Toulmond, F. Zal, P.-M. Sarradin, R. Cosson, J. C. Caprais, C. Arndt, J. O'Brien, J. Guezennec, S. Hourdez, R. Riso, F. Gaill, L. Laubier, and A. Toulmond. 1998. Biology and ecology of the "Pompeii worm" (*Alvinella pompejana* Desbruyères and Laubier), a normal dweller of an extreme deep-sea environment: A synthesis of current knowledge and recent developments. *Deep-Sea Res. II* **45**: 383–422.
- Dixon, D. R., R. Simpson-White, and L. R. J. Dixon. 1992. Evidence for thermal stability of ribosomal DNA sequences in hydrothermal vent organisms. *J. Mar. Biol. Assoc. UK* **72**: 519–527.
- Dobkin, S., and R. S. Manning. 1964. Osmoregulation in two species of *Palaemonetes* (Crustacea: Decapoda) from Florida. *Bull. Mar. Sci. Gulf Caribb.* **14**: 149–157.
- Drach, P. 1939. Mue et cycle d'intermue chez les Crustacés Décapodes. *Ann. Inst. Océanogr.* **19**: 103–391.
- Epifanio, C. E., G. Perovich, A. I. Dittel, and S. C. Cary. 1999. Development and behavior of megalopa larvae and juveniles of the hydrothermal vent crab *Bythograea therymydrion*. *Mar. Ecol. Prog. Ser.* **185**: 147–154.
- Fisher, C. R. 1990. Chemoautotrophic and methanotrophic symbioses in marine invertebrates. *Crit. Rev. Aquat. Sci.* **2**: 399–436.
- Fisher, C. R. 1998. Temperature and sulfide tolerance of hydrothermal vent fauna. *Cah. Biol. Mar.* **39**: 283–286.
- Frederich, M., F. J. Sartoris, W. E. Arntz, and H.-O. Pörtner. 2000. Haemolymph Mg^{2+} regulation in decapod crustaceans: physiological correlates and ecological consequences in polar areas. *J. Exp. Biol.* **203**: 1383–1393.
- Geret, F., N. Rousse, R. Riso, P.-M. Sarradin, and R. P. Cosson. 1998. Metal compartmentalization and metallothionein isoforms in mussels from the Mid-Atlantic Ridge: preliminary approach to the fluid-organism relationship. *Cah. Biol. Mar.* **39**: 291–293.
- Gilles, R. 1970. Osmoregulation in the stenohaline crab "*Libinia emarginata*" Leech. *Arch. Int. Physiol. Biochim.* **78**: 91–99.
- Grassle, J. F. 1986. The ecology of deep-sea hydrothermal vent communities. *Adv. Mar. Biol.* **23**: 301–362. (Cited in Epifanio *et al.*, 1999.)
- Gross, W. J. 1964. Trends in water and salt regulation among aquatic and amphibious crabs. *Biol. Bull.* **127**: 447–466.
- Guinot, D. 1988. Les crabes des sources hydrothermales de la dorsale du Pacifique oriental (campagne *Biocyaris*, 1984). *Oceanol. Acta, Spec. Vol.* **8**: 109–118.
- Guinot, D. 1989. Description de *Segonzacia* gen. nov. et remarques sur *Segonzacia mesatlantica* (Williams): campagne HYDROSLAKE 1988 sur la dorsale médio-Atlantique (Crustacea Decapoda Brachyura). *Bull. Mus. Natl. Hist. Nat.* **11**: 203–231.
- Guinot, D. 1990. *Austino-graea alayseae* sp. nov., Crabe hydrothermal découvert dans le bassin de Lau, Pacifique sud-occidental (Crustacea Decapoda Brachyura). *Bull. Mus. Natl. Hist. Nat.* **11**: 879–903.
- Guinot, D., and M. Segonzac. 1997. Description d'un crabe hydrothermal nouveau du genre *Bythograea* (Crustacea, Decapoda, Brachyura) et remarques sur les Bythograeidae de la dorsale du Pacifique oriental. *Zoosystema* **19**: 121–149.
- Hardy, D., J. Munro, and J.-D. Dutil. 1994. Temperature and salinity tolerance of the soft-shell and hard-shell male snow crab, *Chionoecetes opilio*. *Aquaculture* **122**: 249–265.
- Harris, R. R., and H. Micallef. 1971. Osmotic and ionic regulation in *Potamon edulis*, a fresh water crab from Malta. *Comp. Biochem. Physiol.* **38A**: 769–776.
- Hessler, R. R., and G. D. F. Wilson. 1983. The origin and biogeography of Malacostracan crustaceans in the deep sea. Pp. 227–254 in *Evolution, Time and Space: The Emergence of the Biosphere*, R. W. Sims, J. H. Price, and P. E. S. Whalley, eds. Academic Press, London.
- Ivanoff, A. 1972. *Introduction à l'Océanographie. Tome I: Propriétés Physiques et Chimiques des Eaux de Mer*. Vuibert, Paris. 208 pp.
- Jinks, R. N., B.-A. Battelle, E. D. Herzog, L. Kass, G. H. Renninger, and S. C. Chamberlain. 1998. Sensory adaptations in hydrothermal vent shrimps from the Mid-Atlantic Ridge. *Cah. Biol. Mar.* **39**: 309–312.
- Jones, L. L. 1941. Osmotic regulation in several crabs of the Pacific coast of North America. *J. Cell. Comp. Physiol.* **18**: 79–92.
- Kamamoto, F. I., and K. N. Kato. 1969. The osmotic and chloride regulative capacities of five Hawaiian decapod crustaceans. *Pac. Sci.* **23**: 232–237.
- Lallier, F. H., L. Camus, F. Chausson, and J.-P. Truchot. 1998. Structure and function of hydrothermal vent crustaceans haemocyanin: an update. *Cah. Biol. Mar.* **39**: 313–316.
- Mantel, L. H., and L. L. Farmer. 1983. Osmotic and ionic regulation. Pp. 53–161 in *The Biology of Crustacea, Vol. 5: Internal Anatomy and Physiological Regulation*, L. H. Mantel, ed. Academic Press, New York.
- Mickel, T. J., and J. J. Childress. 1982a. Effects of pressure and temperature on the EKG and heart rate of the hydrothermal vent crab *Bythograea therymydrion* Brachyura. *Biol. Bull.* **162**: 70–82.
- Mickel, T. J., and J. J. Childress. 1982b. Effects of temperature, pressure and oxygen concentration on the oxygen consumption rate of the hydrothermal vent crab *Bythograea therymydrion* Brachyura. *Physiol. Zool.* **55**: 199–207.
- Morritt, D., and J. I. Spicer. 1998. The physiological ecology of talitrid amphipods: an update. *Can. J. Zool.* **76**: 1965–1982.
- Newman, W. A. 1985. The abyssal hydrothermal vent invertebrate fauna: a glimpse of antiquity? *Bull. Biol. Soc. Wash.* **6**: 231–242.
- Péqueux, A. 1995. Osmotic regulation in crustaceans. *J. Crustac. Biol.* **15**: 1–60.
- Péqueux, A., and R. Gilles. 1984. Control of extracellular fluid osmolality in crustaceans. Pp. 18–34 in *Osmoregulation in Estuarine and Marine Animals*, A. Péqueux, R. Gilles, and L. Bolis, eds. Springer, Berlin.
- Potts, W. T. W., and G. Parry. 1963. *Osmotic and Ionic Regulation in Animals*. Pergamon Press, Oxford. 423 pp.
- Powell, M. A., and G. N. Somero. 1986. Adaptations to sulfide by hydrothermal vent animals: sites and mechanisms of detoxification and metabolism. *Biol. Bull.* **171**: 274–290.
- Prosser, C. L. 1973. Inorganic ions. Pp. 79–110 in *Comparative Animal Physiology*, C. L. Prosser, ed. Saunders, Philadelphia.
- Prosser, C. L., and F. A. Brown, Jr. 1965. *Comparative Animal Physiology*. W. B. Saunders, London. 688 pp.
- Robertson, J. D. 1960. Osmotic and ionic regulation. Pp. 317–339 in *Physiology of Crustacea*, Vol. 1, T. H. Waterman, ed. Academic Press, New York.

- Sarradin, P.-M., J.-C. Caprais, P. Briand, F. Gaill, B. Shillito, and D. Desbruyères. 1998. Chemical and thermal description of the environment of the Genesis hydrothermal vent community (13°N, EPR). *Cah. Biol. Mar.* **39**: 159–167.
- Sarradin, P.-M., J.-C. Caprais, R. Riso, R. Kerouel, and A. Aminot. 1999. Chemical environment of the hydrothermal mussel communities in the Lucky Strike and Menez Gwen vent fields, Mid Atlantic Ridge. *Cah. Biol. Mar.* **40**: 93–104.
- Sébert, P., B. Simon, and A. Péqueux. 1997. Effects of hydrostatic pressure on energy metabolism and osmoregulation in crab and fish. *Comp. Biochem. Physiol.* **116A**: 281–290.
- Segonzac, M., M. De Saint Laurent, and B. Casanova. 1993. L'énigme du comportement trophique des crevettes Alvinocarididae des sites hydrothermaux de la dorsale médio-atlantique. *Cah. Biol. Mar.* **34**: 535–571.
- Shaw, J. 1959. Salt and water balance in the East African fresh water crab, *Potamon niloticus* (M. Edw.). *J. Exp. Biol.* **36**: 157–176.
- Sokal, R. R., and F. J. Rohlf. 1981. *Biometry: The Principles and Practice of Statistics in Biological Research*. W. H. Freeman, San Francisco. 859 pp.
- Spencer, A. M., A. H. Fielding, and F. I. Kamemoto. 1979. The relationship between gill NaK-ATPase activity and osmoregulatory capacity in various crabs. *Physiol. Zool.* **52**: 1–10.
- Sternberg, R. V., N. Cumberlidge, and G. Rodriguez. 1999. On the marine sister groups of freshwater crabs (Crustacea: Decapoda: Brachyura). *J. Zool. Syst. Evol. Res.* **37**: 19–38.
- Susanto, G. N., and G. Charmantier. 2000. Ontogeny of osmoregulation in the crayfish *Astacus leptodactylus*. *Physiol. Biochem. Zool.* **73**: 169–176.
- Taylor, E. W., P. J. Butler, and A. Al-Wassia. 1977. The effect of a decrease in salinity on respiration, osmoregulation and activity in the shore crab, *Carcinus maenas* (L.) at different acclimation temperatures. *J. Comp. Physiol.* **119**: 155–170.
- Truchet, M., C. Ballan-Dufrançais, A. Y. Jeantet, J.-P. Lechaire, and R. Cosson. 1998. Le trophosome de *Riftia pachyptila* et *Tevnia jerichonana* (Vestimentifera): bioaccumulations métalliques et métabolisme du soufre. *Cah. Biol. Mar.* **39**: 129–141.
- Truchot, J.-P., and F. H. Lallier. 1998. High CO₂ content in hydrothermal vent water at the Snake Pit area, Mid-Atlantic Ridge. *Cah. Biol. Mar.* **39**: 153–158.
- Tudge, C. C., B. G. M. Jamieson, M. Segonzac, and D. Guinot. 1998. Spermatozoal ultrastructure in three species of hydrothermal vent crab, in the genera *Bythograea*, *Anstinograea* and *Segonzacia* (Decapoda, Brachyura, Bythograeidae). *Invertebr. Reprod. Dev.* **34**: 13–23.
- Tunnicliffe, V. 1988. Biogeography and evolution of hydrothermal-vent fauna in the eastern Pacific Ocean. *Proc. R. Soc. Lond. B* **233**: 347–366.
- Tunnicliffe, V., A. G. McArthur, and D. McHugh. 1998. A biogeographical perspective of the deep-sea hydrothermal vent fauna. *Adv. Mar. Biol.* **34**: 353–442.
- Van Dover, C. L. 1995. Ecology of the Mid-Atlantic Ridge hydrothermal vents. Pp. 257–294 in *Hydrothermal Vents and Processes*, L. M. Parson, C. L. Walker, and D. R. Dixon, eds. Geological Society, London.
- Van Dover, C. L., A. B. Williams, and J. R. Factor. 1984. The first zoeal stage of a hydrothermal vent crab (Decapoda: Brachyura: Bythograeidae). *Proc. Biol. Soc. Wash.* **97**: 413–418.
- Van Dover, C. L., J. R. Factor, A. B. Williams, and C. J. Berg, Jr. 1985. Reproductive patterns of decapod crustaceans from hydrothermal vents. *Bull. Biol. Soc. Wash.* **6**: 223–228.
- Vetter, R. D., M. E. Wells, A. L. Kurtsman, and G. N. Somero. 1987. Sulfide detoxification by the hydrothermal vent crab *Bythograea thermydron* and other decapod crustaceans. *Physiol. Zool.* **60**: 121–137.
- Weast, R. C. 1969. *Handbook of Chemistry and Physics*, 50th Ed. The Chemical Rubber Co., Cleveland, OH. 2033 pp.
- Williams, A. B. 1980. A new crab family from the vicinity of submarine thermal vents on the Galapagos rift (Crustacea: Decapoda: Brachyura). *Proc. Biol. Soc. Wash.* **93**: 443–472.

Escape and Aggregation Responses of Three Echinoderms to Conspecific Stimuli

A. C. CAMPBELL,* S. COPPARD, C. D'ABREO, AND R. TUDOR-THOMAS

School of Biological Sciences, Queen Mary, University of London, Mile End Road, London E1 4NS, UK

Abstract. In marine invertebrates, waterborne chemical stimuli mediate responses including prey detection and predator avoidance. Alarm and flight, in response to damaged conspecifics, have been reported in echinoderms, but the nature of the stimuli involved is not known. The responses of *Asterias rubens* Linnaeus, *Psammechinus miliaris* (Gmelin), and *Echinus esculentus* Linnaeus to conspecifics were tested in a choice chamber against a control of clean seawater (no stimulus). All three species showed statistically significant movement toward water conditioned by whole animals or homogenate of test epithelium. *P. miliaris* and *E. esculentus* displayed a statistically significant avoidance reaction, moving away from conspecific coelomic fluid, gut homogenate, and gonad homogenate. *A. rubens* was indifferent to conspecific coelomic fluid, pyloric cecum homogenate, and gonad homogenate but moved away from cardiac gut homogenate. *P. miliaris* was indifferent to gametes, but the other two species were significantly attracted to them. No species showed preference for one particular side of the chamber during trials to balance water flow. These echinoderms can distinguish between homogenates of conspecific tissues that might be exposed when a predator damages the test, and those that may emanate from the exterior surface during normal activities.

Introduction

Predation is a strong selective force, and failing to escape a predator is much more significant in evolutionary terms than are other selective forces such as failure to mate or achieve an optimal energy intake (Lima and Dill, 1990). Animals use a range of cues to detect predators (*e.g.*, visual,

auditory, olfactory, and tactile), but the value of these cues can be limited in aquatic invertebrates. Turbid inshore waters, for example, may render visual cues vague (Mackie, 1975), and currents can concentrate or dilute chemical ones (Weissburg and Zimmer-Faust, 1993). The efficiency of animals tracking chemical cues is greater in calm flowing water and less in rough turbulent flows (Weissburg and Zimmer-Faust, 1994). Movements, scents, or tactile stimuli can warn of predation risk and can originate from the predator itself or from injured or killed conspecifics (Snyder and Snyder, 1970). Such stimuli may trigger escape responses, while others from intact conspecifics may prompt individuals to aggregate in dense groups where the risk of predation to an individual is reduced (Slater, 1985; Zahavi *et al.*, 1999). Such aggregations occur in other animals such as birds, where a high density of individuals within the aggregation or colony has been shown to be related to decreased frequency of attack by predators (Kruuk, 1964).

Adult echinoderms are sedentary organisms and are vulnerable to a range of predators including mammals, birds, fish, invertebrates, and other echinoderms (Mortensen, 1943; Moore, 1966; Mayo and Mackie, 1976; Bernstein *et al.*, 1981). They are, however, able to counter predation by structural and behavioral means such as the use of spines and globiferous pedicellariae, which are minute, forcep-like appendages that can seize and, in some cases, inject venom into the skin of predators (Campbell, 1983). Such mechanisms reduce the ease with which predators can handle their prey, and two categories of behavioral adaptations serve to counter predation in marine invertebrates (Legault and Himmelman, 1993). These are (1) avoidance adaptations that limit the potential number of encounters with predators; and (2) escape adaptations that reduce the risk of predation when a predator has been detected or encountered. Echinoderms provide good examples of both categories.

Received 23 March 1999; accepted 15 May 2001.

* To whom correspondence should be addressed. E-mail: A.C.Campbell@qmw.ac.uk

Many echinoderms show avoidance behavior such as burrowing (sand dollars, heart urchins, and some starfish; Lawrence, 1987), covering themselves with a layer of shell and sand (sea urchins; Dayton *et al.*, 1977), or sheltering under rocks and in crevices (Orton, 1914). These habits limit the potential for encounters with surface-moving predators. A remarkable avoidance behavior is shown by the echinoid *Strongylocentrotus droebachiensis*. In summer, it avoids a predator, the diurnal-feeding wolffish *Anarhichas lupus*, by foraging at night (Bernstein *et al.*, 1981); in winter, when the wolffish is less active, it forages throughout 24 hours (Bernstein *et al.*, 1981).

Mauzey *et al.* (1968) described the escape reactions of various invertebrate prey species, including other echinoderms, when they encountered predatory starfishes. One of the clearest escape behaviors is the flight response from predators shown by *S. droebachiensis*, which uses its ventral spines to flee when brought into contact with the starfish *Marthasterias glacialis* (Jensen, 1966). This urchin also flees from water conditioned by crabs or lobsters (Bernstein *et al.*, 1981; Mann *et al.*, 1984). Flight responses in the sea urchin *Diadema antillarum* have been initiated by the body fluids of crushed conspecifics (Snyder and Snyder, 1970; Parker and Shulman, 1986).

Aggregation behavior has been widely reported in echinoderms (Reese, 1966), and in some cases aggregations appear to be related to grazing, detrital feeding, and suspension feeding (Sloan and Campbell, 1982). More recently Levitan *et al.* (1992) showed that aggregation can enhance fertilization success in spawning echinoids. Allee (1927) concluded that echinoderm aggregations are the result of a common response to one or more essential environmental factors, such as food availability, and that they do not represent true social groupings. On the other hand, Bernstein *et al.* (1983) believed that aggregation behavior in *S. droebachiensis* functions as an escape device, reducing the risk to individuals because of the sheer numbers present. These authors considered that predatory crabs would find the entire aggregation of urchins more difficult to handle than single individuals.

Although echinoderms have only simple receptor organs, often made up of a few similar receptor cells without ganglia (Pentreath and Cobb, 1972), many species are sensitive to touch, chemicals, and light, and some may respond to pressure changes and vibrations (Campbell, 1983). Various authors (*e.g.*, Bullock and Horridge, 1965; Chia, 1969; Lepper and Moore, 1998) have described the locomotory and defensive responses of asteroids and echinoids to tactile and chemical stimuli. In most species, the mechanoreceptors and chemoreceptors are located superficially in the test epithelium, from where they can monitor tactile and chemical stimuli (Campbell, 1973; Lepper, 1998). The tube feet are also sensitive to touch and chemicals, and are used to

detect food and prey (Sloan and Campbell, 1982). A range of chemicals, of both low and high molecular weight, initiate responses in asteroids and echinoids (Sloan and Campbell, 1982). Responses to these stimuli range from local reflex reactions in the spines, pedicellariae, and tube feet to fully coordinated responses in which the whole organism moves toward or away from a stimulus source. Experimental analyses by Bullock (1965) and Campbell and Laverack (1968) showed that both the peripheral basi-epithelial nerve plexus of the test and the radial nerve cords of the central nervous systems played a role in mediating these responses.

Many echinoderms possess dermal light receptors, but these are anatomically simple (Yoshida, 1966) and, unlike the eyes of insects, molluscs, and vertebrates, do not form detailed images. Spine movements in response to passing shadows are, however, well known in sea urchins (Millott and Takahashi, 1963).

This paper investigates the effects of waterborne stimuli on three common British species, *Asterias rubens* Linnaeus, *Psammechinus miliaris* (Gmelin), and *Echinus esculentus* Linnaeus. We tested the hypothesis that escape and aggregation responses in sea urchins and starfish are triggered by chemical stimuli emanating from the tissues of conspecific animals and, further, that these responses differ according to the source of the stimulus. The three species tested show broadly similar results. By (1) determining whether these animals display escape and aggregation responses when presented with conspecific stimuli and (2) identifying the body tissue or tissues responsible for producing the effective chemical signal, these experiments add to our knowledge of chemical ecology and the role of chemical stimuli in promoting aggregation or avoidance behavior in mobile animals.

Materials and Methods

Specimens of *Asterias rubens*, *Psammechinus miliaris*, and *Echinus esculentus* were collected from the shore and by dredging from the Isle of Great Cumbrae, Scotland. The animals were transferred to a recirculating seawater system aquarium at Queen Mary, University of London. The species were maintained in separate tanks in a 12-h light:12-h dark regime at 11 °C and 34 ppt salinity. The animals were acclimated for 7 days before testing and were fed mussels *ad libitum* (for *A. rubens*) and other epifauna and epiflora (for the echinoids) brought on small rocks from nearby shores. The size classes of animals that were used in the experiments were as follows: *A. rubens*, R (major radius) = 30–50 mm; *P. miliaris*, 20–35 mm test diameter; and *E. esculentus*, 80–120 mm test diameter.

These animals were tested in a choice chamber (see Fig. 1) based on the design of Mann *et al.* (1984), which was chosen because it allowed the test subject to be simulta-

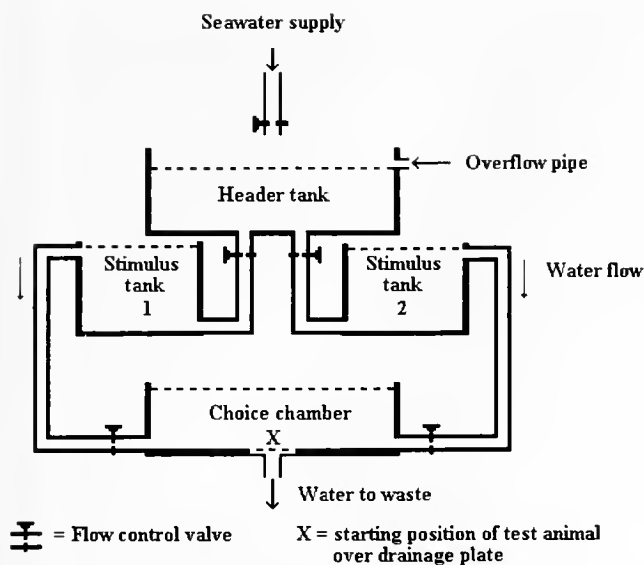


Figure 1. Diagram of the choice apparatus used to test the responses of three echinoderms to waterborne stimuli (not to scale). Internal dimensions of components: header tank 300 mm long, 200 mm wide, and 190 mm deep; stimulus tanks each 175 mm long, 115 mm wide, and 115 mm deep; choice chamber 400 mm long, 160 mm wide, 140 mm deep, and drainage plate diameter 40 mm. Seawater supply to header tank set to overflow constantly; flow tubes to choice chamber set to deliver 0.36 l/min to each side. Flow tubing 8 mm internal diameter.

neously stimulated by two unmixed water bodies. This is impossible in a Y-maze where test animals have to move up the base arm of the Y in a water body containing two elements that may be partly mixed together before the test subjects reach the point of choice. Moreover, some species may move so quickly that they pass into one arm of the Y before making a purely chemically cued choice (Bartel and Davenport, 1956). A significant development in choice apparatus occurred when Pratt (1974) designed a choice chamber to investigate the attraction of prey and the stimulus to attack in the predatory gastropod *Urosalpinx cinerea*. His choice chamber featured two slightly inclined slopes draining centrally in a narrow rectangular chamber and allowed the test animal to be stimulated by two unmixed water bodies at the same time (Pratt, 1974).

In the present work, the header tank, stimulus tanks, and choice chamber itself were all made from clear acrylic plastic. The tubing connecting the tanks (see Fig. 1) was made of flexible plastic with an internal diameter of 8 mm. The header tank acted as the reservoir and supplied the two stimulus tanks with running seawater, which could be adjusted by flow-control valves (see Fig. 1). These two stimulus tanks respectively supplied opposite ends of the choice chamber *via* 1-m-long flexible plastic tubes also fitted with flow-control valves. Each delivered water to the choice chamber at a rate of about 0.36 l/min. The choice chamber itself was a narrow rectangular trough with a perforated

circular drainage plate, 40 mm in diameter, fitted flush to the center of the tank bottom, for wastewater outflow. The chamber measured 400 mm long by 160 mm wide by 140 mm deep (internal measurements).

The choice chamber was positioned on a wet bench close to the sea urchin holding tank, so quick transfers of experimental animals were possible. Clean uncirculated water was used to feed the apparatus during the experiments. However, beforehand, two dyes—green for the left and red for the right—were added simultaneously to each stimulus tank and the flow valves adjusted so that the left and right water flows met exactly in the center of the drainage plate. “Threads” of dye reached the drainage plate within 2 min of the system being set to run. After 5 min there were no pockets of undyed water in the choice chamber, and a front of dyes was clearly visible, with no mixing, over the chamber drainage plate.

To run the experiments, the system was set with similar flow rates of clean seawater entering each side of the choice chamber, thus reducing any confounding effects of rheotaxis. The test animal was placed in the middle of the drainage plate outlet and allowed to acclimate for 1 min. Then, over the next 10 min, 20 ml of test stimulus extract (see below) was introduced directly into the outflow tube of whichever stimulus tank was in use, at the point the tube left the tank. This inevitably led to dilution, which can be estimated over the 10 min of stimulus application as follows: volume of stimulus, 20 ml; volume of water flowing from stimulus tank to choice chamber, 3600 ml ($= 0.36 \text{ l} \times 10 \text{ min}$) = 1:180. Each stimulus was given as 20 doses of 1 ml each, delivered at 30-s intervals. This delivery rate of stimuli helped ensure that the stimulus had equally permeated all parts of the appropriate half of the choice chamber and that the test animals were exposed to as constant a stimulus as possible. When whole animals were used for the stimulus, a pair of starfish or urchins were placed in the appropriate stimulus tank so that seawater flowed over them on its way to the choice chamber. The response of the test animal during this time was observed and recorded. The following responses were possible:

1. Movement towards the stimulus: the test animal moved fully off the drainage base plate into the water body conditioned by the stimulus. The minimum movement for this to be scored as a response was 50 mm for *A. rubens*, 30 mm for *P. miliaris*, and 60 mm for *E. esculentus*, these distances being such that they brought the animals at least partly off the drainage plate and clearly into one water stream. Test animals achieving less distance than this or not moving off the drainage plate within 30 min were scored as having no response. Nearly all of the responding animals moved the full distance from the center of the drainage plate

to the stimulus inflow point, a distance of 200 mm (Fig. 1).

2. Movement away from the stimulus: the animal moved fully off the drainage base plate into the unconditioned water body.
3. No response: part of the animal remained on the drainage base plate or the animal moved to the sides of the choice chamber such that at least part of its body was in line with the base plate.

After each experiment the choice chamber was thoroughly rinsed and cleaned of all animal debris. The chamber was washed through with clean seawater for 5 min between each test to ensure that all residual stimuli were removed. In addition, the end of the choice chamber into which the stimulus was introduced was alternated for each successive test. This was to eliminate the effects of any inequality of flow between the two sides of the apparatus that might cause the test animals to favor one side over the other. No animal was tested more than once each day. Animals were randomly selected from a pool of 50 individuals kept in separate holding tanks according to species. The same animal could have been selected by chance on successive days; in that case, it was assumed that its response to a stimulus was independent between days. We are not aware of any studies that contradict this assumption for starfish.

Forty different animals were exposed to conspecific stimuli in each of eight experiments. Thus data were analyzed with $n = 40$. For each stimulus tested, animals were drawn from the same pool of individuals. The following hypotheses were tested using different experimental stimuli as shown:

1. That the two sides of the choice chamber gave similar flow rates and volumes so that the test animals did not favor one side over the other. This was tested in experiments when no stimulus was used in either side of the chamber. These experiments acted as controls.
2. That intact, whole conspecifics are attractive or repellent. Here conspecifics were used as the stimulus and were placed in one stimulus tank. There was no stimulus in the other.
3. That test homogenate, composed of spines and epidermal tissues from conspecifics (one starfish as well as one large or three small urchins) was attractive or repellent to conspecifics. This material were scraped into a 50-ml glass beaker and ground up thoroughly in 25 ml of seawater, using a glass rod. The mixture was then stirred to suspend all fine material before being added to one stimulus tank. This was to determine whether the chemical cues active in (2) above resided in the epithelium and skeleton of the test and its appendages. Since movement over hard substrates abrades urchin spines (Campbell, pers. obs.), naked

calcite can be exposed to seawater naturally, and the inclusion of calcite in this homogenate is appropriate.

4. That coelomic fluid was attractive or repellent to conspecifics. A syringe was used to draw off 25 ml of coelomic fluid from an arbitrary number of starfish or sea urchins *via* a small hole in the aboral surface. This was to determine the attractive or repellent effects of coelomic fluid that is released from animals broken open by attacking predators.
5. That gut homogenate was attractive or repellent to conspecifics. Gut tissue was carefully removed from halved asteroid (excluding the pyloric caeca) or echinoid tests (all the gut) and placed in a 50-ml glass beaker. The tissue collected from one starfish or large urchin or from five small urchins was ground up in 25 ml of seawater, using a glass rod. The mixture was stirred well to suspend cells and fragments and was tested to determine whether gut tissue, which is exposed during predator attacks, might release chemical stimuli warning conspecifics of predator behavior.
6. That pyloric cecum homogenate (for *A. rubens* only) was attractive or repellent to conspecifics. This was prepared as for (5) above and for a similar purpose.
7. That gonad extract was attractive or repellent to conspecifics. Gonad tissue was carefully removed from one halved test of *A. rubens* or *E. esculentus* (large echinoid), or from five tests of *P. miliaris* (small echinoid), and ground up in 25 ml of seawater, using a glass rod. The mixture was stirred well to suspend cells and fragments. When ripe, gonad tissue may contribute a major part of the contents of the echinoderm body cavity and may be released and consumed when predators break open echinoderm tests (Ormond *et al.*, 1973).
8. That gametes were attractive or repellent to conspecifics. Both male and female gametes were extracted from one large or three small sea urchins by injecting 0.5 ml of 0.5 M KCl through the peristomial membrane to initiate spawning; the animals shed their gametes within a few seconds of injection. The gametes were collected over the 5–15 min spawning period that followed by inverting the urchin over a 50-ml glass beaker filled with seawater and immersing the gonopores. Male and female gametes of *A. rubens* were extracted using the method of Kantanani (1969), in which 30 g of L-methyladenine was dissolved in 2.5 ml of seawater (0.5 ml per arm). Gametes were shed 60 min after injection, collected in seawater, and stirred immediately before use to keep them suspended. Gametes were tested to see if they would stimulate gregarious behavior, which is thought to be important in increasing fertilization success at spawning (Reese, 1966; Levitan *et al.*, 1992).

The significance of the collected data was examined in two ways, using a log-likelihood test. First the numbers of animals moving toward and away from the stimulus in question for each experiment were pooled and tested against those not responding with movements at all. The null hypothesis predicted a ratio of 50:50. This showed whether a significant number of animals moved in response to the stimuli as opposed to not moving. Second, the number of animals moving toward the stimulus in question for each experiment was compared with the number moving away. Again, the null hypothesis predicted a result of 50:50.

Results

Overall, about 75% of the test animals responded to stimuli in the choice chamber within 5 min of the start of each experiment, and 80% had traversed the full length of one arm of the chamber within 30 min. In the first set of experiments (Figs. 2a–c) log-likelihood tests revealed that, with the exception of *Asterias rubens* (where there was a lack of significant response to coelomic fluid) and *Echinus esculentus* (where there was a lack of response to stimulus-free water), all three species displayed significant behavioral responses to eight experimental treatment stimuli in the choice chamber ($P < 0.001$ – $P < 0.025$).

In the second set of experiments (Table 1 and Figs. 3a–c), starfish and urchins tested when no stimulus was introduced to the apparatus failed to display a significant preference for one side or the other of the choice chamber ($P > 0.05$). This control experiment showed that the apparatus lacked any intrinsic bias that might have encouraged test animals to move more to one side than to the other. It therefore confirmed that subsequent choices made by test animals, in response to introduced stimuli, would be meaningful. It also showed that there was effectively no significant response to the direction of water flow. All three species of echinoderm tested were significantly attracted to whole conspecifics ($P < 0.001$ – $P < 0.025$) and to the homogenates of their tests, spines, and epidermal tissues ($P < 0.001$ – $P < 0.01$) (Table 1 and Figs. 3a–c). The sea urchins significantly avoided water bodies containing coelomic fluid, whereas the starfish showed no significant response to them (Table 1 and Figs. 3a–c). All animals avoided homogenates of conspecific gut tissue (Table 1 and Figs. 3a–c). *A. rubens* did not respond to homogenate of its pyloric caeca or gonads, but both sea urchin species were significantly repelled by conspecific gonad homogenates ($P < 0.001$). *P. miliaris* was not significantly attracted to gametes, whereas both *E. esculentus* and *A. rubens* were (Table 1 and Figs. 3a–c).

Discussion

The results show that *Asterias rubens*, *Psammechinus miliaris*, and *Echinus esculentus* generally respond to water-

borne stimuli derived from conspecifics (Table 1), being mainly attracted by whole animals, test homogenate, and gametes and mainly repelled by coelomic fluid, gut, and gonad homogenates. These findings agree with a number of studies which have shown that echinoderms perceive and react to waterborne chemical stimuli (Dix, 1969; Snyder and Snyder, 1970; Campbell, 1983; Mann *et al.*, 1984; Parker and Shulman, 1986). Because these animals have low visual acuity, tactile and chemical cues must be the chief stimuli received by their sensory systems (Sloan and Campbell, 1982). A distance-mediated chemosensory system was suspected for prey detection in *Asterias forbesi*, but could not be definitively demonstrated (Lepper and Moore, 1995, 1998). However, electron microscopy has revealed concentrations of suitable receptors in external epithelium in this species (Lepper, 1998).

Various workers have demonstrated aggregation of conspecific echinoderms both in the field and in the laboratory (McKay, 1945; Reese, 1966; Broom, 1975; Tegner and Dayton, 1976), and the significant attraction we have described is likely to mediate this. Three hypotheses have been put forward to explain aggregation, namely that echinoderms can benefit from it (1) by optimizing feeding, (2) by better resisting the attacks of predators, and (3) by improving fertilization success at spawning (Bernstein *et al.*, 1981; Moore and Campbell, 1985; Levitan *et al.*, 1992). Aggregations of *A. rubens* were studied by Moore and Campbell (1985), who showed that not only were individual starfish attracted by waterborne scents of conspecifics, but foraging starfish were more attractive than nonfeeding ones. Aggregation in *A. rubens* may therefore be a response to optimize food locations, as was shown by Ormond *et al.* (1973) for *Acanthaster planci* and has been described for other animals (Zahavi *et al.*, 1999). Aggregating behavior of *Strongylocentrotus droebachiensis* was also investigated by Bernstein *et al.* (1981, 1983), who found that this species forms dense feeding and nonfeeding groups of up to 100 individuals per square meter.

P. miliaris, in contrast, is often found in small groups of between 2 and 10 in the field (Campbell, unpubl.). Its gregarious behavior could be an adaptation to group defense of feeding areas, enhancing foraging success by locating other individuals already feeding (Stone *et al.*, 1993). However, the small size of the *P. miliaris* aggregations makes them unlikely to be anti-predator mechanisms of the type described by Bernstein *et al.* (1983) for *S. droebachiensis*, where predation risk to an individual might be reduced by putting other conspecifics between it and potential predators (Hamilton, 1971). Such behavior is known for other animals (Zahavi *et al.*, 1999). Laboratory experiments showed that *S. droebachiensis* aggregated in the presence of unspecified crab and lobster predators that were unable to attack them effectively because they could not encircle the aggregation

Figure 2a

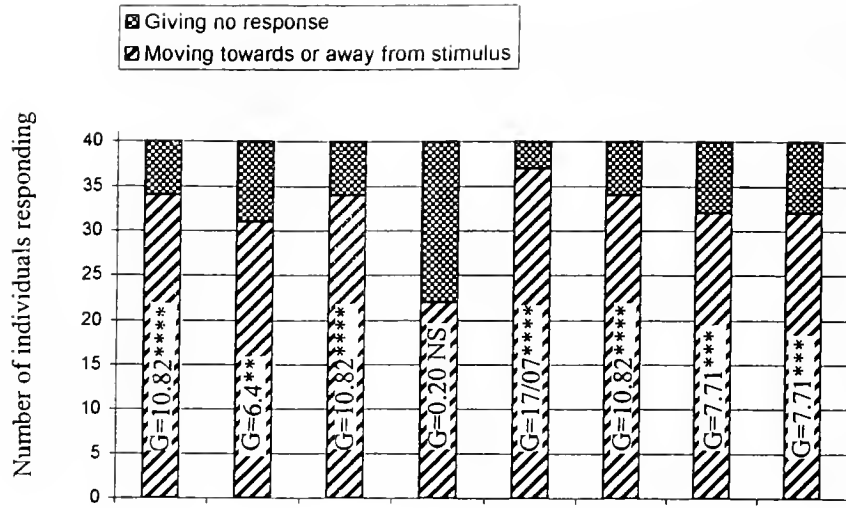


Figure 2b

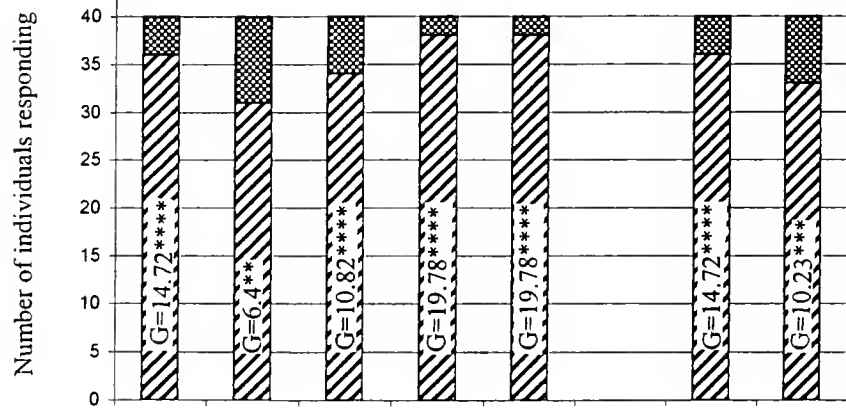


Figure 2c

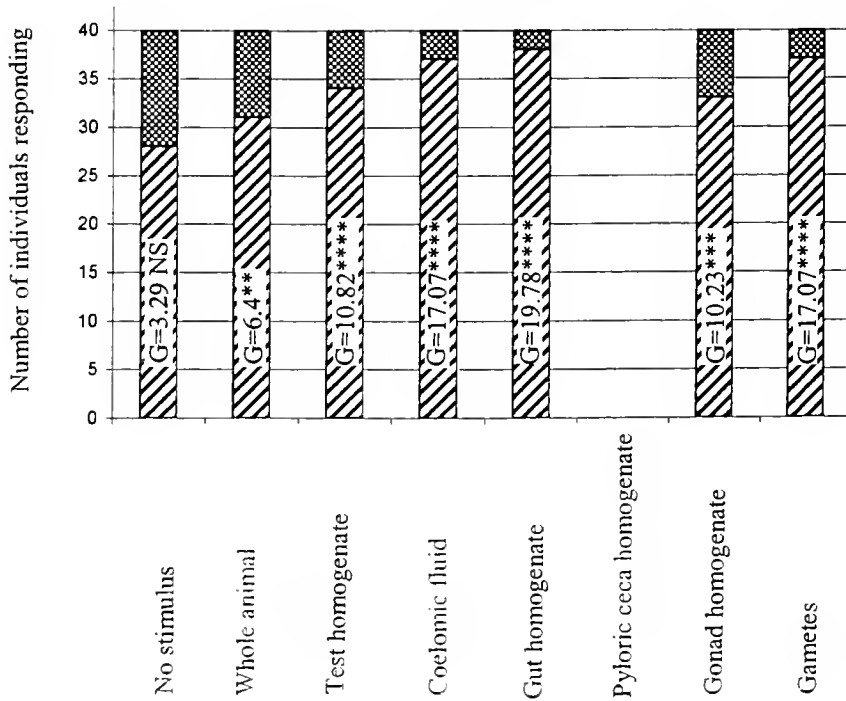


Table 1

Summary of the observed responses of *Asterias rubens*, *Psammechinus miliaris* and *Echinus esculentus* to conspecific stimuli

Stimulus used in choice chamber	No stimulus	Whole animal	Test homogenate	Coelomic Fluid	Gut homogenate	Pyloric cecum homogenate	Gonad homogenate	Gametes
<i>A. rubens</i> moving towards stimulus	18	26	29	10	7	18	16	25
<i>A. rubens</i> moving away from stimulus	16	5	5	12	30	16	16	7
G test value	0.12 NS	15.58****	18.74****	0.18 NS	15.40****	0.12 NS	0 NS	10.76***
<i>P. miliaris</i> moving towards stimulus	17	22	25	5	7	NA	6	19
<i>P. miliaris</i> moving away from stimulus	19	9	9	33	31	NA	30	14
G test value	0.12 NS	5.62**	7.84***	23.08****	16.38****	NA	17.46****	0.76NS
<i>E. esculentus</i> moving towards stimulus	16	24	29	2	3	NA	3	26
<i>E. esculentus</i> moving away from stimulus	12	7	5	35	35	NA	30	11
G test value	0.6 NS	9.86***	18.74****	35.72****	31.68****	NA	25.66****	6.26**

Responses toward stimulus vs. away from stimulus: NS = not significant, $P > 0.05$; * = significant, $P < 0.05$; ** = significant, $P < 0.025$; *** = significant, $P < 0.01$; **** = significant, $P < 0.001$; NA = not applicable.

with their claws (Bernstein *et al.*, 1983). Thus gregarious behavior lowers the intensity of predation and reduces urchin mortality (Bernstein *et al.*, 1983) and, apart from optimizing food locations, these groupings appear to be an effective anti-predator defense.

Orton (1914) found *P. miliaris* living in paired associations of 1 male and 1 female so, alternatively, intraspecific attraction may be explained by spawning aggregation behavior, which is well known for echinoids (Moore, 1966), and which has been shown to increase fertilization success (Levitan *et al.*, 1992). All the specimens in this study were collected in August and maintained at 11 °C. *P. miliaris* is known to breed at Millport from June to August at temperatures of 9 °–11 °C (Jensen, 1966; Sukarno *et al.*, 1979), so it is likely that the individuals tested in these experiments would be susceptible to factors that might enhance reproductive success. The reasons for aggregation in *E. esculentus* are less clear, as there have been fewer investigations of its social behavior than there have been for *A. rubens* and *P. miliaris*. Aggregations of *E. esculentus* have been noted grazing on algal turf (Forster, 1959), and this species is known to migrate inshore and aggregate for spawning (Elmhirst, 1922; Stott, 1931).

The echinoids in the present study all significantly avoided water conditioned with conspecific coelomic fluid, gut homogenate, and gonad homogenate by moving away

from these stimuli ($P < 0.001$) (Table 1). These escape or alarm reactions are similar to those of *Diadema antillarum*, which fled from fluid extracts of damaged conspecifics using its oral spines as supplementary locomotory organs, in a rapid avoidance reaction (Snyder and Snyder, 1970). Although Snyder and Snyder (1970) were unable to verify their field observations by laboratory experiments, our results are consistent with their findings. *S. droebachiensis* also displays an alarm response to water conditioned by crushed conspecifics and predators (Mann *et al.*, 1984), and this characteristic may explain why natural aggregations of this species decreased in number with increasing abundance of the predatory wolffish *Anarhichas lupus* (Bernstein *et al.*, 1981). Presumably, when this fish attacked an urchin, it released chemicals repellent to other echinoids. Using a choice chamber similar to the one in the present study, Mann *et al.* (1984) showed that 79% of active *S. droebachiensis* moved away from crushed conspecifics, while 70% moved away from predators (*Homarus americanus*). These workers found that when active urchins were exposed to water conditioned by either coelomic fluid, gut, or gonad tissue from conspecifics, 80%–87% of the animals exhibited an alarm response. Mann *et al.* (1984) also showed that when the escape reaction was calculated as a percentage of active urchins it was apparently independent of temperature, whereas the food-seeking reaction was temperature-related.

Figure 2. Number of individuals of each species responding to conspecific stimuli with G-test results and significance code for each stimulus type. (a) *Asterias rubens*; (b) *Psammechinus miliaris*; (c) *Echinus esculentus*. NS = 0 > 0.05 * = $P < 0.05$ ** = $P < 0.025$ *** = $P < 0.01$ **** = $P < 0.001$.

Figure 3a

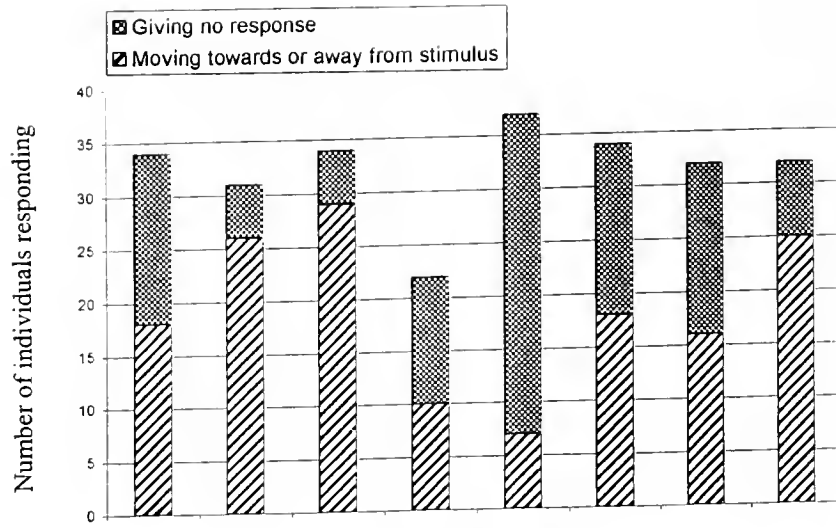


Figure 3b

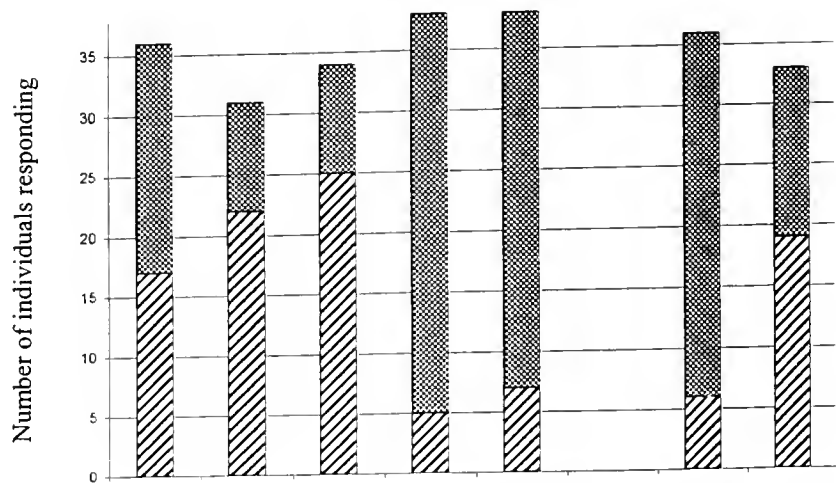
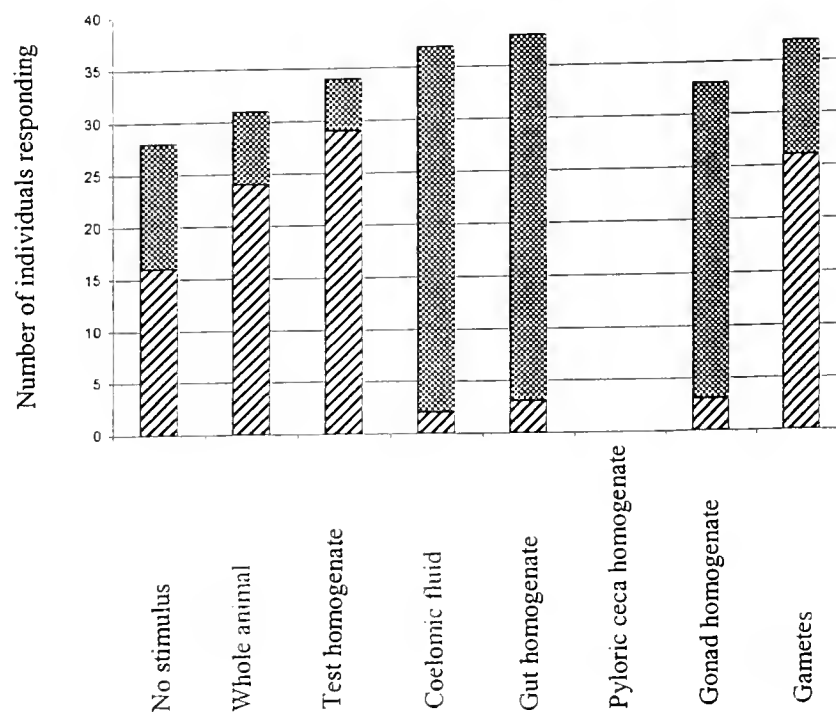


Figure 3c



Thus they suggested that, during the low temperature of winter months, urchin behavior is determined more by the presence of predators than by the distribution of food. The effects of both heterospecific and conspecific body fluids on several species of Caribbean echinoids were examined by Parker and Shulman (1986), who found that the degree of response to conspecific extracts depended on the extent of protection afforded by different microhabitats. Further, there was a correlation between the distance moved by alarmed urchins and the distance they moved from shelter when foraging (Parker and Shulman, 1986). Thus there is a strong implication of predator avoidance in this particular aspect of echinoid behavior.

P. miliaris spends much of its time in protected situations, such as under rocks (Orton, 1929; Jensen, 1966), and makes excursions from these areas to forage on algae and encrusting animals such as sponges, hydroids, bryozoans, and crustaceans (Hancock, 1957). It is during foraging that *P. miliaris* is most vulnerable to predators and that a reliable signal of the presence of a feeding predator will be most advantageous in stimulating the urchin to retreat to safety. The implication of Parker and Shulman's (1986) work may be that the echinoid alarm response to conspecific scents has evolved as an adaptation for escape during foraging periods. The sensitivity to gonad and gut extracts is particularly significant because most predators of echinoids have to break open the test in some way to gain access to the main nutritive elements, the gonads and other viscera. Because *E. esculentus* is a sublittoral species (Orton, 1929), behavioral and ecological observations of this species in the field are less extensive and evaluation of its foraging and escape activities *in situ* is more difficult than for *P. miliaris*, which occurs on the shore. Some echinoderm species form aggregations at spawning time and shed their gametes in synchrony (Moore, 1966). Therefore, why should the urchins be repelled by an extract composed of gonad tissue while not being repelled by gametes, as indicated by the results of this investigation? Possibly the chemical stimulus that caused the urchins to move away from the gonad extract originated in the germinal epithelium or in the nutritive phagocytic tissue. The responses of *A. rubens* to reproductive tissues showed consistencies with those of the echinoids, as starfish were not attracted by gonad homogenate but were by gametes.

In the case of *A. rubens*, gut homogenate (cardiac and pyloric stomach) caused an avoidance response; however, the starfish differed from the urchins in that coelomic fluid did not do so. Possibly *A. rubens*, a known predator and carrion feeder, sometimes acts as a cannibal. Some speci-

mens of *A. rubens* held in the aquaria were seen to eat pyloric ceca previously isolated from other individuals, which accords with Jangoux's (1982) note of cannibalism in this species.

Weissburg and Zimmer-Faust (1993) pointed out that the success of chemically mediated alarm responses in protecting individuals from dangerous situations depends on water turbulence and mixing, because the aquatic environment, as a medium for the transmission of chemical signals, is profoundly affected by hydrodynamics. Every care was taken with our experiments to minimize such disturbances. The use of the dye tests to obtain the correct balance of water flow through the choice chamber allowed us to determine a 10-min regime of stimulus application that subjected the test animals to the most precise stimulus conditions we could obtain. Quantification of the amount of stimulus needed to elicit a response is a desirable but elaborate extension of the experimental procedure, and one that needs to be addressed in future work. Various studies have identified the specific substances to which echinoderms will respond, showing that these animals can react to chemicals such as amino acids, which are present in very low concentrations (Mayo and Mackie, 1976; Sloan and Campbell, 1982; Mann *et al.*, 1984; Lepper and Moore, 1995).

Snyder and Snyder (1970) noted that vinegar produced a flight response in *Diadema antillarum* that was similar to the one initiated by crushed conspecifics. Because crushed heterospecifics had no such effect, they rejected the idea that the escape response was merely due to a change in the chemistry of the water passing over the urchins. Parker and Shulman (1986) found similar results, strengthening the argument for predator avoidance and escape due to extracts from conspecifics. Solandt and Campbell (1998) demonstrated that Caribbean echinoids tested in a choice chamber showed a distinct range of preferences to six algal species, which further supports the idea that these responses are based on choice.

The identification here of clear-cut avoidance and aggregation responses for the two echinoid species shows that they differentiate between, and react to, distinct chemical stimuli under aquarium conditions at a distance of only 1 m. Although the stimulus concentrations are poorly defined, they lie within plausible concentrations for animals living closely together in aggregations or social groups, where one may be seriously damaged by a predator. Our results for *A. rubens* indicate that the distinction between aggregative and repellent effects of various conspecific tissues here is less well defined than it is for the two echinoids, with gut

Figure 3. Number of individuals of each species responding to conspecific stimuli. (a) *Asterias rubens*; (b) *Psammechinus miliaris*; (c) *Echinus esculentus*.

homogenate being the only stimulus that produced a significant avoidance response by the starfish.

Acknowledgments

The authors acknowledge the help and encouragement given by Dr. Maurice Elphick, Dr. Craig Young, and Prof. Paul Tyler. They are indebted to Dr. Carl Smith for his advice on the statistical treatment of the data and to two anonymous referees for their constructive comments.

Literature Cited

- Allee, W. C. 1927. Animal aggregations. *Q. Rev. Biol.* **2**: 367–398.
- Bartel, A. H., and D. Davenport. 1956. A technique for the investigation of chemical responses in aquatic animals. *Br. J. Anim. Behav.* **4**: 117–119.
- Bernstein, B. B., B. E. Williams, and K. H. Mann. 1981. The role of behavioural responses to predators in modifying urchin's (*Strongylocentrotus droebachiensis*) destructive grazing and seasonal foraging patterns. *Mar. Biol.* **63**: 39–49.
- Bernstein, B. B., S. C. Schroeter, and K. H. Mann. 1983. Sea urchin (*Strongylocentrotus droebachiensis*) aggregating behaviour investigated by a subtidal multifactorial experiment. *Can. J. Fish. Aquat. Sci.* **40**: 1975–1986.
- Broom, D. M. 1975. Aggregation behaviour of the brittle-star *Ophiothrix fragilis*. *J. Mar. Biol. Assoc. UK* **55**: 191–197.
- Bullock, T. H. 1965. Comparative aspects of superficial conduction systems in echinoids and asteroids. *Am. Zool.* **5**: 545–562.
- Bullock, T. H., and G. A. Horridge. 1965. *Structure and Function in the Nervous Systems of Invertebrates*. W. H. Freeman, San Francisco.
- Campbell, A. C. 1973. Observations on the activity of echinoid pedicellariae: II. Jaw responses of tridentate and ophiocéphalous pedicellariae. *Mar. Behav. Physiol.* **3**: 17–34.
- Campbell, A. C. 1983. Form and function in pedicellariae. *Echinoderm Stud.* **1**: 139–167.
- Campbell, A. C., and M. S. Laverack. 1968. The responses of pedicellariae from *Echinus esculentus* (L.). *J. Exp. Mar. Biol. Ecol.* **2**: 191–214.
- Chia, E.-S. 1969. Responses of globiferous pedicellariae to inorganic salts in three regular echinoids. *Ophelia* **6**: 203–210.
- Dayton, P. K., R. J. Rosenthal, L. C. Mahen, and T. Antezena. 1977. Population structure and foraging biology of the predaceous Chilean asteroid *Mevenaster gelatinosus* and the escape biology of its prey. *Mar. Biol.* **39**: 361–370.
- Dix, T. 1969. Aggregation in the echinoid *Evechinus chloroticus*. *Pac. Sci.* **23**: 123–124.
- Elmhirst, R. 1922. Habits of *Echinus esculentus*. *Nature* **110**: 667.
- Forster, G. R. 1959. The ecology of *Echinus esculentus* L. Quantitative distribution and rate of feeding. *J. Mar. Biol. Assoc. UK* **38**: 361–367.
- Hamilton, W. D. 1971. Selection of selfish and altruistic behaviour in some extreme models. Pp. 58–91 in *Smithsonian Annual III. Man and Beast: Comparative and Social Behaviour*. J. F. Eisenberg and W. S. Dillon, eds. Smithsonian Institution Press, Washington, DC.
- Hancock, D. A. 1957. The feeding behaviour of the sea urchin *Psammechinus miliaris* (Gmelin) in the laboratory. *Proc. Zool. Soc. Lond.* **129**: 255–262.
- Jangoux, M. 1982. Food and feeding mechanisms: Asterozoa. Pp. 117–159 in *Echinoderm Nutrition*. M. Jangoux and J. N. Lawrence, eds. A. A. Balkema, Rotterdam.
- Jensen, M. 1966. Breeding and growth of *Psammechinus miliaris* (Gmelin). *Ophelia* **7**: 65–78.
- Kanatani, H. 1969. Induction of spawning and oocyte maturation by L-methyladenine in starfishes. *Exp. Cell Res.* **57**: 333–337.
- Kruuk, H. 1964. Predators and anti-predator behaviour of the black-headed gull (*Larus ridibundus* L.). *Behaviour, Supplement XI*. E. J. Brill, Leiden.
- Lawrence, J. M. 1987. *A Functional Biology of Echinoderms*. Croom Helm, Bekenham, UK.
- Legault, C., and J. H. Himmelman. 1993. Relation between escape behaviour of benthic marine invertebrates and the risk of predation. *J. Exp. Mar. Biol. Ecol.* **170**: 55–74.
- Lepper, D. M. E. 1998. Ultrastructure and morphology of the epidermis and tube feet of two echinoderms. P. 46 in *Proceedings of the Ninth International Echinoderm Conference, San Francisco, 5–9 August 1996*. R. Mooi and M. Telford, eds. A. A. Balkema, Rotterdam.
- Lepper, D. M. E., and P. A. Moore. 1995. Chemical ecology of the seastar, *Asterias forbesi*: the role of chemical signals in foraging behaviour. *Chem. Senses* **20**: 729 [Abstract.]
- Lepper, D. M. E., and P. A. Moore. 1998. The role of chemical signals in the foraging behaviour of the sea star *Asterias forbesi*. P. 266 in *Proceedings of the Ninth International Echinoderm Conference, San Francisco, 5–9 August 1996*. R. Mooi and M. Telford, eds. A. A. Balkema, Rotterdam.
- Levitán, D. R., M. A. Sewell, and F.-S. Chia. 1992. How distribution and abundance influence fertilization success in the sea urchin *Strongylocentrotus franciscanus*. *Ecology* **73**: 248–254.
- Lima, S. L., and L. M. Dill. 1990. Behavioural decisions made under the risk of predation: a review and prospectus. *Can. J. Zool.* **68**: 619–640.
- Mackie, A. M. 1975. Chemoreception. Pp. 69–105 in *Biochemical and Biophysical Perspectives in Marine Biology*, Vol. 2. D. C. Malins and J. R. Sargent, eds. Academic Press, London.
- Mann, K. H., J. L. C. Wright, B. E. Welsford, and E. Hatfield. 1984. Responses of the sea urchin *Strongylocentrotus droebachiensis* to waterborne stimuli from potential predators and potential food algae. *J. Exp. Mar. Biol. Ecol.* **79**: 233–244.
- Manzey, K. P., C. Birkland, and P. K. Dayton. 1968. Feeding behaviour of asteroids and escape responses of their prey in the Puget Sound Region. *Ecology* **49**: 603–619.
- Mayo, P., and A. M. Mackie. 1976. Studies of avoidance reactions in several species of predatory British seastars (Echinodermata: Asterozoa). *Mar. Biol.* **38**: 41–49.
- McKay, D. C. G. 1945. Notes on the aggregating marine invertebrates of Hawaii. *Ecology* **26**: 205–207.
- Millott, N., and K. Takahashi. 1963. The shadow reaction of *Diadema antillarum* Philippi. IV. Spine movements and their implications. *Philos. Trans. R. Soc. Lond. B* **246**: 437–470.
- Moore, H. B. 1966. Ecology of echinoids. Pp. 73–85 in *Physiology of Echinodermata*. R. A. Booletoian, ed. Wiley Interscience, New York.
- Moore, R. J., and A. C. Campbell. 1985. An investigation into the behavioural and ecological bases for periodic infestations of *Asterias rubens*. P. 596 in *Proceedings of the Fifth International Echinoderm Conference, Galway, 24–29 September 1984*. B. F. Keegan and B. D. S. O'Connor, eds. A. A. Balkema, Rotterdam.
- Mortensen, T. 1943. *A Monograph of the Echinozoa. Camarodonta II*. C. A. Reitzel, Copenhagen.
- Ormond, R. F. G., A. C. Campbell, S. M. Head, R. J. Moore, P. S. Rainbow, and A. P. Saunders. 1973. Formation and breakdown of aggregations of the crown-of-thorns starfish, *Acanthaster planci* (L.). *Nature* **246**: 167–168.
- Orton, J. H. 1914. On the breeding habits of *Echinus miliaris* with a note on the feeding habits of *Patella vulgata*. *J. Mar. Biol. Assoc. UK* **10**: 254–257.
- Orton, J. H. 1929. On the occurrence of *Echinus esculentus* on the foreshore in the British Isles. *J. Mar. Biol. Assoc. UK* **16**: 289–296.

- Parker, D. A., and M. J. Shulman. 1986.** Avoiding predation: alarm responses of sea urchins to simulated predation on conspecific and heterospecific sea urchins. *Mar. Biol.* **93**: 201–208.
- Pentreath, V. W., and J. L. S. Cobb. 1972.** Neurobiology of Echinodermata. *Biol. Rev.* **47**: 363–392.
- Pratt, D. M. 1974.** Attraction to prey and stimulus attack in the predatory gastropod *Urosalpinx cinerea*. *Mar. Biol.* **27**: 37–45.
- Reese, E. A. 1966.** The complex behavior of echinoderms. Pp. 157–218 in *Physiology of Echinodermata*, R. A. Boolootian, ed. Wiley Interscience, New York.
- Slater, P. J. B. 1985.** *An Introduction to Ethology*. Cambridge University Press, Cambridge.
- Sloan, N. A., and A. C. Campbell. 1982.** Perception of food. Pp. 3–23 in *Echinoderm Nutrition*, M. Jangoux and J. N. Lawrence, eds. A. A. Balkema, Rotterdam.
- Snyder, N., and S. Snyder. 1970.** Alarm response of *Diadema antillarum*. *Science* **168**: 276–278.
- Solandt, J.-L., and A. C. Campbell. 1998.** Habitat selection in Jamaican echinoids. Pp. 821–827 in *Proceedings of the Ninth International Echinoderm Conference, San Francisco, 5–9 August 1996*. R. Mooi and M. Telford, eds. A. A. Balkema, Rotterdam.
- Stone, R. P., C. E. O'Clair, and T. C. Shirley. 1993.** Aggregating behaviour of ovigerous female king crab *Paralithodes camtschaticus*, in Auke Bay, Alaska. *Can. J. Fish. Aquat. Sci.* **50**: 750–758.
- Stott, F. C. 1931.** The spawning of *Echinus esculentus* and some changes in gonad composition. *J. Exp. Biol.* **8**: 133–150.
- Snkarno, R., M. Jangoux, and E. Van Impel. 1979.** Le cycle reproducteur annuel de *Psammechinus miliaris* (Gmelin) (Echinoidea) en Zeelande. Pp. 415–416 in *Echinoderms: Past and Present*, M. Jangoux, ed. A. A. Balkema, Rotterdam.
- Tegner, M. J., and P. K. Dayton. 1976.** Sea urchin recruitment patterns and implications for commercial fishing. *Science* **196**: 324–326.
- Weissburg, M. J., and R. K. Zimmer-Faust. 1993.** Life and death in moving fluids: hydrodynamic effects on chemosensory-mediated predation. *Ecology* **74**: 1428–1443.
- Weissburg, M. J., and R. K. Zimmer-Faust. 1994.** Odor plumes and how blue crabs use them in finding prey. *J. Exp. Biol.* **197**: 349–375.
- Yoshida, M. 1966.** Photosensitivity. Pp. 435–464 in *Physiology of Echinodermata*, R. A. Boolootian, ed. Wiley Interscience, New York.
- Zahavi, A., A. Zahavi, N. Zahavi-Ely, and M. P. Ely. 1999.** *The Handicap Principle: A Missing Piece of Darwin's Puzzle*. Oxford University Press, New York.

Action Potentials Occur Spontaneously in Squid Giant Axons with Moderately Alkaline Intracellular pH

JOHN R. CLAY^{1,*} AND ALVIN SHRIER²

¹ *Laboratory of Neurophysiology, National Institute of Neurological Disorders and Stroke, National Institutes of Health, Bethesda, Maryland 20892; and* ² *Department of Physiology, McGill University, Montreal, Quebec, Canada, H3G1Y6*

Abstract. This report demonstrates a novel finding from the classic giant axon preparation of the squid. Namely, the axon can be made to fire autonomously (spontaneously occurring action potentials) when the intracellular pH (pH_i) was increased to about 7.7, or higher. (Physiological pH_i is 7.3.) The frequency of firing was 33 Hz ($T = 5^\circ$). No changes in frequency or in the voltage waveform itself were observed when pH_i was increased from 7.7 up to 8.5. In other words, the effect has a threshold at a pH_i of about 7.7. A mathematical model that is sufficient to mimic these results is provided using a modified version of the Clay (1998) description of the axonal ionic currents.

Introduction

The electrical response of squid giant axons *in vivo* to environmental stimuli can be characterized as being primarily phasic. For example, the axon fires an action potential once, and only once, in 15 °C seawater in response to a light flash, thereby triggering the rapid, jet-propelled escape of the animal (Otis and Gilly, 1990). A more complicated behavior of the axon occurs in concert with the parallel small axon system (Young, 1939) during the delayed jet escape from chemical stimuli applied at the olfactory organ (Otis and Gilly, 1990). Under these conditions the giant axon fires from one to three action potentials (or none at all). A reduction in temperature to 6 °C, which squid often encounter in deep waters, produces changes in the role of the axon in these behaviors (Neumeister *et al.*, 2000). For example, the axon usually fires twice in response to a light flash at 6 °C (Neumeister *et al.*, 2000). A tonic train of a

relatively large number of action potentials does not appear to be elicited *in vivo*. These results are mirrored by the response of the axon *in vitro* to current stimuli applied with the standard axial wire recording technique. Under these conditions one, and only one, action potential is elicited with a rectangular current pulse, regardless of pulse duration or pulse amplitude (Clay, 1998). Moreover, an action potential is not elicited with a relatively slow depolarizing current ramp (J. R. Clay, unpub. obs.). A rapidly changing stimulus, such as a current step of sufficiently large amplitude, is required.

Given the above results, we were surprised to observe tonic firing of the axon when the pH of the perfusate used during recordings from intracellularly perfused axons was increased to 7.7, or higher. The normal intracellular pH (pH_i) is 7.3 (Boron and DeWeer, 1976). Under these conditions of slightly elevated pH_i , action potentials occurred spontaneously and repetitively. The activity lasted for as long as a few hours in some preparations. An ionic mechanism underlying this observation is proposed.

Materials and Methods

Experiments were performed on internally perfused squid giant axons at the Marine Biological Laboratory, Woods Hole, Massachusetts, using standard axial wire voltage- and current-clamp techniques described elsewhere (Clay and Shlesinger, 1983; Clay, 1998). The intracellular perfusate consisted of 300 mM K glutamate and 400 mM sucrose, with the pH adjusted to the desired level within the 7.2 to 8.5 range by free glutamic acid. In a few experiments the intracellular buffer consisted of 400 mM sucrose, 250 mM KF, and 25 mM K_2HPO_4 ($\text{pH}_i = 7.6\text{--}7.8$). The extracellular solution was either filtered seawater ($\text{pH} = 7.5$) or artificial seawater consisting of 430 mM NaCl, 10 mM KCl, 50 mM

Received 30 November 2000; accepted 28 June 2001.

To whom correspondence should be addressed. E-mail: jrclay@ninds.nih.gov

MgCl₂, 10 mM CaCl₂, and 10 mM Tris-HCl (pH 7.2). These extracellular solutions were used interchangeably given that similar results were obtained in either condition. The temperature was in the 4–6 °C range; in any single experiment it was maintained constant to within 0.1 °C by a Peltier device located within the experimental chamber. Input resistance measurements were made with rectangular current pulses applied to axons in extracellular medium containing tetrodotoxin (TTX, Sigma Chemical Co.) at a final concentration of 1 μM.

Computer simulations of membrane excitability were carried out as described previously (Clay, 1998). The model is given by

$$CdV/dt + (I_K + I_{Na} + I_{NaP} + I_L + I_{K,ir} + I_{stim}) = 0,$$

where V is membrane potential in mV, t is time in ms, C is the specific membrane capacitance ($C = 1 \mu\text{F} \cdot \text{cm}^{-2}$), I_{stim} is the stimulus current ($\mu\text{A} \cdot \text{cm}^{-2}$), and the various ionic current components are described as follows. The sodium ion current is given as in Vandenberg and Bezanilla (1991) with

$$I_{Na} = g_{Na} P_O V (\exp((V - E_{Na})/24) - 1) / ((\exp(V/24) - 1) \times (1 + 0.4 \exp(-0.38V/24)))$$

where $g_{Na} = 107 \text{ mS} \cdot \text{cm}^{-2}$, $E_{Na} = 64 \text{ mV}$, and P_O is the probability that any single Na⁺ channel is in the open state of the Vandenberg and Bezanilla (1991) kinetic scheme. The various rate constants in the model (in ms^{-1}) are as follows:

$$\begin{aligned} a &= 7.55 \exp(0.017(V - 10)), \\ b &= 5.6 \exp(-0.00017(V - 10)), \\ c &= 21.0 \exp(0.06(V - 10)), \\ d &= 1.8 \exp(-0.02(V - 10)), \\ f &= 0.56 \exp(0.00004(V - 10)), \\ g &= \exp(0.00004(V - 10)), \\ i &= 0.0052 \exp(-0.038(V - 10)), \\ j &= 0.009 \exp(-0.038(V - 10)), \\ y &= 22.0 \exp(0.014(V - 10)), \\ z &= 1.26 \exp(-0.048(V - 10)). \end{aligned}$$

The potassium ion current is given by

$$I_K = g_K n(V, t)^8 V (\exp(V/24) - K_s(t)/K_i) / (\exp(V/24) - 1),$$

where $g_K = 62.5 \text{ mS} \cdot \text{cm}^{-2}$, $dn(V, t)/dt = -(\alpha + \beta)n(V, t) - \alpha$, with $\alpha = -0.0075(V + 64) / (\exp(-0.11(V + 64)) - 1)$ and $\beta = 0.075 \exp(-(V + 62)/20)$. This represents a modification of the model of I_K in Clay (1998) in which n^4 kinetics were used. The α and β parameters have also been modified so as to obtain equivalent (or better) descriptions of the I_K results given by the n^4 model in Clay (1998). The K_s parameter, which corresponds to the potassium ion concentration in the restricted space just outside of the axolemma, is given by

$$dK_s/dt = 0.0104I_K - 0.08(K_s - 10) - 5(K_s - 10) / (1 + (K_s - 10)/2)^3.$$

Further details concerning the description of the I_{Na} and I_K components are given in Clay (1998). The background, or time-independent current in the model consists of three terms: the "leak" current, I_L ; a persistent, tetrodotoxin-sensitive sodium ion current I_{NaP} (Rakowski *et al.*, 1985); and an inwardly rectifying potassium ion current, $I_{K,ir}$. The latter, together with I_{NaP} , confers nonlinearity to the background current in the -90 to -60 mV range, similar to that observed experimentally. These components are described by

$$I_{NaP} = 4.5(V/24)(0.03 \exp(V/24) - 0.43) / ((\exp(V/24) - 1) \times (1 + \exp(-(V + 65)/7)));$$

$$I_{K,ir} = 0.24(V + 82) / (1 + 0.05(\exp(0.15(V + 82)))); \text{ and}$$

$$I_L = g_L(V + 49),$$

where g_L is either 0.2 ($\text{pH}_i = 7.3$) or 0.03 ($\text{pH}_i = 8.5$). The formulation for I_{NaP} represents a best fit, by eye, to unpublished measurements of this component kindly provided by R. F. Rakowski (Finch University of Health Sciences/The Chicago Medical School).

The simulations were implemented with a fourth-order Runge-Kutta iteration routine in FORTRAN with a time step of 1 μs.

Results

As noted above, the physiological intracellular pH for squid giant axons is 7.3 ± 0.013 ($\pm\text{SE}$; Boron and DeWeer, 1976). Under these conditions axons are quiescent with a resting potential of about -60 mV . An action potential elicited by a brief current pulse is shown in Figure 1A. A slight oscillatory rebound following the action potential was apparent, as indicated by the arrow in Figure 1A. The effect of changing the intracellular pH to 8.5 is illustrated in Figure 1B and C. A few minutes after the solution change, the membrane potential became oscillatory (inset, Fig. 1B). Moreover, it exhibited a much greater post-excitatory rebound (Fig. 1B). Several minutes later, the amplitude of the spontaneously occurring subthreshold oscillations increased, followed by a train of action potentials that lasted until the experiment was terminated. The result in Figure 1C occurred shortly after the change in pH_i . Similar recordings were obtained at later times in these experiments by clamping the membrane potential at the equilibrium point and then slowly releasing the clamp. The membrane potential remained at the equilibrium point for a few seconds and then began to oscillate spontaneously. The oscillations increased in amplitude until an unending train of action potentials occurred, similar to the result in Figure 1C. Results

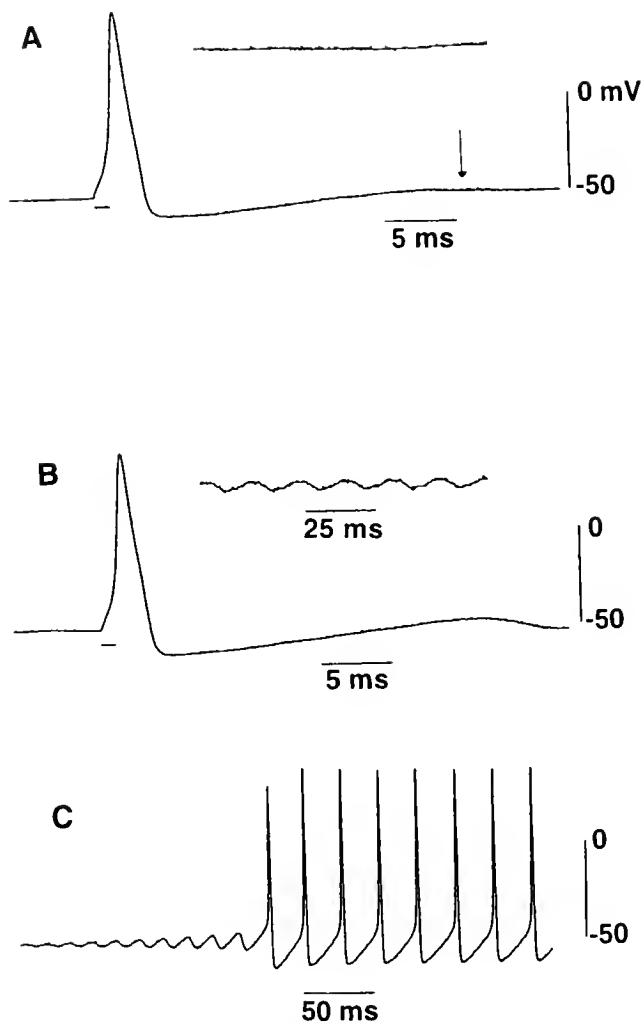


Figure 1. (A) Action potential from a squid giant axon in control conditions ($\text{pH}_i = 7.3$) elicited by a 1-ms, suprathreshold current pulse. The arrow indicates a slight oscillatory rebound after the action potential. The inset illustrates a 100-ms epoch during rest (voltage scale $4\times$). (B) Action potential 2 min after changing to an intracellular buffer with $\text{pH} = 8.5$. The oscillatory rebound was considerably larger, and the membrane potential oscillated about the resting level (inset; voltage scale $4\times$). (C) Initiation of spontaneous firing of action potentials, about 3 min after the change to $\text{pH}_i = 8.5$. The spontaneous activity in this preparation lasted 4 h, at which point the experiment was terminated.

such as those in Figure 1 were observed in 20 out of 24 axons in which the effect was investigated. The frequency of firing at $T = 5^\circ\text{C}$, the temperature at which several of the experiments were performed, was 32.9 ± 6.1 Hz ($n = 8; \pm\text{SD}$).

The pH_i effect was reversible, as illustrated in Figure 2. In this experiment, pH_i was initially 8.3. The axon fired spontaneously (Fig. 2A). The intracellular perfusate was then switched to one having a pH of 7.7 (Fig. 2B). No clear effect on the electrical activity was observed 15 min after the solution change. When the intracellular buffer was changed to one having $\text{pH} = 7.4$, the activity ceased,

although small-amplitude subthreshold oscillations were still observed (Fig. 2C). Spontaneous activity was reestablished when the initial perfusate ($\text{pH}_i = 8.3$) was used (Fig. 2D). These results are consistent with a threshold (all-or-none phenomenon) for autonomous activity with pH_i . The threshold was in the 7.6 to 7.8 range, as indicated by four experiments in which pH_i was changed in 0.2 increments from $\text{pH}_i = 7.2$ to 8.4.

In three experiments on an unrelated topic, spontaneous firing was observed upon initiation of intracellular perfusion with a buffer consisting of 400 mM sucrose, 250 mM KF,

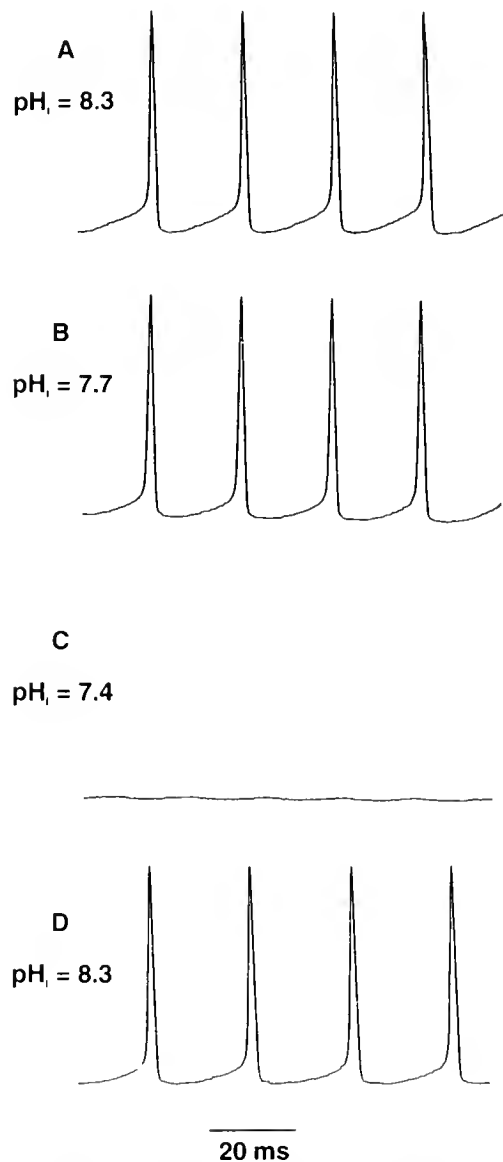


Figure 2. Autonomous activity with $\text{pH}_i = 8.3$ (A) and $\text{pH}_i = 7.7$ (B). No clear effect was apparent with this change in pH . Spontaneous activity ceased with $\text{pH}_i = 7.4$ (C), although subthreshold oscillations were apparent. (D) Spontaneous activity was re-established with $\text{pH}_i = 8.3$. Different preparation than in Figure 1.

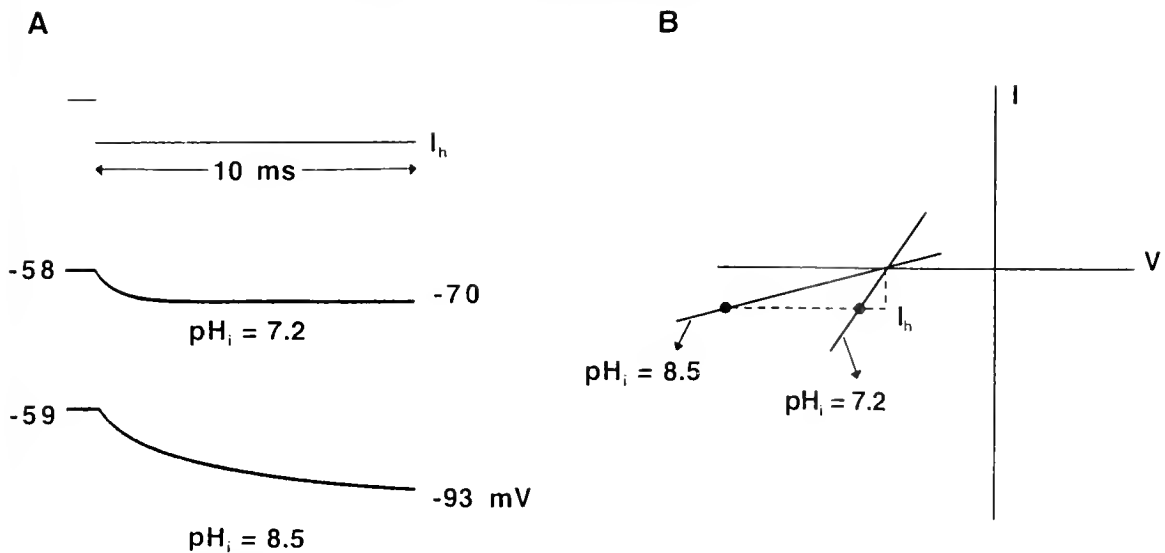


Figure 3. Effect of pH_i on background ("leak") conductance. (A) Membrane potential responses to a $30 \mu\text{A} \cdot \text{cm}^{-2}$ hyperpolarizing current pulse with pH_i = 7.2 and 8.5, as described in the text. (B) Schematic description of the change in the current-voltage relation of the axon which is proposed to explain the results in panel A.

and 25 mM K₂HPO₄ (pH_i = 7.6–7.8). These results demonstrate that the effect was not a function of the buffering system. We primarily used K glutamate which, as Wanke *et al.* (1980a) noted, is appropriate at a concentration of 45 mM for pH in the 9 to 10.8 range. We found that a solution containing 300 mM K glutamate could be stably titrated (with free glutamic acid) down to pH 7.2, which allowed us to cover the pH range of interest (7.2 to 8.5) with a single buffer system containing an anion—glutamate—which is known to be "favorable" for squid giant axons (Adams and Oxford, 1983; Clay, 1988).

The most logical place, *a priori*, to look for the ionic mechanism underlying the pH_i effect would seem to be the classical sodium and potassium ion currents, I_{Na} and I_{K} , respectively, that underlie the action potential (Hodgkin and Huxley, 1952). We looked for an effect of a change in pH_i on I_{Na} in voltage-clamp recordings with pH_i in the 7 to 9 range, but we did not observe any clear effect. An irreversible reduction of I_{Na} inactivation does occur for a pH_i greater than 9.5 (Brodwick and Eaton, 1978), which is outside the range of pH_i we have used. Moreover, blockade of I_{Na} in squid axons by intracellular protons has been observed having pK_a values of 4.6 and 5.8 (Wanke *et al.*, 1980b)—an effect of pH_i which, again, lies outside the range we have used. We are not aware of any report in the literature of an effect of a change in pH_i in the 7 to 9 range on I_{Na} . No such effect was observed in this study.

An increase of pH_i in the 7 to 9 range increases the amplitude of I_{K} at any given depolarization from a holding level of -50 mV (Wanke *et al.*, 1980a), although a similar effect does not occur with relatively negative holding potentials (-80 or -90 mV; Clay, 1990). This holding poten-

tial dependence is consistent with a rightward shift of the I_{K} inactivation curve along the voltage axis as pH_i is increased in the 6 to 10 range (Clay, 1990). The effect—essentially an increase in the number of K⁺ channels available for activation during the action potential—cannot account for pH_i-induced automaticity (simulations not shown).

A clue to the ionic mechanism for pH_i-induced automaticity was provided by input resistance measurements in axons made quiescent with tetrodotoxin (TTX; 1 μM—Fig. 3). The preparation illustrated in Figure 3A rested at -58 mV in TTX with pH_i = 7.2. A hyperpolarizing current pulse 10 ms in duration produced a hyperpolarizing response having a time constant, τ , of 0.7 ms. In an equivalent circuit model of the membrane, this result is equal to the product of the membrane resistance and the membrane capacitance. The specific membrane capacitance is $1 \mu\text{F} \cdot \text{cm}^{-2}$. Consequently, the specific membrane resistivity with $\tau = 0.7$ ms is $0.7 \text{ k}\Omega \cdot \text{cm}^{-2}$, a value that is consistent with the classical small-impedance measurements in figure 23 of Hodgkin and Huxley (1952). The corresponding result for pH_i = 8.5 is shown in the bottom panel of Figure 3A. The change of pH_i from 7.2 to 8.5 produced a slight hyperpolarization of rest potential by about 1 mV. The response to a current pulse of the same amplitude as in pH_i = 7.2 produced a marked increase in membrane hyperpolarization with a much slower response time. Indeed, the response was not yet at the steady-state level at the end of the 10-ms pulse. Similar observations were made in four different preparations. This result is consistent with a reduction of net inward current, as illustrated schematically in Figure 3B. A hyperpolarizing current pulse having an amplitude of I_{h} intersects the current-voltage relation at a much more negative potential with

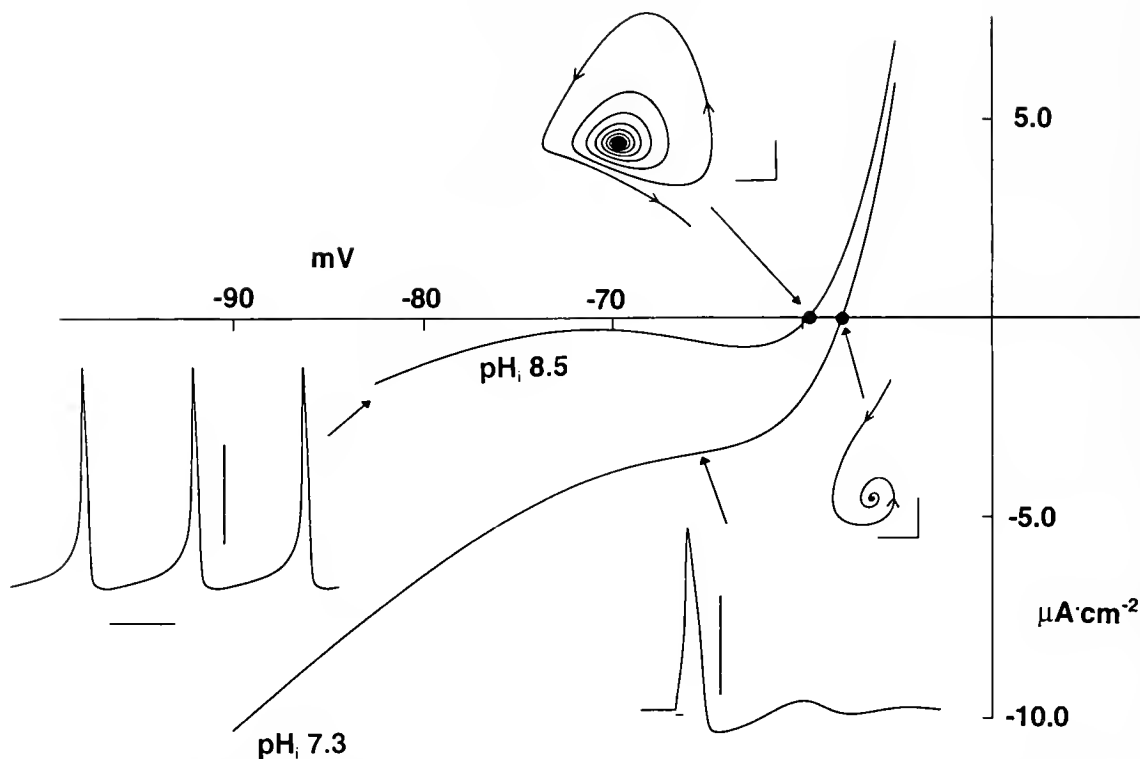


Figure 4. Simulations of pH_i -induced excitability. Steady-state current-voltage relations are shown for $\text{pH}_i = 7.3$ and $\text{pH}_i = 8.5$. The sole difference in the model for the two conditions is in the leak current conductance, which is 0.2 and $0.03 \text{ mS} \cdot \text{cm}^{-2}$ for $\text{pH}_i = 7.3$ and 8.5 , respectively. The equilibrium potential, that is, the point where the current-voltage relation crosses the voltage axis, is stable for $\text{pH}_i = 7.3$, as indicated by the trajectory in the inset adjacent to this point. (The scales are 5 mV and $2 \mu\text{A} \cdot \text{cm}^{-2}$.) An action potential elicited by a suprathreshold current pulse for this condition is shown below the current-voltage relation. (The scales are 50 mV and 1 ms .) The equilibrium point for $\text{pH}_i = 8.5$ is unstable, as illustrated by the adjacent trajectory. (Same scales as the current-voltage trajectory for $\text{pH}_i = 7.3$.) This trajectory spiraled out to the limit cycle described by the spontaneous action potentials shown adjacent to the current-voltage relation. Scales are 50 mV and 20 ms .

$\text{pH}_i = 8.5$ as compared to $\text{pH}_i = 7.2$ (symbols (●) in Fig. 3B). This result suggests that a change of pH_i might affect the third component of the Hodgkin and Huxley (1952) model of the action potential, namely the background, or "leak" current, I_L . In particular, the resistance measurements in Figure 3 imply that the leak component is reduced by an increase in pH_i . This idea has precedence in the work of Bevan and Yeats (1991), who reported the activation of a sustained, nonspecific cation conductance in a subpopulation of rat dorsal root ganglion neurons by extracellular protons. Alkaline pH would reduce the amplitude of this conductance.

The background current in squid giant axons also consists of a small-amplitude tetrodotoxin-sensitive sodium ion current (referred to as I_{NaP}) that is activated at relatively negative potentials, about -80 mV , and has a peak amplitude at -60 mV (Rakowski *et al.*, 1985). This component has a current-voltage relation with a negative slope character at subthreshold potentials, whereas I_L —a net inward current component at subthreshold potentials—has an ap-

proximately linear current-voltage relation. We are proposing that the reduction of I_L with increasing pH_i allows the negative slope character of I_{NaP} to destabilize the equilibrium point (rest potential) of the axon at -60 mV , thereby resulting in autonomous activity. We cannot exclude a pH_i dependence of I_{NaP} . However, the pH_i -induced change in resistance illustrated in Figure 3 is not attributable to changes in I_{NaP} , since those experiments were carried out in the presence of TTX, and as shown below, this resistance change is sufficient to explain the pH_i -induced automaticity.

The mechanism we propose for the result in Figure 3 is illustrated by the simulations and current-voltage relations in Figure 4. These results are based on the equations provided in the Materials and Methods. The steady-state current-voltage relation of the model for control conditions ($\text{pH}_i = 7.3$) for $-90 < V < -55 \text{ mV}$ is shown in Figure 3, along with an action potential (AP) elicited by a brief, suprathreshold current pulse. Only a single AP was elicited in the model even by relatively long-duration current pulses—regardless of pulse amplitude—as in the earlier analysis

(Clay, 1998). The stability of the model for pH_i 7.3 is illustrated by the current-voltage trajectory in the inset of Figure 3 immediately below the pH_i 7.3 equilibrium point. In this simulation the membrane potential was abruptly shifted a few millivolts away from equilibrium conditions. The current-voltage trajectory subsequently spiraled toward the resting potential (stable focus). The effect of changing pH_i to 8.5 is also shown in Figure 3. The *sole* change in the model was a reduction of the leak current conductance, g_L , from 0.2 to 0.03 $\text{mS} \cdot \text{cm}^{-2}$. This change resulted in a hyperpolarization of the equilibrium point from -57.6 to -59.3 mV and a change in its stability properties from a stable to an unstable focus (inset above the voltage axis in Fig. 3). This trajectory spiraled toward a stable limit cycle, that is, autonomous firing, as illustrated by the inset to the left of the current-voltage trajectory, with a frequency of firing of 29.8 Hz.

Discussion

Excitability of the squid giant axon preparation *in vitro* has traditionally been increased by reductions in the extracellular Ca^{2+} concentration (Huxley, 1959; Guttman and Barnhill, 1970). In preliminary experiments, we occasionally observed autonomous activity with $\frac{1}{4}$ normal Ca^{2+} (2.5 mM), but the effect was transient and episodic. In all preparations examined, repetitive firing was not observed either autonomously or with current pulse stimulation 15–20 s after the change to an external medium that was low in Ca^{2+} . Moreover, axons became inexcitable within a few minutes in low Ca^{2+} seawater. This result is not surprising given that low Ca^{2+} external medium is deleterious for neurons (Horn, 1999). The pH_i -induced autonomous activity we report here is reproducible, robust, and long-lasting. In one axon, we observed stable repetitive firing for 4 h (with perfusion both intracellularly and extracellularly to maintain ionic gradients), at which point the experiment was terminated. Consequently, this preparation may be an ideal single-cell neuronal oscillator suitable for investigations concerning mechanisms of rhythmicity.

The ionic model that we propose for the spontaneous activity is novel and counterintuitive, in that the effect is attributable to a *reduction* of inward current, thereby leading to a destabilization of the rest potential by the I_{NaP} component. The result in Figure 2C illustrating subthreshold oscillations that increase in amplitude until the threshold for an action potential is reached is consistent with this aspect of the model. The only stable element both in the preparation and the model is the limit cycle, that is, the trajectory traversed in current-voltage space by the action potential (Winfree, 1980).

Repetitive firing in nerve cells is well known in a number of preparations, such as gastropod neuronal somata (Connor and Stevens, 1971). The rapidly inactivating potassium ion

current, I_A , is believed to play a major role in the activity (Connor and Stevens, 1971). The delayed rectifier, I_K , in squid giant axons also inactivates, as originally shown by Ehrenstein and Gilbert (1966). We think that this kinetic feature does not play a role in our observations because the inactivation kinetics are shifted rightward along the voltage axis by an increase in pH_i (Clay, 1990), and the onset of inactivation at 5°C is too slow to be a factor during the relatively brief times the membrane potential is at depolarized potentials during the action potentials in the pulse train (Clay, 1989). Moreover, g_K inactivation cannot account for the destabilization of the resting potential illustrated in Figure 1C, which we believe is the key feature underlying our results.

To our knowledge, the effect, reported here, of pH_i on excitability in squid axons has not been previously reported. A similar effect with pH_o was noted in passing by Bicher and Ohki (1972) in their work with intracellular pH electrodes. They observed an increase in excitability in the giant axon, including autonomous firing in some preparations, after the pH of the extracellular bathing medium was raised to 9. The change in pH_o caused a few tenths rise in pH_i , which we have shown to be sufficient to induce automaticity. It is tempting to speculate that our observations have physiological relevance, given that they occur within the normal range of pH in the ocean (7.5 to 8.4; Sverdrup *et al.*, 1942), and only slightly above the normal, relatively alkaline, value of 7.3 in the axon (Boron and DeWeer, 1976). Moreover, transient rises in pH in squid blood have been reported in exercising squid (Pörtner *et al.*, 1991), which, based on our work, would favor an increase in neuronal excitability. However, not enough is known about the role of pH_i in squid behavior to make an informed conjecture about the role of the increased excitability *in vivo*, if it indeed occurs.

Acknowledgments

We gratefully acknowledge grant support for this work from the Canadian Institutes for Health Research (A.S.).

Literature Cited

- Adams, D. J., and G. S. Oxford. 1983. Interaction of internal anions with potassium channels of the squid giant axon. *J. Gen. Physiol.* **82**: 429–448.
- Bevan, S., and J. Yeats. 1991. Protons activate a cation conductance in a subpopulation of rat dorsal root ganglion neurons. *J. Physiol. (Lond.)* **433**: 145–161.
- Bicher, H. L., and S. Ohki. 1972. Intracellular pH electrode experiments on the squid giant axon. *Biochim. Biophys. Acta* **255**: 900–904.
- Boron, W. F., and P. DeWeer. 1976. Intracellular pH transients in squid giant axons caused by CO_2 , NH_4 , and metabolic inhibitors. *J. Gen. Physiol.* **67**: 91–112.
- Brodwick, M. S., and D. C. Eaton. 1978. Sodium channel inactivation in squid axon is removed by high internal pH or tyrosine specific reagents. *Science* **200**: 1494–1496.

- Clay, J. R. 1988. Lack of effect of internal fluoride ions on potassium channels in squid giant axons. *Biophys. J.* **53**: 647–648.
- Clay, J. R. 1989. Slow inactivation and reactivation of the K^+ channel in squid axons. A tail current analysis. *Biophys. J.* **55**: 407–414.
- Clay, J. R. 1990. I_K inactivation in squid axons is shifted along the voltage axis by changes in the intracellular pH. *Biophys. J.* **58**: 797–801.
- Clay, J. R. 1998. Excitability of the squid giant axon revisited. *J. Neurophysiol.* **80**: 903–913.
- Clay, J. R., and M. F. Shlesinger. 1983. Effects of external cesium and rubidium on outward potassium currents in squid axons. *Biophys. J.* **42**: 43–53.
- Connor, J. A., and C. F. Stevens. 1971. Prediction of repetitive firing behavior from voltage clamp data on an isolated neuronal somata. *J. Physiol. (Lond.)* **213**: 31–53.
- Ehrenstein, G., and D. L. Gilbert. 1966. Slow changes of potassium permeability in the squid giant axon. *Biophys. J.* **6**: 553–566.
- Guttman, R. S., and R. Barnhill. 1970. Oscillation and repetitive firing in squid axons. *J. Gen. Physiol.* **55**: 104–118.
- Hodgkin, A. L., and A. F. Huxley. 1952. A quantitative description of membrane conductance and its application to conduction and excitation in nerve. *J. Physiol. (Lond.)* **117**: 500–544.
- Horn, R. 1999. The dual role of calcium—Pore blocker and modulator of gating. *Proc. Natl. Acad. Sci. USA* **96**: 3331–3332.
- Huxley, A. F. 1959. Ion movements during nerve activity. *Ann. NY Acad. Sci.* **81**: 221–246.
- Neumeister, H., B. Ripley, T. Preuss, and W. F. Gilly. 2000. Effects of temperature on escape jetting in the squid *Loligo Opalescens*. *J. Exp. Biol.* **203**: 547–557.
- Otis, T. S., and W. F. Gilly. 1990. Jet-propelled escape in the squid *Loligo opalescens*: concerted control by giant and non-giant motor axon pathways. *Proc. Natl. Acad. Sci. USA* **87**: 2911–2915.
- Pörtner, H. O., D. M. Webber, R. G. Boutilier, and R. K. O'Dor. 1991. Acid-base regulation in exercising squid (*Illex illecebrosus*, *Loligo pealei*). *Am. J. Physiol.* **261**: R239–R246.
- Rakowski, R., P. DeWeer, and D. Gadsby. 1985. Threshold channels can account for steady-state TTX-sensitive sodium current of squid axon. *Biophys. J.* **47**: A31.
- Sverdrup, H. U., M. W. Johnson, and R. H. Fleming. 1942. Pp. 194–195 in *The Oceans, Their Physics, Chemistry, and General Biology*. Prentice-Hall, New York.
- Vandenberg, C. A., and F. Bezanilla. 1991. A sodium channel gating model based on single channel, macroscopic ionic, and gating currents in the squid giant axon. *Biophys. J.* **60**: 1511–1533.
- Wanke, E., E. Carbone, and P. L. Testa. 1980a. K^+ conductance modified by a titratable group accessible to protons from the intracellular side of the squid axon membrane. *Biophys. J.* **26**: 319–324.
- Wanke, E., E. Carbone, and P. L. Testa. 1980b. The sodium channel and intracellular H^+ blockage in squid axons. *Nature* **287**: 62–63.
- Winfree, A. T. 1980. *The Geometry of Biological Time*. Springer-Verlag, Berlin.
- Young, J. Z. 1939. Fused neurons and synaptic contacts in the giant nerve fibers of cephalopods. *Philos. Trans. R. Soc. Lond. B* **229**: 465–503.

Molecular Phylogeny of the Model Annelid *Ophryotrocha*

THOMAS G. DAHLGREN^{1,2,*}, BERTIL ÅKESSON², CHRISTOFFER SCHANDER^{2,3},
KENNETH M. HALANYCH¹, AND PER SUNDBERG²

¹*Woods Hole Oceanographic Institution, Biology Department, MS 33, Woods Hole, Massachusetts 02543, USA;* ²*Göteborg University, Department of Zoology, Box 463, 405 90 Göteborg, Sweden; and* ³*University of Copenhagen, Arctic Station, Box 504, DK-3953 Qeqertarsuaq, Greenland*

Abstract. Annelids of the genus *Ophryotrocha* are small opportunistic worms commonly found in polluted and nutrient-rich habitats such as harbors. Within this small group of about 40 described taxa a large variety of reproductive strategies are found, ranging from gonochoristic broadcast spawners to sequential hermaphroditic brooders. Many of the species have a short generation time and are easily maintained as laboratory cultures. Thus they have become a popular system for exploring a variety of biological questions including developmental genetics, ethology, and sexual selection. Despite considerable behavioral, reproductive, and karyological studies, a phylogenetic framework is lacking because most taxa are morphologically similar. In this study we use 16S mitochondrial gene sequence data to infer the phylogeny of *Ophryotrocha* strains commonly used in the laboratory. The resulting mtDNA topologies are generally well resolved and support a genetic split between hermaphroditic and gonochoristic species. Although the ancestral state could not be unambiguously identified, a change in reproductive strategy (*i.e.*, hermaphroditism and gonochorism) occurred once within *Ophryotrocha*. Additionally, we show that sequential hermaphroditism evolved from a simultaneous hermaphroditic ancestor, and that characters previously used in phylogenetic reconstruction (*i.e.*, jaw morphology and shape of egg mass) are homoplastic within the group.

Introduction

Marine annelids belonging to the group *Ophryotrocha* have been used as a laboratory system for much of this century (*e.g.*, Bergh, 1895; Bergmann, 1903; Meek,

1912; Huth, 1933; Hartmann and Lewinski, 1940; Bacci and La Greca, 1953; Bacci, 1965; Åkesson, 1972; Sella, 1988; Vitturi *et al.*, 2000), not least because they are easy to maintain in cultures and have short generation times. *Ophryotrocha* has traditionally been treated as a genus within the eunicimorph family Dorvilleidae (*e.g.*, Fauchald, 1977; Eibye-Jacobson and Kristensen, 1994), but inclusion within the Dorvilleidae has been challenged (Orensanz, 1990). Many ecological (*e.g.*, Åkesson, 1977; Berglund, 1991; Cassai and Prevedelli, 1999), ethological (*e.g.*, Sella, 1991), developmental (*e.g.*, Åkesson, 1967, 1973; Zavarzina and Tzetlin, 1991), and toxicological (*e.g.*, Åkesson, 1970, 1975) studies have been conducted on these worms. Charnov (1982) and Gambi *et al.* (1997) among others, argue that *Ophryotrocha* is a near ideal group for studies of the evolution of sex strategies, since all known forms (gonochorism, sequential and simultaneous hermaphroditism) are represented within a few closely related species.

Since *Ophryotrocha* was first described (Claparède and Mecznikow, 1869), more than 40 species have been added to the group, most of which are reported from shallow, nutrient-rich waters such as harbors (*e.g.*, La Greca and Bacci, 1962; Åkesson, 1976; Paavo *et al.*, 2000). Recent contributions have also shown a considerable diversity in the deep sea (Jumars, 1974; Blake, 1985; Hilbig and Blake, 1991; Lu and Fauchald, 2000). To the best of our knowledge, the Appendix lists all the described species of *Ophryotrocha* with their type locality. Only species from shallow, temperate or tropical waters, however, have been successfully cultured in the laboratory (at present ~20 distinct forms). Among the cultured forms, some of which are yet to be formally described,

Received 15 December 2000; accepted 11 June 2001.

* To whom correspondence should be addressed. E-mail: tdahlgren@whoi.edu

most taxa are morphologically identical; but each is believed to be a distinct species because species crosses failed to produce viable offspring in breeding experiments (Åkesson, 1978, 1984, and unpubl.).

Even though the taxonomical and descriptive morphological literature is extensive (e.g., La Greca and Bacci, 1962; Pfannenstiel, 1972, 1975; Josefsson, 1975; Åkesson, 1978; Oug, 1978, 1990; Blake, 1985; Ockelmann and Åkesson, 1990; Hilbig and Blake, 1991; Lu and Fauchald, 2000; Paavo *et al.*, 2000), there has been but a single study (Pleijel and Eide, 1996) focusing on the phylogenetic history of a broader selection of *Ophryotrocha* species. That study, based on an analysis of 25 morphological characters and 7 electrophoretic protein loci scored for 20 *Ophryotrocha* taxa, described two major clades and suggested that simultaneous hermaphroditism is the plesiomorphic condition for the group as a whole. Basal branching in Pleijel and Eide's tree (1996, Fig. 1B), however, was poorly supported, as depicted by their highly collapsed strict consensus tree. One of the clades found by Pleijel and Eide (1996) is congruent with the gonochoristic *labronica* group previously suggested by Åkesson (1984). On the basis of morphological features, such as similarities in jaw apparatuses and egg-mass morphology, Åkesson (1984) and Ockelmann and Åkesson (1990) also recognized the hermaphroditic "gracilis" and "hartmanni" groups. These taxa form a grade at the base of the most parsimonious tree favored by Pleijel and Eide (1996, Fig. 1A), and they consequently suggested that their similarities are sympleisiomorphic.

Chromosome number and karyological characters were used in an analysis of nine species by Robotti and collaborators (1991). The resulting topology suggested that forms with equal number of chromosomes constitute monophyletic groups. The data also indicated that the distance between *O. robusta* and *O. hartmanni* ($2n = 10$) is larger than the distances between members of the two other groups ($2n = 6$ and $2n = 8$). Further, on the basis of work by Colombera and Lazzaretto-Colombera (1978) suggesting that karyotypes evolved towards reduced chromosome numbers, Robotti *et al.* (1991) proposed that *O. robusta* occupies an ancestral position. The same conclusion was reached by Vitturi and collaborators (2000) in a study of karyotypes of 10 *Ophryotrocha* species.

The evolutionary relationships among 18 *Ophryotrocha* forms were investigated using the mitochondrial 16S rDNA gene. Due to organismal availability, we have focused on intertidal forms that are easily kept in laboratory cultures (Åkesson, 1970, 1975). The present paper builds on the work of Pleijel and Eide (1996) to reconstruct the phylogeny of this model annelid system so that knowledge gained about *Ophryotrocha* may be assessed in a comparative context.

Materials and Methods

Taxa

Eighteen *Ophryotrocha* cultures representing intertidal and shallow-water forms were selected for this study (Table 1). All of these terminal taxa were readily available because they are maintained as laboratory cultures by B.Å. and represent the best-studied members of *Ophryotrocha*. Nine of the eighteen strains included are not formally described as species. Six are referred to by the name under which they will be described, followed by "nom. nud." to indicate their present status as *nomina nuda*, i.e., names not available. The remaining three strains are referred to by the location where they were originally collected. The informally named taxa are not to be regarded as descriptions *sensu* International Code of Zoological Nomenclature (International Commission on Zoological Nomenclature, 1985).

Outgroup terminals were chosen on the basis of recent analyses of eunicimorph and annelid phylogeny (Paxton, 1986; Orensanz, 1990; Eibye-Jacobson and Kristensen, 1994; Rouse and Fauchald, 1997). These taxa include *Hyalinoecia tubicola* (Müller, 1776), *Nothria conchylega* (Sars, 1835), *Eunice pennata* (Müller, 1776), *Dorvillea albomaculata* Åkesson and Rice, 1992, and *Dinophilus gyrociliatus* Schmidt, 1857. Specimens of *H. tubicola*, *N. conchylega*, and *E. pennata* were collected by epibentic dredge, while *Dorvillea albomaculata* and *Dinophilus gyrociliatus* were acquired from laboratory cultures (B.Å.). Locality details are provided in Table 1.

Data collection

The worms were taken from cultures and placed in 70% ethanol. Voucher specimens from the same cultures were fixed in 5% formaldehyde for 1 h and subsequently transferred to 70% ethanol. The voucher specimens are deposited in the Zoological Museum, Copenhagen (ZMUC) and designated the numbers given in Table 1. DNA was extracted by either employing a Chelex protocol (Sundberg and Andersson, 1995) or a standard chloroform/phenol protocol (Doyle and Dickson, 1987). An approximately 400-bp fragment of the mitochondrial large subunit ribosomal RNA gene was amplified with the universal primers 16Sar-L (5'-egcctgtttataaaaacat-3') and 16Sbr-H (5'-ccggtctgaactcagatacgt-3') according to standard protocols (Palumbi, 1996). The amplification profile was 40 cycles of 95 °C for 30 s, 50 °C for 30 s, 72 °C for 45 s with an initial single denaturing step at 95 °C for 2 min, and a final single extension step at 72 °C for 7 min. After spin-column purification (QiaGen, Inc.), the PCR products were sequenced in both directions on a PharmaciaBiotech ALF-Express automated sequencer using the ThermoSequenase kit (AmershamPharmacia) and Cy-5 labeled 16Sar-L and 16Sbr-H

Table 1

Collection data and GenBank accession numbers for *Ophryotrocha* taxa examined

Taxon	Collection site	Coll. year	GenBank Accession Nr	ZMUK Voucher Nr
<i>Dorvillea albomaculata</i> * Åkesson and Rice, 1992	Tarifa, Spain	1990	AF380115	N/A
<i>Dinophilus gyrocoliliatus</i> * Schmidt, 1857	Xiamen, China	1995	AF380116	N/A
<i>Hyalinoecia tubicola</i> (Müller, 1776)	Koster area, Sweden	1997	AF321416	N/A
<i>Nothria conchylega</i> (Sars, 1835)	Koster area, Sweden	1997	AF321417	N/A
<i>Eunice pennata</i> (Müller, 1776)	Koster area, Sweden	1997	AF321418	N/A
<i>O. adherens</i> Paavo <i>et al.</i> , 2000	Kyrenia, Cyprus	1971	AF321419	ZMUC-POL-1110
<i>O. alborana</i> nom. nud.	Algeciras, Spain	1978	AF321420	ZMUC-POL-1111
<i>O. costlowi</i> Åkesson, 1978	Duke, NC, USA	1974	AF321421	ZMUC-POL-1112
<i>O. diadema</i> Åkesson, 1976	L.A. harbor, USA	1972	AF321422	ZMUC-POL-1113
<i>O. gracilis</i> Huth, 1934	Helgoland, Germany	1988	AF321423	ZMUC-POL-1114
<i>O. hartmanni</i> Huth, 1933	Malaga, Spain	1990	AF321424	ZMUC-POL-1115
<i>O. japonica</i> nom. nud.	L.A. harbor, USA	1989	AF321433	ZMUC-POL-1116
<i>O. labronica</i> La Greca and Bacci, 1962	Naples, Italy	1965	AF321425	ZMUC-POL-1117
<i>O. macrovifera</i> nom. nud.	Cyprus	1972	AF321426	ZMUC-POL-1118
<i>O. notoglandulata</i> Pfannenstiel, 1972	Misaki, Japan	1961	AF321427	ZMUC-POL-1119
<i>O. obscura</i> nom. nud.	Pet store, Sweden	1978	AF321436	ZMUC-POL-1120
<i>O. permanni</i> nom. nud.	Indian River, Florida	1991	AF321428	ZMUC-POL-1121
<i>O. puerilis</i> Claparède and Mecznikow, 1869	Malaga, Spain	1990	AF321429	ZMUC-POL-1122
<i>O. robusta</i> nom. nud.	Malaga, Spain	1990	AF321430	ZMUC-POL-1123
<i>O. socialis</i> Ockelmann and Åkesson, 1990	Helsingør, Denmark	1986	AF321431	ZMUC-POL-1124
Eilat-Hurghada	Red Sea	1996	AF321432	ZMUC-POL-1125
Qingdao	Qingdao, China	1995	AF321434	ZMUC-POL-1126
Sanya sp. 2	South Hainan, China	1995	AF321435	ZMUC-POL-1127

* Sequenced by Arne Nygren

primers in accordance with the manufacturer's protocols. GenBank accession numbers are given in Table 1.

Analysis

The sequences were aligned with Clustal X (Thompson *et al.*, 1994) and proofread by eye. Regions that could not be unambiguously aligned were excluded from the analysis. The alignment is deposited at TreeBase and available at <http://phylogeny.harvard.edu/treebase> or from TD. Neighbor-joining (NJ), parsimony, and maximum-likelihood (ML) analyses were conducted with the PAUP*4.0b2 software package (Swofford, 2000). PAUP* was further used for parameter estimations for the ML searches. For NJ, a Kishino-Hasegawa (1989) likelihood test found no significant differences between trees generated under the Jukes-Cantor, Kimura-2-parameter, Tamura-Nei, and general-time-reversible (GTR) models (see Swofford *et al.*, 1996, for a brief description of models). Parsimony trees were inferred from an unweighted character matrix (*i.e.*, the transition/transversion ratio was assumed to be 1 with the heuristic search option using the tree-bisection-reconnection (TBR) branch-swapping algorithm and 100 random-sequence addition replicates. To reduce the computation time of the ML search, the most parsimonious tree was used as

starting tree in the ML heuristic search. The model parameters were estimated from a likelihood analysis of the most parsimonious tree and included a nucleotide model with six substitution types (a GTR model), and among-sites rate heterogeneity used a gamma distribution with shape parameter of 0.30. A GTR model was chosen since it is the most general of the ones mentioned above, all of which are special cases of a GTR (Swofford *et al.*, 1996). Nucleotide frequencies were set to empirical values. Bootstrap analyses for both ML and parsimony employed 1000 iterations.

The four characters—(1) sex strategy, (2) jaw morphology, (3) egg-mass morphology, and (4) diploid number of chromosomes—were chosen in part on the basis of previous efforts to estimate *Ophryotrocha* relationships (*e.g.*, Åkesson, 1984; Robotti *et al.*, 1991; Pleijel and Eide, 1996; Vitturi *et al.*, 2000). MacClade 3.06 (Maddison and Maddison, 1992) was used to manipulate the molecular data, and to map sex strategy and morphological and karyological character state changes on the mtDNA topology. Character states were scored following Pleijel and Eide (1996) except for strains from Eilat-Hurghada, Sanya sp. 2, and Qingdao, which were obtained from the same cultures as the specimens sampled for sequencing. The diploid number of chromosomes is not known for these three forms.

Table 2

Pairwise molecular distances (absolute number of unambiguously aligned substitutions above diagonal and Jukes-Cantor distances below); *Sanya* sp. 2 and *O. obscura* nom. nud. are distinguished in three positions located in the excluded regions of the alignment

	1	2	3	4	5	6	7	8	9	10	11	12	13	14	15	16	17	18	19	20	21	22	23
1 <i>Dorvillea albomaculata</i>		73	60	69	75	69	75	77	75	74	74	81	74	75	79	79	69	65	72	74	83	79	79
2 <i>Dinophilus gyrociliatus</i>	0.32		68	65	79	77	89	79	91	88	80	88	76	83	81	75	77	67	77	80	90	82	82
3 <i>Eumme pennata</i>	0.25	0.30		36	46	73	79	88	70	79	72	92	84	80	93	75	70	72	82	75	94	86	86
4 <i>Hyalinoecia tubicola</i>	0.30	0.28	0.14		40	75	78	84	70	74	78	89	83	76	87	77	74	72	80	76	88	81	81
5 <i>Notria conchylega</i>	0.33	0.35	0.19	0.16		80	77	82	73	83	78	86	81	79	84	84	78	75	76	78	88	81	81
6 <i>O. adherens</i>	0.30	0.35	0.33	0.34	0.37		67	68	63	41	41	70	63	69	66	57	60	23	62	71	65	67	67
7 <i>O. alborana</i> nom. nud.	0.33	0.42	0.36	0.35	0.35	0.29		73	44	77	71	72	67	71	73	70	67	66	69	72	61	73	73
8 <i>O. costlowi</i>	0.34	0.35	0.42	0.39	0.37	0.30	0.32		66	75	80	21	25	29	16	67	48	65	33	29	71	19	19
9 <i>O. diadema</i>	0.33	0.43	0.31	0.31	0.32	0.27	0.18	0.29		62	62	71	69	58	69	58	59	65	69	57	51	67	67
10 <i>O. gracilis</i>	0.33	0.41	0.36	0.33	0.38	0.16	0.35	0.33	0.26		37	76	75	77	60	67	42	76	76	72	77	77	77
11 <i>O. hartmanni</i>	0.33	0.36	0.32	0.35	0.35	0.16	0.31	0.36	0.26	0.15		78	70	77	78	61	68	42	74	76	73	76	76
12 <i>O. labronica</i>	0.37	0.41	0.44	0.42	0.40	0.31	0.32	0.08	0.31	0.34	0.35		25	31	15	68	50	67	31	32	77	11	11
13 <i>O. macrovifera</i> nom. nud.	0.33	0.34	0.39	0.38	0.37	0.27	0.29	0.10	0.30	0.34	0.31	0.10		32	27	67	52	59	24	32	75	27	27
14 <i>O. notoglandulata</i>	0.33	0.38	0.37	0.34	0.36	0.30	0.31	0.11	0.24	0.33	0.35	0.12	0.12		28	66	44	66	34	8	69	28	28
15 <i>O. permanni</i> nom. nud.	0.36	0.37	0.45	0.4	0.39	0.29	0.32	0.06	0.30	0.35	0.35	0.06	0.10	0.11		71	47	66	29	31	70	13	13
16 <i>O. puerilis</i>	0.36	0.33	0.34	0.35	0.39	0.24	0.31	0.29	0.24	0.25	0.26	0.30	0.29	0.29	0.31		62	54	68	66	73	66	66
17 <i>O. robusta</i> nom. nud.	0.30	0.34	0.31	0.33	0.35	0.25	0.29	0.2	0.25	0.29	0.30	0.20	0.21	0.18	0.19	0.26		59	51	43	65	50	50
18 <i>O. socialis</i>	0.28	0.29	0.32	0.32	0.34	0.09	0.29	0.28	0.28	0.17	0.17	0.29	0.25	0.29	0.29	0.22	0.25		62	67	66	67	67
19 <i>Eilat-Hurghada</i>	0.32	0.34	0.38	0.36	0.34	0.26	0.30	0.13	0.30	0.34	0.33	0.12	0.09	0.13	0.11	0.30	0.21	0.26		32	71	32	32
20 <i>O. japonica</i> nom. nud.	0.33	0.36	0.34	0.34	0.35	0.31	0.32	0.11	0.24	0.34	0.34	0.12	0.12	0.03	0.12	0.29	0.17	0.29	0.12		74	29	29
21 Qingdao	0.38	0.42	0.46	0.41	0.41	0.28	0.26	0.31	0.21	0.32	0.32	0.35	0.33	0.30	0.31	0.32	0.28	0.29	0.31	0.33		77	77
22 <i>Sanya</i> sp. 2	0.36	0.37	0.40	0.37	0.37	0.29	0.32	0.07	0.29	0.35	0.34	0.04	0.10	0.11	0.05	0.29	0.20	0.29	0.12	0.11	0.35		0
23 <i>O. obscura</i> nom. nud.	0.36	0.37	0.40	0.37	0.37	0.29	0.32	0.07	0.29	0.35	0.34	0.04	0.10	0.11	0.05	0.29	0.20	0.29	0.12	0.11	0.35	0.00	

Results

The data set consisted of 23 terminal taxa and 485 nucleotide positions. Of the 282 nucleotide positions that could be unambiguously aligned, 55.0% (155 positions) were variable and 45.7% (129 positions) were parsimony informative. Table 2 shows the Jukes-Cantor distances (below diagonal) and absolute distances (above diagonal) for the alignment. Figure 1A shows the highest scoring likelihood tree recovered (Ln likelihood = -2741.47651). More terminal branches were generally well resolved, but support for basal nodes was low (see bootstrap tree, Fig. 1B).

In the ML tree, two large clades emerge. The first, for brevity here called A, is further divided into two clades, A1 and A2. Clade A1 consists of *O. hartmanni*, *O. gracilis*, *O. adherens*, *O. socialis*, and *O. puerilis*; A2 comprises *O. alborana*, *O. diadema*, and "Qingdao." The second major clade, here called B, includes *O. japonica* nom. nud., *O. notoglandulata*, *O. costlowi*, *O. labronica*, *Sanya* sp. 2, *O. obscura* nom. nud., *O. permanni*, *O. macrovifera* nom. nud., *Eilat-Hurghada*, and *O. robusta*. The parsimony and NJ trees (Fig. 2A) differ from the ML tree in the placement of the root. Instead of a monophyletic A group, as in the ML tree, A constitutes a grade where the two clades A1' (excluding *O. puerilis*) and A2, together with *O. puerilis*, lead to B (Fig. 2A). The general topologies are, however, similar in the parsimony, NJ, and ML trees, and most of the nodes are supported over the 50% bootstrap level (Fig. 1B).

In an attempt to assess support for basal nodes, an additional analysis was performed on an alignment of ingroup taxa only (aligning and ML procedures as described above). Inclusion of more distant taxa in an alignment may reduce the nucleotide positions that can be unambiguously aligned, and a more restricted selection of taxa could potentially increase phylogenetic signal by allowing for a "better" alignment (Halanych *et al.*, 1998). The analysis, of the 18 *Ophryotrocha* ingroup taxa only, did reveal higher bootstrap support for internal branches of the tree. This restricted analysis, however, gave lower support or alternative hypotheses for some of the more recent clades. More recent clades in B are less well resolved than in the original analyses, but *O. japonica* nom. nud. and *O. notoglandulata* form a strongly supported monophyletic group (Fig. 2B).

Figure 3 shows an arbitrarily chosen most parsimonious reconstruction (transformation optimization by ACCTRAN) for each of the four characters mapped on the ML tree (Fig. 1A). Evidence of transformation polarity is given from outgroup analysis of mtDNA data, and traced characters are accordingly not scored for outgroup taxa.

Discussion

Ophryotrocha phylogeny was investigated by employing ML, NJ, and parsimony analyses of 16S rDNA data. One alignment of these data included the ingroup and five outgroup taxa and resulted in poor support for basal branching patterns (Fig. 1B). The second data set was limited to the 18 *Ophryotrocha* terminals (*i.e.*, the ingroup) and produced better supported and nearly identical topologies under ML

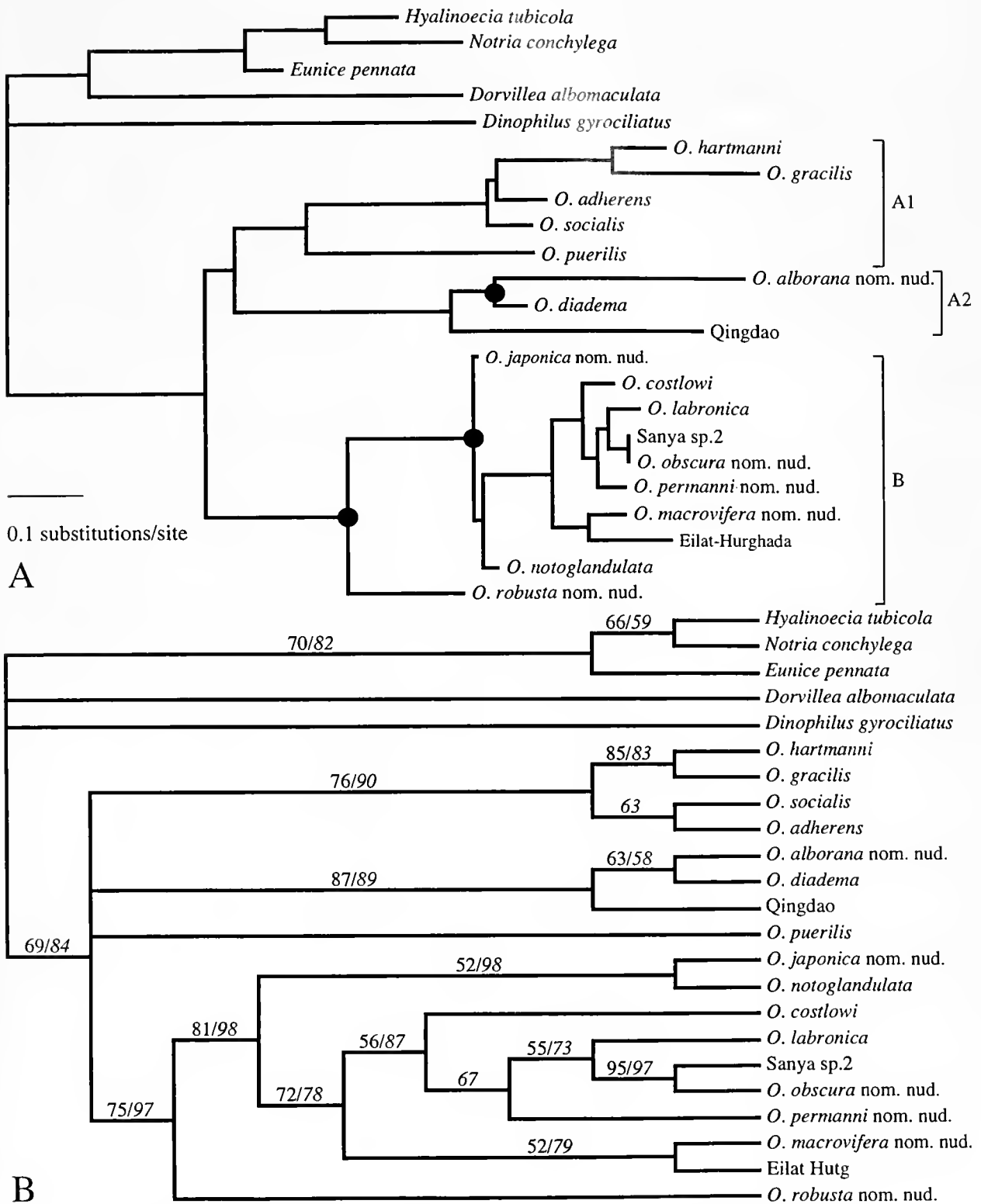


Figure 1. (A) Best maximum likelihood tree. $-\ln = 2741.47651$. Highlighted nodes indicate clades congruent with morphological analysis by Pleijel and Eide (1996). (B) 1000 bootstrap consensus. Numbers in upright type are maximum likelihood and in italic are parsimony support values.

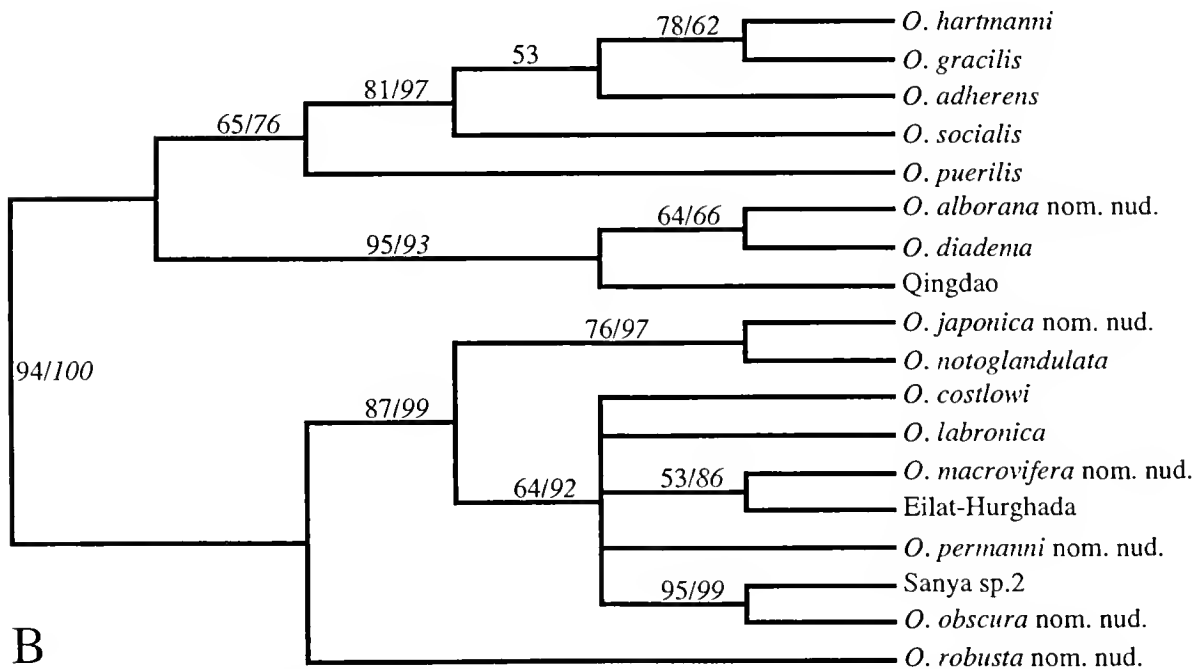
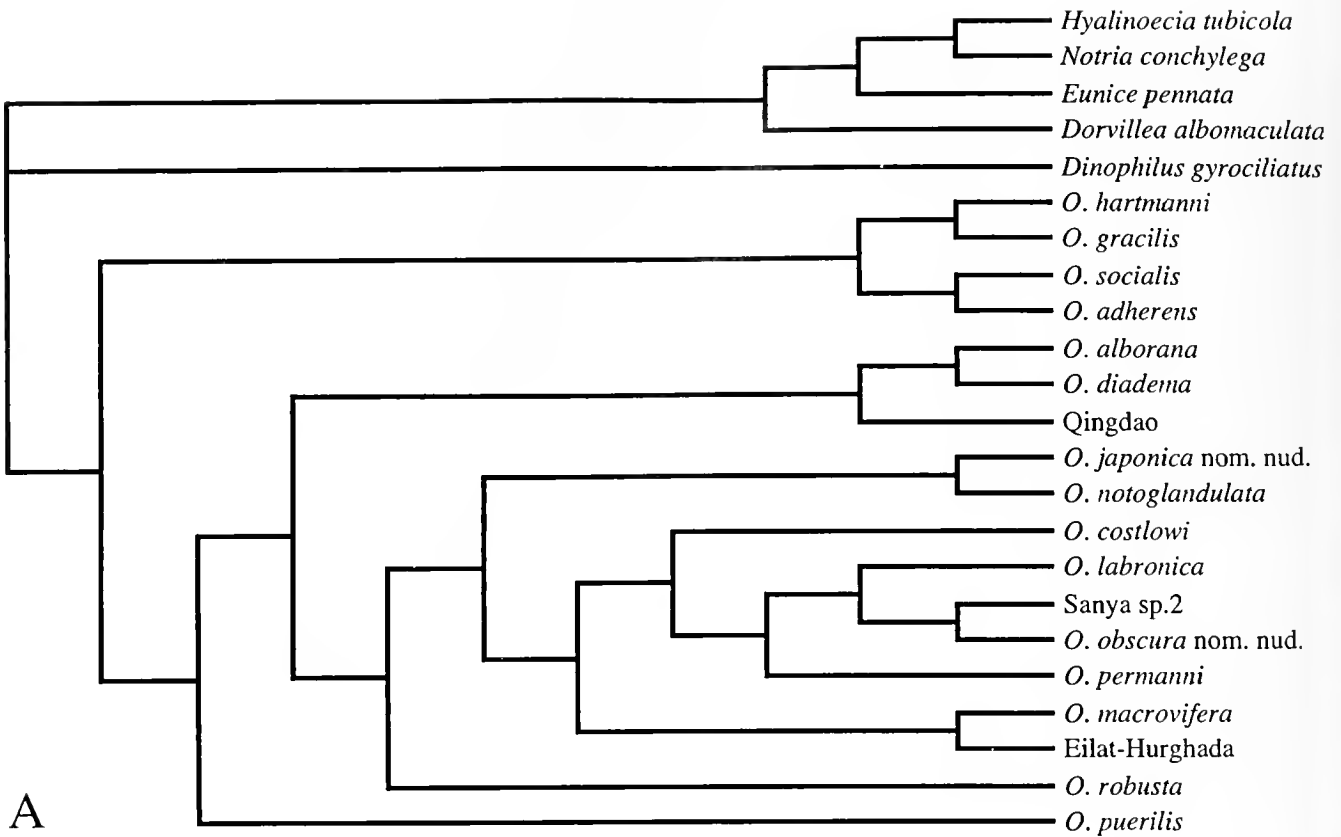


Figure 2. (A) Parsimony and neighbor-joining tree topology. (B) Unrooted bootstrap tree from alignment of ingroup taxa only and drawn to represent the rooting suggested in the original maximum likelihood analysis. Bootstrap values for maximum likelihood in upright type and for parsimony in italic type.

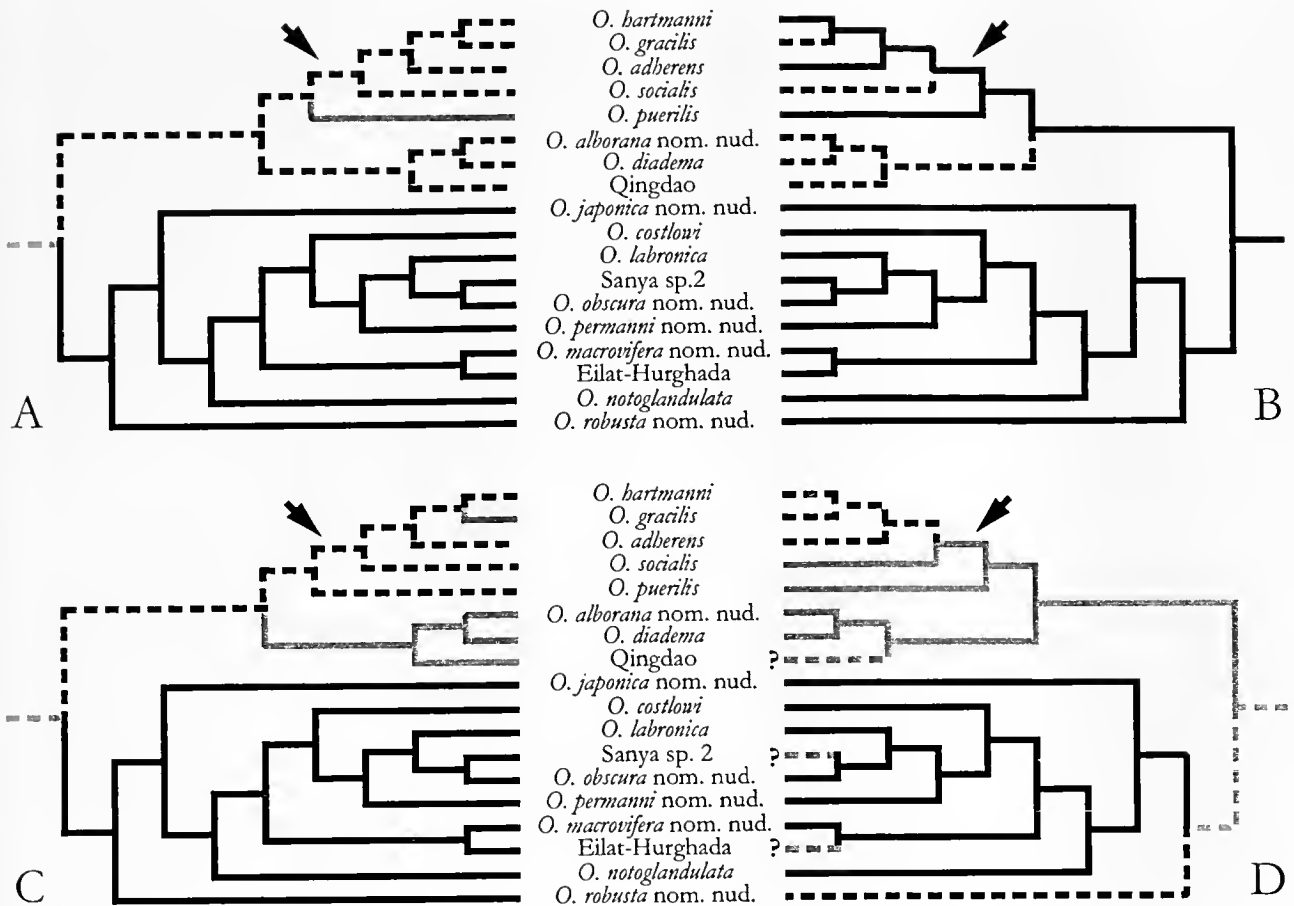


Figure 3. Character transformation hypothesis. Alternative rooting as suggested by parsimony analysis is indicated by an arrow. Dashed gray line depicts equivocal or unknown taxon state. (A) Sex strategy. Full line = gonochorism; dashed line = simultaneous hermaphroditism; gray line = sequential hermaphroditism. (B) Jaws. Full line = P and K-type of jaws; dashed line = presence of P-type only. (C) Shape of egg mass. Full line = tubular; gray line = fusiform; dashed line = irregular. (D) Diploid number of chromosomes. Full line = 6; gray line = 8; dashed line = 10.

and parsimony methods (Fig. 2B). Topologies from the analyses restricted to the ingroup taxa were in overall agreement with the ML and parsimony tree of the first dataset. The problem with alternative hypotheses for placement of the root may be caused by a long branch phenomenon (e.g., Hendy and Penny, 1989) and cannot be conclusively resolved with the data at hand. The parsimony analysis suggests a placement of the root between the (*O. hartmanni*, *O. gracilis*, *O. adherens*, *O. socialis*) clade and the rest of the tree (Fig. 2A), while ML indicates a rooting between the clade of hermaphroditic species and the gonochoristic species clade (Fig. 1A). However, contrary to parsimony, ML methods account for branch-length information and should give a better estimate when the model is accurate (Swofford *et al.*, 1996). Therefore, the discussion below focuses on the ML tree that included 18 ingroup and 5 outgroup taxa.

Figure 1A shows considerable congruence with Pleijel and Eide's (1996) results from an analysis employing mor-

phological, sex strategy, and protein data. Clades supported by both sets of data are indicated with the highlighted nodes in the mtDNA tree (Fig. 1A). However, the topologies differ on the internal branching of *Ophryotrocha* and, possibly, on the placement of the root. The mtDNA ML data gives some support for a deep subdivision in two major clades, but no such subdivision is suggested by Pleijel and Eide (1996). Recent fossil evidence further suggests that *Ophryotrocha* is an old lineage (Eriksson and Lindström, 2000).

The evolution of sex strategies is a debated subject (e.g., Ghiselin, 1969; Charnov, 1982; Maynard Smith, 1982; Hurst, 1992). Our analyses, based on species that are sequential (1) or simultaneous (7) hermaphrodites, and gonochorists (10), suggest that, regardless of the placement of the root, the change from one strategy to the other has taken place only once within the group (Fig. 3A). The ancestral state is, given the available data, ambiguous. The sequential hermaphrodite *O. puerilis* is able to switch sex several times

during life, a feature that is rare among metazoans. Using *O. puerilis* as a model, Premoli and Sella (1995) discussed the ecological constraints necessary for an evolution from sequential to simultaneous hermaphroditism. Our data instead suggest that an evolution in the opposite direction, from simultaneous to sequential hermaphrodites, is more probable within *Ophryotrocha*. Such a scenario is also hinted at by A. Berglund, who—according to Premoli and Sella (1995)—commented that *O. puerilis* is “a modified simultaneous hermaphrodite in which a reversible mechanism of temporal inhibition of one of the two sexual phases has evolved.” The problem of whether gonochorism or hermaphroditism is the ancestral state was also thoroughly discussed by Sella and Ramella (1999). However, they did not take up a definite position.

In addition to reproduction, jaw morphology has been used to understand *Ophryotrocha* relationships. The hindmost pair of maxillary plates in *Ophryotrocha* species can be of two distinct types. Whereas the P-type has a distal row of fang-like denticles, the K-type plates are distally smooth but often of a robust construction (Hartmann and Huth, 1936). Whereas a P-type jaw is found in larvae and juveniles of all species, the character state for adult worms is either P or K (e.g., Ockelmann and Åkesson, 1990). The terminology emanates from the German words “kompliziert” (K-type) and “primitiv” (P-type). Based on reproduction strategy and jaw morphology, Åkesson (1973, 1984) identified the “*labronica*,” the “*hartmanni*,” and the “*gracilis*” groups within *Ophryotrocha*. The “*labronica*” group of sibling species consists of gonochorists with the K-type of jaws; it is well supported by the analysis presented here and represents clade B in Figure 1A. The “*hartmanni*” and “*gracilis*” groups comprise hermaphroditic species. Species belonging to the former group are distinguished by, among other characters, spawning an entirely soft, irregularly shaped egg mass, and the presence of K-type jaws (Ockelmann and Åkesson, 1990). In contrast, the “*gracilis*” group spawns a fusiform egg mass with a hard protective outer layer, and carries P-type jaws only. The monophyly of the two groups of hermaphrodites, “*gracilis*” and “*hartmanni*,” are, however, not validated by the present analysis. On the contrary, the characters “shape of egg mass” and “type of jaws” are homoplasious in all our trees, irrespective of the phylogenetic optimization used (i.e., ML or parsimony) and the placement of the root (Fig. 3B and C). Therefore, in our trees *O. gracilis* is no longer a member of the “*gracilis*” group despite the close points of similarity in reproductive traits and morphology between this species and other members of the group (Ockelmann and Åkesson, 1990; Pleijel and Eide, 1996). A more extensive study seems to be justified.

Cytology and karyology have been extensively studied for a variety of species. Diploid numbers of chromosomes are known for 18 species (Åkesson, 1984; Robotti et al.,

1991; Shaojie and Knowles, 1992) that have $2n = 6$, $2n = 8$ or $2n = 10$. The genome size (measured as picograms of DNA per cell) in 10 studied forms was discontinuously distributed between 0.4 pg (8 taxa), 0.8 (1 taxon) and 1.16 pg (1 taxon) (Sella et al., 1993; Soldi et al., 1994; Gambi et al., 1997). The apparent discontinuous distribution of genome size (i.e., ≈ 0.4 , ≈ 0.8 , or ≈ 1.2) was interpreted as an indication that large parts of the genome are acquired simultaneously (Sella et al., 1993). The increments in genome size, however, do not correspond to increased numbers of chromosomes (Gambi et al., 1997). The position of chromosomal nucleolar organizer regions (NOR) has been characterized and found to be highly polymorphic not only within the genus but also within most of the species (Sella et al., 1995; Vitturi et al., 2000). On the basis of inferred low GC contents and only one pair of NOR carrying chromosomes (studied by fluorescent *in situ* hybridization), Vitturi et al. (2000) suggested that *O. robusta*, with $2n = 10$ and a small genome size (0.4 pg), is plesiomorphic within the group. A basal position of *O. robusta* within the “*labronica*” group is corroborated by the mtDNA data (Fig. 1). Unfortunately, since *O. robusta* is the only studied species with this combination of characters, it is impossible to tell if this is an autapomorphy or a symplesiomorphy.

To summarize, this study presents the first mtDNA gene tree for *Ophryotrocha* species. Examination of the tree, which provides independent data for evaluating the evolution of reproductive strategies, leads us to suggest that hermaphroditism or gonochorism evolved once within studied *Ophryotrocha* taxa and that sequential hermaphroditism evolved from simultaneous hermaphroditism.

Acknowledgments

We are indebted to Arne Nygren for letting us use previously unpublished sequences of *Dorvillea albomaculata* and *Dinophilus gyrotilatus*. Comments by Fredrik Pleijel as well as three anonymous referees helped improve the manuscript. Barbro Löfnertz is acknowledged for assistance in the laboratory. Financial support for this study was provided by Swedish Natural Science Research Council (BÅ, PS), National Science Foundation (DEB-0075618) (KMH), and Knut och Alice Wallenbergs Stiftelse (PS). This is contribution number 10442 to WHOI.

Literature Cited

- Åkesson, B. 1967. On the biology and larval morphology of *Ophryotrocha puerilis* Claparède and Metschnikov (Polychaeta). *Ophelia* **4**: 110–119.
- Åkesson, B. 1970. *Ophryotrocha labronica* as test animal for the study of marine pollution. *Helgol. Wiss. Meeresunters.* **20**: 293–303.
- Åkesson, B. 1972. Sex determination in *Ophryotrocha labronica* (Polychaeta, Dorvilleidae). Pp. 163–172 in *Fifth European Marine Biology Symposium*, B. Battaglia, ed. Piccin Editore, Padova.
- Åkesson, B. 1973. Reproduction and larval morphology of five

- Ophryotrocha* species (Polychaeta, Dorvilleidae). *Zool. Scr.* **2**: 145–155.
- Åkesson, B. 1975. Bioassay studies with polychaetes of the genus *Ophryotrocha* as test animals. Pp. 121–135 in *Sublethal Effects of Toxic Chemicals on Aquatic Animals*, J. H. Koeman and J. J. T. W. A. Strik, eds. Elsevier, Amsterdam.
- Åkesson, B. 1976. Morphology and life cycle of *Ophryotrocha diadema*, a new polychaete species from California. *Ophelia* **15**: 23–35.
- Åkesson, B. 1977. Crossbreeding and geographic races: experiments with the polychaete genus *Ophryotrocha*. *Mikrofauna des Meeresbodens* **61**: 11–18.
- Åkesson, B. 1978. A new *Ophryotrocha* species of the *Labronica* group (Polychaeta, Dorvilleidae) revealed in crossbreeding experiments. Pp. 573–590 in *NATO Conference Series (Marine Science)*, B. Battaglia and J. Beardmore, eds. Plenum Publishing, New York.
- Åkesson, B. 1984. Speciation in the genus *Ophryotrocha* (Polychaeta, Dorvilleidae). Pp. 299–316 in *Polychaete Reproduction*, G. Fischer and H.-D. Pfannenstiel, eds. Gustav Fischer Verlag, Stuttgart.
- Bacci, G. 1965. Sex determination and genetic balance of *Ophryotrocha puerilis*, a hermaphrodite polychaete worm. *Nature* **207**: 1208–1209.
- Bacci, G., and M. La Greca. 1953. Genetic and morphological evidence for subspecific differences between Naples and Plymouth populations of *Ophryotrocha puerilis*. *Nature* **171**: 1115.
- Bergh, R. S. 1895. Neue Untersuchungen über *Ophryotrocha* und über Anneliden-larven. *Zoologische Centralblatt, Leipzig* **2**: 257–263.
- Berglund, A. 1991. To change or not to change sex: a comparison between two *Ophryotrocha* species (Polychaeta). *Evol. Ecol.* **5**: 128–135.
- Bergmann, W. 1903. Untersuchungen über die Eibildung bei Anneliden und Cephalopoden. *Z. Wiss. Zool.* **73**: 278–301.
- Blake, J. A. 1985. Polychaeta from the vicinity of deep-sea geothermal vents in the eastern Pacific. I. Euphrosinidae, Phyllodocidae, Hesionidae, Nereididae, Glyceridae, Dorvilleidae, Orbiniidae, and Maldaniidae. *Bull. Biol. Soc. Wash.* **6**: 67–101.
- Cassai, C., and D. Prevedelli. 1999. Fecundity and reproductive effort in *Ophryotrocha labronica* (Polychaeta: Dorvilleidae). *Mar. Biol.* **133**: 489–494.
- Charnov, E. L. 1982. *Sex Allocation*. Princeton University Press, Princeton, NJ.
- Claparède, D., and E. Mecznirow. 1869. Beiträge zur Kenntnis der Entwickelungsgeschichte der Chaetopoden. *Z. Wiss. Zool.* **19**: 163–205.
- Colombera, D., and I. Lazzaretto-Colombera. 1978. Chromosome evolution in some marine invertebrates. Pp. 487–525 in *Marine Organisms. Genetics, Ecology and Evolution*, B. Battaglia and J. A. Beardmore, eds. Plenum Press, New York.
- Doyle, J. J., and E. Dickson. 1987. Preservation of plant samples for DNA restriction endonuclease analysis. *Taxon* **36**: 715–722.
- Eihye-Jacobsen, D., and R. M. Kristensen. 1994. A new genus and species of Dorvilleidae (Annelida, Polychaeta) from Bermuda, with a phylogenetic analysis of Dorvilleidae, Iphitimidae and Dinophilidae. *Zool. Scr.* **23**: 107–131.
- Eriksson, M., and S. Lindström. 2000. *Ophryotrocha* sp., the first report of a jawed polychaete from the Cretaceous of Skåne, Sweden. *Acta Paleontol. Pol.* **45**: 311–315.
- Fauchald, K. 1977. The polychaete worms. Definitions and keys to the orders, families and genera. *Nat. Hist. Mus. Los Angel. Cty. Sci. Ser.* **28**: 1–188.
- Gambi, M. C., L. Ramella, G. Sella, P. Protto, and E. Aldieri. 1997. Variation in genome size in benthic polychaetes: Systematic and ecological relationships. *J. Mar. Biol. Assoc. U.K.* **77**: 1045–1057.
- Ghiselin, M. T. 1969. The evolution of hermaphroditism among animals. *Q. Rev. Biol.* **44**: 189–208.
- Halanych, K. M., R. A. Lutz, and R. C. Vrijenhoek. 1998. Evolutionary origins and age of vestimentiferan tube-worms. *Cah. Biol. Mar.* **39**: 355–358.
- Hartmann, M., and W. Huth. 1936. Untersuchungen über Geschlechtsbestimmung und Geschlechtsumwandlung von *Ophryotrocha puerilis*. *Zool. Jahrb. Abt. Allg. Zool. Physiol. Tiere* **56**: 389–439.
- Hartmann, M., and G. von Lewinski. 1940. Untersuchungen über die Geschlechtsbestimmung und Geschlechtsumwandlung von *Ophryotrocha puerilis*. III. Die stoffliche Natur der vermännlichenden Wirkung "starker" Weibchen ("Eistoffe"). *Zool. Jahrb. Abt. Allg. Zool. Physiol. Tiere* **60**: 1–12.
- Hendy, M. D., and D. Penny. 1989. A framework for the quantitative study of evolutionary trees. *Syst. Zool.* **38**: 297–309.
- Hilbig, B., and J. A. Blake. 1991. Dorvilleidae (Annelida: Polychaeta) from the U.S. Atlantic slope and rise. Description of two new genera and 14 new species, with generic revision of *Ophryotrocha*. *Zool. Scr.* **20**: 147–183.
- Hurst, L. D. 1992. Intragenomic conflict as an evolutionary force. *Proc. R. Soc. Lond., Biol. Sci.* **248**: 135–140.
- Huth, W. 1933. *Ophryotrocha*-Studien. Zur Cytologie der Ophryotrochen. *Z. Zellforsch. Mikrosk. Anat. Berlin* **20**: 309–381.
- International Commission on Zoological Nomenclature 1985. *International Code of Zoological Nomenclature*, 3rd ed. University of California Press, Berkeley, CA.
- Josefson, A. B. 1975. *Ophryotrocha longidentata* sp.n. and *Dorvillea erucaeformis* (Malmgren) (Polychaeta, Dorvilleidae) from the west coast of Scandinavia. *Zool. Scr.* **4**: 49–54.
- Jumars, P. A. 1974. A generic revision of the Dorvilleidae (Polychaeta), with six new species from the deep North Pacific. *Zool. J. Linn. Soc.* **54**: 101–135.
- Kishino, H., and M. Hasegawa. 1989. Evaluation of the maximum likelihood estimate of the evolutionary tree topologies from DNA sequence data, and the branching order in Hominoidea. *J. Mol. Evol.* **29**: 170–179.
- La Greca, M., and G. Bacci. 1962. Una nuova specie di *Ophryotrocha* delle coste tirreniche. *Boll. Zool.* **29**: 13–23.
- Lu, H., and K. Fauchald. 2000. *Ophryotrocha lipscombae*, a new species and a possible connection between ctenognath and labidognath-prionognath eunican worms (Polychaeta). *Proc. Biol. Soc. Wash.* **113**: 486–492.
- Maddison, W. P., and D. R. Maddison. 1992. *MacClade: Analysis of Phylogeny and Character Evolution*. Sinauer Associates, Sunderland, MA.
- Maynard Smith, J. 1982. *Evolution and the Theory of Games*. Cambridge University Press, Cambridge, United Kingdom.
- Meek, C. F. U. 1912. A metrical analysis of chromosome complexes, showing correlation of evolutionary development and chromatin thread-width throughout the animal kingdom. *Philos. Trans. R. Soc. Lond. B* **203**: 1–74.
- Ockelmann, K. W., and B. Åkesson. 1990. *Ophryotrocha socialis* n.sp., a link between two groups of simultaneous hermaphrodites within the genus (Polychaeta, Dorvilleidae). *Ophelia* **31**: 145–162.
- Orensanz, J. M. 1990. The Eunicemorph polychaete annelids from antarctic and subantarctic seas. Pp. 1–183 in *Antarctic Research Series*, L. S. Kornicker, ed. American Geophysical Union, Washington, D.C.
- Oug, E. 1978. New and lesser known Dorvilleidae (Annelida, Polychaeta) from Scandinavian and northeast American waters. *Sarsia* **63**: 285–303.
- Oug, E. 1990. Morphology, reproduction, and development of a new species of *Ophryotrocha* (Polychaeta: Dorvilleidae) with strong sexual dimorphism. *Sarsia* **75**: 191–201.
- Paavo, B., J. H. Bailey-Broek, and B. Åkesson. 2000. Morphology and life history of *Ophryotrocha adherens* sp. nov. (Polychaeta, Dorvilleidae). *Sarsia* **85**: 251–264.

- Palumbi, S. R. 1996.** Nucleic acid II: the polymerase chain reaction. Pp. 205–247 in *Molecular Systematics*, D. M. Hillis, G. Moritz, and B. K. Mable, eds. Sinauer Associates, Sunderland, MA.
- Paxton, H. 1986.** Generic revision and relationships of the family Onuphidae (Annelida: Polychaeta). *Rec. Aust. Mus.* **38**: 1–74.
- Pfannenstiel, H.-D. 1972.** Eine neue *Ophryotrocha*-Art (Polychaeta, Eunicidae) aus Japan. *Helgol. Wiss. Meeresunters.* **23**: 117–124.
- Pfannenstiel, H.-D. 1975.** *Ophryotrocha natans* n. sp. (Polychaeta, Dorvilleidae): ein Simultanzwitter mit acht männlichen Segmenten aus dem Golf von Aqaba. *Zool. Anz.* **195**: 1–7.
- Pløjel, F., and R. Eide. 1996.** The phylogeny of *Ophryotrocha* (Dorvilleidae: Eunicida: Polychaeta). *J. Nat. Hist.* **30**: 647–659.
- Premoli, M. C., and G. Sella. 1995.** Sex economy in benthic polychaetes. *Ethol. Ecol. Evol.* **7**: 27–48.
- Robotti, C. A., L. Ramella, P. Cervella, and G. Sella. 1991.** Chromosome analysis of nine species of *Ophryotrocha* (Polychaeta: Dorvilleidae). Pp. 625–632 in *Systematics, Biology and Morphology of World Polychaeta*. *Ophelia* Suppl. 5.
- Rouse, G. W., and K. Fauchald. 1997.** Cladistics and polychaetes. *Zool. Scr.* **26**: 139–204.
- Sella, G. 1988.** Reciprocation, reproductive success, and safeguards against cheating in a hermaphroditic polychaete worm, *Ophryotrocha diadema* Åkesson, 1976. *Biol. Bull.* **175**: 212–217.
- Sella, G. 1991.** Evolution of biparental care in the hermaphroditic polychaete worm *Ophryotrocha diadema*. *Evolution* **45**: 63–68.
- Sella, G., and L. Ramella. 1999.** Sexual conflict and mating systems in the dorvilleid genus *Ophryotrocha* and the dinophilid genus *Dinophilus*. *Hydrobiologia* **402**: 203–213.
- Sella, G., C. A. Redi, L. Ramella, R. Soldi, and M. C. Premoli. 1993.** Genome size and karyotype length in some interstitial polychaete species of the genus *Ophryotrocha* (Dorvilleidae). *Genome* **36**: 652–657.
- Sella, G., R. Vitturi, L. Ramella, and M. S. Colomba. 1995.** Chromosomal nucleolar organizer region (NOR) phenotypes in nine species of the genus *Ophryotrocha* (Polychaeta: Dorvilleidae). *Mar. Biol.* **124**: 425–433.
- Shaojie, D., and J. F. Knowles. 1992.** Chromosomes of the polychaete *Ophryotrocha diadema*. *Ophelia* **36**: 195–201.
- Soldi, R., L. Ramella, M. C. Gambi, P. Sordino, and G. Sella. 1994.** Genome size in polychaetes: relationship with body length and life habit. *Mém. Mus. Nat. Paris* **162**: 129–135.
- Sundberg, P., and S. Andersson. 1995.** Random amplified polymorphic DNA (RAPD) and intraspecific variation in *Oerstedtia dorsalis* (Hoplonemertea, Nemertea). *J. Mar. Biol. Assoc. U.K.* **75**: 483–490.
- Swofford, D. L. 2000.** *PAUP* (Phylogenetic Analysis Using Parsimony)*. Sinauer Associates, Sunderland, MA.
- Swofford, D. L., G. J. Olsen, P. J. Waddell, and D. M. Hillis. 1996.** Phylogenetic inference. Pp. 407–514 in *Molecular Systematics*, D. M. Hillis, C. Moritz, and B. K. Mable, eds. Sinauer Associates, Sunderland, MA.
- Thompson, J. D., D. G. Higgins, and T. J. Gibson. 1994.** Clustal W: improving the sensitivity of progressive multiple sequence alignment through sequence weighting, position-specific gap penalties and weight matrix choice. *Nucleic Acids Res.* **22**: 4673–4680.
- Vitturi, R., L. Ramella, M. S. Colomba, V. Caputo, and G. Sella. 2000.** NOR regions of polychaete worms of the genus *Ophryotrocha* studied by chromosome banding techniques and FISH. *J. Heredity* **91**: 18–23.
- Zavarzina, E. G., and A. B. Tzetlin. 1991.** Breeding and larval morphology of *Ophryotrocha dimorphica* Zavarzina & Tzetlin (Polychaeta: Dorvilleidae). *Ophelia* **5**: 411–420.

Appendix

Checklist of described *Ophryotrocha* species with original localities

- O. adherens* Paavo, Bailey-Brock & Åkesson, 2000. Cyprus and Hawaii, littoral.
- O. akessoni* Blake, 1985. Galapagos Rift, East Pacific Basin, deep sea.
- O. atlantica* Hilbig & Blake, 1991. NW Atlantic, slope depths.
- O. baccii* Parenti, 1961. Roscoff, France, littoral.
- O. bifida* Hilbig & Blake, 1991. NW Atlantic, slope depths.
- O. claparedii* Studer, 1878. Kerguelen, littoral.
- O. costlowi* Åkesson, 1978. Beaufort, North Carolina, littoral.
- O. cosmetandra* Oug, 1990. Northern Norway, littoral.
- O. diadema* Åkesson, 1976. Los Angeles harbor, littoral.
- O. dimorphica* Zavarzina & Tzetlin, 1986. Peter the Great Bay, littoral.
- O. dubia* Harmann-Schröder, 1974. North Sea (off Scotland), 68 m.
- O. gerlachi* Hartmann-Schröder, 1974. North Sea (off Denmark), 52 m.
- O. geryonicola* (Esmark, 1874). Skagerack, Kattegat, sublittoral.
- O. globopalpata* Blake & Hilbig, 1990. Juan de Fuca Ridge, deep sea.
- O. gracilis* Huth, 1933. Helgoland, Germany, littoral.
- O. hadalis* Jumars, 1974. Aleutian Trench, deep sea.
- O. hartmanni* Huth, 1933. NE Atlantic, littoral.
- O. irinae* Tzetlin, 1980. Kandalaksha Bay, White Sea, littoral.
- O. kagoshimaensis* Miura, 1997. Kagoshima Bay, Japan, 197 m.
- O. labidion* Hilbig & Blake, 1991. NW Atlantic, slope depths.
- O. labronica* La Greca & Bacci, 1962. Naples, Italy, littoral.
- O. lipscombae* Lu & Fauchald, 2000. NW Atlantic, slope depths.
- O. littoralis* (Levinsen, 1879). Egesminde, Greenland, littoral.
- O. lobifera* Oug, 1978. West Norway, in mud, 50 m.
- O. longidentata* Josefson, 1975. Skagerack, Kattegat, 50–100 m.
- O. maciolekae* Hilbig & Blake, 1991. NW Atlantic, slope depths.

- O. maculata* Åkesson, 1973. Skagerack, Kattegat, 25 m.
- O. mandibulata* Hilbig & Blake, 1991. NW Atlantic, slope depths.
- O. mediterranea* Martin, Abelló & Cartes, 1991. Mediterranean, parasitic, 600–1800 m.
- O. minuta* Levi, 1954. Roscoff, France, littoral.
- O. natans* Pfannenstiel, 1975. Red Sea, littoral.
- O. notialis* (Ehlers, 1908). Southern South America, sublittoral.
- O. notoglandulata* Pfannenstiel, 1972. Japan, littoral.
- O. obtusa* Hilbig & Blake, 1991. NW Atlantic, slope depths.
- O. pachysoma* Hilbig & Blake, 1991. NW Atlantic, slope depths.
- O. paralbidion* Hilbig & Blake, 1991. NW Atlantic, slope depths.
- O. platycephale* Blake, 1985. Guayamas Basin, hydrothermal vents, deep sea.
- O. puerilis puerilis* Claparède & Mecznirow, 1869. Naples, Italy, littoral.
- O. puerilis siberti* (McIntosh, 1885). Plymouth, England, littoral.
- O. scarlatoi* Averincev, 1989. Franz Josefs Land, littoral.
- O. schubrayi* Tzetlin, 1980. Marine aquarium in Moscow, Russia.
- O. socialis* Ockelmann & Åkesson, 1990. Marine aquarium in Helsingør, Denmark.
- O. spatula* Fournier & Conlan, 1994. Arctic Canada, littoral.
- O. vivipara* Banse, 1963. San Juan Archipelago, USA, 22 m.
- O. wubaolingi* Miura, 1997. Kagoshima Bay, Japan, 200 m.

Variable Mate-Guarding Time and Sperm Allocation by Male Snow Crabs (*Chionoecetes opilio*) in Response to Sexual Competition, and their Impact on the Mating Success of Females

AMÉLIE RONDEAU^{1,*} AND BERNARD SAINTE-MARIE^{2,†}

¹*Institut des sciences de la mer de Rimouski (ISMER), Université du Québec à Rimouski, 310 allée des Ursulines, Rimouski, Québec G5L 3A1, Canada; and* ²*Division des invertébrés et de la biologie expérimentale, Institut Maurice-Lamontagne, Pêches et Océans Canada, 850 route de la Mer, C.P. 1000, Mont-Joli, Québec G5H 3Z4, Canada*

Abstract. Two laboratory experiments investigated mate guarding and sperm allocation patterns of adult males with virgin females of the snow crab, *Chionoecetes opilio*, in relation to sex ratio. Although females outnumbered males in treatments, operational sex ratios were male-biased because females mature asynchronously and have a limited period of sexual attractiveness after their maturity molt. Males guarded females significantly longer as the sex ratio increased: the mean time per female was 2.9 d in a 2♂:20♀ treatment compared to 5.6 d in a 6♂:20♀ treatment. Female injury and mortality scaled positively to sex ratio. Males that guarded for the greatest number of days were significantly larger, and at experiment's end had significantly smaller vasa deferentia, suggesting greater sperm expense, than males that guarded for fewer days. In both experiments, the spermathecal load (SL)—that is, the quantity of ejaculate stored in a female's spermatheca—was independent of molt date, except in the most female-biased treatment, where it was negatively related. The SL increased as the sex ratio increased, mainly because females accumulated more ejaculates. However, similarly sized males had

smaller vasa deferentia and passed smaller ejaculates, such that, at a given sex ratio, the mean SL was 55% less in one experiment than in the other. Some females extruded clutches with few or no fertilized eggs, and their median SL (3–4 mg) was one order of magnitude smaller than that of females with well-fertilized clutches (31–50 mg), indicating sperm limitation. Males economized sperm: all females irrespective of sex ratio were inseminated, but to a varying extent submaximally; each ejaculate represented less than 2.5% of male sperm reserves; and no male was fully exhausted of sperm. Sperm economy is predicted by sperm competition theory for species like snow crab in which polyandry exists, mechanisms of last-male sperm precedence are effective, and the probability that one male fertilizes a female's lifetime production of eggs is small.

Introduction

Intrasexual competition for mates is a fundamental characteristic of sexual reproduction (Trivers, 1972). The intensity of sexual competition depends mostly on the operational sex ratio (OSR), which is the number of sexually active males relative to the number of fertilizable females at a given site and time (Emlen and Oring, 1977). In many animal species, females care for progeny and are only briefly and infrequently receptive, giving them a much smaller potential rate of reproduction than males. This causes the OSR to be skewed toward males, a tendency that may be exacerbated if females become receptive asynchronously. As a result, sexual competition is often more intense among males than among females; to enhance their repro-

Received 28 September 2000; accepted 30 May 2001.

* Present address: Division des poissons marins, Centre des pêches du Golfe, Pêches et Océans Canada, C.P. 5030 Moncton, Nouveau Brunswick E1C 9B6, Canada.

† To whom correspondence should be addressed. E-mail: Sainte-MarieB@dfo-mpo.gc.ca

Abbreviations: CW, carapace width; GT, guarding time per female; ESR, effective sex ratio; OSR, operational sex ratio; SL, spermathecal load; VDW, vasa deferentia weight.

ductive success, males may express flexible behaviors, including mate guarding and judicious allocation of sperm (Trivers, 1972; Ridley, 1983; Clutton-Brock and Parker, 1992).

Precopulatory mate guarding is taxonomically widespread, albeit particularly common in the Crustacea, and it may serve to monopolize a female until she is fertilizable (Parker, 1974; Ridley, 1983). Postcopulatory mate guarding occurs mostly in species with direct sperm transfer, and it may help to ensure paternity for the guarding male by preventing rival males from inseminating the female until she has fertilized her eggs or is no longer receptive (Parker, 1970; Smith, 1984). In crustacean species in which female molting and mating are intimately linked, postcopulatory mate guarding may also shield the postmolt female (and the male's reproductive investment) from predators until her shell has hardened enough to offer protection (Hartnoll, 1969; Wilber, 1989; Jivoff, 1997a). Males may vary their mate-guarding pattern in relation to competition and maximize the number of eggs gained during a breeding season by balancing the time spent guarding mates against the time spent searching for new mates (Parker, 1974; Christy, 1987). Theory predicts (Grafen and Ridley, 1983; Yamamura and Jormalainen, 1996) and observations typically confirm (see Jormalainen, 1998) that males respond to increasing sex ratio by guarding females longer.

Judicious sperm-allocation patterns have evolved in part because sperm, spermatophores, and seminal fluid can be in limited supply due to low rates or high costs of production (Dewsbury, 1982; Pitnick and Markow, 1994). Further, males may enhance their reproductive success if they adjust sperm expenditure to the perceived risk of sperm competition, which may vary as a function of sex ratio, potential for polyandry, or female mating history (Parker *et al.*, 1997). Males typically increase sperm expenditure in the presence of larger females and scale the amount of sperm allocated to females positively to the sex ratio and the risk of sperm competition (Gage, 1991; Gage and Barnard, 1996; Wedell and Cook, 1999).

Changes in male competition intensity and male mating patterns may influence female mating success. As competition becomes more intense, the risk of female injury or death may increase due to male harassment and more frequent takeover attempts (*e.g.*, Rowe *et al.*, 1994; Vepsäläinen and Savolainen, 1995). Conversely, when competition is relaxed and postcopulatory guarding is curtailed, postmolt females are more exposed to predators (Wilber, 1989; Jivoff, 1997b). A severe reduction in sperm allocation may lead to sperm limitation and loss of fecundity for females (Pitnick, 1993; MacDiarmid and Butler, 1999).

Although considerable evidence of flexible patterns of sperm allocation exists for terrestrial and freshwater animals with direct sperm transfer, very little is known of this phenomenon in their marine counterparts (Wilber, 1989; Jivoff, 1997b; Sainte-Marie *et al.*, 1997; MacDiarmid and

Butler, 1999). The present study on the snow crab (*Chionoecetes opilio*; Majidae), a marine brachyuran of the northern hemisphere, documents mate guarding and sperm allocation in relation to sex ratio for adult males with virgin females. Male mating strategies predictably are quite flexible in snow crab because the intensity of sexual competition may be highly variable among years as a result of intrinsic, circa-decadal oscillations of 1–2 orders of magnitude in the abundance ratio of adult males to virgin females. Such oscillations arise from the interaction of multiyear variations in year-class strength and of sexual dimorphism in age at maturity, leading to temporally staggered recruitment patterns for adult females and males (Sainte-Marie *et al.*, 1996).

The relationships of mate-guarding time and sperm allocation to sexual competition remain undetermined for snow crab and congeners; however, other aspects of the sexual interactions of males with virgin females are very well documented in the genus *Chionoecetes*. Female snow crabs reach sexual maturity at a terminal molt, which occurs from January to April in the northwest Atlantic (see Alunno-Bruscia and Sainte-Marie, 1998). Males are attracted to pre-mature females by chemical cues (Bouchard *et al.*, 1996; Pelletier *et al.*, 1998) and then engage in courtship and precopulatory mate guarding until the female molts (Watson, 1972; Donaldson and Adams, 1989). Females usually extrude a clutch of eggs within 1–5 d of molting, whether mated or not (Paul and Adams, 1984; Sainte-Marie and Lovrich, 1994). Both fertilized and unfertilized eggs attach to the pleopods: those fertilized are incubated for up to 2 years; those not fertilized are lost within 5–6 months of attachment (Sainte-Marie, 1993; Sainte-Marie and Carrière, 1995; Moriyasu and Lanteigne, 1998). Adult males have a very high potential reproductive rate and can mate effectively with several females in rapid succession (Watson, 1972; Adams and Paul, 1983; Sainte-Marie and Lovrich, 1994). Female asynchronous molting and brief postmolt sexual attractiveness lead to male competition, and adult males that are smaller, have a softer shell, or are missing more pereopods may be displaced from females by more vigorous males (Stevens *et al.*, 1993; Sainte-Marie *et al.*, 1999). Intense male competition also favors polyandry, and female snow crabs during their first breeding period may accumulate in their spermathecae the ejaculates of up to six males (Urbani *et al.*, 1998). Multiple (different males) and repeated (same male) copulations can happen before or shortly after the first egg clutch is extruded (Sainte-Marie *et al.*, 1997, 1999). When multiple mating takes place before oviposition, last-male sperm precedence usually occurs through a combination of sperm displacement and postcopulatory mate guarding (Urbani *et al.*, 1998; Sainte-Marie *et al.*, 2000). The amount of ejaculate stored by females is independent of mate body size (Adams and Paul, 1983; Sainte-Marie and Lovrich, 1994) but is positively related to

number and duration of copulations, which are hypothesized to be influenced by competition intensity (Sainte-Marie *et al.*, 1997).

The present laboratory study of mating behavior in snow crab was guided by three hypotheses: (i) larger males guard more than smaller males, (ii) mate guarding lasts longer at higher than at lower sex ratios, and (iii) females store more sperm as the sex ratio increases. We also measured the effects that changes in male competition intensity and reproductive investment have on the mating success of females. Two mating experiments were conducted to determine if sperm allocation patterns in relation to competition were the same whether sex ratio was manipulated by varying the density of females or of males. Experiments used female-biased treatments to explore the potential for sperm limitation, a major concern where snow crab fisheries remove only large adult males (Kruse, 1993; Elnor and Beninger, 1995).

Materials and Methods

Collection of crabs

Crabs were collected in October of 1996 and 1997 in the Saint Lawrence Estuary (48°33'N, 68°23'W), eastern Canada. The carapace width (CW) of all crabs and the right chela height of males were measured to the nearest 0.1 mm, using a vernier caliper as described in Sainte-Marie and Hazel (1992). Only immature females larger than 40 mm CW were kept, because they are more likely to reach maturity at their next molt. Males retained were adults of 80 to 115 mm CW, at the mid-range of the 40–155 mm CW distribution for adult males, with shells of intermediate condition (*i.e.*, hard exoskeleton with light epibiont fouling). This shell condition prevails from about 8 months to 3 years after the male's terminal molt to adulthood (Sainte-Marie *et al.*, 1995) and coincides with peak sexual competitiveness (Sainte-Marie *et al.*, 1999).

Selected females and males were brought to the Maurice Lamontagne Institute and placed in separate tanks supplied with fresh running seawater. Photoperiod was controlled to reflect the natural light cycle. Crabs were fed excess thawed shrimp (*Pandalus borealis*) and Atlantic herring (*Clupea harengus*) on a semi-weekly basis from the time of capture to the end of the experiments.

Mating experiments

Mating experiments were conducted in 1997 and in 1998. Crabs were used only in the winter after collection. Thus the time elapsed between collection and use in experiments was similar in both years.

The 1997 experiment ran from 31 January to 4 April (64 d) in nine tanks, each with a bottom surface area of 1.14 m²

(390 l). Tanks received fresh running seawater with ranges of temperature (−0.5 to 1.5 °C) and salinity (24.6‰ to 30.2‰) over the duration of the experiment that represented natural conditions for snow crab. Sex ratio was controlled by varying the number of females for a constant number of males: treatments had male-to-female ratios of 2:10 ($n = 3$ replicates), 2:20 ($n = 3$), and 2:30 ($n = 3$). Female and male crabs were allotted to tanks so that their respective size distributions were as similar as possible among all replicates. Immature females were missing no pereopods at the time they were placed in tanks. Some males were missing 1–2 walking legs, but all had two chelae. Excess crabs were held in reserve tanks. Tanks were checked twice daily for the presence of molting females, and any exuvium was removed and measured to determine premolt CW. Several days after a female had molted to maturity and mating behavior had ceased, the female was identified with a numbered plastic tag tied around the coxopodite of a pereopod. During the experiment, dead females were replaced by a female of similar CW and same reproductive stage taken from the reserves. Pre-mature females are called "pubescent," females that have molted to maturity but not yet extruded eggs are called "nulliparous," and females that have laid their first clutch of eggs are called "primiparous." Substitute females were also tagged. At the experiment's end, the CW of primiparous females was measured.

The 1998 experiment ran from 25 January to 30 March (65 d) in 12 tanks, each with a bottom surface area of 2.23 m² (740 l). Tanks were supplied with fresh running seawater ranging from −0.3 to 1.8 °C and from 24.4‰ to 31.3‰ salinity over the duration of the experiment. Sex ratio was controlled by varying the number of males for a constant number of females; male-to-female ratios in treatments were 2:20 ($n = 4$ replicates), 4:20 ($n = 3$), 6:20 ($n = 4$), and 10:20 ($n = 1$). The 2♂:20♀ treatment was common to the 1997 and 1998 experiments. Methods were identical to 1997, except for the following. All males were intact and each was identified with a water-resistant, numbered label fixed to the dorsum. All females in one replicate each of the 2♂:20♀ and 6♂:20♀ treatments were similarly identified with a label that bore a letter. Labels were large enough to be read from a distance but did not impede molting or mating. Each day we determined the number of males that were guarding females and recorded specific mating associations in the two tanks where all crabs were labeled. Guarding males were those grasping a female or copulating.

The high densities of crabs in our treatments, reaching up to 28 crabs m⁻², are not unrealistic. Majid crabs are notorious for their gregarious behavior during the mating season (*e.g.*, DeGoursey and Auster, 1992), and densities of 100 crabs m⁻² have been documented for *Chionoecetes bairdi* (Stevens *et al.*, 1994).

Male reproductive effort

The weight of vasa deferentia (VDW), which include the storage areas for spermatophores and seminal fluid, was determined at the end of experiments to evaluate sperm depletion as a potential indicator of male reproductive effort. Males in the 1997 and 1998 experiments and 16 reserve males (unmated = controls) of 1998 were killed and were injected with, and immersed in, 4% seawater-diluted formalin. Males were subsequently dissected and their vasa deferentia were removed, blotted, and weighed to the nearest milligram.

In 1998 we estimated guarding time for individual females (GT, in days) in each replicate as

$$GT = \sum n\delta_i / N\varphi_m$$

where $n\delta_i$ is the number of males that were guarding a female on the i_{th} day of the experiment and $N\varphi_m$ is the number of females having reached maturity at experiment's end. GT includes both precopulatory and postcopulatory mate guarding, which could not be dissociated under the present experimental conditions. In the two replicates where all crabs were labeled, we determined for each female the time elapsed between the occurrence of first grasping and the maturity molt, and the total number of days she was guarded.

Female mating success

Female mating success was assessed for primiparous females (excluding primiparous substitutes) at the end of experiments by measuring percent fertilized eggs per clutch, clutch weight, and spermathecal load (SL). Injury and death are also components of female mating success, so the number of missing pereopods and the percent mortality of nulliparous and primiparous females were compiled for each replicate.

The percentage of fertilized eggs in a clutch was estimated from a sample of eggs taken from random locations throughout the clutch while the female was alive. Following Carrière (1995), eggs were processed to highlight nuclei for determination of the proportion of divided (= fertilized) eggs per sample. Briefly, eggs were fixed for 1 h in a solution of 97% glucamine-acetate (GA) buffer, 2% formalin, and 1% Triton, and then rinsed in GA buffer. Eggs were then stained for 1 h in a solution of 0.5 μ g Hoechst dye per ml of GA buffer, and were rinsed twice and preserved in GA buffer at 4 °C. A sample typically contained 200–2400 eggs, and divided and undivided eggs were counted under epifluorescent microscopy. Because eggs develop slowly at cold temperatures, their fertilization status cannot be accurately determined before they are 20 d old (Rondeau, 2000), so we sampled only primiparous females older than 20 d

postmolt, reasonably assuming no delay between molt and oviposition.

The female was killed after her eggs were sampled. The remaining clutch was removed, by severing the base of the inner ramus of each pleopod, and preserved in 99% ethanol. The weight of the blotted clutch was measured to the nearest milligram and then was adjusted using correction factors in Rondeau (2000) to account for enclosed pleopod rami and for removed eggs. The right spermatheca was extracted from the female and preserved in 4% seawater-diluted formalin. Subsequently, SL was determined by peeling away the wall of the spermatheca and weighing its blotted content to the nearest 0.1 mg. Total ejaculate stored by a female can be estimated by doubling the SL because delivery of sperm is usually balanced between the two spermathecae (Sainte-Marie and Lovrich, 1994). Females were considered for analyses of SL only if they survived for 3 days after their maturity molt, to ensure they had the opportunity to fully realize their mating potential. After determination of SL, we estimated the number of sperm stored in some spermathecae from the 1998 experiment. To provide an even distribution over the range of SLs for each treatment, 10 spermathecae from each of the 2 δ :20 φ and 10 δ :20 φ treatments were selected before sperm were counted. Our method for counting sperm was to homogenize the spermathecal contents, dilute the homogenate in seawater to a known volume, enumerate the sperm in replicate hemacytometers, and then extrapolate the average sperm count to the total volume (Adams and Paul, 1983; Sainte-Marie and Lovrich, 1994).

Data analysis

For each replicate, the effective sex ratio (ESR) was calculated as

$$ESR = N\delta / (N\varphi_m + N\delta)$$

where $N\delta$ is the number of males and $N\varphi_m$ is the number of mature females available to males during the experiment. Following Emlen and Oring (1977), the operational sex ratio (OSR) was calculated as

$$OSR = \sum [N\delta / (n_i\varphi_j + N\delta)] / D$$

where $N\delta$ is the number of males, $n_i\varphi_j$ is the number of fertilizable females on the i_{th} day, and D is the duration of the experiment in days. To calculate OSR, we somewhat arbitrarily used a fertilizable period of 3 d starting at the maturity molt. Our choice is justified by the fact that when males are present, female snow crabs usually are inseminated and extrude eggs within 6–24 h of molting (Watson, 1972; Sainte-Marie and Lovrich, 1994) but may continue to mate for about 2–3 d after oviposition. However, although males may compete intensively for nulliparous (pre-oviposition) females, there is little or no male competition for females after oviposition (Sainte-Marie *et al.*, 1997, 1999),

Table 1

Mean \pm standard deviation of effective sex ratio (ESR) and of operational sex ratio (OSR, calculated assuming a 3-d fertilizable period for females) for treatments in the 1997 and 1998 mating experiments with snow crab

1997			1998		
Treatment	ESR	OSR	Treatment	ESR	OSR
2♂:30♀	0.06 \pm 0.00	0.69 \pm 0.03	2♂:20♀	0.11 \pm 0.03	0.81 \pm 0.04
2♂:20♀	0.09 \pm 0.01	0.78 \pm 0.03	4♂:20♀	0.18 \pm 0.01	0.89 \pm 0.00
2♂:10♀	0.18 \pm 0.03	0.87 \pm 0.00	6♂:20♀	0.29 \pm 0.06	0.93 \pm 0.02
			10♂:20♀	0.39	0.94

and thus some uncertainty exists as to how the fertilizable period should be defined for calculation of OSR. Given this uncertainty, we preferred to use ESR as a basis for comparison of male reproductive effort and female mating success across treatments. Both ESR and OSR can take on values ranging from 0 (no male) to 1 (no female), with 0.5 representing a balanced sex ratio.

For univariate analyses, we used the mean, standard deviation, and *t* test or analysis of variance (ANOVA) for description and sample comparisons of normally distributed and homoscedastic data (raw or transformed). Otherwise, the median and Mann-Whitney test were used. One-tailed tests were performed when the mean or median was expected *a priori* to be greater in one sample than in the other. Correlation analysis examined trends between pairs of variables such as female size, molt date, guarding time, and SL. Functional relationships between two variables were investigated by regression analysis. When relating VDW or SL to ESR, we used the replicate's mean or median rather than individual values of the dependent variable so that each replicate weighted the regression equally. Analysis of covariance (ANCOVA) was used to compare clutch weight among treatments with CW as the covariate, and VDW and SL between experiments with ESR as the covariate. The assumption of homogeneity of slopes was met if there was no significant interaction between factor and covariate (Sokal and Rohlf, 1995).

In primiparous female snow crabs, SL measured shortly after the mating period is the sum of individual ejaculates received from single or multiple mates, less the amount of ejaculate expended at fertilization (Sainte-Marie *et al.*, 1997). Frequency distributions of \log_{10} SL for replicated treatments were graphed and analyzed using the mixture distribution method of MacDonald and Pitcher (1979) in an attempt to resolve modes representing one or more accumulated ejaculates.

Results

Size of crabs, molting schedule, and operational sex ratio

Immature females ranged from 45.5 to 66.2 mm CW in the 1997 experiment and from 44.2 to 60.5 mm CW in the

1998 experiment; males were 80.4–111.7 mm CW in 1997 and 81.0–113.0 mm CW in 1998. The mean CW of immature females was homogenous among replicates and treatments in each experiment (two-way ANOVA, $F_{8,163} = 0.18$, $P = 0.993$ in 1997 and $F_{11,156} = 1.06$, $P = 0.400$ in 1998), but differed (ANOVA, $F_{1,338} = 20.69$, $P < 0.001$) between 1997 (53.8 mm) and 1998 (51.7 mm). The mean CW of males was homogenous among replicates and treatments in 1997 ($F_{6,9} = 0.68$, $P = 0.671$) and 1998 ($F_{8,41} = 0.32$, $P = 0.953$), and was similar ($F_{1,69} = 2.74$, $P = 0.103$) between 1997 (94.4 mm CW) and 1998 (98.4 mm CW).

The proportion of immature females that molted was 95.6% in the 1997 experiment and 70.0% in the 1998 experiment, and all but two molts achieved maturity. A negative correlation between premolt CW and molt date in 1997 ($r = -0.15$, $n = 186$, $P = 0.037$) and 1998 ($r = -0.26$, $n = 168$, $P < 0.001$) indicated that larger females tended to molt earlier. The first female molt occurred on day 2 and day 5 of the 1997 and 1998 experiments, respectively, and molting continued until the end of each experiment. The cumulative number of molts followed a logistic pattern over time, and about 75% of molts in each treatment occurred over a period of about 25 d. After fitting and comparing logistic regressions, Rondeau (2000) found that 50% of total molts in 1997 occurred on day 20.8 ± 1.0 d in the least female-biased treatment (2♂:10♀), significantly sooner than in treatments with 2♂:20♀ (day 26.2 ± 0.7) and 2♂:30♀ (day 26.8 ± 0.6). In 1998, females also molted sooner in the least female-biased treatment (10♂:20♀, day 33.9 ± 1.9) than in the 6♂:20♀, 4♂:20♀, and 2♂:20♀ treatments (day 43.7 ± 0.7 to 44.3 ± 0.8). ESR and OSR values paralleled male-to-female treatment ratios, but OSR was always biased toward males (Table 1). If the fertilizable period is taken to be 1 d instead of 3 d—to reflect only the usual time between female molt and oviposition when males compete to inseminate a female—then depending on treatment, OSR ranged from 0.77 to 0.96 in 1997 and from 0.93 to 0.98 in 1998.

Female pereopod loss and mortality

Most injury or death of females occurred while they were in the soft postmolt condition. In both experiments, the proportion of primiparous females that was missing 0, 1–2,

Table 2

Percentage of primiparous female snow crabs missing 0, 1–2, or 3 or more pereopods by replicated sex-ratio treatment in the 1997 and 1998 mating experiments (n = number of primiparous females)

Missing pereopods	Treatments					
	1997			1998		
	2♂:30♀	2♂:20♀	2♂:10♀	2♂:20♀	4♂:20♀	6♂:20♀
0	56.8	33.3	53.6	50.8	38.0	9.6
1–2	40.9	41.0	39.3	36.9	38.0	46.2
≥3	2.3	25.7	7.1	12.3	24.0	44.2
n	88	39	28	65	50	52

Females were intact at start of experiment. The number of females in each class of missing pereopods was not independent of treatment (G -test of independence; $P < 0.05$ for both years). Females from one 2♂:20♀ replicate of 1997 were excluded because of incomplete information on number of missing pereopods.

or ≥3 pereopods differed significantly among treatments (Table 2). In 1998, the number of missing pereopods increased relative to the number of males and the sex ratio. In 1997, however, the number of males was held constant and there was no clear pattern between the number of missing pereopods and the sex ratio or female density. Mean mortality of combined nulliparous and primiparous females increased with increasing sex ratio. In the 1997 experiment, mortality reached 6%, 18%, and 20% in the 2♂:30♀, 2♂:20♀, and 2♂:10♀ treatments, respectively. One replicate in the 2♂:20♀ treatment was excluded from computation of mortality because combined nulliparous and primiparous mortality was high (50%). Dead females in this peculiar replicate were shredded, suggesting that one or both males were particularly aggressive. Mortality in the 1998 experiment was 15%, 20%, and 35% in the 2♂:20♀, 4♂:20♀, and 6♂:20♀ treatments, respectively.

Male dominance and mate-guarding patterns

For the 1998 experiment, males were separated *a posteriori* into two groups based on the total number of guarding days accumulated by each male over the course of the experiment. In each replicate, the male that guarded for the greatest number of days was categorized as “dominant” and the other male (or males) was considered to be “subordinate.” Dominant males (mean CW = 102.4 mm, $n = 12$) were as expected larger (one-tailed t test, $t = 1.74$, $P = 0.049$) than subordinate males (mean CW = 97.3 mm, $n = 42$). The average number of days that dominant males guarded in the 1998 experiment did not decline with increasing number of males per treatment (Table 3). Moreover, the decrease in the contribution of dominant males to total number of guarding days was not proportional to the increase in number of males per treatment (Table 3).

Table 3

Cumulative number of guarding days by males, and mean \pm standard deviation of guarding time for individual females (GT), in relation to sex ratio in the 1998 mating experiment with snow crab

Treatment	n	Number of guarding days by male type			Contribution of dominant male to sum of guarding days by all males			Mean GT
		(a) Dominant sum	Dominant mean	(b) All males sum	Observed	Expected	G_{adj} , P	
2♂:20♀	4	88	22.0 \pm 6.1	166	0.53	0.50	0.60, >0.05	2.9 \pm 1.0
4♂:20♀	3	52	17.3 \pm 5.9	124	0.42	0.25	16.87, <0.001	3.1 \pm 0.6
6♂:20♀	4	93	23.2 \pm 8.0	251	0.37	0.17	59.83, <0.001	5.6 \pm 1.9
10♂:20♀	1	18	18	86	0.21	0.10	8.93, <0.01	6.5

The sum of guarding days for the dominant male (a) and for all males (b) in all replicates (n) of each treatment are shown. The dominant male, for which mean \pm standard deviation of guarding days by treatment are given, represents the male that guarded for the greatest number of days in each replicate. Considering only replicated treatments, there was no effect of sex ratio on mean number of guarding days by the dominant male (ANOVA, $F_{2,8} = 0.69$, $P = 0.528$) and a significant effect of sex ratio on mean GT (ANOVA, $F_{2,8} = 6.97$, $P = 0.018$). Observed contribution of dominant males to sum of guarding days for all males is the quotient of (a) over (b); expected contribution of dominant males is the quotient of one over the number of males per treatment. The G -test with William's correction (G_{adj}) verified whether observed contribution departed significantly (P = probability) from expected contribution.

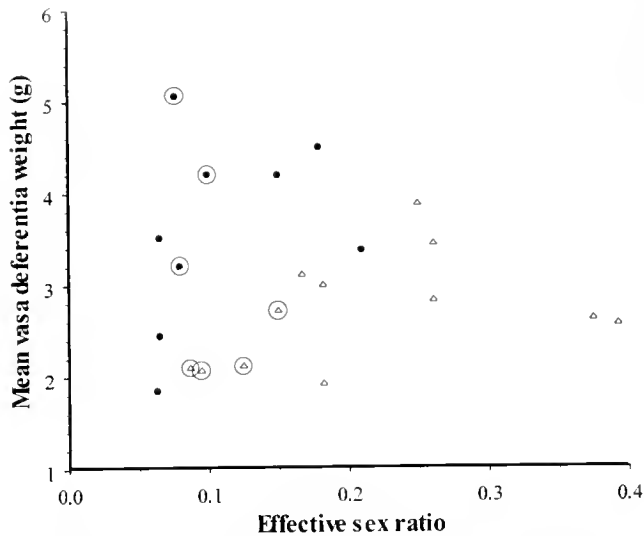


Figure 1. Mean vasa deferentia weight of male snow crabs at end of 1997 (●) and 1998 (△) mating experiments in relation to effective sex ratio by replicate. Encircled values represent replicates of the 2♂:20♀ treatment common to both experiments. Note the outlier (effective sex ratio = 0.08, vasa deferentia weight = 5.06 g) in the 1997 experiment.

As hypothesized, GT increased as the sex ratio (and number of males) increased in the 1998 experiment (Table 3). This increase was not simply a density-dependent effect of more males haphazardly guarding any female. Indeed, based on the two replicates with all crabs labeled, females were grasped for the first time sooner (one-tailed Mann-Whitney test, $U = 8$, $P = 0.002$) before they molted in the 6♂:20♀ treatment (mean 9.4 d, maximum 33 d) than in the 2♂:20♀ treatment (mean 2.8 d, maximum 17 d). Also, dominant males guarded for longer continuous periods prior to the female's molt in the 6♂:20♀ treatment compared to the 2♂:20♀ treatment (one-tailed Mann-Whitney test, $U = 3$, $P = 0.007$), suggesting they mated fewer females as sex ratio increased. There was no correlation between the number of days a female was guarded and the date on which she molted (2♂:20♀, $r = 0.00$, $n = 18$, $P = 1.000$; 6♂:20♀, $r = 0.33$, $n = 10$, $P = 0.353$); therefore, females were guarded as long at the start as at the end of the experiment.

Sperm depletion

Sperm depletion due to mating was suggested by scatterplots showing a weak positive trend between VDW and ESR (Fig. 1), indicating that residual vasa deferentia weight tended to decline with the number of potential mating opportunities for males. ANCOVA on \log_{10} -transformed data showed that the effect of ESR on VDW was significant ($F_{1,17} = 5.33$, $P = 0.034$) and that year and ESR did not interact ($F_{1,17} = 0.12$, $P = 0.738$). The mean VDW adjusted to the overall mean ESR differed between years ($F_{1,18} = 5.49$, $P = 0.031$) and was 35.5% less in 1998 males

(2.45 g) than in 1997 males (3.80 g). Note the outlier in the 1997 experiment (Fig. 1), corresponding to the 2♂:20♀ replicate with unusually high female mortality.

Compelling evidence of sperm depletion was seen in the contrasting patterns of VDW for dominant and subordinate males in 1998 (Fig. 2). Two-way ANOVA excluding the sole 10♂:20♀ replicate indicated that the mean \log_{10} VDW varied with the \log_{10} ESR ($F_{2,37} = 5.78$, $P = 0.007$) and male hierarchy ($F_{1,37} = 7.00$, $P = 0.012$), but there was no interaction between the two factors ($F_{2,37} = 2.17$, $P = 0.129$). The mean VDW was progressively smaller as sex ratio decreased and was less in dominant than in subordinate and control males (Fig. 2), the difference between control and dominant males increasing from 2% to 66% as the sex ratio declined.

Spermathecal load

In every treatment, correlation coefficients were positive between SL and CW and negative between SL and molt date. However, the only significant coefficient was between SL and molt date ($r = -0.31$, $n = 83$, $P = 0.005$) in the most female-biased treatment (2♂:30♀).

As hypothesized, there was a significant positive relationship between SL and ESR in both years (Fig. 3), indicating that females acquired more ejaculate as the sex ratio increased. ANCOVA on \log_{10} -transformed data showed a highly significant effect of ESR on SL ($F_{1,17} = 17.80$, $P = 0.001$) but no interaction between year and ESR ($F_{1,17} = 0.50$, $P = 0.488$). The mean SL adjusted to the overall mean ESR differed between years ($F_{1,18} = 36.41$, $P < 0.001$) and was 55.1% less in 1998 (27.8 mg) than in 1997 (61.9 mg).

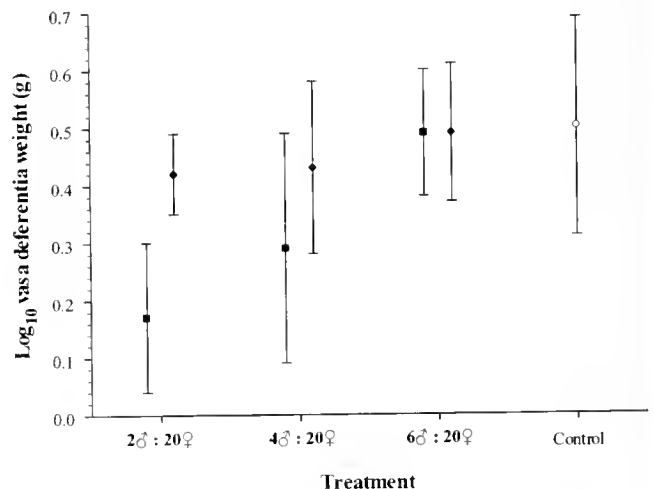


Figure 2. Mean \pm standard deviation of log-transformed vasa deferentia weight of male snow crabs in relation to male mating status (dominant = ■, subordinate = ◆) in the 2♂:20♀, 4♂:20♀ and 6♂:20♀ treatments of the 1998 mating experiment and in comparison to unmated control males.

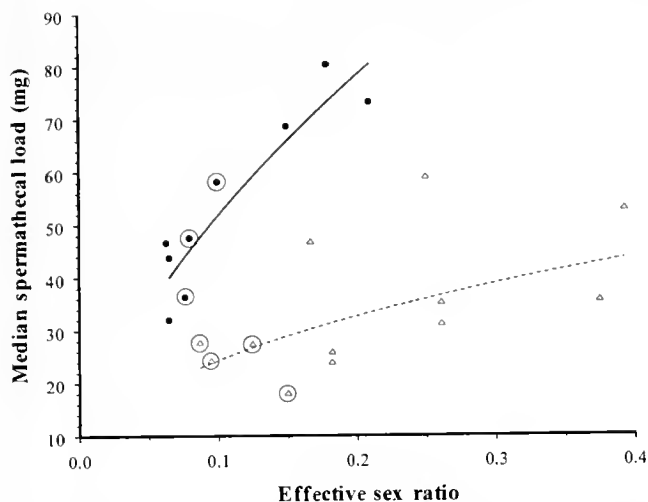


Figure 3. Median of right spermathecal load (SL) of primiparous female snow crabs in relation to effective sex ratio (ESR) per replicate in 1997 and 1998 mating experiments. Regressions fitted to log-transformed data are significant (\bullet 1997: $\log_{10}SL = 0.597 \cdot \log_{10}ESR + 2.310$, $r^2 = 0.80$, $F_{1,8} = 28.25$, $P = 0.001$; \triangle 1998: $\log_{10}SL = 0.425 \cdot \log_{10}ESR + 1.810$, $F_{1,11} = 5.18$, $r^2 = 0.58$, $P = 0.046$). Encircled values represent the 2♂:20♀ treatment common to both experiments.

Frequency distributions of $\log_{10}SL$ of females pooled by experiment produced a similar pattern in 1997 and 1998, consisting of four modes, of which the second was most prominent (Fig. 4). The modes are interpreted as representing spermathecal loads comprising 1, 2, 3, and 4 or more ejaculates. By differencing mean SL for two sequential modes to determine the mean size of successive ejaculates, it was apparent that ejaculates were much smaller in 1998 than in 1997, and that in any given year the size of ejaculates tended to increase with rank of introduction into the spermatheca. Mixture analysis was applied to $\log_{10}SL$ for females pooled by treatment to determine the proportions of females receiving different numbers of ejaculates (Table 4). Two striking features emerged: in the treatments with the highest sex ratio of each experiment (2♂:10♀ in 1997 and 6♂:20♀ in 1998) no female received only one ejaculate; in contrast, in the intermediate and lower sex ratio treatments of each experiment, the proportion of females with four or more ejaculates was null in 1997 or very small in 1998. Some trends between ejaculate size and sex ratio may be biologically meaningful (e.g., the inverse relationship between size of third and fourth ejaculates and sex ratio in 1998) but must be regarded with circumspection given the small sample sizes.

Regression of sperm counts on SL with intercept forced to 0 was significant for the 2♂:20♀ and 10♂:20♀ treatments ($r^2 \geq 0.89$, $n = 10$, and $P < 0.001$ for each regression). Slopes did not differ significantly between the two treatments ($F_{1,17} = 3.12$, $P = 0.095$), so we pooled the data and produced a common regression (Fig. 5).

Clutch weight and percent fertilized eggs

Regression using \log_{10} -transformed data determined a positive relationship between clutch weight and female postmolt CW for each treatment of both experiments ($r^2 \geq 0.59$ and $P < 0.05$ for any given regression). In the 1997 experiment, the slopes of size-fecundity relationships were identical ($F_{2,167} = 0.00$, $P = 0.999$), but the elevations differed ($F_{2,169} = 3.14$, $P = 0.046$) among treatments. Mean clutch weight adjusted to overall mean CW decreased with increasing sex ratio, from 6.77 g in the 2♂:30♀ treatment to 6.47 g in the 2♂:10♀ treatment. In the 1998 experiment, size-fecundity relationships had similar slopes ($F_{3,139} = 1.01$, $P = 0.392$) and elevations ($F_{3,142} = 1.59$, $P = 0.194$) among treatments.

Percent fertilized eggs per clutch followed a dichotomous pattern: either at least 95% of the eggs were fertilized (=

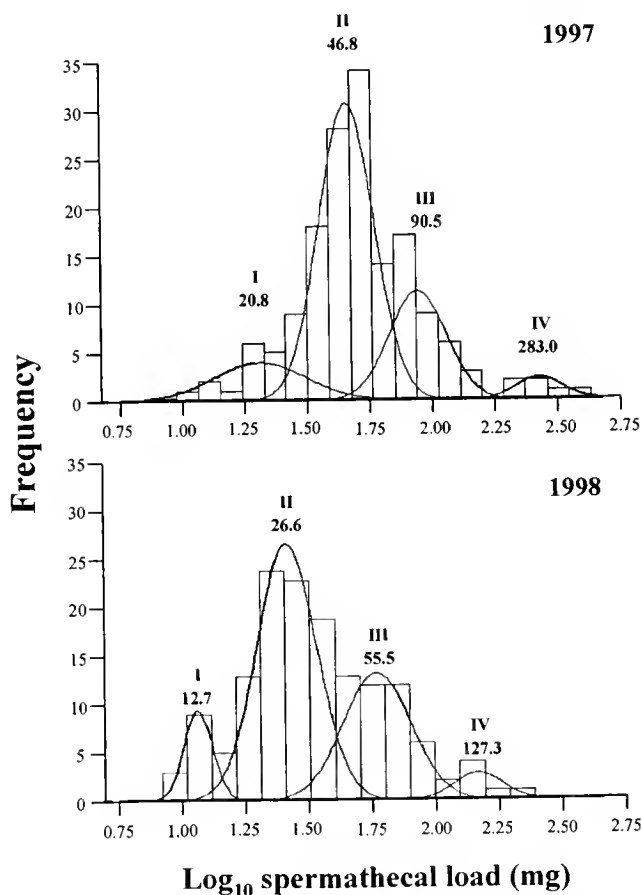


Figure 4. Frequency distribution of right spermathecal load for primiparous female snow crabs in the 1997 and 1998 mating experiments. Four modes were fitted almost perfectly to the distributions in the 1997 ($\chi^2 = 9.78$, $P = 0.913$) and 1998 ($\chi^2 = 2.78$, $P = 0.999$) experiments using the mixture analysis method of MacDonald and Pitcher (1979). Modes are interpreted as representing 1 (mode I), 2 (mode II), 3 (mode III), or 4 or more (mode IV) accumulated ejaculates. The mg-equivalent mean value of each mode appears below the roman numerals.

Table 4

Proportion of primiparous female snow crabs (in boldface) attributed to each of 4 modes identified in frequency distributions of spermathecal loads (see Fig. 4) and mean spermathecal load for each mode (mg, in parentheses) in replicated sex ratio treatments of the 1997 and 1998 mating experiments

Modes	Treatments					
	1997			1998		
	2♂:30♀	2♂:20♀	2♂:10♀	2♂:20♀	4♂:20♀	6♂:20♀
I	0.13 (17.1)	0.12 (20.4)	0.00 (-)	0.11 (11.5)	0.19 (13.9)	0.00 (-)
II	0.72 (42.3)	0.74 (52.5)	0.28 (47.8)	0.76 (26.5)	0.41 (25.8)	0.71 (31.2)
III	0.15 (98.2)	0.14 (115.4)	0.55 (80.2)	0.12 (66.6)	0.35 (56.3)	0.11 (49.9)
IV	0.00 (-)	0.00 (-)	0.17 (255.5)	0.02 (182.4)	0.05 (116.1)	0.18 (86.4)
χ^2	7.10	4.20	2.24	17.52	8.61	12.83
<i>P</i>	0.989	0.980	0.945	0.734	0.929	0.884
<i>n</i>	85	56	31	59	42	39

Goodness of fit (χ^2 value and probability, *P*) is provided for the multiple-mode model that was adjusted by mixture analysis to spermathecal load frequency distributions for each treatment, following methods of MacDonald and Pitcher (1979). The proportion of total females (*n*) attributed to each mode was not independent of treatment (*G*-test of independence on each year, *P* < 0.05).

well-fertilized clutch) or a large proportion to none of the eggs were fertilized (= poorly fertilized clutch). Failure to fertilize most or all eggs apparently resulted from sperm limitation. Indeed, females with poorly fertilized or well-fertilized clutches had median SL values of 4.4 mg (range: 3.0–107.0 mg, *n* = 9) or 49.6 mg (4.4–438.3 mg, *n* = 145) respectively in 1997 (one-tailed Mann-Whitney test, *U* = 137, *P* < 0.001) and of 3.0 mg (0.0–49.8 mg, *n* = 11) or

30.7 mg (10.2–115.1 mg, *n* = 126) respectively in 1998 (*U* = 174, *P* < 0.001).

No clear relationship between fertilization success and sex ratio was found. The proportion of females with poorly fertilized clutches was slightly greater in 1998 (7.8%) than in 1997 (5.8%) and tended to decline with decreasing sex ratio in each year, but differences between years or among treatments within a year were not significant (*G*-test of independence, *P* > 0.05 for all analyses). However, the proportion of females carrying a poorly fertilized clutch may be underestimated due to the criterion of a postmolt age of 20 d for examination of eggs, which excludes females that molted latest and were more likely to have received small amounts of sperm. This may be especially true of the 2♂:30♀ treatment in 1997 due to the negative correlation between SL and molt date, and of the 1998 experiment overall due to a tardy molting schedule.

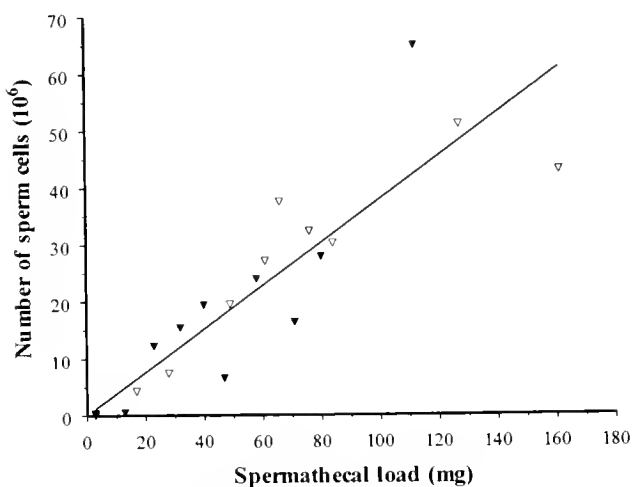


Figure 5. Number of sperm cells (*N*) in relation to the right spermatheca load (SL) of selected primiparous female snow crabs from the 2♂:20♀ (▼) and 10♂:20♀ (▽) treatments of the 1998 mating experiment. A common regression was fitted to the data ($N = 3.788 \cdot 10^5$ SL, *n* = 20, $r^2 = 0.91$, *P* < 0.001).

Discussion

Molting asynchrony combined with brief periods of peak sexual attractiveness for female snow crabs inflated the operational sex ratio (OSR) in our experiments and led to a context of male competition even when females far outnumbered males (Table 1). As expected in such mating systems, males exhibited flexibility in their allocation of time and sperm to females. Below, we discuss how mate-guarding time, sperm depletion, and sperm expenditure varied in relation to sex ratio and male dominance. We close the

discussion by considering the impact of variable patterns of male mating on female mating success.

Duration of mate guarding

Male snow crabs reacted to an increasing sex ratio in the 1998 experiment by guarding females longer, in accordance with theory (Grafen and Ridley, 1983; Yamamura and Jormalainen, 1996) and experimental demonstrations in other brachyuran and anomuran crabs (Wilber, 1989; Jivoff, 1997a; Jivoff and Hines, 1998; Wada *et al.*, 1999). Such a behavior had been inferred for snow crab from *in situ* observations that the proportion of premolt females to postmolt females in mating pairs is greater in years of higher than of lower sex ratio (Sainte-Marie *et al.*, 1999).

Due to different assumptions about female choice and male mate-guarding costs and capability to defend or take over mates, models of mate guarding in the Crustacea have predicted that larger males should associate with females for shorter (*e.g.*, Grafen and Ridley, 1983) or longer (*e.g.*, Elwood and Dick, 1990) periods of time than smaller males. In our study, male snow crabs that accumulated the greatest number of guard days were larger, reflecting in part a size advantage for the defense of females and the ability to displace smaller males (Sainte-Marie *et al.*, 1997). The nonproportional decline in the contribution of the dominant male to total guarding days with increasing number of males (Table 3) suggests that slight male advantages may become increasingly important as the intensity of competition escalates. Accordingly, the range of sizes and conditions of males represented in wild mating pairs was narrower when females were relatively scarce than when they were more abundant (Sainte-Marie *et al.*, 1999).

Sperm depletion

There was clear evidence in our experiments that the sperm reserves of some males were depleted in relation to the number of mating opportunities, as evidenced at the replicate level by progressively smaller mean vasa deferentia weight (VDW) with declining sex ratio (Fig. 1). Moreover, dominant males were significantly more sperm-depleted than subordinate males (Fig. 2), suggesting that the former mated more frequently. This occurred even though the dominant larger males probably had bigger vasa deferentia than the subordinate smaller males at the onset of the experiment, which can be inferred because VDW usually scales positively to male CW (see Sainte-Marie *et al.*, 1995). Part of the difference in VDW with male hierarchy could be due to dominant males charging their vasa deferentia more slowly than subordinate males (see Warner *et al.*, 1995), since energy expenditure and food deprivation may increase with guarding time (Robinson and Doyle, 1985; Sparkes *et al.*, 1996). Furthermore, we posit that the 35% VDW difference in favor of 1997 over 1998 males reflected

sperm depletion through successive breeding periods. Indeed, these males were sampled respectively in the autumn of 1996 and of 1997, 2 and 3 years into a period of intense recruitment of adult females and of declining abundance of large adult males which lasted from 1995 to 1998 (DFO, 2000).

Sperm allocation

Three findings converge to indicate that male snow crabs allocate sperm parsimoniously and partition it among successive matings, a behavior termed sperm economy (Pitnick and Markow, 1994; Shapiro *et al.*, 1994). First, all primiparous females were submaximally inseminated, as evident from the finding that the largest median SL value of 80 mg in our experiments (Fig. 3) was far less than the record mean value of 256 mg determined for wild primiparous females in a year of intense male competition (Sainte-Marie, 1993). Second, in the 1998 experiment even the largest ejaculates passed to females (72 mg, difference between mean SL for modes IV and III in Fig. 4) represented just 2.3% of VDW of control males, and no male fully exhausted his sperm. Third, spermathecal load (SL) was independent of female molt date in all but the most female-biased treatment (2♂:30♀), indicating that sperm depletion was not the usual cause of reduced female sperm reserves at lower sex ratios.

Sperm economy is predicted by sperm competition theory when females can be polyandrous, mechanisms of last-male sperm precedence can be effective, and the probability that one male fertilizes a female's lifetime production of eggs is small (*e.g.*, Pitnick and Markow, 1994; Parker *et al.*, 1997), all of which are attributes of snow crab. The relatively small size of snow crab ejaculates explains why males can equally inseminate several females in rapid succession (Sainte-Marie and Lovrich, 1994). By contrast, the ejaculates of blue crab (*Callinectes sapidus*) represent on average 47% of male gonad volume (Jivoff, 1997b), indicating a sperm-maximizing strategy that correlates with the typically monandrous behavior of females, or otherwise ineffective sperm-precedence mechanisms, and with the generally high probability that one male fertilizes a female's lifetime production of eggs (see Jivoff, 1997a, b). In blue crab, a severe depletion of sperm reserves occurs after just one mating, and males cannot equally inseminate even two females in rapid succession (Jivoff, 1997b; Kendall and Wolcott, 1999).

In snow crab, the coherent pattern of smaller VDW and SL in the 1998 experiment compared to the 1997 experiment for a given effective sex ratio (ESR) (Figs. 1 and 3) indicates that males with relatively smaller gonads pass less ejaculate than males with relatively larger gonads, and this is further evidence of sperm economy. Furthermore, since mean SLs for corresponding modes were distinctly smaller in 1998 compared to 1997 (Fig. 4), but proportions of

females with 1, 2, 3, or 4 or more ejaculates were nearly identical in the common 2♂:20♀ treatment (Table 4), we conclude that the 55% difference in SL between the two years was due mainly to variation in the size of individual ejaculates.

Superimposed on the pattern of SL set by relative vasa deferentia size, in each year SL increased with increasing sex ratio (Fig. 3). This trend resulted from females accumulating more ejaculates of a progressively larger size with increasing rank of insertion into the spermatheca (Fig. 3, Table 4), and it occurred whether sex ratio was controlled by varying the number of females or males. The greater number of ejaculates reflects some combination of more frequent repeated matings (this is certain in 1997, because only two males were used across all treatments) and multiple matings with growing intensity of male competition. The importance of repeated mating relative to polyandry in providing females with larger sperm stores, especially in the 1998 experiment where the number of males was varied across the treatments, will be resolved by genetic analyses using hypervariable microsatellite DNA. Furthermore, the possibility remains that some measure of the variation of SL in relation to sex ratio was due to males adjusting the size of individual ejaculates with changing intensity of competition.

The greater sperm expenditure at higher sex ratios observed in snow crab represents a widespread response of males to the risk of sperm competition (Gage, 1991; Gage and Barnard, 1996; Jivoff, 1997b; Wedell and Cook, 1999). Moreover, the fact that ejaculate size increased with rank of insertion into the spermatheca (Fig. 4) is consistent with predictions and observations for other species that males expend more sperm with previously inseminated females than with virgin females (Cook and Gage, 1995; Jivoff, 1997a; Parker *et al.*, 1997). Increasing the number or size of ejaculates may represent a swamping strategy in species where sperm mixing occurs and all sperm may potentially access eggs (Pitnick and Markow, 1994). However, sperm stratification occurs within the spermathecae of snow crab, and the advantage of introducing a larger ejaculate may be that it will more effectively displace and isolate any previously deposited sperm away from the ovary efferent duct (Sainte-Marie *et al.*, 2000).

The fact that both guarding time and SL were usually independent of female molt date strongly suggests that from the onset of the experiment male snow crabs adopted complementary mate-guarding and sperm-allocation strategies that remained fixed in time. As proposed by Wada *et al.* (1999) for the hermit crab *Pagurus middendorffii*, the rate at which a male encounters females and other males may provide information on the sociosexual context—that is, the potential number of matings to be realized and the degree of male rivalry—that determines in part the male's mating strategy. Similarly, Vepsäläinen and Savolainen (1995)

demonstrated that past OSR experience could condition future male mating behavior in the water strider *Gerris lacustris*. A mate-guarding and sperm-allocation strategy that was established early in the breeding season in reflection of a male's sperm reserves and dominance rank, and of sociosexual context, would allow the male to maximize the number of females that he inseminated. Such a strategy may be maintained even at the expense of reduced fertilization rate per mating (= sperm limitation) "because it is less costly to the male than becoming sperm-depleted before mating opportunities have ceased" (Warner *et al.*, 1995).

Female mating success and sperm limitation

Increasing male sexual competition had both positive and negative effects on female mating success. On one hand, SL increased with increasing sex ratio (Fig. 3); this implies that females had progressively more sperm in storage, given the positive relationship between sperm counts and SL in this study (Fig. 5) as in Sainte-Marie and Lovrich (1994). On the other hand, increasing male competition had adverse effects on the post-mating condition and survival of females. The number of missing pereopods per primiparous female (Table 2) and the percent mortality of the fragile nulliparous and primiparous females increased as the number of males and the sex ratio increased. In the present study, the frequency of injury and mortality may to some extent have been amplified by confinement in the tanks. However, there is field evidence that the number of missing pereopods for primiparous females may vary in relation to the intensity of male competition (Sainte-Marie *et al.*, 1999) and that females are killed by fighting males (Sainte-Marie and Hazel, 1992). Moreover, a negative relationship between female fecundity and sex ratio was seen in the 1997 experiment ($P < 0.05$) and also in the 1998 experiment, although the trend was not significant in the latter (Rondeau, 2000). This decline in fecundity is attributed to the loss of recently extruded, weakly attached eggs during interactions between post-oviposition females and males, which may occur more frequently as male bias in sex ratio increases. These negative effects of male mating activities on female fitness constitute another example of intersexual conflict (Rowe *et al.*, 1994; Vepsäläinen and Savolainen, 1995; Jormalainen, 1998).

Snow crab females incubating a poorly fertilized clutch were apparently sperm-limited, since they had SLs one order of magnitude smaller than those of females incubating a well-fertilized clutch. Similarly, using a subjective index of SL (none, small, or large) on wild female snow crabs, Carrière (1995) found that the proportion of females with well-fertilized clutches increased significantly with extent of spermatheca fullness. In our study, however, there were a few cases where females had a relatively large SL yet a small or null proportion of fertilized eggs. This apparent

inconsistency could arise if a female was mated by another male, after initially mating and laying eggs with a dominant male that was particularly sparing of his sperm.

Sperm limitation occurs naturally when males (i) are too few to inseminate all receptive females, (ii) allocate their sperm too parsimoniously among females, or (iii) do not have time to recharge between matings (Pitnick, 1993; Pitnick and Markow, 1994; Warner *et al.*, 1995; Jivoff, 1997b; MacDiarmid and Butler, 1999). For snow crab, the general cause of sperm limitation was probably sperm economy and in the case of the 30♀:2♂ treatment, additionally, perhaps sperm depletion. Small SLs resulting from unfavorable mating conditions during the female's first breeding season may have negative impacts on her subsequent reproductive activities. Size-fecundity relationships for multiparous (= repeat spawners) females (Sainte-Marie, 1993) and the equation relating sperm counts to SL (Fig. 5) allow estimation of the minimum doubled SL value required for fertilization of a second egg clutch using sperm stored over from a previous breeding period. This value is determined considering that an average of 70 sperm cells are expended to fertilize each oocyte (Sainte-Marie and Lovrich, 1994; Yamasaki *et al.*, 1994). On this basis, 5.2% (1997) and 9.2% (1998) of females did not have enough stored sperm to produce (without re-mating) a second clutch with all eggs fertilized. These are necessarily conservative estimates because mortality of stored sperm may occur between ovipositions (Paul, 1984; Sainte-Marie and Sainte-Marie, 1999). Females with insufficient sperm stores will produce fewer or no fertilized eggs, or they will re-mate at the risk of injury or death (Elnor and Beninger, 1995).

In closing, our study has shown that the mating strategies of male snow crabs are quite flexible, which is adaptive to the widely varying levels of competition intensity and female availability that characterize this species. Our study also points to the potential for sperm limitation to occur in exploited snow crab populations if the removal rates of large males are too high. Indeed, fishing will depress the sex ratio and deplete the most competitive component of the male population. As a result of reduced sexual competition the surviving large males may be subject to sperm depletion through extensive mating, which will exacerbate their sperm-economy behavior. Thus, by contrast to the predominant view in crab fisheries literature that sperm limitation could arise from the number of males becoming insufficient to service all females (see Kruse, 1993; Elnor and Beninger, 1995), the present study revealing the sperm-economy behavior of male snow crabs suggests an insidious process of suboptimal insemination. Further research will consider the implications of sperm economy for the conservation and management of snow crab.

Acknowledgments

This study is part of a M.Sc. thesis from Institut des Sciences de la Mer (ISMER) of Université du Québec à Rimouski, and was supported by a Natural Sciences and Engineering Research Council of Canada (NSERC) grant to B. Sainte-Marie. We thank F. Hazel, M. Levasseur, and M. Carpentier for help in the laboratory. Comments by J.-C. Brêthes, É. Mayrand, and two anonymous reviewers improved this paper at various stages of preparation.

Literature Cited

- Adams, A. E., and A. J. Paul. 1983. Male parent size, sperm storage and egg production in the crab *Chionoecetes bairdi* (Decapoda, Majidae). *Int. J. Invertebr. Reprod.* **6**: 181–187.
- Alunno-Bruscia, M., and B. Sainte-Marie. 1998. Abdomen allometry, ovary development, and growth of female snow crab *Chionoecetes opilio* in the Gulf of Saint Lawrence (Brachyura, Majidae). *Can. J. Fish. Aquat. Sci.* **55**: 459–477.
- Bouchard, S., B. Sainte-Marie, and J. N. McNeil. 1996. Indirect evidence indicates female semiochemicals release male precopulatory behaviour in the snow crab, *Chionoecetes opilio* (Brachyura: Majidae). *Chemoecology* **7**: 39–44.
- Carrière, C. 1995. Insémination et fécondité chez la femelle du crabe des neiges *Chionoecetes opilio* de l'estuaire maritime du Saint-Laurent. Master's thesis, Université du Québec à Rimouski, Rimouski, Canada, 88 pp.
- Christy, J. H. 1987. Competitive mating, mate choice and mating associations of brachyuran crabs. *Bull. Mar. Sci.* **41**: 177–191.
- Clutton-Brock, T. H., and G. A. Parker. 1992. Potential reproductive rates and the operation of sexual selection. *Q. Rev. Biol.* **4**: 437–456.
- Cook, P. A., and M. J. G. Gage. 1995. Effects of risk of sperm competition on the numbers of eupyrene and apyrene sperm ejaculated by the moth *Plodia interpunctella* (Lepidoptera: Pyralidae). *Behav. Ecol. Sociobiol.* **36**: 261–268.
- DeGoursey, R. E., and P. J. Auster. 1992. A mating aggregation of the spider crab (*Libinia emarginata*). *J. Northwest Atl. Fish. Sci.* **13**: 77–82.
- Dewsbury, D. A. 1982. Ejaculate cost and male choice. *Am. Nat.* **119**: 601–610.
- DFO (Department of Fisheries and Oceans, Canada). 2000. Snow crab of the Estuary and Northern Gulf of St. Lawrence (areas 13 to 17). *DFO Science Stock Status Rep.* C4-01 (2000), 13 pp.
- Donaldson, W. E., and A. E. Adams. 1989. Ethogram of behavior with emphasis on mating for the Tanner crab *Chionoecetes bairdi* Rathbun. *J. Crustac. Biol.* **9**: 37–53.
- Elnor, R. W., and P. G. Beninger. 1995. Multiple reproductive strategies in snow crab, *Chionoecetes opilio*: physiological pathways and behavioral plasticity. *J. Exp. Mar. Biol. Ecol.* **193**: 93–112.
- Elwood, R. W., and J. T. A. Dick. 1990. The amorous *Gammarus*: the relationship between precopula duration and size-assortative mating in *G. pulex*. *Anim. Behav.* **39**: 828–833.
- Emlen, S. T., and L. W. Oring. 1977. Ecology, sexual selection, and the evolution of mating systems. *Science* **197**: 215–223.
- Gage, A. R., and C. J. Barnard. 1996. Male crickets increase sperm number in relation to competition and female size. *Behav. Ecol. Sociobiol.* **38**: 349–353.
- Gage, M. J. G. 1991. Risk of sperm competition directly affects ejaculate size in the Mediterranean fruit fly. *Anim. Behav.* **42**: 1036–1037.
- Grafen, A., and M. Ridley. 1983. A model of mate guarding. *J. Theor. Biol.* **102**: 549–567.

- Hartnoll, R. G. 1969. Mating in the Brachyura. *Crustaceana* **16**: 161–181.
- Jivoff, P. 1997a. The relative roles of predation and sperm competition on the duration of the post-copulatory association between the sexes in the blue crab, *Callinectes sapidus*. *Behav. Ecol. Sociobiol.* **40**: 175–186.
- Jivoff, P. 1997b. Sexual competition among male blue crab, *Callinectes sapidus*. *Biol. Bull.* **193**: 368–380.
- Jivoff, P., and A. H. Hines. 1998. Effect of female molt stage and sex ratio on courtship behavior of the blue crab *Callinectes sapidus*. *Mar. Biol.* **131**: 533–542.
- Jormalainen, V. 1998. Precopulatory mate guarding in crustaceans: male competitive strategy and intersexual conflict. *Q. Rev. Biol.* **73**: 275–304.
- Kendall, M. S., and T. G. Wolcott. 1999. The influence of male mating history on male-male competition and female choice in mating associations in the blue crab, *Callinectes sapidus* (Rathbun). *J. Exp. Mar. Biol. Ecol.* **239**: 23–32.
- Kruse, G. H. 1993. Biological perspectives on crab management in Alaska. Pp. 355–384 in *International Symposium on Management Strategies for Exploited Fish Populations*, B. Baxter, ed. Lowell Wakefield Fisheries Symposium Series, University of Alaska Fairbanks, Alaska Sea Grant College Program Report 93-02.
- MacDiarmid, A. B., and M. J. Butler. 1999. Sperm economy and limitation in spiny lobsters. *Behav. Ecol. Sociobiol.* **46**: 14–24.
- MacDonald, P. D. M., and T. J. Pitcher. 1979. Age-groups from size-frequency data: a versatile and efficient method of analysing distribution mixtures. *J. Fish. Res. Board Can.* **36**: 987–1001.
- Moriyasu, M., and C. Lanteigne. 1998. Embryo development and reproductive cycle in the snow crab, *Chionoecetes opilio* (Crustacea: Majidae), in the southern Gulf of St. Lawrence, Canada. *Can. J. Zool.* **76**: 2040–2048.
- Parker, G. A. 1970. Sperm competition and its evolutionary consequences in the insects. *Biol. Rev.* **45**: 525–567.
- Parker, G. A. 1974. Courtship persistence and female-guarding as male time investment strategies. *Behaviour* **48**: 157–184.
- Parker, G. A., M. A. Ball, P. Stockley, and M. J. G. Gage. 1997. Sperm competition games: a prospective analysis of risk assessment. *Proc. R. Soc. Lond. B* **264**: 1793–1802.
- Paul, A. J. 1984. Mating frequency and viability of stored sperm in the Tanner crab *Chionoecetes bairdi* (Decapoda, Majidae). *J. Crustac. Biol.* **4**: 375–381.
- Paul, A. J., and A. E. Adams. 1984. Breeding and fertile period for female *Chionoecetes bairdi* (Decapoda, Majidae). *J. Crustac. Biol.* **4**: 589–594.
- Pelletier, N., A. Fraser, D. Gauthier, M. Laviolette, and M. Moriyasu. 1998. Mise en œuvre d'une méthode pour l'analyse biochimique du mécanisme d'accouplement chez le crabe des neiges (*Chionoecetes opilio*). *Rapp. Tech. Can. Sci. Halieut. Aquat.* **2200**: 25 pp.
- Pitnick, S. 1993. Operational sex ratios and sperm limitation in populations of *Drosophila pachea*. *Behav. Ecol. Sociobiol.* **33**: 383–391.
- Pitnick, S., and T. A. Markow. 1994. Male gametic strategies: sperm size, testes size, and the allocation of ejaculate among successive mates by the sperm-limited fly *Drosophila pachea* and its relatives. *Am. Nat.* **143**: 785–819.
- Ridley, M. 1983. *The Explanation of Organic Diversity. The Comparative Method and Adaptations for Mating*. Clarendon Press, Oxford. 272 pp.
- Robinson, B. W., and R. W. Doyle. 1985. Trade-off between male reproduction (amplexus) and growth in the amphipod *Gammarus lawrencianus*. *Biol. Bull.* **168**: 482–488.
- Rondeau, A. 2000. Économie de sperme par les mâles et succès reproducteur des femelles primipares chez le crabe des neiges, *Chionoecetes opilio*, en fonction du contexte sexuel. Master's thesis, Université du Québec à Rimouski, Rimouski, Canada. 101 pp.
- Rowe, L., G. Arnqvist, A. Sih, and J. J. Krupa. 1994. Sexual conflict and the evolutionary ecology of mating patterns: water striders as a model system. *Trends Ecol. Evol.* **9**: 289–293.
- Sainte-Marie, B. 1993. Reproductive cycle and fecundity of primiparous and multiparous female snow crab, *Chionoecetes opilio*, in the north-west Gulf of Saint Lawrence. *Can. J. Fish. Aquat. Sci.* **50**: 2147–2156.
- Sainte-Marie, B., and C. Carrière. 1995. Fertilization of the second clutch of eggs of snow crab, *Chionoecetes opilio*, from females mated once or twice after their molt to maturity. *Fish. Bull. (Seattle)* **93**: 759–764.
- Sainte-Marie, B., and F. Hazel. 1992. Moulting and mating of snow crabs, *Chionoecetes opilio* (O. Fabricius), in shallow waters of the northwestern Gulf of Saint Lawrence. *Can. J. Fish. Aquat. Sci.* **49**: 1282–1293.
- Sainte-Marie, B., and G. A. Lovrich. 1994. Delivery and storage of sperm at first mating of female *Chionoecetes opilio* (Brachyura: Majidae) in relation to size and morphometric maturity of male parent. *J. Crustac. Biol.* **14**: 508–521.
- Sainte-Marie, G., and B. Sainte-Marie. 1999. Reproductive products in the adult snow crab (*Chionoecetes opilio*). II. Multiple types of sperm cells and of spermatophores in the spermathecae of mated females. *Can. J. Zool.* **77**: 451–462.
- Sainte-Marie, B., S. Raymond, and J.-C. Brêthes. 1995. Growth and maturation of the benthic stages of male snow crab, *Chionoecetes opilio* (Brachyura: Majidae). *Can. J. Fish. Aquat. Sci.* **52**: 903–924.
- Sainte-Marie, B., J.-M. Sévigny, B. D. Smith, and G. A. Lovrich. 1996. Recruitment variability in snow crab (*Chionoecetes opilio*): pattern, possible causes, and implications for fishery management. Pp. 451–478 in *Proceedings of the International Symposium on Biology, Management, and Economics of Crabs from High Latitude Habitats*, B. Baxter, ed. Lowell Wakefield Fisheries Symposium Series, University of Alaska Fairbanks, Alaska Sea Grant College Program Report 96-02.
- Sainte-Marie, B., J.-M. Sévigny, and Y. Gauthier. 1997. Laboratory behavior of adolescent and adult males of the snow crab (*Chionoecetes opilio*) (Brachyura: Majidae) mated noncompetitively and competitively with primiparous females. *Can. J. Fish. Aquat. Sci.* **54**: 239–248.
- Sainte-Marie, B., N. Urbani, J.-M. Sévigny, F. Hazel, and U. Kuhnlein. 1999. Multiple choice criteria and the dynamics of assortative mating during the first breeding season of female snow crab *Chionoecetes opilio* (Brachyura, Majidae). *Mar. Ecol. Prog. Ser.* **181**: 141–153.
- Sainte-Marie, G., B. Sainte-Marie, and J.-M. Sévigny. 2000. Ejaculate-storage patterns and the site of fertilization in female snow crabs (*Chionoecetes opilio*: Brachyura, Majidae). *Can. J. Zool.* **78**: 1902–1917.
- Shapiro, D. Y., A. Marconato, and T. Yoshikawa. 1994. Sperm economy in a coral reef fish. *Thalassoma bifasciatum*. *Ecology* **75**: 1334–1344.
- Smith, R. L., ed. 1984. *Sperm Competition and the Evolution of Animal Mating Systems*. Academic Press, New York. 661 pp.
- Sokal, R. R., and F. J. Rohlf. 1995. *Biometry*, 3rd ed. W. H. Freeman, New York. 887 pp.
- Sparkes, T. C., D. P. Keogh, and R. A. Pary. 1996. Energetic costs of mate guarding behavior in male stream dwelling isopods. *Cecologia* **106**: 166–171.
- Stevens, B. G., W. E. Donaldson, J. A. Haaga, and J. E. Munk. 1993. Morphometry and maturity of paired Tanner crabs, *Chionoecetes bairdi*, from shallow- and deepwater environments. *Can. J. Fish. Aquat. Sci.* **50**: 1504–1516.
- Stevens, B. G., J. A. Haaga, and W. E. Donaldson. 1994. Aggregative mating of Tanner crabs, *Chionoecetes bairdi*. *Can. J. Fish. Aquat. Sci.* **51**: 1273–1280.
- Trivers, R. L. 1972. Parental investment and sexual selection. Pp. 136–

- 179 in *Sexual Selection and the Descent of Man, 1871–1971*, B. Campbell, ed., Aldine Press, Chicago.
- Urbani, N., B. Sainte-Marie, J.-M. Sévigny, D. Zadworny, and U. Kuhnlein. 1998.** Sperm competition and paternity assurance during the first breeding period of female snow crab *Chionoecetes opilio* (Brachyura: Majidae). *Can. J. Fish. Aquat. Sci.* **55**: 1104–1113.
- Vepsäläinen, K., and R. Savolainen. 1995.** Operational sex ratios and mating conflicts between the sexes in the water strider *Gerris lacustris*. *Am. Nat.* **146**: 869–880.
- Wada, S., K. Tanaka, and S. Goshima. 1999.** Precopulatory mate guarding in the hermit crab *Pagurus middendorffii* (Brandt) (Decapoda: Paguridae): effects of population parameters on male guarding duration. *J. Exp. Mar. Biol. Ecol.* **239**: 289–298.
- Warner, R. R., D. Y. Shapiro, A. Marcanato, and C. W. Petersen. 1995.** Sexual conflict: males with the highest mating success convey the lowest fertilization benefits to females. *Proc. R. Soc. Lond. B* **262**: 135–139.
- Watson, J. 1972.** Mating behavior in the spider crab, *Chionoecetes opilio*. *J. Fish. Res. Board Can.* **29**: 447–449.
- Wedell, N., and P. A. Cook. 1999.** Butterflies tailor their ejaculate in response to sperm competition risk and intensity. *Proc. R. Soc. Lond. B* **266**: 1033–1039.
- Wilber, D. II. 1989.** The influence of sexual selection and predation on the mating and postcopulatory guarding behavior of stone crabs (Xanthidae, *Menippe*). *Behav. Ecol. Sociobiol.* **24**: 445–451.
- Yamamura, N., and V. Jormalainen. 1996.** Compromised strategy resolves intersexual conflict over precopulatory guarding duration. *Evol. Ecol.* **10**: 661–680.
- Yamasaki, A., S. Fujita, K. Uchino, and T. Toshima. 1994.** Research into the ecology of snow crabs in the waters off Kyoto Prefecture—IX. Numbers of sperm in the spermathecas of female snow crabs. *Res. Rep. Kyoto Inst. Ocean Fish. Sci.* **17**: 19–24 (*Can. Transl. Fish. Aquat. Sci.* 5663).

The Origins of The Grass Foundation

STEVEN J. ZOTTOLI

*Department of Biology, Williams College, Williamstown, Massachusetts 01267, and
The Marine Biological Laboratory, Woods Hole, Massachusetts 02543*

Introduction

In the fall of 1935, Albert M. Grass and Ellen H. Robinson both came to the Department of Physiology at Harvard Medical School (HMS). This entirely fortuitous confluence of their lives led to their marriage, to a commercial endeavor—the Grass Instrument Company—that would provide equipment of high quality to neuroscientists and other physiologists for over half a century, and finally to the formation of The Grass Foundation, which has benefited the neuroscience community since 1955.

The Department of Physiology at Harvard—the seedbed for these accomplishments—had a deep-rooted commitment to providing both financial and moral support to scientists who were at the beginning of their careers. Albert and Ellen clearly benefited from this commitment, for it generated interactions and collaborations that led to and facilitated the success of the Grass Instrument Company and then the Foundation.

Thus, the origins of The Grass Foundation must be sought, not only in the conjoined histories and proclivities of Albert M. and Ellen R. Grass, but also in scientific and educational developments that took place in the HMS Department of Physiology between 1906 and 1935, well before Albert and Ellen met there. This essay is an attempt to dissect those tangled threads: it ends with a discussion of The Grass Foundation's hallmark program—the Grass Fellowship Program at the Marine Biological Laboratory in Woods Hole, Massachusetts—and the impact that this program has had on neuroscience.

Albert M. Grass and Ellen H. Robinson

Albert Melvin Grass (1910–1992) was born in Quincy, Massachusetts, on September 3, 1910, to Henry J. Grass and Bertha (Martin) Grass. After graduating from Quincy High

School, he funded his college education by working at Samson Electric Company testing and installing the amplifiers and systems that provided sound for films (Marshall, 1980; Henry, 1992). He was successful, both academically and financially, and the B.Sc. degree in electrical engineering was duly awarded by MIT in 1934. Albert remained at MIT to work on servo-mechanisms used to simulate earthquakes in the study of strains acting on model water towers and other structures (Marshall, 1980).

In May of 1935, Frederic A. Gibbs—a research fellow in neurology at the HMS Department of Physiology—contracted with Albert Grass to build a 3-channel electroencephalograph (EEG). Albert and his brother Everett worked in the basement of their father's house and finished the project early in the fall of 1935 (Marshall, 1980; Grass, 1984).

This accomplishment, completed in only three months, led to Albert's being hired as a part-time Research Instrument Engineer by the HMS Department of Physiology, and he remained in that position from 1935 until 1943. As part of this job, he continued to improve the EEG (Grass Instrument Co., 1971; Grass, 1984) and its applications (Grass and Gibbs, 1938). In addition, he worked closely with scientists, tailoring equipment to their needs (*e.g.*, square wave stimulators and amplifiers; Forbes and Grass, 1937; Marshall, 1980).

Ellen Harriet Robinson (1914–2001) was born in Taunton, Massachusetts, on March 29, 1914, the daughter of Laura (Waldron) Robinson and Francis James Robinson. She graduated from Taunton High School in 1931 and went to Radcliffe College, receiving her A.B. degree in Biology in 1935. She continued her education at Harvard University with Morgan "Kelly" Upton (1898–1984) and received a Masters degree from Radcliffe College in 1936; her thesis was entitled "Three Experiments in Audition."

On Upton's recommendation, Ellen decided to immerse herself in "a broader field of brain function" (Marshall,

1995) and began graduate work in the Department of Physiology of HMS in the fall of 1935 (Marshall, 1980, 1995). A special arrangement was made with Radcliffe College so that she could take a course in "Research" (Marshall, 1995), and she was supported by a Porter Fellowship in Physiology (1935–1936) from the American Physiological Society (Howell and Greene, 1938; Fenn, 1963). Alfred C. Redfield (1890–1983) was her initial sponsor on a project entitled "Auditory Action Potentials" (Fenn, 1963; Brobeck *et al.*, 1987), but her work was ultimately conducted under the sponsorship of Hallowell Davis (Kemp *et al.*, 1937; Fenn, 1963). Ellen collaborated with a number of scientists, including Arthur James "Bill" Derbyshire (Grass, 1980), Edward H. Kemp, and Georges Coppée, a Fellow of the C.R.B. Educational Foundation, Institute de Physiologie, Liège. Her studies of the responses of the brainstem to auditory stimulation led to three publications (Kemp and Robinson, 1937; Kemp *et al.*, 1936, 1937).

Ellen Robinson and Albert Grass met in the fall of 1935 and were married on June 28, 1936. Ellen continued as a Ph.D. candidate in the Department of Biology at Harvard University, recording from the auditory cortex of rabbit in the laboratory of the noted physiological psychologist Karl Spencer Lashley (1890–1958). Soon, however, she decided to devote herself "to motherhood and doing whatever I could to help Albert provide equipment to a growing number of scientists" (Marshall, 1995).

The Development of Electroencephalography at the HMS Department of Physiology and the Formation of the Grass Instrument Company

The report of voltage changes recorded through the cranium of humans by Hans Berger (electroencephalogram, EEG; Berger, 1929) and his observations of EEG variations in patients with epilepsy (Berger, 1932; Gibbs *et al.*, 1936) were the basis for continued EEG studies of epilepsy in the United States.

At the time, Stanley Cobb (1887–1968) and William G. Lennox (1884–1960) were experts on epilepsy (*e.g.*, Cobb, 1922; Lennox and Cobb, 1928; Lennox, 1936; see White, 1984, for Cobb's complete bibliography) carrying out their investigations at Harvard Medical School (Hughes and Stone, 1990). In 1929, Cobb offered Frederic A. Gibbs (1903–1992), who had just received his M.D. from Johns Hopkins, a fellowship in neuropathology to work on epilepsy. Gibbs worked in the Lennox lab where he met Erna Leonhardt; the couple were married in 1930 and were collaborators thereafter (Hughes and Stone, 1990).

The Gibbsses wanted to record EEGs from epileptic patients, and Hallowell Davis' engineer, E. Lovett Garceau (1906–1966), had built amplifiers and a portable EEG that could be used for such recordings (Garceau and Davis, 1934, 1935; Garceau and Forbes, 1934). Encouraged by

Cobb, the Gibbsses approached Davis to be a collaborator, and Davis enthusiastically endorsed their plan (White, 1984). With the departure of the engineer, Garceau, and the need for EEG machines with more than one channel, Frederic Gibbs sought out advice at the Massachusetts Institute of Technology. There he met Albert Grass (Marshall, 1980; Grass, 1984). With funding from the Macy Foundation, he contracted with Albert Grass in May of 1935 to "build three channels of EEG amplifiers to drive the Western Union Morse Code inkwriting undulator" (Grass, 1984; Hughes and Stone, 1990).

The Gibbsses went off for the summer to attend the International Congress of Physiologists in Leningrad and Moscow, and to visit Berger and engineer J. F. Tönnies in Germany. In August of 1935, rather late in the summer, Frederic Gibbs mailed a sketch of Tönnies' neuropolygraph (designed for A. Kornmüller's animal studies) to Albert Grass (Grass, 1984; Hughes and Stone, 1990). By that time, the EEG machine being constructed by Albert and Everett Grass in Quincy must have been well along, for when the Gibbsses returned in the fall, it was finished, as mentioned above. This EEG was used by Lennox, Frederic and Erna Gibbs, and Davis in their pioneering investigations, which demonstrated the power of the EEG in the diagnosis of epilepsy (Gibbs *et al.*, 1935, 1936, 1937; Brazier, 1968).

The demand for EEG machines increased markedly during the 1940s. To meet this demand, Albert began to manufacture commercial instruments (Marshall, 1987). Thus, the small business that started in a basement in 1935 continued as a partnership between Albert and Ellen Grass, and ultimately developed and grew to become, 10 years later, the Grass Instrument Company. The success of the Company was due to the balance between Albert's engineering skills and Ellen's scientific expertise, which was critical in the proper design of equipment to meet the needs of neurophysiologists (Fig. 1). Instruments were designed for "convenience, durability and serviceability" (Morison, 1979).

The Grass Instrument Company was never a typical business. In the early years, employees and many of the customers were warm and loyal friends of Albert and Ellen (Morison, 1979), and neurophysiological equipment was loaned to investigators throughout the world, and especially to Grass Fellows and courses at the Marine Biological Laboratory (MBL). To Albert and Ellen, the Company was always meant to contribute "to the development of human knowledge and the search for basic scientific truth." (Grass Instrument Co., 1967). They took great care to ensure that equipment was being properly used for the benefit of the patient. Ricardo Miledi recalls, "When I was in Mexico, I remember on more than one occasion, seeing a letter [from the Grasses] inquiring about doctors that intended to purchase their most advanced EEGs and other equipment. Albert and Ellen were very concerned that their equipment

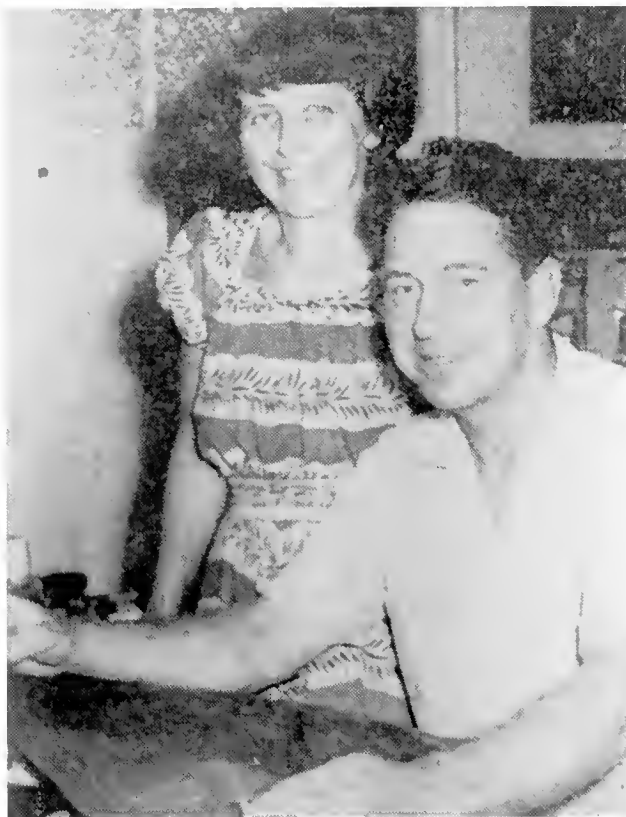


Figure 1. Albert and Ellen Grass in 1955, the year that The Grass Foundation was formed. This picture was copied from a newspaper article entitled "Doctors Told of Findings by Quincy 'Brain' Machine" in the Quincy Patriot Ledger, Saturday, October 8, 1955.

be used wisely for the benefit of the patients and for research, and not merely to extract money from the patients."

Department of Physiology at Harvard Medical School

Albert and Ellen Grass's success was clearly due, in part, to the support they received from established researchers in the Department of Physiology at Harvard Medical School. Walter B. Cannon and Alexander Forbes were especially critical in this regard.

"Speaking personally now," Ellen once said, "Dr. Cannon made very many things possible for Albert and for me. He invested in us at a time when biomedical engineering was indeed in its infancy, and the role for women in science practically negligible" (Grass, 1970).

Walter B. Cannon (1871–1945) served as the George Higginson Professor of Physiology at Harvard Medical School for 36 years (1906–1942). For this entire period, he was chairman of the Department of Physiology and an Emeritus for his last three years. He made many important contributions to our understanding of how the human body functions: the use of Roentgen rays to investigate gastrointestinal motility (Cannon, 1898; Cannon, 1911; Brooks *et*

al., 1975; Barger, 1981), the effects of emotions on the functional state of the body (Cannon, 1915; Davenport, 1981), the basis of surgical shock (Cannon, 1923), the constancy of the internal environment or homeostasis (Cannon, 1939), autonomic neuro-effector systems (Cannon and Rosenblueth, 1937), and the effects of denervation on various tissues (Cannon and Rosenblueth, 1949).

Walter Cannon spent his undergraduate years at Harvard University and continued on at Harvard Medical School, where the faculty held that interested medical students should be encouraged to conduct original research. Thus, in the first semester of his medical training Cannon and fellow student Albert Moser were encouraged by Henry P. Bowditch (1840–1911) to conduct a study on deglutition (Benison *et al.*, 1987). Later, as a third-year medical student, Walter Cannon was approached by William Norton Bullard (1853–1931), a neurologist at Boston City Hospital, who offered to fund further research (Taylor, 1931).

These early research experiences clearly had a profound influence on the development of Cannon's scientific philosophies.

Every man active in investigation has more problems in mind that he can work at himself. A part of his service to the world consists in training others by giving to others these problems to work at under his direction. These "others" are ordinarily his students.—young men who have been stimulated by his example. They are not yet established in life, they require remuneration until they have done enough work to warrant their being taken into independent positions. They should receive during these years of training (which are very likely to be productive of good results in research) sufficient compensation to afford comfortable support (Benison *et al.*, 1987).

Cannon is generally considered to have been exemplary in his scientific conduct and his concern for human welfare (Cannon, 1945; Forbes, 1945; Morison, 1945; Davis, 1975). He "saw that the freedom and beneficence of science could be guaranteed only within the framework of a just society, national and international" (Grass, 1970), and was committed to providing promising young scientists, independent of nationality, the opportunity to participate and contribute to the advancement of science (Morison, 1945).

One such scientist was **Arturo Rosenblueth (1900–1970)**¹ who came to Harvard from Mexico as a Guggenheim Fellow from 1930 to 1932 to work with Cannon. He quickly became Cannon's "favorite son" and secured a position in the Department of Physiology. Their collaborations continued for the next 14 years (e.g., Cannon and Rosenblueth, 1937, 1949).

Cannon and Rosenblueth mentored several scientists who would ultimately become founding and early trustees of The

¹ The names of the founding and early trustees of the Grass Foundation are printed in bold type in this section of the paper. E-mail: Steven.J.Zottoli@Williams.edu.

Table 1

*Founding trustees and early trustees of The Grass Foundation**Founding trustees*

Alexander Forbes
 Albert M. Grass
 Ellen R. Grass
 Frederic A. Gibbs
 William G. Lennox*
 Robert S. Morison
 Arturo Rosenblueth*
 Richard R. Towle
 Robert A. Zottoli

Early trustees

George H. Acheson, 1961
 Donald B. Lindsley, 1958
 Fiorindo A. Simeone, 1968

* Although Lennox and Rosenblueth are not listed as original members of the Corporation in the Constitution and Bylaws of The Grass Foundation, they are recognized as founding members in the minutes of The Grass Foundation.

Grass Foundation (Table 1). **Alexander Forbes (1882–1965)** as a fourth-year medical student was encouraged by Cannon to become involved in research. After receiving his M.D. degree in 1910 from Harvard Medical School, Forbes studied with C. S. Sherrington (1857–1952) for two years, and briefly with Lucas in 1912; afterwards, he returned to Harvard and the Department of Physiology (Fenn, 1969; Davis, 1970; Eccles, 1970). Forbes added a strong engineering background to the department and was continuously at the forefront of technological advances that he applied to neurophysiological investigations. These included the use of the vacuum tube amplifier in conjunction with a string galvanometer to record action currents in nerve and muscle (Forbes and Thacher, 1920, see also Gasser and Newcomer, 1921; Forbes *et al.*, 1931; Grass, 1984; Frank, 1986; Seyfarth, 1996), the study of reflex activity (Forbes, 1922; Davis, 1975; Seyfarth, 1996), and the use of microelectrodes for extracellular recording from cortical cells (Renshaw *et al.*, 1940; Brazier, 1968).

In fact, Forbes' technical and analytical strengths, along with those of Hallowell Davis (Forbes *et al.*, 1931), complemented the more integrative approaches of Cannon and Rosenblueth (Cannon, 1945). Cannon's encouragement of Forbes as a young medical student could not have affected a more appreciative and capable individual. Alexander Forbes quickly adopted the philosophy of encouraging scientists in his own way. He "anonymously supported others in the department of physiology" (Davis, 1970; Seyfarth, 1996).

One of the many young medical students supported by Forbes was Hallowell Davis (1896–1992). He received his B.A. degree in 1918 and the M.D. degree in 1922 from Harvard, worked for a year at Cambridge University in England with Edgar D. Adrian, and then returned to Har-

vard in 1923 as an Instructor in the Department of Physiology (Davis, 1991; Galambos, 1998). Some of his studies at Harvard include the all-or-none nature of the nerve impulse (Davis *et al.*, 1926), the use of the EEG in the study of epilepsy (Gibbs *et al.*, 1935), recordings from single units in the "auditory nerve" of cats (Galambos and Davis, 1943; the recordings turned out to be from cell bodies of the cochlear nucleus, Davis, 1975), and the tolerance of the human ear to loud sounds (Davis *et al.*, 1950). Hallowell Davis would become the sponsor of Ellen Grass' research and an exponent of EEG recording at Harvard.

Donald B. Lindsley (currently Trustee Emeritus) had come to Harvard Medical School with a National Research Council Fellowship to work with Forbes and Davis in 1933. During this period, Lindsley recorded motor unit responses (Lindsley, 1934, 1935a) and pioneered the use of the electromyogram in neuromuscular disorders (*e.g.*, Lindsley, 1935b, 1936; see Lindsley, 1995, for a review).

Arturo Rosenblueth had encouraged **George H. Acheson (1912–2000)**, a first-year medical student, and **Fiorindo A. Simeone (1908–1990)**, a third-year medical student, to consider conducting original research. Both contributed to the scientific productivity in the department (*e.g.*, Rosenblueth and Simeone, 1934, 1938a, b; Acheson, 1938; Acheson *et al.*, 1936, 1942; Simeone *et al.*, 1938) and went on to distinguished medical careers.

Robert Morison (1906–1986) received an undergraduate degree from Harvard in 1930 and the M.D. in 1935. He was encouraged to pursue research by his mentor, Rosenblueth, during his medical school years. "He [Morison] was a man of great and thoughtful learning but one who, above all, wanted to understand the meaning of life and the significance of science for that fundamental issue. He understood what it was to make a moral vocation of one's intellectual work, an effort that requires not only reading, writing, and thinking, but also something else: the living out, in daily life, of the values and virtues that animate that work." (Callahan, 1987). Morison collaborated with many of those present in the Department of Physiology in the 1930s (*e.g.*, Rosenblueth and Morison, 1934; Rosenblueth *et al.*, 1936) and went on to Rockefeller University and then Cornell (Eisner *et al.*, 1986–1987).

The Formation of The Grass Foundation

As the number of requests for financial support of neuroscience endeavors grew, Albert and Ellen recognized that a mechanism must be found to evaluate proposals and make decisions (Morison, 1979). The Grass Charity Trust was formed on December 31, 1948, and charitable disbursements were made after June 27, 1951. This Trust donated most of its assets to The Grass Foundation (The Grass Foundation minutes, 1958), which was formed in 1955 "to assist in advancing knowledge principally in the field of



Figure 2. Four of the original Trustees of The Grass Foundation. From left to right: Albert Grass, Frederic Gibbs, Ellen Grass, Robert Morison, and Erna Gibbs (not a Trustee) at the III International Congress of Electroencephalography and Clinical Neurophysiology held in Boston from August 17–21, 1953.

neurophysiology, and including allied fields of medicine and science" (Article 2 Section 1 of The Grass Foundation Constitution and Bylaws).

As we have seen, most of the founding and early trustees of the Foundation were, at some time in the 1930s, members of the Department of Physiology at Harvard Medical School (Fig. 2; Table 1). This is only fitting, because their commitment to the support of young scientists, their own exemplary performance at the bench, and their concern for human welfare (Morison, 1979) reflect the basic principles that have molded The Grass Foundation. The Foundation currently supports programs within the Society for Neuroscience, at the MBL, and at other institutions. The Grass Fellowship Program at the MBL was one of the first and most important projects of The Grass Foundation, and it continues to flourish.

The Association of Albert and Ellen Grass and The Grass Foundation With the Marine Biological Laboratory at Woods Hole

Albert and Ellen Grass's affinity for the MBL developed over many years and is based on several associations. For example, Alexander Forbes had a natural affection for the Woods Hole area. He spent summers on Naushon Island, which is still owned by the Forbes family, and he was a distinguished investigator at the MBL, publishing research done there with Catharine Thacher (Forbes and Thacher, 1925; Forbes, 1933). Albert Grass was undoubtedly at-

tracted to the MBL because, as a center of neurophysiology, it was regularly visited in the summers by scientists who were actively involved in the development of new equipment. With this common interest, Albert developed lasting friendships with several MBL scientists, including Harry Grundfest (1904–1983) and Stephen Kuffler (1913–1980). Finally, Ellen was drawn to the MBL by her passion for the marine environment and the animals that live there. This passion was particularly evident in her Grass Instrument Company Calendars and the "live displays" presented at the annual meetings of the Society for Neuroscience.

Of the initiatives in support of basic science at the MBL, the Grass Fellowship Program most closely embodies the philosophy of the founding trustees who had "a love for the adventure of new ideas, a priority for assisting young investigators, and a program focus to direct its resources to the growth of neurophysiology" (Grass, 1987). Beginning with two fellows in 1951 under the auspices of the Grass Charity Trust, more than 400 young neuroscientists have spent summers at the MBL conducting independent research.

Established in 1959, the Forbes Lectureship is an integral part of the Grass Fellowship Program. Each summer, the Trustees of The Grass Foundation bring one of the world's outstanding neuroscientists to the MBL "to honor the outstanding achievements of Dr. Alexander Forbes as a pioneer and major contributor to the field of neurophysiology, who has always been an inspired teacher of young students." (The Grass Foundation minutes, December 11, 1958). The

Table 2

Grass Fellows from 1951 to 1961

Year	Fellow
1951	Hal C. Becker Samuel M. Peacock, Jr.
1952	Ellis C. Berkowitz
1953	Donald M. Maynard Y. Zotterman
1954	Daniel D. Hansen David D. Potter
1955	Ricardo Miledi Yutaka Oomura Joaquin Remolina William K. Stephenson
1956	Lionel Adelson
1957	Stanley M. Crain Clarence Hardiman Joan Taylor*
1958	Michael V. L. Bennett John P. Reuben William H. Rickles, Jr.
1959	Shirley H. Bryant Raymond J. Lipicky Charles F. Stevens
1960	Stephen T. Kitai Leslie B. Reynolds
1961	Bernice Grafstein Zach W. Hall Walter Herzog Robert H. Wurtz

* Her fellowship was carried out at UCLA.

Forbes Lecturer not only presents two lectures as part of the MBL's Lecture Series, but also shares space with the Fellows in the Grass Laboratory. Forbes inaugurated the series with a pair of lectures, on "The Growth of Neurophysiology" and on "Electrophysiology of Color Vision."

Many Grass Fellows have gone on to become leaders in neuroscience (Table 2), and many have come back to the MBL as investigators, course directors, instructors, Forbes Lecturers, and as directors and associate directors of the Grass Laboratory.

Ricardo Miledi is an example of a Grass Fellow who has had a major impact on neuroscience. He was born in Mexico City in 1927, received his B.Sc. from the Instituto Científico y Literario, Chihuahua, in 1945 and his M.D. from the Universidad Nacional Autónoma de México in 1955. Miledi and Joaquin Remolina were working with Arturo Rosenblueth and Juan García Ramos at the Instituto Nacional de Cardiología (García Ramos and Miledi, 1953, 1954; Rosenblueth *et al.*, 1954) when Albert Grass and Steve Kuffler came by to visit Rosenblueth. Informed about the Grass Fellowship Program by the visitors, Miledi and Remolina came to the MBL as fellows in 1955 (Fig. 3).

There was no Grass Laboratory or formal program at that time, and fellows generally worked in separate spaces and

did not interact with one another a great deal. Steve Kuffler, Harry Grundfest (1904–1983), and their collaborators were perennial investigators at the MBL, and both were Forbes Lecturers, in 1975 and 1979, respectively. They acted as mentors for Miledi and other Grass Fellows in the early years of the program (Zottoli, 1990). Albert and Ellen Grass would also visit the MBL periodically to make sure that the Grass Fellows had what they needed in the way of equipment, space, and support.

While at the MBL, Miledi worked on lobster and crayfish stretch receptors and the squid giant axon (Miledi, 1957). Miledi has gone on to publish over 460 scientific articles, and he is one of two neuroscientists to be chosen more than once by the Trustees of The Grass Foundation as the Forbes Lecturer (the other is Theodore H. Bullock, in 1963 and 1991). Miledi presented some of his and Bernard Katz's seminal work on neuromuscular transmission at the MBL in 1964 as the sixth Forbes Lecturer. The topic of his two lectures was "Localization of ACh receptors and cholinesterase in muscle fibres." He returned as the Forbes Lecturer in 1990 (Fig. 3) and delivered two lectures on pioneering work that utilized frog oocytes to study native receptors and express exogenous messenger RNA (Kusano *et al.*, 1977, 1982; Barnard *et al.*, 1982). The subject of his two lectures was "How to study the brain using frog oocytes." Dr. Miledi has served two terms as a Trustee of The Grass Foundation (1992–1995; 1997–2000). He is currently a Distinguished Professor in the Department of Neurobiology and Behavior at the University of California, Irvine.

The philanthropic largess of Albert and Ellen goes well beyond the MBL and has benefited the neuroscience community in many other ways. For example, "individuals known to be sound investigators, working under budgetary or foreign exchange difficulties, often found themselves the recipients of indefinite loans" of neurophysiological equipment through the auspices of the Grass Instrument Company (Morison, 1979). Ricardo Miledi remembers, "Joaquin Remolina and I were once asked to make a list of Grass equipment to be bought for the Department of Physiology at the Institute of Cardiology in Mexico. We made a big list that was sent to the Grass Instrument Company and were looking forward, with great excitement, to the day when the equipment would arrive. Then, to our great consternation, there was a big devaluation of the peso and we were asked to send a new order with a good number of items deleted. Later, when the shipment arrived we were all extremely pleased to see that all the items in our original list had arrived and a few extra ones had been included, as if to compensate for our transient worries. I wonder if any other company exists that would do that?"

Albert Grass died in Quincy, Massachusetts, on May 29, 1992, and Ellen died 9 years later on June 14, 2001, also in Quincy. The Grass Foundation that embodies their ideals continues to be committed to providing general support for

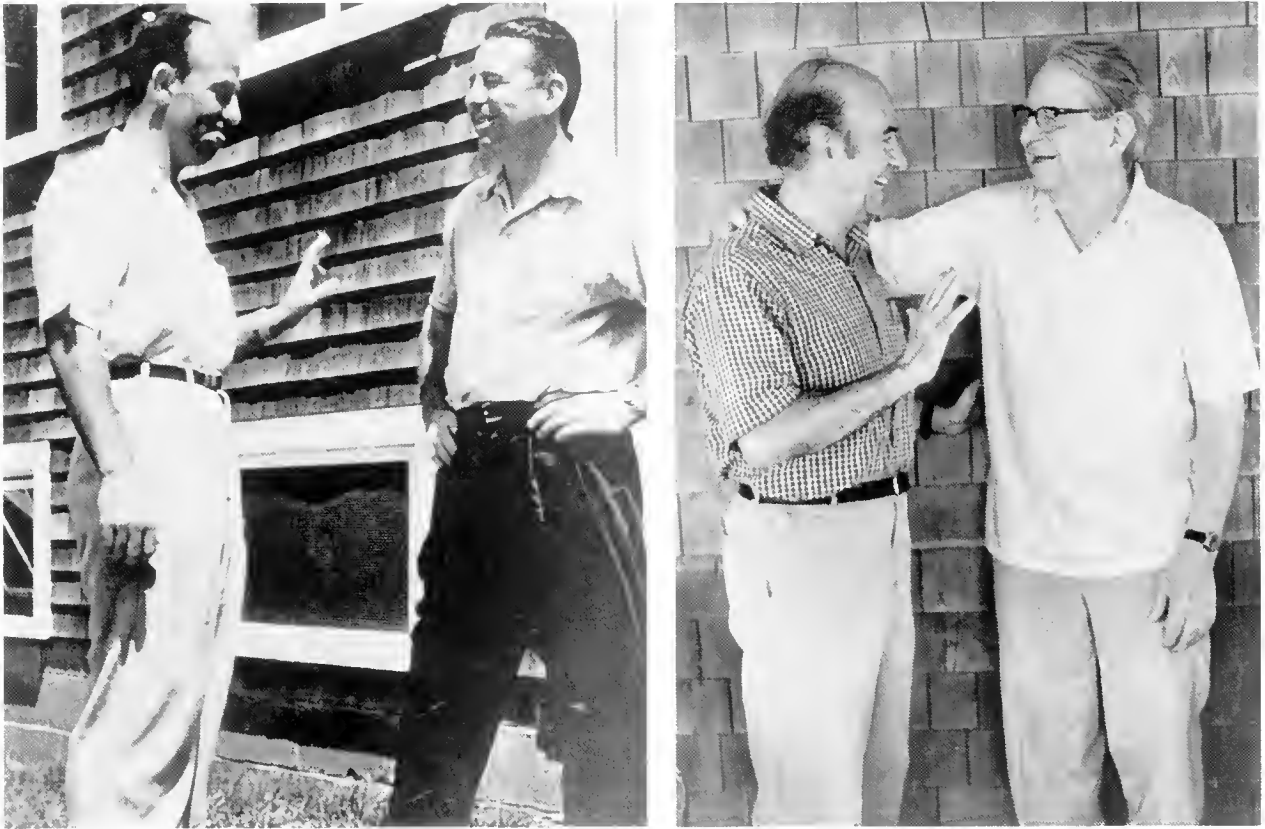


Figure 3. Albert Grass and Ricardo Miledi in Woods Hole, Massachusetts. The picture on the left was taken in 1955 at the Marine Biological Laboratory when Miledi was a Grass Fellow. The picture on the right was a reenactment of the 1955 photograph taken in 1990 at the National Academy of Sciences in Woods Hole when Miledi was a Forbes Lecturer for a second time in 1990. The 1990 photograph was taken by Steve Zottoli.

"excellent science." The tireless efforts of Albert and Ellen to monitor the pulse and flow of neuroscience have led to initiatives in support of the field, especially in helping those in need or just starting out. The greatest achievements of the Foundation's initiatives, such as the Grass Fellowship Program at the MBL, have resulted from the ability of the Trustees to *listen, hear* and *respond* to needs of scientists in a rapidly changing discipline.

Acknowledgments

I would like to thank Ernst-August Seyfarth for his help and support during this project. George Acheson, Ellen Grass, Hank Grass, Ron Hoy, Don Lindsley, Ricardo Miledi, John Reuben, and Richmond Woodward provided important suggestions for the improvement of an earlier version of this manuscript. I also thank Helena Warburg for her efforts in providing biographical information. Mrs. Elin L. Wolfe at the Countway Library of Medicine deserves special mention for the research she did on Catherine Thacher. Finally, I would like to acknowledge the help, enthusiasm, and patience of Mike Greenberg.

Literature Cited

- Acheson, G. H. 1938. The topographical anatomy of the smooth muscle of the cat's nictitating membrane. *Anat. Rec.* **71**: 297-311.
- Acheson, G. H., A. Rosenblueth, and P. F. Partington. 1936. Some afferent nerves producing reflex responses of the nictitating membrane. *Am. J. Physiol.* **115**: 308-316.
- Acheson, G. H., E. S. Lee, and R. S. Morison. 1942. A deficiency in the phrenic respiratory discharges parallel to retrograde degeneration. *J. Neurophysiol.* **5**: 269-273.
- Barger, A. C. 1981. New technology for a new century: Walter B. Cannon and the invisible rays. *Physiologist* **24**: 6-14.
- Barnard, E. A., R. Miledi, and K. Sumikawa. 1982. Translation of exogenous messenger RNA coding for nicotinic acetylcholine receptors produces functional receptors in *Xenopus* oocytes. *Proc. R. Soc. Lond. B* **215**: 241-246.
- Benison, S., A. C. Barger, and E. L. Wolfe. 1987. *Walter B. Cannon: The Life and Times of a Young Scientist*. The Belknap Press of Harvard Univ. Press, Cambridge, MA. 520 pp.
- Berger, H. 1929. Über das Elektroenkephalogramm des Menschen. I. *Arch. Psychiatr.* **87**: 527-570.
- Berger, H. 1932. Über das Elektroenkephalogramm des Menschen. *Arch. Psychiatr.* **97**: 6-26.
- Brazier, M. A. B. 1968. *The Electrical Activity of the Nervous System*. Williams and Wilkins, Baltimore. 317 pp.
- Brobeck, J. R., O. E. Reynolds, and T. A. Appel, eds. 1987. *History of*

- the American Physiological Society, The First Century 1887-1987.* The American Physiological Society, Bethesda, MD.
- Brooks, C. McC., K. Koizumi, and J. O. Pinkston, eds. 1975.** *The Life and Contributions of Walter Bradford Cannon 1871-1945.* SUNY Downstate Medical Center, Brooklyn. 264 pp.
- Callahan, D. 1987.** Robert S. Morison, M.D. Hastings Report February, 1987.
- Cannon, W. B. 1898.** The movements of the stomach as studied by means of the Röntgen rays. *Am. J. Physiol.* **1**: 359-382.
- Cannon, W. B. 1911.** *The Mechanical Factors of Digestion.* Edward Arnold, London. 227 pp.
- Cannon, W. B. 1915.** *Bodily Changes in Pain, Hunger, Fear and Rage.* Appleton, New York. 311 pp.
- Cannon, W. B. 1923.** *Traumatic Shock.* Appleton, New York. 201 pp.
- Cannon, W. B. 1939.** *The Wisdom of the Body.* W. W. Norton, New York. 333 pp.
- Cannon, W. B. 1945.** *The Way of an Investigator.* W. W. Norton, New York. 229 pp.
- Cannon, W. B., and A. Rosenblueth. 1937.** *Autonomic Neuro-Effector Systems.* Macmillan, New York. 229 pp.
- Cannon, W. B., and A. Rosenblueth. 1949.** *The Supersensitivity of Denervated Structures: A Law of Denervation.* Macmillan, New York. 245 pp.
- Cobb, S. 1922.** A case of epilepsy with a general discussion of the pathology. *Med. Clin. North Am.* **5**: 1403-1420.
- Davenport, H. W. 1981.** Signs of anxiety, rage, or distress. *Physiologist* **24**: 1-5.
- Davis, H. 1970.** Alexander Forbes. Pp. 64-66 in *Dictionary of Scientific Biography.* Scribner, New York.
- Davis, H. 1975.** The philosophy of science and the way of investigator. Pp. 186-193 in *The Life and Contributions of Walter Bradford Cannon.* C. McC. Brooks, K. Koizumi and J. O. Pinkston, eds. SUNY Downstate Medical Center, Brooklyn.
- Davis, H. 1991.** *The Professional Memoirs of Hallowell Davis.* Central Institute for the Deaf, St. Louis, MO. 112 pp.
- Davis, H., A. Forbes, D. Brunswick, and A. McH. Hopkins. 1926.** Studies of nerve impulse. II. The question of decrement. *Am. J. Physiol.* **76**: 448-471.
- Davis, H., C. T. Morgan, J. E. Hawkins, Jr., R. Galambos, and F. W. Smith. 1950.** Temporary deafness following exposure to loud tones and noise. *Acta Oto-Laryngol. (Suppl.)* **88**: 1-57.
- Eccles, J. C. 1970.** Alexander Forbes and his achievement in electrophysiology. *Perspect. Biol. Med.* **13**: 388-404.
- Eisner, T., A. M. Srb, and F. A. Long. 1986-1987.** Robert Swain Morison. Cornell University Faculty Memorial Statements.
- Fenn, W. O. 1963.** *History of the American Physiological Society: The Third Quarter Century, 1937-1962.* The American Physiological Society, Washington, DC. Pp. 44-46.
- Fenn, W. O. 1969.** Alexander Forbes. *Biog. Mem. Natl. Acad. Sci.* **40**: 113-141.
- Forbes, A. 1922.** The interpretation of spinal reflexes in terms of present knowledge of nerve conduction. *Physiol. Rev.* **2**: 361-414.
- Forbes, A. 1933.** Conditions affecting the response of the avicularia of *Bugula.* *Biol. Bull.* **65**: 469-479.
- Forbes, A. 1945.** Walter Brandford Cannon (1871-1945). Pp. 349-354 in *Year Book of the American Philosophical Society.* Philadelphia.
- Forbes, A., and A. M. Grass. 1937.** A simple direct-coupled amplifier for action potentials. *J. Physiol.* **91**: 31-35.
- Forbes, A., and C. Thacher. 1920.** Amplification of action currents with the electron tube in recording with the string galvanometer. *Am. J. Physiol.* **52**: 409-471.
- Forbes, A., and C. Thacher. 1925.** Changes in the protoplasm of *Nereis* eggs induced by β -radiation. *Am. J. Physiol.* **74**: 567-578.
- Forbes, A., H. Davis, and J. H. Emerson. 1931.** An amplifier, string galvanometer, and photographic camera designed for the study of action potentials in nerve. *Rev. Sci. Instr.* **2**: 1-15.
- Frank, R. G., Jr. 1986.** The Columbian exchange: American physiologists and neuroscience techniques. *Fed. Proc.* **45**: 2665-2672.
- Galambos, R. 1998.** Hallowell Davis 1896-1992. *Biog. Mem. Nat. Acad. Sci.* **75**: 3-23.
- Galambos, R., and H. Davis. 1943.** The response of single auditory-nerve fibers to acoustic stimulation. *J. Neurophysiol.* **6**: 39-58.
- Garceau, E. L., and H. Davis. 1934.** An amplifier, recording system and stimulation devices for the study of cerebral action currents. *Am. J. Physiol.* **107**: 305-310.
- Garceau, E. L., and H. Davis. 1935.** An ink-writing electroencephalograph. *Arch. Neurol. Psychol.* **34**: 1292-1294.
- Garceau, E. L., and A. Forbes. 1934.** A direct-coupled amplifier for action currents. *Rev. Scient. Instr.* **5**: 10-13.
- García Ramos, J., and R. Miledi. 1953.** Estudios sobre el Flutter y la Fibrilación. IX La Fibrilación Ventricular. *Arch. Inst. Cardio. Mex.* **22**: 805-834.
- García Ramos, J. and R. Miledi. 1954.** La Fibrilación Ventricular. *Bol. San. Mil. Mex.* **7**: 3-24.
- Gasser, H. S., and H. S. Newcomer. 1921.** Physiological action currents in the phrenic nerve. An application of the thermionic vacuum tube to nerve physiology. *Am. J. Physiol.* **57**: 1-26.
- Gibbs, F. A., H. Davis, and W. G. Lennox. 1935.** The electro-encephalogram in epilepsy and in conditions of impaired consciousness. *Arch. Neurol. Psychiatry* **34**: 1133-1148.
- Gibbs, F. A., W. G. Lennox, and E. L. Gibbs. 1936.** The electro-encephalogram in diagnosis and in localization of epileptic seizures. *Arch. Neurol. Psychiatry* **36**: 1225-1250.
- Gibbs, F. A., E. L. Gibbs, and W. G. Lennox. 1937.** Epilepsy: a paroxysmal cerebral dysrhythmia. *Brain* **60**: 377-388.
- Grass, A. M. 1984.** *The Electroencephalographic Heritage.* Grass Instrument Co., Quincy, MA. 41 pp.
- Grass, A. M., and F. A. Gibbs. 1938.** A Fourier transform of the electroencephalogram. *J. Neurophysiol.* **1**: 521-526.
- Grass, E. R. 1970.** Text of the Introduction to the first Cannon lecture supported by the Grass Foundation. Cornell University Medical School, NYC. Tuesday Nov. 17, 1970.
- Grass, J. 1980.** Arthur James "Bill" Derbyshire. Taped interview with "Bill" Derbyshire, August, 1980. UCLA Brain Research Institute, Neuroscience History Resource Project, Oral History Program, Series CON, Code DER.
- Grass, M. 1987.** Alexander Forbes. A handout distributed prior to the annual Forbes Lectures supported by The Grass Foundation at the Marine Biological Laboratory.
- Grass Instrument Co. 1967.** *This is Grass Instrument Company.* Grass Instrument Company Catalogue, 1967, Quincy, MA.
- Grass Instrument Co. 1971.** *Perspectives in Electrophysiological Instrumentation.* 1971 calendar of the Grass Instrument Co., Quincy, MA.
- Henry, M. H. 1992.** In Memoriam, Albert Melvin Grass, 1910-1992. *J. Clin. Neurophysiol.* **9**: 419-421.
- Howell, W. H., and C. W. Greene. 1938.** History of the American Physiological Society Semicentennial, 1887-1937. American Physiological Society, Baltimore, MD.
- Hughes, J. R., and J. L. Stone. 1990.** An interview with Frederic A. Gibbs, M.D. and Erna L. Gibbs. *Clin. Electroencephalogr.* **21**: 175-182.
- Kemp, E. H., and E. H. Robinson. 1937.** Electric responses of the brain stem to bilateral auditory stimulation. *Am. J. Physiol.* **120**: 316-322.
- Kemp, E. H., G. Coppée, and R. Robinson. 1936.** Les voies auditives au niveau de la moelle allongée (Chat). Mise en évidence des synapses nerveuses. *C. R. Soc. Biol.* **122**: 1294-1297.
- Kemp, E. H., G. E. Coppée, and E. H. Robinson. 1937.** Electric

- responses of the brain stem to unilateral auditory stimulation. *Am. J. Physiol.* **120**: 304–315.
- Kusano, K., R. Miledi, and J. Stinnakre. 1977.** Acetylcholine receptors in the oocyte membrane. *Nature* **270**(5639): 739–741.
- Kusano, K., R. Miledi, and J. Stinnakre. 1982.** Cholinergic and catecholaminergic receptors in the *Xenopus* oocyte membrane. *J. Physiol.* **328**: 143–170.
- Lennox, W. G. 1936.** The physiological pathogenesis of epilepsy. *Brain* **59**: 113–121.
- Lennox, W. G., and S. Cobb. 1928.** Epilepsy, from the standpoint of physiology and treatment. *Medicine* **7**: 105–290.
- Lindsley, D. B. 1934.** Inhibition as an accompaniment of the knee jerk. *Am. J. Physiol.* **109**: 181–191.
- Lindsley, D. B. 1935a.** Electrical activity of human motor units during voluntary contraction. *Am. J. Physiol.* **114**: 90–99.
- Lindsley, D. B. 1935b.** Myographic and electromyographic studies of myasthenia gravis. *Brain* **58**: 470–482.
- Lindsley, D. B. 1936.** Electromyographic studies of neuromuscular disorders. *Arch. Neurol. Psychiatry* **36**: 128–157.
- Lindsley, D. B. 1995.** Life and reflections of a psychologist-psychophysiologist from a personal and historical perspective. *Int. J. Psychophysiol.* **20**: 83–141.
- Marshall, L. H. 1980.** Taped interview with Albert Melvin Grass, Nov. 11, 1980, UCLA Brain Research Institute, Neuroscience History Resource Project, Oral History Program, Series CON, Code GRA.
- Marshall, L. H. 1987.** Instruments, techniques, and social units in American neurophysiology, 1870–1950. Physiology in the American Context, 1850–1940. American Physiological Society, Washington, DC.
- Marshall, L. H. 1995.** Taped interview with Ellen R. Grass, Sept. 15, 1995, UCLA Brain Research Institute, Neuroscience History Resource Project, Oral History Program, Series CON, Code GRA.
- Miledi, R. 1957.** The strength latency relation of axons. *Acta Physiol. Latinoamer.* **7**: 155–186.
- Morison, R. S. 1945.** Walter Bradford Cannon in International Affairs. Walter Bradford Cannon 1871–1945: A Memorial Exercise. Held at Harvard Medical School, Monday, Nov. 5, 1945.
- Morison, R. S. 1979.** Albert and Ellen Grass—An Appreciation. Neuroscience Newsletter, Sept. 1979, written 8/1/79.
- Renshaw, B., A. Forbes, and B. R. Morison. 1940.** Activity of isocortex and hippocampus, electrical studies with microelectrodes. *J. Neurophysiol.* **3**: 74–105.
- Rosenblueth, A., and R. S. Morison. 1934.** A quantitative study of the production of sympathin. *Am. J. Physiol.* **109**: 209–220.
- Rosenblueth, A., and F. A. Simeone. 1934.** The interrelations of vagal and accelerator effects on the cardiac rate. *Am. J. Physiol.* **110**: 42–55.
- Rosenblueth, A., and F. A. Simeone. 1938a.** The responses of the superior cervical ganglion to single and repetitive activation. *Am. J. Physiol.* **122**: 688–707.
- Rosenblueth, A., and F. A. Simeone. 1938b.** The action of eserine or prostigmin on the superior cervical ganglion. *Am. J. Physiol.* **122**: 708–721.
- Rosenblueth, A., D. B. Lindsley, and R. S. Morison. 1936.** A study of some decurizing substances. *Am. J. Physiol.* **115**: 53–68.
- Rosenblueth, A., J. García Ramos, and R. Miledi. 1954.** The propagation of impulses of myelinated axons. *J. Cell. Comp. Physiol.* **43**: 347–364.
- Seyfarth, E.-A. 1996.** Ernst Theodor von Brücke (1800–1941) and Alexander Forbes (1882–1965): Chronicle of a transatlantic friendship in difficult times. *Perspect. Biol. Med.* **40**: 45–54.
- Simeone, F. A., W. B. Cannon, and A. Rosenblueth. 1938.** The sensitization of the superior cervical ganglion to nerve impulses by partial denervation. *Am. J. Physiol.* **122**: 94–100.
- Taylor, E. W. 1931.** William Norton Bullard, M.D. 1853–1931. *Arch. Neurol. Psychiatry* **26**: 179–183.
- White, B. V. 1984.** *Stanley Cobb: A Builder of the Modern Neurosciences*. Francis A. Countway Library of Medicine, Boston, 445 pp.
- Zottoli, S. J. 1990.** Taped interview with Ricardo Miledi, July, 1990. Marine Biological Laboratory, Woods Hole, MA.

Reports of Papers Presented at
THE GENERAL SCIENTIFIC MEETINGS
OF THE MARINE BIOLOGICAL LABORATORY,
Woods Hole, Massachusetts
13 to 14 August 2001

Program Chairs:
WILLIAM ECKBERG, Howard University
ROBERT GOULD, New York State Institute for Basic Research
ROBERT PAUL MALCHOW, University of Illinois at Chicago
IVAN VALIELA, Boston University Marine Program

Each of these reports was reviewed by two members of a special editorial board drawn from the research community of Woods Hole, Massachusetts.

Reviewers included scientists from
THE MARINE BIOLOGICAL LABORATORY,
THE WOODS HOLE OCEANOGRAPHIC INSTITUTION,
AND THE NATIONAL MARINE FISHERIES SERVICE.



SHORT REPORTS FROM THE 2001 GENERAL SCIENTIFIC MEETINGS OF THE MARINE BIOLOGICAL LABORATORY

FEATURED REPORT

The Editors

Introduction to the featured report, green fluorescent protein: enhanced optical signals from native crystals. 231

Inoué, Shinya, and Makoto Goda

Fluorescence polarization ratio of GFP crystals. 231

CELL BIOLOGY

Knudson, Robert A., Shinya Inoué, and Makoto Goda

Centrifuge polarizing microscope with dual specimen chambers and injection ports. 234

Tran, P. T., and Fred Chang

Transmitted light fluorescence microscopy revisited. 235

Hernandez, R. V., J. M. Garza, M. E. Graves,

J. L. Martinez, Jr., and R. G. LeBaron

The process of reducing CA1 long-term potentiation by the integrin binding peptide, GRGDSP, occurs within the first few minutes following theta-burst stimulation. 236

Kuhns, William J., Dario Rusciano, Jane Kaltenbach,

Michael Ho, Max Burger, and Xavier Fernandez-Busquets

Up-regulation of integrins $\alpha_3 \beta_1$ in sulfate-starved marine sponge cells: functional correlates. 238

Brown, Jeremiah R., Kyle R. Simonetta, Leslie A. Sandberg, Phillip Stafford, and George M. Langford

Recombinant globular tail fragment of myosin-V blocks vesicle transport in squid nerve cell extracts. 240

Wöllert, Torsten, Ana S. DePina, Leslie A. Sandberg, and George M. Langford

Reconstitution of active pseudo-contractile rings and myosin-II-mediated vesicle transport in extracts of clam oocytes. 241

Clay, John R., and Alan M. Kuzirian

A novel, kinesin-rich preparation derived from squid giant axons. 243

Weidner, Earl

Microsporidian spore sporoplasm dynactin in *Spangua*. 245

Conrad, Mara L., R. L. Pardy, and Peter B. Armstrong

Response of the blood cell of the American horseshoe crab, *Limulus polyphemus*, to a lipopolysaccharide-like molecule from the green alga *Chlorella*. 246

Silver, Robert

LtB₄ evokes the calcium signal that initiates nuclear envelope breakdown through a multi-enzyme network in sand dollar (*Echinarcinus parma*) cells. 248

DEVELOPMENTAL BIOLOGY

Crawford, Karen

Ooplasm segregation in the squid embryo, *Loligo pealeii*. 251

Burbach, J. Peter H., Anita J. C. G. M. Hellemons, Marco Hoekman, Philip Grant, and Harish C. Pant

The stellate ganglion of the squid *Loligo pealeii* as a model for neuronal development: expression of a POU Class VI homeodomain gene, *Rpf-1*. 252

Link, Brian A.

Evidence for directed mitotic cleavage plane reorientations during retinal development within the zebrafish. 254

Smith, Ryan, Emma Kavanagh, Hilary G. Morrison, and Robert M. Gould

Messenger RNAs located in spiny dogfish oligodendrocyte processes. 255

Hill, Susan D., and Barbara C. Boyer

Phalloidin labeling of developing muscle in embryos of the polychaete *Capitella* sp. I. 257

Rice, Aaron N., David S. Portnoy, Ingrid M. Kaatz, and Phillip S. Lobel

Differentiation of pharyngeal muscles on the basis of enzyme activities in the cichlid *Tramitichromis intermedius*. 258

NEUROBIOLOGY

Twig, Gilad, Sung-Kwon Jung, Mark A. Messerli,

Peter J. S. Smith, and Orian S. Shirihai

Real-time detection of reactive oxygen intermediates from single microglial cells. 261

Silver, Robert B., Mahlon E. Kriebel, Bruce Keller, and George D. Pappas

Porocytosis: Quantal synaptic secretion of neurotransmitter at the neuromuscular junction through arranged vesicles. 263

Chappell, Richard L., and Stephen Redenti

Endogenous zinc as a neuromodulator in vertebrate retina: evidence from the retinal slice. 265

Shashar, Nadav, Douglas Borst, Seth A. Ament, William M. Saidel, Roxanna M. Smolowitz, and Roger T. Hanlon
Polarization reflecting iridophores in the arms of the squid *Loligo pealeii* 267

Chiao, Chuan-Chiu, and Roger T. Hanlon
Cuttlefish cue visually on area—not shape or aspect ratio—of light objects in the substrate to produce disruptive body patterns for camouflage. 269

Errigo, M., C. McGuinness, S. Meadors, B. Mittmann, F. Dodge, and R. Barlow
Visually guided behavior of juvenile horseshoe crabs . . . 271

Meadors, S., C. McGuinness, F. A. Dodge, and R. B. Barlow
Growth, visual field, and resolution in the juvenile *Limulus lateral eye*. 272

Kozlowski, Corinne, Kara Yopak, Rainer Voigt, and Jelle Atema
An initial study on the effects of signal intermittency on the odor plume tracking behavior of the American lobster, *Homarus americanus* 274

Hall, Benjamin, and Kerry Delaney
Cholinergic modulation of odor-evoked oscillations in the frog olfactory bulb 276

Zottoli, S. J., D. E. W. Arnolds, N. O. Asamoah, C. Chevez, S. N. Fuller, N. A. Hiza, J. E. Nierman, and L. A. Taboada
Dye coupling evidence for gap junctions between supramedullary/dorsal neurons of the cunner, *Tautoglabrus adspersus*. 277

Kaatz, Ingrid M., and Phillip S. Lobel
A comparison of sounds recorded from a catfish (*Orinocodoras eigenmanni*, Doradidae) in an aquarium and in the field 278

Fay, R. R., and P. L. Edds-Walton
Bimodal units in the torus semicircularis units of the toadfish (*Opsanus tau*). 280

MARICULTURE

Mensingher, Allen F., Katherine A. Stephenson, Sarah L. Pollema, Hazel E. Richmond, Nichole Price, and Roger T. Hanlon
Mariculture of the toadfish *Opsanus tau*. 282

Rieder, Leila E., and Allen F. Mensinger
Strategies for increasing growth of juvenile toadfish. . . . 283

Chikarmane, Hemant M., Alan M. Kuzirian, Ian Carroll, and Robbin Dengler
Development of genetically tagged bay scallops for evaluation of seeding programs 285

ECOLOGY AND POPULATION BIOLOGY

Williams, Libby, G. Carl Noblitt IV, and Robert Buchsbaum
The effects of salt marsh haying on benthic algal biomass 287

Hinckley, Eve-Lyn S., Christopher Neill, Richard McHorney, and Ann Lezberg
Dissolved nitrogen dynamics in groundwater under a coastal Massachusetts forest. 288

Hauxwell, Alyson M., Christopher Neill, Ivan Valiela, and Kevin D. Kroeger
Small-scale heterogeneity of nitrogen concentrations in groundwater at the seepage face of Edgartown Great Pond 290

Novak, Melissa, Mark Lever, and Ivan Valiela
Top down vs. bottom-up controls of microphytobenthic standing crop: role of mud snails and nitrogen supply in the littoral of Waquoit Bay estuaries 292

Fila, Laurie, Ruth Herrold Carmichael, Andrea Shriver, and Ivan Valiela
Stable N isotopic signatures in bay scallop tissue, feces, and pseudofeces in Cape Code estuaries subject to different N loads 294

Grady, Sara P., Deborah Rutecki, Ruth Carmichael, and Ivan Valiela
Age structure of the Pleasant Bay population of *Crepidula fornicata*: a possible tool for estimating horseshoe crab age 296

Kuzirian, Alan M., Eleanor C. S. Terry, Deanna L. Bechtel, and Patrick I. James
Hydrogen peroxide: an effective treatment for ballast water 297

ORAL PRESENTATIONS

Published by title only. 300

Introduction to the Featured Report **Green Fluorescent Protein: Enhanced Optical Signals from Native Crystals**

"The bioluminescent jellyfish *Aequorea* emits 'green' light *in vivo*, whereas the pure photoprotein aequorin extracted from the same organism emits 'blue' light on addition of Ca^{2+} ." Osamu Shimomura made this observation and identified a green fluorescing molecule in 1962; then reported its purification and characterization in 1974 from 30,000 specimens of the hydrozoan jellyfish. The result was green fluorescent protein (GFP), which emits at about 509 nm when it is excited by the blue light (about 460 nm) emitted by aequorin (also purified and characterized by Shimomura). In the jellyfish, this process—called fluorescence resonance energy transfer (FRET)—results in a signal that, because of its longer wavelength, can penetrate farther through the turbidity of natural seawater to its target, which might be, for example, planktonic prey.

The molecular details of GFP emerged about 20 years later (1996) from a pair of independent studies. The laboratories of Roger Tsien and George Phillips, Jr., showed the protein to be an unusual, very regular, barrel-shaped molecule, with its walls (a sheet comprising 11 β -strands) and caps at both ends of the barrel enclosing and protecting a fluorophore composed of post-translationally modified amino acids.

The gene encoding GFP was cloned by Douglas Prasher and associates in 1992. And shortly thereafter (1994), Martin Chalfie and his laboratory showed that the protein, with its fluorophore, could be completely expressed in bacteria, which would (as if they were jellyfish) glow green when excited with blue light. In the same year, Tulle Hazelrigg demonstrated that a suitable gene construct would express a fusion protein including GFP, and that the site of expression could be precisely located in the organism (*Drosophila* in this case), or in a single cell, merely by illumination with blue light. With that critical finding, GFP was quickly recognized, and widely used in developmental, cell, neural, and molecular biology, as a reporter of gene expression and a marker for gene product localization.

Recently, Osamu Shimomura asked Shinya Inoué to produce a photomicrograph of the fluorescence emitted by the needle-shaped crystals of purified, native GFP. Inoué agreed, but thought to examine, as well, the anisotropic properties of the crystals. The novel and surprising results of that investigation are set out in the following short report by Inoué and Makoto Goda. In brief, the fluorescence from excited GFP crystals is polarized, with the resonance vectors oriented parallel to the long axis of the crystals. Moreover, when the excitation is also polarized, the fluorescence measured with an analyzer parallel to the crystal is very much higher (by 20–30 times!) than that measured perpendicular to it.

These observations, combined with structural studies involving X-ray crystallography, should shed more light on GFP function and help us improve our interpretation of FRET imaging. Moreover they suggest that, in investigations where dynamic changes in the orientation of GFP-linked motor or contractile proteins are being followed, the use of polarized light might well increase the sensitivity of the observations.

—The Editors
August 2001

Fluorescence Polarization of GFP Crystals

Shinya Inoué (Marine Biological Laboratory, Woods Hole, Massachusetts 02543) and Makoto Goda¹

Green fluorescence protein (GFP), isolated from the jellyfish, *Aequorea*, purified by column chromatography, and dialyzed against distilled water to remove salts, forms elongated needle-

shaped crystals, about 3- μm to less than 1- μm wide and some 20- to 100- μm long (1). Examined with a polarizing microscope in visible light of wavelength greater than 450 nm, these crystals show a very weak negative birefringence; *i.e.*, their slow axis (larger refractive index) lies perpendicular to the long crystal axis.

¹ AIST, Tokyo, Japan.



Figure 1. Crystals of purified native GFP. (A) Dichroism (anisotropic absorbance) in visible light with crystals appearing green to light brown with the long crystal axis oriented "parallel," and pale blue to white with the long crystal axis oriented "perpendicular," to the polarizer. (In fact, a polarizer and analyzer were used, off-crossed by about five degrees, to accentuate the weak visible light dichroism.) (B, C) Polarization-dependent anisotropy of fluorescence excitation seen in the absence of an analyzer. The polarizer E-vector in Panel B is oriented parallel to the prominent crystal in the middle of the panel. In Panel C, it is oriented perpendicular to the length of the same crystal. Bar = 30 μm .

They also show a weak, but distinct, blue-green dichroism (Fig. 1A).

Illuminated with blue light of less than 450-nm wavelength, the same crystals show a very bright, green fluorescence when viewed through a $527 \pm 15\text{-nm}$ band-pass filter. Surprisingly, the brightness of the fluorescence varied by a ratio of as much as 6:1 when the crystals were illuminated with polarized blue light and ob-

served in the absence of an analyzer (Fig. 1B, 1C). The fluorescence was greatest when the long axis of the crystal lay parallel to the transmission direction of the polarizer E-vector. In other words, the absorption for the exciting light is six times greater with its E-vector polarized parallel to the length of the crystal axis than across. A similarly high ratio and orientation dependence was observed when the crystals were observed with non-polarized illumination but through an analyzer. In other words, the fluorescence emitted by crystals illuminated with non-polarized light is again some six times greater for polarization parallel to the long crystal axis. Between *parallel* polarizer and analyzer, the orientation-dependent fluorescence ratio becomes as high as 20:1 to 30:1, apparently the product of the excitation and emission anisotropies. These extremely high polarization ratios show that the resonance vectors of the dichroic fluorophores are oriented parallel to the long crystal axis, and that there is little loss of energy or alignment during fluorescence excitation and emission. [Even the nucleotide bases in oriented strands of B-form DNA show dichroic ratios of only 4:1 over the wavelength range 240 to 380 nm (2, 3).]

According to detailed X-ray analyses (4, 5), the 11 beta sheets that make up the barrel-shaped exterior of the GFP molecule are arranged helically around the barrel axis, with the barrel length somewhat greater than the diameter. The beta sheets lie at an angle slightly less than 45 degrees to the barrel axis. Thus, in the negatively birefringent GFP crystals, it is likely that the long axes of the barrel-shaped GFP molecules lie more or less across the length of the long crystal axis. In addition, X-ray data show that the chromophore responsible for the fluorescence lies within the beta barrel and is tilted approximately 60 degrees to the long axis of the barrel. The fluorescence polarization that we observe strongly indicates that the fluorophore is arranged with its major absorbing and emission resonance planes (dipoles) oriented parallel to the long axis of the crystal. Combining the data on fluorescence polarization and X-ray analysis, we propose that the beta barrels are regularly packed with the barrel axes tilted some 60 degrees to the length of the crystal, and possibly wound as concentric cylinders around the core of the needle-shaped crystal.

The very high degree of anisotropy for excitation and fluorescence of GFP, as well as the dramatic elevation of the orientation-dependent fluorescence polarization ratio by observation between parallel polars, suggest their potential use as indicators of the orientation of molecules with which the GFP or related chromophores are tightly bound. Our observations may also prove important in using GFP and related compounds in the application of FRET (fluorescence resonance energy transfer) and other measurements of molecular distances and orientations, because the interpretation of these measurements relies on the knowledge, or assumptions, of the orientation-dependent polarizability of the fluorophores. The observations may also be relevant in explaining the efficient energy transfer between aequorin and GFP in the light-emitting organ of the jellyfish itself.

We thank Dr. Osamu Shimomura (Marine Biological Laboratory, Woods Hole) for discussions and providing the pure native GFP crystals, Dr. Kensal Van Holde (Oregon State University) for discussions on an early version of this manuscript, and Dr. Yoshinori Fujiyoshi (Kyoto University) for generous support of this project.

Literature Cited

1. Morise, H., O. Shimomura, F. H. Johnson, and J. Winant. 1974. *Biochemistry* **13**: 2656–2662.
2. Seeds, W. E., and M. H. F. Wilkins. 1950. *Faraday Discuss. Chem. Soc.* **9**: 417–423.
3. Inoué, S., and H. Sato. 1964. Pp. 209–248 in *Molecular Architecture in Cell Physiology*. T. Hayashi, and A. G. Szent-Gyorgyi, eds. Prentice-Hall, Englewood Cliffs, NJ.
4. Ormö, M., A. B. Cubitt, K. Kallio, L. A. Gross, R. Y. Tsien, and S. J. Remington. 1996. *Science* **273**: 1392–1395.
5. Yang, F., L. G. Moss, and G. N. Phillips, Jr. 1996. *Nature Biotechnol.* **14**: 1246–1251.

Reference: *Biol. Bull.* **201**: 234. (October 2001)

Centrifuge Polarizing Microscope with Dual Specimen Chambers and Injection Ports

Robert A. Knudson (Marine Biological Laboratory, Woods Hole, Massachusetts),
Shinya Inoué, and Makoto Goda¹

We reported earlier on a centrifuge polarizing microscope (CPM) that was designed for observing the weak birefringence of organelles and fine structures in living cells as they became stratified and oriented under centrifugal fields of up to 10,500 times Earth's gravitational field. In this earlier model (I), one chamber A contained the specimen under observation, while the contents of the opposed second chamber B, which acted solely to balance the rotor, could not be viewed. We have now improved the CPM so that either chamber can be viewed and selected at the flick of a lever, within the duration of a video frame. In the CPM, an electronic timing circuit synchronizes the firing of the light source laser precisely to the transit of the specimen under the microscope (freezing the image to less than 0.5- μ m specimen motion at up to 11,700 rpm, regardless of the speed of the 16-cm diameter rotor). The timing circuit, in turn, is triggered by the signal from a photodiode that picks up the light originating from a stationary diode laser, and reflected by a small mirror (M1) mounted on the spinning rotor near its axis. The complexity of the electronic timing circuit led us to keep the electronic circuit undisturbed and instead to devise an optical system for switching between the display of the two chambers. To this end, we installed a second timing mirror (M2) on the rotor, exactly opposite the one for chamber A, but tilted up by a few degrees, rather than oriented parallel to the rotor axis as is M1. In front of the photodiode we also placed a mounted pair of small mirrors on a "beam switcher" that could either be flipped up out of the way so that the photodiode would capture the light reflected from M1, or flipped down into position so that light reflected from the tilted mirror M2 would be reflected by the mounted pair of beam-switcher mirrors and enter the photodiode. Thus, depending on the position of the beam switcher, the timing light would enter the photodiode, reflected either from mirror M1 or M2. The timing circuit would then trigger the light source laser at precisely (to within a few nanoseconds) the time point required to display a stable image of the specimen in chambers A or B. The response time of the electronic timing circuit and laser firing device turned out to be so short that no video frames were lost in flipping the beam switcher and capturing the images from either of the two chambers.

Figure 1, left panel, shows the recorded image of sea urchin eggs stratified in a density gradient in chamber A, while the right panel shows density-standard beads (Nycomed Amersham, Oslo, Norway) that reveal the gradient of the identically prepared seawater/Percoll mix in chamber B. As the figure shows, the density of the unfertilized *Arbacia* eggs is approximately 1.060. Immediately after fertilization, the negative birefringence disappears from the membranes stacked in the upper half of the clear zone of the stratified eggs (Fig. 1 and Ref. 2). Concurrently, the (de-jellied) egg becomes lighter over the next minute, presumably by influx of water, and starts to float upward in the gradient until its density is somewhat less than 1.040.

In addition to being able to instantly switch between images from

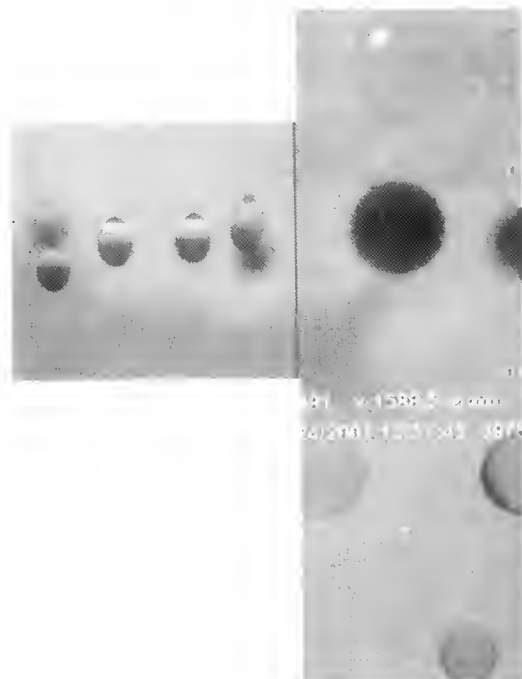


Figure 1. Left: Unfertilized *Arbacia* eggs stratified in chamber A in a seawater/Percoll density gradient. Right: Four sets of beads of standard densities stratified concurrently in the gradient; observed in chamber B. Nominal densities of the beads are, top to bottom: 1.04, 1.06, 1.09, and 1.10.

chambers A and B, we have devised a method for introducing reagents, sperm, etc., into either chamber while the specimen and control are rotating in the CPM. A plastic unit, notched out to pass the timing light for mirrors M1 and M2, was placed over the support post for these mirrors. The unit incorporated an "injection port" drilled along the rotational axis of the rotor, which in turn could be connected through a selection valve, without stopping the rotor, to either of the two thin pieces of plastic tubing leading to chambers A or B. Thus, we can now observe fine structural and density changes—e.g., in marine eggs upon activation—without having to stop the rotor for a period to remove the specimen chamber and introduce the activating agents. Video records resulting from both of these improvements were presented.

We thank Hamamatsu Photonics K.K. and Olympus Optical Co. for generous support of this project.

Literature Cited

- Inoué, S., R. Knudson, M. Goda, K. Suzuki, C. Nagano, N. Okada, H. Takahashi, K. Ichie, M. Iida, and K. Yamanaka. 2001. *J. Microscopy* **201**: 341–356.
- Inoué, S., M. Goda, and R. A. Knudson. 2001. *J. Microscopy* **201**: 357–367.

¹ AIST, Tokyo, Japan.

Reference: *Biol. Bull.* 201: 235–236. (October 2001)

Transmitted Light Fluorescence Microscopy Revisited

P. T. Tran and Fred Chang (Columbia University, Microbiology Department,
701 W. 168th Street, New York, New York 10032)

From its introduction in 1967 by Ploem (1), reflected light fluorescence microscopy, commonly called "epi-fluorescence," has enjoyed wide acceptance. Its optical path is relatively simple: full-spectrum light passing through an excitation filter is reflected by the dichromatic mirror into the objective lens to illuminate the sample; the excited sample emits fluorescent light, which is re-collected by the objective lens and passed through the emission filter to the camera.

The recent development of biosensors based on genetically encoded variants of green fluorescent protein (GFP), coupled with advances in digital, multi-modes, epi-fluorescence microscopy, has introduced new powerful tools for observing protein dynamics and protein-protein interactions at high spatial and temporal resolution within living cells. However, there are some disadvantages inherent in epi-fluorescence microscopy: a) mechanical switching of filter cubes to

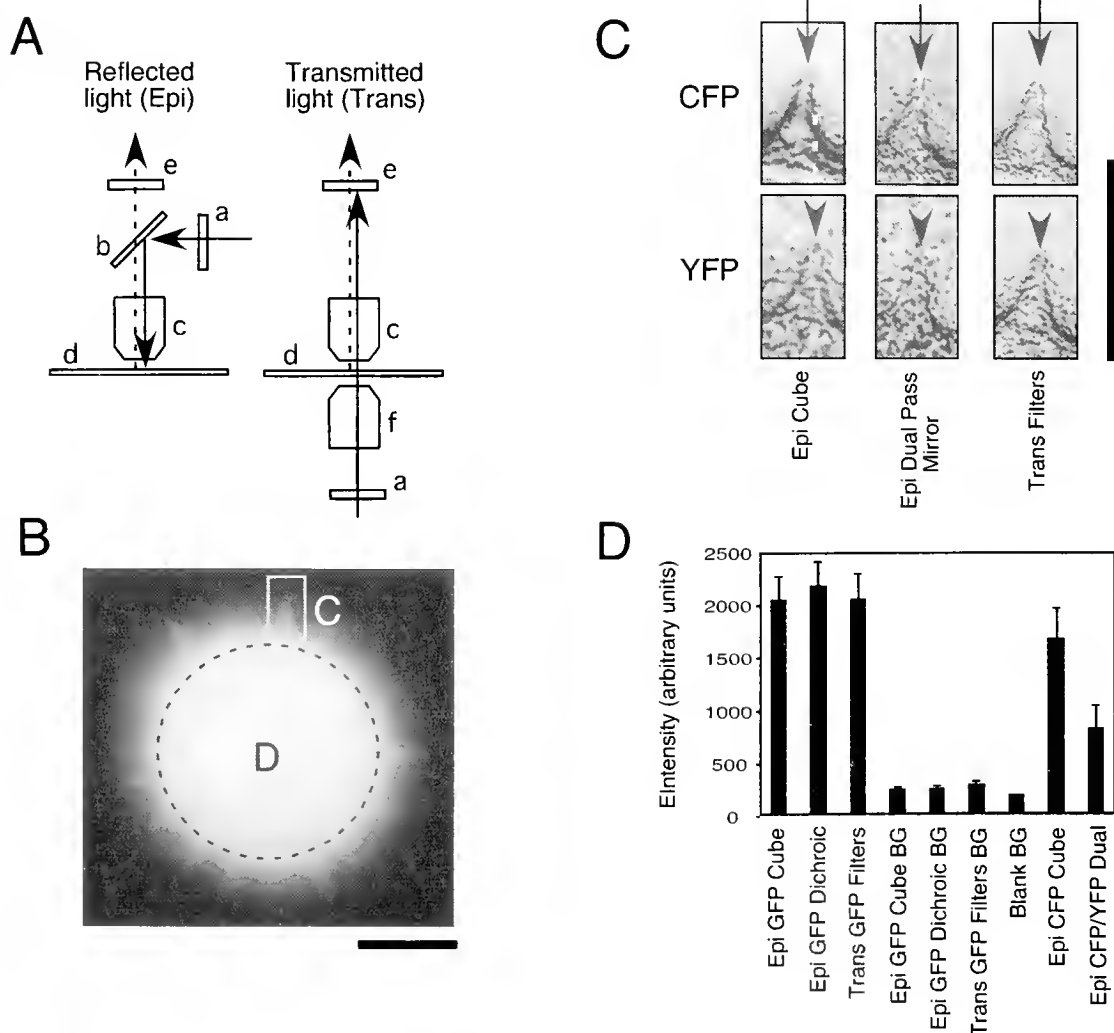


Figure 1. Intensity and image misalignment comparisons between reflected light fluorescence microscopy (epi) and transmitted light fluorescence microscopy (trans). (A) Schematic diagrams of the optical paths of epi- and trans-fluorescence: a-excitation filter, b-dichromatic mirror, c-objective lens, d-specimen, e-emission filter, f-condenser lens. (B) Fluorescent image of a pollen grain. The rectangle C highlights a pollen spike that is used to measure image misalignment. The dashed circle D represents the area of the pollen grain used to measure fluorescent intensity. (C) Positions of a pollen spike (edge-enhanced) imaged with epi- and trans-fluorescence. (D) Mean fluorescence intensities of pollen grain measured with epi- and trans-fluorescence. See text for further details of microscopy set-up. Bar = 10 μ m.

view different color fluorescence can cause misalignment of images; b) multi-pass filter cubes can eliminate the misalignment problem, but may attenuate the emission light; and c) the epi-fluorescent light source cannot be used in combination with transmitted light techniques such as Phase or differential interference contrast (DIC) microscopy.

We investigated the feasibility of using transmitted light fluorescence microscopy (referred to here as "trans-fluorescence") to overcome the limitations of epi-fluorescence described above. In trans-fluorescence, the specimen is excited by light passing through the condenser lens, and the fluorescent emission is captured by the objective lens. This mode eliminates the need for dichromatic mirrors. Trans-fluorescence was pioneered prior to epi-fluorescence but was largely abandoned due to two major drawbacks. In the past, excitation light coming from the condenser lens and going through the objective lens could not be completely blocked by the emission filter, leading to a high background signal. Furthermore, optical alignment and matching of the condenser lens and the objective lens were often difficult, leading to non-optimal fluorescence. However, recent developments in filter technology and automated microscope controls prompted us to test whether trans-fluorescence could provide significant improvement over epi-fluorescence in alignment and fluorescent intensity.

Figure 1A shows schematic diagrams for the epi- and trans-fluorescence optical set-ups. We used a Nikon Eclipse 800 upright microscope with the following attachments. For epi-fluorescence, a first excitation filter wheel (Sutter Instruments, model Lambda 10-2) equipped with band pass excitation filters CFP (436/10 nm), GFP (HQ 525/50 nm), and YFP (535/30 nm) (Chroma Technology) was placed at the epi portal; a corresponding dichromatic mirror for each color protein was placed in the filter cube holder, a Plan Apo 100 \times /1.4 N.A. oil objective lens was used; and a second filter wheel equipped with band pass emission filters CFP (470/30 nm), GFP (HQ 470/40 nm), and YFP (500/20 nm) was placed at the camera port. For trans-fluorescence, minor modifications from the above set-up were required. The excitation filter wheel with appropriate filters was placed at the trans portal; a Universal 1.4 N.A. oil condenser lens was used to illuminate the sample; and all dichromatic mirrors were removed from the optical path. The same 100-watt mercury arc lamp light source was used for illumination in the epi and trans portal. Images of a pollen grain (Carolina Biological) were captured by an Orca-100 cooled CCD digital camera (Hamamatsu Photonics) controlled by the software package OpenLab 3.0 (Improvision). Images were captured at an exposure time of 100 ms.

To compare differences in signal intensity between epi- and trans-fluorescence, we imaged a pollen grain with the GFP filter set using

the two modes. Figure 1B shows the image of the measured pollen grain. The average intensity values of the pollen grain (over area "D"), in 5 separate measurements, were: 2056 ± 224 pollen/252 \pm 23 background for the Epi GFP filter cube, 2190 \pm 221 pollen/257 \pm 25 background for the Epi GFP filter wheels/dichromatic mirror set-up, and 2062 \pm 240 pollen/292 \pm 39 background for the Trans GFP filter set-up (Fig. 1D). We conclude that the fluorescent signal intensities obtained with the epi or trans methods are not different, although the trans method produced slightly higher background intensity. The trans-fluorescent technique is a comparable alternative to epi-fluorescence.

To compare image alignment between epi-fluorescence and trans-fluorescence, we imaged pollen grains sequentially with the CFP and YFP filter sets, using the epi mode and then using the trans mode. Switching between CFP and YFP filter cubes and dichromatic mirrors was done manually, while switching between CFP and YFP filters was automated *via* the filter wheels. Use of the epi mode with manual switches produced a significant lateral shift of up to 1 μ m between the CFP and YFP images (Fig. 1C). The epi mode using automated filter switches with CFP-YFP dual-pass mirror and the trans mode using automated filter switches alone produced no measurable image shift (Fig. 1C). However, the epi mode with CFP-YFP dual-pass mirror attenuated the fluorescent light by 50% compared to the epi mode using filter cube and the trans mode (Fig. 1D). We conclude that the trans mode produces better image alignment than modes using the manual switching of filter cubes; it also produces higher fluorescent intensity compared to the epi mode with a dual-pass mirror.

These studies suggest that transmitted light fluorescence microscopy may be an attractive alternative to reflected light fluorescence microscopy. The advantages of trans-fluorescence include: a) image alignment is better than modes using mechanical switching of filter cubes; b) image fluorescence intensity is comparable to the best epi set-up and is twice as bright as an epi mode using a dual-pass mirror and filter wheels; and c) fluorescence can be combined with Phase or DIC techniques using the same light source.

FC would like to thank the Nikon Corporation for the MBL Nikon fellowship and for providing the microscope equipment used in this analysis. PTT is indebted to Shinya Inoué, Rudolf Oldenbourg, and Ted Salmon for their continued guidance.

Literature Cited

1. Ploem, J. S., and H. J. Tanke. 1987. *Introduction to Fluorescence Microscopy*. Oxford University Press, Oxford.

Reference: *Biol. Bull.* 201: 236-237. (October 2001)

The Process of Reducing CA1 Long-Term Potentiation by the Integrin Peptide, GRGDSP, Occurs Within the First Few Minutes Following Theta-Burst Stimulation

R. V. Hernandez, J. M. Garza, M. E. Graves, J. L. Martinez, Jr., and R. G. LeBaron (University of Texas, Department of Biology and the Cajal Neuroscience Research Center, San Antonio, Texas 78249)

Theta-burst stimulation (TBS) induces Schaffer collateral-CA1 synaptic long-term potentiation (LTP; 1, 2), an experimental model of synaptic plasticity believed to reflect physiological pro-

cesses during normal learning and memory. Various adhesion receptors may play a role in LTP (3), including integrins, transmembrane signaling receptors that link extracellular ligands to the

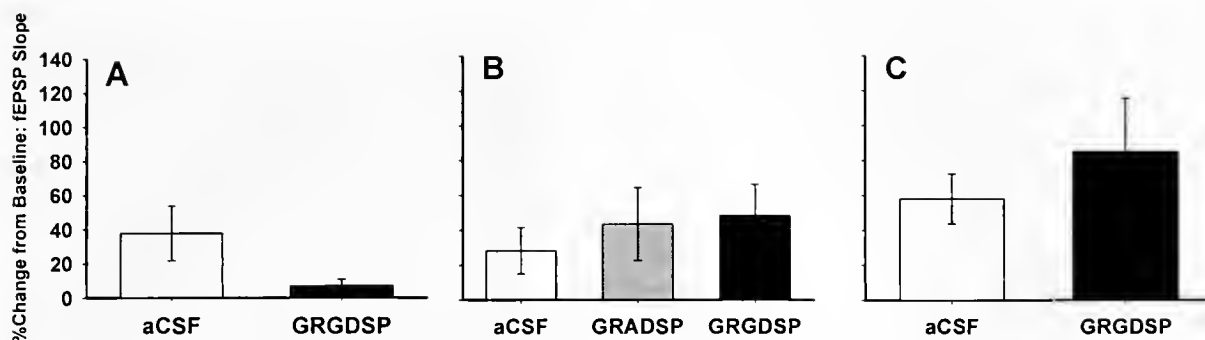


Figure 1. Histograms summarizing the effects of altered integrin-binding by GRGDSP on CA1 LTP. (A) Bath application of 250 μ M GRGDSP for 15 min, starting at 10 min pre-TBS and concluded at 5 min, substantially reduces LTP (solid bar). (B) When 250 μ M GRGDSP (solid bar) or GRADSP (shaded bar) is applied for the 10 min before TBS delivery, with a 30–60 s pre-TBS wash-out, CA1 LTP is not reduced. (C) After robust CA1 LTP is induced, a 40-min bath application of 500 μ M GRGDSP, starting at 5 min post-TBS, fails to reduce LTP. Open bars are aCSF controls.

actin cytoskeleton (4). A principal recognition signal for some integrins is the tripeptide Arg-Gly-Asp (RGD), a sequence found in various extracellular matrix and cell-surface proteins. Indeed, integrin-binding to endogenous ligand is perturbed by the peptide Gly-Arg-Gly-Asp-Ser-Pro (GRGDSP) (5). To assess the role of integrins in LTP, the effect of GRGDSP was tested on the CA1 field excitatory post-synaptic potential (fEPSP) of the rat hippocampus. In previous studies, we found that 250 μ M GRGDSP, half the concentration reported by others (1), was sufficient to significantly reduce LTP (2), even when applied for 15 min during a period that included 10 min pre- to 5 min post-TBS (unpubl. data). Also, application of 250 μ M GRGDSP at 5 or 30 min post-TBS had no effect on CA1 LTP. These results raised questions about the time frame of integrin binding during the process of LTP induction and expression. Current experiments, summarized in graph form in Figure 1, now suggest that a critical period of integrin-binding activity necessary for LTP occurs within the first few minutes following TBS.

Male Sprague-Dawley rats, 30–40 days old, were decapitated and the brains quickly placed in cold artificial cerebral spinal fluid (aCSF) consisting of the following (in mM): 124 NaCl, 2 KCl, 1.25 NaH_2PO_4 , 26 NaHCO_3 , 1 MgCl_2 , 2 CaCl_2 , and 10 dextrose. The brains were cut in 500 μ m horizontal sections, and the hippocampus was dissected away from surrounding cortex. The isolated hippocampal tissue was incubated at room temperature during a 2-h recovery period and then placed on an interface perfusion chamber to record the field potential response. Tissues were bathed in aCSF at a flow rate of 2.0 ml/min and superfused with 95% O_2 /5% CO_2 . All peptides were mixed in aCSF and bath applied through the perfusion system. Pulled-glass electrodes, with an AgCl wire inserted and filled with 150 mM NaCl, served as the recording electrodes. Temperature was maintained at 31–32°C throughout the experiments. Test pulses were evoked every 20 s using a concentric bipolar stimulating electrode.

When 250 μ M GRGDSP was applied—beginning 10 min pre-TBS and concluded at 5 min post-TBS (see Fig. 1A, solid bar; $7.0 \pm 3.8\%$, $n = 3$)—the percent change from baseline of the fEPSP slope, measured at 60 min post-TBS, was substantially reduced when compared with artificial cerebral spinal fluid (aCSF)

controls (Fig. 1A, open bar; $37.8 \pm 16.0\%$, $n = 3$). These experiments replicate previous studies (2) and confirm peptide activity. However, a 10-min application of 250 μ M GRGDSP, with a 30–60 s wash-out immediately before TBS, did not reduce LTP (see Fig. 1B, solid bar; $48.3 \pm 17.9\%$, $n = 3$), as compared with aCSF (Fig. 1B, open bar; $28.2 \pm 13.2\%$, $n = 6$), or 250 μ M of the inactive peptide, GRADSP (Fig. 1B, shaded bar; $43.3 \pm 20.9\%$, $n = 3$; ANOVA, $P > .05$). Finally, to determine whether a decrease in LTP by post-TBS application of GRGDSP may be concentration-dependent within ranges previously tested (1, 2), a 40-min bath application of 500 μ M GRGDSP, beginning 5 min post-TBS, was tested. This concentration also did not decrease CA1 LTP (Fig. 1C, solid bar; $84.7 \pm 30.9\%$, $n = 3$) when compared with aCSF controls (Fig. 1C, open bar; $58.0 \pm 14.3\%$, $n = 7$; t test, $P > .05$).

Based on these new data, we conclude that GRGDSP disrupts LTP within the first few minutes after TBS, and hypothesize that tetanic stimulation may initiate a process that modifies the availability of integrin to bind ligand. The integrin-binding peptide, GRGDSP, is thought to decrease LTP by competing for integrin binding sites in the extracellular matrix that recognize the RGD motif; successful binding by the peptide then disrupts normal integrin function during LTP expression and maintenance. The data presented here, however, suggest that integrins may not be available to bind GRGDSP before TBS, but are quickly and briefly available after TBS.

Supported by a Specialized Neuroscience Research Projects grant (NINDS NS39409; RGL/JLM) and the Ewing Halsell Foundation (JLM).

Literature Cited

1. Stanhli, U., D. Chun, and G. Lynch. 1998. *J. Neurosci.* 18: 3460–3469.
2. LeBaron, R. G., R. V. Hernandez, J. E. Orfila, and J. L. Martinez, Jr. 1999. *Soc. Neurosci. Abstr.* 25: 1495.
3. Benson, D. L., L. M. Schnapp, L. Shapiro, and G. W. Huntley. 2000. *Trends Cell Biol.* 10: 473–482.
4. Hynes, R. O. 1992. *Cell* 69: 11–25.
5. Pierschbacher, M. D., and E. Ruoslahti. 1984. *Nature* 309: 30–33.

Reference: *Biol. Bull.* 201: 238–239. (October 2001)

Up-regulation of Integrins α_3 β_1 in Sulfate-Starved Marine Sponge Cells: Functional Correlates

William J. Kuhns¹, Dario Rusciano², Jane Kaltenbach³, Michael Ho¹,

Max Burger², and Xavier Fernandez-Busquets⁴

(Marine Biological Laboratory, Woods Hole, Massachusetts 02543)

Integrins are a large family of heterodimeric transmembrane glycoproteins that attach cells to fibronectin and collagen and other extracellular matrix proteins of the basement membrane. The attachment is by way of recognition sequences—RGD in the case of fibronectin. The transmembrane and cytoplasmic domains of integrins provide a conduit for outside-in as well as inside-out signaling (1). Integrins or their domains have been highly conserved over many millions of years as judged from their presence in sponges (2). Cell adhesion and motility are regulated by integrins, but the pathways that modulate this function are unclear.

Our previous studies have shown that the properties of adhesion and motility are lost when isolated sponge cells in rotation are deprived of inorganic sulfate (3). We hypothesized that this kind of stress would be likely to cause membrane alterations and would therefore be a useful model for studying integrins and integrin-ligand binding. Herein we describe the effects of sulfate starvation upon the expression of α_3 and β_1 integrins in *Microciona prolifera*, a marine sponge.

Microciona cells were prepared from intact sponge as previously described (3). Aliquots of the cell suspension at a concentration of 2×10^7 /ml were placed in 50-ml centrifuge tubes and spun at low speed in a table model centrifuge at 16°C. The cells were resuspended in either sulfate-free artificial seawater (*i.e.*, less than 10 nM SO_4^{2-}), or in seawater with a normal sulfate concentration (26 mM; + SO_4^{2-}). Each flask was rotated for 8 h; the cells were then centrifuged, the supernatant discarded, and the cell pellets resuspended in fresh ASW, either normal sulfate or sulfate-free. This cycle was repeated four more times.

SDS-PAGE analyses were carried out with lysates prepared by Triton X100 extraction of normal and sulfate-deprived sponge-cell pellets. The proteins separated by gel electrophoresis were probed with rabbit antibodies prepared against integrins α_3 , α_5 , and β_1 following their electro-transfer to nitrocellulose (NC). The NC was cut into seven lanes to account for reference standards (1 lane), integrin staining of (+ SO_4^{2-}) lysate (3 lanes), and integrin staining of (– SO_4^{2-}) lysate (3 lanes). The primary antibodies (rabbit anti-integrins) were applied to their substrates for 1 h and removed, and the NC strips washed with PBS. The secondary reagent (goat anti-rabbit horseradish peroxidase (HRP) conjugate) was applied for 1 h and removed, and the NC was washed again with PBS. Color was developed with ECL reagent at a dilution of 1:1 applied to the NC strips, which were then autoradiographed.

For immunohistochemistry, chemically dissociated cells conditioned in normal or sulfate-free ASW were fixed in 10% formalin ASW and the centrifuged pellets embedded in paraffin as described (3). Tissues were sectioned at 6 μm and stained using mouse monoclonal antibodies (MAB) raised against integrins α_3 and β_1 ; following a wash with PBS, the sections were treated with the secondary antibody (goat anti-mouse HRP conjugate), washed with PBS, and developed with 3', 3' diaminobenzidine. The sections were counterstained for 5 min with Harris' hematoxylin.

The stained Western blots revealed marked differences between the integrins derived from *Microciona* cells prepared in normal ASW and those processed in sulfate-free ASW (Fig. 1a). The expression of α_3 and β_1 integrins was considerably greater in sulfate-free ASW than in normal ASW. The distinction was particularly clear in the case of α_3 integrin, which displayed a single prominent band at about 65 kDa in the (–) lane, whereas the (+) lane displayed a corresponding band at considerably lower intensity. The differences were maintained in the lanes stained with anti-integrin β_1 , but the 65-kDa bands were much more intense. The molecular sizes are somewhat less than those reported in other sponge species (2, 4). The β_1 integrin derived from the sulfate-free lysate also displayed a very dense broad band at 200–205 kDa. The multiplicity of bands could be accounted for, either by cross-reactions between the anti-integrins and non-integrin proteins, or by glycosylation variants of the primary bands. The anti-integrin α_5 failed to react with either cell lysate.

Cell sections stained with integrin MABs generally conformed to the biochemical distinctions. The cells preconditioned in sulfate-free ASW and stained with anti-integrin α_3 displayed many large darkly stained cells along with a considerable amount of stained matrix (Fig. 1b). In contrast, the normal counterpart showed cells and matrix with far less staining intensity, and a more prominent counterstain (Fig. 1c). Similar differences between cells preconditioned in sulfate-free ASW and normal ASW were found in sections stained with anti-integrin β_1 , but the distinctions were less pronounced than those observed in cells stained with anti-integrin α_3 .

This study confirms those of other workers, and it indicates that sponges—the oldest animal phylum with a multicellular lineage—already had membrane structures that provide for controlled reactions between cells, and for cell matrix reactions (2, 4). The inverse correlation between integrin up-regulation and sponge cell motility is of interest and has been described in systems other than the sponge (5). In some cells, the expression of integrins that bind fibronectin RGD is correlated with reduced cellular motility (6). This is important when considering the possible relationships between *Microciona* aggregation fac-

¹ Hospital for Sick Children, 555 University Ave. Toronto, Ontario, Canada M5G 1X8. (Author for correspondence.)

² Friedrich Miescher Institute, Ch 4002, Basel, Switzerland.

³ Mount Holyoke College, Department of Biology, South Hadley, MA 01075.

⁴ Faculty of Pharmacy, University of Barcelona, Barcelona, Spain.

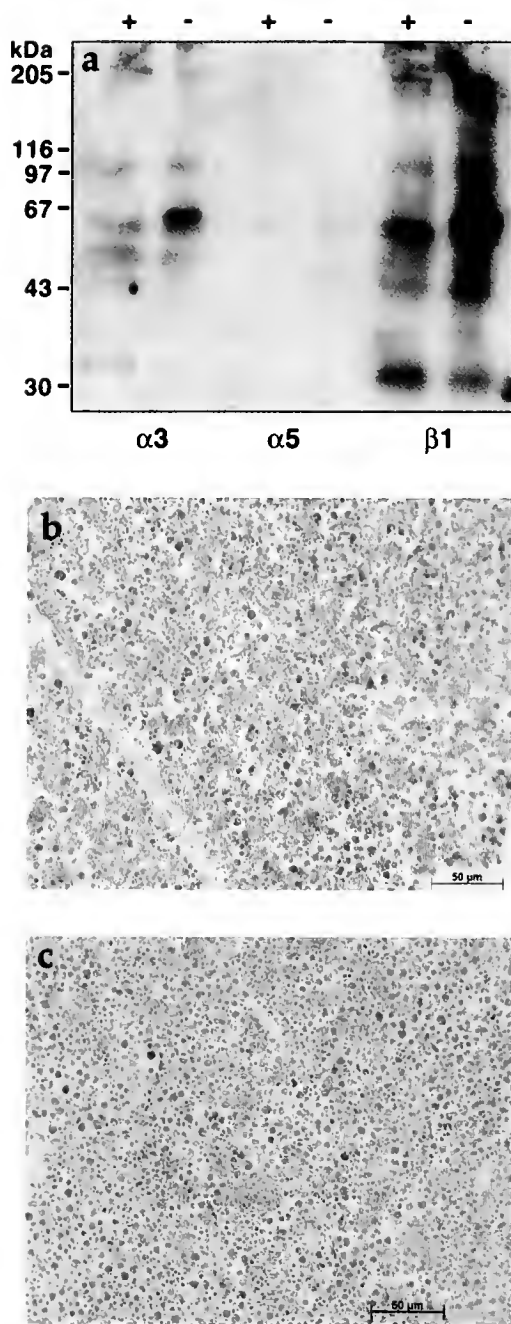


Figure 1. (a) Western blots demonstrating α_3 and β_1 integrins. SDS-PAGE was performed according to the Laemmli buffer systems on gel slabs of $75 \times 100 \times 0.75$ mm, at 125 V, with a Bio-Rad Protean II apparatus at a gel concentration of 10%. The cell lysates were heated in loading buffer at 95°C for 5 min. The wells were charged with 20 μl (100 μg) protein. Reference standards (10 μl) were placed in a separate well; their migration is shown on the left side of the gel. The separated proteins were then electrotransferred to nitrocellulose and probed with anti-integrin rabbit polyclonal antibodies from Bioline Diagnostici srl (Milan, Italy) at a dilution of 1–500. (b, c) Integrin immunohistochemistry; sections were prepared as described in the text. Mouse monoclonal antibodies from BD-Pharmingen were used at a dilution of 1–200. (b) Sulfate-deprived cells. Most large cells treated with anti-integrin α_3 show intense orange-brown staining; widespread moderate staining of the extracellular matrix

tor (MAF), *Microciona* cells, and the $\alpha_3\beta_1$ integrins. MAF proteins that are expressed from cDNA possess RGD binding sequences (see ref. 7, p. 29,548, MAF p3/p4 form C), which could potentially ligate MAF to the integrins to initiate a trans-cellular motility-reduction signal, a strategy distinct from the carbohydrate-carbohydrate binding thought to mediate aggregation. Under usual conditions, the high sugar content of MAF might preclude effective integrin-RGD peptide binding, but this situation might change when cells are exposed to low levels of environmental sulfate. The availability of pure MAF RGD peptide sequences and of integrin peptides may allow for binding correlations between these synthetic compounds and their natural counterparts in normal and sulfate-stressed sponge. The ability to manipulate sponges *in vivo* by sulfate reduction will provide a powerful tool toward a further understanding of signaling pathways and their relationships to adhesion and motility.

Literature Cited

1. Hynes, R. O. 1992. *Cell* 69: 11–25.
2. Pancer, Z., M. Kruse, I. Muller, and W. Muller. 1997. *Mol. Biol. Evol.* 14: 391–398.
3. Kuhns, W., O. Popescu, M. Burger, and G. Misevic. 1995. *J. Cell. Biochem.* 57: 71–89.
4. Wimmer, W., S. Perovic, M. Kruse, H. Schroder, A. Krasko, R. Batel, and W. Muller. 1999. *Eur. J. Biochem.* 260: 156–165.
5. Christopher, R., and Jun-I. in Guan. 2000. *Int. J. Mol. Med.* 2000 5: 575–581.
6. Zhang, Z., A. Morla, K. Vuori, J. Dauer, R. Juliano, and E. Ruoslahti. 1993. *J. Cell Biol.* 122: 235–242.
7. Fernandez-Busquets, X., D. Gerosa, D. Hess, and M. Burger. 1998. *J. Biol. Chem.* 273: 29,545–29,553.

is also noted. (c) Cells preconditioned in normal ASW. Large cell staining is generally less intense; most cells show lighter anti-integrin staining, or they stain more prominently with the hematoxylin counterstain. The extracellular matrix is very lightly stained with anti-integrin α_3 .

Reference: *Biol. Bull.* **201**: 240–241. (October 2001)

Recombinant Globular Tail Fragment of Myosin-V Blocks Vesicle Transport in Squid Nerve Cell Extracts

Jeremiah R. Brown, Kyle R. Simonetta, Leslie A. Sandberg, Phillip Stafford¹, and George M. Langford
(Department of Biological Sciences, Dartmouth College, Hanover, New Hampshire 03755)

Myosin-V, a calmodulin-binding myosin motor, mediates the movement of vesicles on cortical actin filaments in a variety of cell

types. This motor has been shown to transport ER and synaptic vesicles in neurons, melanosomes in melanocytes, and secretory vesicles and the vacuole in yeast. Recent evidence (1) suggests that the globular tail of myosin-V, which binds to the surface of vesicles (2, 3),

¹ Motorola, Inc. Chicago, IL.

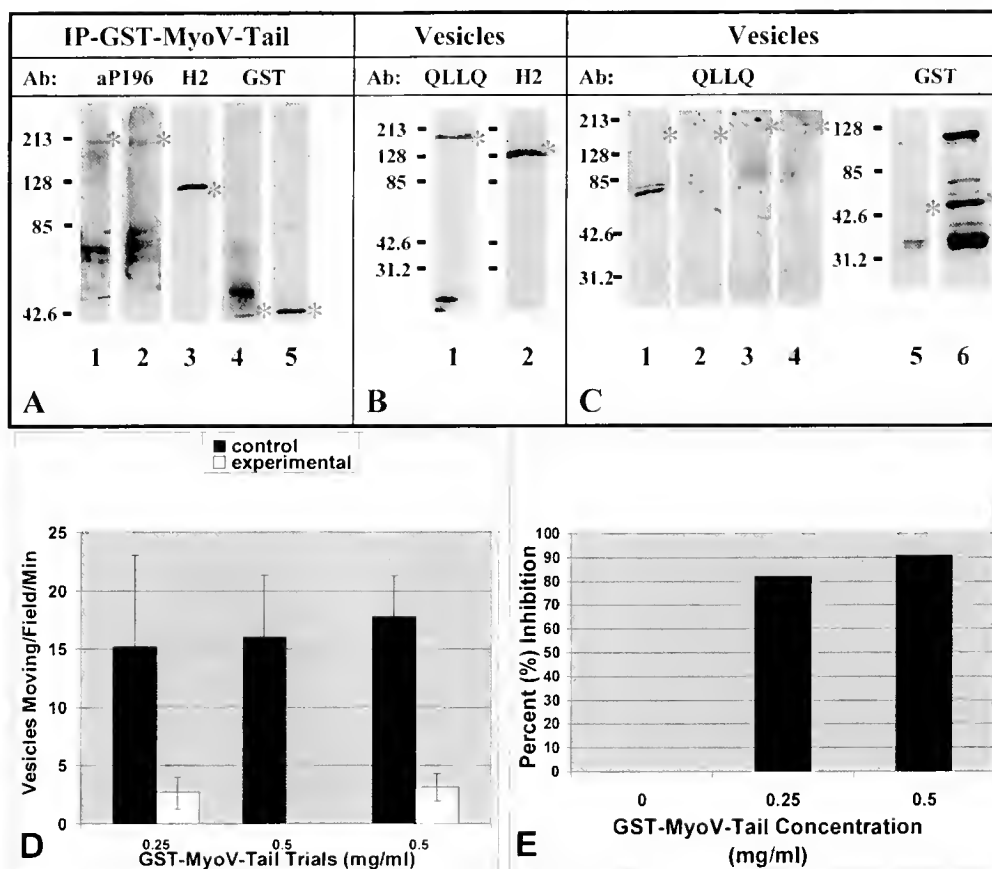


Figure 1. (A) Western blot analyses of immunoprecipitation (IP) experiments using the GST-MyoV-tail. Clarified squid optic lobe homogenate was Triton X-100 extracted, incubated with the recombinant tail fragment for 2 h at 4°C, and recovered using α -GST. (Lane 1) Squid myosin-V enriched fraction (S5B) probed with α -P196, a polyclonal squid myosin-V antibody (* denotes band of interest). (Lane 2) IP-GST-MyoV-tail probed with α -P196. (Lane 3) IP-GST-MyoV-tail probed with α -H2, a monoclonal antibody to the squid kinesin. (Lane 4) IP-GST-MyoV-tail probed with α -GST antibody. (Lane 5) Purified GST-MyoV-tail probed with α -GST. (B) Western blot analyses of sucrose vesicle fractions obtained by running clarified squid brain homogenate on a sucrose density gradient (0.3/0.6/1.5 M gradient; vesicle fraction taken from 0.3/0.6 M interface). (Lane 1) Vesicle fraction probed with α -QLLQ, a polyclonal antibody to the squid myosin-V tail. (Lane 2) Vesicle fraction probed with α -H2. (C) Western blot analyses of vesicle fraction incubation GST-MyoV-tail. The vesicle fraction, prepared by resuspending vesicular pellet from clarified squid brain homogenate, was incubated for 2 h at 4°C with the GST-MyoV-tail. The supernatant and vesicle pellet were analyzed by western blot analyses. (Lane 1) Control supernatant probed with α -QLLQ. (Lane 2) GST-MyoV-tail incubation supernatant probed with α -QLLQ. (Lane 3) Control pellet probed with α -QLLQ. (Lane 4) GST-myosin-V tail incubation probed with α -QLLQ. (Lane 5) GST-MyoV-tail incubation pellet probed with α -GST. (Lane 6) Purified GST-MyoV-tail probed with α -GST. (D) GST-MyoV-tail inhibition experiments. GST-MyoV-tail was added to squid giant axon extracts at time zero. GST was added to the control. Vesicles moving/field/minute (motile activity) was measured for the control at 15 min. Motile activity was measured for the GST-MyoV-tail at 45 min. Each measured for concentrations of 0.25 mg/ml and 0.5 mg/ml. (E) The motile activity at each GST-MyoV-tail concentration compared with the control is plotted as percent (%) inhibition. Percent inhibition determined by comparing 15-minute control time point with the 45-minute experimental time point.

interacts with the microtubule-based motor, kinesin, to form a "hetero-motor" complex on vesicles. The complex of these two motors, one microtubule-based and the other actin-based, is thought to facilitate the movement of vesicular cargo from microtubules to actin filaments. Based on our studies of vesicle transport by these two motors in extracts of squid neurons (4), we hypothesize that one of the functions of the tail-tail interaction is to provide feedback between the two proteins to allow a seamless transition of vesicles from microtubules to actin filaments.

To study the interactions of the globular tail domain of myosin-V to kinesin and to neuronal vesicles, we used a glutathione S-transferase (GST)-tagged globular tail fragment in motility and vesicle-binding experiments. The plasmid for the recombinant tail fragment of mouse myosin-V was provided by Dr. Huang (1). The plasmid contained the GST-labeled mouse AF6/cno tail-globular-domain (GST-MyoV-tail [aa1569 to aa1768] without the coiled medial tail domain). After expression in *E. coli*, the GST-tagged fragment was purified on affinity columns and used in experiments with squid brain extracts and purified vesicles.

The GST-MyoV-tail fragment was identified on blots with a GST antibody (Fig. 1A, lanes 4 and 5; 1C, lanes 5 and 6). To determine whether the GST-MyoV-tail fragment binds squid brain kinesin, squid brain extracts were incubated with GST-MyoV-tail fragments for 2 h at 4°C, and then the GST-labeled fragment was immunoprecipitated with the GST antibody. Blots of the proteins isolated by this immunoprecipitation (IP) showed a kinesin band when probed with the H2 antibody to squid brain kinesin (Fig. 1A, lane 3), establishing that the recombinant mouse myosin-V-tail pulled down native squid kinesin.

The bacterially expressed recombinant globular tail domain of myosin-V was incubated with purified squid brain vesicles to replace native myosin-V. Vesicles were purified by sucrose density gradient from clarified homogenates of squid brain. Vesicle fractions were examined by DIC and fluorescence microscopy after staining with DIOC6, a green fluorescent membrane dye. Overlay of the DIC and fluorescent images demonstrated that the particles observed in the DIC image were membrane structures. The vesicle fractions were analyzed by SDS-PAGE and western blots, and both myosin-V and kinesin were present on these vesicles (Fig. 1B, lanes 1 and 2). A similar vesicle fraction was incubated for 2 h at 4°C with the GST-MyoV-tail fragment. After incubation, blots of the vesicle pellet showed a band for the GST-tagged fragment, indicating binding of the tail domain to vesicles (Fig. 1C, lane 5). Blots of the supernatants,

after the vesicles were pelleted, showed a higher concentration of myosin-V in the GST-MyoV-tail incubation than in the control incubation, indicating displacement of native myosin-V from the vesicles by the recombinant tail (Fig. 1C, lanes 1 and 2).

The recombinant fragment of myosin-V was used in motility assays to determine whether it had replaced native myosin-V on axoplasmic vesicles and blocked transport. The GST-MyoV-tail fragment (0.25 and 0.5 mg/ml) was added to axoplasm in the presence of 5 mM ATP, and the sample was warmed to 24°C. Purified GST was used as a control. Actin-based vesicle transport was quantified by counting the number of vesicles moving/field/min (*v/f/m*, motile activity) at 2 time points during a 1-h incubation. Motile activity for the 0.25 mg/ml trial decreased from 17.5 ± 5.5 to 2.6 ± 1.3 *v/f/m*, and for the 0.5 mg/ml trial, from 16.7 ± 1.7 to 1.5 ± 0.5 *v/f/m* (Fig. 1D). Therefore, the MyoV tail fragment inhibited vesicle transport by 81% and 91%, respectively, and thereby exhibited a dominant negative effect in these functional assays (Fig. 1E). These data show that the recombinant protein blocked the activity of native myosin-V presumably by binding to vesicles and competing away the native myosin-V motors.

The GST-MyoV-tail fragment pulled down kinesin by immunoprecipitation from squid brain homogenates, and it therefore exhibited binding properties of native myosin-V. The GST-MyoV-tail fragment blocked vesicle transport in extracts of the squid giant axon. These data show that the headless myosin-V fragment is an effective inhibitor of vesicle transport in cell extracts and can be used to determine the mechanism of motor recruitment to vesicles. These studies support the hypothesis that tail-tail interactions may be a mechanism for feedback between myosin-V and kinesin, allowing transition of vesicles from microtubules to actin filaments.

Supported by NSF grant MCB9974709 and MBL Josiah Macy Fellowship.

Literature Cited

- Huang, J. D., S. T. Brady, B. W. Richards, D. Stenolen, J. H. Resau, N. G. Copeland, and N. A. Jenkins. 1999. *Nature* 397: 267-270.
- Wu, X., B. Bowers, K. Rao, Q. Wei, and J. A. Hammer III. 1998. *J. Cell Biol.* 143: 1899-1918.
- Reck-Peterson, S. L., P. J. Novick, and M. S. Mooseker. 1999. *Mol. Biol. Cell* 10: 1001-1017.
- Tabb, J. S., B. J. Molyneaux, D. L. Cohen, S. A. Kuznetsov, and G. M. Langford. *J. Cell Sci.* 111: 3221-3234.

Reference: *Biol. Bull.* 201: 241-243. (October 2001)

Reconstitution of Active Pseudo-Contractile Rings and Myosin-II-Mediated Vesicle Transport in Extracts of Clam Oocytes

Torsten Wöllert¹, Ana S. DePina, Leslie A. Sandberg, and George M. Langford

(Department of Biological Sciences, Dartmouth College, Hanover, New Hampshire 03755)

Cell division requires the construction of a contractile ring of actin filaments attached to the plasma membrane at the site of cleavage. Bipolar myosin-II filaments in the contractile ring gen-

erate sliding of anti-parallel bundles of actin filaments, thereby constricting the cell (1). A recent study of cell division in *Dictyostelium* (2) showed that myosin-II filaments are recruited to the contractile ring cell by "cortical flow." The underlying mechanism of cortical flow is not known. We inhibited the motor activity of myosin-II in cell-free extracts of clam (*Spisula solidissima*) oo-

¹ Rostock University, Germany.

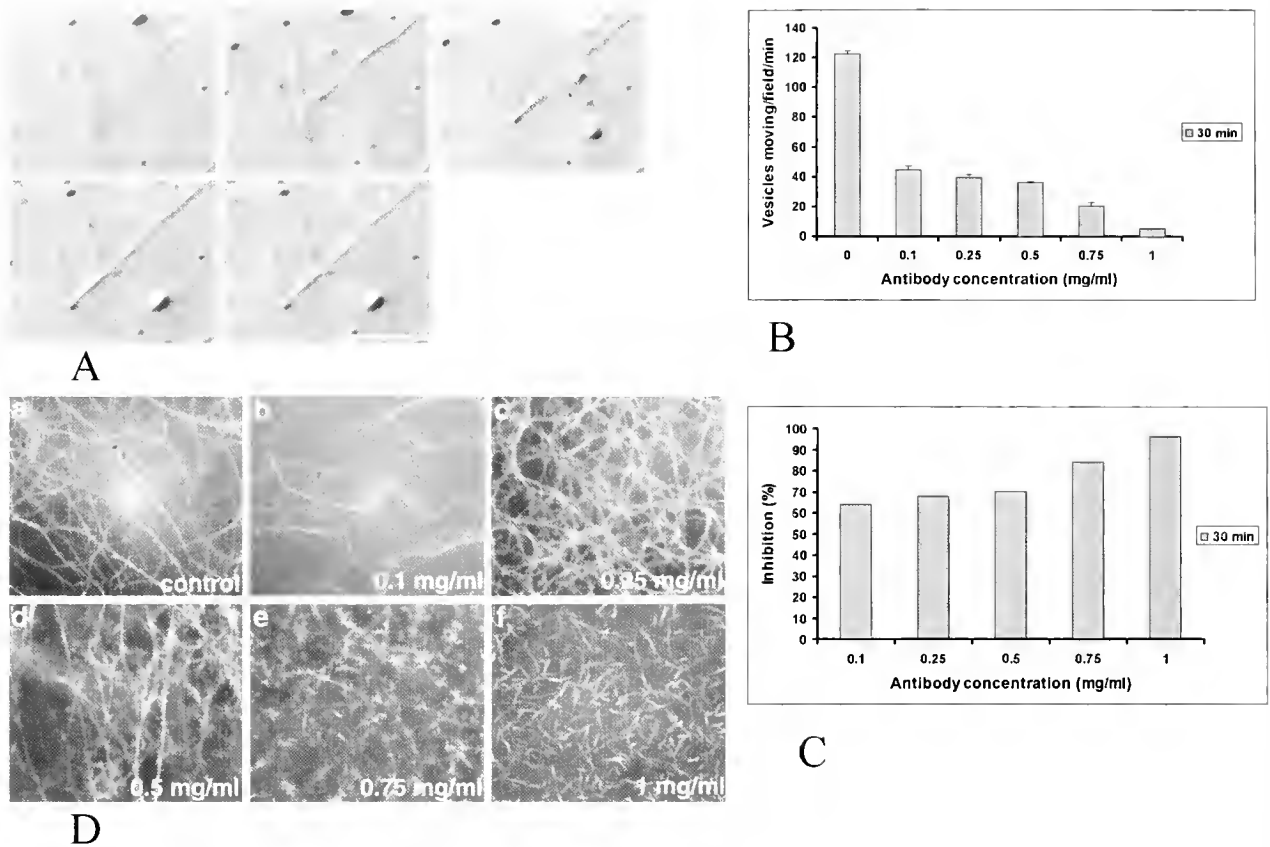


Figure 1. Myosin-II-dependent sliding of actin filament bundles and vesicle transport in clam oocyte extracts. (A) Successive AVEC-DIC images of a sliding actin bundle in a pseudo-contractile ring. The bundle contains 6 or more actin filaments, the limit of detection of video microscopy (5). The tip of the bundle (asterisk) slides toward the lower left as depicted in each successive image captured at 6 s intervals. Bar 10 μm . (B) Antibody inhibition experiments. Inhibition of vesicle transport increased as the myosin-II-specific antibody concentration increased from 0.1 to 1.0 mg/ml. A non-specific rabbit polyclonal (squid myosin-V antibody) was added to the control (labeled 0 mg/ml). (C) Vesicle transport was inhibited by 95% at an antibody concentration of 1.0 mg/ml. (D) Fluorescence images of the 3-D-actin network at 30 min for each concentration of antibody used. Interactive bundles self-organized into a 3-D network in the control and at the low concentrations of antibody. Network formation was blocked at 0.75 and 1.0 mg/ml.

cytes with a function-blocking myosin-II-specific antibody to investigate the mechanism of movement of myosin-II to the contractile ring.

Cytoplasmic extracts were prepared from mature oocytes obtained from gravid female clams (3, 4). The clarified extracts were diluted 2-fold (protein concentration about 15 mg/ml) and adjusted to pH 7.2. Nocodazole (50 μM) was added to the extracts to block microtubule assembly, and an ATP regenerating system was added to maintain ATP levels. The final extract was incubated for 45 min at 18 $^{\circ}\text{C}$ to initiate transition into the meiotic phase of the cell cycle. Rhodamine-phalloidin (0.5 μM) was added to stain the actin filaments, and the myosin II motor activity was monitored by AVEC-DIC and fluorescence microscopy (5).

Actin bundles detectable by AVEC-DIC microscopy assembled spontaneously in the meiotic phase extracts and formed interactive three-dimensional networks or pseudo-contractile rings by a mechanism of self-organization (6). Two types of myosin-dependent movement associated with the actin networks were observed. First, overlapping bundles of actin filaments in the network were observed to slide along each other. The advancing tips of sliding bundles were tracked at speeds greater than 0.2 $\mu\text{m/s}$ for more than

25 μm before disappearing out of the field of view (Fig. 1A). A similar sliding motion produced by bipolar myosin-II filaments is generally accepted as the mechanism by which the contractile ring constricts the cell during cytokinesis. Therefore, these self-organized actin networks or pseudo-contractile rings exhibited one of the principal properties ascribed to the contractile ring.

The second type of motor activity observed in these extracts was the movement of vesicles on actin filaments. In a given video field that measured 25 μm^2 , more than 100 vesicles could be observed moving simultaneously at an average speed of 1.0 $\mu\text{m/s}$ (Fig. 1B, control). On occasion, ER-like networks moved on the actin filaments, but most of the moving particles were individual vesicles that were probably derived from ER during homogenization.

To demonstrate that both filament sliding and vesicle transport were dependent on myosin-II, we performed antibody inhibition experiments with a rabbit-polyclonal antibody raised to myosin-II from clam oocytes. The Protein-A-purified, myosin-II-specific antibody recognized a single band on immunoblots of the oocyte extracts. Inhibition of vesicle transport was determined by comparing motile activity after antibody addition with motile activity in controls. Motile activity was measured by counting the number

of moving vesicles per video field per minute (v/f/m). The control extracts showed high levels of motile activity (122 v/f/m) for periods of 60 min or more. However, addition of the myosin-II-specific polyclonal antibody caused a concentration-dependent inhibition of motile activity (Fig. 1B). Vesicle transport was inhibited by 95% (5 v/f/m) at an antibody concentration of 1 mg/ml (Fig. 1C). The antibody inhibition experiments provided direct evidence that vesicle transport was mediated by myosin-II.

At concentrations of 0.75 and 1.0 mg/ml, the myosin-II-specific antibody inhibited the formation of the 3-D network (Fig. 1D). With fluorescence microscopy, pseudo-contractile rings of actin bundles could be seen in the control extracts, but they were absent at these two antibody concentrations (Fig. 1D). The antibody did not inhibit the assembly of actin filaments but blocked the association of filaments into bundles; therefore, the myosin-II antibody blocked the self-organizing and bundle-sliding activities observed in the control extracts. The concentration of myosin-II in these extracts was estimated to be in the range of 0.1–0.2 mg/ml, so an antibody concentration of 1 mg/ml was about 5-fold higher than the concentration of myosin. The antibody is polyclonal, and only a subset of IgG molecules are expected to bind at sites that block motor function; thus we judge the antibody concentration required for inhibition of filament sliding and vesicle transport to be within the expected range.

The generation of sliding forces between actin filaments is a well-established activity of bipolar filaments of myosin-II. Therefore, the observation that actin filaments self-organized and moved in an anti-parallel fashion in these extracts fits current models of the contractile ring. Sliding of actin filaments is assumed to occur in intact contractile rings, but it has not been observed. These studies provide a direct view of the sliding activity that occurs in self-organized actin networks that mimic contractile rings. Self-organized networks in cell-free extracts such as these may be the only means available to observe myosin-II-mediated sliding of actin bundles like those in the contractile ring.

The other novel observation in these experiments was the myosin-II-dependent movement of vesicles. Myosin-II has not previously been shown to be a vesicle motor. However, the movement of vesicles to the contractile ring has been documented, and myosin-II is known to move toward the equator by cortical flow (2). Myosin-II-mediated vesicle transport on cortical actin filaments may provide a mechanism by which myosin-II filaments arrive at the contractile ring. Such a model is not consistent with several published reports. Yumura and Uyeda (7), for example, demonstrated that myosin-II molecules that lack ATPase activity are recruited to the equator. In addition, headless myosin-II localizes to the equator (8, 9). These observations suggest that myosin filaments are transported as passive passengers to the actin cortex rather than through their own motor activity. Our studies, on the other hand, provide some of the first evidence that myosin-II binds specifically to vesicles and drives vesicle movement. The motor activity of myosin-II may thus be another mechanism by which bipolar myosin-II filaments are recruited to the cortex and to the contractile ring.

Literature Cited

1. Sanger, J. M., and J. W. Sanger. 2000. *Microsc. Res. Tech.* **49**: 190–201.
2. Yumura, S. 2001. *J. Cell Biol.* **154**: 137–145.
3. DePina, A. S., and G. M. Langford. 1999. *Microsc. Res. Tech.* **47**: 93–106.
4. Sandberg, L., P. Stafford, and G. M. Langford. 2000. *Biol. Bull.* **199**: 202–203.
5. Langford, G. M. 2001. *Methods Mol. Biol.* **161**: 31–43.
6. Surrey, T., F. Nedelec, S. Leibler, and E. Karsenti. 2001. *Science* **292**: 1167–1171.
7. Yumura, S., and T. Q. P. Uyeda. 1997. *Mol. Biol. Cell* **8**: 2089–2099.
8. Zang, J. H., and J. A. Spudis. 1998. *Proc. Natl. Acad. Sci. USA* **95**: 13,652–13,657.
9. Naqvi, N. I., K. Eng, K. L. Gould, and M. K. Balasubramanian. 1999. *EMBO J.* **18**: 854–862.

Reference: *Biol. Bull.* **201**: 243–245. (October 2001)

A Novel, Kinesin-Rich Preparation Derived From Squid Giant Axons

John R. Clay¹ and Alan M. Kuzirian (*Marine Biological Laboratory, Woods Hole, Massachusetts 02543*)

Almost 20 years ago, Robert Allen and colleagues (1, 2) observed in squid giant axons a relatively large number of “submicroscopic” particles moving with velocities consistent with fast axonal transport. These observations were made with video-enhanced contrast-differential interference contrast microscopy (1), a methodology which had just been developed. The particles were estimated to be 30–50 nm in diameter, and they were proposed to be anatomical correlates of small vesicles apparent in electron micrographs of Hodge and Adelman (3). We recently published additional evidence in support of this view (4). Moreover, we demonstrated with immunocytochemistry that a small fraction of these vesicles contain the delayed rectifier K⁺ channel.

This channel is also present in the axolemma, where it underlies the repolarization phase of the nerve impulse (“action potential”; 4, 5). These vesicles appear not to be targeted to the axon terminals since they do not contain synaptic vesicle proteins and are not clathrin coated (4, 6). We have developed novel methodology for isolating them from axoplasm (4). The initial step used in these procedures is highlighted in this report.

The medial giant axons were dissected from squid provided by the Marine Resources Center of the Marine Biological Laboratory, and the axoplasm was extruded using standard techniques (7; Fig. 1). A small amount of buffer was added (1 μ l per cm length of axon) which contained 10 mM Na acetate, 10 mM HEPES (pH 7.2) with 1M glucose, so that the osmolarity was 980 mOsm. Similar results were obtained with a buffer consisting of 440 mM K glutamate, 5 mM EGTA, and 10 mM HEPES (4). Axoplasm and buffer were immediately placed in a small, thick-walled polycar-

¹ National Institute of Neurological Disorders and Stroke, National Institutes of Health, Bethesda, MD 20892.

bonate centrifuge tube (0.2 ml fill volume, Beckman Instruments, Inc., Palo Alto, CA) and spun in an ultracentrifuge (Sorvall RC-M120GX) for 5–6 min at 35,000 g_{av} (Fig. 1). A typical preparation consisted of axoplasm pooled from 30 axons in lots of six to minimize the time between dissection of the axons and the centrifugation step. Centrifugation yielded approximately equal volumes of translucent materials that we refer to as residual axoplasm and clear supernatant (Fig. 1).

A standard Eppendorf laboratory centrifuge having maximal centrifugal force of 14,000 g_{av} was not sufficient to produce the result described above. A force about 2 to 3 times larger was required. Specifically, the result shown was obtained with a force in the range of 25,000 to 40,000 g_{av} . This step appears to be a measure of the structural integrity of squid axoplasm. The result illustrated in Figure 1 has not typically been obtained in August, when squid viability is known to be poor—and, in our experience, viability of the axoplasm is also poor. At those times the axoplasm collapses into a small pellet (approximately 1% of the size of the residual axoplasm illustrated in Fig. 1) with a supernatant volume equal to that of residual axoplasm plus supernatant obtained at other times of the year. A similar result was obtained when chaotropic buffer, such as 0.5 M K iodide, was added to the axoplasm.

The supernatant (Fig. 1) is rich in low-molecular-weight proteins, as determined by SDS-PAGE with Coomassie blue staining (Fig. 2, lane a). In particular, it contains tubulin and actin (Fig. 2; arrows 2 and 3, respectively), which was confirmed by immunoblots (not shown) with anti-tubulin and anti-actin (Calbiochem, La Jolla, CA). Neurofilament proteins were not detected in an immunoblot using the antibodies described by Grant and colleagues (8). The supernatant also contains heat shock protein (Hsc70; [9]; arrow 1 in Fig. 2), as demonstrated with an immunoblot with anti-Hsc70 (Stressgen, Victoria, BC, Canada). Of particular note is the abundance of the microtubule-based motor protein kinesin in the supernatant. This protein was not detectable with SDS-PAGE either with Coomassie blue or silver staining, but was readily apparent by immunoblot (lane b, Fig. 2; anti-kinesin [Chemicon, Temecula, CA]). We estimate that 20%–40% of the total kinesin in axoplasm is contained in the supernatant of our preparation, based on densitometer tracings of immunoblots of the supernatant and residual axoplasm. Immunoblots and single-channel record-

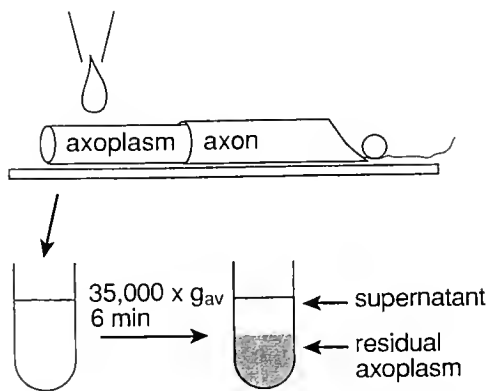


Figure 1. Illustration of the experimental procedure used in this study.

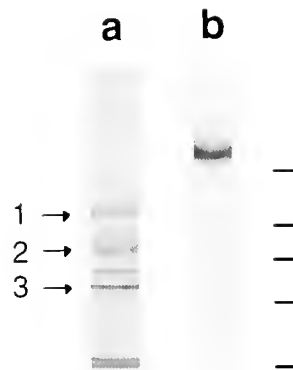


Figure 2. (a.) SDS-PAGE of the supernatant stained with Coomassie blue. Arrows 1, 2, and 3 correspond to heat shock protein (Hsc70; the lower band of the doublet by the arrow), tubulin, and actin, respectively. (b.) Immunoblot of the supernatant with anti-kinesin, detected with enhanced chemiluminescence. The lines on the right are molecular weight markers corresponding to 98, 64, 50, 36, and 16 kDa, top to bottom, respectively.

ings obtained by adding an aliquot of supernatant to one side of an artificial lipid bilayer (4) demonstrated that the supernatant also contains K^+ channels. In addition to kinesin, all the other proteins (Hsc70, neurofilaments, actin, and tubulin) except for K^+ channels were detected in residual axoplasm.

We believe that the kinesin in the supernatant is largely, or perhaps entirely, bound to small vesicles such as those illustrated in figure 4 of our previous work (4). Kinesin has also been found in soluble fractions of *in vitro* preparations (10). In those studies the tissue was homogenized, a procedure which we avoided. We handled the axoplasm gently until the spin at 35,000 g_{av} , which we believe strips small vesicles from microtubules and any other elements to which they may be attached. The vesicles then float into the supernatant because of their buoyancy. A centrifugal force of 35,000 g_{av} is not nearly sufficient to bring them down into a pellet (4).

Our technique provides a vesicle preparation (vesicles destined for the axolemma) that is free of one of the major contaminants of vesicle preparations: neurofilament proteins. The preparation also contains a significant amount of actin and tubulin, which we believe are not associated with the vesicles. A small fraction of the heat shock protein is bound to the vesicles (unpubl. obs.), which appears to be a key factor in further purification of the vesicles (4). This preparation may be of interest to other investigators in the cellular motility field.

We gratefully acknowledge Phil Grant for his gift of neurofilament protein antibodies.

Literature Cited

1. Allen, R. D., J. Metzuzals, I. Tasaki, S. T. Brady, and S. P. Gilbert. 1982. *Science* 218: 1127–1129.
2. Brady, S. T., R. J. Lasek, and R. D. Allen. 1982. *Science* 218: 1129–1131.
3. Hodge, A. J., and W. J. Adelman. 1980. *J. Ultrastruct. Res.* 70: 220–241.
4. Clay, J. R., and A. M. Kuzirian. 2000. *J. Neurobiol.* 45: 172–184.
5. Hodgkin, A. L., and A. F. Huxley. 1952. *J. Physiol. (Lond.)* 116: 449–472.

6. de Waegh, S., and S. T. Brady. 1989. *J. Neurosci. Res.* **23**: 433–440.
7. Brown, A., and R. J. Lasek. 1990. Pp. 235–302 in *Squid as Experimental Animals*. D. L. Gilbert, W. J. Adelman, Jr., and J. M. Arnold, eds., Plenum Press, New York.
8. Grant, P., D. Tseng, R. M. Gould, H. Gainer, and H. C. Pant. 1995. *J. Comp. Neurol.* **356**: 311–326.
9. Tsai, M.-Y., G. Morfini, G. Szebenyi, and S. T. Brady. 2000. *Mol. Biol. Cell* **11**: 2161–2173.
10. Hollenbeck, P. J. 1989. *J. Cell Biol.* **108**: 2335–2342.

Reference: *Biol. Bull.* **201**: 245–246. (October 2001)

Microsporidian Spore/Sporoplasm Dynactin in *Spraguea*

Earl Weidner (Biological Sciences, Louisiana State University, Baton Rouge, Louisiana 70803)

Intracellular protistan parasites have evolved a diversity of adaptations for survival and replication within host cell vacuoles. Some of these adaptations require specific membrane-inserted or surface-attached proteins on the vacuolar envelopes. However, intracellular microsporidian parasites are not in vacuoles; rather, they locate directly in contact with the host cell cytoplasm. This position in the host cytoplasm may be partly due to their means of entry through injection by an invasion tube. Within the microsporidian genus *Spraguea*, the parasites are confined to neuronal fiber axoplasms in the central nervous system of anglerfish, genus *Lophius*. The supramedullary neurons are frequently parasitized by *Spraguea*, and the colonies locate in the proximal regions of fibers adjoining the nerve cell bodies. The supramedullary neurons send fibers to the cutaneous areas in fish (1). Recent studies of puffer fish, genus *Takifuga*, indicate that these fibers innervate the cutaneous mucous glands (2); this observation is supported by our preliminary investigations on anglerfish. The mucous gland domains of anglerfish skin are the most common sites where infective *Spraguea* spores activate and discharge their sporoplasms. Mucus is a major activator of *Spraguea* spores and is a primary factor in

effecting spore discharge (3). So the sporoplasms are likely to be introduced directly into the nerve endings surrounding the cutaneous glands in anglerfish. However, established infections of *Spraguea* are always found at the proximal end of the supramedullary nerve. Our laboratory has therefore hypothesized that *Spraguea* sporoplasms are equipped with surface proteins that support sporoplasm transport up the fiber to the neuronal cell body area. This study was therefore designed to probe for a dynactin-dynein assemblage because this motor is minus-end-directed and can effect linkups between membrane and microtubules.

To search for dynactin-dynein motor molecules in *Spraguea* sporoplasms, purified spores were incubated in 0.1 M HEPES buffer (pH 7.0) and transferred to glass coverslips. The spores were activated to discharge their sporoplasms by a method described earlier (3). The discharged sporoplasms retain their attachment to the glass during subsequent washing episodes that remove unfired and discharged spores; the wash solution was 0.1% concanavalin A made up in 0.1 M HEPES (pH 7.0).

The isolated sporoplasms were subjected to optical probes and Western blots using antibodies to dynactin peptides p^{150glued}, p⁵⁰,

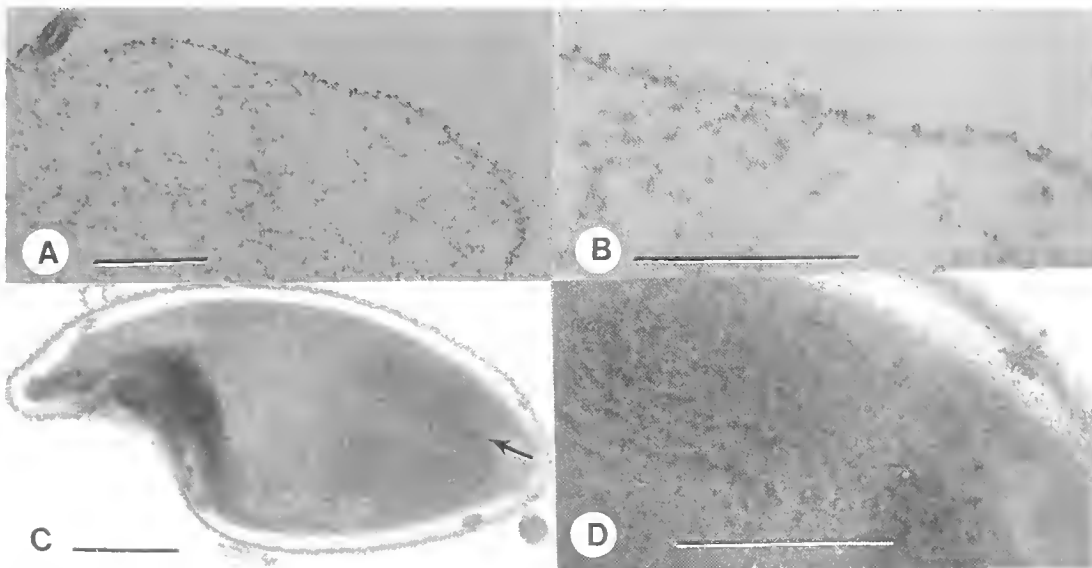


Figure 1. *Spraguea* spp. sporoplasm with peroxidase label directly against p^{150glued}. Sporoplasms are exceedingly permeable and thus devoid of some internal matrix; however, the sporoplasm surfaces were consistently labeled with external peroxidase probe (A). (B) This image is a higher magnification of A. (C) The sporoplasm is within an unfired spore and the peroxidase label is within the polaroplast (arrow). (D) This is an enlarged image of C. Bar scales represent 0.25 μm .

Arp1 and intermediate dynein chains. The Western blots to *Sprague* sporoplasm proteins indicated that, whether whole sporoplasm samples were tested, or only the sporoplasm outer membrane isolates, all four of these peptides were present. Ultrastructural immunolabeling with an antibody-peroxidase probe for p^{150glued} showed the label binding uniformly over the sporoplasm surface (Fig. 1A, B). These results were also supported by immunogold labeling and immunofluorescence (not shown). Since I hypothesized that the dynactin assemblage should be associated with the membrane within unfired spores, tests were made to determine where the dynactin is located in such spores. Spores were prefixed with 1% glutaraldehyde and subsequently partially disrupted by the shearing action of a glass homogenizer. These spores were then subjected to the p^{150glued} antibody probe, and this was visualized with a second antibody coupled to peroxidase. The results showed that the label reacts within the polaroplast domain

(Fig. 1C, D). The position of the dynactin within the polaroplast supports an old idea: that the spore discharges a tube through which the membrane of the polaroplast everts to form the sac. The cytoplasm and nucleus are thought to be introduced into the everted polaroplast-derived sac. That the sporoplasm membrane is a secondhand membrane derived from the polaroplast organelle is supported by the absence of cholesterol in the outer envelope (3) and the absence of lectin-binding molecules (unpubl. obs.).

Literature Cited

1. Funakoshi, K., T. Abe, and R. Kishida. 1995. *J. Comp. Neurol.* **358**: 552–562.
2. Funakoshi, K., T. Kadota, Y. Atobe, M. Nakano, R. Goris, and R. Kishida. 1998. *Neurosci. Lett.* **258**: 171–174.
3. Weidner, E., and A. Findley. 1999. *Biol. Bull.* **197**: 270–271.

Reference: *Biol. Bull.* **201**: 246–247. (October 2001)

Response of the Blood Cell of the American Horseshoe Crab, *Limulus polyphemus*, to a Lipopolysaccharide-like Molecule from the Green Alga *Chlorella*

Mara L. Conrad (Department of Biology, Hunter College, New York, New York 10021),
R. L. Pardy¹, and Peter B. Armstrong²

The granular amebocyte is the single cell type in the general circulation of the horseshoe crab, *Limulus polyphemus*, and functions as the most important element in the immune system of the animal. The cytoplasm of the cell is packed with granules containing multiple immune effector proteins and peptides (1). Degranulation of the amebocyte, with the concomitant release of this complex of antimicrobial effectors, can be elicited by specific secretagogues such as bacterial lipopolysaccharide (LPS) (2). LPS is an essential component of the cell wall of all gram-negative bacteria and is an indicator molecule for the presence of these bacteria. Although LPS had previously been thought to be unique to gram-negative bacteria, a similar molecule has recently been found in the eukaryotic green algae, *Chlorella*, strain NC64A, maintained in bacteria-free culture (3). Algal LPS, like bacterial LPS, is composed of lipid A, ϵ -myristic acid, and 2-keto-3-deoxy-D-manno-octulosonic acid (KDO). This material gels the *Limulus* amebocyte lysate, a standard test for LPS (3). However, its biological activities are essentially uncharacterized.

Does algal LPS operate as an agonist of exocytosis of the granular amebocyte? Algal LPS was prepared as described previously (3). To evaluate the ability of the granular amebocyte to react to algal LPS, cultured horseshoe crab blood cells were challenged with algal or bacterial LPS, and the extent of exocytosis was evaluated by microscopic inspection (2). The animal was chilled for 2 h at 4 °C and bled (cardiac puncture with a 20-gauge needle) directly onto microscope coverslips

submerged in cold LPS-free 3% NaCl. The cells were allowed to attach to the coverslips for 5 min; then the coverslips were assembled into perfusion chambers (with the cell-coated slips supported above glass slides with chips of #1½ coverslips) as described by Armstrong and Rickles (2). The chambers were perfused with bacterial or algal LPS in 3% NaCl + 10 mM CaCl₂, at room temperature, and observed over time either with a Nikon inverted phase contrast microscope, or a Zeiss phase contrast microscope equipped with a Nikon Coolpix digital camera. Control cultures were perfused with LPS-free 3% NaCl + 10 mM CaCl₂. All glassware used was rendered LPS-free by heating at 180–200 °C for at least 4 h. Alternately, blood was collected directly into prechilled, virgin 35 × 10 mm plastic petri dishes containing 2 ml of LPS-free 3% NaCl, 1 drop of blood per dish. After allowing 5 min for the cells to attach to the dish, the culture was renewed with 2 ml fresh 3% NaCl. Blood plasma accelerates the exocytosis response in the absence of LPS (4), and its removal stabilizes the cells from spontaneous degranulation. Three percent NaCl was replaced with test solutions containing LPS in 3% NaCl + 10 mM CaCl₂. Ca⁺⁺ is required for cell flattening and a robust reaction to endotoxin. As before, the extent of exocytosis was determined by microscopic inspection.

The granular amebocyte responds positively to algal LPS (degranulation occurs), but the cell requires a concentration about 10 times higher than for bacterial LPS (*E. coli* Serotype 0127:B8, Sigma Cat # L-3129). Bacterial LPS provokes a vigorous exocytosis response at 5 µg/ml, causing the majority of the cells to degranulate within 20 min of exposure, whereas the cultured blood cell requires 50 µg/ml of algal LPS to initiate a similar response within that period (Fig. 1).

¹ School of Biological Sciences, University of Nebraska, Lincoln, NE 68583.

² Department of Molecular and Cellular Biology, University of California, Davis, CA 95616.

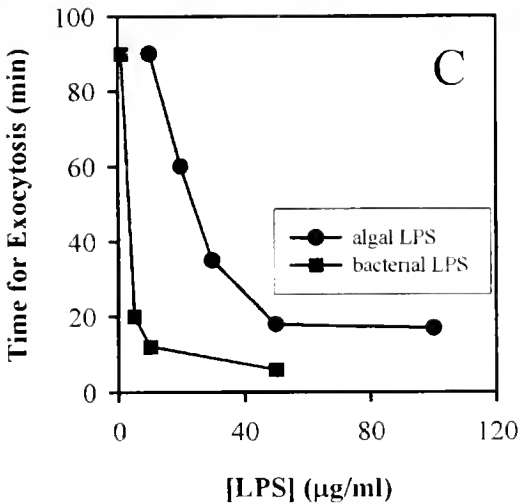
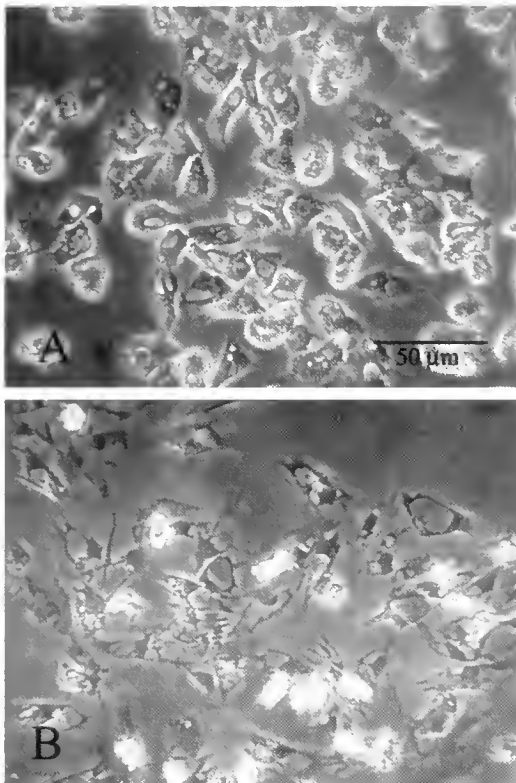


Figure 1. Stimulation of exocytosis of substratum-attached, cultured *Limulus* amoebocytes by algal LPS. (A) Prior to exposure, the cells are flattened on the culture surface and retain their secretory granules, which are observable as the small spherical vesicles that pack the cytoplasm surrounding the nucleus. (B) Thirty min after exposure to 30 µg/ml algal LPS, all of the substrate-attached cells have degranulated. The flattened cells show large internal lacunae, which are the sites of fusion of the membranes of the secretory granules with the plasma membrane. The contracted shiny cells in (B) are situated above the focal plane of the substratum-attached cells. These are fully granulated blood cells that have separated from the culture surface and are now migrating on the surface of the coagulin clot formed from materials secreted by the substrate-attached cells. Cells that have lost their attachment to the solid culture substratum are refractory to stimulation by bacterial LPS (2) and, as shown here, to algal LPS. (C) The response to algal LPS occurs more rapidly at higher concentrations of the agonist and requires about 10 times more LPS than does the response to bacterial LPS.

Limulus amoebocytes generate eicosanoid metabolites (5). The eicosanoids—oxygenated metabolites of the C20 polyunsaturated fatty acids, 20:3n-6, 20:4n-6, and 20:5n-3—operate as second messengers in activating cellular defense reactions to bacterial infection in insects. Exposure of blood cells to the eicosanoid biosynthesis inhibitor naproxin, an inhibitor of cyclooxygenase, abolished the LPS-induced nodulation response by the blood cells of the beetle, *Zophobas* (6). Consistent with a role for the eicosanoids in signaling in the amoebocyte, naproxin (1 mM) inhibited the exocytosis response of the cultured *Limulus* amoebocyte both to algal and to bacterial LPS.

The response of the granular amoebocyte to algal LPS is interesting, both for the characterization of a LPS-like molecule from algae, and for a better understanding of the immune system of the animal. In this latter regard, algal colonization and subsequent erosion of the carapace of the horseshoe crab appears to be an important cause of mortality of the adult animal (7), so it is of interest to characterize the different ways by which the immune system can interact with algae. Our documentation of the parallel activities of algal and bacterial LPS in the induction of the exocytotic response of the granular amoebocyte indicates that both molecules are capable of activating this important pathway of immunity in *Limulus*. This is the first demonstration that the LPS-like agent from an alga mediates LPS-like biological activities.

We thank Mr. Jim Barkes of Nikon for assistance with microscopy and Dr. Norman Wainwright and Ms. Alice Childs for conducting LAL assays of algal LPS. This research was supported by NSF Grant MB 26771 (to PBA) and a fellowship from the Hunter College-Howard Hughes Medical Institute Undergraduate Education Program (to MLC).

Literature Cited

- Iwanaga, S., and S.-i. Kawabata. 1998. *Front. Biosci.* 3: d973–d984.
- Armstrong, P. B., and F. R. Rickles. 1982. *Exp. Cell Res.* 140: 15–21.
- Royce, C. L., and R. L. Pardy. 1996. *J. Endotoxin Res.* 3: 437–444.
- Armstrong, P. B. 1980. *J. Cell Sci.* 44: 243–262.
- MacPherson, J. C., J. G. Pavlovich, and R. S. Jacobs. 1996. *Biochim. Biophys. Acta* 1303(2): 127–136.
- Bedick, J. C., R. L. Pardy, R. W. Howard, and D. W. Stanley. 2000. *J. Insect Physiol.* 46: 1481–1487.
- Liebovitz, L., and G. A. Lewbart. 1987. *Biol. Bull.* 173: 430 (abstract).

Reference: *Biol. Bull.* 201: 248–250. (October 2001)

LtB₄ Evokes the Calcium Signal That Initiates Nuclear Envelope Breakdown through a Multi-enzyme Network in Sand Dollar (*Echinarcinus parma*) Cells

Robert B. Silver (Departments of Radiology, Pharmacology and Physiology, Wayne State University School of Medicine, Detroit, Michigan; Decision and Information Sciences Division, Argonne National Laboratory, Argonne, Illinois; and Marine Biological Laboratory, Woods Hole, Massachusetts)

In our ongoing study of cell division control, we have shown that a calcium signal that is required for mitosis and that precedes nuclear envelope breakdown (NEB) arises from perinuclear endomembrane vesicles which are derived from a subset of the endoplasmic reticulum (1–5). Analyses of the calcium signals indicate that 1) this pre-NEB calcium signal occurs in microdomains; 2) the signals emitted at individual microdomains are not coherent; and 3) neither calcium nor its agonist diffuses more than 1 μm from the site of agonist production and calcium release (4, 6, 7). Prompted by those analyses, we posited and subsequently showed that leukotriene B₄ (LtB₄) (8) evokes the release of calcium *in vivo* and *in vitro* in a stereospecific fashion and functions as an important intracellular signal (5, 9, 10).

To approach the mechanism by which the calcium signal is controlled on the perinuclear vesicles, we have shown that 1) an enzyme network, that includes PLA₂ and the 5-lipoxygenase pathway enzymes, glutathione reductase, two forms of glutathione S-transferase (including a presumptive leukotriene C₄ synthase), and enzymes of the oxidative pentose phosphate and glycolytic pathways are also present on the calcium regulatory endomembranes of the prophase MA (11, 12); and 2) that phospholipase C activity is absent from prophase MA, thereby excluding 1,4,5-inositol trisphosphate as the agonist that evokes the pre-NEB calcium signal (5, 12).

In this paper, we report that the perinuclear calcium-independent PLA₂ activity occurs on perinuclear vesicles within the minute before the pre-NEB calcium signal, and thus is present in the right time and location to be associated with the pre-NEB calcium signal. We have also found phosphofructokinase (PFK) activity on the calcium regulatory vesicles isolated from native prophase mitotic apparatus. Finally, we have developed a model that incorporates the measured kinetics of enzymes found on those vesicles. This model tracks the production of numerous products, including LtB₄, and the emission of the calcium signal from single vesicles. The timing of events seen in the model is consistent with the deterministic nature of the pre-NEB calcium signal.

This study was conducted with eggs and cells from embryos in the first and second cell cycle, and isolated native prophase MA. Gametes were obtained from mature adult sand dollars (*Echinarcinus parma*) as previously described (3, 4, 13, 14). The temperature of the gametes and embryos was maintained between 11 ° and 15 °C throughout the experimental procedure. Quantitative direct-pressure microinjection studies were performed as previously described (3, 4). Imaging of PLA₂ activity *in vivo* was performed with the self-quenching PLA₂ substrate PED6 (15) in the following fashion. Unquenched derivative of PED6 was found uniformly distributed in the cytoplasm of the injected cell. For injection with substrate (*i.e.*, 2–10 μl of 1–2 $\mu\text{g}/\mu\text{l}$ PED6), cells

were viewed with the multispectral video light microscope. Following microinjection, they were transferred to a Zeiss 510 confocal light microscope system. The cells tolerated this level of injected PED6 and the inter-microscope transfer procedure. Special care was taken to reduce the photonic load on the cells—thereby reducing the effects of photobleaching and eliminating phototoxicity—while maintaining high spatial and temporal resolution. Cells were observed in Multi-Track mode of a Zeiss 510 confocal microscope configured for concurrent viewing of fluorescein and rhodamine fluorescent emissions and differential interference contrast of the specimen. With Multi-Track, we were able to simultaneously assess PLA₂ activity in the fluorescein emission channel, the formation of lipofuscin due to photon-induced lipid peroxidation of membranes in the rhodamine emission channel, and cell structure with differential interference contrast. Typically, images were recorded at a frequency of 1 image per min (0.0167 Hz). Images were recorded, processed, and then archived in TIFF format on CD-ROM.

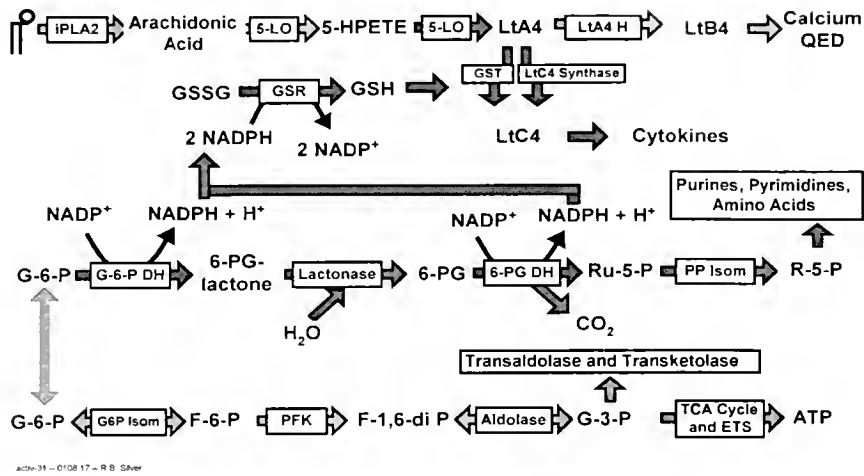
Assays for phosphofructokinase activity were performed using modifications of the methods described by Kemp (16, 17). Reaction volumes were kept to 2 ml, activities of aldolase and glyceraldehyde-3-phosphate dehydrogenase were 10-fold less than those used by Kemp (16, 17), temperature was maintained at 11–12 °C, and spectrophotometry was performed with an HP 8453 diode array spectrophotometer. Modeling was performed in WinSAAM using Michaelis-Menten kinetics for each of the enzymes listed as part of the network. The kinetics values (*e.g.*, Km and Vmax) were obtained in this laboratory with endomembrane subfractions prepared from isolated native prophase mitotic apparatus as first developed in this laboratory (*e.g.*, 12, 13).

In vivo hydrolysis of PED6, a self-quenching fluorescent phospholipid substrate for PLA₂, was monitored by confocal light microscopy imaging. The observed PLA₂ activity was detected on discrete perinuclear vesicles seven minutes prior to NEB in the second cell cycle of sand dollar embryos. This activation, which occurs in the same region as the pre-NEB calcium signal (1, 3, 15), just precedes the pre-NEB calcium signal that occurs 6 min before NEB (4, 6, 7). This activation also occurs during the period when NEB in these cells is inhibitable by antagonists of PLA₂ (*e.g.*, 7,7-dimethyl-5,8-eicosadienoic acid, bromoenol lactone), 5-lipoxygenase and leukotriene A₄ hydrolase (5, 10, 12). Hydrolysis of PED6, on perinuclear vesicular membranes, was also observed to precede NEB in the third and fourth cell cycles of those embryos. Thus, the location of PLA₂ activity, which generates the initial precursor for LtB₄, coincides with the pre-NEB calcium signal (3–6).

Several enzyme activities have been observed on perinuclear endomembranes of prophase mitotic apparatus (*cf.* Fig. 1A; 1–4).

Panel A

Activation Pathways of Metabolic Network



Panel B

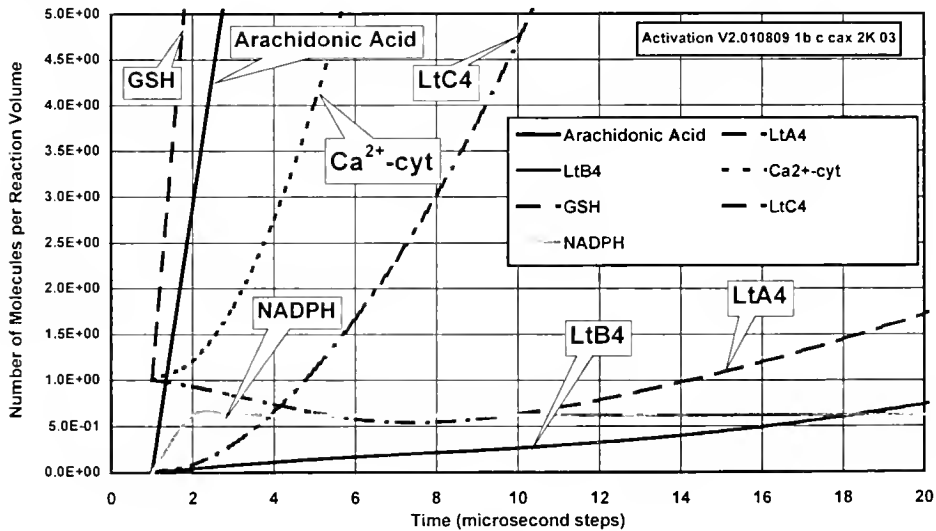


Figure 1. (A) A schematic of the metabolic model for regulation of the calcium signal that occurs as a prerequisite for nuclear envelope breakdown. The enzymes noted have been identified by enzymatic activity, and in some cases by immunoassays and sensitivity of the pre-NEB calcium signal, NEB and mitosis to pharmacological antagonists (e.g., 14, 18). (B) The first 20 μ s of output of the model for starting conditions that included 1 mM ATP and 1 mM fructose-6-phosphate. This model assumes that for every LtB₄ produced, 200 calcium ions are released from a vesicle lumen to the cytosol. Furthermore, the model assumes no lag time for mechanisms of LtB₄ evoking calcium release from the vesicle lumen. Therefore, it appears that the rise in cytosolic calcium occurs immediately upon the start of metabolism, and not because of the action of LtB₄. Note the rapid rise and leveling of NADPH and later drop in LtA₄ levels that are to be expected given their nature as precursor relationships in the production of LtB₄ as depicted in Fig. 1A. above.

To better understand the spatial and temporal relationships among these enzymes, a mathematical model was developed that permits assessment of enzyme catalyzed metabolic flow amongst compartments. The model incorporates the Michaelis-Menten kinetics we have measured in the calcium regulatory endomembrane subfraction of prophase mitotic apparatus for the phospholipase A₂-5-lipoxygenase pathway, glutathione reductase and glutathione-S-transferase, and the oxidative pentose phosphate pathways. Other

enzyme activities that we have observed in prophase mitotic apparatus (e.g., creatine kinase, myosin, and kinesin) were also incorporated in the model. The model, at present, assumes that a single copy of each enzyme in the reaction scheme (Fig. 1A) is present on a single 100-nm spherical vesicle resident within a cube 0.5 μ m on a side—a so-called "Unit Reaction Volume" based on ultrastructural observations (e.g., 1, 18). The value of 0.5 μ m was taken from the measured mean free spacing amongst the vesicles

in the aster (1, 18). The model also assumes an immediate effect of agonist (LtB_4) upon calcium release from vesicles. The output of this model (mentioned above) evokes a calcium signal detectable with high sensitivity aequorin (e.g., 4–6) within 250 μs of the start of PLA_2 activity, assuming a single calcium ion is released per LtB_4 produced. When the model was modified to consider a ratio of 100–200 calcium ions released per agonist produced, a calcium signal detectable with the high sensitivity aequorin we use to visualize the pre-NEB calcium signal (e.g., 4, 5) is generated in less than 6 μs (Fig. 1B).

To extend the hypothesis that an integrated metabolic network is involved in production of LtB_4 , isolated endomembrane subfractions from prophase mitotic apparatus were assayed for phosphofructokinase (PFK) activity. The calcium regulatory endomembrane subfraction of the prophase mitotic apparatus exhibited abundant PFK activity, but little or no PFK activity was detected on the other three endomembrane density subfractions. Under standard reaction conditions that included 1 mM ATP and concentrations of fructose-6-phosphate ranging from 0.1 nM through 1 mM, the K_m and V_{max} of this PFK activity were determined to be 1.38 μM and 46.0 $\mu\text{M}/\text{mg}$ protein/min, respectively. This relationship, of V_{max} being less than K_m , indicates that ATP inhibits the PFK activity, which is consistent with behavior of PFKs isolated from other sources (e.g., 16, 17). Taken together with our earlier finding of hexose monophosphate isomerase and aldolase activities on these membranes, it is now apparent that glycolysis is one of four metabolic pathways that are present and active on the calcium regulatory endomembranes.

The results presented in this paper reveal that the first enzymatic step in LtB_4 production occurs at the right place and time for the pre-NEB calcium signal. In addition, we have found that PFK activity is part of a network of enzymes on perinuclear vesicles that regulate production of LtB_4 as an agonist of the discrete pre-NEB calcium signal (5, 12). Lastly, results of our model support the concept that these networked enzymes act rapidly and are probably clustered on the vesicles. This represents the first report of the presence of pre-NEB, calcium-independent PLA_2 activity on perinuclear endomembranes, the first demonstration of

PFK activity on perinuclear membranes, and the first report of a model that incorporates the enzyme network that appears to regulate nuclear envelope breakdown through a calcium signal and supports the hypothesis that LtB_4 is the agonist for pre-NEB calcium signal and cell activation (5).

Research grant support by NSF (MCB-99082680) and the Burroughs Wellcome Fund (1002768) is gratefully acknowledged. Thanks are extended to Drs. John R. Hummel, Howard Rasmussen, and Raoul F. Reiser for their helpful comments and advice during these studies, and to the reviewers for their helpful suggestions in the refinement of the manuscript.

Literature Cited

1. Silver, R. B., R. D. Cole, and W. Z. Cande. 1980. *Cell* **19**: 505–516.
2. Silver, R. B. 1986. *Proc. Natl. Acad. Sci. USA* **83**: 4302–4306.
3. Silver, R. B. 1989. *Dev. Biol.* **131**: 11–26.
4. Silver, R. B. 1996. *Cell Calcium* **20**: 161–179.
5. Silver, R. B. 1999. *FASEB J.* **13**: S209–S215.
6. Silver, R. B., A. P. Reeves, B. P. Kelley, and W. J. Fripp. 1996. *Biol. Bull.* **191**: 278–279.
7. Llinás, R., M. Sugimori, and R. B. Silver. 1992. *Science* **256**: 677–679.
8. Samuelsson, B. 1983. *Science* **220**: 568–575.
9. Silver, R. B., J. B. Oblak, G. S. Jeun, J. J. Sung, and T. C. Dutta. 1994. *Biol. Bull.* **187**: 242–244.
10. Silver, R. B. 1995. *Biol. Bull.* **189**: 203–204.
11. Silver, R. B., L. A. King, and A. F. Wise. 1998. *Biol. Bull.* **195**: 209–210.
12. Silver, R. B., and N. M. Deming. 1999. *Biol. Bull.* **197**: 268–270.
13. Silver, R. B. 1986. *Methods Enzymol.* **134**: 200–217.
14. Silver, R. B. 1997. Pp. 83.1–20 in *Cells: A Laboratory Manual*. CSHL Press, Cold Spring Harbor, NY.
15. Hendrickson, H. S., E. K. Hendrickson, I. D. Johnson, and S. A. Farber. 1999. *Anal. Biochem.* **276**: 27–35.
16. Kemp, R. G. 1975a. *Methods Enzymol.* **42**: 67–71.
17. Kemp, R. G. 1975b. *Methods Enzymol.* **42**: 71–77.
18. Silver, R. B., M. S. Saft, A. R. Taylor, and R. D. Cole. 1983. *J. Biol. Chem.* **258**: 13,287–13,291.

Reference: *Biol. Bull.* **201**: 251–252. (October 2001)

Ooplasm Segregation in the Squid Embryo, *Loligo pealeii*

Karen Crawford (Department of Biology, St. Mary's College of Maryland, St. Mary's City, Maryland 20686)

After fertilization, squid egg ooplasm streams toward the animal pole to create a clear lens-shaped blastodisc cap where meroblastic cleavage occurs (1). Exposing the embryo to cold (4 °C) after fertilization inhibits blastodisc formation (2), suggesting that microtubules may be associated with this ordered movement of cytoplasm (3). Although microtubules have been correlated with cytoplasmic movements that follow fertilization in amphibians (4), ascidians (5), and annelids (6), these embryos do not form blastodisc caps and, unlike the squid, they undergo complete or holoblastic cleavage. Interestingly, ooplasmic segregation, blastodisc cap formation, and meroblastic cleavage all take place in the zebrafish embryo, but here microfilaments and not microtubules have been shown to direct the segregation of ooplasm from the yolk (7).

To clarify the role of the cytoskeleton during early development in squid, embryos cultured at 20 °C in petri dishes lined with 0.2% agarose (Sigma, Type II) and filled with Millipore-filtered seawater (MFSW), were treated 30 min after *in vitro* fertilization (8) with either 0.01–20 µg/ml of the microfilament inhibitor cytochalasin D (Sigma) (3 trials, 50 to 75 embryos per dish) or 0.5–10 µg/ml of the microtubule inhibitor colchicine (Sigma) (6 trials, 50 to 75 embryos per dish). Stock solutions of each inhibitor were prepared in dimethyl sulfoxide (DMSO) (Sigma), and DMSO (0.1%) was therefore added to MFSW as a control. Embryos were observed for at least 4 h after fertilization during blastodisc formation and after incubation overnight at 17 °C.

Embryos cultured in MFSW (Fig. 1a) or MFSW and DMSO (Fig. 1d) formed normal 40–50 µm thick blastodiscs by 4 h and underwent normal cleavage and early development. Blastodisc cap formation occurred in all embryos treated with 0.01, 0.05, 0.1, 0.5, 1.0, 2.0, 4.0, and 10.0 µg/ml cytochalasin D; however, at all but the lowest concentration of microfilament inhibitor, the entire cortical yolk cell membrane appeared disrupted by the presence of small and large vesicles of cytoplasm (Fig. 1c). This result was similar to what had previously been reported in squid (9). Normal yolk cell membranes were observed in 45% of the embryos treated with 0.05 µg/ml cytochalasin D, while all yolk membranes appeared similar to the control in the 0.01 µg/ml group. It is important to note that embryos from these different treatment groups failed to undergo normal development. In contrast, colchicine prevented ooplasm segregation and blastodisc formation in all embryos cultured at concentrations of 10.0, 7.5, and 5.0 µg/ml, although the thin layer of cytoplasm present prior to fertilization was maintained (Fig. 1b). Embryos cultured in 2.5 µg/ml all formed thinner, <20 µm, blastodisc caps by 4 h but failed to retain them after culture overnight. While blastodisc caps (30–35 µm) formed in the cultures treated with 1.0 and 0.5 µg/ml colchicine, after overnight culture these caps were either lost or reduced to small abnormal shaped discs or sacs of cytoplasm at the animal pole. Normal cleavage and development were never observed in any embryos treated with cytoskeletal inhibitors. Normal blasto-

disc cap formation and cleavage occurred in all embryos treated with DMSO (0.1%) (Fig. 1d).

These results suggest that a microtubule-associated mechanism is responsible for ooplasm segregation and blastodisc formation in the squid. Although microfilaments do not seem to be required for ooplasm movement to the blastodisc, the disruption of the cortical yolk cell membrane by cytochalasin D suggests that they may have a role in stabilizing the yolk cell membrane or regulating cortical cytoplasm flow toward the animal cap. In contrast, microtubules do not seem to be involved in ooplasm segregation and blastodisc formation in the zebrafish embryo (10), where microfilaments have been shown to direct ooplasm flow along streamers of cytoplasm within the central region of the yolk cell. Interestingly, in embryos of another fish, medaka, both microtubules and microfilaments have been shown to be involved in ooplasm segregation. In this fish, not only did cytochalasin D inhibit blastodisc formation, but colchicine treatment also resulted in less directed ooplasm movements (11). Thus it seems, in medaka, microfilaments and microtubule networks may function in concert during ooplasm segregation.

One possible clue to understanding the subtle similarities and differences observed in embryos of these fish and the squid may be found when the location of ooplasm within the unfertilized egg and the route of cytoplasmic flow are considered. In contrast to the central flow of ooplasm in zebrafish, ooplasm flow in medaka occurs cortically along meridional pathways (11). Similarly, in the squid embryo, where microtubular arrays can be visualized by antibody labeling, the ooplasm flow to the cortex of the yolk cell surface is restricted to the outermost cortical layer of cytoplasm (unpubl. results). With antibodies to β -tubulin, unfertilized eggs were observed to possess circular swirls of tubulin staining within the cortex. Yolk just below this thin layer did not label for β -tubulin. After fertilization, these patterns change and β -tubulin-rich streams oriented toward the animal pole are formed along the outer cortex of the embryo. Perhaps the reliance on two supporting cytoskeletal mechanisms within the cortex to move ooplasm to the blastodisc, as shown in medaka, is characteristic of eggs that possess a dense central yolk and cortical ooplasm, and may underlie this process in the squid embryo. With this possibility in mind, it will be important to reexamine these elements in other embryos where microtubules alone, or in concert with microfilaments, have been linked to ooplasm segregation and movement following fertilization. In addition, further analysis of microtubule and microfilament arrays during ooplasm segregation and in the presence of cytoskeletal inhibitors will further extend our understanding of the mechanism of blastodisc formation and early development in the squid embryo.

This work was supported by a Faculty Development Grant from St. Mary's College of Maryland to Karen Crawford and would not have been possible without Dr. Robert Baker and his laboratory group at the Marine Biological Laboratory.

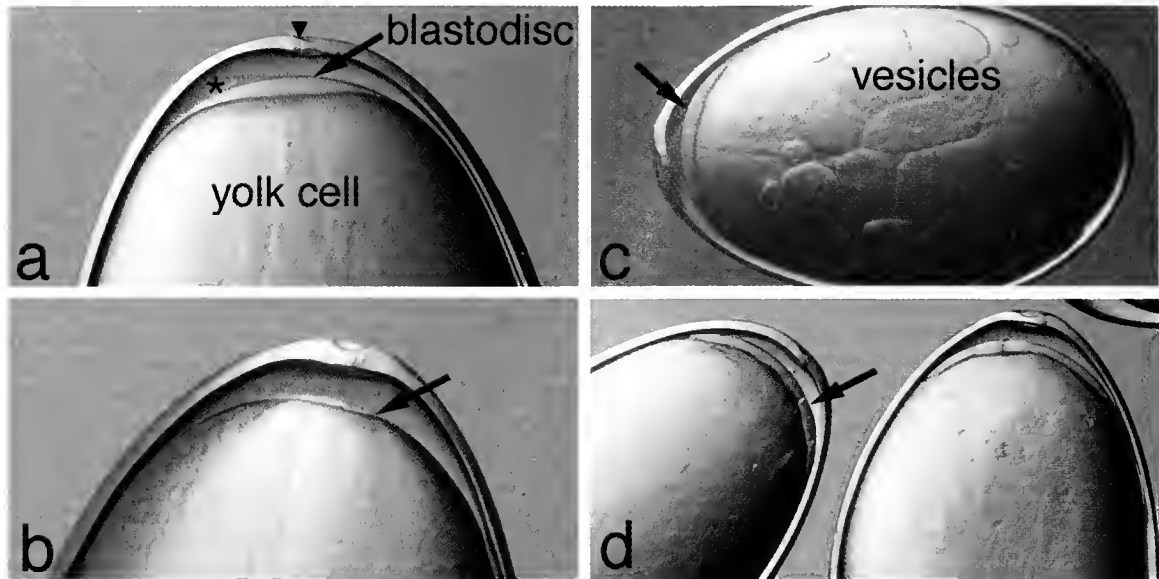


Figure 1. Colchicine inhibits ooplasm segregation and blastodisc cap formation in the squid embryo. (a) Normal blastodisc cap formation 3 h post-fertilization, lateral view (65 \times) (an arrowhead marks the micropyle and chorion, an * marks the polar bodies, the yolk cell is labeled, and arrows indicate the blastodisc in each panel). (b) Embryo treated with 5.0 μ g/ml colchicine, 5 h post-fertilization, lateral view (65 \times). Note the inhibition of ooplasm segregation and blastodisc cap formation. (c) Embryo treated with 0.05 μ g/ml cytochalasin D (45 \times). Although this embryo has formed a normal blastodisc, perturbation of the yolk cell membrane is demonstrated by the presence of large vesicles. (d) Control embryos treated with DMSO (0.1%) undergo blastodisc cap formation and cleave normally, 8 h post-fertilization (45 \times). Note the presence of cleavage furrows in these embryos.

Literature Cited

1. Arnold, J. M. 1968. *Dev. Biol.* **18**: 180–197.
2. Crawford, K. 2000. *Biol. Bull.* **199**: 207–208.
3. Yahara, I., and F. Kakimoto-Sameshima. 1978. *Cell* **15**: 251–259.
4. Houliston, E., and R. P. Elinson. 1991. *Development* **112**: 107–117.
5. Sawada, T., and G. Shatten. 1989. *Dev. Biol.* **132**: 331–342.
6. Eckberg, W. R. 1981. *Differentiation* **19**: 55–58.
7. Leung, C. F., S. E. Webb, and A. L. Miller. 1998. *Develop. Growth Differ.* **40**: 313–326.
8. Klein, K. C., and L. A. Jaffe. 1984. *Biol. Bull.* **167**: 518.
9. Arnold, J. M., and L. D. Williams-Arnold. 1974. *J. Embryol. Exp. Morphol.* **31**: 1–25.
10. Leung, C. F., S. E. Webb, and A. L. Miller. 2000. *Dev. Growth Differ.* **42**: 29–40.
11. Abraham, V. C., S. Gupta, and R. A. Fluck. 1993. *Biol. Bull.* **184**: 115–124.

Reference: *Biol. Bull.* **201**: 252–254. (October 2001)

The Stellate Ganglion of the Squid *Loligo pealeii* as a Model for Neuronal Development: Expression of a POU Class VI Homeodomain Gene, *Rpf-1*

J. Peter H. Burbach¹ (Rudolf Magnus Institute of Neurosciences, Utrecht, The Netherlands), Anita J. C. G. M. Hellemons¹, Marco Hoekman¹, Philip Grant², and Harish C. Pant²

A major challenge in developmental neurobiology is to understand how neuronal systems are specified, for example, how transmitter phenotype and connectivity are established during develop-

ment. Molecular cascades of transcription factors and growth factors direct neuronal specification (1). How they operate in terminal differentiation and adult networks is poorly understood. To complement our research to characterize molecular cascades in complex neuronal systems such as midbrain dopaminergic and hypothalamic systems in the mouse (2, 3, 4), we have turned to a non-mammalian neuronal system that has a functionally and morphologically more homogeneous structure. That structure is the stellate ganglion of the squid *Loligo pealeii*. It is a compacted

¹ Department of Medical Pharmacology, Rudolf Magnus Institute of Neurosciences, University Medical Center Utrecht, Utrecht University, 3584CG Utrecht, The Netherlands.

² Laboratory of Neurochemistry, NINDS, NIH, Bethesda, MD 20892.

A

<i>Loligo pealeii</i>	RPF-1	PQALEILNQHF EK NTHPSGAELTELSENLSYDREVV RV
comparison		PQALEILN-HFEKNTHPSG-E+TE++E-L+YDREVV RV
Human	RPF-1	PQALEILNAHF EK NTHPSGQEMTEIAEKLNYDREVV RV

B

<i>Loligo pealeii</i>	Phox2	AQLKELEKAF AETHYPDIYTREEI AMKIDLTEARVQVW
comparison		AQLKELE+ -FAETHYPDIYTREE+A+KIDLTEARVQVW
Mouse	Phox2a	AQLKELERVFAETHYPDIYTREELALKIDLTEARVQVW

Figure 1. Partial amino acid sequences of homeodomain proteins predicted from cloned PCR fragments obtained from the stellate ganglion of the squid *Loligo pealeii*. The degenerate PCR primers were those used in mammalian brain (2, 3); upstream, 5'-GMRSCGMSAVMGSACMMBCCTTYAC-3'; downstream, 5'-TGGTTYMRVAAAYCGYHGMGCMARRTG-3'. Sequences without primer-coded sequence are shown and compared with the mammalian homologs retina-derived POU factor-1 (RPF-1) of man (A), and Phox2a of mouse (B). In the comparison, identical amino acids are shown and substitutions by physicochemically similar amino acids indicated by +. The predicted RPF-1 protein sequence of *Loligo pealeii* shows a 31/38 identity and a 35/38 similarity to the human protein. Phox 2 shares a 34/38 identity and 37/38 similarity to mouse Phox2a.

cluster of neurons that innervates the muscles of the mantle through the giant nerve fiber system and controls the jet-propelled escape response of the squid (5). The aim of this study was to identify homeodomain genes expressed in the stellate ganglion and to correlate their expression with development of the ganglion.

Working from the concept that transcription factors involved in terminal neuronal differentiation are still operating in the adult system, as demonstrated in mammalian brain (2, 3, 4), we cloned homeodomain transcripts from the dissected stellate ganglion of the squid *Loligo pealeii* using RT-PCR with degenerated primers designed to conserved motifs in paired-like homeodomain genes (2, 3). Two homeodomain transcripts were identified from 40 cloned PCR fragments (Fig. 1). One fragment (1 out of 40 clones) predicted a homeodomain protein that was highly homologous to a POU class VI homeodomain gene product recently identified in man (6): retina-derived POU factor-1 (RPF-1). The other fragment (6 clones out of 40) was highly similar to the paired-like homeodomain genes *phox2a* and *phox2b*, also termed *arix/pmx* (7). Both types of homeodomain genes have been implicated in the specification of neuronal systems of the mouse. *Phox2* genes are required for normal development of central and peripheral components of the autonomous nervous system, while *rpf-1* has been implicated in the development of amacrine and retinal ganglion cells (6, 7). Other clones represented non-homeodomain-containing genes, including abundant transcripts like alpha-tubulin, actin, and collagen.

We chose to determine the embryonic expression of the *rpf-1* gene further by a whole mount *in situ* hybridization protocol using DIG-labeled cRNA (8), since initial experiments indicated specific labeling for *rpf-1*, but no signals for *phox2*. Comparison of anti-sense and sense probes showed specific expression of the squid *rpf-1* gene in dorsal structures in the mantle in stage 27 embryos of the squid. Comparison to histologically stained sections of squid

embryos (9) indicated that the labeled structures are part of the stellate ganglion. No other neural or non-neuronal structures were labeled at this developmental stage. In earlier stages (22 to 25), results suggested expression in the developing eye. These results suggest that this *rpf-1* gene is expressed in the developing and adult stellate ganglion of the squid.

Genes like *rpf-1* and others may have a role in developmental events in the stellate ganglion, such as establishment of connectivity and giant axon formation, as well as participating in regulation and maintenance of the adult giant fiber system. If interference with its expression, for example by introduction of morpholinos (10), can be achieved, the role of the *rpf-1* gene and other homeodomain genes can be established and can serve as a starting point to delineate molecular cascades in developing neurons.

Part of this research was performed at the Marine Biological Laboratory, Woods Hole, Massachusetts, and supported by an MBL Fellowship sponsored by the Baxter Postdoctoral Fellowship Fund, MBL Associates Fund, James A. and Faith Miller Memorial Fund, and the H. B. Steinbach Fellowship Fund.

Literature Cited

- Jessell, T. M. 2000. *Nat. Rev. Genet.* 1: 20–29.
- Smidt, M. P., H. S. van Schaick, C. Lanctot, J. J. Tremblay, J. J. Cox, A. A. van der Kleij, G. Wolterink, J. Drouin, and J. P. H. Burbach. 1997. *Proc. Natl. Acad. Sci. USA* 94: 13,305–13,310.
- Smidt, M. P., C. H. Asbreuk, J. J. Cox, H. Chen, R. L. Johnson, and J. P. H. Burbach. 2000. *Nat. Neurosci.* 3: 337–341.
- Burbach, J. P. H., S. M. Luckman, D. Murphy, and H. Gainer. 2001. *Physiol. Rev.* 81: 1197–1267.
- Martin, R. 1965. *Z. Zellforsch. Mikrosk. Anat.* 67: 77–85.
- Zhou, H., T. Yoshioka, and J. Nathans. 1996. *J. Neurosci.* 16: 2261–2274.

7. Stanke, M., D. Junghans, M. Geissen, C. Goridis, U. Ernberger, and H. Rohrer. 1999. *Development* **126**: 4087–4094.
8. Green, C. B., A. J. Durston, and R. Morgan. 2001. *Mech. Dev.* **101**: 105–110.
9. Grant, P., D. Tseng, R. M. Gould, H. Gainer, and H. C. Pant. 1995. *J. Comp. Neurol.* **356**: 311–326.
10. Ando, H., T. Furuta, R. Y. Tsien, and H. Okamoto. 2001. *Nat. Genet.* **28**: 317–325.

Reference: *Biol. Bull.* **201**: 254–255. (October 2001)

Evidence for Directed Mitotic Cleavage Plane Reorientations During Retinal Development within the Zebrafish

Brian A. Link (*Marine Biological Laboratory, Woods Hole, Massachusetts 02543*)

The vertebrate retina develops from a single layer of elongated cells—the optic cup neuroepithelium. At the time of optic cup formation, individual neuroepithelial cells are multipotent and can give rise to any of the cell types found within the differentiated retina (1). As the optic cup neuroepithelium proliferates, the repertoire of cell type fates becomes restricted. Retinal cell specification, the commitment to differentiate as one particular cell type, occurs at or following the final cell division. The underlying mechanisms of cellular specification that generate the diversity of retinal cell types are unknown.

In many invertebrate epithelial cell types, as well as the rat neuroepithelium, the plane of cell division is regulated during development by rapidly reorienting the metaphase chromosomal plane relative to the plane formed by the cellular sheet (2, 3). With regard to cellular specification, particular metaphase orientations often correlate with specific cell fates for each daughter cell. Underlying this correlation, studies in both *Caenorhabditis elegans* and *Drosophila melanogaster* have demonstrated that the orientation of the mitotic cleavage plane can dictate whether asymmetrically distributed mRNAs or proteins are inherited equally or unequally by the two daughter cells (4). Whether vertebrate retinal cells regulate their mitotic cleavage plane through metaphase reorientations is addressed in this study.

To assess metaphase chromosomal plane orientations in a vertebrate retina, newly fertilized zebrafish embryos (1–8 cell stage) were injected with 5 nl of plasmid DNA (0.1 $\mu\text{g}/\mu\text{l}$) encoding a fusion protein of histone H2B and GFP (H2B::GFP) (5). At this concentration, expression was mosaic. This fusion protein associates with chromosomes throughout the cell cycle in an inert manner, thus fluorescently labeling a subset of the embryo's cell nuclei. At 22 hours post fertilization (hpf), injected embryos were prepared for time-lapse microscopy. Zebrafish were anesthetized with MS222 (to inhibit spontaneous movements), treated with 0.2 mM 1-phenyl-2-thiourea (to block pigmentation), and embedded in 1.5% agarose (to immobilize the embryo). Labeled proliferating retinal neuroepithelial cells were imaged using a 40 \times water immersion objective on an upright epifluorescent microscope. Z-series, 50–60 μm in depth, were collected with a cooled CCD camera at intervals of 1–2 min over periods of 10–24 h. At 22 hpf, the retinoblast pool in zebrafish is expanding because all cells of the optic cup neuroepithelium are proliferative with an 8–10 h cell cycle (6).

Mitoses were observed at the apical border of the neuroepithelium adjacent to the retinal pigment epithelium (RPE). Only mi-

totic cells unobstructed by other labeled cells were scored. A proportion (8/86) of these observable mitoses showed cleavage plane reorientations (Fig. 1). For all cells, the time required to progress from metaphase (initial chromatin condensation) to cell division (end of karyokinesis) showed a range of 9 to 16 min with a mean of 12.8 ± 2.1 min. No significant difference in this time was observed between cells that reoriented their metaphase plate and cells that did not (12.5 ± 2.7 min vs. 12.8 ± 2.1 min). Interestingly, each cell that did rotate spindles shifted its chromosomes by 90° so that the plane of cell division was perpendicular to the plane of the neuroepithelial sheet. Cells that did not rotate metaphase chromosomes also cleaved with the axis of separation perpendicular to the RPE-neuroepithelial border.

These results demonstrate that the plane of cell division within a vertebrate retinal neuroepithelium can be rapidly reoriented, and in a directed fashion. Rotations of the metaphase spindle ensured that all 86 cell divisions occurred perpendicular to the RPE-neuroepithelial border. This consistency in final cell division plane suggests that during proliferative phases of retinal development, perpendicular cleavages are actively maintained. Although the significance of retinal metaphase rotations has not been probed in this study, the relationship of spindle rotations to cell fate decisions in other systems is intriguing. Furthermore, similar to invertebrates, asymmetric distribution of proteins has also been observed in vertebrates. For example Numb, an intracellular signal-modifying protein, is localized in a polarized fashion for several neuronal precursor cell types including the rat retinal neuroepithelium (7).

The main result of these studies is the demonstration of mitotic cleavage plane reorientations in a vertebrate retina. More generally, by observing mitotic behaviors *in situ* within a living embryo, cell cycle parameters such as M-phase length or mitotic spindle behavior can be measured directly for individual cells, and heterogeneity can be assessed. This has not been possible with traditional population studies that use cell cycle markers in tissue sections. This experimental system also provides the framework to integrate studies of cleavage plane orientation, asymmetric distribution of mRNA or protein, and cell fate decisions in a single biological context. Lastly, the genetic manipulability of zebrafish will enable mechanistic studies for each of these processes.

This work was funded by generous support from the Grass Foundation. The author also thanks John Dowling, Scott Fraser, and Reinhard Köster for their generosity and advice.

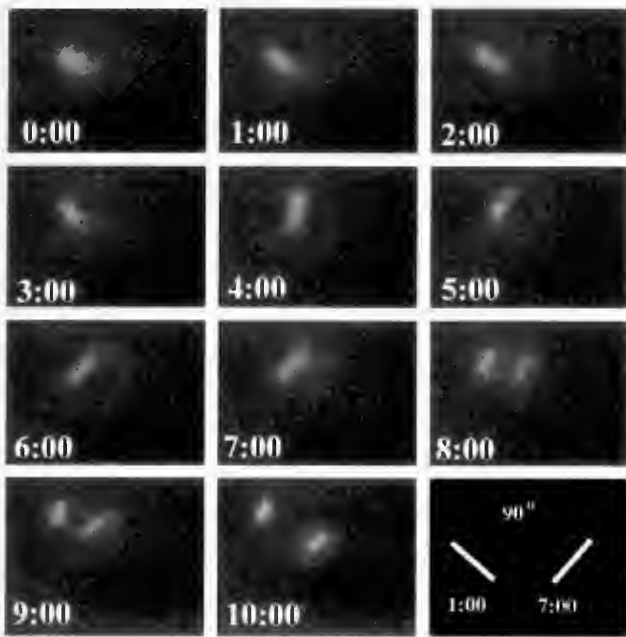


Figure 1. Time lapse analysis of a cell labeled with H2B::GFP shows metaphase chromosomal plane reorientation in a mitotic retinal neuroepithelial cell. The panel in the lower right models the 90° reorientation shift in axis from 1 to 7 minutes. The RPE-neuroepithelial border is located in the upper right corner for each image. Time in minutes is listed in the bottom left for each image.

Literature Cited

- Harris, W. A. 1997. *Curr. Opin. Genet. Dev.* 7: 651–658.
- Guo, S., and K. Kemphues, 1996. *Curr. Opin. Genet. Dev.* 6: 408–415.
- Adams, R. 1996. *J. Neurosci.* 16: 7610–7618.
- Lu, B., L. Jan, and Y.-N. Jan. 2000. *Annu. Rev. Neurosci.* 23: 531–556.
- Köster, R., and S. Fraser. 2001. *Dev. Biol.* 233: 329–346.
- Hu, M., and S. Easter. 1999. *Dev. Biol.* 207: 309–321.
- Cayouette, M., A. Whitmore, G. Jeffery, and M. Raff. 2001. *J. Neurosci.* 21: 5643–5651.

Reference: *Biol. Bull.* 201: 255–256. (October 2001)

Messenger RNAs Located in Spiny Dogfish Oligodendrocyte Processes

Ryan Smith¹, Emma Kavanagh², Hilary G. Morrison³, and Robert M. Gould²

(N. Y. S. Institute for Basic Research in Developmental Disabilities, Staten Island, New York)

Oligodendrocytes, the myelin-forming cells in the CNS, synthesize proteins in two distinct locations: the cell body, and in each process where myelin sheaths form. Morphologically these “outer tongue” processes are cytoplasmic channels that run along the outer surface of each myelin sheath. In mammals, myelin basic protein (MBP), a major constituent of compact myelin, is synthesized in these processes and moves rapidly (within minutes) into compact myelin. Proteins synthesized in the cell body take roughly 30 minutes to incorporate into compact myelin.

To place MBP in each sheath, oligodendrocytes synthesize protein in many (up to 40, [1]) cytoplasmic processes. We recently identified many other proteins (nearly 100, based on cDNA sequences representing mRNAs enriched in myelin) that are synthesized in rat oligodendrocyte processes using a combination of subcellular fractionation and suppression subtractive hybridization

(2, 3). To broaden our understanding of the role that local protein synthesis plays in myelination, we applied the same approach to identify proteins synthesized in oligodendrocyte processes of an elasmobranch, the spiny dogfish (*Squalus acanthias*). We already found (Gould, unpubl.) that MBP was not synthesized in dogfish oligodendrocyte processes by *in situ* hybridization, since the mRNA is retained in the oligodendrocyte soma and not transported to the cells’ processes.

We prepared “driver” and “tester” cDNAs from total homogenate and myelin for the subtractive hybridization experiment. Briefly, three female spiny dogfish were killed with an overdose of anesthetic. Their brains were removed and homogenized in a buffered hyperosmotic sucrose (1.2 M) solution; previously we had found that mRNAs located in oligodendrocyte processes are trapped more effectively in myelin vesicles homogenized with hyperosmotic homogenization solution (3). A portion of the homogenate was extracted for RNA (represents the entire population of RNAs in the dogfish brain and is the source of “driver”) with TRI reagent (Molecular Research Center). Buffer was added to the remaining homogenate to reduce the osmolarity to 0.85 M sucrose, the sample was placed in an ultracentrifuge tube, overlaid

¹ Marine Models in Biological Research Program, Woods Hole, MA.

² N. Y. S. Institute for Basic Research in Developmental Disabilities, Staten Island, NY.

³ Josephine Bay Paul Center for Comparative Molecular Biology and Evolution, Marine Biological Laboratory, Woods Hole, MA.

Table 1

Distribution of cDNAs obtained by subtractive hybridization

A. Distribution of the cDNA sequences

Classification	Quantity	Percentage of Total
Related to known cDNAs	21	28.4%
Mitochondrial genome	21	28.4%
Unrelated to known cDNAs	32	43.2%
Total	74	

B. Distribution of known cDNA sequences

cDNA	Species	Size (bp)	Matches
B-catenin	Human	450	371/440 (84%)
POMC (9)	Shark	177–407	<i>e.g.</i> , 405/407 (99%)
HspA5 (2)	Mouse	583–602	<i>e.g.</i> , 236/283 (83%)
Dihydropyrimidinase-like	Human	617	457/617 (74%)

SINE	Shark	718	149/163 (91%)
B-spectrin	Human	227	65/78 (83%)
Ribosomal protein L1	Zebrafish	134	34/37 (91%)
Ig heavy chain	Shark	500	35/38 (91%)
Evx2/Hox (4)	Shark	514–826	<i>e.g.</i> , 126/155 (81%)

Note. Matches are taken directly from the BLAST search results, except for dihydropyrimidinase-like protein, where an intervening region (384) bases were included from both the subject and query sequences. Parentheses: more than one hit. Range in Size field corresponds to lowest/highest size of multiple-hit cDNA.

with 0.25 M sucrose, and centrifuged (100,000 × g for 3.5 h). Myelin vesicles floating on the 0.85 M sucrose were collected, and myelin fraction RNA was prepared with TRI reagent (Molecular Research Center) and used to prepare "tester." Messenger RNA was prepared from both homogenate and myelin fraction RNAs (MicroPoly(A) Purist™ mRNA purification kit, Ambion). Homogenate and myelin mRNAs were then converted to "driver" and "tester" cDNA, and a subtraction product (enriched in cDNAs that represent mRNAs enriched in myelin) was prepared with PCR-Select™ cDNA Subtraction Kit (CLONTECH) according to the manufacturer's protocol. Several products were amplified by PCR, subcloned into pGEM T Easy vector (Promega), and clones were taken to prepare plasmids (minipreps). The cDNAs were sequenced in the Josephine Bay Paul Center for Comparative Molecular Biology and Evolution at the Marine Biological Laboratory in Woods Hole, Massachusetts.

In all, 74 sequences were analyzed (BLAST (N) search of the GenBank non-redundant database) (Table 1). Unlike rat cDNAs (prepared in the same fashion), which mainly represented MBP and myelin-associated oligodendrocytic basic protein (MOBP) mRNAs (1), none of the dogfish cDNA represented MBP or MOBP homologs. As with rat, about half were unrelated to mRNAs in the current GenBank database, and high portions were derived from mitochondrial DNA. Only four of the known sequences, β -catenin, proopiomelanocortin (POMC), heat shock protein A5 (HspA5), and dihydropyrimidinase-like protein, matched sequences in the GenBank database throughout. The portions of

HspA5 that matched the human sequence were 3'-coding. The non-coding portion was less conserved. Small portions of five other cDNAs—SINE, β -spectrin, ribosomal protein L1, evx2, and Ig heavy chain—matched known sequence in the GenBank database.

To confirm that these cDNAs represent mRNAs located in oligodendrocyte processes, Northern blot studies are needed to show that the mRNAs are enriched in myelin. Complementary *in situ* hybridization studies are planned to further locate the mRNAs to oligodendrocyte processes. In summary, our results suggest that the population of mRNAs transported to spiny dogfish oligodendrocyte processes is large and varied. Comparative studies are planned to find out if β -catenin, POMC, Hsp5a and dihydropyrimidinase-like protein are expressed in rat oligodendrocytes and if some of the cDNAs identified in rat oligodendrocyte processes are expressed in spiny dogfish processes.

This study was supported by grants from the National Multiple Sclerosis Society (RMG) and the National Science Foundation (RS and RMG).

Literature Cited

1. Peters, A., and C. C. Proskauer. 1969. *Anat. Rec.* 163: 243.
2. Gould, R. M., C. M. Freund, F. Palmer, and D. L. Feinstein. 2000. *J. Neurochem.* 74: 1834–1844.
3. Gould, R. M., C. M. Freund, J. Engler, and H. G. Morrison. 2000. *Biol. Bull.* 199: 215–217.

Reference: *Biol. Bull.* **201**: 257–258. (October 2001)

Phalloidin Labeling of Developing Muscle in Embryos of the Polychaete *Capitella* sp. I

Susan D. Hill (Department of Zoology, Michigan State University, East Lansing, Michigan 48824) and Barbara C. Boyer¹

Capitella sp. I, previously considered part of the *Capitella capitata* complex (1), is a small polychaete annelid that can be maintained in culture with ease (J.P. Grassle, Institute of Marine and Coastal Sciences, Rutgers University, pers. comm.). Lecithotrophic eggs are deposited in a maternal brood tube and can be readily harvested at different stages of development. Larvae emerge from the brood tube after approximately 8 days as many-segmented metatrochophores, each bearing a protroch and telotroch, the classic trochophore stage being bypassed. The free-swimming metatrochophores are non-feeding and are competent to settle and metamorphose within a few hours of emergence. Metamorphosis in this species is not morphologically dramatic, but includes a pronounced elongation, loss of trochal bands and accompanying locomotory changes, and a transition from non-feeding to feeding. Postmetamorphic growth involves a general enlargement of the worm and addition of segments in a growth zone immediately anterior to the terminal pygidium.

The development of muscle patterns in soft-bodied bilaterian animals is not well understood, with most recent information coming from investigations of acoelomate flatworms (2, 3) and the medicinal leech, a derived annelid (4, 5). Segmentation between annelids and arthropods has traditionally been considered to be homologous; however, the recent assignment of annelids to the Lophotrochozoa and arthropods to the Ecdysozoa, brings this homology into question. A study of muscle development in a more ancestral annelid would be useful in furthering our understanding of the ontogenetic and evolutionary origins of segmentation, as well as the cellular interactions involved in muscle patterning and innervation during embryogenesis. To this end we are investigating early muscle development in *Capitella* sp. I. Staged embryos were removed from the brood tube and labeled with rhodamine-phalloidin following the procedure used by Reiter *et al.* (2) to detect actin filaments in developing muscle of turbellarian flatworms. Specimens were observed with an Olympus BX60 fluorescence microscope and imaged using an Olympus Magnifire digital camera (model S99860).

Muscle development proceeds from anterior to posterior. As the stomodeum forms, a ventral arc of muscle becomes apparent in the lower lip. Phalloidin binding continues dorsally until the mouth is surrounded (Fig. 1a). Approximately three days after fertilization, longitudinal muscles of the body wall begin to form. Initially eight longitudinal muscles appear in the following sequence: (1) four dorsal strands that will reach from the prostomium to the pygidium begin to develop; (2) two latero-

ventral muscles form at the lateral edges of the stomodeum (Fig. 1a), then come together at the apex of the prostomium (Fig. 1b); (3) these two lateroventral muscles also grow posteriorly, extending ventrally from the stomodeum into the pygidium (Fig. 1b); (4) medially, a second pair of midventral muscles (Fig. 1b) grows posteriorly from the stomodeum. Subsequently two additional lateral muscles form (Fig. 1b). Longitudinal muscles initially appear as thread-like single strands which thicken as more strands are added.

After initial differentiation of longitudinal muscles, circular muscles begin to develop, appearing first in the peristomial region. One band forms in the lateral stomodeal region, while a second passes immediately posterior to the stomodeum. Additional circular muscle bands are added sequentially from anterior to posterior corresponding to the metameric pattern of the developing larva (Fig. 1b, c). Development of circular muscles seems to be initiated in the ventrolateral region of the embryo, between the midventral muscles (MV) and the lateroventral muscles (LV). The circular muscles appear as complete bands ventrally before they are seen dorsally. A few closely spaced circular fibers also become visible in the telotrochal region. At this time there is a gap between the more anterior circular muscles and these telotrochal bands.

As development continues, both longitudinal and circular muscles become more massive with the addition of more strands. Circular muscle formation continues posteriorly (Fig. 1c), filling the gap between the developing circular muscles and telotrochal bands. The number of telotrochal bands also increases.

During larval development additional muscles—longitudinal, intrasegmental, oblique, setal sac fibers, etc.—are added so that the muscle pattern in newly emerged metatrochophores is very complex (Fig. 1d). Since metamorphosis occurs without major structural changes, these larval muscles form the basis of the adult musculature.

Mesoderm formation in polychaetes is attributed to two teloblasts, derivatives of the 4d blastomere, which reside between the posterior ectoderm and the lining of the developing gut (6). Segmentation is believed to occur as successive blocks of mesoderm are formed. Currently segmentation in polychaetes is being investigated in a number of laboratories (7, 8, 9) using several genetic markers. Our results show that the circular muscles that differentiate in the larval trunk anterior to the telotroch are iterated sequentially from anterior to posterior. We suggest that the phalloidin-staining telotrochal bands are the nascent segmental muscles of the growth zone.

This work was supported in part by the Union College Faculty Research Fund. The authors gratefully acknowledge the generous assistance of Dr. William Eckberg in creating the figure.

¹ Department of Biological Sciences, Union College, Schenectady, NY 12308

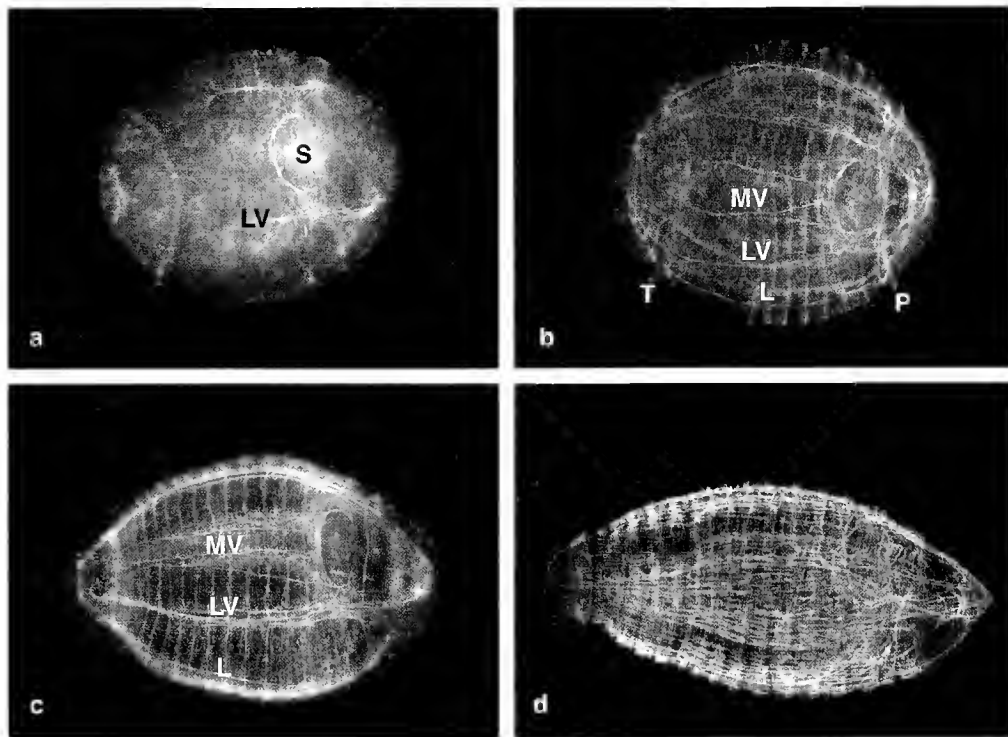


Figure 1. (a) Ventral view of an early embryo ($240 \times 175 \mu\text{m}$) showing the stomodeum (S) with phalloidin labeling of the lower lip and lateroventral muscles (LV). (b) Ventral view showing the prototroch (P), telotroch (T), paired midventral muscles (MV), lateroventral muscles (LV), and lateral muscles (L). Circular musculature formation is incomplete, with a gap between the most posterior circular muscle band and the telotroch. (c) Ventrolateral view showing thickened midventral (MV) and lateroventral (LV) muscles. Circular muscle bands are complete to the telotroch. L = lateral muscle. (d) Metatrochophore showing greatly increased complexity of the larval musculature.

Literature Cited

- Grassle, J. P., and J. F. Grassle. 1976. *Science* 192: 567–569.
- Reiter, D., B. Boyer, P. Ladurner, G. Mair, W. Salvenmoser, and R. Rieger. 1996. *Roux's Arch. Dev. Biol.* 205: 410–423.
- Ladurner, P., and R. Rieger. 2000. *Dev. Biol.* 222: 359–375.
- Jellies, J. 1990. *Trends Neurosci.* 13: 126–131.
- Jellies, J., and W. B. Kristan, Jr. 1988. *J. Neurosci.* 8: 3317–3326.
- Anderson, D. T. 1966. *Acta Zool.* Bd XLVII: 1–42.
- Seaver, E. C., and S. D. Hill. 1999. *Am. Zool.* 39: 77A.
- Werbrock, A. H., D. A. Meiklejohn, A. Sainz, J. H. Iwasa, and R. M. Savage. 2001. *Dev. Biol.* 235: 476–488.
- Seaver, E. C., D. A. Paulson, S. Q. Irvine, and M. Q. Martindale. 2001. *Dev. Biol.* 236: 195–209.

Reference: *Biol. Bull.* 201: 258–260. (October 2001)

Differentiation of Pharyngeal Muscles on the Basis of Enzyme Activities in the Cichlid *Tramitichromis intermedius*

Aaron N. Rice, David S. Portnoy, Ingrid M. Kaatz, and Phillip S. Lobel (Boston University Marine Program, Marine Biological Laboratory, Woods Hole, Massachusetts 02543)

One of the key morphological features of cichlid fishes is their highly developed pharyngeal jaw complex used in feeding (1). Although many studies focused on the anatomy (2) and function (1) of pharyngeal muscles, the potential physiological differences between them have not been examined in detail. The purpose of this paper is to investigate the capacity for anaerobic activity of the muscles in the pharyngeal jaw complex, and to assess whether they

are all the same functional type. Finding different types would suggest that various muscles in the complex may have functions other than mastication.

Bass *et al.* (3) demonstrated that fundamentally different types of muscles can be distinguished by the activity level of energetic enzymes. Assaying these enzymes in muscles tissues can indicate whether a muscle functions primarily through aerobic or anaerobic

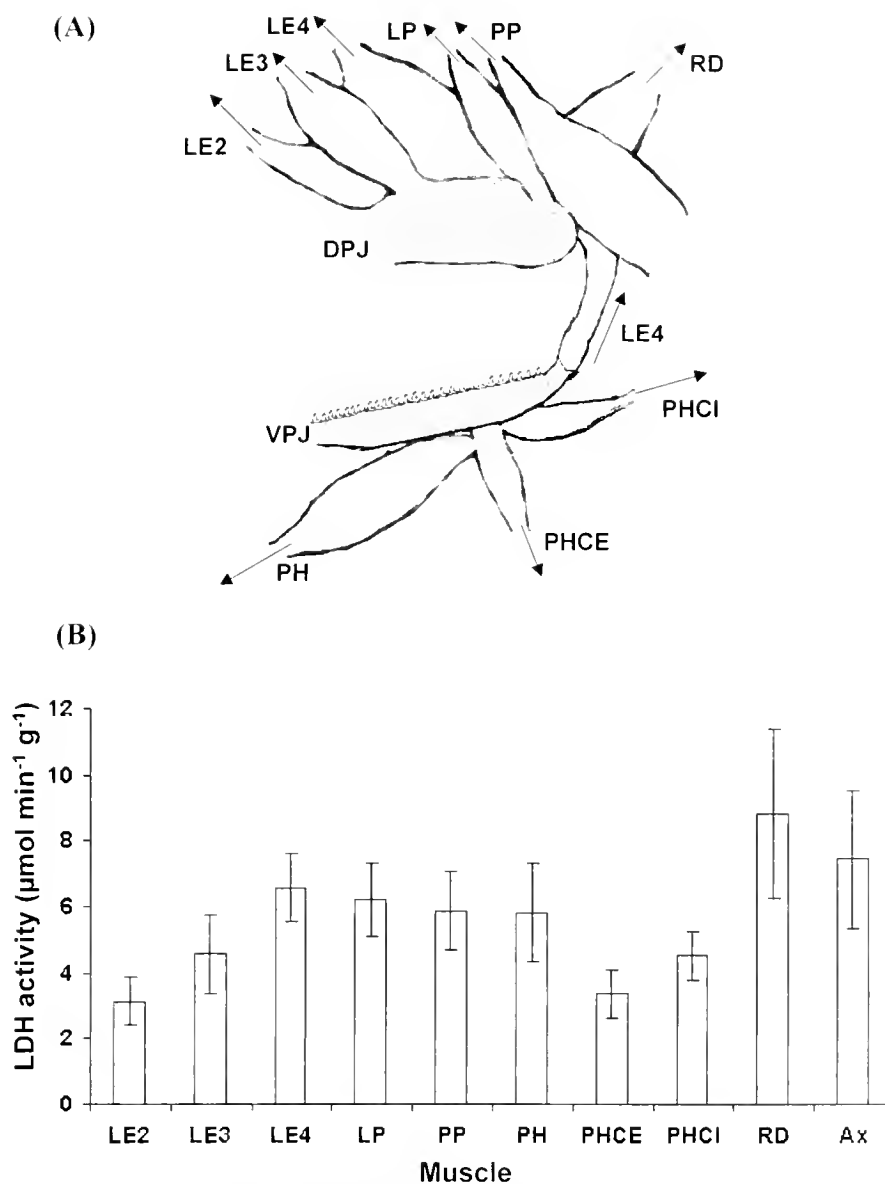


Figure 1. (A) The *Tramitichromis intermedius* pharyngeal muscles. Arrows indicate the direction of movement of the pharyngeal jaws due to muscular contraction. Abbreviations are as follows: LE2, levator externus 2; LE3, levator externus 3; LE4, levator externus 4; LP, levator posterior; PP, protractor pectoralis; PH, pharyngochoyoides; PHCE, pharyngocleithralis externus; PHCI, pharyngocleithralis internus; RD, retractor dorsalis; DPJ, dorsal pharyngeal jaw; VPJ, ventral pharyngeal jaw. (B) Enzymatic activities of L-lactate dehydrogenase from different *T. intermedius* pharyngeal muscles.

pathways. Comparative analysis between muscles can further elucidate the degree of functional specialization that these tissues have undergone relative to other muscles in the body. This technique has been employed in a variety of different taxa—for example, fishes (4), frogs (5), and bats (6)—to demonstrate functional differences between muscle types.

Captive-bred *Tramitichromis intermedius* (born in July 2000 from wild-caught parents from Lake Malawi, Africa) were kept in 75-gallon aquaria. Fish were euthanized with MS-222, and the opercles were removed. Muscles involved in movement of the dorsal and ventral pharyngeal jaws were removed and weighed: levator externi 2, 3, 4 (LE2, LE3, LE4), levator posterior (LP), protractor pectoralis (PP), pharyngochoyoides (PH), pharyngo-

cleithralis externus (PHCE), pharyngocleithralis internus (PHCI), and retractor dorsalis (RD) (Fig. 1A). Axial muscle (Ax) from the tail was also removed and served as a comparison for fast-twitch muscle. Muscle nomenclature follows Liem (1). Tissues were homogenized in 1 ml of buffer (7.5 mM Tris and 1 mM EGTA, pH 7.6), and analyzed for activities of L-lactate dehydrogenase (LDH; E.C. 1.1.1.27), in order to indicate capacity for anaerobic respiration. Using a Perkin-Elmer Lambda 3B UV/Vis spectrophotometer, enzymes were assayed using 50 mM TEA, 5 mM EGTA, 0.15 mM NADH, 0.24 mM pyruvate, pH 7.6, at 340 nm. Enzyme activities were calculated as micromoles of product per minute per gram of tissue (4), and differences between muscle groups were analyzed using a one-way ANOVA.

The mean (\pm SE) LDH activities of the muscles were as follows: LE2: 3.15 ± 0.71 , LE3: 4.56 ± 1.19 , LE4: 6.57 ± 1.02 , LP: 6.20 ± 1.12 , PP: 5.87 ± 1.18 , PH: 5.82 ± 1.48 , PHCE: 3.38 ± 0.73 , PHCI: 4.52 ± 0.72 , RD: 8.83 ± 2.57 , Ax: 7.44 ± 2.09 (Fig. 1B). These results show that the pharyngeal muscles examined differ significantly in levels of LDH activity ($n = 8$, $P = 0.0152$). A post-hoc Fisher's Protected Least Significant Difference test revealed that significant differences existed between Ax and PHCE ($P = 0.0469$), LE2 and RD ($P = 0.0143$), LE3 and RD ($P = 0.0374$), PHCE and RD ($P = 0.0355$).

The differences in LDH activity in this muscle complex shows that several muscles examined have different capacities for anaerobic activity. Functional muscle types can be differentiated on the basis of enzyme activities by comparing ratios between activities of aerobic and anaerobic enzymes. Without determining aerobic activity, we cannot conclusively demonstrate that the muscles examined are different functional types. These preliminary data suggest that more than one muscle type may be present, but analysis of the aerobic capacity is necessary.

The presence of different muscle types would suggest that the pharyngeal complex may be performing a dual function. In addition to mastication, the pharyngeal jaws have also been hypothesized to function in sound production (7). Spectrograms of sounds produced by cichlids (8) suggest that this behavior involves very

rapid muscle contraction and occlusion of the pharyngeal jaws mediated by rapid muscle contraction (7). These muscles would need to be capable of powerful burst activity, as opposed to more slow-twitch muscles involved in mastication. Observable differences in enzymatic properties of pharyngeal muscles are further representative of the complexity of this structure, and perhaps the result of its dual function.

This project would not have been possible without the valuable advice of B. D. Sidell, C. R. Bevier, and R. Voigt. Research was supported by a grant from the Army Research Office (DAAG55-91-1-0304) to PSL.

Literature Cited

1. Liem, K. F. 1974. *Syst. Zool.* **22**: 425-441.
2. Anker, G. C. 1978. *Neth. J. Zool.* **28**: 234-271.
3. Bass, A., D. Brdiczka, P. Eyer, S. Hofer, and D. Pette. 1969. *Eur. J. Biochem.* **10**: 198-206.
4. West, J. L., J. R. Bailey, V. M. F. Almeida-Val, A. L. Val, B. D. Sidell, and W. R. Driedzic. 1999. *Can. J. Zool.* **77**: 690-696.
5. Bevier, C. R. 1995. *Physiol. Zool.* **68**: 1118-1142.
6. Yacoe, M. E., J. W. Cummings, P. Myers, and G. K. Creighton. 1982. *Am. J. Physiol.* **242**: R189-R194.
7. Lobel, P. S. 2001. *J. Aquatic. Aquat. Sci.* **9**: 89-108.
8. Lobel, P. S. 1998. *Environ. Biol. Fishes* **52**: 443-452.

Reference: *Biol. Bull.* 201: 261–262. (October 2001)

Real-Time Detection of Reactive Oxygen Intermediates From Single Microglial Cells

Gilad Twig^{1,2}, Sung-Kwon Jung³, Mark A. Messerli³, Peter J. S. Smith³, and Orian S. Shirihai³

A growing body of evidence indicates that activation of microglia (macrophages resident in brain) aggravates the inflammatory process and thus can contribute significantly to the progression of various neurodegenerative diseases (1). As with other tissue-specific macrophages, microglia are thought to exert some of their cytotoxic effects through the production of reactive-oxygen-intermediates (ROI). For example, β -amyloid, an abundant component of amyloid ("senile") plaques, was shown to induce the production of ROI by cultured microglia within 1–2 min (2). Any damage caused to surrounding tissue by microglial cells is mainly dependent upon the magnitude of the gradient of ROI that is generated on the surface of the cell's membrane. Therefore, quantification at a high spatial and temporal resolution of ROI distribution in the microenvironment of an activated microglial cell is important for the assessment of neurotoxicity.

The enzyme responsible for the generation of ROI in an oxidative burst in microglial cells is NADPH oxidase, which transfers an electron from a single cytoplasmic NADPH molecule to an oxygen molecule, producing superoxide anion (O_2^-). O_2^- and its dismutation product, hydrogen peroxide (H_2O_2), diffuse away from the microglial cells and have the potential to oxidize cellular components in neighboring cells, including proteins, lipids, and DNA (3). However, H_2O_2 is a much more stable product than O_2^- and therefore can be used as a reliable indicator for detection of an oxidative burst.

The self-referencing technique has the capacity to detect, with high spatial and temporal resolution, concentration gradients of specific molecules surrounding single cells (4, 5). In the current investigation, we used an H_2O_2 -sensitive microprobe as a sensor of ROI production by microglia cells. To test the feasibility of the self-referencing technique for the detection of ROI from single microglial cells, we activated the NADPH oxidase machinery with phorbol-12-myristate-13-acetate (PMA), a potent activator of this enzyme (6).

H_2O_2 microsensors were prepared as described previously for oxygen sensors, but with slight modification (7). Briefly, 25- μ m diameter platinum (Pt) wires were immersed in an aqueous solution of 4 M KCN and 1 M NaOH and then etched down to \sim 2 μ m diameter by the application of square waves (amplitude, 4.0 V; period, 4 ms). The etched Pt wires were inserted into pulled glass capillaries, insulated with optical adhesive, and then coated with 10% cellulose acetate. The total tip diameter of the sensor was about 3 μ m. For all measurements, the sensor was polarized at +0.60 V against a Ag/AgCl reference electrode; its sensitivity was 0.85 ± 0.12 pA/ μ M (mean \pm SD, $n = 4$). Although the sensor can potentially detect other ROI beside

H_2O_2 (such as nitric oxide and O_2^-), H_2O_2 was probably the major component of the concentration gradient, considering its longer half-life time and the composition of the media (<100 μ M L-arginine).

Purified microglia were isolated from rat brains, as described elsewhere (8), and were plated into 35-mm diameter culture dishes at a density of 3000 cells/ml to allow a distribution of single cells (one cell where no other cells can be detected within a range of \sim 200 μ m).

Figure 1A demonstrates the experimental protocol that we used to detect H_2O_2 production in a single microglial cell. In the presence of culture medium only, no significant H_2O_2 efflux was detected in the close vicinity of the cell (Fig. 1A, trace (a), 5, 15 μ m). However, 10 min after adding PMA (final concentration of 130 nM), a measurement from the same location detected an H_2O_2 efflux of 0.46 pmol/cm²/s. The magnitude of the H_2O_2 efflux was inversely related to the distance from cell surface (traces (c–g) in Fig. 1A) and was nearly zero when the microprobe was moved 40 μ m from the cell surface (trace (g) in Fig. 1A). Similar results to those shown in Figure 1 were obtained in 80% of the isolated microglial cells (12 out of 15) when PMA was added to the solution; in the remaining 20% no H_2O_2 was detected. The range of peak flux was 0.22 pmol/cm²/s (SD \pm 0.17) and the average threshold detection distance was 22.4 μ m (SD \pm 4.2) ($n = 12$). The average latency for response was 4.3 min and in all the responding cells the time period of detectable gradient exceeded 30 min.

To ensure that the signal detected by the probe originated from the production of ROI, catalase, an enzyme that hydrolyzes H_2O_2 , was added to the bath. Catalase significantly attenuated the H_2O_2 efflux regardless of the distance from the cell surface (Fig. 1A: compare (h) with (i) and Fig. 1B: compare closed with open circles).

The present study demonstrates that a self-referencing microsensor can detect H_2O_2 changes in the nano-molar range near the surface of a single microglial cell. Though numerous assays are available to measure an oxidative burst within macrophages, the self-referencing technique is unique in providing the ability to measure the microenvironment around a single cell or cluster of cells in real-time and with high spatial and temporal resolution. Because microglial cells can enhance neurotoxicity of the surrounding tissue, this assay may be useful for quantifying the potential contribution of endogenous microglial-induced activators in neurodegenerative diseases.

We thank Paul Malchow, Jeffery Laskin, and Solomon Graf for critical reading of the manuscript. This study was supported by the Grass Foundation Fellowship in Neurophysiology to G. Twig and by NIH grant NCRR P41 RRO1395 to PJS Smith.

¹ The Bruce Rappaport Faculty of Medicine, Technion, Israel.

² Grass Laboratory and ³ BioCurrents Research Center, Marine Biological Laboratory, Woods Hole, MA.

Literature Cited

1. Gonzalez-Scarano, F., and G. Baltuch. 1999. *Annu. Rev. Neurosci.* 22: 219-240.
2. Bianca, V. D., S. Dusi, E. Bianchini, I. Dal Pra, and F. Rossi. 1999. *J. Biol. Chem.* 274: 15,493-15,499.
3. J. S. Weiss. 1989. *N. Engl. J. Med.* 320: 365-376.
4. Smith, P. J. S., and J. Trimarchi. 2001. *Am. J. Physiol.* 280: C1-C11.
5. Smith, P. J. S., K. Hammar, D. M. Porterfield, R. H. Sanger, and J. R. Trimarchi. 1999. *Microsc. Res. Tech.* 46: 398-417.
6. Khanna, R., L. Roy, X. Zhu, and L. C. Schlichter. 2001. *Am. J. Physiol.* 280: C796-C806.
7. Jung, S.-K., W. Gorski, C. A. Aspinwall, L. M. Kauri, and R. T. Kennedy. 1999. *Anal. Chem.* 71: 3642-3649.
8. Shirihai, O., P. J. S. Smith, K. Hammar, and D. Dagan. 1998. *Glia* 23: 339-348.

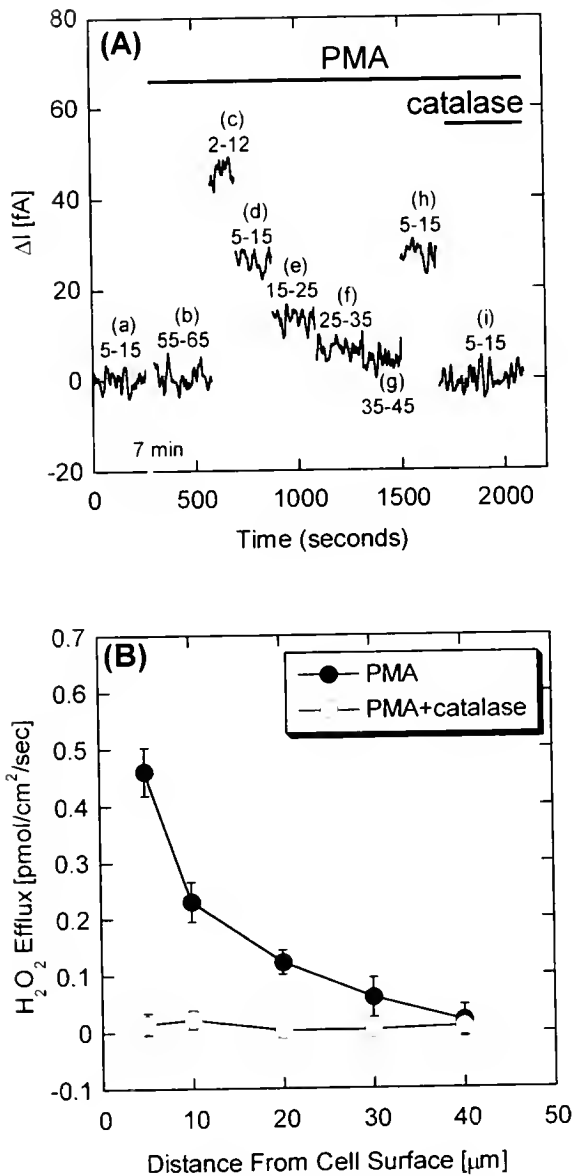


Figure 1. Self-referencing H_2O_2 measurement of a single microglial cell. (A) The difference in current values detected by the microelectrode when self-referencing at different distances from the cell surface. In all traces, the excursion (distance of the probe in the self-referencing format) was $10 \mu m$, and the number on the top of each trace represents the two positions of the microsensors in μm . Note that addition of PMA (upper solid horizontal line) induced a significant elevation in H_2O_2 efflux [(a) vs. (c-g)] and that in the presence of catalase (0.19 mg/ml) the H_2O_2 efflux was abolished [(i) vs. (h)]. Trace (b) is a "background" measure taken $60 \mu m$ away from the cell. (B) The relationships between H_2O_2 efflux and the average distance from a membrane surface in the presence of PMA; data from the same cell shown in (A). Note that application of catalase abolishes the H_2O_2 efflux.

Reference: *Biol. Bull.* 201: 263–264. (October 2001)

Porocytosis: Quantal Synaptic Secretion of Neurotransmitter at the Neuromuscular Junction Through Arrayed Vesicles

Robert B. Silver^{1,2}, Malilon E. Kriebel³, Bruce Keller³, and George D. Pappas^{2,4}

We have developed a new hypothesis for secretion, particularly at the neuromuscular junction and CNS synapses. Our interpretation of secretion—which is consistent with the structural organization of the neuromuscular junction reported by McMahan and co-workers (1)—is based upon the porocytosis hypothesis (2, 3), in which the postsynaptic quantal response results from presynaptic neurotransmitter secretion from many docked vesicles, rather than from a single vesicular exocytotic event (*cf.* 4, 5). In the mechanism we propose, presynaptic vesicles are arrayed at two levels: 1) vesicles are anchored to the active zones of the plasma membrane and juxtaposed to calcium ion-selective channels by proteins such as SNAREs (6) to make a unit; and 2) these vesicle-ion channel-SNARE-membrane-containing units are arranged in spatially periodic arrays. We envision that the organization of the arrayed active zone material at the frog neuromuscular junction described by Harlow and co-workers (1), and the array that we discuss, are one and the same entity. We view this secretory “organelle” (1), which we have called the “synaptomere” (3), to be the unit of secretion, much as the sarcomere is the unit of contraction. The synaptomere contains a scaffold that would prevent vesicular fusion into the terminal membrane and would maintain vesicles in the linear array so that vesicle and terminal unit membranes are in apposition to the receptors on the postsynaptic fold. This arrangement is extendable to synapses, although the fine level of organization of the array structure may vary among secretory systems.

The porocytosis mechanism we propose provides a quantum of neurotransmitter, but without the need to invoke fusion of a single vesicle membrane with the (presynaptic) plasma membrane. The small observed coefficient of variation (<3%) in end plate potentials indicates that there are only about 200 release sites (9), each of which secretes one quantum per action potential (2, 7, 8, 9). The 200 sites found on a small muscle fiber establish a maximum quantitative limit of 1 site per micrometer terminal length for the number of secretory organelles at the neuromuscular junction (2, 7, 9) and excludes a single vesicle quantum mechanism. Our mathematical modeling efforts have shown that release of neurotransmitter *via* the quantal vesicular fusion mechanism would result in a coefficient of variation of 14% to 30%. In summary, the notion that neurotransmitter release is mediated through a “single quantum-single vesicle” mechanism would appear to be precluded (2, 3).

Strong physiological evidence supports the concept that the repeating components of the synaptomere function as units, each secreting one packet of transmitter (10). Most importantly, the ratio of the large to small class of transmitter packets (MEPPs and sub-MEPPs), and the number of subunits composing the larger class, is readily changed with many treatments and conditions (10), showing that the two classes share the same sub-unit. Decreasing extracellular calcium decreases MEPP frequency and decreases the number of subunits in the MEPP (Fig. 1). In normal calcium, there is a very small percentage of sub-MEPPs, while in reduced calcium concentration most MEPPs are of the sub-MEPP class. A postsynaptic effect is ruled out because the modal size of the sub-MEPP has not changed. Thus, these data indicate that the number of secreting pores in the array is calcium-dependent. The concept that a single vesicle would release only a portion of its contents per flicker is supported by other studies. Neher (11) calculated that a flicker of a pore would secrete about 8% of the contents of a small vesicle. Rahamimoff and Fernandez (12) proposed that a cationic transmitter could exchange with Na ions through a fusion pore to generate the sub-MEPP. In the porocytosis array model, the 200 physiologically described release sites of a neuromuscular junction defined by Katz and Miledi (13) are the synaptomeres, and the attractive “organelles” described by Harlow and co-workers (1).

What then is the functional significance of the vesicle array of the neuromuscular junction? A two-tiered hierarchical array of vesicles is observed at the neuromuscular junction. Calcium acts within microdomains during a millisecond timeframe to evoke the release of neurotransmitter from docked vesicles across two bilayers (14). We believe that the calcium ions, with a mobility that is restricted in space and time, establishes a “salt-bridge” among adjacent lipid molecules, and in doing so, establishes a pore that spans the lipid bilayers of both the vesicle and plasma membrane. That pore will be maintained as long as calcium levels are sufficiently high. Upon the reduction of calcium levels (*i.e.*, within a millisecond), the liaison of calcium and lipid is disengaged, and the lipid molecules are freed to rotate and spread readily by diffusion, thus resulting in closure of the transient pore (16). We believe that, aside from the mechanism known as “constitutive secretion” (15), this porocytotic mechanism extends beyond the synapse, to include nearly if not all cellular secretory processes.

The observed constancy of the amount of neurotransmitter secreted with nerve stimulation, attested to by the small value of the coefficient of variance of EPPs, can only be explained by release of small amounts of neurotransmitter molecules from arrays of vesicles at each release site of the neuromuscular junction. Since the coefficient of variation of the quantal packet is a function of 1/square root of the number of contributing vesicles, and there are 30–50 in an array, a standard amount of secretion is guaranteed by the array with each action potential. The array notion is so robust

¹Departments of Radiology, Pharmacology and Physiology, Wayne State University School of Medicine, Detroit, MI; Decision and Information Sciences Division, Argonne National Laboratory, Argonne, IL.

²Marine Biological Laboratory, Woods Hole, MA.

³Department of Neuroscience and Physiology, SUNY Upstate Medical University, Syracuse, NY 13210.

⁴Psychiatric Institute, and Department of Anatomy and Cell Biology, College of Medicine, University of Illinois, Chicago, IL 60612.

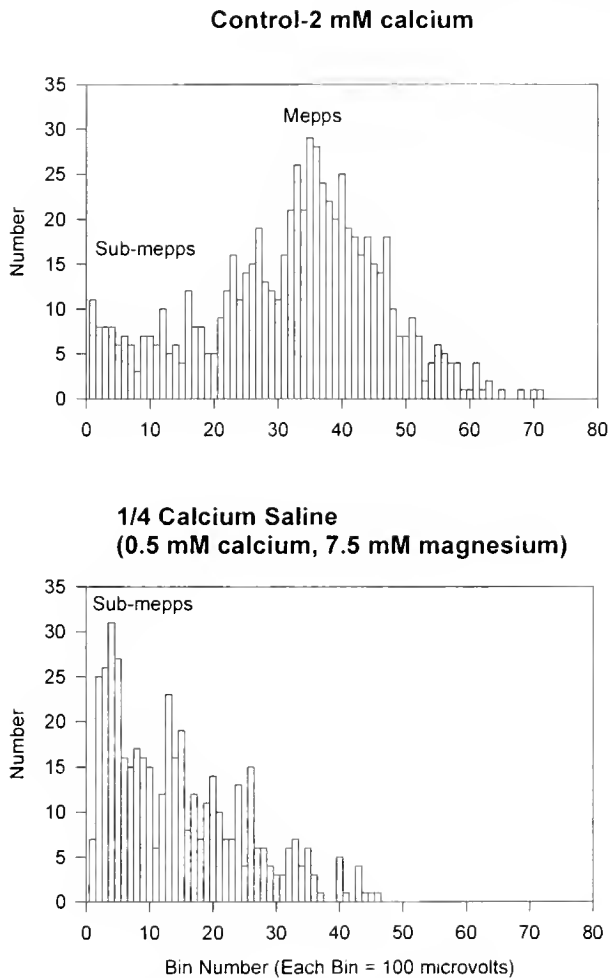


Figure 1. The effect of calcium concentration on MEPP amplitudes and on the ratio of sub-MEPPs to MEPPs in skate electrocytes. Top Panel: Control in normal saline with 2 mM calcium external to a cell stimulated to generate 1 MEPP/s. Note the small percentage of sub-MEPPs. Bottom Panel: The effect of low (1/4 normal) calcium concentration saline (0.5 mM CaCl_2 , 7.5 mM MgCl_2) and stimulation at a rate of 1 MEPP/s. Note that most MEPPs are of the sub-MEPP class. A postsynaptic effect is ruled out because the modal size of the sub-MEPP has not changed.

in maintaining a standard packet size, that vesicle contents may vary from full to empty. Since 60% of the acetylcholine in the synapse is present in the cytosol (17, 18), transporters on the vesicle membrane would continuously "fill" vesicles. In addition, acetylcholine is readily available for transporters because synthe-

sis, mediated by acetyl-O-transferase, is known to occur on the cytoplasmic surface of the vesicle membrane (19). In addition, it is likely that, concurrently, there are mechanisms for docking and undocking vesicles that are independent of secretion, each process having its own identifiable rate constants. Small variations in amounts of neurotransmitter released are readily accommodated by modulating (e.g., through small changes in calcium dynamics) the amount released from many vesicles whose diameters are observed to vary by 3% to 10% (20, 21). Most importantly, the array concept permits quantal size to be frequency-dependent. Thus, to achieve the observed characteristic constancy of "quantal release" (i.e., MEPP size), the synapse must rely on secretion through many vesicles within an array of vesicles. The porocytosis mechanism we have proposed uniquely meets these requirements. We believe that the porocytosis mechanism extends to secretion in other non-synaptic systems.

Literature Cited

1. Harlow, M. L., D. Ress, A. Stoschek, R. M. Marshall, and U. J. McMahan. 2001. *Nature* **409**: 479–484.
2. Kriebel, M. E., B. Keller, J. Holsapple, G. Q. Fox, and G. D. Pappas. 2000. *Neuroscientist* **6**: 422–427.
3. Kriebel, M. E., B. Keller, R. B. Silver, G. Q. Fox, and G. D. Pappas. 2001. *Brain Res.* (In press).
4. Heuser, J. E., T. S. Reese, and D. M. Landis. 1981. *J. Neurocytol.* **3**: 109–131.
5. Heuser, J. E., and T. S. Reese. 1974. *J. Cell Biol.* **88**: 564–580.
6. Sudhof, T. C. 2000. *Neuron* **28**: 317–320.
7. del Castillo, J., and B. Katz. 1954. *J. Physiol.* **124**: 560–573.
8. Quastel, D. M. J. 1997. *Biophysical J.* **72**: 728–753.
9. Kriebel, M. E., and B. Keller. 1999. *Cell Biol. Int.* **23**: 527–532.
10. Kriebel, M. E. 1988. Pp. 537–566 in *Handbook of Experimental Pharmacology*. Springer-Verlag, Berlin.
11. Neher, E. 1993. *Nature* **363**: 497–498.
12. Rahamimoff, R., and J. M. Fernandez. 1997. *Neuron* **18**: 17–27.
13. Katz, B., and R. Miledi. 1979. *Proc. R. Soc. Lond. B* **205**: 369–378.
14. Llinás, R. 1999. *The Squid Giant Synapse: A Model for Chemical Transmission*. Oxford University Press, New York.
15. Blasquez, M., and K. L. Shennan. 2000. *Biochem. Cell Biol.* **78**: 181–191.
16. Menikh, A., P. G. Nyholm, and J. M. Boggs. 1997. *Biochemistry* **36**: 3438–3447.
17. Zimmerman, H., and C. R. Denston. 1977. *Neuroscience* **2**: 695–714.
18. Zimmermann, H. 1982. Pp. 241–259 in *Neurotransmitter Vesicles*. Academic Press, New York.
19. Eder-Colli, L., and S. Amato. 1985. *Neuroscience* **15**: 577–589.
20. Fox, G. Q. 1996. *Cell Tissue Res.* **284**: 303–316.
21. Fox, G. Q., and M. E. Kriebel. 1994. *Brain Res.* **660**: 113–128.

Reference: *Biol. Bull.* 201: 265–267. (October 2001)

Endogenous Zinc as a Neuromodulator in Vertebrate Retina: Evidence From the Retinal Slice

Richard L. Chappell (Hunter College, CUNY, 695 Park Ave., New York, New York 10021)
and Stephen Redenti¹

Studies of the transretinal electroretinogram (ERG) of the skate (*Raja erinacia*) eyecup have provided evidence that endogenous zinc plays a role as a neuromodulator in vertebrate retina (1). With GABA receptor activity blocked by 200 μM picrotoxin, superfusion of the zinc chelating agent histidine (100 μM) increased by about 2-fold the ON (b-wave) and OFF (d-wave) components of the ERG. In addition, as shown first in the salamander retina (2) and more recently in mammalian retinas (3, 4), an accumulation of zinc has been localized to the base of the photoreceptors in skate (5). These observations support the suggestion that zinc, co-released with glutamate from photoreceptor terminals, may serve as

a neuromodulator in the outer plexiform layer of the vertebrate retina. By acting on the receptor terminal to reduce calcium entry, zinc could serve as a feedback signal to modulate transmitter release (2). If this is the case, one would expect to observe an effect of histidine application on the conductance of second-order cells in the retina of the skate.

We have tested this hypothesis by the use of whole-cell, patch-clamp recordings from horizontal cells in the skate retinal slice preparation. The slices ($\sim 200 \mu\text{m}$ thick) from the all-rod retina of the skate were positioned on a glass slide and visualized using a fixed-stage microscope equipped with a water-immersion objective and Nomarski differential interference contrast optics. Whole-cell patch recordings were obtained under conditions of steady ambient illumination from horizontal cells of the inner nuclear

¹ Ph.D. Program in Biology, The Graduate School and University Center, CUNY, 365 Fifth Ave., New York, NY 10016.

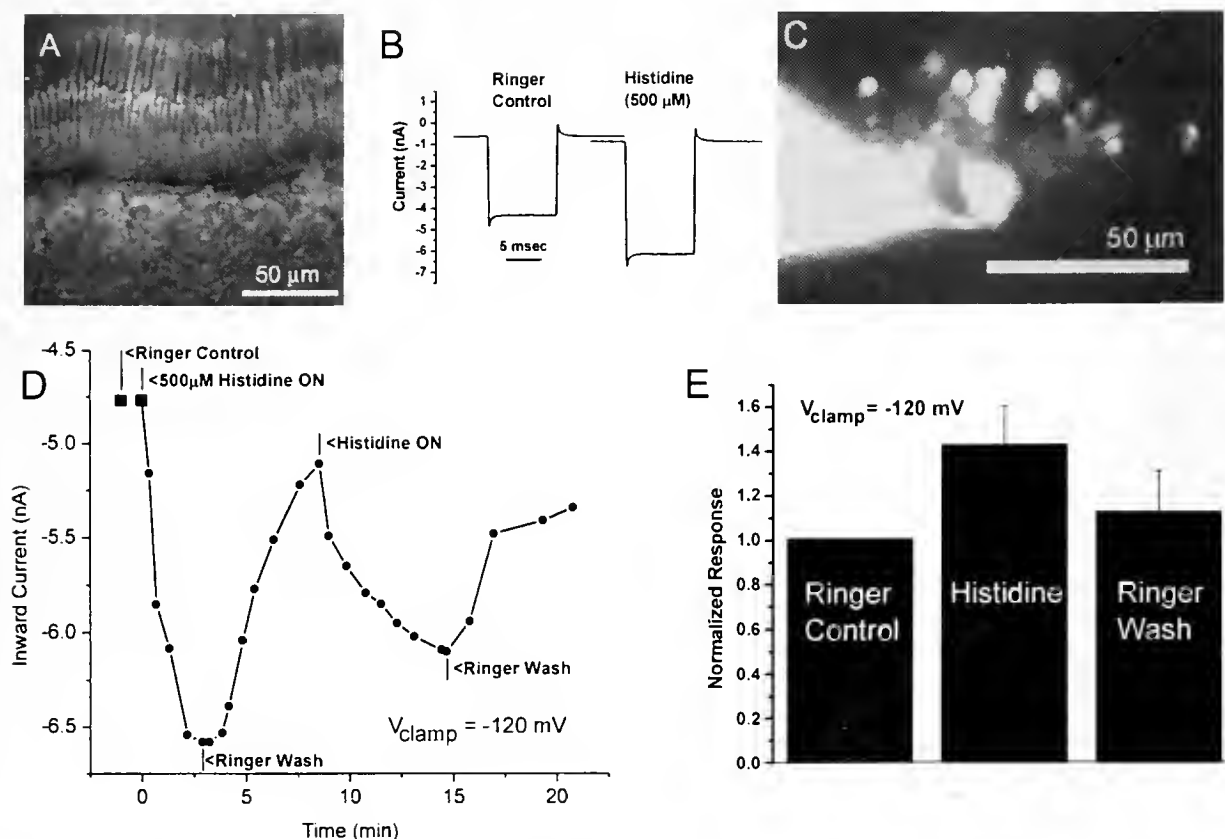


Figure 1. (A) Light micrograph of a 200- μm retinal slice from skate retina. (B) Whole-cell voltage-clamp recordings from a skate horizontal cell during 10 ms steps from a holding potential of -40 mV to -120 mV in control Ringer solution and after 2 min in 500 μM histidine. (C) Fluorescence micrograph of a skate horizontal cell recorded and stained with Lucifer yellow in the retinal slice during whole-cell patch-clamp. (D) Time course of horizontal cell conductance increase upon histidine application during a 100 ms step to a potential of $V_c = -120 \text{ mV}$ from a -40 mV holding potential represented by measured voltage-clamp inward currents. After a Ringer wash, the conductance recovers. (E) Horizontal cell currents measured in histidine ($n = 6$) and subsequent Ringer wash ($n = 5$) at $V_c = -120 \text{ mV}$ normalized to current in control Ringer. Mean \pm SEM.

layer, located below the base of the photoreceptors (Fig. 1A). Glass capillary electrodes, pulled to a resistance of 2 to 4 megohms, were filled with a standard skate internal solution (5) and the fluorescent dye, Lucifer yellow (0.3%). In addition, cesium chloride (204 mM) was added to suppress potassium currents. Holding potentials of -40 mV were used, thus avoiding the transient outward currents seen in these cells when they are held at more negative potentials (6). This simplified the analysis of the relationship between membrane conductance and photoreceptor transmitter release. The preparation was superfused with a continuous flow of skate-modified Ringer solution (5) at approximately 1 ml per min. This could be rapidly exchanged with a Ringer solution to which histidine (100 or 500 μ M) had been added. The higher concentration provided a faster increase in histidine concentration in the experimental chamber, but the ratios of the current increases measured were found to be independent of drug concentration.

Responses to 10 ms steps in voltage (Fig. 1B) were obtained from horizontal cells like the one shown in the fluorescence micrograph of Figure 1C. Note the brightly stained bulbous terminals suggestive of the knob-like endings observed in sections of Golgi-stained skate external horizontal cells (6). To monitor currents during solution changes, it was convenient to hold the cell at -40 mV and step the voltage to -120 mV. Applying histidine (500 μ M) for 2 min produced a 40% increase in the inward current as compared with that obtained in Ringer (Fig. 1B). Using a different protocol, in which the duration of the -120 mV step was 0.1 s, the time course of the current changes during 500 μ M histidine applications and Ringer washes was measured and plotted (Fig. 1D). Each point represents the average of data from 3 successive steps, except for the "Ringer Control" points (square symbols) where 9 successive steps have been averaged. The initial increase in inward current observed in histidine approached saturation in less than 3 min. When the solution was returned to Ringer for a period of 5 min, 81% recovery was observed. A subsequent histidine application followed by Ringer wash gave comparable results.

Data similar to that shown in Figure 1D were obtained from 6 horizontal cells, normalized to the current measured at $V_c = -120$ mV in control Ringer solution, and averaged (Fig. 1E). The inward current increased 42% in histidine at $V_c = -120$ mV; when returned to Ringer, the increment in current was reduced by 72%.

Since the skate horizontal cell has no ligand-gated GABA receptors (7), the well known effect of zinc on these receptors is not relevant, as it is for salamander horizontal cells (2). Glutamate receptors of skate horizontal cells have not been studied, but the possibility that zinc is acting directly on horizontal cells to reduce their permeability seems remote. Retinal horizontal cell glutamate receptors have been identified as AMPA/kainite receptors (8), although metabotropic glutamate receptors have been reported in one case (9). AMPA/kainite receptors studied on neurons elsewhere in the nervous system are generally enhanced by zinc at low concentrations (10, 11). Similar observations have been reported for retinal horizontal cells (12), but most studies have shown no effect of zinc on these cells (2, 13, 14), with one exception, where currents were reduced (15). For example, a zinc concentration of 50 μ M—while high enough to block glutamate release from

salamander photoreceptors—showed no effect on horizontal cell responses to applied glutamate (2). Similarly, it is important to note that, as a chelating agent, histidine, which has a much higher affinity for Zn^{2+} than for Ca^{2+} and is not membrane-permeable, would be expected to reduce, not increase, the ERG response if it were acting directly to reduce calcium entry needed for photoreceptor transmitter release (1).

The skate horizontal cell can serve as a glutamate electrode, monitoring the amount of photoreceptor transmitter released; *i.e.*, an increase in photoreceptor transmitter release will be reflected in an increase in horizontal cell conductance. With these considerations in mind, we interpret the increase in membrane conductance observed in the presence of histidine to represent an increase in photoreceptor transmitter release. We believe that this effect is due to the chelation by histidine of endogenous zinc. Thus, in the presence of histidine, the inhibitory feedback process is suppressed, calcium entry into the receptor terminals is increased, and transmitter release is enhanced.

This mechanism probably represents an important component of "neural" adaptation, comprising processes that are distinct from those governed directly by the bleaching and generation of rhodopsin (16, 17). Moreover, it may well provide insight into mechanisms of response dynamics, such as the surround enhancement effects observed with dynamically-modulated spots of light (18, 19), as well as phenomena referred to as suppressive rod-cone interaction in amphibians (20), cat (21, 22), and man (23).

Supported by NIH Grant EY00777, PSC/CUNY Grants 622450031 and 632130032, as well as by an NIH/RISE (Research Institute for Scientific Enhancement) GM60665 award to Hunter College and by NIGMS grants 2T34 GM07823 (MARC) and R25 GM56945. Research Centers in Minority Institutions award RR-03037 from the National Center for Research Resources of the National Institutes of Health, which supports the infrastructure of the Biological Sciences Department at Hunter College, is also acknowledged. The contents are solely the responsibility of the authors and do not necessarily represent the official views of the NCRR/NIH.

Literature Cited

1. Rosenstein, F. J., R. W. Miller, and R. L. Chappell. 2001. *Investig. Ophthalmol. Vis. Sci.* **42**: S668.
2. Wu, S. M., X. Qiao, J. L. Noehels, and X. L. Yang. 1993. *Vision Res.* **33**: 2611–2616.
3. Kaneda, M., M. Mochizuki, K. Aoki, and A. Kaneko. 1997. *J. Gen. Physiol.* **110**: 741–747.
4. Akagi, T., M. Kaneda, K. Ishii, and T. Hashikawa. 2001. *J. Histochem. Cytochem.* **49**: 87–96.
5. Qian, H., L. Li, R. L. Chappell, and H. Ripps. 1997. *J. Neurophysiol.* **78**: 2402–2412.
6. Malchow, R. P., H. Qian, H. Ripps, and J. E. Dowling. 1990. *J. Gen. Physiol.* **95**: 177–198.
7. Malchow, R. P., and H. Ripps. 1990. *Proc. Natl. Acad. Sci. USA* **87**: 8945–8949.
8. Wu, S. M., and B. R. Maple. 1998. *Vision Res.* **38**: 1371–1384.
9. Gafka, A. C., K. S. Vogel, and C. L. Linn. 1999. *Neuroscience* **90**: 1403–1414.
10. Bresink, L., B. Ebert, C. G. Parsons, and E. Mutschler. 1996. *Newopharmacology* **35**: 503–509.

11. Lin, D. D., A. S. Cohen, and D. A. Coulter. 2001. *J. Neurophysiol.* **85**: 1185–1196.
12. Yang, X.-L., L. Ping, T. Lu, Y. Shen, and M.-H. Han. 2001. *Prog. Brain Res.* **131**: 277–293.
13. Schmidt, K.-F. 1999. *Neurosci. Lett.* **262**: 109–112.
14. Shen, Y., and X.-L. Yang. 1999. *Neurosci. Lett.* **259**: 177–180.
15. McMahon, D. G., D.-Q. Shang, L. Ponomareva, and T. Wagner. 2001. *Prog. Brain Res.* **131**: 419–436.
16. Dowling, J. E., and H. Ripps. 1970. *J. Gen. Physiol.* **69**: 57–75.
17. Green, D. G., J. E. Dowling, I. M. Siegel, and H. Ripps. 1975. *J. Gen. Physiol.* **65**: 483–502.
18. Chappell, R. L., K.-I. Naka, and M. Sakuranaga. 1985. *J. Gen. Physiol.* **86**: 423–453.
19. Chappell, R. L. 2001. *Prog. Brain Res.* **131**: 177–184.
20. Frumkes, T. E., and T. Eysteinnsson. 1987. *J. Neurophysiol.* **57**: 1361–1383.
21. Pflug, R., R. Nelson, and P. K. Ahnelt. 1990. *J. Neurophysiol.* **64**: 313–325.
22. Nelson, R., R. Pflug, and S. M. Baer. 1990. *J. Neurophysiol.* **64**: 326–340.
23. Frumkes, T. E., G. Lange, N. Denny, and I. Beczkowska. 1992. *Vis. Neurosci.* **8**: 83–89.

Reference: *Biol. Bull.* **201**: 267–268. (October 2001)

Polarization Reflecting Iridophores in the Arms of the Squid *Loligo pealeii*

Nadav Shashar (Hebrew University, Interuniversity Institute for Marine Sciences, P.O. Box 469, Eilat 88103, Israel), Douglas T. Bors¹, Seth A. Ament¹, William M. Saidel², Roxanna M. Smolowitz¹, and Roger T. Hanlon¹

Distinct polarization body patterns have been recorded in cephalopods. In cuttlefish (*Sepia officinalis*) and squid (*Loligo pealeii*) these patterns are postulated to constitute a discrete communication channel that may be “hidden” from some of their predators (1, 2). In squid, the patterns of polarization are most prominent as long, narrow stripes along the arms (3). Examination of the skin of *L. pealeii* has now revealed very localized rows of iridophore cells that are reflecting and polarizing incident light and thus producing these patterns. Topical application of acetylcholine (ACh) to the arms of *L. pealeii* induced a change in the polarization reflection, as in other squid species (4). Moreover, silver staining and acetylcholinesterase histochemistry suggest that these iridophores are under direct neural control, unlike any known cephalopod iridophore.

Reflection and polarization of incident light by squid iridophores is accomplished by layers of intracellular platelets that are positioned parallel to each other (5). The spectrum (color) of the reflection can change from red/pink to blue and depends upon the distance between platelets, the orientation of the platelets, and the direction of viewing (6, 7). In squid dermis, iridophores have been found heretofore only beneath the layer of chromatophores (4). Iridophores are found in many parts of squid skin, but in most species they are especially abundant on the mantle. Because the polarization patterns in *Loligo pealeii* are created within very localized areas on the arms (Fig. 1B), we examined the skin in those areas and looked for structures that could potentially reflect light to produce polarization patterns.

For *in vitro* examination, pieces of fresh skin containing the polarizing sections were stretched to original size onto a paraffin-coated petri dish filled with chilled filtered seawater. The tissue was then examined with a Zeiss SVII dissecting microscope equipped with a polarization indifferent digital camera, under depolarized epi-illumination, and with a rotating linear polarizing filter (Polaroid HN38S) installed in the outgoing light path. Three

consecutive images were then taken with the filter set at preset angles (arbitrarily defined as 0°, 45°, and 90°). The images were then analyzed with custom-made software, and the polarization characteristics of the reflected light were determined.

For morphology, arms were preserved in 10% formalin in buffered seawater for 3 d and, after washing, they were cut, mounted, and transferred to 70% ETOH. Samples were then sectioned at 40–200 μm intervals and stained with Mayer's hematoxylin and eosin, Masson's trichrome, and silver (Holmes' silver nitrate method). Sectioning and processing arm tissue for acetylcholinesterase histochemistry was done according to the method of Mesulam and Van Hoesen (8), using the acetylthiocholine medium specified by Geneser-Jensen and Blackstad (9). Images were then observed with a Zeiss Axioplan microscope equipped with an internal scaling and calibration system.

Strong partially linearly polarized reflection could be identified in specific lines along the animals' arms (Fig. 1A–D) and was often associated with physical colors such as blue or pink. Microscopic examination of skin tissue at these locations revealed the existence of a new type of iridophore. These reflecting cells were located in very narrow areas of the skin, $60 \pm 26 \mu\text{m}$ ($n = 24$) underneath the skin surface, and organized as long stripes. Cell length was $267 \pm 131 \mu\text{m}$ ($n = 22$), and cell width was $14.8 \pm 7.2 \mu\text{m}$ ($n = 26$). These long stripes of iridophores are consistent with the red and highly polarizing iridophores reported by Mäthger and Denton (7), but the squid arm iridophores are much narrower. Unlike other squid iridophores, which are found beneath the chromatophore layer, these cells were situated above the chromatophores (Fig. 1E). Platelets [$1.8 \pm 1.2 \mu\text{m}$ wide and $14.1 \pm 6.4 \mu\text{m}$ long ($n = 138$)] were set in an angle inside the cell and were organized parallel to each other with a variability of $7.9^\circ \pm 4.0^\circ$ ($n = 25$). Inter-platelet space was $1.2 \pm 0.7 \mu\text{m}$ ($n = 150$), providing for an average density of 30.8 ± 9.0 platelets per $100 \mu\text{m}$.

Previous studies have never furnished evidence of innervated squid iridophores (4). This is surprising considering the speed with which changes in color—even iridescent color—occur in cephalopods. Hanlon *et al.* (4) found that iridophores in the squids *Lolliguncula brevis* and *Loligo plei* became iridescent when treated with ACh, but no nerve fibers were found adjacent to or

¹ Marine Resources Center, Marine Biological Laboratory, Woods Hole, MA 02543.

² Dept. of Biology, Rutgers, the State University of New Jersey, Camden, NJ 08102.

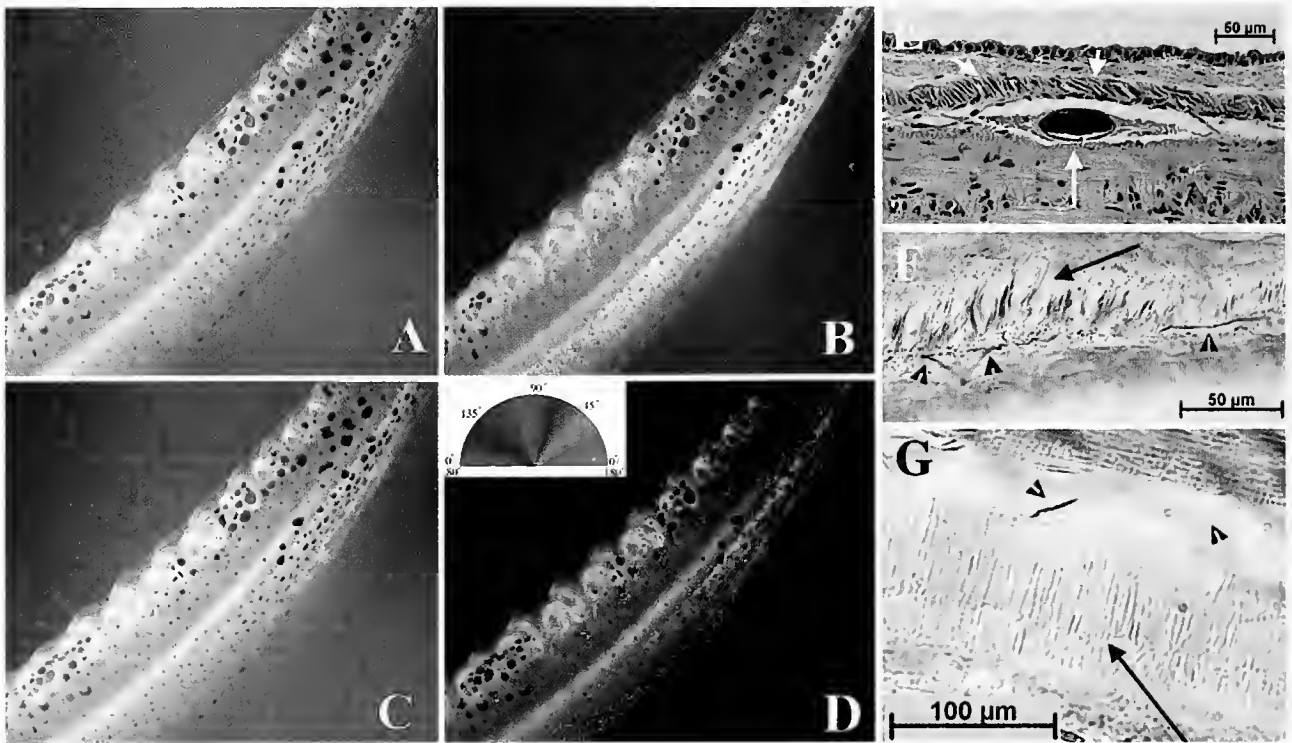


Figure 1. An arm of a squid as seen in normal light (A); through a linear polarizer set at 45° to the orientation of maximal polarized reflection (B); as a black and white image of A, which is presumably what a color-blind, polarization-insensitive predator would see (C); and when % polarization is coded into saturation (the color image) and orientation of polarization is encoded into hue (the scale)—note that the polarization reflection is very localized into a specific stripe along the arm (D). Light microscopy of cross sections in squid arms with H&E staining (E) shows iridophores (short arrows) above the chromatophores (long arrow), which is a novel arrangement. In (F), a DIC image of a silver-stained section which indicates potential nerve fibers (short arrows) immediately adjacent to or on an iridophore (long arrow). In (G), acetylcholinesterase staining (short arrows) adjacent to an iridophore cell (long arrow) also indicates potential locations of innervation.

near the iridophore cells. They therefore surmised that ACh would diffuse to the iridophore cell surfaces, would bind to ACh receptors there and thus would induce an ultrastructural change in the platelets to produce iridescence.

However, polarization patterns on cephalopods change in just a second or two, suggesting neural rather than hormonal control. Topical application of 10^{-3} M ACh to isolated skin patches induced polarization reflections. Silver staining revealed nerve fibers in very close proximity to the iridophores (Fig. 1F), suggesting that these cells may be innervated directly. Finally, staining for acetylcholinesterase revealed specific active areas at the attachment of potential nerve fibers to the iridophores (Fig. 1G).

Our results present quite a different cellular structure—and potential control mechanism—in which a polarization pattern is produced in the arms of squid. The control of these structures, and the significance of polarization patterns to squids, remain to be investigated.

We thank Michael Mitchell for sectioning some samples, John Messenger and William Kier for evaluating some microscopic tissue samples, and Louis Kerr and Rudi Rottenfusser for micros-

copy assistance. This study was sponsored by NSF grant IBN 9722805, BSF grant 1999040, and an MBL fellowship to NS.

Literature Cited

- Hanlon, R. T., M. R. Maxwell, N. Shashar, E. R. Loew, and K.-L. Boyle. 1999. *Biol. Bull.* 197: 49–62.
- Shashar, N., P. S. Rutledge, and T. W. Cronin. 1996. *J. Exp. Biol.* 199: 2077–2084.
- Shashar, N., and R. T. Hanlon. 1997. *Biol. Bull.* 193: 207–208.
- Hanlon, R. T., K. M. Cooper, B. U. Budelmann, and T. C. Pappas. 1990. *Cell Tissue Res.* 259: 3–14.
- Mirow, S. 1972. *Z. Zellforsch. Mikrosk. Anat.* 125: 176–190.
- Cooper, K. M., R. T. Hanlon, and B. U. Budelmann. 1990. *Cell Tissue Res.* 259: 15–24.
- Mäthger, L. M., and E. J. Denton. 2001. *J. Exp. Biol.* 204: 2103–2118.
- Mesulam, M. M., and G. W. Van Hoesen. 1976. *Brain Res.* 109: 152–157.
- Geneser-Jensen, F. A., and T. W. Blackstad. 1971. *Z. Zellforsch. Mikrosk. Anat.* 114: 460–481.

Reference: *Biol. Bull.* 201: 269–270. (October 2001)

Cuttlefish Cue Visually on Area—Not Shape or Aspect Ratio—of Light Objects in the Substrate to Produce Disruptive Body Patterns for Camouflage

Chuan-Chin Chiao¹ and Roger T. Hanlon (Marine Biological Laboratory, Woods Hole, Massachusetts 02543)

Cephalopods have at least 20 body patterns for camouflage, yet these can be organized into four categories: uniform, stipple, mottle, and disruptive (1). Among them, disruptive coloration is probably the most striking because it breaks up the animal's body outline by visual deception (2). Cuttlefish produce (by direct neural control of chromatophores) an array of white skin components that produce a disruptive coloration on their bodies, and this helps them achieve camouflage as it is defined by Endler (3). "A colour or pattern is cryptic if it resembles a random sample of the visual background as perceived by the predator at the time and place at which the prey is most vulnerable to predation." The so-called "White square" on the dorsal mantle of cuttlefish represents a random sample of white background objects (Fig. 1) that are common in marine habitats, thereby distracting the attention of visual predators away from the body outline (2). How do cuttlefish "decide" to switch to disruptive coloration, and what sensory cues are involved? We developed a non-invasive assay that monitors motor output (*i.e.*, the body pattern of the cuttlefish) resulting from different visual inputs (computer-generated artificial substrates). Although many aspects of cephalopod vision are known (4), little is known about the visual features of the substrate that elicit disruptive coloration. A recent study (5) of young cuttlefish, *Sepia pharaonis*, showed that the size, contrast, and number of white squares on a black background are the main visual features that cause cuttlefish to switch from general resemblance of the substrate to disruptive coloration. In this study, we examine the shapes and aspect ratios of white objects on black backgrounds that lead cuttlefish to show disruptive coloration.

Five young cuttlefish, *Sepia pharaonis* (8–10 cm mantle length, 10 weeks old), were reared from eggs in the laboratory of the National Research Center for Cephalopods (University of Texas Medical Branch, Galveston) and were maintained in the Marine Resources Center at the Marine Biological Laboratory, Woods Hole, Massachusetts. Each animal was placed in a running seawater tank (25 cm × 40 cm × 10 cm) and was restricted by a four-wall divider (inside covered by black cloth to prevent light reflection) to an area (20 cm × 26 cm) where various computer-generated backgrounds (laminated to be waterproof) were presented as the substrate. Acclimation to the tank was gauged by the cessation of excessive swimming and hovering movements and by the chronic expression of a stable body pattern. A digital video camera was used to record the body patterning of *S. pharaonis* over a period of 30 min (*i.e.*, record 2 s for every 1-min interval;

total 60 s for each cuttlefish on each substrate). Although cuttlefish cannot perfectly match backgrounds that are completely artificial, they do show various grades of disruptive patterns based on certain visual features of these substrates. Thus, it was possible to quantify the body patterns corresponding to the shapes or areas of the white objects in the black background. A simple system for grading patterns was used to assess an animal's responses to different substrates (see Ref. 5 for details). The assigned grades were: 1 = uniformly stippled pattern; 2 = indistinct pattern; 3 = disruptive pattern. Grading was conducted by playing the videotape and assigning a grade (1–3; whole integers only) every 10 s. Since all tapes were 60 s long, six grades were assigned for each animal on each substrate. The combined mean values (and overall standard deviation) of all animals were plotted in Figure 1.

Six different shapes of medium-sized white objects (same area, 1.53 cm²) were tested to determine whether they would elicit disruptive coloration (Fig. 1). Two control images were also used: large circle and large square (same area, 13.80 cm²), which are too large to elicit the White square in the cuttlefish. The generation of disruptive or uniform skin patterns in the cuttlefish did not depend on the shape and aspect ratio of white objects (Fig. 1). Although shapes with equal aspect ratio (*i.e.*, circle, hexagon, pentagon, square, and triangle—all generally similar to the shape of White square on the mantle) did not affect the display of a disruptive body pattern, we were surprised that the elongated oval shape also elicited the White square and disruptive coloration. This indicates that cuttlefish may integrate the whole area of white objects to determine the display of disruptive coloration, regardless of the shapes and aspect ratios of white objects.

Cuttlefish live in much more complex environments than these computer-generated backgrounds, and the ability to display appropriately camouflaged body patterns is critical to survival of this soft-bodied creature. We are gradually learning how cuttlefish use certain features of the visual background to decide upon the type of camouflage that will avoid detection by predators. The sophisticated skin of cephalopods provides a novel system with which to study visual perception and decision-making (6). Further studies should be aimed at exploring these processes on more natural backgrounds.

We thank Janice Hanley, Bill Mebane, James Carroll, Hazel Richmond, and Nicole Gilles for help with cuttlefish rearing and maintenance. CCC is grateful for the support from Richard Masland of Harvard. This paper is dedicated to Ellen Grass (the Grass Foundation), who staunchly and enthusiastically supported young scientists studying all aspects of neurobiology and behavior.

¹ Howard Hughes Medical Institute, 50 Blossom Street, Wellman 429, Massachusetts General Hospital, Boston, MA 02114.

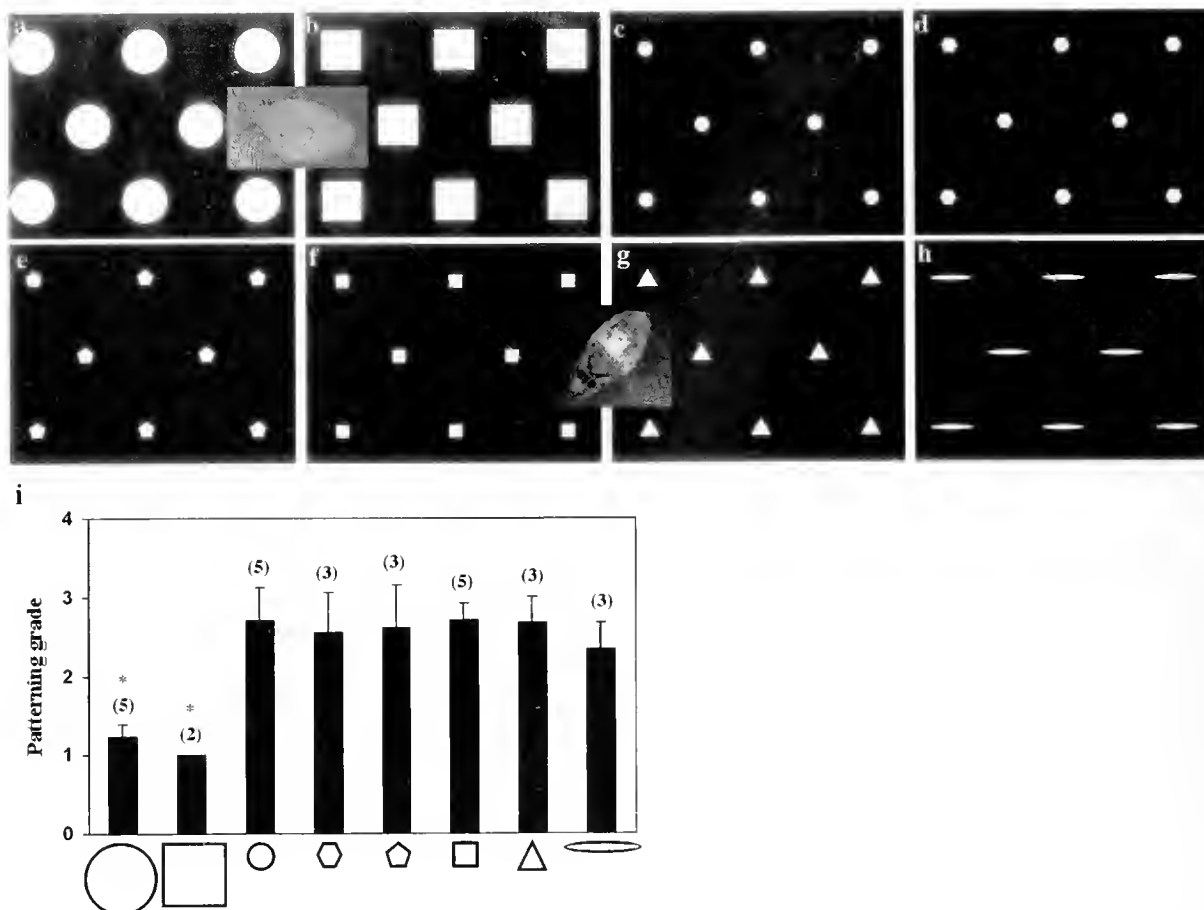


Figure 1. Two large control images (a,b) on which the cuttlefish (centered) did not show its White square. For five images (c–g), cuttlefish were expected to—and did—show White square disruptive coloration. On one image (h) they were not expected to elicit White square due to its highly different aspect ratio, yet they did. (i) A summary of results from all eight images. Patterning grade 3 is disruptive. The number enclosed in parentheses indicates the number of cuttlefish tested. Results of the first two images were significantly different from the remaining six images ($P < 0.00001$).

Literature Cited

- Hanlon, R. T., and J. B. Messenger. 1988. *Philos. Trans. R. Soc. Lond. B* 320: 437–487.
- Hanlon, R. T., and J. B. Messenger. 1996. *Cephalopod Behaviour*. Cambridge University Press, Cambridge.
- Endler, J. A. 1991. Pp. 169–196 in *Behavioural Ecology. An Evolutionary Approach*. J. R. Krebs and N. B. Davies, eds. Blackwell Scientific Publications, Oxford.
- Messenger, J. B. 1991. Pp. 364–397 in *Evolution of the Eye and Visual System*. J. R. Cronly-Dillon and R. L. Gregory, eds. Macmillan Press, London.
- Chiao, C.-C., and R. T. Hanlon. 2001. *J. Exp. Biol.* 204: 2119–2125.
- Packard, A. 1995. Pp. 331–367 in *Cephalopod Neurobiology*. N. J. Abbott, R. Williamson, and L. Maddock, eds. Oxford University Press, New York.

Reference: *Biol. Bull.* 201: 271–272. (October 2001)

Visually Guided Behavior of Juvenile Horseshoe Crabs

M. Errigo¹, C. McGuinness², S. Meadors³, B. Mittmann⁴, F. Dodge⁵, and R. Barlow⁵
(Marine Biological Laboratory, Woods Hole, Massachusetts 02543)

The horseshoe crab, *Limulus polyphemus*, has long been an admirable model for vision research. More than 70 years of research on the physiological properties of the *Limulus* lateral eye have uncovered fundamental mechanisms of visual function common to many animals, including humans (1, 2). Less attention has been given to the role of the lateral eyes in the animal's behavior. Initial field studies showed that adult males use their eyes to find mates, whereas adult females avoid mate-like objects (3). Our attempts to study these behaviors in the laboratory were not successful because adults do not exhibit them in captivity (R. Barlow, pers. obs.). We therefore turned our attention to juvenile *Limulus* and report here an investigation of their visually guided behavior both in the field and in the laboratory.

We first studied visually guided behavior of juvenile crabs on tidal flats (0.3–1 m depth) of the North Monomoy Island Wildlife Refuge, Chatham, Cape Cod, Massachusetts. Because juvenile as well as adult animals are most active on the submerged flats during high tides, we restricted our observations to these periods. We selected 1-year-old juveniles, born in the spring of 2000 (stages VI to X; prosoma widths: 16–39 mm). Their compound lateral eyes contain from 500 to 600 ommatidia, or about half the number of the adult eye. When a moving juvenile crab was located, we placed a high-contrast cylindrical object (7.6 cm diameter; 15 cm high) on the bottom 15 to 45 cm in front of the animal. Twenty-three of the 26 animals tested changed direction and avoided the object; the other 3 stopped and buried themselves. A low-contrast, gray object of the same size and placement evoked avoidance behavior in 14 of 20 animals. Five animals continued straight and hit the object, and one stopped and buried itself. Most animals appeared to respond to objects placed in front of them because they could see them, with the black object being more visible than the gray one. However, we could not eliminate the possibility that they detected a disturbance in the water when the objects were placed in front of them.

To examine the visually guided behavior of juveniles under more controlled conditions, we placed them in shallow seawater troughs (40 cm × 50 cm; 3 cm water depth; 2 cm sand depth) under ambient diurnal lighting in the Marine Biological Laboratory, Woods Hole, Massachusetts. To test the animals, we transferred 10 of them to a trough of the same size, containing seawater (3 cm depth) but no sand. The lack of sand prevents them from burying themselves and enhances their locomotor activity. We simulated the illumination of an overcast cloudy day by reflecting light from a white diffusing surface located above the trough. The

level of illumination at the water's surface was 1.0 cd/m². After giving the animals time (~30 min) to acclimate to the new trough without sand, we videotaped their behavior in the vicinity of a high contrast (black) cylindrical object (diameter: 6.5 cm) placed in the center of the trough. After 5 min, the object was removed for 5 min or replaced with a transparent object of the same size. This sequence of 5-min test intervals was repeated for about 1 h, and then the animals were returned to their sand-filled troughs. We digitized the video recordings at 2 frames/sec and traced the paths of animals on a transparent sheet attached to the monitor. Using NIH Image software, we also measured their "distance of closest approach" to the objects (4). The distance at which animals began to turn from the object ("turning distance," see Ref. 4) was difficult to judge with precision and was therefore not measured. All animals appeared about equally active. We did not track specific individuals.

Figure 1 shows that juvenile horseshoe crabs avoided the black object (a), but not the transparent one (b). Only twice did an animal contact the black object, whereas animals contacted and circled the transparent object many times. In the absence of an object, they moved about through all areas of the trough. For purposes of demonstration, we show only 30 traced paths for each of the two conditions containing targets. Each traced path begins and ends near the sides of the trough because we did not include the animals' movements along the sides of the trough.

The "distance of closest approach" of an animal to an object provides a measure of how well they can see (4). This is the distance from the center of the animal to the center of the object (4). NIH Image was used to make these measurements. The data in Figure 1(a) yield an average distance of closest approach of 11.4 ± 3.1 cm ($n = 30$). The greatest distance was 18.3 cm, suggesting that the crabs can see the black object at this distance. The transparent object (Fig. 1b) is apparently invisible to the animals because they run into it. After contacting the object, they tend to circle it one or more times before moving away.

This study presents the first evidence that juvenile horseshoe crabs can see. Their avoidance of high-contrast objects is similar to that observed for adult females (4). The previous study suggested that adult females migrating to shallow waters to build nests search for unoccupied areas and thus avoid dark, female-size objects. Juveniles may turn away from dark objects because they represent potential predators. Adult males avoided dark objects only if they were held overhead (R. Barlow, pers. obs.). Adult males may view overhead objects as predators in the same way that juveniles view dark objects on the bottom. We cannot relate the specific behaviors we observe to the sex of the 1-year-old juveniles because their sex is not known. Horseshoe crabs acquire external sexual features when they reach maturity, at about six years of age. Perhaps all the juveniles we tested were females and avoided high-contrast objects as they do in adult life. Or the juveniles we tested could have been

¹ Boston University Marine Program.

² Syracuse University.

³ University of South Carolina.

⁴ Humboldt-Universität, Berlin.

⁵ SUNY Upstate Medical University.

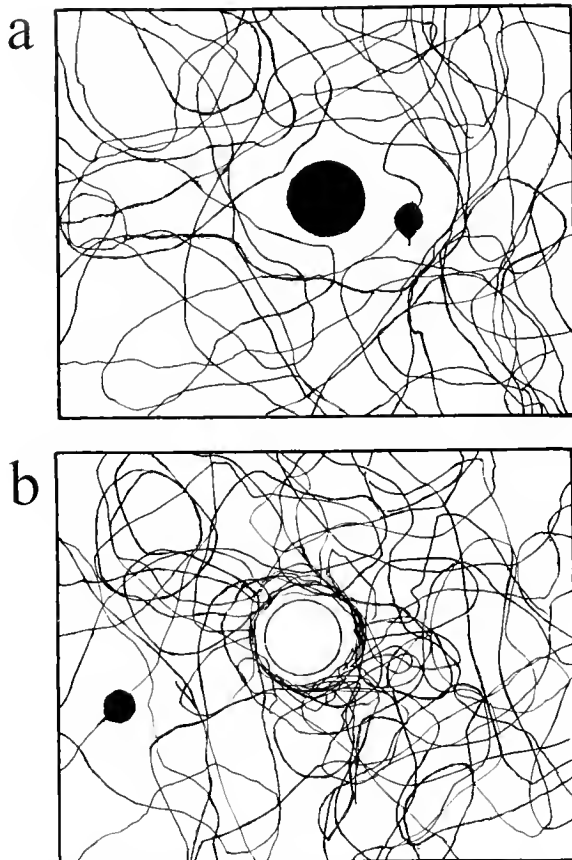


Figure 1. (a) Thirty tracings of the paths of 10 juvenile *Limulus* in a trough containing a high-contrast black cylinder. This figure illustrates the avoidance behavior of the juvenile crabs in the presence of a high-contrast object. The small black spot represents the relative size of a crab. (b) Thirty tracings of the paths of 10 juvenile *Limulus* in a trough containing a clear cylinder. This figure illustrates the inability of the crabs to detect a low-contrast object visually. Again, the small black spot represents the relative size of a crab.

Reference: *Biol. Bull.* **201**: 272–274. (October 2001)

Growth, Visual Field, and Resolution in the Juvenile *Limulus* Lateral Eye

*S. Meadors*¹, *C. McGuinness*², *F. A. Dodge*³, and *R. B. Barlow*³
 (Marine Biological Laboratory, Woods Hole, Massachusetts 02543)

When a trilobite larval *Limulus* hatches from an egg, it begins to forage with the locomotor abilities of an adult but not with the vision of an adult. Its lateral eyes have fewer than 2% of the photoreceptors possessed by an adult. Our understanding of the way an adult horseshoe crab sees its environment is now sufficiently advanced that its visual processes can be mathematically modeled (1). Guided by this model, we have set out to examine

a mix of males and females, and not yet at the time in life when males change their response to visual objects in front of them from avoidance to attraction.

Supported by grants from the National Science Foundation, National Eye Institute and the National Institutes of Mental Health. C. McGuinness and S. Meadors received REU Fellowships from the National Science Foundation.

Literature Cited

1. Ratliff, F. 1974. *Studies on Excitation and Inhibition in the Retina*. The Rockefeller University Press, New York.
2. Barlow, R. B., J. M. Hitt, and F. A. Dodge. 2001. *Biol. Bull.* **200**: 169–176.
3. Barlow, R. B., L. C. Ireland, and L. Kass. 1982. *Nature* **296**: 65–66.
4. Powers, M. K., R. B. Barlow, and L. Kass. 1991. *Visual Neurosci.* **7**: 179–189.

how the lateral eye and visually guided behavior develop. Here we report on how photoreceptors, or ommatidia, are added during development, and how the eyes of juvenile crabs sample visual space.

We collected eggs from nests on tidal flats of Cape Cod, Massachusetts, from June 4 to 12, 2001 and maintained them under natural diurnal lighting in Petri dishes in the laboratory. In 3–4 weeks the eggs hatched into trilobite larvae, or Stage I crabs (3 mm wide), and 4 weeks later the larvae molted into Stage II crabs (5.5 mm wide). To analyze the ommatidial array at both stages, we photographed the eyes with a Zeiss Axiocam attached

¹ University of South Carolina.

² Syracuse University.

³ SUNY Upstate Medical University.

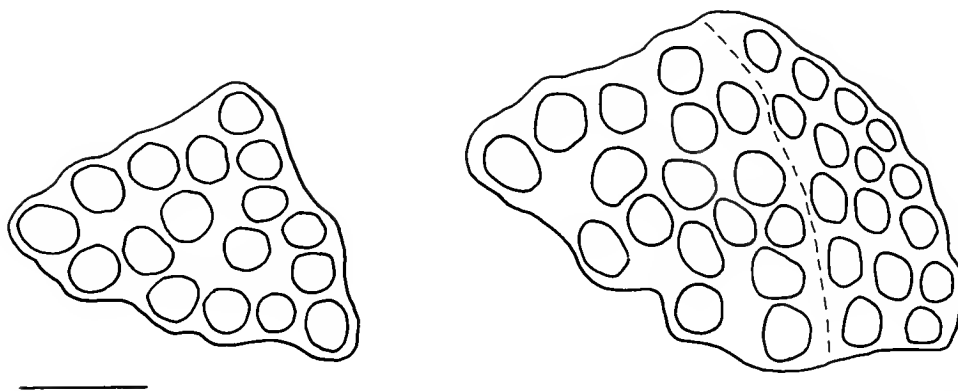


Figure 1. Scale drawings of a lateral eye of a Stage I *Limulus* before (left) and after molting to Stage II (right). The solid lines denote the borders of the eyes, and the ovals indicate the size and location of ommatidia. In both drawings, the apex to the left, with the largest ommatidia, is posterior. The dashed line marks the visible division between the older Stage I and newer Stage II regions of the eye. Scale bar is 50 μm .

to an Axioplan II compound microscope. The array is clearly distinguishable in some parts of the eye but is partially obscured in others by retinal pigmentation. We analyzed photographs taken at various eye orientations to resolve and reconstruct the arrays of lateral eyes in Stage I and II crabs.

Lateral eyes of trilobite larvae (Stage I) approximate an equilateral triangle (100–120 μm on a side) containing 14 to 17 ommatidia (Fig. 1). We observed a gradient of ommatidial diameters within the array, with the largest ommatidium at the posterior apex, and the smallest at the base. In the larval eye in Figure 1 (left), the diameters of the largest and smallest ommatidia are 26 μm and 15 μm , respectively.

When trilobite larvae molt to Stage II crabs, another triangular array of ommatidia is added to the anterior edge of the lateral eyes (Fig. 1, right). The eyes of two Stage II crabs yielded counts of 29 and 33 ommatidia, or about twice the number in the eyes of trilobite larvae. The new triangular array now has an apex pointing anteriorly, and a partition between Stage I and Stage II ommatidia is distinguishable (dashed line in Fig. 1). Corneal lenses are visible in Stage II, but not in Stage I, suggesting that trilobite larvae have no directional vision. Indeed, we do not know whether either Stage I or II crabs can see.

Juvenile horseshoe crabs (stages VI [16 mm wide] to X [40 mm]) were also collected on tidal flats of Cape Cod from June 4 to 12, 2001. We maintained them under diurnal lighting in shallow troughs in the laboratory. They were fed, and their water was changed weekly. To assess the growth of their lateral eyes, we placed five scars along the anterior and ventral edges of the cornea with a sharp metallic needle (diameter 50 μm). Using a Zeiss SV11 stereoscope, we photographed the scarred eyes before and after each animal molted. We also photographed their molted shells to supplement the original records of their eyes.

To assess the visual field of the juvenile eye, we adapted the method of Herzog and Barlow (2). With the high magnification of a stereomicroscope, we identified the ommatidium whose optic axis was aligned with that of the microscope. By changing the orientation of the molt, we measured the optic axes of numerous ommatidia and determined the visual field of the eye as well as its

resolution in various parts of the visual field. We analyzed the growth of the lateral eye at various stages and found, as others have, that the eye adds ommatidia at each molt (3, 4).

When a Stage IX crab (30 mm wide) molted to a Stage X crab (38 mm), its right lateral eye increased from 1.8 to 2.2 mm along the anteroposterior axis, adding approximately 90 ommatidia (490 to 580) in agreement with morphometric data of Waterman (3). The diameter of ommatidia in the medial and posterior regions of the eye increased from 64 μm to 78 μm . Scars along the anterior edge shifted posteriorly, revealing the addition of 5 columns of about 90 small ommatidia (52 μm in diameter). This result supports previous observations that the lateral eye grows by adding new photoreceptors at its anterior edge (4). A similar result was reported for the dragonfly eye using the same scarring technique (5). Curiously, the ventral scars moved dorsally by about 5 ommatidial diameters. This movement is not associated with the addition of new ommatidia because the number of ommatidia medial and posterior to the scars was the same in both the molt and the crab. Apparently the outer scarred cornea of the Stage X crab had not grown as much as the underlying matrix of lens facets.

A juvenile crab has about the same visual field as an adult, but samples it differently. This can be demonstrated by locating the unique "index" ommatidium, which is the ommatidium with its optic axis horizontal and normal to the body axis of the crab. It is located near the center of the adult eye, but in a more posterior position in juveniles. The younger the crab, the more posterior is the location of the index ommatidium. For example, 22% of ommatidia in a Stage VIII eye lie posterior to the index ommatidium, whereas 35% do in a Stage XII eye. Consequently, juveniles sample the anterior region of visual space with a greater proportion of ommatidia than an adult eye. However, they do so with about half the horizontal resolution (0.05 cycles/deg, Ref. 2) of an adult because they possess fewer columns of ommatidia. On the other hand, juveniles have about the same vertical resolution as an adult (0.1 cycles/deg above, and 0.2 cycles/deg below the horizon) because they possess vertical columns with about the same number of ommatidia (23 to 26) as an adult.

Pulsatile growth of the eye at the anterior edge modifies its view

of the world after each molt. That is, ommatidia viewing the most anterior region of the animal's visual space now sample a more lateral region of visual space. As a consequence, the retinotopic map in the brain must undergo comparable rearrangements to accommodate inputs from new ommatidia sampling visual space in front of the animal. The retinotopic map has been determined for adult animals at the first two synaptic layers in the brain (6), but that of the juvenile remains to be studied. The retinotopic map must be plastic to accommodate the changing retinal mosaic as the eye grows.

Supported by grants from the National Science Foundation, National Eye Institute, and the National Institutes of Mental Health. C. McGuinness and S. Meadors received REU Fellowships from the National Science Foundation. We thank the

Monomoy National Wildlife Refuge, Morris Island, Chatham, Massachusetts.

Literature Cited

1. Passaglia, C. L., F. A. Dodge, and R. B. Barlow. 1998. *J. Neurophysiol.* **80**: 1800–1815.
2. Herzog, E. H., and R. B. Barlow. 1992. *Vis. Neurosci.* **9**: 571–580.
3. Waterman, T. H. 1954. *J. Morphol.* **54**: 125–158.
4. Marler, J. J., R. B. Barlow, L. Eisele, and L. Kass. 1983. *Biol. Bull.* **165**: 541.
5. Sherk, T. E. 1978. *J. Exp. Zool.* **203**(2): 183–200.
6. Chamberlain, S. C., and R. B. Barlow. 1982. *J. Neurophysiol.* **48**: 505–520.

Reference: *Biol. Bull.* **201**: 274–276. (October 2001)

An Initial Study on the Effects of Signal Intermittency on the Odor Plume Tracking Behavior of the American Lobster, *Homarus americanus*

Corinne Kozlowski¹, Kara Yopak², Rainer Voigt² (Boston University Marine Program, Woods Hole, Massachusetts) and Jelle Atema²

Chemical signals are used by organisms for communication and location of food, mates, and shelters. The spatial and temporal distribution of these signals is shaped primarily by environmental conditions. Turbulent odor dispersal causes intermittency in the chemical signal even when the source emits continuously. Therefore, animals that use chemical cues to localize odor sources must overcome signal intermittency. The ability of lobsters to track continuously released odor plumes has been well-described (1). Lobsters may be using one or a combination of two possible mechanisms to locate an odor source: (a) odor-gated rheotaxis, which would cause the animal to move upstream, using the mean current for orientation once a chemical signal is detected (2), and (b) eddy-chemotaxis, which would require an animal to use the internal chemical and hydrodynamic fine structure of an odor plume to locate the source (3). The mechanisms lobsters use to overcome signal intermittency are still unknown. Male moths use a sequence of upwind surges and horizontal casting to locate a female releasing pheromone (4). In the presence of an odor source, tsetse flies perform a series of overshoots followed by 180° turns until they come within 1 m of the source (5). In more turbulent odor plumes, blue crabs decrease their locomotor activity and stop and turn more frequently (6). Here we explore how lobsters track odor plumes with a controlled increase in intermittency.

Lobsters (*Homarus americanus*), ranging in carapace length from 77.5 mm to 98.5 mm, were caught locally and kept in separate holding tanks with running seawater. Twice weekly the animals were fed about 2 g of squid. As in previous studies, this small amount was thought to increase their motivation to track an

odor source, consisting of 100 ml squid rinse/l seawater. Each lobster was tested in a flume (1.8 m × 5.5 m × 0.5 m experimental arena) with a mean flow rate of 4.5 cm/s. Each lobster was blindfolded; a white dot of nail polish on the carapace served as a reference point to digitize the track. After a 20-min acclimation period, each lobster was placed into a shelter 6 m downstream from a jet source releasing odor at 100 ml/min through a nozzle with a 2-mm ID ($Re = 200$). The trial began once the lobster began exhibiting tracking behavior (antennule flicking and antennae waving) in the downstream patch field as visualized with dye; it ended once the animal was less than one body length away from the source, or after 20 min. Animals that tracked a continuous jet plume (Fig. 1A) were randomly tested with odor pulses (1 cm in length) with gaps of about 5-cm (Fig. 1B) and 10-cm (Fig. 1C) between them. Dye visualization showed that interpulse gaps were maintained for 2 to 3 m from the source; farther downstream, the pulses merged due to turbulent dispersal in the flume. Fresh seawater entered into the flume during each trial to minimize odor accumulation, and the flume was drained and refilled each night. All trials were videotaped and digitized using the Metamorph® Imaging System (Version 3.5, Universal Imaging Corporation) for analysis. Walking speed, heading, and turning angles were then calculated for each track.

Under all three plume conditions (continuous, pulsed with 5-cm gaps, and pulsed with 10-cm gaps), heading and turning angles remained constant with distance from the source for the successful tracks; 84.5% of heading angles ranged from -40° to 40° , and 86.9% of turning angles ranged from -20° to 20° . Source localization success decreased with increasing gap length: 10 out of 33 lobsters successfully tracked the continuous jet plume (Fig. 1A), while 7 of these 10 tracked the plume with 5-cm gaps (Fig. 1B), and only 4 tracked the plume with 10-cm gaps (Fig. 1C). Generally, lobsters emerged slowly from the shelter area (orientation

¹ Bowling Green State University, Laboratory for Sensory Ecology, Bowling Green, OH 43403-0212.

² Boston University Marine Program, Marine Biological Laboratory, Woods Hole, MA 02543.

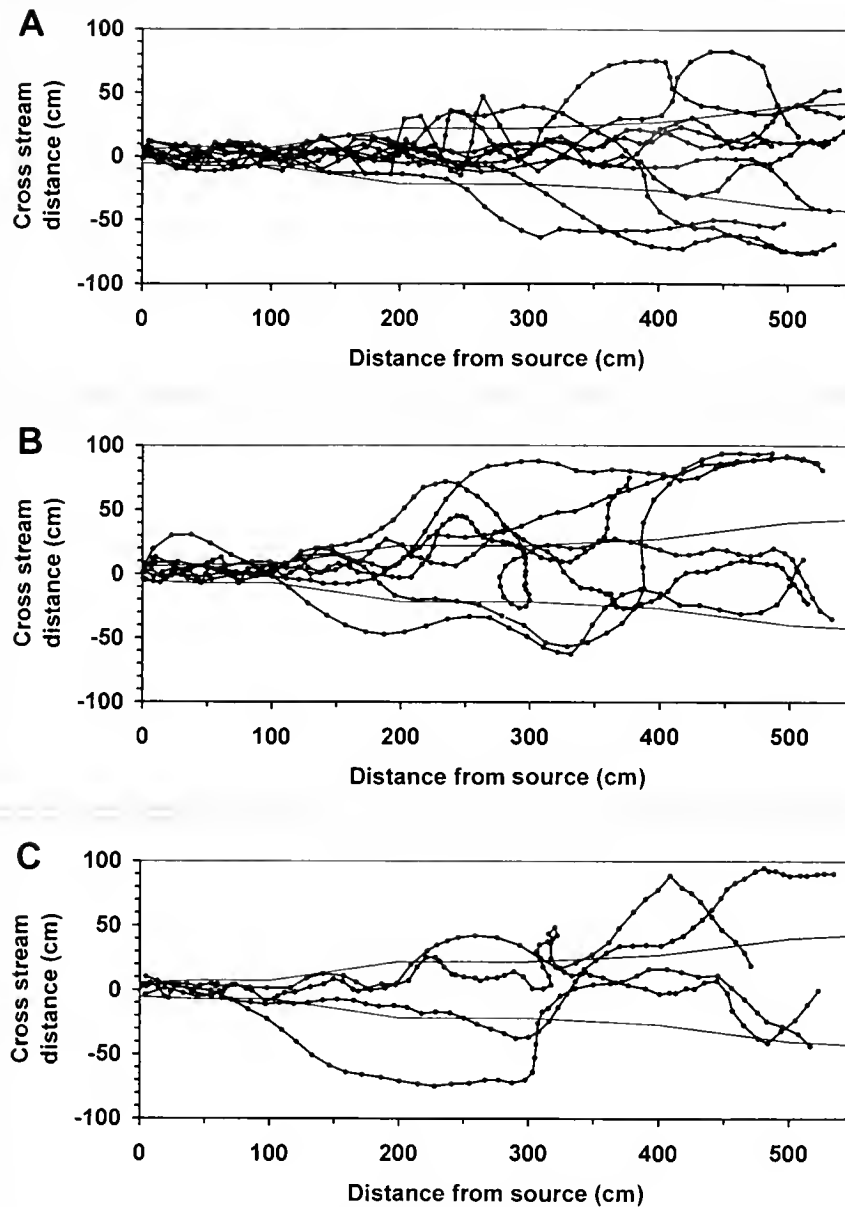


Figure 1. Individual tracks under plume conditions with continuous release (A, $N = 10$) and deliberate gaps of 5 cm (B, $N = 7$), and 10 cm (C, $N = 4$). Solid lines indicate approximate boundaries of the odor plume, as visualized with dye. Odor source is located at ($x = 0$ cm, $y = 0$ cm, $z = 9$ cm); shelter is located at ($x = 550$ cm, $y = 0$ cm).

phase, 3 to 6 m from the source). Under continuous plume conditions (Fig. 1A), walking speed then increased during the subsequent tracking phase (1 to 3 m) and decreased again as the animal approached the odor source (0 to 1 m). During the tracking phase and final approach, lobsters mostly stayed within the plume boundaries (20% of animals spent more than 5 s outside of the suggested plume area). Overall, the 10 lobsters that successfully tracked under continuous plume conditions (Fig. 1A) seemed to show a straighter approach to the source (higher linearity index; 68% had a linearity index equal to or greater than 0.9) than when tested

under intermittent plume conditions (Fig. 1B, C) (57% had a linearity index equal to or greater than 0.9). In contrast, in plumes with deliberate gaps (Fig. 1B, C), walking speed remained constant with distance from the source and *increased* during the final approach; 81.8% of animals walked outside of the plume boundaries for at least 5 s during the tracking and final approach phases. Mean walking speed decreased with an increase in gap length. Most lobsters that did not locate the odor source in plumes with deliberate gaps walked along the wall or did not leave the shelter. Two lobsters showed tracking behav-

ior downstream from the odor source (2) but then lost the odor plume upstream in the jet field.

These results suggest that successfully tracking lobsters use similar walking paths independent of signal intermittency. Counter-turning or casting behavior as described for moths (4) was rarely observed. However, tracking success dropped with increasingly intermittent signal conditions. It appears that lobsters require a minimal signal encounter rate to continue tracking the plume successfully to the source. The fact that lobsters stayed mostly within the odor plume boundaries further suggests that they use its internal fine structure for guidance.

First and second authors are listed alphabetically; both authors contributed to the experiment equally and in the same manner.

This study was supported by NSF REU Grant (OCE-0097498) to CK and KY, and ONR Grant (N00014-981-0822) to JA.

Literature Cited

1. Moore, P. A., N. Scholz, and J. Atema. 1991. *J. Chem. Ecol.* **17**: 1293–1307.
2. Baker, C. F., and J. C. Montgomery. 1999. *Polar Biol.* **21**: 305–309.
3. Atema, J. 1998. *Biol. Bull.* **195**: 179–180.
4. Vickers, N. J., and T. C. Baker. 1996. *J. Comp. Physiol. A* **178**: 831–847.
5. Bursell, E. 1984. *Physiol. Entomol.* **9**: 133–137.
6. Weissburg, M. J., and R. K. Zimmer-Faust. 1994. *J. Exp. Biol.* **197**: 349–375.

Reference: *Biol. Bull.* **201**: 276–277. (October 2001)

Cholinergic Modulation of Odor-Evoked Oscillations in the Frog Olfactory Bulb

Benjamin Hall (Marine Biological Laboratory, Woods Hole, Massachusetts 02543) and Kerry Delaney¹

The vertebrate olfactory bulb (OB) receives sensory information from peripheral odorant receptors and transmits this information to other cortical regions. OB output is encoded in the spiking patterns of the primary OB neurons—the mitral and tufted mitral cells (MTCs)—which project directly to higher cortical centers. The activity of the MTCs is determined both by patterns of odorant receptor activation and by interactions with intrinsic inhibitory interneurons within the OB. OB output is thus shaped by the two major classes of interneurons: the periglomerular cells (PGs) and the granule cells (GCs). GCs make distributed reciprocal dendrodendritic synaptic contacts along the secondary dendrites of MTCs and, via GABA release, provide both feedback and feedforward inhibition of the primary neurons (1). In addition, these reciprocal circuits are thought to be the site of generation of odor-evoked oscillations in the OB. In vertebrates, including frogs, GC dendrites receive prominent cholinergic innervation from the basal forebrain, mediated in the GC layer by muscarinic acetylcholine (mACh) receptors (2). Although studies have investigated the effects of ACh modulation in the OB in response to nerve activation and at the MTC to GC synapse in slice preparations, the effect of mACh agonists on natural odorant-evoked oscillations in the OB is unknown (3, 4).

We examined odor-evoked oscillatory responses in the frog olfactory bulb using an *in vitro* nose and brain preparation, in which we can maintain intact the olfactory circuitry from nose to cortex (5). We bath-applied the mACh agonist oxotremorine and monitored local field potential (LFP) electrodes placed in the external plexiform layer of the OB to examine the effect of this mACh agonist on odor-evoked activity.

Airborne odorants were delivered to the exposed nares (within ≈ 3 mm) by means of electrically controlled pressure pulses (0.5 psi–1.5 psi/50–300 ms) that introduced a pulse of clean charcoal-filtered air through a saturated odorized volume (amyl acetate) or

via addition of an odorized bolus into a continuous clean airstream. Oxotremorine (sesquifumarate salt) was mixed fresh daily in regular Ringer's solution and bath-applied at 100 μ M. Bicuculline was aliquoted in distilled water and diluted (1000-fold) in Ringer's to 10 μ M.

Odor-evoked oscillations in the frog OB, recorded in the external plexiform layer, consisted of an initial biphasic component (0–300 ms) followed by a slow wave envelope (1 to 2 s in duration) and a superimposed fast oscillation (≈ 7 –12 Hz) (Fig. 1A). The parameters of the odor-evoked response are consistent with our previous observations and similar to observations in turtle OB (5, 6). The fast oscillation was completely and reversibly blocked by bath application of the GABA_A antagonist bicuculline (10 μ M), demonstrating that GABA_A inhibition is required to maintain these oscillations (data not shown). Analysis of LFP recordings determined that oxotremorine had two distinct effects on the OB LFP response. First, it enhanced the initial component (0–300 ms) of the olfactory response by $\approx 25\%$ ($126.6 \pm 4.2\%$; mean \pm SE; $n = 16$ trials in four animals; $P < 0.001$) (Fig. 1B); second, it increased the power of the frequency spectrum of LFP recordings between 2 and 10 Hz by 75% ($175.2 \pm 8.1\%$; mean \pm SE; $n = 16$ trials in four animals) (Fig. 1C).

In conclusion, the *in vitro* preparation of frog nose and brain is a system which, by offering access for stimulating electrodes to the forebrain nuclei from which these fibers arise, permits us to study the effects of centrifugal ACh release in the OB. Our data here, showing enhancement of the LFP in the OB, predict that mACh receptor activation may improve the spatial coherence of OB activity. We speculate that one function for this mACh modulation may be to drive synchrony of the OB output necessary for plasticity at the level of lateral (olfactory) cortex.

This project was generously supported by the Grass Foundation and by the Canadian Institutes of Health Research. BH would like to thank all of the Grass Fellows and Kim Hoke and Melissa Vollrath for their comments on the manuscript.

¹ Simon Fraser University, Burnaby, British Columbia, Canada V5A 1S6.

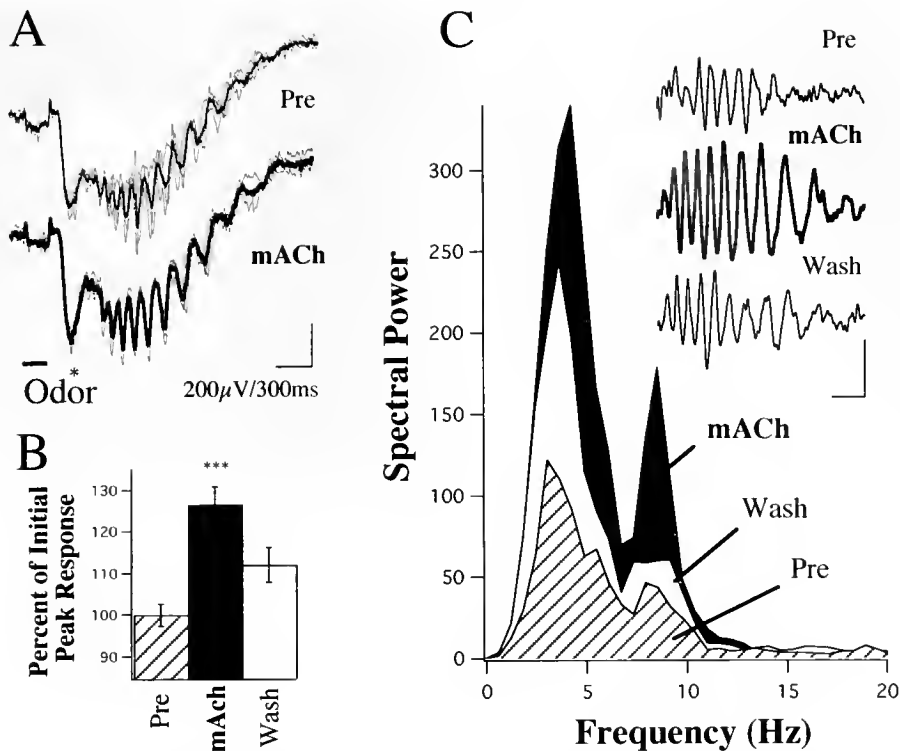


Figure 1. Effects of the muscarinic acetylcholine (mACh) receptor agonist oxotremorine (100 μ M) on the odor-evoked local field potential (LFP) response in frog olfactory bulb. (A) The characteristic response to odor application at the nose (200 ms-bar) was an initial, typically biphasic, component followed by a slow wave and superimposed fast (7–12 Hz) oscillations. (B) Bath application of the mACh agonist increased the peak amplitude of the initial component (* in A). (C) Power spectral density analysis of the LFP showed increased power in the presence of the mACh agonist between 2 and 10 Hz. Inset in C shows representative averages of three single traces in each condition showing the fast oscillation high-pass filtered to 3.5 Hz (scale bar as in A).

Literature Cited

1. Shepherd, G. M., and C. A. Greer. 1990. Pp. 133–169 in *The Synaptic Organization of the Brain*, G. M. Shepherd, ed., Oxford University Press, New York.
2. Crespo, C., J. M. Blasco-Ibanez, J. G. Brinon, J. R. Alonso, M. I. Dominquez, and F. J. Martinez-Guijarro. 2000. *Eur. J. Neurosci.* 12(11): 3963–3974.
3. Castillo, P. E., A. Carleton, J. D. Vincent, and P. M. Lledo. 1999. *J. Neurosci.* 19(21): 9180–9191.
4. Elaagouby, A., N. Ravel, and R. Gervais. 1991. *Neuroscience* 45(3): 653–662.
5. Delaney, K. R., and B. J. Hall. 1996. *J. Neurosci. Methods* 68(2): 193–202.
6. Lam, Y. W., L. B. Cohen, M. Wachowiak, and M. R. Zochowski. 2000. *J. Neurosci.* 20(2): 749–762.

Reference: *Biol. Bull.* 201: 277–278. (October 2001)

Dye Coupling Evidence for Gap Junctions Between Supramedullary/Dorsal Neurons of the Cunner, *Tautoglabrus adspersus*

S. J. Zottoli, D. E. W. Arnolds, N. O. Asamoah, C. Chevez, S. N. Fuller, N. A. Hiza, J. E. Nierman, and L. A. Taboada (Department of Biology, Williams College, Williamstown, Massachusetts 01267)

Many teleost fish have neurons whose somata lie on the surface of the medulla oblongata (supramedullary neurons), the spinal cord (dorsal cells), or both. The somata of these neurons in the cunner, *Tautoglabrus adspersus*, are arranged in a single, median, longitudinal row, from the posterior end of the fissura rhomboidalis through the anterior portion of the spinal cord (1). Comparative physiological studies in the cunner and other teleost fish have

indicated that these cells make electrotonic connections with one another (2). To test the hypothesis that gap junctions exist between these cells, we have injected individual supramedullary/dorsal cells with Lucifer yellow and looked for dye coupling with neighboring neurons.

Cunner, 7.3–10.5 cm in body length, were initially anesthetized in 0.03% ethyl-m-aminobenzoate; when respiration ceased, they

were transferred to a holding chamber where a 0.015% solution of the anesthetic was passed through the mouth and over the gills of the fish. The caudal portion of the medulla oblongata and rostral spinal cord were exposed, and a microelectrode filled with Lucifer yellow (Sigma; 5% in distilled water) was inserted into the soma of only one neuron. Since the neurons exposed in this area of the central nervous system could either be in a supramedullary position or a spinal cord position, we will refer to the cells as supramedullary/dorsal neurons. The dye was iontophoresed (-10 nA of current was pulsed for 200 ms at a rate of 3/s) for about 1 h. About 1 h after injection the fish were perfused with 10% phosphate-buffered formalin. The brain and spinal cord were then dissected out, dehydrated, and cleared with methyl salicylate. The whole brain was viewed with a fluorescent microscope.

The somata of supramedullary/dorsal cells are visible on the surface of the brain with the aid of a dissecting microscope. In seven fish, a single soma was located and filled with dye. Lucifer yellow traveled from the filled cell to adjacent ones in three of the seven fish. One cell rostral and two cells caudal to the filled cell contained dye in two fish. In the third fish two cells rostral to the filled cell contained dye (Fig. 1). In the four cases where there was no apparent dye transfer between neurons, the intensity of the fill appeared similar to that of filled neurons in which dye coupling did occur. To control for the possibility that extracellular leakage of the dye might label neurons other than the one being filled, a single dorsal gill was penetrated with a dye-filled microelectrode in two fish. The electrode was withdrawn to just outside the cell membrane and Lucifer yellow was iontophoresed extracellularly for 1 h, the fish was perfused, and the brain processed as described above. No dye was localized to any cell.

The transfer of Lucifer yellow from one supramedullary/dorsal cell to others provides morphological evidence for the existence of gap junctions. The lack of dye coupling in four fish does not necessarily mean that gap junctions do not exist between supramedullary/dorsal cells in these fish. For example, there may be a wide distribution of sites of electrical coupling, or Lucifer yellow may not have crossed the gap junctions (3, 4). When dye coupling occurred, the fall-off in dye concentration from the filled cell to adjacent neurons was large, so more distal neurons may be equally well coupled but not contain dye. The cunner has between 35 and 40 supramedullary/dorsal cells. Electrical coupling measurements will help determine the extent of coupling between this group of



Figure 1. Lucifer yellow injection of a single supramedullary/dorsal cell in the cunner. The cell on the far right was iontophoretically filled with dye; after fixation, dehydration, and clearing, the whole brain was viewed with a fluorescent microscope. The soma of the filled neuron gives rise to a single process that extends ventrally and bifurcates near the bottom of the photomicrograph. Two other rostral somata (arrows) contain dye as well, providing support for the existence of gap junctions between these cells. This is a sagittal view of the brain with dorsal up and rostral to the left. Calibration bar = 100 μ m.

neurons. Supramedullary/dorsal cells in the cunner are sensitive to tactile stimulation (5). Our results predict that neurons that are electrotonically coupled will fire synchronously with sufficient tactile stimulation.

This work was supported in part by Howard Hughes Medical Institute and Essel Foundation grants to Williams College.

Literature Cited

1. Sargent, P. E. 1899. *Anat. Anz.* 15: 212–225.
2. Bennett, M. V. L. 1960. *Biol. Bull.* 119: 303.
3. Murphy, A. D., R. D. Hadley, and S. B. Kater. 1983. *J. Neurosci.* 3: 1422–1429.
4. Peinado, A., R. Yuste, and L. C. Katz. 1993. *Neuron* 10: 103–114.
5. Zottoli, S. J., F. R. Akanki, N. A. Hiza, D. A. Ho-Sang, Jr., M. Motta, X. Tan, K. M. Watts, and E.-A. Seyfarth. 1999. *Biol. Bull.* 197: 239–240.

Reference: *Biol. Bull.* 201: 278–280. (October 2001)

A Comparison of Sounds Recorded From a Catfish (*Orinocodoras eigenmanni*, Doradidae) in an Aquarium and in the Field

Ingrid M. Kaatz and Phillip S. Lobel (Boston University Marine Program, Marine Biological Laboratory, Woods Hole, Massachusetts 02543)

Parvulescu (1) raised concerns regarding the suitability of a small glass aquarium for characterizing fish sounds based upon a theoretical consideration of sound echoes. Four out of eight authors who cited this paper most recently noted that small aquaria have complex acoustics, and the other four described the aquarium

environment as yielding imprecise and poor quality sound recordings. Further advances in the study of sound production and communication in fishes require studies in controlled laboratory environments. Recently, Lugli (2) noted that waveforms and sound spectra were similar for field- and aquarium-recorded goby sounds.

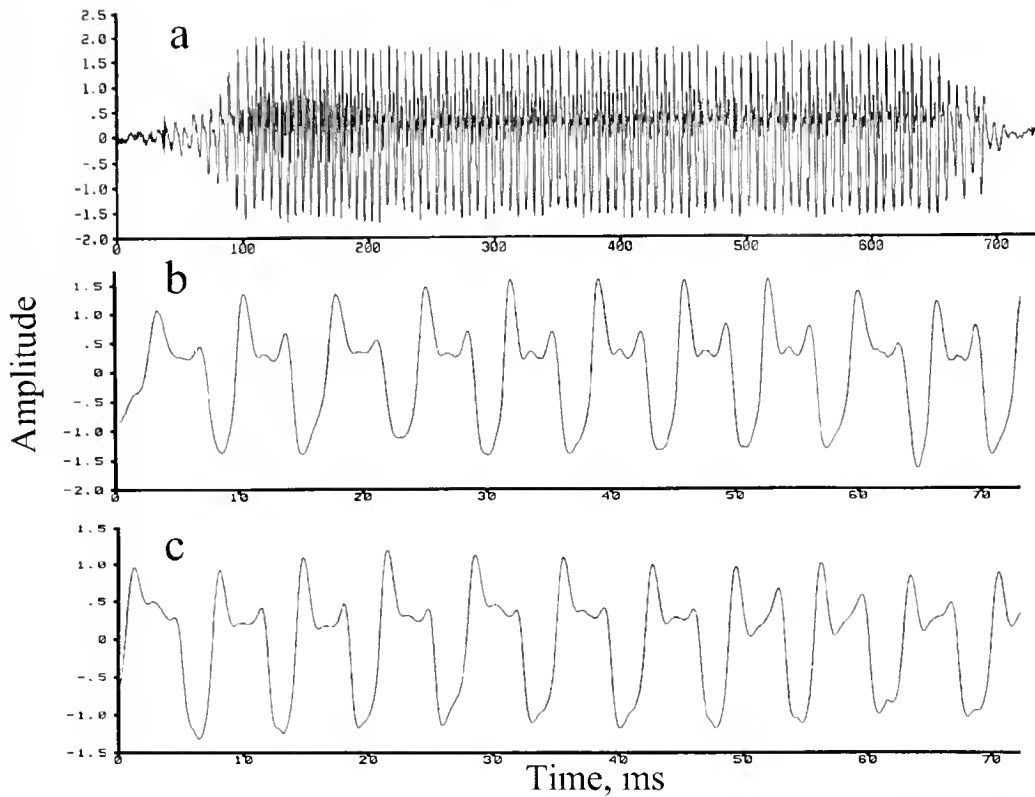


Figure 1. Swimbladder disturbance sounds for three different individuals of a doradid catfish, *Orinocodoras eigenmanni*: (a) waveform of one entire sound, field recording, (b) expanded waveform of 10 pulses, field recording (c) expanded waveform of 10 pulses, aquarium recording. The time scale differs between the top (a) and bottom two plots (b & c) by a factor of 10.

Okumura *et al.* (3) observed that artificially generated sounds recorded close to a hydrophone were free from acoustic artifacts. Whether more complex, natural fish sounds would also be artifact-free requires testing. We elicited sounds from a catfish and compared field and aquarium recordings which were specifically made close to the signal source.

We analyzed sounds produced by the swimbladder mechanism of a catfish in the disturbance context (fish are restrained by a human hand) underwater. Similar sounds were produced by the same fish in conflicts over resting sites (4). Many fishes that produce sounds in intraspecific behavioral contexts also "release" these sounds when restrained (5). We chose swimbladder sounds because they are a common mechanism of sound production for many fishes (6, 7).

We recorded sounds of nine individuals of a wild-caught neotropical catfish, the doradid *Orinocodoras eigenmanni*. Standard length ranged from 5.7 to 8.5 cm. Each individually recognizable fish was recorded twice in both recording environments. Recordings were conducted during 10 July–6 August 1992. Fish were positioned 7.5 cm from a hydrophone and 23 cm under the water surface. Fish were held with their left side toward and their swimbladder centered on the midpoint of the hydrophone. In the field (Jenkins Pond, Falmouth, MA) fish were recorded in a containment net. The net had a 60-cm diameter and 60-cm maximum depth. Water depth at the dock field site (Jenkins Pond) was 90 cm over a sand bottom. Aquarium recordings were conducted in a

10-gallon glass aquarium on a grass lawn near the pond. The hydrophone was suspended in the center of the water-filled aquarium. Fish were held in the same relative position to the hydrophone and water surface as in the field. Temperatures for recording dates in the aquarium and in the field were not different (24.7 ± 0.6 aquarium, 25.2 ± 0.3 field; $n = 3$). Sounds were recorded using a tape recorder (SONY Model WM-D6C: frequency response 40–15,000 Hz ± 3 dB). The hydrophone was pressure sensitive and had a frequency response range of 10 to 3,000 Hz (BioAcoustics, see 8 for specifications). The acoustic analysis software SIGNAL (Engineering Systems, Belmont, MA) was used to digitize and analyze sounds (sampling rate 25 kHz). We only analyzed sounds which had clear pulse structure. Both recording environments occasionally yielded some sounds with obscured pulse number and waveform patterns, due to spurious background noise or fish movements.

Spectrograms of over 800 sounds were evaluated (580 field, 275 aquarium). The catfish produced similar numbers of sounds in both recording environments. A minimum of ten sounds were produced by each individual on each sampling date. The same types of sounds were produced by individuals in both recording environments. Sound duration ranged from 30 ms to 2,400 ms.

In order to assess whether sounds were altered in the aquarium environment compared to the field, we compared waveforms visually and pulse durations statistically for sounds from both recording environments. Waveforms of sound pulses for field and

aquarium showed the same shapes (Fig. 1). No artifacts were noted. Pulse duration was measured for one sound per individual ($n = 9$) for seven pulses in the center third of the sound where pulse peak amplitudes were consistent. Individual pulse durations ranged from 6 to 7 ms and were not significantly different between field and aquarium environments (one way ANOVA). For aquarium-recorded sounds, the pulse duration mean was 6.5 (SE 0.07, $n = 63$). For field-recorded sounds, the pulse duration mean was 6.5 (SE 0.07, $n = 63$).

Disturbance context swimbladder sounds of a catfish showed no differences in pulse waveform or pulse duration when recorded close to a hydrophone in both field and small aquarium recording environments. Kastberger (9) observed that for field recordings of doradid sounds, pulse pattern was unchanged for up to 30 cm. Many fishes initiate sound production in close proximity to conspecifics (10, 11). These results suggest that a small aquarium environment can provide sound recordings that accurately represent the sounds a fish produces in the field, yielding reliable acoustic measurements.

The research was supported by the SUNY-ESF Barbara Sussman fund and Sigma Xi. Thanks to John Beckerly for providing aquarium space, and Matt Bohling, Eric Horgan and David Mann

for technical assistance. Supported in part by Army Research Office Grant DAAG-55-98-1-0304.

Literature Cited

1. Parvulescu, A. 1967. Pp. 7–14 in *Marine Bio-acoustics*, vol. 2. Pergamon Press, Oxford.
2. Lugli, M., G. Pavan, P. Torricelli, and L. Bobio. 1995. *Environ. Biol. Fishes* 43: 219–231.
3. Okumura, T., T. Akamatsu, and H. Y. Yan. 2001. *Bioacoustics* (in press).
4. Kaatz, I. M. 1999. Ph.D. dissertation, SUNY College of Environmental Science and Forestry, Syracuse, NY. Pp. 162–213.
5. Fish, M. P., and W. H. Mowbray. 1970. Pp. 1–207 in *Sounds of the Western North Atlantic Fishes*. The Johns Hopkins Press, Baltimore.
6. Schneider, H. 1967. Pp. 135–158 in *Marine Bio-Acoustics*, vol. 2. Pergamon Press, New York.
7. Tavolga, W. N. 1971. Pp. 135–205 in *Fish Physiology*, vol. 5. Academic Press, New York.
8. Kaatz, I. M., and P. S. Lobel. 1999. *Biol. Bull.* 197: 241–242.
9. Kastberger, G. 1977. *Zool. Jahrb. Physiol.* 81: 281–309.
10. Ladich, F. 1997. *Mar. Freshw. Behav. Physiol.* 29: 87–108.
11. Myrberg, A. A., Jr. 1981. Pp. 395–424 in *Hearing and Sound Communication in Fishes*. Springer-Verlag, New York.

Reference: *Biol. Bull.* 201: 280–281. (October 2001)

Bimodal Units in the Torus Semicircularis of the Toadfish (*Opsanus tau*)

R. R. Fay and P. L. Edds-Walton (Parnly Hearing Institute, Loyola University Chicago, 6525 N. Sheridan Rd., Chicago, Illinois 60626)

We have been investigating aspects of auditory processing and directional hearing in the toadfish *Opsanus tau*. We have shown that the saccule is an auditory endorgan that encodes both frequency and direction of a sound source (1). This information is sent via the VIIIth nerve to nuclei in the medulla, in particular, the descending octaval nucleus (1). Our previous work on cells in the descending octaval nucleus in *Opsanus tau* has revealed that most are highly directional (1) and that these directional auditory cells project to the midbrain. The torus semicircularis (TS) is a sensory processing site in the midbrain of fishes and amphibians. Nucleus centralis in the TS receives input from auditory areas in the medulla, and nucleus ventrolateralis receives input from lateral line areas in the medulla (2). Here we report some preliminary results from extracellular recordings of auditory cells in the TS.

Our protocol is described in detail elsewhere (1). In brief, the toadfish is anesthetized and immobilized (pancuronium bromide injection and lidocaine applied topically), and the dorsal surface of the midbrain is exposed. Following surgery, the fish is placed in a cylindrical dish filled with fresh seawater and is secured with a head holder. The water surface in the dish lies just below the surgical opening in the skull. The dish is part of a three-dimensional shaker table that provides sinusoidal motion of the animal with the surrounding water along linear pathways to simulate the particle motion component of underwater sound at appropriate frequencies (50–300 Hz) and levels, in the horizontal and mid-sagittal planes at specified angles (0°, 30°, 60°, 90°, 120°, 150° in

each plane). In addition, we tested for external mechanoreceptive sensitivity (tentatively identified as lateral line) by producing hydrodynamic disturbances using puffs of air at the water surface along the length of the fish in the absence of an auditory stimulus. Units were classified as responding to hydrodynamic stimuli if the evoked spike rate was two standard deviations or more above the mean background rate.

For extracellular recording we used pulled glass electrodes with tip sizes of 3–5 μm and resistances of 3–10 M Ω . Our recording sites in the TS were confirmed in two ways. First, we used neurobiotin-filled electrodes (4% in 3 M NaCl) to mark the location of the first auditory cell analyzed. Second, the location of the electrode at all recording sites was plotted using the scale on a three-dimensional micromanipulator (accuracy to 10 μm). The neurobiotin was visualized using standard ABC immunohistochemistry (Vector Labs) in 50- μm floating sections, which were then placed on slides, dehydrated, and coverslipped.

We have recorded from 71 units in the TS. Of the cells that responded to the auditory stimuli, we have found that 33% have auditory sensitivity only and 67% respond to both auditory and hydrodynamic stimulation. Units unresponsive to auditory stimuli but responsive to hydrodynamic stimuli were observed frequently, but were not analyzed further. Figure 1 illustrates the responses of two TS units to varying levels of whole-body vibration in three orthogonal directions and to the hydrodynamic assay for putative lateral line sensitivity. Some units demonstrate a relatively large

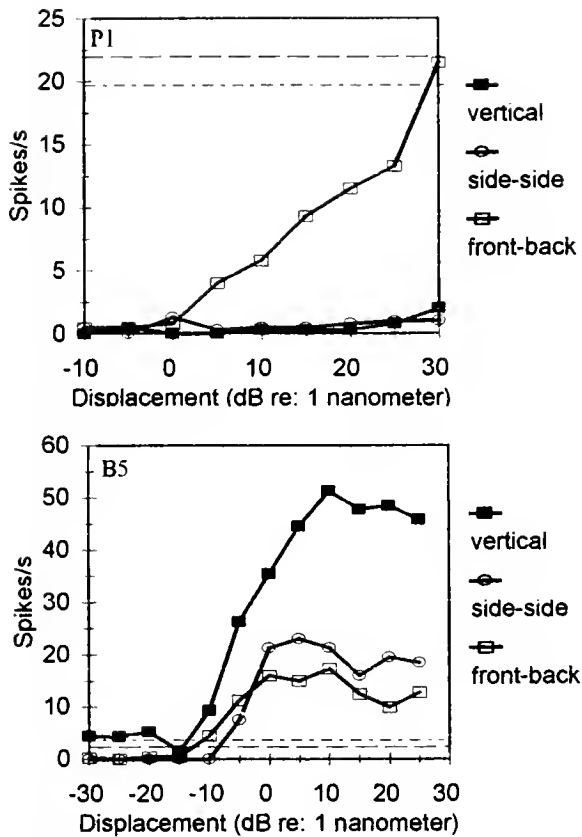


Figure 1. Responses of cells in the torus semicircularis of the toadfish. Spike rate versus stimulus level (displacement) is shown for two cells (P1, B5) in response to whole-body linear translatory motion at 100 Hz in three orthogonal axes. Also shown is the spike rate for P1, B5 during hydrodynamic stimulation ipsilateral (dash-dot line) and contralateral (dash line) to the left hemisphere of the brain. The hydrodynamic stimulus consisted of repeated water disturbances along the length of the fish, and the data plotted are average spike rates for comparison with the other stimuli. P1 has a strong bimodal response. (Spontaneous rate of 0.5 spikes/s for both P1 and B5.)

response to hydrodynamic stimulation compared with auditory (e.g., P1 in Fig. 1), while others respond little if at all to the hydrodynamic stimulus (e.g., B5 in Fig. 1). Both units of Figure 1 are highly sensitive and directional with respect to the vibrational axes producing the greatest responses: P1 responds best in the front-back axis with a displacement threshold of 3 dB re: 1 nm; and B5 is most responsive to vertical motion with a displacement threshold of -10 dB re: 1 nm.

The origin of the bimodal sensitivity may be the convergence of auditory and lateral line inputs to some of the cells in the TS from nuclei in the medulla, or bimodal sensitivity may result from connections between nucleus centralis and nucleus ventrolateralis within the TS. Our preliminary anatomical data indicate extensive opportunities for interactions among cells in the two nuclei of the TS. We are currently evaluating the locations of medullary projection cells that were back-filled with neurobiotin following injection at TS sites with bimodal response characteristics.

Supported by an R01 grant from NIH, NIDCD to R.R.F. and from an NIH, NIDCD Program Project Grant to the Parmlly Hearing Institute.

Literature Cited

1. Edds-Walton, P. L., R. R. Fay, and S. M. Highstein. 1999. *J. Comp. Neurol.* 411: 212-238.
2. McCormick, C. A. 1999. Pp. 155-217 in *Springer Handbook of Auditory Research: Comparative Hearing: Fish and Amphibians*, A. N. Popper and R. R. Fay, eds. Springer-Verlag, New York.

Reference: *Biol. Bull.* 201: 282–283. (October 2001)

Mariculture of the Toadfish *Opsanus tau*

Allen F. Mensinger¹ (University of Minnesota-Duluth, Duluth, Minnesota, 55812), Katherine A. Stephenson², Sarah L. Pollema², Hazel E. Richmond¹, Nichole Price¹, and Roger T. Hanlon¹

In response to declining stocks of toadfish in local waters around Cape Cod, Massachusetts, a toadfish mariculture program was initiated in the summer of 1998 (1); the aims were to provide researchers at the Marine Biological Laboratory (MBL) with sufficient numbers (approximately 400 per year) of this valuable biomedical research model (2, 3) while lessening pressure on native stocks. The goal was

to raise fish to the target size of 25 cm and 500 gm within three years. In the first year of the program, culture methods were developed, and the effects of temperature and stocking density on toadfish growth were monitored; a preliminary report was published in 1999 (1). We continued to observe and monitor this captive population through the summer of 2001. This paper summarizes the growth rates and mortalities of these three-year fish.

Briefly, two toadfish nests (with guardian males) were transported to the Marine Resources Center of the MBL from Waquoit Bay, Massachusetts in July 1998. Approximately 400 juvenile fish

¹ Marine Biological Laboratory, Woods Hole, MA 02543.

² Biology Department, 10 University Drive, University of Minnesota-Duluth, Duluth, MN 55812.

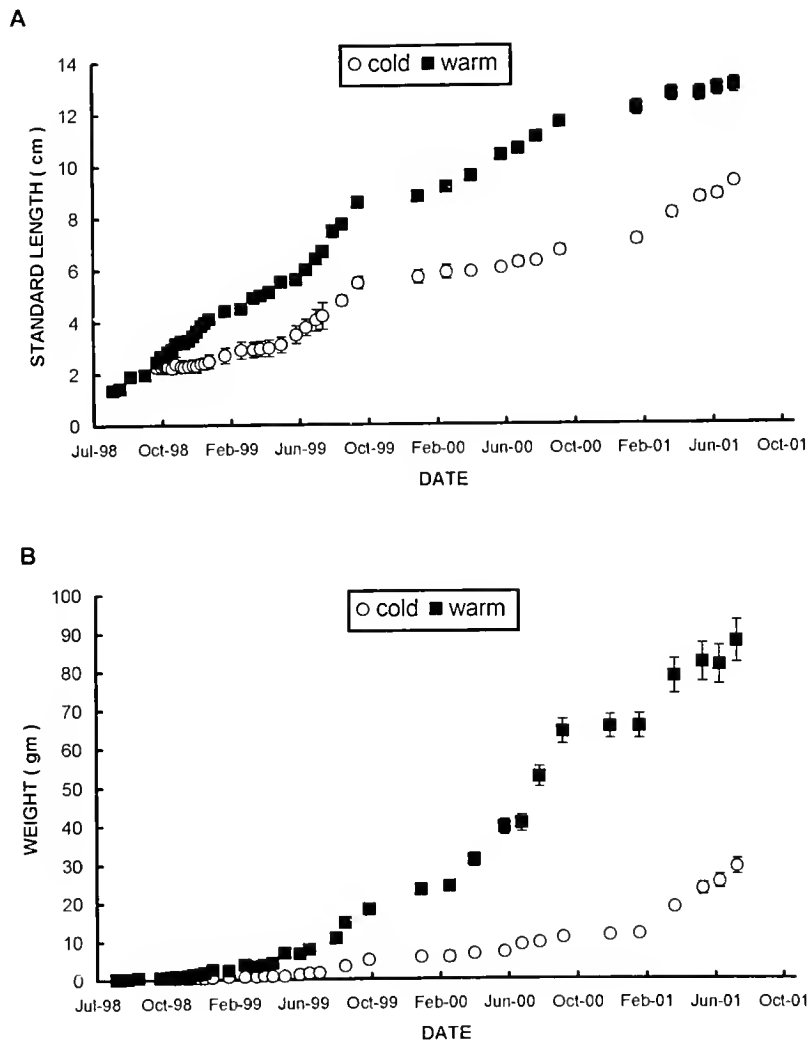


Figure 1. Standard length (A) and weight (B) of maricultured toadfish plotted as a function of time for about three years. Data points represent mean values of fish raised at cold (circle) and warm (square) temperatures (see the text for specific temperatures). Error bars = 1 SE.

detached from both nests in August 1998. In October 1998, 100 of the juvenile fish were selected for mariculture and placed in shallow fiberglass tanks (130 × 70 × 10 cm). Fish were raised at two different temperatures, and their growth was monitored. Half the fish were maintained at "cold" temperatures (15.8° ± 0.4 °C average weekly temperature), which have proven successful for maintaining adult toadfish in captivity. The remaining fish were maintained at "warm" (19.6° ± 0.8 °C) temperatures in an effort to increase growth rate. Stocking densities ranged from 10 to 40 toadfish m⁻². Fish initially were fed live adult *Artemia* that had been bathed in a nutritional supplement (Super Selco). After six months of culture, the diet was switched to chopped pieces of squid and butterfish. At the conclusion of the first year, the warm-water fish averaged 6.4 ± 0.1 cm in length and weighed 13.0 ± 0.3 g, and the cold-water fish averaged 4.0 ± 0.5 cm and 1.7 ± 0.0 g (1). Survival rate was 78%, with many of the mortalities attributed to the cannibalistic nature of batrachadoids (4).

At the conclusion of year one, the juvenile fish were transferred to large, fiberglass tanks measuring either 3.7 × 2.4 m or 3.7 × 1.8 m. The water level in each tank was maintained at 13 cm. Pieces of PVC pipe (diameter 7 to 10 cm) were provided as shelters for the fish. The temperature regimes were maintained (warm and cold), but fish from the different densities were combined after being sorted by size to prevent cannibalism. The fish were distributed to the tanks at a density of 1.8 to 2.4 fish m⁻². The two- and three-year age classes were maintained on a prepared diet consisting mainly of chopped squid and butterfish and were fed three times per week.

During the second year of culture, the average weekly temperatures were 19.4 °C (warm) and 16.9 °C (cold). In year three, the average warm-water temperature was 20.2 °C. Because the cold-water fish continued to be small, they were switched to the "warm" water in February of 2001; as a result, the average weekly temperature for these fish was 19.2 °C during year three.

After 24 months of culturing, the warm-water fish averaged 10.6 ± 0.2 cm and weighed 40.5 ± 2.1 g, and the cold-water fish averaged 6.2 ± 0.7 cm and 9.0 ± 0.6 g. By the end of the third year, the warm fish had grown to an average standard length of 13.0 ± 0.3 cm (range 9.5 to 15.5 cm) and average weight of 87.7 ± 5.5 g (25 to 136 g). The cold-water population continued to display slower growth, with the average fish measuring 9.3 ± 0.2 cm (8.4 to 10.8 cm) and 29.2 ± 2.0 g (15 to 45 g) in year three (Fig. 1).

Survival rates remained high, following the initial 78% rate in year one. Approximately two-thirds of the original fish remained alive after

24 months, and 60% survived through July 2001. The size segregation instituted in the summer of 1999 greatly reduced cannibalism.

Our eventual goal is to eliminate field collection through the successful spawning and rearing of captive fish. However, the age of sexual maturity among the Cape Cod population has never been firmly established. Five females in the warm-water tanks became gravid in the spring of 2001, and at least one successfully deposited scores of eggs inside a PVC pipe, suggesting that the onset of sexual maturity for female toadfish is less than three years. Unfortunately, for unknown reasons, these eggs failed to develop. The onset of sexual maturity in the males remains to be determined.

In summary, we have demonstrated that toadfish can be raised in captivity for at least three years. At the current maximal growth rate of 5 cm/year, we estimate that the fish will need at least five to six years to attain the desired size range of 25 to 30 cm, thus making the project impractical in terms of cost and time.

One of the main impediments to faster growth is the virtual cessation of growth during the winter (Fig. 1). Previous observations led us to hypothesize that keeping the fish at temperatures about 15 °C above ambient during the winter would circumvent this "hibernation." Because this expectation has proved incorrect, future attempts will focus on temperature and photoperiod. Preliminary evidence shows that newly detached juvenile toadfish raised at 26° to 29 °C grow significantly faster than fish raised at 20 °C (5). We also plan to manipulate the photoperiod during the winter to stimulate year-round growth.

We wish to thank Waquoit Bay National Estuarine Research Reserve for use of their facilities, and J. Hanley and B. Mebane for assistance in tank maintenance. Support was provided by the Marine Models in Biological Research Program, University of Minnesota Grant in Aid, NASA Life Science Fellowship, MBL Associates Fellowship and NIH grant DC01837.

Literature Cited

1. Tang, K. Q., N. N. Price, M. D. O'Neill, A. F. Mensinger, and R. T. Hanlon. 1999. *Biol. Bull.* 197: 247-248.
2. Mensinger, A. F., and S. M. Highstein. 1999. *J. Comp. Neurol.* 410: 653-676.
3. Mensinger, A. F., D. J. Anderson, C. J. Buchko, M. A. Johnson, D. C. Martin, P. A. Tresco, R. B. Silver, and S. M. Highstein. 2000. *J. Neurophysiol.* 83: 611-615.
4. Mensinger, A. F., and J. F. Case. 1991. *Biol. Bull.* 181: 181-188.
5. Rieder, L. E., and A. F. Mensinger. 2001. *Biol. Bull.* 201: 283-285.

Reference: *Biol. Bull.* 201: 283-285. (October 2001)

Strategies for Increasing Growth of Juvenile Toadfish

Leila E. Rieder^{1,2} and Allen F. Mensinger¹ (University of Minnesota-Duluth, Duluth, Minnesota 55812)

A toadfish mariculture program was initiated in the summer of 1998 at the Marine Biological Laboratory, Woods Hole, Massa-

chusetts. The purpose of this program was to reduce pressure on the native toadfish population while providing researchers with a year-round supply of appropriately sized animals. Although the toadfish have proven to be amenable to year-round culturing (survival rates were 60% to 70% during the initial three years (1, 2)), their growth was slower than that of conspecifics inhabiting

¹ Marine Biological Laboratory, Woods Hole, MA 02543.

² Columbia High School, East Greenbush, NY 12061.

southern portions of the geographical range (3). Therefore, in an effort to accelerate growth, the effects of temperature and diet were investigated in toadfish that had recently detached from their nests.

Four nests with guardian males were transported from Waquoit Bay, Massachusetts, to the Marine Biological Laboratory in June of 2001. The fish for this experiment were selected from a single nest. Fish began to detach from the nest during the first week of July, and feeding was initiated on July 9. Nine 40-l glass aquaria filled with fresh, filtered seawater were used for the study. The aquaria were placed in a 3×3 matrix on a large aquarium stand. Each contained 3 cm of sand overlying an air-powered undergravel filter and had an overhead fluorescent light (14/10 L/D cycle). Water temperature was maintained at 23°, 26°, or 29 °C in each set of three aquaria. About 30% to 50% of the aquarium water was changed daily by slowly adding fresh seawater. Fish were randomly selected from the 400+ juveniles that detached from the nest, and 10 fish were placed in each aquarium. An additional 25 fish were placed in a shallow 1-m² fiberglass tray and provided with fresh running seawater at 20 °C.

Fish were maintained on three diets: live, prepared, and prepared plus. Live food consisted mainly of adult *Artemia* treated with a nutritional supplement (Super Selco) and supplemented with live mysids or newly hatched *Fundulus* sp. The prepared diet consisted of small chunks (approximately 3 mm \times 4 mm) of squid, clam, or mussel. The prepared plus diet consisted exclusively of small pieces of squid supplemented with crushed commercial fish food (5 mm pellets, Aquatic Eco-Systems). The three tanks at each temperature were fed one of the diets exclusively. Control fish in the fiberglass tanks were fed live *Artemia* treated with Super Selco supplemented with mysids.

Experimental fish were fed an average of 6 days per week, and control fish were fed about 4 times per week. For live food, the daily ration was sufficient that fish would terminate feeding prior to prey extermination, and live prey was often observed in the tanks 24 h after feeding. For the prepared diets, the food was impaled on a copper wire (28 gauge) affixed to a glass rod and was waved in front of the fish until it was eaten. Fish were fed once per day, and individual fish were presented with food continuously until refusal. To ensure that all fish on prepared diets were fed, individual fish were visually checked for extended abdomens.

Fish were weighed and measured prior to the initiation of feeding on July 9. Standard length averaged 1.7 ± 0.02 cm; weight averaged 0.17 ± 0.01 g. There was no significant difference in size among the experimental and control aquaria (ANOVA: $P = 0.14$; all statistical analysis was performed with GraphPad InStat version 4.10 for Windows 95, GraphPad Software, San Diego, CA). All fish were weighed and measured again after 3 weeks of feeding. Figure 1 shows the standard length and weight distribution for the three temperatures and diets plus the control.

Examination of the standard lengths of fish kept at 23 °C did not reveal any size difference among the three diets (ANOVA: $P = 0.13$). However, at both 26 °C and 29 °C, fish eating both prepared food diets were significantly longer than ones maintained on live food (ANOVA: $P < 0.05$). When the experimental tanks were compared with the controls, fish fed the prepared diet at all three temperatures and fish given the prepared plus diet at 26 and 29 °C were significantly larger than controls (ANOVA: $P < 0.05$).

Examination of weight at each temperature revealed that at

23 °C, the fish on both prepared diets were significantly heavier than those consuming live prey (ANOVA: $P < 0.01$). At both 26 and 29 °C, fish fed both prepared diets were larger than fish on the live diet (ANOVA: $P < 0.001$). When treatments were compared against controls, fish maintained on the prepared diet at all three temperatures and fish fed the prepared plus diet at the two higher temperatures were significantly larger than controls (ANOVA: $P < 0.05$).

The results indicate that toadfish growth can be accelerated compared to our previous mariculture methods (1, 2), by increasing water temperature and by substituting a diet of prepared food for one of live food. Previous mariculture efforts (1, 2) required 90 days for toadfish to attain the size and weight that fish in the current experiment reached in 21 days. Survival was high (98%) and the elevated temperatures were not detrimental to fish health. This is not surprising because the range of the conspecifics extends to Florida, and, locally, temperatures of 25 to 30 °C are not uncommon during summer months in shallow Cape Cod estuaries.

The objective of this experiment was to determine new strategies to accelerate juvenile toadfish growth. Therefore, the experiment was designed to compare our new methodology to our previous culture techniques. Thus, control fish were placed in shallow fiberglass trays rather than in 40-l aquaria. Although every effort was made to make the experimental tanks identical, small

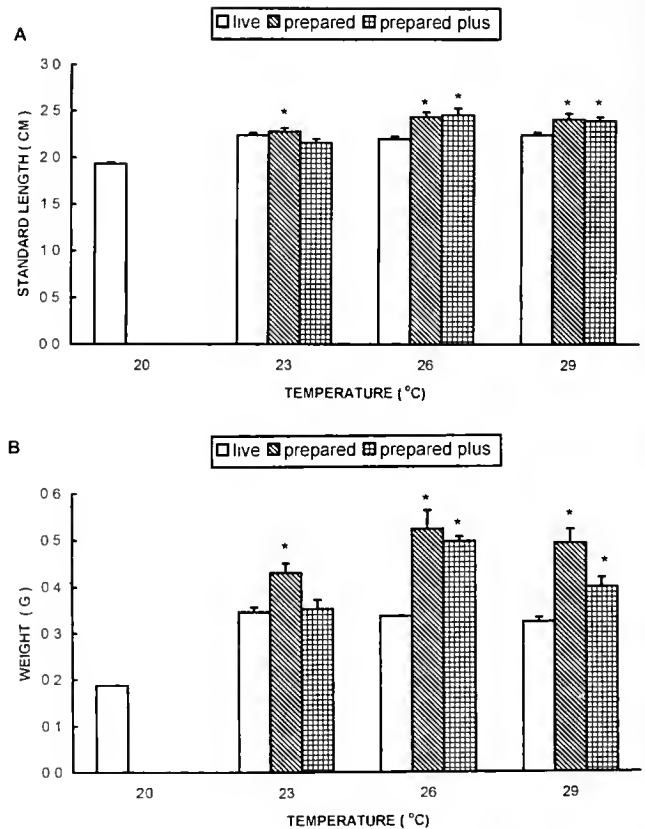


Figure 1. The bars represent the average standard length (A) and weight (B) for each diet at a specific temperature for juvenile toadfish. Asterisks indicate significantly different means compared to controls (ANOVA: $P < 0.05$). Error bars = 1 SE.

variations in each tank (water chemistry, ambient light, vibration) were not examined and may have subtly influenced individual fish. Finally, the energy expenditure (foraging vs. "hand" feeding) between the live and prepared diets will need to be addressed in the future.

The fish in our experiment grew fastest when fed the prepared diets. However, because hand-feeding hundreds to thousands of juvenile toadfish is not practical, we are attempting to refine the feeding techniques to reduce or eliminate this time-consuming step. The 4- and 5-week-old toadfish have begun foraging, indicating that the food presentation may only be needed during the first month.

Reference: *Biol. Bull.* **201**: 285–286. (October 2001)

Development of Genetically Tagged Bay Scallops for Evaluation of Seeding Programs

Hemant M. Chikarmane, Alan M. Kuzirian (*Marine Biological Laboratory, Woods Hole, Massachusetts*), Ian Carroll¹, and Robbin Dengler (*Marine Biological Laboratory, Woods Hole, Massachusetts*)

The bay scallop *Argopecten irradians* (Lamarck 1819) is harvested commercially and recreationally throughout its range along the east and Gulf coasts of North America. At its peak, the Massachusetts harvest exceeded 1200 metric tons with a monetary value of \$11 million (1). On Martha's Vineyard, bay scallop harvests are an important economic commodity and can represent, depending upon the size of the catch and price per pound, between 4% and 10% of the island's annual economy (2).

Argopecten irradians irradians, the northern bay scallop, and the southern subspecies (*A. i. concentricus*, *A. i. amplicostatus*) exhibit extreme natural variability in harvestable stocks from year to year; but, in general, natural populations have declined over the past quarter century (1). Harvest data from Cape Cod, Martha's Vineyard, and Massachusetts as a whole, compiled from 1965 to 1997, reveal that the maximum harvests (in bushels) occurred in the 1980s, but that scallop harvests have dropped precipitously since 1985 (3).

The variability and population declines are attributed to predation and habitat loss, to harmful algal blooms, and to the species' short life (1, 4, 5). The consequent economic pressures have led to increased emphasis on scallop aquaculture, development of field grow-out techniques, transplantations, and seeding programs using hatchery- or field-collected seed (1, 6). However, the notion that these efforts contribute significantly to population stabilizations is poorly supported by hard evidence (3, 7).

One of the difficulties in ascertaining the success of seeding or stock enhancement programs is that seeded animals cannot be distinguished from the natural population. The colored tags used for shrimp and fin fish are not useful for scallops. Allozyme differences were insufficient to discriminate between native and transplanted animals (8). In contrast, DNA-based molecular markers are excellent at distinguishing between subpopulations (9) and also have the great advantage of being neutral, while not generating artifacts due to predator preferences or survival. In this paper,

We thank the Waquoit Bay National Estuarine Research Reserve for use of their facilities. We thank H. Richmond, J. Hanley, and B. Mebane for help with aquarium set-up. We thank C. Taylor for education assistance. Funded by NIH grant DC01837.

Literature Cited

1. Tang, K. Q., N. N. Price, M. D. O'Neill, A. F. Mensinger, and R. T. Hanlon. 1999. *Biol. Bull.* **197**: 247–248.
2. Mensinger, A. F., K. A. Stephenson, S. L. Pollema, H. E. Richmond, N. Price, and R. T. Hanlon. 2001. *Biol. Bull.* **201**: 282–283.
3. Wilson, C. A., J. M. Dean, and R. Radtke. 1982. *J. Exp. Mar. Biol. Ecol.* **62**: 251–259.

we report progress in the development of scallops with molecular tags—an aid in the evaluation of stock enhancement programs.

We chose to develop RAPD (Random Amplification of Polymorphic DNA) genetic markers that can be detected by the polymerase chain reaction (PCR) (10). RAPD-PCR has the great advantage that DNA sequence information is not required for the development of useful markers.

Representative adult bay scallops were initially collected from Nantucket Island and, more recently, from Martha's Vineyard. Mantle tissue was sampled after the valves opened spontaneously. This procedure does not kill the animal, which can then be kept alive for mating experiments. After the tissue was thoroughly rinsed to remove extraneous biological material, DNA was purified from it. DNA purification procedures, RAPD-PCR protocols, and electrophoresis conditions have been described previously (11). Fifteen primers were screened for amplifiability and reproducibility, and the relative frequency of bands was determined. Results for two primers are shown in Table 1. In both cases, the larger size bands were present at higher relative frequencies when compared with those of the smaller size bands. Figure 1 shows a represen-

Table 1

Relative marker frequencies in the population, for primers AGGTCCTGA (10 bands) and GAAGCGCGAT (9 bands)

Band number	AGGTCCTGA	GAAGCGCGAT
10	1.0	—
9	1.0	1.0
8	1.0	0.9
7	1.0	0.8
6	0.3	0.5
5	0.6	0.5
4	0.3	0.1
3	0.4	0.2
2	0.4	0.4
1	0.2	0.1

¹ Brown University, Providence, RI.

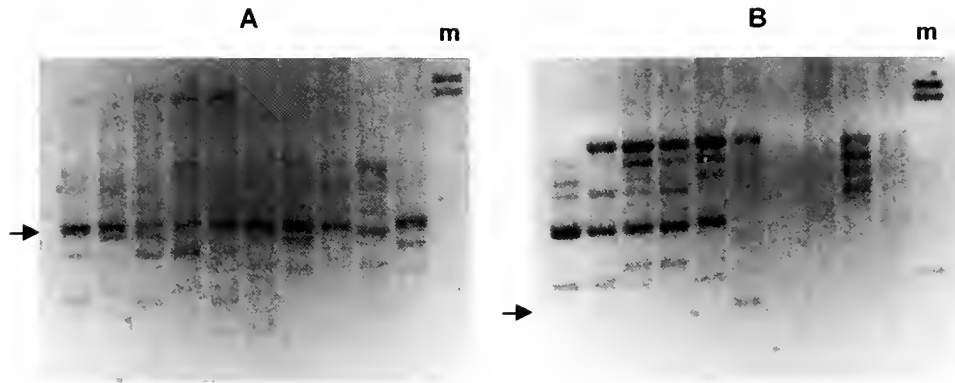


Figure 1. Representative RAPD-PCR profiles with Primer AGGTCCTGA (Panel A), and Primer GAAGCGCGAT (Panel B). Arrows point to a high frequency marker in Panel A, and a low frequency marker in Panel B. 'm' is a Lambda HindIII DNA size ladder.

tative gel image for the same two primers. Panel A shows an example of a RAPD marker that occurs at 100% frequency in the test population. Panel B shows a RAPD marker that appears at low frequency in the same population.

The breeding of marked scallops was a challenge. Bay scallops are simultaneous hermaphrodites, so inbreeding bay scallops carrying selected markers should have been relatively easy. Six animals were spawned by immersion in 1 mM serotonin, or by temperature shock (12), and self-fertilization was allowed to occur. Several hundred embryos were obtained in each case and were cultured in roller bottles. None of them survived to adulthood, indicating that self-crosses result in little or no survival of the F_1 progeny. This inbreeding depression confirms the results of Karney (pers. comm.) and Stiles *et al.* (13).

To circumvent this problem, we performed bulk matings with adults carrying distinctive markers. Crosses were done with four selected groups of 10 to 25 individuals. These have now gone through two generations, and are being screened. Animals testing positive for the high frequency marker (arrow, Fig. 1) will be conditioned and spawned. From the results obtained thus far, bulk mating of animals carrying selected markers appears to be the best approach to genetically tagging *Argopecten*.

Field trials will be carried out by transplanting animals carrying the selected marker into test areas where the marker is absent or present at a very low level, and then determining the relative frequency of the tag in sampled animals. To the best of our knowledge, this is the first attempt to tag a cultured mollusc species with molecular markers for the evaluation of seeding programs. If this proof-of-principle experiment is successful, it can be extended to commercial aquacultured species such as *Placopecten magellanicus*, *Mya arenaria*, and *Mercenaria mercenaria*.

This work was supported in part by a grant from the MIT/WHOI Sea Grant Program to A.M.K. and H.M.C. (Project: R/A-34).

H.M.C. and A.M.K. are indebted to Dr. Dale Leavitt of SEMAC and Rick Karney of the Martha's Vineyard Shellfish Group for assistance and advice. We thank the Marine Resources Center, Marine Biological Laboratory, for providing facilities for maintenance of the scallops.

Literature Cited

1. National Marine Fisheries Service. 2001. *Annual Commercial Landing Statistics*. [Online]. Available: http://www.st.nmfs.gov/st1/commercial/landings/annual_landings.html [August 2001].
2. Karney, R. 1991. Pp. 308–312 in *An International Compendium of Scallop Biology and Culture*. S. E. Shumway and P. A. Sandifer, eds. World Aquaculture Society, Baton Rouge, LA.
3. Macfarlane, S. L. 1999. *South Eastern Massachusetts Aquaculture Center (SEMAC) Technical Report 99-01*: 1–73.
4. Arnold, W. S., D. C. Marelli, C. P. Bray, and M. M. Harrison. 1998. *Mar. Ecol. Prog. Ser.* 170: 143–157.
5. Short, F. T., B. W. Ibelings, and C. DenHartog. 1998. *Aquat. Bot.* 30: 295–304.
6. Tettelbach, S. T. 1991. Pp. 164–175 in *An International Compendium of Scallop Biology and Culture*. S. E. Shumway and P. A. Sandifer, eds. World Aquaculture Society, Baton Rouge, LA.
7. Marelli, D. C., and W. S. Arnold. 1998. *J. Shellfish Res.* 17: 332.
8. Krause, M. K. 1992. *J. Shellfish Res.* 11: 199.
9. De Wolf, H., T. Backeljau, and R. Verhagen. 1998. *Heredity* 81: 486–492.
10. Williams, J. G. K., A. R. Kubelik, K. J. Livak, J. A. Rafalski, and S. V. Tingey. 1990. *Nucleic Acids Res.* 18: 6531–6535.
11. Chikarmane, H. M., A. M. Kuzirian, R. Kozlowski, M. Kuzirian, and T. Lee. 2000. *Biol. Bull.* 199: 227–228.
12. Ram, J. L., G. W. Crawford, J. U. Walker, J. J. Mojares, N. Patel, P. P. Fong, and K. Kyozuka. 1993. *J. Exp. Zool.* 265: 587–598.
13. Stiles, S., J. Choromanski, D. Schweitzer, and Q-Z. Xue. 1996. *J. Shellfish Res.* 16: 461.

Reference: *Biol. Bull.* **201**: 287–288. (October 2001)

The Effects of Salt Marsh Haying on Benthic Algal Biomass

Libby Williams, (The College of Wooster, Wooster, Ohio), G. Carl Noblitt IV¹, and Robert Buchsbaum²

Salt marsh haying is a traditional activity on East Coast salt marshes and is still carried out on a large scale (over 400 hectares regularly) throughout Plum Island Sound, located in northeastern Massachusetts.

The removal of approximately 90% of the aboveground biomass of the salt marsh by haying may alter many ecological processes within the salt marsh (1). One such process is the production of benthic algae. Estrada *et al.* (1974) found that nutrients and light are critical controls on the amount of benthic algae present (2). When a thick grass canopy shades the algae, their growth is limited not by nutrients but rather by the available light. However, when little grass canopy is present, benthic algal growth is limited by the available nutrients. Grazers are also likely to determine the amount of algal standing crop. In this project we tested the hypothesis that there should be a marked increase in benthic algal biomass after an area has been hayed because the algae is no longer limited by the available light.

We took core samples at three marsh sites, each about 1 to 2 hectares in area. Two of these are regularly subjected to haying, and one is an unhayed reference area. The reference area (PUH) has not been hayed for at least 25 years. One hayed site (EPH) was last hayed two summers ago (1999). At PUH and EPH, six 1-m² quadrats were placed randomly in two different vegetation zones, *Spartina alterniflora* (low marsh) and *Spartina patens* (high marsh) sites. Three quadrats in each vegetation zone at each area were cleared of aboveground vegetation by clipping, and three were left as unclipped reference quadrats. The second hayed site (HAY) was hayed in June 2001 before sampling began. At HAY, we established three 1-m² quadrats within *Spartina patens* zones that had just been cleared of vegetation by the hayer.

Six sediment cores (3-cm diameter, 1-cm depth) were taken from each quadrat at day 0, day 7, day 14, and day 30 after clipping

(or haying). The six sediment cores were then pooled together into two sets of three cores. At the end of the 30-day sampling period, the aboveground plant biomass from the quadrats within the hayed and reference sites was removed to measure the regrowth of the vegetation during the experimental period. The material from the sites was then dried and weighed. The benthic chlorophyll was extracted and measured from the pooled core samples using the method of Lorenzen (3).

We used HOBO HLI light intensity loggers to determine the relative amount of light reaching the sediment surface at both the treatment and reference sites.

We found no difference between the benthic algal chlorophyll in the area that was hayed two summers ago and the area that has not been hayed for 25 years. Consequently, we pooled and treated the two areas as replicates in further analyses. Furthermore, we found no statistically consistent increase in algal biomass over the 30 days of the experiment in the clipped or hayed treatments. In addition, there was not a significant difference in benthic algal biomass between *S. alterniflora* (low marsh) and *S. patens* (high marsh) zones regardless of whether they were clipped or not (Fig. 1).

The benthic chlorophyll concentrations in the June 2001 hayed area were significantly higher than the benthic chlorophyll in the unclipped treatments (ANOVA, $F = 3.330$, $P = 0.039$). However, neither the benthic algal chlorophyll present in the hayed area nor that in the reference quadrats was significantly different from that present in the clipped quadrats. The results suggest that haying on a large scale, but not small-scale removal of the plant canopy, increases the amount of benthic algae present.

Based on a limited number of light measurements, there is a direct relationship between the percentage of light reaching the sediment surface and benthic chlorophyll concentrations within each quadrat (Fig. 2). In addition, it appears that there is an inverse relationship between the plant biomass of each quadrat and the benthic chlorophyll concentration (Fig. 2).

¹ Governor Dummer Academy, Byfield, MA.

² Massachusetts Audubon Society, Wenham, MA.

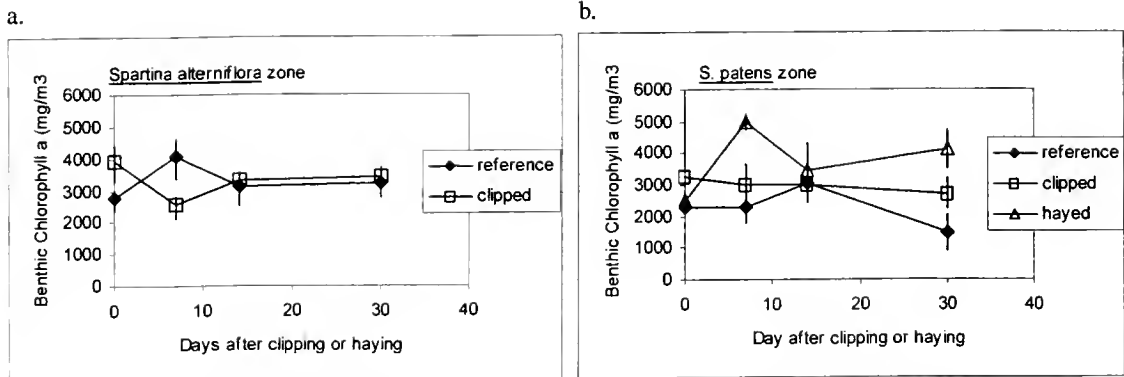


Figure 1. Benthic algal biomass (mg chlorophyll per m³) in two different vegetation zones after clipping or haying.

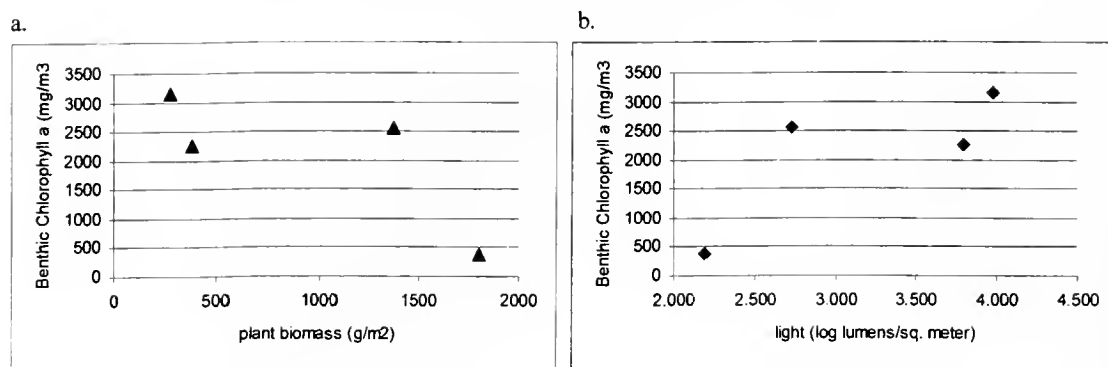


Figure 2. Relationships between benthic algal biomass, incident light to the marsh surface, and aboveground plant biomass.

The benthic algal biomass is distributed very patchily throughout each site. As a result, even though six core samples were taken on each sampling day, more samples might be needed to truly estimate the actual biomass of each quadrat. The tremendous variability—not only within each area but also within each quadrat—confounds the algal chlorophyll measurements.

It is possible that significant algal growth occurred, but the algae were grazed heavily and thus did not show an actual increase in biomass. It is also possible that our removal of aboveground plant biomass resulted in desiccation of the marsh surface. Desiccation could limit algal growth directly and by preventing the remineralization of nutrients necessary for future algal growth.

Regrowth of marsh plants in the hayed site occurred particularly rapidly (to more than 70% of the biomass of an *S. patens* reference) over the 30 days of the experiment. Thus any stimulation of

algal growth by increased light due to haying is likely to be short term.

The Plum Island Estuary LTER and a Research Experience for Undergraduates NSF fellowship supported this research. Thanks to Robert H. Garritt and Kris Tholke for guidance on the chlorophyll analyses and to Charles G. Hopkins for advice on experimental design.

Literature Cited

1. Greenbaum, A., and A. Giblin. 2000. *Biol. Bull.* 199: 225–226.
2. Estrada, M., I. Valiela, and J. M. Teal. 1974. *J. Exp. Mar. Biol. Ecol.* 14: 47–56.
3. Lorenzen, C. J. 1967. *Limnol. Oceanogr.* 12: 343–346.

Reference: *Biol. Bull.* 201: 288–290. (October 2001)

Dissolved Nitrogen Dynamics in Groundwater Under a Coastal Massachusetts Forest

Eve-Lyn S. Hinckley, Christopher Neill, Richard McHorney¹, and Ann Lezberg (The Ecosystems Center, Marine Biological Laboratory, Woods Hole, Massachusetts 02543)

Land uses, such as agriculture and residential development, have greatly influenced the amount of nitrogen (N) transported from coastal watersheds to receiving estuaries. This is a concern to ecologists and management groups in coastal regions such as Cape Cod, Martha's Vineyard, and Nantucket, where precipitation percolates rapidly through sandy glacial sediments in the vadose zone (unsaturated layer between the soil and aquifer), causing rapid vertical transport of N to the aquifer (saturated layer) and horizontal movement of N to coastal waters (1, 2). In many forested watersheds, ammonium (NH_4^+) and nitrate (NO_3^-) are transported to receiving estuaries in low amounts relative to dissolved organic N (DON), which includes organic acids and other compounds (3, 4). However, in human-altered systems, high amounts of inorganic N, particularly in the form of NO_3^- , are often transported to aquatic systems, elevating primary production (5). To make management

decisions for coastal areas with high anthropogenic N inputs, it is important to study systems in which human influences are minimal so that background N transformations can be identified.

Our goal in this study was to quantify N concentrations and to identify N transformations in groundwater moving along a known flow path in a forested system with a known land-use history, minimal septic inputs, and no overland flow. We measured the relative concentrations of dissolved N species (NH_4^+ , NO_3^- , and DON) in throughfall, soil solution in the vadose (unsaturated) zone, and groundwater from an oak forest on Job's Neck peninsula in Edgartown, Massachusetts. We also measured N concentrations at the seepage face of the Edgartown Great Pond estuary which lies roughly 500–1000 m downgradient in the groundwater flowpath from the forest.

We collected throughfall, and water from the vadose zone, aquifer, and seepage face from June 2000 to August 2001 and analyzed samples for NH_4^+ , NO_3^- , and DON concentrations. We used spatially extensive sampling to capture fine-scale differences

¹ The Nature Conservancy, Plymouth, MA 02360.

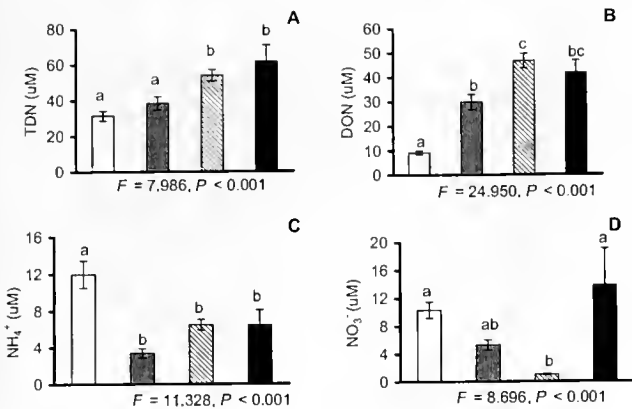


Figure 1. Mean concentrations of TDN, DON, NH₄⁺, and NO₃⁻ in water inputs to and outputs from the forest. □ = Throughfall, ▨ = Vadose zone, ▩ = Aquifer, ■ = Seepage face. Means represent the average concentrations of samples taken from June 2000–August 2001. Only samples for which all three N analyses were completed are included. Throughfall N = 72, Vadose zone N = 79, Aquifer N = 138, Seepage face N = 62. Bars are ± 1 SE and letters above bars indicate significant difference to the P < 0.001 level.

in vegetation and topography: 60 throughfall collection units and 50 zero-tension lysimeters installed at 40-cm depth in a stratified random pattern throughout the forest, 40 iron piezometers installed to the water table along the groundwater flow paths, and 34 points for shallow groundwater discharge sampling at the seepage face of Edgartown Great Pond. All water samples were filtered with ashed (2 h at 550 °C) Whatman GF/F filters and frozen in 60-ml polyethylene bottles until analyzed colorimetrically for NH₄⁺, NO₃⁻, and TDN concentrations (TDN was analyzed by persulfate digestion). DON concentrations were calculated by subtracting NH₄⁺ + NO₃⁻ from TDN concentrations of each sample. We used a one-way analysis of variance and a Tukey’s post-hoc test to determine statistical differences between means (at 0.05 level of significance). All statistical analyses were performed using SYSTAT (SPSS Inc., 1997, Version 7.0).

TDN increased significantly (P < 0.001) from 31.44 ± 2.71 µM in throughfall to 54.08 ± 3.21 µM in the aquifer (Fig. 1A). DON was the principal component of dissolved N in the vadose zone, aquifer, and at the seepage face (Table 1). These data are consistent with other studies that show dominance of DON in soil solution and groundwater of forested watersheds (3, 4). DON increased significantly (P < 0.001) from 9.15 ± 0.76 µM in throughfall inputs to 46.63 ± 2.96 µM in the aquifer (Fig. 1B). Most DON consists of organic acids and other compounds that originate in the upper layers of the forest floor and move to groundwater during periods of heavy precipitation (4, 6). There was no significant difference between DON concentrations in the aquifer and at the seepage face, suggesting that further removal or accumulation of DON may not occur as groundwater moves horizontally to receiving waters.

NH₄⁺ decreased significantly (P < 0.001) from 11.97 ± 1.48 µM in throughfall to 3.38 ± 0.50 µM in the vadose zone (Fig. 1C). This suggests that plants or microbes in the rooting zone immobilized NH₄⁺. NH₄⁺ concentrations were higher in the aquifer and

the seepage face compared with the vadose zone, but these differences were not significant and suggest that little additional NH₄⁺ uptake occurs below the 40-cm depth at which the vadose zone samples were collected. NH₄⁺ composed about 12% of TDN in the aquifer, indicating some export of NH₄⁺-N could occur as groundwater moves to the seepage face (Table 1). NH₄⁺ movement from the vadose zone to the aquifer is consistent with data from other coastal systems with sandy soils on Cape Cod and may be caused by low soil pH and low soil cation exchange capacity (2). These characteristics may cause NH₄⁺ to be more mobile in forests with very coarse-textured soils compared with other upland forests on finer-textured soils (7, 8).

NO₃⁻ decreased significantly (P < 0.001) from 10.33 ± 1.16 µM in throughfall to 0.99 ± 0.08 µM in the aquifer (Fig. 1D). NO₃⁻ was about 2% of TDN in the aquifer (Table 1), indicating that very little NO₃⁻ moves from the plant-rooting zone to the aquifer. In the aquifer, concentration of NO₃⁻ was also lower than NH₄⁺, which suggests low rates of nitrification along the flowpath from soil solution to the aquifer. This pattern is consistent with NH₄⁺ and NO₃⁻ concentrations measured in soil solution and groundwater in Cape Cod coastal forests (2, 6).

NO₃⁻ increased significantly (P < 0.001) from 0.99 ± 0.08 µM in the aquifer to 13.79 ± 5.26 µM at the seepage face (Fig. 1D). NO₃⁻ concentrations were highly variable but this overall pattern suggested that NO₃⁻ from additional sources was detected at some locations along the Edgartown Great Pond shoreline. There are several possible explanations for this result. Long-distance transport of NO₃⁻ from septic discharges farther inland are possible but, we feel, unlikely, given the relative hydrological isolation of Job’s Neck, the west-to-east groundwater movement under the forest, and our measurements of higher NO₃⁻ concentrations at the southern (coastal) end of the pond shoreline. It is also possible that increases in NO₃⁻ result from zones of oxidation of NH₄⁺ or DON to NO₃⁻ within the seepage face, or from inputs of fixed N derived from the N-fixing shrub *Myrica pensylvanica*, which is present at many places along the pond shoreline.

From these findings, we conclude that: (1) relatively low NH₄⁺ and NO₃⁻ and high DON are transported from the forest to the coastal pond, (2) incomplete retention of NH₄⁺ above the aquifer and comparatively low NO₃⁻ concentrations in the aquifer, and (3) there is the possibility that in some places the seepage face may contribute a small amount of NO₃⁻ to discharging groundwater rather than remove it, because of NH₄⁺ or DON oxidation or N inputs derived from N-fixing species. These findings can serve as a baseline for understanding how N transformations change with increasing human development and a shift toward a greater proportion of NO₃⁻ reaching the seepage face from the coastal aquifer.

Table 1

Percentage of TDN for each N species measured

	NH ₄ ⁺	NO ₃ ⁻	DON
Throughfall	38.1	32.8	29.1
Vadose zone	8.8	13.7	77.6
Aquifer	12.0	1.8	86.2
Seepage face	10.4	22.3	67.3

This research was supported by the Mellon Foundation. We thank Tom Chase and Mike Dunphy of The Nature Conservancy and the Kohlberg family for allowing us to work on their property.

Literature Cited

1. Valiela, I., M. Geist, J. McClelland, and G. Tomasky. 2000. *Biogeochemistry* 49: 277–293.
2. Lajtha, K., B. Seely, and I. Valiela. 1995. *Biogeochemistry* 28: 33–54.
3. Hedin, L., J. Armesto, and A. Johnson. 1995. *Ecology* 76: 493–509.
4. Qualls, R., B. Haines, and W. Swank. 1991. *Ecology* 72: 254–266.
5. Valiela, I., G. Collins, J. Kremer, K. Lajtha, M. Geist, B. Seely, J. Brawley, and C. Sham. 1997. *Ecol. Appl.* 7: 358–380.
6. Seely, B., K. Lajtha, and G. Salvucci. 1998. *Biogeochemistry* 42: 326–343.
7. Vitousek, P., and W. Reiners. 1979. *Science* 204: 469–474.
8. Gorham, E., P. Vitousek, and W. Reiners. 1979. *Annu. Rev. Ecol. and Syst.* 10: 53–84.

Reference: *Biol. Bull.* 201: 290–292. (October 2001)

Small-Scale Heterogeneity of Nitrogen Concentrations in Groundwater at the Seepage Face of Edgartown Great Pond

Alyson M. Hauxwell¹, Christopher Neill, Ivan Valiela, and Kevin D. Kroeger (Ecosystems Center and Boston University Marine Program, Marine Biological Laboratory, Woods Hole, Massachusetts 02543)

Groundwater transports nitrogen to receiving estuaries (1, 2), but the details of nitrogen exchange, transformations, and losses are insufficiently known (3). We examined small-scale heterogeneity of salinity, ammonium (NH₄), nitrate (NO₃), dissolved organic nitrogen (DON), and boron in both vertical and horizontal profiles near the sandy seepage face of Edgartown Great Pond (Martha's Vineyard, Massachusetts). The water level of this pond is managed by dredging an outlet to release accumulated groundwater; from April to June 2001 the pond was open to the sea. Sampling for this study was done in June 2001. We focused on nitrogen because of its role in limiting estuarine production (4), and on boron because it can be used as a tracer of both wastewater (5) and seawater (6). Relationships among these solutes allow inquiry as to sources of the materials and identity of some major processes (5).

To describe in detail the pattern of distributions of the solutes, we collected groundwater samples along three parallel transects running perpendicular to shore from 4.5 m upland to 1.5 m beyond the shoreline of Edgartown Great Pond (Fig. 1A, B, C). Each transect consisted of seven points, each sampled at about 16 cm, 41 cm, 66 cm, 91 cm, and 116 cm below the ground surface. We collected 125 ml of water from each point using a well point piezometer and pressure pump. The samples were filtered through 47-mm glass fiber filters to remove particulates. We measured salinity using a refractometer and ammonium concentrations using the alkaline phenol method. Nitrate and TDN concentrations were measured on a Lachat autoanalyzer using the Quick Chem method, and DON was determined by subtracting NH₄ and NO₃ concentrations from TDN concentrations for each sample. Ward Laboratories (Kearney, NE) determined boron concentrations on a subset of the samples.

Salinity (Fig. 1A) and ammonium (Fig. 1B) concentrations in groundwater increased seaward. In contrast, NO₃ (Fig. 1C) concentrations decreased seaward. Vertical cross-sections of concentrations (Fig. 1D, E, F) along the top transect shown in Figure 1 (A, B, C) suggest how groundwater flow interacts with horizontal transportation to determine the small-scale patterns of concentra-

tion across the seepage face of this estuary (Fig. 1D, E, F). Salinity of groundwater was 0‰ and increased to 17‰–19‰ under the pond, about half the salinity of the pond (28‰) (Fig. 1D). The contours suggest that the fresh groundwater flows over the saltier water, and discharges in a seepage face a few meters wide. Ammonium concentrations were highest under the pond and at increasing depths, with one high value under land (Fig. 1E). NH₄ concentrations increase as salinities increase beyond 13‰ (Fig. 1G). This increase is not due to NH₄ imported from land to the pond, or from the pond (the pond has a concentration of only 2 μM NH₄). Nitrate concentrations were highest landward and decreased offshore, with a smaller peak seaward (Fig. 1F). DON did not change significantly through each transect (data not shown) and decreased only slightly with increasing depth.

One possible explanation for the high NH₄ associated with salty water may be that the pond bottom shares the vertical pattern of high NH₄ concentrations characteristic of anoxic coastal sediments, with upward diffusion of NH₄ regenerated within the sediments by decay of buried organic matter (7). This explanation seems implausible because 1) none of the water samples had a sulfide odor, hence were not anoxic, and 2) it is difficult to explain the peak in NO₃ concentrations if we simply had freshwater continually flowing toward the seepage face. Perhaps a more plausible idea is that during the open-to-the-sea stage of the year, seawater intrudes into the pore space in sediments at the seepage face, and the Na⁺ displaces NH₄ previously adsorbed to particles. Such a mechanism has been invoked in the displacement of radium from many shorelines (8). This mechanism also has the advantage that it will account for the NO₃ peak shoreward of the NH₄ peak: during the open-pond phase, saltwater may force its way landward, and nitrification could transform the exchanged NH₄ into NO₃ as the porewater moves landward. In most other such estuaries tidal forces may repeat the pattern that occurs once a year in Edgartown Great Pond and probably hide the local pattern of concentrations. This pond hence provides a slow-motion view of what probably occurs twice daily in tidal dominated estuaries.

The high NO₃ concentrations landward are likely to be associated with a wastewater source (Fig. 1H); the concentrations of NO₃ are too high to be atmospheric nitrogen passing through soil (W.

¹ University of Michigan, Ann Arbor, MI 48109.

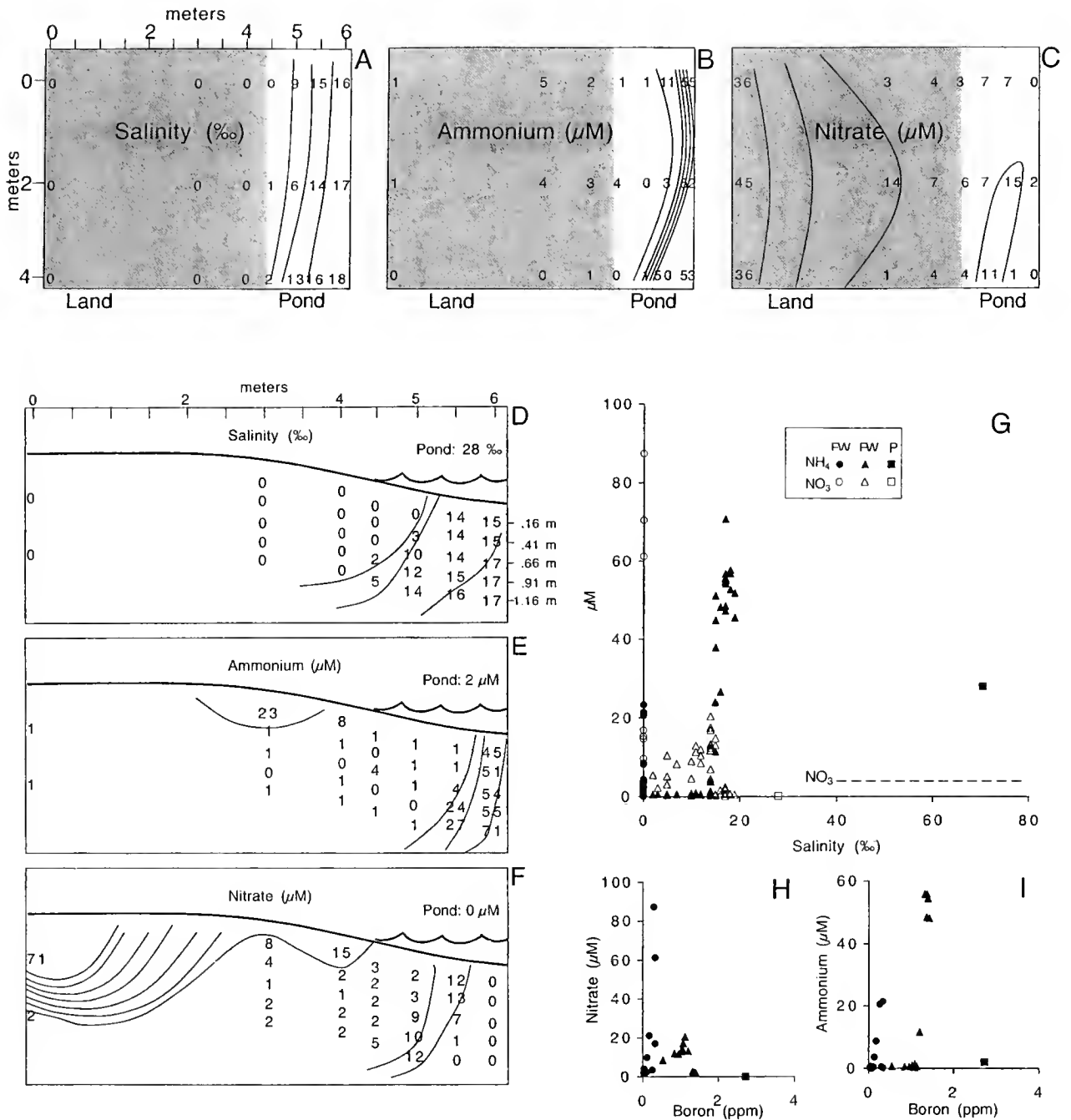


Figure 1. (A, B, C) Plan view of transects where each value is an average for all depths at the location showing (A) salinity (contour line interval 5‰); (B) NH_4 (contour line interval 20 μM); (C) NO_3 (contour line interval 10 μM). Gray area is land and white area is water. (D, E, F): Cross-section of transect Figure 1 (A, B, C) showing (D) salinity (contour line interval 5‰); (E) NH_4 (contour line interval 20 μM); (F) NO_3 (contour line interval 10 μM). (G) NH_4 (open shapes) and NO_3 (closed shapes) concentrations versus salinity for freshwater (●), estuarine water (▲), and pond water (■). Dashed line is peak NO_3 value from soil sources (Pabich *et al.*, unpubl. data). (H) Boron concentrations versus NO_3 concentrations for fresh, estuarine, and pond water. (I) Boron concentrations versus NH_4 concentrations for fresh (FW), estuarine (EW), and pond water (P).

Pabich *et al.*, unpubl. data), and show higher boron concentrations than would be likely in uncontaminated sediments (Fig. 1H). The pattern of boron concentrations supports the idea that in freshwater the high NO_3 peak derives from some source on land, probably wastewater. Boron concentrations within a septic plume can have

ranges above 0.2 ppm boron (5). In saltier groundwater, some other process produces the smaller peak in concentration under the pond (Fig. 1H)—in our view, nitrification of the displaced NH_4 .

Concentrations of solutes in groundwater were variable normal to the shoreline. The presence of small-scale transient NH_4 and

NO₃ fronts that are the result of local processes in the fresh-seawater mixing zone at the interface can alter ideas as to how we estimate land-derived N loads, and can provide insight into the processes that transfer nitrogen between fresh and saltwater. Understanding this heterogeneity is important for establishing a meaningful sampling protocol to estimate nitrogen loading to an estuary and for interpreting the likely sources.

This research was funded by a National Science Foundation-Research Experience for Undergraduates Grant (OCE-0097498). Special thanks to Ann Lezberg and Eve Hinckley for help with chemistry protocols and to Marci Cole and Joanna York for their endless help in the lab. Also thanks to William Wilcox of the Martha's Vineyard Commission and the Kohlberg family for use of their land.

Reference: *Biol. Bull.* 201: 292–294. (October 2001)

Top-down vs. Bottom-up Controls of Microphytobenthic Standing Crop: Role of Mud Snails and Nitrogen Supply in the Littoral of Waquoit Bay Estuaries

Melissa Novak¹, Mark Lever, and Ivan Valiela (Boston University Marine Program, Marine Biological Laboratory, Woods Hole, Massachusetts 02543)

Top-down and bottom-up processes are important in the regulation of primary productivity. In shallow estuaries, the mud snail *Ilyanassa obsoleta* may exert strong top-down forces on the biomass of microphytobenthos (1, 2), and nutrient availability in the sediments may also affect microphytic biomass (3, 4, 5, 6). We examined the relative importance of top-down and bottom-up effects by experimentally manipulating mud snail densities and porewater nutrient concentrations.

Twenty cages were set up in Sage Lot Pond in Waquoit Bay, Massachusetts. The cages were placed in two rows of 10, paralleling the shoreline on sandy, subtidal sediments, approximately 7 cm below mean low tide level. The cages were constructed from plastic boxes (23 cm × 23 cm × 8 cm). The bottom was removed and windows were cut into the lid and sides. The windows allowed water exchange and minimized artifacts caused by interference with water flow. To prevent the escape of enclosed snails, each window was covered with a 4-mm polypropylene mesh. Each cage was pushed into the sediment to a depth of approximately 5 cm.

To determine the significance of bottom-up effects, 10 cages were treated using "diffusers" made of polypropylene microcentrifuge tubes with holes drilled into their sides, filled with controlled-release fertilizer (9.7% NH₄⁺, 8.3% NO₃⁻, 6% P₂O₅). In each cage, nine tubes were evenly spaced and fully pushed into the sediment, so that the top was 1 cm below the sediment surface. The nutrient additions were equivalent to 60 g N/m² and 8.7 g P/m².

The success of the fertilizer treatment was established by sampling porewater from six randomly selected locations within each cage at day 0, 7, 14, 28, and 38. All porewater samples were pooled samples collected from the entire upper 1 cm of sediment

Literature Cited

1. Valiela, I., G. Collins, J. Kremer, K. Lajtha, M. Geist, B. Seely, J. Brawley, and C. H. Sham. 1997. *Ecol. Appl.* 7: 358–380.
2. Giblin, A. E., and A. G. Gaines. 1990. *Biogeochemistry* 10: 309–328.
3. Portnoy, J. W., B. L. Nowicki, C. T. Roman, and D. W. Urish. 1998. *Water Res.* 34: 3095–3104.
4. Howarth, R. W. 1988. *Annu. Rev. Ecol. Syst.* 19: 89–110.
5. Westgate, E. J., K. D. Kroeger, W. J. Pabich, and I. Valiela. 2000. *Biol. Bull.* 199: 221–223.
6. Barth, S. R. 2000. *Appl. Geochem.* 15: 937–952.
7. Valiela, I. 1995. P. 437 in *Marine Ecological Processes*. Springer-Verlag, New York.
8. Moore, W. S. 2000. *J. Geophys. Res.* 105: 117–122.

using sippers constructed from modified 10-ml polyethylene syringes. Samples were filtered through 47-mm glass fiber filters with 0.7 μm pore sizes. Concentrations of phosphate were determined using a spectrophotometer (7), ammonium following a fluorometric method (8), and nitrate by using a LACHAT auto analyzer following the QuikChem method.

To assess top-down effects, densities of 0, 20, 50, 100, and 200 snails per cage were randomly assigned to different cages. The mean ambient density of mud snails in the area at time 0 was 97 snails/cage ($s = 4.14$). Each experimental density was applied to two cages in each of the fertilized and control treatments. Snails were recounted after each sampling to ensure that densities were maintained throughout the experimental period.

To measure the response of benthic microphytes to fertilization and snail density treatments, six core samples were taken from each cage at each sampling date. Each coring device consisted of a cut-off 10-ml syringe with a diameter of 0.95 cm and length of 2.5 cm. Chlorophyll *a* concentrations were analyzed spectrophotometrically (9).

Both the fertilization and snail density treatments were effective. Nutrient concentrations in the upper layer of sediments in the fertilized cages were significantly higher than in control plots (Fig. 1a, b, c) (one-tailed *t* test: phosphate, $P < 0.009$; ammonium, $P < 0.004$; nitrate, $P < 0.03$). We note that concentrations of nutrients in estuarine sediments often exceed those found in our samples (10), but our concentrations are within the range we find in the upper 1 cm of sandy substrate in Waquoit Bay sub-estuaries (M. Lever, unpubl. data). The snail counts in the various cages remained constant over the course of the experiment.

Linear regressions of chlorophyll *a* concentrations vs. time were used to calculate rates of change of the microphyte biomass in each cage. These rates were then plotted against snail density for both

¹ University of Rhode Island, Kingston, RI 02881.

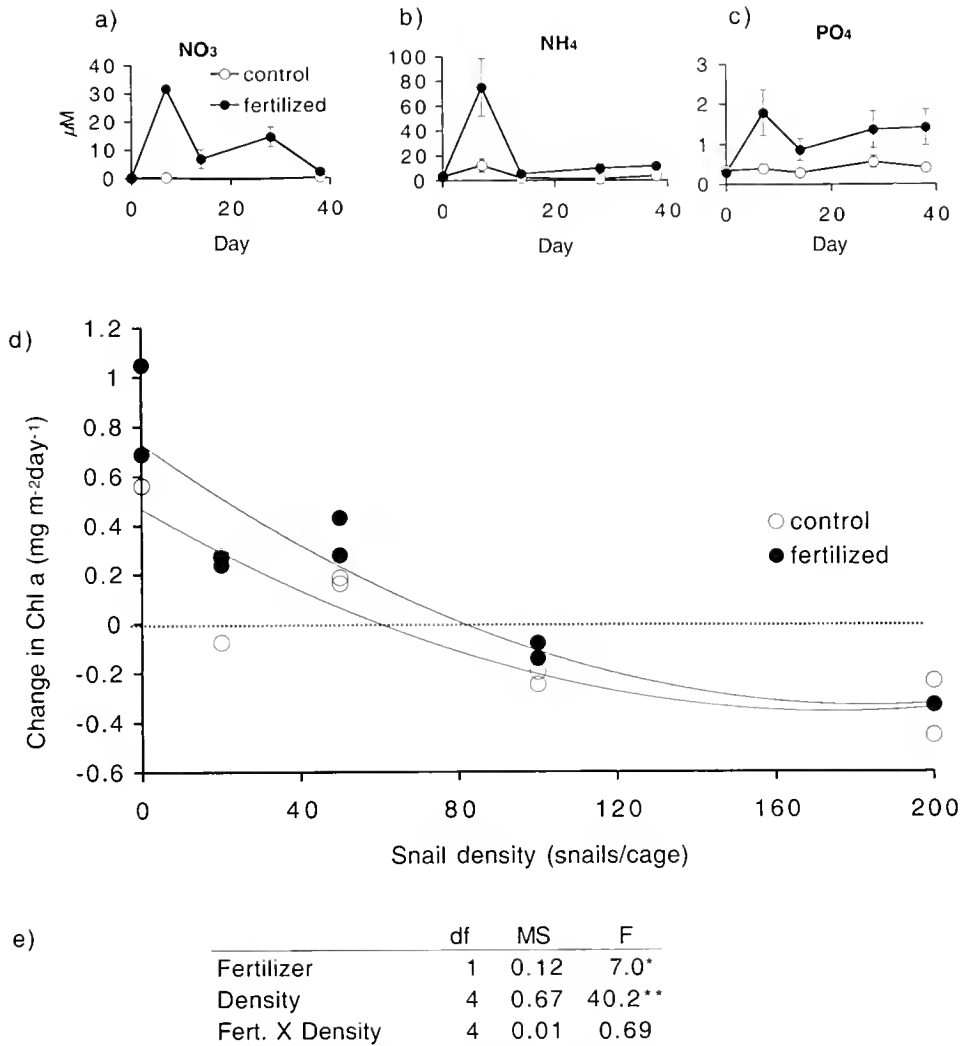


Figure 1. (a–c) Time courses of nitrate (a), ammonium (b), and phosphate (c) concentrations in pore water in control and fertilized cages. (d) Change in chlorophyll a as a function of snail density. Data points are calculated from regressions of change in chlorophyll over time for individual cages. (e) Two-way ANOVA of the results of chlorophyll response to the fertilizer and density treatments. * indicates significance at P = 0.05; ** indicates significance at P = 0.01.

fertilized and control treatments (Fig. 1d). A two-way ANOVA showed that both snail densities and nutrient concentrations had significant effects on chlorophyll a concentrations (Fig. 1e).

In terms of the effect of herbivore density, we interpret the results of Fig. 1d to suggest that 1) lower snail densities allowed increases in microphytobenthic biomass (note the position of the dashed horizontal line showing no change), and 2) snail densities exceeding the ambient of 97 snails per cage reduced microphyte biomass. These results suggest that mud snails can control abundance of their food, which means, perhaps, that field densities are poised at a level that does not deplete the food supply.

In terms of the effect of nutrient supply, the addition of nutrients significantly increased microphytobenthic biomass (Fig. 1e). In spite of the trends suggested by Fig. 1d, the response of microphyte biomass to fertilization was not significantly larger at lower snail densities (Fig. 1e). The results were insufficient to allow us to discern the possible interaction between grazing pressure and nutrient supply, in part because there were only two levels of the

nutrients examined, and because even in the fertilized sediments concentrations were relatively low.

The results of this experiment suggest that both bottom-up and top-down processes can be potentially important controls of benthic microphytes in estuarine sediments. Further experiments in which a broader range of fertilizer loads is applied will help to determine the relative importance of top-down vs. bottom-up controls.

Jennifer Wolf helped with the fieldwork. This work was supported by NSF-Research Experience for Undergraduates Grant OCE-0097498.

Literature Cited

1. Pace, M. L., S. Shimmel, and W. M. Darley. 1979. *Estuar. Coast. Mar. Sci.* 9: 121–134.
2. Connor, M. S., J. M. Teal, and J. Valiela. 1982. *J. Exp. Mar. Biol. Ecol.* 65: 29–45.
3. Admiraal, W., H. Peletier, and H. Zomer. 1982. *Estuar. Coast. Shelf Sci.* 14: 471–487.

4. MacIntyre, H. L., R. J. Geider, and D. C. Miller. 1996. *Estuaries* 19: 186–201.
5. van Raalte, C. D., I. Valiela, and J. M. Teal. 1976. *Limnol. Oceanogr.* 21: 862–872.
6. Granéli, E., and K. Sundbäck. 1985. *J. Exp. Mar. Biol. Ecol.* 85: 253–268.
7. Strickland, J. D. H., and T. R. Parsons. 1972. Pp. 49–64 in *A Practical Handbook of Sea Water Analysis*, Fisheries Research Board of Canada, Ottawa.
8. Holmes, R. M., A. Aminot, R. Kerouel, B. A. Hooker, and B. J. Peterson. 1999. *Can. J. Fish. Aquat. Sci.* 56: 1801–1808.
9. Lorenzen, C. J. 1967. *Limnol. Oceanogr.* 12: 343.
10. Valiela, I. 1995. Pp. 59–78 in *Marine Ecological Processes*, Springer, New York.

Reference: *Biol. Bull.* 201: 294–296. (October 2001)

Stable N Isotopic Signatures in Bay Scallop Tissue, Feces, and Pseudofeces in Cape Cod Estuaries Subject to Different N Loads

Laurie Fila¹, Ruth Herrold Carmichael, Andrea Shriver, and Ivan Valiela (Boston University Marine Program, Marine Biological Laboratory, Woods Hole, Massachusetts 02543)

Scallops (*Argopecten irradians*) feed on particulates in estuaries, and their growth and survival may depend on the quality and quantity of food particles available (1, 2). To a significant degree, particle supply in shallow estuaries such as those on Cape Cod depend on rates of land-derived N load (3). Linkages between estuarine organisms and terrestrial loadings have been studied in various ways, including stable isotopic techniques. Isotopic fractionation leads to detectable shifts created by microbial transformations, trophic steps, as well as to differences due to source of the N (4, 5).

In this paper we apply isotopic analyses and experiments with introduced scallops to define the rate at which scallops acquire the signature of the estuary in which they are located; we examine whether scallop tissues differ from the signatures of pseudofeces and feces ejected by scallops, and whether differences in N-loading rates and sources to different estuaries result in corresponding differences in the signature of scallops within the estuaries. Finally, we use results of the introduced scallop experiments to see if differences in $\delta^{15}\text{N}$ signature acquisition are related to differences in growth or survival of the scallops.

We compared the acquisition of $\delta^{15}\text{N}$ signatures by scallops incubated in two estuaries of Waquoit Bay, Cape Cod, receiving different N inputs. Childs River (CR) has a loading rate of $601 \text{ kg N ha}^{-1} \text{ y}^{-1}$. Sage Lot Pond (SLP) has a loading rate of $14 \text{ kg N ha}^{-1} \text{ y}^{-1}$. The difference in N load between these estuaries is due to different levels of urbanization in their watersheds, and the differences in wastewater contributions to these two estuaries result in different isotopic signatures in the N entering the estuaries from land (5, 6). Juvenile scallops (40–50 mm) were obtained from Taylor Seafood, Fairhaven, Connecticut. In each estuary we placed four plastic-coated wire cages, each containing 20 scallops. Cages were secured 10 cm above the sediment surface in 1 m of water at mean low tide.

To monitor the acquisition of the $\delta^{15}\text{N}$ signature in tissue and ejecta over time, we removed one cage of scallops from each estuary on days 3, 6, 12, and 24. Animals were immediately placed in filtered seawater for 24 hours to clear their guts. Feces and pseudofeces were filtered through pre-ashed, 7- μm Whatman

GF/F filters. Scallop tissue was dissected from the shell and dried at 60 °C overnight. Ejecta were acidified to remove carbonates, and samples not collected on filters were homogenized.

We determined the $\delta^{15}\text{N}$ signatures of potential food sources, particulate organic matter in water (POM, or seston) and sediments. In each estuary, we sampled the water column and sediments near the cages on days 0, 3, 6, 12, and 24. Water column samples were processed in the same manner as ejecta. The top 1 cm of sediment was sampled using a 5-cc syringe as a corer. We combined four sediment cores for each sample. Sediment samples were acidified and homogenized. All samples were analyzed using a Europa Scientific Integra mass spectrometer at the University of California-Davis.

To determine scallop growth over time, length of shells of animals from each cage were measured with vernier calipers accurate to 0.1 mm. The number of dead scallops per cage were counted on each collection day.

The $\delta^{15}\text{N}$ values of tissue from scallops grown in each estuary were initially 9.23‰ and during the course of the field incubation approached $\delta^{15}\text{N}$ values of POM in water and sediments, corrected by an expected trophic fractionation of 3‰ (4) (Fig. 1A, B). For example, if scallops in CR were feeding only on sediments, we extrapolate that the scallops, at the measured rate of change in tissue signature, would converge on the mean sediment signature (corrected by a 3‰ trophic fractionation) in 93 days. Similarly, if the scallops were feeding on only seston, the convergence would take place in 60 days. For the scallops in SLP, the convergence time would be shorter: 47 days and 36 days, respectively.

To examine whether scallops eject fractionated food particles, we compared the $\delta^{15}\text{N}$ signature of ejecta (feces + pseudofeces) to the $\delta^{15}\text{N}$ signature of food supply from each estuary. Lighter $\delta^{15}\text{N}$ signatures for food in SLP corresponded to lighter $\delta^{15}\text{N}$ signatures in ejecta from the scallops grown in SLP, while heavier $\delta^{15}\text{N}$ food signatures in CR corresponded to heavier ejecta signatures from the CR scallops (Fig. 1C). In both estuaries, the $\delta^{15}\text{N}$ signature of ejecta was equal to or heavier than that of potential food sources (Fig. 1C). In addition, $\delta^{15}\text{N}$ signatures of ejecta were lighter than $\delta^{15}\text{N}$ signatures of tissue in CR [8.75‰–9.85‰ (Fig. 1A)] and SLP [0.07‰–9.23‰ (Fig. 1B)]. The 2‰–3‰ enrichment from food to ejecta agrees with trophic level fractionation reported in the literature. The relative similarity between the $\delta^{15}\text{N}$ signatures of seston and sediments makes

¹ Mount Holyoke College

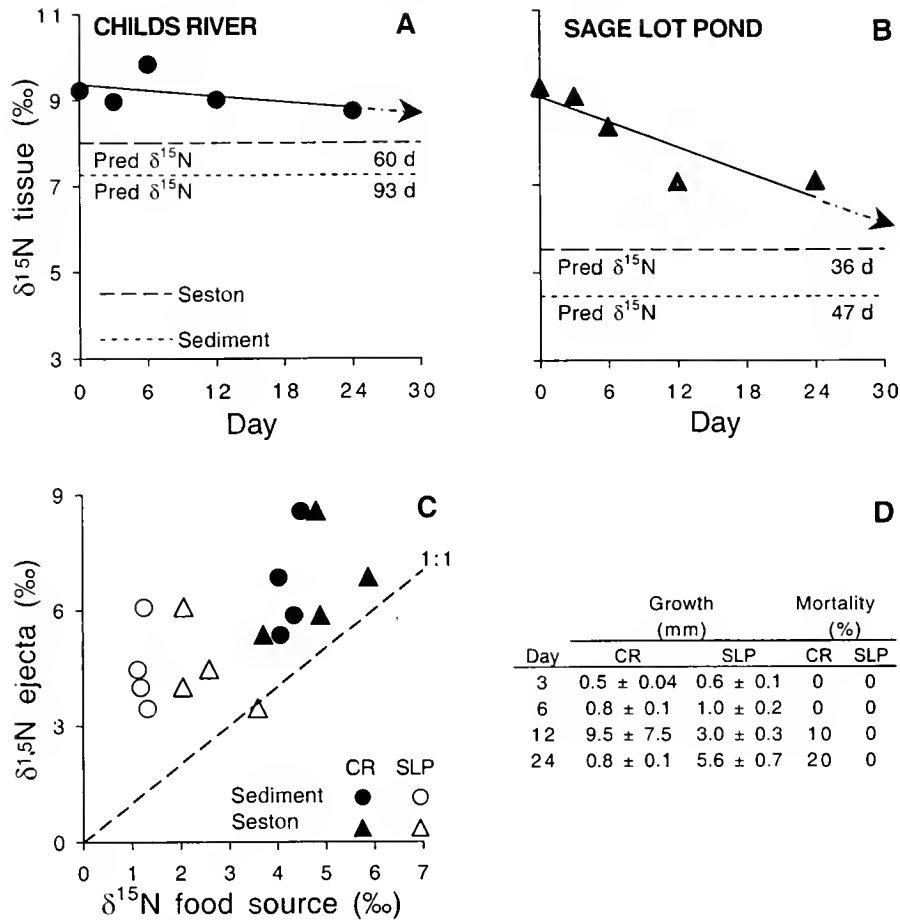


Figure 1. (A, B) $\delta^{15}\text{N}$ signature of tissue from scallops grown in Childs River (A) and Sage Lot Pond (B) vs. time. CR regression: $y = -0.02x + 9.37$, $F = 1.08$ ns. SLP regression: $y = -0.10x + 9.01$, $F = 10.85^*$. Predicted $\delta^{15}\text{N}$ signature lines for tissue are derived from mean seston and sediment signatures, +3% to correct for trophic shift. The lines represent predicted ultimate tissue signatures for scallops assuming exclusive consumption of either food source. (C) $\delta^{15}\text{N}$ signature of scallop ejecta (feces + pseudofeces) is generally heavier than that of food sources (seston and sediment). (D) Mean (\pm std. error) scallop growth (measured as cumulative change in shell length) and mortality over time, in each study estuary. Mean growth was calculated using a subsampling of the individuals in the cage ($n = 10$).

it difficult, however, to determine which food source contributed most to the diet of scallops during this study.

The faster rate at which SLP scallops approached predicted $\delta^{15}\text{N}$ signatures of their food sources (Fig. 1A, B) may be related to the faster growth of scallops in SLP (Fig. 1D). SLP scallops grew more quickly and achieved greater length than CR scallops (Fig. 1D). Mean growth rates (from incremental growth data) are 0.24 ± 0.03 mm/day for SLP, and 0.14 ± 0.01 mm/day for CR. In addition, no scallops in SLP died during the study, whereas those in CR reached 20% mortality by day 24 (Fig. 1D). The data suggest that conditions in CR were less favorable for scallops than conditions in SLP. This could be related to lower water quality in CR (7), which could have lowered feeding rate and possibly altered the rate of internal turnover of nitrogen within the scallop tissue.

Scallop $\delta^{15}\text{N}$ signatures moved toward the signatures of their presumed food sources at a rate suggesting they would converge with trophic-shift-corrected $\delta^{15}\text{N}$ food signatures in 1–3 months of

feeding. Material ejected by scallops had heavier $\delta^{15}\text{N}$ signatures than potential food signatures but lighter than tissue signatures. The increased wastewater N load in CR coincided with a slower convergence of tissue signatures to trophic-shift-corrected food signatures, lowered growth, and increased mortality.

Thanks to Marci Cole, Gabby Tomasky, Joanna York, and Marshall Otter for technical assistance, and the residents of 71 Childs River Road for providing site access. This work was supported by NSF-Research Experience for Undergraduates Grant OCE-0097498 and the Five College Coastal and Marine Sciences Program's participation in the Woods Hole Marine Sciences Consortium.

Literature Cited

1. Cahalan, J., S. E. Siddall, and M. W. Luckenback. 1989. *J. Exp. Mar. Biol. Ecol.* 129: 45–60.
2. Rheault, R. B., and M. A. Rice. 1996. *J. Shellfish Res.* 15: 271–283.

3. Valiela, I., G. Tomasky, J. Hauxwell, M. L. Cole, J. Cebrián, and K. D. Kroeger. 2000. *Ecol. Appl.* 10: 1006–1023.
4. Peterson, B., and B. Fry. 1987. *Annu. Rev. Ecol. Syst.* 18: 293–320.
5. McClelland, J., I. Valiela, and R. Michener. 1997. *Limnol. Oceanogr.* 42: 930–937.
6. Valiela, I., M. Geist, J. McClelland, and G. Tomasky. 2000. *Biogeochemistry* 49: 277–293.
7. Valiela, I., K. Foreman, M. LaMontagne, D. Hersh, J. Costa, P. Peckol, B. DeMeo-Anderson, C. D'Avanzo, M. Babione, C.-H. Sham, J. Brawley, and K. Lajtha. 1992. *Estuaries* 15: 433–457.

Reference: *Biol. Bull.* 201: 296–297. (October 2001)

Age Structure of the Pleasant Bay Population of *Crepidula fornicata*: A Possible Tool For Estimating Horseshoe Crab Age

Sara P. Grady, Deborah Rutecki, Ruth Carmichael, and Ivan Valiela (Boston University Marine Program,
Marine Biological Laboratory, Woods Hole, Massachusetts 02543)

Crepidula fornicata, the common slipper shell, lives on rocks, horseshoe crabs (*Limulus polyphemus*), and other hard surfaces, often in stacks of one animal atop another. Unlike many other gastropods, they tend to remain sessile, and as they grow, their shells contour to the substrate (1). The association between horseshoe crabs and *C. fornicata* offers the possibility to use the slipper shell as a tool to determine the ages and average lifespan of horseshoe crabs (2). Knowing this information would be helpful for trying to understand horseshoe crab ecology for use in conservation efforts.

It is difficult to directly estimate horseshoe crab age because horseshoe crabs lack any hard parts that could be sectioned and analyzed for growth rings. Their chitinous exoskeleton is molted with decreasing frequency until a theoretical "terminal molt" (3). There are also a variety of sizes within visually estimated age classes because growth is very slow or stops in adults (3).

Other methods have been suggested for aging horseshoe crabs, including qualitative aging criteria and tagging studies. From the results of tagging studies it has been estimated that horseshoe crabs live 9 to 12 years before maturity and 5 to 7 years as adults, for a total lifespan of 14 to 19 years (4). These age spans are consistent with the prediction of Botton and Ropes (2) based on laboratory work using *C. fornicata* as a proxy for horseshoe crab age.

C. fornicata could indicate age of host horseshoe crabs if 1) horseshoe crabs have a terminal molt or do not molt often as adults, 2) *C. fornicata* remain on the same horseshoe crab, and 3) *C. fornicata* age can be determined with some degree of accuracy (5). It is also assumed that *C. fornicata* attach to a host horseshoe crab as soon as the new cuticle hardens.

Botton and Ropes (2) used a regression proposed by Walne (1) of *C. fornicata* length to age to quantitatively estimate the ages of horseshoe crabs. These *C. fornicata* were used to formulate this regression without comparison to a local population of horseshoe crabs, since the *C. fornicata* data was from England and horseshoe crabs were not measured at all.

In this study we measured shell length of *C. fornicata* and prosomal width of *Limulus polyphemus* in Pleasant Bay, Chatham, Massachusetts. We measured 496 crabs and their corresponding *C. fornicata*, with the number of *C. fornicata* per crab ranging widely from 1 to 30, with an average of 4 per crab. From these data we fitted cohorts of *C. fornicata* to a size-frequency distribution. We also related size of *C. fornicata* to prosomal width of *L.*

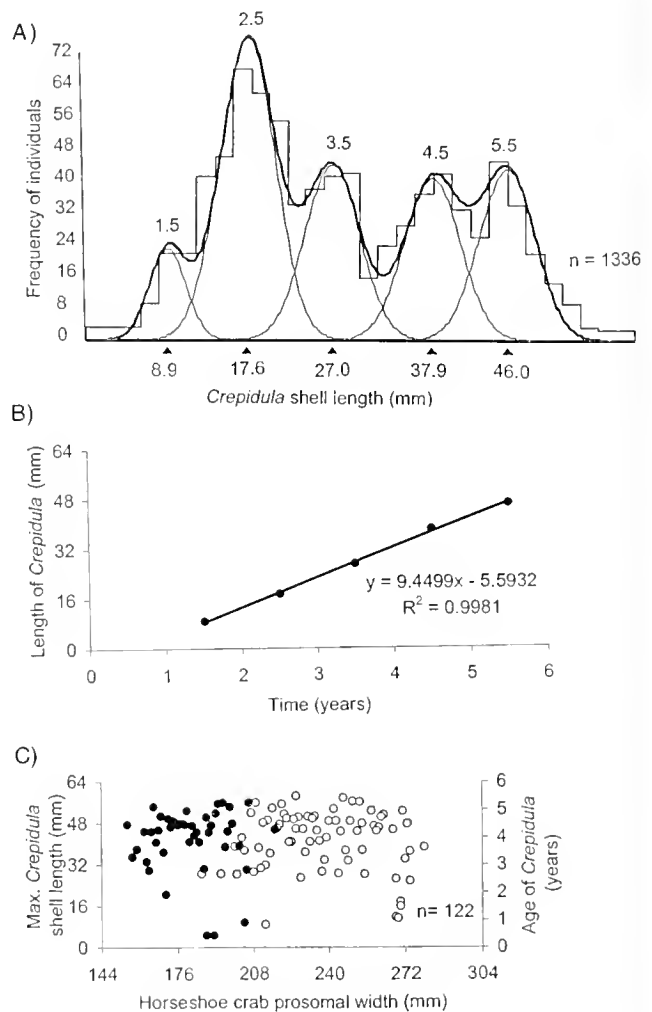


Figure 1. (A) Cohorts of Pleasant Bay population of *Crepidula fornicata*: 8.9 mm (~1.5 y), 17.6 mm (~2.5 y), 27.0 mm (~3.5 y), 37.9 mm (~4.5 y), and 46.0 mm (~5.5 y). (B) *C. fornicata* length vs. age; extrapolation data from Botton and Ropes (2). (C) Length of largest *C. fornicata* on horseshoe crabs of different prosomal width. Filled circles (●) represent males, open circles (○) represent females.

polyphemus to see if *C. fornicata* could provide a proxy for *L. polyphemus* size and age.

The analysis of cohorts demonstrated that *C. fornicata* in Pleasant Bay can be divided into 5 size cohorts (Fig. 1A), with *C. fornicata* of approximately 4–6 mm in length appearing to represent the most recent spatfall. The cohorts differed in abundance, reflecting different magnitudes of recruitment from year to year. Growth rates in this study did not decrease with increased size and age (Fig. 1B). This may be due to low numbers of larger (50 mm +) and older *C. fornicata*. Published data of sizes and ages (1, 2) match those found in this study, and thus confirm the conversion from size to age of the *C. fornicata*. The largest *C. fornicata* found resident on a horseshoe crab was 58 mm. This size *C. fornicata* could be from 8–11 years old (2).

There was no evident relationship between maximum length and age of *C. fornicata* and size of the host horseshoe crabs (Fig. 1C). Male horseshoe crabs were consistently smaller than females, but in both sexes the length and presumed age of *C. fornicata* varied greatly, and was independent of the size of the crab.

It is not possible to establish a strong relationship between true horseshoe crab length and the length of the *C. fornicata* upon it. At most the data of Figure 1C support that a minimum age can be calculated by adding the maximum *C. fornicata* length on a given horseshoe crab to the minimum age of horseshoe crabs at maturity. Using 9 years as the age at maturity (4), the crabs in this study were from 12 to 17 years old.

This study was funded by the Woods Hole Marine Science Consortium and a grant from the Friends of Pleasant Bay.

Literature Cited

1. Walne, P. R. 1956. *Fish. Investig.* 6: 1–50.
2. Botton, M. L., and J. W. Ropes. 1988. *J. Shellfish Res.* 7: 407–412.
3. Shuster, C. 1950. Third rept. investigations of methods of improving the shellfish resources of Massachusetts. *WHOI Contr. No. 564*: 18–23.
4. Shuster, C. 1982. Pp. 1–52 in *Physiology and Biology of Horseshoe Crabs*. Alan R. Liss, New York.
5. Ropes, J. 1961. *Trans. Am. Fish. Soc.* 90: 79–80.

Reference: *Biol. Bull.* 201: 297–299. (October 2001)

Hydrogen Peroxide: An Effective Treatment for Ballast Water

Alan M. Kuzirian, Eleanor C. S. Terry, Deanna L. Bechtel, (Marine Biological Laboratory, Woods Hole, Massachusetts 02543), and Patrick L. James¹

Introduced species have been a problem in the marine and coastal environments for centuries. Historically, many of these introductions have a strong geophysical component often associated with natural disasters. However, in more recent times, “man, the supreme meddler” (1) has dramatically changed the rate, number, and geography of exotic species invasions through importation, transportation, intentional releases related to agriculture or aquaculture, as well as unintentional escapes. During the last century, the problem has dramatically accelerated with the advent of modern high-speed freighters and their methods of ballast water exchange.

Transport and discharge of biocontaminated ballast water constitutes a major route (29%) by which potentially invasive species—from plants and algae to fish, invertebrates, planktonic and bacterial micro-organisms, and even potential pathogens—are introduced into coastal waters worldwide. It is estimated that 3000 species are transported daily *via* ballast water (National Research Council, 2000). The Great Lakes have experienced the introduction of at least 129 non-indigenous species (2), while the San Francisco Bay estuary has recorded 234 exotic species with at least an additional 125 cryptogenic species (3). At the current estimated rate, a new species is introduced into the ecosystem every 14 weeks (3).

The problem is not confined to the United States but occurs worldwide. One noteworthy example is the introduction of the western Atlantic ctenophore, *Mnemiopsis leidyi*, into the Black and Azov Seas in 1987 and 1988, respectively. This invader has been

blamed for a 20-fold decrease in zooplankton biomass, the subsequent sharp decline in anchovy and other pelagic fish stocks, and a marked disruption in these ecosystems (4).

The United Nations International Maritime Organization (IMO), established in 1991, developed a voluntary ballast water exchange (BWE) at sea policy that has now become mandatory (5). BWE is carried out either by draining and refilling the ballast tanks or by continuous flushing equivalent to three volume exchanges. The policy is based upon the rationale that coastal organisms will not survive at sea and vice versa, so BWE is simpler, less costly, and thus preferable to controls implemented before departure or upon arrival (*i.e.*, land-based treatments). Unfortunately, BWE is only 90%–95% effective, and the exchange itself can be dangerous in foul weather or can produce excessive hull stress. Therefore, alternative ballast water treatments are being sought.

Some current technologies available for ballast water treatment include filtration, cyclone or hydrotech-drum settling, UV, ultrasonics, and heat. Additional secondary treatment methods include biocides, ozone, electric pulse or pulse plasma, deoxygenation, and biological. Some of the biocidal methods involve the storage of dangerous chemicals and cause unacceptably high levels of corrosion (*e.g.*, hypochlorite). However, hydrogen peroxide, generated on-site at low (safe) concentrations, precludes these hazards and is more cost-effective than the sophisticated and high-energy-demanding equipment necessary for ozone generation. Neutral hydrogen peroxide has been effective in a number of studies, but only at moderately high concentrations (10–50 ppm; [6]), for planktonic and some small neustonic organisms. Because most marine organisms and bacteria cannot tolerate pH extremes (7), hydrogen peroxide combined with elevated pH (alkaline hydrogen

¹ Eltron Research, Inc., Boulder, CO.

peroxide) has the potential to produce synergistic effects useful for treating ballast water. Since alkaline peroxide has not been investigated for this application, and it is the consequence of the proposed generating process, we undertook a toxicological laboratory study to test the effects of alkaline peroxide on plankton. This study is designed to complement the development of an electrolytic cell (based on patented technology [8]) that is capable of producing alkaline hydrogen peroxide. An upscale design of the cell has been proposed for use onboard ship to treat ballast water to reduce the potential introduction of invasive species.

Plankton were collected from the local waters off Woods Hole, Massachusetts, by the Aquatic Resources Department of the Marine Biological Laboratory (MBL). Indigenous zooplankters (Table 1) were used in this study. The faunal composition of the plankton varied between collections, but the majority were dominated by crustaceans, both planktonic adults and larvae of benthic species. Particular attention was directed toward the effects of alkaline peroxide on the ctenophore, *Mnemiopsis leidyi*, a known invasive species (see above), which made up over 90% of many plankton collections.

The following treatment regimes were tested: 1) natural seawater (NSW) at elevated pH (using NaOH, 8.5, 9.0, 9.5, or 10); and 2) NSW at the four elevated pHs with the addition of 1, 3, or 10 ppm (=mg/l) of hydrogen peroxide (3% USP grade). Hydrogen peroxide was added first, the pH adjusted (with NaOH), and the solutions allowed to equilibrate for 30 min (the solution at pH 10 with 10 ppm peroxide precipitated and was removed from the testing matrix). The pH was re-adjusted before the addition of mixed zooplankton (minimum of 25 animals/condition). Times for 50% (LD50) and 100% mortality (mortality time) were recorded. Mortality time was defined as the point when all of the plankton species ceased movement and became unresponsive to tactile stimuli. To ensure the accuracy of mortality time determinations, all animals were returned to NSW (via serial dilution) after each treatment to test for recovery. LD50s were also calculated and compared with mortality times; the values averaged 43% of the 100% mortality times. Since 100% mortality was the desired outcome, the data were reported using that method. Plankton left in

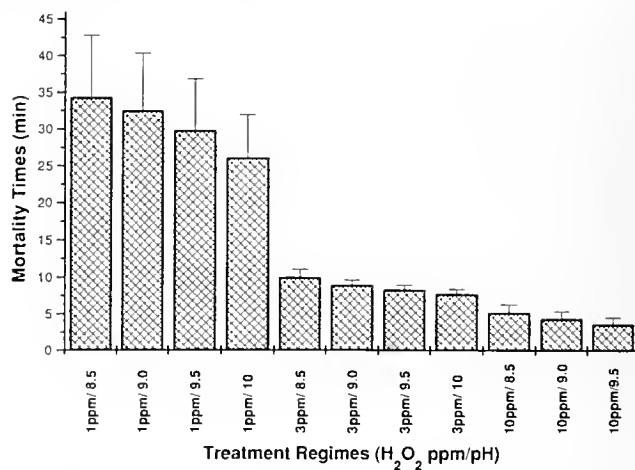


Figure 1. Combined effects of pH and peroxide on mixed plankton. Mortality times (i.e., time to 100% mortality) were recorded when all swimming activity had ceased and all of the animals were unresponsive to tactile stimuli. Animals were subsequently placed in natural seawater (NSW) and observed for recovery as a test of these end points. No recovery was observed.

NSW (pH 7.8–8.0) served as controls. There were at least six replicates for each treatment.

The ctenophore, *Mnemiopsis leidyi*, was tested with the same treatment regimes. Because of their size and buoyancy, even when dead, for accuracy it was necessary to record mortality times when the compound cilia of the comb rows and the cilia in the digestive tract both ceased beating. The test animals were placed back into NSW and observed for signs of recovery. All data were analyzed statistically using ANOVA or Student's *t* paired comparisons.

Plankton placed in NSW with elevated pHs all survived for at least 24 h, and the majority of those in pH 8.5–9.5 were alive for as long as three days. Only those animals at pH 10 did not survive beyond 24 h. *Mnemiopsis* responded similarly.

When solutions containing mixed plankton and alkaline peroxide were tested, no significant differences were found between pH values within each peroxide concentration (ANOVA: *F* values < 2; *P* > 0.2) (Fig. 1). However, for each peroxide concentration, there were significant decreases in mortality times (Student's *t* paired comparisons: *t* > 4.7; *P* < 0.001). Similar results were obtained with *Mnemiopsis*; i.e., there were no pH effects within each peroxide concentration (ANOVA: *F* < 1.8; *P* > 0.15). However, increases in peroxide concentrations significantly shortened mortality times (Fig. 2). When animals were placed in 10 ppm peroxide, beating of all the comb rows immediately stopped; and within seconds, the activity of the digestive cilia also ceased. Therefore, the effects of this concentration were not graphed. The difference between the means of the two peroxide concentrations (1 and 3 ppm) was highly significant, with Student's *t* value *t* > 11.5 with *P* < 0.001.

The results indicate that, up to pH 10, the increased alkalinity has little toxic effect on either mixed plankton or ctenophores; and survivorship after 24 h was equal to NSW controls. Hydrogen peroxide, even at 1 ppm, had a mean (100%) mortality time of 30 min for mixed plankton samples; and for the ctenophores, the times were even shorter ($\times 3.7$). Peroxide at 3 ppm was three times

Table 1

List of major taxa of species present in the mixed plankton samples

Phylum Cnidaria	<i>Ovalipes ocellatus</i>
Class Hydrozoa	(zoa, megalops stages)
<i>Pennaria</i> sp. (Medusae)	Procellanid zoea
	Calanoid copepods
Phylum Ctenophora	Euphausiids, spp.
<i>Mnemiopsis leidyi</i>	Mysid shrimp, spp.
Phylum Annelida	Phylum Mollusca
Class Polychaeta	Class Bivalvia
<i>Platynereis</i> sp.	Various larval spp.
(epitoke stages and eggs)	
Phylum Arthropoda	Phylum Chordata
Class Crustacea	Class Osteichthyes
<i>Homarus americanus</i>	Syngnathidae sp.
(advanced larval stages)	Various larval spp.

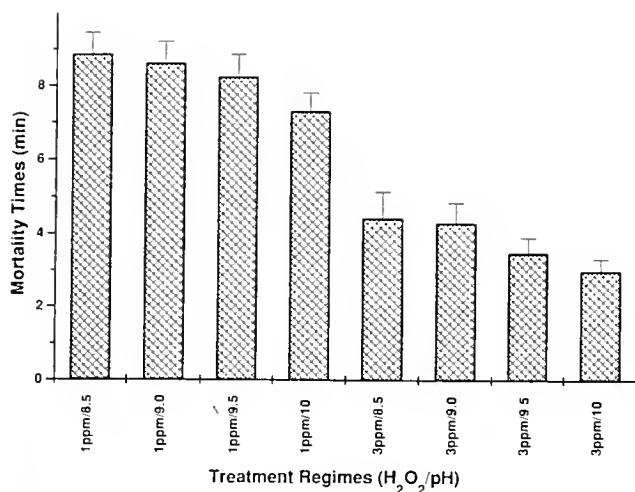


Figure 2. Effects of pH and peroxide concentrations on the ctenophore, *Mnemiopsis leidyi*.

more efficient at disinfection than 1 ppm for plankton and approximately twice as effective for the comb jellies. When 10 ppm peroxide was used with mixed plankton, the mortality times decreased again, this time at twice the rate. The within-treatment variance was extremely low for both the 3- and 10-ppm peroxide, and thus the means between the two treatment regimes were highly significant. For the ctenophore *Mnemiopsis*, 10-ppm peroxide was essentially lethal upon contact (<1 min).

In summary, the data from these tests indicate that NSW at pHs slightly elevated above that of ambient, and containing concentrations of 1 ppm hydrogen peroxide, can be lethal to plankton composed of a wide phylogenetic mix of species (Table 1). It was

interesting to discover that a concentration of 3-ppm peroxide has effects comparable to ozone levels (2.2 ppm) when tested on larvae of the nudibranch mollusc, *Hermisenda crassicornis* (9). The short exposures (*i.e.*, mortality times) required at this concentration of peroxide should encourage the development and implementation of an onboard electrolytic system capable of generating the required peroxide levels at rates sufficient to treat ballast water of ships during uptake at sea or in coastal waters. This device would provide an efficient, low-energy cost treatment for ballast water, and would preclude the bulk and danger of storing concentrated biocide chemicals on board ships.

This research was supported by a Phase I, SBIR/EPA grant (68-D-01-017) to Eltron Research, Inc.

Literature Cited

1. Laycock, G. 1966. *The Alien Animals*. Natural History Press, Garden City, NY.
2. Mills, E. L., J. H. Leach, J. T. Carlton, and C. L. Secor. 1993. *J. Great Lakes Res.* **19**: 1-54.
3. Cohen, A. N., and J. T. Carlton. 1998. *Science* **279**: 555-558.
4. Kideys, A. E. 1994. *J. Mar. Syst.* **5**: 171-181.
5. Carlton, J. T. 1992. Pp. 23-26 in *Introductions and Transfers of Marine Species*, R. DeVoe, ed. South Carolina Sea Grant Consortium, Charleston, SC.
6. Laughton, R., T. Moran, and G. Brown, n.d. *Pollutech Technical Papers* [Online]. Available: <http://www.pollutech.com/papers/p22.htm> [22 August 2001].
7. Oemcke, D. 1999. *The Treatment of Ship's Ballast Water*. Ecoports Monography Series 18. Ports Corporation of Queensland, Brisbane. P. 102.
8. White, J., M. Schultz, and A. Sammells. 1997. United States Patent, US-5645700.
9. Kuzirian, A. M., C. T. Tamse, and M. Heath. 1990. *Biol. Bull.* **179**: 227.

Published by Title Only

Aldrich, Stephen, R. Gil Pontius, Jr., Takashi Tada, and Luc Claessens

Influence of land use on nitrate loading in the Ipswich River Watershed, Massachusetts

Clay, John

Action potentials occur spontaneously in squid giant axons with moderately alkaline intracellular pH

Denton, Jerod, and J. C. Leiter

Identification of CO₂-chemosensitive and non-chemosensitive neurons in the right parietal ganglion of the pulmonate snail, *Helix aspersa*

Heck, Diane, Lydia Louis, and Jeffrey Laskin

17-beta-estradiol modulates gastrulation in the sea urchin *Arbacia punctulata*

Jaffe, Lionel

Action potential velocities along working heart muscles are highly conserved and may be calcium based

Martel, David, Rainer Voigt, and Jelle Atema

The *Limulus* worm (*Bdelloura candida*) prefers individual horseshoe crab (*Limulus polyphemus*) odor

Unis, Jennifer, Christopher Neill, and Richard McHorney

Predicting groundwater flow rate at Edgartown Great Pond on Martha's Vineyard, Massachusetts: salinity and groundwater flow at the seepage face of a coastal pond

Biomimetic Engineering Conference

March 3-8, 2002

Sandestin, Florida

Biological organisms exhibit sophisticated crystal engineering capabilities that underlie the remarkable material properties of mineralized tissues such as bone and teeth, and the beautiful and functional nacre of molluscs and abalone. Increasing interest is being paid to nature's processing strategies, particularly by materials scientists looking for bio-inspired methods to engineer unique ceramics coatings or composites for use in magnetic, optical, biomedical, and protective coatings applications. In particular, the engineering of hard tissues may benefit from biomimetic approaches since the benign conditions allow for the incorporation of biomolecular compounds into the organic/inorganic composite during fabrication.

On the other hand, there is great interest from the biomedical community because the disruption of normal biomineralization processes may lead to pathological conditions, such as in arteriosclerotic plaque formation, encrustation of biomaterials (such as urinary catheters and artificial heart valve calcification), kidney stone buildup, dental calculus formation, or bone and tooth demineralization.

The main objective of this conference is to bring together scientists, physicians, and engineers in a relaxed environment, with talks designed to bridge the gap between researchers in this interdisciplinary field.

This groundbreaking conference will have sessions that deal with (a) Biomineralization in Nature: Vertebrates and Invertebrates (Inspiration for Design Principles), (b) Organic Modulators of Crystallization: Templated Nucleation and Crystal Growth Modification, (c) Engineering Strategies: Bioinspired Materials and Novel Physicochemical Properties, and (d) Applications of Biomimetic Materials: Devices and Processes.

Each day will open with a keynote address to highlight the day's topics; each of the sessions will include eight to ten presentations, with afternoons left free for ad hoc meetings and informal discussions. An evening poster session will also promote dialogue among the attendees.

The Chair of the Conference is Dr. Allison A. Campbell of the Pacific Northwest National Laboratory in Richland, Washington, and the Co-Chair is Prof. Laurie Gower of the University of Florida in Gainesville.

Additional information about this Conference — and a registration form — can be found at www.engfnd.org.

The United Engineering Foundation is located at Three Park Avenue, 27th Floor, New York, NY 10016-5902; Tel: 212-591-7836, Fax: 212-591-7441, E-mail: engfnd@aol.com

MARINE RESOURCES CENTER

MARINE BIOLOGICAL LABORATORY • WOODS HOLE, MA 02543 • (508)289-7700

WWW.MBL.EDU/SERVICES/MRC/INDEX.HTML



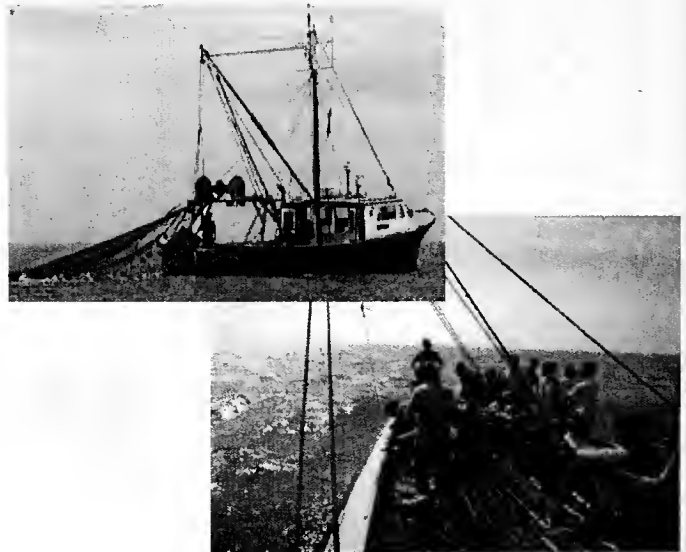
zebrafish facilities

Animal and Tissue Supply for Education & Research

- 150 aquatic species available for shipment via online catalog: <<http://www.mbl.edu/animals/index.html>>; phone: (508)289-7375; or e-mail: specimens@mbi.edu
- zebrafish colony containing limited mutant strains
- custom dissection and furnishing of specific organ and tissue samples

MRC Services Available

- basic water quality analysis
- veterinary services (clinical, histopathologic, microbial services, health certificates, etc.)
- aquatic systems design (mechanical, biological, engineering, etc.)
- educational tours and collecting trips aboard the R/V Gemma



Using the MRC for Your Research

- capability for advanced animal husbandry (temperature, light control, etc.)
- availability of year-round, developmental life stages
- adaptability of tank system design for live marine animal experimentation



What makes our bio-imaging software great? The people behind the product.



Senior Application Scientist Dr. Neal Gliksman assists customers during the May 2001 Customer Training Course at Universal Imaging Institute.

With the growing complexity of applications and devices, bio-imaging has never been more challenging.

That's why educators call on us to support imaging courses at Marine Biological Laboratory, Cold Spring Harbor Laboratory, Mt. Desert Island Biological Laboratory and other locations. They want the best for their students and we give them our best.

Only Universal Imaging provides this level of complete coverage to so many courses. Our customers see this dedication every day. In the world of bio-imaging support, no one is as Universal.

To register for our next course, go to www.universal-imaging.com/resources/training.cfm

Come see us at
**the Society for Neuroscience
30th Annual Meeting
San Diego, CA
Booth 1042**



UNIVERSAL IMAGING CORPORATION
Working to Improve Your Image
www.universal-imaging.com/people
610-873-5610

Software and Systems for:

- 6-D Imaging
- Brightness Measurements
- Colocalization
- Cell-based Screening
- Intracellular Calcium, pH, etc. Ratio Imaging
- FRET
- Morphometry
- Motion Analysis
- Time-Lapse and more...

Makers of



MetaMorph®

Marine Biological Laboratory

2002 Course Offerings

Advances In Genome Technology & Bioinformatics

October 6 - November 1

Analytical & Quantitative Light Microscopy

May 9 - May 17

Biology of Parasitism: Modern Approaches

June 13 - August 10

Embryology: Concepts & Techniques In Modern Developmental Biology

June 16 - July 27

Frontiers In Reproduction: Molecular & Cellular Concepts & Applications

May 19 - June 29

Fundamental Issues In Vision Research

August 11 - August 24

Medical Informatics

1st Session: May 26 - June 2

2nd Session: September 29 - October 6

Methods In Computational Neuroscience

August 4 - September 1

Microbial Diversity

June 16 - August 2

Microinjection Techniques In Cell Biology

May 21 - May 28

Molecular Biology of Aging

July 30 - August 17

Molecular Mycology: Current Approaches to Fungal Pathogenesis

August 12 - August 30



Substantial financial assistance is available for many of our courses!

For more information contact:

Carol Hamel,
Admissions Coordinator
(508) 289-7401
admissions@mbledu
<http://courses.mbl.edu>

The MBL is an EEO/Affirmative Action Institution

Neural Development & Genetics of Zebrafish

August 18 - August 31

Neural Systems & Behavior

June 16 - August 10

Neurobiology

June 16 - August 17

Neuroinformatics

August 17 - September 1

Optical Microscopy & Imaging In the Biomedical Sciences

October 9 - October 18

Physiology: The Biochemical & Molecular Basis of Cell Signaling

June 16 - July 27

Rapid Electrochemical Measurements In Biological Systems


May 9 - May 13

Summer Program In Neuroscience, Ethics, & Survival (SPINES)

June 15 - July 13

Workshop on Molecular Evolution

July 28 - August 9



ZEISS
LSM 510 META

Opening

doors to new worlds

The Next Generation:

Laser Scanning Microscope LSM 510
META for multi-channel fluorescence
in single and multiphoton microscopy

META - a unique confocal
microscope detector will separate
overlapping fluorescence dyes
for sharp, crosstalk free images.

Apioplan 2
imaging

Carl Zeiss MicroImaging, Inc.
One Zeiss Drive
Thornwood, NY 10594

1.800.233.2343
micro@zeiss.com
www.zeiss.com/micro



Volume 201

Number 3

THE BIOLOGICAL BULLETIN



DECEMBER 2001

Published by the Marine Biological Laboratory

<http://www.biolbull.org>





THE BIOLOGICAL BULLETIN ONLINE

The Marine Biological Laboratory is pleased to announce that the full text of *The Biological Bulletin* is available online at

<http://www.biolbull.org>

The Biological Bulletin publishes outstanding experimental research on the full range of biological topics and organisms, from the fields of Neurobiology, Behavior, Physiology, Ecology, Evolution, Development and Reproduction, Cell Biology, Biomechanics, Symbiosis, and Systematics.

Published since 1897 by the Marine Biological Laboratory (MBL) in Woods Hole, Massachusetts, *The Biological Bulletin* is one of America's oldest peer-reviewed scientific journals.

The journal is aimed at a general readership, and especially invites articles about those novel phenomena and contexts characteristic of intersecting fields.

The Biological Bulletin Online contains the full content of each issue of the journal, including all figures and tables, beginning with the February 2001 issue (Volume 200, Number 1). The full text is searchable by keyword, and the cited references include hyperlinks to Medline. PDF files are available beginning in February 2000 (Volume 198,

Number 1), some abstracts are available beginning with the October 1976 issue (Volume 151, Number 2), and some Tables of Contents are online beginning with the October 1965 issue (Volume 129, Number 2).

Each issue will be placed online approximately on the date it is mailed to subscribers; therefore the online site will be available prior to receipt of your paper copy. Online readers may want to sign up for the eTOC (electronic Table of Contents) service, which will deliver each new issue's table of contents *via* e-mail. The web site also provides access to information about the journal (such as Instructions to Authors, the Editorial Board, and subscription information), as well as access to the Marine Biological Laboratory's web site and other publications.

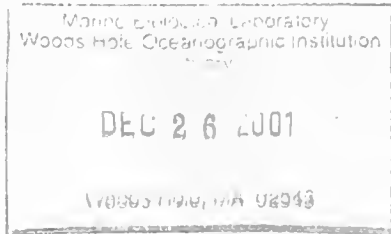
There is currently a free trial period for access to *The Biological Bulletin*. Once the free trial period ends on January 31, 2002, individuals and institutions who are subscribers to the journal in print or are members of the Marine Biological Laboratory Corporation will be able to activate an online subscription. All other access (*e.g.*, to Abstracts, eTOCs, searching, Instructions to Authors) will remain freely available. Online access will be included in the print subscription price.

<http://www.biolbull.org>

Made to my exact specifications.



Here's how the BX2's modular design came through for me. First, the 8 position universal condenser offers the flexibility to choose from brightfield, darkfield and phase. Next, it's assortment of DIC prisms makes it possible to match the optical image shear to the specimen, achieving the optimal balance of contrast and resolution. Finally, the motorized nosepiece, Z-drive, condenser, illuminator and filter wheels are fully integrated through the user-friendly software package. So digital images can now be acquired, processed and analyzed faster than before. Now let's move on.



And yours. And yours.



Picture yourself sitting here, looking into your Olympus BX2 research microscope, your fluorescence requirements having been met. Specifically: The aspherical collector lens produces a fluorescence intensity that's twice as bright as others. The unique excitation balancers improve visualization of multiple labels. The six-position filter turret makes single and multiband imaging faster and simpler. And the rectangular field stop, another Olympus exclusive, protects the specimen by exposing only the precise area being imaged. With all this modularity and flexibility, my BX2 microscope is also your BX2 microscope.



Now modularity really comes into play. The Olympus FLUOVIEW laser scanning microscope offers 5 imaging channels, intuitive operation and high productivity. The BX2 is the only confocal microscope with a Metal Matrix Condenser, static and thermal stability for use of 3D microscopy, time-lapse observation and high-end digital imaging, resulting in a complete confocal system. It's the optimal solution.

BX²

Research Microscope Series

OLYMPUS
FOCUS ON LIFE

Visit us at www.olympusamerica.com or call 1-800-451-8236.

Cover

Two striking features of the open ocean are the lack of obvious physical features and the extraordinary clarity of the water, in which visibility extends to about 100 meters. Animals that live in this pelagic realm are, of course, extremely vulnerable to being seen, identified as food, and eaten. To meet the challenge of predation, oceanic animals have evolved various tactics for hiding in an environment that precludes hiding. Effective adaptations include counterillumination, countershading, and mirrored sides; but the most apt mechanism is surely whole-body transparency—an emulation of the habitat. Therefore, although transparency is rare on land or in coastal waters, it is extremely common in the open ocean and is closely tied to the pelagic lifestyle.

On the cover of this issue is a photograph of an octopus, *Vitreledonella richardi*, which spends its entire life swimming in the subtropical and tropical regions of the world's oceans at depths of 200–1000 meters. Not only are most of its tissues highly transparent, but it is further modified for camouflage: its non-transparent elongated gut and eyes are continually oriented vertically and thus cast a min-

imal shadow toward potential predators that may be cruising below. (Credits: photo by David Wrobel, Monterey Bay Aquarium).

For many years, the biology of animals like *Vitreledonella* was completely overlooked. Most transparent species are fragile, and they are therefore destroyed by the sampling nets deployed from oceanographic vessels. In a sense, therefore, these cryptic organisms were hidden from biologists, as well as from their predators. The development of manned and robotic submersibles, blue water diving techniques, and optical equipment that is both portable and reliable has greatly increased our knowledge of these animals and their transparency.

In this issue, Sönke Johnsen reviews our current understanding of biological transparency. This field—still in its infancy—includes empirical studies by marine and fresh-water biologists, but especially work on such camouflage-breaking visual abilities as ultraviolet and polarization vision. Theoretical and empirical research into the physical basis of biological transparency is also being carried out, much of it driven by the need to prevent and treat lapses in ocular transparency, such as cataracts.

THE BIOLOGICAL BULLETIN

DECEMBER 2001

Editor	MICHAEL J. GREENBERG	The Whitney Laboratory, University of Florida
Associate Editors	LOUIS E. BURNETT R. ANDREW CAMERON CHARLES D. DERBY MICHAEL LABARBERA	Grice Marine Biological Laboratory, College of Charleston California Institute of Technology Georgia State University University of Chicago
Section Editor	SHINYA INOUÉ, <i>Imaging and Microscopy</i>	Marine Biological Laboratory
Online Editors	JAMES A. BLAKE, <i>Keys to Marine Invertebrates of the Woods Hole Region</i> WILLIAM D. COHEN, <i>Marine Models Electronic Record and Compendia</i>	ENSR Marine & Coastal Center, Woods Hole Hunter College, City University of New York
Editorial Board	PETER B. ARMSTRONG ERNEST S. CHANG THOMAS H. DIETZ RICHARD B. EMLET DAVID EPEL KENNETH M. HALANYCH GREGORY HINKLE NANCY KNOWLTON MAKOTO KOBAYASHI ESTHER M. LEISE DONAL T. MANAHAN MARGARET MCFALL-NGAI MARK W. MILLER TATSUO MOTOKAWA YOSHITAKA NAGAHAMA SHERRY D. PAINTER J. HERBERT WAITE RICHARD K. ZIMMER	University of California, Davis Bodega Marine Lab., University of California, Davis Louisiana State University Oregon Institute of Marine Biology, Univ. of Oregon Hopkins Marine Station, Stanford University Woods Hole Oceanographic Institution Cereon Genomics, Cambridge, Massachusetts Hiroshima University of Economics, Japan Scripps Inst. Oceanography & Smithsonian Tropical Res. Inst. University of North Carolina Greensboro University of Southern California Kewalo Marine Laboratory, University of Hawaii Institute of Neurobiology, University of Puerto Rico Tokyo Institute of Technology, Japan National Institute for Basic Biology, Japan Marine Biomed. Inst., Univ. of Texas Medical Branch University of California, Santa Barbara University of California, Los Angeles
Editorial Office	PAMELA CLAPP HINKLE VICTORIA R. GIBSON CAROL SCHACHINGER WENDY CHILD	Managing Editor Staff Editor Editorial Associate Subscription & Advertising Secretary

Published by
MARINE BIOLOGICAL LABORATORY
WOODS HOLE, MASSACHUSETTS

<http://www.biolbull.org>

Genomic Research Leaders Choose Microway® Scalable Clusters

Eos Biotechnology, Marine Biological Laboratory, Millennium Pharmaceuticals, Mount Sinai Medical School, NIH, Pfizer, and Rockefeller University All Choose Microway Custom Clusters and Workstations for Reliability, Superior Technical Support and Great Pricing.

- 1.4 GHz Dual Athlon, 1.7 GHz Pentium 4, or 1 GHz Dual Pentium III in 1U or 2U Clusters
- Dual Alpha 833 MHz Clusters and Towers
For maximum price/performance choose our Alpha 1U 833 MHz, 4 MB DDR Cache CS20, 4U UP2000+ or 4U 264DP RuggedRack™
- Myrinet, Gigabit Ethernet or Dolphin Wulffkit High Speed Low Latency Interconnects
- RAID and Fibre Channel Storage Solutions

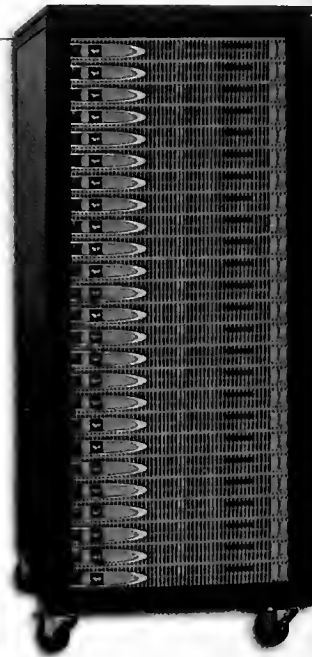


Microway® Screamer™
Dual Alpha UP2000-
833 MHz, 4MB Cache in
RuggedRack™ Chassis
with RRR™ Redundant
Power Supply

Microway has earned an excellent reputation since 1982. If you need a quality product that is fine tuned and built to last, from a company that will be around to support you for years to come, Microway is The Number One Choice.

Microway has delivered high-performance computing products since 1982, when our pioneering software made it possible to use an 8087 in the IBM-PC. In 1987 we created the world's first PC parallel processing systems. Since then, our QuadPuter™ architecture has migrated from Transputers to i860s and finally to Alphas in 1995. Over the past three years, we engineered and delivered over 300 clusters that utilized MPI running on Linux. As a software developer and hardware manufacturer, we know the value of extensive testing and validation. We are experts at configuring and validating the low latency interconnects we employ in our clusters. Our technical support is legendary — the systems we sell arrive at your site and WORK! Los Alamos chose Microway to maintain and upgrade its I44 node Alpha Avalon Cluster because of our reputation. Large clusters we have sold include 400+ nodes at the University of Wisconsin and 250+ nodes at Rockefeller University.

Microway offers three Athlon/Pentium enclosures—1U, 2U and tower, plus five Alpha configurations—1U, 3U, 4U RuggedRack™, QuadPuter™ and full tower. Our 264DP includes two 21264's with up to 4 GB of memory in our custom 4U RuggedRack, which features front accessible redundant power supplies and hard disks. This rugged configuration was chosen by the U.S. Navy for onboard use. We also offer a dual Alpha UP2000+ running at 833MHz with 2GB of memory. Our QuadPuter chassis holds 4 Alpha processors and up to 4GB memory. The 1U CS20 dual Alpha (at right) is the highest density computational platform available.



"Most Powerful, Highest Density Computational Platform On the Planet"

Microway Scalable 25 Node
50 Processor Cluster Using CS20 Dual
833 MHz Alphas and Myrinet Interconne
Yielding Peak Throughput of 82.5 Gigaflo

Microway is API-Networks' Top North American Channel Partner.



"I have ordered numerous Alpha and Intel-based servers and workstations from Microway running both Tru64 UNIX and Linux. We have been very happy with both the performance and great value of Microway's products. The major UNIX vendors don't come close to Microway in this regard, and we have also found that Microway provides better value than other Linux hardware vendors. I have also used Microway's tech support and was pleased with their response. We've been using their systems for over a year and have had only a couple of minor incidents which were dealt with promptly."

— David Kristofferson, Ph.D., MBA,
Director of Information Systems, Eos Biotechnology, Inc.

Find out why over 75% of Microway's sales come from repeat customers. Please call 508-746-7341 for a technical salesperson who speaks your language!

Visit us at www.microway.com



Microway
Technology you can count on™

CONTENTS

VOLUME 201, No. 3: DECEMBER 2001

REVIEW

- Johnsen, Sönke**
Hidden in plain sight: the ecology and physiology of
organismal transparency 301

RESEARCH NOTE

- Hibbett, David S., and Manfred Binder**
Evolution of marine mushrooms. 319

CELL BIOLOGY

- Leys, Sally P., and Bernard M. Degnan**
Cytological basis of photoresponsive behavior in a
sponge larva. 323

PHYSIOLOGY AND BIOMECHANICS

- Shimomura, Osamu, Per R. Flood, Satoshi Inouye,
Bruce Bryan, and Akemi Shimomura**
Isolation and properties of the luciferase stored in
the ovary of the scyphozoan medusa *Periphylla pe-
riphylla*. 339

SYMBIOSIS AND PARASITOLOGY

- Toller, W. W., R. Rowan, and N. Knowlton**
Zooxanthellae of the *Montastraea annularis* species
complex: patterns of distribution of four taxa of *Sym-
biodinium* on different reefs and across depths 348
- Toller, W. W., R. Rowan, and N. Knowlton**
Repopulation of zooxanthellae in the Caribbean corals
Montastraea annularis and *M. faveolata* following
experimental and disease-associated bleaching. 360

ECOLOGY AND EVOLUTION

- Helmuth, Brian S. T., and Gretchen E. Hofmann**
Microhabitats, thermal heterogeneity, and patterns
of physiological stress in the rocky intertidal zone. 374
- Rossi, Sergi, and Mark J. Snyder**
Competition for space among sessile marine inverte-
brates: changes in HSP70 expression in two Pacific
cnidarians 385

DEVELOPMENT AND REPRODUCTION

- Bishop, Cory D., and Bruce P. Brandhorst**
NO/cGMP signaling and HSP90 activity repress
metamorphosis in the sea urchin *Lytechinus pictus*. 394
- Furuya, Hidetaka, F. G. Hochberg, and Kazuhiko Tsuneki**
Developmental patterns and cell lineages of vermi-
form embryos in dicyemid mesozoans 405
- Kossevitch, Igor A., Klaus Herrmann, and Stefan Berking**
Shaping of colony elements in *Laomedea flexuosa*
Hinks (Hydrozoa, Thecaphora) includes a temporal
and spatial control of skeleton hardening 417

NEUROBIOLOGY AND BEHAVIOR

- Dufort, Christopher G., Steven H. Jury, James M. Newcomb,
Daniel F. O'Grady III, and Winsor H. Watson III**
Detection of salinity by the lobster, *Homarus america-
nus*. 424
- * * *
- Index for Volume 201** 435

THE BIOLOGICAL BULLETIN

THE BIOLOGICAL BULLETIN is published six times a year by the Marine Biological Laboratory, 7 MBL Street, Woods Hole, Massachusetts 02543.

Subscriptions and similar matter should be addressed to Subscription Manager, THE BIOLOGICAL BULLETIN, Marine Biological Laboratory, 7 MBL Street, Woods Hole, Massachusetts 02543. Subscription per year (six issues, two volumes): \$260 for libraries; \$105 for individuals. Subscription per volume (three issues): \$130 for libraries; \$52.50 for individuals. Back and single issues (subject to availability): \$45 for libraries; \$20 for individuals.

Communications relative to manuscripts should be sent to Michael J. Greenberg, Editor-in-Chief, or Pamela Clapp Hinkle, Managing Editor, at the Marine Biological Laboratory, 7 MBL Street, Woods Hole, Massachusetts 02543. Telephone: (508) 289-7428. FAX: 508-289-7922. E-mail: pclapp@mbl.edu.

<http://www.biobull.org>

THE BIOLOGICAL BULLETIN is indexed in bibliographic services including *Index Medicus* and MEDLINE, *Chemical Abstracts*, *Current Contents*, *Elsevier BIOBASE/Current Awareness in Biological Sciences*, and *Geo Abstracts*.

Printed on acid free paper,
effective with Volume 180, Issue 1, 1991.

POSTMASTER: Send address changes to THE BIOLOGICAL BULLETIN, Marine Biological Laboratory, 7 MBL Street, Woods Hole, MA 02543.

Copyright © 2001, by the Marine Biological Laboratory
Periodicals postage paid at Woods Hole, MA, and additional mailing offices.
ISSN 0006-3185

INSTRUCTIONS TO AUTHORS

The Biological Bulletin accepts outstanding original research reports of general interest to biologists throughout the world. Papers are usually of intermediate length (10–40 manuscript pages). A limited number of solicited review papers may be accepted after formal review. A paper will usually appear within four months after its acceptance.

Very short, especially topical papers (less than 9 manuscript pages including tables, figures, and bibliography) will be published in a separate section entitled "Research Notes." A Research Note in *The Biological Bulletin* follows the format of similar notes in *Nature*. It should open with a summary paragraph of 150 to 200 words comprising the introduction and the conclusions. The rest of the text should continue on without subheadings, and there should be no more than 30 references. References should be referred to in the text by number, and listed in the Literature Cited section in the order that they appear in the text. Unlike references in *Nature*, references in the Research Notes section should conform in punctuation and arrangement to the style of recent issues of *The Biological Bulletin*. Materials and Methods should be incorporated into appropriate figure legends. See the article by Lohmann *et al.* (October 1990, Vol. 179: 214–218) for sample style. A Research Note will usually appear within two months after its acceptance.

The Editorial Board requests that regular manuscripts conform to the requirements set below; those manuscripts that do not conform will be returned to authors for correction before review.

1. **Manuscripts.** Manuscripts, including figures, should be submitted in quadruplicate, with the originals clearly marked. (Xerox copies of photographs are not acceptable for review purposes.) The submission letter accompanying the manuscript should include a telephone number, a FAX number, and (if possible) an E-mail address for the corresponding author. The original manuscript must be typed in no smaller than 12 pitch or 10 point, using double spacing (*including* figure legends, footnotes, bibliography, etc.) on one side of 16- or 20-lb. bond paper, 8 by 11 inches. Please, no right justification. Manuscripts should be proofread carefully and errors corrected legibly in black ink. Pages should be numbered consecutively. Margins on all sides should be at least 1 inch (2.5 cm). Manuscripts should conform to the *Council of Biology Editors Style Manual*, 5th Edition (Council of Biology Editors, 1983) and to American spelling. Unusual abbreviations should be kept to a minimum and should be spelled out on first reference as well as defined in a footnote on the title page. Manuscripts should be divided into the following components: Title page, Abstract (of no more than 200 words), Introduction, Materials and Methods, Results, Discussion, Acknowledgments, Literature Cited, Tables, and Figure Legends. In addition, authors should supply a list of words and phrases under which the article should be indexed.

2. **Title page.** The title page consists of a condensed title or running head of no more than 35 letters and spaces, the manuscript title, authors' names and appropriate addresses, and footnotes

listing present addresses, acknowledgments or contribution numbers, and explanation of unusual abbreviations.

3. **Figures.** The dimensions of the printed page, 7 by 9 inches, should be kept in mind in preparing figures for publication. We recommend that figures be about 1 times the linear dimensions of the final printing desired, and that the ratio of the largest to the smallest letter or number and of the thickest to the thinnest line not exceed 1:1.5. Explanatory matter generally should be included in legends, although axes should always be identified on the illustration itself. Figures should be prepared for reproduction as either line cuts or halftones. Figures to be reproduced as line cuts should be unmounted glossy photographic reproductions or drawn in black ink on white paper, good-quality tracing cloth or plastic, or blue-lined coordinate paper. Those to be reproduced as halftones should be mounted on board, with both designating numbers or letters and scale bars affixed directly to the figures. All figures should be numbered in consecutive order, with no distinction between text and plate figures and cited, in order, in the text. The author's name and an arrow indicating orientation should appear on the reverse side of all figures.

Digital art: *The Biological Bulletin* will accept figures submitted in electronic form; however, digital art must conform to the following guidelines. Authors who create digital images are wholly responsible for the quality of their material, including color and halftone accuracy.

Format. Acceptable graphic formats are TIFF and EPS. Color submissions must be in EPS format, saved in CMKY mode.

Software. Preferred software is Adobe Illustrator or Adobe Photoshop for the Mac and Adobe Photoshop for Windows. Specific instructions for artwork created with various software programs are available on the Web at the Digital Art Information Site maintained by Cadmus Professional Communications at <http://cpc.cadmus.com/dal/>

Resolution. The minimum requirements for resolution are 1200 DPI for line art and 300 for halftones.

Size. All digital artwork must be submitted at its actual printed size so that no scaling is necessary.

Multipanel figures. Figures consisting of individual parts (e.g., panels A, B, C) must be assembled into final format and submitted as one file.

Hard copy. Files must be accompanied by hard copy for use in case the electronic version is unusable.

Disk identification. Disks must be clearly labeled with the following information: author name and manuscript number; format (PC or Macintosh); name and version of software used.

Color: *The Biological Bulletin* will publish color figures and plates, but must bill authors for the actual additional cost of printing in color. The process is expensive, so authors with more than one color image should—consistent with editorial concerns, especially citation of figures in order—combine them into a single plate to reduce the expense. On request, when supplied with a copy of a color illustration, the editorial staff will provide a pre-publication estimate of the printing cost.

4. **Tables, footnotes, figure legends, etc.** Authors should follow the style in a recent issue of *The Biological Bulletin* in

preparing table headings, figure legends, and the like. Because of the high cost of setting tabular material in type, authors are asked to limit such material as much as possible. Tables, with their headings and footnotes, should be typed on separate sheets, numbered with consecutive Roman numerals, and placed after the Literature Cited. Figure legends should contain enough information to make the figure intelligible separate from the text. Legends should be typed double spaced, with consecutive Arabic numbers, on a separate sheet at the end of the paper. Footnotes should be limited to authors' current addresses, acknowledgments or contribution numbers, and explanation of unusual abbreviations. All such footnotes should appear on the title page. Footnotes are not normally permitted in the body of the text.

5. **Literature cited.** In the text, literature should be cited by the Harvard system, with papers by more than two authors cited as Jones *et al.*, 1980. Personal communications and material in preparation or in press should be cited in the text only, with author's initials and institutions, unless the material has been formally accepted and a volume number can be supplied. The list of references following the text should be headed Literature Cited, and must be typed double spaced on separate pages, conforming in punctuation and arrangement to the style of recent issues of *The Biological Bulletin*. Citations should include complete titles and inclusive pagination. Journal abbreviations should normally follow those of the U. S. A. Standards Institute (USASI), as adopted by BIOLOGICAL ABSTRACTS and CHEMICAL ABSTRACTS, with the minor differences set out below. The most generally useful list of biological journal titles is that published each year by BIOLOGICAL ABSTRACTS (BIOSIS List of Serials; the most recent issue). Foreign authors, and others who are accustomed to using THE WORLD LIST OF SCIENTIFIC PERIODICALS, may find a booklet published by the Biological Council of the U.K. (obtainable from the Institute of Biology, 41 Queen's Gate, London, S.W.7, England, U.K.) useful, since it sets out the WORLD LIST abbreviations for most biological journals with notes of the USASI abbreviations where these differ. CHEMICAL ABSTRACTS publishes quarterly supplements of additional abbreviations. The following points of reference style for THE BIOLOGICAL BULLETIN differ from USASI (or modified WORLD LIST) usage:

A. Journal abbreviations, and book titles, all underlined (for italics)

B. All components of abbreviations with initial capitals (not as European usage in WORLD LIST e.g., *J. Cell. Comp. Physiol.*, NOT *J. cell. comp. Physiol.*)

C. All abbreviated components must be followed by a period, whole word components *must not* (i.e., *J. Cancer Res.*)

D. Space between all components (e.g., *J. Cell. Comp. Physiol.*, not *J.Cell.Comp.Physiol.*)

E. Unusual words in journal titles should be spelled out in full, rather than employing new abbreviations invented by the author. For example, use *Rit Vísindafjélag Íslendinga* without abbreviation.

F. All single word journal titles in full (e.g., *Veliger*, *Ecology*, *Brain*).

G. The order of abbreviated components should be the same as the word order of the complete title (*i.e.*, *Proc.* and *Trans.* placed where they appear, not transposed as in some BIOLOGICAL ABSTRACTS listings).

H. A few well-known international journals in their preferred forms rather than WORLD LIST or USASI usage (*e.g.*, *Nature*, *Science*, *Evolution* NOT *Nature, Lond.*, *Science, N.Y.*; *Evolution, Lancaster, Pa.*)

6. **Reprints, page proofs, and charges.** Authors may purchase reprints in lots of 100. Forms for placing reprint orders are sent with page proofs. Reprints normally will be delivered about 2 to 3 months after the issue date. Authors (or delegates for foreign authors) will receive page proofs of articles shortly before publication. They will be charged the current cost of printers' time for corrections to these (other than corrections of printers' or editors' errors). Other than these charges for authors' alterations, *The Biological Bulletin* does not have page charges.

CONTENTS for Volume 201

No. 1: AUGUST 2001

RESEARCH NOTE

- Seibel, Brad A., and David B. Carlini**
Metabolism of pelagic cephalopods as a function of habitat depth: a reanalysis using phylogenetically independent contrasts 1

NEUROBIOLOGY AND BEHAVIOR

- Herberholz, Jens, and Barbara Schmitz**
Signaling *via* water currents in behavioral interactions of snapping shrimp (*Alpheus heterochaelis*) 6

PHYSIOLOGY AND BIOMECHANICS

- Reddy, P. Sreenivasula, and B. Kishori**
Methionine-enkephalin induces hyperglycemia through eyestalk hormones in the estuarine crab *Scylla serrata* 17
- Mogami, Yoshihiro, Junko Ishii, and Shoji A. Baba**
Theoretical and experimental dissection of gravity-dependent mechanical orientation in gravitactic microorganisms 26

SYMBIOSIS AND PARASITOLOGY

- Hanten, Jeffrey J., and Sidney K. Pierce**
Synthesis of several light-harvesting complex 1 polypeptides is blocked by cycloheximide in symbiotic chloroplasts in the sea slug, *Elysia chlorotica* (Gould): A case for horizontal gene transfer between alga and animal? 34
- McCurdy, Dean G.**
Asexual reproduction in *Pygospio elegans* Claparède (Annelida, Polychaeta) in relation to parasitism by *Lepocreadium setiferoides* (Miller and Northup) (Platyhelminthes, Trematoda) 45

DEVELOPMENT AND REPRODUCTION

- Stewart-Savage, J., Aimee Phillippi, and Philip O. Yund**
Delayed insemination results in embryo mortality in a brooding ascidian 52

CELL BIOLOGY

- Ballarin, Lorian, Antonella Franchini, Enzo Ottaviani, and Armando Sabbadin**
Morula cells as the major immunomodulatory hemocytes in ascidians: evidences from the colonial species *Botryllus schlosseri* 59

ECOLOGY AND EVOLUTION

- Halanych, Kenneth M., Robert A. Feldman, and Robert C. Vrijenhoek**
Molecular evidence that *Sclerolinum brattstromi* is closely related to vestimentiferans, not to frenulate pogonophorans (Siboglinidae, Annelida) 65
- Ponczek, Lawrence M., and Neil W. Blackstone**
Effect of cloning rate on fitness-related traits in two marine hydroids 76
- Meidel, Susanne K., and Philip O. Yund**
Egg longevity and time-integrated fertilization in a temperate sea urchin (*Strongylocentrotus droebachiensis*) 84
- Wares, J. P.**
Biogeography of *Asterias*: North Atlantic climate change and speciation. 95

SYSTEMATICS

- Gershwin, Lisa-ann**
Systematics and biogeography of the jellyfish *Aurelia labiata* (Cnidaria: Scyphozoa) 104

* * *

- Annual Report of the Marine Biological Laboratory R1**

No. 2: OCTOBER 2001

RESEARCH NOTE

- Maier, Ingo, Christian Hertweck, and Wilhelm Boland**
Stereochemical specificity of lamoxirene, the sperm-releasing pheromone in kelp (Laminariales, Phaeophyceae) 121

PHYSIOLOGY AND BIOMECHANICS

- Johnson, Amy S.**
Drag, drafting, and mechanical interactions in canopies of the red alga *Chondrus crispus* 126

- Thompson, Joseph T., and William M. Kier**
Ontogenetic changes in fibrous connective tissue organization in the oval squid, *Sepioteuthis lessoniana* Lesson, 1830 136

- Thompson, Joseph T., and William M. Kier**
Ontogenetic changes in mantle kinematics during escape jet locomotion in the oval squid, *Sepioteuthis lessoniana* Lesson, 1830 154

- Martinez, Anne-Sophie, Jean-Yves Toullec, Bruce Shillito, Mireille Charmantier-Daures, and Guy Charmantier**
Hydromineral regulation in the hydrothermal vent crab *Bythograea thermydron* 167

NEUROBIOLOGY AND BEHAVIOR

- Campbell, A. C., S. Coppard, C. D'Abreo, and R. Tudor-Thomas**
Escape and aggregation responses of three echinoderms to conspecific stimuli 175

- Clay, John R., and Alvin Shrier**
Action potentials occur spontaneously in squid giant axons with moderately alkaline intracellular pH 186

SYSTEMATICS

- Dahlgren, Thomas G., Bertil Åkesson, Christoffer Schander, Kenneth M. Halanych, and Per Sundberg**
Molecular phylogeny of the model annelid *Ophryotrocha* 193

ECOLOGY AND EVOLUTION

- Rondeau, Amélie, and Bernard Sainte-Marie**
Variable mate-guarding time and sperm allocation by male snow crabs (*Chionoecetes opilio*) in response to sexual competition, and their impact on the mating success of females 204

BIOGRAPHY

- Zottoli, Steven J.**
The origins of The Grass Foundation 218

SHORT REPORTS FROM THE 2001 GENERAL SCIENTIFIC MEETINGS OF THE MARINE BIOLOGICAL LABORATORY

FEATURED REPORT

- The Editors**
Introduction to the featured report. green fluorescent protein: enhanced optical signals from native crystals 231

- Inoué, Shinya, and Makoto Goda**
Fluorescence polarization ratio of GFP crystals. 231

CELL BIOLOGY

- Knudson, Robert A., Shinya Inoué, and Makoto Goda**
Centrifuge polarizing microscope with dual specimen chambers and injection ports 234

- Tran, P. T., and Fred Chang**
Transmitted light fluorescence microscopy revisited. 235

- Hernandez, R. V., J. M. Garza, M. E. Graves, J. L. Martinez, Jr., and R. G. LeBaron**
The process of reducing CA1 long-term potentiation by the integrin binding peptide, GRGDSP, occurs within the first few minutes following theta-burst stimulation. 236

- Kuhns, William J., Dario Rusciano, Jane Kaltenbach, Michael Ho, Max Burger, and Xavier Fernandez-Busquets**
Up-regulation of integrins $\alpha_3 \beta_1$ in sulfate-starved marine sponge cells: functional correlates 238

- Brown, Jeremiah R., Kyle R. Simonetta, Leslie A. Sandberg, Phillip Stafford, and George M. Langford**
Recombinant globular tail fragment of myosin-V blocks vesicle transport in squid nerve cell extracts 240

- Wöllert, Torsten, Ana S. DePina, Leslie A. Sandberg, and George M. Langford**
Reconstitution of active pseudo-contractile rings and myosin-II-mediated vesicle transport in extracts of clam oocytes 241

- Clay, John R., and Alan M. Kuzirian**
A novel, kinesin-rich preparation derived from squid giant axons 243

- Weidner, Earl**
Microsporidian spore/sporoplasm dynactin in *Spraguea* 245

- Conrad, Mara L., R. L. Pardy, and Peter B. Armstrong**
Response of the blood cell of the American horseshoe crab, *Limulus polyphemus*, to a lipopolysaccharide-like molecule from the green alga *Chlorella*. 246

- Silver, Robert**
LiB₄ evokes the calcium signal that initiates nuclear envelope breakdown through a multi-enzyme network in sand dollar (*Echinarracnius parma*) cells 248

DEVELOPMENTAL BIOLOGY

- Crawford, Karen**
Ooplasm segregation in the squid embryo, *Loligo pealeii*. 251

- Burbach, J. Peter H., Anita J. C. G. M. Hellemons, Marco Hoekman, Philip Grant, and Harish C. Pant**
The stellate ganglion of the squid *Loligo pealeii* as a model for neuronal development: expression of a POU Class VI homeodomain gene, *Rpf-1* 252

Link, Brian A.
Evidence for directed mitotic cleavage plane reorientations during retinal development within the zebrafish 254

Smith, Ryan, Emma Kavanagh, Hilary G. Morrison, and Robert M. Gould
Messenger RNAs located in spiny dogfish oligodendrocyte processes 255

Hill, Susan D., and Barbara C. Boyer
Phalloidin labeling of developing muscle in embryos of the polychaete *Capitella* sp. I. 257

Rice, Aaron N., David S. Portnoy, Ingrid M. Kaatz, and Phillip S. Lobel
Differentiation of pharyngeal muscles on the basis of enzyme activities in the cichlid *Tramitichromis intermedius* 258

NEUROBIOLOGY

Twig, Gilad, Sung-Kwon Jung, Mark A. Messerli, Peter J. S. Smith, and Orian S. Shirihai
Real-time detection of reactive oxygen intermediates from single microglial cells 261

Silver, Robert B., Mahlon E. Kriebel, Bruce Keller, and George D. Pappas
Porocytosis: Quantal synaptic secretion of neurotransmitter at the neuromuscular junction through arrayed vesicles 263

Chappell, Richard L., and Stephen Redenti
Endogenous zinc as a neuromodulator in vertebrate retina: evidence from the retinal slice 265

Shashar, Nadav, Douglas Borst, Seth A. Ament, William M. Saidel, Roxanna M. Smolowitz, and Roger T. Hanlon
Polarization reflecting iridophores in the arms of the squid *Loligo pealeii* 267

Chiao, Chuan-Chin, and Roger T. Hanlon
Cuttlefish cue visually on area—not shape or aspect ratio—of light objects in the substrate to produce disruptive body patterns for camouflage 269

Errigo, M., C. McGuinness, S. Meadors, B. Mittmann, F. Dodge, and R. Barlow
Visually guided behavior of juvenile horseshoe crabs 271

Meadors, S., C. McGuinness, F. A. Dodge, and R. B. Barlow
Growth, visual field, and resolution in the juvenile *Limulus* lateral eye 272

Kozlowski, Corinne, Kara Yopak, Rainer Voigt, and Jelle Atema
An initial study on the effects of signal intermittency on the odor plume tracking behavior of the American lobster, *Homarus americanus* 274

Hall, Benjamin, and Kerry Delaney
Cholinergic modulation of odor-evoked oscillations in the frog olfactory bulb 276

Zottoli, S. J., D. E. W. Arnolds, N. O. Asamoah, C. Cbevez, S. N. Fuller, N. A. Hiza, J. E. Nierman, and L. A. Taboada
Dye coupling evidence for gap junctions between supramedullary/dorsal neurons of the cunner, *Tautoglabrus adspersus* 277

Kaatz, Ingrid M., and Phillip S. Lobel
A comparison of sounds recorded from a catfish (*Orinocodoras eigenmanni*, Doradidae) in an aquarium and in the field 278

Fay, R. R., and P. L. Edds-Walton
Bimodal units in the torus semicircularis units of the toadfish (*Opsanus tau*) 280

MARICULTURE

Mensingher, Allen F., Katherine A. Stephenson, Sarah L. Pollema, Hazel E. Richmond, Nichole Price, and Roger T. Hanlon
Mariculture of the toadfish *Opsanus tau* 282

Rieder, Leila E., and Allen F. Mensinger
Strategies for increasing growth of juvenile toadfish 283

Chikarmane, Hemant M., Alan M. Kuzirian, Ian Carroll, and Robbin Dengler
Development of genetically tagged bay scallops for evaluation of seeding programs 285

ECOLOGY AND POPULATION BIOLOGY

Williams, Libby, G. Carl Noblitt IV, and Robert Buchsbaum
The effects of salt marsh haying on benthic algal biomass 287

Hinckley, Eve-Lyn S., Christopher Neill, Richard McHorney, and Ann Lezberg
Dissolved nitrogen dynamics in groundwater under a coastal Massachusetts forest 288

Hauxwell, Alyson M., Christopher Neill, Ivan Valiela, and Kevin D. Kroeger
Small-scale heterogeneity of nitrogen concentrations in groundwater at the seepage face of Edgartown Great Pond 290

Novak, Melissa, Mark Lever, and Ivan Valiela
Top down vs. bottom-up controls of microphytobenthic standing crop: role of mud snails and nitrogen supply in the littoral of Waquoit Bay estuaries 292

Fila, Laurie, Ruth Herrold Carmichael, Andrea Shriver, and Ivan Valiela
Stable N isotopic signatures in bay scallop tissue, feces, and pseudofeces in Cape Cod estuaries subject to different N loads 294

Grady, Sara P., Deborah Rutecki, Ruth Carmichael, and Ivan Valiela
Age structure of the Pleasant Bay population of *Crepidula fornicata*: a possible tool for estimating horseshoe crab age 296

Kuzirian, Alan M., Eleanor C. S. Terry,
Deanna L. Bechtel, and Patrick I. James

Hydrogen peroxide: an effective treatment for ballast
water 297

Published by title only 300

No. 3: DECEMBER 2001

REVIEW

Johnsen, Sönke
Hidden in plain sight: the ecology and physiology of
organismal transparency 301

RESEARCH NOTE

Hibbett, David S., and Manfred Binder
Evolution of marine mushrooms. 319

CELL BIOLOGY

Leys, Sally P., and Bernard M. Degnan
Cytological basis of photoresponsive behavior in a
sponge larva. 323

PHYSIOLOGY AND BIOMECHANICS

Shimomura, Osamu, Per R. Flood, Satoshi Inouye,
Bruce Bryan, and Akemi Shimomura
Isolation and properties of the luciferase stored in
the ovary of the scyphozoan medusa *Periphylla pe-
riphylla* 339

SYMBIOSIS AND PARASITOLOGY

Toller, W. W., R. Rowan, and N. Knowlton
Zooxanthellae of the *Montastraea annularis* species
complex: patterns of distribution of four taxa of *Sym-
biodinium* on different reefs and across depths 348

Toller, W. W., R. Rowan, and N. Knowlton
Repopulation of zooxanthellae in the Caribbean cor-
als *Montastraea annularis* and *M. faveolata* following
experimental and disease-associated bleaching. . . . 360

ECOLOGY AND EVOLUTION

Helmuth, Brian S. T., and Gretchen E. Hofmann
Microhabitats, thermal heterogeneity, and patterns
of physiological stress in the rocky intertidal zone. . . 374

Rossi, Sergi, and Mark J. Snyder
Competition for space among sessile marine inverte-
brates: changes in HSP70 expression in two Pacific
cnidarians 385

DEVELOPMENT AND REPRODUCTION

Bishop, Cory D., and Bruce P. Brandhorst
NO/cGMP signaling and HSP90 activity repress
metamorphosis in the sea urchin *Lytechinus pictus*. . . 394

Furuya, Hidetaka, F. G. Hochberg, and Kazuhiko Tsuneki
Developmental patterns and cell lineages of vermi-
form embryos in dicyemid mesozoans 405

Kossevitch, Igor A., Klaus Herrmann, and Stefan Berking
Shaping of colony elements in *Laomedea flexuosa*
Hinks (Hydrozoa, Thecaphora) includes a temporal
and spatial control of skeleton hardening 417

NEUROBIOLOGY AND BEHAVIOR

Dufort, Christopher G., Steven H. Jury, James M. Newcomb,
Daniel F. O'Grady III, and Winsor H. Watson III
Detection of salinity by the lobster, *Homarus america-
nus*. 424

* * *

Index for Volume 201 435

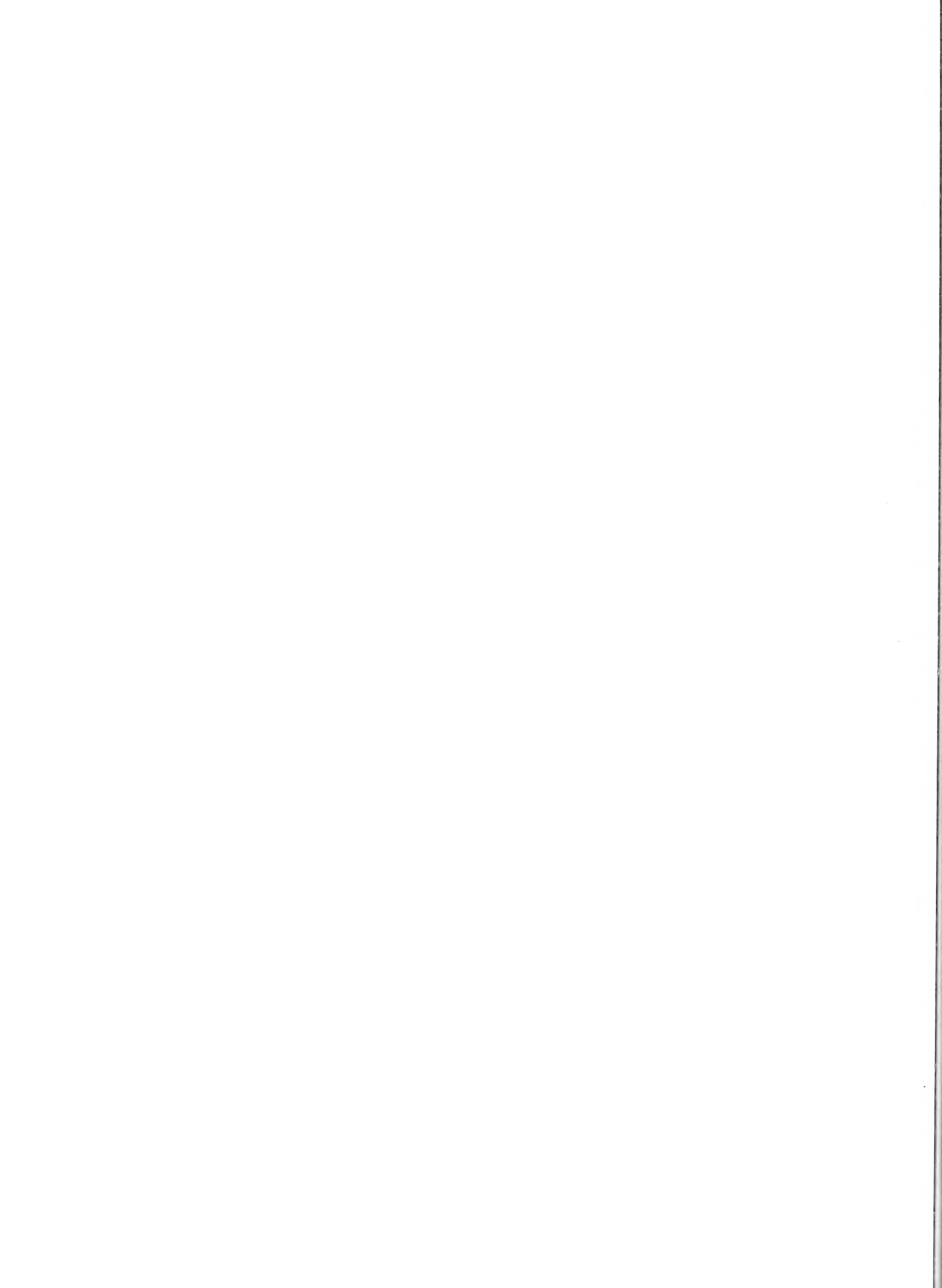
Notice to Subscribers

2002 SUBSCRIPTION RATES FOR *THE BIOLOGICAL BULLETIN*

Prices include print and electronic versions

	Libraries	Individuals
Per year (six issues, two volumes):	\$260.00	\$105.00
Per volume (three issues):	\$130.00	\$ 52.50
Back and single issues: (subject to availability)	\$ 45.00	\$ 20.00

For additional information, please contact our subscription secretary at the Marine Biological Laboratory, 7 MBL Street, Woods Hole, MA 02543; tel: (508) 289-7402; e-mail: wchild@mbl.edu. Visit our new website at www.biolbull.org



Hidden in Plain Sight: The Ecology and Physiology of Organismal Transparency

SÖNKE JOHNSEN*

Biology Department, Woods Hole Oceanographic Institution, Woods Hole, Massachusetts

Abstract. Despite the prevalence and importance of transparency in organisms, particularly pelagic species, it is a poorly understood characteristic. This article reviews the current state of knowledge on the distribution, ecology, and physical basis of biological transparency. Particular attention is paid to the distribution of transparent species relative to their optical environment, the relationship between transparency and visual predation, the physics of transparency, and what is known about the anatomical and ultrastructural modifications required to achieve this condition. Transparency is shown to be primarily a pelagic trait, uncommon in other aquatic habitats and extremely rare on land. Experimental and theoretical studies in terrestrial, freshwater, and marine ecosystems have shown that transparency is a successful form of camouflage, and that several visual adaptations seem to counter it. The physical basis of transparency is still poorly understood, but anatomical observations and mathematical models show that there are various routes to transparency. Future avenues for research include examination of the ultrastructure and optical properties of transparent tissue, exploring the link between transparent species and special visual modifications in the species they interact with, and analysis of the evolution of transparency using comparative methods.

Introduction

Transparency is a fascinating and surprisingly common characteristic that has received little attention because the majority of transparent species are found only in the pelagic regions of the open ocean. In these regions, however, the prevalence and diversity of transparent species is remarkable, ranging from the relatively well-known medusae and

ctenophores to transparent polychaetes, gastropods, and fish (Fig. 1). Transparency is one of the few forms of camouflage possible in a habitat with no surfaces to match or hide behind. It is also the only form of camouflage, and one of the few adaptations, that involve the entire organism. Although the importance of transparency has been mentioned many times by pelagic ecologists, it is a relatively unstudied characteristic (Hardy, 1956; Fraser, 1962; McFall-Ngai, 1990; Meyer-Rochow, 1997).

This review synthesizes the current knowledge on the distribution, ecology, and physical basis of biological transparency. It is divided into five sections. The first section reviews the phylogenetic distribution of transparent species. The second section reviews and attempts to explain the relationship between transparent species and their optical environment. The third section links transparency to visibility; reviews terrestrial, freshwater, and marine studies of transparency and visual predation, including the use of special visual adaptations; and lists known active uses of transparency. The fourth section presents the underlying optical principles of transparency and then applies these principles to the various anatomical and ultrastructural modifications seen in transparent tissues. The final section suggests several avenues for future research.

Phylogenetic Distribution

The phylogenetic distribution of transparent animals is diverse, uneven, and strongly influenced by environment. Although significant levels of tissue transparency are found in a wide array of organisms (Figs. 1, 2), most transparent species are found in the following 10 groups, all of which are pelagic: cubozoans, hydromedusae, non-beroid ctenophores, hyperiid amphipods, tomopterid polychaetes, pterotracheid and carinariid heteropods, pseudothecosomatous pteropods, cranchiid squid, thaliaceans, and chaetognaths.

Received 30 May 2001; accepted 30 August 2001.

* Current address: Biology Department, Box 90338, Duke University, Durham, NC 27708. E-mail: sjohnsen@duke.edu

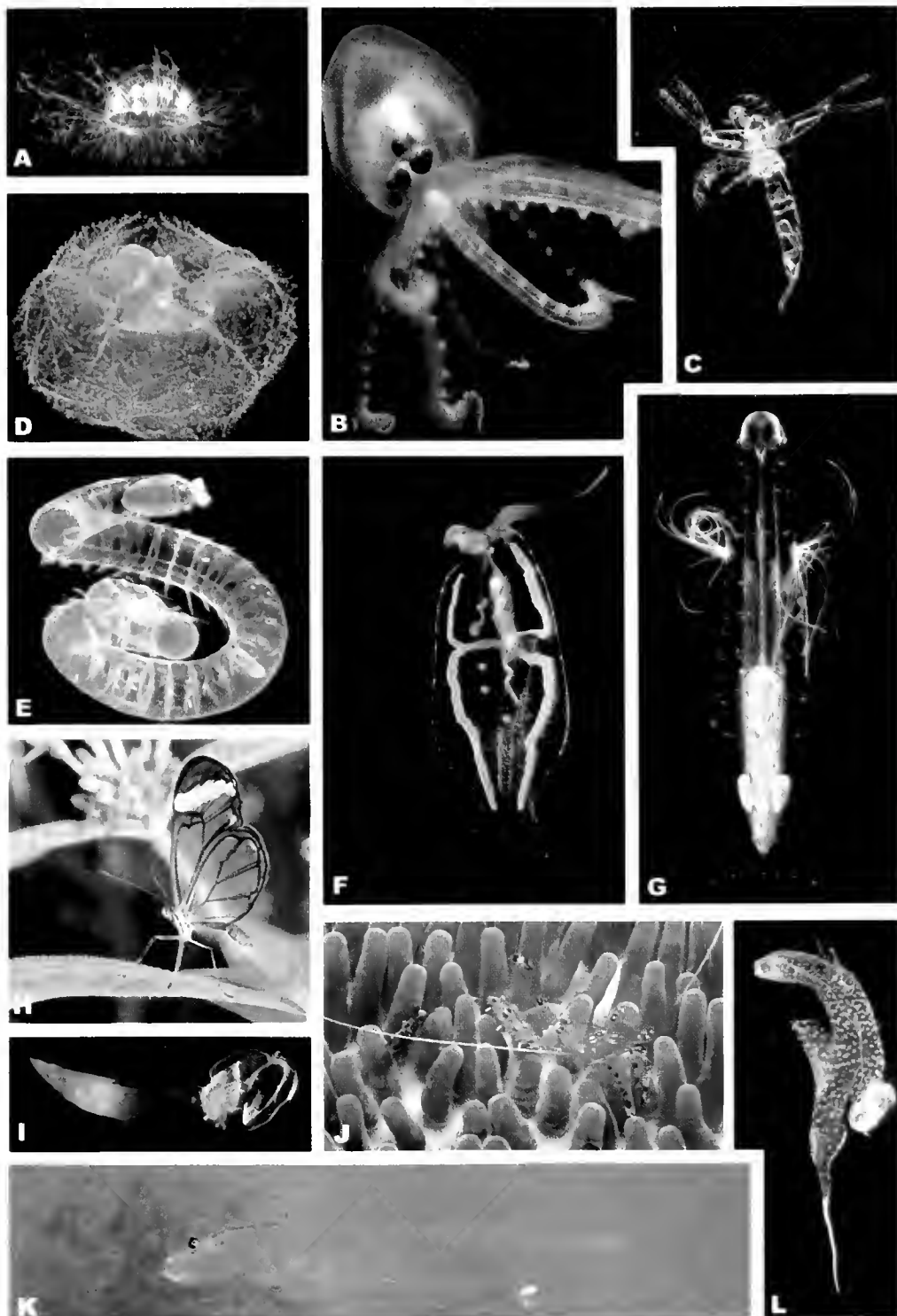


Figure 1. Assemblage of transparent animals. (A) *Amphogona apicata* (hydromedusa), (B) *Amphitretus pelagicus* (octopus), (C) *Leptodora kindtii* (freshwater cladoceran), (D) *Planctosphaera pelagica* (hemichordate larva), (E) *Naides cantrainii* (polychaete), (F) *Phylliroë bucephala* (nudibranch), (G) *Pterosagitta draco* (chaetognath), (H) *Greta oto* (neotropical butterfly), (I) *Bathochordens charon* (larvacean), (J) *Periclimenes holthuisi* (shrimp), (K) *Bathophilus* sp (larva of deep-sea fish), (L) *Cardiopoda richardi* (heteorpod). Credits as follows: A, D, E, G, I, K, L—Laurence P. Madin; B, F—Steven Haddock; C—Wim Van Egmond; H—Randy Emmitt; J—Jeff Jeffords.

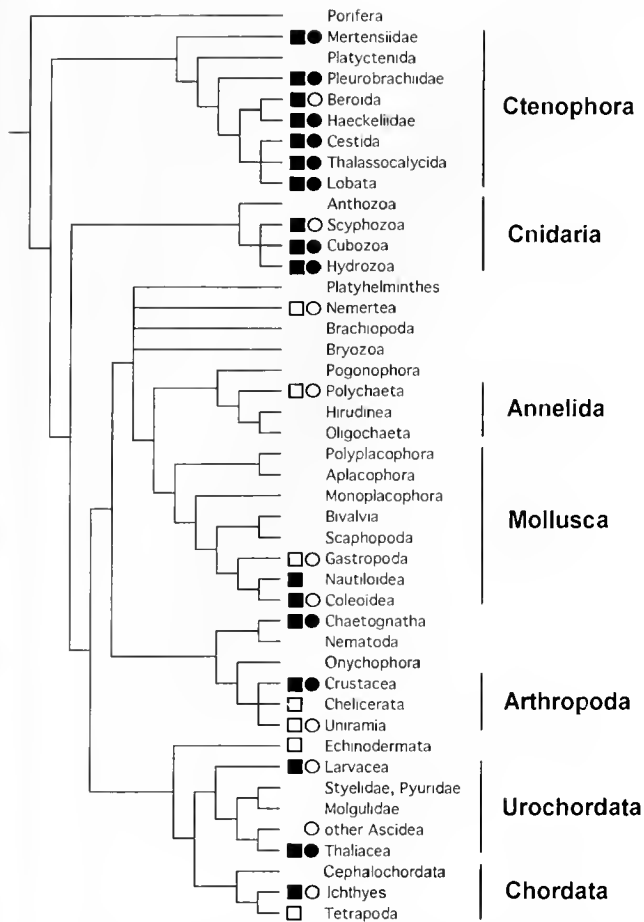


Figure 2. Transparency and pelagic existence mapped onto a phylogeny of the major phyla in the Animalia. Open square indicates pelagic existence is rare within adults of the group; filled square indicates pelagic existence is common. Open circle indicates transparency is rare within adults of the group; filled circle indicates transparency is common. Interrelationships of phyla taken from Halanych and Passamaneck (2001). Relationships within phyla taken from the following: Cnidaria (Bridge *et al.*, 1995), Ctenophora (Podar *et al.*, 2001), Annelida (McHugh, 2000), Mollusca (Wingstrand, 1985; Scheltema, 1993), Urochordata (Swalla *et al.*, 2000), Chordata (Nelson, 1994). The phylogeny of the Arthropoda is controversial and so is left as a polytomy. Taxa are resolved to different levels to maximize information about the distribution of transparency. Therefore Ctenophora is resolved to family level, while Nematoda, which has no transparent members, is unresolved. Gastropoda and Polychaeta are left unresolved because a resolution showing the distribution of transparency would make the figure too complex.

Most benthic, neustonic, and terrestrial groups have very few transparent members, although there are exceptions.

The following phyletic review of transparency was compiled with the aid of specialists in different taxa and environments (see acknowledgments) and is subject to several constraints. First, because nearly all small, unpigmented objects are transparent (for reasons described later), this section considers only species with transparent regions larger than 5 mm. Therefore certain phyla (*e.g.*, Rotifera, Gastrotricha) and most larvae and freshwater taxa are not

covered. Second, because aquatic species from transparent groups that are found at aphotic depths tend to be strongly pigmented (usually red, orange, or black) (Hardy, 1956; Herring and Roe, 1988), only terrestrial taxa and aquatic taxa at euphotic and dysphotic depths are considered. Euphotic and dysphotic regions possess enough solar radiation for photosynthesis and vision, respectively. In the clearest waters, the lower bounds of the two regions are 200 and 1000 m. Finally, infaunal or endoparasitic species, in which transparency could not have any optical function (*e.g.*, Echiura, Sipuncula, Nematomorpha), are not covered.

Eight phyla—Porifera, Nematoda, Pogonophora, Onychophora, Brachiopoda, Bryozoa, Platyhelminthes, and Echinodermata—appear to have no transparent adults. The first seven of these are exclusively benthic, neustonic, or terrestrial (Faubel, 1984; May, 1994). Echinodermata is benthic with few exceptions (Miller and Pawson, 1990). Possible examples of transparency in these phyla, such as hexactinellid sponges and certain benthopelagic holothurians (*e.g.*, *Peniagone diaphana*, *Irpa ludwigi*) are better described as unpigmented and translucent (*i.e.*, milky) rather than transparent.

With the exception of the beroids, ctenophores at euphotic and dysphotic depths are generally transparent (Mayer, 1912; Harbison *et al.*, 1978). Guts, papillae, and other small features are sometimes strongly pigmented, and the comb rows iridesce in directional illumination, but the bulk of the body is often extraordinarily transparent. Beroid ctenophores tend to be opaque, due to the presence of thousands of giant muscle fibers within the mesoglea (Hernandez-Nicaise, 1991), though smaller specimens of certain species (*e.g.*, *Beroe gracilis*) can be transparent.

Transparency in the Cnidaria is mostly found in cubozoans, hydromedusae, and siphonophores. Cubozoans are all highly transparent (Matsumoto, 1995). Hydromedusae tend to be highly transparent, though often with pigmented guts or gonads (Russell, 1953; Kramp, 1959) (Fig. 1A). Siphonophores follow a similar pattern with the exception of neustonic species (*e.g.*, *Physalia*), which are often blue, and members of the benthic family Rhodaliidae, which are opaque (Totton, 1965; Herring, 1967; Pugh, 1983). Scyphozoans, in contrast and for unknown reasons, are generally opaque and pigmented (Mayer, 1910; Russell, 1970; Wrobel and Mills, 1998). No anthozoans are transparent.

Among the Annelida, transparency is found only among the pelagic polychaetes (Fig. 1E). Five phyllodocidacean families (Alciopidae, Lopadorrhynchidae, Pontodoridae, Tomopteridae, and Typhloscolecidae) and two flabelligerid families (Flotidae and Poeobiidae) are dominated by transparent species (Usechakov, 1972; Glasby *et al.*, 2000). The degree of transparency varies between the different families, with the tomopterids and alciopids highly transparent and the flabelligerids less so. The remaining pelagic family,

Isopilidae, apparently does not have transparent members (Uschakov, 1972; Glasby *et al.*, 2000).

Several genera of polystyliferous pelagic nemerteans are transparent (Pelagonemertes, Pilonemertes) (P. Roe, California State University Stanislaus, pers. comm.). However, pigmented food in their highly branched guts often seriously reduces any cryptic benefit. No species of benthic nemerteans is known to be transparent (Roe, pers. comm.).

Transparency in the Mollusca is complex. Although the phylum as a whole is overwhelmingly benthic and opaque, it contains several pelagic groups that are dominated by transparent species (Van der Spoel, 1976; Lalli and Gilmer, 1989). The Mollusca also contains pelagic groups that are entirely opaque, and at least one transparent benthic genus. The Aplacophora, Monoplacophora, Polyplacophora, Bivalvia, and Scaphopoda are exclusively benthic and opaque. Among gastropods, the exclusively pelagic pterotracheid and carinariid heteropods, pseudothecosomatous pteropods, and phylliroid nudibranchs are highly transparent (Figs. 1F, L). However, the janthinid snails, atlantid heteropods, euthecosomatous and gymnosomatous pteropods, and glaucid nudibranchs are all opaque, despite also being pelagic taxa (Van der Spoel, 1976; Lalli and Gilmer, 1989). Benthic gastropods are opaque, with the exception of several species of the nudibranch *Melibe*, which have transparent oral hoods that are used to catch crustaceans (Von W. Kjer-schow-Agersborg, 1921). Among cephalopods, transparency is found only in octopus and squid. Although no benthic octopi are transparent, the pelagic families Amphitretidae and Vitreledonellidae are highly transparent (Ijema and Ikeda, 1902; Joubin, 1918) (Fig. 1B). None of the genera of the four families of the pelagic argonautoid octopods are transparent, and the pelagic Bolitaenidae are better described as translucent (Nesis, 1982). The benthopelagic cirrate octopods are all opaque and often strongly pigmented. Among the exclusively pelagic squid, only the Cranchiidae and small specimens of certain chiroteuthids (*e.g.*, *Chiroteuthis*) display any significant transparency. *Vampyroteuthis* and the Sepioidea are opaque.

Species in the Chaetognatha are pelagic and highly transparent, with the exception of the benthic Spadellidae and certain species at the lower end of the dysphotic zone (Fig. 1G). The spadellids are opaque due to the presence of transverse muscles and pigmentation (Bone and Duvert, 1991).

With the exception of the wings of certain satyrid and ithomiid butterflies and sphingid moths (*e.g.*, *Greta oto*, *Cephonodes hylas*) (Papageorgis, 1975; Yoshida *et al.*, 1997) (Fig. 1C) and the large pelagic larvae of certain freshwater insects (*e.g.*, *Chaoborus*), transparency in the Arthropoda appears to be limited to aquatic crustaceans. As in the Mollusca, the distribution of transparency in crustaceans is complex, with many major groups containing both transparent and non-transparent forms. The only group that

is truly dominated by transparent forms is the exclusively pelagic Hyperidea (Amphipoda) (Bowman and Gruner, 1973; Vinogradov *et al.*, 1996). The hyperiids, which are commensal on gelatinous zooplankton (Madin and Harbison, 1977; Laval, 1980), can be extraordinarily transparent and often have special modifications to increase their transparency (*e.g.*, Land, 1981; Nilsson, 1982). The generally benthic or terrestrial groups (*e.g.*, Decapoda, Gammaridea, Cirripedia, Stomatopoda, Isopoda) are primarily opaque, but with many exceptions among pelagic and benthopelagic subgroups (*e.g.*, some Pasiphaeaid shrimp, various species of cleaner shrimp, the sergestid *Lucifer*, the isopod *As-tacilla*, the phyllosoma larvae of *Palinurus*, the anemone shrimp *Periclimenes*) (Fig. 1J). As is true of cnidarians and ctenophores, many transparent pelagic crustaceans have red-pigmented guts and gonads, particularly at dysphotic depths (Hardy, 1956; Herring and Roe, 1988). Transparency is fairly common in freshwater crustaceans, but only a few species, mostly highly modified cladocerans, are larger than 5 mm (*e.g.*, *Leptodora*, *Bythotrephes*) (Fig. 1C).

Most transparent urochordates are found in the exclusively pelagic Thaliacea, which comprises the pyrosomids, salps, and doliolids (Godeaux *et al.*, 1998). Pyrosomids are opaque, while salps and doliolids, excepting large individuals of *Thetys vagina*, are highly transparent. Among the exclusively benthic Ascidea, transparency is observed in several genera of the order Enterogona (*e.g.*, *Ciona*, *Clavelina*), some of which are predatory (*e.g.*, *Megalodico-pia hians*) (Sanamyan, 1998). The larvaceans generally have small opaque bodies and long transparent tails, but with few exceptions (*e.g.*, *Bathochordeus*) are smaller than 5 mm (L. P. Madin, Woods Hole Oceanographic Institution, pers. comm.) (Fig. 1I).

Although adults in the Hemichordata are infaunal and opaque, the larval form of *Planctosphaera pelagica* has a diameter of 25 mm and is highly transparent (Hart *et al.*, 1994) (Fig. 1D). This organism, known only in this form, appears to have a prolonged larval stage and is well adapted to a pelagic existence.

No tetrapod chordate is transparent, but a number of fish are. Transparent adults are scattered throughout marine and freshwater teleosts, but are common only in the freshwater family Ambassidae (glassfish) (Johnson and Gill, 1995). Commonly known examples from other families include the glass catfish *Kryptopterus bicirrhus* (Siluridae) and *Parailia pellucida* (Schilbeidae), the cardinalfish genus *Rhabdamia* (Apogonidae), the clingfish *Alabes parvulus* (Cheilobranchidae), and the glass knifefish *Eigenmannia virescens* (Sternopygidae) (Briggs, 1995; Ferraris, 1995; Johnson and Gill, 1995). In addition, the pelagic larvae of many freshwater and marine fish are often highly transparent (Breder, 1962; Meyer-Rochow, 1974) (Fig. 1K). The most striking of these are the leptocephalous larvae of elopomorphs. These leaf-shaped larvae incorporate gelatinous material in

their bodies and quickly grow to lengths of up to 50 cm (Pfeiler, 1986). Most larval fish lose their transparency upon metamorphosis, some within 24 hours. The only possible tetrapod candidates, the glass frogs (Centrolenidae), have transparent skin on their ventral side, but opaque organs and a strongly pigmented dorsal surface (reviewed by McFall-Ngai, 1990).

Transparency and Environment

As can be seen from Figure 2 and the previous section, transparency has evolved multiple times and is almost exclusively a pelagic trait. Organismal transparency (rather than simply ocular) is extremely rare on land, rare in the aquatic benthos, uncommon in aphotic regions, somewhat more common in dysphotic and neustonic habitats, and ubiquitous at euphotic depths in clear water. The rarity of terrestrial transparency is probably due to the low refractive index of air, the presence of gravity, and high levels of ultraviolet radiation. The distribution of transparency in aquatic habitats appears to be correlated with the distribution of successful visual predation and crypsis strategies.

Terrestrial transparency

The extreme rarity of terrestrial transparency is probably due to the problem of reflections. The invisibility of a transparent object depends in part on the difference between its refractive index and the refractive index of the surrounding medium. A large difference causes surface reflections that substantially increase visibility. For example, an ice sculpture, while transparent, is highly visible due to surface reflections. At normal incidence, the fraction of incident light that is reflected (R) is

$$R = \left(\frac{n_1 - n_2}{n_1 + n_2} \right)^2, \quad (1)$$

where n_1 and n_2 are the refractive indices of the object and the surrounding medium. The refractive index of biological tissue is roughly proportional to density and ranges from 1.35 (cytoplasm) to about 1.55 (densely packed protein) (Charney and Brackett, 1961; Chapman, 1976). The refractive index of seawater depends on temperature and salinity, but is about 1.34. For these values, the surface reflection of a transparent organism in air (2%–5%) is roughly 10-fold to 2000-fold greater than its surface reflection in seawater (0.001%–0.7%). Although some nongaseous compounds with refractive indices slightly less than that of seawater exist (e.g., trifluoroacetic acid, $n = 1.28$), the refractive index of water is the lower limit for biological materials. Therefore successful crypsis using transparency is unlikely in terrestrial habitats. Other likely contributing factors are the increased levels of ultraviolet radiation on land, which

require protective pigmentation, and the need for supporting skeletal structures that are often opaque.

Distribution of aquatic transparency

Transparency is common in pelagic species at euphotic and dysphotic depths. Almost all non-transparent pelagic taxa are either camouflaged by small size (e.g., atlantid heteropods, euthecosomatous and gymnosomatous pteropods, glaucid nudibranchs, copepods, ostracods) or mirrored surfaces (e.g., fish, cephalopods), or are protected by fast swimming speeds (e.g., fish, cephalopods, shrimp) or chemical or physical defenses (e.g., scyphozoans, janthinid snails, *Nautilus*) (Hamner, 1996). The primary explanation for the prevalence of transparency in this environment is that it is the only form of camouflage in the pelagic realm that is successful from all viewpoints and at all depths. Cryptic coloration (e.g., countershading) is generally successful only from a given viewpoint and at a given depth (Munz and McFarland, 1977; Johnsen, 2002). Mirrored sides are successful at euphotic and upper dysphotic depths and for most viewpoints, although not from directly above or below (Herring, 1994; Denton, 1990). Counterillumination tactics are metabolically expensive and successful only during moonlit nights or at dysphotic depths.

The relative rarity of transparency in benthic and neustonic habitats is puzzling. Both benthic and neustonic species tend to be pigmented to match the surface below them—benthic animals matching the substrate and neustonic species matching the upwelling radiance (deep blue in oceanic water, brown in shallow freshwater) (David, 1965; Herring, 1967; Cheng, 1975; Guthrie, 1989). The rarity of transparency in benthic habitats is possibly due to two factors. First, pigmentation may be less costly to the animal than transparency, since it requires fewer modifications. However, a varied background requires the ability to detect and match a range of patterns and colors, a process done automatically by transparency camouflage. A second possibility is that even perfectly transparent objects tend to cast highly conspicuous shadows, due to distortion of the light by the higher refractive index of the tissue. These shadows, invisible in pelagic habitats, may render transparency ineffective for benthic species.

Neither of these factors, however, can account for the relative rarity of transparency in neustonic species. The two major hypotheses for the pigmentation of neustonic species are photo-protection and crypsis (Herring, 1967; Zaitsev, 1970). Although ultraviolet (UV) radiation is quite high at the surface of any aquatic habitat, there is no evidence that the pigmentation in neustonic species absorbs strongly at UV wavelengths. In addition, there are compounds, such as mycosporine-like amino acids, that strongly absorb at UV but not visible wavelengths (Karentz *et al.*, 1991). The fact that neustonic pigmentation often matches the upwelling

radiation strongly suggests that at least part of its function is crypsis. However, the blue or brown pigmentation is successfully cryptic only from above, or possibly from the side (Munz and McFarland, 1977; Johnsen, 2002), whereas neustonic individuals are most likely to be viewed from below. From this angle, any individual is silhouetted by the bright downwelling light, rendering cryptic coloration useless. Predation from above (e.g., avian) appears to mostly involve larger species (Zaitsev, 1970). As Herring (1967) concluded, no functional explanation of pigmentation in neustonic species is entirely satisfactory, and more data on the UV absorption of the pigments and the structure of the neustonic food web is needed.

As mentioned above, transparent species are rare at aphotic depths, generally being replaced by species with whole-body red or black pigmentation (Hardy, 1956; Herring and Roe, 1988; McFall-Ngai, 1990). At these depths, visual predation by solar light is sometimes replaced by visual predation based on directed bioluminescence. Because the spectra of photophores are generally void of red wavelengths (Widder *et al.*, 1983), neither red nor black surfaces can be seen by bioluminescent "searchlights." If the red or black coloration absorbs more than 99.5% of the directed bioluminescence, it may be more cryptic than transparency because even a perfectly transparent object causes surface reflections. However, because the reflected light is a small fraction of a dim source, the background light levels must be extremely low for the reflection to be visible. For example, the radiant intensity of the suborbital photophores of the Panama snaggletooth (*Borostomias panamensis*) is on the order of 10^{10} photons \cdot s $^{-1}$ \cdot sr $^{-1}$ (Mensing and Case, 1997). If this light strikes a transparent individual with a refractive index of 1.37 (10% protein), one can determine from equation (1) that about 0.01% of the photons are reflected back to the viewer. Therefore the background light levels must be 10^6 photons \cdot s $^{-1}$ or lower. For upward viewing this occurs at about 750 m in oceanic water (using absorption and attenuation values from the equatorial Pacific (Barnard *et al.*, 1998) and radiative transfer software (Hydrolight 4.1, Sequoia Scientific)). At these depths, horizontal and upward radiances are 3% and 0.5% of the downward radiance (Denton, 1990), so the equivalent depths for successful viewing using horizontal and downward bioluminescence are 650 and 600 m. For viewers with brighter bioluminescent "searchlights" or targets with higher refractive index, the depths are less. For example, the chitinous cuticle of a transparent hyperiid amphipod ($n = 1.55$) reflects 0.5% of the light and would be visible at 625, 525, and 475 m for upward, horizontal, and downward-directed bioluminescence, respectively. Truly opaque objects, such as guts and digestive organs, reflect a much higher percentage of light and are visible at even shallower depths. This may explain why many opaque and high re-

fractive index organs are pigmented at shallower depths than those at which whole-body pigmentation is observed.

Visibility and Visual Predation

Although some transparent species may only have trophic interactions with blind taxa, the majority either prey on or are preyed upon by at least some species with well-developed visual systems (Harbison *et al.*, 1978; Alldredge and Madin, 1982; Alldredge, 1984; Madin, 1988; Lalli and Gilmer, 1989; Pages *et al.*, 1996; Baier and Purcell, 1997; Madin *et al.*, 1997; Purcell, 1997; Harbison, unpublished literature review of gelatinivory in vertebrates). Since transparent animals are often more delicate and less agile than their visually orienting predators or prey, their success in predator/prey interactions with these animals depends critically upon their visibility and in particular their sighting distance (the maximum distance at which they are detectable by an animal relying on visual cues). Prey with short sighting distances reduce their encounters with visually orienting predators (Greene, 1983). "Ambush" predators (e.g., medusae, siphonophores, cydippid ctenophores) with short sighting distances increase their chances of entangling visually orienting prey before being detected and avoided. Raptors (e.g., chaetognaths, heteropods) with short sighting distances increase their chances of getting within striking distance without being detected.

Transparency and contrast

The visibility of a transparent individual generally depends more on its contrast than on its size (Mertens, 1970; Hemmings, 1975; Lythgoe, 1979). The inherent contrast (contrast at zero distance) at wavelength λ is defined as

$$C_o(\lambda) = \frac{L_o(\lambda) - L_b(\lambda)}{L_b(\lambda)}, \quad (2)$$

where $L_o(\lambda)$ is the radiance of the object and $L_b(\lambda)$ is the radiance of the background, both viewed a short distance from the object (Hester, 1968; Mertens, 1970; Jerlov, 1976). The absolute value of contrast decreases exponentially with distance according to

$$|C(\lambda)| = |C_o(\lambda)| \cdot e^{-(K_L(\lambda) - c(\lambda))d}, \quad (3)$$

where $|C(\lambda)|$ is the absolute value of apparent contrast at distance d from the object, $K_L(\lambda)$ is the attenuation coefficient of the background radiance, and $c(\lambda)$ is the beam attenuation coefficient of the water (adapted from Mertens, 1970; Lythgoe, 1979). The maximum distance at which the object is still detectable is

$$d_{\text{sighting}}(\lambda) = \frac{\ln\left(\frac{|C_o(\lambda)|}{C_{\text{min}}(\lambda)}\right)}{c(\lambda) - K_L(\lambda)}, \quad (4)$$

where $C_{\min}(\lambda)$ is the minimum contrast threshold of the viewer. An animal can indirectly affect $c(\lambda) = K_L(\lambda)$ by moving into a different water type or controlling the angle from which it is viewed, but it can only directly decrease its sighting distance by decreasing its inherent contrast. The inherent contrast of a transparent organism from an arbitrary viewpoint depends on its light-scattering properties and the characteristics of the underwater light field (Chapman, 1976), so it is difficult to model exactly. In general, however, pelagic objects have the greatest sighting distances when viewed from below, and are often viewed from this angle (Mertens, 1970; Munz, 1990; Johnsen, 2002). The transparency, $T(\lambda)$, of an object is the fraction of light of wavelength λ that passes unabsorbed and unscattered through it. Therefore, for the upward viewing angle

$$T(\lambda) = \frac{L_o(\lambda)}{L_b(\lambda)}, |C_o(\lambda)| = 1 - T(\lambda),$$

$$\text{and } d_{\text{sighting}}(\lambda) = \frac{\ln\left(\frac{1 - T(\lambda)}{C_{\min}(\lambda)}\right)}{c(\lambda) - K_L(\lambda)}. \quad (5)$$

Thus, the relationship between transparency and sighting distance is not linear and depends also on the contrast sensitivity of the viewer. Optimal minimum contrast thresholds have been determined for man (0.01), cat (0.01), goldfish (0.009–0.05), cod (0.02), rudd (0.03–0.07), roach (0.02), and bluegill (0.003–0.007) (Lythgoe, 1979; Douglas and Hawryshyn, 1990). It is important to note, however, that because these values depend on many aspects of the experimental situation (*e.g.*, temperature, target size, position of stimulus on retina, whether one eye or two was used, assessment method), they are not directly comparable (Douglas and Hawryshyn, 1990). For example, the minimum contrast threshold increases as the light level decreases. For example, the minimum contrast threshold of cod (*Gadus morhua*) increases from 0.02 at the surface to nearly 0.5 at 650 m in clear water ($10^{-7} \text{ W sr}^{-1} \text{ m}^{-2}$) (Anthony, 1981). Therefore, animals that are detectable near the surface may become undetectable at depth.

Empirical studies

The only empirical research on terrestrial transparency is a study on predation of neotropical butterflies showing that transparent species were mostly found near the ground, where they were presumably maximally cryptic (Papageorgis, 1975). A subsequent study, however, did not confirm this (Burd, 1994).

Most of the research on the relationship between transparency and visual predation has been performed in freshwater systems. Early studies by Zaret (1972) on fish predation on two morphs of transparent daphnia (*Ceriodaphnia cornuta*) showed that predation was higher on the morph

with larger eyes. When the “small-eye” morph was then fed India ink, creating a “super eye spot” in the gut, the predation preferences of the fish switched. Zaret also found that the small-eye morph had a greatly reduced reproductive potential and hypothesized that it was maintained in natural populations due to its reduced visual predation pressure. Later Zaret and Kerfoot (1975) showed that predation on a different transparent cladoceran (*Bosmina longirostris*) did not depend on body size but on the size of the opaque eye spot; they concluded that the important variable in visual predation was not body size, as previously assumed, but apparent body size. This conclusion has been supported by several subsequent studies (*e.g.*, Confer *et al.*, 1978; Wright and O’Brien, 1982; Hessen, 1985). Kerfoot (1982) measured the transparency, palatability, and sighting distances (for pumpkinseed fish) of several species of transparent freshwater zooplankton and found that transparency was correlated with palatability and inversely correlated with sighting distance. He proposed that visual predation by freshwater fishes has driven zooplankton in two opposing directions—palatable groups being selected for decreased visibility through decreased size, increased transparency, or both; unpalatable groups being selected for increased visibility through increased size, intense pigmentation, or both. O’Brien and Kettle (1979) examined the countervailing selective pressures of tactile predation (selecting for large prey) and visual predation (selecting for small prey) on two species of *Daphnia*. They found that these species increased their actual size, but not their apparent size, by developing morphs with large transparent armored sheaths. Giguere and Northcote (1987) repeated the India ink studies of Zaret (1972) in a more natural way by examining the effect of a full gut on the predation of transparent prey. They found that ingested prey increased the predation of *Chaoborus* larvae by 68% and suggested that this increased risk was at least partially responsible for the sinking of the animals after nocturnal feeding.

In contrast to the relatively abundant freshwater studies, fewer feeding studies on transparency exist for marine ecosystems. Tsuda *et al.* (1998), in a feeding study similar to Giguere and Northcote’s, found that predation on transparent copepods roughly doubled when their guts were full; he also suggested that predation risk due to gut visibility may be an important factor contributing to vertical migration in transparent zooplankton. Brownell (1985) and Langsdale (1993) both found that eye pigmentation significantly increased the vulnerability of transparent fish larvae to predation. Thetmeyer and Kils (1995) examined the effect of attack angle on the visibility of transparent mysids to hermit crab predators and found that they were most visible when viewed from above or below and least visible when viewed horizontally. Finally, Utne-Palm (1999) found that the sighting distances for transparent copepods (to goby pred-

ators) were significantly lower than the sighting distances for pigmented copepods.

Most of the research on transparency in marine ecosystems has concentrated on physical measurements of transparency and modeling its relationship to visibility. Greze (1963, 1964) was the first to describe the importance of transparency in visual predation. Using relatively crude equipment, he measured the average transparency of various dinoflagellates, siphonophores, copepods, and larvaceans and presented a model, which, unfortunately, was inaccurate, relating the measurements to sighting distance. Using a spectrophotometer, Chapman (1976) measured the transparency of several medusae (*Polyorchis*, *Chrysaora*, *Aurelia*) as a function of wavelength (from 200 to 800 nm). He found that transparency was relatively constant over the visual and infrared range and then dropped dramatically at ultraviolet wavelengths. Chapman also modeled the relationship between transparency, reflectivity, and visibility as a function of viewing angle, showing that the visibility of any object that is not 100% transparent depends strongly on the viewing angle and the underwater radiance distribution. Forward (1976), in a study of shadow responses in crab larvae, measured the transparency of the larvae's ctenophore predator, *Mnemiopsis leidyi*, and showed that the ctenophores were sufficiently opaque to cause a defensive response in individuals below them. More recently, Johnsen and Widder (1998, 2001) measured the ultraviolet (280–400 nm) and visible (400–700 nm) transparency of 50 epipelagic and mesopelagic Atlantic species from seven phyla (Cnidaria, Ctenophora, Annelida, Mollusca, Crustacea, Chaetognatha, Chordata) and modeled the relationship between transparency and sighting distance using analyses similar to those given in the previous section. They found that transparency is generally constant over the visual range, with longer wavelengths slightly more transparent. Deep-water animals tended to have constant and high transparency at UV wavelengths, whereas near-surface animals showed rapidly decreasing and low transparency in the UV. The relationship between transparency and visibility was complex and depended strongly on the contrast sensitivity of the viewer. Many mesopelagic animals were found to be far more transparent than necessary for complete invisibility.

Visual adaptations to increase contrast of transparent animals

The importance of transparency in predator/prey interactions is also demonstrated by the special visual adaptations seen in pelagic animals. The three best studied of these are UV vision, polarization vision, and viewing at certain angles. In addition to their possible other functions, all three of these can "break" the camouflage of transparency.

UV vision (documented down to ~320 nm) has been

demonstrated in many aquatic species; it has been conservatively estimated that there is sufficient UV light for vision down to 100 m in clear ocean water (reviewed by Losey *et al.*, 1999, and Johnsen and Widder, 2001). Visual pigments with UV sensitivity have been found in dozens of species of marine and freshwater fish (reviewed by Douglas and Hawryshyn, 1990; Jacobs, 1992; Goldsmith, 1994; and Johnsen and Widder, 2001). Among arthropods, UV vision has been demonstrated in stomatopods, cladocerans, copepods, decapods, and horseshoe crabs (Wald and Krainin, 1963; Marshall and Oberwinkler, 1999; Flamarique *et al.*, 2000). Finally, and surprisingly, UV sensitivity is found in at least one mesopelagic alciopid polychaete and four mesopelagic decapod crustaceans (Wald and Rayport, 1977; Frank and Case, 1988).

Three primary functions for UV vision have been hypothesized (Losey *et al.*, 1999): (1) intraspecific communication, (2) enhanced detection of opaque prey (silhouetted against the relatively bright UV background), and (3) enhanced detection of transparent prey. Due to higher light scattering or the presence of UV-protective compounds, many visibly transparent tissues are opaque at UV wavelengths (Douglas and Thorpe, 1992; Thorpe *et al.*, 1993; Johnsen and Widder, 2001). Several researchers have hypothesized that UV vision is primarily used to improve detection of transparent prey (Loew *et al.*, 1993; Cronin *et al.*, 1994; McFarland and Loew, 1994; Loew *et al.*, 1996; Sandstroem, 1999), and Browman *et al.* (1994) have shown that the presence of UV light improves the search behavior of certain UV-sensitive zooplanktivorous fish. The presence of UV sensitivity in planktivorous but not in non-planktivorous life stages of salmonids (reviewed by Tovee, 1995) and the correlation between UV vision and planktivory in coral reef fish (McFarland *et al.*, unpubl. data) suggest that UV vision is often used to increase the contrast of transparent planktonic prey.

Therefore, near-surface transparent species may have to satisfy the conflicting selective pressures of camouflage and protection from radiation damage. The increased visibility due to photo-protective carotenoid and melanin pigmentation in high-UV freshwater environments has been studied for many years (Hairston, 1976; Luecke and O'Brien, 1981, 1983; Byron, 1982; Hobaek and Wolf, 1991; Hansson, 2000; Miner *et al.*, 2000). These studies have shown several novel solutions, such as inducible pigmentation mediated by the relative levels of UV radiation and visual predation, restriction of pigmentation to vital organs, and the use of a photoprotective compound that also decreases visibility. Only two studies have examined marine systems (Morgan and Christy, 1996; Johnsen and Widder, 2001), and only the latter has explored the effect of nonvisible UV protective pigments on UV visibility. In this study, near-surface zooplankton displayed significantly greater UV absorption than deep-dwelling zooplankton, but the effect of UV absorption on UV visibility was less than expected because the mea-

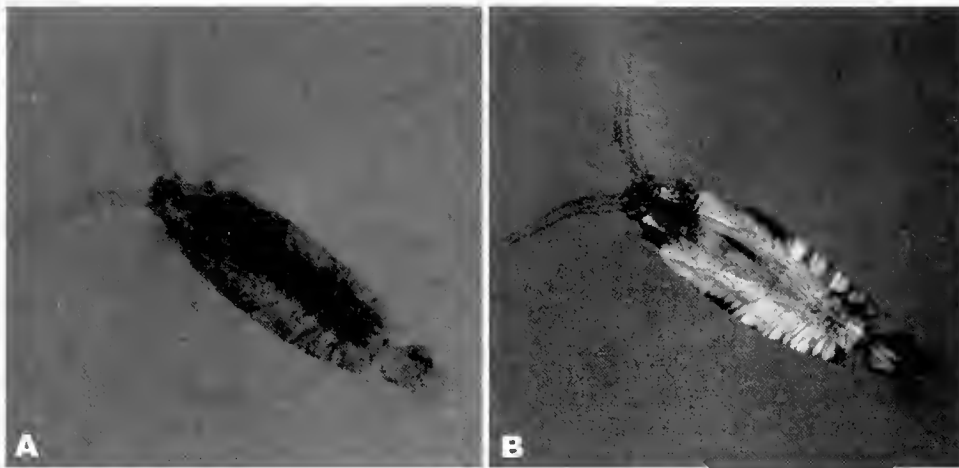


Figure 3. Copepod (*Labidocera*) viewed under (A) unpolarized transmitted light, and (B) crossed polarizers. The copepod is more distinct in (B) due to the presence of birefringent muscle and connective tissue. Because the background underwater illumination is polarized, a viewer with polarization vision may be able to visualize the contrast increase from (A) to (B). Courtesy of Nadav Shashar.

sured UV absorption was generally significantly greater in the UVB than in the UVA (where UV vision occurs), and because the highest UV absorption was often found in less transparent individuals.

The conflict between UV protection and UV concealment may have important ecological implications in light of reports of decreasing ozone levels at polar, temperate, and tropical latitudes and concomitant increases in UVB radiation (measured at 10%–20% per decade at temperate latitudes) (Solomon, 1990; Smith *et al.*, 1992; Stolarski *et al.*, 1992). A responsive increase in UV-protective pigmentation (at either an individual or population level) increases visibility at UV and possibly visible wavelengths, potentially resulting in increased predation or decreased feeding success. A responsive increase in depth may decrease access to prey, phytoplankton, or warmer water. Given the importance of transparent zooplankton to the trophic ecology of the pelagic realm (*e.g.*, Madin *et al.*, 1997; Purcell, 1997), either response may have significant effects.

A second visual adaptation that can increase the contrast of transparent predators or prey is polarization vision. Underwater light is polarized, particularly in the horizontal direction (Waterman, 1981). A transparent object can affect this polarization in two ways: it can depolarize it entirely or, if the object is birefringent, it can rotate the plane of polarization (Lythgoe and Hemmings, 1967; Fineran and Nicol, 1978). Either change is potentially detectable by a polarization-sensitive visual system (Fig. 3), which may explain the prevalence of polarization sensitivity in underwater crustaceans and cephalopods (Waterman, 1981). Despite the enormous potential of this field, only one study has tested this possibility (Shashar *et al.*, 1998). This study showed that squid (*Loligo pealei*) preferentially attacked

birefringent plastic beads over non-birefringent beads, although they were otherwise indistinguishable.

The final adaptation is behavioral rather than physiological and relies on the special optical properties of the air-water interface. Due to refraction at the water's surface, the hemispherical sky is compressed into a region 97° across, known as Snell's window. Any transparent object just outside the edge of this window is more conspicuous because it refracts and reflects some of the light from within the window, but is seen against the relatively dark background of water outside the window (Lythgoe, 1979). As with polarization sensitivity, this contrast enhancer, while potentially quite important, has only been tested once. Janssen (1981) showed that the attack angles of the blueback herring (*Alosa aestivalis*) were closely distributed around the outside edge of Snell's window.

Active uses of transparency

Although transparency seems to be primarily designed for passive crypsis, a few examples exist of more active uses of this trait. The physonect siphonophores *Athorybia rosacea* and *Aglama okeni* are mostly transparent, but they have pigmented regions mimicking copepods and larval fish that are apparently used as lures (Purcell, 1980, 1981). Therefore, animals approaching the small lures cannot detect the large individual that is also present. Other siphonophores appear to have exploited temporal changes in transparency for defense. The calycophoran siphonophores *Hippopodius hippopus* and *Vogtia* are normally transparent, but they rapidly become opaque when disturbed, presumably as a defensive startle response (Mackie, 1996).

The Physical Basis of Transparency

General principles

Transparency differs from other forms of crypsis and most adaptations in general in that it involves the entire organism. Therefore, many or all the tissues must be specialized for transparency. How this is achieved and how the modifications are compatible with life are only just beginning to be understood. The following sections explain the physics of transparency and then discuss the few theoretical and fewer empirical biological studies that have been performed.

An organism or tissue is transparent if it neither absorbs nor scatters light (Kerker, 1969). The majority of organic molecules do not absorb visible light (Tardieu and Delaye, 1988), and measurements of the wavelength dependence of light attenuation in 52 species of transparent zooplankton show no evidence of visible absorption bands in the transparent regions (Chapman, 1976; Johnsen and Widder, 1998, 2001). Therefore, except for necessarily opaque tissues (*e.g.*, gut, retina) and the special case of UV transparency, the primary barrier to transparency in organic tissue appears to be light scattering.

Scattering is caused by discontinuities in refractive index. A nonabsorbing substance with a homogeneous refractive index is transparent. Biological tissue has many refractive-index discontinuities, due to the varying proportions and densities of its components. For example, the refractive index of lipids is higher than that of cytoplasm (Meyer, 1979). Therefore, plasma membranes, lipid droplets, and organelles with extensive folded membranes (*e.g.*, mitochondria, Golgi apparatus, and endoplasmic reticulum) have a higher refractive index than the surrounding cytoplasm. Organelles with dense protein concentrations, such as peroxisomes and lysosomes, also have a higher refractive index than the surrounding cytoplasm, as do nuclei, due to their high concentrations of nucleic acids. Even gelatinous organisms containing large amounts of water have sufficient complexity to scatter light, as evidenced by their opacity after death. In addition to these internal discontinuities, there is also the large discontinuity defined by the surface of the organism. As a photon passes through regions of different refractive indices, its direction is altered. Given enough direction changes, the tissue, though nonabsorbing, will be opaque. Common examples of nonabsorbing, highly scattering, opaque substances are milk, clouds, snow, and the sclera (white) of the eye.

Therefore, transparent animals must be adapted to scatter as little light as possible. Because the refractive indices of organic molecules are generally closely correlated with density (Ross, 1967), chemical adaptations are unlikely, and the problem is essentially a structural one.

Anatomical adaptations

Although most of the adaptations for transparency are observable only at the electron microscopy level, some are visible to the naked eye. These can be divided into the cloaking of tissues that cannot be made transparent and body flattening (Fig. 4).

Eyes and guts cannot be made transparent. Eyes must absorb light to function and guts are betrayed by their contents, since even transparent prey become visible during digestion. The eyes of transparent animals have been camouflaged in various ingenious ways. Many hyperiid amphipods have enormous eyes, covering most of their head, and could be betrayed by their large, pigmented retinas. However, the retinal signature is masked using either of two strategies. In some hyperiids (*e.g.*, *Phronima*), the light is directed from the large eyes to highly compact retinas using transparent fiber optic cables of complex optical design (Land, 1981; Nilsson, 1982) (Fig. 4B). Conversely, the retina of the hyperiid *Cystisoma* is thinned, expanded, situated directly behind the cornea, and therefore indistinct (Fig. 4A). Many transparent molluscs camouflage their eyes with mirrors, because mirrors in the open ocean reflect only more ocean and so are invisible (Herring, 1994). Others, particularly the transparent cranchiid squid, use counterillumination to mask the shadows of their eyes seen from below (Fig. 4D) (Voss, 1980). Land (1992) suggested that the elongated eyes of transparent octopi function to minimize the shadow of the eye from below. A final adaptation that has not been explored is the separation of the eyes using long stalks (*e.g.*, cranchiid and phyllosoma larvae), thereby minimizing the characteristic signature of two eyes side by side (Fig. 4F).

Similarly ingenious adaptations exist for minimizing the visibility of the opaque guts. Many transparent animals have elongated, vertically oriented, and sometimes reflective guts, including pterotracheid heteropods, cranchiid squid, transparent octopi, and hyperiid amphipods (Seapy and Young, 1986; Land, 1992; Vinogradov *et al.*, 1996; Young *et al.*, 1998). The shape and orientation minimizes the profile of the gut when viewed from above or below. The reflective coating minimizes the contrast of the gut when viewed from other angles. Seapy and Young (1986) showed that pterotracheids and cranchiids actively maintained the vertical orientation of their guts while altering the orientation of their bodies (Fig. 4C, D). A converse approach, seen in many salps, ctenophores, and medusae, is the possession of compact, spherical guts. Although not as cryptic from below, a sphere has the minimum average projected area when averaged over all potential viewing angles (Johnsen and Widder, 1999). Finally, as is found in eyes, the shadows of the opaque guts of certain species are masked using counterilluminating bioluminescence. For example, the mostly transparent midwater shrimp *Sergestes similis* masks

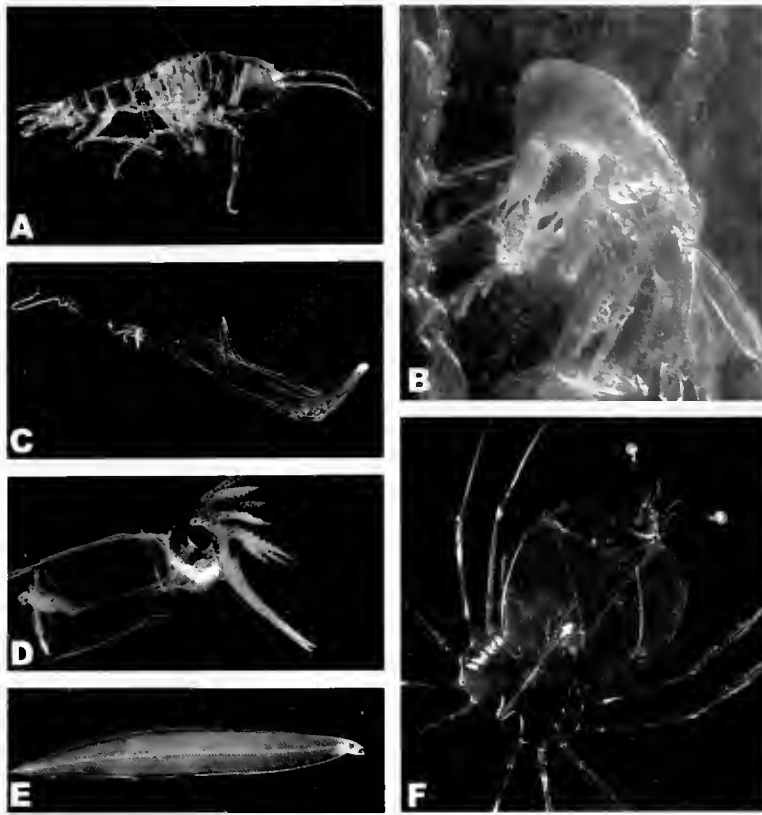


Figure 4. Various anatomical modifications that reduce the visibility of transparent animals. (A) Thin and extended retina directly behind cornea reduces the opacity of the eyes of the hyperiid amphipod *Cystisoma*. (B) Although the eyes of the hyperiid *Phronima* are large, the light is directed to the compact retinae using transparent fiber optic guides. (C) and (D) The guts of the heteropod *Pterotrachea* and the cranchiid squid *Taonius pavo* are elongated, mirrored, and vertical to minimize their visibility. (E) and (F) The bodies of leptocephalous and phyllosoma larvae are highly flattened to minimize light attenuation. Credits: A, B, E—Laurence Madin; C, D—Edith Widder; F—Tamara Frank.

the shadow of its digestive organs in this fashion (Warner *et al.*, 1979).

Many guts of transparent animals, if not mirrored, are pigmented. This is hypothesized to mask the presence of bioluminescent prey but may also serve as cryptic coloration, particularly since the color often approximates the optimally cryptic shade for a given depth (Johnsen, 2002).

Finally, some animals simply ingest substances that remain clear. The highly transparent larva of the phantom midge (*Chaoborus*) sucks out clear fluids from its prey (Kerfoot, 1982). Therefore, the gut remains transparent and does not need to be camouflaged.

Light attenuation in tissue, whether due to absorption or scattering, is exponential. For example, if a 1-cm-thick section of tissue is 60% transparent, then 2 cm is 36% transparent, and 3 cm is 22% transparent. Conversely, a 1-mm-thick section of the same tissue is 95% transparent. Therefore, transparency can be achieved through extreme body flattening. This adaptation has the additional advantage of also camouflaging the animal when it is observed edge-on. Flattening is observed in many transparent animals

including cestid ctenophores, phylliroid nudibranchs, many freshwater cladocerans, hyperiid amphipods, phyllosoma and stomatopod larvae, and the leptocephalous larvae of fish (Mayer, 1912; Zaret, 1981; Pfeiler, 1986; Lalli and Gilmer, 1989; Vinogradov *et al.*, 1996) (Fig. 4E, F). In certain cases, the flattening is extreme. The phyllosoma larvae of *Palinurus* are about 50 mm across and less than 1 mm thick (Fig. 4F). In many cases, body flattening may serve additional functions, such as more efficient swimming in fish and phylliroid nudibranchs, or increased surface area for gas exchange in cestid ctenophores.

Transparency and ultrastructure

The primary modifications for transparency, however, are ultrastructural and can only be seen with electron microscopy. The modifications depend on the tissue, which can be divided into three groups: external surface, extracellular matrix, and cellular tissue.

As mentioned above, the external surface of even a perfectly transparent organism reflects light due to the change

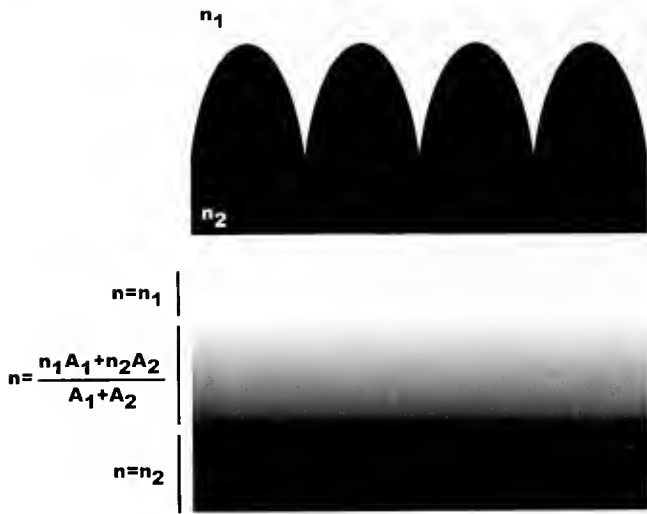


Figure 5. Photons impinging from above on an irregular surface with protrusions smaller than half a wavelength of light experience a gradual change in refractive index rather than a sharp discontinuity. n_1 is the refractive index of the external medium, n_2 is the index of the surface of the organism (e.g., cuticle). The refractive index at a given horizontal plane within the protrusion layer equals the average refractive index, which is given by the equation in the figure, where A_1 and A_2 are the respective areas of the external and organismal regions in that plane. The gradual shift in refractive index can reduce or eliminate surface reflections.

in refractive index. These reflections can be reduced or eliminated by covering the surface with submicroscopic protrusions (Miller, 1979; Wilson and Hutley, 1982). Because the protrusions are submicroscopic, they do not scatter light, but instead mimic a material of an intermediate refractive index. At the tips of the protrusions, the refractive index is that of the external medium. At the base, the index is that of the organism. At intermediate heights, the index varies smoothly and depends on the relative projected areas of the protrusions and the external medium (Fig. 5). These structures, known as "moth eye" surfaces, are found on the eyes of certain, particularly nocturnal, lepidopterans, dipterans, and caddisflies, where they are believed to camouflage the large eyes and increase sensitivity (by reducing reflected light) (reviewed by Miller, 1979; Parker *et al.*, 1998). They are also found on the wings of transparent lepidopterans, and in certain species (e.g., *Cephonodes hylas*) have been shown to reduce their visibility (Yoshida *et al.*, 1997).

The transparency of many extracellular tissues may depend on the counterintuitive notion that, although a completely homogeneous refractive index is sufficient for transparency, it is not always necessary. A transparent tissue can have components with many different refractive indices, so long as the average refractive index is constant over distances equal to half the wavelength of the incident light or more (Benedek, 1971). More precisely, scattering and light attenuation are low if the spatial distribution of refractive index has no Fourier components with wavelengths greater

than one half the wavelength of light. This low scattering is due to extensive destructive interference of the scattered light from the various scatterers. What is observed instead is a slower speed of light through the material. In short, scattering (in the presence of heavy destructive interference) is the source of refractive index. In glass, for example, each of the various molecules scatter light, but due to destructive interference no scattered light is observed and the beam is not attenuated. This theory has been invoked to explain the transparency of the mammalian cornea and lens (Benedek, 1971; Tardieu and Delaye, 1988; Vaezy and Clark, 1994). In both tissues, a substance with a high refractive index (collagen fibers in the cornea and crystalline proteins in the lens) is embedded within a substance with a low refractive index. The substance with the high refractive index is packed so densely that steric and other repulsive interactions force a local ordering of the scatterers (Tardieu and Delaye, 1988). The ordering exists only over distances on the order of several diameters of the scatterers, but it is sufficient to drastically reduce scattering. In the case of N identical scatterers, the total scattering cross-section, C_{total} , is given by

$$C_{\text{total}} = NC_{\text{sca}}S(\phi), \quad (6)$$

where C_{sca} is the scattering cross-section of an individual scatterer, ϕ is the volume concentration of the scatterers ($V_{\text{scatterers}}/V_{\text{total}}$), and $S(\phi)$ is the structure factor. The structure factor gives the amount of reduction in total scattering due to destructive interference caused by local ordering. In general, $S(\phi)$ is complex or unknown (see Benedek, 1971), but in the simpler case of small scatterers (radius ≤ 70 nm) it is

$$S(\phi) = \frac{(1 - \phi)^4}{1 + 4\phi + 4\phi^2 - 4\phi^3 + \phi^4} \quad (\text{Delaye and Tardieu, 1983}). \quad (7)$$

A concentration of scatterers of 30% reduces the total scattering to 10% of the value calculated under the assumption of no destructive interference of scattered light. A concentration of 60% reduces the scattering to less than 1% of the value calculated assuming no destructive interference. Figure 6 shows the total scattering cross-section of a solution of small particles plotted against their volume concentration. As the volume concentration increases there are more scatterers, but also more destructive interference. The maximum light scattering occurs at 13% concentration and then decreases as the concentration increases (see Benedek (1971) and Tardieu and Delaye (1988) for further details). This theory has been experimentally confirmed using solutions of lens proteins (Bettleheim and Siew, 1983). The solution becomes cloudier with increasing concentration, until a volume concentration of about 13%, after which it becomes clearer.

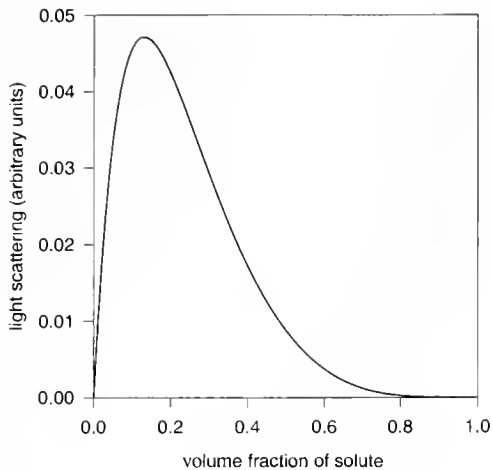


Figure 6. The amount of light scattering of a solution of small, identical scatterers plotted against their concentration (by volume). The scattering peaks when the concentration equals 13%.

Many extracellular and some cellular tissues (*e.g.*, muscle) of transparent organisms may meet these requirements. Although studies of the extracellular matrices and muscle of transparent animals are fairly rare, ultrastructural data exist for hydromedusae, siphonophores, ctenophores, chaetognaths, transparent ascidians, pyrosomas, doliolids, and salps (De Leo *et al.*, 1981; Weber and Schmid, 1985; Franc, 1988; Hernandez-Nicaise, 1991; Shinn, 1997; Hirose *et al.*, 1999). The fact that all of these appear homogeneous under light microscopy strongly suggests that they have few Fourier components greater than one half the wavelength of light. However, rigorous analyses have not been performed.

Although the above theory may explain the transparency of extracellular structures, it cannot adequately account for the transparency of cellular tissue. Reduction of scattering by destructive interference relies on dense packing of similar objects. In the two cases where this theory has been successfully applied (lens and cornea), the tissues are highly simplified. The mammalian lens, in particular, has been drastically modified for transparency (Goldman and Benedek, 1967; Philipson, 1973; Tardieu and Delaye, 1988). Most of the lens cells lack nuclei, mitochondria, and other organelles and, in fact, are little more than containers for dense concentrations of a few different proteins. The cells rely entirely on the surrounding cells for metabolic support and maintenance. Similarly, the cornea is a tightly packed array of collagen fibers with very few support cells and cannot maintain itself. These modifications are obviously incompatible with life when employed throughout an entire organism.

The only investigation of the basis of transparency in more complex cellular tissue is a theoretical treatment by Johnsen and Widder (1999). This study assumed that a cell requires given total volumes of various components. It then determined how to apportion, distribute, and shape the

volumes to minimize light scattering. The study found that the size of the components was most important, followed by the refractive index and, distantly, by the shape (Fig. 7; Table 1). A similar analysis was performed assuming that a cell requires a given total surface area of certain components, with similar results. Because a group of smaller particles within a wavelength of light of each other behave roughly like one larger particle (Thiele, 1998), clustering particles can change the total amount of scattering. For example, if several lysosomes have radii near the critical

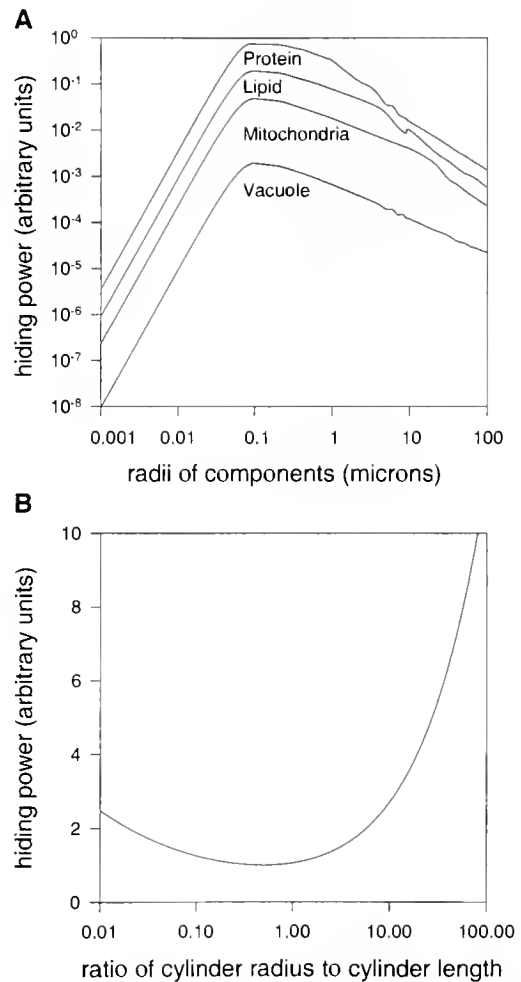


Figure 7. (A) The hiding power (opacity) for a given volume of material as a function of refractive index and the size of the smaller volumes into which it is divided. Hiding power is $S \cdot (1 - \langle \cos \theta \rangle)$, where S is the total amount of light scattering and $\langle \cos \theta \rangle$ is the average cosine of the angle into which the light is scattered. Therefore, backscattered light has a higher hiding power than forward scattered light. Material is assumed to be embedded in cytoplasm ($n = 1.35$). The refractive indices are vacuole—1.34, mitochondria—1.42, lipid—1.49, protein—1.62. (B) Hiding power plotted against shape for a large cylinder of constant volume averaged over all possible orientations relative to the incident light. Shape is given as the ratio between the radius of the cylinder and the length. Scattering is minimal when the radius equals half the length of the cylinder (*i.e.*, when the cylinder is most spherical).

Table 1

Ultrastructural predictions for transparent cellular tissue: the left column lists the various parameters in order of their importance to tissue transparency; the right column lists the predictions for the given parameter under a constant volume constraint; particles are considered clustered if they are within a wavelength of light of each other

Parameter	Predictions
Size of particles into which substance is subdivided	Particles will have radii either greater or less than 100 nm
Clustering or dispersion of particles	Small particles will be dispersed; large particles will be clustered
Refractive index of particles	All particles will have low relative refractive indices
Shape for particles with radii less than the wavelength of light	Particle shape will be arbitrary
Shape for particles with radii comparable to the wavelength of light	Predictions are highly case-specific
Shape for particles with radii greater than the wavelength of light	Particles will be spherical

radius (see Fig. 7; Table 1), they can be clustered to reduce the total amount of light scattering. Shape is surprisingly unimportant. For particles smaller than the wavelength of light, shape is irrelevant (Johnsen and Widder, 1999). For larger particles, the change in scattering as an object shifts from needle-shaped to disk-shaped is quite small relative to the enormous changes due to size (Fig. 7B).

Table 2 lists the predictions for actual cell components to scatter a minimum amount of blue-green light. For each component, a range of size and refractive index is given. All the components are considered to be primarily bound by

constant-volume constraints, with the exception of mitochondria. Since mitochondrial functioning depends heavily on membrane surface, it is considered to be bound by constant-surface-area constraints (see above). The refractive index of the cytoplasm is assumed to be 1.35. The refractive indices of the components are highly approximate and based on values of 1.62 for protein, 1.49 for lipid, and 1.34 for saline. In cases where a given prediction cannot be applied (*e.g.*, dividing a nucleus into smaller nuclei, changing the shape of a microtubule), no prediction is made. All predictions assume that the size and refractive index of a given

Table 2

Predictions for a typical cell that scatters a minimum amount of light: the predictions cover the shape, distribution (many and small, few and large), and refractive index of the cellular components

Component	Constraint	Size	Index	Predictions
Actin filaments, intermediate filaments, microtubules	Volume	4 nm, 5 nm, 12 nm	1.55–1.62	Shape: not applicable Distribution: dispersed Refractive index: low
Ribosomes	Volume	15 nm	1.55–1.62	Shape: arbitrary Distribution: dispersed Refractive index: low
Transport vesicles	Volume	15–50 nm	1.49–1.62	Shape: arbitrary Distribution: many, small, and dispersed Refractive index: low
Lysosomes, peroxisomes	Volume	0.1–0.25 μm	1.49–1.62	Shape: difficult to predict Distribution: many, small, and dispersed Refractive index: low
Lipid droplets	Volume	0.1–10 μm	1.49–1.62	Shape: arbitrary (if droplets are large, then spherical) Distribution: many, small, and dispersed Refractive index: low
Mitochondria	Surface area	0.25–10 μm	1.42–1.49	Shape: difficult to predict Distribution: many, small, and dispersed Refractive index: low
Nucleus	Volume	1.5–5 μm	1.42–1.49	Shape: spherical Distribution: not applicable Refractive index: low
Large vacuole	Volume	5–15 μm	1.34–1.62	Shape: spherical Distribution: few, large, and clustered Refractive index: low

component must remain within the range given. None of these predictions have been tested, although the morphological techniques are relatively straightforward.

In summary, although the physics of light scattering is well understood, the field of organismal transparency is still in its infancy. The few theoretical and empirical studies suggest that there are several routes to transparency, many of which probably operate concurrently. For example, the transparency of leptocephalous larvae may be due to body flattening, ordered packing within the gelatinous core, a very thin muscle layer, and possibly modifications within the cellular tissue itself. Other animals, such as phyllosoma larvae, may rely entirely on their extreme flattening. However, the actual modifications and their proximate and ultimate costs are, for the most part, unknown.

Future Directions

Transparency is currently a field with more questions than answers. Almost every major aspect of its study is a fruitful avenue for future research, but several topics are critical for future understanding of this adaptation. First, the structural predictions must be tested using morphological and optical measurements of transparent tissue. The unlikely possibility that organic molecules in transparent organisms have altered their refractive indices needs to be tested. More images of transparent animals under UV and polarized light are needed to evaluate the hypotheses of special camouflage breakers in planktivores, as are more feeding studies in both freshwater and marine ecosystems. Finally, as more phylogenies of pelagic groups become available, comparative methods should be used to explore the evolution of this extraordinary trait.

Acknowledgments

I thank the following for information on the transparency of specific groups: Martin Angel, Daphne Fautin, Tamara Frank, Steven Haddock, Richard Harbison, Peter Herring, Dina Leech, Laurence Madin, Marianne Moore, Karen Osborn, David Pawson, Pamela Roe, Clyde Roper, Michael Vecchione, Janet Voight, and Edith Widder. I also thank Ken Halanych and Yale Passamanek for pointing out relevant phylogenetic literature and software, and Kristina Fjeld, Tamara Frank, and Laurence Madin for a critical reading of the manuscript. The images for Figures 1, 3, and 4 were generously provided by Tamara Frank, Steven Haddock, Jeff Jeffords, Laurence Madin, Nadav Shashar, and Edith Widder. This work was funded in part by grants to SJ from The Rinehart Coastal Research Center, the Reuben F. and Elizabeth B. Richards Endowed Fund, the Penzance Endowed Fund, and the Grayce B. Kerr Fund. This is contribution number 10555 of the Woods Hole Oceanographic Institution.

Literature Cited

- Aldredge, A. L. 1984.** The quantitative significance of gelatinous zooplankton as pelagic consumers. Pp. 407–434 in *Flows of Energy and Materials in Marine Ecosystems*, M. J. R. Fasham, ed. Plenum Press, New York.
- Aldredge, A. L., and L. P. Madin. 1982.** Pelagic tunicates: unique herbivores in the marine plankton. *Bioscience* **32**: 655–663.
- Anthony, P. D. 1981.** Visual contrast thresholds in the cod *Gadus morhua*. *J. Fish Biol.* **19**: 87–103.
- Baier, C. T., and J. E. Purcell. 1997.** Trophic interactions of chaetognaths, larval fish, and zooplankton in the South Atlantic Bight. *Mar. Ecol. Prog. Ser.* **146**: 43–53.
- Barnard, A. H., W. S. Pegau, and J. R. V. Zaneveld. 1998.** Global relationships of the inherent optical properties of the oceans. *J. Geophys. Res.* **103**: 24955–24968.
- Benedek, G. B. 1971.** Theory of the transparency of the eye. *Appl. Opt.* **10**: 459–473.
- Bettleheim, F. A., and E. L. Siew. 1983.** Effect of change in concentration upon lens turbidity as predicted by the random fluctuation theory. *Biophys. J.* **41**: 29–33.
- Bone, Q., and M. Duvert. 1991.** Locomotion and buoyancy. Pp. 32–44 in *The Biology of Chaetognaths*, Q. Bone, H. Kapp, and A. C. Pierrot-Bults, eds. Oxford University Press, New York.
- Bowman, T., and H. E. Gruner. 1973.** The families and genera of Hyperidea (Crustacea: Amphipoda). *Smithson. Contrib. Zool.* **146**: 1–60.
- Breder, C. M. 1962.** On the significance of transparency in osteichthid fish eggs and larvae. *Copeia* **1962**: 561–567.
- Bridge, D., C. W. Cunningham, R. DeSalle, and L. W. Buss. 1995.** Class-level relationships in the phylum Cnidaria: molecular and morphological evidence. *Mol. Biol. Evol.* **12**: 679–689.
- Briggs, J. C. 1995.** Clingfishes. Pp. 142–144 in *Encyclopedia of Fishes*, J. R. Paxton and W. N. Eschmeyer, eds. Academic Press, New York.
- Browman, H. I., I. Novales-Flamarique, and C. W. Hawryshyn. 1994.** Ultraviolet photoreception contributes to prey search behaviour in two species of zooplanktivorous fishes. *J. Exp. Biol.* **186**: 187–198.
- Brownell, C. L. 1985.** Laboratory analysis of cannibalism by larvae of the Cape anchovy *Engraulis capensis*. *Trans. Am. Fish Soc.* **114**: 512–518.
- Burd, M. 1994.** Butterfly wing colour patterns and flying heights in the seasonally wet forest of Barro Colorado Island, Panama. *J. Trop. Biol.* **10**: 601–610.
- Byron, E. R. 1982.** The adaptive significance of calanoid copepod pigmentation: a comparative and experimental analysis. *Ecology* **63**: 1871–1886.
- Chapman, G. 1976.** Reflections on transparency. Pp. 491–498 in *Coe-lenterate Ecology and Behavior*, G. O. Mackie, ed. Plenum Press, New York.
- Charney, E., and F. S. Brackett. 1961.** The spectral dependence of scattering from a spherical alga cell and its implication for the state of organization of the light accepting pigments. *Arch. Biochem. Biophys.* **92**: 1–12.
- Cheng, L. 1975.** Marine pleuston—animals at the sea-air interface. *Oceanogr. Mar. Biol. Annu. Rev.* **13**: 181–212.
- Confer, J. L., G. L. Howick, M. H. Corzette, S. L. Kramer, S. Fitzgibbon, and R. Landerbert. 1978.** Visual predation by planktivores. *Oikos* **31**: 27–37.
- Cronin, T. W., N. J. Marshall, R. L. Caldwell, and N. Shashar. 1994.** Specialization of retinal function in the compound eyes of mantis shrimps. *Vision Res.* **34**: 2639–2656.
- David, P. M. 1965.** The surface fauna of the ocean. *Endeavour* **24**: 95–100.
- Delaye, M., and A. Tardieu. 1983.** Short-range order of crystallin proteins accounts for eye lens transparency. *Nature* **302**: 415–417.

- De Leo, G., E. Patricolo, and G. Frittitta. 1981. Fine structure of the tunic of *Ciona intestinalis* L. II. Tunic morphology, cell distribution and their functional importance. *Acta Zool.* **62**: 259–271.
- Denton, E. J. 1990. Light and vision at depths greater than 200 meters. Pp. 127–148 in *Light and Life in the Sea*, P. J. Herring, A. K. Campbell, M. Whitfield, and L. Maddock, eds. Cambridge University Press, New York.
- Douglas, R. H., and C. W. Hawryshyn. 1990. Behavioral studies of fish vision: an analysis of visual capabilities. Pp. 373–418 in *The Visual System of Fish*, R. H. Douglas and M. B. A. Djamgoz, eds. Chapman and Hall, New York.
- Douglas, R. H., and A. Thorpe. 1992. Short-wave absorbing pigments in the ocular lenses of deep-sea teleosts. *J. Mar. Biol. Assoc. UK* **72**: 93–112.
- Faubel, A. 1984. On the geographical occurrence of pelagic polyclad turbellarians. *Cah. Biol. Mar.* **25**: 153–168.
- Ferraris, C. J. 1995. Catfishes and knifefishes. Pp. 106–112 in *Encyclopedia of Fishes*, J. R. Paxton and W. N. Eschemeyer, eds. Academic Press, New York.
- Fineran, B. A., and J. A. C. Nicol. 1978. Studies on the photoreceptors on *Anchoa mitchilli* and *A. hepsetus* (Engraulidae) with particular reference to the cones. *Philos. Trans. R. Soc. Lond. B* **283**: 25–60.
- Flamarique, I. N., H. I. Browman, M. Belanger, and K. Boxaspen. 2000. Ontogenetic changes in visual sensitivity of the parasitic salmon louse *Lepeophtheirus salmonis*. *J. Exp. Biol.* **203**: 1649–1659.
- Forward, R. B., Jr. 1976. A shadow response in a larval crustacean. *Biol. Bull.* **151**: 126–140.
- Franc, J. M. 1988. The mesoglea of ctenophores. *Bull. Soc. Zool. Fr.* **113**: 347–351.
- Frank, T. M., and J. F. Case. 1988. Visual spectral sensitivities of bioluminescent deep-sea crustaceans. *Biol. Bull.* **175**: 261–273.
- Fraser, J. 1962. *Nature Adrift: The Story of Marine Plankton*. G. T. Foulis, London.
- Giguere, L. A., and T. G. Northcote. 1987. Ingested prey increase risks of visual predation in transparent *Chaoborus* larvae. *Oecologia* **73**: 48–52.
- Glasby, C. J., P. A. Hutchings, K. Fauchald, H. Paxton, G. W. Rouse, C. W. Russell, and R. S. Wilson. 2000. Polychaeta. Pp. 1–296 in *Polychaetes and Allies: The Southern Synthesis*, P. L. Beesley, G. J. B. Ross, and C. J. Glasby, eds. CSIRO Publishing, Melbourne.
- Godeaux, J., Q. Bone, and J. C. Braconnot. 1998. Anatomy of Thaliacea. Pp. 1–24 in *The Biology of Pelagic Tunicates*, Q. Bone, ed. Oxford University Press, New York.
- Goldman, J. N., and G. B. Benedek. 1967. The relationship between the morphology and transparency in the nonswelling corneal stroma of the shark. *Investig. Ophthalmol.* **6**: 574–600.
- Goldsmith, T. H. 1994. Ultraviolet receptors and color vision: evolutionary implications and dissonance of paradigms. *Vision Res.* **34**: 1479–1488.
- Greene, C. H. 1983. Selective predation in freshwater zooplankton communities. *Int. Rev. Gesamten Hydrobiol.* **68**: 297–315.
- Greze, V. N. 1963. The determination of transparency among planktonic organisms and its protective significance. *Dokl. Akad. Nauk. SSSR* **151**: 435–438.
- Greze, V. N. 1964. The transparency of planktonic organisms in the equatorial part of the Atlantic Ocean. *Okeanologiya* **4**: 125–127.
- Guthrie, M. 1989. *Animals of the Surface Film*. Richmond Publishing, Slough, U.K.
- Hairston, N. 1976. Photoprotection by carotenoid pigments in the copepod *Diatomus nevadensis*. *Proc. Natl. Acad. Sci.* **73**: 971–974.
- Halanych, K. M., and Y. Passamanek. 2001. A brief review of metazoan phylogeny and future prospects in Hox-research. *Am. Zool.* (In press).
- Hamner, W. M. 1996. Predation, cover, and convergent evolution in epipelagic oceans. Pp. 17–37 in *Zooplankton: Sensory Ecology and Physiology*, P. H. Lenz, D. K. Hartline, J. E. Purcell, and D. L. Macmillan, eds. Overseas Publishers Association, Amsterdam.
- Hansson, L. 2000. Induced pigmentation in zooplankton: a trade-off between threats from predation and ultraviolet radiation. *Proc. R. Soc. Lond. B.* **267**: 2327–2331.
- Harbison, G. R., L. P. Madin, and N. R. Swanberg. 1978. On the natural history and distribution of oceanic ctenophores. *Deep-Sea Res.* **25**: 233–256.
- Hardy, A. C. 1956. *The Open Sea, Its Natural History: The World of Plankton*. Houghton Mifflin, Cambridge, MA.
- Hart, M. W., R. L. Miller, and L. P. Madin. 1994. Form and feeding mechanism of a living *Planctosphaera pelagica* (phylum Hemichordata). *Mar. Biol.* **120**: 521–533.
- Hemmings, C. C. 1975. The visibility of objects underwater. Pp. 359–374 in *Light as an Ecological Factor*, G. C. Evans, R. Bainbridge, and O. Rackham, eds. Blackwell, Oxford.
- Hernandez-Nicaise, M.-L. 1991. Ctenophora. Pp. 359–418 in *Microscopic Anatomy of the Invertebrates Volume II: Placozoa, Porifera, Cnidaria, and Ctenophora*, F. W. Harrison and J. A. Westfall, eds. John Wiley, New York.
- Herring, P. J. 1967. The pigments of plankton at the sea surface. *Symp. Zool. Soc. Lond.* **19**: 215–235.
- Herring, P. J. 1994. Reflective systems in aquatic animals. *Comp. Biochem. Physiol. A* **109**: 513–546.
- Herring, P. J., and H. S. J. Roe. 1988. The photoecology of pelagic oceanic decapods. *Symp. Zool. Soc. Lond.* **59**: 263–290.
- Hessen, D. O. 1985. Selective zooplankton predation by pre-adult roach (*Rutilus rutilus*): the size-selective hypothesis versus the visibility-selective hypothesis. *Hydrobiologia* **124**: 73–79.
- Hester, F. J. 1968. Visual contrast thresholds of the goldfish (*Carassius auratus*). *Vision Res.* **8**: 1315–1335.
- Hirose, E., S. Kimura, T. Itoh, and J. Nishikawa. 1999. Tunic morphology and cellulosic components of pyrosomas, doliolids, and salps (Thaliacea, Urochordata). *Biol. Bull.* **196**: 113–120.
- Hobaek, A., and H. G. Wolf. 1991. Ecological genetics of Norwegian *Daphnia*. 2. Distribution of *Daphnia longispina* genotypes in relation to short-wave radiation and water colour. *Hydrobiologia* **225**: 229–243.
- Ijema, I., and S. Ikeda. 1902. Notes on a specimen of *Amphitretus* obtained in the Sagami Sea. *Annot. Zool. Jpn.* **4**: 5–101.
- Jacobs, G. H. 1992. Ultraviolet vision in vertebrates. *Am. Zool.* **32**: 544–554.
- Janssen, J. 1981. Searching for zooplankton just outside Snell's window. *Limnol. Oceanogr.* **26**: 1168–1171.
- Jerlov, N. G. 1976. *Marine Optics*. Elsevier, New York.
- Johnsen, S. 2002. Cryptic and conspicuous coloration in the pelagic environment. *Proc. R. Soc. Lond. B* **269**(1). (In press).
- Johnsen, S., and E. A. Widder. 1998. Transparency and visibility of gelatinous zooplankton from the northwestern Atlantic and Gulf of Mexico. *Biol. Bull.* **195**: 337–348.
- Johnsen, S., and E. A. Widder. 1999. The physical basis of transparency in biological tissue: ultrastructure and the minimization of light scattering. *J. Theor. Biol.* **199**: 181–198.
- Johnsen, S., and E. A. Widder. 2001. Ultraviolet absorption in transparent zooplankton and its implications for depth distribution and visual predation. *Mar. Biol.* **138**: 717–730.
- Johnson, G. D., and A. C. Gill. 1995. Perches and their allies. Pp. 181–196 in *Encyclopedia of Fishes*, J. R. Paxton and W. N. Eschemeyer, eds. Academic Press, New York.
- Joubin, L. 1918. Études préliminaires sur les Cephalopodes recueillis au cours des croisières de S. A. S. le Prince de Monaco 6e Note: *Vitreledonella richardi* Joubin. *Bull. Inst. Oceanogr.* **340**: 1–40.

- Karentz, D., F. S. McEuen, M. C. Land, and W. C. Dunlap. 1991. Survey of mycosporine-like amino acid compounds in Antarctic marine organisms: potential protection from ultraviolet exposure. *Mar. Biol.* **108**: 157–166.
- Kerfoot, W. C. 1982. A question of taste: crypsis and warning coloration in freshwater zooplankton communities. *Ecology* **63**: 538–554.
- Kerker, M. 1969. *The Scattering of Light and Other Electromagnetic Radiation*. Academic Press, New York.
- Kramp, P. L. 1959. The hydromedusae of the Atlantic Ocean and adjacent waters. *Dana-Rep.* **46**: 1–283.
- Lalli, C. M., and R. W. Gilmer. 1989. *Pelagic Snails*. Stanford University Press, Palo Alto, CA.
- Land, M. F. 1981. Optics of the eyes of *Phronimo* and other deep-sea animals. *J. Comp. Physiol. A* **145**: 209–226.
- Land, M. F. 1992. A note on the elongated eye of the octopus *Vitreledonella richardi*. *J. Mar. Biol. Assoc. UK* **72**: 89–92.
- Langsdale, J. R. M. 1993. Developmental changes in the opacity of larval herring, *Clupea harengus*, and their implications for vulnerability to predation. *J. Mar. Biol. Assoc. UK* **73**: 225–232.
- Larson, R. J. 1976. Cubomedusa: feeding, functional morphology, behavior and phylogenetic position. Pp. 237–246 in *Coelenterate Ecology and Behavior*, G. O. Mackie, ed. Plenum Press, New York.
- Laval, P. 1980. Hyperiid crustaceans as parasitoids associated with gelatinous zooplankton. *Oceanogr. Mar. Biol.* **18**: 11–56.
- Loew, E. R., and W. N. McFarland. 1990. The underwater visual environment. Pp. 1–44 in *The Visual System of Fish*, R. H. Douglas and M. B. A. Djangoz, eds. Chapman and Hall, New York.
- Loew, E. R., W. N. McFarland, E. L. Mills, and D. Hunter. 1993. A chromatic action spectrum for planktonic predation by juvenile yellow perch, *Perca flavescens*. *Can. J. Zool.* **71**: 384–386.
- Loew, E. R., R. A. McAlary, and W. N. McFarland. 1996. Ultraviolet visual sensitivity in the larvae of two species of marine atherinid fishes. Pp. 195–210 in *Zooplankton: Sensory Ecology and Physiology*, P. H. Lenz, D. K. Hartline, J. E. Purcell, and D. L. Macmillan, eds. Gordon and Breach, Amsterdam.
- Loosey, G. S., T. W. Cronin, T. H. Goldsmith, D. Hyde, N. J. Marshall, and W. N. McFarland. 1999. The UV visual world of fishes: a review. *J. Fish. Biol.* **54**: 921–943.
- Luecke, C., and W. J. O'Brien. 1981. Phototoxicity and fish predation: selective factors in color morphs in *Heterocope*. *Limnol. Oceanogr.* **26**: 454–460.
- Luecke, C., and W. J. O'Brien. 1983. Photoprotective pigments in a pond morph of *Daphnia middendorffiana*. *Arctic* **36**: 365–368.
- Lythgoe, J. N. 1979. *The Ecology of Vision*. Clarendon Press, Oxford.
- Lythgoe, J. N., and C. C. Hemmings. 1967. Polarized light and underwater vision. *Nature* **213**: 893–894.
- Mackie, G. O. 1996. Defensive strategies in planktonic coelenterates. Pp. 435–446 in *Zooplankton: Sensory Ecology and Physiology*, P. H. Lenz, D. K. Hartline, J. E. Purcell, and D. L. Macmillan, eds. Overseas Publishers Association, Amsterdam.
- Madin, L. P. 1988. Feeding behavior of tentaculate predators: in situ observations and a conceptual model. *Bull. Mar. Sci.* **43**: 413–429.
- Madin, L. P., and G. R. Harbison. 1977. The associations of Amphipoda Hyperiidea with gelatinous zooplankton—I. Associations with Salpidae. *Deep-Sea Res.* **24**: 449–463.
- Madin, L. P., J. E. Purcell, and C. B. Miller. 1997. Abundance and grazing effects of *Cyclosalpa bakeri* in the subarctic Pacific. *Mar. Ecol. Prog. Ser.* **157**: 175–183.
- Marshall, N. J., and J. Oberwinkler. 1999. The colourful world of mantis shrimp. *Nature* **401**: 873–874.
- Matsumoto, G. I. 1995. Observations on the anatomy and behavior of the cubozoan *Carybdea rastonii* Haacke. *Mar. Freshw. Behav. Physiol.* **26**: 139–148.
- May, R. M. 1994. Biological diversity: differences between land and sea. *Philos. Trans. R. Soc. Lond. B.* **343**: 105–111.
- Mayer, A. G. 1910. *Medusae of the World III: The Scyphomedusae*. Carnegie Institution of Washington, Washington, DC.
- Mayer, A. G. 1912. *Ctenophores of the Atlantic Coast of North America*. Carnegie Institution of Washington, Washington, DC.
- McFall-Ngai, M. J. 1990. Crypsis in the pelagic environment. *Am. Zool.* **30**: 175–188.
- McFarland, W. N., and E. R. Loew. 1994. Ultraviolet visual pigments in marine fishes of the family Pomacentridae. *Vision Res.* **34**: 1393–1396.
- McHugh, D. 2000. Molecular phylogeny of the Annelida. *Can. J. Zool.* **78**: 1873–1884.
- Mensinger, A. F., and J. F. Case. 1997. Luminescent properties of fishes from nearshore California basins. *J. Exp. Mar. Biol. Ecol.* **210**: 75–90.
- Mertens, L. E. 1970. *In-Water Photography: Theory and Practice*. John Wiley, New York.
- Meyer, R. A. 1979. Light scattering from biological cells: dependence of backscatter radiation on membrane thickness and refractive index. *Appl. Opt.* **18**: 585–588.
- Meyer-Rochow, V. B. 1974. Leptocephali and other transparent fish larvae from the south-eastern Atlantic ocean. *Zool. Anz.* **192**: 240–251.
- Meyer-Rochow, V. B. 1997. Wenn Unsichtbares sichtbar wird: durchsichtige Tiere—transparente Gewebe. *Nat. Mus.* **127**: 121–127.
- Miller, J. E., and D. L. Pawson. 1990. Swimming sea cucumbers (Echinodermata: Holothuroidea): a survey, with analysis of swimming behavior in four bathyl species. *Smithson. Contrib. Mar. Sci.* **35**: 1–18.
- Miller, W. H. 1979. Intraocular filters. Pp. 69–144 in *Handbook of Sensory Physiology*, Vol. 7/6A, H. Autrum, ed. Springer, New York.
- Miner, G. B., S. G. Morgan, and J. R. Hoffman. 2000. Postlarval chromatophores as an adaptation to ultraviolet radiation. *J. Exp. Mar. Biol. Ecol.* **249**: 235–248.
- Morgan, S. G., and J. H. Christy. 1996. Survival of marine larvae under the countervailing selective pressures of photodamage and predation. *Limnol. Oceanogr.* **41**: 498–504.
- Munz, W. R. A. 1990. Stimulus, environment and vision in fishes. Pp. 491–511 in *The Visual System of Fish*, R. H. Douglas and M. B. A. Djangoz, eds. Chapman and Hall, New York.
- Munz, F. W., and W. N. McFarland. 1977. Evolutionary adaptations of fishes to the photic environment. Pp. 194–274 in *The Visual System in Vertebrates*, F. Crescitelli, ed. Springer-Verlag, New York.
- Nelson, J. S. 1994. *Fishes of the World*. John Wiley, New York.
- Nesis, K. N. 1982. *Cephalopods of the World*. T. F. H. Publications, Neptune City, NJ.
- Nilsson, D. E. 1982. The transparent compound eye of *Hyperia* (Crustacea): examination with a new method for analysis of refractive index gradients. *J. Comp. Physiol. A* **147**: 339–349.
- O'Brien, W. J., and D. Kettle. 1979. Helmets and invisible armor: structures reducing predation from tactile and visual planktivores. *Ecology* **60**: 287–294.
- Pages, F., M. G. White, and P. G. Rodhouse. 1996. Abundance of gelatinous carnivores in the nekton community of the Antarctic polar frontal zone in summer 1994. *Mar. Ecol. Prog. Ser.* **141**: 139–147.
- Papageorgis, C. 1975. Mimicry in neotropical butterflies. *Am. Sci.* **63**: 522–532.
- Parker, A. R., Z. Hegedus, and R. A. Watts. 1998. Solar-absorber antireflector on the eye of an Eocene fly (45 Ma). *Proc. R. Soc. Lond. B* **265**: 811–815.
- Pfeiler, E. 1986. Towards an explanation of the developmental strategy in leptocephalous larvae of marine teleost fishes. *Environ. Biol. Fishes* **15**: 3–13.
- Philipson, B. 1973. Changes in the lens related to the reduction of transparency. *Exp. Eye Res.* **16**: 29–39.

- Podar, M., S. H. D. Haddock, M. L. Sogin, and G. R. Harbison. 2001. A molecular phylogenetic framework for the phylum Ctenophora using 18S rRNA genes. *Mol. Biol. Evol.* (In press).
- Pugh, P. R. 1983. Benthic Siphonophores: a review of the family Rhodaliidae (Siphonophora, Physonectae). *Philos. Trans. R. Soc. Lond. B* 301: 165–300.
- Purcell, J. E. 1980. Influence of siphonophore behavior on their natural diets; evidence for aggressive mimicry. *Science* 209: 1045–1047.
- Purcell, J. E. 1981. Selective predation and caloric consumption by the siphonophore *Rosacea cymbiformis* in nature. *Mar. Biol.* 63: 283–294.
- Purcell, J. E. 1997. Pelagic cnidarians and ctenophores as predators: selective predation, feeding rates and effects on prey populations. *Ann. Inst. Oceanogr.* 73: 125–137.
- Ross, K. F. A. 1967. *Phase Contrast and Interference Microscopy*. Edward Arnold, London.
- Russell, F. R. S. 1953. *The Medusae of the British Isles*. Cambridge University Press, Cambridge.
- Russell, F. R. S. 1970. *The Medusae of the British Isles II: Pelagic Scyphozoa*. Cambridge University Press, Cambridge.
- Sanamyan, K. 1998. Ascidians from the north-western Pacific region. 5. Phlebobranchia. *Ophelia* 49: 97–116.
- Sandstrom, A. 1999. Visual ecology of fish—a review with special reference to percids. *Fiskeriverk Rapp.* 2: 45–80.
- Scheltema, A. H. 1993. Aplousobranchia as progenetic aculiferans and the coelomate origin of mollusks as the sister taxon of Sipuncula. *Biol. Bull.* 184: 57–78.
- Seapy, R. R., and R. E. Young. 1986. Concealment in epipelagic pterotracheid heteropods (Gastropoda) and cranchiid squids (Cephalopoda). *J. Zool. Lond.* 210: 137–147.
- Shashar, N., R. T. Hanlon, and A. Petz. 1998. Polarization vision helps detect transparent prey. *Nature* 393: 222–223.
- Shinn, G. L. 1997. Chaetognatha. Pp. 103–220 in *Microscopic Anatomy of Invertebrates, Volume 15: Hemichordata, Chaetognatha, and the Invertebrate Chordates*, F. W. Harrison and E. E. Ruppert, eds. John Wiley, New York.
- Smith, R. C., B. B. Prézélin, K. S. Baker, R. R. Bidigare, N. P. Boucher, T. Coley, D. Karentz, S. MacIntyre, H. A. Matlick, D. Menzies, M. Ondrusek, Z. Wan, and K. J. Waters. 1992. Ozone depletion: ultraviolet radiation and phytoplankton biology in Antarctic waters. *Science* 255: 952–959.
- Solomon, S. 1990. Progress toward a quantitative understanding of Antarctic ozone depletion. *Nature* 347: 347–354.
- Stolarski, R. S., R. Bojkov, L. Bishop, C. Zerefos, J. Stachelin, and J. Zawodny. 1992. Measured trends in stratospheric ozone. *Science* 256: 342–349.
- Swalla, B. J., C. B. Cameron, L. S. Corley, and J. R. Garey. 2000. Urochordates are monophyletic within the deuterostomes. *Syst. Biol.* 49: 52–64.
- Tardieu, A., and M. Delage. 1988. Eye lens proteins and transparency: from light transmission theory to solution x-ray structural analysis. *Annu. Rev. Biophys. Biophys. Chem.* 17: 47–70.
- Thetmeyer, H., and U. Kils. 1995. To see and not be seen: the visibility of predator and prey with respect to feeding behavior. *Mar. Ecol. Prog. Ser.* 126: 1–8.
- Thiele, E. S. 1998. Light scattering by complex microstructures in the resonant regime. Ph.D. dissertation, University of Pennsylvania.
- Thorpe, A., R. H. Douglas, and R. J. W. Truscott. 1993. Spectral transmission and short-wave absorbing pigments in the fish lens—I. Phylogenetic distribution and identity. *Vision Res.* 33: 289–300.
- Totton, A. K. 1965. *A Synopsis of the Siphonophora*. British Museum, London.
- Tovee, M. J. 1995. Ultra-violet photoreceptors in the animal kingdom: their distribution and function. *Trends Ecol. Evol.* 10: 455–460.
- Tsuda, A., H. Saito, and T. Hirose. 1998. Effect of gut content on the vulnerability of copepods to visual predation. *Limnol. Oceanogr.* 43: 1944–1947.
- Uschakov, P. V. 1972. *Fauna of the U.S.S.R. Polychaetes. Vol. 1. Polychaetes of the Suborder Phyllocladiformia of the Polar Basin and the Northwestern Part of the Pacific: Families Phyllocladidae, Alciopidae, Tomopteridae, Typhloscoleicidae, and Lacydentiidae*. Akademiya NAUK SSSR, New Series 102, B. E. Bykhorskii, ed. [Translated from Russian by the Israel Program for Scientific Translations, Jerusalem, 1974.]
- Utne-Palm, A. C. 1999. The effect of prey mobility, prey contrast, turbidity and spectral composition on the reaction distance of *Gobiusculus flavescens* to its planktonic prey. *J. Fish Biol.* 54: 1244–1258.
- Vaezy, S., and J. I. Clark. 1994. Quantitative analysis of the microstructure of the human cornea and sclera using 2-D Fourier methods. *J. Microsc.* 175: 93–99.
- Van der Spoel, S. 1976. *Pseudothecosomata, Gymnosomata and Heteropoda*. Bohn, Scheltema and Holkema, Utrecht.
- Vinogradov, M. E., A. F. Volkov, and T. N. Semanova. 1996. *Hyperiid Amphipods (Amphipoda, Hyperiidea) of the World Oceans*. Smithsonian Institution Libraries, Washington, DC.
- Von W. Kjerschow-Agersborg, H. P. 1921. Contribution to the knowledge of the nudibranchiate mollusk, *Melibe leonina* (Gould). *Am. Nat.* 55: 222–253.
- Voss, N. A. 1980. A generic revision of the Cranchiidae (Cephalopoda: Oegopsida). *Bull. Mar. Sci.* 30: 365–412.
- Wald, G., and J. M. Krainin. 1963. The median eye of *Limulus*: an ultraviolet photoreceptor. *Proc. Natl. Acad. Sci.* 50: 1011–1017.
- Wald, G., and S. Rayport. 1977. Vision in annelid worms. *Science* 196: 1434–1439.
- Warner, J. A., M. I. Latz, and J. F. Case. 1979. Cryptic bioluminescence in a midwater shrimp. *Science* 203: 1109–1110.
- Waterman, T. H. 1981. Polarization sensitivity. Pp. 281–469 in *Handbook of Sensory Physiology*, Vol. 7/6B, H. Autrum, ed. Springer, New York.
- Weber, C., and V. Schmid. 1985. The fibrous system in the extracellular matrix of hydromedusae. *Tissue Cell* 17: 811–822.
- Widder, E. A., M. I. Latz, and J. F. Case. 1983. Marine bioluminescence spectra measured with an optical multichannel detection system. *Biol. Bull.* 165: 791–810.
- Wilson, S. J., and M. C. Hutley. 1982. The optical properties of 'moth eye' antireflection surfaces. *Optica Acta* 7: 993–1009.
- Wingstrand, K. G. 1985. On the anatomy and relationships of Recent Monoplacophora. *Galathea Rep.* 16: 7–94.
- Wright, D. L., and W. J. O'Brien. 1982. Differential location of *Chaoborus* larvae and *Daphnia* by fish: the importance of motion and visible size. *Am. Midl. Nat.* 108: 68–73.
- Wrobel, D., and C. Mills. 1998. *Pacific Coast Pelagic Invertebrates: A Guide to Common Gelatinous Animals*. Sea Challengers, Monterey Bay Aquarium, Monterey Bay, CA.
- Yoshida, A., M. Motoyama, A. Kosaku, and K. Miyamoto. 1997. Antireflective nanoprotuberance array in the transparent wing of a hawkmoth. *Cephanodoes hylas*. *Zool. Sci.* 14: 737–741.
- Young, R. E., M. Vecchione, and D. T. Donovan. 1998. The evolution of coleoid cephalopods and their present biodiversity and ecology. *S. Afr. J. Mar. Sci.* 20: 393–420.
- Zaitsev, V. P. 1970. *Marine Neustonology*. Keter Press, Jerusalem.
- Zaret, T. M. 1972. Predators, invisible prey, and the nature of polymorphisms in the Cladocera (Class Crustacea). *Limnol. Oceanogr.* 17: 171–184.
- Zaret, T. M. 1981. Lateral compression and visibility in cladocerans. *Limnol. Oceanogr.* 26: 965–970.
- Zaret, T. M., and W. C. Kerfont. 1975. Fish predation on *Bosmina longirostris*: body size selection versus visibility selection. *Ecology* 56: 232–237.

Evolution of Marine Mushrooms

DAVID S. HIBBETT* AND MANFRED BINDER

Biology Department, Clark University, 950 Main Street, Worcester, Massachusetts 01610

Fungi make up one of the most diverse, ecologically important groups of eukaryotes. The vast majority of fungi are terrestrial, but the chytridiomycetes, a basal group of fungi, includes flagellated, unicellular, aquatic forms, and it is likely that this was the ancestral condition of the group (1). The more derived groups of fungi—zygomycetes, ascomycetes, and basidiomycetes—are all predominantly filamentous and terrestrial, and lack flagellated cells at any stage of the life cycle. Within the basidiomycetes, the most conspicuous group is the homobasidiomycetes, which includes about 13,000 described species of mushrooms and related forms. Eleven species of homobasidiomycetes (in eight genera) occur in marine or freshwater habitats. To resolve the relationships among terrestrial and aquatic homobasidiomycetes, we assembled a data set of ribosomal DNA (rDNA) sequences that includes 5 aquatic species and 40 terrestrial species. Phylogenetic trees obtained using parsimony and maximum likelihood (ML) methods suggest that there have been three or four independent transitions from terrestrial to aquatic habitats within the homobasidiomycetes. Three of the marine taxa in our data set are associated with mangroves, suggesting that these ecosystems provide a common evolutionary stepping-stone by which homobasidiomycetes have reinvaded aquatic habitats.

One of the major themes in the evolution of eukaryotes is the repeated transition from aquatic to terrestrial habitats that has occurred in several major clades, including fungi, plants, and animals. In a classic paper, Pirozynski and Malloch (2) suggested that fungi and plants were the first eukaryotes to colonize the land, and that this ecological shift was made possible by the establishment of mycorrhizal symbioses (associations involving fungal hyphae and plant roots). This hypothesis has been bolstered by the recent

discovery of spores of putatively mycorrhizal fungi from the Ordovician (3). Fungi have radiated extensively in terrestrial habitats, where they play pivotal ecological roles, as decayers, pathogens, and symbionts of plants and animals.

One group of fungi that is elegantly adapted to life on the land is the homobasidiomycetes. Adaptations to terrestrial habitats displayed by some homobasidiomycetes include rootlike rhizomorphs that allow the fungi to forage along the forest floor, drought-resistant sclerotia, and tough, perennial fruiting bodies. Aerial spore dispersal in homobasidiomycetes is accomplished by a forcible discharge mechanism termed ballistospory. However, several lineages of terrestrial homobasidiomycetes have lost ballistospory, including puffballs and other forms with enclosed spore-bearing structures.

Aquatic homobasidiomycetes include four species that have retained ballistospory and seven species that have lost ballistospory. The ballistosporic forms can be tentatively assigned to certain terrestrial groups on the basis of the morphology of spores and fruiting bodies (4–12). However, the aquatic homobasidiomycetes that have lost ballistospory have no obvious close relatives among terrestrial groups. This taxonomically enigmatic assemblage includes several marine genera that have elongate or appendaged spores, which superficially resemble the spores of many aquatic ascomycetes (4, 5; Fig. 1).

To resolve the relationships among terrestrial and aquatic homobasidiomycetes, we assembled a data set that includes 4 marine species, 1 freshwater species, and 40 diverse terrestrial species (Fig. 2). The heterobasidiomycete “jelly fungus” *Auricularia auricula-judae* was included for rooting purposes. The data set contains sequences of four rDNA regions, including nuclear and mitochondrial small and large subunit rDNA (3.8 kb total). Four species in the data set lack the mitochondrial large subunit rDNA sequence (Fig. 2). Sequences from 38 terrestrial species and one marine species, *Nia vibrissa*, were drawn from earlier studies (13, 14).

Received 19 July 2001; accepted 30 August 2001.

* To whom correspondence should be addressed. E-mail: dhibbett@black.clarku.edu

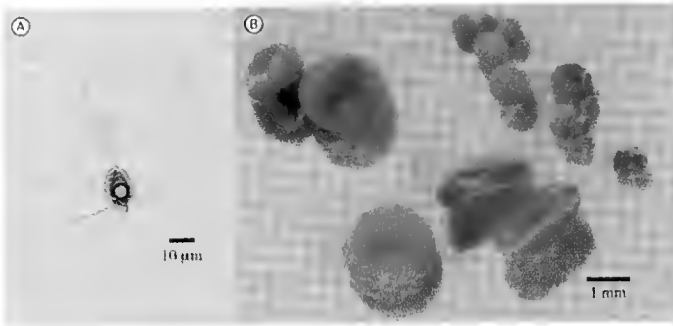


Figure 1. Appendaged spore (A) and enclosed fruiting bodies (B) of the marine homobasidiomycete *Nia vibrissa*.

Parsimony analysis (15) resulted in two shortest trees (5175 steps, consistency index (CI) = 0.372, retention index (RI) = 0.410), and ML analysis resulted in one optimal tree ($-\ln L = 29962.65066$; Fig. 2). In all trees, the aquatic species occur in four separate lineages (Fig. 2). There are two equally parsimonious reconstructions of shifts between terrestrial and aquatic habitats (on all three trees). One reconstruction suggests that there have been four independent transitions from terrestrial to aquatic habitats (Fig. 2A), whereas the other reconstruction suggests that there have been three shifts to aquatic habitats and one reversal from aquatic to terrestrial habitats (Fig. 2B). Under the latter scenario, the terrestrial species *Cyphellopsis anomala* would be derived from marine ancestors.

All of the aquatic species in our data set are nested in a strongly supported group (parsimony bootstrap = 90%/ML bootstrap = 99%) called the euagarics clade, which has been estimated to contain roughly 7400 species (57%) of homobasidiomycetes (Fig. 2; 16). Most members of the euagarics clade are typical mushrooms, with a cap, gills, and (often) a stalk. Familiar taxa in our data set include the cultivated button mushroom *Agaricus bisporus* and the mycorrhizal “fly agaric” *Amanita muscaria*. The ancestor of the euagarics clade was probably a gilled mushroom (14), but contemporary aquatic fungi bear scant resemblance to such forms, as described below.

Three marine species in our data set, *Halocyphina villosa*, *Calathella mangrovei*, and *Physalacria maipoensis* are ballistosporic, have exposed spore-bearing surfaces, and occur in intertidal mangrove communities. *Halocyphina villosa* and *Calathella mangrovei* produce “cyphelloid” fruiting bodies, which are minute (ca. 0.3–1.0 mm diameter), cup-shaped structures, whereas *Physalacria maipoensis* produces a “capitate” fruiting body, which has a globose head on a short stalk (ca. 0.5–2.5 mm high; 8, 9, 11). The genera *Calathella* and *Physalacria* each include terrestrial species, as well as the marine species sampled here (9, 11). *Halocyphina* contains only one species, but Ginns and Malloch

(8) suggested that it could be closely related to the terrestrial cyphelloid genera *Henningsomyces* or *Rectipilus*. Consistent with this prediction, our results suggest that the terrestrial cyphelloid genera *Henningsomyces* and *Cyphellopsis* are closely related to marine homobasidiomycetes (Fig. 2).

The remaining aquatic species in our dataset, *Nia vibrissa* (marine) and *Linnoperdon incarnatum* (freshwater), have lost ballistospory and produce spores inside minute (ca. 0.3–1.2 mm diameter), enclosed, puffball-like fruiting bodies (5, 7, 17, 18; Fig. 1). *Nia vibrissa* is further distinguished by having appendaged basidiospores (Fig. 1). *Nia vibrissa* and *Linnoperdon incarnatum* bear a superficial resemblance to terrestrial puffballs, but their phylogenetic relationships have been obscure. Our results indicate that *Nia vibrissa* is strongly supported (bootstrap = 99%/100%) as the sister group of *Halocyphina villosa* (Fig. 2). The precise placement of *Linnoperdon incarnatum* is not resolved with confidence, although it is strongly supported as a member of the euagarics clade (bootstrap = 90%/99%; Fig. 2).

The close relationship of *Nia vibrissa* and *Halocyphina villosa* could not have been predicted based on morphology. Aside from their small size and marine habit they have no distinguishing features in common. Moreover, *Halocyphina villosa* occurs in mangroves, whereas *Nia vibrissa* and the related species *N. epidermoidea* and *N. globospora* have been collected on fully submerged substrates, including driftwood and the wreckage of a sunken ship, and have been isolated by baiting with submerged wooden test panels, *Spartina* culms, horsehair, and feathers (17, 19–22). Nevertheless, the *Nia*-*Halocyphina* clade is strongly supported and is nested in another strongly supported clade (bootstrap = 100%/100%) that includes the mangrove-inhabiting species *Calathella mangrovei* and two terrestrial species, *Cyphellopsis anomala* and *Favolaschia intermedia* (Fig. 2). With its appendaged spores, enclosed fruiting body, and habit on submerged substrates, *Nia vibrissa* is the most derived member of this clade. Transformations leading to the evolution of this unusual basidiomycete probably involved a shift from terrestrial to periodically immersed to fully submerged substrates, loss of ballistospory, and evolution of appendaged spores and an enclosed fruiting body. Significantly, the cyphelloid fruiting body of *Halocyphina villosa* is enclosed during parts of its ontogeny, and at maturity the opening of the fruiting body is partially covered by interwoven hyphae (8, 18). Thus, the mangrove-inhabiting *Halocyphina villosa* appears to be morphologically and ecologically intermediate between *Nia vibrissa* and terrestrial cyphelloid forms, such as *Cyphellopsis anomala*.

In the mangroves where they occur, *Calathella mangrovei*, *Halocyphina villosa*, and *Physalacria maipoensis* are all periodically submerged in seawater (4, 5, 8, 11). *Physalacria maipoensis*, however, has also been found in adjacent upland forests that are not inundated (9).

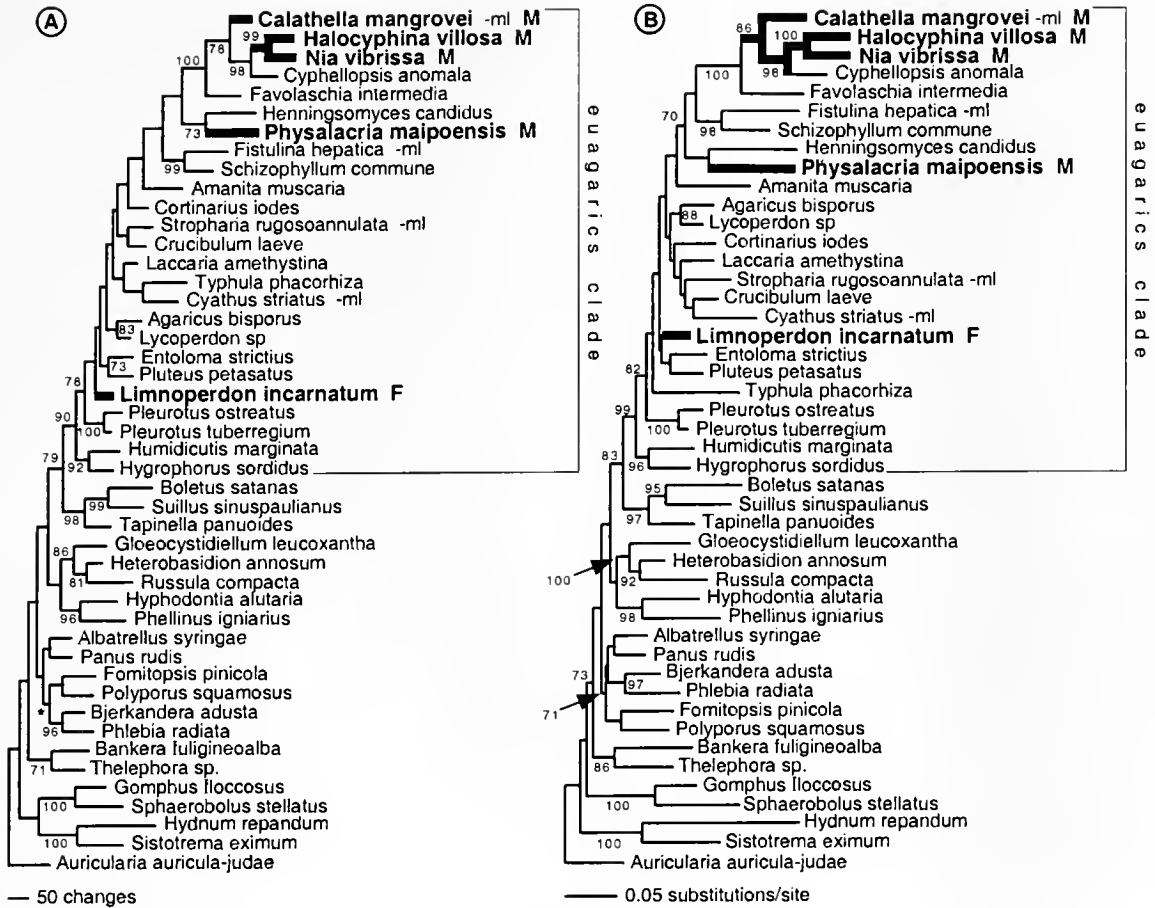


Figure 2. Phylogenetic relationships of terrestrial, marine, and freshwater homobasidiomycetes inferred from nuclear and mitochondrial ribosomal DNA (rDNA) sequences, and alternative reconstructions of the history of shifts between terrestrial and aquatic habitats. (A) One of two phylogenetic trees inferred using parsimony (asterisk indicates the one node that collapses in the strict consensus tree). (B) Phylogenetic tree inferred using maximum likelihood (ML). Names of aquatic taxa are in bold type; M = marine, F = freshwater. Taxa marked -ml lack mitochondrial large subunit rDNA sequences. Bootstrap values are indicated next to branches (only values above 70% are shown). Branch shading indicates reconstruction of ancestral habitats; thin lines = terrestrial, thick lines = aquatic. The parsimony tree (A) shows a reconstruction of habitat shifts that involves four independent transitions from terrestrial to aquatic habitats. The ML tree (B) shows an equally parsimonious reconstruction of ancestral states that involves three transitions from terrestrial to aquatic habitats, and one reversal. Methods: DNA was isolated from cultured mycelium, and nuclear and mitochondrial rDNA regions were amplified and sequenced using protocols and primers that have been reported elsewhere (13, 14). Sequences were aligned by eye in the PAUP* (15) data editor. After excluding 185 positions that were deemed to be ambiguously aligned, the data set included 3574 aligned positions, of which 1267 were variable and 827 were parsimony-informative. Parsimony analysis used 1000 heuristic searches with random taxon addition sequences, tree bisection-reconnection (TBR) branch-swapping, and MAXTREES set to autoincrease, with all characters and transformations equally weighted. Bootstrapped parsimony analysis used 1000 replicates with one heuristic search per replicate, with other settings as in the baseline analysis. ML analysis used the HKY85 model of sequence evolution, with empirical base frequencies, transition-transversion bias set to 2, and among-site rate heterogeneity modeled on a discrete gamma distribution, with four rate classes and shape parameter α set to 0.5. The ML analysis used a heuristic search, with the trees obtained in the parsimony analysis used as starting trees for branch swapping with TBR. Bootstrapped ML analyses used 100 replicates, with one heuristic search per replicate, using a starting tree generated with neighbor-joining (Kimura two-parameter distances), and TBR branch swapping. A time limit of 1 hour per bootstrap replicate was enforced. Sequences have been deposited in GenBank (accession numbers AF426948-AF426970, which should be consulted for strain data) and the data set has been deposited in TreeBASE (accession number S666).

Inderbitzin and Desjardin (9) regarded *Physalacria maipoensis* as "halotolerant," and suggested that it is closely related to certain terrestrial species of *Physalacria*. It is

tempting to speculate that *Physalacria maipoensis* represents an early stage in the transition from terrestrial to marine environments in homobasidiomycetes.

Acknowledgments

We are indebted to E. B. Gareth Jones, who provided a collection of *Calathella mangrovei*; Patrick Inderbitzin, who provided a culture of *Physalacria maipoensis*; and Karen Nakasone, who provided a culture and confirmed the identification of *Favolaschia intermedia*. This work was supported by the National Science Foundation.

Literature Cited

1. Barr, D. J. S. 2001. Chytridiomycota. Pp. 93–112 in *The Mycota VII. Part A. Systematics and Evolution*. Springer-Verlag, Berlin.
2. Pirozynski, K. A., and D. W. Malloch. 1975. The origin of land plants: a matter of mycotrophism. *Biosystems* 6: 153–164.
3. Redecker, D., R. Kodner, and L. Graham. 2000. Glomalean fungi from the Ordovician. *Science* 289: 1920–1921.
4. Hyde, K. D., V. V. Sarma, and E. B. G. Jones. 2000. Morphology and taxonomy of higher marine fungi. Pp. 172–204 in *Marine Mycology—A Practical Approach*. Fungal Diversity Press, Hong Kong.
5. Kohlmeyer, J., and E. Kohlmeyer. 1979. *Marine Mycology—The Higher Fungi*. Academic Press, New York.
6. Desjardin, D. E., L. Martínez-Peck, and M. Rajchenberg. 1995. An unusual psychrophilic aquatic agaric from Argentina. *Mycologia* 87: 547–550.
7. Escobar, G. A., D. E. McCabe, and C. W. Harpel. 1976. *Limnoperdon*, a floating gasteromycete isolated from marshes. *Mycologia* 68: 874–880.
8. Ginns, J., and D. W. Malloch. 1977. *Halocyphina*, a marine basidiomycete (Aphylliphorales). *Mycologia* 69: 53–58.
9. Inderbitzin, P., and D. E. Desjardin. 1999. A new halotolerant species of *Physalacria* from Hong Kong. *Mycologia* 91: 666–668.
10. Jones, E. B. G. 1986. *Digitatispora lignicola* sp. nov. A new marine lignicolous basidiomycotina. *Mycotaxon* 27: 155–150.
11. Jones, E. B. G., and R. Agerer. 1992. *Calathella mangrovii* sp. nov. and observations on the Mangrove fungus *Halocyphina villosa*. *Bot. Mar.* 35: 259–265.
12. Porter, D., and W. F. Farnham. 1986. *Mycaureola dilseae*, a marine basidiomycete parasite of the red alga, *Dilsea carnosa*. *Trans. Br. Mycol. Soc.* 87: 575–582.
13. Binder, M., D. S. Hibbett, and H. P. Mofitoris. 2001. Phylogenetic relationships of the marine gasteromycete *Nia vibrissa*. *Mycologia* 93: 679–688.
14. Binder, M., and D. S. Hibbett. 2001. Higher level phylogenetic relationships of homobasidiomycetes (mushroom-forming fungi) inferred from four rDNA regions. *Mol. Phylogen. Evol.* (in press).
15. Swofford, D. L. 2001. *PAUP* Phylogenetic Analysis Using Parsimony and Other Methods*, Version 4.0b8. Smithsonian Institution and Sinauer Associates, Sunderland, MA.
16. Hibbett, D. S., and R. G. Thorn. 2001. Basidiomycota: Homobasidiomycetes. Pp. 121–168 in *The Mycota VII. Part B. Systematics and Evolution*. Springer-Verlag, Berlin.
17. Jones, A. M., and E. B. G. Jones. 1993. Observations on the marine gasteromycete *Nia vibrissa*. *Mycol. Res.* 97: 1–6.
18. Nakagiri, A., and T. Ito. 1991. Basidiocarp development of the cyphelloid gasteroid aquatic basidiomycetes *Halocyphina villosa* and *Limnoperdon incarnatum*. *Can. J. Bot.* 69: 2320–2327.
19. Barata, M., M. C. Basilo, and J. L. Baptista-Ferreira. 1997. *Nia globospora*, a new marine gasteromycete on baits of *Spartina maritima* in Portugal. *Mycol. Res.* 101: 687–690.
20. Leightley, L. E., and R. A. Eaton. 1979. *Nia vibrissa*—a marine white rot fungus. *Trans. Br. Mycol. Soc.* 73: 35–40.
21. Rees, G., and E. B. G. Jones. 1985. The fungi of a coastal sand dune system. *Bot. Mar.* 28: 213–220.
22. Rossello, M. A., and E. Descals. 1993. *Nia epidermoidea*, a new marine gasteromycete. *Mycol. Res.* 97: 68–70.

Cytological Basis of Photoresponsive Behavior in a Sponge Larva

SALLY P. LEYS^{1,*} AND BERNARD M. DEGNAN²

¹ *Department of Biology, University of Victoria, British Columbia, Canada, V8W 3N5; and* ² *Department of Zoology and Entomology, University of Queensland, Brisbane, QLD 4072 Australia*

Abstract. Ontogenetic changes in the photoresponse of larvae from the demosponge *Reneira* sp. were studied by analyzing the swimming paths of individual larvae exposed to diffuse white light. Larvae swam upward upon release from the adult, but were negatively phototactic until at least 12 hours after release. The larval photoreceptors are presumed to be a posterior ring of columnar monociliated epithelial cells that possess 120- μm -long cilia and pigment-filled protrusions. A sudden increase in light intensity caused these cilia to become rigidly straight. If the light intensity remained high, the cilia gradually bent over the pigmented vesicles in the adjacent cytoplasm, and thus covered one entire pole of the larva. The response was reversed upon a sudden decrease in light intensity. The ciliated cells were sensitive to changes in light intensity in larvae of all ages. This response is similar to the shadow response in tunicate larvae or the shading of the photoreceptor in *Euglena* and is postulated to allow the larvae to steer away from brighter light to darker areas, such as under coral rubble—the preferred site of the adult sponge on the reef flat. In the absence of a coordinating system in cellular sponges, the spatial organization and autonomous behavior of the pigmented posterior cells control the rapid responses to light shown by these larvae.

Introduction

Light, gravity, current, and chemical cues enable the larvae of many marine invertebrates to locate the habitat that will best ensure their success as adults (Grave, 1926; Ryland, 1960; Thorson, 1964; Forward and Costlow, 1974; Brewer, 1976; Young and Chia, 1982; Miller and Hadfield, 1986; Svane and Young, 1989; Pawlik, 1992). Thus, eye-

spots are well developed in many bilaterian larvae (see Eakin, 1968, 1972; Burr, 1984), and signals received by these and other sensory organs are apparently translated into behavior *via* the larval nervous system (Thomas *et al.*, 1987; Kempf *et al.*, 1997; Murphy and Hadfield, 1997; Hadfield *et al.*, 2000). The role of photosensory systems in the larval behavior of basal metazoans is less well documented. Although ocelli are well developed in cnidarian medusae and polyps (Thomas and Edwards, 1991), the putative photoreceptors that have been identified in planulae are simple monociliated sensory cells with electron-dense granules (Weis *et al.*, 1985; Thomas *et al.*, 1987). Presumably the neurons underlying the ciliated epithelium of cnidarian planulae are involved in assessing the environment (Chia and Koss, 1979; Martin and Chia, 1982; Thomas *et al.*, 1987), but there is currently no evidence for synaptic signaling between presumptive photoreceptors and other cells. Poriferan larvae are considered to be even more simply constructed than planulae in that they lack neurons.

Porifera is the only metazoan phylum that lacks neurons (Pavans de Ceccatty, 1974a, b; Mackie, 1979). Furthermore, despite one report suggesting electrical coupling between two reaggregated cells from dissociated adult tissue (Loewenstein, 1967), there is no evidence that sponges have gap junctions, which would allow the rapid conduction of behavioral signals between cells (Green and Bergquist, 1982; Lethias *et al.*, 1983). Members of the subphylum Symplasma, the Hexactinellida, are the only sponges known to be capable of rapid behavior (Lawn *et al.*, 1981; Mackie *et al.*, 1983). Because hexactinellid tissue is mostly syncytial (Leys, 1995), the electrical signals that cause concurrent shutdown of flagellar activity propagate along the membrane of the continuum (Leys and Mackie, 1997; Leys *et al.*, 1999).

Behavior in cellular sponges, the Demospongiae and Cal-

Received 21 December 2000; accepted 22 October 2001.

* To whom correspondence should be addressed. E-mail: spleys@uvic.ca

careca, is limited to gradual contraction of the tissues (McNair, 1923; Vacelet, 1966; Pavans de Ceccatty, 1969, 1976; Mackie, 1979; Lawn, 1982) and variations in pumping patterns (Reiswig, 1971), for which chemical or mechanical coordination are invoked. Although the mechanisms for coordinated behaviors are apparently absent, cellular sponge larvae do exhibit rapid responses to external stimuli. The responses of sponge larvae to light, gravity, and current have been reported since the early 1900s (reviewed in Wapstra and van Soest, 1987).

Photokinesis, one of the most tangible aspects of sponge larval behavior, is best known from studies on parenchymellae larvae of demosponges (Warburton, 1966; Bergquist and Sinclair, 1968; Bergquist *et al.*, 1970; Wapstra and van Soest, 1987; Woollacott, 1990, 1993; Maldonado and Young, 1996, 1999). Typically, these larvae are oblong and heavily ciliated. The parenchymellae of different species are distinguished primarily by the presence or absence of cilia at the poles of the larva, of a ring of longer cilia at one end, or of pigmented cells at one end. Unfortunately, the pattern of ciliation or pigmentation on larvae smaller than 500 μm is difficult to determine accurately by light microscopy, and relatively few larvae have been characterized by electron microscopy (Evans, 1977; Simpson, 1984; Woollacott and Hadfield, 1989; Harrison and De Vos, 1991; Kaye and Reiswig, 1991; Amano and Hori, 1992; Woollacott, 1990, 1993; Fell, 1997). Furthermore, only a few investigators have taken an experimental approach to sponge larval behavior (Jaecle, 1995; Woollacott and Hadfield, 1996; Maldonado and Young, 1996, 1999; Maldonado *et al.*, 1997); most studies report only anecdotal observations.

The cellular mechanisms underlying sponge larval behavior have yet to be addressed: how does an animal lacking nerves and communicating junctions between its cells respond so agilely to light and other stimuli? This paper addresses the ontogenetic change in the light response and its cytological basis in the parenchymella larva of the demosponge *Reneira* sp.

Materials, Methods, and General Observations

Collection and maintenance of specimens

Adult specimens of the sponge *Reneira* sp. (Porifera, Demospongiae, Haplosclerida, Chalinidae) were collected in February, April, August, and December, 1999, from the reef flat in Shark Bay on Heron Is. Reef, Great Barrier Reef (23°26'N, 151°03'E). The sponges were maintained in shaded aquaria in seawater pumped from the reef slope.

Systematics

The identification of this sponge as *Reneira* sp. was confirmed by taxonomists at the Queensland Museum. However, as this species has not yet been formally de-

scribed, a brief description is given here. The sponge is grey or olive brown, and its texture is firm due to a well-developed anisotropic reticulate network of primary spongin that is cored by paucispicule to multispicule tracts of oxeas 80–100 μm long by 1 μm wide. Oscula are slightly raised above the surface of the sponge, which is formed by a typical chalinid isodictyal reticular network that is tangential to the surface. We have deposited a voucher specimen and photograph in the Poriferan Collection in the Queensland Museum (QM G315611). The North Atlantic genus *Reneira* has been variously called *Haliclona* or *Adocia* in the past, and most recently taxonomists have formally transferred the genus *Reniera* to *Haliclona* (de Weerd, 1986). Although the Pacific species of these genera have not been revised recently (J. Hooper, Queensland Museum, Australia; pers. comm.), the behavior and structure of the *Reneira* sp. larvae studied here appear to be very similar to those reported for other chalinids, and even most haplosclerids (Wapstra and van Soest, 1987).

Habitat and description of adult sponges

The sponge forms encrustations 1–3 cm thick on the underside of coral rubble, which is home to numerous other encrusting and grazing animals. The coral is just submerged at low tide and is approximately 3 m deep at high tide.

The brood chambers of *Reneira* sp. are typically located in the lowest portion of the sponge closest to the coral substrate (Fig. 1a). *Reneira* sp. is reproductive year round (Ley and Degnan, unpubl. data), but although sponges collected in all seasons contained brood chambers, sponges collected in August had the least number and released the fewest larvae. The chambers are up to 1 cm^2 in diameter and contain 20 to 150 embryos, 600–900 μm long, in a wide range of developmental stages (Fig. 1b). Spermatocysts were found in only 2 of more than 100 sponges that were collected and sectioned during all collection periods.

Description of the larvae

The larvae of *Reneira* sp. are cream colored with a dark ring of pigment-containing cells around the posterior end; in fact, the dark pigmented ring defines the posterior end (Fig. 1b, c). The outer layer of the larva consists primarily of monociliated cells possessing 20- μm -long cilia (hereafter called short lateral cilia), but there are two protruding bare patches, one each at the poles of the larva. The bare patch at the anterior end is 55–60 μm in diameter, and that at the posterior end is 140–160 μm in diameter and lies inside the pigmented ring (Fig. 1c, d). The anterior border of the pigmented ring is marked by a ring of cells that contain pigment vesicles but also give rise to 120–150- μm long cilia (hereafter called long posterior cilia) (Fig. 1c, d). These latter structures are more appropriately described as cilia

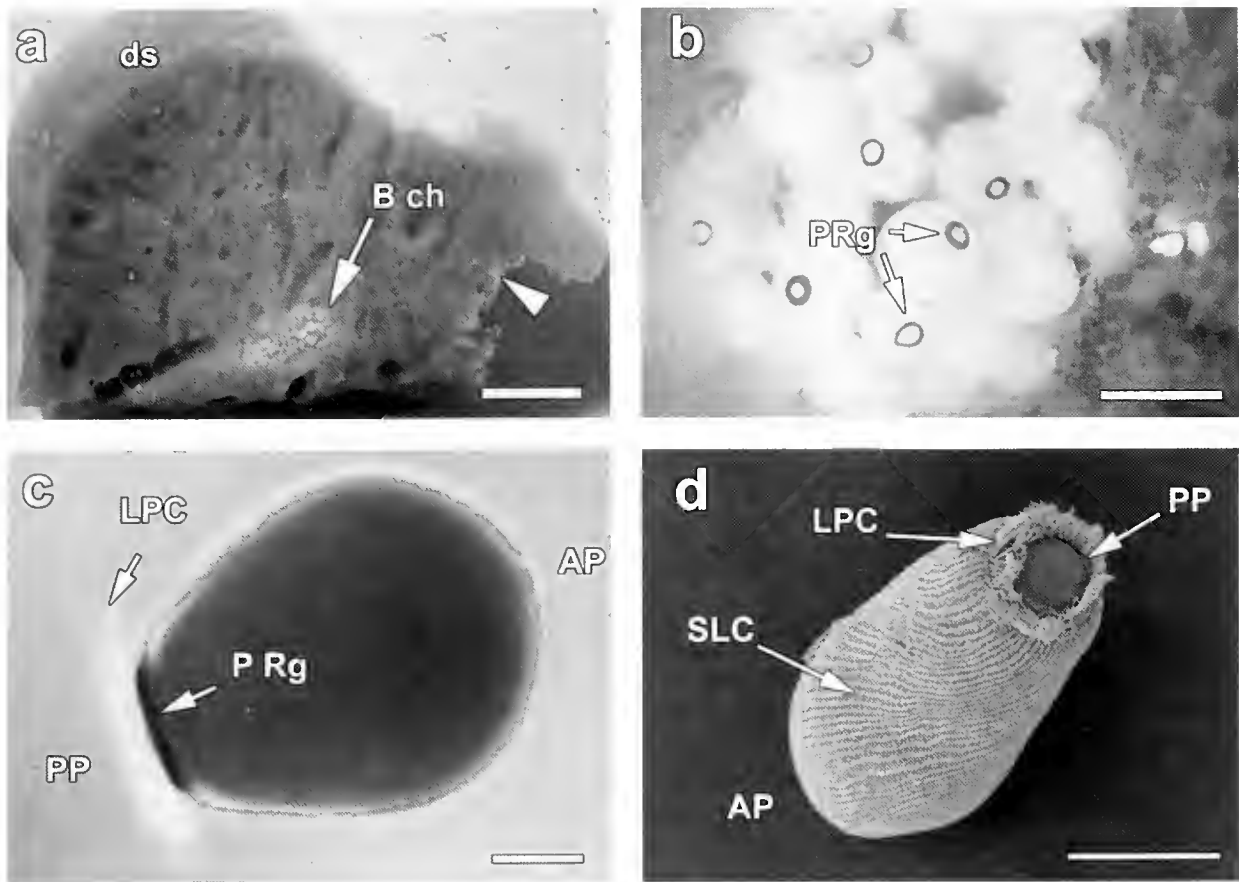


Figure 1. Brood chambers and embryos of *Reneira* sp. in various stages of development (a–c: light microscopy; d: scanning electron microscopy). (a) A section of the adult sponge that was attached at its lower edge to the coral substrate (arrowhead) shows a brood chamber (B ch) with embryos and larvae. Bar: 1 cm. Dermal surface, ds. (b) Embryos and larvae in a brood chamber clearly showing the pigment ring (PRg) at one pole. Bar: 1 mm. (c) A swimming larva showing the dark pigmented ring (PRg) and long posterior cilia (LPC) at the posterior swimming pole (PP), and a protrusion at the anterior swimming pole (AP). Bar: 100 μ m. (d) A larva showing the long posterior cilia (LPC), the unciliated posterior pole (PP), and the lines of short lateral cilia (SLC) arrested by fixation during their beat in metachronal waves. Bar: 250 μ m.

rather than flagella because their motion is whiplike; they do not propagate quasi-sinusoidal waves (Alberts *et al.*, 1989).

Laboratory experiments on larval phototaxis

The larvae were maintained individually in 2 ml of 0.2- μ m-filtered seawater in 12-well multiwell dishes at room temperature (about 22 °C). At various times after release—*i.e.*, 0, 2, 4, 6, 12, 24, and 48 hours—individual larvae were pipetted into a rectangular aquarium (15 \times 20 cm) containing 0.2- μ m-filtered seawater (Fig. 2a). Pipetting was not observed to affect the swimming behavior of the larvae. The rectangular aquarium (the test chamber) was immersed in seawater in a second aquarium, which was blackened on all but one side to reduce reflected light (after Wendt and Woollacott, 1999). Light from a cold light source (Volpi Intralux 5000) was passed through a diffuser made of acrylic plastic into the inner test chamber, such that a

gradient of light was created in the horizontal direction from the front to the back of the test chamber ($950 \mu\text{M} \cdot \text{photons} \cdot \text{m}^{-2} \cdot \text{s}^{-1}$ to $<1 \mu\text{M} \cdot \text{photons} \cdot \text{m}^{-2} \cdot \text{s}^{-1}$). The radiance at the side closest to the light was at the same level recorded at the edge of the underside of a coral boulder at low tide on the reef flat in bright sunlight during the day (Fig. 2b). Light measurements were made in the field and in experimental aquaria with a LI-COR underwater quantum sensor (LI-192SA, LI-COR Inc., Nebraska). Ambient light in the room where measurements were made was $1.8 \mu\text{M} \cdot \text{photons} \cdot \text{m}^{-2} \cdot \text{s}^{-1}$. A glass plate was placed above the test chamber, and the changing position of the larva in the test chamber was recorded for one minute with a nonpermanent felt marker; these records were later transcribed onto paper. Between tests, the larvae were maintained away from direct light in their multiwell dish, at 22 °C.

The initial direction swum by each larva was recorded

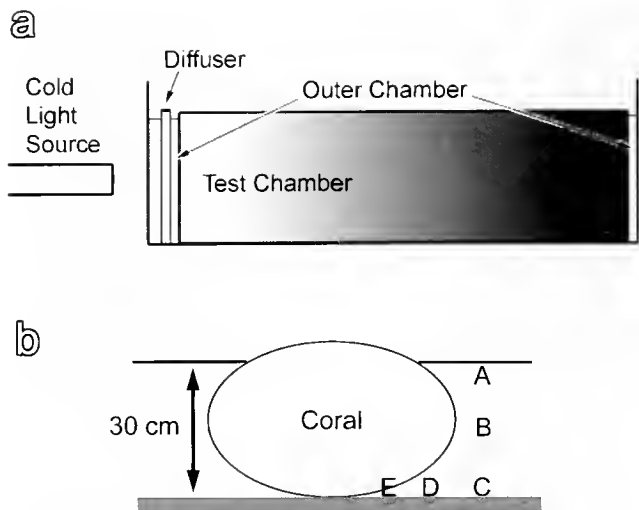


Figure 2. (a) The experimental apparatus for measuring the phototaxis of individual larvae in response to horizontal light from a cold light source shining through a diffuser of acrylic plastic. A test chamber containing filtered seawater is immersed in seawater contained in an outer chamber, which is blackened on all sides except that facing the light source. Larvae were dropped by pipette into the inner test chamber in which there was a gradient of light in the horizontal direction (left to right in the diagram) of $950 \mu\text{M} \cdot \text{photons} \cdot \text{m}^{-2} \cdot \text{s}^{-1}$ to $<1 \mu\text{M} \cdot \text{photons} \cdot \text{m}^{-2} \cdot \text{s}^{-1}$. See methods for further details. (b) Light intensities on the reef flat during a sunny day were recorded at 5 positions (A–E) around coral rubble that was in 30 cm of water at low tide. The average of 10 measurements at each position is given in $\mu\text{M} \cdot \text{photons} \cdot \text{m}^{-2} \cdot \text{s}^{-1}$. A: 1906.5; B: 1354; C: 785.8; D: 57.9; E: 9.4. The substrate below the coral was sand.

and plotted as a circular distribution. The mean angle swum by the larvae in each age group (*i.e.*, 0–48 h) was calculated, and the measure of randomness was tested using the nonparametric Rayleigh test [a high z value, or an r value approaching 1, indicates the data are highly grouped (Zar, 1984)].

Video and light microscopy

Live larvae were observed with an Olympus SZH dissecting microscope with a 1X plan lens, and with an Olympus BX60 compound microscope equipped with an Olympus C35 AD4 photoautomat. New glass coverslips (22×22 mm) were placed on the bottom of a 5-cm-diameter plastic petri dish, and individual larvae were pipetted forcefully onto this surface, causing them to adhere by their anterior end for up to 5 min. During this period, light levels could be manipulated, and the cilia could be observed. Cold light was shone on the posterior end of the larva. Other larvae that had adhered to the dish or coverslip were transected medially, creating an anterior portion and a posterior portion with its pigment ring and long posterior cilia intact. Although mucus and cellular material from the wound was initially caught in the cilia, these debris disappeared after several minutes: then cilia on both the anterior and posterior por-

tions continued their normal beating, and both halves rotated as they did prior to being cut. If the posterior half of a bisected larva was placed with the pigment ring facing upward, it would continue to rotate on the spot indefinitely. Light from a cold light source was shone at the pigmented ring and long posterior cilia on the posterior end of the bisected larva from either the left or right side of the microscope stage. The ciliary beat was recorded using a Panasonic digital CCD video camera and a National time-lapse VCR (AG6010) in real-time recording mode. The intensity of light from the cold light source was measured in seawater on the dissecting microscope base with a LI-COR underwater quantum sensor.

The effect of elevated KCl (10–50 mM) on beating of cilia was tested; ciliary beating was recorded by video CCD.

Electron microscopy

Larvae were fixed for ultrastructural observations in a fixative cocktail consisting of 1% OsO_4 and 2% glutaraldehyde in 0.45 M sodium acetate buffer (pH 6.4) with 10% sucrose (Leys and Reisinger, 1998). For scanning electron microscopy, fixed larvae were dehydrated in a graded ethanol series, critical-point-dried with CO_2 , and coated with gold in an Edwards S150B sputter coater. Up to five larvae were mounted on each stub with clear nail polish and viewed in a Hitachi S-3500N scanning electron microscope at the University of Victoria.

For transmission electron microscopy, the fixed larvae were dehydrated in a graded ethanol series to 70%, stained with 0.5% uranyl acetate in 70% ethanol *en bloc* overnight, desilicified in 4% hydrofluoric acid in 70% ethanol, and then embedded in Epon (Taab 812). Semithin and thin sections were cut on either a Reichert UM2 or a Leica Ultracut T ultramicrotome. Semithin sections were stained with Richardson's (Richardson *et al.*, 1960), mounted in Histoclad, viewed with a Zeiss Axioskop compound microscope, and photographed with a digital DVC camera using Northern Eclipse software. Thin sections were stained with lead citrate and viewed with a JOEL 1010 transmission electron microscope at the University of Queensland, or with a Hitachi 7000 transmission electron microscope at the University of Victoria.

Results

Larval release and swimming behavior

If sponges were placed in an aquarium without flowing seawater, larvae were released at all times of the day, either within 30 min of collection, or when the brood chambers were cut open with a scalpel. Upon release, the larvae swam out of the oscula and directly upward until they reached the surface of the aquarium. In the presence of light, the larvae generally swam forward continuously, corkscrewing or ro-

Table 1

Ontogenetic change in swimming speed of Reneira sp. larvae

Age of larva (h post release)	0	2	4	6	12	24
Mean swimming speed (cm/s)	0.14	0.18	0.16	0.12	0.12	0.07
Number	19	19	19	15	16	11
SD	0.081	0.087	0.099	0.110	0.095	0.072
Variance	0.0066	0.0076	0.0098	0.0122	0.0091	0.0052
<i>t</i> test	Zero-h larvae vs. 24-h larvae			2-h larvae vs. 24-h larvae		
<i>P</i>	0.0043			0.0001		

tating clockwise (as observed from the posterior end of the larva), with occasional bursts of acceleration for periods of several seconds. Larvae responded to light in an identical manner in all seasons.

If undisturbed, larvae in the laboratory would swim at the surface of the seawater for the first 2–3 h after release. Thereafter, they tended to remain at the bottom of their dish moving forward slowly or rotating in one spot with the anterior end upward. However, as soon as the dish was disturbed by light or movement, larvae younger than 2 days old would begin swimming vigorously forward, often at the surface of the water. They were energetic swimmers for 12 h, until they began a creeping phase along the substrate prior to settlement and metamorphosis. Whereas undisturbed larvae metamorphosed 12 to 24 h after release, larvae that were disturbed periodically generally did not metamorphose until 48 hours after release or longer. Some disturbed larvae never metamorphosed and eventually died after one week. Of more than 100 larvae observed, three swam in the reverse direction with the long posterior cilia leading.

Ontogenetic response of Reneira sp. larvae to unidirectional light

Young larvae (<12 hours old) stimulated by light swam energetically in the mid-water column or on the surface of the test aquarium and stopped when they reached a point at which the light intensity fell, from approximately 10%, to 0.1% of the original intensity (from $73 \mu\text{M} \cdot \text{photons} \cdot \text{m}^{-2} \cdot \text{s}^{-1}$ to $1 \mu\text{M} \cdot \text{photons} \cdot \text{m}^{-2} \cdot \text{s}^{-1}$). Older larvae (>12 h old) swam slowly along the substrate away from the light source and continued swimming until they reached the end of the test aquarium, regardless of light intensity. The mean velocities of newly released larvae (0 h) and of 2-h-old larvae stimulated by light were significantly faster than those of day-old larvae (Table 1).

The great majority of newly released larvae (0 h old) were negatively phototactic in response to unidirectional light [mean angle swum (α) = 193°], but a few larvae in this age cohort swam erratically, showing no preference for swimming direction ($r = 0.6$) (Fig. 3). Larvae aged 2, 4, and 6 h were all strongly negatively phototactic (Fig. 3).

The mean angle swum by larvae in response to light shone from zero degrees was 163° ($r = 0.9$) for 2-h-old larvae, 160° ($r = 0.82$) for 4-h-old larvae, and 174° ($r = 0.85$) for 6-h-old larvae. At 12 h after release, active larvae were still swimming directly away from light [mean angle swum (α) = 187°], while less active larvae swam in spirals in one place and were only weakly phototactic, if at all. By 24 h after release from the brood chambers, the swimming directions of larvae were highly varied ($\alpha = 1.637$; $r = 0.233$). All 48-h-old larvae showed little swimming activity and sank to the bottom of the test aquarium rotating gently in one spot (Fig. 3).

Response of larval cilia

Most larval cilia are $20 \mu\text{m}$ long and beat in a pattern of metachronal waves that proceeds obliquely around the larva from anterior to posterior pole (Fig. 1d). This beat is unceasing, and the pattern of beat did not change when the larva was prodded or even cut in half. Moreover, these cilia did not respond to changes in light intensity or increased levels of KCl.

The circular band or ring of long posterior cilia circumscribing the unciliated posterior pole beat either intermittently or in a single wave in a counterclockwise direction (as viewed from the posterior of the larva). The beat of these long cilia was unaffected by mechanical stimuli, but when the larva was transected medially, so as to isolate the posterior portion, these cilia stopped beating, apparently because they were tangled in mucus and cellular debris released from the wound. The debris disappeared within a few minutes, and the long posterior cilia resumed their beat. Treatment with seawater containing 10 and 30 mM KCl had no effect on the long cilia, but treatment with seawater containing 50 mM KCl caused the long posterior cilia to stop beating and the larva to stop swimming for several seconds.

The beat of the long posterior cilia halted instantly when the light intensity abruptly increased or decreased. With a sudden increase in light intensity (2.3 to $19.5 \mu\text{M} \cdot \text{photons} \cdot \text{m}^{-2} \cdot \text{s}^{-1}$; 19.5 to $57.7 \mu\text{M} \cdot \text{photons} \cdot \text{m}^{-2} \cdot \text{s}^{-1}$; 57.7 to $100.9 \mu\text{M} \cdot \text{photons} \cdot \text{m}^{-2} \cdot \text{s}^{-1}$; 100.9 to $144.2 \mu\text{M} \cdot$

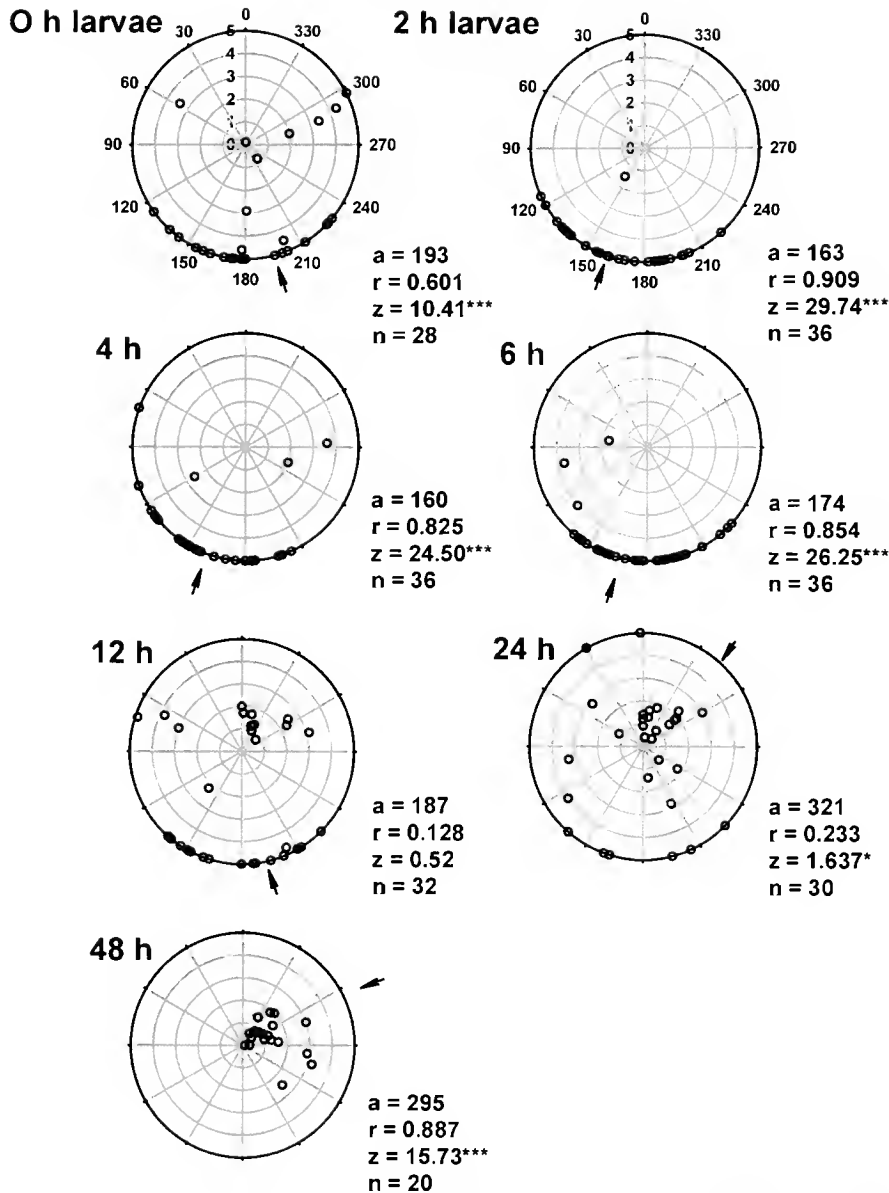


Figure 3. Circular histograms showing the directions swum by individual larvae in response to diffuse light shining from zero degrees (see methods for a complete description). The mean angle swum by larvae of an age cohort is given (a) and is shown with an arrow. A Raleigh's test (z) determined the degree of dispersion of the data; highly grouped data [a high value of z, or a regression (r) approaching 1] are significant (***) at $P < 0.001$. The number of larvae (n) used at each time point is given. The distance swum by larvae is given in centimeters and displayed as distance from the center of the circle. The great majority of larvae younger than 12 h old swam directly away from the light source, while 12-h-old larvae either swam directly away from the light or were indifferent. The majority of day-old larvae showed no clear phototaxis, while 2-day-old larvae sank to the bottom of the test aquarium and rotated in one spot.

photons \cdot m $^{-2}$ \cdot s $^{-1}$), these cilia immediately straightened and remained straight for several seconds (Fig. 4). If the light intensity remained high for longer than 5 s, the ring of long posterior cilia gradually bent down over the bare posterior pole; the cilia constituting the ring responded sequentially, producing a wavelike motion. The ciliary ring remained bent until the light intensity was gradually re-

duced, whereupon the cilia began to beat freely again, as though swimming. If the light intensity was suddenly reduced by reversing the gradients described above, the ciliary ring rapidly bent over the bare posterior pole. If the light remained low for more than 5 s, the cilia slowly straightened again in a wavelike motion and remained rigidly extended until the light intensity was gradually increased. The re-

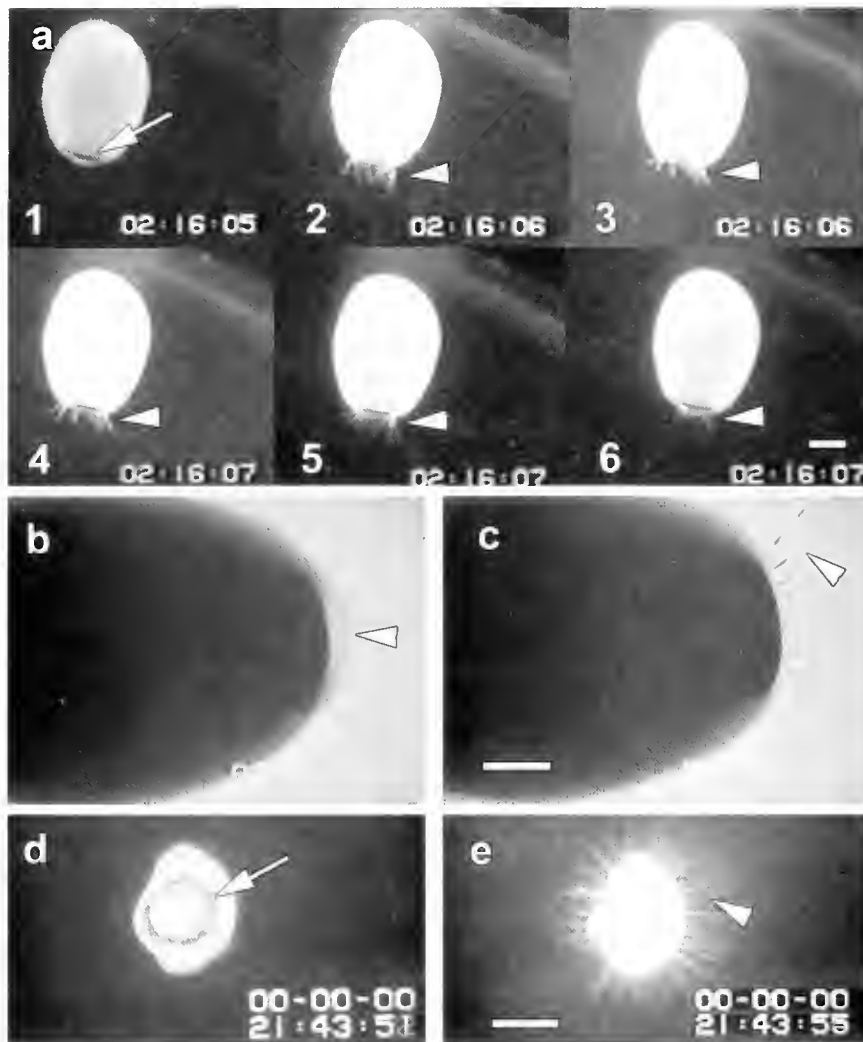


Figure 4. The response of the ring of long posterior cilia to a rapid increase or decrease in light intensity (video microscopy). The time that each video frame was captured is shown in the bottom right-hand corner of each image in hours, minutes, and seconds. The rate of straightening and bending of the ring of long posterior cilia shown in all parts of this figure was controlled by the rate that light intensity was increased and decreased. See methods for details. (a) Frame 1: The cilia are bent over the pigment ring (the dark line indicated by the arrow) in response to a previous sudden reduction of light intensity. Frames 2–3: Upon an abrupt increase in light intensity, the long posterior cilia that constitute the ciliary ring (arrowheads) rapidly straighten and remain rigidly extended (frame 3). Frames 4–6: When the light intensity is suddenly reduced, the ciliary ring (arrowheads) rapidly bends down over the pigment ring. (b, c) The ciliary response was viewed with a compound microscope. The long posterior cilia (arrowheads) are bent over the pigment ring when light is abruptly reduced (b), and straighten when the light intensity is rapidly increased (c). (d, e) The long posterior cilia on the posterior portion of a bisected larva still respond to an abrupt increase and decrease in light intensity. (d) The cilia are bent over the pigment ring (arrow) after a previous sudden decrease in light intensity. (e) With an abrupt increase in light intensity the cilia (arrowhead) straighten. Bar: a, d, e: 100 μm ; b, c: 50 μm .

sponse of the long posterior cilia to changes in light intensity was instantaneous, and the ciliary ring could be made to straighten and bend in unison as fast as a shutter in front of the cold light source could be opened and closed. If the shutter was opened and closed at a slower rate, the cilia straightened and bent more slowly, but still in unison.

The long posterior cilia on isolated posterior portions of

the larva, or on posterior portions in which the ciliary ring had been completely bisected, responded in an identical manner. The response of these cilia became increasingly slow in larvae older than 24 h, but even a larva that had settled on its anterior end and was undergoing metamorphosis would continue to move its long posterior cilia in response to changes in light intensity.

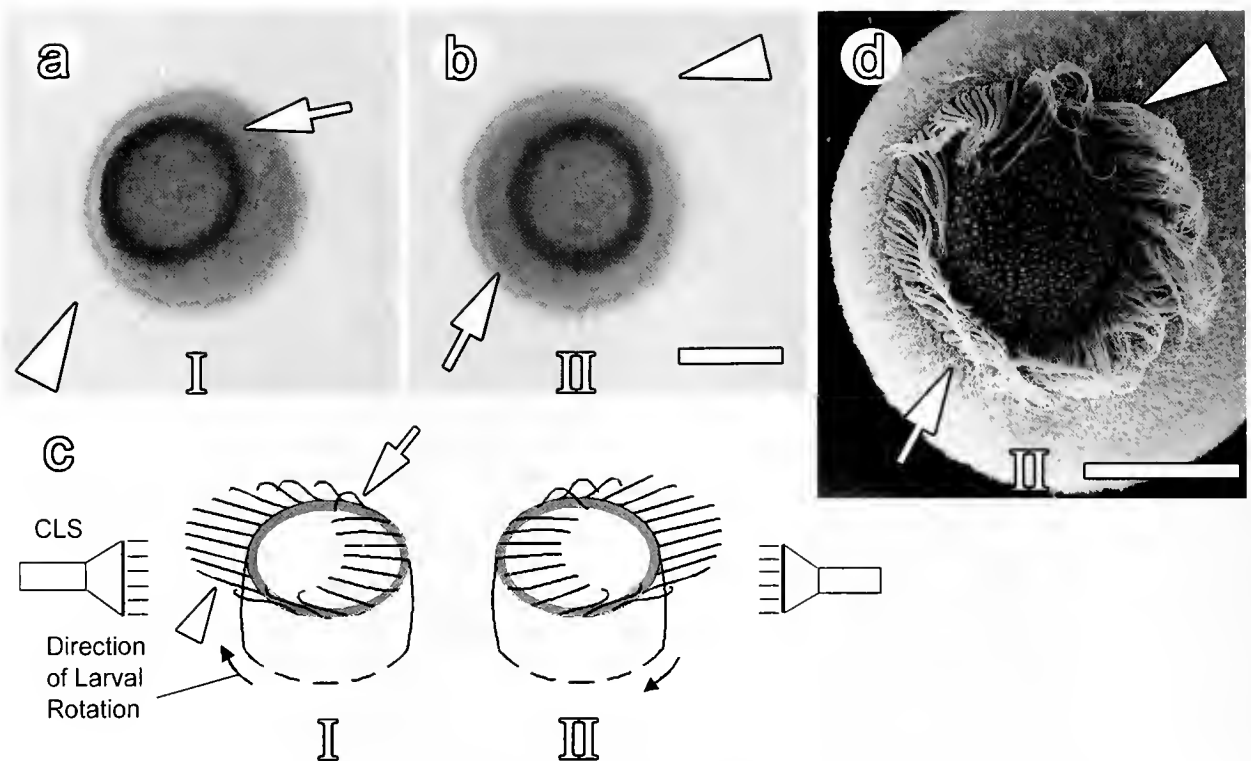


Figure 5. Ciliary movement in "half" (bisected) larvae that were rotating while illuminated from the left (I) or right (II) side. (a, b) Frames from a video recording of the posterior portion of a bisected larva rotating in the same spot while illuminated from the left (a) and right (b) as diagrammed in (c). As the larva rotates in a clockwise direction the cilia straighten (arrowheads) when they are closest to the cold light source (CLS), and bend (arrows) over the pigment ring and bare posterior pole when they are farthest from the light source. Magnification of (a) and (b) is the same. (d) A scanning electron micrograph of a larva that was fixed while rotating in illumination from the right shows that the cilia are straight (arrow) on the right and bent (arrowhead) over the pigmented ring on the left. Bar: a, b, d: 100 μm .

Light shining parallel to the bench top, from either the left or right side of the microscope stage, onto the posterior end of a bisected larva that was rotating in one spot, caused the long posterior cilia closest to the light source to straighten, and those farthest from the light source to bend (Fig. 5). The bisected larvae completed a full rotation once every 1.5–2 s; each long posterior cilium straightened at the instant it reached the side closest to the light source, and bent at the instant it reached the side furthest from the light source. This experiment was readily repeatable with any number of bisected larvae.

Larval ultrastructure

Semithin longitudinal sections of the larva revealed three layers (Fig. 6a, b). Uniciliated columnar epithelial cells form the outer layer that constitutes all but the anterior and posterior poles. These cells have two zones: a basal region with a nucleus (2 μm long) and electron-lucent inclusions (0.66 μm in diameter), and an apical region that is rich in mitochondria and gives rise to a 20- μm -long cilium (Fig. 6c). Large mucous cells occur throughout the epithelial

layer (Fig. 6c). In the anterior third of the larva, flask-shaped ciliated cells are regularly interspersed among the columnar epithelial cells. These cells have a large, centrally located nucleus, numerous small clear vesicles in the cytoplasm, and possess a cilium that arises from a deep indentation in the apical surface of the cell (Fig. 6d).

Underlying the layer of columnar epithelial cells is a region of cells and collagen that is arranged circumferentially around the larva, perpendicular to the longitudinal axis, giving the impression of a belt or girdle of cells (Fig. 6b). This sheet of cells is interrupted only at the posterior end of the larva. These long, narrow cells contain spherulous inclusions (Fig. 6f). The interior of the larva is composed of at least four cell types, which are aligned along the anterior-posterior axis of the larva and are surrounded by a thick layer of collagen fibers and a single type of rod-shaped bacteria that was present in all specimens sectioned (Fig. 6e, inset). The anterior end of the larva is bare (Fig. 7) and is formed of large, almost cuboidal cells filled with very small (0.08–0.25 μm), clear vesicles (Fig. 7b, c). Although most of these cells appear to lack cilia, occasional cilia were seen

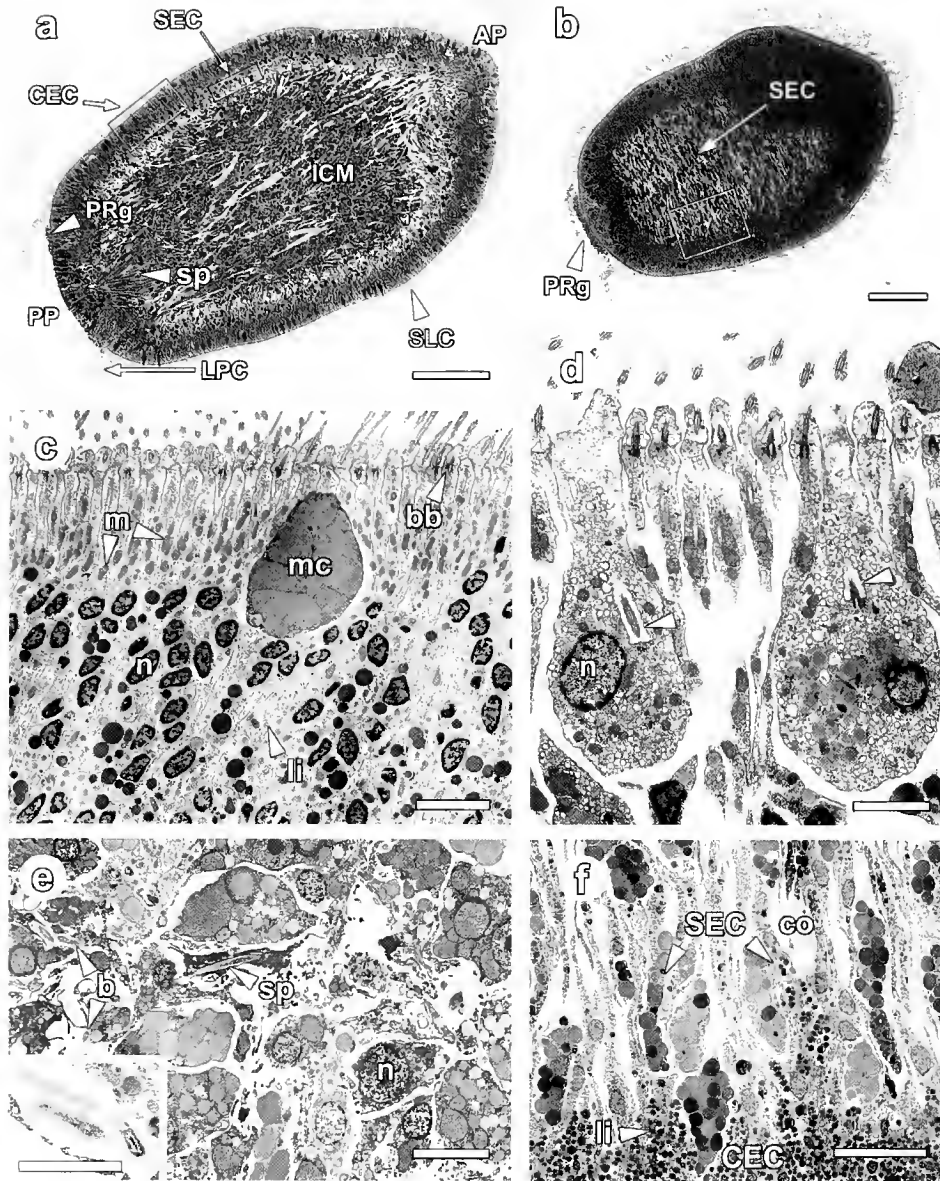


Figure 6. The structure and ultrastructure of *Reneira* sp. larvae (a, b: light microscopy; c-f: electron microscopy). (a) A longitudinal section through a 2-h-old larva shows that short (20- μm -long) lateral cilia (SLC) arise from columnar epithelial cells (CEC) except at the anterior pole (AP) and posterior pole (PP), which are bare. Long posterior cilia (LPC) arise from pigment-filled columnar epithelial cells primarily in the anterior portion of the pigment ring (PRg). Inside the CECs is a layer of subepithelial cells (SEC) that run circumferentially around the larva. Cells in the central region (inner cell mass, ICM) are aligned along the anterior-posterior axis of the larva. Spicules (sp) are evident at the posterior pole. The region in the box is shown in (c). Bar a, b: 100 μm . (b) A tangential longitudinal section through the edge of a 2-h-old larva shows that the subepithelial cells (SEC) are aligned perpendicular to the A-P axis of the larva. The region in the box is shown in (f). Pigment ring, PRg. (c) Columnar epithelial cells from the region of the larva shown in the box in (a); mitochondria, m; mucous cell, mc; basal body of the cilia, bb; nucleus, n; light inclusions, li. Bar: 4 μm . (d) Flask-shaped epithelial cells that occur towards the anterior end of the larva possess a large centrally located nucleus (n) and a cilium that arises from a deep invagination in the cell (arrowheads). Bar: 2 μm . (e) Cells of the inner cell mass. Spicules, sp; nucleus, n; extracellular rod-shaped bacteria, b (inset). Bar: 5 μm ; inset: 2 μm . (f) Subepithelial cells (SEC) from the region shown in the box in (b) lie in a dense bed of collagen (co). Light inclusions (li) can be seen in the bases of the columnar epithelial cells (CEC). Bar: 10 μm .

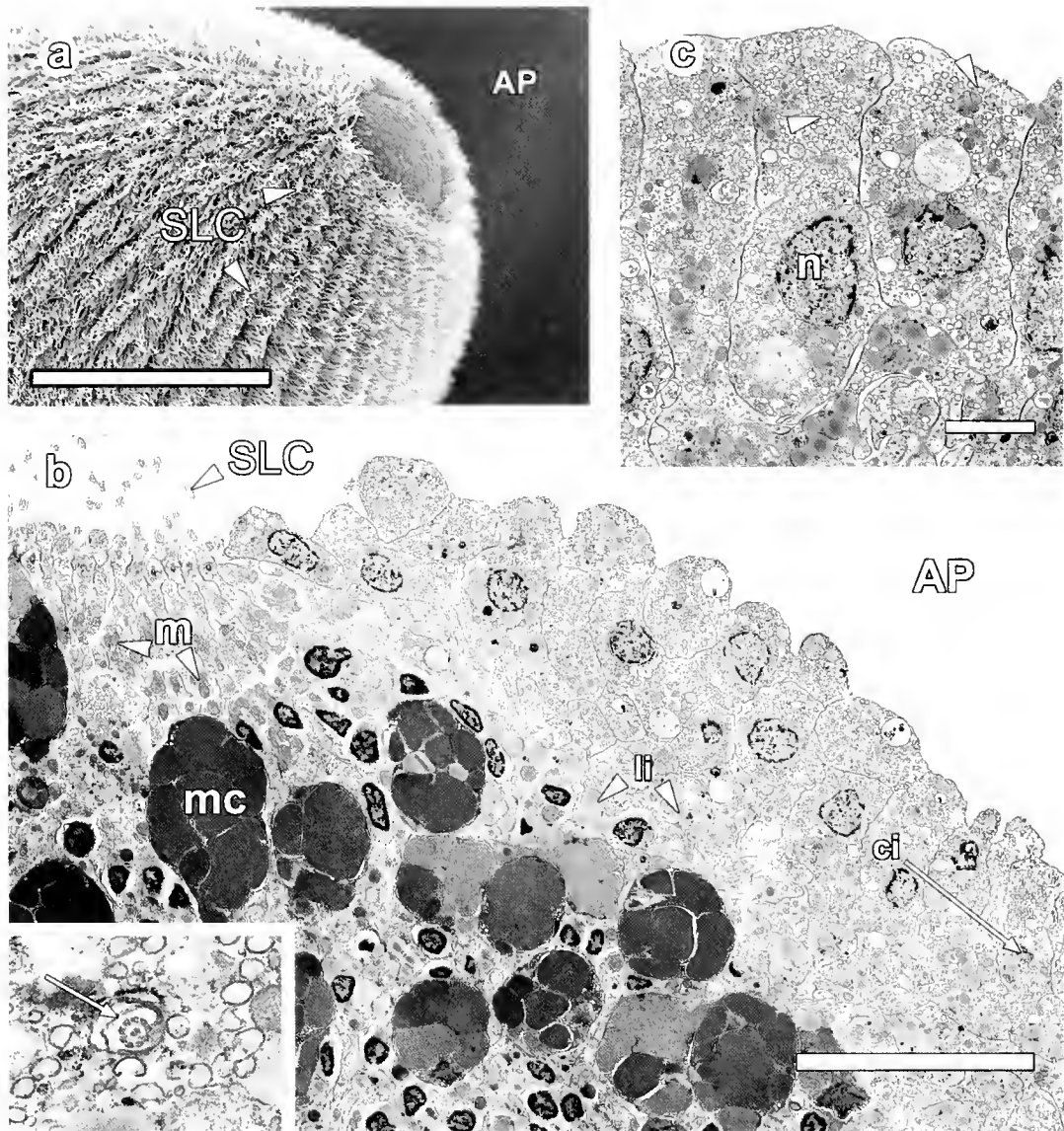


Figure 7. Ultrastructure of the anterior pole of *Reneira* sp. larvae. (a) A scanning electron micrograph of a 2-h-old larva shows that the anterior pole (AP) is bare of cilia, and that the short lateral cilia (SLC) are preserved in bands illustrating the metachronal waves entrained by their beating when alive. Bar: 100 μm . (b) A transmission electron micrograph of a region near the edge of the anterior pole of a 48-h-old larva. The short lateral cilia (SLC) mark the end of the columnar epithelial cells at the anterior pole (AP). The anterior-most cells are generally nonciliated, but the occasional cilium (ci, arrow; inset) can be found deep within the cells. Mucous cells, mc; mitochondria, m; light inclusions, li. Bar: 10 μm . (c) Magnification of the cuboidal cells at the anterior end of a newly released (zero hour) larva shows numerous clear vesicles (arrowheads), n, nucleus. Bar: 2 μm .

arising from deep invaginations in the apical surface of the cuboidal cells (Fig. 7b, inset).

At the posterior end of the larva, large cells containing electron-dense, mucus-like inclusions protrude slightly from the bare posterior pole (Fig. 8). At the boundary between these large posterior cells and the columnar epithelial cells with short cilia lie the pigmented cells bearing the long cilia (Fig. 8a). Electron-dense pigment vesicles occur throughout the length of these cells and in the pro-

trusions of their apical surfaces that extend over the base of the neighboring cells, covering the basal portions of the long posterior cilia (Fig. 8, 9a). The posterior-most pigment-filled cells appear to lack cilia, but otherwise most pigmented cells also give rise to a long posterior cilium (Fig. 8, 9a). No obvious changes in the number or size of pigment vesicles, or the area they occupy in the cell protrusions, could be found in thin sections of the posterior of newly released larvae and 2- to 3-day-old larvae. Further, neither

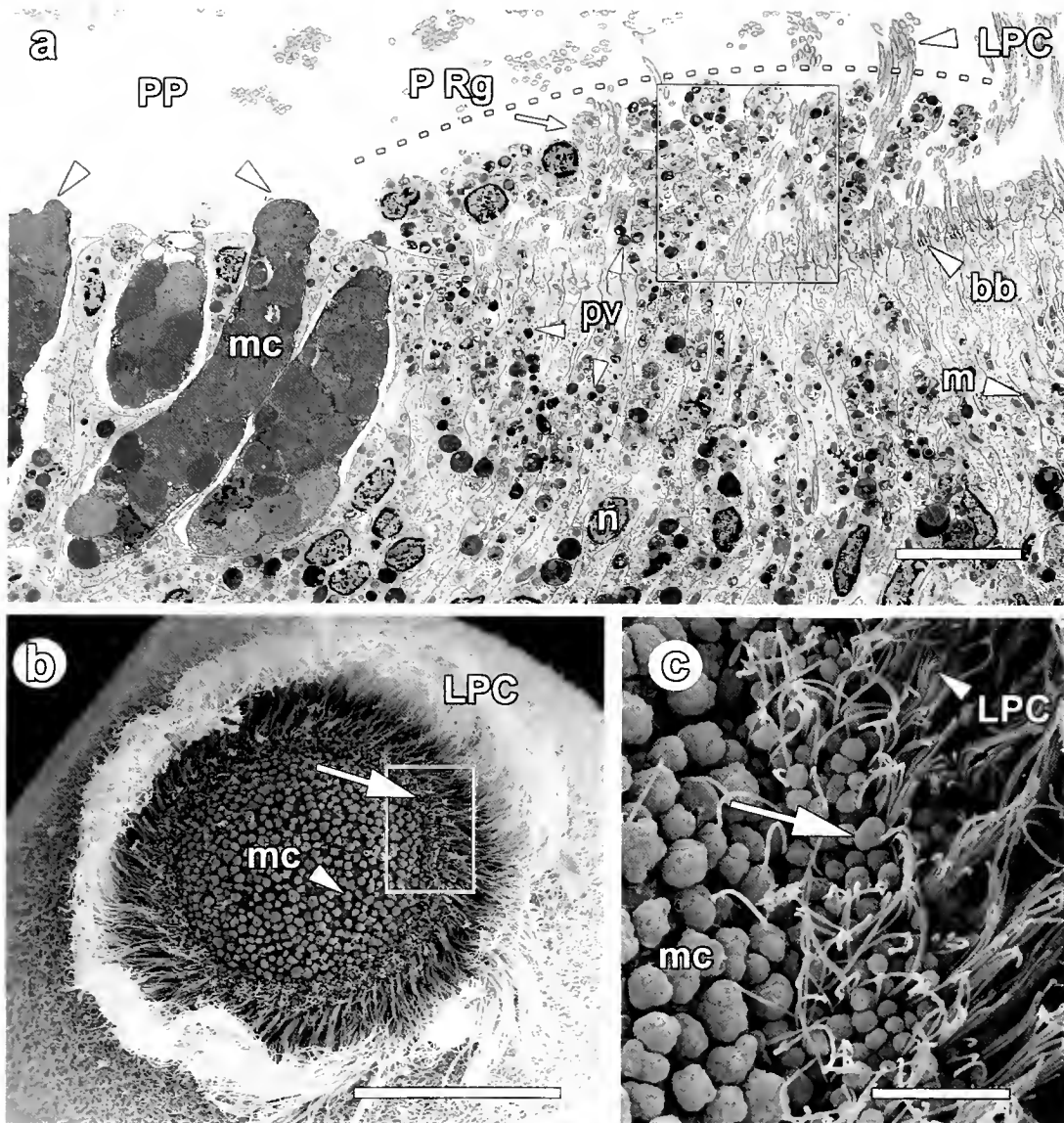


Figure 8. Ultrastructure of the posterior pole of *Renciera* sp. larvae. (a) The posterior pole (PP) is formed in part of large mucus-like cells (mc) that protrude slightly from the posterior end (arrowheads). The pigment ring (PRg, dashed line) is formed of columnar epithelial cells with protrusions (arrow) at their apical surface. These cells contain numerous pigment vesicles (pv) throughout their length and in the apical protrusions. The long posterior cilia (LPC) arise primarily from the anterior-most of these cells. Magnification of the region in the box is shown in Figure 9a. Mitochondria, m; basal bodies of the cilia, bb; nucleus, n. Bar: 5 μ m. (b) A scanning electron micrograph of the posterior pole of a larva that has been fixed while exposed to an abrupt increase in light intensity to cause the long posterior cilia to straighten. Note also that the mucus-like cells (mc) protrude slightly from the posterior end (arrowhead), and that most long posterior cilia (LPC) are anterior to the pigment-filled protrusions (arrow). Magnification of the region in the box is shown in (c). Bar: 100 μ m. (c) A scanning electron micrograph of the region of the pigment ring shown in the box in (b). Mucus-like cells (mc) protrude from the posterior pole, and pigment-filled protrusions (arrow) lie at the base of, and slightly posterior to, the long posterior cilia (LPC). Bar: 20 μ m.

the number of pigmented cells nor the general histology of the posterior end in older larvae changed. The structure of the basal bodies and of the basal portions of the long posterior cilia did not appear to be different from those of the short lateral cilia (Fig. 9b, c).

Discussion

This report presents the first demonstration that sudden changes in light intensity cause an instantaneous response in the cilia of a sponge larva. This, together with the demon-

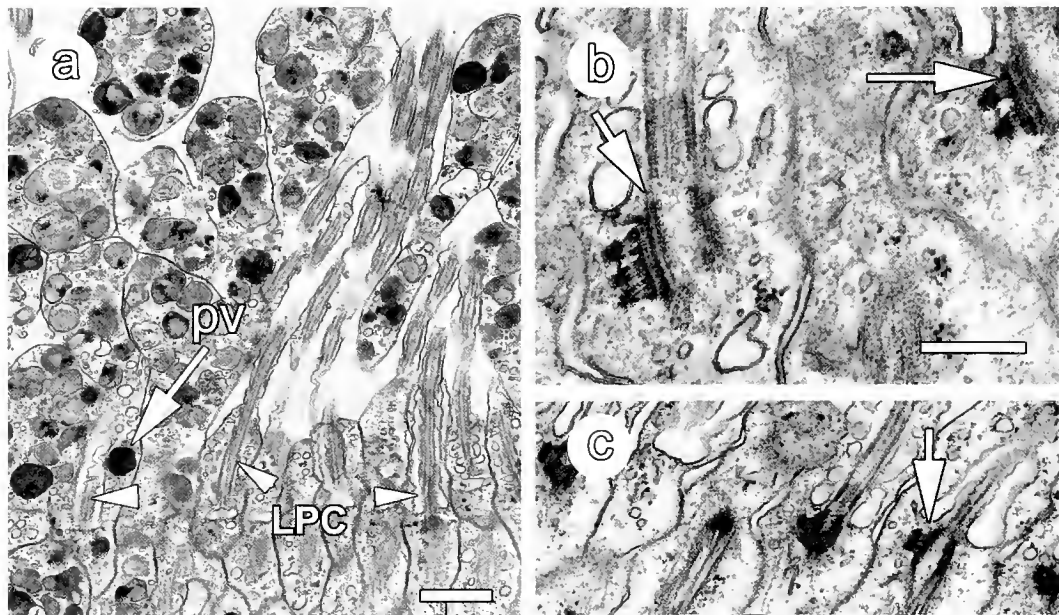


Figure 9. Details of the pigmented cells and ciliated cells in and near the pigment ring (transmission electron microscopy). (a) Magnification of the boxed region in Figure 8a showing that at least some pigment-filled vesicles (pv; arrow) are in protrusions of the same cells that give rise to the long posterior cilia (LPC, arrowheads). Protrusions of the apical surface of other cells in the ciliated ring are also in view in this section. Bar: 1 μm . (b) Basal bodies (arrows) of the long posterior cilia. (c) Basal bodies (arrow) of the short lateral cilia. Bar b, c: 0.5 μm .

stration that light shining at an oblique angle on the long posterior cilia of a rotating larva causes the cilia nearest the light to straighten and those furthest from the light to bend as the larva rotates, implicates the posterior pigment ring and the band of long cilia in steering the sponge larva away from bright light.

Sponge larval "behavior"

Given that cellular sponges lack neurons and gap junctions (Pavans de Ceccatty, 1974a; Mackie, 1979; Lethias *et al.*, 1983; Green and Bergquist, 1982; Woollacott, 1993), sponge larval behavior is usually explained as being due to the physical attributes of the larva. For example, many sponge larvae are reported to swim directly upward after release from the adult (Bergquist and Sinclair, 1968; Wapstra and van Soest, 1987), although there is no evidence that sponge larvae possess gravity or pressure sensors, such as statoysts, or a conduction system that would allow them to translate such messages rapidly into behavior. However, Warburton (1966) suggested that the ability of young larvae to swim to the top of a tube of seawater each time it was inverted, whether illuminated from above or below, could be caused by a differential weighting of the larva at the posterior end. Indeed, as in many species, spicules develop at the posterior end of *Reneira* sp. larvae after their release from the adult, and Maldonado *et al.* (1997) provided ex-

perimental evidence that differential weighting, caused by the presence of spicules at the posterior end in some larvae, is correlated with positive geotaxis and rheotaxis.

The beating of cilia in metachronal waves that run obliquely around the long axis of the larva is often thought to be a result of coordinated behavior (Borojevic, 1969). However, the entrainment of cilia into metachronal waves in many animal systems has been demonstrated to be caused by viscous coupling among cilia (Sleigh, 1974). A very small number of *Reneira* sp. larvae do swim backwards, suggesting that reversal of the direction of metachronal waves is possible in *Reneira*.

Phototaxis and the shadow response

Neither of the above examples of sponge larval behavior suggests that sensory receptors are involved. For this reason, the role of the long posterior cilia in *Reneira* sp. larvae in responding to changes in light intensity, and thus in steering the larva away from the light, is intriguing. Although photoreceptors have often been implicated in the phototaxis of sponge larvae (Kaye and Reisswig, 1991; Woollacott, 1990, 1993; Maldonado and Young, 1996, 1999), the mechanism by which this might occur has not been explored by any of these authors.

The different responses of old and young larvae when swimming into a shaded region of a test chamber has been

noted previously. Maldonado *et al.* (1997) suggested that older larvae are more sensitive to light than newly released larvae, because they continue to swim long after they have moved into a shaded region. *Reneira* sp. larvae exhibited a similar behavior. However, qualitative analysis of the ultrastructure of the posterior end of larvae of all ages revealed no changes in the number of pigment vesicles, the area of the cells occupied by pigment vesicles, or the number of long posterior cilia. Furthermore, the long posterior cilia responded to changes in light intensity in larvae of all ages, including those undergoing metamorphosis, although the response became more sluggish in older larvae. Another interpretation is that, upon entering a shaded area, the younger larvae exhibit a "shadow response"—a photokinetic response that changes the level of activity rather than the direction of movement. The function of the shadow response has been examined in some detail in ascidian tadpole larvae (Woodbridge, 1924; Grave, 1944; Young and Chia, 1985; Svane and Young, 1989) where it appears to influence the settlement patterns of larvae, and in the hydrozoan medusa *Polyorchis penicillatus* where it is involved in vertical diurnal migration (Spencer and Arkett, 1984; Arkett, 1985). The immediate response of the long posterior cilia of *Reneira* sp. larvae to a sudden decrease in light—bending to cover the pigmented ring and posterior pole—is also suggestive of a shadow response. If larvae exhibited this response when entering a region of greatly diminished light (such as under a rock on the reef flat), the larva would stop swimming forward. This suggests that, contrary to the conclusion drawn by Maldonado *et al.* (1997), older larvae are, in fact, less sensitive than younger larvae to changes in light intensity.

The light receptor

Ciliary or rhabdomeric photoreceptors have been described in all invertebrate phyla except Porifera (Eakin, 1968, 1972; Burr, 1984). Both Tuzet (1973) and Amano and Hori (1992) have suggested that the cruciform cells in developing amphiblastulae, the larvae of calcareous sponges, are photoreceptive, but no studies have confirmed this function in larval behavior. The morphology of photoreceptors in basal metazoan groups is unstudied recently, but the work of Eakin (1968, 1972) suggests that the simplest photoreceptors, known from the Cnidaria, are monociliated cells surrounded by cells containing pigment vesicles. The pigment cells in *Reneira* sp. that give rise to the long posterior cilia are similar in structure to the simple photoreceptors described in the hydromedusan *Leuckartiara octona* (Singla, 1974) and to sensory cells that may be photoreceptors in the planulae of *Hydractinia echinata* (Thomas *et al.*, 1987; Weis *et al.*, 1985) and *Phialidium (Clytia) gregarium* (Thomas *et al.*, 1987).

The surface of the pigment cells protrudes out over the

surrounding epithelium forming a dark ring on the posterior side of the long cilia. This band of pigment would effectively block light coming from across the bare posterior pole from reaching the basal portion of the cilium (Figs. 8, 9). It appears that although the posterior-most pigment-containing cells may lack cilia, most cells possess both pigment and a long cilium. Although the location of the photoreceptor is currently unknown (future work using microspectrophotometry to determine its location being planned), the cilium is probably both the receptor and effector, as in the well-studied green unicell *Euglena* (Eakin, 1972; Naitoh and Eckert, 1974; Neuman and Hertel, 1994). The effect of increased external potassium ion concentration in causing temporary arrest of the long cilia in *Reneira* sp. larvae suggests that depolarization of the membrane potential, and possible influx of calcium into the cilium, is the mechanism behind the shadow response of sponge larvae. The phenomenon of reversal or inhibition of ciliary beating due to calcium ion influx resulting from membrane depolarization, is well known in protists (reviewed by Naitoh and Eckert, 1974; Eckert *et al.*, 1976), ctenophores, anthozoans, bivalve gills, echinoderm pleutei, and pelagic tunicates (reviewed in Aiello, 1974).

As indicated earlier, unlike planulae, parenchymellae lack neurons or gap junctions that would allow coordination of signals between the cells with long cilia. Instead, each posterior ciliated cell probably responds independently to changes in light intensity. On the basis of the overt responses of the long posterior cilia to abrupt changes in light intensity, and the asymmetric response of the long posterior cilia to light shining on the cilia from the side, as shown in Figure 5, we hypothesize that the larva steers by the subtle photokinetic responses of each ciliated cell to the light, as diagrammed in Figure 10. As the larva rotates through the water, the base of those cilia on the side opposite the direction of the light would be shadowed by pigment, thus triggering a shadow response, which would cause those cilia to bend and cover the pigmented ring (Fig. 10 B arrowhead). Again, as the larva rotates, cilia whose bases are exposed to light would straighten and beat (Fig. 10 B arrow), thus steering the larva away from the light. In this manner, no coordination between cells is required to steer the larva. Rather, a cumulative effect is achieved by the slightly different angle at which each cilium is exposed to or shaded from light. Phototaxis in *Euglena* is thought to be based similarly on the shading of its photoreceptor (Doughty, 1993). However, as steering in *Euglena* has also been shown to depend largely upon polarized light (Creutz and Diehn, 1976; Häder, 1993), such mechanisms of receiving light cues should also be considered in further investigations of the photoreceptor in sponge larvae.

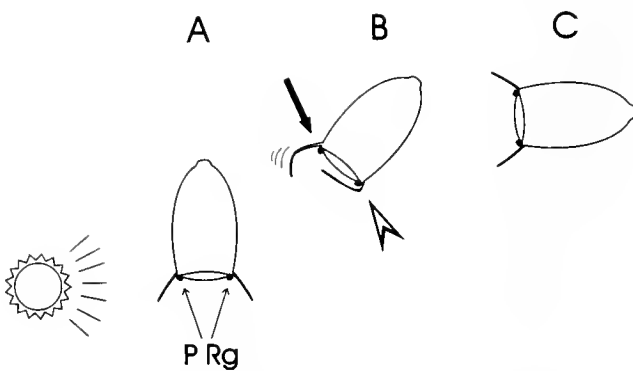


Figure 10. Diagram describing the suggested mechanism by which the pigment ring and long posterior cilia allow *Reneira* sp. larvae to steer away from a light source. (A) As the larva rotates, light from one side of the larva impinges on the base of the cilia closest to the light, but is blocked by the pigment ring from the cilia furthest away from the light. (B) Cilia exposed to the light (arrow) straighten or beat rapidly, depending on the extent of their exposure; those hidden from the light by pigment (arrowhead) undergo a shadow response and bend over the pigment ring. (C) The individual response of each cilium to light as the larva rotates causes a graded response taking the larva away from the source of light.

Coordination of behavior and cellular differentiation in sponge larvae

Cellular differentiation is integral to the behavior of *Reneira* sp. larvae. Five regions of the larva are distinctly differentiated (Fig. 11). The outer ciliated columnar epithelial layer of the larva is separated from the cells in the central region by a sheath or band of circumferential cells. A radial or circumferential sheath has been described in many parenchymella larvae as a subepithelial cell layer (Meewis, 1941; Brien, 1973; Woollacott, 1993). Although it has been suggested that the cells in this layer have a secretory function (Meewis, 1941), it is equally possible that, in light of the paucity of cell-cell junctions in these larvae, the circumferential subepithelial cells give structural support to the larva during release from the parent and during swimming. The cells of the anterior pole are differentiated in *Reneira* sp. larvae as well. Both the monociliated ciliated flask-shaped cells that occur towards the anterior end of the larva and the large cuboidal cells at the anterior pole have numerous small clear vesicles and may therefore have a secretory function. However, the presence of a cilium arising from a deep invagination in both cell types is also reminiscent of some sensory cells in gastropod larvae (e.g., Kempf *et al.*, 1997). This anterior region attaches to the substratum at settlement in *Reneira* sp. larvae. Finally, although the function of the large cells at the posterior pole remains unclear, the pigmented epithelial cells from which arise the long posterior cilia are clearly differentiated to steer the larva away from light.

The resulting picture of the sponge larva is not one typically conjured up of a parazoan, an "almost metazoan."

The *Reneira* sp. larva is an ensemble of differentiated and pluripotential cells arranged in stereotypic patterns along both central-lateral and anterior-posterior axes (Fig. 11). The spatial arrangement of differentiated cell types in the larva, with their specific functions and behaviors, plays a central role in guiding the larva to a suitable settlement location. Clearly this grade of multicellular organization is built by the functioning of multiple transcriptional networks during embryogenesis and larval development. Although a variety of regulatory genes are known to exist in sponge genomes (e.g., Degnan *et al.*, 1993, 1995; Seimiya *et al.*, 1994; Coutinho *et al.*, 1994; Kruse *et al.*, 1994; Hoshiyama *et al.*, 1998), and even though they may be locally expressed in the larva, it is unclear whether conserved genes involved in bilaterian development are operating in a similar manner in sponges. Analysis of the sponge larva and its embryogenesis may enable the identification of developmental genes and processes that are shared among all metazoans, helping us to understand the earliest steps in animal evolution.

Acknowledgments

We thank the director and staff at Heron Island Research Station for use of facilities for portions of this study, Dr. J. Hooper and Mr. J. Kennedy for identification of the sponge, Dr. W. Dennison for use of his LI-COR underwater quantum sensor, and the Great Barrier Reef Marine Park Authority for permission to conduct research on Heron Island Reef. This research was supported by an Australian Research Council grant to BMD, and a Natural Sciences and Engineering Research Council (NSERC Canada) Postdoctoral Fellowship to SPL.

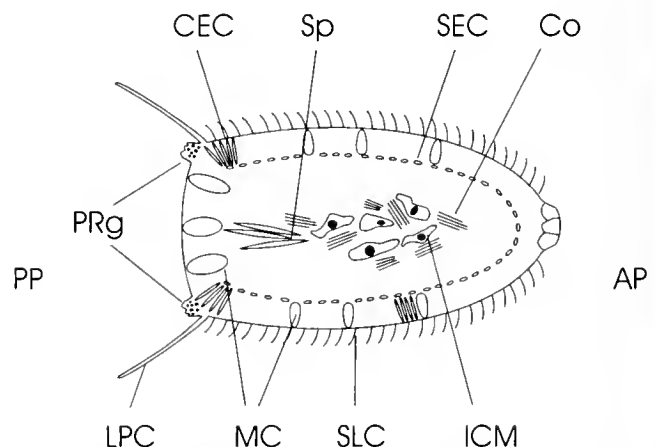


Figure 11. Schematic diagram of cellular differentiation in *Reneira* larvae. PP, posterior pole; AP, anterior pole; MC, mucous cell; PRg, pigment ring; LPC, long posterior cilia; SLC, short lateral cilia; CEC, columnar epithelial cells; SEC, subepithelial cells; ICM, inner cell mass; Co, collagen; Sp, spicules.

Literature Cited

- Aiello, E. 1974. Control of ciliary activity in Metazoa. Pp. 353–376 in *Cilia and Flagella*, M. A. Sleight, ed. Academic Press, London.
- Alberts, B., D. Bray, J. Lewis, M. Raff, K. Roberts, and J. D. Watson. 1989. *Molecular Biology of the Cell*. Garland Publishing, New York.
- Amano, S., and I. Hori. 1992. Metamorphosis of calcareous sponges I. Ultrastructure of free-swimming larvae. *Invertebr. Reprod. Dev.* **21**: 81–90.
- Arnett, S. A. 1985. The shadow response of a hydromedusan (*Polysorchis penicillatus*): behavioral mechanisms controlling diel and ontogenetic vertical migration. *Biol. Bull.* **169**: 297–312.
- Bergquist, P. R., and M. E. Sinclair. 1968. The morphology and behavior of larvae of some intertidal sponges. *N. Z. J. Mar. Freshw. Res.* **2**: 426–437.
- Bergquist, P. R., M. E. Sinclair, and J. J. Hogg. 1970. Adaptation to intertidal existence: reproductive cycles and larval behavior in Demospongiae. *Zool. Soc. Lond.* **25**: 247–271.
- Borojevic, R. 1969. Étude due développement et de la différenciation cellulaire d'éponges calcaires calcinéennes (genres *Clathrina* et *Asandra*). *Ann. Embryol. Morphog.* **2**: 15–36.
- Brewer, R. H. 1976. Larval settling behavior in *Cyanea capillata* (Cnidaria: Scyphozoa). *Biol. Bull.* **150**: 183–199.
- Brien, P. 1973. Les Démospogones. Pp. 133–461 in *Traité de Zoologie*, P.-P. Grassé, ed. Masson Cie, Paris.
- Burr, A. H. 1984. Evolution of eyes and photoreceptor organelles in the lower phyla. Pp. 131–178 in *Photoreception and Vision in Invertebrates*, M. A. Ali, ed. Plenum Press, New York.
- Chia, F.-S., and R. Koss. 1979. Fine structural studies of the nervous system and the apical organ in the planula larva of the sea anemone *Anthopleura elegantissima*. *J. Morphol.* **160**: 275–298.
- Coutinho, C. C., J. Seack, G. Van de Vyver, R. Borojevic, and W. E. G. Mueller. 1994. Origin of the metazoan bodyplan: characterization and functional testing of the promoter of the homeobox gene *EmH-3* from the freshwater sponge *Ephydatia muelleri* in Mouse 3T3 cells. *Biol. Chem.* **379**: 1243–1251.
- Creutz, C., and B. Diehn. 1976. Motor responses to polarized light and gravity sensing in *Euglena gracilis*. *J. Protozool.* **23**: 552.
- de Weerd, W. H. 1986. A systematic revision of the North-Eastern Atlantic shallow-water Haplosclerida (Porifera, Demospongiae). Part II. Chalinidae. *Beaufortia* **36**: 81–165.
- Degnan, B. M., S. M. Degnan, T. Naganuma, and D. E. Morse. 1993. The *ets* multigene family is conserved throughout the Metazoa. *Nucleic Acids Res.* **21**: 3479–3484.
- Degnan, B. M., S. M. Degnan, A. Giusti, and D. E. Morse. 1995. A *hox/hom* homeobox gene in sponges. *Gene* **155**: 175–177.
- Doughty, M. J. 1993. Step-up photophobic response of *Euglena gracilis* at different irradiances. *Acta Protozool.* **32**: 73–77.
- Eakin, R. M. 1968. Evolution of photoreceptors. Pp. 194–242 in *Evolutionary Biology*, T. Dobzhansky, M. K. Hecht, and W. C. Steere, eds. Appleton-Century-Crofts, New York.
- Eakin, R. M. 1972. Structure of invertebrate photoreceptors. Pp. 625–684 in *The Photochemistry of Vision*, J. A. Dartnall, ed. Springer, Berlin.
- Eckert, R., Y. Naitoh, and H. Machermer. 1976. Calcium in the bioelectric and motor functions of *Paramecium*. Pp. 233–256 in *Calcium in Biological Systems*, C. J. Duncan, ed. Cambridge University Press, London.
- Evans, C. W. 1977. The ultrastructure of larvae from the marine sponge *Halicondria moorei* Bergquist (Porifera, Demospongiae). *Cah. Biol. Mar.* **18**: 427–433.
- Fell, F. E. 1997. Poriferans, the sponges. Pp. 39–54 in *Embryology. Constructing the Organism*, S. F. Gilbert and A. M. Raunio, eds. Sinauer Associates, Sunderland, MA.
- Forward, R. B. J., and J. D. J. Costlow. 1974. The ontogeny of phototaxis by the crab *Rhithropanopeus harrisi*. *Mar. Biol.* **26**: 27–33.
- Grave, C. 1926. *Mogulo citrina* (Alder and Hancock). Activities and structure of the free-swimming larva. *J. Morphol. Physiol.* **42**: 453–471.
- Grave, C. 1944. The larva of *Styela (cynthia) partita*: structure, activities and duration of life. *J. Morphol.* **75**: 173–191.
- Green, C. R., and P. R. Bergquist. 1982. Phylogenetic relationships within the invertebrata in relation to the structure of septate junctions and the development of occluding junctional types. *J. Cell Sci.* **53**: 270–305.
- Häder, D.-P. 1993. Simulation of phototaxis in the flagellate *Euglena gracilis*. *J. Biol. Phys.* **19**: 95–108.
- Hadfield, M. G., E. A. Meleshkevitch, and D. Y. Boudko. 2000. The apical sensory organ of a gastropod veliger is a receptor for settlement cues. *Biol. Bull.* **198**: 67–66.
- Harrison, F. W., and L. De Vos. 1991. Porifera. Pp. 29–89 in *Microscopic Anatomy of Invertebrates. Volume 2. Placozoa, Porifera, Cnidaria, and Ctenophora*. F. W. Harrison and J. A. Westfall, eds. Wiley-Liss, New York.
- Hoshiyama, D., H. Suga, N. Iwabe, M. Koyanagi, N. Nikoh, K. Kuma, F. Matsuda, T. Honjo, and T. Miyata. 1998. Sponge *Pax* cDNA related to *Pax 2-5-8* and ancient gene duplications in the *Pax* family. *J. Mol. Evol.* **47**: 640–648.
- Jaekle, W. B. 1995. Transport and metabolism of alanine and palmitic acid by field-collected larvae of *Tedania ignis* (Porifera, Demospongiae): estimated consequences of limited label translocation. *Biol. Bull.* **189**: 159–167.
- Kaye, H. R., and H. M. Reiswig. 1991. Sexual reproduction in four Caribbean commercial sponges. III. Larval behavior, settlement and metamorphosis. *Invertebr. Reprod. Dev.* **19**: 25–35.
- Kemp, S. C., L. R. Page, and A. Pires. 1997. Development of serotonin-like immunoreactivity in the embryos and larvae of nudibranch mollusks with emphasis on the structure and possible function of the apical sensory organ. *J. Comp. Neurol.* **386**: 507–528.
- Kruse, M., A. Mikoc, H. Cetkovic, V. Gamulin, B. Rinkevich, I. M. Mueller, and W. E. G. Mueller. 1994. Molecular evidence for the presence of a developmental gene in the lowest animals: identification of a homeobox-like gene in the marine sponge *Geodia cydonium*. *Mech. Ageing Dev.* **77**: 43–54.
- Lawn, I. D. 1982. Porifera. Pp. 49–72 in *Electrical Conduction and Behavior in 'Simple' Invertebrates*, G. A. B. Shelton, ed. Clarendon Press, Oxford.
- Lawn, I. D., G. O. Mackie, and G. Silver. 1981. Conduction system in a sponge. *Science* **211**: 1169–1171.
- Lethias, C., R. Garrone, and M. Mazzorana. 1983. Fine structure of sponge cell membranes: comparative study with freeze-fracture and conventional thin section methods. *Tissue Cell* **15**: 523–535.
- Leys, S. P. 1995. Cytoskeletal architecture and organelle transport in giant syncytia formed by fusion of hexactinellid sponge tissues. *Biol. Bull.* **188**: 241–254.
- Leys, S. P., and G. O. Mackie. 1997. Electrical recording from a glass sponge. *Nature* **387**: 29–31.
- Leys, S. P., and H. M. Reiswig. 1998. Nutrient transport pathways in the neotropical sponge *Aplysina*. *Biol. Bull.* **195**: 30–42.
- Leys, S. P., G. O. Mackie, and R. W. Meech. 1999. Impulse conduction in a sponge. *J. Exp. Biol.* **202**: 1139–1150.
- Loewenstein, W. R. 1967. On the genesis of cellular communication. *Dev. Biol.* **15**: 503–520.
- Mackie, G. O. 1979. Is there a conduction system in sponges? *Colloq. Int. Cent. Natl. Rech. Sci.* **291**: 145–151.
- Mackie, G. O., I. D. Lawn, and M. Pavans de Ceccatty. 1983. Studies on hexactinellid sponges. II. Excitability, conduction and coordination

- of responses in *Rhabdocalypus dawsoni* (Lambe 1873). *Philos. Trans. R. Soc. Lond. B* **301**: 401–418.
- Maldonado, M., and C. M. Young. 1996.** Effects of physical factors on larval behavior, settlement and recruitment of four tropical demosponges. *Mar. Ecol. Prog. Ser.* **138**: 169–180.
- Maldonado, M., and C. M. Young. 1999.** Effects of the duration of larval life on postlarval stages of the demosponge *Sigmadocia caerulea*. *J. Exp. Mar. Biol. Ecol.* **232**: 9–21.
- Maldonado, M., S. B. George, C. M. Young, and I. Vaquerizo. 1997.** Depth regulation in parenchymella larvae of a demosponge: relative roles of skeletogenesis, biochemical changes and behavior. *Mar. Ecol. Prog. Ser.* **148**: 115–124.
- Martin, V. J., and F.-S. Chia. 1982.** Fine structure of a scyphozoan planula, *Cassiopeia xamachana*. *Biol. Bull.* **163**: 320–328.
- McNair, G. T. 1923.** Motor reactions of the fresh-water sponge *Ephydatia fluviatilis*. *Biol. Bull.* **44**: 153–166.
- Meewis, H. 1941.** L'embryogenèse des éponges siliceuses. *Ann. Soc. R. Zool. Belg.* **72**: 126–149.
- Miller, S. E., and M. G. Hadfield. 1986.** Ontogeny of phototaxis and metamorphic competence in larvae of the nudibranch *Phestilla sibogae* Bergh (Gastropoda: Opisthobranchia). *J. Exp. Mar. Biol. Ecol.* **97**: 95–112.
- Murphy, B. F., and M. G. Hadfield. 1997.** Chemoreception in the nudibranch gastropod *Phestilla sibogae*. *Comp. Biochem. Physiol. A Comp. Physiol.* **118**: 727–735.
- Naitoh, Y., and R. Eckert. 1974.** The control of ciliary activity in Protozoa. Pp. 305–352 in *Cilia and Flagella*, M. A. Sleigh, ed. Academic Press, New York.
- Neumann, R., and R. Hertel. 1994.** Purification and characterization of a riboflavin-binding protein from flagella of *Euglena gracilis*. *Photochem. Photobiol.* **60**: 76–83.
- Pavans de Ceccatty, M. 1969.** Les systèmes des activités motrices, spontanées et provoquées des Éponges. *C. R. Acad. Sci. Ser. III Sci. Vie.* **269**: 596–599.
- Pavans de Ceccatty, M. 1974a.** Coordination in sponges. The foundations of integration. *Am. Zool.* **14**: 895–903.
- Pavans de Ceccatty, M. 1974b.** The origin of the integrative systems: a change in view derived from research on coelentrates and sponges. *Perspect. Biol. Med.* **17**: 379–390.
- Pavans de Ceccatty, M. 1976.** Cellular movements and pathways of coordination in the sponges. *Bull. Soc. Zool. Fr.* **100**: 154.
- Pawlik, J. R. 1992.** Chemical ecology of the settlement of benthic marine invertebrates. *Oceanogr. Mar. Biol. Annu. Rev.* **30**: 273–335.
- Reiswig, H. M. 1971.** In situ pumping activities of tropical demospongiae. *Mar. Biol.* **9**: 38–50.
- Richardson, K. C., L. Jarett, and E. H. Finke. 1960.** Embedding in epoxy resins for ultrathin sectioning in electron microscopy. *Stain Technol.* **35**: 313–323.
- Ryland, J. S. 1960.** Experiments on the influence of light on the behavior of polyzoan larvae. *J. Exp. Biol.* **37**: 783–800.
- Seimiya, M., H. Ishiguro, K. Miura, Y. Watanabe, and Y. Kurosawa. 1994.** Homeobox-containing genes in the most primitive metazoa, the sponges. *Eur. J. Biochem.* **221**: 219–225.
- Simpson, T. L. 1984.** *The Cell Biology of Sponges*. Springer-Verlag, New York.
- Singla, C. L. 1974.** Ocelli of hydromedusae. *Cell Tissue Res.* **149**: 413–429.
- Sleigh, M. A. 1974.** Metachronism of cilia of Metazoa. Pp. 287–304 in *Cilia and Flagella*, M. A. Sleigh, ed. Academic Press, New York.
- Spencer, A. N., and S. A. Arkett. 1984.** Radial symmetry and the organization of central neurones in a hydrozoan jellyfish. *J. Exp. Biol.* **110**: 69–90.
- Svane, I., and C. M. Young. 1989.** The ecology and behavior of ascidian larvae. *Oceanogr. Mar. Biol. Annu. Rev.* **27**: 45–90.
- Thomas, M. B., and N. C. Edwards. 1991.** Cnidaria: Hydrozoa. Pp. 91–183 in *Microscopic Anatomy of Invertebrates*, F. W. Harrison and J. A. Westfall, eds. Wiley-Liss, New York.
- Thomas, M. B., G. Freeman, and V. J. Martin. 1987.** The embryonic origin of neurosensory cells and the role of nerve cells in metamorphosis in *Phialidium gregarium* (Cnidaria, Hydrozoa). *Invertebr. Reprod. Dev.* **11**: 265–287.
- Thorson, G. 1964.** Light as an ecological factor in the dispersal and settlement of larvae of marine bottom invertebrates. *Ophelia* **1**: 167–208.
- Tuzet, O. 1973.** Éponges calcaires. Pp. 27–132 in *Traité de Zoologie*, P.-P. Grassé, ed. Mason Cie, Paris.
- Vacelet, J. 1966.** Les cellules contractiles de l'éponge cornée *Verongia cavernicola* Vacelet. *C. R. Acad. Sc. Ser. III, Sci. Vie* **263**: 1330–1332.
- Wapstra, M., and R. W. M. van Soest. 1987.** Sexual reproduction, larval morphology and behavior in demosponges from the southwest of the Netherlands. Pp. 281–307 in *Taxonomy of Porifera*, J. Vacelet and N. Boury-Esnault, eds. Springer-Verlag, Berlin.
- Warburton, F. E. 1966.** The behavior of sponge larvae. *Ecology* **47**: 672–674.
- Weis, V. M., D. R. Keene, and L. W. Buss. 1985.** Biology of hydractinid hydroids. 4. Ultrastructure of the planula of *Hydractinia echinata*. *Biol. Bull.* **168**: 403–418.
- Wendt, D. E., and R. M. Woollacott. 1999.** Ontogenies of phototactic behavior and metamorphic competence in larvae of three species of *Bugula* (Bryozoa). *Invertebr. Biol.* **118**: 75–84.
- Woodbridge, H. 1924.** *Botryllus schlosseri* (Pallas); the behavior of the larva with special reference to the habitat. *Biol. Bull.* **47**: 223–230.
- Woollacott, R. M. 1990.** Structure and swimming behavior of the larva of *Halichondria melanadocia* (Porifera: Demospongiae). *J. Morphol.* **205**: 135–145.
- Woollacott, R. M. 1993.** Structure and swimming behavior of the larva of *Haliclona tubifera* (Porifera: Demospongiae). *J. Morphol.* **218**: 301–321.
- Woollacott, R. M., and M. G. Hadfield. 1989.** Larva of the sponge *Dendrilla cactus* (Demospongiae: Dendroceratida). *Trans. Am. Microsc. Soc.* **108**: 410–413.
- Woollacott, R. M., and M. G. Hadfield. 1996.** Induction of metamorphosis in larvae of a sponge. *Invertebr. Biol.* **115**: 257–262.
- Young, C. M., and F.-S. Chia. 1982.** Ontogeny of phototaxis during larval development of the sedentary polychaete, *Serpula vermicularis* (L.). *Biol. Bull.* **162**: 457–468.
- Young, C. M., and F.-S. Chia. 1985.** An experimental test of shadow response function in ascidian tadpoles. *J. Exp. Mar. Biol. Ecol.* **85**: 165–175.
- Zar, J. H. 1984.** *Biostatistical Analysis*. Prentice Hall, Englewood Cliffs, NJ.

Isolation and Properties of the Luciferase Stored in the Ovary of the Scyphozoan Medusa *Periphylla periphylla*

OSAMU SHIMOMURA^{1,*}, PER R. FLOOD², SATOSHI INOUE³,
BRUCE BRYAN⁴, AND AKEMI SHIMOMURA¹

¹Marine Biological Laboratory, Woods Hole, Massachusetts 02543; ²Bathybiologica A.S., N-5081 Bergen, Norway; ³Yokohama Research Center, Chisso Corporation, 5-1 Okawa, Kanazawa-ku, Yokohama 236, Japan; and ⁴Prolume Ltd., 1085 William Pitt Way, Pittsburgh, Pennsylvania 15238

Abstract. Bioluminescence of the medusa *Periphylla* is based on the oxidation of coelenterazine catalyzed by luciferase. *Periphylla* has two types of luciferase: the soluble form luciferase L, which causes the exumbrellar bioluminescence display of the medusa, and the insoluble aggregated form, which is stored as particulate material in the ovary, in an amount over 100 times that of luciferase L. The eggs are especially rich in the insoluble luciferase, which drastically decreases upon fertilization. The insoluble form could be solubilized by 2-mercaptoethanol, yielding a mixture of luciferase oligomers with molecular masses in multiples of approximately 20 kDa. Those having the molecular masses of 20 kDa, 40 kDa, and 80 kDa were isolated and designated, respectively, as luciferase A, luciferase B, and luciferase C. The luminescence activities of *Periphylla* luciferases A, B, and C were $1.2\sim 4.1 \times 10^{16}$ photon/mg · s, significantly higher than any coelenterazine luciferase known, and the quantum yields of coelenterazine catalyzed by these luciferases (about 0.30 at 24 °C) are comparable to that catalyzed by *Oplophorus* luciferase (0.34 at 22 °C), which has been considered the most efficient coelenterazine luciferase until now. Luciferase L (32 kDa) could also be split by 2-mercaptoethanol into luciferase A and an accessory protein (approx. 12 kDa), as yet uncharacterized. Luciferases A, B, and C are highly resistant to inactivation: their luminescence activities are only slightly diminished at pH 1 and pH 11 and are enhanced in the presence of 1~2 M guanidine hydrochloride; but they are less stable to heating than luciferase L, which is practically unaffected by boiling.

Introduction

The bioluminescent deep-sea medusa *Periphylla periphylla* is widely distributed in the oceans. It is especially abundant in certain Norwegian fjords, where large specimens are commonly found—up to 20 cm in diameter, 25 cm in height, and weighing over 600 g (Fosså, 1992). Unlike hydrozoan medusas, which contain calcium-sensitive photoproteins, the glow of the scyphozoan *Periphylla periphylla* is due to a luciferin-luciferase reaction involving coelenterazine (a luciferin) and *Periphylla* luciferase. The luciferase of *Periphylla* occurs as a soluble enzyme and as an insoluble particulate matter (Shimomura and Flood, 1998). The soluble form is found mainly in the exumbrellar epithelia of the dome and lappets and in the dome mesoglea. The particulate matter (about 0.5–1 μm in size) occurs abundantly in maturing ovarian eggs, and the total amount of luciferase activity in this form per medusa is far greater than the activity of the soluble form. The soluble form, extracted and purified from the lappets, is an unusually heat-stable luciferase, called luciferase L (32 kDa). The highly active particulate matter obtained from the ovary was partially solubilized and extracted with a buffer containing 2 M guanidine hydrochloride, then purified. The enzyme obtained was highly resistant to various denaturants, and it was designated luciferase O (75 kDa).

We recently found that the treatment of the ovarian particulate with 2-mercaptoethanol solubilizes the luciferase and markedly increases its activity. Moreover, we also found that the solubilized luciferase was a mixture of various molecular species having different molecular weights. These and other lines of evidence suggested that the partic-

Received 30 April 2001; accepted 1 October 2001.

* To whom correspondence should be addressed: E-mail: shimomur@mbi.edu

Table 1

An example of the purification of luciferases A, B, and C from 40 g of ovaries, showing the progress of purification

Step	Method		Total activity (10 ⁶ LU)	Specific activity (10 ⁶ LU/A _{280, 1cm})
1	2-Mercaptoethanol treatment and extraction		50	Not measured
2	Ether-650 hydrophobic interaction chromatography		25	Not measured
3	Superdex 200 gel filtration	A	4.3	0.3
		B	4.6	0.7
		C	3.2	0.3
4	SP-Sepharose anion exchange chromatography	A	2.6	7
		B	3.8	12
		C	2.5	25
5	SP-650 anion exchange chromatography	A	1.9	21
		B	2.8	24
		C	2.1	30
6	Superdex 200 gel filtration	A	1.2	13
		B	1.6	20
		C	1.2	27

1 LU (light unit) corresponds to 5.5×10^8 photons/s.

ulate material could be the storage form of aggregated luciferase. The present work was undertaken to clarify the chemical nature of luciferase in those aggregates. We have isolated three new molecular species of *Periphylla* luciferase from the ovaries of *Periphylla*, and named them luciferases A, B, and C, respectively. The methods of extraction and purification, and the properties of these luciferases are described and discussed in this paper; we also present a new method of preparing luciferase L.

Materials and Methods

Measurement of luminescence activity of luciferase

Luminescence intensity and total light were measured with an integrating photometer model 8020 (Pelagic Electronics, Falmouth, Massachusetts) calibrated with the *Cypridina* bioluminescence reaction (Shimomura and Johnson, 1970). In the assay of luciferase activity, 3 ml of 1 M NaCl/0.05% BSA/20 mM Tris-HCl (pH 7.8) containing 10 μ l of 0.1 mM methanolic coelenterazine was added to a luciferase sample (2–50 μ l) at 24 °C (this is the standard assay condition), and luminescence intensity was measured. Because coelenterazine was present in large excess and luciferase was stable, the rate of the reaction (and thus light emission) was essentially zero-order. One light unit (LU) of luciferase activity on this instrument corresponded to a luminescence intensity of 5.5×10^8 photons/s. The specific activity of a luciferase sample is defined as "luciferase activity in LU or photons/s, divided by A_{280 nm, 1 cm}" except as noted.

Extraction and purification of luciferase from ovaries

The following is only a general plan of the procedure of purification, because experiments were often modified due

to unavoidable variations in the starting materials. At each step of column chromatography, active side fractions were re-chromatographed, and any good fractions recovered were added to the main fractions. In the purification of luciferases A, B, and C (Steps 3–5, below), any side fractions of a target luciferase that contained a different molecular species were combined with a batch of the corresponding luciferase species for further purification. The yields of luciferase at each purification step are shown in Table 1.

Step 1: The specimens of *Periphylla* were collected on board R/V *Håkon Mosby* by vertical plankton-net hauls and midwater trawling in Lurefjorden, western Norway. The ovaries and other organs were excised from live specimens, and stored at –75 °C. Frozen ovary (40 g) was thawed and homogenized with a Bamix mixer MI22 (Clark National Products, San Dimas, California) in 80 ml of 10 mM phosphate buffer (pH 6.6). The homogenate was then centrifuged at $12,000 \times g$ for 10 min at 0 °C. The supernatant was discarded, and the pellets were homogenized in 80 ml of 20 mM acetate buffer (pH 5.4) containing 1 M KCl and 25 mM 2-mercaptoethanol. This mixture was left standing at 0 °C for 3 or 4 h, during which the activity of the sample increased approximately 4-fold. Centrifugation of the mixture gave a clear supernatant (Extract 1). The pellets were mixed with 80 ml of 20 mM acetate buffer (pH 4.8) containing 1 M KCl and were left standing at 0 °C for 3 or 4 h, then centrifuged to give Extract 2. This extraction was repeated two more times in the same manner, except that the standing time was increased, each time, to 1 day; Extracts 3 and 4 were thus produced.

Step 2: Extracts 1 and 2 were combined, and ammonium sulfate was added to make 2.4 M. The solution was adsorbed on a column of Toyopearl Ether-650M (Supelco, Bellefonte, PA; 2.5 cm \times 7 cm). The column was washed

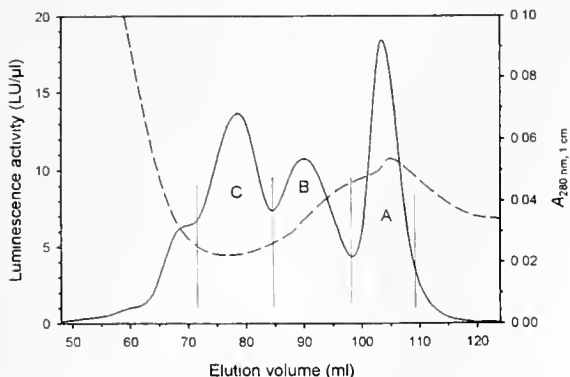


Figure 1. An example of the third-step gel filtration on Superdex 200 Prep. Elution curves are shown for luminescence activity (solid line) and the value of $A_{280 \text{ nm}, 1 \text{ cm}}$ (dashed line). A, B, and C are the peaks of luciferases A, B, and C, respectively. The fractions constituting each of these peaks were combined for further purification.

with 2.2 M ammonium sulfate/20 mM acetate buffer (pH 4.8) at room temperature, then luciferase was eluted with 1.8 M ammonium sulfate/20 mM acetate buffer (pH 4.8), and the active fractions were collected. Luciferase fractions that were eluted with ammonium sulfate concentrations lower than 1.8 M were not used in this study. Extracts 3 and 4 were chromatographed on the Ether-650M column in the same manner. All of the active fractions were combined, made up to 2.4 M ammonium sulfate, and then adsorbed on a column of Ether-650M (1.5 cm \times 3.5 cm). The adsorbed luciferase was eluted with 0.5 M KCl/0.01% lauroylcholine chloride (LCC)/20 mM acetate buffer (pH 4.8), giving about 6 ml of concentrated luciferase solution.

Step 3: Size-exclusion chromatography was carried out on a column of Superdex 200 Prep (Pharmacia; 1.5 cm \times 72 cm) with 1 M KCl/0.01% LCC/20 mM acetate buffer (pH 4.8) as the eluent. On each run, 3 ml of the sample were injected and the effluent was collected in 2-ml fractions. The fractions were separated into 3 groups—luciferases A, B and C (see Fig. 1)—according to their elution volume, and all the fractions from the same group were combined.

Step 4: Cation-exchange chromatography was carried out on a column of SP Sepharose High Performance (Pharmacia; 1 cm \times 6 cm) at room temperature. The eluate from the third step was diluted with two volumes of 0.01% LCC/20 mM acetate buffer (pH 5.5), then adsorbed onto the column. After washing the column with 0.5 M KCl/0.01% LCC/20 mM acetate buffer (pH 5.5), elution was done with a linear gradient of 1.3 M KCl/0.7 M guanidine hydrochloride/0.01% LCC/20 mM acetate buffer (pH 5.5), that increased from 0% to 100% in 23 min.

Step 5: Cation-exchange chromatography was repeated with Toyopearl SP-650M (Supelco; 1 cm \times 6 cm). The eluate of the fourth step was diluted with three volumes of 0.01% LCC/20 mM acetate buffer (pH 5.5) and was adsorbed onto the column. The elution was done in the same

manner as in the fourth step. Step 5 effectively eliminated the tailing UV-absorbing impurities that were seen in the fourth step.

Step 6: Size-exclusion chromatography was performed on a column of Superdex 200 Prep (1 cm \times 48.5 cm) in 1 M KCl/20 mM acetate buffer (pH 4.8); 1 ml of sample was injected in each run.

An improved alternative to Steps 1 and 2: Ovarian tissue (6 g) was briefly homogenized with 20 ml of 10 mM phosphate buffer (pH 6.8), then centrifuged at 20,000 \times g for 10 min, and the supernatant was discarded. The precipitate was mixed with 6 ml of 1 M KCl/1 M guanidine hydrochloride/50 mM acetate buffer (pH 5.4), heated at 80 $^{\circ}$ C for 1 min, and then centrifuged again. The supernatant, which contained 10^6 LU of luciferase activity and a large amount of protein, was not used. The precipitate was mixed with 4 ml of 1 M KCl/0.025% BSA/0.3% 2-mercaptoethanol/50 mM acetate buffer (pH 5.4), and left standing at 0 $^{\circ}$ C for 20 h. Centrifugation of the mixture produced a clear supernatant with a luciferase activity of 2.9×10^6 LU. Extraction of the precipitate with 1 ml of 1 M KCl/50 mM acetate (pH 5.4) gave an additional luciferase activity of 3.6×10^5 LU. This alternative method has three advantages: (1) the product obtained has a markedly higher purity than that obtained in Step 2 above; (2) the ratio of luciferases A:B:C can be changed by altering the concentration of 2-mercaptoethanol and the reaction time, because luciferase C progressively dissociates into B and A; and (3) a significant activity loss caused by the use of high concentrations of ammonium sulfate can be avoided.

A modified method for preparing luciferase L

Only the dome mesoglea (average weight 300 g each), with the thin pigmented layer on the surface removed, were used. The lappets contained greater concentrations of luciferase L, but they were not used because the surface pigment, which drastically decreases the yield of luciferase, is difficult to remove. Cleaned dome mesoglea (500 g) were homogenized in 500 ml of water with 0.3 g of BSA. The homogenate was mixed with 3 teaspoonfuls of Whatman CDR (cell debris remover) and filtered on a Büchner funnel. The filtrate was diluted with two volumes of 10 mM acetate buffer (pH 4.8) and filtered through a column of SP-650M (2.5 cm \times 8 cm). Luciferase adsorbed at the top of the column was eluted with 0.5 M NaCl/0.025% BSA/10 mM acetate buffer (pH 4.8), giving approximately 50 ml of luciferase solution (40,000 LU; this could be safely stored at -70° C, if necessary). The solution was neutralized (pH 7.0) with dibasic sodium phosphate, made up to 2.5 M with ammonium sulfate, and then adsorbed on an Ether-650M column, as described in Step 2 above. The column was washed successively with 15 ml each of 2 M and 1 M ammonium sulfate made with 10 mM phosphate buffer (pH

7.1), and the luciferase L was eluted with 0.5 M ammonium sulfate/acetate buffer (pH 4.8). The material was further purified by chromatography on the columns of SP-650M and Superdex 200, in basically the same manner as reported previously (Shimomura and Flood, 1998). The final yield of purified luciferase L from approximately 5 kg of cleaned domes was 400,000 LU.

Assay of the luciferase in single eggs, embryos, and juveniles

The specimens were frozen in dry ice on board ship immediately after collection. A single frozen specimen was ground thoroughly in a cold aluminum oxide mortar and pestle with 2 ml of 10 mM phosphate buffer (pH 7.0) containing 0.05% BSA. Fifty microliters of this ground suspension was used to measure the total amount of luciferase activity. The rest of the suspension was centrifuged at $20,000 \times g$ for 10 min, and the amount of soluble luciferase in 50 μ l of the supernatant was then determined. After the supernatant was discarded, the precipitate was mixed with 2 ml of 20 mM acetate buffer (pH 5.5), containing 0.05% each of BSA and LCC (lauroylcholine chloride) 1 M KCl, and 25 mM 2-mercaptoethanol. This extraction/solubilization with 2-mercaptoethanol continued overnight at 0 °C. The total amount of luciferase activity in 50 μ l of this suspension was then measured. After this suspension was centrifuged at $20,000 \times g$ for 10 min, the amount of soluble luciferase in 50 μ l of the supernatant was assayed.

Results

Purification of the three molecular species of Periphylla luciferase from ovary

The insoluble, aggregated form of luciferase was successfully solubilized with 2-mercaptoethanol, presumably by the splitting of disulfide bonds. However, the purification of the solubilized luciferase was difficult, mainly because of certain unusual characteristics of luciferase: its inactivation by dilution—particularly when high concentrations of ammonium sulfate were diluted, its irreversible binding to almost anything, and its expected loss of activity by enzymatic degradation in the early stages of purification.

Because the luciferase bound irreversibly to most chromatographic adsorbents, these materials were unsuitable for purification; indeed their use led to large, often complete, loss of enzyme activity. After extensive tests, a few kinds of adsorbent were found to be relatively safe under certain conditions. At first, BSA was used in the purification of luciferase L to minimize the activity loss, although a protein additive is clearly undesirable in the purification of a protein. However, we have recently found that cationic detergents, such as LCC, effectively prevent the inactivation of luciferase preparations, although the tight binding of the

detergent may cause certain complications by altering the properties of proteins. Guanidine hydrochloride (1–2 M) was also highly effective at stabilizing luciferase.

Because of their “sticky” nature, luciferase molecules in crude and partially purified preparations probably exist in complexed forms, bound to some impurities in the solution. Thus, the chromatographic behavior of luciferase in crude preparations may differ from that of pure luciferase, and the behavior of luciferase may change as purification progresses. For example, hydrophobic interaction columns, such as Ether-650M and Butyl Sepharose (Pharmacia), can be used with crude luciferase but not for highly purified luciferase. Similarly, a gel filtration column of Superdex 200 Prep is reliable in most stages of purification, but not with completely pure luciferase.

The purification of the solubilized luciferases from 40 g of ovaries involved over 50 column chromatography runs (summarized in Table 1). In Step 5, the elution curve plotted with luciferase activity and that plotted with $A_{280 \text{ nm}, 1 \text{ cm}}$ value were practically parallel for all three species of luciferase (data not presented), indicating that they were highly pure. The results of Step 6 show decreases in the specific activity, possibly due to two combined effects: the loss of luciferase by adsorption onto the column, and an actual decrease in specific activity; both decreases were caused by the omission of LCC from the buffer used. Assuming that a solution with $A_{280 \text{ nm}, 1 \text{ cm}}$ equal to 1.0 contains 1 mg/ml of luciferase, the yields of purified luciferases at Step 5 (Table 1) are 0.09 mg, 0.12 mg, and 0.07 mg for luciferase A, B, and C, respectively. When Steps 1 and 2 were replaced by the alternative method, the specific activities at Step 4 became 2–3 times higher than those at Step 5 in the original method, although the protein purities remained on comparable levels.

Molecular properties of luciferases A, B, and C

The molecular weights of luciferases A, B, and C were estimated by gel filtration on the same Superdex 200 Prep column that was used in Step 6 to purify the luciferases; 0.005% LCC was added to the buffer to minimize adsorption onto the column. The results (Fig. 2) indicated the molecular masses of luciferases A, B, and C to be 19 kDa, 40 kDa, and 80 kDa, respectively. After treating the proteins for 1 day at room temperature with an elution buffer containing 25 mM 2-mercaptoethanol, the main peaks of all the proteins were found at the same position—that corresponding to 19 kDa. This result suggests that luciferases B and C are the dimer and tetramer, respectively, of luciferase A, and that the molecular masses of luciferase A is about 20 kDa, rather than 19 kDa. During the process of purification, three other luciferase species, corresponding to 60 kDa, 120 kDa, and 160 kDa, were observed as relatively minor components. These were not purified.

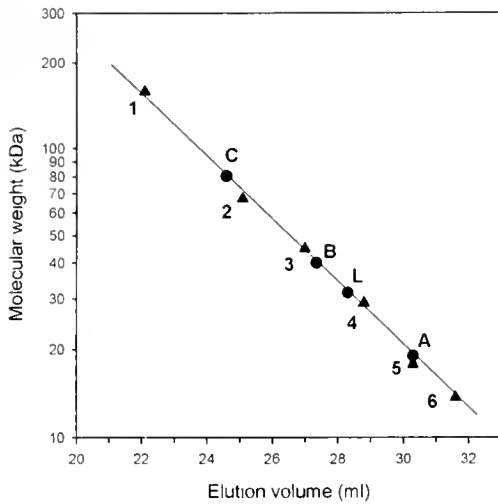


Figure 2. Molecular weight estimation of luciferases A, B, C, and L. The gel filtration was carried out on a column of Superdex 200 Prep (1×48.5 cm), in 20 mM acetate buffer (pH 4.8), containing 1 M KCl and 0.01% laurylcholine chloride. Calibration standards: aldolase (1), BSA (2), ovalbumin (3), carbonic anhydrase (4), myoglobin (5), ribonuclease A (6).

SDS-PAGE (polyacrylamide gel electrophoresis) analysis of luciferases A, B, and C under reducing condition (with 2-mercaptoethanol) showed only one major band corresponding to a molecular mass of 24 kDa (Fig. 3); thus, the purity of these proteins and the oligomeric nature of luciferases B and C are verified. Although the molecular mass of the luciferase monomer obtained by gel filtration (19 kDa) does not match well with that obtained by SDS-PAGE (24 kDa), we chose to use the value of 20 kDa for luciferase A (and 40 kDa and 80 kDa for luciferases B and C) as a reasonable approximation, pending the determination of its precise value in the future. We also note here that luciferase L (32 kDa) also yielded luciferase A upon treatment with 2-mercaptoethanol (Fig. 3; see Discussion).

The spectral properties of luciferase A, B, and C were practically identical with those of luciferase L; their absorption and fluorescence spectra indicate that the luciferases are simple proteins, without any chromophore that absorbs or fluoresces in the visible region.

Enzymatic properties

The enzymatic properties of luciferases A, B, and C are generally similar to those of luciferase L previously reported (Shimomura and Flood, 1998), but with some notable differences. Thus, the luminescence intensity of luciferase A was highest at 27 °C, and those of luciferases B and C at 30 °C, whereas the luminescence intensity of luciferase L showed no maximum, but steadily increased as the temperature was lowered to almost 0 °C (Fig. 4). A clear difference was also found in their heat stabilities (Fig. 5). Luciferase L is extremely stable to heat, with almost no loss of luminescence activity after

being heated at 95 °C for 2 min. Luciferases A, B, and C are less stable, showing activity losses of 50% or more under the same conditions; the loss seems to be greater with the luciferase species of larger size.

The effects of pH on the luminescence of luciferases A, B, and C were similar to that of luciferase L, showing an optimum at pH 8.0. All *Periphylla* luciferases are highly stable at acidic and alkaline pHs (Fig. 6). The influence of salt concentration on the luminescence activities of luciferases A, B, and C appears essentially the same as that for luciferase L, showing that the optimum salt concentration is about 1 M (Fig. 7). The effect of the concentration of coelenterazine on luminescence intensity is presented in Figure 8, and the Michaelis constants of luciferases A, B, and C calculated from these data are about 0.2 μ M, which is significantly lower than the value for luciferase L (1.1 μ M).

Like luciferase L, luciferases A, B, and C were strongly inhibited by Cu^{2+} ; but they were not inhibited by thiol agents. Inhibition of luciferase L by thiol agents reported previously (Shimomura and Flood, 1998) must be incorrect because purer preparations showed lesser inhibition; the inhibition seen earlier could have been caused by the activation of thiol-activated proteases.

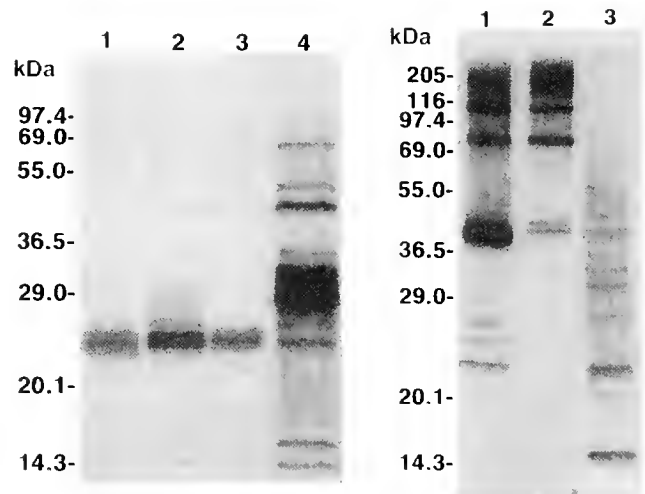


Figure 3. SDS-PAGE analysis of luciferases A, B, C, and L. The electrophoresis was carried out under reducing condition for luciferases A, B, C, and L (left panel, lanes 1, 2, 3, and 4, respectively) and under nonreducing condition for luciferases B, C, and L (right panel, lanes 1, 2, and 3, respectively), by the method of Laemmli (1970) using 12% gel; the protein bands were visualized by silver staining. Approximate amounts of protein used: luciferases A, B, and C, 0.3–1.2 μ g; luciferase L, 10 μ g. Marker proteins (not shown): myosin (205 kDa), β -galactosidase (116 kDa), phosphorylase b (97.4 kDa), BSA (69 kDa), glutamic dehydrogenase (55 kDa), lactic dehydrogenase (36.5 kDa), carbonic anhydrase (29 kDa), trypsin inhibitor (20.1 kDa), lysozyme (14.3 kDa). Note that the 15-kDa band of lane 4 (left panel) corresponds to the 14.5-kDa band of lane 3 (right panel), in both color and position; the accessory protein of luciferase L is shown as the weak 14-kDa band in lane 4, left panel.

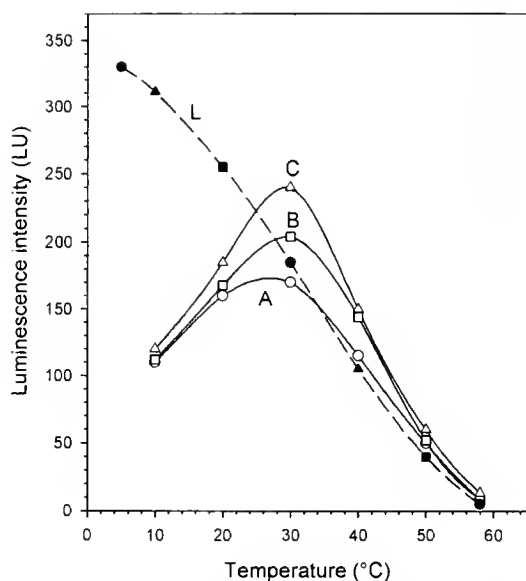


Figure 4. Effect of temperature on the luminescence intensities of coelenterazine catalyzed by luciferases A, B, C, and L. The measurements were done in 20 mM Tris-HCl buffer (pH 7.8), containing 1 M NaCl and 0.05% BSA (the standard buffer). The luminescence reaction was started by the addition of 10 μ l of 0.1 mM methanolic coelenterazine. The amount of sample used for measuring each point: luciferase A, 170 LU; luciferase B, 190 LU; luciferase C, 210 LU; luciferase L, 210 LU.

Luminescence reaction of coelenterazine and its analogs catalyzed by luciferases A, B, and C

The spectra of the luminescence of coelenterazine catalyzed by luciferase A, B, and C were all identical with that of luciferase L, showing a peak at 465 nm. The specific activity (quanta emitted per second, divided by $A_{280\text{ nm}, 1\text{ cm}}$) of the materials obtained in Step 5, Table 1, was 1.21×10^{16} photons/s for luciferase A, 1.32×10^{16} photons/s for luciferase B, and 1.65×10^{16} photons/s for luciferase C, under the standard assay conditions. However, significantly higher specific activities were obtained when the purification included the alternative method for Steps 1 and 2: 3.6×10^{16} photons/s and 4.1×10^{16} photons/s for luciferases A and B, respectively (the yield of luciferase C was low). The maximum specific activities obtainable with high concentrations of coelenterazine (over 2 μ M) should be roughly twice these values, based on the data of Figure 8 (note that the coelenterazine concentration in the standard assay is about 0.3 μ M). As a reference to these data, the maximum specific activity of luciferase L reported previously was 8×10^{13} photons/s (Shimomura and Flood, 1998). The quantum yields of coelenterazine in the luminescence reaction catalyzed at 24 °C by luciferases A, B, and C were 0.287, 0.291, and 0.296, respectively, compared with 0.14 previously reported for luciferase L.

All known coelenterazine luciferases can catalyze the luminescent oxidation of various coelenterazine analogs,

causing luminescence in various intensities—from a negligibly low level to a level several times higher than that of coelenterazine (Inouye and Shimomura, 1997; Nakamura *et al.*, 1997). Using *Periphylla* luciferases A, B, and C, none of more than 20 analogs tested gave a luminescence intensity higher than that of coelenterazine, and only four analogs emitted significant levels of luminescence, each giving the same intensity with the three luciferase oligomers. These four analogs had a substitution at the 2 or 6 position of the imidazopyrazinone ring of coelenterazine, and their relative luminescence intensities, taking coelenterazine as 100%, were: 2- $\text{CH}_2\text{C}_6\text{H}_5$, 95%; 2- $\text{CH}_2\text{C}_6\text{H}_{11}$, 21%; 6- $\text{C}_6\text{H}_4\text{NH}_2$ (*p*), 20%; 6- $\text{C}_6\text{H}_4\text{NHCH}_3$ (*p*), 31%.

Luciferase O

Luciferase O (about 75 kDa) had previously been obtained from the ovary by extraction with a buffer solution containing 2 M guanidine hydrochloride (Shimomura and Flood, 1998). On the basis of a chromatographic comparison on a Superdex 200 Prep column, this material was found to be a mixture containing luciferase C (80 kDa) as the main component; the preparation also contained some luciferase oligomers of 60 kDa and 120 kDa and impurity proteins.

Discussion

Distribution of luciferase

Periphylla becomes luminescent when coelenterazine is oxidized in the presence of luciferase in certain tissues of

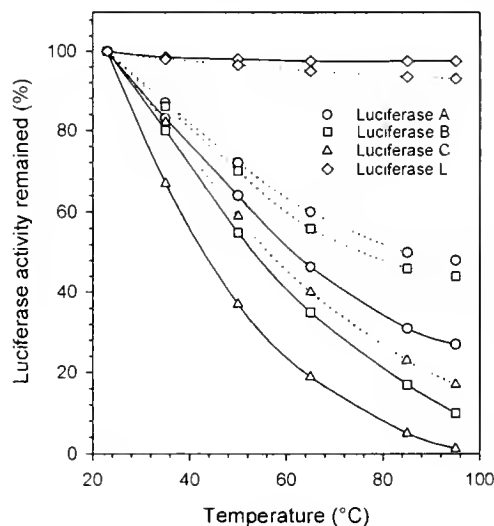


Figure 5. Stability of luciferases A, B, C, and L at various temperatures in 20 mM Tris-HCl buffer (pH 7.8) containing 1 M NaCl and 0.05% BSA (solid lines) or 0.01% lauroylcholine chloride (dotted lines). The buffer (1 ml) containing a luciferase sample was added into a glass test tube that had been soaked and pre-equilibrated in a water bath of a desired temperature. After 2 min, the test tube was briefly cooled in cold water, and the luciferase activity in 10 μ l of the sample solution was measured at 24 °C by the standard assay method.

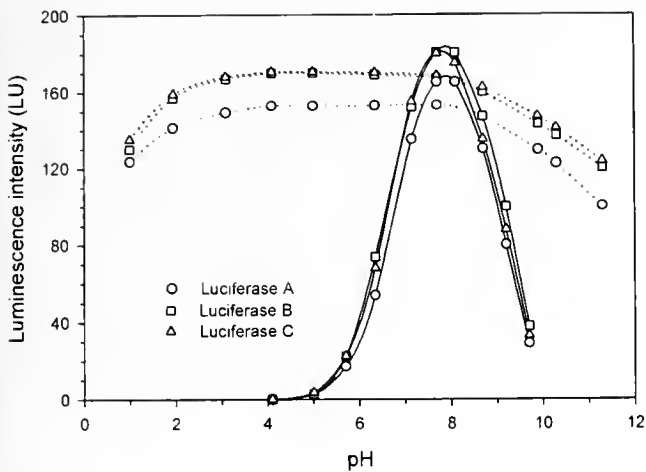


Figure 6. Effect of pH on the light intensity of the luminescence of coelenterazine catalyzed by luciferases A, B, and C, and on the stability of the same luciferases. The effect on light intensity (solid lines) was measured in 50 mM phosphate buffers, pH 4.1-7.25, or 50 mM Tris-HCl buffers, pH 7.1-9.7, all containing 1 M NaCl, 0.025% BSA, and 10 μ l of 0.1 mM methanolic coelenterazine. For measuring the effect on stability (dotted lines), luciferase samples were left standing for 30 min at room temperature, in 0.1 ml of a solution having various pH values, then luminescence intensity was measured under the standard condition (pH 7.8). The solutions used were 0.1 M HCl, 0.01 M HCl, 0.01 M acetic acid, 50 mM phosphate, 50 mM Tris-HCl, 0.01 M NH_3 , and 0.01 M NaOH, all containing 1 M NaCl and 0.025% BSA. The amount of luciferases used for measuring each point were luciferase A, 150 LU; luciferases B and C, 170 LU.

this organism. The luciferase occurs in a soluble form (luciferase L) and also as an insoluble aggregate. The soluble form is responsible for the *in vivo* bioluminescence of the animal and is distributed widely, not only in the epithelial photocytes but also in the mesoglea of the large coronal dome. The insoluble form exists in the particulate matter distributed abundantly in the ovary, particularly in the eggs. The size of the particles, measured by differential filtration, was larger than 0.2 μ m and smaller than 2 μ m; the actual size is probably close to the low end of this range according to previous microscopic observation (Flood *et al.*, 1996). Like soluble luciferase L, the particulate matter is highly active in catalyzing the luminescence of coelenterazine, but its involvement in the *in vivo* bioluminescence is uncertain. The luciferase activity of particulate matter is increased several times by solubilization using 2-mercaptoethanol, which yields soluble luciferase oligomers, such as luciferases A, B, and C.

The total luciferase activity existing in one gram of the dome mesoglea, lappet, and ovary was approximately 100 LU, 1000 LU, and 7×10^5 LU, respectively. Taking account of the quantity of tissue in each organ in the body, these figures suggest that the amount of luciferase stored in the ovary is more than 100 times the total amount of luciferase L in the whole body of a female medusa. The facts that the luciferase is complexed in a stepwise fashion

(dimer, tetramer, etc.) and that these oligomers occur in discrete subcellular particles suggest that the luciferase is being stored for later use. In the case of the male medusae, an insoluble aggregated form of luciferase was not found in the testes, but we are unable to conclude that such a luciferase is absent until all other internal organs have been tested.

Luciferase in the eggs and during early development

In the eggs, the particulates containing aggregated luciferase are in the cortical layer (Flood *et al.*, 1996). The total content of luciferase in one egg is extremely large for its small size (1 μ g or 5×10^{-11} mole/egg; calculated from the data in Table 2), and the luciferase is mostly the aggregated form. Unexpectedly, the eggs contained a negligibly small amount of coelenterazine (1×10^{-14} mole/egg), but some coelenterazine may have been spent by the luminescence reaction that occurs during the preparation of the material.

Unlike most medusae, *Periphylla periphylla* develops directly from egg to medusa without an intermediary, sessile polyp stage (Martinussen *et al.*, 1997; Jarms *et al.*, 1999). The data of Table 2 suggest that the amount of luciferase in the eggs decreases drastically upon fertilization, reaching a minimum at a late embryonic or early juvenile stage (about 3% of the initial amount). Therefore, the biosynthesis of luciferase must start at a later stage of development, because large adult specimens contain large amounts of luciferase. We may see the first sign of such biosynthesis in juveniles with a dome diameter of 8-10 mm. During these juvenile stages, we also see the first differentiation of exumbrellar epithelial photocytes with basically the same organization

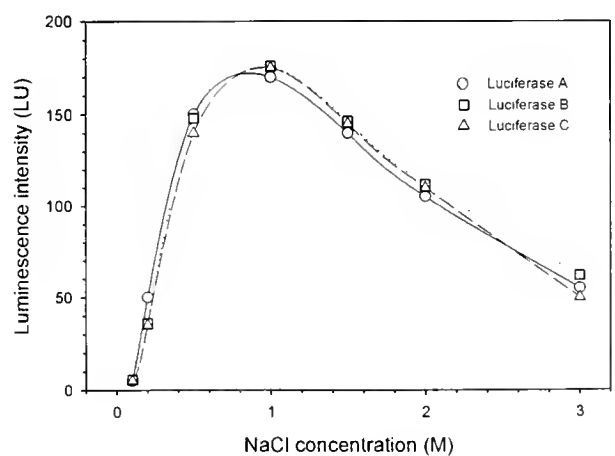


Figure 7. Effect of salt concentration on the luminescence intensity of coelenterazine catalyzed by luciferases A, B, and C. The measurements were done in 20 mM Tris-HCl buffer (pH 7.8) containing various concentrations of NaCl, 0.05% BSA, and 10 μ l of 0.1 mM methanolic coelenterazine. With NaCl concentration lower than 0.2 M, the intensity gradually decreased by the inactivation of luciferase. For the measurement of each point, 170 LU of each luciferase was used.

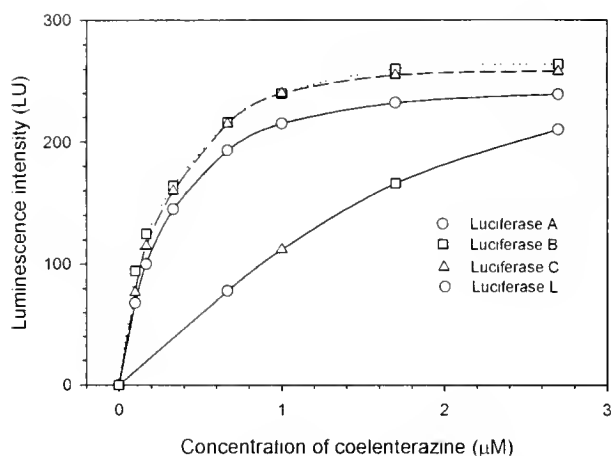


Figure 8. Effect of coelenterazine concentration on the luminescence catalyzed by luciferases A, B, C, and L. The measurements were done in the standard buffer. The amounts of sample used were the same as in Figure 6 for luciferases A, B, and C. The data for luciferase L were taken from the previous report (Shimomura and Flood, 1998).

as those found in the adult medusae (Flood, unpubl. obs.). The decrease of luciferase in the eggs, described above, is puzzling and intriguing. Why does the egg contain a large amount of luciferase in the first place? What is the function or purpose of this luciferase?

A similar phenomenon has been observed in the eggs of bioluminescent hydrozoan medusae that contain a Ca^{2+} -sensitive photoprotein, a complex of oxygenated coelenterazine and an enzyme. In those eggs, the amount of photoprotein slowly declines during the development of the planula larva, and then markedly declines when the planula undergoes metamorphosis to become a polyp (Freeman and Ridgway, 1987).

Properties of luciferases A, B, and C

The present results indicate that luciferases B (40 kDa) and C (80 kDa) are the dimer and tetramer, respectively, of

the luciferase A monomer (20 kDa). The specific luminescence activities of luciferases A, B, and C were in a range of $1.2\sim 4.1 \times 10^{16}$ photons/s, showing a tendency to increase slightly as the oligomer size increases. This is the highest specific activity ever reported for a luciferase whose substrate is coelenterazine; the highest in the past was that of the luciferase of the deep-sea shrimp *Oplophorus* (1.75×10^{15} photons/s) (Shimomura *et al.*, 1978).

The specific activity of purified luciferases A, B, and C can vary in a complex manner, depending upon the method of purification and the history of handling; and an increase in the purity is sometimes accompanied by a decrease in the specific activity. Furthermore, the dilution of a solution containing high concentrations of ammonium sulfate always causes a marked decrease in the activity, whereas the addition of 1-2 M guanidine hydrochloride or 0.01% cationic detergent (such as LCC or hexadecyltrimethylammonium bromide) to a luciferase solution often results in an increase in activity. On the other hand, luciferases A, B, and C are highly resistant to inactivation by heat, extreme pHs, and denaturants, such as 4 M guanidine hydrochloride, detergents, and organic solvents. Thus, luciferase A, B, and C are distinctly different from all previously known coelenterazine luciferases that are easily inactivated. The facts noted here may suggest that *Periphylla* luciferase has a unique and unusual tertiary structure, and that the luciferases isolated by us are mixtures of two or more molecular species having conformationally different structures (having different activities) that are not easily separable by chromatography.

The luminescence quantum yields of coelenterazine in the presence of luciferases A, B, and C were close to 0.30 at 24 °C, one of the highest values among coelenterazine luciferases. The quantum yields for other coelenterazine luciferases are *Oplophorus* luciferase, 0.34 at 22 °C (Shimomura *et al.*, 1978), and *Renilla* (sea pansy) luciferase, 0.11 at 23 °C (Inouye and Shimomura, 1997). The high

Table 2

Average luciferase content in single specimens of eggs, embryos, and juveniles

Sample	Before 2-ME treatment		After 2-ME treatment	
	Soluble (Luciferase L)	Total	Soluble (Luciferase A, B, C)	Total (mean \pm SD)
Egg, dissected from ovary (7)	46	4760	17,400	19,300 \pm 3,000
Egg, liberated ^a (5)	35	1350	4,200	5,010 \pm 3,500
Early embryo ^b (5)	18	730	2,990	3,380 \pm 1,750
Late embryo ^c (3)	38	173	620	603 \pm 50
Juvenile, 4-5 mm ^d (6)	16	205	460	490 \pm 431
Juvenile, 8-10 mm ^d (5)	162	370	784	824 \pm 375

Luciferase activity was assayed before and after treatment with 25 mM 2-mercaptoethanol (2-ME) and shown in light units (LU). The number of samples tested is shown in parentheses.

^a Collected by plankton net. ^b Yolky throughout, with minute grooves for later development of lappets and tentacles. ^c Trace of pigmentation around mouth, still with yolk in stomach. ^d Dome diameter.

efficiency of *Periphylla* bioluminescence suggests that luciferase A might be useful as a highly sensitive reporter.

The nature of luciferase L

The specific luminescence activity of luciferase L previously reported (8×10^{13} photons/s) is more than two orders of magnitude lower than that of luciferases A, B, or C (more than 10^{16} photons/s), raising doubts about the purity of the luciferase L sample previously reported (Shimomura and Flood, 1998). SDS-PAGE analysis of a sample of luciferase L (Fig. 3) showed that the sample contained only a trace of luciferase A (shown as a weak 24-kDa band) and a large amount of other proteins (an intense broad band of 28-34 kDa), indicating that the purity of the sample was indeed very low, probably about 1%. Such a condition could have arisen from the extremely small amount of luciferase L, as well as from the difference in the initial extracts: luciferase L was purified from an extract containing all soluble proteins, whereas luciferase A, B, and C were purified only from the proteins that were solubilized by 2-mercaptoethanol.

A pure sample of luciferase L (32 kDa), if available, could not, on the basis of its molecular weight, be a simple oligomer of the luciferase A monomer (20 kDa) notwithstanding that it yielded luciferase A by treatment with 2-mercaptoethanol. Thus, luciferase L must be a complex of the luciferase A plus another protein (about 12 kDa). The presence of this accessory protein was confirmed by SDS-PAGE as a band corresponding to 14 kDa (Fig. 3). One of the functions of the accessory protein, apparently, is to solubilize the luciferase, because luciferase L is the only naturally soluble form of luciferase existing in *Periphylla*. The accessory protein, however, has other important functions as judged from the data presently obtained. One of these functions pertains to thermal properties, modifying the temperature-luminescence intensity curve to emit the strongest luminescence at an unusually low temperature, near 0 °C (Fig. 4), and significantly increasing the stability of luciferase activity at high temperatures (Fig. 5). The adaptation of a low-temperature luminescence system as a means of enhancing light emission is understandable for an organism that lives in the deep sea at 3 to 7 °C, but it is puzzling that the accessory protein makes the luciferase L heat-stable to such an unusual level that it withstands even boiling.

Recently, an accessory protein was also found in the luciferase of *Oplophorus* (Inouye *et al.*, 2000). The native form of this luciferase (about 106 kDa) was found to be a complex of two proteins, one 19 kDa and the other 35 kDa. The luciferase function was found in the 19-kDa protein, whereas the role of the 35-kDa accessory protein remains unknown.

The quantum yield of coelenterazine in the presence of luciferase L was previously reported as 0.14 (Shimomura

and Flood, 1998), in contrast to the value of about 0.30 for luciferases A, B, or C. The quantum yield value of luciferase L should be reexamined because it was obtained by an unconventional method that is certainly affected by the impurities that destroy coelenterazine and decreases quantum yield. With a pure preparation of luciferase L, the specific activity and the quantum yield are probably close to those of luciferases A, B, and C. Uncertainties concerning luciferase L and the role of the accessory protein will not be completely clarified until pure preparations of luciferase L become available.

Acknowledgments

The *Periphylla* material used in this work was collected aboard the R/V *Håkon Mosby* during a cruise organized in March 2000 by Professor Ulf Båmstedt, University of Bergen. Financial support was received from the National Science Foundation (MCB-9722982).

Literature Cited

- Flood, P. R., J.-M. Bassot, and P. J. Herring. 1996. The microscopical structure of the bioluminescence system in the medusa *Periphylla periphylla*. Pp. 149–153 in *Bioluminescence and Chemiluminescence: Molecular Reporting with Photons*, J. W. Hastings, L. J. Kricka, and P. E. Stanley, eds. John Wiley, Chichester, UK.
- Fosså, J.-H. 1992. Mass occurrence of *Periphylla periphylla* (Scyphozoa, Coronata) in a Norwegian fjord. *Sarsia* **77**: 237–251.
- Freeman, G., and E. B. Ridgway. 1987. Endogenous photoproteins, calcium channels and calcium transients during metamorphosis in hydrozoans. *Roux's Arch. Dev. Biol.* **196**: 30–50.
- Inouye, S., and O. Shimomura. 1997. The use of *Renilla* luciferase, *Oplophorus* luciferase and apoaequorin as bioluminescent reporter protein in the presence of coelenterazine analogues as substrate. *Biochem. Biophys. Res. Commun.* **233**: 349–353.
- Inouye, S., K. Watanabe, H. Nakamura, and O. Shimomura. 2000. Secretional luciferase of the luminous shrimp *Oplophorus graciliorostris*: cDNA cloning of a novel imidazopyrazinone luciferase. *FEBS Lett.* **481**: 19–25.
- Jarms, G., U. Båmstedt, H. Tiemann, M. B. Martinussen, and J. H. Fosså. 1999. The holopelagic life cycle of the deep-sea medusa *Periphylla periphylla* (Scyphozoa, Coronata). *Sarsia* **84**: 55–65.
- Laemmli, U. K. 1970. Cleavage of structural proteins during the assembly of the head of bacteriophage T4. *Nature* **227**: 680–685.
- Martinussen, M. B., G. Jarms, U. Båmstedt, and P. R. Flood. 1997. Livssyklusen til *Periphylla periphylla*. *Årsmote for Norske Havforskernes forening*, Bergen 1997. (Abstract).
- Nakamura, H., C. Wu, A. Murai, S. Inouye, and O. Shimomura. 1997. Efficient bioluminescence of bisdeoxycoelenterazine with the luciferase of a deep-sea shrimp *Oplophorus*. *Tetrahedron Lett.* **38**: 6405–6406.
- Shimomura, O., and P. R. Flood. 1998. Luciferase of the scyphozoan medusa *Periphylla periphylla*. *Biol. Bull.* **194**: 244–252.
- Shimomura, O., and F. H. Johnson. 1970. Mechanisms in the quantum yield of *Cypridina* bioluminescence. *Photochem. Photobiol.* **12**: 291–295.
- Shimomura, O., T. Masugi, F. H. Johnson, and Y. Haneda. 1978. Properties and reaction mechanism of the bioluminescence system of the deep-sea shrimp *Oplophorus graciliorostris*. *Biochemistry* **17**: 994–998.

Zooxanthellae of the *Montastraea annularis* Species Complex: Patterns of Distribution of Four Taxa of *Symbiodinium* on Different Reefs and Across Depths

W. W. TOLLER^{1,3}, R. ROWAN^{2,*}, AND N. KNOWLTON^{1,3}

¹Marine Biology Research Division 0202, Scripps Institution of Oceanography, University of California San Diego, La Jolla, California 92093-0202; ²University of Guam Marine Laboratory, Mangilao, Guam 96923; and ³Smithsonian Tropical Research Institute, Apartado 2072, Balboa, Republic of Panama

Abstract. Corals of the *Montastraea annularis* complex host several different dinoflagellates in the genus *Symbiodinium*. Here we address two questions arising from our previous studies of these associations on an offshore reef. First, do the same taxa and patterns of association (*Symbiodinium* A and B found in higher irradiance habitats than *Symbiodinium* C) occur on an inshore reef? Second, does *M. franksi* at the limits of its depth range host only *Symbiodinium* C, as it does at intermediate depths? In both surveys, a new *Symbiodinium* taxon and different patterns of distribution (assayed by analyses of small ribosomal subunit RNA genes [srDNA]) were observed. Inshore, a taxon we name *Symbiodinium* E predominated in higher irradiance habitats in *M. franksi* and its two sibling species; the only other zooxanthella observed was *Symbiodinium* C. Offshore, *M. franksi* mainly hosted *Symbiodinium* C, but hosted *Symbiodinium* A, B, C, and E in shallow water and *Symbiodinium* E and C in very deep water. *Symbiodinium* E may be stress-tolerant. Observed srDNA heterogeneity within samples of *Symbiodinium* B, C, and E is interpreted as variation across copies within this multigene family. Experimental bleaching of *Symbiodinium* C supported this interpretation. Thus sequences from natural samples should be interpreted cautiously.

Introduction

Coral reefs are the most biologically diverse marine habitats. Underpinning this diversity are the reef-building corals themselves, which are obligate, mutualistic symbioses between coral animals and dinoflagellates (commonly called zooxanthellae). This partnership between heterotrophic hosts and phototrophic symbionts allows corals to thrive in shallow, nutrient-poor tropical seas, and deposit calcium carbonate in amounts large enough to build reefs (reviewed in Muscatine and Porter, 1977; Falkowski *et al.*, 1984; Barnes and Chalker, 1990; Muller-Parker and D'Elia, 1997).

Coral taxonomy at the species level, although occasionally frustrating (Knowlton and Jackson, 1994; Veron, 1995), has generally been sufficient to describe overall diversity and to define experimental subjects. This taxonomy seldom, however, has considered zooxanthellae, because it was widely assumed that one species of coral associates with only one species of zooxanthella—in other words, that host taxonomy identified both partners. Zooxanthellae are diverse (*e.g.*, Schoenberg and Trench, 1980; Rowan, 1998), and it is now recognized that some species of corals associate with multiple species of zooxanthellae (Rowan and Knowlton, 1995; Rowan, 1998). Thus corals identified as members of the same species may not in fact be equivalent at the whole organism (holobiont) level, and the taxonomic identities of zooxanthellae may be as ecologically important as those of their hosts.

As far as is known, zooxanthellae in reef-building corals are members of the genus *Symbiodinium* (Rowan, 1998), which includes four species described as *in vitro* cultures (Freudenthal, 1962; Trench and Blank, 1987). Several other

Received 9 February 2000; accepted 5 July 2001.

*To whom correspondence should be addressed. E-mail: rowan@uog9.uog.edu

Abbreviations: RFLP, restriction fragment length polymorphism; rDNA, ribosomal RNA genes; srDNA, small ribosomal subunit RNA genes.

cultured isolates of *Symbiodinium* have been named informally, but most members of the genus remain uncultured and undescribed (Rowan, 1998). Nevertheless, sequences and restriction fragment length polymorphism (RFLP) of genes that encode ribosomal RNA (rDNA) can be used to distinguish some taxa of *Symbiodinium* and to study ecological relationships among host, symbiont, and habitat diversity (Rowan and Powers, 1991a, b; Rowan and Knowlton, 1995; Rowan *et al.*, 1997; Baker and Rowan, 1997; Hill and Wilcox, 1998; Darius *et al.*, 1998; Baker, 1999). The present study uses genes that encode small ribosomal subunit RNA (srDNA).

Our earlier work concerned zooxanthellae of the sibling coral species *Montastraea annularis*, *M. faveolata*, and *M. franksi*, which are the dominant reef-building corals in the Western Atlantic (Goreau, 1959). On an offshore reef in the San Blas Islands of Panama, we found that both *M. annularis* and *M. faveolata* associate with three distinct taxa of *Symbiodinium* (A, B, and C; see Rowan and Knowlton, 1995; Rowan *et al.*, 1997). *Symbiodinium* A and B, or both, are predominant in tissue exposed to high irradiance (shallower water or colony tops). *Symbiodinium* C is predominant in shaded tissue (deeper water or colony sides), and mixtures of *Symbiodinium* A and/or B with C occur between these extremes. Colonies of *M. franksi*, in contrast, were found to host only *Symbiodinium* C (Rowan and Knowlton, 1995); however, this coral species was not found at shallow depths on this reef. These observations led to two questions addressed here. First, do these symbiont taxa and patterns of association occur on other types of reef? Second, does the deeper distribution of *M. franksi* reflect an inability by this species to host those taxa of *Symbiodinium* with which *M. annularis* and *M. faveolata* associate in shallow water?

We also discuss some concerns about using srDNA to identify the *Symbiodinium* that we collected. Although srDNA was heterogeneous in samples of *Symbiodinium* B, C, and E, we found no evidence to suggest that the zooxanthellae in each of these samples were heterogeneous. We suspect that srDNA in these *Symbiodinium* is a heterogeneous multigene family, as is rDNA in some other dinoflagellates (Scholin *et al.*, 1993; Scholin and Anderson, 1994, 1996). We discuss practical implications of this suspicion for the use of srDNA as a taxonomic character.

Materials and Methods

Field collections and study sites

Corals were identified in the field by colony-level characters (Weil and Knowlton, 1994). Apparently healthy colonies, separated from one another by >2 m, were sampled with hammer and 1/2-in (#12) steel hole punch, yielding a coral core with about 1.3 cm² of live colony surface. Cores were wrapped in aluminum foil and frozen in a cryogenic dry shipper (chilled with liquid nitrogen). Many colonies of

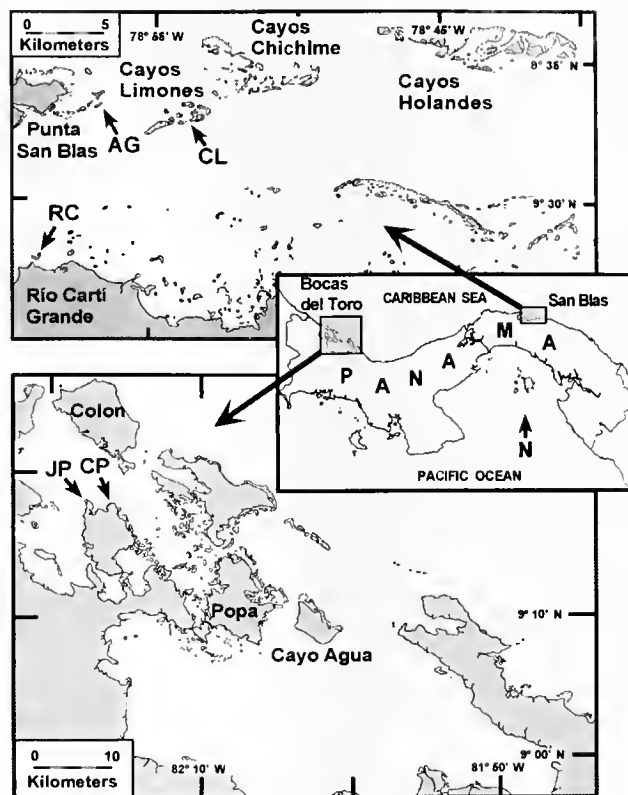


Figure 1. Collecting localities in the San Blas Archipelago (upper panel) and Bocas del Toro (lower panel), Republic of Panama (inset). Arrows with initials identify places where corals were sampled: AG, Aguadargana reef; RC, Río Cartí; CL, Cayos Limones; JP, Juan Point; CP, Cocos Point. Data from Aguadargana reef were reported previously (Rowan and Knowlton, 1995; Rowan *et al.*, 1997).

Montastraea annularis and *M. faveolata* were sampled both on their tops and on their sides to obtain samples from relatively high- and low-irradiance tissues (respectively) within a colony (Rowan *et al.*, 1997). Most colonies of *M. franksi* were sampled at only one location because their relatively flat morphologies made a distinction between colony top and side superfluous.

Coral colonies were sampled at three sites in the Republic of Panama (Fig. 1) between October 1997 and October 1998:

(1) Río Cartí, San Blas. We sampled from a small coastal fringing reef adjacent to the mouth of a major river (Río Cartí Grande). During May to December, such nearshore sites are periodically subjected to heavy freshwater runoff and riverine sediments (Clifton *et al.*, 1997; D'Croze *et al.*, 1999). *Montastraea* species occur at Río Cartí from the barely subtidal to a depth of about 12 m, where hard substrate is replaced by soft-bottom sediments. We sampled the tops of all encountered colonies (*M. annularis*, $n = 4$; *M. faveolata*, $n = 20$; *M. franksi*, $n = 19$); 30 of these were also sampled on their sides.

(2) Cayos Limones, San Blas. These reefs are located 15

km north of mainland Panama and are not strongly influenced by terrestrial runoff (D'Croz *et al.*, 1999). We sampled from a relatively steep, leeward fringing reef that ends abruptly at depths between 35 and 40 m in soft sediments (see fig. 9 in Robertson and Glynn, 1977). On this reef, *M. franksi* is common below 8 m, and it is the dominant coral (with *Agaricia lamarcki*) below 15 m. We sampled *M. franksi* throughout its depth range (4 to 38 m, $n = 78$ colony tops).

(3) Bocas del Toro. Juan Point and Cocos Point reefs are located in the semienclosed lagoon of Bahía Almirante in the Province of Bocas del Toro. Like Río Cartí, these sites are affected by high rainfall and river outflow throughout much of the year. On many of the reefs in this area, *M. franksi* is the most abundant member of the *M. annularis* complex. We made a limited collection at depths of 1–15 m for comparative purposes, consisting of 1 top sample of *M. annularis*, 10 of *M. franksi*, and 3 of *M. faveolata*.

Observations of srDNA heterogeneity within samples of *Symbiodinium* C (see Results) prompted us to investigate the stability of these genotypes under stress. We identified 11 colonies of *M. annularis* (each colony consisting of a cluster of columns) that hosted heterogeneous RFLP genotypes of *Symbiodinium* C. After an initial sample, columns (one per colony) were transplanted from their natural habitat (*ca.* 10–14 m depth) to 1 m depth at either Cayos Limones ($n = 4$ transplants) or Aguadargana ($n = 7$ transplants) reefs (Fig. 1), where they bleached. Columns were sampled again after 4 days (Cayos Limones) or 40 days (Aguadargana). Transplants and determinations of zooxanthellar numbers were conducted as described in Toller *et al.* (2001). In the present study, however, we did not sample corals further (*i.e.*, during zooxanthellar repopulation; see Toller *et al.*, 2001).

Identification of zooxanthellae

Zooxanthellae were isolated and identified as described previously (Rowan and Powers, 1991b; Rowan and Knowlton, 1995). srDNAs were obtained by PCR amplification with a "host-excluding" primer pair (ss5 and ss3Z) or with universal primers (ss5 and ss3), and then characterized by restriction enzyme digestion. The host-excluding primer pair does not amplify known host srDNAs (Rowan and Powers, 1991b; unpubl. obs.), but does amplify srDNAs from a phyletic group that is much larger than *Symbiodinium* (McNally *et al.*, 1994; Toller *et al.*, 2001). All samples were assayed using host-excluding primers, and about one-third of them were also analyzed with universal primers. Data obtained from the two kinds of amplifications were always in agreement.

Every sample was analyzed by digesting amplified srDNA with *Dpn* II and with *Taq* I, which differentiate *Symbiodinium* A, B, and C by RFLP (Rowan and Powers,

1991a; Rowan and Knowlton, 1995; Rowan *et al.*, 1997). RFLPs were diagnosed by comparison to genotype standards, which were obtained by PCR amplification from cloned srDNAs of *Symbiodinium* A, B, and C, all isolated from *M. annularis* (Rowan and Knowlton, 1995), and from *Symbiodinium* E (from *M. faveolata*, this study). These cloned genotype standards are denoted hereafter as A⁰, B⁰, C⁰, and E⁰⁻¹. We use the superscript zero to indicate srDNA clones, as opposed to taxa of *Symbiodinium*; clones obtained from different samples of the same taxon of *Symbiodinium* are distinguished by numbers (*e.g.*, E⁰⁻¹ and E⁰⁻²; see below). Because universal PCR primers amplify coral host srDNA when it is present (Rowan and Powers, 1991b), a cloned srDNA from *M. annularis* (clone H⁰; see below) was used as an additional standard in RFLP analyses of these amplifications. Where RFLP analyses indicated mixtures of *Symbiodinium* A, B, C, or E in a sample, relative abundance (greater than or less than 50% of the total) was estimated by comparison to standard mixtures prepared from cloned srDNAs (Rowan and Knowlton, 1995; Rowan *et al.*, 1997; see Fig. 4).

srDNA was cloned from three samples of *Symbiodinium* E; clone E⁰⁻¹ is from *M. faveolata* (from Río Cartí, 3 m depth), clone E⁰⁻² is from *M. franksi* (from Cayos Limones, 38 m), and clone E⁰⁻³ is from the coral *Siderastrea siderea* (from Portobelo, Panama, 6 m). Amplified srDNAs (DNA for clone E⁰⁻¹ by universal PCR primers; DNAs for clones E⁰⁻² and E⁰⁻³ by host-excluding PCR primers) were gel-purified, ligated into pGEM-T Easy Vector (Promega Corporation, Madison, WI), and then transformed into *Escherichia coli* according to manufacturer's recommendations. From each ligation, 4–12 clones were characterized by amplifying srDNAs with host-excluding PCR primers and then digesting the PCR products with *Dpn* II, with *Taq* I, and with *Hae* III. Each cloned RFLP genotype was compared to the RFLP of its corresponding natural sample. srDNA of *M. annularis* was obtained with universal PCR primers from sperm DNA (Lopez *et al.*, 1999) and cloned (clone H⁰) as described above.

Clones E⁰⁻¹, E⁰⁻², and E⁰⁻³ were sequenced completely, as were cloned genotype standards A⁰, B⁰, and C⁰ (from which only partial sequences had been obtained previously; Rowan and Knowlton, 1995) and clone H⁰. Plasmids were prepared using QIAprep Spin Miniprep kits (Qiagen, Inc., Valencia, CA) according to manufacturer's recommendations, and sequences were determined for both DNA strands using Big Dye Terminator sequencing kits (PE Corporation, Norwalk, CT) with vector sequencing primers T7 and M13-Reverse, and with srDNA sequencing primers 18F1 (5'-AGCTCGTAGTTGGATTCTG-3'), 18F2 (5'-TTAATTTGACTCAACACGGG-3'), 18R1 (5'-AGTCAAA-TTAAGCCGCAGGC-3') or 18-R1X (5'-GTTGAGTCA-AATTAAGCCGC-3'), and 18R2 (5'-ATATACGCTA-TTGAGCTGG-3'). Reactions were analyzed with an ABI

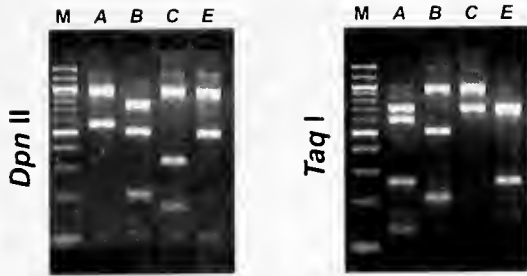


Figure 2. RFLP genotypes A, B, C, and E of *Symbiodinium* obtained from different colonies of *Montastraea franksi*. srDNAs were amplified with host-excluding PCR primers and digested with *Dpn* II (left) and with *Taq* I (right). Lane M contains DNA fragment size standards of (top to bottom) 1500 base pairs (bp), 1200 bp, and then 1000 bp to 100 bp in 100-bp increments.

373 sequencer (Applied Biosystems, Foster City, CA) and complete sequences were assembled using SeqEd software (Applied Biosystems). RFLP genotypes of cloned srDNAs were obtained from their sequences using Gene Construction Kit software (Textco, Inc., West Lebanon, NH). Note that we used only partial srDNA sequences in some analyses (Fig. 3); the full-length srDNA sequences were deposited in GenBank (<http://www.ncbi.nlm.nih.gov/>; accession numbers AF238256-AF238258, AF238261-AF238263, and AF238267).

For phylogenetic analysis, we aligned partial srDNA sequences (Rowan and Powers, 1992) with Clustal X software (Thompson *et al.*, 1997) and used neighbor-joining reconstruction (Saitou and Nei, 1987). The following srDNA sequences were obtained from GenBank: *Symbiodinium microadriaticum* (M88521), *Symbiodinium* #8 (M88509), *Symbiodinium* sp. PSP1-05 (AB016578), s11-2xba (U20961), s20-2xba (U20962), 37-4xba (U20959), 86-5xba (U20960), a12-5xba (U20954), a8-5xba (U20955), 175-5xba (U20952), 178-6xba (U20956), 33-6xba (U20958), a1-5xba (U20953), 178-8xba (U20957), *Gymnodinium beii* (U37366), *Gyrodinium galatheanum* (M88511), *Gymnodinium simplex* (M88512), and *Polarella glacialis* (AF099183). srDNA sequences from *Symbiodinium* C2 [clone C2⁰⁻¹ (AF238259) and clone C2⁰⁻² (AF238260)] are from Toller *et al.* (2001). A partial sequence of zooxanthellar srDNA from the coral *Montipora patula* is from a previous study (Rowan and Powers, 1991a).

To investigate srDNA variation within our samples of *Symbiodinium* in greater detail, we selected representative samples of each *Symbiodinium* taxon from each host coral species (*M. annularis*, *M. faveolata*, *M. franksi*) and made additional RFLP analyses. Different samples (from different colonies) of *Symbiodinium* A ($n = 10$), B ($n = 12$), C ($n = 12$), and E ($n = 12$) were analyzed with a panel of 12 restriction enzymes, used one at a time. These enzymes were *Dpn* II, *Taq* I, *Alw* I, *Bst*U I, *Hae* III, *Hha* I, *Hinf* I, *Mse* I, *Msp* I, *Nci* I, *Sau*96 I, and *Sty* I. Samples of *Symbiodinium*

E were investigated further with the enzymes *Alu* I, *Bsp*1286 I, *Mae* III, *Mnl* I, *Sfa*N I, and *Tsp*45 I. We chose the latter enzymes based on RFLP differences among clones E⁰⁻¹, E⁰⁻², and E⁰⁻³. All enzymes were purchased from New England Biolabs, Inc. (Beverly, MA) except for *Mae* III (Roche Diagnostics Corp., Indianapolis, IN).

Results

Identification of *Symbiodinium* E

Routine analyses of srDNAs with *Dpn* II and with *Taq* I revealed a zooxanthella in our surveys (see below) that was different from *Symbiodinium* A, B, and C (Fig. 2). We call this new RFLP genotype E (D has been assigned to a sponge symbiont [Carlos *et al.*, 1999]). Cloned genotype E srDNAs (E⁰⁻¹, E⁰⁻², and E⁰⁻³ from *Montastraea faveolata*, *M. franksi*, and *Siderastrea siderea* respectively) were more than 99% similar in sequence to one another, and more than 96% similar to srDNAs of *Symbiodinium* A, B, and C that were cloned from *M. annularis* (genotype standards A⁰, B⁰, and C⁰). A neighbor-joining analysis of partial srDNA sequences (Fig. 3) places genotype E srDNAs within *Symbiodinium* (defined by cultured *S. microadriaticum* and *Symbiodinium* #8 [Rowan,

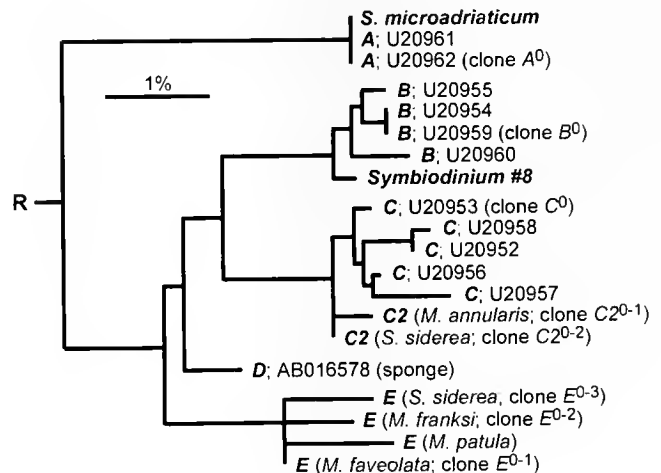


Figure 3. Inferred phylogenetic relationships among srDNAs from different zooxanthellae. Partial srDNA sequences (Rowan and Powers, 1992) were grouped by the neighbor-joining method (Saitou and Nei, 1987). *Symbiodinium microadriaticum* and *Symbiodinium* #8 are cultured zooxanthellae (Rowan and Powers, 1992). A, B, and C (followed by GenBank accession numbers) are from *Montastraea annularis* (Rowan and Knowlton, 1995); three of these correspond to standard clones A⁰, B⁰, and C⁰ (this study). Two srDNAs labeled C2 (hosts and clone numbers in parentheses) are from Toller *et al.* (2001). D (followed by GenBank accession number) is from a sponge (Carlos *et al.*, 1999). srDNAs labeled E (host and clone numbers in parentheses) are from this study, except for that from the coral *Montipora patula*, which is from Rowan and Powers (1991a). The branch labeled R (to the left) indicates the root for this tree, obtained by including srDNA sequences from the dinoflagellates *Gymnodinium beii*, *Gyrodinium galatheanum*, *Gymnodinium simplex*, and *Polarella glacialis* (not shown).

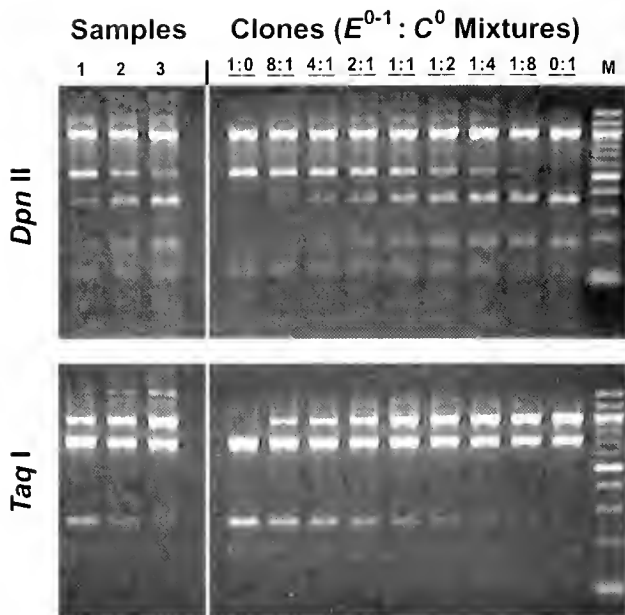


Figure 4. RFLP genotypes of mixtures of *Symbiodinium* E and C. Samples of zooxanthellae are from *Montastraea faveolata* (samples 1, 2) and *M. franksi* (sample 3); other lanes are clones E^{0-1} and C^0 singly (1:0 and 0:1, respectively) and mixed together in molar ratios ranging from 8:1 to 1:8, to obtain standards. srDNAs were amplified with host-excluding PCR primers and then digested with *Dpn* II (top panel) and with *Taq* I (bottom panel). By visual inspection, samples 1-3 contain both *Symbiodinium* E and C, in ratios of about 4:1, 1:1.5, and 1:4, respectively. Lane M contains DNA size standards, as in Figure 2.

1998); separate from *Symbiodinium* A, B, and C; and close to a zooxanthellar srDNA from the coral *Montipora patula*, an srDNA that previously could not be assigned to either *Symbiodinium* A, B, or C (Rowan and Powers, 1991a). srDNA from *Symbiodinium* D, a dinoflagellate cultured from the sponge *Haliclona koremella* (Carlos *et al.*, 1999), is not similar to genotype E (Fig. 3). Thus, genotype E represents a distinct taxon of zooxanthella—*Symbiodinium* E.

Some samples of zooxanthellae (see below) had RFLP genotypes that implied mixtures of *Symbiodinium* E and C, based on comparisons to RFLP genotypes of synthetic mixtures of cloned genes (srDNA clones E^{0-1} and C^0 ; Fig. 4). As with mixtures of *Symbiodinium* A, B, or C described previously (Rowan and Knowlton, 1995; Rowan *et al.*, 1997), the apparent ratio of *Symbiodinium* E to *Symbiodinium* C in different samples varied, and did not depend on which restriction enzyme was used to differentiate these two genotypes (*e.g.*, Fig. 4, *Dpn* II digests versus *Taq* I digests).

Distribution of different taxa of *Symbiodinium*

At Río Cartí, *M. franksi* was observed with only two taxa of zooxanthellae—*Symbiodinium* E and C—and the same two taxa were obtained from *M. faveolata* and *M. annularis*

(Fig. 5) at this reef. *Symbiodinium* E was the predominant zooxanthella from all three *Montastraea* species: it occurred in 35 of 43 corals and was the only zooxanthella detected in 18 of these. In *M. franksi* and *M. faveolata*, *Symbiodinium* E was more common in higher irradiance habitats (colonies at 1-3 m depth, tops of colonies at 3-6 m depth) than in lower irradiance habitats (colony sides at 3-6 m depth and generally below 6 m); *Symbiodinium* C exhibited the converse pattern (Fig. 5). Samples from *M. annularis* ($n = 4$) showed the same top and side pattern of zooxanthellar distribution within colonies (Fig. 5), although our small sample size precludes an examination across depth. A zonation pattern was often observed in comparisons of tops and sides from the 16 doubly sampled colonies that had the two types of zooxanthellae. In 12 of these colonies, the ratio of *Symbiodinium* E:C decreased from top to side, in three there was no clear difference in the ratios, and in only one colony did the ratio increase from top to side.

At Cayos Limones, *M. franksi* associated primarily with *Symbiodinium* C (Fig. 6), which was the only taxon of zooxanthella observed between 6.5 and 33 m depth ($n = 53$ colonies): this result is consistent with the previous study (Rowan and Knowlton, 1995) of *M. franksi* from depths

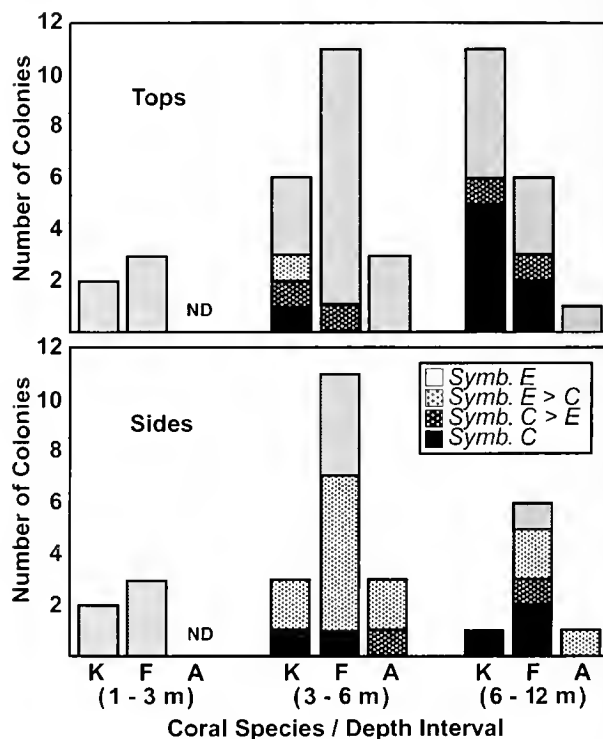


Figure 5. Occurrences of *Symbiodinium* C and E (assayed by RFLP, see Fig. 4) in colonies of *Montastraea franksi* (K), *M. faveolata* (F), and *M. annularis* (A) living in three depth intervals at Río Cartí. Top samples (upper histogram) were taken from 43 corals; 30 of these were also sampled on their sides (lower histogram). There are no data (ND) from *M. annularis* in the shallowest depth interval because no colonies were encountered there.

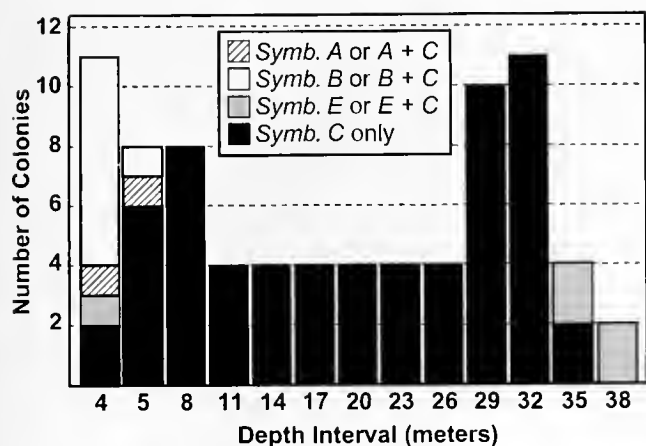


Figure 6. Occurrences of *Symbiodinium* A, B, C, and E in tops of colonies of *Montastraea franksi* living at Cayos Limones. Shallow depth intervals are 3.5–4.5 m (labeled 4) and 4.5–6 m (labeled 5); other depth intervals are 3 m wide on the centers indicated. Samples were scored as containing *Symbiodinium* A, B, C, and/or E, according to the key. More samples were analyzed at the ends of the depth range, where more than one taxon of *Symbiodinium* was observed.

between 6 and 11 m at Aguadargana, another nearby off-shore reef (Fig. 1). However, in the shallowest and deepest colonies of *M. franksi*, different taxa of zooxanthellae were observed. Between 4 and 6 m, colonies contained, in order of decreasing frequency of occurrence, *Symbiodinium* B, C, A, and E. With the exception of *Symbiodinium* E in one colony, this distribution of taxa resembles that found in *M. annularis* at similar depths at Aguadargana reef (Rowan and Knowlton, 1995; Rowan *et al.*, 1997). Samples from four of the six deepest colonies of *M. franksi* (35–38 m depth) contained *Symbiodinium* E only; the other two colonies contained *Symbiodinium* C only (Fig. 6). At both the shallow and deep extremes, colonies of *M. franksi* were relatively small, encrusting forms (<0.5 m diameter).

To find out if the congeners of *M. franksi* at Cayos Limones also host *Symbiodinium* E at their lower depth limits, we sampled the deepest colonies of *M. annularis* ($n = 23$) and *M. faveolata* ($n = 5$) that we could find. They were not very deep (12–17 m and 13–15 m, respectively), and like *M. franksi* at the same depths, contained *Symbiodinium* C only (not shown).

In our limited sample of corals from two reefs at Bocas del Toro (1–15 m depth), *M. franksi* was found with *Symbiodinium* E only (1 colony), with *Symbiodinium* E and C (4 colonies), with *Symbiodinium* C only (2 colonies), or with *Symbiodinium* A only (3 colonies). *M. faveolata* was found with *Symbiodinium* C only (2 colonies) or with *Symbiodinium* A only (1 colony). The single encountered colony of *M. annularis* contained *Symbiodinium* A. We did not observe *Symbiodinium* B in any of these samples.

Other diversity in zooxanthellar srDNAs

The routine RFLP analyses (with *Dpn* II and *Taq* I) reported above indicated that all samples of zooxanthellae in this study contained srDNAs of either *Symbiodinium* A, B, C, or E, or mixtures thereof, as defined by our standard, cloned srDNA genotypes (A^0 , B^0 , C^0 , E^{0-1}). However, when zooxanthellar srDNAs were analyzed in greater detail (with additional restriction enzymes; see Methods and Materials), samples of *Symbiodinium* B, C, and E (but none of 10 tested samples of *Symbiodinium* A) were found to contain additional srDNAs that could not be attributed to genotypes A^0 , B^0 , C^0 , E^{0-1} , or to host srDNA. These other srDNAs appeared as additional DNA fragments in restriction digests, as described below.

Twelve selected samples of *Symbiodinium* E and clones E^{0-1} , E^{0-2} , and E^{0-3} were all indistinguishable in digests with *Dpn* II (examples in Fig. 7, *Dpn* II panel) and with *Taq* I (not shown). In digests with *Mae* III, however, all of these samples had an additional DNA fragment in relatively low abundance (arrow in Fig. 7, *Mae* III panel) that was not part of the RFLP genotype of clones E^{0-1} and E^{0-2} , but which was in the RFLP genotype of clone E^{0-3} . Thus, these samples apparently contained at least two srDNAs—one defined in *Mae* III digests by clones E^{0-1} and E^{0-2} , the other by clone E^{0-3} . Similarly, an additional band in digests of sample srDNAs with *Mnl* I (arrow in Fig. 7, *Mnl* I panel) apparently represents the RFLP genotype of clone E^{0-1} (versus clones E^{0-2} and E^{0-3}). Digestion of samples with *Alu* I also yielded an additional DNA fragment (arrow in Fig. 7, *Alu* I panel), and digestion of cloned srDNAs with *Alu* I showed that the genotype of clone E^{0-2} is unique. In all, additional bands like those shown in Figure 7 (arrows) were observed in 7 of 18 different restriction enzyme digestions (other digests not shown) of the 12 tested samples of *Symbiodinium* E. Therefore, srDNA in these samples of *Symbiodinium* E was clearly heterogeneous. This heterogeneity did not, however, vary qualitatively nor quantitatively among the tested samples (*e.g.*, Samples 1–3 in Fig. 7). Thus, clones E^{0-1} , E^{0-2} , and E^{0-3} , which are different (Fig. 7; see also Fig. 3), were obtained from indistinguishable samples of zooxanthellae.

As with *Symbiodinium* E, srDNA heterogeneity was observed in all tested samples of *Symbiodinium* B. Two digests (out of 12) revealed heterogeneity—*Hha* I and *Sty* I (examples in Fig. 8). In each of these, the additional fragments (arrows in Fig. 8) imply an srDNA with one restriction site gain relative to clone B^0 . Interestingly, a cloned srDNA from *Symbiodinium* B (*Symbiodinium* #8 isolated from a Hawaiian anemone [*Aiptasia pulchella*] Rowan and Powers, 1992) has both additional sites (S8 in Fig. 8; schematic genotype on the right), suggesting that samples of *Symbiodinium* B from other hosts may also exhibit srDNA heterogeneity. In our samples of *Symbiodinium* B from *Montastraea*, within-sample srDNA heterogeneity did not vary among the 12 tested samples (*e.g.*, samples 1–4 in Fig. 8).

In the case of *Symbiodinium* C, srDNAs in all of 12 tested

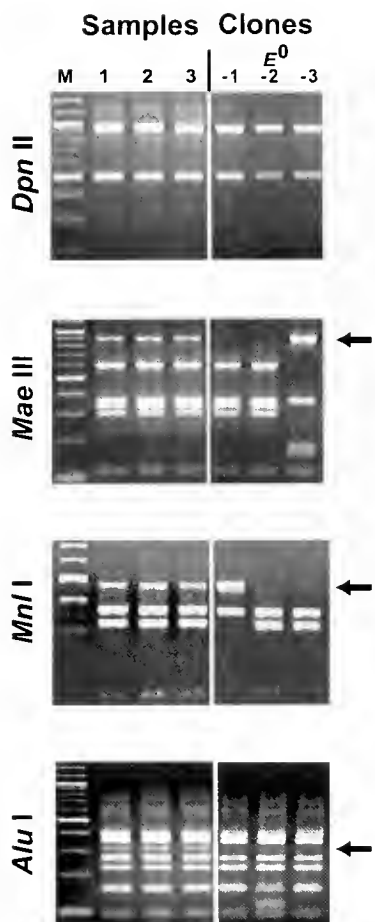


Figure 7. Examples of srDNA heterogeneity within samples of *Symbiodinium* E. srDNAs were amplified (with host-excluding PCR primers) from different samples of *Symbiodinium* E (lanes 1-3) and from srDNA clones E⁰⁻¹, E⁰⁻², and E⁰⁻³ (as indicated) and then digested with *Dpn* II, *Mae* III, *Mnl* I, and *Alu* I (indicated on the left). On the right, arrows identify the positions of additional DNA fragments in lanes 1-3 that indicate srDNA heterogeneity (see text). In *Mae* III and *Mnl* I digestions, these bands were also observed in one of the three clones: for *Alu* I digestions no clone contains the indicated band. Samples are from *Montastraea franksi* (lane 1), from *M. faveolata* (lane 2), and from *M. annularis* (lane 3). Lane M contains DNA size markers as in Figure 2.

samples were also heterogeneous. However, unlike *Symbiodinium* E and B (above), within-sample srDNA heterogeneity in *Symbiodinium* C varied both qualitatively (e.g., compare samples 3-5 in *Dpn* II panel, Fig. 9) and quantitatively (e.g., compare Samples 1-5 in *Hinf* I panel, Fig. 9) among samples. srDNA heterogeneity was observed in as few as one or as many as six different digests (examples in Fig. 9) among the 12 samples tested. That additional variation suggested that some or all samples might have contained more than one genotype of *Symbiodinium*.

We made two analyses that might have supported this hypothesis. First, because mixtures of *Symbiodinium* A, B, C, or E vary in proportion at different locations within a coral colony (Rowan and Knowlton, 1995; Rowan *et al.*,

1997; Results), we analyzed multiple samples from colonies of *M. annularis* in which *Symbiodinium* C had been observed previously. In 14 colonies (each consisting of a cluster of columns), we sampled one column on its top and on its side: srDNA genotypes were indistinguishable in every top-versus-side comparison (not shown). We also sampled the tops of one or two additional columns in 13 of these colonies, and again saw no differences in zooxanthellar RFLP genotype within any colony (not shown). Second, we speculated that if the additional srDNAs did represent distinct, co-occurring zooxanthellae, their relative abundance might change under stress (e.g., as in Rowan *et al.*, 1997). Transplantation of columns from deep to shallow

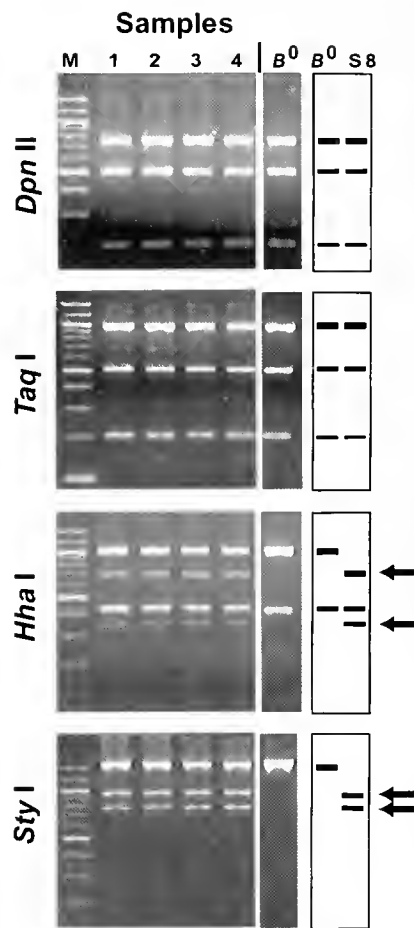


Figure 8. Examples of srDNA heterogeneity within samples of *Symbiodinium* B. srDNAs were amplified (with host-excluding PCR primers) from different samples of *Symbiodinium* B (lanes 1-4) and from srDNA clone B⁰ and then digested with *Dpn* II, *Taq* I, *Hha* I, and *Sty* I (indicated on the left). On the right are schematic RFLP genotypes of clone B⁰ and of an srDNA clone from *Symbiodinium* #8 (S8), obtained from its sequence (Rowan and Powers, 1992). Arrows next to the schematics identify DNA fragments that, in digestions of srDNA from these samples of zooxanthellae, are additional to the DNA fragments of clone genotype B⁰. Samples are from *Montastraea annularis* (lanes 1, 2), *M. faveolata* (lane 3), and *M. franksi* (lane 4). Lane M contains DNA size markers as in Figure 2.

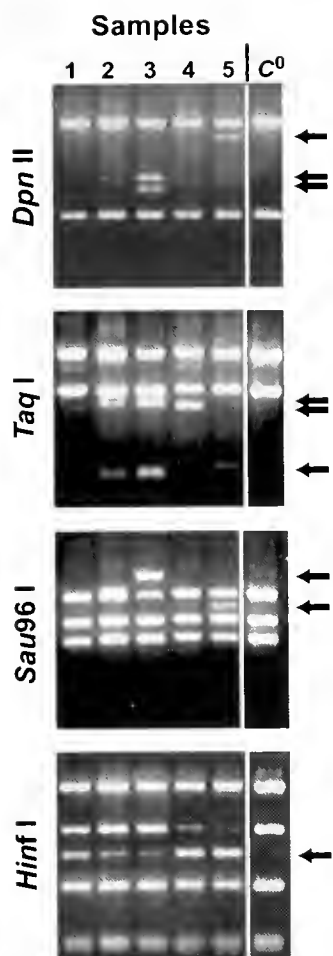


Figure 9. Examples of srDNA heterogeneity within samples of *Symbiodinium C*. srDNAs were amplified (using host-excluding PCR primers) from different samples of *Symbiodinium C* (lanes 1-5) and from srDNA clone C⁰ (lane C⁰) and then digested with *Dpn II*, *Taq I*, *Sau96 I*, and *Hinf I* (indicated on the left). Arrows on the right identify DNA fragments that, in digests of srDNA from these samples of zooxanthellae, are additional to the DNA fragments of clone genotype C⁰. Samples are from *Montastraea annularis* (3), *M. faveolata* (1, 2, 4) and *M. franksi* (5).

habitats resulted in bleaching of all columns, and effectively reduced zooxanthellar numbers (70% reduction on average). However, neither acute stress (5 days) nor prolonged stress (ca. 40 days) of zooxanthellae altered the RFLP genotypes that were observed (examples in Fig. 10)—the relative abundance of distinct srDNAs had not changed compared to samples taken prior to transplantation.

Discussion

Four taxa of *Symbiodinium* in the *Montastraea annularis* complex

Previous surveys of zooxanthellar diversity in *Montastraea annularis*, *M. faveolata*, and *M. franksi* (Rowan and Knowlton, 1995; Rowan *et al.*, 1997) are now shown to be

incomplete. In surveys of additional habitats and depths, we found (i) a fourth taxon of *Symbiodinium* (E) that was not previously reported in these corals, (ii) differences in the distribution of zooxanthellae at offshore and coastal reefs, and (iii) multiple taxa of zooxanthellae in *M. franksi*, which previously had been found to contain only *Symbiodinium C*.

Groups A, B, C, and E constitute the known diversity of coral-associated *Symbiodinium* (Rowan, 1998; this study), and *M. annularis*, *M. faveolata*, and *M. franksi* all associate with at least one member of each of these groups. This is a remarkable amount of taxonomic diversity—at least 12 distinct symbioses—in what was previously (Knowlton *et al.*, 1992; Rowan and Knowlton, 1995) regarded as one species of coral hosting one species of zooxanthella. Moreover, this diversity is not randomly distributed, suggesting that what was once viewed as a single quintessential generalist (Connell, 1978) is in fact a complex assemblage of ecologically more specialized entities.

Our observations from Cayos Limones now enable us to refute the speculation that *M. franksi* associates exclusively with *Symbiodinium C*—this host coral can and does form symbioses with *Symbiodinium A*, B, and E. However, at this offshore reef, the latter host-zooxanthella combinations are observed only at the margins of this coral's depth distribution (Fig. 6): shallow (*Symbiodinium B* > A > E) and very deep (*Symbiodinium E*; discussed further below). Other-

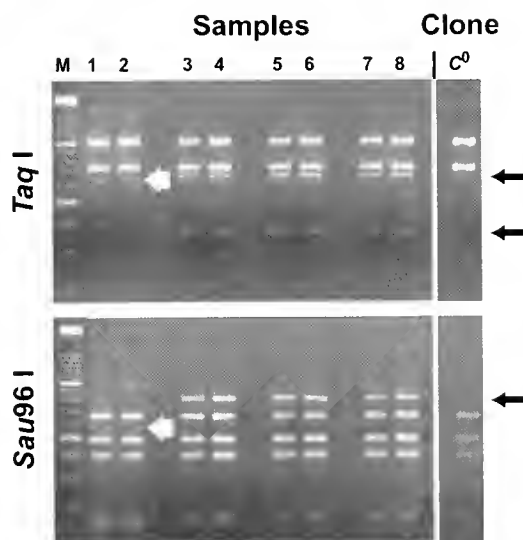


Figure 10. srDNA heterogeneity in samples of *Symbiodinium C* from four colonies of *Montastraea annularis* before and after experimental stress (see text). srDNAs were amplified (using host-excluding PCR primers) from samples of zooxanthellae (lanes 1-8) and from srDNA clone C⁰ (lane C⁰) and then digested with *Taq I* (top panel) and with *Sau96 I* (bottom panel). Arrows identify DNA fragments that are additional to those of genotype C⁰. Samples were taken from the same colony before (lane 1) and after (lane 2) stress. Samples 3 and 4 are from another colony, before and after stress (respectively), as are samples 5 and 6 and samples 7 and 8. Lane M contains DNA fragment size standards of (top to bottom) 2642 base pairs (bp), and 1500 bp to 100 bp in 100-bp increments.

wise, *M. franksi* hosts *Symbiodinium* C throughout nearly all of its depth range (Fig. 6), where colony growth is robust. Although in shallow water the distributions of zooxanthellae (mostly *Symbiodinium* A and B) are similar in *M. franksi*, *M. faveolata*, and *M. annularis*, the small size of *M. franksi* colonies in shallow water may reflect a relatively poor physiological fit between this coral host and these zooxanthellae.

The main question posed by our new results is why all three species in the *Montastraea annularis* species complex at a coastal site (Río Cartí) host predominantly *Symbiodinium* E at higher irradiance (Fig. 5), instead of *Symbiodinium* A or B, as found at offshore reefs (Rowan and Knowlton, 1995; Rowan *et al.*, 1997; Fig. 6). One possible explanation is that this coastal site is characterized by environmental stress to which *Symbiodinium* E is more tolerant than are *Symbiodinium* A or B. High irradiance is a stress that may exacerbate (Brown, 1997) the many other kinds of stress found in nearshore environments (*e.g.*, fluctuations in temperature, salinity, nutrients, sediments, and underwater irradiance; see Bowden, 1983; Kirk, 1994). All of these factors can affect the stability of coral-algal symbioses (Falkowski *et al.*, 1993; Brown, 1997; Wesseling *et al.*, 1999). In the San Blas Archipelago (Fig. 1), nearshore effects associated with freshwater runoff are limited to a relatively narrow coastal band and do not reach our offshore study sites at Aguadargana and Cayos Limones (D'Croz *et al.*, 1999). *Symbiodinium* E was also common in *Montastraea* within a large coastal lagoon at Bocas del Toro, Panama (Fig. 1), an area of exceptionally high rainfall where water quality is also likely to be dominated by coastal effects.

A second (and perhaps related) question asks why *Symbiodinium* E was distributed differently at Cayos Limones, where it was common not at high irradiance but rather in the very deepest colonies of *M. franksi* (Fig. 6). Perhaps shallow and deep populations of *Symbiodinium* E are different species of zooxanthella, although we did not find any evidence to support this (see following section). Instead, we suggest that *Symbiodinium* E was actually not distributed so differently at these two sites. In both cases it was associated with marginal habitat: at great depth where *M. franksi* colonies are not large and where the reef itself disappears into sediment (Cayos Limones), and along the coast near a large river, where coral reefs are poorly developed or absent (Río Cartí). Bleaching-associated stress may be common in both habitats, due to occasional smothering by sediments in the former (*e.g.*, Wesseling *et al.*, 1999) and to near-shore conditions in the latter (see above). We propose that the *Symbiodinium* E we observed represents a taxon of zooxanthella that occurs in certain habitats not because it performs best in those habitats, but because it tolerates them, whereas *Symbiodinium* A, B, and C do not. According to this idea, *Symbiodinium* E is rare or absent from other

habitats not because it performs poorly in them, but because *Symbiodinium* A, B, and C are better adapted to those habitats and somehow exclude it.

Anecdotal observations are consistent with our interpretation of *Symbiodinium* E as a stress-tolerant zooxanthella. We observed *Symbiodinium* E (diagnosed by *Dpn* II and *Taq* I digests of srDNA) in *M. faveolata* in the Bahamas (not shown), in four of seven colonies that were relatively unbleached during a natural bleaching event (D. Zawada, Scripps Institution of Oceanography, pers. comm.). We also found that *Symbiodinium* E—but not *Symbiodinium* B or C—was adept at repopulating severely bleached corals in experiments (Toller *et al.*, 2001). These experimental results suggest that, in addition to tolerating stress, *Symbiodinium* E may also be good at colonizing corals whose zooxanthellar communities have been severely disrupted by stress.

Observations of zooxanthellae related to *Symbiodinium* E in other hosts and seas imply that this taxon, like the taxa *Symbiodinium* A, B, and C (Rowan, 1998), may represent a group (clade) of zooxanthellae. Those observations include the corals *Montipora patula* in Hawaii (Rowan and Powers, 1991a; Fig. 3), *Acropora palifera* in Australia (R. R., unpubl. obs.), *Pocillopora damicornis* in the eastern Pacific (Baker, 1999), *Goniastrea aspera* in Thailand (A. Douglas, University of York, pers. comm.), and the giant clam *Hippopus hippopus* in Australia (R. R., unpubl. obs.). In the context of our hypothesis that *Symbiodinium* E is stress tolerant in *Montastraea*, it is notable that *G. aspera* occurs on reef flats—an environment that is stressful for corals, and where coral bleaching events occur regularly (Brown *et al.*, 2000). Similarly, in *P. damicornis*, *Symbiodinium* E was disproportionately common in unbleached colonies during an El Niño-related bleaching event (*Symbiodinium* D of Baker [1999] has an RFLP pattern that is indistinguishable from that of *Symbiodinium* E from *Montastraea* in three restriction enzyme digests; A. Baker, Wildlife Conservation Society, pers. comm.). These observations suggest that other members of the clade *Symbiodinium* E may also be stress tolerant.

The hypothesis that *Symbiodinium* E is a relatively stress-tolerant zooxanthella is based on circumstantial evidence, and should be tested in experiments in which environmental factors are controlled and physiological responses are measured. Descriptive studies of unmanipulated corals are, however, indispensable for framing realistic hypotheses in the first place.

Taxonomic interpretation of variation in zooxanthellar srDNA

We recognize the RFLP genotype E as a distinct taxon—*Symbiodinium* E—for the following reasons: (i) RFLP genotype E was common, and many samples contained only

this genotype (Fig. 5); (ii) the nonrandom distribution of RFLP genotype E (Figs. 5 and 6) strongly implies that it represents a distinct organism with distinct ecological attributes; and (iii) phylogenetic analyses of genotype E srDNAs place them within *Symbiodinium*, but distinct from srDNAs of genotypes A, B, and C (Fig. 3), which, by the same reasoning, represent distinct taxa of *Symbiodinium* (Rowan, 1998). In practice, these four taxa of *Symbiodinium* are readily identified by comparison to cloned srDNAs (RFLP genotypes A⁰, B⁰, C⁰, and E⁰⁻¹) digested with the enzymes *Dpn* II and *Taq* I.

By analyzing zooxanthellar srDNA with additional restriction enzymes, we found that samples containing srDNA of RFLP genotype B⁰, C⁰, or E⁰⁻¹ also contained at least one additional srDNA of a different RFLP genotype (examples in Figs. 7-9). What do these additional srDNAs represent, taxonomically? Like an srDNA in genotype C* (Rowan and Knowlton, 1995), they appear to be from *Symbiodinium* (and not some other type of organism) because (i) they were distinguishable in fewer than one-half of different restriction digests, (ii) many of them seemed to represent simple, single restriction site changes compared to a cloned srDNA (not shown), and (iii) different srDNAs from samples of *Symbiodinium* E (Fig. 3) or of C* (Rowan and Knowlton, 1995) differed relatively little in sequence.

Do these additional srDNAs represent distinct species or strains of *Symbiodinium*? In the case of *Symbiodinium* E and B, no evidence suggests that they do. Specifically, these srDNAs were not observed by themselves, nor did they vary in relative abundance from sample to sample (Figs. 7 and 8). This contrasts with observations on srDNAs of RFLP genotypes A⁰, B⁰, C⁰ and E⁰⁻¹, which occur alone, and also mix in a range of proportions (e.g., *Symbiodinium* C and E, Fig. 4; Rowan and Knowlton, 1995; Rowan *et al.*, 1997).

Because srDNA is a multigene family in eukaryotes, srDNA heterogeneity (as seen within samples of *Symbiodinium* B and E) can reside in one organism—including dinoflagellates (Scholin *et al.*, 1993; Scholin and Anderson, 1994, 1996)—among gene-family members (Hillis and Dixon, 1991). We favor this as an explanation for our data because it is parsimonious compared to the alternative of multiple strains of zooxanthellae that for some reason always co-occur in the same relative proportion. Testing this hypothesis requires the analysis either of one dinoflagellate (e.g., Yeung *et al.*, 1996) or of a clonal culture (e.g., Scholin *et al.*, 1993; Rowan *et al.*, 1996).

Heterogeneity of srDNA within samples of *Symbiodinium* C was more intriguing because sample-to-sample variation was observed among colonies (Fig. 9). That observation suggested that different srDNAs within any one sample could represent different strains of *Symbiodinium*. If so, that sample-to-sample variation might also appear within one coral colony, either from place to place or time to time, especially before *versus* after an environmental

change. We found no such variation (e.g., Fig. 10) in corals hosting *Symbiodinium* C, which again is consistent with the hypothesis that srDNA heterogeneity is a property of individual zooxanthellae. Different patterns of srDNA heterogeneity seen among samples of *Symbiodinium* C from different corals (Fig. 9) are different zooxanthellar genotypes, but we do not know if these differences are biologically significant (e.g., Scholin and Anderson, 1994, 1996).

Independent of its source, within-sample srDNA heterogeneity limits the information that can be obtained from srDNA sequences. This limitation is apparent in our analysis of *Symbiodinium* E. The sequence of clone E⁰⁻¹ implies that our RFLP analyses, using 18 enzymes (examples in Fig. 7), surveyed about 220 nucleotide positions (not shown). Heterogeneity was detected with seven enzymes, which implies a within-sample srDNA sequence diversity of about 3% (7 of 220 nucleotide positions). We do not know how this diversity is distributed; possibilities range from two srDNAs that differ at 7 of 220 positions (ca. 3% different srDNAs, similar to the difference between srDNAs of *Symbiodinium* A and B [Rowan and Powers, 1992]) to seven srDNAs that differ from one another at 1 of 220 positions (ca. 0.4% different srDNAs). Differences among srDNA clones E⁰⁻¹, E⁰⁻², and E⁰⁻³ fall within this range, and there is no reason to expect any cloned srDNA to represent our samples of *Symbiodinium* E with any greater precision. Moreover, the PCR creates chimeric DNA molecules when mixed templates are amplified, and many clones obtained from those PCR products will be artifacts (Bradley and Hillis, 1997; Wintzingerode *et al.*, 1997; Darius *et al.*, 1998).

Sequences of srDNAs obtained (as clones) from *Symbiodinium* in the *M. annularis* species complex are summarized in Figure 3. Because we have evidence for only four taxa—A, B, C, and E—the multiple branches within groups B, C, and E represent sequence variation within, not among, taxa. An exception to this statement is the pair of sequences labeled C2⁰⁻¹ and C2⁰⁻², which came from an experimentally bleached *M. annularis* and from an unmanipulated colony of the coral *Siderastrea siderea*, respectively (see Toller *et al.*, 2001). Ecological data and RFLP analyses strongly imply that C2⁰⁻¹ and C2⁰⁻² represent a taxon (*Symbiodinium* C2) that is distinct from the taxon *Symbiodinium* C found commonly in unmanipulated *Montastraea* (Toller *et al.*, 2001). We stress that this taxonomic difference could not be inferred from srDNA sequence data alone, given the levels of srDNA heterogeneity within samples of *Symbiodinium* C and C2 (Toller *et al.*, 2001).

In conclusion, the problem of fully interpreting srDNA variation in natural samples of *Symbiodinium* is challenging. By themselves, srDNA sequence data contributed relatively little to understanding zooxanthellar diversity in *Montastraea*. RFLP data were much more informative, not the least because they revealed the informational limits of

srDNA sequences. Many samples of zooxanthellae from these species of coral contained more than one taxon of *Symbiodinium* (Figs. 4 and 5; Rowan *et al.*, 1997), a phenomenon that would have been difficult to understand from srDNA sequences alone. RFLP data are easily obtained, at reasonable cost, from many samples of zooxanthellae, which allows ecological data to inform taxonomic decisions.

Acknowledgments

We thank the Kuna Nation and the Republic of Panama (Autoridad Nacional del Ambiente, Departamento de Cuarentena Agropecuaria del Ministerio de Desarrollo Agropecuario, and Recursos Marinos) for permission to collect and export specimens. Many thanks to Javier Jara for tireless field assistance and to Juan Maté for help with the deep collections of *M. franksi*. Thanks to Ursula Anlauf and Suzanne Williams for advice. Thanks to Ralf Kersanach and David Kline for coral DNA and advice. David Zawada provided samples from the Bahamas. R. R. thanks Chris Hein and Uma Narayan for hospitality in California. This research was supported by the Andrew W. Mellon Foundation, the Smithsonian Tropical Research Institute, the Scripps Institution of Oceanography, and the National Institutes of Health.

Literature Cited

- Baker, A. C. 1999. Symbiosis ecology of reef-building corals. Ph.D. dissertation, University of Miami, 120 pp.
- Baker, A. C., and R. Rowan. 1997. Diversity of symbiotic dinoflagellates (zooxanthellae) in scleractinian corals of the Caribbean and Eastern Pacific. *Proc. Eighth Int. Coral Reef Symp.* 2: 1301–1306.
- Barnes, D. J., and B. E. Chalker. 1990. Calcification and photosynthesis in reef-building corals and algae. Pp. 109–131 in *Ecosystems of the World Vol. 25: Coral Reefs*, Z. Dubinsky, ed. Elsevier, New York.
- Bowden, K. F. 1983. *Physical Oceanography of Coastal Waters*. Ellis Horwood, Chichester, United Kingdom.
- Bradley, R. D., and D. M. Hillis. 1997. Recombinant DNA sequences generated by PCR amplification. *Mol. Biol. Evol.* 14: 592–593.
- Brown, B. E. 1997. Coral bleaching: causes and consequences. *Coral Reefs* 16: Suppl. S129–S138.
- Brown, B. E., R. P. Dunne, M. S. Goodson, and A. E. Douglas. 2000. Bleaching patterns in reef corals. *Nature* 404: 142–143.
- Carlos, A. A., B. K. Baillie, M. Kawachi, and T. Maruyama. 1999. Phylogenetic position of *Symbiodinium* (Dinophyceae) isolates from tridacnids (Bivalvia), cardids (Bivalvia), a sponge (Porifera), a soft coral (Anthozoa), and a free-living strain. *J. Phycol.* 35: 1054–1062.
- Clifton, K. E., K. Kim, and J. L. Wulff. 1997. A field guide to the reefs of Caribbean Panama with an emphasis on Western San Blas. *Proc. Eighth Int. Coral Reef Symp.* 1: 167–184.
- Connell, J. H. 1978. Diversity in tropical rain forests and coral reefs. *Science* 199: 1302–1310.
- Darius, H. T., C. Dauga, P. A. D. Grimont, E. Chungue, and P. M. V. Martin. 1998. Diversity in symbiotic dinoflagellates (Pyrrhophyta) from seven scleractinian coral species: restriction enzyme analysis of small subunit ribosomal RNA genes. *J. Eukaryot. Microbiol.* 45: 619–627.
- D'Croz, L., D. R. Robertson, and J. A. Martinez. 1999. Cross-shelf distribution of nutrients, plankton, and fish larvae in the San Blas Archipelago, Caribbean Panama. *Rev. Biol. Trop.* 47: 203–215.
- Falkowski, P. G., Z. Dubinsky, L. Muscatine, and J. W. Porter. 1984. Light and the bioenergetics of a symbiotic coral. *Bioscience* 34: 705–709.
- Falkowski, P. G., Z. Dubinsky, L. Muscatine, and L. R. McCloskey. 1993. Population control in symbiotic corals. *Bioscience* 43: 606–611.
- Freudenthal, H. D. 1962. *Symbiodinium* gen. nov. and *Symbiodinium microadriaticum* sp. nov., a zooxanthella: taxonomy, life cycle, and morphology. *J. Protozool.* 9: 45–52.
- Goreau, T. F. 1959. The ecology of Jamaican coral reefs I. Species composition and zonation. *Ecology* 40: 67–90.
- Hill, M., and T. Wilcox. 1998. Unusual mode of symbiont repopulation after bleaching in *Anthosignella varians*: acquisition of different zooxanthellae strains. *Symbiosis* 25: 279–289.
- Hillis, D. M., and M. T. Dixon. 1991. Ribosomal DNA: molecular evolution and phylogenetic inference. *Q. Rev. Biol.* 66: 411–454.
- Kirk, J. T. O. 1994. *Light and Photosynthesis in Aquatic Ecosystems*, 2nd ed. Cambridge University Press, Cambridge.
- Knowlton, N., and J. B. C. Jackson. 1994. New taxonomy and niche partitioning on coral reefs: jack of all trades or master of some? *Trends Ecol. Evol.* 9: 7–9.
- Knowlton, N., E. Weil, L. A. Weigt, and H. M. Guzmán. 1992. Sibling species in *Montastraea annularis*, coral bleaching, and the coral climate record. *Science* 255: 330–333.
- Lopez, J. V., R. Kersanach, S. A. Rehner, and N. Knowlton. 1999. Molecular determination of species boundaries in corals: genetic analysis of the *Montastraea annularis* complex using amplified fragment length polymorphisms and a microsatellite marker. *Biol. Bull.* 196: 80–93.
- McNally, K. L., N. S. Govind, P. E. Thomé, and R. K. Trench. 1994. Small-subunit ribosomal DNA sequence analyses and a reconstruction of the inferred phylogeny among symbiotic dinoflagellates (Pyrrhophyta). *J. Phycol.* 30: 316–329.
- Muller-Parker, G., and C. F. D'Elia. 1997. Interactions between corals and their symbiotic algae. Pp. 96–113 in *Life and Death of Coral Reefs*, C. Birkeland, ed. Chapman & Hall, New York.
- Muscatine, L., and J. W. Porter. 1977. Reef corals: mutualistic symbioses adapted to nutrient-poor environments. *Bioscience* 27: 454–460.
- Robertson, D. R., and P. W. Glynn. 1977. Field guidebook to the reefs of San Blas Islands, Panama. *Third Int. Symp. Coral Reefs*, University of Miami, Florida. 15 pp.
- Rowan, R. 1998. Diversity and ecology of zooxanthellae on coral reefs. *J. Phycol.* 34: 407–417.
- Rowan, R., and N. Knowlton. 1995. Intraspecific diversity and ecological zonation in coral-algal symbiosis. *Proc. Natl. Acad. Sci. USA* 92: 2850–2853.
- Rowan, R., and D. A. Powers. 1991a. A molecular genetic classification of zooxanthellae and the evolution of animal-algal symbioses. *Science* 251: 1348–1351.
- Rowan, R., and D. A. Powers. 1991b. Molecular genetic identification of symbiotic dinoflagellates (zooxanthellae). *Mar. Ecol. Prog. Ser.* 71: 65–73.
- Rowan, R., and D. A. Powers. 1992. Ribosomal RNA sequences and the diversity of symbiotic dinoflagellates (zooxanthellae). *Proc. Natl. Acad. Sci. USA* 89: 3639–3643.
- Rowan, R., S. M. Whitney, A. Fowler, and D. Yellowlees. 1996. Rubisco in marine symbiotic dinoflagellates: form II enzymes in eukaryotic oxygenic phototrophs encoded by a nuclear multigene family. *Plant Cell* 8: 539–553.
- Rowan, R., N. Knowlton, A. Baker, and J. Jara. 1997. Landscape

- ecology of algal symbionts creates variation in episodes of coral bleaching. *Nature* **388**: 265–269.
- Saitou, N., and M. Nei. 1987. The neighbor-joining method: a new method for reconstructing phylogenetic trees. *Mol. Biol. Evol.* **4**: 406–425.
- Schoenberg, D. A., and R. K. Trench. 1980. Genetic variation in *Symbiodinium* (= *Gymnodinium*) *microadriaticum* Freudenthal, and specificity in its symbiosis with marine invertebrates. III. Specificity and infectivity of *Symbiodinium microadriaticum*. *Proc. R. Soc. Lond. B* **207**: 445–460.
- Scholin, C. A., and D. M. Anderson. 1994. Identification of group- and strain-specific genetic markers for globally distributed *Alexandrium* (Dinophyceae). I. RFLP analysis of SSU rRNA genes. *J. Phycol.* **30**: 744–754.
- Scholin, C. A., and D. M. Anderson. 1996. LSU rDNA-based RFLP assays for discriminating species and strains of *Alexandrium* (Dinophyceae). *J. Phycol.* **32**: 1022–1035.
- Scholin, C. A., D. M. Anderson, and M. L. Sogin. 1993. Two distinct small-subunit ribosomal RNA genes in the North American toxic dinoflagellate *Alexandrium fundyense* (Dinophyceae). *J. Phycol.* **29**: 209–216.
- Thompson, J. D., T. J. Gibson., F. Plewniak, F. Jeanmougin, and D. G. Higgins. 1997. The ClustalX windows interface: flexible strategies for multiple sequence alignment aided by quality analysis tools. *Nucleic Acids Res.* **24**: 4876–4882.
- Toller, W. W., R. Rowan, and N. Knowlton. 2001. Repopulation of zooxanthellae in the Caribbean corals *Montastraea annularis* and *M. faveolata* following experimental and disease-associated bleaching. *Biol. Bull.* **201**: 360–373.
- Trench, R. K., and R. J. Blank. 1987. *Symbiodinium microadriaticum* Freudenthal, *S. goreauii* sp. nov., *S. kawagutii* sp. nov. and *S. pilosum* sp. nov.: gymnodinioid dinoflagellate symbionts of marine invertebrates. *J. Phycol.* **23**: 469–481.
- Veron, J. E. N. 1995. *Corals in Space and Time: The Biogeography and Evolution of the Scleractinia*. UNSW Press, Sydney, Australia.
- Weil, E., and N. Knowlton. 1994. A multi-character analysis of the Caribbean coral *Montastraea annularis* (Ellis and Solander, 1786) and its two sibling species, *M. faveolata* (Ellis and Solander, 1786) and *M. franksi* (Gregory, 1895). *Bull. Mar. Sci.* **55**: 151–175.
- Wesseling, L. A. J., Uychiaoco, P. M., Alino, T., Aurin, and J. E. Vermaat. 1999. Damage and recovery of four Philippine corals from short-term sediment burial. *Mar. Ecol. Prog. Ser.* **176**: 11–15.
- Wintzingerode, F. v., U. B. Göbel, and E. Stackebrandt. 1997. Determination of microbial diversity in environmental samples: pitfalls of PCR-based rRNA analysis. *FEMS Microbiol. Rev.* **21**: 213–229.
- Yeung, P. K. K., K. F. Kong, F. T. W. Wong, and J. T. Y. Wong. 1996. Sequence data for two large-subunit rRNA genes from an Asian strain of *Alexandrium catenella*. *Appl. Environ. Microbiol.* **62**: 4199–4201.

Repopulation of Zooxanthellae in the Caribbean Corals *Montastraea annularis* and *M. faveolata* following Experimental and Disease-Associated Bleaching

W. W. TOLLER^{1,3}, R. ROWAN^{2,*}, AND N. KNOWLTON^{1,3}

¹Marine Biology Research Division 0202, Scripps Institution of Oceanography, University of California San Diego, La Jolla, California 92093-0202; ²University of Guam Marine Laboratory, Mangilao, Guam 96923; and ³Smithsonian Tropical Research Institute, Apartado 2072, Balboa, Republic of Panama

Abstract. Caribbean corals of the *Montastraea annularis* species complex associate with four taxa of symbiotic dinoflagellates (zooxanthellae; genus *Symbiodinium*) in ecologically predictable patterns. To investigate the resilience of these host-zooxanthella associations, we conducted field experiments in which we experimentally reduced the numbers of zooxanthellae (by transplanting to shallow water or by shading) and then allowed treated corals to recover. When depletion was not extreme, recovering corals generally contained the same types of zooxanthellae as they did prior to treatment. After severe depletion, however, recovering corals were always repopulated by zooxanthellae atypical for their habitat (and in some cases atypical for the coral species). These unusual zooxanthellar associations were often (but not always) established in experimentally bleached tissues even when adjacent tissues were untreated. Atypical zooxanthellae were also observed in bleached tissues of unmanipulated *Montastraea* with yellow-blotch disease. In colonies where unusual associations were established, the original taxa of zooxanthellae were not detected even 9 months after the end of treatment. These observations suggest that zooxanthellae in *Montastraea* range from fugitive opportunists and stress-tolerant generalists (*Symbiodinium* A and E) to narrowly adapted specialists (*Symbiodinium* B and C), and may undergo succession.

Introduction

Scleractinian reef-building corals are obligate, mutualistic symbioses involving heterotrophic coral animals (hosts) and phototrophic dinoflagellate endosymbionts in the genus *Symbiodinium* (commonly called zooxanthellae). Scleractinian corals (Wells, 1956; Veron, 1995; Cairns, 1999) and zooxanthellae (Trench, 1997; Rowan, 1998) are both taxonomically diverse groups. Their symbioses, however, are restricted to a small and specific subset of the myriad combinations that theoretically might exist (Trench, 1988, 1993). Presumably this host-symbiont specificity is shaped by natural selection, which favors those combinations that perform well and can perpetuate themselves effectively (Trench, 1988; Rowan and Powers, 1991a; Buddemeier and Fautin, 1993). Hypotheses about coral-zooxanthellar specificity were originally shaped by the belief that corals (as individuals or as species) associate with only one species of *Symbiodinium* (Trench, 1988, 1993; see Buddemeier and Fautin, 1993). Accordingly, any direct interactions among different species of *Symbiodinium* were thought to result in one species of zooxanthella consistently "winning" and therefore specifically and exclusively populating its host (Fitt, 1985a; Trench, 1988, 1993).

In contrast to this view, we found that individual colonies of coral in the *Montastraea annularis* species complex often contain more than one taxon of *Symbiodinium* (Rowan and Knowlton, 1995; Rowan *et al.*, 1997; Toller *et al.*, 2001). At Aguadargana reef in the San Blas Islands of Panama (see fig. 1 in Toller *et al.*, 2001), colonies of *M. annularis* host *Symbiodinium* B (or rarely, *Symbiodinium* A) in tissues exposed to high irradiance, and they host *Symbiodinium* C

Received 9 February 2000; accepted 5 July 2001.

*To whom correspondence should be addressed. E-mail: rowan@uog9.uog.edu

Abbreviations: RFLP, restriction fragment length polymorphism; srDNA, small subunit ribosomal RNA gene; YBD, yellow-blotch disease.

in tissues exposed to low irradiance. Colonies of *M. faveolata* exhibit a similar pattern except that *Symbiodinium* A and B are both common at high irradiance in these corals (Rowan and Knowlton, 1995; Rowan *et al.*, 1997). Nearby at Rfo Carti (a near-shore habitat; see fig. 1 in Toller *et al.*, 2001), members of the *Montastraea annularis* complex host *Symbiodinium* E in tissues exposed to high irradiance and host *Symbiodinium* C otherwise (Toller *et al.*, 2001). Thus on these two reefs, corals at shallower depths, which experience both high (on the colony top, exposed to downwelling irradiance) and low (on colony sides) irradiance, typically host both high- (*Symbiodinium* A and/or B or *Symbiodinium* E) and low- (*Symbiodinium* C) irradiance-associated zooxanthellae simultaneously. (On another offshore reef, *Symbiodinium* E also occurs in some of the deepest colonies of *M. franksi*, possibly as a result of sediment-associated stress [Toller *et al.*, 2001]).

Several observations suggest that interactions among different taxa of *Symbiodinium* within one colony of *Montastraea* may be dynamic. First, coral growth causes slow changes in irradiance microenvironments (*e.g.*, corallites moving from tops to sides of *M. annularis* columns), and the specificity of different zooxanthellae for different irradiance environments (above) implies that zooxanthellar communities will change in response to these irradiance changes. Second, experimental manipulations of irradiance gradients within colonies of *M. annularis* hosting *Symbiodinium* B and C resulted in changes in the distribution of these zooxanthellae (Rowan *et al.*, 1997). Finally, the proportions of *Symbiodinium* A, B, and C in *Montastraea* changed during a coral bleaching event (Rowan *et al.*, 1997).

The present study tested the ability of zooxanthellar symbioses in *M. annularis* and in *M. faveolata* to reestablish typical patterns of association after being disturbed. Because zooxanthellae in unmanipulated corals have such environmentally predictable patterns of distribution (above), we hypothesized that disturbed zooxanthellar populations would re-establish the same patterns of association, directly. To disturb zooxanthellae, we treated corals with low light (*e.g.*, Franzisket, 1970) or with high light (*e.g.*, Dustan, 1979), both of which caused corals to lose zooxanthellae (to bleach). Corals were then allowed to recover. We also studied the zooxanthellar communities of unmanipulated corals that exhibited yellow-blotch disease and associated reductions in zooxanthellar numbers.

Materials and Methods

Experimental manipulations

Experiments were conducted between October 1997 and October 1998 at Aguadargana reef, San Blas Archipelago, Republic of Panama (see fig. 1 in Toller *et al.*, 2001). Time courses of experiments (not always optimal) were dictated

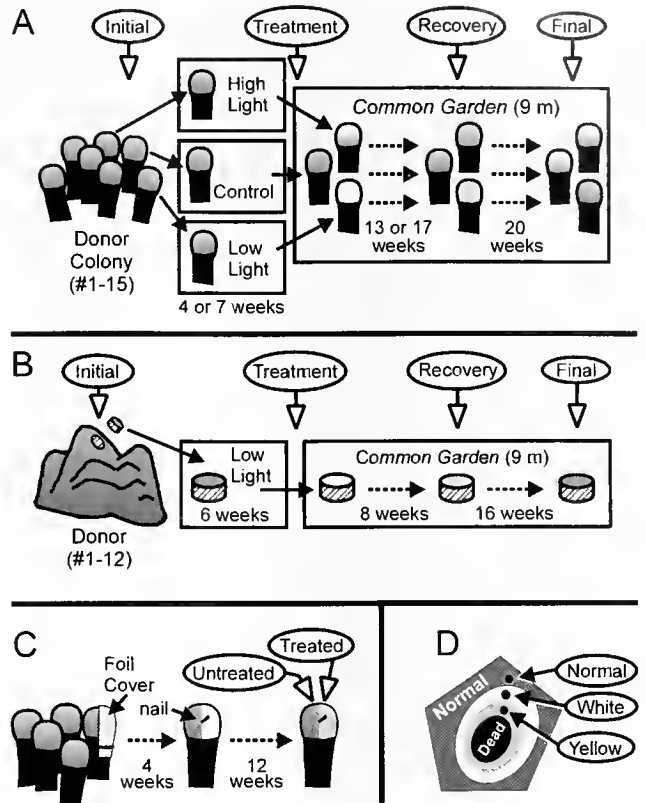


Figure 1. Experimental and sampling designs. (A) Experiment I, in which three columns (gray is live tissue; black is nonliving base) from each of 15 donor colonies of *Montastraea annularis* living at 9–10 m depth (#1–15, corresponding to Corals 1–15 in Figs. 3 and 4) were transplanted to 1 m depth (box labeled High Light), to 9 m depth (Control), and to a cave (Low Light) for treatment for a period of 4 (Colonies 11–15) or 7 (Colonies 1–10) weeks; corals were then transplanted to common gardens at 9 m depth. Samples of zooxanthellae (Initial, Treatment, Recovery, Final) were taken at the times indicated (open arrows); longer times apply to Colonies 1–10; shorter times to Colonies 11–15. (B) Experiment II, in which cores cut from 12 colonies of *M. faveolata* (#1–12, corresponding to Corals 1–12 in Fig. 5) were transplanted to caves (Low Light) for 6 weeks, and then to a common garden at 9 m depth. Samples of zooxanthellae (Initial, Treatment, Recovery, Final) were taken (open arrows) at the times indicated. (C) Experiment III, in which one column on each of 14 colonies of *M. annularis* was half-covered with aluminum foil for 4 weeks, then uncovered for 12 weeks (nail marks the treatment boundary), and then sampled on the top of each half (open arrows, Untreated and Treated; data in Fig. 6). (D) Schematic of yellow-blotch disease (YBD) on *Montastraea* (polygon), showing concentric halos of yellow (light gray color) and bleached (white color) tissue around dead skeleton (Dead), and surrounded by normally pigmented tissue (Normal). Black dots and arrows indicate places where zooxanthellae were sampled (Normal, White, Yellow; data in Fig. 7).

by the imminent closure of the Smithsonian Institution's field station. Experiments used parts of apparently healthy, large colonies of *Montastraea annularis* (Experiments I and III) and *M. faveolata* (Experiment II), as described below and in Figure 1. These large donor coral colonies were separated from one another by more than 5 m. Coral tissues

were sampled with a #6 hole punch, which yields a sample (small core) with about 0.24 cm² of coral tissue, or with a #12 hole punch (ca. 1.3 cm² of tissue). These samples were wrapped in aluminum foil and frozen in a cryogenic dry shipper (chilled with liquid nitrogen) in the field, and then stored in the laboratory at -80 °C until analysis.

Experiment I (Fig. 1A). In December 1997, three columns of similar size (ca. 7–10 cm diameter) were collected from each of 10 colonies of *M. annularis* living at a depth of 9–10 m. (Colonies of *M. annularis* consist of clusters of columns, each of which is covered distally with living tissue; see Fig. 1A.) The columns were broken off at their nonliving bases, labeled, and a sample (#6 hole punch) was taken from the top of each one (Initial samples). The three columns from each colony were then distributed among three treatments: one was transplanted to an open site on the reef crest at a depth of about 1 m (high-light treatment; High Light in Fig. 1A); one was transplanted to a cave at 14 m (low-light treatment; Low Light in Fig. 1A); and one was transplanted to an open site at 9 m (treatment control; Control in Fig. 1A). The cave was a crevice (ca. 2.5 m deep, ca. 1.5 m wide, and <1 m high) that was completely shaded from downwelling irradiance, largely shaded from other irradiance, and lacked conspicuous photosynthetic organisms. For low-light treatment, coral columns were mounted upright on PVC posts set in blocks of concrete, using nylon cable ties to secure the columns at their nonliving bases. These blocks then were placed in the back of the cave. Control and high-light-treated coral columns were affixed in an upright position to wire grids using cable ties, and these grids were secured to the reef by wedging them into substrate and covering them with rubble.

After 7 weeks of treatment, all coral columns were collected, assessed visually, and sampled (#6 hole punch; Treatment samples). They were then mounted on wire grids in an upright position and placed in a common garden at 9 m depth, with unobstructed irradiance, for the remainder of the experiment. There were six grids, each with five columns arranged analogously to a Latin square with respect to treatment. After 17 weeks, all columns were assessed and sampled again (#6 hole punch; Recovery samples). Nine of the 30 columns were assessed and sampled once more (#6 hole punch; Final samples) after a total of 37 weeks in the common garden; the other 21 columns had been lost to vandals by that time. All samples (Initial, Treatment, Recovery, and Final) were taken from the tops of columns, within an area (ca. 7 cm²) over which zooxanthellar identities do not vary much or at all in unmanipulated columns of *M. annularis* (Rowan *et al.*, 1997).

A second experiment was done (starting in January 1998) at a different location (ca. 0.5 km away). The second experiment differed from the first one only as follows: five colonies (15 coral columns) of *M. annularis* were used, treatment was for 4 rather than 7 weeks, Recovery samples

were obtained after 13 rather than 17 weeks, and Final samples were obtained (from all columns) after a total of 33 rather than 37 weeks.

Experiment II (Fig. 1B). In October 1997, one core was removed from each of 12 large (> 1.5 m tall and wide) colonies of *M. faveolata* living at depths of 1–9 m, using a pneumatic drill fitted with a 44-mm hole saw (resulting cores had ca. 12.6 cm² of live tissue and were ca. 5 cm in height). At this time, tissue samples (Initial samples) were taken immediately adjacent to the coring sites with a steel hole punch (#12). Coral cores were then transplanted among three small caves (Low Light, as above) on the reef (7–11 m depth), where they were secured with plastic cable ties to masonry nails pounded into reef framework. Cores occupied the back (darkest) portion of the caves and were mounted upside-down on the cave ceilings.

After 6 weeks of low-light treatment in caves, coral cores were collected and assessed visually; tissue samples were taken from each coral core at a haphazardly selected location away from the core's perimeter (#6 hole punch; Treatment samples). Cores were then attached to cleared reef substrate at 9 m depth with epoxy putty (Z-Spar Splash Zone, Kop-Coat, Inc., Pittsburgh, PA), facing upward under unobstructed natural irradiance. After 8 weeks in this common garden and then again after another 16 weeks, coral cores were assessed and sampled again (#6 hole punch; Recovery samples and Final samples, respectively). In the latter case (Final samples), only eight coral cores were sampled—the four others were lost.

Experiment III (Fig. 1C). In January 1998, individual columns of *M. annularis* were each half-covered with a shield of aluminum foil. This treatment bisected each column vertically into two morphologically equivalent halves, one of which was covered by foil and therefore low-light treated (Treated) and the other of which was exposed to natural irradiance (Untreated). Each shield was molded to its column, lifted off slightly (<0.5 cm), and secured to the column's nonliving base with nylon cable ties. A shield was placed on one column of each of 15 colonies living at depths of 2–4 m (shallow group), and on one column of each of 15 colonies living at depths of 7–9 m (deep group). Shields were removed after 4 weeks, at which time treatment boundaries were marked by gently tapping two small steel nails into opposite sides of each column. After another 12 weeks, columns were assessed visually and a pair of tissue samples was taken from the top of each, 2 cm apart and on either side of the treatment boundary (#6 hole punch; Treated and Untreated samples, Fig. 1C).

Yellow-blotch disease

In October 1997 and January 1998 at Cayos Limones, San Blas (see fig. 1 in Toller *et al.*, 2001), we found a number of colonies of *Montastraea* that appeared to have

“yellow-blotch disease” (YBD; Santavy *et al.*, 1999). Some colonies had only one or two small lesions (*ca.* 10–30 cm wide), which usually consisted of a patch of exposed skeleton surrounded by a halo (typically *ca.* 1–3 cm wide) of yellow living tissue, which in turn was surrounded by a halo (typically ≤ 2 cm wide) of white (bleached) tissue; lesions were surrounded by apparently healthy tissue (see Fig. 1D). Other colonies were mostly dead, in which case a patch of normal tissue was surrounded by a band of bleached tissue inside a band of yellow tissue.

Using a steel hole punch (#12), we took samples from five colonies of *M. franksi* (one lesion per colony), from six colonies of *M. faveolata* (one or two lesions per colony), and from one colony of *M. annularis* (two lesions). Two samples were taken at every lesion—one of normally pigmented tissue and one of yellow tissue nearby (≤ 3 cm apart; Normal and Yellow, respectively; see Fig. 1D). At five lesions we also sampled the white tissue that was between yellow and normal tissue (White; see Fig. 1D).

Progression of YBD was monitored in 12 colonies of *M. faveolata*. On 25 January 1998, two small nails were driven into the bare skeleton next to one YBD lesion in each colony. The two nails defined a line parallel to the lesion edge, and the distance between that line and the lesion edge (living, yellow tissue) was measured with a pair of calipers. We also measured the distance to normally pigmented tissue, along the same vector. These measurements were repeated 5 months later (28 May 1998).

Laboratory methods

Zooxanthellae were isolated from frozen samples as described previously (Rowan and Powers, 1991b; Rowan and Knowlton, 1995), except that skeletal cores or fragments, after being stripped of tissue, were broken apart with a steel spatula and then washed with isolation buffer. That wash was combined with the tissue that had been stripped from the sample previously. At this point, one-tenth of each sample was fixed in 10% formalin and stored at 4 °C for cell counts, which were obtained from eight subsamples of each sample by hemacytometry. The rest of each sample was used to prepare DNA as described previously (Rowan and Powers, 1991b; Rowan and Knowlton, 1995).

Zooxanthellae in each sample were identified by restriction fragment length polymorphism (RFLP) genotypes of small ribosomal subunit RNA genes (srDNA), as described previously (Rowan and Powers, 1991b; Toller *et al.*, 2001). Each sample was analyzed at least twice—once by srDNA amplification with universal PCR primers (ss3 and ss5; Rowan and Powers, 1991b), and once by srDNA amplification with host-excluding PCR prim (ss3Z and ss5; Rowan and Powers, 1991b; Toller *et al.*, 2001). All amplified srDNAs were digested with *Dpn* II and with *Taq* I, and then compared to standard srDNA genotypes of *Symbiodinium*

A, B, C, and E (srDNA clones A⁰, B⁰, C⁰, and E⁰⁻¹, amplified and digested the same way; see Toller *et al.*, 2001). RFLP genotypes C2 (in two samples) and C (in 12 samples) were compared in greater detail using a total of 12 restriction enzymes: *Alu* I, *Bst*N I, *Bst*U I, *Dpn* II, *Hae* III, *Hha* I, *Hinf* I, *Mbo* I, *Mse* I, *Msp* I, *Sau*96 I, and *Taq* I.

Samples that contained more than one zooxanthellar RFLP genotype were compared to a series of synthetic mixtures of cloned srDNAs (srDNA clones A⁰, B⁰, C⁰, and E⁰⁻¹ and srDNA clone C2⁰⁻¹, see below) to estimate the relative abundance of each genotype in the sample (Rowan *et al.*, 1997; Toller *et al.*, 2001). For graphical presentation, these estimates were multiplied by the sample's total cell number (see above) to estimate the number of cells of each genotype in the sample, and these values were then converted to numbers of cells per square centimeter of live coral surface (number of zooxanthellae/cm² in Figs. 3–7).

Samples with low numbers of zooxanthellae ($< 4 \times 10^5$ cells/cm² of coral) yielded little zooxanthellar srDNA when srDNAs were PCR-amplified in the usual manner. To obtain more srDNA from such samples in Experiment I, we used two rounds of amplification (Roux, 1995) as follows. Sample srDNAs were amplified with host-excluding PCR primers over 34 cycles of the PCR. Aliquots (10 μ l) of those amplifications were electrophoresed on agarose gels (1.0% Nuseive GTG; FMC BioProducts, Rockland, ME), and faint bands of srDNA were excised and added to 100 μ l of water. These gel-purified srDNAs were heated to 65 °C for 2 min, and then 1 μ l of each one was PCR-amplified with host-excluding primers in the same manner. The resulting re-amplified srDNAs were then analyzed as described above.

srDNA with an RFLP genotype distinct from *Symbiodinium* A⁰, B⁰, C⁰, and E⁰⁻¹, here called C2, was cloned and sequenced using methods described previously (Toller *et al.*, 2001). It was amplified with host-excluding PCR primers from a colony of *M. annularis* in Experiment III (clone C2⁰⁻¹) and from an unmanipulated colony of the coral *Siderastrea siderea* (clone C2⁰⁻²). DNA sequences were deposited in GenBank [<http://www.ncbi.nlm.nih.gov/>; accession numbers AF238259 (C2⁰⁻¹), AF238260 (C2⁰⁻²)].

Results

RFLP genotypes of zooxanthellae in experimental corals

Using the restriction enzymes *Dpn* II and *Taq* I, we scored six different RFLP genotypes of srDNA in samples of zooxanthellae (Fig. 2). As explained below, genotypes A, B, C, C2, and E represent the taxa *Symbiodinium* A, B, C, C2, and E. RFLP genotype N (Fig. 2, lane N⁰⁻¹) is not a taxon of *Symbiodinium* and is instead related to protozoa of the phylum Apicomplexa (Toller *et al.*, in press). Using our methods (above), genotype N was observed only in six corals—all of these from Experiment I (low-light treatment) and only in samples taken immediately after treatment (see

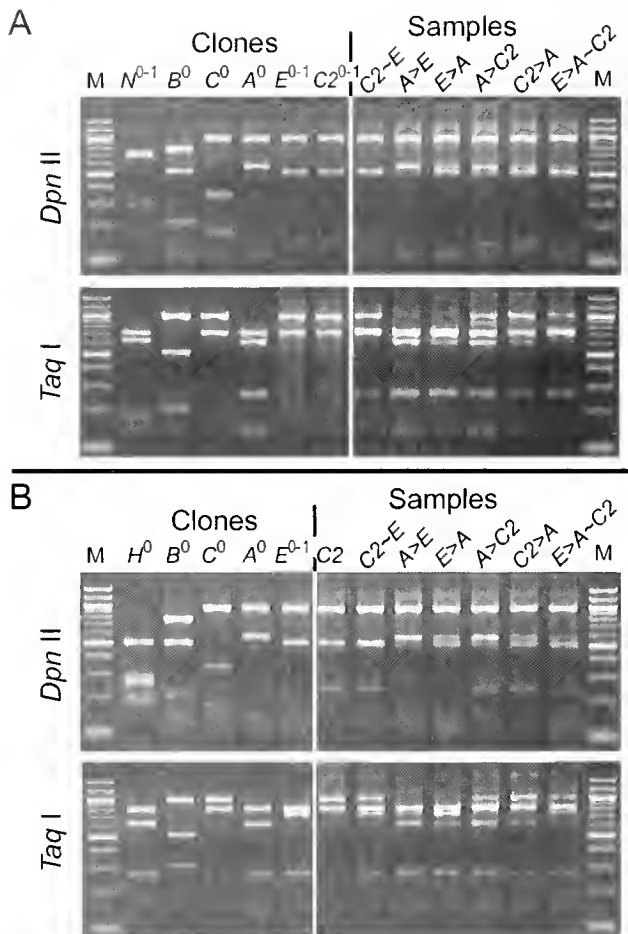


Figure 2. RFLP genotypes of *Symbiodinium*. The same srDNAs were amplified with host-excluding PCR primers (A) and with universal PCR primers (B), and then digested with *Dpn* II (upper panels) and with *Taq* I (lower panels). Clones are srDNA standards for genotype *N* (clone N^{0-1} ; see Results), *Montastraea annularis* (clone H^0), *Symbiodinium* B (clone B^0), *Symbiodinium* C (clone C^0), *Symbiodinium* A (clone A^0), *Symbiodinium* E (clone E^{0-1}), and *Symbiodinium* C2 (clone $C2^{0-1}$). Samples are zooxanthellae from *Montastraea* scored as *Symbiodinium* C2 (B; C2), *Symbiodinium* C2 and *Symbiodinium* E in approximately equal amounts (A and B; C2~E), more *Symbiodinium* A than *Symbiodinium* E (A and B; A > E), more *Symbiodinium* E than *Symbiodinium* A (A and B; E > A), more *Symbiodinium* A than *Symbiodinium* C2 (A and B; A > C2), more *Symbiodinium* C2 than *Symbiodinium* A (A and B; C2 > A), and *Symbiodinium* A and C2 in approximately equal amounts with more *Symbiodinium* E (A and B; E > A~C2). Lane M contains DNA fragment size standards of (top to bottom) 1500 base pairs (bp), 1200 bp, and then 1000 bp to 100 bp in 100-bp increments.

below). Further observations on genotype *N* are presented elsewhere (Toller *et al.*, in press).

The srDNA genotypes of *Symbiodinium* A, B, C, and E are represented by cloned srDNAs A^0 , B^0 , C^0 , and E^{0-1} (respectively), and these genotypes differ from one another in both *Dpn* II and *Taq* I digests (Toller *et al.*, 2001; Fig. 2A, B). RFLP genotype C2, represented in Figure 2A by a cloned srDNA ($C2^{0-1}$; below) and in Figure 2B by a sample

of zooxanthellae (C2), has not been found in unmanipulated colonies of *Montastraea annularis* and *M. faveolata* (Rowan and Knowlton, 1995; Rowan *et al.*, 1997; Toller *et al.*, 2001; this study and unpubl. obs.). Genotype C2 is distinguished from genotypes C and E only when both *Dpn* II and *Taq* I digests are examined together (Fig. 2A, B).

srDNA of genotype C2 appears to lack a *Dpn* II restriction site relative to srDNA of genotype C (Fig. 2). Defined by this character, genotype C2 was found previously in various other species of host (R. Rowan and W. Toller, unpubl. obs.). Cloned srDNAs C^0 (which represents *Symbiodinium* C; Toller *et al.*, 2001), $C2^{0-1}$ (genotype C2 from Experiment III), and $C2^{0-2}$ (genotype C2 from *Siderastrea siderea*, collected nearby) differed from one another in nucleotide sequence by about 0.9% (not shown; see also Toller *et al.*, 2001). That amount of srDNA sequence difference could imply that these three clones represent three species of *Symbiodinium* (e.g., McNally *et al.*, 1994), or one species of *Symbiodinium* in which srDNA is heterogeneous (see Toller *et al.*, 2001).

We further compared the two samples from which clones $C2^{0-1}$ and $C2^{0-2}$ were obtained to 12 samples of *Symbiodinium* C (samples in fig. 9 in Toller *et al.*, 2001) by digesting srDNAs with 12 restriction enzymes (listed in Materials and Methods). The two samples of genotype C2 were indistinguishable and differed from *Symbiodinium* C only in *Dpn* II (above) and *Mse* I digests (not shown). This analysis also showed that srDNA was heterogeneous in all samples, which means that zooxanthellae in the samples cannot be described precisely by sequences of cloned srDNA (i.e., clones C^0 , $C2^{0-1}$, and $C2^{0-2}$; see above and Toller *et al.*, 2001). Nevertheless, RFLP data indicate that genotype C2 represents a taxon of zooxanthella, *Symbiodinium* C2, that is distinct from the *Symbiodinium* C that occurs commonly in *M. annularis* and *M. faveolata*.

Examples of RFLP genotypes that we interpreted as mixtures of taxa of *Symbiodinium* are shown on the right side of Figure 2 (Samples). The figure compares data obtained by amplifying srDNAs with host-excluding (Fig. 2A) versus universal (Fig. 2B) PCR primers because, using *Dpn* II and *Taq* I, both sets of data are needed to distinguish mixtures of genotypes A and C2 (e.g., Fig. 2, A > C2 and C2 > A) from mixtures of genotypes A, C2, and E (e.g., Fig. 2, E > A~C2). Universal PCR primers also amplify coral host srDNA (Fig. 2B, clone H^0), but none was detected in the samples of zooxanthellae shown in Figure 2B.

Experiment I

The experimental units were individual coral columns taken from 15 donor colonies of *M. annularis* (see Fig. 1A). Below, a column is identified by the colony from which it came and by its treatment group (e.g., Colony 1, High Light). Columns 1–10 were in the first experimental group;

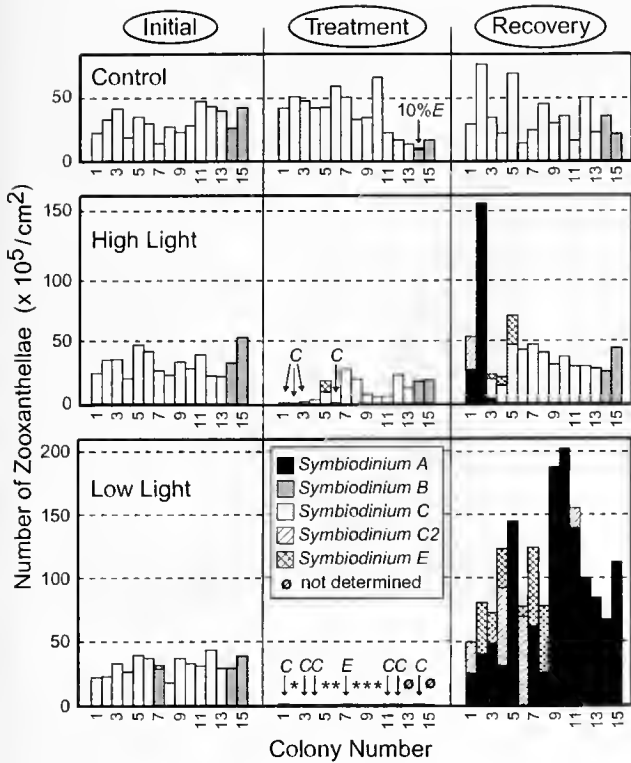


Figure 3. Zooxanthellae observed in *Montastraea annularis* in Experiment I. Panels labeled Control (top), High Light (middle), and Low Light (bottom) present data from corals in the treatments labeled as such in Figure 1A. Panel divisions labeled Initial, Treatment, and Recovery (in ovals at top) present data from samples labeled as such in Figure 1A (ovals with open arrows). Colony Number (horizontal axes) identifies data obtained from different coral columns; data with the same Colony Number within a panel are different samples from the same column; data with the same Colony Number in different panels are samples from different columns taken from the same donor coral colony (see Fig. 1A). Colonies 1–10 are from the first experimental group, and colonies 11–15 are from the second experimental group (see Methods). Bars indicate the taxa of zooxanthellae (by shade, according to the key in the middle panel) and the number of zooxanthellae (by height, normalized to 1 cm² of coral surface) observed in each sample. Where bars are too short to be legible, zooxanthellar identities are given by the arrows labeled C (*Symbiodinium* C), E (*Symbiodinium* E), and 10% E (together with 90% *Symbiodinium* B). Samples in which zooxanthellae were not identified are indicated with a theta (θ). Samples that contained RFLP genotype N (see text) are indicated with asterisks (*).

Columns 11–15 were in the second group (see Materials and Methods). Before treatment, samples from most coral columns contained *Symbiodinium* C (Fig. 3, Initial). Exceptions were two donor colonies that yielded only *Symbiodinium* B (Fig. 3, Initial; Colonies 14 and 15 in all treatment groups), and one column that yielded *Symbiodinium* B with a small amount of *Symbiodinium* E (Fig. 3, Initial; Colony 7, Low Light). Initial zooxanthellar numbers in the three treatment groups (Control, High Light, and Low Light; Fig. 3) were indistinguishable ($31.5 \pm 10.1 \times 10^5$, $31.9 \pm$

9.80×10^5 , and $31.4 \pm 7.10 \times 10^5$ zooxanthellae/cm² of coral, respectively).

Zooxanthellar numbers decreased after treatment. Samples from high-light-treated coral columns (Fig. 3, High Light, Treatment) had, on average, 29% as many zooxanthellae as did samples from controls ($10.7 \pm 9.0 \times 10^5$ versus $36.6 \pm 17.5 \times 10^5$ zooxanthellae/cm² [means \pm standard deviations]; Wilcoxon signed rank test, $P < 0.001$). Two high-light-treated columns (Colonies 14 and 15; with *Symbiodinium* B before treatment) appeared normal; the other 13 (with *Symbiodinium* C before treatment) were pale or bleached, but only on their tops and south-facing (sun-facing) sides. All low-light-treated columns (Fig. 3, Low Light, Treatment) were white, and samples from them had, on average, only about 2.5% as many zooxanthellae as did samples from controls ($0.90 \pm 1.4 \times 10^5$ versus $36.6 \pm 17.5 \times 10^5$ zooxanthellae/cm²; Wilcoxon signed rank test, $P < 0.001$). Zooxanthellar identities did not change in samples from the tops of coral columns in the control group after 4 or 7 weeks (Fig. 3, Control, Treatment versus Initial), with one exception. That exception was Colony 14, which yielded only *Symbiodinium* B initially but yielded *Symbiodinium* B with a small amount of *Symbiodinium* E 4 weeks later. In high-light-treated columns one change was observed (Fig. 3, High Light, Treatment versus Initial); Colony 5 initially yielded *Symbiodinium* C but yielded roughly equal parts of *Symbiodinium* C and *Symbiodinium* E immediately after treatment.

Identities of zooxanthellae were difficult to determine in low-light-treated coral columns at the end of treatment, presumably because these columns contained so few zooxanthellae (above). Two rounds of PCR amplification (see Materials and Methods) allowed 13 samples to be analyzed (Fig. 3, Low Light, Treatment); no srDNA was obtained from the other two samples. Six samples contained *Symbiodinium* C, one contained *Symbiodinium* E (Colony 7, which contained some *Symbiodinium* E initially), and six yielded only a non-*Symbiodinium* RFLP genotype (genotype N; see above).

After a total time of 17 or 24 weeks, zooxanthellar numbers and RFLP genotypes in samples from the control group were similar to initial conditions; Colony 14 once again yielded only *Symbiodinium* B (Fig. 3, Control; Initial, Treatment, Recovery). High-light-treated columns, which had then spent 13 or 17 weeks in their original, deeper environment (Fig. 3, High Light, Recovery) regained coloration (11 normal, 4 pale on tops only) and zooxanthellar numbers (Recovery versus Treatment: $45.4 \pm 34.2 \times 10^5$ versus $10.7 \pm 9.0 \times 10^5$ zooxanthellae/cm²; Wilcoxon signed rank test, $P < 0.001$). At this time, zooxanthellar numbers in samples from high-light-treated columns were similar to those in samples from controls ($45.4 \pm 34.2 \times 10^5$ versus $35.2 \pm 18.5 \times 10^5$ zooxanthellae/cm², respectively; Wilcoxon signed rank test, $P > 0.1$).

Thirteen or 17 weeks after the end of treatment, 10 of 15 high-light-treated coral columns had the same taxa of *Symbiodinium* that they contained before treatment, but 5 of 15 coral columns apparently contained different taxa of *Symbiodinium* than they began with (Fig. 3, High Light, Recovery). One of these taxonomic differences had been observed at the end of treatment (Colony 5). The other four changes (Fig. 3, High Light, Initial versus Recovery) were *Symbiodinium* C to *Symbiodinium* A and C2 (Colony 1); *Symbiodinium* C to *Symbiodinium* A (Colony 2); *Symbiodinium* C to *Symbiodinium* C, A, and E (Colony 3); and *Symbiodinium* C to *Symbiodinium* C and E (Colony 4). These four columns represented four of the five columns with the lowest numbers of zooxanthellae following treatment.

All low-light-treated coral columns experienced major changes in zooxanthellar populations after 13 or 17 weeks back in their original environment (Fig. 3, Low Light, Recovery). Zooxanthellar numbers were about 100-fold higher than after treatment (Recovery versus Treatment: $111 \pm 45.2 \times 10^5$ versus $0.90 \pm 1.4 \times 10^5$ zooxanthellae/cm²; Wilcoxon signed rank test, $P < 0.001$), and were about 3-fold higher than in the control group ($35.2 \pm 18.5 \times 10^5$ zooxanthellae/cm²; Wilcoxon signed rank test, $P < 0.001$). Only Colony 2 appeared normal; the other 14 columns, despite their large numbers of zooxanthellae, were still pale at this time (May 1998).

No low-light-treated coral column contained the same zooxanthellae that it had originally (Fig. 3, Low Light, Recovery versus Initial). Eight of them contained mixtures of taxa, and *Symbiodinium* A was predominant, followed by *Symbiodinium* E and C2; *Symbiodinium* C and B were not detected (Fig. 3, Low Light, Recovery). The predominance of *Symbiodinium* A was observed primarily in Colonies 11–15 (sampled 13 weeks after treatment); among Colonies 1–10 (sampled 17 weeks after treatment) only four samples contained more than 50% *Symbiodinium* A.

Twenty-four of the above coral columns ($n = 8$ colonies) were sampled again, for the last time, 33 or 37 weeks after treatment. At this time (18 October 1998), many unmanipulated colonies of *M. annularis*, *M. faveolata*, and *M. franksi* living at depths of 8–14 m at our study site were pale or bleached on their upper surfaces. Weekly mean sea-surface temperatures near our study site ranged between 29.4 °C and 29.9 °C from 26 August to 7 October (9.5 °N, 78.5 °W; data from Integrated Global Ocean Services System, <http://ingrid.ldgo.columbia.edu/SOURCES/IGOSS>). Historically, temperatures this high are associated with coral bleaching at our study site (see fig. 3e in Rowan *et al.*, 1997). Moreover, most of the summer of 1998 was unusually warm: from the first week of May through the first week of October (23 weeks) in the years 1981 to 1997 (but excluding 1983 and 1995, when corals bleached), there were an average of 3.5 weeks of average sea-surface temperature at or above 29.0 °C near our study site; for this period in 1998, there were 16 such weeks (data

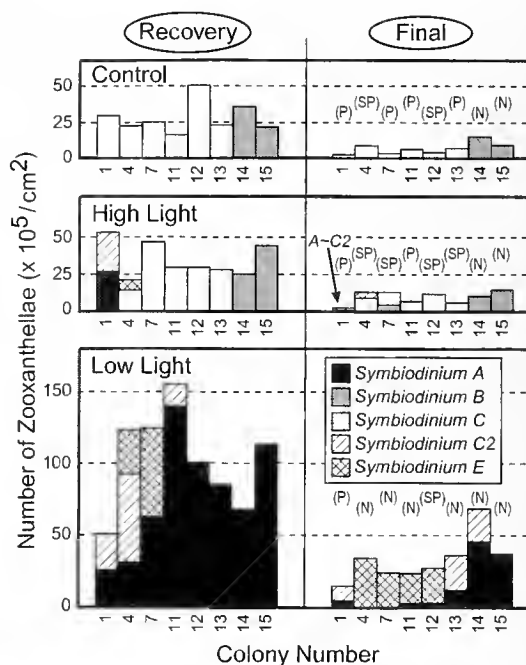


Figure 4. Zooxanthellae observed in *Montastraea annularis* at the last two sampling times of Experiment I. Data are presented as in Figure 3, using the same system to number colonies. Data under Recovery (oval, above) are the same data from Figure 3, and data under Final (oval, above) are from samples from the same corals 20 weeks later (see Fig. 1A). When Final samples were collected, corals were scored as normal (N), slightly pale (SP), or pale (P).

from IGOSS, as above). However, bleaching appeared to be less severe than in October 1995 (Rowan *et al.*, 1997; pers. obs.) in terms of the number of colonies of *Montastraea* affected, the number of species of coral affected, and the extent to which individual corals were bleached.

Results are presented in Figure 4 (Final), in comparison to Recovery samples (13 or 17 weeks after treatment) from the same columns (data from Fig. 3). When final samples were collected, six of eight control coral columns appeared pale or slightly pale [labeled (P) and (SP), respectively, in Fig. 4] on top, as were six of eight high-light-treated columns (Fig. 4, Final); the other two columns in each group hosted *Symbiodinium* B and appeared normal [labeled (N)]. Twenty weeks earlier (Recovery) only one of these 16 columns appeared pale (Colony 1, High Light) and all others appeared normal. As suggested by the increase in numbers of pale colonies, average zooxanthellar numbers decreased and were about 5-fold lower than in the previous samples (Final versus Recovery: control columns, 6.7 ± 4.0 versus $35.2 \pm 18.5 \times 10^5$ zooxanthellae/cm²; high-light-treated columns, 9.4 ± 4.3 versus $45.4 \pm 34.2 \times 10^5$ zooxanthellae/cm²; Wilcoxon signed rank tests, $P = 0.01$).

In contrast, only two low-light-treated coral columns (Colonies 1 and 12) appeared pale or slightly pale in October, and six appeared normal (Fig. 4, Low Light, Final). All

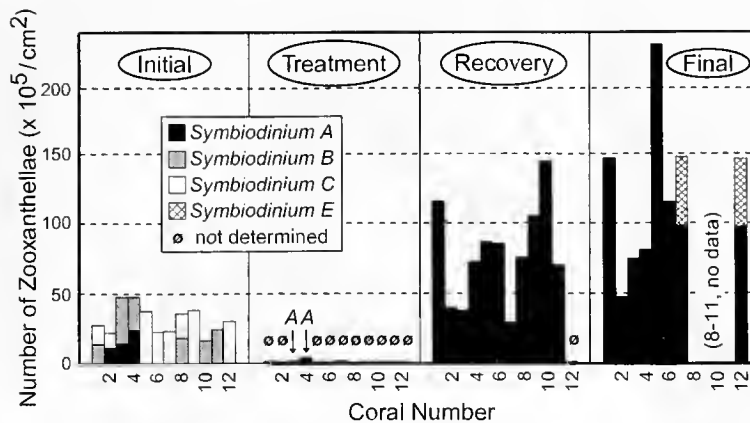


Figure 5. Zooxanthellae observed in *Montastraea faveolata* before and after low-light treatment (Experiment II). The data are presented as in Figures 3 and 4, for the experiment diagrammed in Figure 1B; there was no control group in this experiment. Corals 8–11 were lost before Final samples were collected (8–11, no data).

eight of these columns were pale 20 weeks earlier. Contrary to expectation, the overall increase in pigmentation was accompanied by an average decrease of about 3-fold in zooxanthellar number (Final versus Recovery; 33.6 ± 16.1 versus $111 \pm 45.2 \times 10^5$ zooxanthellae/cm²; Wilcoxon signed rank test, $P < 0.02$), to numbers comparable to those in control, normally pigmented columns at previous sampling times (e.g., Fig. 4, Low Light, Final versus Control, Recovery).

Final samples from control columns contained the same taxa of *Symbiodinium* that were observed previously in those columns (Fig. 4; Control, Recovery). This was also true for most high-light-treated columns, although in one of these *Symbiodinium* B was found with *Symbiodinium* C (Fig. 4, High Light, Final; Colony 7), whereas only *Symbiodinium* C was detected in that column previously. In contrast, we found different zooxanthellae (relative to Recovery) in six of eight low-light-treated columns (Fig. 4, Low Light, Final versus Recovery). In final samples from low-light-treated corals overall, *Symbiodinium* A declined, *Symbiodinium* E increased to become predominant, and *Symbiodinium* C2 appeared in different columns, compared to samples taken 20 weeks earlier. *Symbiodinium* C and B were not detected.

Experiment II

Cores taken from colonies of *M. faveolata* (see Fig. 1B; these cores are hereafter referred to as "corals") living at depths between 1 and 9 m contained a variety of zooxanthellar taxa before treatment (*Symbiodinium* A, B, C; Fig. 5, Initial), as expected based on earlier surveys (Rowan and Knowlton, 1995; Rowan *et al.*, 1997). After low-light treatment, all 12 corals were white and contained, on average, about 2.6% as many zooxanthellae as they began with (Fig. 5, Treatment versus Initial; $0.8 \pm 1.0 \times 10^5$ versus $30.8 \pm$

10.2×10^5 zooxanthellae/cm², respectively; Wilcoxon signed rank test, $P = 0.002$). Zooxanthellae were identified in only two samples; both contained *Symbiodinium* A, and were from corals that had mixtures of A and B before treatment (Corals 3 and 4; Fig. 5).

Eight weeks after the end of treatment, zooxanthellar numbers were about 2-fold higher than before treatment (Fig. 5, Recovery versus Initial; $71.6 \pm 40.5 \times 10^5$ versus $30.8 \pm 10.2 \times 10^5$ zooxanthellae/cm², respectively; Wilcoxon signed rank test, $P = 0.01$). Corals 1 and 6 appeared normal, Coral 12 was bleached (and had very few zooxanthellae; Fig. 5, Recovery), and the other eight corals appeared pale. Only *Symbiodinium* A was detected at this time (Fig. 5, Recovery), in contrast to the typical pattern for *M. faveolata* in this habitat, which host *Symbiodinium* C (Rowan and Knowlton, 1995).

Eight corals were sampled after a further 16 weeks in their common garden (24 weeks total time after the end of treatment, at the end of May 1998, prior to the bleaching event noted above). Six of them appeared normal and two (Corals 5 and 6) were pale. Zooxanthellar numbers remained high on average ($111.1 \pm 55.6 \times 10^5$ zooxanthellae/cm²). Samples from six corals contained only *Symbiodinium* A; samples from the other two corals contained *Symbiodinium* A and E (Fig. 5, Final).

Experiment III

When the foil treatment shields (see Fig. 1C) were removed, all treated tissues were white. Adjacent tissues that had not been covered appeared normal, and borders between the white (treated) tissue and the normal (untreated) tissue were sharp. Many corals had suffered partial mortality in covered areas during treatment; further observations were made only on those in which more than 50% of the treated tissue appeared healthy ($n = 5$ in the shallow group; $n = 9$

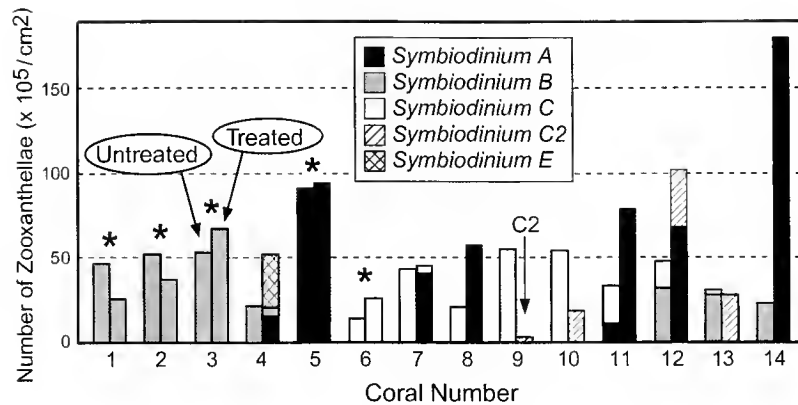


Figure 6. Zooxanthellae observed in untreated and in treated parts of the same column of *Montastraea annularis* (Experiment III; see Fig. 1C). Corals 1–5 lived at 2–4 m depth, Corals 6–14 lived at 7–9 m depth. Data from untreated (Untreated) and from treated (Treated) parts of the same coral column are paired (left bar and right bar, respectively, as shown for Coral 3). Asterisks (*) identify coral columns in which samples from both treated and untreated tissue appeared normal (see text). Otherwise, data are presented as in Figures 3–5.

in the deep group). To avoid additional stress to the corals, no samples were taken immediately after treatment.

The corals had different appearances 12 weeks after treatment. In four shallow corals and one deep coral (Fig. 6, asterisks; Corals 1, 2, 3, 5, and 6) it appeared that normal pigment had spread from untreated into treated tissue by about 2–3 cm, so that treatment boundaries were no longer apparent. In these corals, samples taken from either side of the treatment boundary (see Fig. 1C, Treated and Untreated) were normally pigmented; they also had similar numbers of zooxanthellae, of the same taxon of *Symbiodinium*. The taxa were those expected in shallower (Corals 1, 2, 3, 5; *Symbiodinium* B or A) and deeper (Coral 6; *Symbiodinium* C) colonies of *M. annularis* at this location (Rowan and Knowlton, 1995; Rowan *et al.*, 1997).

In the other nine corals (Fig. 6; Corals 4, 7–14) treatment boundaries were still obvious 12 weeks after treatment. Untreated tissues appeared normal, whereas treated tissues were unevenly pigmented and pale overall, and samples taken from either side of the treatment boundary had different taxa of *Symbiodinium*. Untreated halves contained the expected taxa (*Symbiodinium* B, C, or, rarely in deeper water, some A); treated halves contained, in order of decreasing occurrence, *Symbiodinium* A, C2, E, and B or C (Fig. 6; Corals 4, 7–14). In samples from three of these nine corals (Corals 4, 7, and 11), the taxon of *Symbiodinium* found in the untreated half was also found in the treated half, but—except where that taxon was *Symbiodinium* A (Colony 11)—it was relatively minor in the treated tissue. Zooxanthellar numbers were variable among samples from treated halves (Fig. 6); overall, there was no significant difference in zooxanthellar numbers in samples from treated *versus* untreated halves of corals.

Disease-associated disturbance of zooxanthellae

We marked YBD lesions in 12 colonies of *M. faveolata* and observed that mortality progressed by 11 ± 6 mm (mean \pm standard deviation) during 5 months. Yellow and white halos (see Fig. 1D) progressed in concert with mortality. Thus, as YBD spreads across a coral, it appears that tissue first loses zooxanthellae (white), then partially recovers zooxanthellae (yellow), and then dies. Average numbers of zooxanthellae in samples of normal ($31.8 \pm 10.1 \times 10^5$ zooxanthellae/cm²), white ($3.7 \pm 1.8 \times 10^5$ zooxanthellae/cm²), and yellow ($24.6 \pm 16.1 \times 10^5$ zooxanthellae/cm²) tissues confirmed that hypothesis.

With one exception (Fig. 7; Colony 9), normal and yellow samples from the same lesion contained different taxa of *Symbiodinium*. Samples of normal tissues contained the taxa that are common in unaffected corals at these depths (Rowan and Knowlton, 1995; Rowan *et al.*, 1997; Toller *et al.*, 2001)—predominantly *Symbiodinium* C—and yellow tissues contained predominantly *Symbiodinium* A (estimated at $\geq 50\%$ of the total in samples from 12 of 15 lesions; Fig. 7). Yellow tissue also often (9 of 15 samples; Fig. 7) contained the zooxanthellae found in the adjacent normal tissue. We could identify zooxanthellae in two samples of white tissue (Colony 3 and Lesion 7-1, Fig. 7); they contained mixtures of the taxa found in the adjacent normal (*Symbiodinium* C) and yellow (*Symbiodinium* A) tissues.

Discussion

Taxonomic identities of zooxanthellae

In laboratory studies of establishment or re-establishment of symbiosis between *Symbiodinium* and host animals, sources of zooxanthellae are under full experimental control

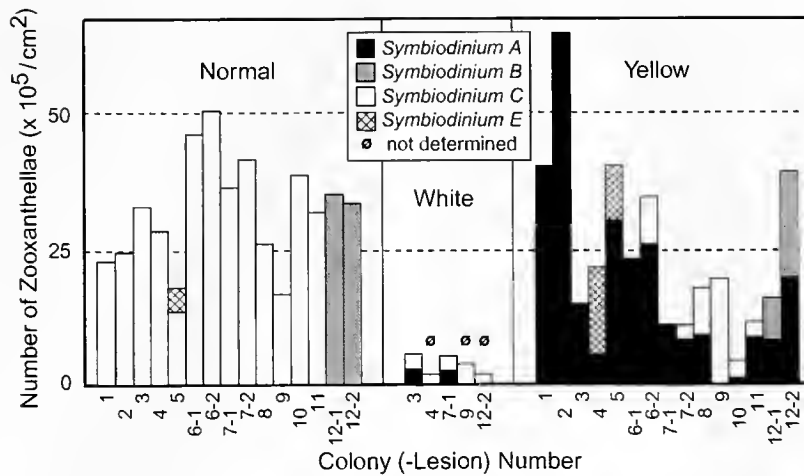


Figure 7. Zooxanthellae associated with yellow-blotch disease (YBD). Lesions of YBD were sampled in 12 affected coral colonies (Colony Number, 1–12), one lesion per colony (most colonies) or two lesions per colony (Colonies 6, 7, and 12 only; Colony-Lesion Numbers 6-1 and 6-2, 7-1 and 7-2, 12-1 and 12-2). At every lesion, samples were taken from Normal and Yellow tissues as diagrammed in Figure 1D. Samples of White tissue (see Fig. 1D) were obtained from five of the lesions only. Each bar represents data from one sample, presented as in Figures 3–6. Coral species were *Montastraea franksi* (Colonies 1–5), *M. faveolata* (Colonies 6–11), and *M. annularis* (Colony 12).

(e.g., Kinzie and Chee, 1979; Schoenberg and Trench, 1980; Colley and Trench, 1983; Davy *et al.*, 1997). In contrast, corals in our field experiments were exposed to uncharacterized natural populations of *Symbiodinium*. Here, the identities of zooxanthellae in re-established symbioses are certain only to the extent that zooxanthellar taxonomy is certain.

Our study compared zooxanthellae that were identified by *Dpn* II- and *Taq* I-generated RFLP genotypes of srDNA, and this method does not discriminate all species of *Symbiodinium* (Rowan, 1998; Toller *et al.*, 2001). For example, three known species of *Symbiodinium* A—*S. microadriaticum* (GenBank accession number M88521), *S. pilosum* (X62650), and *S. corcolorum* (L13717)—would be indistinguishable in this analysis. Nevertheless, where the same zooxanthellar RFLP genotype was detected in a coral both before and after treatment (e.g., Fig. 3, High Light, Colonies 6–15), parsimony argues that the coral hosted the same species of *Symbiodinium* throughout the experiment. On the other hand, no taxonomic uncertainty affects our observation that many re-established symbioses involved changes; when compared samples of zooxanthellae differed with respect to RFLP genotypes A, B, C, or E (e.g., Fig. 3, Low Light; Fig. 5), it is clear that the samples contained different species of *Symbiodinium* (Rowan, 1998; Toller *et al.*, 2001).

Disturbance and re-establishment of zooxanthellar symbioses

Where our experiments were conducted, *Symbiodinium* B predominates in *Montastraea annularis* at higher irradiance,

Symbiodinium A and B predominate in *M. faveolata* at higher irradiance, and *Symbiodinium* C predominates in both species of coral at lower irradiance (Rowan and Knowlton, 1995; Rowan *et al.*, 1997). This predictable pattern suggests that host-symbiont specificity is defined largely by the interaction of each host-zooxanthella combination with its environment (*sensu* Buddemeier and Fautin, 1993). This led us to hypothesize that, under a constant environment, host-symbiont specificity should be directly re-established following acute disturbance.

We found some evidence for this in Experiment I, in that most (10 of 15) of high-light-treated columns of *M. annularis* were repopulated with the same zooxanthellae that existed prior to treatment (*Symbiodinium* C or B; Fig. 3, High Light, Colonies 6–15). However, the host-zooxanthella specificity was not re-established in the other high-light-treated columns, which contained at least some different zooxanthellae (*Symbiodinium* A, E, and C2; Fig. 3, High Light, Colonies 1–5) after recovery. In these five corals, treatment had led to significantly fewer zooxanthellae than in the other 10 corals (5.0×10^5 cells/cm² vs. 13.6×10^5 cells/cm², respectively; $P < 0.05$, Mann-Whitney test). This suggests that coral-zooxanthella associations may or may not be re-established following disturbance, depending on the magnitude of zooxanthellar depletion.

This conclusion is supported by the results of Experiment I, in which none of the previously observed coral-zooxanthella associations were re-established in low-light-treated *M. annularis*. Zooxanthellae were severely depleted in these corals during treatment (to ca. 1×10^5 cells/cm² on aver-

age), and all corals were repopulated by completely different zooxanthellae (*Symbiodinium* A, E, and C2; Fig. 3, Low Light, Recovery), even 9 months after treatment (Fig. 4). A similar result was obtained by low-light treatment of *M. faveolata* in Experiment II, although in that experiment the re-establishment of symbioses was not tested under a constant environment; after being treated with low light, most corals were also transplanted to a new environment. In that new environment (9 m depth), unmanipulated *M. faveolata* host *Symbiodinium* C (Rowan and Knowlton, 1995; unpubl. obs.), whereas re-established symbioses involved *Symbiodinium* A or A and E (Fig. 5).

We hypothesized that new taxa (*Symbiodinium* A, E, or C2) following severe bleaching (Experiments I and II) would not become established if untreated zooxanthellae (resident *Symbiodinium* B or C populations) were abundant near bleached tissues (zooxanthellae are thought to be translocated within colonies, among coral polyps, via their gastrovascular systems [e.g., Gladfelter, 1983; Gateño *et al.*, 1998]). In Experiment III, the results from 5 of the 14 half-bleached columns were consistent with this hypothesis: bleached tissues were repopulated with zooxanthellae that apparently originated from untreated tissues (Fig. 6, Corals 1, 2, 3, 5, 6). Together with the observations on the spread of pigmentation (Fig. 6, Results), this indirect evidence suggests that zooxanthellae are translocated into bleached tissues in some cases. However, in the majority of tested cases (9 of 14), new zooxanthellae did become established: *Symbiodinium* A, E, and/or C2 repopulated treated tissues (Fig. 6, Corals 4, 7–14), despite the proximity (≤ 7 polyps away; see Weil and Knowlton, 1994) of untreated zooxanthellae (*Symbiodinium* C, with one exception). When new zooxanthellae became established, they were observed more frequently in the deeper habitat (8 of 9 columns in the deep group vs. 1 of 5 in the shallow group), and when resident zooxanthellae were *Symbiodinium* C (rather than *Symbiodinium* B)—our data do not resolve which factor had the greater influence. Nevertheless, these observations clearly show that a reservoir of adjacent zooxanthellae, whether *Symbiodinium* C or B, is not sufficient to prevent the establishment of new host-zooxanthella associations in bleached tissues.

We do not know where the new *Symbiodinium* in re-established symbioses came from. For most experimental corals, the fact that these zooxanthellae were not detected initially or after treatment is not good evidence that they were truly absent. This is because an srDNA genotype must be at least 5% of the total to be detected reliably (e.g., for values of ca. 12%, see fig. 4 in Toller *et al.*, 2001; fig. 2B in Rowan *et al.*, 1997). Thus, corals that had ca. 1×10^5 cells/cm² of *Symbiodinium* C after low-light treatment (Fig. 3, Low Light, Treatment; also see Results) also may have contained up to about 5×10^3 cells/cm² of *Symbiodinium* A, E, or C2 that went undetected. With a hypothetical

doubling time of 5 days (e.g., Wilkerson *et al.*, 1988), 5×10^3 zooxanthellae/cm² become 150×10^5 zooxanthellae/cm² after only 8 weeks. Thus, even where only *Symbiodinium* C was detected right after treatment (Fig. 3, Low Light, Treatment; Colonies 1, 3, 4, 11, 12, and 14), there might have been enough *Symbiodinium* A, E, and/or C2 present to found the established symbioses observed 13 or 17 weeks later.

On the other hand, no data show that treated corals did not acquire *Symbiodinium* A, E, and C2 for the first time during recovery. Free-living *Symbiodinium* may be attracted specifically to hosts lacking zooxanthellae (Fitt, 1985b). Juveniles of host species that do not transmit zooxanthellae vertically (e.g., *Montastraea*; Szmant, 1991) must be colonized, and the ability of adult hosts to pick up *Symbiodinium* from the environment has been documented for bleached anemones (Kinzie *et al.*, 2001) and for juvenile giant clams originally inoculated with cultured zooxanthellae (Belda-Baillie *et al.*, 1999; also see Fitt, 1984).

Regardless of where *Symbiodinium* A, E, and C2 came from, they fared well compared to any *Symbiodinium* C or B that remained in corals after low-light treatment. For example, the about 1×10^5 cells/cm² of *Symbiodinium* C that six corals in Experiment I contained after treatment (Fig. 3, Low Light, Treatment; Colonies 1, 3, 4, 11, 12, and 14) would have been observed in re-established symbioses if they had doubled only three or four times during 13 or 17 weeks (doubling times of 23–29 days; a slow rate of growth for zooxanthellae in general [Wilkerson *et al.*, 1988]). Thus, the identities of re-established symbioses in these six corals resulted not only from the proliferation, acquisition, or both of *Symbiodinium* A, E, or C2, but also from the failure of *Symbiodinium* C to proliferate.

Competition and succession in zooxanthellar communities

In general, the first phototrophs to colonize disturbed habitat are transient and eventually replaced by competitively superior species that dominate thereafter. This process is called succession (Odum, 1969; Connell and Slatyer, 1977; Huston and Smith, 1987), and it might eventually have led from *Symbiodinium* A, E, and C2 to *Symbiodinium* C or B, and thus restored the host-symbiont specificity observed in nature. We did not observe this hypothetical succession of zooxanthellae. However, the only corals we followed for more than 17 weeks after treatment (Fig. 4, Final: 33 or 37 weeks after treatment) experienced a natural bleaching event (Results) that apparently reduced populations of *Symbiodinium* C by about 80% in control and high-light-treated *M. annularis*; *Symbiodinium* B may have been affected also (Fig. 4, Final vs. Recovery). It seems unlikely that *Symbiodinium* C or B would have proliferated in low-light-treated corals during the same period of time.

Thus, unfavorable conditions might explain why succession was not observed.

Hypotheses on the mechanisms of plant succession invoke genetic differences in the abilities of species to compete for resources such as water, light, and nutrients, supplies of which decrease as succession proceeds (e.g., Huston and Smith, 1987; Tilman, 1988; Wilson, 1999). Zooxanthellae in unmanipulated corals cannot be water-limited, nor can they extensively shade one another (Drew, 1972), but they probably are nutrient-limited (Rees, 1991; Falkowski *et al.*, 1993). In contrast, severely bleached corals may be nutrient-rich zooxanthellar habitats because the waste products of coral heterotrophy go largely unutilized (e.g., Szmant-Froelich and Pilson, 1977; Muscatine and D'Elia, 1978); competition among zooxanthellae for nutrients may be minimal in this case. Competition should increase, however, as zooxanthellar biomass increases, and the zooxanthellar genotype that competes for nutrients best should ultimately prevail, regardless of its rate of growth in the absence of competition or its initial abundance (e.g., Huston and Smith, 1987; Tilman, 1988).

In *M. annularis* and *M. faveolata* living at 9 m depth at our study site, those efficient, specialized, but comparatively slowly growing zooxanthellae might be *Symbiodinium* C and B. In contrast, *Symbiodinium* A, E, and C2 seem to have played the role of early successional, rapidly proliferating opportunists in our experiments. In Experiment II, *Symbiodinium* A reached large numbers in only 8 weeks (Fig. 5, Recovery; see also Fig. 3, Low Light). Opportunistic behavior by *Symbiodinium* A has also been observed in *M. annularis* and *M. faveolata* during a natural coral bleaching event (Rowan *et al.*, 1997) and in mixed *in vitro* cultures of *Symbiodinium* (Rowan, 1998; Carlos *et al.*, 1999). Our observation of *Symbiodinium* E in *Montastraea* living in a marginal habitat near our study site (Río Cartí; see Toller *et al.*, 2001) also suggests a weed-like ecology. Similarly, the unusual association of *Symbiodinium* C2 with *M. annularis* (Results) suggests that our experimental treatment enabled this zooxanthella to exploit a host species with which it does not commonly associate. We note, however, in the cases of both *Symbiodinium* A and E, it is unknown whether different observations involved one or several species of zooxanthella (see discussion on taxonomy, above).

Stability of zooxanthellar communities and coral bleaching

During natural episodes of coral bleaching (reviewed in Brown, 1997), even severely bleached colonies of *M. annularis* retain at least 10% of their pre-bleaching population of zooxanthellae (Porter *et al.*, 1989; Fitt *et al.*, 2000), which represents at least four times as many zooxanthellae as our low-light-treated corals had. Thus, the dramatic changes in species of *Symbiodinium* that we observed fol-

lowing low-light treatment of *M. annularis* and *M. faveolata* are unlikely to be common in nature. Mild coral bleaching or seasonal fluctuations in numbers of zooxanthellae in normal years (Stimson, 1997; Fagooonee *et al.*, 1999; Fitt *et al.*, 2000) involve lesser depletions of zooxanthellae, comparable to those observed in high-light-treated *M. annularis* in which communities of *Symbiodinium* did not change (Fig. 3, High Light, Colonies 6–10). Nevertheless, two high-light-treated corals that retained about 15% and 20% (Fig. 3, Colonies 4 and 5, respectively) of their zooxanthellae after treatment apparently did acquire detectable amounts of *Symbiodinium* E as a result of treatment. This suggests that severe natural bleaching episodes might modify communities of *Symbiodinium* in *M. annularis*, at least in part.

If infrequent, natural bleaching events at our study site (e.g., Lasker *et al.*, 1984; Rowan *et al.*, 1997) do allow *Symbiodinium* E or C2 to proliferate in *M. annularis* and *M. faveolata* from time to time, the effect must be transient or slight. These host-zooxanthella combinations are rarely encountered in unmanipulated corals from this reef (Rowan and Knowlton, 1995; Rowan *et al.*, 1997; this study), despite occasional coral bleaching. On the other hand, at a nearby coastal site (Río Cartí), where stresses that can induce coral bleaching may be severe and frequent (Toller *et al.*, 2001), disturbance appears to have a widespread effect on host-zooxanthella association. In high-irradiance habitats, *M. faveolata* and *M. annularis* at Río Cartí associate predominantly with *Symbiodinium* E—an opportunistic taxon of zooxanthella (above) that may also be stress-resistant (Toller *et al.*, 2001). In this environment, these host-zooxanthella associations resemble the persistence of early-to-mid successional phototrophs under conditions of chronic disturbance (Odum, 1969; Horn, 1974; Huston and Smith, 1987).

Buddemeier and Fautin (1993) proposed that bleaching allows corals to replace their zooxanthellae with different, better ones (see also Baker, 1999, 2001; Kinzie *et al.*, 2001). According to this "adaptive bleaching hypothesis," such replacements are driven by environmental change, which simultaneously makes some host-zooxanthella combinations less well adapted and other combinations better adapted than they had been. Baker (2001) found that the mortality of corals challenged with prolonged environmental change (transplantation) was reduced when they acquired new zooxanthellae, but these new host-zooxanthella associations were only established after coral bleaching. Similarly, our experiments indicate that severe bleaching allowed corals to associate with new zooxanthellae: *Symbiodinium* A, E, or C2 replaced *Symbiodinium* C or B in *Montastraea* (see above). However, in our experiments, environmental change was not a prerequisite; instead, *Symbiodinium* A, E, or C2 proliferated in the very environment that *Symbiodinium* C or B apparently thrive in (Figs. 3 and

5: Recovery). Although our experiments did not include prolonged environmental change and therefore was not a direct test of the adaptive bleaching hypothesis, they do show that testing this hypothesis may not be straightforward—severe coral bleaching may favor zooxanthellar replacements, irrespective of environmental change.

Disease-related disturbance of zooxanthellar symbioses

Symbiodinium A especially and also *Symbiodinium E* proliferated in the bleached tissues of corals with yellow-blotch disease (Fig. 7, Yellow). These zooxanthellae apparently gave many lesions of YBD their distinctive yellow color, and they were fugitives in the strict sense because their habitat was ephemeral. Our measurements suggest that their habitat lasted an average of about 5 months. Nonetheless, continuous progression of YBD across a coral would provide a large amount of habitat for these fugitive zooxanthellae to occupy.

Our findings explain the "yellow" in YBD, but they do not address the cause of the pathology. Most colonies we encountered were in two clusters that were surrounded widely by unaffected corals, which suggested an infectious agent with limited dispersal. YBD may have more than one etiology: our experimental results imply that it would arise when anything spread through a coral and disturbed stress-sensitive communities of zooxanthellae (*Symbiodinium B* or *C*) without actually killing the host immediately. One agent might even be a "rogue" (parasitic) genotype of *Symbiodinium A* that prospered at the expense of its coral host.

Acknowledgments

We thank the Kuna Nation and the Republic of Panama (Autoridad Nacional del Ambiente, Departamento de Cuarentena Agropecuaria del Ministerio de Desarrollo Agropecuario, and Recursos Marinos) for permission to collect and export specimens. Many thanks to Javier Jara for tireless field assistance and cell counts, Ursula Anlauf, Ralf Kersanach, Mike McCartney, and Suzanne Williams provided valuable advice. Mick Wilson and Dave Wilson assisted with field manipulations. R. R. thanks Chris Hein and Uma Narayan for hospitality in California. This research was supported by the Andrew W. Mellon Foundation, the Smithsonian Tropical Research Institute, the National Institutes of Health, and the Scripps Institution of Oceanography.

Literature Cited

- Baker, A. C. 1999. Symbiosis ecology of reef-building corals. Ph.D. dissertation, University of Miami. 120 pp.
- Baker, A. C. 2001. Reef corals bleach to survive change. *Nature* **411**: 765–766.
- Belda-Baillie, C. A., M. Sison, V. Silvestre, K. Villamor, V. Monje, E. D. Gomez, and B. K. Baillie. 1999. Evidence for changing symbiotic algae in juvenile tridacnids. *J. Exp. Mar. Biol. Ecol.* **241**: 207–221.
- Brown, B. E. 1997. Coral bleaching: causes and consequences. *Coral Reefs* **16**: S129–S138.
- Buddemeier, R. W., and D. G. Fautin. 1993. Coral bleaching as an adaptive mechanism. *Bioscience* **43**: 320–326.
- Cairns, S. D. 1999. Species richness of recent Scleractinia. *Atoll Res. Bull.* **459**: 1–12.
- Carlos, A. A., B. K. Baillie, M. Kawachi, and T. Maruyama. 1999. Phylogenetic position of *Symbiodinium* (Dinophyceae) isolates from tridacnids (Bivalvia), cardiiids (Bivalvia), a sponge (Porifera), a soft coral (Anthozoa), and a free-living strain. *J. Phycol.* **35**: 1054–1062.
- Colley, N. J., and R. K. Trench. 1983. Selectivity in phagocytosis and persistence of symbiotic algae by the scyphistoma stage of the jellyfish *Cassiopeia xamachana*. *Proc. R. Soc. Lond. B* **219**: 61–82.
- Connell, J. H., and R. O. Slatyer. 1977. Mechanisms of succession in natural communities and their role in community stability and organization. *Am. Nat.* **111**: 1119–1144.
- Davy, S. K., I. A. N. Lucas, and J. R. Turner. 1997. Uptake and persistence of homologous and heterologous zooxanthellae in the temperate sea anemone *Cereus pedunculatus* (Pennant). *Biol. Bull.* **192**: 208–216.
- Drew, E. A. 1972. The biology and physiology of alga-invertebrate symbioses. II. The density of symbiotic algal cells in a number of hermatypic corals and alcyonarians from various depths. *J. Exp. Mar. Biol. Ecol.* **9**: 71–75.
- Dustan, P. 1979. Distribution of zooxanthellae and photosynthetic chloroplast pigment of the reef-building coral *Montastrea annularis* Ellis and Solander in relation to depth on a West Indian coral reef. *Bull. Mar. Sci.* **29**: 79–95.
- Fagoonee, L., H. B. Wilson, M. P. Hassell, and J. R. Turner. 1999. The dynamics of zooxanthellae populations: a long-term study in the field. *Science* **283**: 843–845.
- Falkowski, P. G., Z. Dubinsky, L. Muscatine, and L. R. McCloskey. 1993. Population control in symbiotic corals. *Bioscience* **43**: 606–611.
- Fitt, W. K. 1984. The role of chemosensory behavior of *Symbiodinium microadriaticum*, intermediate hosts and host behavior in the infection of coelenterates and molluscs with zooxanthellae. *Mar. Biol.* **81**: 9–17.
- Fitt, W. K. 1985a. Effect of different strains of the zooxanthella *Symbiodinium microadriaticum* on growth and survival of their coelenterate and molluscan hosts. *Proc. Fifth Int. Coral Reef Congr. (Tahiti)*, **6**: 131–136.
- Fitt, W. K. 1985b. Chemosensory responses of the symbiotic dinoflagellate *Symbiodinium microadriaticum* (Dinophyceae). *J. Phycol.* **21**: 62–67.
- Fitt, W. K., F. K. McFarland, M. E. Warner, and G. C. Chilcoat. 2000. Seasonal patterns of tissue biomass and densities of symbiotic dinoflagellates in reef corals and relation to coral bleaching. *Limnol. Oceanogr.* **45**: 677–685.
- Franzisket, L. 1970. The atrophy of hermatypic reef corals maintained in darkness and their subsequent regeneration in light. *Int. Rev. Hydrobiol.* **55**: 1–12.
- Gateño, D., A. Israel, Y. Barki, and B. Rinkevich. 1998. Gastrovascular circulation in an octocoral: evidence of significant transport of coral and symbiont cells. *Biol. Bull.* **194**: 178–186.
- Gladfelter, E. H. 1983. Circulation of fluids in the gastrovascular system of the reef coral *Acropora cervicornis*. *Biol. Bull.* **165**: 619–636.
- Horn, H. S. 1974. The ecology of secondary succession. *Annu. Rev. Ecol. Syst.* **5**: 25–37.
- Huston, M., and T. Smith. 1987. Plant succession: life history and competition. *Am. Nat.* **130**: 168–198.
- Kinzie, R. A., III, and G. S. Chee. 1979. The effect of different

- zooxanthellae on the growth of experimentally reinfected hosts. *Biol. Bull.* **156**: 315–327.
- Kinzie, R. A., III, M. Takayama, S. R. Santos, and M. A. Coffroth. 2001.** The adaptive bleaching hypothesis: experimental tests of critical assumptions. *Biol. Bull.* **200**: 51–58.
- Lasker, H. R., E. C. Peters, and M. A. Coffroth. 1984.** Bleaching of reef coelenterates in the San Blas Islands, Panama. *Coral Reefs* **3**: 183–190.
- McNally, K. L., N. S. Govind, P. E. Thomé, and R. K. Trench. 1994.** Small-subunit ribosomal DNA sequence analyses and a reconstruction of the inferred phylogeny among symbiotic dinoflagellates (Pyrrhophyta). *J. Phycol.* **30**: 316–329.
- Muscantine, L., and C. F. D'Elia. 1978.** The uptake, retention, and release of ammonium by reef corals. *Limnol. Oceanogr.* **23**: 725–734.
- Odum, E. P. 1969.** The strategy of ecosystem development. *Science* **164**: 262–270.
- Porter, J. W., W. K. Fitt, H. J. Spero, C. S. Rogers, and M. W. White. 1989.** Bleaching in reef corals: physiological and stable isotope responses. *Proc. Natl. Acad. Sci. USA* **86**: 9342–9346.
- Rees, T. A. V. 1991.** Are symbiotic algae nutrient deficient? *Proc. R. Soc. Lond. B* **243**: 227–234.
- Roux, K. H. 1995.** Optimization and troubleshooting in PCR. Pp. 53–62 in *PCR Primer: A Laboratory Manual*. C. W. Dieffenbach and G. S. Dveksler, eds. Cold Spring Harbor Laboratory Press, New York.
- Rowan, R. 1998.** Diversity and ecology of zooxanthellae on coral reefs. *J. Phycol.* **34**: 407–417.
- Rowan, R., and N. Knowlton. 1995.** Intraspecific diversity and ecological zonation in coral-algal symbiosis. *Proc. Natl. Acad. Sci. USA* **92**: 2850–2853.
- Rowan, R., and D. A. Powers. 1991a.** A molecular genetic classification of zooxanthellae and the evolution of animal-algal symbioses. *Science* **251**: 1348–1351.
- Rowan, R., and D. A. Powers. 1991b.** Molecular genetic identification of symbiotic dinoflagellates (zooxanthellae). *Mar. Ecol. Prog. Ser.* **71**: 65–73.
- Rowan, R., N. Knowlton, A. Baker, and J. Jara. 1997.** Landscape ecology of algal symbionts creates variation in episodes of coral bleaching. *Nature* **388**: 265–269.
- Santavy, D. L., E. C. Peters, C. Quirolo, J. W. Porter, and C. N. Bianchi. 1999.** Yellow-blotch disease outbreak on reefs of the San Blas Islands, Panama. *Coral Reefs* **18**: 97.
- Schoenberg, D. A., and R. K. Trench. 1980.** Genetic variation in *Symbiodinium* (*Gymnodinium*) *microadriaticum* Freudenthal, and specificity in its symbiosis with marine invertebrates. III. Specificity and infectivity of *S. microadriaticum*. *Proc. R. Soc. Lond. B* **207**: 445–460.
- Stimson, J. 1997.** The annual cycle of density of zooxanthellae in the tissues of field and laboratory-held *Pocillopora damicornis* (Linnaeus). *J. Exp. Mar. Biol. Ecol.* **214**: 35–48.
- Szmant, A. M. 1991.** Sexual reproduction by the Caribbean corals *Montastrea annularis* and *M. cavernosa*. *Mar. Ecol. Prog. Ser.* **74**: 13–25.
- Szmant-Froelich, A., and M. E. Q. Pilson. 1977.** Nitrogen excretion by colonies of the temperate coral *Astrangia danae* with and without zooxanthellae. *Proc. Third Int. Coral Reef Symp.* **1**: 418–423.
- Tilman, D. 1988.** *Plant Strategies and the Dynamics and Structure of Plant Communities*. Princeton University Press, Princeton, NJ.
- Toller, W. W., R. Rowan, and N. Knowlton. 2001.** Zooxanthellae of the *Montastraea annularis* species complex: patterns of distribution of four taxa of *Symbiodinium* on different reefs and across depths. *Biol. Bull.* **201**: 348–359.
- Toller, W. W., R. Rowan, and N. Knowlton. In press.** Genetic evidence for a protozoan (phylum Apicomplexa) associated with corals of the *Montastraea annularis* species complex. *Coral Reefs*.
- Trench, R. K. 1988.** Specificity in dinomastigote-marine invertebrate symbioses: an evaluation of hypotheses of mechanisms involved in producing specificity. Pp. 325–346 in *Cell to Cell Signals in Plant, Animal and Microbial Symbiosis*. S. Scannerini, D. C. Smith, P. Bonfante-Fasolo, and V. Gianninazzi-Pearson, eds. NATO Advanced Research Workshop on Cell to Cell Signals in Plant, Animal, and Microbial Symbiosis (1987; Turin, Italy). Springer-Verlag, Berlin.
- Trench, R. K. 1993.** Microalgal-invertebrate symbioses: a review. *Endocytobiosis Cell Res.* **9**: 135–175.
- Trench, R. K. 1997.** Diversity of symbiotic dinoflagellates and the evolution of microalgal-invertebrate symbioses. *Proc. Eighth Int. Coral Reef Symp.* **2**: 1275–1286.
- Veron, J. E. N. 1995.** *Corals in Space and Time: The Biogeography and Evolution of the Scleractinia*. UNSW Press, Sydney, Australia.
- Weil, E., and N. Knowlton. 1994.** A multi-character analysis of the Caribbean coral *Montastraea annularis* (Ellis and Solander, 1786) and its two sibling species, *M. faveolata* (Ellis and Solander, 1786) and *M. franksi* (Gregory, 1895). *Bull. Mar. Sci.* **55**: 151–175.
- Wells, J. W. 1956.** Scleractinia. Pp. 328–444 in *Treatise in Invertebrate Paleontology, Part F*, R. C. Moore, ed. Geological Society of America and University of Kansas Press, Lawrence, KS.
- Wilkinson, F. P., D. Kobayashi, and L. Muscantine. 1988.** Mitotic index and size of symbiotic algae in Caribbean reef corals. *Coral Reefs* **7**: 29–36.
- Wilson, S. D. 1999.** Plant interactions during secondary succession. Pp. 611–632 in *Ecosystems of the World, Vol. 16: Ecosystems of Disturbed Ground*, L. R. Walker, ed. Elsevier, New York.

Microhabitats, Thermal Heterogeneity, and Patterns of Physiological Stress in the Rocky Intertidal Zone

BRIAN S. T. HELMUTH^{1,*} AND GRETCHEN E. HOFMANN²

¹ *Department of Biological Sciences, University of South Carolina, Columbia, South Carolina 29208;*
and ² *Department of Biology, Arizona State University, Tempe, Arizona 85287-1501*

Abstract. Thermal stress has been considered to be among the most important determinants of organismal distribution in the rocky intertidal zone. Yet our understanding of how body temperatures experienced under field conditions vary in space and time, and of how these temperatures translate into physiological performance, is still rudimentary. We continuously monitored temperatures at a site in central California for a period of two years, using loggers designed to mimic the thermal characteristics of mussels, *Mytilus californianus*. Model mussel temperatures were recorded on both a horizontal and a vertical, north-facing microsite, and in an adjacent tidepool. We periodically measured levels of heat shock proteins (Hsp70), a measure of thermal stress, from mussels at each microsite. Mussel temperatures were consistently higher on the horizontal surface than on the vertical surface, and differences in body temperature between these sites were reflected in the amount of Hsp70. Seasonal peaks in extreme high temperatures ("acute" high temperatures) did not always coincide with peaks in average daily maxima ("chronic" high temperatures), suggesting that the time history of body temperature may be an important factor in determining levels of thermal stress. Temporal patterns in body temperature during low tide were decoupled from patterns in water temperature, suggesting that water temperature is an ineffective metric of thermal stress for intertidal organisms. This study demonstrates that spatial and temporal variability in thermal stress can be highly complex, and "snapshot" sampling of temperature and biochemical indices may not always be a reliable method for defining thermal stress at a site.

Introduction

Temperature is one of the most important abiotic determinants of organismal distribution and physiological performance in the rocky intertidal zone (Orton, 1929a, b; Doty, 1946; Hutchins, 1947; Carefoot, 1977; Bertness, 1981; Wethey, 1983, 1984; Menge and Olson, 1990; Williams and Morrill, 1995). Animals and algae in this environment are exposed to rapidly fluctuating and often extreme temperatures, and recent studies have shown that exposure to high temperatures can have significant physiological consequences to these organisms (Hofmann and Somero, 1995, 1996a, b; Stillman and Somero, 1996; Roberts *et al.*, 1997; Chapple *et al.*, 1998; Tomanek and Somero, 1999; Buckley *et al.*, 2001; Dahlhoff *et al.*, 2001; Snyder *et al.*, 2001). Several studies have further indicated that thermal stress can have significant ecological consequences, and that exposure to stressful conditions varies both in space and in time in the rocky intertidal zone. For example, Wethey (1983, 1984) demonstrated that the competitive dominance of one species of barnacle over another varied with substratum angle, presumably as an indirect effect of thermal or desiccation stresses on the relative physiological performance of each species. Menconi *et al.* (1999) found that community structure at an intertidal site in the Mediterranean varied as much as a function of substratum angle as it did as a function of tidal height. Dahlhoff *et al.* (2001) showed that temporal variability in physiological stress had significant effects on the foraging ability of an intertidal gastropod. However, despite a robust and growing body of literature on the physiological ecology of intertidal organisms, we are just beginning to understand on a mechanistic basis how body temperature variation influences physiological performance and, ultimately, how physiological performance contributes to the ecological interactions of intertidal organisms.

Received 30 April 2001; accepted 11 September 2001.

* To whom correspondence should be addressed. E-mail: helmuth@biol.sc.edu

Our understanding of temperature effects on intertidal organisms is limited by at least three gaps in our knowledge of the ecological physiology of the rocky intertidal zone. First, although the ecological community is gaining appreciation and insight into the significance of organismal body temperatures under natural field conditions (*e.g.*, Elvin and Gonor, 1979; Wethey, 1983, 1984; Bell, 1995; Williams and Morrill, 1995; Helmuth, 1998, 1999; Dahlhoff *et al.*, 2001), more attention needs to be paid to the complexity of determining spatial and temporal patterns of body temperatures in the intertidal. While it is submerged, an ectothermic invertebrate is likely to have a temperature fairly similar to that of the surrounding water. In contrast, during aerial exposure, climatic factors such as air temperature, wind speed, solar radiation, and relative humidity interact to drive the flux of heat into and out of an organism's body (Johnson, 1975; Bell, 1995; Helmuth, 1998, 1999). As a result, temperature extremes during low tide can far exceed those experienced during submersion, and an organism's body temperature can be substantially different from the temperature of the surrounding air (Helmuth, 1998). Furthermore, heat fluxes are to some extent determined by the size and morphology of the organism. As a result, organisms exposed to identical climatic conditions can experience different body temperatures (*e.g.*, Porter and Gates, 1969; Porter *et al.*, 1973; Helmuth, 1998), and an animal's "thermal regime" is determined in part by its own morphology.

Second, even though accurate determinations of body temperature can be made, the physiologically significant aspect of the "thermal signal" of environmental temperature (*e.g.*, maximum, minimum, average, time history) is unknown. Investigations of the plasticity of physiological processes, such as the environmental induction of heat shock proteins (*e.g.*, Buckley *et al.*, 2001) and the relationship between oxygen consumption and temperature (Widdows, 1976), have documented that invertebrates are responsive to a changing thermal environment in a regulatory manner and therefore must sense environmental temperature. Additional studies have coupled relatively short-term measurements of body temperature to physiological indicators of thermal stress (*e.g.*, Hofmann and Somero, 1995; Tomanek and Somero, 1999; Dahlhoff *et al.*, 2001; Snyder *et al.*, 2001). However, we still do not understand what aspect of environmentally driven body temperature variation is physiologically significant in these ectothermic organisms.

Finally, only recently have advances in technology allowed for measurement of body temperatures as a function of microhabitat over long time scales. Deploying instrumentation in the rocky intertidal zone is notoriously difficult due to damage from waves, and only recently have commercially available instruments become sufficiently small and robust to be deployed for long periods of time. Furthermore, because of the influence of a temperature logger's (or organism's) size, mass, and morphology on the temperature

that it records, temperature measurements relevant to intertidal organisms are scarce, and those that exist are not necessarily accurate proxies for the body temperatures of all organisms at that site. Thus, there are relatively few data sets that provide information as to how microscale features of intertidal substrata influence organismal body temperature (except see Wethey, 1983, 1984; Williams and Morrill, 1995; Helmuth and Denny, 1999).

As a first step in addressing these complex issues, we have integrated the fine-scale measurement of organismal body temperature with the analysis of a bioindicator of physiological stress. Specifically, in the current study, we present temperature data recorded by loggers designed to mimic the body temperatures of a competitively dominant mussel, *Mytilus californianus*, and collected over a period of 2 years at a site in central California (Monterey Bay). We couple these data with periodic measurements of isoforms of the 70-kDa heat shock protein (Hsp) gene family, a molecular chaperone that has been used routinely as a bioindicator of stress (see Feder and Hofmann, 1999, for a review), and explore the inherent difficulty in linking patterns in thermal signals in the field to physiological indicators of stress. We further examine the effects of substratum angle on body temperature and levels of thermal stress to address the question of how body temperature and thermal stress vary over small spatial scales in the intertidal.

Our results demonstrate that while biochemical indicators of stress are potentially a very powerful tool for examining the role of environmental variation in driving organismal physiology, we still do not yet have a complete understanding of what aspects of the thermal environment drive the transcriptional activation of stress protein genes. Similarly, high spatial and temporal variability in patterns of body temperatures necessitate caution when extrapolating from short-term measurements of temperature or Hsp production in the intertidal. Namely, while the use of biochemical indicators of stress and concomitant measurements of temperature can potentially serve as an effective link between the ecology and physiology of intertidal organisms, such studies require detailed measurements of body temperature, and an awareness of the potential role of thermal history in driving physiological stress in the rocky intertidal zone.

Materials and Methods

Temperature measurements and logger design

Mussel temperatures were recorded using temperature loggers deployed on the shores adjacent to the Hopkins Marine Station in Pacific Grove, California (37°18.0' N, 54°15.5' W), from October 1998 to October 2000. Loggers were deployed in the centers of small mussel beds at two microsites in the mid- to high intertidal zone (mean lower low water + 1.7 m): a horizontal, upward-facing microsite

and a vertical, north-facing site. Sites were located within 20 cm of one another, in an area judged to be moderately wave-exposed. A third logger was deployed at the bottom of a nearby tidepool (about 1.5 m × 1 m × 15 cm deep) from July 1999 to June 2000.

Because the same morphological factors that determine heat flux to intertidal plants and animals and drive differences in their body temperatures can also affect heat flux to temperature loggers, we used loggers imbedded in physical models of mussels to collect temperature data. Thus, for example, larger, more massive loggers have a larger thermal inertia than do smaller loggers, and they may not always record peaks in body temperature experienced by animals with a faster thermal response time (Helmuth, 1998). Matching the thermal characteristics of a temperature logger to those of the organism in question is therefore critical, and a single type of logger is unlikely to be an effective proxy for all organisms at an intertidal site. We therefore deployed temperature loggers of a size (60–75 mm) and shape comparable to those of real mussels, and we matched their thermal response characteristics (mass × specific heat) to living animals. From October 1998 to May 2000, empty shells of *Mytilus californianus* (~75 mm in length) were filled with silicone sealant and fitted with a thermistor cable. The recording tip of the thermistor was placed in the center of the silicone-filled mussel shell. The thermistor was then connected to an Onset Corporation Stowaway logger encased in a waterproof housing. Mussels were attached to the substratum in the middle of small beds, in approximate growth position, using marine epoxy (Z-spar). Because of the high rate of damage to thermistor cables, thermistor loggers were replaced in May 2000 with a similar logger designed entirely of epoxy plastic, where the logger (an Onset Corporation Tidbit logger) was encased inside of the fake mussel. Again, the product of mass × specific heat of the plastic logger in the fake mussel was similar to that of a living mussel. Both loggers recorded temperatures to an accuracy and resolution of 0.3 °C, and recorded average temperatures at intervals of 5 to 10 min (preliminary studies indicated that changes in body temperature were slow enough that this sampling interval would capture all peaks). Because logger design was thought to have a significant effect on the temperature recorded only while the logger was exposed to air and not while completely submerged, unmodified Onset Corp. Tidbit loggers were used to record tidepool temperatures.

On 25 days from October 1998 to May 1999, the external logger temperature was compared to the temperatures of living mussels. An infrared thermocouple (Omega Corp.) was used to record the external temperature of the logger, and of 5–10 mussels in the surrounding bed. Results of the 82 comparisons indicated that loggers recorded temperatures that were, on average, within 0.75 °C of those of living mussels, and were usually within 1 standard deviation of the

average of the living mussels (correlation analysis indicated a 1:1 curve fit with an R^2 value of 0.94). Temperature data were collected on days in which logger and mussel temperatures ranged from ~11 °C to 27 °C. The loggers were thus thought to serve as a reliable proxy for body temperature, although comparisons were not made for the uppermost range of temperatures observed throughout the year (30–34 °C). Furthermore, because loggers were sealed, they potentially ignored any effects of evaporative cooling due to mussel gaping. However, Bayne *et al.* (1976) showed that aerial respiration by *M. californianus* is generally only effective when relative humidity approaches 100%, when evaporative cooling cannot occur (Helmuth, 1998, 1999). Preliminary experiments (T. Fitzhenry and Helmuth, unpubl. data) also suggest that this species does not gape as a means of evaporatively cooling; nonetheless, this potential complication requires further investigation.

To compare the effects of logger design on temperature recorded, an unmodified Tidbit logger was deployed in the horizontal mussel bed from July 1999 to October 2000. Average and maximum daily temperatures recorded by the unmodified logger were then compared to those recorded by the adjacent physical model.

Temperature analyses

Because of the large number of data points collected by the loggers, temperatures were summarized for each microsite on a monthly basis. Monthly maxima were divided into two categories, each broadly representing a different potential source of thermal stress. "Acute" exposure to high temperature was defined as the absolute maximum temperature experienced by a logger at each site, on a monthly basis (Fig. 1). In contrast, as a measure of "chronic" or repeated exposure to high temperature, the average daily maximum was calculated (Fig. 1). Similarly, the monthly extreme minimum was recorded and average daily minimum was calculated. Other metrics included the daily average temperature (including both aerial and submerged temperatures) and the temperature at high tide (a measure of water temperature). Except for monthly maxima and minima, in which a single point was used for each month, standard deviations of daily average, average daily maximum, average daily minimum, and temperature at high tide were recorded as a metric of variability between days within a month.

Western blot analysis of *Hsp70* isoforms

Five specimens of *Mytilus californianus* (length ~50 mm) were collected at each microsite on four dates: 6 July 1999, 24 September 1999, 21 January 2000, and 8 May 2000. Mussels were immediately dissected, and samples of gill tissue were stored at -80 °C until they could be ana-

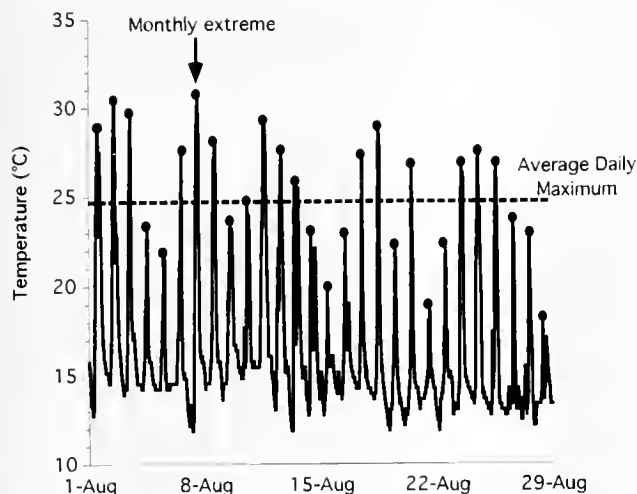


Figure 1. Example of fluctuations in temperature experienced over one month (August 1999) at the horizontal microsite. Daily maxima were calculated from temperature data collected every 5 to 10 min. The highest daily maximum was recorded as the monthly extreme ("acute") high temperature at each site. The average of the daily maxima was calculated as a measure of "chronic" high temperature exposure. Similarly, average daily minima and monthly minima were calculated.

lyzed. Western blotting was employed to determine the levels of both the constitutive and inducible isoforms of Hsp70 in the samples. Hsp70 western blots were performed as described by Hofmann and Somero (1995) except that wet electrophoretic transfer at 30 V for 15 h was used during the western protocol (transfer buffer = 20 mM Tris, 192 mM glycine, 20% methanol). Equal amounts of protein (10 μ g total protein) were separated on 7.5% polyacrylamide gels. A sample of purified Hsc70 (10 ng of bovine Hsc70; Stressgen) was included on each gel as a positive control, and as an internal standard to allow comparison of multiple western blots. Immunodetection was performed using an anti-Hsp70 rat monoclonal antibody that cross-reacts with the cognate and inducible forms of Hsp70 (Affinity Bioreagents; MA3-001). Western blots were developed using an enhanced chemiluminescence protocol according to the manufacturer's instructions (ECL Western Blot Reagent; Amersham) and visualized on a Fluor-S MultiImager (BioRad). Band intensity from each western blot was quantified using Quantity One software. Protein determinations of the gill extracts were performed using a modified Bradford protein assay (Pierce Coomassie Plus).

Levels of Hsp as a function of microsite and of collection date were compared using a two-way analysis of variance. *Post-hoc* comparisons of the effect of season within site, and the effect of site within season, were conducted using a series of one-way ANOVAs with Fisher's PLSD test. Levels of the two isoforms of Hsp70 (Hsp72 and Hsc75, see below) were analyzed separately.

Results

Temperature analysis

Although the study area was superficially judged to be only moderately wave-exposed, wave forces at the sites were often severe (Helmuth and Denny, 1999) and frequently resulted in the loss of or damage to loggers. Gaps in the data sets are therefore present, particularly during winter months when wave forces were greatest. Summary statistics for months in which fewer than 3 weeks of data were collected are thus not reported.

From 11 December 1999 to 6 May 2000, the only loggers recovered at the horizontal site were the unmodified Tidbit loggers. A correlation analysis from days on which both the unmodified and modified loggers were present at the horizontal site ($n = 329$ days) indicated that temperatures recorded by the unmodified logger could be used to predict those recorded by the physical models ($R^2 = 0.96$). An offset value (+0.46 $^{\circ}$ C) calculated from the correlation analysis was used to predict maximum daily temperature for the missing 149 days, and an offset of +0.15 $^{\circ}$ was used to predict average daily temperature. No correction was required for predicting minimum temperatures. On any given day, however, maximum temperatures recorded by the two loggers differed by as much as 4.7 $^{\circ}$ C, with an average difference of 1.3 $^{\circ}$ C. The correlation between the unmodified logger and the logger on the north-facing substratum was too poor to be useful for days in which the logger at that site was missing.

The highest annual temperatures at the horizontal microsite (Fig. 2a) were recorded in May 1999 (33.8 $^{\circ}$ C on 23 May) and August 2000 (33.8 $^{\circ}$ C on 10 August). The highest levels of "chronic" high temperature exposure (average daily maxima) at this microsite were recorded in August 1999 (24.4 $^{\circ}$ C), and in June 2000 (24.2 $^{\circ}$ C; Fig. 2a). Thus, the levels of these two metrics of temperature exposure were out of phase with one another, most obviously in 1999 (Fig. 2a). In contrast, on the north-facing site, both the highest average daily maximum and the yearly extreme high temperature (29.1 $^{\circ}$ C on 10 August) occurred in August 1999 (Fig. 2b); insufficient data were collected to assess the timing of the extremes at the north-facing microsite in 2000. Minimum temperatures were comparable between the north-facing and horizontal microsites, and tended to occur during aerial exposure after sunset. Notably, two freeze (or near freeze) events were recorded on the early evenings of 22 and 23 December 1998, with loggers on the north-facing sites recording temperatures of about -0.6 to -0.9 $^{\circ}$ C. A large disturbance in the mussel bed was recorded a few weeks later; whether it was precipitated by the freeze is unknown (Helmuth and M. W. Denny, Stanford University, unpubl. data).

Temperatures were consistently higher at the horizontal site than at the north-facing site (Figs. 3 and 4). On average,

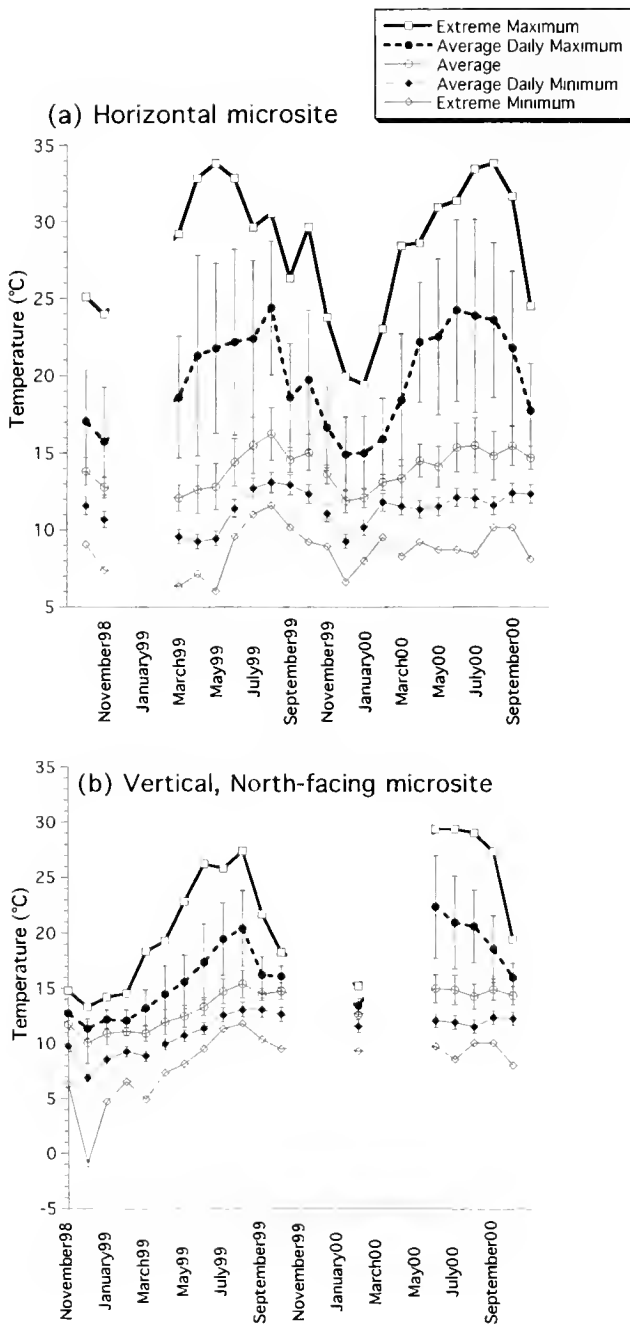


Figure 2. Temperature statistics recorded at the (a) horizontal microsite and (b) vertical, north-facing microsite from November 1998 to October 2000. Temperature data from January to May 2000 at the horizontal microsite were extrapolated from an unmodified logger placed in the bed. Yearly maxima at the horizontal site occurred in May 1999 and August 2000. In contrast, peaks in the average daily maximum ("chronic" temperature exposure) at this site occurred in August 1999 and June 2000. Standard deviations indicate the amount of variability within each month, except for monthly extremes and minimums, for which a single point was recorded during each month-long interval. At the north-facing site (b) the yearly maximum and the highest average daily maximum occurred in August 1999. Note the incidence of an unusual freeze event in December 1998.

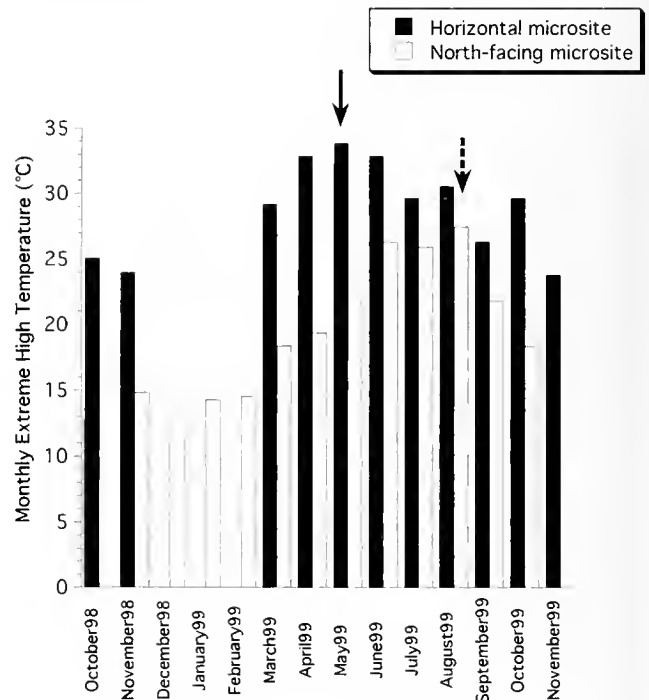


Figure 3. Comparison of monthly high extreme temperatures recorded on horizontal and north-facing microsites. Monthly extrema were always highest on the horizontal substrate, in some months by 10 °C or more. The seasonal timing of temperature maxima varied between sites, occurring in May 1999 on the horizontal site and in August 1999 on the vertical site (indicated by arrows).

extreme maximum monthly temperatures recorded on the horizontal site were 6.75 °C hotter than those on the vertical site; the difference in extreme high monthly temperatures between the horizontal and vertical sites ranged from a high of 13.5 °C in April 1999 to a low of 1.9 °C in June 2000 (Fig. 3). Average daily maxima calculated for each month were also higher on the horizontal site, with an average difference of 3.6 °C, ranging from 1.7 °C in October 2000 to 6.8 °C in April 1999 (Fig. 4).

Temperatures recorded in the tidepool were not as high as those on the exposed horizontal microsite, but in general exceeded those recorded on the aerially exposed vertical face (Fig. 5). Both the yearly extreme high temperature maximum (29.8 °C on 2 August 1999) and the highest average daily maximum (24.5 °C) in the tidepool were recorded in August 1999 (Fig. 5). Water temperatures (recorded by the loggers at high tide) were highest in August through October 1999 and July through September 2000 (~15 °C), and displayed a pattern that was markedly different from any of those recorded during aerial exposure (Fig. 6).

Heat shock protein analysis

To compare the physiological status of mussels from the different microsites, the cellular levels of isoforms of the

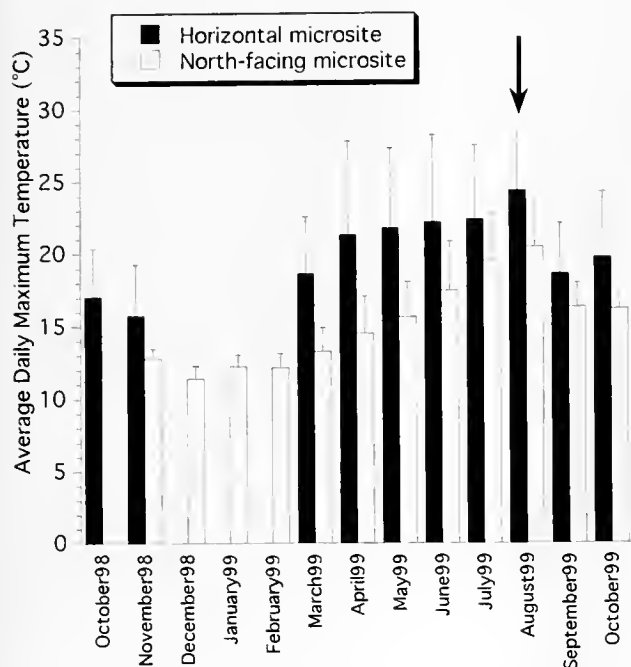


Figure 4. Comparison of average daily maxima recorded at the two aerially exposed sites. Again, levels of "chronic" high temperature exposure were highest on the horizontal substratum. In both cases, highest yearly levels in 1999 occurred in August.

70-kDa Hsp gene family were measured in gill tissue of mussels collected in each season of the year—in July and September 1999, and January and May 2000. Figures 7 and 8 show relative endogenous levels of isoforms of Hsp70 in two groups that separate on SDS-PAGE, a 72-kDa band (Fig. 7) and a 75-kDa band (Fig. 8). Although the precise identity of the separate proteins that compose the two sets is unknown and cannot be determined using one-dimensional electrophoresis, the two isoforms display changes that to some degree correspond to the temperature exposure of *Mytilus*. In previous studies, the 72-kDa band varied significantly with the thermal history of the mussel, with higher levels in summer than in winter; in contrast, the higher molecular mass band varied less as a function of season (Hofmann and Somero, 1995; Roberts *et al.*, 1997). Therefore, we have expressed the data using the two sets of isoforms as separate indicators, where the 75-kDa band (hereafter Hsc75) reflects constitutive levels of Hsp expression and the 72-kDa band (hereafter Hsp72) reflects a stress-inducible subset of the 70-kDa Hsps.

Overall, levels of the 70-kDa molecular chaperones in mussel gill varied significantly as a function of microsite (Table 1; Figs. 7, 8). Regardless of season, levels of Hsp72 were always significantly greater in mussels on the horizontal substratum than in mussels attached to the north-facing surfaces of rocks (ANOVA; $P = 0.0001$; Fig. 7; Table 1). However, there was no consistent pattern for Hsc75 (Fig. 8).

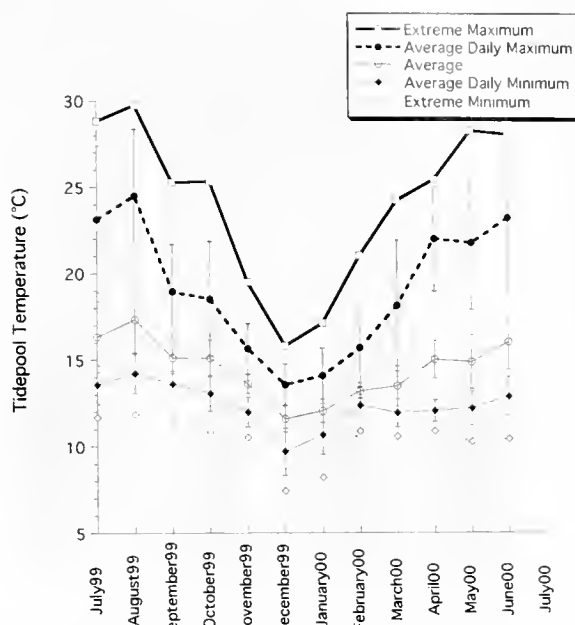


Figure 5. Temperature recorded in a small tidepool. As expected, temperature extremes were buffered relative to the aerially exposed horizontal substratum. However, high temperature extremes were higher than those on the aerially exposed, north-facing site, with yearly extremes reaching nearly 30 °C.

Compared to north-facing mussels, the horizontal mussels had significantly higher levels of Hsc75 only in January ($P = 0.012$). In July, Hsc75 levels in the two groups were

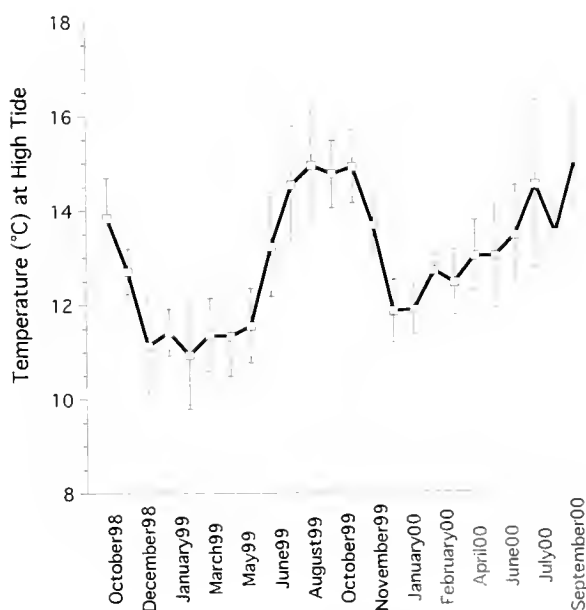


Figure 6. Patterns in water temperature recorded during high tide. The seasonal pattern in water temperature is markedly different in both magnitude and timing from those recorded in any of the microsites during aerial exposure.

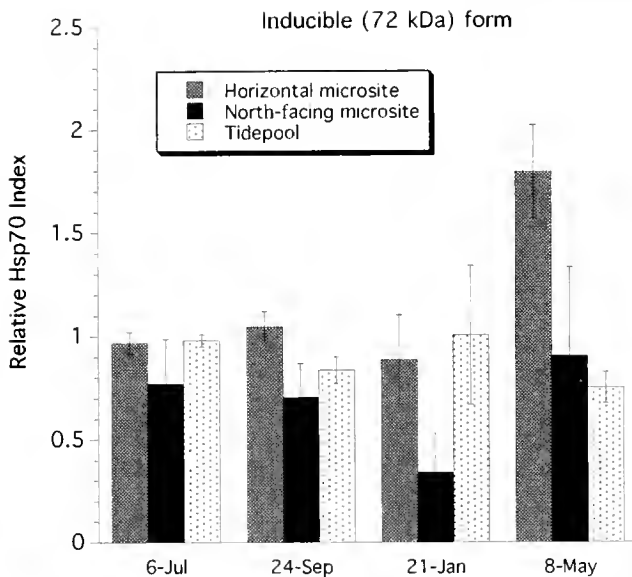


Figure 7. "Inducible" (72-kDa isoform) levels of heat shock protein from mussels collected at each of the three sites. See Table 1 for statistical results, and Table 2 for temperature conditions experienced by mussels prior to each collection. In general, inducible forms were significantly higher in mussels from the horizontal site than in mussels from the north-facing site. Differences between the aerially exposed mussels and mussels from the tidepool were less consistent.

equivalent, and in the other two months the levels were significantly lower in the horizontal mussels than in the north-facing mussels (September, $P = 0.0001$; May, $P = 0.0001$; Fig. 8).

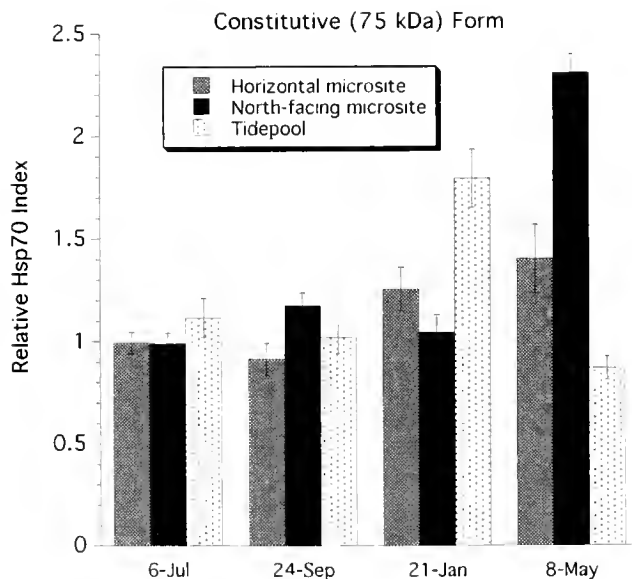


Figure 8. "Constitutive" (75-kDa isoform) levels of stress proteins from mussels at each site. Constitutive forms are thought to be affected by multiple physiological parameters and do not necessarily change with thermal stress. See Table 1 for results of statistical analysis.

Table 1

Results of statistical analyses of the 72-kDa form of Hsp 70

Effect of Site within Collection Date*	
6 July 1999	H = TP > N ($F = 4.12, P = 0.0400$)
24 September 1999	H > TP = N ($F = 12.14, P = 0.0013$)
21 January 2000	H = TP > N ($F = 9.64, P = 0.0030$)
8 May 2000	H > TP = N ($F = 19.85, P = 0.0002$)
Effect of Collection Date within Site	
Horizontal	May > July = Sept. = Jan. ($F = 33.0, P = 0.0001$)
North-facing	July = Sept. = May > Jan. ($F = 4.0, P = 0.0270$)
Tidepool	July = Sept. = Jan. = May ($F = 2.4, P = N.S.$)

Overall analysis using a two-factor ANOVA indicated a significant effect of collection date ($F = 10.0, P = 0.0001$), Site ($F = 28.2, P = 0.0001$) and a significant interaction term ($F = 9.23, P = 0.0001$). A series of one-way ANOVAs with Fisher's PLSD *post hoc* tests were used to discern the effects of site within collection date, and of collection date within site.

* H, horizontal; TP, tidepool; N, north-facing.

In a comparison of tidally exposed and constantly submerged individuals, there were no obvious differences or trends in either Hsp72 or Hsc75 levels between the horizontal and north-facing mussels and mussels that were permanently immersed in a tidepool (Figs. 7, 8). Hsp72 levels were greater in horizontal mussels in September and May as compared to tidepool mussels, but these levels were equal in July and January (Fig. 7). Hsp72 levels in tidepool mussels were equivalent to north-facing levels in May and September, but tidepool mussels had significantly greater levels in July and January than did their north-facing counterparts. For Hsc75, levels in mussels from the tidepool were greater than those in horizontal mussels in September, July, and January, and significantly lower than in mussels from horizontal surfaces in May. Levels of Hsc75 from tidepool mussels were significantly greater than in north-facing mussels in July and January, and significantly lower than in north-facing mussels in May and September.

Finally, the three microsites displayed variation in levels of the 70-kDa Hsp bioindicators as a function of time of collection (Figs. 7, 8). For the horizontal mussels, Hsp72 levels were higher in May than in any other month; however, all three other months (July, September, and January) were not significantly different from each other (Fig. 7). In contrast, the mussels from the north-facing substratum had their lowest levels of Hsp72 in January; the difference between January and the other months was statistically significant. Hsp72 levels in gill from north-facing mussels were not significantly different amongst the July, September, and May collections. With respect to Hsc75, horizontal mussels in September and July had equivalent but lower

Table 2

Temperature measurements conducted during the week prior to each mussel collection

	Horizontal	North-facing	Tidepool
30 June–6 July 1999	19.8 (25.1)	20.5 (26.3)	22.0 (26.3)
18–24 September 1999	21.1 (26.3)	17.1 (19.1)	20.7 (25.3)
15–21 January 2000	13.0 (15.3)	N.R.	14.9 (16.1)
2–8 May 2000	20.9 (30.0*)	14.2 (22.0)	19.0 (26.6)

Both the average daily maximum temperature and the extreme temperature (in parentheses) recorded during that week are given (°C).

* The 30 °C temperature recorded on May 8 was for a very brief period of time (<20 min.).

levels than in January and May; north-facing mussels displayed the highest values in May as compared to all other months, which were not significantly different from each other. Interestingly, the tidepool mussels exhibited no seasonal effect on Hsp72 levels (Fig. 7), but they did show some variation in Hsc75 levels (Fig. 8). Specifically, the levels of Hsc75 in May and September were equivalent to each other but significantly lower than in the months of July and January ($P = 0.001$); July and January levels were not significantly different from each other.

A comparison between the maximum temperature exposure in the week prior to collection (Table 2) and the levels of Hsp72 (Fig. 7), shows that inducible Hsp levels generally increased with maximum temperature exposure, but the correlation was not as good as might be expected (Fig. 9). A regression of Hsp72 with maximum temperature indicated a significance level of $P = 0.03$ (Statview; $F = 7.66$) when both north-facing and horizontal mussels were considered (note that the temperature datum for the January north-facing site was assumed to be no higher than that on the horizontal site). Tidepool data (not shown) generally fell along the same trend line, but reduced the significance level to $P = 0.059$ ($F = 4.55$).

Discussion

Intertidal organisms live at the margins of the marine and terrestrial environments and must contend with the changing physical conditions of both regimes. Recently, much attention has been paid to the influence of seawater temperature, and in particular to changes in seawater temperature as a result of climate, on changes in intertidal communities (e.g., Barry *et al.*, 1995; Sagarin *et al.*, 1999). However, few studies have investigated the importance of aerial exposure to intertidal organisms in a changing thermal environment (but see Denny and Paine, 1998). Clearly, extremes in body temperature (both high and low) experienced during exposure to air far exceed those occurring during high tide. Depending on the zonal height of the organism, the duration of exposure to air can be as long as or even longer than the submersion time.

An important question that remains to be answered is, how important to an organism's physiological performance is thermal stress during low tide as opposed to the effects of water temperature during submersion? Previous evidence suggests that some intertidal organisms slow their metabolic rates during aerial exposure, and in some cases resort to anaerobic metabolism (e.g., Bayne *et al.*, 1976). Work by Sanford (1999) has suggested that the rate of predation by the sea star *Pisaster* is driven by water temperature and appears to be unrelated to air temperature. In contrast, measurements of Hsp production show that the temperatures at which Hsps are induced occur almost exclusively during low tide (e.g., Roberts *et al.*, 1997; Tomanek and Somero, 1999), and that the deficit to the protein pool can have a significant effect on the animal's scope for growth (Roberts *et al.*, 1997). Mass mortalities due to thermal stress also have been reported primarily as a result of extremes in temperature experienced during exposure to air (e.g., Glynn, 1968; Suchanek, 1978; Tsuchiya, 1983; Liu and Morton, 1994; Williams and Morrill, 1995). Understanding the relative importance of thermal stress during submersion *versus* during aerial exposure is therefore key if we are to decipher

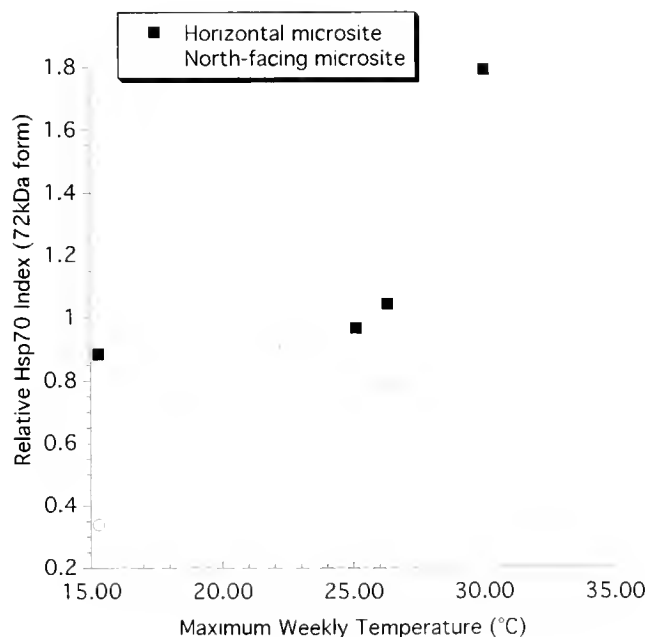


Figure 9. Comparison of Hsp72 ("inducible form") levels vs. the maximum temperature recorded in the week prior to collection. As a result of data logger failure, no temperature data were collected on the north-facing site prior to the January collection. For the purposes of this figure, we thus assume that the north-facing site was no hotter (15.3 °C) than the horizontal site where temperatures were recorded. A simple regression reveals a significant relationship between Hsp72 and maximum temperature ($P = 0.03$; $F = 7.66$), although it should be noted that the relationship is significant primarily because of the large spike in Hsp72 production observed in May.

and predict the effects of climate, and of climate change, on intertidal communities.

Our results show that patterns in body temperature experienced during low tide cannot be predicted on the basis of measurements of nearshore water temperature. Similarly, preliminary evidence (Helmuth, unpubl. data) suggests that air temperature is also an ineffective proxy for body temperature. This observation is pertinent because air and water temperatures are frequently the dominant metrics used to estimate patterns in thermal stress in the intertidal zone (e.g., Barry *et al.*, 1995; Menge *et al.*, 1997; Sagarin *et al.*, 1999; Denny and Paine, 1998; Sanford, 1999; Thompson *et al.*, 2000). Furthermore, as our data indicate, high spatial variability due to substratum angle can lead to large differences in body temperatures. Single measurements of temperature, and particularly those based on water or air temperature, cannot be used to define thermal stress at an intertidal site or to compare multi-year trends in community structure as a function of climate change.

Our study also points out gaps in our understanding of what aspect of the thermal environment drives organismal stress and of how organisms respond to temporally varying environmental signals. Widdows (1976), for example, showed that, when acclimated to cyclic temperatures, *Mytilus edulis* decreased its amplitude of response of filtration rate and oxygen consumption to changing temperatures. More relevant to our study, previous research has shown that the threshold induction temperature and the total cellular pools of Hsps in mussels changed as a function of season and thermal acclimation in the laboratory (Roberts *et al.*, 1997; Buckley *et al.*, 2001). Although these studies clearly demonstrate an effect of thermal history on the physiology and regulation of the heat shock response, the mechanism that couples variation in environmental temperature with the physiological response is unknown. Surprisingly, even in the heat shock biology of model cells, there is no consensus about how the thermal signal is transduced from the membrane, through protein kinase cascades to the nucleus (e.g., Lin *et al.*, 1997; Ng and Bogoyevitch, 2000; Han *et al.*, 2001). As ecological physiologists, if we are ever to determine the pathway of signal transduction of temperature in an organism in nature, we must first understand the physiologically important aspect of temperature.

Thus, one of the goals of this study was to bridge the gap between temperature exposure in nature and a predictable molecular response, the heat shock response. Our results highlight the complexity of examining an environmentally induced gene expression event in organisms in a natural population. Although there are some instances in which the Hsp levels "match" the predicted result (Fig. 9), there are others in which the correspondence is poor. For example, as expected, mussels living on horizontal substrata consistently had higher levels of Hsp72, the inducible isoform of the 70-kDa Hsp gene family, than did mussels on north-

facing substrata (Fig. 7, Tables 1, 2). In contrast, seasonal differences in Hsp production (Fig. 7) were less easily interpreted and did not always display the pattern observed in other studies of intertidal mussels. For example, levels of Hsp72 in mussels from the horizontal microsite were nearly as high (albeit more variable) in January as in July (Fig. 7), even though recorded body temperatures were considerably higher in July than in January (Table 2). On the other hand, higher temperatures recorded in May (Table 2) were reflected in Hsp72 production during this time period (Figs. 7, 9), and appear to be most closely related to differences in extreme temperature (30 vs. 25 °C; Table 2). These patterns, and in particular the patterns observed in Hsp75 production, suggest again that there are numerous factors at work in the control of chaperone levels and that thermal stress may not be the only factor driving variation in Hsp expression. Specifically, other physiological stressors such as hypoxia and desiccation may contribute to temperature's influence on Hsp induction (see Feder and Hofmann, 1999). Furthermore, our study shows that the seasonal timings of potential stressors do not always act in concert, and that the timing of "acute" and "chronic" high temperature exposures varies with substratum angle. The thermal landscape is highly variable, and conclusions drawn from any given study could depend on the sampling regime (e.g., effects of substratum angle). Extreme caution must be exercised when collecting samples over limited spatial and temporal scales as a means of defining thermal stress at a site.

Our data also address the inherent complexity of using Hsps as biomarkers in the environment. In general, the heat shock response is subject to complex regulation in the cell (Kline and Morimoto, 1997; Ali *et al.*, 1998; Morimoto, 1998; Zhong *et al.*, 1998). The nature of Hsp gene activation can change with the length and severity of the thermal stress (see Lindquist, 1986, for a review; see also Yost *et al.*, 1990), and Hsp70 mRNA stability varies as a function of temperature (Petersen and Lindquist, 1988, 1990). In fact, Hsps are thought to control their own expression *via* a negative feedback loop, making the cellular pools and the induction points interrelated (e.g., DiDominico *et al.*, 1982; Craig and Gross, 1991; Shi *et al.*, 1998). Furthermore, once the Hsps are synthesized, they are also subject to decay just like any other protein, and their half-life is influenced by the thermal conditions of the cell. In combination, all the mechanistic and complex regulatory aspects of the heat shock response make for a system that not only is sensitive to temperature but also is directly influenced by temperature, just like any other biomolecular process in a cell. Thus, for example, mussels exposed to lower chronic levels of high temperature may produce inducible forms of Hsp at a lower acute temperature level than will mussels that were acclimated to high average daily maxima. Thus, a hot day that is preceded by a week of relatively mild days may elicit a very different physiological response than an extreme tempera-

ture exposure that follows several days of gradually increasing daily maxima. In summary, the effects of both extreme temperature events (acute temperature exposure) and of the thermal history (e.g., chronic temperature exposure) are likely to be important, but we do not yet sufficiently understand the molecular consequences of temperature variation or how variation in signal transduction and in gene expression would alter the pools of Hsps.

In some ways our study raises more questions than it answers. Defining "thermal stress" at any given site is likely to be complex. Substratum angle can have an enormous effect on the magnitude, timing, and thermal history of temperature. Because ectothermic organisms influence their body temperatures at least partially through their size and morphology, two organisms at one site might experience different patterns in the thermal signal, particularly if they are mobile (e.g., Orton, 1929a). Thermal stress may therefore be organism-specific, rather than site-specific (Menge and Olson, 1990). Finally, care must be taken to account for the thermal conditions occurring during the collection period. Thermal stress experienced during low tide results from the interaction between terrestrial climate and the timing of low tides as set by the tidal series (Orton, 1929a; Helmuth, 1999). For example, sites separated by tens of kilometers have been predicted to experience temperature maxima that differ by several degrees due to the timing of low tide during the hottest times of the year; organisms at sites where low tide occurs at noon may experience much higher temperatures than those at sites where low tide occurs in the morning (Helmuth, 1998, 1999). Inter-annual and decadal-scale variations in tidal exposure have also been predicted to occur (Denny and Paine, 1998). The coupling of biochemical indicators of stress with detailed measurements of temperature may be effective in predicting the role of climate in driving the ecology of rocky intertidal communities, and in predicting the effects of climate change on these ecosystems. However, for ecologists, the temptation to base large-scale comparisons of the role of thermal stress on limited measurements of stress proteins must be balanced by a knowledge of the role of the organism's "cellular thermostat" in driving its physiological response to temperature change. Conversely, physiologists must have a better grasp of how temperatures change in nature if we are to extrapolate from controlled laboratory experiments to conditions in the field. Thus, while there is no simple mechanism for linking patterns in temperature to patterns in physiological stress, the merger of these levels of approach promises to be fruitful for understanding the effects of climate on the rocky intertidal zone.

Acknowledgments

The authors thank Matthew Wright, Sean P. Place, and Megan Dueck for technical assistance with sample prepara-

tion and western blot analysis, Michael O'Donnell for assistance in the field, and Morgan Timmerman-Helmuth for her help in editing the manuscript. In addition, we thank Hopkins Marine Station of Stanford University and its Director, Dr. George N. Somero, for access to the study field sites, and Dr. Mark Denny for his advice and insight. This research was supported in part by National Science Foundation grants IBN 9985878 to BSTH, IBN 0096100 to GEH, and NSF 0083369 to GEH and BSTH.

Literature Cited

- Ali, A., S. Bharadwaj, R. O'Carroll, and N. Ovsenek. 1998. Hsp90 interacts with and regulates the activity of Heat Shock Factor 1 in *Xenopus* oocytes. *Mol. Cell Biol.* **18**: 4949–4960.
- Barry, J. P., C. H. Baxter, R. D. Sagarin, and S. E. Gilman. 1995. Climate-related, long-term faunal changes in a California rocky intertidal community. *Science* **267**: 672–675.
- Bayne, B. L., C. J. Bayne, T. C. Carefoot, and R. J. Thompson. 1976. The physiological ecology of *Mytilus californianus* Conrad. 2. Adaptation to low oxygen tension and air exposure. *Oecologia* **22**: 229–250.
- Bell, E. C. 1995. Environmental and morphological influences on thallus temperature and desiccation of the intertidal alga *Mastocarpus papillatus* Kützinger. *J. Exp. Mar. Biol. Ecol.* **191**: 29–55.
- Bertness, M. D. 1981. Predation, physical stress, and the organization of a tropical rocky intertidal hermit crab community. *Ecology* **62**: 411–425.
- Buckley, B. A., M. E. Owen, and G. E. Hofmann. 2001. Adjusting the thermostat: changes in the threshold induction temperature for heat shock protein genes in mussels from the genus *Mytilus*. *J. Exp. Biol.* **204** (In press).
- Carefoot, T. 1977. *Pacific Seashores: a Guide to Intertidal Ecology*. University of Washington Press, Seattle, WA.
- Chapple, J. P., G. R. Smerdon, R. J. Berry, and A. J. S. Hawkins. 1998. Seasonal changes in stress-70 protein levels reflect thermal tolerance in the marine bivalve *Mytilus edulis* L. *J. Exp. Mar. Biol. Ecol.* **229**: 53–68.
- Craig, E. A., and C. A. Gross. 1991. Is Hsp70 the cellular thermometer? *Trends Biochem. Sci.* **16**: 135–140.
- Dahlhoff, E. P., B. A. Buckley, and B. A. Menge. 2001. Feeding of the rocky intertidal predator *Nucella ostrina* along an environmental stress gradient. *Ecology* **82**: 2816–2829.
- Denny, M. W., and R. T. Paine. 1998. Celestial mechanics, sea-level changes, and intertidal ecology. *Biol. Bull.* **194**: 108–115.
- DiDominico, B. J., G. E. Bugaisky, and S. Lindquist. 1982. Heat shock and recovery are mediated by different translational mechanisms. *Proc. Natl. Acad. Sci. USA* **79**: 6181–6185.
- Doty, M. S. 1946. Critical tide factors that are correlated with the vertical distribution of marine algae and other organisms along the Pacific Coast. *Ecology* **27**: 315–328.
- Elvin, D. W., and J. J. Gonor. 1979. The thermal regime of an intertidal *Mytilus californianus* Conrad population on the central Oregon coast. *J. Exp. Mar. Biol. Ecol.* **39**: 265–279.
- Feder, M. E., and G. E. Hofmann. 1999. Heat-shock proteins, molecular chaperones, and the stress response. *Annu. Rev. Physiol.* **61**: 243–282.
- Glynn, P. W. 1968. Mass mortalities of echinoids and other reef flat organisms coincident with midday, low water exposures in Puerto Rico. *Mar. Biol.* **1**: 226–243.
- Han, S. I., S. Y. Oh, S. H. Woo, K. H. Kim, J.-H. Kim, H. D. Kim, and H. S. Kang. 2001. Implication of a small GTPase Rac 1 in the activation of c-Jun N-terminal kinase and heat shock factor in response to heat shock. *J. Biol. Chem.* **276**: 1889–1895.

- Helmuth, B. S. T. 1998. Intertidal mussel microclimates: Predicting the body temperature of a sessile invertebrate. *Ecol. Monogr.* **68**: 29–52.
- Helmuth, B. 1999. Thermal biology of rocky intertidal mussels: quantifying body temperatures using climatological data. *Ecology* **80**: 15–34.
- Helmuth, B., and M. W. Denny. 1999. Measuring scales of physical stress in the rocky intertidal. *Am. Zool.* **39**: 114A (abstract).
- Hofmann, G. E., and G. N. Somero. 1995. Evidence for protein damage at environmental temperature: seasonal changes in levels of ubiquitin conjugates and Hsp70 in the intertidal mussel *Mytilus trossulus*. *J. Exp. Biol.* **198**: 1509–1518.
- Hofmann, G. E., and G. N. Somero. 1996a. Interspecific variation in thermal denaturation of proteins in the congeneric mussels *Mytilus trossulus* and *M. galloprovincialis*: evidence from the heat-shock response and protein ubiquitination. *Mar. Biol.* **126**: 65–75.
- Hofmann, G. E., and G. N. Somero. 1996b. Protein ubiquitination and stress protein synthesis in *Mytilus trossulus* occurs during recovery from tidal emersion. *Mol. Mar. Biol. Biotechnol.* **5**: 175–184.
- Hutchins, L. W. 1947. The bases for temperature zonation in geographical distribution. *Ecol. Monogr.* **17**: 325–335.
- Johnson, S. E. II. 1975. Microclimate and energy flow in the marine rocky intertidal. Pp. 559–587 in *Perspectives of Biophysical Ecology*. D. M. Gates and R. B. Schmerl, eds. Springer-Verlag, New York.
- Kline, M. P., and R. I. Morimoto. 1997. Repression of the heat shock factor 1 transcriptional activation domain is modulated by constitutive phosphorylation. *Mol. Cell. Biol.* **17**: 2107–2115.
- Lin, L. Z., Z.-W. Hu, J. H. Chin, and B. B. Hoffman. 1997. Heat shock activates c-Sre tyrosine kinases and phosphatidylinositol 3-kinase in NIH3T3 fibroblasts. *J. Biol. Chem.* **272**: 31196–31202.
- Lindquist, S. 1986. The heat shock response. *Annu. Rev. Biochem.* **55**: 1151–1191.
- Liu, J. H., and B. Morton. 1994. The temperature tolerances of *Tetraclita squamosa* (Crustacea: Cirripedia) and *Septifer virgatus* (Bivalvia: Mytilidae) on a sub-tropical rocky shore in Hong Kong. *J. Zool. Lond.* **234**: 325–339.
- Menconi, M., L. Benedetti-Cecchi, and F. Cinelli. 1999. Spatial and temporal variability in the distribution of algae and invertebrates on rocky shores in the northwest Mediterranean. *J. Exp. Mar. Biol. Ecol.* **233**: 1–23.
- Menge, B. A., and A. M. Olson. 1990. Role of scale and environmental factors in regulation of community structure. *Trends Ecol. Evol.* **5**: 52–57.
- Menge, B. A., B. A. Daley, P. A. Wheeler, E. Dahlhoff, E. Sanford, and P. T. Strub. 1997. Benthic-pelagic links and rocky intertidal communities: bottom-up effects on top-down control? *Proc. Natl. Acad. Sci.* **94**: 14,530–14,535.
- Morimoto, R. I. 1998. Regulation of the heat shock transcriptional response: cross talk between a family of heat shock factors, molecular chaperones, and negative regulators. *Genes Dev.* **12**: 3788–3796.
- Ng, D. C. H., and M. A. Bogoyevitch. 2000. The mechanism of heat shock activation of ERK mitogen-activated protein kinases in the interleukin 3-dependent ProB cell line BaF3. *J. Biol. Chem.* **275**: 40,856–40,866.
- Orton, J. H. 1929a. Observations on *Patella vulgata* Part III. Habitat and habits. *J. Mar. Biol. Assoc. UK* **16**: 277–288.
- Orton, J. H. 1929b. On the occurrence of *Echinus esculentus* on the foreshore in the British Isles. *J. Mar. Biol. Assoc. UK* **16**: 289–296.
- Petersen, R. B., and S. Lindquist. 1988. The *Drosophila* Hsp70 message is rapidly degraded at normal temperatures and stabilized by heat shock. *Genes* **72**: 161–168.
- Petersen, R. B., and S. Lindquist. 1990. Differential mRNA stability: A regulatory strategy for Hsp70 synthesis. Pp. 83–91 in *Posttranscriptional Control of Gene Expression*. J. E. G. McCarthy and M. F. Tuite, eds. Springer-Verlag, New York.
- Porter, W. P., and D. M. Gates. 1969. Thermodynamic equilibria of animals with environment. *Ecol. Monogr.* **39**: 245–270.
- Porter, W. P., J. W. Mitchell, W. A. Beckman, and C. B. DeWitt. 1973. Behavioral implications of mechanistic ecology. Thermal and behavioral modeling of desert ectotherms and their microenvironment. *Oecologia* **13**: 1–54.
- Roberts, D. A., G. E. Hofmann, and G. N. Somero. 1997. Heat-shock protein expression in *Mytilus californianus*: acclimatization (seasonal and tidal-height comparisons) and acclimation effects. *Biol. Bull.* **192**: 309–320.
- Sagarin, R. D., J. P. Barry, S. E. Gilman, and C. H. Baxter. 1999. Climate-related change in an intertidal community over short and long time scales. *Ecol. Monogr.* **69**: 465–490.
- Sanford, E. 1999. Regulation of keystone predation by small changes in ocean temperature. *Science* **283**: 2095–2097.
- Shi, Y., D. D. Mosser, and R. I. Morimoto. 1998. Molecular chaperones as HSF1-specific transcriptional repressors. *Genes Dev.* **12**: 654–666.
- Snyder, M. J., E. Girvetz, and E. P. Mulder. 2001. Induction of marine mollusc stress proteins by chemical or physical stress. *Arch. Environ. Contam. Toxicol.* **41**: 22–29.
- Stillman, J. H., and G. N. Somero. 1996. Adaptation to temperature stress and aerial exposure in congeneric species of intertidal porcelain crabs (genus *Petrochelidon*): correlation of physiology, biochemistry and morphology with vertical distribution. *J. Exp. Biol.* **199**: 1845–1855.
- Suchanek, T. II. 1978. The ecology of *Mytilus edulis* L. in exposed rocky intertidal communities. *J. Exp. Mar. Biol. Ecol.* **31**: 105–120.
- Thompson, R. C., M. F. Roberts, T. A. Norton, and S. J. Hawkins. 2000. Feast or famine for intertidal grazing molluscs: a mis-match between seasonal variations in grazing intensity and the abundance of microbial resources. *Hydrobiologia* **440**: 357–367.
- Tomaneck, L., and G. N. Somero. 1999. Evolutionary and acclimation-induced variation in the heat-shock responses of congeneric marine snails (genus *Tegula*) from different thermal habitats: implications for limits of thermotolerance and biogeography. *J. Exp. Biol.* **202**: 2925–2936.
- Tsuchiya, M. 1983. Mass mortality in a population of the mussel *Mytilus edulis* L. caused by high temperature on rocky shores. *J. Exp. Mar. Biol. Ecol.* **66**: 101–111.
- Wetley, D. S. 1983. Geographic limits and local zonation: the barnacles *Semibalanus (Balanus)* and *Chthamalus* in New England. *Biol. Bull.* **165**: 330–341.
- Wetley, D. S. 1984. Sun and shade mediate competition in the barnacles *Chthamalus* and *Semibalanus*: a field experiment. *Biol. Bull.* **167**: 176–185.
- Widdows, J. 1976. Physiological adaptation of *Mytilus edulis* to cyclic temperatures. *J. Comp. Physiol.* **105**: 115–128.
- Williams, G. A., and D. Morritt. 1995. Habitat partitioning and thermal tolerance in a tropical limpet, *Cellana grata*. *Mar. Ecol. Prog. Ser.* **124**: 89–103.
- Yost, H., R. B. Petersen, and S. Lindquist. 1990. RNA metabolism: strategies for regulation in the heat shock response. *Trends Genet.* **6**: 223–227.
- Zhong, M., A. Orosz, and C. Wu. 1998. Direct sensing of heat and oxidation by *Drosophila* heat shock transcription factor. *Mol. Cell* **2**: 101–108.

Competition for Space Among Sessile Marine Invertebrates: Changes in HSP70 Expression in Two Pacific Cnidarians

SERGI ROSSI* AND MARK J. SNYDER†

*University of California, Davis, and Bodega Marine Laboratory,
P.O. Box 247, Bodega Bay, California 94923*

Abstract. The role of stress proteins—either constitutive (HSC) or inducible (HSP)—of the HSP70 family in intra- and interspecific competition for space was examined in two sessile Pacific cnidarians. *Anthopleura elegantissima*, an intertidal anemone, and *Corynactis californica*, a subtidal corallimorpharian, express HSP70 in the absence of apparent physical stress. HSP70 protein expression is concentrated in the tentacles of *A. elegantissima* when the animal is exposed to contact with other benthic organisms. Under the same conditions, however, HSP concentrations are similar in the body and tentacles of *C. californica*. When two different clones of *A. elegantissima* interact in the field, the outside polyps (warriors) express more HSP70 than the inside ones (2.4 versus 0.6 ng HSP70/ μ g Protein). When different *C. californica* clones interact, HSP70 expression in the outside and inside polyps is similar (1.5 versus 1.8 ng HSP70/ μ g P) and is fairly constant in the corallimorpharian in the different interspecific encounters. HSP70 expression is related to the different kinds of aggression encountered by both cnidarians. HSP70 expression may be involved in the recovery of tissues damaged by the allelochemical, cytotoxic, or corrosive substances produced by different enemies. *C. californica* clones appear prepared for war, as evidenced by the high constant expression of HSP70 in the polyps. *A. elegantissima* exhibits differential HSP70 expression depending on the identity of each neighboring intra- or interspecific sessile competitor. We propose that stress pro-

teins can be used to quantify space competition or aggression among sessile marine invertebrates.

Introduction

Space on which to live is often the most limiting resource in marine hard-substratum environments, and patchiness has evolved under the influence of intense competition for living space (Connell, 1961; Pequegnat, 1964; Paine, 1971; Dayton, 1971; Jackson, 1977). Once established, organisms can show aggressive behavior (Chadwick, 1987) that may be especially intense in cryptic environments where free space is almost nonexistent.

In benthic environments, sponges, ectopods, cnidarians, and ascidians can produce biologically active substances that may be destructive to enemies during space competition (Whittaker and Feeny, 1973; Uriz *et al.*, 1991). These organisms aggregate in patches that can dominate hard-bottom substrates (Sutherland, 1978; Chornesky, 1983; Chadwick, 1987, 1991; Chadwick and Adams, 1991; Langmead and Chadwick, 1999a, b, among others). Growth is often slow in such organisms, and interactions between competitors are often nonevident. It is difficult to quantify competitive interactions *in situ*, and the manipulation of organisms is frequently essential to demonstrate the potential effects of space competition (Schoener, 1983). For example, investigators have rarely observed agonistic interactions in wild anemones (*A. xanthogrammica*), although these organisms frequently exhibit such behavior in forced situations (Sebens, 1984). The quantification of damage from encounters between such organisms and the identification of potential mechanisms used to counter the effect of such aggression have proved difficult. Most studies have dealt with the organismal responses to the attack and the

Received 26 January 2001; accepted 22 May 2001.

* Current address: Institut de Ciències del Mar, Passeig Nacional, s/n, 08003 Barcelona, Spain.

† To whom correspondence should be addressed. E-mail: mjsnyder@ucdavis.edu

consequent aggressive behavior displayed by individuals. Few workers have focused on the capacities, and implied mechanisms, for tissue recovery following aggressive interactions. We hypothesize that components of the stress response such as HSPs may provide evidence of the intensity of competitive interactions and are one of the mechanisms by which cnidarians recover from or prepare their tissues for the effects of competitive or aggressive interactions.

HSPs enhance cell survival by reducing the accumulation of damaged or abnormal polypeptides within cells (Feder and Hofmann, 1999). However, whether all wild organisms routinely, occasionally, or seldom express inducible HSPs is unknown. For marine invertebrates, most investigators have examined the effects of thermal variations on constitutive (HSC70) and inducible (HSP70) responses (Feder and Hofmann, 1999). Competitive interactions between sessile organisms can elicit HSP responses due to protein damage following the excretion of harmful substances by one or both competitors (Uriz *et al.*, 1991; Turon *et al.*, 1996; Wiens *et al.*, 1998). One index of tolerance to aggressive sessile organisms could be the presence and abundance of mechanisms (such as HSPs) that would resist or ameliorate the damage inflicted on cellular components by the potential space competitor. Furthermore, once HSP can be related to space competition, no manipulation will be necessary to test such hypotheses. HSP expression could then be a quantitative tool to examine competitive interactions in the field without human interference.

To determine whether HSP expression patterns could be related to competitive interactions in marine hard-bottom sessile invertebrates, two Pacific cnidarians were chosen for study: the intertidal anemone *Anthopleura elegantissima* and the subtidal corallimorpharian *Corynactis californica*. *A. elegantissima* forms contiguous aggregations composed of individuals of a single clone, the products of asexual reproduction (Francis, 1973b; Sebens, 1982a, b). Free zones are created where competition between clones occurs through the outside polyps of the aggregation (called "warriors," Francis, 1973a). Compared with polyps in the center of the clone, the warriors have larger and more abundant acrorhagi (specialized nonfeeding tentacles) and lack mature gonads (Francis, 1973b, 1976). The aggressive response is not directly involved in either defense against predators or capture of prey (Francis, 1973b), but functions in the competition for space. We hypothesize that *A. elegantissima* warriors may exhibit higher HSP levels than interior clonemates because they interact more frequently with competitors.

In the subtidally distributed *C. californica*, the polyps have no distinctive roles within each clone (Chadwick, 1987). Although the physiology of this group is not as well understood as that of anemones, several studies have described the competition for space and the specific responses to aggression in corallimorpharians (Chadwick, 1987, 1991;

Chadwick and Adams, 1991; Langmead and Chadwick, 1999a, b). Space competition experiments demonstrate that *C. californica* influences the abundance and population structure of other cnidarians by means of its aggressive behavior (Chadwick, 1987, 1991; Chadwick and Adams, 1991). We sought to determine whether the high aggression in this species is related to elevated HSP levels as preparation for possible damage resulting from such interspecies encounters.

We tested two main hypotheses in this work: first, that stress produced by space competition can induce HSP expression to counter the effects of aggressive neighbors; second, that HSP expression can provide a quantitative assay for space competition in sessile invertebrates.

Materials and Methods

Animals and treatments

Anthopleura elegantissima and *Corynactis californica* were collected from the Bodega Bay area and held in the running seawater system of the Bodega Marine Laboratory. All animals were held in ambient seawater (13–15 °C) and fed adult brine shrimp or frozen seafood. The seawater from the Bodega Bay area is considered clean, and the animals used in these experiments are considered to have had minimal contact with anthropogenic chemicals that are known to induce HSP expression (McCain *et al.*, 1988). All experiments (aquarium and field) were done in September–October 1998 and 1999 to avoid seasonal differences in cnidarian behavior. Each experiment, whether forced interactions in an aquarium or *in situ* interaction, was designed to assess the effects of neighboring competition for space on HSP70 expression.

Forced aquarium experiments

The first experiment examined HSP70 protein expression in *A. elegantissima* and *C. californica* in a forced situation. Six isolated polyps of each species (attached to stones, no physical stress induced) were moved into contact with each other (*i.e.*, one polyp of *A. elegantissima* against one polyp of *C. californica*). After 24 h, tentacle samples from three individuals of each species were removed and frozen in liquid nitrogen. To quantify the differences between tentacles and body, the other three polyps of each species were sampled 48 h later, frozen in liquid nitrogen, and then assayed for HSP70 level by methods detailed below. As controls, isolated polyp tentacles ($n = 5-6$, no interacting species) of *A. elegantissima* and *C. californica* were likewise sampled in the aquarium.

In situ intraspecific competition

We assessed HSP70 expression related to competition for space in a natural environmental situation (*i.e.*, in natural

clones in the field). Because collection and transport of animals to artificial holding conditions can stimulate a stress response (Sharp *et al.*, 1994; Roberts *et al.*, 1997), clones of *A. elegantissima* and *C. californica* were located and sampled from the Bodega Bay Jetty from a minimum 2 m below the 0 tide level (permanently submerged). This avoided significant desiccation, changes in temperature, fluctuations in salinity and pH, and other effects that are typical of the environment for the intertidal *A. elegantissima* but not for the subtidal *C. californica*.

For the *A. elegantissima* intraspecific competition experiments, clones were located by scuba and photographed (Nikonos V camera, 35-mm lens with macro 1:1 or close-up lens). Polyps of each clone were sampled ($n = 3$, tentacles) from the outside (touching the competitor) and the inside (touching only the same clone, 10–20 cm from the outside polyps). Samples were dissected, kept in 13 °C seawater for no longer than 30 min before freezing in liquid nitrogen, and stored at –70 °C. As a control to assess whether HSP70 levels were affected by the extra 30-min tissue incubation in ambient seawater before freezing, the following experiment was performed. Individual tentacle samples were obtained from three individuals of two clones exposed to elevated temperatures in the intertidal zone (elevated HSP70 is found in these conditions, Snyder and Rossi, unpubl. obs.). Each sample was divided into three parts, of which two were immediately frozen in liquid nitrogen and the third was submerged in ambient seawater for 40 min prior to freezing as above.

For the *C. californica* intraspecific competition experiments, six clones were located and sampled as above. Color varies greatly between different clonal aggregations, which is useful in distinguishing clones that show potential intraspecific competition. Outside and inside polyps (tentacle crowns) of each clone were sampled to compare interacting (<2.5 mm apart) and non-interacting individuals (5–10 cm apart from the outside ones).

Interspecific competition

To examine the effects that different space competitors in the benthic substrata have on HSP70 protein levels, we chose two genera of algae that compete for space with *A. elegantissima* and *C. californica* and two intertidal and two subtidal invertebrates for *A. elegantissima* and *C. californica*, respectively. The sampled and photographed anemone clones were always submerged (as described before).

Four clones of *A. elegantissima* and three of *C. californica* that were interacting with a calcareous red alga (*Lithothamnium* sp.) were dissected (outside and inside clone tentacles). Another alga interacting with both cnidarians was a fleshy green alga (*Ulva* sp.), and six clones of each cnidarian were sampled as above.

In the high subtidal, common space competitors of *A.*

elegantissima are the anemone *A. xanthogrammica* and the cirriped *Balanus amphitrite*. Five *A. elegantissima* clones interacting with *A. xanthogrammica* were sampled in the outside and inside parts of the clones. For *B. amphitrite*, three clones competing for space were likewise sampled. For *C. californica*, the subtidal organisms chosen (sponge *Haliclona permollis*; ascidian *Synoicum parfustis*) were considered potentially more aggressive than the fleshy algae. Six *C. californica* clones were chosen for their clear interactions with *H. permollis*, and polyps of the outside and inside part of each clone were dissected. For *S. parfustis*, the interaction of the clones was observed in four populations in the dive area, and outside and inside polyps were sampled.

HSP70 measurements

The western immunoblotting for HSP70 expression was done as follows. Frozen tentacle samples (stored at –70 °C) were individually homogenized in 0.2 ml of buffer K containing 5 mM NaHPO₄, 40 mM HEPES (pH 7.4), 5 mM MgCl₂, 70 mM potassium gluconate, 150 mM sorbitol, and 1% SDS. Homogenates were centrifuged 10 min at 10,000 × *g*, and the supernatants were combined with equal volumes of SDS sample buffer (Laemmli, 1970) and boiled for 5 min. Supernatant protein levels were determined by BioRad DC assay, and 20 μg of tentacle protein was loaded in each gel lane. For each blot, 50 ng of standard HSP70 protein (human, StressGen) was included. Discontinuous SDS gels (1 mm) were 6.2% for the stacking gel and 12% for the resolving gel. After running for 2 h at 150 V, SDS gels were electroblotted onto PDVF membranes (for 1 h at 100 V). The protein bands in each western blot were visualized by staining with Ponceau S. HSP70 protein was detected with mouse monoclonal anti-HSP70 (SPA-822, StressGen, Victoria, BC); the secondary antibody was goat-anti-mouse IgG, conjugated to peroxidase (Sigma), and was visualized with ECL reagents (Amersham) and exposure of blots to X-ray film.

Blot band intensities were compared by scanning the X-ray films and analyzing the scans with the NIH Image software package. For each blot, the scanned intensity of the HSP was normalized against the intensities of the HSP70 protein standard from that blot; that is, the NIH Image datum point was divided by the intensity of the HSP70 standard.

Results

Anthopleura elegantissima and *Corynactis californica* express a single HSP70 or HSP70 protein (Fig. 1). In other eukaryotes, the HSP70-DnaK protein family comprises multiple proteins, more than one of which may be detected by the antibody. For the sake of convenience, we will collectively term these as "HSP70." The inclusion of protease inhibitors did not affect HSP70 levels (Fig. 1A,

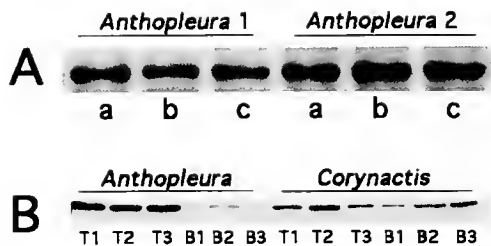


Figure 1. Western blots of HSP70 levels in *Anthopleura elegantissima* and *Corynactis californica*: comparison of tentacles under different sampling conditions and body without tentacles. In (A), triplicate tentacle samples were taken from two *A. elegantissima* individuals; (a) the first of the triplicate samples was immediately frozen in liquid nitrogen, (b) duplicate of (a) with the addition of protease inhibitors prior to homogenization, and (c) third sample from each anemone kept in a sample bag submerged at 13 °C for 40 min prior to freezing in liquid N₂. In (B), three individuals from each species were divided into tentacles only or body minus tentacles prior to homogenization.

Anthopleura 1 and 2, a versus b); therefore they were omitted from our studies during the homogenization steps. The 30-min ambient seawater submersion of subtidal tentacle samples prior to freezing had no effect compared with immediate freezing (Fig. 1A, *Anthopleura 1* and 2, c versus a and b). In comparing tentacles of the same polyp 24 h after the first forced interaction between the two cnidarian species in the laboratory, no differences were observed ($F(3, 8) = 2.0$, $P < 0.1929$) (Fig. 2). Two days later, HSP70 levels in *A. elegantissima* tentacle were 4 times greater than before (4.0 ± 0.5 ng HSP70/ μ g P in the tentacles; 0.0 ± 0.1 ng HSP70/ μ g P in the body, power of test = 0.87), but no differences were detected in *C. californica* tentacles (1.7 ± 0.9 ng HSP70/ μ g P in the tentacles; 0.8 ± 0.9 ng HSP70/ μ g P in the body) (Fig. 2). Differences between tentacles and body were found in *A. elegantissima* but not in *C. califor-*

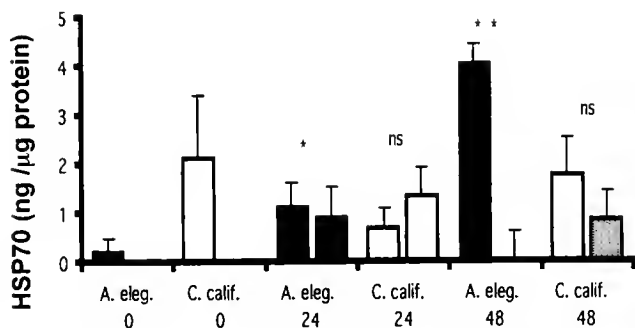


Figure 2. HSP70 expression in tentacles of *Anthopleura elegantissima* and *Corynactis californica* at time 0, 24 h after the first contact of the cnidarians (*A. eleg.* clones 1 and 2, black and stippled; *C. calif.* Clones 1 and 2, white and stippled), and 48 h later in both tentacles and body (without tentacles, stippled) of the same polyps in *A. elegantissima* and *C. californica*. The bars are +1 standard deviation of 3–6 samples. Asterisks indicate significant differences between groups ($P \leq 0.05$); ns indicates a lack of significant differences between groups.

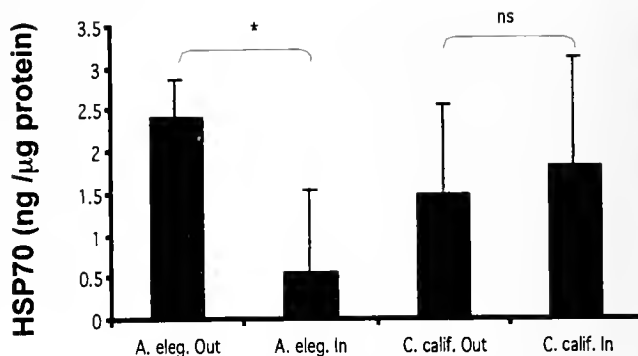


Figure 3. Intraspecific competition. HSP70 expression between tentacles of the inside and outside polyps in *Anthopleura elegantissima* and *Corynactis californica* in intraspecific conditions. The bars are +1 standard deviation of 4–5 clones. Asterisks indicate significant differences between groups ($P \leq 0.05$); ns indicates a lack of significant differences between groups.

nica (Fig. 1; $F(3, 8) = 18.55$, $P < 0.0006$, power of test = 0.98). Algal symbionts are at the highest concentration in *A. elegantissima* oral disk (Fitt *et al.*, 1982; Weis and Levine, 1996); these data imply that we are measuring HSP70 responses in animal tissue. No such differences were found in the corallimorpharian, which lacks algal symbionts.

HSP70 levels in isolated polyps were also examined under the same conditions (no contact with any other invertebrate). *A. elegantissima* tentacles had very low expression (0.2 ± 0.3 ng HSP70/ μ g P) compared with the previous contact experiments. *C. californica* had high expression (2.1 ± 1.3 ng HSP70/ μ g P) even when there was no direct (contact) aggression present. Comparing this analysis with the anemone–corallimorpharian experiments, no differences were found between HSP70 expressions in *C. californica*. There were differences in the HSP70 expression of polyps between the two cnidarians when they were compared together ($F(1, 9) = 10.81$, $P < 0.0094$).

The mean distance between competitors in field studies as determined from the photographs was 2.4 ± 0.9 mm ($n = 17$). This distance is clearly within the range that *A. elegantissima* tentacle crowns sway during seawater movements (Francis, 1973a). The results of intraspecific competition in selected patches of both cnidarians are shown in Figure 3. There were clear differences in *A. elegantissima* HSP70 expression between the outside warrior polyps and the inside ones (in contact, 2.4 ± 0.5 ng HSP70/ μ g P; no contact, 0.6 ± 0.7 ng HSP70/ μ g P; $F(3, 20) = 3.93$, $P < 0.0234$, power of test = 0.82) when two clones of the same species interacted. Interestingly, *C. californica* had similar HSP70 amounts in polyps of different clones (outside 1.5 ± 1.1 ng HSP70/ μ g P; inside 1.8 ± 1.3 ng HSP70/ μ g P).

The regular cnidarian HSP70 expression in both outside and inside polyps of the clone in different competition–for-space situations is illustrated in Figure 4. *A. elegantissima*

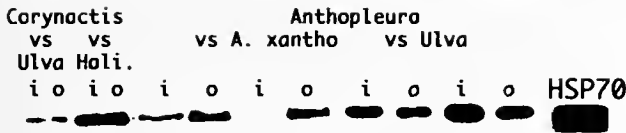


Figure 4. Western blot of HSP70 levels in *Anthopleura elegantissima* and *Corynactis californica* tentacles from inside not interacting (i) and outside interacting (o) analyzed with competitors in the field. *C. californica* competitors were *Ulva* sp. and *H. permollis*. *A. elegantissima* competitors were *A. xanthogrammica* and *Ulva* sp.

had more HSP70 in the warriors than in the inside clone polyps in general, depending on the competing species (Fig. 4). In Figure 5A, B we show HSP70 levels when both cnidarians interacted with the same competitors in the field: crustose red (*Lithothamnium* sp.) and fleshy green (*Ulva* sp.) algae. Contact with *Lithothamnium* (Fig. 5A) resulted in higher HSP70 expression in the outside *A. elegantissima* clone polyps (warriors, 2.4 ± 1.2 ng HSP/ μ g P; inside ones 0.5 ± 0.4 ng HSP/ μ g P, $F(3, 10) = 4.82$, $P < 0.025$, power of test = 0.80). No differences were found between the inside and outside *C. californica* polyps in interactions with either algal species (outside 1.2 ± 0.4 ng HSP/ μ g P; inside 1.5 ± 0.5 ng HSP/ μ g P).

Neither cnidarian showed any significant difference in HSP70 between inside and outside polyps (Fig. 5B). In *A. elegantissima*, the inside polyps (1.0 ± 0.8 ng HSP70/ μ g P) were similar to the outside ones (0.6 ± 0.6 ng HSP70/ μ g P). The expression was also similar for both clone polyps in *C. californica* (outside 1.2 ± 0.6 ng HSP70/ μ g P; inside $1.3 \pm$

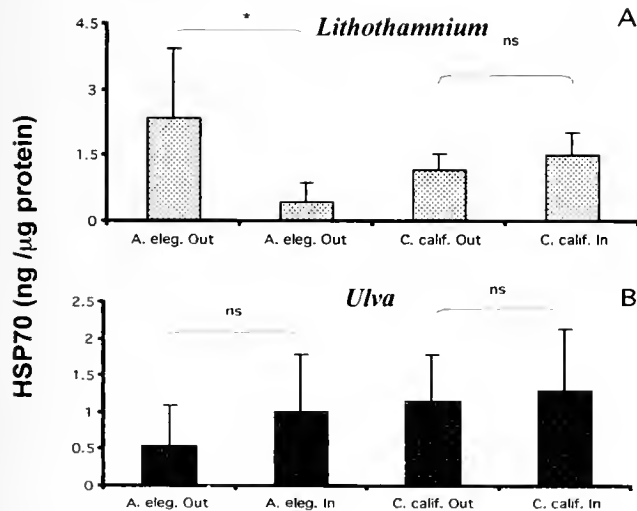


Figure 5. Interspecific competition I. HSP70 expression between tentacles of the inside and outside polyps in *Anthopleura elegantissima* and *Corynactis californica* in contact with calcareous red (*Lithothamnium* sp.) (A) and fleshy green (*Ulva* sp.) (B) algae. The bars are +1 standard deviation of 4–6 clones. Asterisks indicate significant differences between groups ($P \leq 0.05$); ns indicates a lack of significant differences between groups.

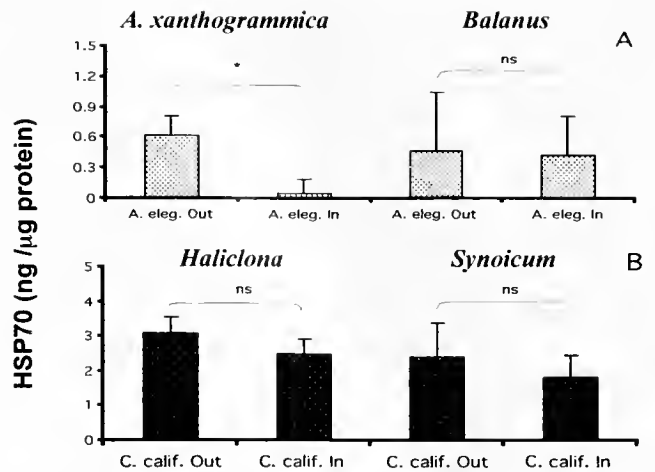


Figure 6. Interspecific competition II. HSP70 expression between tentacles of the inside and outside polyps in *Anthopleura elegantissima* and *Corynactis californica* with different competitors. (A) *A. elegantissima* against *A. xanthogrammica* and *Balanus*; (B) *C. californica* against *Haliclona permollis* and *Synoicum parfustis*. The bars are +1 standard deviation of 3–5 clones. Asterisks indicate significant differences between groups ($P \leq 0.05$); ns indicates a lack of significant differences between groups.

0.8 ng HSP70/ μ g P). *C. californica* HSP70 expression was always the same in the outside and inside polyps (1 – 1.8 ng HSP70/ μ g P) in encounters with either *A. elegantissima*, other *C. californica* clones, or either algal species.

For *A. elegantissima*, two intertidal competitors were tested in submersed conditions: *A. xanthogrammica* and *Balanus amphitrite* (Fig. 6A). Encounters with *A. xanthogrammica* resulted in higher HSP70 in *A. elegantissima* outside polyps (0.6 ± 0.2 ng HSP70/ μ g P; inside ones 0.1 ± 0.1 ng HSP70/ μ g P, $F(3, 12) = 2.88$, $P < 0.048$, power of test = 0.99). However, HSP70 levels were low compared with other situations (interactions with calcareous algae or other *A. elegantissima* clones). No differences in HSP70 level were found with the *B. amphitrite* interactions (outside 0.5 ± 0.6 ng HSP70/ μ g P; inside 0.4 ± 0.4 ng HSP70/ μ g P).

Differences in *C. californica* HSP70 levels occurred when potential encounters and fights for space were against the sponge *Haliclona permollis* or the ascidian *Synoicum parfustis* (Fig. 6B). HSP70 expression was the same in the outside and inside polyps, but was slightly higher than with other competitors. Both sponge and ascidian appear to activate higher HSP70 expression (*H. permollis* outside 3.1 ± 0.5 ng HSP70/ μ g P; inside 2.5 ± 0.5 ng HSP70/ μ g P; *S. parfustis* outside 2.4 ± 1.0 ng HSP70/ μ g P; inside 1.8 ± 0.6 ng HSP70/ μ g P). Again, no significant differences were found between inside and outside polyps. When comparing the response of this cnidarian against the sponge and the ascidian with all the other encounters, significant HSP70 differences were found ($F(5, 79) = 18.58$, $P < 0.00001$). HSP70 expression in the sponge and ascidian

encounters was 2.2 ± 0.7 ng HSP70/ μ g P, and in all the other encounters (*A. elegantissima* and *C. californica*, calcareous and fleshy algae) the HSP70 level was 1.3 ± 0.6 ng HSP70/ μ g P.

Discussion

Anthopleura elegantissima and *Corynactis californica* express HSP70 without physical stress (e.g., from temperature, desiccation, changes in pH) or pollution stress (e.g., due to heavy metals, organochlorines). There are few examples of cnidarian HSP expression patterns, and all are directly (Bosch *et al.*, 1988; Bosch and Praetzel, 1991; Sharp *et al.*, 1994) or indirectly (Hayes and King, 1995; Sharp *et al.*, 1997; coral bleaching) related to temperature stress. This is the first set of observations relating aquatic invertebrate HSP levels to biological stress and relating cnidarian HSP expression to parameters other than temperature.

There were significant differences in HSP70 levels between the two cnidarians, and these depended on the particular competing species. Perhaps the aggressive behavior of *C. californica* (Chadwick, 1987, 1991; Chadwick and Adams, 1991) causes cellular damage, thereby increasing HSP70 expression levels in *A. elegantissima* tentacles (Fig. 2) in the first aquarium experiments. *C. californica* extrudes mesenterial filaments upon contact with nonfood species, suggesting that this behavior is used in interspecies aggressive encounters (Chadwick, 1987; Chadwick and Adams, 1991). Prolonged contact with *C. californica* mesenterial filaments kills the competitor. In this forced situation, no stresses other than contact between polyps appear to affect the tentacles of both cnidarians. In comparison with isolated (non-interacting) *A. elegantissima* polyps (Fig. 2), the expression of HSP70 is nearly 20 times greater after 48 h of interspecific interactions. The differences shown between tentacle crown and whole body in *A. elegantissima* were not found in *C. californica*.

The more striking result is the lack of differences between the solitary and interacting *C. californica* polyps in the aquarium experiences (in Fig. 2, compare 24 and 48 h). The expression of HSP70 is high and very constant in the three interspecific encounters (1.3–2.1 ng HSP70/ μ g P). One explanation could be that the aggressive behavior of some corallimorpharians requires cellular protection to counter the effect of the competing species' response (Chadwick, 1987; Langmead and Chadwick, 1999a, b). After a period of contact with *C. californica*, *A. elegantissima* moved away via pedal locomotion, suggesting that the specialized aggressive structures of the anemone were ineffective against the corallimorpharian (Francis, 1973a, b; Chadwick, 1987).

Strong intraspecific competition has been clearly demonstrated between clones of *A. elegantissima* (Francis, 1973a,

b; Ayre and Grossberg, 1995, 1996). Contact between genetically different individuals of this species initiates elaborate behaviors involving acrorhagial contact (leaving patches of tissue containing high numbers of nematocysts) and results in damage to one or both competitors. In addition, anemones of the genus *Anthopleura*, including *A. xanthogrammica* (discussed below), produce cytolytic and sodium-channel toxins that presumably damage cellular constituents such as proteins following contact (Bernheimer and Lai, 1985; Cline and Wolowyk, 1997; Kelso and Blumenthal, 1998). These toxic mechanisms could explain the high HSP70 levels found in the examined clones (Fig. 3). The outside warrior polyps bordering neighboring clones have more HSP70 than the inside ones. Sessile organisms discontinuously fight for space, depending on growth and reproductive cycles, the age of competitors, or the nature of the enemies (Connell, 1961; Jackson, 1977; Chadwick, 1991). Perhaps when warrior polyps encounter a "known" competitor (i.e., in this case a different clone of the same species), they become "prepared for war," producing HSP70 levels high enough to avoid serious cellular damage when real interactions begin. Alternatively, some interactions have already caused some tissue damage, resulting in higher HSP70.

No differences in HSP70 expression were expected in interactions between *A. elegantissima* and a fleshy green alga (*Ulva* sp., Fig. 5B). This algal type escapes from direct competition for space by growing as rapidly as nutrients and light levels permit (Lewis, 1964; Paine, 1971). No direct interactions were evident, and the low HSP70 levels found in the outside interacting polyps of these clones seem to confirm their absence, although algae in this genus are capable of producing harmful secondary compounds (Paine, 1990; Whitfield *et al.*, 1999). In the case of *Lithothamnium* sp. (Fig. 5A), it is known that coralline algae grow slowly (Steneck, 1986; Garrabou and Ballesteros, 2000) and can synthesize allelochemicals (as do some other red algae) to compete for space (Whitfield *et al.*, 1999). Perhaps the anemone better detects or is more affected by these *Lithothamnium* chemicals than by those produced by *Ulva*.

A. xanthogrammica is a common intertidal competitor with *A. elegantissima* for space (Francis, 1973b; Sebens, 1984). This solitary anemone elicits aggression in *A. elegantissima* (Francis, 1973b) but does not display the same mechanisms of defense. Observations made by Sebens (1984) support the idea that aggression is common between these two species, which explains the higher levels of HSP70 in the outside *A. elegantissima* polyps in these interactions (Fig. 6A). *Balanus amphitrite*, another common space competitor, seems to have no effect on HSP70 expression (Fig. 6A). It is possible that the lack of effect was due to exposure to small individual cirripeds, and it would be interesting to examine *A. elegantissima* clones that are in competition for space with larger clumps of barnacles.

In *C. californica*, HSP70 levels are similar in outside and inside clone polyps. Therefore the corallimorpharian does not distinguish between the exposed (outside polyps) and nonexposed (inside polyps) areas of the clone. More importantly, even without apparent interactions (Fig. 2), *C. californica* expresses HSP70 at constant levels (1–2 ng HSP70/ μg P). In this species, intraspecific competition results in HSP70 levels that are within the “normal” range (Fig. 3), and there is no aggressive behavior in intraspecific contacts (Chadwick, 1987). Perhaps the key to interpreting HSP70 expression as a mechanism of competence in *C. californica* is the finding that the highest HSP70 levels were found in polyps interacting with *Haliclona* or *Syonicum* (Fig. 6B). Also of importance is that these differences between interacting and non-interacting polyps were significant. It is known that sponges and ascidians use chemical substances to defend themselves or attack potential foes competing for substrata (Green, 1977; Suchanek *et al.*, 1985; Thompson *et al.*, 1985; Turon *et al.*, 1996, 1998; Becerro *et al.*, 1997). We suggest that HSP70 expression differences found when the encounter involves ascidians or sponges may reflect the aggressive toxic substances used by these enemies (Uriz *et al.*, 1991).

C. californica appears to be always “prepared for war” by its aggressive behavior (Chadwick, 1991). Another organism that exhibits this strategic use of stress proteins (by maintaining a basal level of HSP expression) is the desert-dwelling ant *Cataglyphis*. This ant presynthesizes HSPs at relatively low nest temperatures to limit damage from heat shock on the desert floor. Coupled with continued HSP production at higher temperatures, this protects the ant from the high temperatures it experiences when foraging in daytime (Gehring and Wehner, 1995). Perhaps the presynthesis of HSP70 in *C. californica* provides protection from neighbors that intermittently excrete harmful substances. Alternatively, the constant HSP70 levels might protect the corallimorpharian against its own aggressive substances, which it uses to catch prey and to fight for space (Chadwick, 1987). The aggressive behavior of *C. californica* includes the extrusion of mesenteric filaments containing gland cells that secrete strong proteolytic enzymes and nematocysts that may inject cytolytic toxins into prey or enemies (Van Praet, 1985).

Because of the high cost of the HSP expression and its occasional harmful effect if constantly highly expressed (Feder *et al.*, 1992; Krebs and Feder, 1997), we suggest that expression varies depending on the kind of neighboring competitor or enemy. Furthermore, *A. elegantissima* also expresses high levels of HSP70 in response to physical factors, especially temperature (Rossi and Snyder, unpubl. obs.). The anemone has to “share” HSP70 expression between biological (*e.g.*, competition for space) and physical (*e.g.*, temperature) factors.

It is also possible that other stress proteins contribute to

the responses against biological phenomena such as competitive interactions for space in the benthic environment. For example, unexpected low-molecular-weight HSP70 homologs have been found in other cnidarians (Sharp *et al.*, 1994). HSP60 has known roles in thermal acclimation of the cnidarians *Hydra vulgaris* and *Acropora grandis* (Bosch *et al.*, 1988; Fang *et al.*, 1997). The use of SPA-822 HSP70 antiserum can possibly underestimate the number of HSP70 isoforms, and consequently may explain the finding of single HSP70 proteins by our methods. However, we have successfully used the same antiserum and measured two and three to four different HSP70 isoforms in larval lobsters, (*Homarus americanus*), and juvenile abalone (*Haliotis rufescens*) and adult mussels (*Mytilus galloprovincialis*) respectively (Snyder and Mulder, 2001; Snyder *et al.*, 2001).

Many questions remain unanswered, such as the identity of the harmful substances or aggressive behaviors that activate HSP70 expression in competitive interactions among sessile marine invertebrates. Among the likely candidates for cellular damaging allelochemicals are cnidarian sodium-channel toxins (Kelso and Blumenthal, 1998), cytotoxic and cytolytic factors (Bernheimer and Lai, 1985; Cline and Wolowyk, 1997), and an array of toxic alkaloids found in cnidarians and sponges (*e.g.*, Djura and Faulkner, 1980; Koh and Sweatman, 2000). Such chemicals can diffuse and act at some distance from the source or can be deposited on neighboring organisms by direct contact (*e.g.*, Schmitt *et al.*, 1995; Slatery *et al.*, 1997). Further studies of HSP proteins may provide important information about the consequent distribution and hierarchy of species in the rocky benthos.

With this work we propose HSP70 expression as a tool for evaluating space competition among sessile marine invertebrates, without manipulative experiments. From our results, it is clear that the expression of the stress proteins depends on both the particular competing species and the interacting life stages of each competitor. The energy required to repair tissue damage cannot be used for other processes such as reproduction and growth. It will be interesting to measure how the amount of energy an organism devotes to growth and reproduction varies with the level of HSP produced during prolonged competition for space.

Acknowledgments

The manuscript was improved by the comments of Drs. Josep-María Gili, Cadet Hand, and several anonymous reviewers. This work was supported by the National Sea Grant College Program, National Oceanic and Atmospheric Administration, U.S. Department of Commerce, under grant number NA66RG0477, project number R/A-108, through the California Sea Grant College Program and an F.P.I. fellowship from “Ministerio de Educación y Ciencia” to S.R. through the DGICYT grants PB94-0014-C02-01 and

PB98-0496-C03-01. The views expressed herein are those of the authors and do not necessarily reflect the views of NOAA or any of its sub-agencies. The U.S. Government is authorized to reproduce and distribute this publication for governmental purposes. Contribution 2136 from the Bodega Marine Laboratory, University of California at Davis.

Literature Cited

- Ayre, D. J., and R. K. Grosberg. 1995. Aggression, habituation, and clonal coexistence in the sea anemone *Anthopleura elegantissima*. *Am. Nat.* **146**: 427–453.
- Ayre, D. J., and R. K. Grosberg. 1996. Effects of social organization on inter-clonal dominance relationships in the sea anemone *Anthopleura elegantissima*. *Anim. Behav.* **51**: 1233–1245.
- Becerro, M. A., X. Turon, and M. J. Uriz. 1997. Multiple functions for the secondary metabolites in encrusting marine invertebrates. *J. Chem. Ecol.* **23**: 1527–1547.
- Bernheimer, A. W., and C. Y. Lai. 1985. Properties of a cytolytic toxin from the sea anemone. *Stoichacys kenti*. *Toxicon* **23**: 791–800.
- Bosch, T. C. G., and G. Praetzel. 1991. The heat shock response in *Hydra*: immunological relationships of hsp60, the major heat shock protein of *Hydra vulgaris*, to the ubiquitous hsp70 family. *Hydrobiologia* **216/217**: 513–517.
- Bosch, T. C. G., S. M. Krylow, H. R. Bode, and R. E. Steele. 1988. Thermotolerance and synthesis of heat shock proteins; these responses are present in *Hydra attenuata* but absent in *Hydra oligactis*. *Proc. Natl. Acad. Sci. USA* **85**: 7927–7931.
- Chadwick, N. E. 1987. Interspecific aggressive behavior of the corallimorpharian *Corynactis californica* (Cnidaria: Anthozoa): effects on sympatric corals and sea anemones. *Biol. Bull.* **173**: 110–125.
- Chadwick, N. E. 1991. Spatial distribution and the effects of competition on some temperate Scleractinia and Corallimorpharia. *Mar. Ecol. Prog. Ser.* **70**: 39–48.
- Chadwick, N. E., and C. Adams. 1991. Locomotion, asexual reproduction and the killing of corals by the corallimorpharian *Corynactis californica*. *Hydrobiologia* **216/217**: 263–269.
- Chornesky, E. A. 1983. Induced development of sweeper tentacles on the reef coral *Agaricia agaricites*: a response to direct competition. *Biol. Bull.* **165**: 569–581.
- Cline, E. I., and M. W. Wołowyk. 1997. Cardiac stimulatory, cytotoxic and cytolytic activity of extracts of sea anemones. *Int. J. Pharmacogn.* **35**: 91–98.
- Connell, J. H. 1961. The influence of interspecific competition and other factors on the distribution of the barnacle *Chthamalus stellatus*. *Ecology* **42**: 315–328.
- Dayton, P. K. 1971. Competition, disturbance, and community organization: the provision and subsequent utilization of space in a rocky intertidal community. *Ecol. Monogr.* **41**: 351–389.
- Djura, P., and D. J. Faulkner. 1980. Metabolites of the marine sponge *Dercitus* sp. *J. Org. Chem.* **45**: 735–737.
- Fang, L.-s., S.-p. Huang, and K.-l. Lin. 1997. High temperature induces the synthesis of heat-shock proteins and the elevation of intracellular calcium in the coral *Aeropora grandis*. *Coral Reefs* **16**: 127–131.
- Feder, M. E., and G. E. Hofmann. 1999. Heat-shock proteins, molecular chaperones, and the stress response: evolutionary and ecological physiology. *Annu. Rev. Physiol.* **61**: 243–282.
- Feder, M. E., J. M. Rossi, J. Solomon, N. Solomon, and S. Lindquist. 1992. The consequences of expressing *hsp70* in *Drosophila* cells at normal temperatures. *Genes Dev.* **6**: 1402–1413.
- Fitt, W. K., R. L. Pardy, and M. M. Littler. 1982. Photosynthesis, respiration, and contribution to community productivity of the symbiotic sea anemone *Anthopleura elegantissima* (Brandt, 1835). *J. Exp. Mar. Biol. Ecol.* **61**: 213–232.
- Francis, L. 1973a. Clone specific segregation in the sea anemone *Anthopleura elegantissima*. *Biol. Bull.* **144**: 64–72.
- Francis, L. 1973b. Intraspecific aggression and its effect on the distribution of *Anthopleura elegantissima* and some related sea anemones. *Biol. Bull.* **144**: 73–92.
- Francis, L. 1976. Social organization within clones of the sea anemone *Anthopleura elegantissima*. *Biol. Bull.* **150**: 361–376.
- Garrabou, J., and J. Ballesteros. 2000. Growth of *Mesophyllum alternans* and *Lithophyllum frondosum* (Corallines, Rhodophyta) in the northwestern Mediterranean. *Eur. J. Phycol.* **35**: 1–10.
- Gehring, W. J., and R. Wehner. 1995. Heat shock protein synthesis and thermotolerance in *Cataglyphis*, an ant from the Sahara desert. *Proc. Natl. Acad. Sci. USA* **92**: 2994–2998.
- Green, G. 1977. Ecology of toxicity in marine sponges. *Mar. Biol.* **40**: 207–215.
- Hayes, R. L., and C. M. King. 1995. Induction of 70-kD heat shock protein in scleractinian corals by elevated temperature: significance for coral bleaching. *Mol. Mar. Biol. Biotechnol.* **4**: 36–42.
- Ireland, C. M., D. M. Roll, T. F. Molinski, T. C. McKee, T. M. Zahriskie, and J. C. Swersey. 1988. Uniqueness of the marine chemical environment: categories of marine natural products from invertebrates. Biomedical importance of marine organisms. *Mem. Calif. Acad. Sci.* **13**: 41–57.
- Jackson, J. B. C. 1977. Competition on marine hard substrata: the adaptive significance of solitary and colonial strategies. *Am. Nat.* **111**: 743–767.
- Kelso, G. J., and K. M. Blumenthal. 1998. Identification and characterization of novel sodium channel toxins from the sea anemone *Anthopleura xanthogrammica*. *Toxicon* **36**: 41–51.
- Koh, E. G. L., and H. Sweatman. 2000. Chemical warfare among scleractinians: bioactive natural products from *Tubastraea faulkneri* Wells kill larvae of potential competitors. *J. Exp. Mar. Biol. Ecol.* **251**: 141–160.
- Krebs, R., and M. E. Feder. 1997. Deleterious consequences of Hsp70 overexpression in *Drosophila melanogaster* larvae. *Cell Stress Chaperones* **2**: 60–71.
- Laemmli, U. K. 1970. The cleavage of structural proteins during assembly of the head of bacteriophage T4. *Nature* **227**: 680–685.
- Langmead, O., and N. E. Chadwick. 1999a. Marginal tentacles of the corallimorpharian *Rhodactis rhodostoma*. 1. Role in competition for space. *Mar. Biol.* **134**: 479–489.
- Langmead, O., and N. E. Chadwick. 1999b. Marginal tentacles of the corallimorpharian *Rhodactis rhodostoma*. 2. Induced development and long-term effects on coral competitors. *Mar. Biol.* **134**: 491–500.
- Lewis, J. R. 1964. *The Ecology of Rocky Shores*. English Universities Press, London.
- McCain, B. B., D. W. Brown, M. M. Krahn, M. S. Myers, R. C. Clark, S.-L. Chan, and D. C. Malins. 1988. Marine pollution problems, North American West Coast. *Aquat. Toxicol.* **11**: 143–162.
- Paine, R. T. 1971. A short-term experimental investigation of resource partitioning in a New Zealand rocky intertidal habitat. *Ecology* **52**: 1096–1106.
- Paine, R. T. 1990. Benthic macroalgal competition: complications and consequences. *J. Phycol.* **26**: 12–17.
- Pequegnat, W. E. 1964. The epifauna of a California siltstone reef. *Ecology* **45**: 272–283.
- Roberts, D. A., G. E. Hofmann, and G. N. Somero. 1997. Heat shock protein expression in *Mytilus californianus*: acclimatization (seasonal and tidal-height comparisons) and acclimation effects. *Biol. Bull.* **192**: 309–320.
- Schmitt, T. M., M. E. Hay, and N. Lindquist. 1995. Constraints on

- chemically mediated coevolution: multiple functions for seaweed secondary metabolites. *Ecology* **76**: 107–123.
- Schoener, T. W. 1983. Field experiments on interspecific competition. *Am. Nat.* **122**: 240–285.
- Sebens, K. P. 1982a. The limits to indeterminate growth: an optimal size model applied to passive suspension feeders. *Ecology* **63**: 209–222.
- Sebens, K. P. 1982b. Asexual reproduction in *Anthopleura elegantissima* (Anthozoa:Actinaria): seasonality and spatial extent of clones. *Ecology* **63**: 434–444.
- Sebens, K. P. 1984. Agonistic behavior in the intertidal sea anemone *Anthopleura xanthogrammica*. *Biol. Bull.* **166**: 457–472.
- Sharp, V. A., D. Miller, J. C. Bythell, and B. E. Brown. 1994. Expression of low molecular weight HSP 70 related polypeptides from the symbiotic sea anemone *Anemonia viridis* Forskall in response to heat shock. *J. Exp. Mar. Biol. Ecol.* **179**: 179–193.
- Sharp, V. A., B. E. Brown, and D. Miller. 1997. Heat shock protein (HSP70) expression in the tropical reef coral *Goniopora djiboutiensis*. *J. Therm. Biol.* **22**: 11–19.
- Slattery, M., M. T. Hamann, J. B. McClintock, T. L. Perry, M. P. Pnglisi, and W. Y. Yoshida. 1997. Ecological roles for water-borne metabolites from Antarctic soft corals. *Mar. Ecol. Prog. Ser.* **161**: 133–144.
- Snyder, M. J., and E. P. Mulder. 2001. Environmental endocrine disruption in decapod crustacean larvae: Hormone titers, cytochrome P450, and stress proteins. *Aquat. Toxicol.* **55**: 177–190.
- Snyder, M. J., E. Girvetz, and E. P. Mulder. 2001. Stress protein induction by chemical exposures in molluscs. *Arch. Environ. Contam. Toxicol.* **41**: 22–29.
- Steneck, R. S. 1986. The ecology of coralline algal crusts: convergent patterns and adaptative strategies. *Annu. Rev. Ecol. Syst.* **17**: 273–303.
- Suchanek, T. H., R. C. Carpenter, J. D. Witman, and C. D. Harvell. 1985. Sponges as important space competitors in deep Caribbean coral reef communities. Pp. 55–59 in *The Ecology of Deep and Shallow Coral Reefs*, M. L. Reaka, ed. *Symposia Series for Undersea Research* 3(1), NOAA/NURP, Rockville, MD.
- Sutherland, J. P. 1978. Functional roles of *Schizoporella* and *Styela* in the fouling community at Beaufort, North Carolina. *Ecology* **59**: 257–264.
- Thompson, J. E., R. P. Walker, and D. J. Faulkner. 1985. Screening and bioassays for biologically-active substances from forty marine sponge species from San Diego, California USA. *Mar. Biol.* **88**: 11–21.
- Turon, X., M. A. Becerro, M. J. Uriz, and J. Llopis. 1996. Small-scale associations measures in epibenthic communities as a clue for allelochemical interactions. *Oecologia* **108**: 351–360.
- Turon, X., J. Tarjuelo, and M. J. Uriz. 1998. Growth dynamics and mortality of the encrusting sponge *Crambe crambe* (Poecilosclerida) in contrasting habitats: correlation with population structure and investment in defense. *Funct. Ecol.* **12**: 631–639.
- Uriz, M. J., D. Martín, X. Turón, E. Ballesteros, R. Hughes, and C. Acebal. 1991. An approach to the ecological significance of chemically mediated bioactivity in Mediterranean benthic communities. *Mar. Ecol. Prog. Ser.* **70**: 175–188.
- Van-Praet, M. 1985. Nutrition of sea anemones. *Adv. Mar. Biol.* **22**: 65–99.
- Weis, V. M., and R. P. Levine. 1996. Differential protein profiles reflect the different lifestyles of symbiotic and aposymbiotic *Anthopleura elegantissima*, a sea anemone from temperate waters. *J. Exp. Biol.* **199**: 883–892.
- Whitfield, F. B., F. Helidoniotis, K. J. Shaw, and D. Svoronos. 1999. Distribution of bromophenols in species of marine algae from eastern Australia. *J. Agric. Food Chem.* **47**: 2367–2373.
- Whittaker, R. H., and P. P. Feeny. 1973. Allelochemicals: chemical interaction between species. *Science* **171**: 757–768.
- Wiens, M., C. Koziol, H. M. A. Hassanein, R. Batel, H. C. Schröder, and W. E. G. Müller. 1998. Induction of gene expression of the chaperones 14-3-3 and HSP70 by PCB 118 (2,3',4,4',5-pentachlorobiphenyl) in the marine sponge *Geodia cydonium*: novel biomarkers for polychlorinated biphenyls. *Mar. Ecol. Prog. Ser.* **165**: 247–257.

NO/cGMP Signaling and HSP90 Activity Represses Metamorphosis in the Sea Urchin *Lytechinus pictus*

CORY D. BISHOP AND BRUCE P. BRANDHORST*

*Department of Molecular Biology and Biochemistry, Simon Fraser University,
Burnaby, British Columbia V5A 1S6, Canada*

Abstract. Nitric oxide (NO) signaling repressively regulates metamorphosis in two solitary ascidians and a gastropod. We present evidence for a similar role in the sea urchin *Lytechinus pictus*. NO commonly signals *via* soluble guanylyl cyclase (sGC). Nitric oxide synthase (NOS) activity in some mammalian cells, including neurons, depends on the molecular chaperone heat shock protein 90 (HSP90); this may be so in echinoid larvae as well. Pluteus larvae containing juvenile rudiments were treated with either radicicol L- or D-nitroarginine-methyl-ester (L-NAME and D-NAME), or 1H-[1,2,4]oxadiazolo[4,3-a]quinoxalin-1-one (ODQ), inhibitors of HSP90, NOS, and sGC, respectively. In all instances, drug treatment significantly increased the frequency of metamorphosis. SNAP, a NO donor, suppressed the inductive properties of L-NAME and biofilm, a natural inducer of metamorphosis. NADPH diaphorase histochemistry indicated NOS activity in cells in the lower lip of the larval mouth, the preoral hood, the gut, and in the tube feet of the echinus rudiment. Histochemical staining coincided with NOS immunostaining. Microsurgical removal of the oral hood or the pre-oral hood did not induce metamorphosis, but larvae lacking these structures retained the capacity to metamorphose in response to ODQ. We propose that the production of NO repressively regulates the initiation of metamorphosis and that a sensory response to environmental cues reduces the production of NO, and consequently cGMP, to initiate metamorphosis.

Introduction

Many species of sea urchin undergo maximal indirect development (Davidson, 1991). Embryonic development generates a bilaterally symmetrical feeding pluteus larva that bears no resemblance to an adult sea urchin. After a period of growth in the plankton, an adult rudiment forms on the left side of the larva, within the vestibule. Once competence is reached, and in response to appropriate cues, the pluteus larva settles and undergoes a radical transformation into a pentaradially symmetrical juvenile sea urchin. The initial events of this transformation, as described for *Lytechinus pictus*, are completed within an hour (Cameron and Hinegardner, 1974, 1978; Pearse and Cameron, 1991). Briefly, the larval arms bend away from the vestibule, from which the tube feet of the rudiment extend, allowing podial attachment to the substratum. The rudiment becomes exposed to the exterior and then everts. The larval epithelium, including that of the arms, contracts and collapses onto the aboral surface of the juvenile, involving drastic changes in cell shape. The vestibular epithelium extends to cover the aboral surface, forming the epithelium of the juvenile and enclosing degenerating larval cells. Extensive remodeling of internal structures such as the digestive tract continue for several days as the juvenile begins the reproductive stage of its life cycle as a benthic feeder.

Competent echinoid larvae will settle and initiate metamorphosis if provided with a hard surface covered with an appropriate organic film, particularly a microbial film (reviewed by Strathmann, 1987; Pearse and Cameron, 1991; also see Discussion). In the absence of such cues, some species delay metamorphosis (Caldwell, 1972; Cameron and Hinegardner, 1974). When placed in clean glass or plastic dishes with fresh seawater, *L. pictus* larvae rarely metamorphose. This allows experimental investigation of the induction of metamorphosis. The mechanism by which

Received 17 November 2000; accepted 7 September 2001.

* To whom correspondence should be addressed. Email: brandhor@sfu.ca

Abbreviations: D-NAME, D-nitroarginine-methyl-ester; GA, geldanamycin; GBD, geldanamycin binding domain; HSP90, heat shock protein 90; L-NAME, L-nitroarginine-methyl-ester; NO, nitric oxide; NOS, nitric oxide synthase; ODQ, 1H-[1,2,4]oxadiazolo[4,3-a]quinoxalin-1-one; RD, radicicol; sGC, soluble guanylyl cyclase; SNAP, S-nitroso-N-acetylpenicillamine.

external cues are detected and transduced into the initiation of metamorphosis remains poorly understood, but apparently involves a neurosensory response. Further, it is not clear whether larval or juvenile sensory perception (or both) is responsible for transducing external signals under natural conditions. Evidence for the involvement of neural responses from both the larva and the juvenile has been reported. Electrical stimulation of the oral ganglion or the apical neuropile of *Dendroaster excentricus* larvae induced metamorphosis (Burke, 1983). In contrast, observation of settling behaviors and the prevention of settling (and consequently of metamorphosis) in the presence of inducers clearly demonstrates a role for the juvenile sensory apparatus in *L. pictus* (Cameron and Hinegardner, 1974; Burke, 1980; our observations). Investigations of the molecular and anatomical basis of signaling events that regulate echinoid metamorphosis can thus be placed in this historical context.

Nitric oxide synthase (NOS) catalyzes the conversion of L-arginine to L-citrulline with the production of the gas nitric oxide (NO). NOS expression and NO function have been documented in both nervous and non-nervous tissues alike across a range of eukaryotic organisms, indicating their antiquity and importance in regulating many cellular processes (Schulte *et al.*, 1998; Cueto *et al.*, 1996; Kuzin *et al.*, 1996; Czar *et al.*, 1997). That NO is diffusible through biological membranes suggests that it may have served as a primitive signaling system between cells before more elaborate mechanisms of cell adhesion and receptor-based signaling evolved. In mammalian cells, NOS activity *in vivo* requires interaction with heat shock protein 90 (HSP90) (Garcia-Cardena *et al.*, 1998; Bender *et al.*, 1999). We recently reported that metamorphosis of two species of ascidian tadpole larvae is induced by drugs that inhibit the activity of the protein chaperone HSP90, NOS, or soluble guanylyl cyclase (sGC) (Bishop *et al.*, 2001). Among larval tissues, NOS activity is concentrated in the tail muscle cells of the ascidian tadpole *Cnemidocarpa finmarkiensis*. Removal of the tail stimulates metamorphosis of the head, consistent with there being a signal, probably NO, from the tail that represses metamorphosis. NOS produces NO, a gaseous signaling molecule whose most common effector is sGC (Garthwaite *et al.*, 1995; Salter *et al.*, 1996; Hebeiss and Kilbinger, 1998). Thus, inhibition of NOS often results in a corresponding reduction of cGMP (McDonald and Murad, 1996, for review). Metamorphosis of the marine gastropod *Ilyanassa obsoleta* was also reported to be induced by inhibition of NOS activity (Froggett and Leise, 1999), indicating that NO may repress metamorphosis in a variety of animals.

To further test the idea that NO-mediated repression of metamorphosis occurs widely within the bilaterian clade, we used the sea urchin *L. pictus*. We report that NO/cGMP signaling is an important regulator of the events surrounding the transition of form from the larva to the juvenile in *L.*

pictus, that it is downstream from a natural inductive cue, and that this regulation may be dependent upon HSP90 function. NOS was detected in both larval and juvenile organs; such organs may be involved in sensing or transducing the response to natural inductive cues.

Materials and Methods

Obtaining and culturing larvae

Specimens of *Lytechinus pictus* were purchased from Marinus (Long Beach, CA) and held in recirculating seawater tanks. Eggs were induced to shed by intracoelomic injection of 0.5 mol KCl, then washed and fertilized. Embryos in Millipore (0.45 μ m) filtered seawater (MFSW) at 16 °C containing 50 μ g/ml penicillin and streptomycin were continuously stirred at 20 or 60 rpm using plastic paddles. After hatching, the embryos were collected by filtration on 93- μ m-mesh Nitex and resuspended in fresh MFSW; this washing procedure was repeated frequently throughout larval growth, and the concentration of larvae was gradually reduced to 1/ml or less. Algae were obtained from the Northeast Pacific Culture Collection (NEPCC) at the University of British Columbia, Vancouver. Either a mix of *Pyrenomonas salina* (NEPCC strain 076; Center for Culture of Marine Phytoplankton (CCMP) strain 3C) and *Dunaliella tertiolecta* (NEPCC strain 001; CCMP strain 1320) or only the latter were fed to plutei every 2-3 days in quantities such that most algae had been ingested as of the next feeding.

Pharmacological inhibition

L-NAME (L-nitroarginine-methyl-ester) and its enantiomer D-NAME, radicicol (RD), and ODQ (1H-[1,2,4]oxadiazolo[4,3-a]quinoxalin-1-one) were obtained from Sigma Chemical Corp. (St. Louis, MO). Because there is variation in the rate of development of the juvenile rudiment, individual *L. pictus* plutei were selected by examination under a stereomicroscope and transferred to wells of 24-well plastic culture dishes (Flow Labs, McLean, VA). Larvae were selected for experiments based on the presence of a large, pigmented rudiment having well developed spines and tube feet. Each well contained about 10 larvae in 2 ml MFSW or experimental solutions in MFSW. To quadruplicate sets of these selected larvae were added L-NAME, D-NAME, RD, ODQ, or MFSW in 1- or 2-ml final volumes. Metamorphosis was monitored using a stereomicroscope; it was scored if the larval epithelium had collapsed on top of an everted juvenile. The activity of tube feet was used as an indicator of larval vitality. The concentrations of L-NAME, RD, and ODQ used in the experiments reported here were chosen because they elicited a metamorphic response in ascidian larvae (Bishop *et al.*, 2001). L-NAME and D-NAME were prepared as 1 M stocks in water and diluted to a final concentration of 1-10 mM with MFSW. ODQ was prepared

as a 100 mM stock in DMSO and diluted into MFSW to 50 μ M. RD was prepared as a 5 mM stock in DMSO and diluted into MFSW to 5 μ M. SNAP (S-nitroso-N-acetylpenicillamine) was prepared as a 100 mM stock in DMSO and diluted to 0.1 mM in MFSW. For RD, ODQ, and SNAP treatments, experimental and control wells all contained a final concentration of 0.1% DMSO; this concentration of DMSO did not have any inductive properties. Unless significant metamorphosis was observed sooner, experiments were scored at 24, 48, and sometimes 72 h. A low frequency of spontaneous metamorphosis was observed for larvae placed in plastic dishes; this response tends to occur shortly after the assessment of a larvae and its transfer into a well. If such a response was observed before the addition of drugs, juveniles were removed.

To create a natural inductive cue, glass syracuse dishes were submerged for several days in recirculating tanks containing natural seawater. Ten larvae were exposed to the substrate in MFSW either in the presence or absence of 0.1 mM SNAP. Results shown are from a single experiment.

Microsurgical removal of oral hoods and pre-oral hoods was accomplished using a fine-edged stainless steel pin (Fine Science Tools, Vancouver, BC) fused to a glass pipette. Dissected oral and pre-oral hoods retained their capacity to swim. Quadruplicate sets of 5 larvae or hoods per well (a total of 20 operations) were used for each experiment.

All experiments were tested for statistical significance by performing a one-tailed Student's *t* test with the assumption of homoscedastic variance. In all graphs (made using Microsoft Excel 97), the asterisks denote statistical significance; *P* values are provided in the figure legends. Specific statistical comparisons are described in the figure legends.

NADPH histochemistry and NOS immunohistochemistry

The NADPH diaphorase staining protocol described by Weinberg *et al.* (1996) was used with modifications. Larvae were fixed in 2% glutaraldehyde and 1% formaldehyde in sodium phosphate buffer for 1 h at room temperature. Formaldehyde was freshly prepared by dissolving paraformaldehyde (EM grade, Ted Pella, CA) in MFSW, adjusting the pH to 7.4, and then diluting in PB to 1%. After rinsing with PB, fixed larvae were incubated in 0.4 mg/ml nitroretazolium blue substrate with 2 mg/ml NADPH from 2 to 16 h at 37 °C. As a negative control, specimens were incubated in 50% ethanol for 2 h and then incubated in nitroretazolium blue in the absence of NADPH; no staining was observed under these conditions. Under the fixation conditions used, NOS is the only diaphorase expected to be active (Weinberg *et al.*, 1996). Stained larvae were examined as whole mounts by microscopy or were dehydrated in a graded ethanol series, embedded in polyester wax (BDH Laboratory Supplies, Poole, England), and sectioned at 8 μ m.

Sectioned larvae were examined using an Olympus Vanox microscope, and images were captured using a Sony DXC-950 3CCD camera.

Universal anti-NOS (Affinity Bioreagents, Golden, CO) polyclonal rabbit antibody was used to detect NOS in growing and mature larvae. Larvae were fixed for 2 h at room temperature in 4% formaldehyde (prepared as outlined above). Fixed larvae were blocked with PB saline containing 5% bovine serum albumin and 0.1% Triton-X-100 and then incubated in 1:100 anti-NOS overnight at 4 °C. Larvae were incubated in secondary antibody (goat anti-rabbit-Alexa 568, Molecular Probes, Eugene OR) for 2 h at room temperature and then rinsed, mounted, and viewed on a Zeiss LSM 410 confocal microscope. Images were processed using Adobe Photoshop 5.5 or 6.0.

Results

Inhibitors of nitric oxide synthase, guanylyl cyclase, and HSP90 induce metamorphosis

Treatment of larvae with the NOS inhibitor L-NAME induced a significant increase in the frequency of metamorphosis in comparison with larvae treated with seawater (Fig. 1A) or D-NAME (Fig. 1B). In a time-course experiment, the frequency of metamorphosis was scored every hour for 6 h (Fig. 1B). Some larvae responded rapidly (within 2 h) to either L- or D-NAME but others required several hours. Because D-NAME is used as an inactive enantiomer of L-NAME, the observed inductive property of D-NAME was unexpected and substantial, although less so than for L-NAME (Fig. 1). To confirm that the inductive properties of L-NAME or D-NAME were due to a reduction in NO levels, larvae were co-incubated with L-NAME or D-NAME and the NO donor SNAP. At a 10-fold lower concentration than L-NAME or D-NAME, SNAP completely suppressed their inductive properties (Fig. 1A). In a variation of that experiment, SNAP was added 4 h after L-NAME had been added. This also resulted in the suppression of metamorphosis (Fig. 2).

Marine biofilms consisting of bacteria and other microorganisms have previously been shown to induce metamorphosis in *L. pictus* larvae (Cameron and Hindgardner, 1974). This is considered to be a cue that approximates that of a natural benthic environment. We exposed larvae to a biofilm grown in recirculating tanks (containing natural seawater from local sources) in the presence or absence of SNAP to test whether NO signaling was downstream of a sensory pathway that is responsive to a natural cue. SNAP suppressed the inductive properties of the biofilm in a reversible manner (Fig. 3). SNAP was effective at suppressing metamorphosis among larvae that had been exposed to biofilm for several hours, but had not yet metamorphosed (Fig. 3).

Soluble guanylyl cyclase (sGC) is the most common downstream effector of NO signaling (Salter *et al.*, 1996;

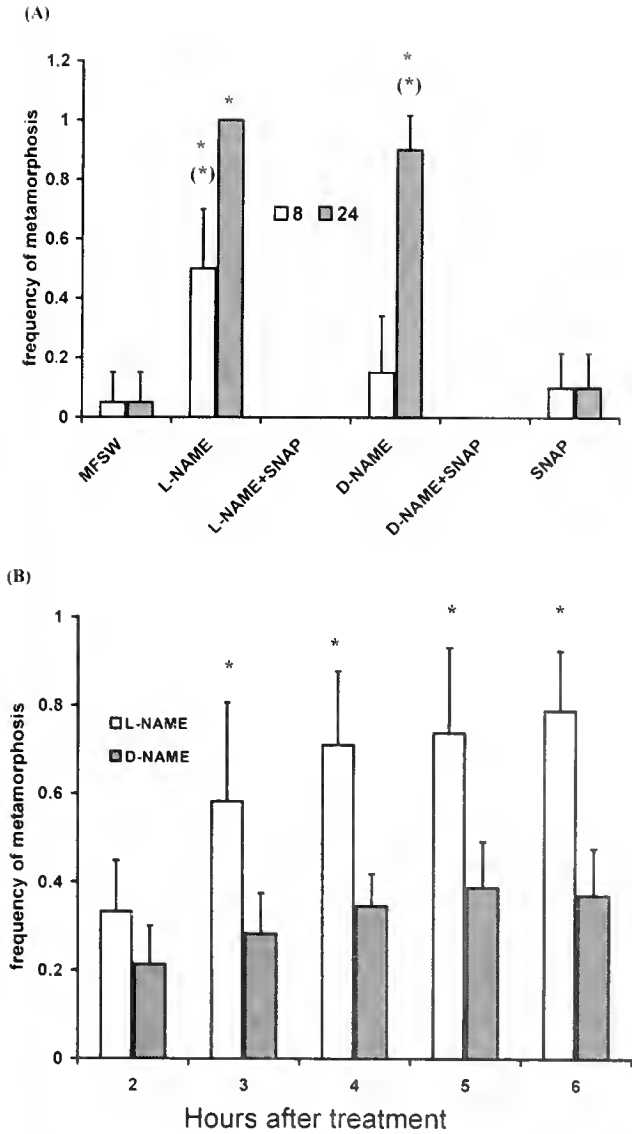


Figure 1. L-NAME and D-NAME treatments induce metamorphosis in a time-dependent fashion; SNAP suppresses their inductive properties. (A) Larvae were incubated in 1 mM L-NAME or D-NAME or co-incubated with 0.1 mM SNAP. The frequency of metamorphosis was scored after 8 and 24 h. Asterisks indicate a significant difference between larvae treated with L-NAME or D-NAME and seawater controls ($P_{1,8} < 0.004$; $P_{1,24} < 6.9 \times 10^{-7}$; $P_{1,24} < 3.2 \times 10^{-5}$; $n = 4$). Asterisks in parentheses indicate a significant difference between L-NAME and L-NAME + SNAP or D-NAME and D-NAME + SNAP ($P_{1,8} < 0.002$; $P_{1,24} < 3.0 \times 10^{-6}$; $n = 4$). The value from a statistical comparison between I_{24} and $I_1 + S_{24}$ cannot be calculated, since the respective means are 1 and 0 with no variation. (B) The frequency of metamorphosis was monitored the hour, for 6 h. Asterisks indicate a significant difference in the frequency of metamorphosis between larvae treated with 1 mM L-NAME or D-NAME. ($P_3 < 0.03$; $P_4 < 0.004$; $P_5 < 0.01$; $P_6 < 0.002$; $n = 4$).

Hebeiss and Kilbinger, 1998). To test the involvement of cGMP signaling in *L. pictus* metamorphosis, we incubated larvae in ODQ. There was a significant increase in the frequency of metamorphosis in comparison with controls in

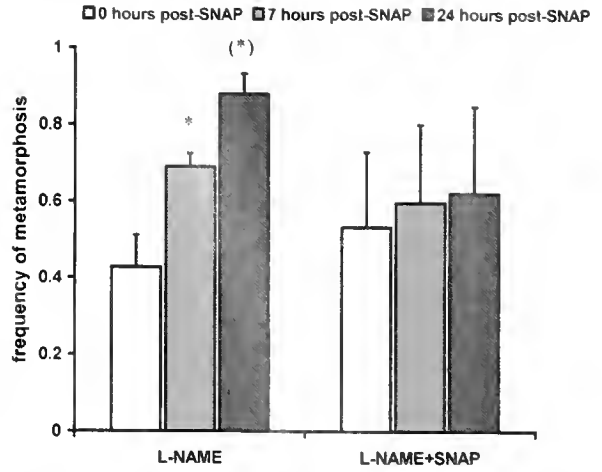


Figure 2. SNAP can suppress metamorphosis after the addition of L-NAME. Eight wells (10 larvae/well) were incubated with L-NAME. After 4 h, the frequency of metamorphosis reached approximately 0.5, then 0.1 mM SNAP was added to four of the wells. The frequency of metamorphosis was scored 7 and 24 h thereafter. The asterisk indicates a significant difference between time points in the frequency of metamorphosis among larvae treated with L-NAME ($P_{0,7h} < 0.02$; $P_{7,24h} < 0.0005$; $n = 4$). The asterisk in parentheses indicates a significant difference in the frequency of metamorphosis between larvae treated with L-NAME and L-NAME + SNAP after 24 h ($P_{24} < 0.03$).

MFSW (Fig. 4). In another experiment, larvae were treated with radicicol, an inhibitor of HSP90 function. Radicicol and geldanamycin frequently lead to a decrease in the activity or abundance of HSP90's client proteins (Yen *et al.*, 1994; Schulte *et al.*, 1998). Therefore, based on a hypothesized interaction of HSP90 and NOS in urchins, and the observation that inhibiting NOS activity induces metamorphosis, we expected that treatment with RD would increase

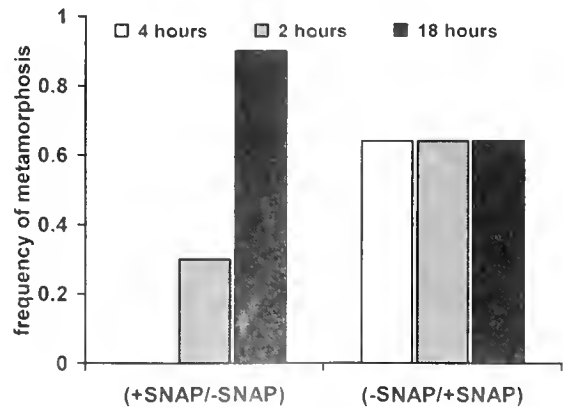


Figure 3. SNAP suppresses the inductive properties of biofilm in a reversible manner. Larvae were exposed to a biofilm in the presence or absence of 0.1 mM SNAP. After 4 h the conditions were reversed such that SNAP was washed out of the dish that contained it and added to the dish that lacked it. The frequency of metamorphosis was scored at 2 and 18 h thereafter (i. e., 6 and 22 h, respectively after initial exposure to biofilm). This experiment was not amenable to statistical analysis.

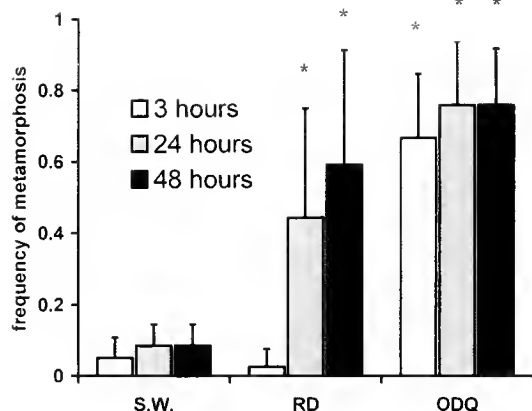


Figure 4. Inhibitors of HSP90 or sGC induce metamorphosis. Larvae were treated with 0.1% DMSO (control), 5 μ M RD, or 50 μ M ODQ. The frequency of metamorphosis was monitored after 3, 24, and 48 h. Asterisks indicate a significant difference in the frequency of metamorphosis of larvae treated with RD or ODQ compared to controls. ($P_{RD24} \leq 0.01$; $P_{RD48} \leq 0.02$; $n = 4$). ODQ caused a significant increase within 3 h ($P_{ODQ3} \leq 0.0004$; $n = 4$), with no further significant increase.

the frequency of metamorphosis over the untreated controls, and it did (Fig. 4). We have not measured directly whether RD reduces the activity of NOS.

NOS activity is present in neurons of larval tissues and tube feet of the rudiment

The NADPH diaphorase histochemical assay was used under conditions specific for vertebrate NOS enzymes. Whole larvae were stained and observed; some were then fixed and sectioned before examination by microscopy. Feeding larvae stained for diaphorase activity in the lower lip of the mouth, mid- and hindgut, at the tips of postoral arms, and in cells within the lobe between the anterolateral arms. These sites of NADPH diaphorase activity most likely represent sites of NOS activity. Larvae having large rudiments resembling those used for the inhibitor assays were also sectioned and stained. As shown in Figure 5, diaphorase activity was found in a variety of structures. Stained cells were found within the larval gut epithelium (Fig. 5A-C). The basioepithelial nerve plexus of juvenile tube feet was intensely stained and appeared to extend processes to the outer surfaces of the tube foot (Fig. 5D, E). Stained cells were observed at the tips of larval arms (Fig. 5F) and in the pre-oral hood (Fig. 5A). Stained cells, often having a neuronal appearance, were observed in epaulettes (Fig. 5G) and the lower lip of the larval mouth (Fig. 5H-J).

We stained larvae with anti-NOS antibodies to see whether sites of NADPH activity were coincident with the location of NOS. Prominent staining was observed in the lower lip of the mouth (Fig. 5K) and in some cells situated in the pre-oral hood (not shown). Stained cells in the lower lip are roughly symmetrically arranged around the pharyn-

geal lumen. The number of immunoreactive cells in the lower lip was variable from larva to larva. It is not clear if this perceived variation was due to variation in the actual number of NOS-positive cells in this region or in the sensitivity of immunostaining. Since the variation was observed among larvae in individual immunostaining experiments, the former possibility is more likely. To gain a three-dimensional perspective on the organization of NOS-positive cells in the lower lip of the mouth, serial optical sections were captured and projected as three-dimensional images (Fig. 5L, M). In agreement with histochemically stained sections, these cells extend processes toward the apical surface of the oral epithelium. We also saw a general correspondence between histochemical and immunohistochemical staining in other tissues (data not shown), indicating that sites of NADPH diaphorase activity correspond to sites of NOS expression.

Dendroaster excentricus pluteus larvae contain cells that express catecholamines in the lower lip of the mouth; this region was thus termed an oral ganglion (Burke, 1983). Removal of the oral hood (OH), which includes the oral ganglion, induced metamorphosis (Burke 1983). That observation and the expression of NOS in the oral ganglion cells of *L. pictus* larvae led to the hypothesis that these cells repress metamorphosis *via* their production of NO. To test this idea, we microsurgically removed either the entire OH or the pre-oral hood (PH) from mature larvae and scored the frequency of metamorphosis. This operation did not induce metamorphosis of *L. pictus* after 6 h (not shown), so L-NAME was added to see if larvae lacking the OH or the PH had retained their capacity to undergo metamorphosis. Neither postoperative larvae nor the OH and PH were responsive to L-NAME at concentrations that induced metamorphosis in intact control larvae (Fig. 6A). To further test if the postoperative larvae and the dissected tissues had retained the capacity to metamorphose, we added 50 μ M ODQ after 14 h of incubation in L-NAME. This resulted in a very rapid metamorphic response (Fig. 6A). The OH and PH did not initially undergo epithelial collapse typical of intact metamorphosing larvae, although they did so within 24 h (data not shown). Microscopic analysis indicated that the OH and PH were not necrotic, but rather they had undergone genuine cellular rearrangements characteristic of the epithelium of metamorphosing larvae. Therefore, microsurgical removal of the OH or the PH did not lead to metamorphosis of postoperative larvae, and apparently decreased their capacity to respond to NOS inhibition but not sGC inhibition. Dissected OH and PH tissues underwent rearrangements typical of metamorphosing larvae, but only after a protracted period in drug.

Discussion

Independent pharmacological inhibition of NOS, HSP90, and sGC led to a significant increase in the frequency of

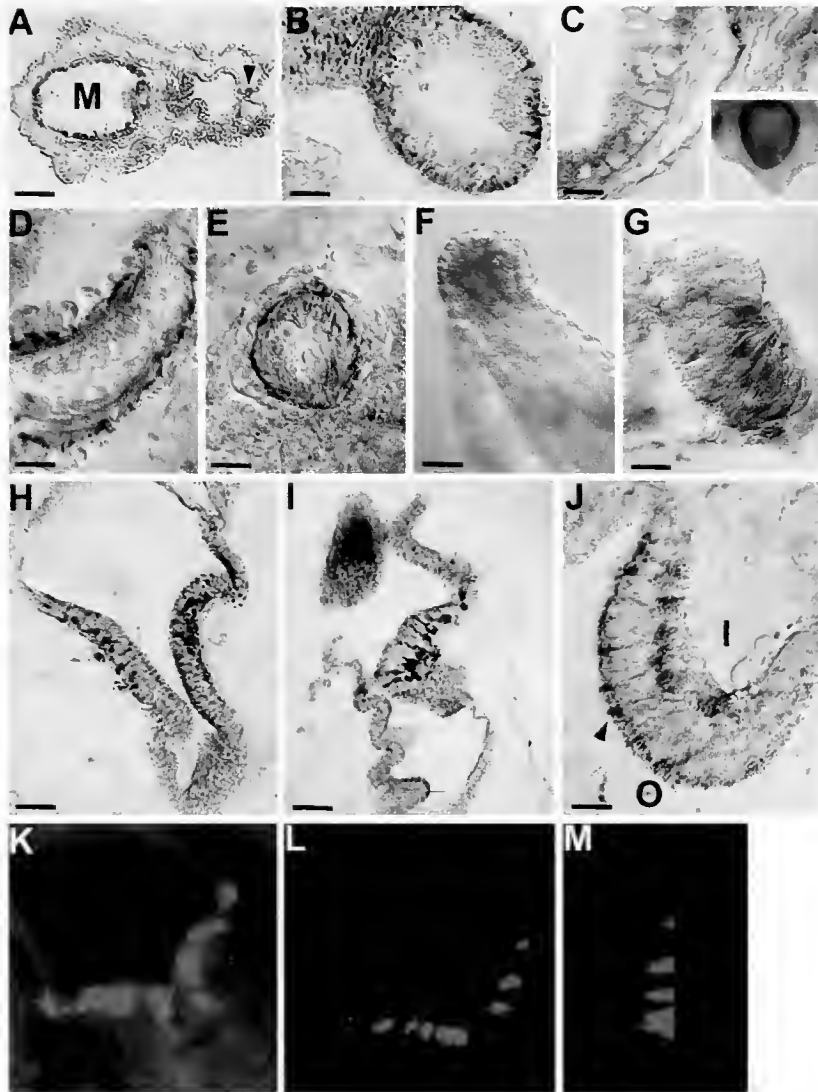


Figure 5. NOS expression in larvae was analyzed by NADPH diaphorase histochemistry and NOS immunohistochemistry. (A) Section of a 26-day larva showing dark blue staining in the fore and mid-gut (M) and in a cell in the pre-oral hood (arrowhead). (B) Oblique longitudinal section showing the arrangement of stained mid-gut epithelial cells. (C) Higher magnification cross section showing staining in the basal portion of columnar epithelial cells lining the mid-gut. The inset shows a low magnification whole-mount view of a stained larval mid-gut. (D) Longitudinal section of a tube foot from a juvenile rudiment contained in a larva. Stained cells of the basioepithelial nerve plexus are tightly apposed to the ectodermal epithelium. (E) Slightly oblique transverse section of a tube foot showing stained nerve plexus with possible projections to the outer surface of the epithelium. (F) Whole-mount staining of a post-oral larval arm from a 26-day-old larva. (G) Section of an epaulette showing staining in cells at the distal tip. (H) Frontal section of the larval mouth showing stained cells. (I) Lateral section of the oral hood and mouth. (J) Higher magnification view of the oral epithelium showing basal position of stained cell bodies. O = outside and I = inside. Axon-like projections having bulbous termini (arrowhead) extend to the ciliated apical surface. Scale bars: 40 μm in A inset of C; 20 μm in B, F, H, and I; 8 μm in C-E, G, J. (K-M) NOS immunostaining. (K) Mouth of a larva. Only cells in the lower lip are immunoreactive. (L) 3-D projection of NOS-positive oral cells. (M) Same projection as (L) but rotated to show cell polarity. Apical side of the oral epithelium (outside of larva) is to the left. Sharp line at the right demarcates the end of the confocal stack. Scale bars are not available for K-M.

metamorphosis of *L. pictus* larvae. These results are consistent with our model for the signaling system that regulates the initiation of metamorphosis in ascidians: cells having NOS activity (probably dependent upon interaction with HSP90) release NO that stimulates the activity of

guanylyl cyclase to produce cGMP that inhibits metamorphosis (Bishop *et al.*, 2001). This proposal is also based, in part, on evidence that NO represses metamorphosis in a gastropod (Froggett and Leise, 1999; Leise *et al.*, 2001). Natural inductive cues may be operating *via* receptor-based

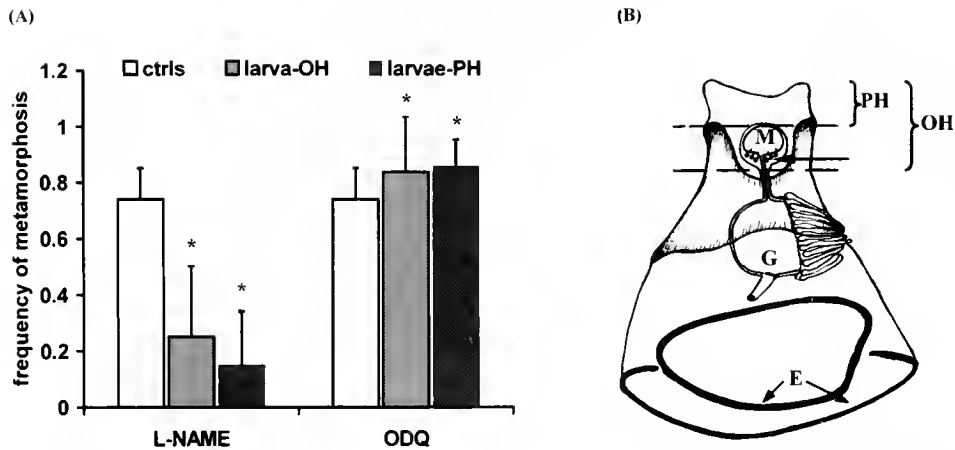


Figure 6. (A) Removal of the entire oral hood or the pre-oral hood does not induce metamorphosis and diminishes the response to L-NAME, but not ODQ. L-NAME was added to postoperative larvae (POL) and the dissected fragments 6 h after surgery. After 14 h in L-NAME, the metamorphic response was significantly reduced in comparison with intact control larvae in L-NAME. Asterisks indicate significant differences between the frequency of metamorphosis of intact and postoperative larvae (POL) ($P_{\text{Larvae minus OH}} < 0.02$; $P_{\text{Larvae minus PH}} < 0.002$). ODQ was added to both POL and dissected fragments, and the frequency of metamorphosis was scored. After 2 h, ODQ rapidly induced metamorphosis. Asterisks indicate a significant difference between POL before and after ODQ treatment ($P_{\text{Larvae minus the oral hood}} < 0.006$; $P_{\text{Larvae minus the preoral hood}} < 0.0003$). (B) A schematic drawing of a *Lytechinus pictus* larva indicating the position of NOS-positive cells found in the lower lip of the mouth (arrow) and the point at which portions of the larvae were surgically removed. Dashed lines indicate the plane of the cuts. NOS-positive oral cells are removed along with the entire oral but not with the pre-oral hood. Arms are virtually absent in well-fed, stirred larvae. PH = pre-oral hood; OH = oral hood; M = mouth; G = gut; E = epaulettes.

sensory perception that is upstream of NO/cGMP signaling. A low-molecular-weight, water-soluble compound isolated from biofilm has inductive properties in *L. pictus* (Cameron and Hinegardner, 1974).

Frequently, some of the treated larvae did not respond by initiating metamorphosis, even after longer incubations (72 h in some cases). In similar experiments, we have found that a fraction of selected larvae do not respond to dishes coated with microbial film. The fraction of resistant larvae in such experiments was variable (not shown), but similar to the fraction resistant to potent drug treatments such as ODQ (Fig. 4). Variation in response to inducers, whether natural or otherwise, may represent variation in sensitivity of sensory perception, levels of NO repression, or response to a reduction of NO signaling (or a combination thereof) among larvae of a clutch and among clutches. Perhaps the resistant larvae had not achieved competence to undergo metamorphosis, despite the morphological similarity of their rudiments to those that did metamorphose. In fact, in some cases, larvae containing less well developed rudiments were responsive to drugs, whereas those with large, highly pigmented rudiments were not. It is clear that competence does not strictly correspond to the presence of a fully formed rudiment within the larva. Assessing competence is problematic in that one does not know whether a lack of response is due to lack of competence or failure to respond to an inductive cue.

To our knowledge, the concept of competence does not

describe a specific biological state in any marine invertebrate having planktotrophic larvae and benthic adults. Larvae with no rudiments or abnormal rudiments do not respond to inducers of metamorphosis (Cameron and Hinegardner, 1978; CDB, unpubl. obs.), so competence in urchins represents a discrete change in the physiological state of the larva that is related to the growth and development of the juvenile. Competence is a phenomenon that requires further investigation and should be considered in all studies on the regulation of metamorphosis. The acquisition of competence coincides with the initiation of metamorphosis in some animals, but not in others (Birkeland *et al.*, 1971; Degnan *et al.*, 1997; Bishop *et al.*, 2001). This indicates that the fitness consequences associated with the timing of, and substrate choice during, settling and metamorphosis vary. What other signaling systems may be contributing to the timing events surrounding life cycle transformations? Studies on thyroxine in echinoids suggest its involvement in the evolutionary loss of larval feeding. The addition of exogenous thyroxine leads to a reduction of larval structures and the time to metamorphosis in *D. excentricus* (J. Hodin, Friday Harbor Laboratories, and A. Heyland, University of Florida; pers. comm.). It will be interesting to know if and how NO/cGMP and hormonal signals interact to regulate the timing of life cycle transformations in echinoids.

Between different clutches, we have observed a striking difference in the response of larvae to NOS inhibition.

Increased sensitivity is manifested as a more rapid response given that identical concentrations of L-NAME and D-NAME were used. We cannot rule out other variations in culturing conditions, such as larval densities and food. The data on NO signaling presented here are from the clutch that was the most sensitive to NOS inhibition. This clutch often responded to NOS inhibition within 2 h, whereas another clutch often took 24-48 h to show a significant effect. The source of this variation is not clear.

We have shown that D-NAME has inductive properties that are suppressed by SNAP, indicating that application of D-NAME also leads to a decrease in NO. Although D-NAME is often used as an inactive negative control for L-NAME treatment, we propose that it does inhibit NOS, but less effectively than L-NAME; others have also noted this activity (Babal *et al.*, 2000). Therefore, D-NAME should be used as a less active enantiomer of L-NAME, not an inactive enantiomer. The extent to which D-NAME is useful as a control for L-NAME treatment will depend on the sensitivity of the experimental system to NO reduction and the concentration of drug used.

There was a lag in the response to radicicol after the beginning of treatment. Radicicol competes with ATP for binding to HSP90, thereby inhibiting its function in binding and folding proteins (Schulte *et al.*, 1998; Sharma *et al.*, 1998). As a protein chaperone, HSP90 interacts with members of several signal transduction pathways (reviewed by Pratt, 1998). In concert with accessory proteins, HSP90 promotes the folding and maintenance of the active state of several known client proteins (Aligue *et al.*, 1994; Whitesell *et al.*, 1994; Nathan and Lindquist, 1995; reviewed by Caplan, 1999). NOS activity in some mammalian cells, including neurons, requires an interaction with HSP90; all three vertebrate isoforms of NOS are degraded in the presence of geldanamycin (GA), another HSP90 inhibitor (Joly *et al.*, 1997; Garcia-Cardena *et al.*, 1998; Bender *et al.*, 1999). Like RD, this agent inhibits HSP90 function by competing with ATP for binding (Promrodou *et al.*, 1997). When the folding function of HSP90 is impaired by inhibitory drugs such as RD and GA, its client proteins (which are often in complexes including HSP90) may be caught in a partially folded state that is then recognized by the ubiquitin-proteasome protein degradation machinery (reviewed by Pratt, 1998; Caplan, 1999). Thus, some client proteins are expected to be degraded or lose activity after HSP90 activity is inhibited. In this circumstance, a response to inhibition of HSP90 would not be expected until its activity had become limiting and its critical client proteins had lost activity or decayed. Such a lag in response was observed for three HSP90 inhibitors that induced metamorphosis when applied to ascidian larvae (Bishop *et al.*, 2001). Thus, we consider this lag to be a consequence of the mechanism by which RD probably leads to a decline in NOS activity.

However, a direct demonstration of interaction between HSP90 and NOS in urchins is warranted.

All of the biochemical characterizations concerning the inhibitory properties of anti-HSP90 drugs have been conducted with vertebrate cells. It is relevant to assess whether RD is likely to have the same effect on *L. pictus* HSP90 as it does on vertebrate HSP90. The crystal structure of a geldanamycin-HSP90 complex has been determined (Stebbins *et al.*, 1997). The geldanamycin binding domain (GBD) is 43% conserved at the amino acid level between vertebrates and *E. coli*; the aspartic acid residue (Asp93) is absolutely conserved among all HSP90 homologs from 35 species. A hydrogen bond network between Asp93 and the carbamate group of GA has been suggested by structural and functional studies to play the most critical role in the binding of HSP90 to GA (Schnur *et al.*, 1995; Stebbins *et al.*, 1997). Thus, it is probable that GA has similar inhibitory properties on HSP90 from all organisms. RD and GA share no structural similarities, but RD can compete with GA for binding to the N-terminal portion of HSP90 that contains the GBD (Schulte *et al.*, 1998). Moreover, like GA treatment, RD depletes cells of known HSP90 client proteins (Schulte *et al.*, 1998). It is reasonable then to expect a set of highly conserved intermolecular interactions between the GBD of HSP90 of different organisms and RD and hence, a highly conserved mechanism of inhibition of HSP90 by RD. Consistent with this conclusion, GA and RD had similar effects on the initiation of ascidian metamorphosis (Bishop *et al.*, 2001) and morphogenetic movements during sea urchin embryonic development (CB, unpubl. obs.).

Under natural circumstances, the initiation of metamorphosis by competent *L. pictus* larvae results from a sensory response to appropriate environmental cues. Minimally, this is a biochemical cue, although a hard surface is usually required (Cameron and Hinegardner, 1974). It is not clear what cells or organs are involved in transducing this chemo- and mechanosensory perception into a metamorphic response. The rate of biphasic potentials recorded from the larval body or near the rudiment increases more in response to a substrate "conditioned" with a microbial film than to an unconditioned substrate (Satterlie and Cameron, 1985). This suggests that both the larval and juvenile neural systems are responsive to environmental stimuli. We have not tested whether the drugs used herein can induce metamorphosis in the absence of contact with a hard surface, but the suppression by SNAP of the inductive properties of biofilm demonstrate that NO signaling is downstream of sensory perception leading to metamorphic events.

Various experiments have attempted to address how metamorphosis is initiated and coordinated. The results can differ among echinoid species. Although many species require a hard surface for settlement before metamorphosis, larvae of the sand dollar *D. excentricus* suspended in sea-

water can be induced to metamorphose by a heat-labile, low-molecular-weight compound extracted from the sand of a bed of adults (Highsmith, 1982; Burke, 1983, 1984). Low-voltage electrical stimulation of the oral ganglion on the lower lip of the larval mouth or the apical neuropile between the preoral and anterolateral arms on the preoral hood region of the *D. excentricus* larva induced metamorphosis (Burke, 1983). These sensitive larval areas have axonal connections (Burke, 1983), and there is a ciliary patch on the pre-oral hood that may have a sensory function (Nakajima, 1986). Electrical stimulation of the oral ganglion has been reported to induce metamorphosis in several echinoids, including *L. pictus* (Burke and Gibson, 1986), although Cameron and Hinègardner (1974) reported otherwise for *L. pictus*. The difference in these results may be methodological. Recently, Beer *et al.* (2001) reported that cells in the lower lip of the larval mouth of the sea urchin *Psammechinus miliaris* develop immunoreactivity to a serotonin antibody. We found staining for NOS protein and NOS activity in cells that appear to be neurons in the lower lip of the mouth, corresponding to the region of the oral ganglion (Burke, 1983), and in cells of the preoral hood, perhaps corresponding to the apical neuropile (Burke, 1983). When Burke (1983) excised the oral hood of *D. excentricus*—including the oral ganglion and apical neuropile—both fragments of the larva rapidly began metamorphosis, but this did not occur when only the preoral hood—lacking the oral ganglion—or larval arms—lacking both sites—were excised. The excised preoral hood and remaining larva were able to respond to a chemical cue for metamorphosis, but isolated larval arms did not (Burke, 1983). Isolated larval arms of some species, including *D. excentricus*, can be induced to contract by treatment with divalent ionophores or the neural transmitters adrenalin, noradrenalin, and dopamine (Burke, 1982, 1983). Dopamine induced only a few whole *D. excentricus* larvae to initiate metamorphosis, suggesting the local response of arms can be inhibited centrally.

On the basis of his experiments, Burke (1983) proposed that there is a mutually inhibitory control of metamorphosis between the oral hood and remainder of the *D. excentricus* larva that is switched off in response to an appropriate cue (or electrical stimulation). The inhibitory region of the oral hood appears to be localized to the larval mouth (Burke, 1983), while the preoral and remaining regions of the larva must have sensory receptors for the chemical cue that induces metamorphosis. Data from histological sectioning and optical reconstructions of the *L. pictus* oral epithelium stained for NOS suggest that nitrergic neurons may reside within this epithelium, possibly performing a sensory role related to feeding or metamorphosis. These NOS-expressing cells were considered as candidate NO-signaling centers. We removed the pre-oral hood or the entire oral hood. In the former case, most of the oral cells remained with the

larva; in the latter, they were removed (see Fig. 6B). In direct contrast to *D. excentricus*, *L. pictus* did not metamorphose in response to the removal of the oral hood, a basic distinction between these two species. Moreover, both classes of *L. pictus* postoperative larvae were less sensitive to NOS inhibition than were the intact controls, but they apparently retained their sensitivity to inhibition of sGC. In Figure 6A, ODQ was added directly to wells containing postoperative larvae that had been treated with L-NAME for 14 h; there may have been an additive effect of the two drugs. Accordingly, when tested separately, a five-fold excess of L-NAME or ODQ is required to induce metamorphosis of larvae lacking the oral hood over concentrations that induce metamorphosis of control larvae (CDB, unpubl. obs.). These experiments are difficult to interpret with respect to Burke's model of mutual inhibition, but they do suggest the involvement of cells in the oral hood of *L. pictus* in a pathway that regulates metamorphosis by NO/cGMP signaling.

The regulatory role of these and other NOS-expressing cells in larvae or juveniles may be additive. In *L. pictus*, the tube feet of the rudiment appear to have sensory receptors that may be involved in inducing metamorphosis (Burke, 1980). We found intense staining for NOS activity in the nerve plexus lining the outer epithelial layer of the tube feet of the rudiment. NO has been implicated in the relaxation of adult tube feet (Billack *et al.*, 1998). The presence of NOS in cells associated with other structures that may have a sensory role (the pre-oral hood, the tips of the anterolateral arms and epaulettes) suggests that the drugs we used act on one or more of these groups of cells to inhibit their production of NO. Indeed, microsurgical and expression data indicate that multiple larval structures and perhaps juvenile structures transduce sensory information, by NO/cGMP signaling, which leads to the initiation of metamorphosis. The frequency of metamorphosis of larvae of *L. variegatus* was increased by excess potassium or calcium ions (Cameron *et al.*, 1989). Metamorphosis of *Strongylocentrotus purpuratus* larvae was induced by treatment with calcium ionophore A23187 or quercetin, an inhibitor of a [Ca,Mg]-ATPase (Klein *et al.*, 1985). Ionic fluxes may play a role, perhaps in coordinating cellular responses (Burke, 1983; Pearse and Cameron, 1991). Some mammalian isoforms of NOS (endothelial and neuronal) are dependent on Ca²⁺ for their activation (Mayer *et al.*, 1998). The inductive properties of Ca²⁺ flux may relate to the role of Ca²⁺ in the regulation of NOS activity.

With this report, there is now evidence that NO plays a repressive role in regulating the initiation of metamorphosis in a protostome (*Ilyanassa*) and three deuterostomes (two ascidians and an echinoid) (Froggett and Leise, 1999; Bishop *et al.*, 2001). NO is involved in metamorphosis of larvae that do not grow before metamorphosis and retain much of the larval tissue (ascidians), larvae that grow as

swimming veliger larvae but do not undergo profound changes upon metamorphosis (*Ilyanassa*), and larvae that undergo extensive growth and catastrophic metamorphosis in which most larval tissues are degraded and replaced by a radically different juvenile (echinoids). NO, a universal and ancient signaling molecule in eukaryotes, may have a role in regulating metamorphosis in a wide diversity of animals.

Sea urchin larvae are optically clear and can easily be cultured in large numbers. This fact, and a rich experimental literature on settling and metamorphosis, make echinoids a useful system with which to investigate the neuroanatomical basis for the regulation of metamorphosis. These features and our findings provide a basis for a more focused experimental effort to identify which cells or organs repress metamorphosis by NO production in *L. pictus*.

Acknowledgments

This research was funded by a Research Grant from the Natural Sciences and Engineering Research Council of Canada. We thank Robert Burke, Andrew Cameron, and Victor Vacquier for helpful discussions, and two anonymous reviewers for useful comments.

Literature Cited

- Aligue, R., H. Akhavan-Niak, and P. Russell. 1994. A role for Hsp90 in cell cycle control: Wee 1 tyrosine kinase activity requires interaction with Hsp90. *EMBO J.* **13**: 6099–6106.
- Babal, P., O. Pechanova, and I. Bernatova. 2000. Long-term administration of D-NAME induces hemodynamic and structural changes in the cardiovascular system. *Physiol. Res.* **49**: 47–54.
- Beer, A.-J., C. Moss, and M. Thorndyke. 2001. Development of serotonin-like and SALMFamide-like immunoreactivity in the nervous system of the sea urchin *Psammechinus miliaris*. *Biol. Bull.* **200**: 268–280.
- Bender, A. T., A. M. Silverstein, D. R. Demady, K. C. Kanelakis, S. Noguchi, W. C. Pratt, and Y. Osawa. 1999. Neuronal nitric oxide synthase is regulated by the hsp90-based chaperone system *in vivo*. *J. Biol. Chem.* **274**: 1472–1478.
- Billack, B., J. D. Laskin, P. T. Heck, W. Trönl, M. A. Gallo, and D. E. Heck. 1998. Alterations in cholinergic signaling modulate contraction of isolated sea urchin tube feet: potential role of nitric oxide. *Biol. Bull.* **195**: 196–197.
- Birkeland, C., F. S. Chia, and R. R. Strathmann. 1971. Development, substrate selection, delay of metamorphosis and growth in the sea star, *Mediaster aequalis* Stimpson. *Biol. Bull.* **141**: 99–108.
- Bishop, C. D., W. R. Bates, and B. P. Brandhorst. 2001. Regulation of metamorphosis in ascidians involves NO/cGMP signaling and HSP90. *J. Exp. Zool.* **289**: 374–384.
- Burke, R. 1980. Podial sensory receptors and the induction of metamorphosis in echinoids. *J. Exp. Mar. Biol. Ecol.* **47**: 223–234.
- Burke, R. 1982. Echinoid metamorphosis: retraction and resorption of larval tissues. Pp. 513–518 in *Echinoderms: Proceedings of the International Echinoderms Conference, Tampa Bay, 14–17 September 1981*, J. M. Lawrence, ed. A. A. Balkema, Rotterdam.
- Burke, R. 1983. Neural control of metamorphosis in *Dendroaster excentricus*. *Biol. Bull.* **164**: 176–188.
- Burke, R. 1984. Pheromonal control of metamorphosis in the Pacific sand dollar, *Dendroaster excentricus*. *Science* **255**: 442–443.
- Burke, R. D., and A. W. Gibson. 1986. Cytological studies for the studies of larval echinoids with notes on methods for inducing metamorphosis. *Methods Cell Biol.* **27**: 295–308.
- Caldwell, J. W. 1972. Development, metamorphosis, and substrate selection of the larvae of the sand dollar, *Mellita quinques perforata*. M.Sc. Thesis, University of Florida, Gainesville.
- Cameron, R. A., and R. T. Hinegardner. 1974. Initiation of metamorphosis in laboratory-cultured sea urchins. *Biol. Bull.* **146**: 335–342.
- Cameron, R. A., and R. T. Hinegardner. 1978. Early events of metamorphosis in sea urchins; description and analysis. *J. Morphol.* **157**: 21–32.
- Cameron, R. A., T. R. Tosteson, and V. Hensley. 1989. The control of sea urchin metamorphosis: ionic effects. *Dev. Growth. Differ.* **31**: 589–594.
- Caplan, A. J. 1999. Hsp90's secrets unfold: new insights from structural and functional studies. *Trends Cell Biol.* **9**: 262–268.
- Cueto, M., O. Hernández-Perera, R. Martín, M. L. Bentura, J. Rodrigo, S. Lamas, and M. P. Golvano. 1996. Presence of nitric oxide synthase activity in roots and nodules of *Lupinus albus*. *FEBS Lett.* **398**: 59–64.
- Czar, M. J., M. D. Galigniana, A. M. Silverstein, and W. B. Pratt. 1997. Geldanamycin, heat shock protein 90-binding benzoquinone ansamycin, inhibits steroid-dependent translocation of the glucocorticoid receptor from the cytoplasm to the nucleus. *Biochemistry* **36**: 7776–7785.
- Davidson, E. H. 1991. Spatial mechanisms of gene regulation in metazoan embryos. *Development* **113**: 1–26.
- Degnan, B. M., D. Souter, S. M. Degnan, and S. C. Long. 1997. Induction of metamorphosis with potassium ions requires the development of competence and an anterior signaling centre in the ascidian *Herdmania momus*. *Dev. Genes Evol.* **206**: 370–376.
- Froggett, S. J., and E. M. Leise. 1999. Metamorphosis in the marine snail *Ilyanassa obsoleta*, yes or NO? *Biol. Bull.* **196**: 57–62.
- García-Cardena, G., R. Fan, V. Shah, R. Sorrentino, G. Cirino, A. Papapetropoulos, and W. C. Sessa. 1998. Dynamic activation of endothelial nitric oxide synthase by Hsp90. *Nature* **392**: 821–824.
- Garthwaite, J., E. Southam, C. L. Boulton, E. B. Neilsen, K. Schmidt, and B. Mayer. 1995. Potent and selective inhibition of nitric oxide-sensitive guanylyl cyclase by 1H-[1,2,4]oxadiazolo[4,3-a]quinoxalin-1-one. *Mol. Pharmacol.* **48**: 184–188.
- Hebeiss, K., and H. Kilbinger. 1998. Nitric oxide-sensitive guanylyl cyclase inhibits acetylcholine release and excitatory motor transmission in the guinea-pig ileum. *Neuroscience* **82**: 623–629.
- Highsmith, R. C. 1982. Induced settlement and metamorphosis of sand dollar (*Dendroaster excentricus*) larvae in predator-free sites: adult sand dollar beds. *Ecology* **63**: 320–337.
- Joly, G. A., M. Ayres, and R. G. Kilbourn. 1997. Potent inhibition of inducible nitric oxide synthase by geldanamycin, a tyrosine kinase inhibitor, in endothelial, smooth muscle cells, and in rat aorta. *FEBS Lett.* **403**: 40–44.
- Klein, W. H., C. D. Carpenter, L. Philpotts, and B. P. Brandhorst. 1985. The sea urchin Spec family of calcium binding proteins: characterization and consideration of possible roles in larval development. Pp. 272–295 in *The Cellular and Molecular Biology of Invertebrate Development*, R. Sawyer and R. Showman, eds. University of South Carolina Press, Columbia, SC.
- Kuzin, B., I. Roberts, N. Peunova, and G. Enikolopov. 1996. Nitric oxide regulates cell proliferation during *Drosophila* development. *Cell* **87**: 639–649.
- Leise, E. M., K. Thavaradhara, N. R. Durham, and B. E. Turner. 2001. Serotonin and nitric oxide regulate metamorphosis in the marine snail *Ilyanassa obsoleta*. *Am. Zool.* **41**: 258–267.
- Mayer, B., S. Pfeiffer, A. Schrammel, D. Koesling, K. Schmidt, and F.

- Brunner, 1998.** A new pathway of nitric oxide/cGMP signaling involving S-nitroglutathione. *J. Biol. Chem.* **273**: 3264–3270.
- McDonald, L. J., and F. Murad. 1996.** Nitric oxide and cyclic GMP signaling. *Proc. Soc. Exp. Biol. Med.* **211**: 1–6.
- Nakajima, Y. 1986.** Presence of a ciliary patch in preoral epithelium of sea urchin plutei. *Dev. Growth Differ.* **28**: 243–249.
- Nathan, D. F., and S. Lindquist. 1995.** Mutational analysis of Hsp90 function: interactions with a steroid receptor and a protein kinase. *Mol. Cell. Biol.* **15**: 3917–3925.
- Pearse, J. S., and R. A. Cameron. 1991.** Echinodermata: Echinoidea. Pp. 513–662 in *Reproduction of Marine Invertebrates*, Vol. VI, A. C. Giese, J. S. Pearse, and V. B. Pearse, eds. The Boxwood Press, Pacific Grove, CA.
- Pratt, W. B. 1998.** The hsp90-based chaperone system: involvement in signal transduction from a variety of hormone and growth factor receptors. *Proc. Soc. Exp. Biol. Med.* **217**: 420–434.
- Promrodou, C., S. M. Roe, R. O'Brien, J. E. Ladbury, P. W. Piper, and L. H. Pearl. 1997.** Identification and structural characterization of the ATP/ADP-binding site in the HSP90 molecular chaperone. *Cell* **90**: 65–75.
- Salter, M., P. J. Strijbos, S. Neale, C. Duffy, R. L. Follenfant, and J. Garthwaite. 1996.** The nitric oxide-cyclic GMP pathway is required for nociceptive signalling at specific loci within the somatosensory pathway. *Neuroscience* **73**: 649–655.
- Satterlie, R. A., and R. A. Cameron. 1985.** Electrical activity at metamorphosis in larvae of the sea urchin *Lytechinus pictus* (Echinoidea: Echinodermata). *J. Exp. Zool.* **235**: 197–204.
- Schnur, R. C., M. L. Corman, R. J. Gallaschun, B. A. Cooper, M. F. Dee, J. L. Doty, M. L. Muzzi, J. D. Moyer, C. I. DiOrio, E. G. Barbacci, P. E. Miller, A. T. O'Brien, M. J. Morin, B. A. Foster, V. A. Pollack, D. M. Savage, D. E. Sloan, L. R. Pustilnik, and M. P. Moyer. 1995.** Inhibition of the oncogene product p185(erbB-2) in vitro and in vivo by geldanamycin and dihydrogeldanamycin derivatives. *J. Med. Chem.* **38**: 3806–3812.
- Schulte, T. W., S. Akinaga, S. Soga, W. Sullivan, B. Stensgard, D. Toft, and L. M. Neckers. 1998.** Antibiotic radicicol binds to the N-terminal domain of Hsp90 and shares important biologic activities with geldanamycin. *Cell Stress Chaperones* **3**: 100–108.
- Sharma, S. V., T. Agatsuma, and H. Nakano. 1998.** Targeting of the protein chaperone HSP90 by the transformation suppressing agent radicicol. *Oncogene* **16**: 2639–2645.
- Stebbins, C. E., A. A. Russo, C. Schneider, N. Rosen, F. U. Hartl, and N. P. Pavletich. 1997.** Crystal structure of an Hsp90-geldanamycin complex: targeting of a protein chaperone by an antitumor agent. *Cell* **89**: 239–250.
- Strathmann, M. F. 1987.** *Reproduction and Development of Marine Invertebrates of the Northern Pacific Coast*. University of Washington Press, Seattle.
- Weinberg, R. J., J. G. Valtschanoff, and H. H. W. Schmidt. 1996.** The NADPH diaphorase histochemical stain. Pp. 237–248 in *Methods in Nitric Oxide Research*, M. Feelisch and J. S. Stamler, eds. Wiley and Son, Chichester, United Kingdom.
- Whitesell, L., E. G. Mimnaugh, B. D. Costa, C. E. Myers, and L. M. Neckers. 1994.** Inhibition of heat shock protein Hsp90-pp60^{v-src} heteroprotein complex formation by benzoquinone ansamycins: essential role for stress proteins in oncogenic transformation. *Proc. Natl. Acad. Sci. USA* **91**: 8324–8328.
- Yen, A., S. Soong, H. J. Kwon, M. Yoshida, T. Beppu, and S. Varvayannis. 1994.** Enhanced cell differentiation when RB is phosphorylated and down-regulated by radicicol, a src-kinase inhibitor. *Exp. Cell Res.* **214**: 163–171.

Developmental Patterns and Cell Lineages of Vermiform Embryos in Dicyemid Mesozoans

HIDETAKA FURUYA¹, F. G. HOCHBERG², AND KAZUHIKO TSUNEKI¹

¹*Department of Biology, Graduate School of Science, Osaka University, Toyonaka, Osaka 560-0043, Japan; and* ²*Department of Invertebrate Zoology, Santa Barbara Museum of Natural History, 2559 Puesta del Sol Road, Santa Barbara, California 93105-2936*

Abstract. Patterns of cell division and cell lineages of the vermiform embryos of dicyemid mesozoans were studied in four species belonging to four genera: *Conocyema polymorpha*, *Dicyema apalachiensis*, *Microcyema vespa*, and *Pseudicyema nakaoi*. During early development, the following common features were apparent: (1) the first cell division produces prospective cells that generate the anterior peripheral region of the embryo; (2) the second cell division produces prospective cells that generate the posterior peripheral region plus the internal cells of the embryo; (3) in the lineage of prospective internal cells, several divisions ultimately result in cell death of one of the daughter cells. Early developmental processes are almost identical in the vermiform embryos of all four dicyemid genera. The cell lineages appear to be invariant among embryos and are highly conserved among species. Species-specific differences appear during later stages of embryogenesis. The number of terminal divisions determines variations in peripheral cell numbers among genera and species. Thus, the numbers of peripheral cells are fixed and hence species-specific.

Introduction

All members of the phylum Dicyemida are found in the renal sacs of benthic cephalopod molluscs (Nouvel, 1947; McConnaughey, 1951; Hochberg, 1990). Their bodies consist of the smallest number of cells among multicellular animals (usually 10 to 40) and are organized in a very simple fashion. Although recent studies have revealed that they might not be truly primitive animals deserving the name of mesozoans (Katayama *et al.*, 1995; Kobayashi *et al.*, 1999), they are still one of the most

interesting groups of lower invertebrates. Each species is characterized by a fixed number of cells. The somatic cells therefore undergo a limited number of species-specific divisions during embryogenesis. The analysis of embryonic cell lineages in dicyemids is intriguing, since it may provide clues towards an understanding of the simplest patterns of cell differentiation in multicellular animals. A comparative study of cell lineage and developmental processes among related species of dicyemids is also relevant to advance our understanding of morphological evolution in these simple animals.

Dicyemids produce two distinct types of embryos: vermiform embryos from an asexual agamete and infusoriform embryos from fertilized eggs (Furuya *et al.*, 1996). From the standpoint of morphological evolution, the vermiform embryo is the more pertinent target for study because its shape is similar to that of an adult. The cell lineage of vermiform embryos has been fully documented in only two dicyemids, *Dicyema acuticephalum* and *D. japonicum* (Furuya *et al.*, 1994). Among other species, cell lineages have been described only to a limited extent in *Microcyema vespa* and *Pseudicyema truncatum* (Lameere, 1919; McConnaughey, 1938; Schartau, 1940; Nouvel, 1947; Bogomolov, 1970; Lapan and Morowitz, 1975). Details of cell lineage in the phylum as a whole remain to be determined.

In this paper we describe the pattern of cell divisions and cell lineages in the embryogenesis of vermiform embryos in dicyemids belonging to four genera: *Conocyema polymorpha*, *Dicyema apalachiensis*, *Microcyema vespa*, and *Pseudicyema nakaoi*. Our data reveal that cell lineages in vermiform embryos are highly conserved among species; but species-characteristic features appear in the later embryogenesis, and these are related to morphological evolution and speciation.

Materials and Methods

Specimens of *Conocyema polymorpha* van Beneden, 1882, *Dicyema apalachiensis* Short, 1962, *Microcyema vespa* van Beneden, 1882, and *Pseudicyema truncatum* (Whitman, 1883) were examined in the collections of the Department of Invertebrate Zoology, Santa Barbara Museum of Natural History, Santa Barbara, California. *Conocyema polymorpha*, found in *Octopus vulgaris*, was collected by Henri Nouvel in the Mediterranean Sea (Nouvel, 1947). *Microcyema vespa* and *P. truncatum*, found in *Sepia officinalis*, were also collected by Nouvel in the Mediterranean Sea (Nouvel, 1947). *Dicyema apalachiensis*, found in *Octopus joubini*, was collected by Robert B. Short in the Gulf of Mexico off Florida (Short, 1962).

Specimens of *Pseudicyema nakaoui* Furuya, 1999, were prepared for this study. A total of 57 host cuttlefishes, *Sepia esculenta*, were purchased in the western part of Japan. When dicyemids were detected in the kidney of the host cuttlefish, small pieces of renal appendages with attached dicyemids were removed and smeared on slide glasses. The smears were fixed immediately in Bouin's fluid for 24 h and then stored in 70% ethyl alcohol. The fixed smears were stained in Ehrlich's hematoxylin and counterstained in eosin. Stained smears were mounted using Entellan (Merck).

Embryos within the axial cell of parent nematogens were observed with the aid of a light microscope under an oil-immersion objective at a magnification of 2000 diameters. Cells were identified by their position within the embryo, their size, and the intensity of stain taken up by the nucleus and cytoplasm. By careful examination, we were able to identify each swollen nucleus that was about to divide and each metaphase figure in terms of the cell that was about to divide into two daughter cells. Each developing embryo was sketched at three optical depths, and three-dimensional diagrams were reconstructed from these sketches. Measurements and drawings were made with the aid of an ocular micrometer and a drawing tube (Olympus U-DA), respectively. Fully formed embryos consisted at most of 23 cells, and special techniques such as injection of a tracer and videoscropy were not required for determination of the cell lineage. Early divisions of the vermiform embryos examined in this study were the same as those of *Dicyema acuticephalum* and *D. japonicum* (see Furuya et al., 1994). The terminology of cells used by Furuya et al. (1994) was adopted in designating the cells in the present paper.

Results

In the Dicyemida, two adult forms, the nematogen and the rhombogen, develop asexually from an agamete (axoblast) through a vermiform embryo within the axial cell of parent nematogens (Fig. 1).

Microcyema vespa

Agamete diameter is about 6 μm . The first division is meridional and unequal, producing two daughter cells, A and B. Cell B becomes the mother cell of the peripheral cells of the embryo's head. The second division involves only cell B. This division is occasionally skipped. It is extremely unequal, producing two daughter cells that are quite different in size. The smaller of these two cells ultimately degenerates without contributing to embryogenesis. The third division, involving cell A, is latitudinal and equal, producing two daughter cells, 2A and 2a. Cell 2A is the mother cell of peripheral cells in the tail, and cell 2a is the prospective axial cell. In the 2a lineage, extremely unequal divisions occur at around the 5- and 7-cell stages. The resultant much smaller daughter cells remain attached to the larger daughter cells until they ultimately degenerate without contributing to embryogenesis. The fourth division, involving cell 2B, is meridional and equal, producing two daughter cells, 3B and 3B. At this 4-cell stage, two pairs of cells, 2A-2a and 3B-3B, are arranged crosswise with respect to one another. The furrow of the fourth division coincides with the plane of bilateral symmetry of the embryo. The pattern of division and the cell lineage are the same for the descendants of cell 3B and those of cell 3B. The fifth division, involving cell 2A, is latitudinal and equal; resulting in the 5-cell embryo. The plane of cell division coincides with the plane of bilateral symmetry, and it separates the right cell 3A from the left cell 3A. These cells do not divide further but become the two peripheral cells of the tail region, known as the utropolar cells (Figs. 2a-c, 3a).

The pattern of cell division beyond the 5-cell stage changes from spiral to bilateral. After the 5-cell stage, divisions occur not one by one but in pairs, and the divisions become almost synchronized. Subsequent developmental stages thus proceed with odd numbers of cells, yielding, for example, a 7-cell embryo, and so on.

The sixth division is extremely unequal. Both the 3B and 3B cells divide, and they produce a pair of large cells and a pair of much smaller daughter cells. The smaller cells degenerate and eventually disappear. At around the 5-cell stage, cell 2a, the prospective axial cell, undergoes an extremely unequal division. The resultant smaller cell degenerates and eventually disappears. The seventh division is equal, and results in the 7-cell embryo. Cells 4B and 4B divide and produce two pairs of daughter cells, 5B¹ and 5B² plus 5B¹ and 5B², respectively. The future anterior-posterior axis of the embryo corresponds almost exactly to the 5B¹-3A axis at the 7-cell stage. About the 7-cell stage, cell 3a, the prospective axial cell, undergoes an extremely unequal division. The resulting smaller cells degenerate and eventually disappear.

After the seventh division, the order of division is not necessarily identical among developing embryos. The

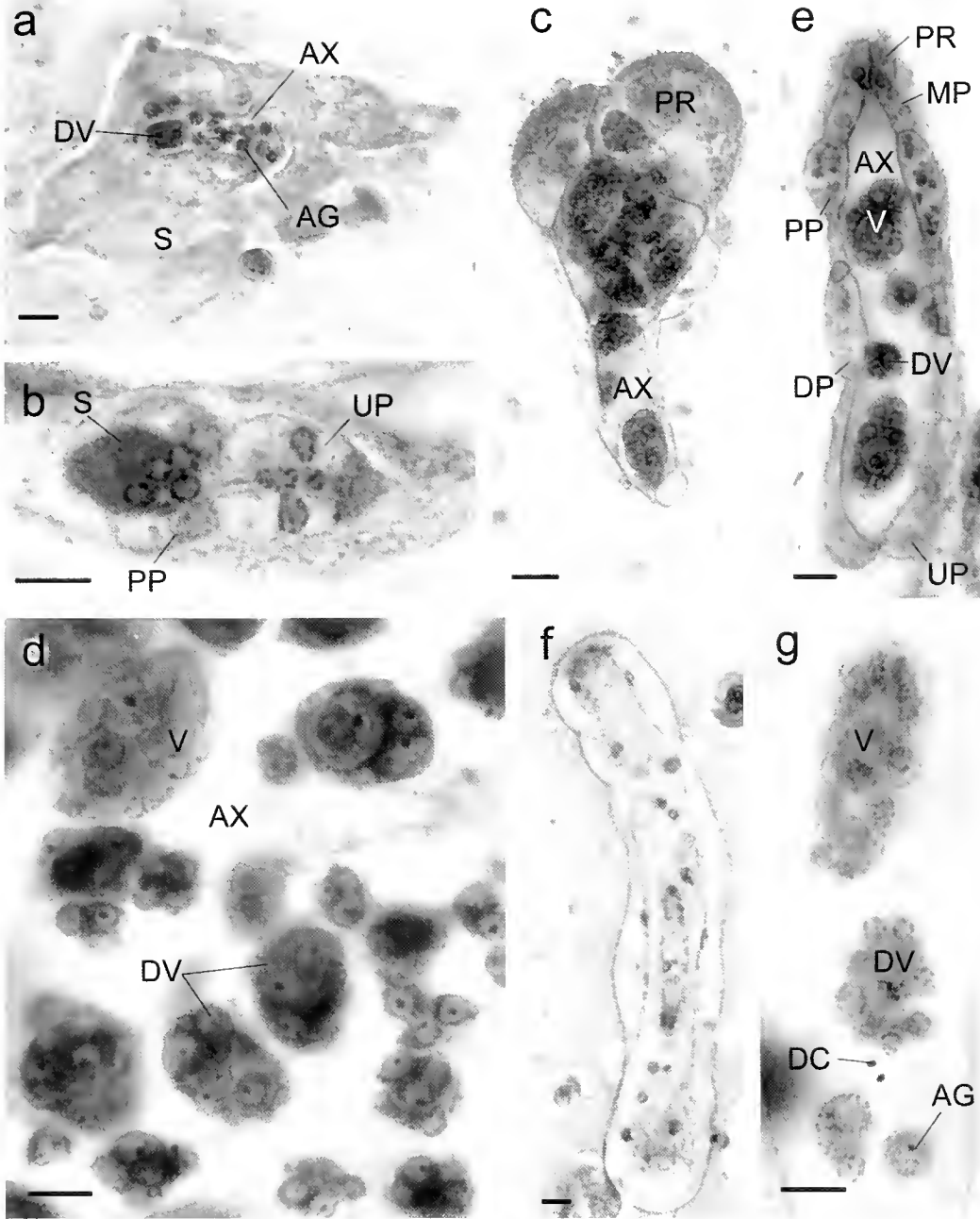


Figure 1. Light micrographs of nematogens in four species of dicyemids. Scale bars represent 10 μm . Abbreviations: AG, agamete; AX, axial cell; DC, degenerating cell; DP, diapolar cell; DV, developing vermiform embryo; MP, metapolar cell; PP, parapolar cell; PR, propolar cell; S, syncytium; UP, uropolar cell; V, vermiform embryo. *Microcyema vespa*: (a) whole body of a young individual; (b) a vermiform embryo in the axial cell of the nematogen. *Conoecyema polymorpha*: (c) whole body of a nematogen; (d) developing vermiform embryos in the axial cell of the nematogen. *Dicyema apalachiensis*: (e) whole body of the nematogen. *Pseudicyema nakaoi*: (f) whole body of a nematogen; (g) developing vermiform embryos in the axial cell of the nematogen.

$5B^1$ cell pair divides equally and produces two pairs of daughter cells, $6B^{11}$ and $6B^{12}$ plus $6B^{11}$ and $6B^{12}$. The $5B^2$ cell pair divides equally and produces two pairs of daughter cells, $6B^{21}$ and $6B^{22}$ plus $6B^{21}$ and $6B^{22}$. Nei-

ther pair divides further, and they form the anterior part of the embryo (Fig. 2a, b). The $6B^{22}$ cell pair develops into the parapolar cells, while the $6B^{11}$, $6B^{12}$, and $6B^{21}$ cell pairs eventually form a syncytium, which is more

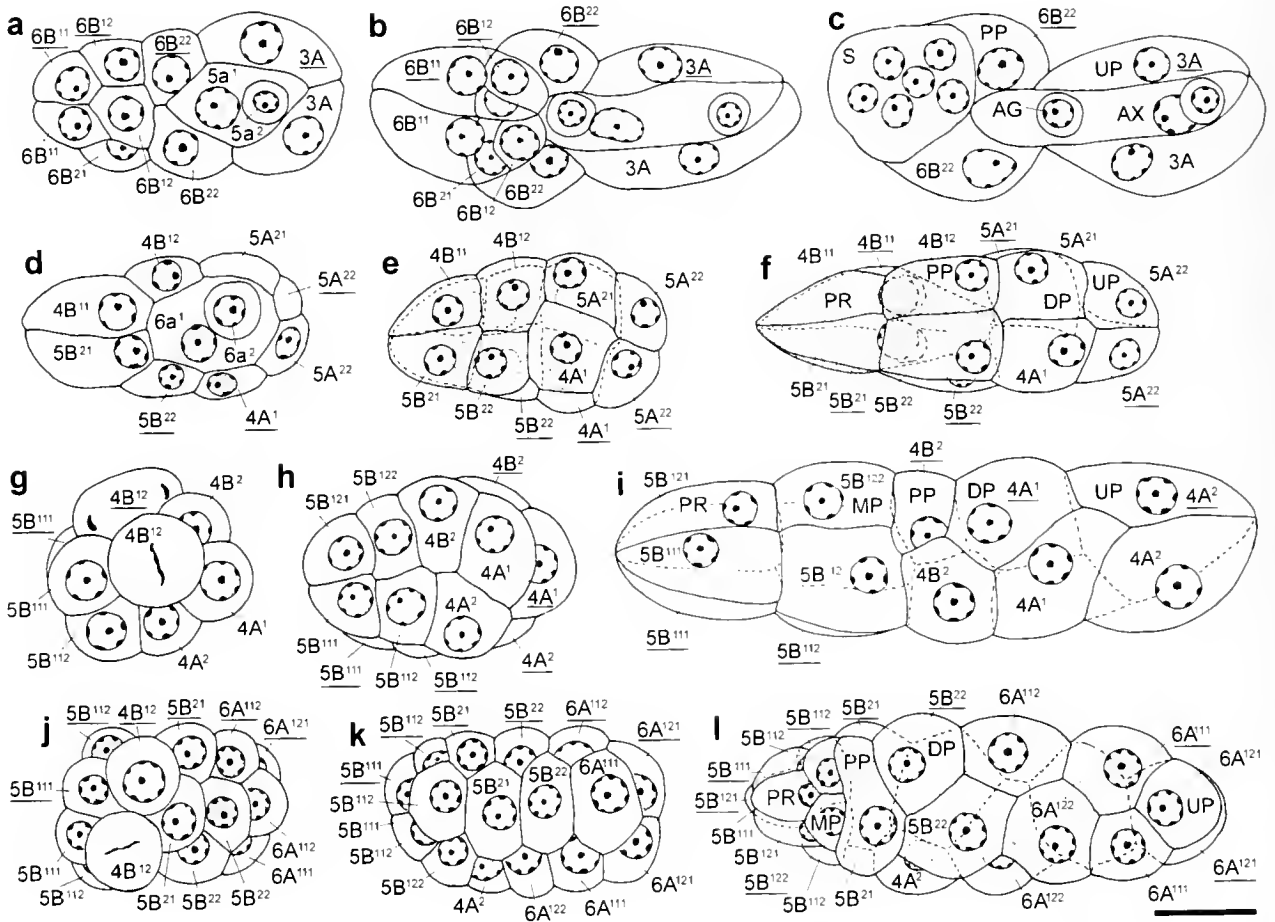


Figure 2. The late-stage vermiform embryos of four species of dicyemids. Scale bar represents 10 μm . Cilia are omitted. See text for explanations of cell division notations. Other abbreviations: AG, agamete; AX, axial cell; DP, diapolar cell; MP, metapolar cell; PR, propolar cell; PP, parapolar cell; S, syncytium; UP, uropolar cell. *Microcyema vespa*: (a) a late-stage embryo (sagittal optical section)—note an agamete ($5a^2$) in the cytoplasm of an axial cell ($5a^1$); (b) a late-stage embryo (sagittal optical section); (c) formed embryo (sagittal optical section)—pairs of $6B^{11}$, $6B^{12}$, and $6B^{21}$ cells form a syncytium (S) that is more conspicuously stained with hematoxylin. *Conocyema polymorpha*: (d) a late-stage embryo (sagittal optical section)—note an agamete ($6a^2$) incorporated in the cytoplasm of an axial cell ($6a^1$); (e) a late-stage embryo (lateral view); (f) formed embryo (lateral view)—pairs of $4B^{11}$ and $5B^{21}$ cells form propolar cells (PR) that are more conspicuously stained with hematoxylin. *Dicyema apalachiensis*: (g) 13-cell stage—note an anaphase figure of $4B^{12}$ cell and a metaphase figure of $4B^{12}$ cell; (h) 15-cell stage—the $5B^{111}$ and $5B^{121}$ pairs form the propolar cells (PR), while the $5B^{112}$ and $5B^{122}$ pairs form another type of polar cell, the metapolar cell (MP); (i) formed embryo (lateral view)—propolar cells and metapolar cells are more conspicuously stained with hematoxylin. *Pseudicyema nakaoi*: (j) 22-cell stage—note a metaphase figure in $4B^{12}$ cell—the plane of this division, in contrast to the divisions of $4B^{12}$ pair (Fig. 2g), are oblique to the anterior-posterior axis, and as the result, cells of the propolar tier alternate with cells of the metapolar tier (see Fig. 2k, l); (k) a late-stage embryo (lateral view); (l) formed embryo (lateral view)—propolar cells and metapolar cells are more conspicuously stained with hematoxylin.

conspicuously stained with hematoxylin than the other cells (Fig. 1b). The two parapolar cells cover more than half of the syncytium (Fig. 2c). As peripheral cells are formed, the prospective axial cell, 4a, divides unequally. The large anterior cell, $5a^1$, undergoes no further divisions and becomes the axial cell, while the smaller posterior cell, $5a^2$, is incorporated into the axial cell and

becomes an agamete (Fig. 2a). At this stage, cilia are first evident on the peripheral cells. Cilia on the external surface of the syncytium are directed anteriorly and are more densely distributed than on other peripheral cells.

The fully formed embryo consists of three types of cells: peripheral cells, one syncytial cell, and an axial cell, which contains two agametes (Figs. 1b, 2c). The

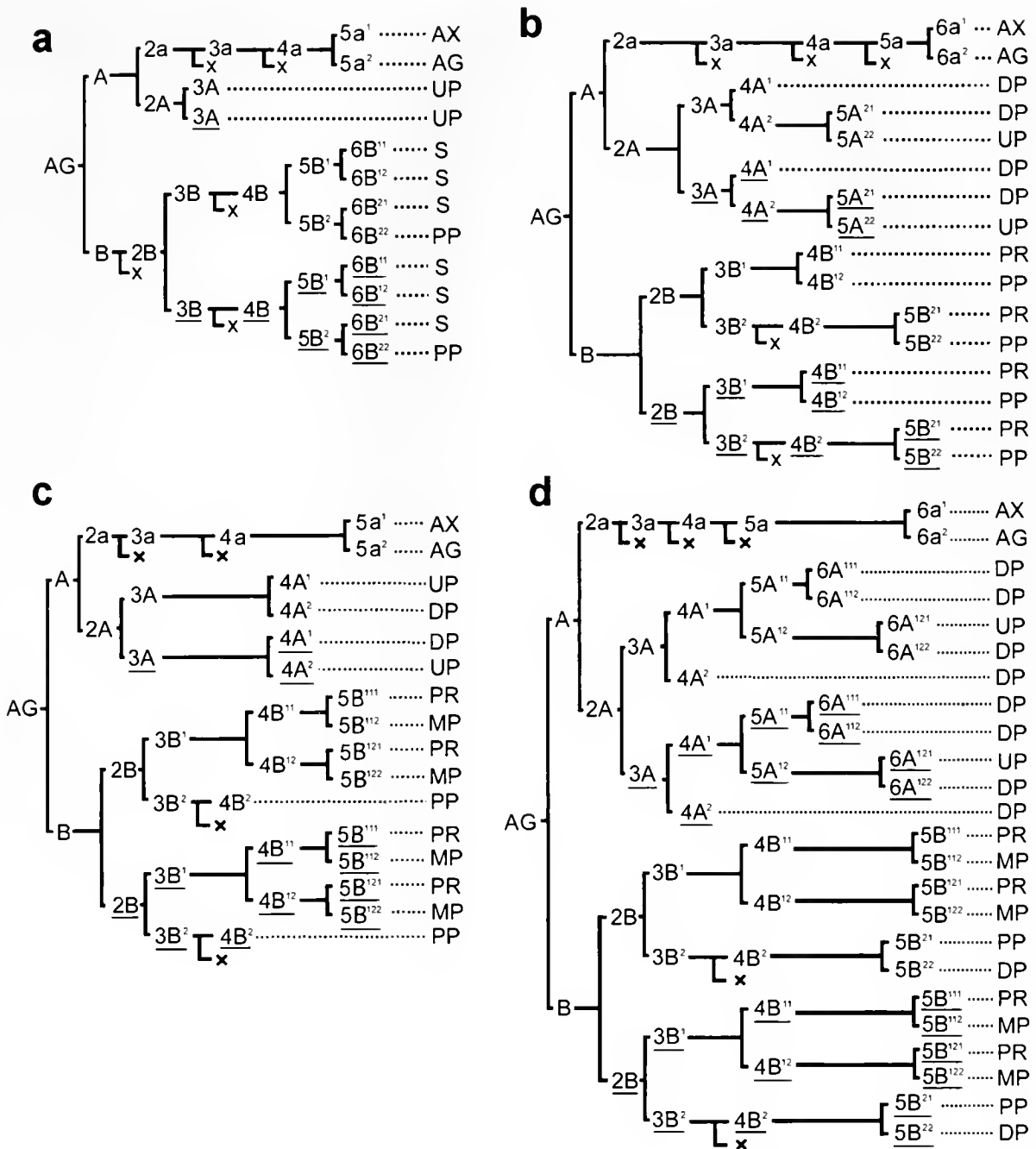


Figure 3. Cell lineages of vermiform embryos. A cross (x) indicates that a cell, formed as the result of an unequal division, degenerates and does not contribute to the formation of the embryo. See text for explanations of cell division notations. Other abbreviations: AG, agamete; AX, axial cell; DP, diapolar cell; MP, metapolar cell; PP, parapolar cell; PR, propolar cell; S, syncytium; UP, uropolar cell. (a) *Microcyema vespa*; (b) *Conocyema polymorpha*; (c) *Dicyema apalachiensis*; (d) *Pseudicyema nakaoui*.

peripheral cells are composed of two parapolar cells and two uropolar cells. The swollen cephalic head region consists of a calotte and two parapolar cells. The calotte is a syncytium. The trunk is composed of two uropolar cells. Further development involves growth and enlargement of the syncytium and branching of the axial

cell (Fig. 1a). Total length, excluding cilia, of the fully formed vermiform embryo is about 50 μm , and the width is about 20 μm . The cell lineage of the vermiform embryo is summarized in Figure 3a. No variations in cell lineage were found in more than 50 embryos examined.

Conocyema polymorpha

Agamete diameter is about 7 μm . The first division is meridional and unequal, producing two daughter cells that are slightly different in size, A and B. The larger cell B becomes the mother cell of the peripheral cells of the embryo's head (propolar and parapolar cells). The second division involves only the smaller cell A. This division is latitudinal and equal, producing two daughter cells, 2A and 2a. Cell 2A is the mother cell of the peripheral cells of the posterior trunk and tail, and cell 2a is the prospective axial cell (Fig. 3b). In the 2a lineage, extremely unequal divisions occur at around the 5-, 11-, and 13-cell stages (Fig. 3b), and the resultant much smaller daughter cells remain attached to the larger daughter cells until they ultimately degenerate without contributing to embryogenesis. The third division, involving cell B, is meridional and equal, producing two daughter cells, 2B and 2B. At this 4-cell stage, two pairs of cells, 2A-2a and 2B-2B, are arranged crosswise with respect to one another. The furrow of the third division coincides with the plane of bilateral symmetry of the embryo. The pattern of division and the cell lineage are the same for the descendants of cell 2B and those of cell 2B (Fig. 3b). The fourth division, involving cell 2A, is meridional and equal, resulting in the 5-cell embryo. The plane of cell division again coincides with the plane of bilateral symmetry, and it separates the right cell 3A from the left cell 3A. The pattern of cell division and the cell lineage are the same for descendants of cell 3A and for those of cell 3A (Fig. 3b).

The pattern of cell division beyond the 5-cell stage changes from spiral to bilateral. Beyond the 5-cell stage, divisions occur not one by one but in pairs, and they become almost synchronized. Subsequent developmental stages thus proceed with odd numbers of cells.

At around the 5-cell stage, cell 2a, the prospective axial cell, undergoes an extremely unequal division. The resultant smaller cell degenerates and finally disappears. The fifth cell division is equal and results in the 7-cell embryo. Thus, cells 2B and 2B divide and produce two pairs of daughter cells, 3B¹ and 3B² plus 3B¹ and 3B², respectively. The future anterior-posterior axis of the embryo corresponds almost exactly to the 3B¹-3A axis at the 7-cell stage. The sixth division is slightly unequal. Cells 3A and 3A divide into two pairs of daughter cells, 4A¹ and 4A² plus 4A¹ and 4A². Cells 4A² and 4A² are the smallest cells at this stage. In addition to the 2a lineage, cells 3B² and 3B² undergo unequal divisions, each generating a pair of cells, one large and one much smaller. The smaller cells degenerate and finally disappear, although they remain in place on the developing embryo until later stages.

The 3B¹ pair divide equally into 4B¹¹ and 4B¹² pairs. These cells undergo no further divisions. The 4B¹¹ pair become the propolar cells, and the 4B¹² pair become the parapolar cells (Figs. 2e, f). The cell in the 2a lineage (cell

3a) is incorporated into the inside of the embryo, and the 3B¹ pair divide and rearrange their descendants. At around the 11-cell stage, the 3a cell undergoes an extremely unequal division.

The 13-cell stage is achieved by equal divisions of cells 4A² and 4A². The resultant 5A²¹ and 5A²² pairs undergo no further divisions and become diapolar cells and uropolar cells, respectively. Soon after these divisions, the 4B² pair divide equally into two pairs of daughter cells, 5B²¹ and 5B²² plus 5B²¹ and 5B²². The 5B²¹ and 5B²² pair undergo no further divisions and become the propolar cells and parapolar cells, respectively (Fig. 2e, f). At around the 13-cell stage, the prospective axial cell 4a undergoes an extremely unequal division.

At the final stage of embryogenesis, the prospective axial cell, 5a, divides unequally. The large anterior cell, 6a¹, undergoes no further divisions and becomes the axial cell, while the smaller posterior cell, 6a², is incorporated into the axial cell and becomes an agamete (Fig. 2d).

The fully formed vermiform embryo of *Conocyema polymorpha* consists of 14 peripheral cells and one axial cell, which contains one or two agametes (Fig. 2f). The head peripheral cells are composed of four propolar cells and parapolar cells. The propolar cells have short, dense cilia and form the calotte, which is more conspicuously stained with hematoxylin than the other cells. Four diapolar cells make up the trunk peripheral cells. The caudal peripheral cells are uropolar cells. The length, excluding cilia, of the fully formed embryo is about 25 μm , and the width is about 10 μm . The cell lineage of the vermiform embryo is summarized in Figure 3b. No variations in cell lineage were found in more than 80 embryos examined.

Dicyema apalachiensis

Agamete diameter is about 5.5 μm . The first division is meridional and equal, producing two daughter cells of equal size. The subsequent patterns of development and cell lineage up to the 7-cell stage are the same as those described for *Conocyema polymorpha*.

At the 7-cell stage, cells 3B² and 3B² undergo unequal divisions, each generating a pair of cells, one large and one much smaller cell. The 9-cell stage is achieved by unequal divisions of cells 3B¹ and 3B¹. The resultant small cells, 4B¹¹ and 4B¹¹, divide again into two pairs of daughter cells, 5B¹¹¹ and 5B¹¹² plus 5B¹¹¹ and 5B¹¹², in the anterior part of the embryo (Fig. 2g-i). Almost simultaneously, the resultant large cells, 4B¹² and 4B¹², divide again into two pairs of daughter cells, 5B¹²¹ and 5B¹²² plus 5B¹²¹ and 5B¹²², in the anterior part of the embryo (Fig. 2h, i). These cells undergo no further divisions, and the 5B¹¹¹ and 5B¹²¹ pairs become the propolar cells, while the 5B¹¹² and 5B¹²² pairs become the metapolar cells. The cell in the 2a lineage (cell 4a) is

incorporated into the inside of the embryo, and the other cells, $4B^{11}$ and $4B^{12}$, divide and rearrange their descendants.

At the 9-cell stage, cells $3A$ and $3A$ divide equally into two pairs of daughter cells, $4A^1$ and $4A^2$ plus $4A^1$ and $4A^2$. They do not divide further: the $4A^1$ pair become the uropolar cells, and the $4A^2$ pair become the diapolar cells (Fig. 3c). At the final stage of embryogenesis, the prospective axial cell, $4a$, divides unequally. The large anterior cell, $5a^1$, becomes the axial cell, and the smaller posterior cell, $5a^2$, is incorporated into the axial cell and becomes an agamete.

The vermiform embryo of *Dicyema apalachiensis* consists of 14 peripheral cells and one axial cell, which contains one or two agametes. The peripheral cells of the head region are composed of four propolar cells, four metapolar cells, and two parapolar cells. The propolar and metapolar cells have short, dense cilia and form the calotte. Two diapolar cells make up the trunk peripheral cells. Two caudal peripheral cells are uropolar cells. The length, excluding cilia, of the fully formed embryo is about 30 μm , and the width is about 10 μm . The cell lineage of the vermiform embryo is summarized in Figure 3c. No variations in cell lineage were found in more than 50 embryos examined.

Pseudicyema nakaoui

Agamete diameter is about 6.5 μm . The first division is equal, producing two daughter cells of equal size. The subsequent patterns of development and cell lineage up to the 9-cell stage are the same as those described for *Dicyema apalachiensis* (see Fig. 3c).

At the 9-cell stage, cells $3B^2$ and $3B^2$ undergo extremely unequal divisions, each generating a pair of cells, one large and one much smaller cell. The smaller cells resulting from this division degenerate and finally disappear. In the 2a line, unequal divisions occur at around the 5-, 9-, and 11-cell stages (Fig. 3d). The pattern of development and cell lineages up to the 9-cell stage are the same in both *P. truncatum* and *P. nakaoui*. Further development was not studied in *P. truncatum*, because adequate material was not available.

After the unequal divisions of the $3B^2$ pair, cell pairs $4A^1$ and $3B^1$ undergo equal divisions almost simultaneously and produce two pairs of daughter cells, $5A^{11}$ and $5A^{12}$ plus $4B^{11}$ and $4B^{12}$, to form the 13-cell-stage embryo. At around the 13-cell stage, the prospective axial cell, $4a$, undergoes an unequal cell division. The $5A^{11}$ pair divide equally and produce two pairs of daughter cells, $6A^{111}$ and $6A^{112}$ plus $6A^{111}$ and $6A^{112}$. The plane of this division is parallel to the anterior-posterior axis, in contrast to the previous division, which occurs parallel to the perpendicular axis. As a result, cells $6A^{111}$ and $6A^{111}$ are situated on the left and right sides of the embryo, respectively.

At the 15-cell stage, cell pairs $4B^2$ and $5A^{12}$ undergo equal divisions almost simultaneously, and produce two pairs of daughter cells, $5B^{21}$ and $5B^{22}$ plus $6A^{121}$ and $6A^{122}$,

to form the 19-cell-stage embryo. These pairs undergo no further divisions. Cell pair $5B^{21}$ become the parapolar cells, and the $5B^{22}$ pair become the anterior diapolar cells (Fig. 3d). Cell pair $6A^{121}$ become the uropolar cells, and the $6A^{122}$ pair become the posterior diapolar cells (Fig. 3d).

At the 19-cell stage, the $4B^{11}$ and $4B^{12}$ pairs divide equally into two pairs of daughter cells, $5B^{111}$ and $5B^{112}$ plus $5B^{121}$ and $5B^{122}$, in the anterior part of the embryo (Fig. 2k, l). These divisions proceed cell by cell. The daughter cells undergo no further divisions, and the $5B^{111}$ and $5B^{121}$ pairs become the propolar cells, while the $5B^{112}$ and $5B^{122}$ pairs become the metapolar cells (Fig. 2j). The planes of these divisions, in contrast to the previous division, are oblique to the anterior-posterior axis. As the result, cells of the propolar tier alternate with cells of the metapolar tier (Fig. 2k, l).

At the final stage of embryogenesis, the prospective axial cell, $5a$, divides unequally. The large anterior cell, $6a^1$, becomes the axial cell, and the smaller posterior cell, $6a^2$, is incorporated into the axial cell and becomes an agamete.

The fully formed vermiform embryo of *P. nakaoui* consists of 22 peripheral cells and one axial cell, which contains one agamete. The peripheral cells of the head region are composed of four propolar cells, four metapolar cells, and two parapolar cells. The propolar and metapolar cells have dense short cilia and form the calotte. Ten diapolar cells make up the trunk peripheral cells. Two caudal peripheral cells are uropolar cells. The body length, excluding cilia, of the fully formed embryo is about 70 μm , and the body width is about 16 μm . The cell lineage of the vermiform embryo is summarized in Figure 3d. No variations in cell lineage were found in more than 50 embryos examined.

Discussion

Patterns of development of the vermiform embryos of four species of dicyemids belonging to four genera, namely *Microcyema vespa*, *Conocyema polymorpha*, *Dicyema apalachiensis*, and *Pseudicyema nakaoui*, were studied in detail. In the embryogenesis of each species, cell divisions proceed without variation and result in fully formed embryos with a definite number and arrangement of cells. The process of development of vermiform embryos is very simple and seems to be programmed similarly to that of infusoriform embryos and infusorigens (Furuya *et al.*, 1992b, 1993, 1995). Seven different cell lineages including those of two previously described species, *D. acuticephalum* and *D. japonicum* (Figs. 3, 4; see also Furuya *et al.*, 1994), could be compared. Early developmental processes up to the 7-cell stage are almost identical in vermiform embryos examined in this study and those of *D. acuticephalum* and *D. japonicum* (Figs. 5, 6).

Our results are different from earlier reports with respect to the timing of cell-fate specification (Lameere, 1919;

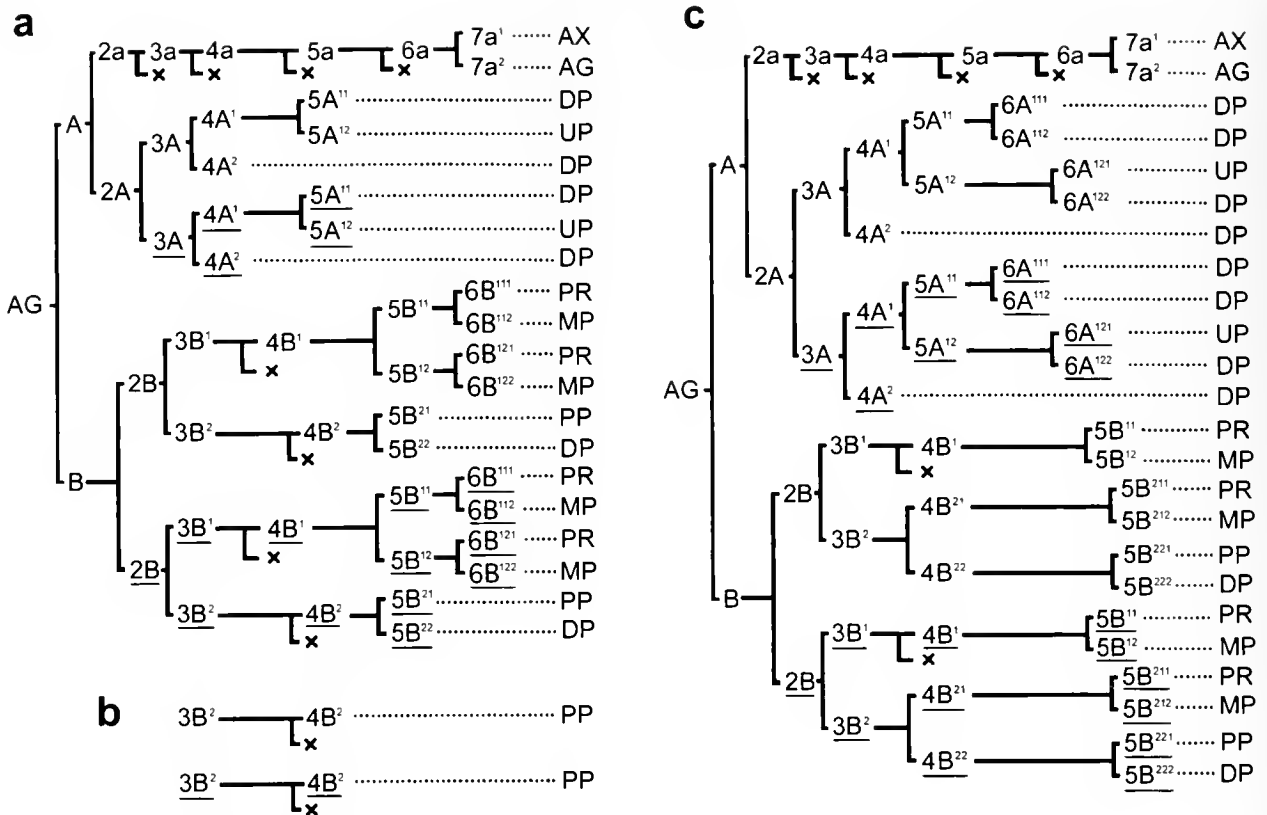


Figure 4. Cell lineages of vermiform embryos in *Dicyema acuticephalum* and *D. japonicum* (modified from Furuya *et al.*, 1994). A cross (x) indicates that a cell resulting from an unequal division degenerates and does not contribute to the formation of the embryo. Abbreviations: AG, agamete; AX, axial cell; DP, diapolar cell; MP, metapolar cell; PP, parapolar cell; PR, propolar cell; UP, uropolar cell. (a) *D. acuticephalum* with 18 peripheral cells; (b) *D. acuticephalum* with 16 peripheral cells; (c) *D. japonicum*.

Gersch, 1938; McConnaughey, 1951). According to Lameere (1919), in *M. vespa* and *P. truncatum* the first division is unequal, and as a result two daughter cells of different sizes are produced. One of the daughter cells (usually the larger one) is described as a prospective axial cell, and the other is regarded as the mother cell of the peripheral cells. However, in all species examined, we found that the prospective axial cell was produced at the second division, not at the first division. Gersch (1938) and McConnaughey (1951) also claimed that the prospective axial cell is produced at the first division in *D. typus*, *D. balamuthi*, *Dicyemenea abelis*, and *Dicyemenea californica*. Although the possibility that two types of first division exist cannot be excluded in this study, the results of those early observations remain to be confirmed.

Early developmental pattern and cell lineage

Comparisons of developmental processes and cell lineages among various species of dicyemids reveal conser-

vative features in the early development. Although dicyemids from different host species and geographically different distributions were compared, the developmental processes and cell lineages are almost identical from an agamete to the 7-cell stage (Fig. 5). Cell-fate segregation appears in the very early stages of embryogenesis. Three types of prospective cells that form the body of embryos, such as the agamete, the axial cell, and the peripheral cells, can be identified as early as the 3-cell stage. In the development of vermiform embryos, cell fates may be initially segregated. This conserved feature among species may represent the basic plan in forming bodies of vermiform embryos (Fig. 6). These features in cell lineage suggest that the early developmental processes have persisted through the evolution of dicyemids. Vermiform embryos develop in the confined space of an axial cell located within the parent nematogen. This peculiar habitat thus may constrain the developmental process, as well as limit the size and number of cells that compose the body. As a result, development may appear to be conserved.

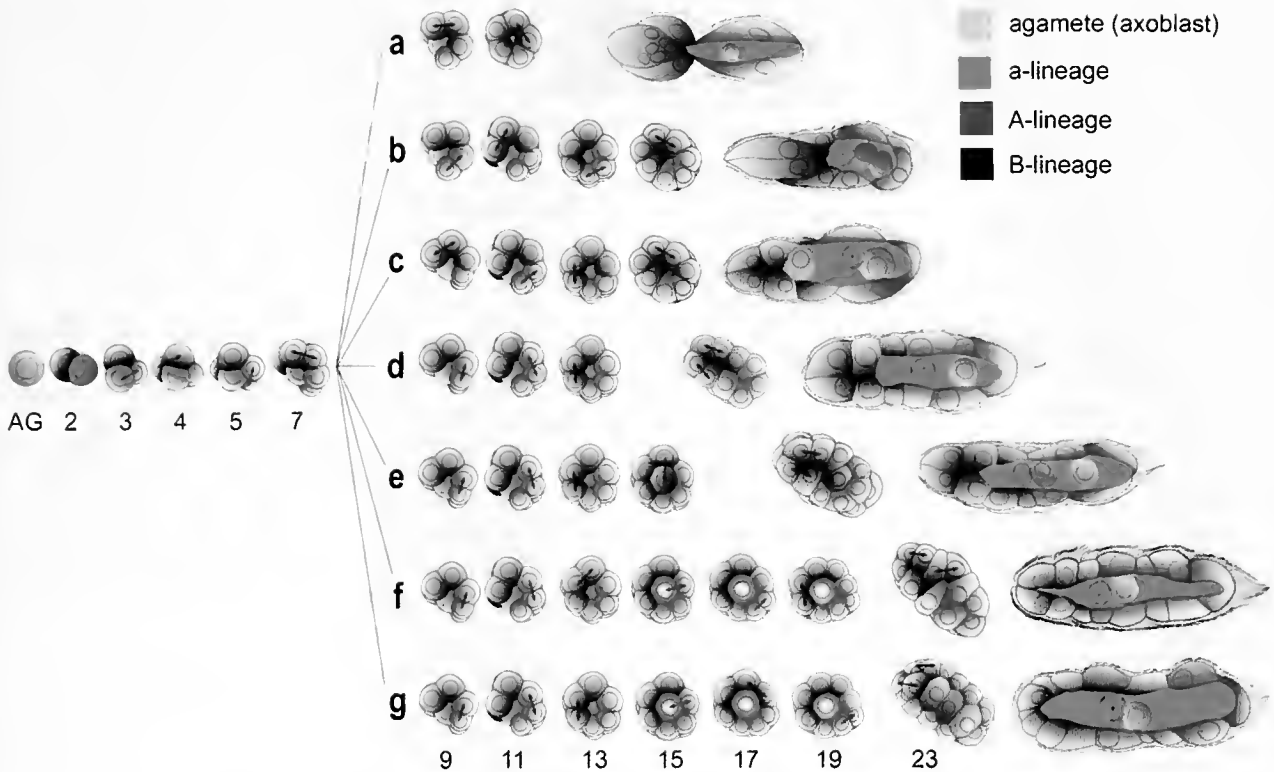


Figure 5. Developmental processes of vermiform embryos in several species of dicyemids. The developmental patterns and cell lineages from the agamete (AG) to 7-cell stage are identical among the species. The numerals in the bottom row represent cell number stages in the development. Arrows in the developing embryos indicate daughter cells that were produced by the preceding division. (a) *Microcyema vespa*; (b) *Conocyema polymorpha*; (c) *Dicyema apalachiensis*; (d) *D. acuticephalum* with 16 peripheral cells; (e) *D. acuticephalum* with 18 peripheral cells; (f) *D. japonicum*; (g) *Pseudicyema nakaioi*.

Variations of terminal divisions in cell lineages

Species-specific patterns of development and cell lineages appear in the later stages of embryogenesis. The most striking difference is seen in terminal divisions in the cell lineage that give rise to variations in peripheral cell numbers. For instance, species-specific differences in the peripheral cell number between *Dicyema acuticephalum* and *D. japonicum* can be attributed to the number of divisions of the 4A¹ pair (Fig. 4; Furuya *et al.*, 1994). In other species, additional terminal divisions occur toward the end of the establishment of another cell lineage as well. The various numbers of terminal divisions, which are genetically determined, clearly play a significant role in the morphogenesis of vermiform embryos and may be correlated with speciation in the dicyemids.

In most species of dicyemids, vermiform embryos have a constant number of peripheral cells. However, some species of dicyemids, such as *Dicyema acuticephalum*, *D. bilobum*, *D. benthocopi*, *D. erythrum*, *D. lycidoceum*, and *D. rhadinum*, have a variable number of peripheral cells (Nouvel, 1947; Couch and Short, 1964; Hochberg and Short, 1970;

Furuya *et al.*, 1992a; 1994; Furuya, 1999). Such intraspecific variation in peripheral cell numbers could be attributed to minor differences in numbers of terminal divisions in certain cell lineages (compare Fig. 4a and b).

In the developmental patterns of vermiform embryos, the cell lineages do not vary, and the terminal divisions usually occur bilaterally. Thus, several even numbers of peripheral cells are formed as the result of a pair of terminal divisions in both the 2A- and B-cell lineages. In species that have a variable number of peripheral cells, such as *Dicyema erythrum*, *D. lycidoceum*, and *D. rhadinum*, some peaks are evident in even numbers of peripheral cells (see tables in Furuya, 1999). The number of terminal divisions may not be strictly programmed in these exceptional species.

Later development and larval morphology

In the evolution of dicyemids, various types of vermiform embryos must have been produced as deviations from a common developmental pattern. Unusual species, such as *Microcyema vespa* and *Conocyema polymorpha*, not only differ morphologically from other dicyemids but are distinct

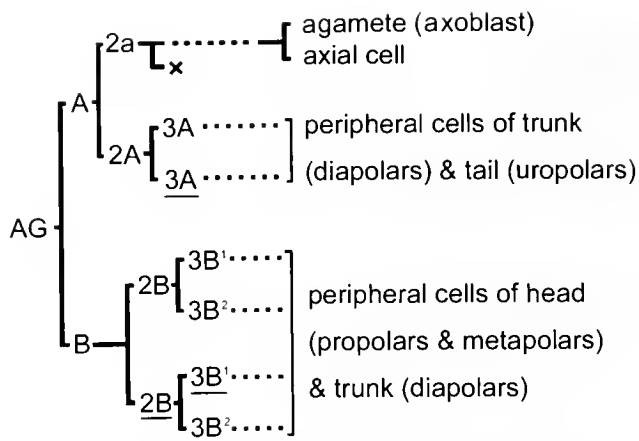


Figure 6. A common cell lineage in all the vermiform embryos examined. At the first division, an agamete (AG) divides to produce two daughter cells, A and B. Cell A divides into two daughter cells. Cell 2a is a mother cell for both an axial cell and agamete. Descendants of cell 2A form the peripheral cells of both trunk and tail. Descendants of cell B form the peripheral cells of both the head and anterior trunk. A cell formed by unequal division degenerates and does not contribute to the formation of the embryo.

in the later stages of development. As shown in the cladogram (Fig. 7), these two species of dicyemids are clearly distinct and separate when compared with the clade composed of the genera *Dicyema* and *Pseudicyema*. Some changes that occur in cell lineages certainly are reflected in morphological features.

The genus *Pseudicyema*, as diagnosed by Nouvel (1933), is morphologically very similar to *Dicyema*. As a result, it occasionally has been treated as a subgenus of *Dicyema* (Hochberg, 1990). The difference between *Pseudicyema* and *Dicyema* depends on whether cells of the propolar tier are alternate or opposite with respect to the cells in the metapolar tier. The developmental processes in these genera are different only in the terminal cell lineage and the pattern of cell divisions at the final stage of embryogenesis. On the basis of cell lineages, differences between *Dicyema* and *Pseudicyema* are within the range of inter-species differences in *Dicyema*, as shown in the cladogram. However, as far as calotte configuration and the process of calotte formation are concerned, *Dicyema* and *Pseudicyema* can be clearly identified as separate groups. Although cell lineage is an important character, it may not necessarily help to determine the definition of genera. Detailed comparative studies on cell lineages and organization of infusoriform embryos are also indispensable in separating dicyemid taxa.

In recent years, it has been argued that the evolution of morphological features requires alterations in developmental processes. In dicyemids, the cell lineage of *Microcyema vespa* is closer to a conservative lineage than in other genera in the phylum, but vermiform embryos of *M. vespa* show a distinctive form not seen in other genera. It is possible that

in *M. vespa* the developmental process may be truncated, resulting in a simple cell lineage and a body organization with a very small number of peripheral cells. However, changes in cell lineage may not always contribute to morphological characters. For example, there are some differences in the later cell lineage between *Dicyema acuticephalum* and *D. apalachiensis*, but these dicyemids are very similar in general body shape.

Cell death

McConnaughey (1951) described chromatin elimination from the prospective axial cell. In *Dicyema acuticephalum* and *D. japonicum*, what appears to be a mass of eliminated chromatin is actually a small cell that is produced as the result of an extremely unequal division (Furuya *et al.*, 1994). In *Pseudicyema truncatum* and *Microcyema vespa*, Lameere (1919) noted that the prospective axial cell underwent an unequal division and that the smaller daughter cell itself divided once or twice to produce two or four small

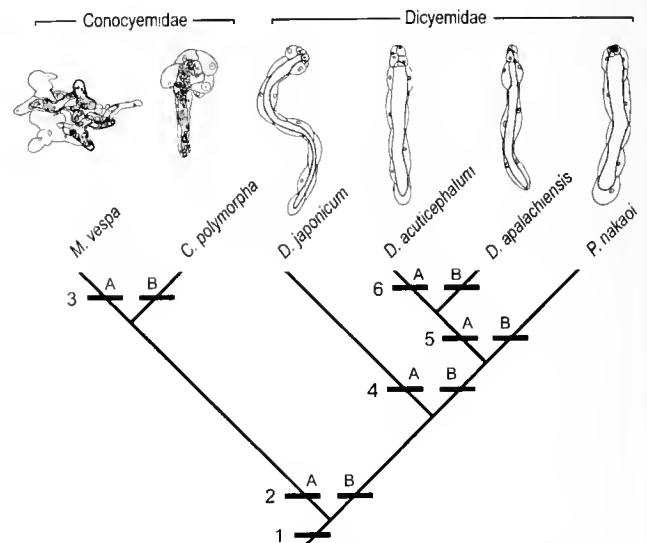


Figure 7. Cladogram of six species of dicyemids based on cell lineages of the vermiform embryos. These dicyemids might have been derived from an ancestor that had a basic cell lineage as shown in Figure 6. Modifications in cell lineages might result in diversity of morphology giving rise to two separate families, namely, Conocyemidae and Dicyemidae. Sketches at top of cladogram indicate the size and shape of the whole bodies of adult stages of each species. Bars represent modifications of the different cell lineages as follows: (1) Early development as shown in Figure 6. (2A) Calotte is formed with a tier of polar cells. (2B) Calotte is formed with two tiers of polar cells; propolars and metapolars present. (3A) Calotte forms a syncytium; diapolars absent. (3B) Calotte is cellular; diapolars present. (4A) Calotte is formed from both 3B¹- and 3B²-cell lineages. (4B) Calotte is formed only from 3B¹-cell lineage. (5A) Propolars are located perpendicularly above metapolars. (5B) Propolars are obliquely oriented to metapolars. (6A) Cell death occurs both in 3B¹- and 3B²-cell lineages. (6B) Cell death occurs only in 3B²-cell lineages; both 4A¹- and 4A²-cells undergo no further divisions.

Table 1

The number of cell divisions in each cell lineage

Dicyemid	Peripheral cell number	A-cell lineage		B-cell lineage	Total cell divisions
		A-cell lineage	a-cell lineage		
<i>Microcyema vespa</i>	10	2	3 (2)	10 (3*)	15 (5)
<i>Conocyema polymorpha</i>	14	6	4 (3)	9 (2)	19 (5)
<i>Dicyema apalachiensis</i>	14	4	3 (2)	11 (2)	18 (4)
<i>Dicyema acuticephalum</i>	16 [#]	6	5 (4)	13 (4)	24 (8)
<i>Dicyema acuticephalum</i>	18 [#]	6	5 (4)	15 (4)	26 (8)
<i>Dicyema japonicum</i>	22 [#]	10	5 (4)	13 (2)	28 (6)
<i>Pseudicyema nakaoui</i>	22	10	4 (3)	13 (2)	27 (5)

The numbers in parentheses represent the number of extremely unequal cell divisions.

* One cell division was not consistently observed.

From Furuya *et al.* (1994).

cells that do not degenerate. We were able to examine the details of these small cells in several dicyemids, including the species studied by Lameere. In contrast to Lameere's observation, the small cell does not undergo further divisions. In his report, the small cells were exclusively derived from a prospective axial cell (a-cell lineage), but we recognized they are formed in both the a-cell and B-cell lineages, as recognized in the previous study of *D. acuticephalum* and *D. japonicum*.

The small cells eventually die and are eliminated without contributing to the embryogenesis. This is considered to be a programmed cell death as described in the development of infusoriform embryos (Furuya *et al.*, 1992b). In the dicyemids examined, extremely unequal divisions take place four to eight times during embryogenesis (Table 1). The number of such divisions is as definite according to species as the number of peripheral cells. In the a-cell lineage, much programmed cell death appears frequently in dicyemids that consist of a large number of peripheral cells. It seems possible that successive, extremely unequal divisions in the a-cell lineage may be required to maintain an increased amount of cytoplasm in the large axial cell. The axial cell retains most of the cytoplasm of the mother cell and enlarges after each cell division. In most dicyemids, the axial cell elongates as peripheral cell numbers increase. Thus, peripheral cell number appears to be correlated to the number of programmed cell deaths.

The B-cell lineage gives rise to the head region, in which cell death occurs in all dicyemids examined. In contrast, no cell death was observed in the A-cell lineage. The A-cell lineage gives rise to the trunk and tail region, which are composed of standard peripheral cells. Programmed cell death in dicyemids appears in cell lineages associated with remarkably differentiated cells, *e.g.*, the axial cell and calotte cells. Thus, cell death may be intimately involved in the advanced characteristic differentiation of cells.

Several features in developmental pattern and cell lineages among species

The early development of dicyemids is conservative and may be summarized as follows: (1) the first cell division produces prospective cells that generate the anterior peripheral region of the embryo; (2) the second cell division produces prospective cells that generate the posterior peripheral region plus the internal cells within the embryo; (3) in the lineage of prospective internal cells, several divisions ultimately result in the death of one of the daughter cells. Developmental processes to the 7-cell stage are almost identical in the vermiform embryos of the four genera examined (Figs. 5, 6).

In contrast, distinct species-specific differences appear in the order and number of terminal divisions of peripheral cells. Most of the changes in terminal divisions can be correlated with individual body length. Generic differences appear in the number of cells that contribute to the calotte during the final stage of embryogenesis. Distinct morphological features typically emerge following a final cell division or after the embryo escapes from the axial cell of the adult. Subsequent processes, proceeding without cell divisions, are cell differentiation in the head region and cell elongation in the trunk region.

On the basis of cell lineage, a simple cladogram was constructed (Fig. 7). Cell lineages from an agamete to the 7-cell stage were almost identical among species (bar 1). The terminal of B-cell lineage indicates some variation among species. In the family Conocyemidae, a calotte is formed with a tier of polar cells (bar 2A), whereas in the Dicyemidae a calotte consists of two tiers of polar cells, propolars and metapolars (bar 2B). Thus, the tree indicates that two clusters initially separate to form two families. In *Microcyema*, a calotte and peripheral cells form a syncytium (bar 3A), but in *Conocyema* a calotte is cellular and diapolars are present (bar 3B). In *Dicyema japonicum*, the calotte

is formed in 3B¹- and 3B²-cell lineages (bar 4A), but in *D. acuticephalum*, *D. apalachiensis*, and *Pseudicyema nakaai* the calotte is formed only in 3B¹-cell lineage (bar 4B). The orientation of propolars to metapolars separates *Pseudicyema* from *Dicyema*. In *Pseudicyema*, propolars are obliquely oriented to metapolars (bar 5B). In *Dicyema*, propolars are located perpendicularly above metapolars (bar 5A). In *D. acuticephalum*, cell death occurs both in 3B¹- and in 3B²-cell lineages (bar 6A), but in *D. apalachiensis* it occurs only in 3B²-cell lineage (bar 6B). Based on the above criteria, separation of the dicyemids into two families may be justified; however, the generic state of *Pseudicyema* apparently warrants further study.

Acknowledgments

We wish to express our gratitude to the late Dr. Yutaka Koshida, Professor Emeritus of Osaka University, for his continual advice and valuable suggestions on the biology of dicyemids. This study was supported in part by research grants from the Nakayama Foundation for Human Science, Japan Society for the Promotion of Science (no. 12740468), and the Santa Barbara Museum of Natural History.

Literature Cited

- Bogomolov, S. I. 1970.** On the question of the type of cleavage in the dicyemids. Pp. 22–33 in *Questions of Evolutionary Morphology and Biocenology*. Kazan University Press, Kazan, Russia.
- Couch, J. A., and R. B. Short. 1964.** *Dicyema bilobum* sp. n. (Mesozoa: Dicyemidae) from the northern Gulf of Mexico. *J. Parasitol.* **50**: 641–645.
- Furuya, H. 1999.** Fourteen new species of dicyemid mesozoans from six Japanese cephalopods, with comments on host specificity. *Species Diversity* **4**: 257–319.
- Furuya, H., K. Tsuneki, and Y. Koshida. 1992a.** Two new species of the genus *Dicyema* (Mesozoa) from octopuses of Japan with notes on *D. misakiense* and *D. acuticephalum*. *Zool. Sci.* **9**: 423–437.
- Furuya, H., K. Tsuneki, and Y. Koshida. 1992b.** Development of the infusoriform embryo of *Dicyema japonicum* (Mesozoa: Dicyemidae). *Biol. Bull.* **183**: 248–257.
- Furuya, H., K. Tsuneki, and Y. Koshida. 1993.** The development of the hermaphroditic gonad in four species of dicyemid mesozoans. *Zool. Sci.* **10**: 455–466.
- Furuya, H., K. Tsuneki, and Y. Koshida. 1994.** The development of the vermiform embryos of two mesozoans. *Dicyema acuticephalum* and *Dicyema japonicum*. *Zool. Sci.* **11**: 235–246.
- Furuya, H., K. Tsuneki, and Y. Koshida. 1996.** The cell lineages of two types of embryo and a hermaphroditic gonad in dicyemid mesozoans. *Dev. Growth Differ.* **38**: 453–463.
- Gersch, J. 1938.** Der Entwicklungszyklus der Dicyemiden. *Z. wiss. Zool.* **151**: 515–605.
- Hochberg, F. G. 1990.** Diseases caused by protists and metazoans. Pp. 47–202 in *Diseases of Marine Animals, Vol. III*. O. Kinne, ed. Biologische Anstalt Helgoland, Hamburg.
- Hochberg, F. G., and R. B. Short. 1970.** *Dicyemenea littlei* sp. n. and *Dicyema benthocopi* sp. n.: dicyemid Mesozoa from *Benthocopus megellonicus*. *Trans. Am. Microsc. Soc.* **89**: 216–224.
- Katayama, T., H. Wada, H. Furuya, N. Satoh, and M. Yamamoto. 1995.** Phylogenetic position of the dicyemid mesozoa inferred from 18S rDNA sequences. *Biol. Bull.* **189**: 81–90.
- Kobayashi, M., H. Furuya, and W. H. Holland. 1999.** Dicyemids are higher animals. *Nature* **401**: 762.
- Lameere, A. 1919.** Contributions à la connaissance des Dicyémides. *Bull. Biol. Fr. Belg.* **53**: 234–275.
- Lapan, E. A., and H. J. Morowitz. 1975.** The dicyemid Mesozoa as an integrated system for morphogenetic studies. 1. Description, isolation and maintenance. *J. Exp. Zool.* **193**: 147–160.
- McConnaughey, B. H. 1938.** The dicyemid Mesozoa. *J. Entomol. Zool.* **30**: 1–12.
- McConnaughey, B. H. 1951.** The life cycle of the dicyemid Mesozoa. *Univ. Calif. Publ. Zool.* **55**: 295–336.
- Nouvel, H. 1933.** Recherches sur la cytologie, la physiologie et la biologie des Dicyémides. *Ann. Inst. Océanogr. Monaco* **13**: 165–255.
- Nouvel, H. 1947.** Les Dicyémides. 1^{re} partie: systématique, générations, vermiformes, infusorigène et sexualité. *Arch. Biol. Paris* **58**: 59–220.
- Schartau, O. 1940.** Der Entwicklungszyklus von *Microcyema vespa* van Beneden (Heterocyemidae). *Pubbl. Stn. Zool. Napoli* **18**: 118–128.
- Short, R. B. 1962.** Two new dicyemid mesozoans from the Gulf of Mexico. *Tulane Stud. Zool.* **9**: 101–111.

Shaping of Colony Elements in *Laomedea flexuosa* Hinks (Hydrozoa, Thecaphora) Includes a Temporal and Spatial Control of Skeleton Hardening

IGOR A. KOSSEVITCH¹, KLAUS HERRMANN^{2,*}, AND STEFAN BERKING²

¹Department of Invertebrate Zoology, Biology Faculty, Moscow State University, Moscow 119899, Russia; and ²Zoologisches Institut, Universität zu Köln, Weyertal 119, 50923 Köln, Germany

Abstract. The colonies of thecate hydroids are covered with a chitinous tubelike outer skeleton, the perisarc. The perisarc shows a species-specific pattern of annuli, curvatures, and smooth parts. This pattern is exclusively formed at the growing tips at which the soft perisarc material is expelled by the underlying epithelium. Just behind the apex of the tip, this material hardens. We treated growing cultures of *Laomedea flexuosa* with substances we suspected would interfere with the hardening of the perisarc (L-cysteine, phenylthiourea) and those we expected would stimulate it (dopamine, *N*-acetyldopamine). We found that the former caused a widening of and the latter a reduction in the diameter of the perisarc tube. At the same time, the length of the structure elements changed so that the volume remained almost constant. We propose that normal development involves a spatial and temporal regulation of the hardening process. When the hardening occurs close to the apex, the diameter of the tube decreases. When it takes place farther from the apex, the innate tendency of the tip tissue to expand causes a widening of the skeleton tube. An oscillation of the position at which hardening takes place causes the formation of annuli.

Introduction

The fragile, almost beautiful pattern of hydrozoa colonies attracts every observer's interest. There are many variations reminiscent of plumes, plants, or minute trees. At closer examination the pattern of the colonies is fixed by a rigid outer skeleton, the chitinous perisarc. We are interested in how this perisarc is shaped.

Inside the perisarc is a hollow tube of soft tissue composed of two cell layers separated by an extracellular matrix, the mesogloea. This matrix is flexible. In general, a colony comprises two parts: a net of tubes (stolons or hydrorhiza) generally fixed to a substratum, and shoots (hydrocauli) emerging vertically from these stolons in a more or less regular pattern. The shoots bear polyps (hydranths) with which the animals catch their prey. All parts of the colony are covered with the perisarc. In thecates, the polyp expands out of the tubelike endings of the perisarc covering (Fig. 1).

The perisarc of the stolons is an almost uniform tube that is flattened at the site of tight contact to the substratum. The perisarc of the shoots in *Laomedea flexuosa* Hinks, used in this research, forms a repetitive pattern (Fig. 1). One element of the shoot—the internode—consists of two sequences of annuli separated by a smooth, slightly bent tube and followed by the finely structured housing (hydrotheca) of the polyp. The sequence, the number, and the size of the pattern elements are almost invariant and species specific (Kosevich, 1990). The exact composition of the perisarc is unknown, but it appears to contain up to 30% of chitin (Jeuniaux, 1963; Holl *et al.*, 1992).

Both the stolon and the shoot tubes increase in length exclusively at their tips (Kühn, 1914; Hyman, 1940). Hence, the pattern of the perisarc emerges exclusively at that site. Close to the apex of the elongating tube, this material is rather soft and flexible. Its shape is exactly that of the underlying tissue. The perisarc material “hardens” some dozens of micrometers proximal to the apex, and from that time onward it has a fixed shape. The pattern of the perisarc is a time recording of the activity of the tissue in the tip.

Our interest is to learn how the perisarc is shaped. One possibility is that in the course of growth, cell-cell interactions

Received 5 February 2001; accepted 26 July 2001.

* To whom correspondence should be addressed. E-mail: k.herrmann@uni-koeln.de

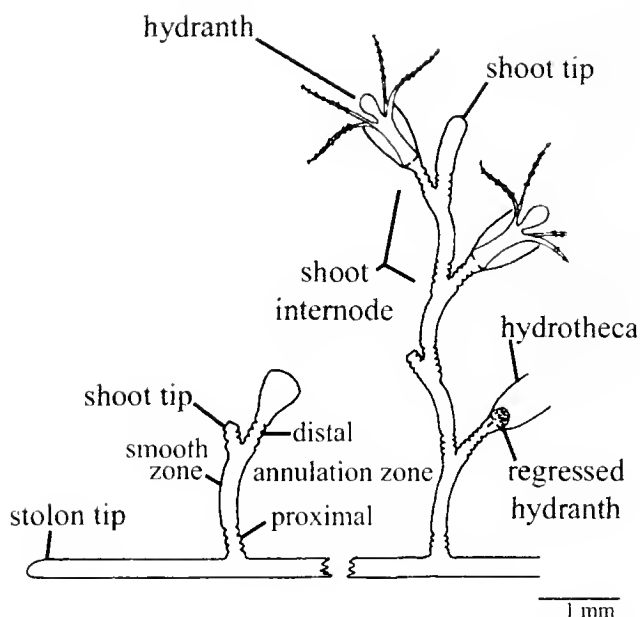


Figure 1. A colony of *Laomedea flexuosa* illustrating the perisarc and two hydranths.

cause a differential curving of the tip surface, and that this pattern is simply fixed by the perisarc. In this case the time at which the perisarc hardens has no influence on the shape of the perisarc. But shaping could also involve a differential pattern in time and space of perisarc hardening. When the perisarc hardens closer to the apex, the diameter of the growing tube should decrease thereafter. But when hardening takes place more distantly, the diameter can increase due to the tendency of the tissue in the apex to expand.

To test whether a differential hardening of the perisarc could play a role in the process of shaping, we treated the colonies with substances that could be expected to either support or to antagonize the hardening process. The effects we observed indicate that both a spatial and temporal pattern of perisarc hardening is involved in the shaping of the perisarc.

Materials and Methods

Animals

Colonies of *Laomedea flexuosa* Hincks (Thecophora, Campanulariidae) were cultured on glass microscope slides in artificial seawater (Tropic Marine, 1000 mOsmol, pH 8.2–8.3) in a 5-l aquarium at 18 °C. The animals were fed daily with *Artemia salina* nauplii.

Test system

Shoots with newly emerged tips were used as test systems. Shoots including 4 to 6 distal internodes were isolated from the colony 2–4 h after feeding. The pieces were used immediately.

The treatment was performed in 4-ml petri dishes. Normally, the treatment lasted for 14 to 36 h. Under such conditions the shoot tip completed the formation of the internode in about 20 to 24 h. The animals were not fed during the course of the experiment. However, the tips of fed and unfed specimens grew with the same speed (Kossevitch, 1991). The medium was not changed. The results were scored at different times, starting 14 h after the beginning of the treatment. Measurements were made by means of an ocular micrometer. The proximal internodes of the isolated shoots that had completed their development before the start of the experiment served as the control, and were termed untreated.

Chemicals used for treatments

The stock solutions of the following chemicals were prepared in distilled water: 10 mM/l dopamine (Sigma), 10 mM/l *N*-acetyldopamine (Sigma), 5 mM/l phenylthiourea (Sigma), 0.1% Calcofluor white (Fluorescent Brightener 28 [Sigma]). The following stock solutions were prepared in seawater: 10 mM/l L-cysteine (Sigma), adjusted to pH 8.2–8.3, each time freshly prepared; staining solution for phenol compounds with fast red salt (Chroma, Stuttgart) according to Romeis (Clara, after Romeis, 1968), treatment for 3 to 5 min under visual control; 0.001% Congo red (Merck) and Evans blue (Merck), treatment for 5 to 15 min under visual control; 4% formaldehyde (Merck), treatment for 24 h.

Statistics

The significance of differences between data obtained following the various treatments was calculated by means of the *F*-test and the one-tailed *t* test.

Results

Architecture of the stolon tip and the shoot tip

The stolon and the shoot tip differ in size. During formation of the smooth part of a shoot, the tissue tube in the tip is about 160–250 μ m in diameter and is in tight contact with the perisarc over a length of 250–350 μ m (the perisarc is translucent). The tissue tube in the stolon tip is 200–300 μ m in diameter and is in tight contact with the perisarc over a length of 300–500 μ m. In both cases, adjacent to that region the tissue tube is much smaller in diameter and has tight contact with the perisarc at only a few positions.

The mode of perisarc formation

The composition of the perisarc is not well known but includes chitin and proteins (Jeuniaux, 1963; Chapman, 1973). The proteins of related species were found to contain a high concentration of disulfide bonds (Chapman, 1937; Bouillon and Levi, 1971). Phenol compounds are expected

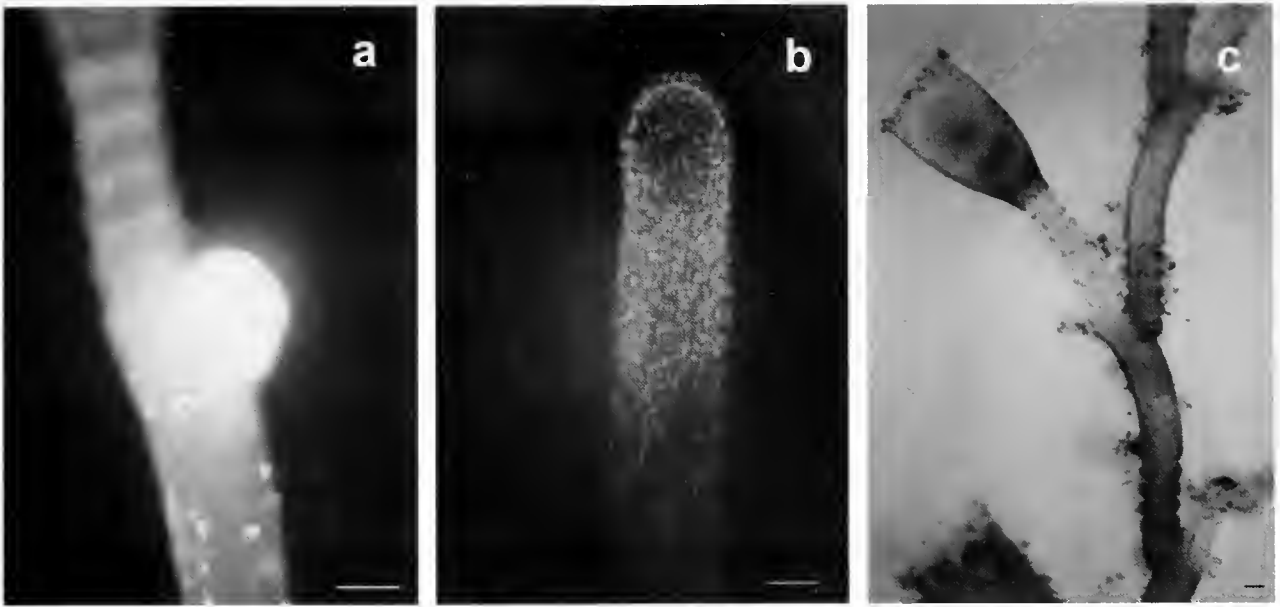


Figure 2. *Laomedea flexuosa* stained with various compounds. (a) A shoot stained with Calcofluor white. Note that the new tip is strongly stained, but the staining in the previously formed internode occurs in patches. (b) A stolon tip stained with formaldehyde. Note the decrease in the brightness of the fluorescence in the proximal direction. (c) Shoot perisarc stained with 1mM of dopamine. The proximal part of the internode and of the hydrotheca are well stained, but the distal annulation zone is almost unstained. The scale bar represents 100 μm .

to play a role in the hardening by causing a crosslinking between the proteins and the chitin (Knight, 1970).

Figure 2a shows the result of staining with Calcofluor white, which stains various carbohydrate fibrils, including amorphous chitin (Compère, 1996). The treatment stains the perisarc of the tip and in particular the outer surface of all ectodermal cells in the tip, that is, in the region in which all ectodermal cells contact the perisarc. Proximal to the tip, the ectoderm is not in close contact with the perisarc. In this region, the surface of the ectoderm, staining is observed to be in the shape of patches. The diameter of such a patch corresponds to the diameter of one or several ectodermal cells. The perisarc in the proximal part shows very little staining. No correlation between the spatial pattern of stained cells and the perisarc pattern could be detected. It appears that perisarc material is almost continuously secreted by the epithelial cells along the whole shoot, with the cells in the tip being the most active ones. That correlates with the finding that in old parts of the colony the perisarc is thicker than in younger parts. For example, the thickness of the perisarc wall in the smooth part of the internodes was found to change from proximal (the eldest) towards distal (the youngest) as follows (in μm): 11.95–8.34–7.56–6.10–4.39–3.17. Note that the distal part is stained but the proximal is not.

After formaldehyde was applied, a fluorescent stain appeared in cells of the ectoderm or at their surface. The stained cells were more numerous within the tip, but were

also found in smaller numbers along the whole tissue proximal to the tip (Fig. 2b). This result may indicate the presence of phenol compounds, which are known to play a role in the hardening process or sclerotization of the chitin-containing exoskeletons of various animals, including cnidarians (Knight, 1968, 1970; Holl *et al.*, 1992).

Although the perisarc looks almost uniform within an internode, it is not. Treatment with dyes including dopamine, fast red salt, Evans blue, and Congo red revealed a distinct pattern of staining of the perisarc. The most intense and spatially different staining was obtained with dopamine (Fig. 2c). The staining intensity decreases gradually from the most proximal position to the distal end of the smooth part. The distal annulated zone is not stained, whereas in the hydrotheca the staining is intense again. In elder internodes the pattern is identical, but the staining is *deeper*. Thus, the pattern of staining does not correspond simply to the thickness of the perisarc wall. Because of the chemical nature of the various agents and their binding specificity, we argue that these substances bind to phenol compounds, which may have played a role in cross-linking the proteins and the chitin in the skeleton (*cf.* Holl *et al.*, 1992).

The influence of L-cysteine on shoot patterning

L-cysteine is able to interfere with the formation of disulfide bonds between and within proteins. Thus, the application of L-cysteine may antagonize perisarc hardening if

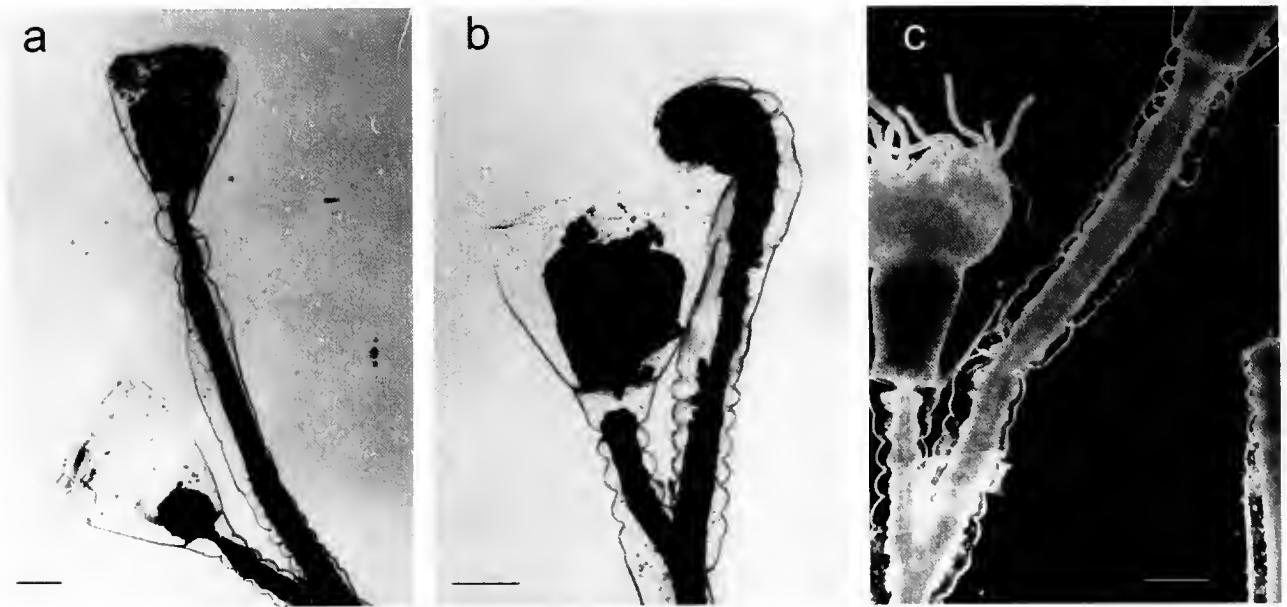


Figure 3. Alteration of the shoot perisarc shape due to treatment with L-cysteine and phenylthiourea. Treatment with 1 mM/l of L-cysteine. (a); 2 mM/l of L-cysteine (b); 0.25 mM/l of phenylthiourea (c). Note that the proximal annulation zone is smoothed, the smooth part is crumbled, and the distal annulation zone is smoothed and widened. Compare the normal pattern elements on the left side of each graph. The scale bar represents 100 μm .

the formation of disulfide bonds is involved in this process. In addition, L-cysteine impedes the formation of diphenols (Horowitz *et al.*, 1970). Diphenolic compounds including dopamine and *N*-acetyldopamine were shown to be involved in the sclerotization of the cuticle of insects (Kramer *et al.*, 1987; Sugumaran, 1987).

Treatment of shoots with L-cysteine greatly altered the shape of the perisarc. The perisarc tube widened, crumbled, and displayed folds at unusual positions (Fig. 3a, b). The smooth part and the distal annulated zone were especially affected. Most important, the annuli of the distal part, which form after the onset of the treatment, were not separated by the usual deep indentations, but displayed a much smoother pattern. (Compare as internal control the old pattern elements that formed before the start of treatment [Fig. 3]). The effect was observed following application of up to 1–2 mM/l of L-cysteine. Concentrations ten times higher caused the tissue to disintegrate.

Although the shape of the perisarc was altered to a great degree, the sequence of the pattern elements—such as the proximal annulated zone, the smooth part, the distal annulated zone, and the hydrotheca—was laid down as usual. It appears that even the volume of these elements was not significantly changed. Thus, the applied concentrations of L-cysteine did not strongly affect the pattern-forming processes in the tissue, but rather adversely affected the normal perisarc hardening. Due to the L-cysteine treatment, the perisarc remained soft for a longer period of time, allowing

external and internal mechanical forces to produce the observed malformations.

The influence of phenylthiourea on stolon and shoot patterning

Phenylthiourea, due to its sulfhydryl moiety, was also expected to interfere with the hardening of the perisarc. As was found for L-cysteine, phenylthiourea hinders the formation of diphenols by interaction with the monophenol monooxygenases (Lerch, 1983). Treatment of shoots by application of 0.25–0.5 mM/l of phenylthiourea resulted in the formation of bent and crumpled pattern elements. In particular, the distal annulated zone and the smooth part of the shoot were affected (Fig. 3c). Following treatment with L-cysteine, the annuli were not separated by the usual deep indentations but displayed a much smoother pattern. The sequence of pattern elements was unchanged.

Dopamine

The diphenol dopamine is an intermediate on the way to those diphenols that are involved in cross-linking of components of the cuticle in insects. In *L. flexuosa* Knight (1970) found dopamine and a phenoloxidase. He suggested that both substances generate quinones that react to cross-link structural proteins. We found that 0.1 mM/l of dopamine reduced the maximal diameter of both the smooth part and the distal annulated zone. At the same time, the length

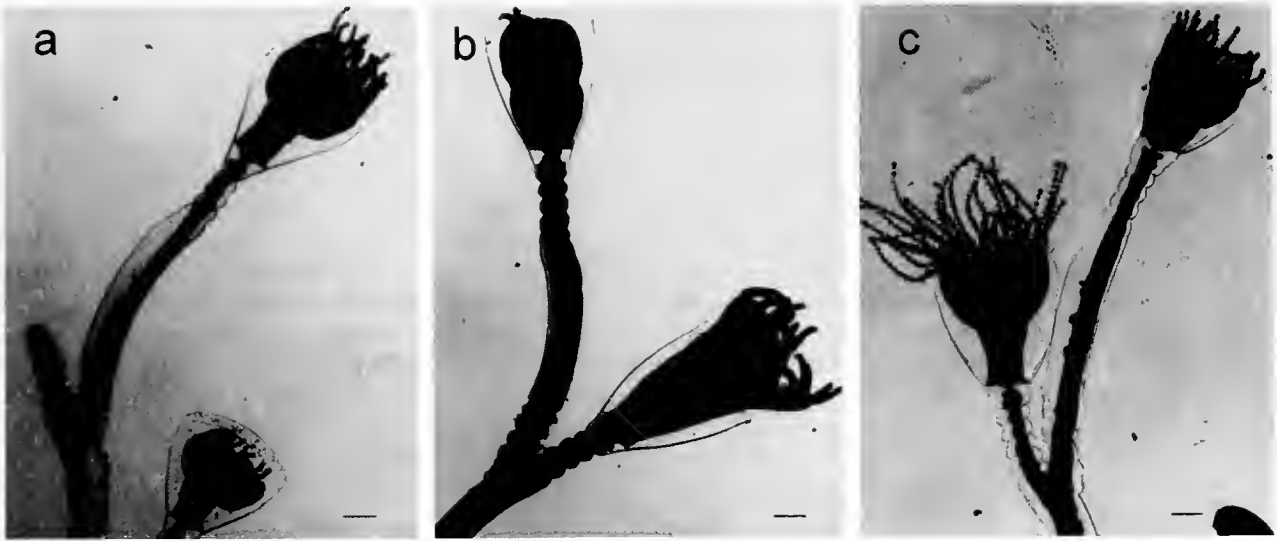


Figure 4. Alteration of the shoot perisarc shape due to treatment with dopamine and *N*-acetyldopamine. (a) Treatment with 0.1 mM/l of dopamine (b) Untreated control (c) Treatment with 0.1 mM/l of *N*-acetyldopamine. Note that the smooth part and the distal annulation zone are increased in length, and the proximal annulation zone is irregular in shape due to treatment with *N*-acetyldopamine. Compare Fig. 4b as control. The scale bar represents 100 μ m.

of these pattern elements increased (Fig. 4a, Fig. 5). In the annulated zone, the ratio between the maximal outer diameter of the annuli and the diameter of the furrow between adjacent annuli remained almost unchanged (not shown). In the proximal annulated zone, the effect was less pronounced. One reason may be the short interval between the onset of treatment and the formation of the proximal annuli. Further, the composition of the perisarc may play a role. The resultant staining of the perisarc was strong in the

proximal annulated zone and almost absent in the distal annulated zone (Fig. 2c).

N-acetyldopamine

In insects, *N*-acetyldopamine is thought to be an intermediate between dopamine and the diphenols used for cross-linking of the cuticle (Kramer *et al.*, 1987; Sugumaran, 1987). Knight (1970), however, suggested that the mecha-

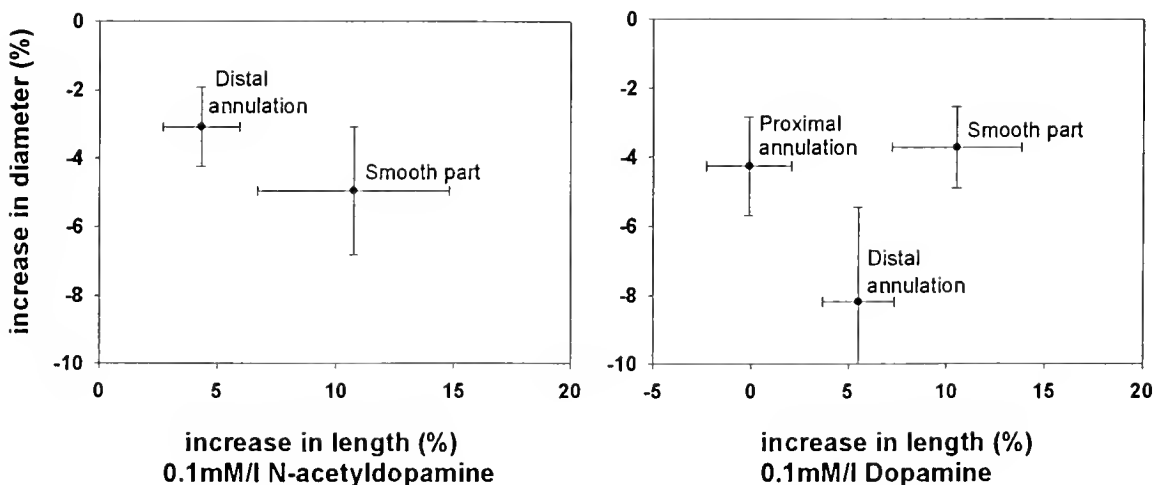


Figure 5. Treatments of growing tips with dopamine and *N*-acetyldopamine change the diameter-to-length ratio of the structural elements of a shoot internode. A concentration of 0.1 mM/l of the compounds was applied. The graphs show the changes in the size (dimensions) of the internode parts. The data are given as percent of increase as compared to the respective control, the previously formed internode. The bars indicate the standard deviation of the mean. dopamine, two experiments, $n = 9, 10$, and *N*-acetyldopamine $n = 7$.

nism of sclerotization of the hydroid perisarc differs from that of insects, because he failed to detect *N*-acetyldopamine and phenolic- β -glucosides in hydroids. In *L. flexuosa*, a concentration of 0.1 mM of *N*-acetyldopamine caused the smooth part and the annuli of the distal annulated zone to become narrower and longer (Figs. 4a, b; Fig. 5). Further, as observed for the treatment with dopamine, the ratio between the maximal outer diameter of the annuli and the diameter of the furrow between adjacent annuli remained almost unchanged. Unlike dopamine, *N*-acetyldopamine strongly affected the proximal annulated zone, eliminating its regular annulation pattern (Fig. 4c). *N*-acetyldopamine may act faster than dopamine.

There is no indication of an unspecific, cytotoxic action of the chemicals. One can see in the figures that the older colony elements are unaffected by the treatment: polyps stretch out of their hydrotheca, and they are able to catch their prey. The hydrothecae formed during treatment with the chemicals are well shaped, and living polyps formed with tentacles.

Discussion

The delicate species-specific pattern of a thecate colony is laid down exclusively at the growing tip. At this site, the tissue has permanent contact with the expelled soft material from which the outer skeleton, the perisarc, is formed. Some dozen micrometers proximal to the apex of the tip, the perisarc hardens, which fixes the pattern of the perisarc.

It is obvious that the soft material is molded by the outer shape of the underlying tissue. This outer shape is determined by the property and activity of the cells that built the tissue tube, particularly those cells that produce the growing tip. In the tip, the tissue moves back and forth rhythmically. This phenomenon, termed growth pulsation, has been studied extensively (Belousov *et al.*, 1992).

The staining with Calcofluor white suggests that the amorphous perisarc material that eventually forms fibrils, including chitin fibrils, is secreted by almost all the ectodermal epithelial cells of the growing tip, as well as by some epithelial cells along the body axis. The phenolic compounds, which Knight contended to be involved in the cross-linking of the perisarc, appear to be contained in so-called tanning cells (Knight, 1970). These cells are concentrated in the tip and also exist in lower density in the proximal parts. They have no broad contact with the outer surface of the epithelial sheet of the growing tip and are embedded between the epithelial cells (Knight, 1970).

Our data suggest that a differential hardening of the perisarc is involved in the shaping of the perisarc tube. We treated a growing culture with substances that we expected, from their chemical nature, to affect the hardening process. Phenylthiourea and L-cysteine were expected to impede the hardening; dopamine and *N*-acetyldopamine were expected

to support it. The putative "softeners" caused a crumbling and a widening of the perisarc. Of particular importance is that the constrictions between the annuli were smoothed out in the distal annulated zone. The putative "hardeners" caused the perisarc tube in all internode parts to become narrower and longer. The applied concentration of the various chemicals was apparently not toxic to the animals: in the presence of the chemicals the polyp and the hydrotheca of the internode formed normally and the polyps behaved normally—for example, in stretching out to catch their prey.

We suggest that the composition of the soft perisarc material surrounding the apex changes with time. The nature of the compounds is largely unknown. In insects, low-molecular-weight catechols such as *N*-acetyldopamine and *N*- β -alanyldopamine are involved in sclerotization. These are converted to quinones, which react in cross-linking proteins (for general review see Waite, 1990). Knight (1970) proposed a different mechanism of action for *Laomedea flexuosa*: failing to detect the mentioned substances, he detected dopamine instead, and suggested that it was active in sclerotization. Waite (1990) stated that "this should be taken with caution since the entire animal was methanol-extracted." In organisms other than insects, dopa-containing proteins are thought to cause the sclerotization through a process of "autotanning" (Smyth, 1954; Brown, 1952; Pryor, 1962) in which the dopa moieties are converted to quinones. Additional molecules—of chitin, collagen, fibroin, or cellulose, for example—are necessary as "fillers." This mode of sclerotization is well-distributed throughout the animal kingdom, and Waite and coworkers (1990) found dopa-containing proteins in the cnidarian *Pachygerianthus fimbriatus*. Our results do not help resolve the question of which mode of sclerotization acts in *L. flexuosa*. We know, however, that the concentration of one or several of the components changes rhythmically during the growth of the shoot internode. These rhythms are much slower than those of the aforementioned growth pulsations. If the hardening occurs closer to the apex, the diameter of the ring-shaped border between the hard and the soft perisarc decreases, forcing the tissue to squeeze through this opening. Under these conditions, the perisarc tube elongates with a reduced diameter. A widening of the diameter needs at least two prerequisites: the hardening has to happen more distally from the apex than before, and the tissue of the apex must form a bulb. Evidence for bulb formation may be that the tissue tube in both the tip of the stolon and the tip of the shoot has a tight contact to the perisarc, while in proximal regions the tissue tube is much smaller than the inner lumen of the perisarc tube. Further, the shoot and the stolon occasionally form a bulb at the wound after cutting (Kossevitch, unpubl. obs.).

In the process of annulus formation, the zone of hardening may move rhythmically closer to and then farther away from the apex. This may occur in either a continuous or a

stepwise manner. When a hydrotheca starts to form, the zone of hardening lags behind in relation to the apex of the protruding tissue. That causes a widening of the tissue tube and subsequently of the perisarc tube as well.

In *L. flexuosa*, the observed bending of the tube in the smooth part of the internode (cf. Fig. 1) may be the result of an asymmetry in the hardening of the perisarc along the circumference of the tip. It may occur closer to the tip apex at the side that faces the shoot axis, imposing a spatial control of hardening in addition to the temporal control.

In other animals with an exoskeleton, such as arthropods, the integument may be shaped by changes in the hardening process together with changes in the pressure of the tissue against the forming integument. In arthropods other than thecate hydrozoa, the hardening can start at various positions and can spread at different speeds from those positions. The resultant shape of the integument can thus be more complex than in hydrozoa.

The various treatments we applied caused the perisarc to bend, to fold, and to crumble. However, the sequence of the pattern elements up to hydrotheca formation was as normal as possible. The volume of the tissue responsible for the formation of the corresponding element was largely unchanged. The decrease in the diameter of the perisarc tube was compensated for by the elongation of the tube. This indicates that the very tip determines the sequence of pattern elements. The respective decisions of the tip were not influenced by (1) the chemicals applied in the concentrations noted, (2) the disturbance of the shape and movements of the tissue in the tip, (3) the shape of the tissue tube in a more proximal region, nor (4) the altered tension and pressure of the proximal tissue on the tissue in the very tip. These four points are in agreement with the observation that the experimentally isolated shoot tip continued the patterning program of the perisarc tube up to the formation of the polyp's housing. The tissue itself was transformed into only the apical part of the polyp; the proximal part of the perisarc tube was free of tissue (Kosevich, 1991).

Acknowledgments

This work was in part supported by the Deutscher Akademischer Austauschdienst (PKZ A/98/40374) for I.A.K.

Literature Cited

- Belousov, L. V., J. A. Labas, and N. I. Kazakova. 1992. Growth pulsations in hydroid polyps: kinematics, biological role and cytophysiology. Pp. 183–193 in *Oscillations and Morphogenesis*, L. Rensing, ed. Marcel Dekker, New York.
- Bouillon, J., and C. Levi. 1971. Structure et ultrastructure des attaches

hydranthes-hydrothèques chez les polypes Thecata. *Z. Zellforsch.* **121**: 218–231.

- Brown, C. H. 1952. Some structural proteins of *Mytilus edulis*. *Q. J. Microsc. Sci.* **93**: 487–502.
- Chapman, G. 1973. A note on the composition of some coelenterate exoskeletal materials. *Comp. Biochem. Physiol.* **45B**: 279–282.
- Chapman, S. S. 1937. Localization of -SH and -S-S- in *Obelia geniculata*. *Growth* **1**: 299.
- Compère, P. 1996. Cytochemical labelling of chitin. Pp. 66–87 in *Chitin in Life Sciences*, M. M. Giraud-Guille, ed. Jacques André Publisher, Lyon, France.
- Holl, S. M., J. Schaefer, W. M. Goldberg, K. J. Kramer, T. D. Morgan, and T. L. Hopkins. 1992. Comparison of black coral skeleton and insect cuticle by a combination of carbon-13 NMR and chemical analyses. *Arch. Biochem. Biophys.* **292**: 107–111.
- Horowitz, N. H., M. Fling, and G. Horn. 1970. Tyrosinase (*Neurospora crassa*). *Methods Enzymol.* **17A**: 615–620.
- Hyman, H. 1940. *The Invertebrates: Protozoa through Ctenophora*. McGraw-Hill, New York. Pp. 400–497.
- Jeuniaux, C. 1963. *Chitine et Chitinolyse. Un chapitre de la biologie moléculaire*. P. Masson, Paris.
- Knight, D. P. 1968. Cellular basis for quinone tanning of the perisarc in the thecate hydroid *Campanularia* (= *Obelia*) *flexuosa* Hinks. *Nature* **218**: 584–586.
- Knight, D. P. 1970. Sclerotization of the perisarc of the caliptoblastic hydroid, *Laomedea flexuosa*. I. The identification and localization of dopamine in the hydroid. *Tissue Cell* **2**: 467–477.
- Kosevich [Kossevitch], I. A. 1990. Development of stolon's and stem's internodes in hydroid genera *Obelia* (Campanulariidae). *Vestn. Mosk. Univ. Biol.*, **N 3**: 26–32. [In Russian; English summary.]
- Kosevich [Kossevitch], I. A. 1991. Comparison of upright's and stolon's tips function in hydroid colony *Obelia loveni* (Allm.) (Campanulariidae). *Vestn. Mosk. Univ. Biol.*, **N 2**: 44–52. [In Russian; English summary.]
- Kramer, K. J., T. L. Hopkins, J. Schaefer, T. D. Morgan, J. R. Garbow, G. S. Jacob, E. O. Stejskal, and R. D. Speirs. 1987. Mechanisms of insect cuticle stabilization. How do tobacco hornworms do it? Pp. 331–355 in *Molecular Entomology*, J. H. Law, ed. Alan R. Liss, New York.
- Kühn, A. 1914. Entwicklungsgeschichte und Verwandtschaftsbeziehungen der Hydrozoen. I. Teil: Die Hydroiden. *Ergebnisse Fortschr. Zool.* **4**: 1–284.
- Lerch, K. 1983. Neurospora tyrosinase: structural, spectroscopic and catalytic properties. *Mol. Cell Biochem.* **52**: 125–138.
- Pryor, M. G. M. 1962. Sclerotization. Pp. 371–396 in *Comparative Biochemistry*, Vol. IV, M. Florkin and H. S. Mason, eds. Academic Press, New York.
- Romeis, B. 1968. *Mikroskopische Technik*. R. Oldenbourg, Munich, Germany.
- Smyth, J. D. 1954. A technique for the histochemical demonstration of polyphenoloxidase and its application to eggshell formation in helminths and byssus formation in *Mytilus*. *O. J. Microsc. Sci.* **95**: 139–152.
- Sugumaran, M. 1987. Quinone methide sclerotization. Pp. 357–367 in *Molecular Entomology*, J. H. Law, ed. Alan R. Liss, New York.
- Waite, J. H. 1990. The phylogeny and chemical diversity of quinone-tanned glues and varnishes. *Comp. Biochem. Physiol.* **97B**: 19–29.

Detection of Salinity by the Lobster, *Homarus americanus*

CHRISTOPHER G. DUFORT, STEVEN H. JURY¹, JAMES M. NEWCOMB²,
DANIEL F. O'GRADY III, AND WINSOR H. WATSON III³

*Zoology Department and Center for Marine Biology, University of New Hampshire,
Durham, New Hampshire 03824*

Abstract. Changes in the heart rates of lobsters (*Homarus americanus*) were used as an indicator that the animals were capable of sensing a reduction in the salinity of the ambient seawater. The typical response to a gradual (1 to 2 ppt/min) reduction in salinity consisted of a rapid increase in heart rate at a mean threshold of 26.6 ± 0.7 ppt, followed by a reduction in heart rate when the salinity reached 22.1 ± 0.5 ppt. Animals with lesioned cardioregulatory nerves did not exhibit a cardiac response to changes in salinity. A cardiac response was elicited from lobsters exposed to isotonic chloride-free salines but not to isotonic sodium-, magnesium- or calcium-free salines. There was little change in the blood osmolarity of lobsters when bradycardia occurred, suggesting that the receptors involved are external. Furthermore, lobsters without antennae, antennules, or legs showed typical cardiac responses to low salinity, indicating the receptors are not located in these areas. Lobsters exposed to reductions in the salinity of the ambient seawater while both branchial chambers were perfused with full-strength seawater did not display a cardiac response until the external salinity reached 21.6 ± 1.8 ppt. In contrast, when their branchial chambers were exposed to reductions in salinity while the external salinity was maintained at normal levels, changes in heart rate were rapidly elicited in response to very small reductions in salinity (down to 29.5 ± 0.9 ppt in the branchial chamber and 31.5 ± 0.3 ppt externally). We conclude that the primary receptors responsible for detecting reductions in salinity in *H. americanus* are located within or near the branchial chambers and are primarily sensitive to chloride ions.

Introduction

Several studies have provided evidence for osmolarity or salinity receptors in crustaceans, but the location of such receptors and the precise ionic stimuli that activate them are not fully understood. In a study designed to localize the salinity receptors of the green crab *Carcinus maenas*, Hume and Berlind (1976) selectively exposed different parts of crabs to seawater with a salinity of 15 ppt. They concluded that the salinity receptors were located in or near the excurrent opening of the branchial chambers. In the crayfish *Procambarus simulans*, the branchial chamber also appears to be the location of receptors that mediate cardiovascular responses to changes in salinity (Larimer, 1964). Although the antennae and antennules of lobsters are exquisitely sensitive to a wide range of chemicals (Tierney *et al.*, 1988; Johnson *et al.*, 1989; see review by Atema and Voigt, 1995), it is unclear whether they play a role in sensing salinity. During Hume and Berlind's (1976) investigation of salinity detection in *C. maenas*, removal of the antennae and antennules had no effect. In contrast, Lagerspetz and Mattila (1961), demonstrated that the antennules and antennae played an important role in the detection of low salinity in the isopod *Asellus* sp. and the amphipod *Gammarus oceanicus*, and Tazaki and Tanino (1973) concluded that the antennae of the spiny lobster *Panulirus japonicus* have mechanoreceptors that also function as osmoreceptors. There is also evidence that the legs of crustaceans have receptors that provide important information about salinity. The porcelain crab *Porcellana platycheles* is able to discriminate between water of different salinities by using its walking legs (Davenport and Wankowski, 1973), and Schmidt (1989) recorded electrophysiological responses to changes in salinity from sensilla on the legs of *C. maenas*. Thus, there is some limited evidence for receptors capable of sensing salinity changes in crustaceans, but the locations

Received 27 April 2000; accepted 21 July 2001.

¹ Current address: SUNY-New Paltz, New Paltz, NY 12561.

² Current address: Georgia State University, Atlanta, GA 30303.

³ To whom correspondence should be addressed. E-mail: whw@cisunix.unh.edu

of these receptors and the transduction mechanisms involved are poorly understood.

Little is known about how marine invertebrates detect changes in salinity. The bivalves *Mytilus edulis* and *Scrobicularia plana* close their shells in response to salinity reductions, and the receptors controlling these shell closures are primarily sensitive to Na^+ , Mg^{++} , Ca^{++} , and possibly Cl^- , rather than to osmolarity (Davenport, 1981; Akberali and Davenport, 1982). However, there is also evidence for osmoreceptors in both marine molluscs and crustaceans (Davenport, 1972; Davenport and Wankowski, 1973; Tazaki, 1975; Schmidt, 1989). One goal of this study was to determine whether lobsters detect reductions in salinity by using a transduction mechanism that is sensitive to changes in the concentration of certain ions, or one that responds to alterations in ambient osmolarity.

Homarus americanus, the American lobster, is an excellent organism in which to investigate responses to changing salinity, both in terms of the sensory processes involved and how this behavior is adaptive in certain habitats. Although the American lobster is generally considered to be stenohaline and intolerant to salinities below 25 ppt (Dall, 1970), adult and juvenile lobsters are known to inhabit salt marshes, bays, and estuaries that are characterized by frequent fluctuations in salinity (Thomas and White, 1969; Munro and Therriault, 1983; Able *et al.*, 1988; Jury *et al.*, 1995; Howell *et al.*, 1999; Watson *et al.*, 1999; reviewed by Charmantier *et al.*, 2001). For example, lobsters are regularly found in the Great Bay Estuary, New Hampshire, where the salinity is normally between 22 and 28 ppt in the summer but routinely drops below 15 ppt each spring (Loder *et al.*, 1983; Short, 1992; Watson *et al.*, 1999). After heavy storms, the salinity can also fall to less than 5 ppt (Jury *et al.*, 1995), a value below the lower lethal limit for adult lobsters, which is from 8 to 14 ppt, depending on temperature, oxygen and acclimation conditions (McLeese, 1956). Moreover, even if lobsters are able to survive short-term exposure to low salinity, the resulting physiological stress may have deleterious long-term effects on growth or reproduction (Jury *et al.*, 1994a; Houchens, 1996).

Field studies have shown that lobster movements in estuaries tend to be correlated with seasonal changes in temperature and salinity (Munro and Therriault, 1983; Watson *et al.*, 1999), or with storms that cause substantial decreases in salinity (Jury *et al.*, 1995). Laboratory studies have also demonstrated that both adult lobsters (Jury *et al.*, 1994b) and larval lobsters (Scarratt and Raine, 1967) avoid low-salinity water. For example, when given a choice between two passageways, one containing water held at a low salinity (10–15 ppt) and one at a higher salinity (20–25 ppt), 93% of the lobsters tested moved through the high-salinity passageway. Lobsters also moved out of their shelters if the salinity in those shelters was lowered below 12.5 ppt (Jury *et al.*, 1994b). This avoidance response to low salinity strongly suggests that lobsters possess the ability to detect

decreases in either osmolarity or the concentrations of specific ions.

It is well known that many crustaceans will exhibit a drop in heart rate (bradycardia) or ventilation rate (apnea) in response to novel stimuli (Maynard, 1960; McMahon, 1999). Therefore, as was pointed out by Florey and Kreibel (1974), heart rate "can serve as a most sensitive indicator of sensory perception and it could well be used in studies on perceptual physiology." For example, Larimer (1964) showed that crayfish exhibited changes in heart rate when exposed to (1) solutions low in oxygen; (2) different concentrations of NaCl and L-glutamic acid; and (3) sudden changes in temperature. A cardiac assay was also used by Offutt (1970) to measure the ability of *H. americanus* to detect sounds of different frequencies, and by Jury and Watson (2000) to measure the thermosensitivity of *H. americanus*.

In the present study, we employed a cardiac assay to demonstrate that lobsters are able to sense drops in salinity of greater than 4 ppt. Although removal of the legs, antennae, and antennules had little impact on their responsiveness, selective perfusion of the branchial chamber revealed that this is the most likely location of receptors sensitive to changes in salinity. Finally, by exposing lobsters to seawater deficient in certain ions, we determined that lobsters probably detect changes in salinity by monitoring the concentration of chloride rather than by sensing changes in osmolarity.

Materials and Methods

Adult (>82 mm carapace length), intermolt lobsters of both sexes were captured in research traps in the Gulf of Maine, near New Castle, New Hampshire. They were held in recirculating tanks at a salinity of 32 ppt and a temperature of 12 to 14 °C for up to 2 weeks prior to use. Throughout this paper, "normal" seawater refers to full-strength (along the NH coast), 32 ppt seawater.

Cardiac assay

Changes in heart and ventilation rates were used as indicators that lobsters sensed an alteration in their environment. Two pairs of wire electrodes, insulated except at the tips, were inserted through the carapace of each lobster and then fastened to the shell with tape and cyanoacrylate glue. Typically, one pair was implanted through the dorsal carapace on either side of the heart, and the second pair was inserted through the lateral carapace over the scaphognathites (gill bailers). The electrodes were connected to an impedance converter (UFI, Morro Bay, CA) that produced analog signals proportional to the magnitude of the movements of the heart or gill bailer. The impedance converter output was then digitized using a MacLab analog-to-digital interface (AD Instruments, Grand Junction, CO), and this digitized signal was recorded on a Macintosh computer. In

some cases, data were also recorded on an AstroMed Dash 4 polygraph (Grass Instruments, Quincy, MA).

Lobsters were placed individually in a 3-l light-tight acrylic plastic chamber that was continuously perfused with cooled (12 to 14 °C) normal seawater taken from a large holding aquarium. The experimental chamber was connected by tubing to two 1-l stimulus bottles, one containing experimental (0 ppt) water, and the other containing control seawater (32 ppt). Valves were used to control whether the lobster received an experimental or a control stimulus. During the ion-sensitivity experiments (see subsequent section of Materials and Methods), the experimental water consisted of solutions that were isotonic to the seawater in the recording chamber (950–1050 mOsm) but deficient in one or more specific ions. The temperature of the water in the stimulus bottles was held constant by placing them in a 25-l water bath that was maintained at the same temperature as the chamber holding the lobster.

Lobsters were secured in the chamber with elastic bands fastened loosely across their dorsal carapace and left overnight to adjust to this new environment. Previous studies have indicated that cardiac responses are more pronounced and are elicited with smaller stimulus intensities when lobsters are left in the chamber overnight instead of being tested shortly after electrode implantation (Offutt, 1970; Florey and Kriebel, 1974; Jury and Watson, 2000).

All lobsters were first tested to determine whether their heart rates altered in response to tactile stimulation, 10^{-4} betaine (Atema and Voigt, 1995), or shadows (Larimer, 1964). Only lobsters that exhibited a cardiac response to these stimuli were used in subsequent experiments. A Quicktime video showing a lobster cardiac response to a low-salinity stimulus can be viewed at the following website: <http://zoology.unh.edu/faculty/win/winvideos.htm>.

Salinity detection threshold

In this experiment, 30 lobsters (15 male, 15 female) were tested for their ability to sense changes in salinity. For each animal, the salinity in the recording chamber was gradually lowered from a starting value of 32 ppt to less than 20 ppt, at a rate of 1–2 ppt/min, while heart and scaphognathite rates were continuously recorded. To monitor salinity, a piece of tubing was placed in the experimental chamber near the inhalent opening to the lobster's branchial chamber. Throughout the experiment water from this area of the chamber continuously dripped out of this tubing. At 1-min intervals, the salinity of the water flowing from this tubing was determined, in parts per thousand, using a refractometer. It took 10 s for water to flow from the chamber to the end of the tubing, and data were adjusted for this time lag.

During these experiments, under these controlled conditions, the heart rates were very stable, deviating less than 4% from one minute to the next. Thus, a sudden, stimulus-induced increase or decrease in heart rate was very obvious

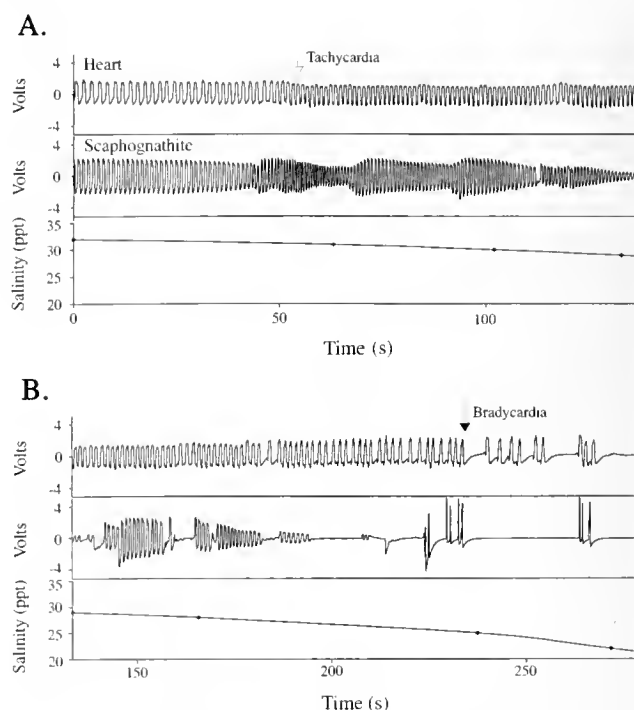


Figure 1. Impedance recordings (in volts) of heart and scaphognathite activity during reductions in salinity for a typical test animal. The salinity was decreased at a rate of 1–2 ppt/min. (A) The initial response was typically a rapid increase in heart rate, or tachycardia, which took place in this experiment at a salinity of 31 ppt and was accompanied by an increase in ventilation rate, as can be seen in the scaphognathite recording. Initiation of tachycardia is indicated by the open arrow. (B) As the salinity was decreased further, to 25 ppt, the lobster responded with a rapid decrease in heart rate, or bradycardia. Initiation of bradycardia is indicated by the closed arrow. Bradycardia was usually accompanied by a decrease in ventilation rate (*i.e.*, apnea).

(see Fig. 1 for example). However, even under the most stable conditions, occasionally lobsters will spontaneously skip a heartbeat, or ventilate their gill bailers in the reverse direction, which is often accompanied by a small change in heart rate. Therefore, to avoid counting these events as responses to salinity drops, we set a more obvious and conservative criterion for designating a change in rate as either a tachycardia or bradycardia response. This criterion was either an increase or a decrease of at least 25% from the baseline heart rate that lasted for more than 10 s. When a cardiac response occurred, the salinity measured at the beginning of the response (taking into account the time lag) was considered to be the salinity detection threshold (SDT) for that animal. All results are reported as a mean \pm SEM.

Ion sensitivity assay

To determine which ions were used to detect differences in salinity, cardiac responses were measured while exposing lobsters ($n = 37$) to artificial saline solutions that were deficient in one or more specific ions. Most lobsters were

exposed to at least two different salines, yielding a total of 61 trials. All artificial saline solutions were isotonic with seawater, so the osmolarity did not change as they were introduced into the experimental chamber, but the concentrations of certain ions did change.

Each artificial saline solution was deficient in one, or a combination, of the following ions: sodium, chloride, magnesium, and calcium. The solutions tested were: 550 mM sodium bicarbonate, 530 mM sodium acetate, 530 mM sodium phosphate, 590 mM choline chloride, and 530 mM sodium chloride, as well as artificial seawater (423 mM NaCl, 9 mM KCl, 9.27 mM CaCl₂, 22.94 mM MgCl₂, 25.50 mM MgSO₄, 2.14 mM NaHCO₃), sodium-free seawater (9.40 mM KCl, 9.00 mM CaCl₂, 22.10 mM MgCl₂, 25.60 mM MgSO₄, 455 mM choline chloride, and 2.10 mM KHCO₃) and chloride-free seawater (25.50 mM MgSO₄, 2.14 mM NaHCO₃, 422.30 mM NaNO₃, 9.69 mM KNO₃, and 9.27 mM Ca(NO₃)₂). The pH of most solutions was adjusted to 7.6–7.7 with hydrogen chloride, acetic acid, sodium hydroxide, or potassium hydroxide, depending on the ions being tested. A few solutions, such as sodium acetate and choline chloride, were allowed a larger pH range (6.7–8.1), because adjusting the pH would alter the concentration of either Na⁺, K⁺, or Cl⁻ ions, as well as the overall osmolarity. In separate tests, lobsters did not exhibit cardiac responses when only the pH of natural seawater was changed over the range 6.2 to 8.1.

Blood osmolarity experiments

These experiments were carried out to determine whether significant changes in hemolymph osmolarity take place during the type of salinity reduction protocol used in the salinity detection studies. Individual lobsters ($n = 8$) were placed in the experimental chamber, and the salinity was decreased at a rate of 1.5 ppt/min. Before the salinity was decreased, and every 2 min during the study, the lobster was quickly removed from the chamber and 0.3 ml of hemolymph was removed from the base of one of the walking legs using a 1-ml tuberculin syringe and a 26-gauge needle. Because all SDTs in previous experiments occurred less than 16 min after exposure to low salinity, these experiments were conducted for 16 min. Hemolymph samples were placed in 1-ml eppendorf tubes on ice. Seawater samples were also taken from the experimental chamber every 2 min and placed in tubes on ice. Control lobsters ($n = 8$) were subjected to a similar protocol, except that the salinity of the seawater was kept constant. The osmolarities of all the hemolymph and water samples were measured using a Wescor vapor-pressure osmometer. The heart and ventilation rates were not measured from these lobsters because the repetitive blood sampling caused dramatic changes in heart rate that were not related to reductions in salinity.

Cardioregulatory nerve lesions

To determine whether changes in heart activity are mediated by the cardioresgulatory nerves, three groups of lobsters were tested for cardiac responses to salinity changes. The first group of lobsters ($n = 5$) had their cardioresgulatory nerves cut (lesion); the second group ($n = 5$) had the same operation as the first group except that their cardioresgulatory nerves were left intact (sham); and the third group ($n = 5$) was handled, but did not undergo an operation (control). The baseline heart rates of all lobsters were recorded for more than 1 h before surgery and again at least 4 days after surgery, to determine if lesioning the cardioresgulatory nerves had any effect on baseline heart rates. Once baseline heart rates were recorded, all lobsters were then tested for a cardiac response to reduced salinity. All recordings were carried out as described above, after lobsters had become accustomed to the recording chamber overnight.

Lesions were performed as described in Guirguis and Wilkens (1995). Briefly, a small (3-cm²) rectangular piece of dorsal carapace just above the heart was removed, and superficial cuts were made with fine scissors through the connective tissue along the border of the opening. The shell was then replaced and secured with tape and cyanoacrylate glue.

Ablations

First, the SDTs of the experimental lobsters ($n = 15$) were determined by the cardiac assay method. Then, after chilling the animals for 30 min, their antennae ($n = 5$), antennules ($n = 5$), or all walking legs ($n = 5$) were removed. After at least 4 weeks of recovery in a flow-through tank at the UNH Coastal Marine Laboratory, the lobsters were tested again to determine the salinity reduction necessary to elicit bradycardia.

Selective perfusion of the branchial chambers

Since the branchial chamber cannot be isolated by lesioning, a different technique was employed to determine whether this region is receptive to reductions in salinity. Both branchial chambers of six lobsters were cannulated with polyethylene (PE) tubing (1.57 mm I.D.). Four lengths of PE tubing were inserted into each branchial chamber through small holes drilled in the carapace near the dorsal edge of the branchial chambers and glued into place. These four lengths of tubing were connected to a flow divider, which in turn was connected to a valve that permitted the perfusion of each branchial chamber with either normal seawater or reduced-salinity water. A fifth length of PE tubing (1.19 mm I.D.) was inserted through the shell posterior to the exhalant area of each branchial chamber to monitor water salinity. As in all previously described experiments, lobsters were left in the experimental chamber.

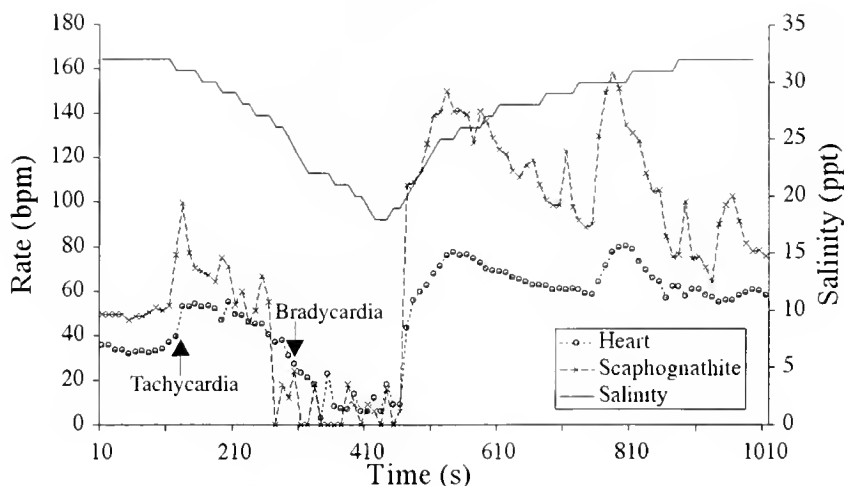


Figure 2. Changes in heart and scaphognathite rates in response to changes in salinity. As in Figure 1, salinity was decreased at a rate of 1–2 ppt/min. Each heart and scaphognathite data point is an average of 10 s of data from a digital ratemeter, while each salinity data point comes from a single refractometer measurement each min. Initial heart and scaphognathite rates were 35 and 50 bpm, respectively. Tachycardia first occurred at 31 ppt (upward arrow) and was accompanied by an increase in ventilation rate. When the salinity reached a value of 22 ppt, the lobster responded with bradycardia (downward arrow). The bradycardia response was accompanied by apnea. Shortly after the salinity began to increase, both heart and scaphognathite rates rebounded to levels well above baseline and then slowly recovered towards baseline over time.

with normal seawater flowing through both the branchial chambers and the experimental chamber (tank), overnight. The next day, lobsters were exposed to the following treatments. (1) Normal seawater (32 ppt) was perfused through the tank while the salinity in the branchial chambers was gradually reduced. (2) The salinity in the tank was reduced while the branchial chambers were perfused with normal seawater. (3) The salinity in the tank was reduced and no solutions were perfused through the branchial chamber, as in a typical salinity-reduction experiment. Treatment #1 was always carried out last; the other two treatments were randomized. Animals were given at least 1 h to recover between treatments. Water from both branchial chambers and the experimental chamber dripped into a reserve tank through PE tubing so that salinity could be sampled each minute using a refractometer.

Results

Control heart rates and cardiac response controls

After overnight acclimation in the experimental chamber, the lobsters tested before their salinity detection threshold (SDT) was measured ($n = 32$) had a mean heart rate of 52.2 ± 3.3 beats/min (bpm). The heart rates of lobsters under these control conditions were very consistent, and thus changes in heart rate in response to drops in salinity were quite evident and easy to identify. For example, in a separate experiment (cardioregulatory nerve lesion controls), when we averaged the heart rates for 5 consecutive min, in 10 different lobsters, the mean standard deviation

was only 1.2 bpm, or a 4% deviation from the average heart rate (48.4 bpm).

In response to a variety of novel stimuli, 30 of the 32 lobsters tested exhibited a transient bradycardia that was usually, although not always, accompanied by a reduction in ventilation rate (apnea). Stimuli which were effective in eliciting bradycardia included 10^{-4} M betaine, shadows, and tactile stimulation of the carapace. The abrupt and transient reductions in heart rate typically lasted 30 to 120 s, although on one occasion the heart rate stayed below baseline for 10 min. None of the lobsters showed any response to control applications of full-strength ambient seawater, which was true in all subsequent experiments as well. Only lobsters that exhibited a cardiac response to novel stimuli were tested for their response to changes in salinity.

Responses to a reduction in salinity

All the lobsters tested for their response to a reduction in salinity exhibited a dramatic change in heart rate when the salinity detection threshold was reached. The typical response was an increase, followed by a decrease, in heart rate (Figs. 1, 2). The initial tachycardia lasted for 178.0 ± 13.0 s ($n = 22$ because not all lobsters tested responded with an increase in heart rate) and was often, but not always, accompanied by a significant increase in ventilation rate. On average, heart rate increased significantly from 45.0 ± 3.0 to 66.9 ± 2.9 bpm or 48% (paired t test, $P < 0.0001$, $n = 22$). The bradycardia that occurred next was usually accompanied by a transient decrease in scaphognathite pumping

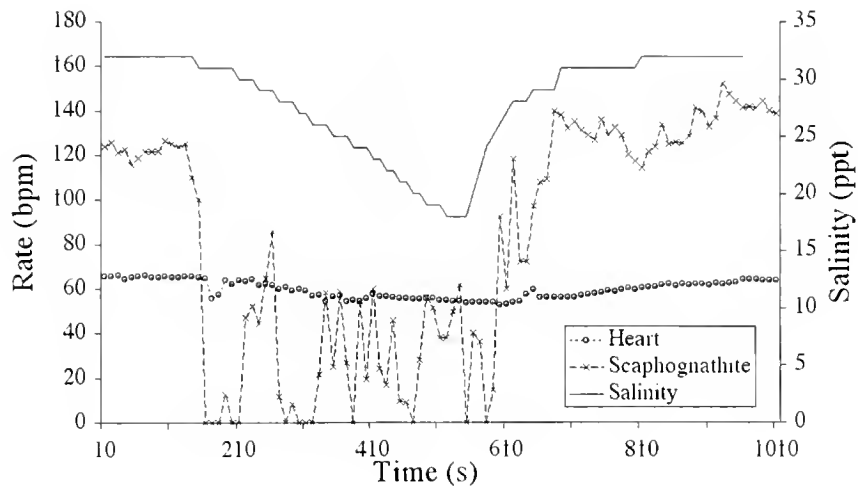


Figure 3. Heart and scaphognathite rates during a drop in salinity for a lobster with lesioned cardioregulatory nerves. The baseline heart and scaphognathite rates were 63 and 120 bpm, respectively. When the salinity reached 31 ppt, the scaphognathite rate dropped suddenly and continued a pattern of intermittent stops and starts until the salinity increased again. Over the course of the salinity drop, heart rate declined slowly to 53 bpm, a decrease of 16% from baseline, and then slowly increased back to baseline. Similar results with four additional lobsters indicate that cardiac responses to changes in salinity are mediated by the cardioregulatory nerves.

(Fig. 2). During bradycardia, the heart rate fell significantly from 50.3 ± 3.1 to 17.0 ± 1.33 bpm (paired *t* test, $P < 0.0001$, $n = 30$, a 66% decrease in rate) and remained below baseline for 123.0 ± 8.2 s. Following bradycardia, heart and ventilation rates usually increased above baseline for several minutes before full recovery (Fig. 2).

Seventy-three percent (22 of 30) of the lobsters exhibiting cardiac responses to drops in salinity expressed a biphasic change in heart rate; 27% expressed a bradycardia response with no tachycardia. Tachycardia, when present, always preceded the bradycardia and always occurred before the salinity reached 25 ppt. Although the bradycardia response was much more reliable, occurring in every lobster tested, it did not occur until the salinity had dropped to nearly 20 ppt. It is possible that the lobsters not exhibiting tachycardia may already have been in an excited state, because their average baseline heart rate was 64.6 ± 6.1 bpm and animals expressing tachycardia in response to reduced salinity increased their heart rate to 66.9 ± 2.9 . In contrast, animals that did display a tachycardia response had a mean initial heart rate of 45.0 ± 3.0 . Due to the more reliable nature of the bradycardia response, it was used in the ablation and ion-sensitivity experiments as an indicator that lobsters sensed changes in salinity.

Salinity detection threshold

Lobsters first expressed a tachycardia response when the salinity had fallen to 26.6 ± 0.7 ($n = 22$), representing a 5.4 ppt drop in salinity relative to ambient levels (32.0 ± 0.2 ppt). The salinity at which the tachycardia response occurred did not differ significantly (unpaired *t* test, $P > 0.5$)

from females (26.3 ± 0.7 ppt) to males (26.9 ± 1.1 ppt). The bradycardia response in the 30 animals tested occurred at 22.1 ± 0.5 ppt, which represents an average drop of 9.9 ppt from the ambient salinity. For the lobsters that showed both bradycardia and tachycardia responses, the salinity at which bradycardia occurred was significantly lower than that at which tachycardia occurred (paired *t* test, $P < 0.001$). The SDT for bradycardia was also significantly higher (unpaired *t* test, $P < 0.05$) for females (23.1 ± 0.4 ppt) than for males (21.0 ± 1.0 ppt).

Involvement of cardioregulatory nerves

Under control conditions, prior to treatment, there was no significant difference ($P = 0.9775$, one-way ANOVA) between the baseline heart rates of control ($n = 5$, 43.7 ± 5.5 bpm), experimental ($n = 5$, 45.3 ± 4.0 bpm), and sham-lesioned lobsters ($n = 5$, 44.9 ± 6.9 bpm). After recovery from treatment (4–7 days), the heart rates of both the sham and lesioned groups were elevated in comparison to the control group, but this difference was not statistically significant ($P = 0.2994$, one-way ANOVA: control 40.8 ± 6.7 bpm; experimental 56.6 ± 7.8 bpm; sham-lesioned 51.3 ± 6.2 bpm). Lobsters in the control and sham groups ($n = 10$) all exhibited bradycardia in response to a 1 to 2 ppt/min reduction in salinity before the salinity in the experimental chamber reached 20 ppt. There was no significant difference ($P = 0.2362$, unpaired *t* test) in the mean SDTs of these two groups of lobsters (30.4 ± 1.7 ppt for controls and 25.8 ± 3.2 ppt for sham lesions). None of the lesioned animals ($n = 5$) exhibited bradycardia in response to salinity reductions down to 20 ppt (Fig. 3). Two of the 5

lesioned animals showed a slow decrease in heart rate during the course of the salinity reduction, but the magnitude of these rate decreases did not qualify them as a bradycardia under our criteria (Fig. 3). Interestingly, all of the lesioned lobsters exhibited reductions in ventilation rates during the course of the salinity reduction (Fig. 3). The salinity at which lesioned lobsters reduced their ventilation rates was not significantly different ($P = 0.8930$, one-way ANOVA), from that of control or sham-lesioned lobsters (control $n = 3$ [because scaphognathite records were poor in 2 of the 5 lobsters], 28.3 ± 2.6 ppt; lesion $n = 5$, 26.6 ± 2.2 ppt; sham-lesion $n = 5$, 26.4 ± 3.2 ppt), suggesting that the salinity response elements in the nervous system had been activated, but the lobsters were unable to modify their heart rates due to the lesions.

Ion sensitivity

Most (21 of 24) of the lobsters exposed to isotonic solutions lacking chloride showed a typical bradycardia response (Fig. 4). However, cardiac responses were seen in only 2 of 19 lobsters exposed to isotonic solutions lacking other ions, but containing chloride (Fig. 4). Statistically, the occurrence of a bradycardia was significantly dependent on the lack of chloride (Fig. 4). For example, lobsters did not exhibit bradycardia when exposed to an isotonic solution of choline chloride, but they did upon exposure to solutions of

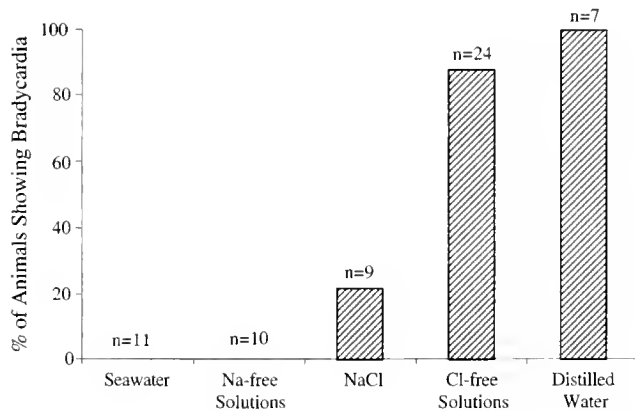


Figure 4. Percentage of trials ($n = 61$) in which lobsters exhibited bradycardia responses when exposed to natural and artificial solutions containing various amounts of certain ions. Lobsters did not usually respond when exposed to solutions containing chloride, such as seawater (natural [$n = 7$, 32 ppt] and artificial [$n = 4$]), sodium-free solutions (choline chloride [$n = 7$] and sodium-free seawater [$n = 3$]), and NaCl ($n = 9$). However, lobsters did usually exhibit bradycardia when exposed to solutions lacking chloride, such as distilled water ($n = 7$) and chloride-free solutions (sodium bicarbonate [$n = 8$], sodium acetate [$n = 7$], sodium phosphate [$n = 5$], and chloride-free seawater [$n = 4$]). Statistically, the occurrence of bradycardia was significantly dependent on the lack of chloride (Fisher's exact test, $P < 0.0001$). Each lobster ($n = 37$) was usually subjected to one to four different solutions, with sufficient time between solutions for the heart to recover to its baseline rate (> 2 h). Distilled water, when used, was always the last solution tested.

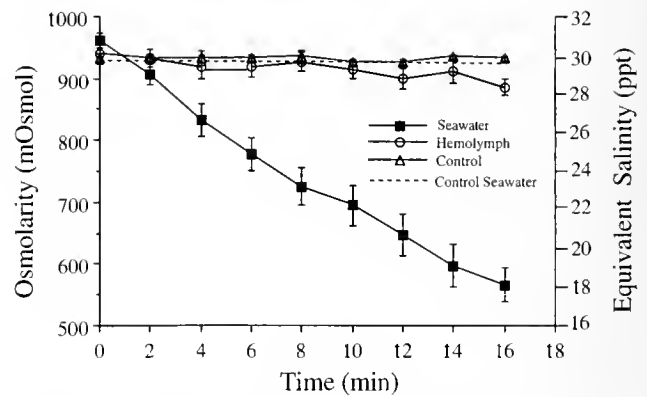


Figure 5. Comparison of the osmolarity of ambient seawater and lobster hemolymph during a typical salinity-reduction experiment. Blood samples and water samples were taken every 2 min, from eight lobsters, and averaged (\pm SEM). Control hemolymph values are also shown for eight lobsters held at a constant salinity for 16 min. There was no statistically significant difference between the hemolymph osmolarity of control and experimental animals after 10 min. However, after 16 min there was a slight, but statistically significant, difference. Equivalent salinity values, in parts per thousand, are shown on the right-hand vertical axis for comparison.

sodium phosphate and sodium acetate. Lobsters also expressed bradycardia in chloride-free but not in sodium-free artificial seawater. Thus, when only chloride was missing they detected a change, but when some combination of sodium, calcium, and magnesium was missing they responded as if the solution was normal seawater. The only exceptions were two lobsters that responded when exposed to NaCl solutions. It is not clear why they responded and seven other lobsters did not. These experiments indicate that (1) a change in osmolarity is not required for lobsters to sense a change in salinity; and (2) as long as chloride is present at normal concentrations, lobsters do not sense changes in the concentrations of other ions.

Changes in blood osmolarity as ambient salinity is reduced

In these experiments, the salinity of the seawater in the experimental chamber was reduced from 31 to 18 ppt over 16 min, and the osmolarity of lobster hemolymph and the seawater in the chamber were measured every 2 min. The control study was identical, except the salinity was not changed. After 10 min there was no statistically significant change (2-way ANOVA with replication $P > 0.10$) in the blood osmolarity of the test animals ($n = 8$) when compared to the blood osmolarity of control lobsters ($n = 8$) (Fig. 5). For comparison, in the salinity reduction experiments, the external salinity had dropped almost to 20 ppt after 10 min, which was usually sufficient to elicit a bradycardia response. After 16 min there was a small but statistically significant difference (2-way ANOVA with replication, $P < 0.01$) in experimental blood osmolarity

compared to controls (Fig. 5). Thus, although it is possible that sensitive internal receptors could detect this slight decrease in blood osmolarity, the time course and magnitude of the change—in comparison to the response of the lobsters—make it more likely that external salinity receptors detect the more robust declines that occur in the ambient seawater.

Ablation experiments

Lobsters with antennules ($n = 5$), antennae ($n = 5$), or walking legs ($n = 5$) ablated were responsive to declining salinity both before and after removal of these putative receptor sites (Fig. 6). There was no statistically significant difference between the mean SDTs obtained before and after removal of these structures (paired t test, $P > 0.5$ in all three groups; antennae $P = 0.94$, antennules $P = 0.30$, legs $P = 0.80$).

Branchial perfusion

Both branchial chambers in six lobsters were cannulated so that the salinity could be differentially controlled in both the branchial chambers and the experimental chamber. The day after cannulation, when the lobsters were exposed to different treatments, the mean heart rate of the lobsters was 51.8 ± 6.3 bpm. The SDTs were then determined in response to (1) a typical drop in external salinity; (2) a drop in external salinity with the branchial chambers perfused with normal salinity seawater; and (3) perfusion of the branchial chambers with low-salinity seawater while exposing the animal to normal seawater.

When these cannulated lobsters were exposed to a typical drop in external salinity, with no seawater perfusion of their branchial chambers, their SDT was 26.7 ± 1.4 ppt. During these experiments, the salinities in both branchial chambers and the experimental chamber were recorded each minute. These data showed that the salinity in the branchial cham-

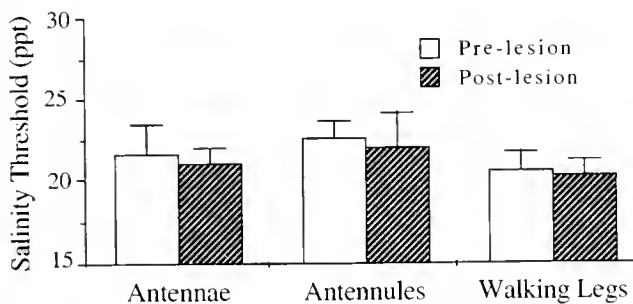


Figure 6. Mean salinity detection thresholds (SDTs) for pre- and post-lesion lobsters. The salinity level at which bradycardia occurred was measured prior to removal of antennules, antennae, and legs (pre-lesion SDT), and then compared to values obtained 4 weeks after ablations (post-lesion SDT). Five lobsters were tested after ablation of each putative receptor site. There were no statistically significant differences between any of the means (paired t test, $P > 0.5$).

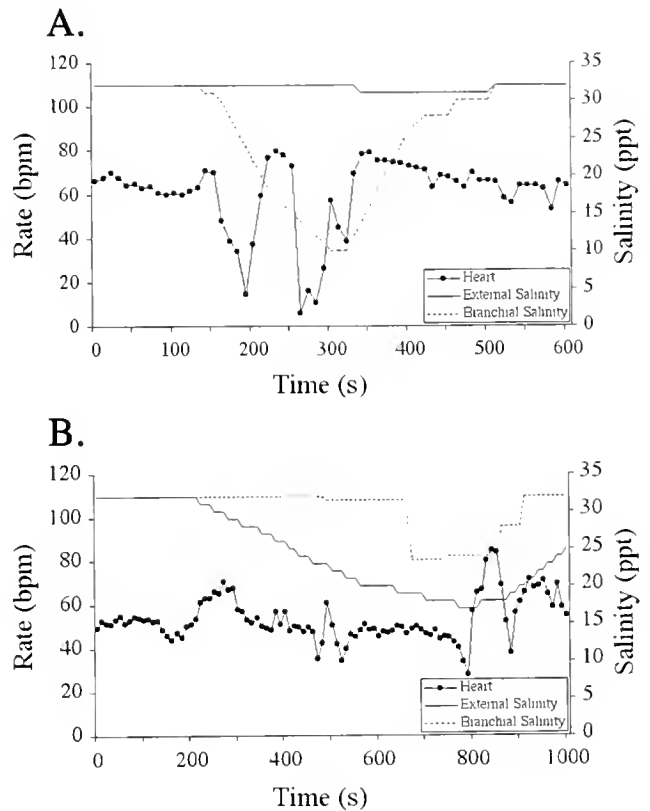


Figure 7. Cardiac responses of two lobsters to (A) perfusion of the branchial chambers with low-salinity water while providing the experimental chamber with normal seawater; and (B) perfusion of the branchial chambers with normal seawater while the salinity in the experimental tank was lowered. In both experiments, the salinity in the branchial chambers and the experimental tank was recorded every minute. The heart rates shown were averaged every 10 s. Compare how fast the lobster responded when low-salinity water was perfused directly into its branchial chambers with how long it took the other lobster to respond when the salinity in its branchial chambers was maintained close to 32 ppt, while the salinity in the experimental tank was lowered.

bers was always 1–2 ppt higher than the changes in salinity recorded in the ambient seawater. For example, in one lobster, the salinity in the branchial chambers was 28.0 ppt when the SDT was 26.7 ppt.

Perfusing the branchial chambers with normal seawater while dropping the external salinity caused the cardiac response to occur at an average external salinity of 21.6 ± 1.8 ppt (Fig. 7), which was lower than the SDT obtained from these same lobsters during the typical experiment described above. However, this difference in thresholds was not statistically significant (Mann-Whitney U test, $P = 0.06$). At the time the lobsters showed a cardiac response, the salinity in their branchial chambers was still significantly higher than the external salinity (Mann-Whitney U test, $P < 0.05$) due to the perfusion with normal seawater. However, it had decreased to a value of 29.0 ± 1.2 ppt due to dilution with the lower salinity water in the experimental tank that was being pumped through the branchial chambers

by the scaphognathites. In contrast, when the salinity in the branchial chambers was lowered, while the lobster was being perfused with normal seawater, a cardiac response was expressed almost immediately, when the branchial chamber salinity had only dropped to 29.5 ± 0.9 ppt and the external salinity had only been reduced to 31.5 ± 0.3 ppt. Interestingly, in all three experiments, there was no statistically significant difference between the salinity values in the branchial chambers when a cardiac response took place (repeated measures ANOVA, $P > 0.5$ ($P = .66$)). These data, taken together, suggest that some, if not all, of the salinity receptors are located in or near the branchial chambers.

Discussion

The ability of American lobsters to detect changes in salinity was examined by monitoring heart and ventilation rates while exposing the animals to a gradual reduction in salinity, either in the ambient seawater or in water directly flowing into the branchial chambers. The typical response to a reduction in salinity consisted of tachycardia followed by bradycardia. In the first set of experiments, tachycardia occurred when the salinity had decreased from 32 to 26.6 ± 0.7 ppt, whereas bradycardia was not expressed until the salinity dropped to 22.1 ± 0.5 ppt. During direct perfusion of the branchial chamber, bradycardia was elicited in response to very small drops in salinity (SDT = 29.5 ± 0.9 , measured in the branchial chamber); when the branchial chambers were perfused with normal seawater while the external salinity was dropped, lobsters were less responsive than during control experiments. These data suggest that the primary salinity receptors mediating the cardiac responses investigated in this study are located in or very near the branchial chambers.

In the behavioral avoidance experiments conducted by Jury *et al.* (1994b), lobsters first became restless and started to move out of their shelters when the salinity in their shelters dropped below 18 ppt. These observations, along with observations of lobsters during cardiac assays and more recent electrocardiogram recordings obtained from freely moving lobsters (D. O'Grady, University of New Hampshire, unpubl. data), indicate that the bradycardia response, and not the more sensitive tachycardia response, is more often correlated with avoidance behaviors. Therefore, even though lobsters can detect relatively small reductions in salinity, which may cause them to become aroused and may increase their heart rate, they may not exhibit avoidance behaviors until the salinity drops to about 18 ppt, a level well below that necessary to elicit bradycardia. Thus, as suggested by McGaw and McMahan (1996) and Guirguis and Wilkens (1995), bradycardia is probably a shock or startle response, indicating that animals sense a potentially dangerous stimulus and are initiating an avoidance behavior.

We suggest that tachycardia is one of the earliest indicators that lobsters have sensed a change in salinity, and that this sensory input leads to arousal and a readiness for a change in behavior. Most of the lobsters in our study that did not exhibit tachycardia had elevated heart rates before the stimulus was applied, so they may already have been in a relatively excited state. In *Callinectes sapidus*, the blue crab, drops in salinity trigger a similar tachycardia, and the available data suggest this increase in heart rate facilitates certain behaviors associated with low osmolarity (McGaw and Reiber, 1998). Lobsters induced to walk on a treadmill exhibit a very rapid increase in heart rate at the onset of activity, which is comparable to the changes observed in our experiments (Guirguis and Wilkens, 1995; Rose *et al.*, 1998; O'Grady *et al.*, 2001). This increase is mediated by the cardioregulatory nerves, and as in our experiments, the tachycardia is probably an arousal response that helps prepare the lobster for activity.

Although the physiological role of brief changes in heart and ventilation rates is not obvious, the physiological role of long-term changes is clear. Increased oxygen uptake and enhanced circulation of the hemolymph are necessary to serve the metabolic demands associated with osmoregulation (Jury *et al.*, 1994a; Houchens, 1996), locomotion (Guirguis and Wilkens, 1995; Rose *et al.*, 1998), and higher temperatures (S. Schreiber, University of New Hampshire, unpubl. data). Under these circumstances, the initial and rapid changes in heart rate appear to be mediated by the cardioregulatory nerves, whereas circulating hormones appear to be involved in long-term modulation (Guirguis and Wilkens, 1995; McMahan, 1999; Jury and Watson, 2000; O'Grady *et al.*, 2001).

Marine animals may sense drops in ambient salinity by detecting a change in osmolarity (Davenport, 1972; Davenport and Wankowski, 1973; Tazaki, 1975; Schmidt, 1989), or they may utilize a sensory mechanism that is sensitive to the concentration of one or more of the ions present in seawater (Davenport, 1981; Akberali and Davenport, 1982). One further possibility is that a change in osmolarity could alter the responsiveness of another type of receptor. For example, in *Callinectes sapidus*, the sensitivity of olfactory sensilla decreases in low-salinity water because the osmotic stress causes the outer dendritic segments to change size (Gleeson *et al.*, 1996, 1997). However, in the two species of molluscs that have been studied in the most detail, *Mytilus edulis* and *Scrobicularia plana*, and in two crustaceans, *Carcinus maenas* (Hume and Berlind, 1976) and *Homarus americanus* (present study), the salinity detection systems involved are sensitive to the concentration of certain ions rather than to overall osmolarity. Both molluscs are primarily sensitive to sodium, magnesium, and calcium, and only slightly responsive to changes in chloride levels (Davenport, 1981; Akberali and Davenport, 1982). Hume and Berlind (1976) were unable to determine if any single ion was detected during salinity reductions in *Carcinus maenas*. In

contrast, the lobsters in the present study exhibited the typical low-salinity response when exposed to saline solutions lacking chloride, even though the osmolarity of the artificial saline was identical to that of seawater. Moreover, they did not exhibit that response when exposed to solutions that lacked other ions but contained appropriate concentrations of chloride ions. Thus, although marine crustaceans may employ any of several mechanisms to detect changes in salinity, the American lobster appears to detect drops in salinity by monitoring changes in the concentration of chloride ions.

This study provides evidence that at least some salinity receptors in lobsters are located in or near the branchial chamber. A similar conclusion was reached by Hume and Berlind (1976) for *Carcinus maenas* and by Larimer (1964) for crayfish. Previous studies of various crustaceans have suggested that osmoreceptors might be located on the antennules or antennae (Lagerspetz and Mattila, 1961; Van Weel and Christofferson, 1966; Tazaki and Tanino, 1973), and the dactyls (Case *et al.*, 1960; Davenport, 1972; Davenport and Wankowski, 1973; Schmidt, 1989). However, in this investigation we did not find any evidence that the antennules, antennae, or legs were necessary for the detection of salinity changes in *Homarus americanus*.

There may be internal receptors for salinity or osmolarity in lobsters, but three lines of evidence strongly implicate external receptors. First, there was no statistically significant change in blood osmolarity during the first 10 min of our experiments, even though changes in heart rate typically occur within the first 5 min, when the external salinity had been reduced by 6 to 8 ppt. Second, when the branchial chamber was perfused with low-salinity water while the rest of the animal was exposed to normal seawater, bradycardia occurred very rapidly in response to very small drops in salinity. Finally, when the branchial chamber was selectively perfused with normal seawater, animals became less responsive to changes in external salinity. Their eventual response was typically correlated with a slight decrease in the branchial chamber salinity, which was difficult to maintain at 32 ppt when the external salinity reached low levels. Thus, while the available evidence suggests that external salinity receptors probably exist, further studies are clearly needed to better localize and characterize these sensory structures.

Lobsters inhabit estuarine and coastal habitats where storms and spring runoff often produce large drops in salinity that may last for days or weeks (Charmantier *et al.*, 2001). This puts a tremendous demand upon the limited ability of the animals to osmoregulate, causing a marked increase in metabolism and, at salinities less than 10 ppt, extensive mortality (McLeese, 1956; Thomas and White, 1969; Jury *et al.*, 1994a; Houchens, 1996). The avoidance responses to drops in salinity that lobsters exhibit in the laboratory probably serve in their natural habitat to move them to an area that might have a higher salinity (Jury *et al.*,

1994b, 1995). Although we have used bradycardia as an assay for detection of salinity and possibly as an index of an impending avoidance response, the true adaptive significance of this response still needs to be resolved. In the field, bradycardia would probably be triggered when reductions in salinity are rapid, long-lasting, or of sufficient magnitude to cause osmoregulatory stress. During the spring runoff season in the Great Bay estuary, the salinity typically drops at a rate of 0.2 ppt/min; the rate of decrease is probably even greater during a storm with heavy rains (see the UNH/CICEET IDEMS website: www.ciceet.unh.edu). It is likely that lobsters would detect such a change, and their reaction would be twofold. First, they would avoid the low-salinity water and seek deeper water, closer to the coast, that would have a higher salinity (Jury *et al.*, 1994b, 1995). Second, they would increase their metabolism and heart and ventilation rates to help fuel the Na^+/K^+ -ATPases necessary to keep their blood osmolarity higher than the ambient water (Jury *et al.*, 1994a; Charmantier *et al.*, 2001). The metabolic demands of these behavioral and physiological adaptations are likely to be too large to allow both to occur simultaneously. Results from recent studies, in which we measured locomotion, ventilation, and heart rates while exposing lobsters to gradual drops in salinity, indicate that when they are faced with this dilemma, lobsters will eventually stop walking and give priority to osmoregulation (D. O'Grady, University of New Hampshire, unpubl. data). Field studies are necessary to further test this hypothesis and clarify how lobsters regulate their heart and ventilation rates in response to naturally occurring changes in their environment.

Acknowledgments

We thank the anonymous reviewers whose comments greatly improved the manuscript. We also thank Hunt Howell for his input on, and assistance with, all aspects of this work, John Sasner for his advice during the early stages of this study, Mike Kinnison for his preliminary studies in the Spaulding Lab, Noel Carlson for his help at the Coastal Marine Laboratory, and Ed Millman for his meticulous editing. Special thanks to Glenn Crossin for his aid in fine-tuning the bradycardia assay and Mary Calhoun for patience, driving, and support. This project was supported by USDA (Hatch) and NOAA (Sea Grant) grants to WHW and Hunt Howell, as well as funds from the UNH Marine Program and Graduate School. It is contribution number 376 of the Center for Marine Biology/Jackson Estuarine Laboratory series.

Literature Cited

- Able, K. W., K. L. Heck, Jr., M. P. Fahay, and C. T. Roman. 1988. Use of salt-marsh peat reefs by small juvenile lobsters on Cape Cod, Massachusetts. *Estuaries* 11: 83–86.
- Akberali, H. B., and J. Davenport. 1982. The detection of salinity changes by the marine bivalve mollusc *Scrobicularia plana* (da Costa) and *Mytilus edulis* L. *J. Exp. Mar. Biol. Ecol.* 58: 59–71.

- Atema, J., and R. Voigt. 1995. Behavior and sensory biology. Pp. 313-348 in *Biology of the Lobster*. Homarus americanus J. R. Factor, ed. Academic Press, New York.
- Case, J., G. F. Gwillian, and F. Hanson. 1960. Dactyl chemoreceptors of brachyurans. *Biol. Bull.* 119: 308.
- Charmantier, G., C. Haond, J.-H. Lignot, and M. Charmantier-Daures. 2001. Ecophysiological adaptation to salinity throughout a life cycle: a review in homarid lobsters. *J. Exp. Biol.* 204: 967-977.
- Dall, W. 1970. Osmoregulation in the lobster *Homarus americanus*. *J. Fish. Res. Board Can.* 27: 1123-1130.
- Davenport, J. 1972. Salinity tolerances and preferences in the porcelain crab, *Porcellana platycheles* and *P. longicornis*. *Mar. Behav. Physiol.* 1: 123-138.
- Davenport, J. 1981. The opening response of mussels (*Mytilus edulis*) exposed to rising seawater concentrations. *J. Mar. Biol. Assoc. UK* 61: 667-678.
- Davenport, J., and J. Wankowski. 1973. Pre-immersion salinity-choice behavior in *Porcellana platycheles*. *Mar. Biol.* 22: 313-316.
- Florey, E., and M. E. Kriebel. 1974. The effects of temperature, anoxia and sensory stimulation on the heart rate of unrestrained crabs. *Comp. Biochem. Physiol.* 48A: 285-300.
- Gleeson, R. A., L. M. McDowell, and H. C. Aldrich. 1996. Structure of the aesthetasc (olfactory) sensilla of the blue crab, *Callinectes sapidus*: transformations as a function of salinity. *Cell Tissue Res.* 284: 279-288.
- Gleeson, R. A., M. G. Wheatly, and C. L. Reiber. 1997. Perireceptor mechanisms sustaining olfaction at low salinities: insight from the euryhaline blue crab *Callinectes sapidus*. *J. Exp. Biol.* 200: 445-456.
- Guirguis, M. S., and J. L. Wilkens. 1995. The role of the cardioregulatory nerves in mediating heart rate responses to locomotion, reduced stroke volume, and neurohormones in *Homarus americanus*. *Biol. Bull.* 188: 179-185.
- Houchens, C. R. 1996. A comparison of the osmoregulatory capabilities of estuarine and coastal populations of the American lobster, *Homarus americanus*. Master's thesis, University of New Hampshire, 76 pp.
- Howell, W. H., W. H. Watson III, and S. H. Jury. 1999. Skewed sex ratio in an estuarine lobster (*Homarus americanus*) population. *J. Shellfish Res.* 18: 193-201.
- Hume, R. I., and A. Berling. 1976. Heart and scaphognathite rate changes in a euryhaline crab, *Carcinus maenas*, exposed to dilute environmental medium. *Biol. Bull.* 150: 241-254.
- Johnson, B. R., R. Voigt, and J. Atema. 1989. Response properties of lobster chemoreceptor cells: response modulation by stimulus mixtures. *Physiol. Zool.* 62: 559-579.
- Jury, S. H., and W. H. Watson III. 2000. Thermosensitivity of the lobster, *Homarus americanus*, as determined by cardiac assay. *Biol. Bull.* 199: 257-264.
- Jury, S. H., M. T. Kinnison, W. H. Howell, and W. H. Watson III. 1994a. The effects of reduced salinity on lobster (*Homarus americanus* Milne Edwards) metabolism: implications for estuarine populations. *J. Exp. Mar. Biol. Ecol.* 176: 167-185.
- Jury, S. H., M. T. Kinnison, W. H. Howell, and W. H. Watson III. 1994b. The behavior of lobsters in response to reduced salinity. *J. Exp. Mar. Biol. Ecol.* 180: 23-37.
- Jury, S. H., W. H. Howell, and W. H. Watson III. 1995. Lobster movements in response to a hurricane. *Mar. Ecol. Prog. Ser.* 119: 305-310.
- Lagerspetz, K., and M. Mattila. 1961. Salinity reactions of some fresh- and brackish-water crustaceans. *Biol. Bull.* 120: 44-53.
- Larimer, J. 1964. Sensory-induced modifications of ventilation and heart rate in crayfish. *Comp. Biochem. Physiol.* 12: 25-36.
- Loder, T. C., J. A. Love, C. E. Penniman, and C. D. Neefus. 1983. Long-term environmental trends in nutrient and hydrographic data from the Great Bay Estuarine System, New Hampshire-Maine. University of New Hampshire Marine Program, UNH-MP-D/TR-SG-83-6. 65 pp.
- Maynard, D. M. 1960. Circulation and heart function. Pp. 161-226 in *The Physiology of Crustacea*, Vol. 1, T. H. Waterman, ed. Academic Press, New York.
- McGaw, I. J., and B. R. McMahon. 1996. Cardiovascular responses resulting from variation in external salinity in the dungeness crab, *Cancer magister*. *Physiol. Zool.* 69: 1384-1401.
- McGaw, I. J., and C. L. Reiber. 1998. Circulatory modification in the blue crab *Callinectes sapidus*, during exposure and acclimation to low salinity. *Comp. Biochem. Physiol.* 121A: 67-76.
- McLeese, D. W. 1956. Effects of temperature, salinity and oxygen on the survival of the American lobster. *J. Fish. Res. Board Can.* 13: 247-272.
- McMahon, B. R. 1999. Intrinsic and extrinsic influences on cardiac rhythms in crustaceans. *Comp. Biochem. Physiol.* 124A: 539-547.
- Munro, J., and J. Therriault. 1983. Migrations saisonnières du homard (*Homarus americanus*) entre la côte et les lagunes des Îles-de-la-Madeleine. *Can. J. Fish. Aquat. Sci.* 40: 905-918.
- Offutt, G. C. 1970. Acoustic stimulus perception by the American lobster, *Homarus americanus* (Decapoda). *Experientia* 26: 1276-1278.
- O'Grady, D. F., S. H. Jury, and W. H. Watson III. 2001. The use of a treadmill to study the relationship between locomotion, ventilation and heart rate in the lobster, *Homarus americanus*. *Mar. Freshw. Res.* (In press).
- Rose, R. A., J. L. Wilkens, and R. L. Walker. 1998. The effects of walking on heart rate, ventilation rate and acid-base status in the lobster *Homarus americanus*. *J. Exp. Biol.* 201: 2601-2608.
- Scarratt, D. J., and G. E. Raine. 1967. Avoidance of low salinity by newly hatched lobster larvae. *J. Fish. Res. Board Can.* 24: 1403-1406.
- Schmidt, M. 1989. The hair-peg organs of the shore crab, *Carcinus maenas* (Crustacea, Decapoda): ultrastructure and functional properties of sensilla sensitive to changes in seawater concentration. *Cell Tissue Res.* 257: 609-621.
- Short, F. T., ed. 1992. *The Ecology of the Great Bay Estuary, New Hampshire and Maine: An Estuarine Profile and Bibliography*. NOAA Coastal Ocean Program Publ. 222 pages.
- Tazaki, K. 1975. Sensory units responsive to osmotic stimuli in the antennae of the spiny lobster, *Panulirus japonicus*. *Comp. Biochem. Physiol.* 51A: 647-653.
- Tazaki, K., and T. Tanino. 1973. Responses of osmotic concentration changes in the lobster antenna. *Experientia* 29: 1090-1091.
- Thomas, M. L. H., and G. N. White. 1969. Mass mortality of estuarine fauna at Biddeford P. E. associated with abnormally low salinities. *J. Fish. Res. Board Can.* 26: 701-704.
- Tierney, A. J., R. Vnigt, and J. Atema. 1988. Response properties of chemoreceptors from the medial antennular filament of the lobster *Homarus americanus*. *Biol. Bull.* 174: 364-372.
- Van Weel, P. B., and J. P. Christofferson. 1966. Electrophysiological studies on perception in the antennules of certain crabs. *Physiol. Zool.* 39: 317-325.
- Watson, W. H. III, A. Vetrovs, and W. H. Howell. 1999. Lobster movements in an estuary. *Mar. Biol.* 134: 65-75.

INDEX

A

- Acetylcholine, muscarinic, 276
 Actin, 240, 241
 Action potentials occur spontaneously in squid giant axons with moderately alkaline intracellular pH, 186
 Age structure of the Pleasant Bay population of *Crepidula fornicata*: a possible tool for estimating horseshoe crab age, 296
 Aggregation, 175
 Aggression, 385
 Aging, 296
 ÅKESSON, BERTIL, see Thomas G. Dahlgren, 193
 Alga, 34, 121, 126, 287
 Alkaline intracellular pH, 186
 AMIENT, SETH A., see Nadav Shashar, 267
 Ammonium, 288
 An initial study on the effects of signal intermittency on the odor plume tracking behavior of the American lobster, *Homarus americanus*, 274
 Animal-algal symbiosis, 348, 360
 Annelida, 193
Anthopleura, 385
 Aquarium, acoustics in, 278
Arbacia eggs, 234
Argopecten, 285
 ARMSTRONG, PETER B., see Mara L. Conrad, 246
 ARNOLDS, D. E. W., see S. J. Zottoli, 277
 Array, 263
 ASAMOAH, N. O., see S. J. Zottoli, 277
 Ascidian, 52
 Asexual reproduction, 45
 Asexual reproduction in *Pygospio elegans* Claparède (Annelida, Polychaeta) in relation to parasitism by *Lepocreadium setiferoides* (Miller and Northup) (Platyhelminthes, Trematoda), 45
Asterias, 95, 175
 ATEMA, JELLE, see Corinne Kozłowski, 274
Aurelia, 104
 Auditory processing, 280
 Axonal transport, 240, 243
 Axoplasmic vesicle, 243

B

- BABA, SHOJI A., see Yoshihiro Mogami, 26
 BALLARIN, LORIANO, ANTONELLA FRANCHINI, ENZO OTTAVIANI, AND ARMANDO SABBADIN, Morula cells as the major immunomodulatory hemocytes in ascidians: evidences from the colonial species *Botryllus schlosseri*, 59
 Ballast water, 297
 BARLOW, R., see M. Errigo, 271; S. Meadors, 272
 Bay scallop, 285
 BECHTEL, DEANNA L., see Alan M. Kuzirian, 297
 Behavior, 6, 271, 323, 424
 Benthic alga, 287
 BERKING, STEFAN, see Igor A. Kossevitch, 417
 Bimodal units in the torus semicircularis units of the toadfish (*Opsanus tau*), 280
 BINDER, MANFRED, see David S. Hibbett, 319
 Biogeography, 95, 104
 Biogeography of *Asterias*: North Atlantic climate change and speciation, 95
 Bioluminescence, 339
 Biomass, 292

- Biomechanics, 126
 BISHOP, CORY D., AND BRUCE P. BRANDHORST, NO/cGMP signaling and HSP90 activity repress metamorphosis in the sea urchin *Lytechinus pictus*, 394
 BLACKSTONE, NEIL W., see Lawrence M. Ponczek, 76
 Blastodisc, 251
 BOLAND, WILHELM, see Ingo Maier, 121
 BORST, DOUGLAS, see Nadav Shashar, 267
Botryllus, 59
 BOYER, BARBARA C., see Susan D. Hill, 257
 BRANDHORST, BRUCE P., see Cory D. Bishop, 394
 BROWN, JEREMIAH R., KYLE R. SIMONETTA, LESLIE A. SANDBERG, PHILLIP STAFFORD, AND GEORGE M. LANGFORD, Recombinant globular tail fragment of myosin-V blocks vesicle transport in squid nerve cell extracts, 240
 BRYAN, BRUCE, see Osamu Shimomura, 339
 BUCHSBAUM, ROBERT, see Libby Williams, 287
 Buoyancy, sea urchin egg, 234
 BURBACH, J. PETER H., ANITA J. C. G. M. HELLEMONS, MARCO HOEKMAN, PHILIP GRANT, AND HARISH C. PANT, The stellate ganglion of the squid *Loligo pealeii* is a model for neuronal development: expression of a POU Class VI homeodomain gene *Rpf-1*, 252
 BURGER, MAX, see William J. Kuhns, 238
Bythograea, 167

C

- CA1, 236
 Calcium, 248, 263
 Camouflage, 269, 301
 CAMPBELL, A. C., S. COPPARD, C. D'ABREO, AND R. TUDOR-THOMAS, Escape and aggregation responses of three echinoderms to conspecific stimuli, 175
Capitella, 257
 Cardiac, 424
 CARLINI, DAVID B., see Brad A. Seibel, 1
 CARMICHAEL, RUTH, see Laurie Fila, 294; Sara P. Grady, 296
 CARROLL, IAN, see Hemant M. Chikarmane, 285
 β -catenin, 255
 Catfish, 278
 Cell
 division, 241
 lineage, 405
 Centrifuge microscope, 234
 Centrifuge polarizing microscope with dual specimen chambers and injection ports, 234
 Cephalopod, 1, 136, 154, 186, 240, 251, 267
 cGMP signaling, 394
 CHANG, FRED, see P. T. Tran, 235
 CHAPPELL, RICHARD L., AND STEPHEN REDENTI, Endogenous zinc as a neuromodulator in vertebrate retina: evidence from the retinal slice, 265
 CHARMANTIER, GUY, see Anne-Sophie Martinez, 167
 CHARMANTIER-DAURES, MIREILLE, see Anne-Sophie Martinez, 167
 CHEVEZ, C., see S. J. Zottoli, 277
 CHIAO, CHUAN-CHIN, AND ROGER T. HANLON, Cuttlefish cue visually on area—not shape or aspect ratio—of light objects in the substrate to produce disruptive body patterns for camouflage, 269
Chionoecetes opilio, 204
 CHIKARMANE, HEMANT M., ALAN M. KUZIRIAN, IAN CARROLL, AND ROBBIN DENGLE, Development of genetically tagged bay scallops for evaluation of seeding programs, 285

Chloride, 424
 Chloroplast, 34
 Choice chamber, 175
 Cholinergic modulation of odor-evoked oscillations in the frog olfactory bulb, 276
 Cichlidae, 258
 Clam oocyte extract, 241
 CLAY, JOHN R., AND ALAN M. KUZIRIAN, A novel, kinesin-rich preparation derived from squid giant axons, 243
 CLAY, JOHN R., AND ALVIN SHRIER, Action potentials occur spontaneously in squid giant axons with moderately alkaline intracellular pH, 186
 Climate change, 374
 Clonal biology, 76
 Cnidaria, 104, 385
 Coelenterate, 339
 Cohort analysis, 296
 Collagen, 136, 154
 Colonial animal, 76
 A comparison of sounds recorded from a catfish (*Orinocodoras eigenmanni*, Doradidae) in an aquarium and in the field, 278
 Competition, 385
 Competition for space among sessile marine invertebrates: changes in HSP70 expression in two Pacific cnidarians, 385
 CONRAD, MARA L., R. L. PARDY, AND PETER B. ARMSTRONG, Response of the blood cell of the American horseshoe crab, *Limulus polyphemus*, to a lipopolysaccharide-like molecule from the green alga *Chlorella*, 246
 Conspecific stimuli, 175
 Contractile ring, 241
 COPPARD, S., see A. C. Campbell, 175
 Coral
 bleaching, 348, 360
 reef, 348, 360
 Cortical flow, 241
Corynactis, 385
 Crab, 17, 167, 204
 CRAWFORD, KAREN, Ooplasm segregation in the squid embryo, *Loligo pealeii*, 251
Crepidula fornicata, 296
 Cuttlefish, 269
 Cuttlefish cue visually on area—not shape or aspect ratio—of light objects in the substrate to produce disruptive body patterns for camouflage, 269
 Cytokinesis, 241
 Cytological basis of photoresponsive behavior in a sponge larva, 323
 Cytoskeleton, 251

D

D'ABREO, C., see A. C. Campbell, 175
 DAHLGREN, THOMAS G., BERTIL ÅKESSON, CHRISTOFFER SCHANDER, KENNETH M. HALANYCH, AND PER SUNDBERG, Molecular phylogeny of the model annelid *Ophryotrocha*, 193
 Deep sea, 1
 DEGNAN, BERNARD M., see Sally P. Leys, 323
 DELANEY, KERRY, see Benjamin Hall, 276
 Delayed insemination results in embryo mortality in a brooding ascidian, 52
 DENGLER, ROBBIN, see Hemant M. Chikarmane, 285
 DEPINA, ANA S., see Torsten Wöllert, 241
 Detection of salinity by the lobster, *Homarus americanus*, 424
 Development, 272, 285, 405
 Development of genetically tagged bay scallops for evaluation of seeding programs, 285
 Developmental patterns and cell lineages of vermiform embryos in dicyemid mesozoans, 405
 Dichroism, 231
 Dicyemid, 405
 Differentiation of pharyngeal muscles on the basis of enzyme activities in the cichlid *Tamniichromis intermedius*, 258
 Dinoflagellate, 348, 360

Dissolved nitrogen dynamics in groundwater under a coastal Massachusetts forest, 288
 Dissolved organic nitrogen, 288
 Disturbance, 360
 DODGE, F., see M. Errigo, 271; S. Meadors, 272
 Dorsal cell, 277
 Drag, 126
 Drag, drafting, and mechanical interactions in canopies of the red alga *Chondrus crispus*, 126
 DUFORT, CHRISTOPHER G., STEVEN H. JURY, JAMES M. NEWCOMB, DANIEL F. O'GRADY III, AND WINSOR H. WATSON III, Detection of salinity by the lobster, *Homarus americanus*, 424
 Dye coupling, 277
 Dye coupling evidence for gap junctions between supramedullary/dorsal neurons of the cunner, *Tautoglabrus adspersus*, 277

E

Echinoderm, 175
Echnus, 175
 EDDS-WALTON, P. L., see R. R. Fay, 280
 Eddy chemotaxis, 274
 EEG, 218
 Effect of cloning rate on fitness-related traits in two marine hydroids, 76
 The effects of salt marsh haying on benthic algal biomass, 287
 Egg
 Arbacia, 234
 longevity, 84
 Egg longevity and time-integrated fertilization in a temperate sea urchin (*Strongylocentrotus droebachiensis*), 84
 Elastic energy storage, 136
 Electrical activity, spontaneous, 186
 Electrotonic coupling, 277
Elysia, 34
 Embryo loss, 52
 Endogenous zinc, 265
 Endogenous zinc as a neuromodulator in vertebrate retina: evidence from the retinal slice, 265
 Endosymbiosis, 34
 Endotoxin, 246
 Epi-fluorescence, 235
 Epibiont, 296
 ERRIGO, M., C. MCGUINNESS, S. MEADORS, B. MITTMANN, F. DODGE, AND R. BARLOW, Visually guided behavior of juvenile horseshoe crabs, 271
 Escape, 175
 jet, 154, 252
 Escape and aggregation responses of three echinoderms to conspecific stimuli, 175
 Estuarine crab, 17
 Estuary, 290, 292
 Evidence for directed mitotic cleavage plane reorientations during retinal development within the zebrafish, 254
 Evolution of marine mushrooms, 319
 Exocytosis, 246
 Extracts, 240
 Eye, 272

F

FAY, R. R., AND P. L. EDDS-WALTON, Bimodal units in the torus semicircularis units of the toadfish (*Opsanus tau*), 280
 FELDMAN, ROBERT A., see Kenneth M. Halanych, 65
 FERNANDEZ-BUSQUETS, XAVIER, see William J. Kuhns, 238
 Fertilization, 52, 84, 234
 FILA, LAURIE, RUTH HERROLD CARMICHAEL, ANDREA SHRIVER, AND IVAN VALIELA, Stable N isotopic signatures in bay scallop tissue, feces, and pseudofeces in Cape Cod estuaries subject to different N loads, 294
 Fingerprinting, 285
 FLOOD, PER R., see Osamu Shimomura, 339
 Flow, 126

Fluorescence
 microscopy, 231
 polarization, 231
 Fluorescence polarization ratio of GFP crystals, 231
 Fractionation, 294
 FRANCHINI, ANTONELLA, see Lorian Ballarin, 59
 Free radicals, 261
 FRET, 231
 FULLER, S. N., see S. J. Zottoli, 277
 Fungi, 319
 FURUYA, HIDETAKA, F. G. HOCHBERG, AND KAZUHIKO TSUNEKI, Developmental patterns and cell lineages of vermiform embryos in dicyemid mesozoans, 405

G

Gap junction, 277
 GARZA, J. M., see R. V. Hernandez, 236
 Genetic tag, 285
 GERSHWIN, LISA-ANN, Systematics and biogeography of the jellyfish *Aurelia labiata* (Cnidaria: Scyphozoa), 104
 GFP, 231
 Gill current, 6
 GODA, MAKOTO, see Shinya Inoué, 231; Robert A. Knudson, 234
 GOULD, ROBERT M., see Ryan Smith, 255
 GRADY, SARA P., DEBORAH RUTECKI, RUTH CARMICHAEL, AND IVAN VALIELA, Age structure of the Pleasant Bay population of *Crepidula fornicata*: a possible tool for estimating horseshoe crab age, 296
 GRANT, PHILIP, see J. Peter H. Burbach, 252
 Grass
 Fellowships, 218
 Foundation, 218
 Instrument Company, 218
 GRAVES, M. E., see R. V. Hernandez, 236
 Gravity, 26
 Grazer inclusion, 292
 Green fluorescence protein, 231
 Groundwater, 288, 290
 Growth, visual field, and resolution in the juvenile *Limulus* lateral eye, 272
 Gulf of Maine, 45

H

HALANYCH, KENNETH M., see Thomas G. Dahlgren, 193
 HALANYCH, KENNETH M., ROBERT A. FELDMAN, AND ROBERT C. VRIENHOEK, Molecular evidence that *Sclerolium brattstromi* is closely related to vestimentiferans, not to frenulate pogonophorans (Siboglinidae, Annelida), 65
 HALL, BENJAMIN, AND KERRY DELANEY, Cholinergic modulation of odor-evoked oscillations in the frog olfactory bulb, 276
 HANLON, ROGER T., see Nadav Shashar, 267; Chuan-Chin Chiao, 269; Allen F. Mensinger, 282
 HANTEN, JEFFREY J., AND SIDNEY K. PIERCE, Synthesis of several light-harvesting complex I polypeptides is blocked by cycloheximide in symbiotic chloroplasts in the sea slug, *Elysia chlorotica* (Gould): a case for horizontal gene transfer between alga and animal?, 34
 Hardening, 417
 Harvard Medical School, 218
 HAUXWELL, ALYSON M., CHRISTOPHER NEILL, IVAN VALIELA, AND KEVIN D. KROEGER, Small-scale heterogeneity of nitrogen concentrations in groundwater at the seepage face of Edgartown Great Pond, 290
 Hay, salt marsh, 287
 Hearing, 280
 Heat shock protein, 374, 385, 394
 HELLEMONS, ANITA J. C. G. M., see J. Peter H. Burbach, 252
 HELMUTH, BRIAN S. T., AND GRETCHEN E. HOFMANN, Microhabitats, thermal heterogeneity, and patterns of physiological stress in the rocky intertidal zone, 374
 Hemocyte, 59
 HERBERHOLZ, JENS, AND BARBARA SCHMITZ, Signaling via water currents in behavioral interactions of snapping shrimp (*Alpheus heterochaelis*), 6

Hermaphroditism, 193
 HERNANDEZ, R. V., J. M. GARZA, M. E. GRAVES, J. L. MARTINEZ, JR., AND R. G. LEBARON, The process of reducing CA1 long-term potentiation by the integrin binding peptide, GRGDSP, occurs within the first few minutes following theta-burst stimulation, 236
 HERRMANN, KLAUS, see Igor A. Kossevitch, 417
 HERTWECK, CHRISTIAN, see Ingo Maier, 121
 HIBBETT, DAVID S., AND MANFRED BINDER, Evolution of marine mushroomrooms, 319
 Hidden in plain sight: the ecology and physiology of organismal transparency, 301
 HILL, SUSAN D., AND BARBARA C. BOYER, Phalloidin labeling of developing muscle in embryos of the polychaete *Capitella* sp. 1, 257
 HINCKLEY, EVE-LYN S., CHRISTOPHER NEILL, RICHARD MCHORNEY, AND ANN LEZBERG, Dissolved nitrogen dynamics in groundwater under a coastal Massachusetts forest, 288
 Hippocampus, 236
 HIZA, N. A., see S. J. Zottoli, 277
 HO, MICHAEL, see William J. Kuhns, 238
 HOCHBERG, R. G., see Hidetaka Furuya, 405
 HOEKMAN, MARCO, see J. Peter H. Burbach, 252
 HOFMANN, GRETCHEN E., see Brian S. T. Helmuth, 374
 Homeodomain gene, 252
 Host response, 45
 HSP70, 385
 HSP90, role of, 394
Hydractinia, 76
 Hydrogen peroxide, 297
 Hydrogen peroxide: an effective treatment for ballast water, 297
 Hydroid, 76
 Hydromineral regulation in the hydrothermal vent crab *Bythograea thermydron*, 167
 Hydrostatic skeleton, 136, 154
 Hydrothermal vent, 167

I

Iyanassa obsoleta, 292
 Immunity, invertebrate, 246
 Immunology, 59
 Independent contrast, 1
 INOUÉ, SHINYA, AND MAKOTO GODA, Fluorescence polarization ratio of GFP crystals, 231
 INOUÉ, SHINYA, see Robert A. Knudson, 234
 INOUE, SATOSHI, see Osamu Shimomura, 339
 Integrins, 236, 238
 Invasive species, 297
 Iridophore, 267
 ISHII, JUNKO, see Yoshihiro Mogami, 26
 Isolation and properties of the luciferase stored in the ovary of the scyphozoan medusa *Periphylla periphylla*, 339
 Isotope, 294

J

JAMES, PATRICK J., see Alan M. Kuzirian, 297
 Jellyfish, 104
 JOHNSEN, SÖNKE, Hidden in plain sight: the ecology and physiology of organismal transparency, 301
 JOHNSON, AMY S., Drag, drafting, and mechanical interactions in canopies of the red alga *Chondrus crispus*, 126
 JUNG, SUNG-KWON, see Gilad Twig, 261
 JURY, STEVEN H., see Christopher G. Dufort, 424

K

KAATZ, INGRID M., AND PHILLIP S. LOBEL, A comparison of sounds recorded from a catfish (*Orinocodorus eigenmanni*, Doradidae) in an aquarium and in the field, 278
 KAATZ, INGRID M., see Aaron N. Rice, 258
 KAITENBACH, JANE, see William J. Kuhns, 238

- KAVANAGH, EMMA, see Ryan Smith, 255
 KELLER, BRUCE, see Robert B. Silver, 263
 KIER, WILLIAM M., see Joseph T. Thompson, 136, 154
 Kinesin, 243
 KISHORI, B., see P. Sreenivasula Reddy, 17
 KNOWLTON, N., see W. W. Toller, 348, 360
 KNUDSON, ROBERT A., SHINYA INOUÉ, AND MAKOTO GODA, Centrifuge polarizing microscope with dual specimen chambers and injection ports, 234
 KOSSEVITCH, IGOR A., KLAUS HERRMANN, AND STEFAN BERKING, Shaping of colony elements in *Laomedea flexuosa* Hinks (Hydrozoa, Thecophora) includes a temporal and spatial control of skeleton hardening, 417
 KOZLOWSKI, CORINNE, KARA YOPAK, RAINER VOIGT, AND JELLE ATEMA, An initial study on the effects of signal intermittency on the odor plume tracking behavior of the American lobster, *Homarus americanus*, 274
 KRIEBEL, MAHLON E., see Robert B. Silver, 263
 KROEGER, KEVIN D., see Alyson M. Hauxwell, 290
 KUHNS, WILLIAM J., DARIO RUSCIANO, JANE KALTENBACH, MICHAEL HO, MAX BURGER, AND XAVIER FERNANDEZ-BUSQUETS, Up-regulation of integrins $\alpha_3 \beta_1$ in sulfate-starved marine sponge cells: functional correlates, 238
 KUZIRIAN, ALAN M., see John R. Clay, 243; Hemant M. Chikarmane, 285
 KUZIRIAN, ALAN M., ELEANOR C. S. TERRY, DEANNA L. BECHTEL, AND PATRICK I. JAMES, Hydrogen peroxide: an effective treatment for ballast water, 297

L

- Laminariales, 121
 LANGFORD, GEORGE M., see Jeremiah R. Brown, 240; Torsten Wöllert, 241
Laomedea, 417
 Larva, 323
 development of, 394
 gastrula, 26
 Lateral line, 280
 LEBARON, R. G., see R. V. Hernandez, 236
 Leukotriene B₄, 248
 LEVER, MARK, see Melissa Novak, 292
 LEYS, SALLY P., AND BERNARD M. DEGNAN, Cytological basis of photoreponsive behavior in a sponge larva, 323
 LEZBERG, ANN, see Eve-Lyn S. Hinckley, 288
Limulus, 246, 271, 272, 296
 LINK, BRIAN A., Evidence for directed mitotic cleavage plane reorientations during retinal development within the zebrafish, 254
 Lipopolysaccharide, 246
 LOBEL, PHILLIP S., see Aaron N. Rice, 258; Ingrid M. Kaatz, 278
 Lobster, 274, 424
 Local field potential, 276
 Locomotion, 136, 154
 LiB₄ evokes the calcium signal that initiates nuclear envelope breakdown through a multi-enzyme network in sand dollar (*Echinarcinus parma*) cells, 248

M

- Macrophage, 261
 MAIER, INGO, CHRISTIAN HERTWECK, AND WILHELM BOLAND, Stereochemical specificity of lamoxirene, the sperm-releasing pheromone in kelp (Laminariales, Phaeophyceae), 121
 Mangrove, 319
 Mariculture, 282, 283
 Mariculture of the toadfish *Opsanus tau*, 282
 Marine Biological Laboratory
 and the Grass Foundation, 218
 Annual Report, v. 200(1), R1
 General Scientific Meetings, Short Reports, 227
 MARTINEZ, ANNE-SOPHIE, JEAN-YVES TOULUEC, BRUCE SHILLITO, MIREILLE CHARMANTIER-DAURES, AND GUY CHARMANTIER, Hydromineral regulation in the hydrothermal vent crab *Bythograea theryndron* 167
 MARTINEZ, J. L., JR., see R. V. Hernandez, 236

- Mating success, 204
 Maximum likelihood, 193
 MBL, see Marine Biological Laboratory
 MCCURDY, DEAN G., Asexual reproduction in *Pygospio elegans* Claparède (Annelida, Polychaeta) in relation to parasitism by *Lepocreadium setiferoides* (Miller and Northup) (Platyhelminthes, Trematoda), 45
 MCGUINNESS, C., see M. Errigo, 271; S. Meadors, 272
 MCHORNEY, RICHARD, see Eve-Lyn S. Hinckley, 288
 MEADORS, S., C. MCGUINNESS, F. A. DODGE, AND R. BARLOW, Growth, visual field, and resolution in the juvenile *Limulus* lateral eye, 272
 MEADORS, S., see M. Errigo, 271
 Mechanoreception, 280
 MEIDEL, SUSANNE K., AND PHILIP O. YUND, Egg longevity and time-integrated fertilization in a temperate sea urchin (*Strongylocentrotus droebachiensis*), 84
 MENSINGER, ALLEN F., see Leila E. Rieder, 283
 MENSINGER, ALLEN F., KATHERINE A. STEPHENSON, SARAH L. POLLEMA, HAZEL E. RICHMOND, NICHOLE PRICE, AND ROGER T. HANLON, Mariculture of the toadfish *Opsanus tau*, 282
 Mesozoa, 405
 Messenger RNAs located in spiny dogfish oligodendrocyte processes, 255
 MESSERLI, MARK A., see Gilad Twig, 261
 Metabolism, 1
 Metabolism of pelagic cephalopods as a function of habitat depth: a reanalysis using phylogenetically independent contrasts, 1
 Metamorphosis, 394
 Methionine-enkephalin induces hyperglycemia through eustalk hormones in the estuarine crab *Scylla serrata*, 17
 Microhabitats, thermal heterogeneity, and patterns of physiological stress in the rocky intertidal zone, 374
 Microphytobenthos, 292
 Microscope
 centrifuge, 234
 polarizing, 234
 Microscopy, 231, 235
 Microsporidian dynactin, 245
 Microsporidian spore/sporoplasm dynactin in *Spraguea*, 245
 Midbrain, 280
 Midwater, 1
 Mitosis, 248
 MITTMANN, B., see M. Errigo, 271
 Model, 248
 MOGAMI, YOSHIHIRO, JUNKO ISHII, AND SHOJI A. BABA, Theoretical and experimental dissection of gravity-dependent mechanical orientation in gravitactic microorganisms, 26
 Molecular
 evolution, 255
 phylogeny, 193
 systematics, 319
 Molecular evidence that *Sclerolimum brattstromi* is closely related to vestimentiferans, not to frenulate pogonophorans (Siboglinidae, Annelida), 65
 Molecular phylogeny of the model annelid *Ophryotrocha*, 193
Montastraea annularis, 348, 360
 Morphology, 126, 104
 MORRISON, HILARY G., see Ryan Smith, 255
 Morula cells as the major immunomodulatory hemocytes in ascidians: evidences from the colonial species *Botryllus schlosseri*, 59
 Mud snail, 292
 Muscle
 development, 257
 physiology, 258
 Mutualism, 348, 360
 Mycology, 319
 Myosin
 II, 241
 V, 240
Mytilus californianus, 374

N

- NEILL, CHRISTOPHER, see Eve-Lyn S. Hinckley, 288; Alyson M. Hauxwell, 290
- Neural adaptation, 265
- Neuroepithelium, 254
- Neuronal development, 252
- Neuromodulator, 265
- Neuromuscular junction, 263
- Neurophysiology, 218
- NEWCOMB, JAMES M., see Christopher G. Dufort, 424
- NIERMAN, J. E., see S. J. Zottoli, 277
- Nitrate, 288
- Nitric oxide, 394
- Nitrogen, 288
loading, 290, 294
- NO/cGMP signaling and HSP90 activity repress metamorphosis in the sea urchin *Lytechinus pictus*, 394
- NOBLITT, G. CARL, IV, see Libby Williams, 287
- NOVAK, MELISSA, MARK LEVER, AND IVAN VALIELA, Top down vs. bottom-up controls of microphytobenthic standing crop: role of mud snails and nitrogen supply in the littoral of Waquoit Bay estuaries, 292
- A novel, kinesin-rich preparation derived from squid giant axons, 243
- Nuclear envelope breakdown, 248
- Nutrient, 292

O

- O'GRADY, DANIEL F., III, see Christopher G. Dufort, 424
- Odor tracking behavior, 274
- Odor-gated rheotaxis, 274
- Olfaction, 276
- Oligodendrocyte, 255
- Ontogenetic changes in fibrous connective tissue organization in the oval squid, *Sepioteuthis lessoniana* Lesson, 1830, 136
- Ontogenetic changes in mantle kinematics during escape jet locomotion in the oval squid, *Sepioteuthis lessoniana* Lesson, 1830, 154
- Ontogeny, 136, 154
- Ooplasm segregation in the squid embryo, *Loligo pealeii*, 251
- Ophryotrocha*, 193
- Opioid peptide, 17
- Optics, 301
- Orientation, 26
- The origins of The Grass Foundation, 218
- Oscillation, 276
- Osmolarity, 424
- Osmoregulation, 167
- OTTAVIANI, ENZO, see Lorian Ballarin, 59

P

- PANT, HARISH C., see J. Peter H. Burbach, 252
- PAPPAS, GEORGE D., see Robert B. Silver, 263
- Paramecium*, 26
- Parasitism, 45
- PARDY, R. L., see Mara L. Conrad, 246
- Pelagic, 1
- Peptide, opioid, 17
- Perisarc, 417
- Phaeophyceae, 121
- Phalloidin labeling of developing muscle in embryos of the polychaete *Capitella* sp. 1, 257
- Pharyngeal jaw, 258
- Pheromone, 121
- PHILLIPPI, AIMEE, see J. Stewart Savage, 52
- Photoreceptor, 323
feedback, 265
- Phototaxis, 323
- Phylogenetics, 65
- Phylogeny, 1, 193
- PIERCE, SIDNEY K., see Jeffrey J. Hanten, 34
- Plankton, 297

- Pleasant Bay, 296
- Pleistocene, 95
- Plum Island Sound, 287
- Podocoryna*, 76
- Pogonophora, 65
- Polarization reflecting iridophores in the arms of the squid *Loligo pealeii*, 267
- Polarization
microscope, 234
vision, 267
- POLLEMA, SARAH L., see Allen F. Mensinger, 282
- Polychaete, 193
larva, 257
- Polygamy, 204
- PONCZEK, LAWRENCE M., AND NEIL W. BLACKSTONE, Effect of cloning rate on fitness-related traits in two marine hydroids, 76
- Population biology, 104
- Porifera, 323
- Porocytosis, 263
- Porocytosis: quantal synaptic secretion of neuro-transmitter at the neuromuscular junction through arrayed vesicles, 263
- PORTNOY, DAVID S., see Aaron N. Rice, 258
- Potentiality, long-term, 236
- PRICE, NICOLE, see Allen F. Mensinger, 282
- The process of reducing CA1 long-term potentiation by the integrin binding peptide, GRGDSP, occurs within the first few minutes following theta-burst stimulation, 236
- Proopiomelanocortin, 255
- Psammochinus*, 175

Q

- Quantum, 263

R

- Rana pipiens*, 276
- 16S rDNA, 65
- 18S rDNA, 65
- Real-time detection of reactive oxygen intermediates from single microglial cells, 261
- Receptor, 424
- Recombinant globular tail fragment of myosin-V blocks vesicle transport in squid nerve cell extracts, 240
- Reconstitution of active pseudo-contractile rings and myosin-II-mediated vesicle transport in extracts of clam oocytes, 241
- REDDY, P., SREENIVASULA, AND B. KISHORI, Methionine-enkephalin induces hyperglycemia through eyestalk hormones in the estuarine crab *Scylla serrata*, 17
- REDENTI, STEPHEN, see Richard L. Chappell, 265
- Reflection, 267
- Repopulation of zooxanthellae in the Caribbean corals *Montastraea annularis* and *M. faveolata* following experimental and disease-associated bleaching, 360
- Reproduction, 193
asexual, 45
sexual, 121
- Reproductive success, 45
- Resolution, 272
- Response of the blood cell of the American horseshoe crab, *Limulus polyphemus*, to a lipopolysaccharide-like molecule from the green alga *Chlorella*, 246
- Retina, 272
development of, in zebrafish, 254
slice, 265
- Ribosomal RNA genes, 348
- RICE, AARON N., DAVID S. PORTNOY, INGRID M. KAATZ, AND PHILLIP S. LOBEL, Differentiation of pharyngeal muscles on the basis of enzyme activities in the cichlid *Tramitichromis intermedius*, 258
- RICHMOND, HAZEL E., see Allen F. Mensinger, 282

- RIEDER, LEILA E., AND ALLEN F. MENSINGER, Strategies for increasing growth of juvenile toadfish, 283
- Rocky intertidal zone, 374
- RONDEAU, AMÉLIE, AND BERNARD SAINTE-MARIE, Variable mate-guarding time and sperm allocation by male snow crabs (*Chionoecetes opilio*) in response to sexual competition, and their impact on the mating success of females, 204
- ROSSI, SERGI, AND MARK J. SNYDER, Competition for space among sessile marine invertebrates: changes in HSP70 expression in two Pacific cnidarians, 385
- ROWAN, R., see W. W. Toller, 348, 360
- RUSCIANO, DARIO, see William J. Kuhns, 238
- RUTECKI, DEBORAH, see Sara P. Grady, 296

S

- SABBADIN, ARMANDO, see Lorian Ballarín, 59
- SAIDEL, WILLIAM M., see Nadav Shashar, 267
- SAINTE-MARIE, BERNARD, see Amélie Rondeau, 204
- Salinity, 424
- Salt marsh, 287
- SANDBERG, LESLIE A., see Jeremiah R. Brown, 240; Torsten Wöllert, 241
- Scallop, 294
- SCHANDER, CHRISTOFFER, see Thomas G. Dahlgren, 193
- SCHMITZ, BARBARA, see Jens Herberholz, 6
- Sclerolimum*, 65
- Scyphozoa, 104
- Scylla*, 17
- Sea slug, 34
- Sea urchin, 26, 84, 394
- Secretion, 263
- Segmentation, 257
- SEIBEL, BRAD A., AND DAVID B. CARLINI, Metabolism of pelagic cephalopods as a function of habitat depth: a reanalysis using phylogenetically independent contrasts, 1
- Self-referencing, 261
- Sensory processing, 280
- Sex ratio, 204
- Sexual
 competition, 204
 reproduction, 121
- Shaping of colony elements in *Laomedea flexuosa* Hinks (Hydrozoa, Thecophora) includes a temporal and spatial control of skeleton hardening, 417
- SHASHAR, NADAV, DOUGLAS BORST, SETH A. AMENT, WILLIAM M. SAIDEL, ROXANNA M. SMOLOWITZ, AND ROGER T. HANLON, Polarization reflecting iridophores in the arms of the squid *Loligo pealeii*, 267
- SHILLITO, BRUCE, see Anne-Sophie Martinez, 167
- SHIMOMURA, AKEMI, see Osamu Shimomura, 339
- SHIMOMURA, OSAMU, PER R. FLOOD, SATOSHI INOUE, BRUCE BRYAN, AND AKEMI SHIMOMURA, Isolation and properties of the luciferase stored in the ovary of the scyphozoan medusa *Periphylla periphylla*, 339
- SHIRIHAI, ORIAN S., see Gilad Twig, 261
- SHRIER, ALVIN, see John R. Clay, 186
- SIRIVER, ANDREA, see Laurie Fila, 294
- Siboglinidae, 65
- Signaling, 6
- Signaling *via* water currents in behavioral interactions of snapping shrimp (*Alpheus heterochaelis*), 6
- SILVER, ROBERT B., MAHLON E. KRIEBEL, BRUCE KELLER, AND GEORGE D. PAPPAS, Porocytosis: quantal synaptic secretion of neuro-transmitter at the neuromuscular junction through arrayed vesicles, 263
- SILVER, ROBERT, LiB_4 evokes the calcium signal that initiates nuclear envelope breakdown through a multi-enzyme network in sand dollar (*Echinarcinus parma*) cells, 248
- SIMONETTA, KYLE R., see Jeremiah R. Brown, 240
- Skate, 265
- Small-scale heterogeneity of nitrogen concentrations in groundwater at the seepage face of Edgartown Great Pond, 290
- SMITH, PETER J. S., see Gilad Twig, 261
- SMITH, RYAN, EMMA KAVANAGH, HILARY G. MORRISON, AND ROBERT M. GOULD, Messenger RNAs located in spiny dogfish oligodendrocyte processes, 255
- SMOLOWITZ, ROXANNA M., see Nadav Shashar, 267
- Snow crab, 204
- SNYDER, MARK J., see Sergi Rossi, 385
- Sound, swimbladder
- Speciation, 95
- Sperm
 depletion, 204
 economy, 204
 limitation, 204
- Sponge, 323
- Spontaneous electrical activity, 186
- Squid, 240, 251, 252, 267
 giant axon, 186, 252
- Stable N isotope, 294
- Stable N isotopic signatures in bay scallop tissue, feces, and pseudofeces in Cape Cod estuaries subject to different N loads, 294
- STAFFORD, PHILIP, see Jeremiah R. Brown, 240
- The stellate ganglion of the squid *Loligo pealeii* is a model for neuronal development: expression of a POU Class VI homeodomain gene *Rpf-1*, 252
- STEPHENSON, KATHERINE A., see Allen F. Mensinger, 282
- Stereochemical specificity of lamosirene, the sperm-releasing pheromone in kelp (Laminariales, Phaeophyceae), 121
- STEWART-SAVAGE, J., AIMEE PHILLIPPI, AND PHILIP O. YUND, Delayed insemination results in embryo mortality in a brooding ascidian, 52
- Strategies for increasing growth of juvenile toadfish, 283
- Stress protein, 374, 385, 394
- Subtractive hybridization, 255
- SUNDBERG, PER, see Thomas G. Dahlgren, 193
- Supramedullary neurons, 277
- Symbiodinium*, 348, 360
- Synaptic
 plasticity, 236
 vesicle, 263
- Synthesis of several light-harvesting complex I polypeptides is blocked by cycloheximide in symbiotic chloroplasts in the sea slug, *Elysia chlorotica* (Gould): a case for horizontal gene transfer between alga and animal?, 34
- Systematics, 104
- Systematics and biogeography of the jellyfish *Aurelia labiata* (Cnidaria: Scyphozoa), 104

T

- TABOADA, L. A., see S. J. Zottoli, 277
- Teleost, 282
- Temporal pattern, 52
- TERRY, ELEANOR C. S., see Alan M. Kuzirian, 297
- Theoretical and experimental dissection of gravity-dependent mechanical orientation in gravitactic microorganisms, 26
- Thermal stress, 374
- THOMPSON, JOSEPH T., AND WILLIAM M. KIER, Ontogenetic changes in fibrous connective tissue organization in the oval squid, *Sepioteuthis lessoniana* Lesson, 1830, 136
- THOMPSON, JOSEPH T., AND WILLIAM M. KIER, Ontogenetic changes in mantle kinematics during escape jet locomotion in the oval squid, *Sepioteuthis lessoniana* Lesson, 1830, 154
- Toadfish, 282, 283
- TOLLER, W. W., R. ROWAN, AND N. KNOWLTON, Repopulation of zooxanthellae in the Caribbean corals *Montastraea annularis* and *M. faveolata* following experimental and disease-associated bleaching, 360
- TOLLER, W. W., R. ROWAN, AND N. KNOWLTON, Zooxanthellae of the *Montastraea annularis* species complex: patterns of distribution of four taxa of *Symbiodinium* on different reefs and across depths, 348
- Top down vs. bottom-up controls of microphytobenthic standing crop: role of mud snails and nitrogen supply in the littoral of Waquoit Bay estuaries, 292
- TOULLEC, JEAN-YVES, see Anne-Sophie Martinez, 167

TRAN, P. T., AND FRED CHANG, Transmitted light fluorescence microscopy revisited, 235
 Trans-fluorescence, 235
 Transmitted light fluorescence microscopy revisited, 235
 Transparency, 301
 TSUNEKI, KAZUHIKO, see Hidetaka Furuya, 405
 TUDOR-THOMAS, R., see A. C. Campbell, 175
 TWIG, GILAD, SUNG-KWON JUNG, MARK A. MESSERLI, PETER J. S. SMITH, AND ORIAN S. SHIRIHAI, Real-time detection of reactive oxygen intermediates from single microglial cells, 261

U

Ultrastructure, 301
 Up-regulation of integrins $\alpha_3 \beta_1$ in sulfate-starved marine sponge cells: functional correlates, 238

V

VALIELA, IVAN, see Alyson M. Hauxwell, 290; Melissa Novak, 292; Laurie Fila, 294; Sara P. Grady, 296
 Variable mate-guarding time and sperm allocation by male snow crabs (*Chionoecetes opilio*) in response to sexual competition, and their impact on the mating success of females, 204
Vaucheria, 34
 Ventilation, 424
 Vermiform embryo, 405
 Vesicle transport, 240, 241
 Vision, 271, 301
 Visual
 cue, 269
 field, 272
 predation, 301
 Visually guided behavior of juvenile horseshoe crabs, 271

VOIGT, RAINER, see Corinne Kozlowski, 274
 VRIJENHOEK, ROBERT C., see Kenneth M. Halanych, 65

W

Waquoit Bay, 292, 294
 WARES, J.P., Biogeography of *Asterias*: North Atlantic climate change and speciation, 95
 WATSON, WINSOR H., III, see Christopher G. Dufort, 424
 WEIDNER, EARL, Microsporidian spore/sporoplasm dynactin in *Spraguea*, 245
 WILLIAMS, LIBBY, G. CARL NOBLITT IV, AND ROBERT BUCHSBAUM, The effects of salt marsh hay on benthic algal biomass, 287
 WÖLLERT, TORSTEN, ANA S. DEPINA, LESLIE A. SANDBERG, AND GEORGE M. LANGFORD, Reconstitution of active pseudo-contractile rings and myosin-II-mediated vesicle transport in extracts of clam oocytes, 241

Y

YOPAK, KARA, see Corinne Kozlowski, 274
 YUND, PHILIP O., see J. Stewart Savage, 52; Susanne K. Meidel, 84

Z

Zebrafish retinal development, 254
 Zooxanthella, 348, 360
 Zooxanthellae of the *Montastraea annularis* species complex: patterns of distribution of four taxa of *Symbiodinium* on different reefs and across depths, 348
 ZOTTOLI, S. J., D. E. W. ARNOLDS, N. O. ASAMOAH, C. CHEVEZ, S. N. FULLER, N. A. HIZA, J. E. NIERMAN, AND L. A. TABOADA, Dye coupling evidence for gap junctions between supramedullary/dorsal neurons of the cunner, *Tautoglabrus adspersus*, 277
 ZOTTOLI, STEVEN J., The origins of The Grass Foundation, 218

Biomimetic Engineering Conference

March 3-8, 2002

Sandestin, Florida

Biological organisms exhibit sophisticated crystal engineering capabilities that underlie the remarkable material properties of mineralized tissues such as bone and teeth, and the beautiful and functional nacre of molluscs and abalone. Increasing interest is being paid to nature's processing strategies, particularly by materials scientists looking for bio-inspired methods to engineer unique ceramics coatings or composites for use in magnetic, optical, biomedical, and protective coatings applications. In particular, the engineering of hard tissues may benefit from biomimetic approaches since the benign conditions allow for the incorporation of biomolecular compounds into the organic/inorganic composite during fabrication.

On the other hand, there is great interest from the biomedical community because the disruption of normal biomineralization processes may lead to pathological conditions, such as in arteriosclerotic plaque formation, encrustation of biomaterials (such as urinary catheters and artificial heart valve calcification), kidney stone buildup, dental calculus formation, or bone and tooth demineralization.

The main objective of this conference is to bring together scientists, physicians, and engineers in a relaxed environment, with talks designed to bridge the gap between researchers in this interdisciplinary field.

This groundbreaking conference will have sessions that deal with (a) Biomineralization in Nature: Vertebrates and Invertebrates (Inspiration for Design Principles), (b) Organic Modulators of Crystallization: Templated Nucleation and Crystal Growth Modification, (c) Engineering Strategies: Bioinspired Materials and Novel Physicochemical Properties, and (d) Applications of Biomimetic Materials: Devices and Processes.

Each day will open with a keynote address to highlight the day's topics; each of the sessions will include eight to ten presentations, with afternoons left free for ad hoc meetings and informal discussions. An evening poster session will also promote dialogue among the attendees.

The Chair of the Conference is Dr. Allison A. Campbell of the Pacific Northwest National Laboratory in Richland, Washington, and the Co-Chair is Prof. Laurie Gower of the University of Florida in Gainesville.

Additional information about this Conference — and a registration form — can be found at www.engfnd.org.

The United Engineering Foundation is located at Three Park Avenue, 27th Floor, New York, NY 10016-5902; Tel: 212-591-7836, Fax: 212-591-7441, E-mail: engfnd@aol.com

THE BIOLOGICAL BULLETIN

2002 Subscription Rates Volumes 202-203

*Paid Subscriptions include both print and electronic subscriptions at: www.biolbull.org

	Institutional*	Individual*
One year subscription (6 issues - 2 volumes)	\$260.00	\$105.00
Single volume (3 issues)	\$130.00	\$52.50
Single Issues	\$ 45.00	\$20.00

*Surface delivery included in above prices.

For prompt delivery, we encourage subscribers outside the U.S. to request airmail service.

Airmail Delivery Charge

U.S. and Canada:	\$ 25.00
Mexico:	\$ 60.00
All other locations:	\$100.00

Orders Must Be Prepaid in U.S. Dollars, Check Payable to The Marine Biological Laboratory

About *The Biological Bulletin*

ISSN: 0006-3185

Frequency: Bimonthly

Number of issues per year: 6

Months of Publication: February, April, June, August, October, December

Subscriptions entered for calendar year

Volume indexes contained in June and December issues

Annual report of the Marine Biological Laboratory contained in August issue

Most back issues available

Claims handled upon receipt

No agency discounts

Internet:

www.biolbull.org

Please address orders to:

Wendy Child

Subscriptions

The Biological Bulletin

Marine Biological Laboratory

7 MBL Street

Woods Hole, MA 02543-1015 U.S.A.

Fax: 508-289-7922 Tel: 508-289-7402 Email: wchild@mbl.edu

Published by the Marine Biological Laboratory

Woods Hole, Massachusetts, 02543 U.S.A.

THE BIOLOGICAL BULLETIN
(www.biolbull.org)
2002 SUBSCRIPTION FORM
(VOLUMES 202-203, 6 ISSUES)

All subscriptions run on the calendar year; price includes both print and online journals.

(please print)

NAME: _____

INSTITUTION: _____

ADDRESS: _____

CITY: _____ STATE: _____

POSTAL CODE: _____ COUNTRY: _____

TELEPHONE: _____ FAX: _____

E-MAIL ADDRESS: _____

Please send me a 2002 subscription to *The Biological Bulletin* at the rate indicated below:

Individual: \$105.00 (6 ISSUES)

Institutional: \$260.00 (6 ISSUES)

Individual: \$ 52.50 (3 ISSUES)

Institutional: \$130.00 (3 ISSUES)

Check one: February, April, June or August, October, December

Please send me the following back issue(s): _____

Individual: at \$20.00 (PER ISSUE)

Institutional: at \$45.00 (PER ISSUE)

Delivery Options

_____ Surface Delivery (Surface delivery is included in the subscription price.)

_____ Air delivery (Please add the correct amount to your payment.)

U.S. and Canada: \$25.00 Mexico: \$60.00 All other locations: \$100.00

Payment Options

_____ Enclosed is my check or U.S. money order for \$ _____ made payable to The Marine Biological Laboratory

_____ Please send me an invoice. (Note: Payment must be received before subscription commences.)

_____ Please charge my VISA, MasterCard Discover Card \$ _____

Account No.: _____ Exp. Date: _____

Signature: _____ Date: _____

Return this form with your check or credit card information to:

Marine Biological Laboratory

Subscription Office ♦ The Biological Bulletin ♦ 7 MBL Street ♦ Woods Hole, MA 02543-1015

MARINE RESOURCES CENTER

MARINE BIOLOGICAL LABORATORY • WOODS HOLE, MA 02543 • (508)289-7700

WWW.MBL.EDU/SERVICES/MRC/INDEX.HTML



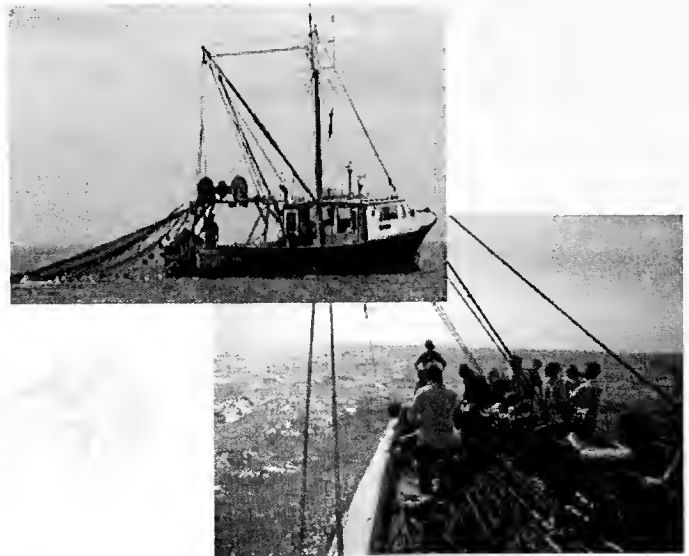
zebrafish facilities

Animal and Tissue Supply for Education & Research

- 150 aquatic species available for shipment via online catalog: <<http://www.mbl.edu/animals/index.html>>; phone: (508)289-7375; or e-mail: specimens@mbi.edu
- zebrafish colony containing limited mutant strains
- custom dissection and furnishing of specific organ and tissue samples

MRC Services Available

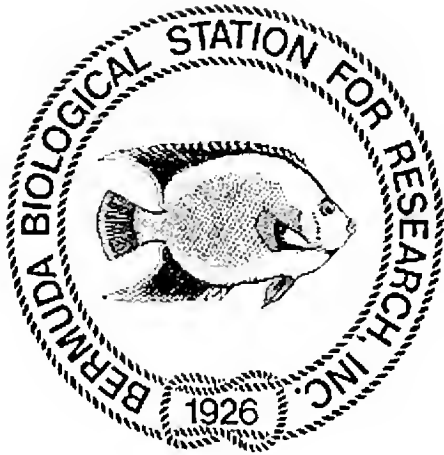
- basic water quality analysis
- veterinary services (clinical, histopathologic, microbial services, health certificates, etc.)
- aquatic systems design (mechanical, biological, engineering, etc.)
- educational tours and collecting trips aboard the R/V Gemma



Using the MRC for Your Research

- capability for advanced animal husbandry (temperature, light control, etc.)
- availability of year-round, developmental life stages
- adaptability of tank system design for live marine animal experimentation





"Chemosensory Neurobiology in the Marine Environment"

a 3-week summer course at the
Bermuda Biological Station for Research
June 16-July 5, 2002

Faculty

Dr. Hank Trapido-Rosenthal, Bermuda Biological
Station for Research
Dr. Charles Derby, Georgia State University

We will study chemosensory neurobiology in the marine environment at the physiological, biochemical, and molecular levels. Lectures will deal with chemoreception in a variety of marine organisms. In laboratory exercises and research projects the olfactory system of the spiny lobster, *Panulirus argus*, will serve as the main teaching and research tool. Emphasis is on experimental techniques and approaches to the study of chemosensory biology. Receptor cell electrophysiology, immunocytochemistry, BrdU labeling of cell proliferation, biochemistry of receptor and perireceptor phenomena, and molecular biology (PCR, sequencing, and other techniques) will be taught and applied to the study of novel research questions relating to chemical sensing, including basic function and applications (e.g. environmental biology).

The course is designed to benefit graduate students and advanced undergraduates with interests in organismal, systems, cellular, or molecular biology.

Competitive scholarships are available to cover tuition, room, and board.

For more information or applications, see
<http://www.bbsr.edu/Education/summercourses/summercourses.html>

For questions, contact the instructors:

Charles Derby

Dept. of Biology, Georgia State University, P. O. Box 4010

Atlanta, GA 30302-4010

cderby@gsu.edu

(404) 651-3058 (office)

<http://www.gsu.edu/~biocdd/>

or

Hank Trapido-Rosenthal

Bermuda Biological Station for Research, 17 Biological Lane

Ferry Reach, GE01, Bermuda

hank@sargasso.bbsr.edu

(441) 297-1880

http://www.bbsr.edu/About_BBSR/Faculty_Profiles/hank/hank.html/

2081 32

2002 SUMMER RESEARCH FELLOWSHIPS

FUNDING AVAILABLE FOR SUMMER RESEARCH AT THE MARINE BIOLOGICAL LABORATORY

The Marine Biological Laboratory is pleased to announce the availability of funding for Summer Research Fellowships in 2002 for junior or senior investigators holding a Ph.D., M.D., or equivalent degree. These prestigious awards provide costs for research and housing, and also enable Fellows to benefit from the rich intellectual and interactive environment of the scientific community at the MBL.

Proposals for Fellowship support will be considered in, but are not limited to, the following fields of investigation:

Cellular & Molecular Physiology **Parasitology**
Developmental Biology **Microbiology**
Neurobiology **Molecular Biology**
Ecology

In addition, specific Fellowships also provide state-of-the-art microscopy support.

ADDITIONAL INFORMATION IS AVAILABLE ON OUR WEB-SITE:

<http://www.mbl.edu/fellowships>

APPLICATION DEADLINE FOR
FELLOWSHIPS IS JANUARY 15, 2002

FOR APPLICATION FORMS AND ADDITIONAL INFORMATION, PLEASE CONTACT:

Sandra Kaufmann, Fellowship Coordinator
(508)289-7441, skaufman@mbl.edu

*Applications are encouraged from women and
members of underrepresented minorities.*

The MBL is an EEO/Affirmative Action Institution



Marine Biological Laboratory, 7 MBL Street, Woods Hole, Massachusetts 02543-1015

OGL-OCEAN GENOME LEGACY

■ Team Leader

A new not-for-profit foundation devoted to the preservation, distribution and evolutionary genomics of DNA from marine organisms is seeking a Team Leader.

The successful candidate will have a Ph.D. in cell or molecular biology, 4+ years' experience in molecular biology, and be highly motivated to work at the bench. Responsibilities will include the assembly of a small team of scientists for the long-term preservation of marine organism DNA, development of tissue culture techniques for marine invertebrate cells, construction of genome libraries, and evolutionary genomics of special marine transition groups.

The OGL laboratory will be temporarily located at New England Biolabs, Inc., Beverly, MA until a new facility is constructed in Ipswich, MA.

*Applicants should send a resume and three references to:
Carol Ann Zapustas, New England Biolabs, Inc.,
32 Tozer Road, Beverly, MA 01915.*

OCEAN GENOME LEGACY



An Equal Opportunity Employer.

Marine Biological Laboratory

2002 Course Offerings

**Advances In Genome Technology &
Bioinformatics**
October 6 - November 1

Analytical & Quantitative Light Microscopy
May 9 - May 17

Biology of Parasitism: Modern Approaches
June 13 - August 10

**Embryology: Concepts & Techniques In
Modern Developmental Biology**
June 16 - July 27

**Frontiers In Reproduction: Molecular &
Cellular Concepts & Applications**
May 19 - June 29

Fundamental Issues In Vision Research
August 11 - August 24

Medical Informatics
1st Session: May 26 - June 2
2nd Session: September 29 - October 6

Methods in Computational Neuroscience
August 4 - September 1

Microbial Diversity
June 16 - August 2

Microinjection Techniques In Cell Biology
May 21 - May 28

Molecular Biology of Aging
July 30 - August 17

**Molecular Mycology: Current Approaches
to Fungal Pathogenesis**
August 12 - August 30



Substantial financial assistance is
available for many of our courses!

For more information contact:
Carol Hamel,
Admissions Coordinator
(508) 289-7401
admissions@mbl.edu
<http://courses.mbl.edu>

The MBL is an EEO/Affirmative Action Institution

**Neural Development & Genetics
of Zebrafish**
August 18 - August 31

Neural Systems & Behavior
June 16 - August 10

Neurobiology
June 16 - August 17

Neuroinformatics
August 17 - September 1

**Optical Microscopy & Imaging In the
Biomedical Sciences**
October 9 - October 18

**Physiology: The Biochemical & Molecular
Basis of Cell Signaling**
June 16 - July 27

**Rapid Electrochemical Measurements In
Biological Systems**
May 9 - May 13

**Summer Program In Neuroscience, Ethics,
& Survival (SPINES)**
June 15 - July 13

Workshop on Molecular Evolution
July 28 - August 9

Marine Biological Laboratory, 7 MBL Street, Woods Hole, MA 02543



LSM 510 META

A ioplan 2
imaging

Opening

doors to new worlds

The Next Generation:

Laser Scanning Microscope LSM 510
META for multi-channel fluorescence
in single and multiphoton microscopy

META - a unique confocal
microscope detector will separate
overlapping fluorescence dyes
for sharp, crosstalk free images.

Carl Zeiss MicroImaging, Inc.
One Zeiss Drive
Thornwood, NY 10594

1.800.233.2343
micro@zeiss.com
www.zeiss.com/micro





MBL WHOI LIBRARY



WH 1839 U

